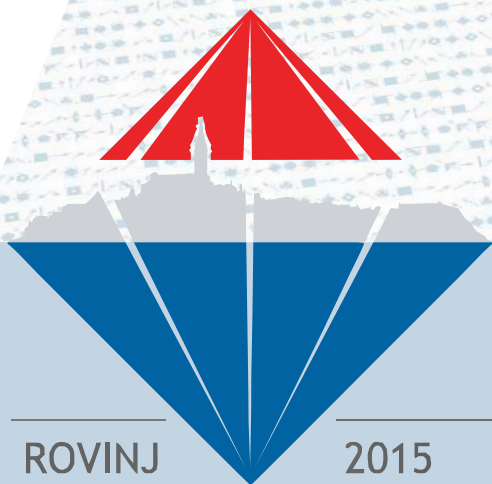


29th European Crystallographic Meeting

23rd-28th August 2015

Rovinj
Croatia

Book
of
abstracts



ROVINJ

2015

ECM29
CROATIA

29th European
Crystallographic
Meeting

Book of Abstracts

Plenary lectures

PL-2 Graphene future emerging technology

Andrea Ferrari¹

1. Cambridge Graphene Centre Engineering Department,
University of Cambridge, UK

email: acf26@eng.cam.ac.uk

Disruptive technologies are usually characterised by universal, versatile applications, which change many aspects of our life simultaneously, penetrating every corner of our existence. In order to become disruptive, a new technology needs to offer not incremental, but dramatic, orders of magnitude improvements. Moreover, the more universal the technology, the better chances it has for broad base success. Does graphene have a chance to become the next disruptive technology? Can graphene be the material of the 21st century? Are the properties of graphene so unique to overshadow the unavoidable inconveniences of switching to a new technology, a process usually accompanied by large R&D and capital investments? In spite of the inherent novelty associated with graphene and the lack of maturity of graphene technology, a roadmap can be envisaged, including short-term milestones, and some medium- to long-term targets, intrinsically less detailed, but potentially even more disruptive. This should guide the transition towards a technological platform underpinned by graphene, with opportunities in many fields and benefits to society.

Keywords: graphene

PL-1 Serial crystallography with X-ray free-electron laser pulses

Henry Chapman¹

1. Center for Free-Electron Laser Science, DESY / Universität Hamburg, Hamburg, Germany

email: henry.chapman@desy.de

The pulses from X-ray free-electron lasers are a billion times brighter than the brightest synchrotron beams available today. When focused to micron dimensions, such a pulse destroys any material, but the pulse terminates before significant atomic motion can take place. This mode of “diffraction before destruction” yields structural information at resolutions better than 2 Å, from proteins that cannot be grown into large enough crystals or are too radiation sensitive for high-resolution crystallography. This has opened up a new methodology of serial femtosecond crystallography that yields radiation damage-free structures without the need for cryogenic cooling of the sample. The method has begun to yield new structures and has the potential to increase the rate at which structures can be solved. Ultrafast pump-probe studies of photoinduced dynamics in proteins or other materials can also be studied. Irreversible reactions can be studied, synchronised with the short pulses, with new sample being constantly replenished. We have yet to reach the limit of the smallest samples that can be studied this way, and many innovations indicate the feasibility of single molecule diffractive imaging.

Keywords: X-ray free-electron lasers, serial femtosecond crystallography

Keynote lectures

KN-1 Crystal structures of amino acids: investigations into CSD

Carl Henrik Gørbitz¹

1. Department of Chemistry, University of Oslo

email: c.h.gorbitz@kjemi.uio.no

After the discovery of X-ray diffraction by crystals, amino acids were among the first organic compounds to have their solid state structures investigated. After a short introduction dealing with the early history of crystal structure determination, this keynote will present the main results of a systematic review of more than 3500 entries for alpha-amino acids in the Cambridge Structural Database. This includes an overview of various experimental techniques and conditions, a classification of amino acid structures, and a discussion of their acid-base properties leading to a series of different protonation states. For each such state essential structural elements are described, especially hydrogen bonding preferences and coordination to metal ions. Finally, the concepts of polymorphism and phase transitions as the result of extreme temperatures or pressures are discussed, with reference to recent work.

Keywords: amino acid, crystal structure, database, hydrogen bonding, polymorphism, metal complexes

KN-2 Keeping muscle proteins in shape: The moonlighting function of the UNC-45 chaperone

Tim Clausen¹

1. Institute of Molecular Pathology (IMP), Vienna, Austria

email: tim.clausen@imp.ac.at

Muscle development and function rely on the correct assembly of contractile units called the sarcomeres. Their main components, thin (actin) and thick (myosin) filaments are organized in a precisely ordered, quasi-crystalline protein framework that mediates muscle contraction. Although the overall architecture of the sarcomere has been studied in detail, little is known about its complicated assembly process. In particular, the mechanism of myosin incorporation into thick filaments is poorly understood.

The UCS (UNC-45/CRO1/She4) chaperones play an evolutionarily conserved role in promoting myosin-dependent processes including cytokinesis, endocytosis, RNA transport and muscle development. To investigate the protein machinery orchestrating myosin folding and assembly, we performed a comprehensive analysis of *Caenorhabditis elegans* UNC-45. Our structural and biochemical data demonstrate that UNC-45 can form linear protein chains offering multiple binding sites for co-working chaperones and client proteins. Accordingly, Hsp70 and Hsp90, which bind to the TPR domain of UNC-45, could act in concert and with defined periodicity on captured myosin molecules. We thus propose that UNC-45 represents a novel type of filament assembly factor that is capable of coupling myosin folding with myofilament formation.

As for the assembly, also the degradation of muscle myosin is relatively little understood. The U-box containing E3 ligase UFD-2, which is one of the most abundant proteins in embryonic cardiomyocytes, is implicated in this process. New data from our lab reveal the molecular mechanism of UFD-2 in myosin homeostasis. We show that UFD-2 employs UNC-45 as an adaptor protein to target and ubiquitinate the muscle myosin in a highly specific manner. These data suggest that UNC-45 is situated at the interface of myosin folding and degradation pathways. On one side, it interacts with its partner chaperones Hsp70 and Hsp90 to fold and assemble myosin molecules. On the other side, UNC-45 can team up with UFD-2 to ubiquitinate and quality-control damaged myosin proteins. Accordingly, UNC-45 is a central player in the triage system channeling myosin molecules into refolding and ubiquitination pathways, thereby determining the fate of the myosin protein in different cellular situations.

Keywords: protease, chaperone, filament assembly, myosin, UNC-45, UFD-2

KN-3 High pressure synchrotron radiation crystallography, from organic conductors to chemistry in the lower mantleHanfland Michael¹¹. European Synchrotron Radiation Facility, 71, avenue des Martyrs, CS 40220, 38043 Grenoble, France

email: hanfland@esrf.fr

ID09A is a state of the art high pressure diffraction beamline at the ESRF. It uses monochromatic diffraction with large area detectors. Powder and single crystal diffraction experiments can be performed at high pressures in diamond anvil cells, permitting accurate determination of crystallographic properties of the investigated samples. Soon ID09A will be replaced by a new and improved beamline, ID15B. Recent technical advances have significantly added to the utility of single crystal X-ray diffraction experiments at high pressures [1]. New ways of supporting diamond anvils, like Boehler Almax anvils [2], have considerably increased the volume of accessible reciprocal space. Use of Helium or Neon as pressure transmitting medium extends substantially the practicable pressure range. Flat panel detectors have noticeably decreased the data collection time and increased the accuracy. Data can be collected at low and high temperatures. Even single crystal diffraction experiments with laser heating have become possible [3]. Here we will present several examples to illustrate the recent progress.

Work performed in collaboration with M. Merlini, Università degli Studi di Milano, Italy

[1] M. Merlini, M. Hanfland, High Pressure Research 2013 33, 511.

[2] R. Boehler, K. DeHantsetters, High Pressure Research 2004 24, 391.

[3] L. Dubrovinsky, T. Boffa-Ballaran, K. Glazyrin, A. Kurnosov, D. Frost, M. Merlini, M. Hanfland, V.B. Prakapenka, P. Schouwink, T. Pippinger, N. Dubrovinskaia, High Pressure Research 2010 30, 620.

Keywords: high pressure, crystallography

KN-4 Structure and mechanism of respiratory complex I, a giant molecular proton pumpLeonid Sazanov¹¹. Institute of Science and Technology Austria, Klosterneuburg, 3400, Austria

email: sazanov@ist.ac.at

NADH-ubiquinone oxidoreductase (complex I) is the first and largest enzyme in the respiratory chain of mitochondria and many bacteria. It couples electron transfer between NADH and ubiquinone to the translocation of four protons across the membrane. It is a major contributor to the proton flux used for ATP generation in mitochondria, being one of the key enzymes essential for life as we know it. Mutations in complex I lead to the most common human genetic disorders. It is an L-shaped assembly formed by membrane and hydrophilic arms. Mitochondrial complex I consists of 44 subunits of about 1 MDa in total, whilst the prokaryotic enzyme is simpler and generally consists of 14 conserved "core" subunits. We use the bacterial enzyme as a "minimal" model to understand the mechanism of complex I. We have determined the first atomic structures of complex I, starting with the hydrophilic domain, followed by the membrane domain and, finally, the recent structure of the entire *Thermus thermophilus* complex (536 kDa, 16 subunits, 9 Fe-S clusters, 64 TM helices). Structures suggest an unusual mechanism of coupling between electron transfer in the hydrophilic domain (involving ~ 90 Å long chain of 7 conserved Fe-S clusters) and proton translocation in the membrane domain, via long-range (up to ~200 Å) conformational changes. It resembles a steam engine, with coupling elements (akin to coupling rods) linking parts of this molecular machine. I will discuss our current work, which is aimed at elucidating the molecular details of the coupling mechanism through determination of structures of the complex in different redox states with various bound substrates/inhibitors, using both X-ray crystallography and new cryo-EM methods.

Keywords: respiratory complex I, giant molecular proton pump

KN-5 Evolution of symmetry-broken states in the pseudo-gap regimes of nickelates and cuprates

Emil Bozin¹

¹ Condensed Matter Physics and Materials Science Department, Brookhaven National Laboratory, Upton, New York, USA

email: bozin@bnl.gov

Realization that many emerging phenomena, such as colossal magnetoresistance and unconventional superconductivity to name but a few, may be governed by complex disorder exemplifies the importance of utilization of local probes sensitive to short range correlations. To that effect the knowledge of the local atomic structure may reveal relevant nanometer lengthscale footprints important for more comprehensive understanding of the character of symmetry broken states. Atomic pair distribution function (PDF) is one of the few experimental methods that can speak to this problem. Systematic approach in charting both long and short range structural orders, on an equal footing, across the (x, T) phase diagram of materials emerges as a powerful identification tool for grasping the relevance and hierarchy of length scales reflecting competing and/or coexisting orders, such as that seen in e.g. $\text{La}_{1-x}\text{Ca}_x\text{MnO}_3$. Revealing the nature of the symmetry broken states and fluctuations of short-range order in strongly correlated electron systems in general and in the pseudo-gap (PG) phase of cuprates in particular, remains instrumental in understanding the underlying physical properties.

Mounting experimental evidence suggests that the PG phase of cuprates may represent an electronic state in which the four-fold rotational symmetry (C_4) of the CuO_2 planes is broken (down to at least C_2), pointing to stripe or nematic character. Here the former is referred to as orthogonally equivalent, and the later as orthogonally inequivalent (OI) state. Recent neutron total scattering based results extending the systematic approach to the nickelate and cuprate systems will be presented. In order to benchmark the sensitivity of powder-based methods for this class of problems, we initially explored T-evolution of structural effects associated with the melting of well-established stripe order in $\text{La}_{1.67}\text{Sr}_{0.33}\text{NiO}_4$ across the charge-order temperature, T_{co} . In this model stripe system structural features sensitive to both long and short range stripe order are identified, further suggesting that dynamic charge-stripe correlations survive to $T \sim 2T_{\text{co}}$. Encouraged by these observations, underdoped $\text{La}_{2-x}\text{Ba}_x\text{CuO}_4$ that hosts stripes was studied next over a range of doping and temperature. PDF and complementary inelastic neutron scattering measurements reveal that dynamic nanoscale OI-type tilt correlations do persist well above T_{co} and peak coincidentally near $x = 0.125$, where stripe order is the strongest.

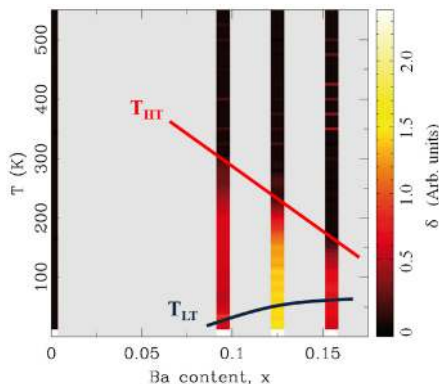


Figure 1. (x, T) evolution of the nanoscale dynamic broken symmetry state, expressed through parameter δ obtained from PDF analysis. Solid lines mark structural transition temperature: T_{IT} (red) and T_{LT} (blue). After E. S. Bozin *et al.*, Phys. Rev. B 91, 054521 (2015).

Keywords: superconductivity, neutron scattering, nanoscale, pair distribution function, broken symmetry states

KN-6 Structure of a bacterial α -macroglobulin reveals mimicry of eukaryotic innate immunity

Andrea Dessen^{1,2}

1. Institut de Biologie Structurale (IBS), Grenoble, France

2. Laboratório Nacional de Biociências (LNBio), Campinas, Brazil

email: Andrea.Dessen@ibs.fr

Alpha-2-macroglobulins (A2Ms) are plasma proteins that trap and inhibit a broad range of proteases and are major components of the eukaryotic innate immune system. Surprisingly, A2M-like proteins were identified in pathogenically invasive bacteria and species that colonize higher eukaryotes. Bacterial A2Ms are located in the periplasm where they are believed to provide protection to the cell by trapping external proteases through a covalent interaction with an activated thioester. Our work reveals the crystal structures and characterization of *Salmonella typhimurium* A2M in different states of thioester activation. The structures reveal thirteen domains whose arrangement displays high similarity to proteins involved in eukaryotic immune defense. A structural lock mechanism maintains the stability of the buried thioester, a requirement for its protease trapping activity. These findings indicate that bacteria have developed a rudimentary innate immune system whose mechanism mimics that of eukaryotes.

Keywords: bacterial infection, immunity, macroglobulin, crystal structure

KN-7 Solving chemistry puzzles in molecules and crystals through charge and spin density analyses

Carlo Gatti¹

1. CNR-ISTM, Istituto di Scienze e Tecnologie Molecolari del CNR, via Golgi 19, 20133 Milano, Italy

email: carlo.gatti@istm.cnr.it

Being based on a quantum observable and (easily) measurable quantity, the Electron Density (ED) based descriptors retain the great advantage of enabling a comparison of theoretical predictions with experimental results on the same grounds, and regardless of the specific tools used to obtain the observable itself. EDs derived from X-Ray structure factors or from *in vacuo* and in crystal wavefunctions will be considered during the talk. On top of customarily used ED topological descriptors [1], this lecture will mostly focus on the Source Function (SF) tool [2,3], and on the Reduced Density Gradient analysis, introduced by Johnson [4] as a convenient instrument to characterize non covalent interactions (NCIs) *in vacuo* (and recently also made available for [5] and applied to [6-7] NCIs in crystals). The SF enables one to view chemical bonding and other chemical paradigms under a new perspective [3]. Its extension [8] to the electron spin density (ESD) provides special insights on how spin information is transmitted from paramagnetic to non-magnetic centers. Use of the mentioned ED-based descriptors to help solving chemistry puzzles, like the issue of S hypervalency in the $[\text{SO}_4]^{2-}$ anion [9], the NC bond length inversion in a thiazete-1,1-dioxide crystal [10], the detection of electron correlation effects [11] and of NCIs nature in molecular organic crystals [5-6] and the distinction of *magnetic* from *relaxation* contributions in ESD transmission [8] will be shown.

[1] *Modern Charge Density Analysis*, C. Gatti and P. Macchi (Eds), Springer 2012

[2] R.F.W. Bader, C. Gatti, *Chem. Phys. Lett.* **287**, 233-238 (1998)

[3] C. Gatti, *Struct. Bond.* **147**, 193-286 (2012)

[4] E.R. Johnson et al. *J. Am. Chem. Soc.* **132**, 6498-6506 (2010)

[5] G. Saleh, L. Lo Presti, C. Gatti, D. Ceresoli, *J. Appl Cryst* **46**, 1513-1517 (2013)

[6] G. Saleh, C. Gatti*, L. Lo Presti * and J. Contreras-García, *Chem. Eur. J.*, **18**, 15523-15536 (2012)

[7] G. Saleh, C. Gatti*, L. Lo Presti* , *Comp.Theor. Chem.* **998**, 148-163 (2012)

[8] C. Gatti, A. M. Orlando, L. Lo Presti, *Chemical Science*, 2015, DOI: 10.1039/C4SC03988B

[9] M.S. Schmökel, S. Cenedese, J. Overgaard, M.R.V. Jørgensen, Y-S Chen, C. Gatti*, Dietmar Stalke,* and Bo B. Iversen*, *Inorg. Chem.* **51**, 8607-8616 (2012)

[10] L. Lo Presti,* A. Orlando, L. Loconte, R. Destro, E. Ortoleva, R. Soave, C. Gatti*, *Cryst. Growth and Design*, **14**, 4418-4429 (2014)

[11] C. Gatti, G. Saleh, L. Lo Presti, invited feature article to be submitted to *Acta Cryst B*

Keywords: electron density, electron spin density, chemical descriptors, source function, reduced density gradient

KN-8 Quasicrystals in soft condensed matterRon Lifshitz¹1. Raymond & Beverly Sackler School of Physics & Astronomy,
Tel Aviv University

email: ronlif@tau.ac.il

Recent years have shown a resurgence of scientific interest in quasicrystals, perhaps amplified by the award of the 2011 Nobel Prize in Chemistry to Dan Shechtman; yet mostly driven by breakthroughs in unlocking their crystal structure [1], and by the expanding scope of the field owing to the advent of a host of new experimental systems exhibiting aperiodic long-range order. Among these are soft-matter quasicrystals whose building blocks—rather than being individual atoms—are composed of large synthesized particles such as macromolecules, block co-polymers, nanoparticles, and colloids [2-5]. At these dimensions it is possible to design the interaction between particles, manipulate their positions, or even artificially place them at pre-assigned locations. It may also be possible to track the dynamics of individual particles, and in the optical domain even observe quantum wave functions. Consequently, these mesoscopic-scale quasicrystals provide rich and versatile platforms for the fundamental study of the basic physics of quasicrystals. At the same time they hold the promise for new applications based on artificial or self-assembled nanomaterials with unique physical properties that take advantage of the lack of periodicity, such as novel photonic metamaterials.

After giving a brief overview of the rapidly expanding field of soft-matter quasicrystals, I shall demonstrate how a quantitative understanding of their thermodynamic stability [6] has given us the ability to control the self-assembly of a variety periodic and aperiodic soft-matter crystals (at the moment only on the computer) and has led to the numerical discovery of a novel phase—a so-called "cluster quasicrystal" [7]. If time permits, I shall describe the design of nonlinear photonic quasicrystals for optical frequency-conversion applications [8].

[1] Takakura, Pay Gomez, Yamamoto, de Boissieu, Tsai (2007) *Nature Materials* **6**, 58.

[2] Zeng, Ungar, Liu, Percec, Dulcey, & Hobbs (2004) *Nature* **428**, 157.

[3] Hayashida, Dotera, Takano, & Matsushita (2007) *Phys. Rev. Lett.* **98**, 195502.

[4] Talapin, Shevchenko, Bodnarchuk, Ye, & Murray (2009) *Nature* **461**, 964.

[5] Mikhael, Roth, Helden, & Bechinger (2008) *Nature* **454**, 501.

[6] Lifshitz & Diamant (2007) *Phil. Mag.* **87**, 3021; Barkan, Diamant, & Lifshitz (2011) *Phys. Rev. B* **83**, 172201.

[7] Barkan, Engel, & Lifshitz (2014) *Phys. Rev. Lett.* **113**, 098304.

[8] Lifshitz, Arie, & Bahabad (2005) *Phys. Rev. Lett.* **95**, 133901.

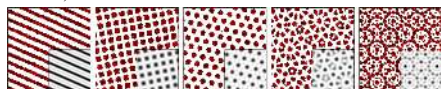


Figure 1. Self-assembled cluster crystals. Red particles represent molecules. Gray-scale images display the same structures, as

predicted by mean-field theory. From left to right: stripes, 4-fold and 6-fold periodic crystals, 10-fold and 12-fold quasicrystals. Reprinted from Ref. [7].

Keywords: quasicrystals, aperiodic crystals, soft matter, macromolecules, nanoparticles, block co-polymers, colloids, self assembly, photonic crystals, metamaterials

KN-9 Crystallographic studies on correlated electron systems under non-ambient conditionsKaren Friese¹¹ Jülich Centre for Neutron Science, Research Centre Jülich, Germany

email: k.friese@fz-juelich.de

Structural characteristics like symmetry, interatomic distances, or thermal movements of the atoms are closely related to the properties of a material. Correlated electron systems exhibiting novel magnetic properties, a superior optical and electric performance or superconductivity have excellent prospects as advanced materials. However, the establishment of reliable structure/property relationships is often difficult due to complications in the crystal structure determination process. This talk will concentrate on two classes of materials which are characterized by a strong coupling of charge, spin and/or lattice degrees of freedom. The first part will be centered on the behaviour of the crystal and magnetic structures of magnetocaloric compounds. In these materials, which can be used for advanced refrigeration technologies, the application of a magnetic field leads to changes in the magnetic entropy and adiabatic temperature. The magnetocaloric transition is usually accompanied by a structural transition and the response of the lattice to the onset of magnetic ordering is of key importance for the understanding of the underlying mechanism of the magnetocaloric effect. The second example will concentrate on mixed-valence compounds. Here, charge ordering can lead to significant changes of the coordination spheres of the aliovalent ions and lead to drastic changes in the underlying crystal structures often reflected in first-order phase transitions. Multiparametric studies on both systems performed at neutron and synchrotron source will be presented. Apart from the variation of temperature and chemical composition, hydrostatic pressure plays a key role in these studies as it permits to drastically influence the interatomic distances in the materials and can thus help to better understand the underlying mechanisms of the observed phenomena.

Keywords: Correlated electron systems, phase transitions, hydrostatic pressure, magnetic interactions, charge order

KN-10 Advanced electron crystallography through imagingSandra Van Aert¹¹ Electron Microscopy for Materials Science (EMAT), Universiteit Antwerpen, Belgium

email: sandra.vanaert@uantwerpen.be

New developments in the field of nanoscience and nanotechnology drive the need for advanced quantitative materials characterisation techniques that can be applied to complex nanostructures. The physical properties of these nanostructures are controlled by composition and chemical bonding, but also by the positions of the atoms. Indeed, changing the interatomic distances by picometers can turn an insulator into a conductor. Because of the presence of defects, interfaces and surfaces, the locations of atoms deviate from their equilibrium bulk positions giving rise to strain. In order to study nanostructures, transmission electron microscopy (TEM) is an excellent technique because of the strong interaction of electrons with small volumes of matter providing local information on the material under study. Over the past few years, remarkable high-technology developments in the lens design greatly improved the image resolution. Nowadays, a resolution of the order of 50 pm can be achieved. For most atom types, this exceeds the point where the electrostatic potential of the atoms is the limiting factor. Furthermore, new data collection geometries are emerging that allow one to optimise the experimental settings. In addition, detectors behave more and more as ideal quantum detectors. In this manner, the microscope itself becomes less restricting and the quality of the experimental images is mainly set by the unavoidable presence of electron counting noise and environmental disturbances. In order to measure the atom positions and atom types as accurately and precisely as possible from atomic resolution TEM image, quantitative methods are required. To reach this goal, the use of statistical parameter estimation theory is of great help. This methodology allows one to measure 2D atomic column positions with subpicometer precision, to measure compositional changes at interfaces, to count atoms with single atom sensitivity, and to reconstruct 3D atomic structures. Using current state-of-the-art experimental examples, it will be shown how statistical parameter estimation techniques can be used to overcome the traditional limits set by modern TEM. The precision that can be achieved in this quantitative manner far exceeds the resolution performance of the instrument. This opens up a whole new range of possibilities to understand and characterise nanostructures at the atomic level and to help developing innovative materials with revolutionary interesting properties.

Keywords: electron microscopy, quantitative imaging

KN-11 Crystallization and gelation: orthogonal self-assembly far from equilibrium

Jonathan Steed¹

1. Department of Chemistry, Durham University, UK

email: jon.steed@durham.ac.uk

A vast and diverse array of organic compounds and coordination complexes form gels by hierarchical self-assembly either because of hydrophobic effects in water or by more directional interactions such as hydrogen bonding in less polar solvents. Of recent interest is the emergence of metal-, anion and salt-containing gelators based on small-molecule 'low molecular weight gelators (LMWG)'. Particular attractions of LMWGs to the scientific community are the reversible nature of the interactions between the gelator molecules, the wide (essentially unlimited) range of solvents that can be gelled and the possibility of tuning the gels' behaviour by introducing responsive or switching functionality. Gels derived from LMWGs have been proposed in a range of applications and include templation of nanoparticles and nanostructures, drug delivery and as crystal growth media. This presentation focuses on the use of concepts borrowed from anion host-guest chemistry to control and trigger the materials properties of small molecule (supramolecular) gels. We show how concepts firmly rooted in supramolecular host-guest chemistry and supramolecular self-assembly can be married with the materials science of soft matter in order to utilise a molecular-level understanding of supramolecular chemistry to control and manipulate bulk materials properties. This 'evolution' has been described in a recent review,¹ and the application of these kinds of switchable gels as novel media for pharmaceutical crystal growth has recently been described.²

Steed, J. W. *Chem. Soc. Rev.* **2010**, 39, 3686.

Kumar, D. K.; Steed, J. W. *Chem. Soc. Rev.* **2014**, 43, 2080.



Figure 1. Carbamazepine crystals growing in a supramolecular gel

Keywords: gel, supramolecular, pharmaceutical

KN-12 Molecular structure and luminescent propertiesPaul R. Raithby¹¹. Department of Chemistry, University of Bath, UK

email: p.r.raithby@bath.ac.uk

Luminescence can either take the form of fluorescence, emission of a photon from a singlet excited state, or phosphorescence, emission from an excited triplet state. The fluorescent emission normally occurs on a much faster timescale than phosphorescence. Being able to exploit phosphorescence emission enhances the emission efficiency, since there are three accessible triplet states for each singlet state. However, in order to achieve this singlet to triplet intersystem crossing has to occur. This is facilitated by the presence of heavy transition metals, such as osmium, iridium or platinum, with their associated high spin-orbit coupling. Thus, there has been considerable interest in platinum(II) poly-yne complexes and polymers which display excellent phosphorescence properties. These materials take the form of platinum(II) dimers linked by an aromatic or heteroaromatic linker group, or related polymers (Figure 1a).¹ In these systems we have found it possible to tune the electronic band gap, and the luminescent properties, by changing the donor/acceptor properties of the linker group, its length and the properties of auxiliary ligands on the metal centres.² More recently, we have found that related platinum(II) pincer complexes (Figure 1b) show changes in their colour and luminescent properties depending on how they pack in the solid-state. This packing, and hence the luminescence, can be modified by the introduction of various solvents and volatile organic compounds into the crystal. These colour changes occur on a sub-second time scale providing a new class of rapid-acting sensors.

References ¹ Chawdhury, N.; et. al. *J. Chem. Phys.* **1999**, *110* (10), 4963–4970. ² Devi, L. S.; et. al. *Macromolecules* **2009**, *42* (4), 1131–1141.

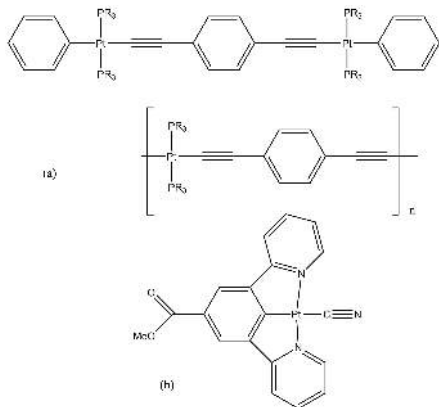


Figure 1. Figure 1. The structures of (a) the platinum (II) diynes and poly-ynes, and (b) the structures of some platinum (II) pincer complexes.

Keywords: Platinum (II), Diynes, Poly-ynes, Pincer complexes, Luminescence, X-ray crystal structures

KN-13 Structure determination revisitedGeorge M. Sheldrick¹¹. Institute of Inorganic Chemistry, Göttingen, Germany

email: gsheldr@shelx.uni-ac.gwdg.de

Recent developments in the experimental phasing of both small and macromolecules with the SHELX programs will be discussed. In both cases the amount of user input required has been reduced to an absolute minimum.

The new program SHELXT (released August 2014) for small molecule structure solution requires only the unit-cell, Laue group, reflection data and an approximate indication of which elements might be present. The phase problem is solved for data expanded to space group P1 and the resulting phases are then used to determine the true space group. This is much more robust than conventional methods based on systematic absences etc. The integrated electron density enables most elements to be identified correctly.

The programs SHELXC, SHELXD and SHELXE apply the SAD, MAD, SIRAS, SIR and RIP methods for experimental phase determination followed by density modification and iterative poly-alanine tracing. SHELXE may also be used to improve borderline molecular replacement solutions. The statically linked SHELX programs have zero dependencies - no libraries, other programs or environment variables are required - and are available free for academic use for Windows, Linux and MacOSX systems. Further details may be found on the SHELX homepage.

Keywords: SHELX, Phase problem, Experimental phasing

KN-14 Trapping a transient state in DNA mismatch repair: the MutS/MutL sliding clamp loads MutL on DNA

Titia K. Sixma¹

1. Division of Biochemistry Netherlands Cancer Institute, Amsterdam, Netherlands

email: t.sixma@nki.nl

Flora S. Groothuizen¹, Ines Winkler², Michele Cristóvão², Alexander Fish¹, Herrie H.K. Winterwerp¹, Annet Reumer¹, Andreas D. Marx², Nicolaas Hermans³, Robert A. Nicholls⁴, Garib N. Murshudov⁴, Joyce H.G. Lebbink³, Peter Friedhoff², Titia K. Sixma¹

¹Netherlands Cancer Institute (NKI), Amsterdam, the Netherlands,

²Justus-Liebig-University, Giessen,

Germany, ³ErasmusMC, Rotterdam, the Netherlands,

⁴LMB, Cambridge, UK

To avoid mutations in the genome, DNA replication is followed by DNA mismatch repair (MMR). This process starts when a MutS homolog recognizes a mismatch and undergoes an ATP-dependent transformation to an elusive sliding clamp state. How this transient state promotes MutL homolog recruitment and activation of repair is unclear.

Here we present the crystal structure of the MutS/MutL complex where we trap this transient state, by making use of highly specific single-cysteine crosslinking. The resulting structures (4.7-7.6 Å) have surprisingly large conformational changes that were validated by FRET, binding studies and mutagenesis and interpreted in terms of the MMR cycle.

The structure captures MutS in the sliding clamp conformation, where tilting of the MutS subunits across each other pushes DNA into a new channel, and reorientation of the connector domain creates an interface for MutL with both MutS subunits. Our work explains how the sliding clamp promotes loading of MutL onto DNA, to activate downstream effectors. We thus elucidate a crucial mechanism that ensures that MMR is initiated only after detection of a DNA mismatch.

Keywords: Low resolution refinement, crosslinking, DNA repair, FRET, SPR, MutS, MutL

KN-15 Molecular mechanisms of RNA polymerase I and III transcription

Christoph W. Müller¹

1. European Molecular Biology Laboratory (EMBL), Heidelberg, Germany

email: cmueller@embl.de

RNA polymerase (Pol) I and Pol III mainly synthesize the non-coding RNA components required for ribosome assembly and protein synthesis in eukaryotes. Pol I synthesizes precursor rRNA that is subsequently processed into 25S, 18S and 5.8S rRNA, while Pol III produces small RNAs such as tRNA, 5S RNA and U6 snRNA. The Pol I and Pol III transcription initiation machineries are carefully regulated in healthy cells, while misregulation of Pol I and Pol III transcription is observed in a variety of cancers. Our group uses an integrated structural biology approach combining X-ray crystallography, single-particle electron microscopy and chemical crosslinking mass spectrometry to study the Pol I and Pol III enzymes and their transcription initiation complexes. We have determined the crystal structure of the 14-subunit RNA polymerase I from *Saccharomyces cerevisiae* at 3.0 Å resolution. The Pol I structure shows a very wide DNA-binding cleft that is occupied by an extended loop mimicking DNA. The Pol I-specific subunits A12.2 and A49-A34.5 provide additional functionality to the enzyme. The crystal structure of Pol I will be compared to the cryo-electron microscopy structure of the 17-subunit Pol III enzyme. Recruitment of Pol III to tRNA-encoding genes requires the general transcription factors (TF) IIIB and IIIC. TFIIIC is a multi-subunit protein composed of two subcomplexes. We used chemical cross-linking mass spectrometry to determine the overall architecture of TFIIIC and to position crystal structures corresponding to about 2/3 of the entire TFIIIC complex.

Keywords: RNA polymerases, transcription, multi-subunit complexes, integrated structural biology

KN-16 Ultrafast dynamics in condensed matter

Matias Bargheer^{1,2}

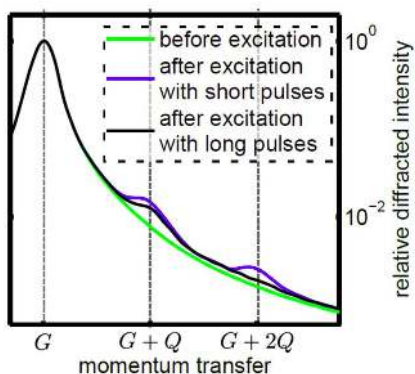
1. Institute of Physics and Astronomy, University of Potsdam
2. Helmholtz Zentrum Berlin für Materialien und Energie

email: matias.bargheer@helmholtz-berlin.de

This lecture will give an introduction to the field of ultrafast x-ray diffraction (UXRD) and related techniques such as inelastic or diffuse x-ray scattering. Generally, we excite molecules or solids by ultrashort light pulses and monitor the dynamics on the natural timescale of atomic motion, i.e. with a resolution of about 100 femtoseconds. The idea is to generate movies that teach us how energy flows in complex material systems. The main body of the lecture will discuss very recent experimental progress in the field using both laser-based plasma x-ray sources and synchrotron radiation. As a tutorial example, we demonstrate how UXRD can monitor the inhomogeneous excitation of metallic thin films and the associated generation of hyper-sound waves. This process is used to tailor giant phonon-wavepackets with a well defined wavevector, although localized to few tens of nanometers. We not only observe the generation and decay of these phonons directly by UXRD. We can even monitor nonlinear phonon-phonon interaction in real time. As a second very recent research area monitors the structural changes of rare earth metals after heating with ultrashort laser pulses. The transient lattice strain can be used as a local ultrafast thermometer, that tells us about the heat flow within a multilayered sample, where a very large fraction of the heat can be trapped in antiferromagnetic excitations (magnons and fluctuations). We discuss the complex lattice dynamics induced by various stress contributions from anharmonic lattice heat expansion to forces induced by the magnetic exchange interaction. In the vicinity of the Neel temperature we observe critical behavior in the observed relaxation timescales that are connected with fluctuations at the phase transition.

Figure 1. Experimental data showing the Bragg peak of a single crystal (green) and how it changes when a phonon with wavevector q (black) is written into the crystal. When the second harmonic at $2q$ is present as well, it can be monitored at the respective momentum transfer.

Keywords: Ultrafast X-ray Diffraction, Inelastic Scattering, Phonons, anharmonic, nonlinear, femtosecond, antiferromagnet, ferromagnet, exchange interaction, heat transport, magnons, fluctuations



Oral presentations

MS1. Recent experimental developments in synchrotron macromolecular crystallography

Chairs: Gordon Leonard, Marjolein Thunnissen

MS1-O1 Serial synchrotron crystallography experiments at EMBL beamline P14 at PETRA III

Thomas R. Schneider¹, Gleb Bourenkov¹, Cornelius Gati², Henry N. Chapman², Lars Redecke³, Ulrich Zander⁴, Jose' A. Marquez², Florent Cipriani⁴, Thomas R. Schneider¹

1. European Molecular Biology Laboratory (EMBL), Hamburg Outstation, Notkestrasse 85, 22607 Hamburg, Germany

2. Center for Free-Electron Laser Science (CFEL), Deutsches Elektronensynchrotron (DESY), Notkestrasse 85, 22607 Hamburg, Germany

3. University of Lübeck, Institute of Biochemistry, Ratzeburger Allee 160, 23538 Lübeck, Germany

4. European Molecular Biology Laboratory (EMBL), Grenoble Outstation, 6 Rue Jules Horowitz, 38042 Grenoble, France

email: thomas.schneider@embl-hamburg.de

Beamline P14 on PETRA III (DESY, Hamburg) offers a high flux micro-focused beam for extracting diffraction data from crystals with linear dimensions of less than 10 μm . At an energy of 12 keV, the beamline can deliver on the order of 5×10^{12} photons/s into a $5 \times 5 \mu\text{m}^2$ focal spot corresponding to an X-ray dose of approximately 100 MGy deposited into a typical macromolecular crystal per second. At this dose-rate, the lifetime of a macromolecular crystal reduces to several hundred ms at cryo-genic temperatures and several ten ms at room temperature.

Being able to extract the entire diffraction information from a crystal on a sub-second time-scale allows applying the serial crystallography paradigm - originally developed for FEL-based experiments [Chapman et al. (2012) *Nature* 470:73] - to synchrotron data collection. In serial crystallography, a carrier containing many small crystals is systematically exposed to the X-rays. Irrespective of whether or not crystalline material is in the exposed sub-volume or not, each sub-volume of the carrier is sampled with an X-ray dose sufficient to extract a

maximum of diffraction data. All acquired frames are then filtered, integrated, and scaled using custom-made processing software such as CrystFEL [White et al. (2012) *J. Appl. Cryst.* 45:335] resulting in the assembly of a set of structure factor amplitudes against which a crystallographic model can be refined.

On P14, we have performed Serial Synchrotron Crystallography 'SSX' experiments both at cryogenic and at ambient temperature. At cryogenic temperature, a cryo-cooled suspension of small ($1 \times 1 \times 10 \mu\text{m}^3$) crystals of Cathepsin B was mounted in a standard crystallographic loop [Gati et al. (2014), *IUCrJ* 1:87]. At ambient temperature, small (10-20 μm linear dimensions) crystals of Insulin were grown in low-background CrystalDirectTM crystallization plates [Cipriani et al. (2012) *Acta Cryst.* D68:1393] for *in situ* data collection from the crystallization drops. For both cases, diffraction data were collected from hundreds of crystals via a continuous series of parallel helical scans as implemented in the MD3 diffractometer resulting in data sets against which models were refined.

The SSX data collection strategy is available via the MxCuBE v2 user interface installed on P14.

We will present results obtained with the SSX strategy, discuss current possibilities for difficult to crystallize systems, and extrapolate to the future.

Keywords: serial crystallography, radiation damage

MS1-O2 The long-wavelength macromolecular crystallography beamline I23 at Diamond Light Source

Ramona Duman¹, Armin Wagner¹, Vitaliy Mykhaylyk¹

1. Diamond Light Source, Diamond House DH2-53, Chilton, Didcot, OX11 0DE, United Kingdom

email: ramona.duman@diamond.ac.uk

The Long-Wavelength MX Beamline I23 at Diamond Light Source will be the first dedicated beamline for long-wavelength phasing experiments from macromolecular crystals. By exploiting the weak anomalous differences from sulfur or phosphorus present in proteins or RNA/DNA molecules the crystallographic phase problem can be experimentally solved by anomalous diffraction methods based on their intrinsic signal without labeling the crystals with additional anomalous scatterers. Additionally, anomalous contrast can be used to unambiguously identify biologically important ions such as Ca^{2+} , K^+ or Cl^- . The beamline operates in a core wavelength range from 1.5 to 4 Å, offering a complementary setup to the suite of already five existing MX beamlines at Diamond. To minimize absorption and scattering effects, the complete beamline including sample, goniometer and detector is operated in vacuum. A large curved Pilatus 12M detector allows access to diffraction data up to $2\theta = \pm 100^\circ$. Sample cooling is realized by a conductive path from a pulse tube cryo-cooler through the kappa goniometer.

The challenges of in-vacuum long-wavelength macromolecular crystallography and the opportunities by extending the wavelength range towards the sulfur and phosphorus K-absorption edges will be discussed and first results from the beamline will be presented.

Keywords: long-wavelength crystallography, native SAD, synchrotron beamline

MS1-O3 *In vacuo* X-ray data collection from graphene-wrapped protein crystals

Anna J. Warren¹, Adam D. Crawshaw², Jose Trincao¹, Pierre Aller¹, Simon Alcock¹, Ioana Nistea¹, Gwyndaf Evans¹

1. Diamond Light Source, Harwell Science and Innovation Campus, Didcot, OX11 0DE, UK

2. Institute for Cell and Molecular Biosciences, Faculty of Medical Science, Newcastle University, Newcastle upon Tyne, NE2 4HH, UK

email: anna.warren@diamond.ac.uk

The focus in macromolecular crystallography is moving towards more challenging target proteins, often leading to smaller crystals and more challenging data collection conditions. Sources of X-ray background start to become more of an issue with a decrease in crystal volume as this is accompanied by a reduction in diffraction intensity. One method of reducing X-ray background is to place samples in an evacuated environment; however crystals are prone to dehydration. A series of experiments have been run on test crystals in which it has been possible to collect room temperature data on graphene-wrapped crystals in a rough vacuum. Further tests were also carried out on graphene-wrapped crystals exposed to different relative humidities and to a chemically harsh environment to confirm the effectiveness of graphene as a protective layer against dehydration.

Keywords: graphene, crystal mounting, microcrystallography

MS1-O4 Sulfur SAD phasing at the Photon Factory macromolecular crystallography beamlines in Japan

Yusuke Yamada^{1,2}, Naohiro Matsugaki^{1,2}, Dorothee Liebschner¹, Masahiko Hiraki^{2,3}, Ayaka Harada^{1,2}, Miki Senda^{1,2}, Hisayoshi Makio¹, Toshiya Senda^{1,2}

1. Structural Biology Research Center and Photon Factory, Institute of Materials Structure Science, High Energy Accelerator Research Organization (KEK)

2. School of High Energy Accelerator Science, The Graduate University for Advanced Studies (SOKENDAI)

3. Mechanical Engineering Center, High Energy Accelerator Research Organization (KEK)

email: yusuke.yamada@kek.jp

Sulfur SAD phasing is a method to determine phases by measuring anomalous signals from light atoms such as sulfur and phosphor, which are naturally contained in the most of macromolecular crystals. This method has an advantage that any heavy-atom substitutions are not necessary for phase determination. Structural Biology Research Center in KEK has promoted this promising phasing technique to user community by developing a dedicated beamline and peripheral technologies such as sample mounting methods and automated data analysis pipeline. BL-1A is one of the five macromolecular crystallography beamlines at the Photon Factory (PF), and has been operated since 2010. The beamline was designed from the beginning to take full advantage of X-ray beams at around 3 Å aiming to explore the applicability of long wavelength for sulfur SAD phasing. The beam was highly focused at the sample to reduce unwanted scattering from the solvent around microcrystals. The available long wavelength of BL-1A is ranging from 2.7 to 3.5 Å. The advantage of larger anomalous signals from light atoms can be easily spoiled by severe absorption of the beam by air around the sample, which is one of the practical difficulties in performing accurate SAD experiment with longer wavelength. To mitigate the absorption effects, a bulky standing chamber was recently introduced in order to operate the whole diffractometer system in helium, where a helium cold stream is continuously supplied and recycled. A dedicated sample changer was developed to minimize the contamination of air during the exchange process. The setup allows simple beamline operation thanks to the experimental environment common at any available wavelength. PreMo is an experimental data management system in the PF macromolecular crystallography beamlines. This also has a capability to process a diffraction data set collected at the beamlines and proceed to further analysis as a data analysis pipeline. In the presentation, an overview of the current status and future plan of the beamline and peripheral technology developments will be given. De-novo structural solutions by sulfur SAD phasing at the beamline are shown as well as methodological studies performed with various wavelengths to discuss the feasibility of extending the wavelength range.

Keywords: sulfur SAD, beamline, macromolecular crystallography

MS1-O5 3-D Data Collection strategy accounting radiation damage

Alexander N. Popov¹

1. ESRF, BP-220, Grenoble, 38043, France

email: apopov@esrf.fr

Use of micro-beams for diffraction data collection from the often in-homogeneously diffracting crystals of macromolecules allows improving the ratio of measured signal to noise and increases achievable resolution. In order to utilize the advantages of micro-beam conditions, all available material of a crystal must be used for measurements thus reducing the inevitable radiation damage effects. For this purpose, the sample during or between X-ray exposures is translated (e.g. helical or multi-positional data collection strategies). The optimum choice of crystal displacements and data collection parameters obviously should be defined by accounting the shape and the sizes of a crystal. Here we would like to present next step in the development of the program BEST [Bourenkov, G.P. & Popov, A.N. (2010). *Acta Cryst. D*66, 409-419.] intended for optimal planning of data collection. The new version of the program is based on the use of approximate 3D model of a crystal. Diffraction intensity at any moment of data collection is calculated as the sum of diffraction intensities from crystal voxels taking into account the profile of primary X-ray beam and the dose absorbed by each voxel. Such modelling significantly improves the accuracy of predicted data statistics (also for data collection involving rotation without translations), and allows selecting the best trajectory of the crystal movements.

Keywords: BEST, radiation damage, data collection

MS2. X-ray free electron lasers (XFEL) in macromolecular crystallography

Chairs: Janos Hajdu, Adrian Mancuso

MS2-O1 High-resolution native structure analyses of supramacromolecular complexes susceptible to radiation damage

Hideo Ago¹, Kunio Hirata^{1,2}, Go Ueno¹, Masaki Yamamoto¹,
Kyoko Shinzawa-Itoh³, Tomitake Tsukihara^{2,3,4}, Shinya
Yoshikawa⁵, Michihiro Suga⁵, Fusamichi Akita⁵, Jian-Ren Shen⁵

1. RIKEN SPring-8 Center
2. Japan Science and Technology Agency, CREST
3. University of Hyogo
4. Osaka University
5. Okayama University

email: ago@spring8.or.jp

In protein crystallography, radiation damage free structure determination is not necessarily achieved, even when the data is collected at cryogenic temperatures. The active sites of metalloproteins are especially susceptible to radiation damage due to changes in the oxidation states of catalytically important ions. Therefore, native structural determination of the active site of such metalloproteins is an important challenge in protein crystallography.

Recently we successfully determined the radiation damage free high-resolution structure of bovine heart cytochrome c oxidase (CcO) ⁽¹⁾ and cyanobacteria photosystem II (PSII) ⁽²⁾. Both CcO and PSII are supramacromolecular complexes containing metal ions as catalysts of their redox reactions. Radiation damage free diffraction data was collected using femtosecond crystallography. To improve diffraction resolution, large crystals, as opposed to micro-crystals popular in serial femtosecond crystallography, were used. In this presentation I talk the goniometer based data collection system developed at SACLA (SPring-8 Angstrom Compact free-electron LAser) and the damage free crystal structures of CcO and PSII.

(1) Hirata, K. *et al.* (2014) *Nature Methods* **11**, 734–736. (2) Suga, M. *et al.* (2015) *Nature* **517**, 99–103.

Keywords: femtosecond crystallography, radiation damage, metalloprotein

MS2-O2 Data processing for serial crystallography: recent developments in CrystFEL

Thomas A. White¹

1. Center for Free-Electron Laser Science, Deutsches Elektronen-Synchrotron DESY, Hamburg

email: thomas.white@desy.de

The technique of serial femtosecond crystallography has emerged over the last few years as a particularly successful application of X-ray free-electron laser (XFEL) sources. Data processing for this technique, which starts with the diffraction patterns and from them derives estimates of the structure factor moduli, requires some modifications to the conventional methods and is an area of active and ongoing research. Very recently, exciting progress has been made towards increasing the quality of data which can be obtained from a given number of diffraction patterns in a serial crystallography experiment [1,2], which may eventually allow new types of experiment to be performed. The CrystFEL software suite [3] has been made available as free and open-source software to address the needs of this technique, including these recent improvements, in a user-oriented manner along with suitable documentation, tutorials and usage guidelines. This talk will discuss recent progress in this area, including a look at new features and improvements in recent versions of CrystFEL. [1] M. Uervirojnangkoorn, O. B. Zeldin, A. Y. Lyubimov, J. Hattne, A. S. Brewster, N. K. Sauter, A. T. Brunger, W. I. Weis. *eLife* 2015;10.7554/eLife.05421 [2] T. A. White. "Post-refinement method for snapshot serial crystallography". *Phil. Trans. Roy. Soc. B* 369 (2014) 20130330. [3] T. A. White, R. A. Kirian, A. V. Martin, A. Aquila, K. Nass, A. Barty and H. N. Chapman. "CrystFEL: a software suite for snapshot serial crystallography". *J. Appl. Cryst.* 45 (2012), p335–341.

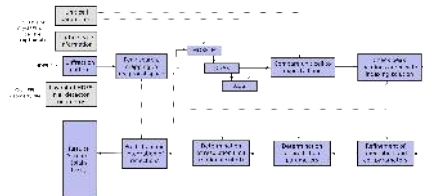


Figure 1. Fully automated indexing and integration pipeline implemented in CrystFEL for each frame of diffraction data, corresponding to one X-ray pulse.

Keywords: XFEL, serial femtosecond crystallography, data processing

MS2-O3 Improving resolution in serial crystallography

Kartik Ayyer¹, Oleksandr M. Yefanov¹, Dominik Oberthuer^{1,2}, Shatabdi Chowdhury³, Lorenzo Galli^{1,2}, Valerio Mariani¹, Shibom Basu³, Jesse Coe³, Chelsie E. Conrad³, Raimund Fromme³, Katerina Doerner^{1,3}, Matthias Frank⁴, Daniel James⁵, Christopher Kupitz^{3,6}, Markus Metz², Garrett Nelson⁵, Xavier L. Paulraj², Kenneth Beyerlein¹, Marius Schmidt⁴, Iosifina Sarrou⁷, John C.H. Spence², Uwe Weierstall⁵, Thomas A. White¹, Jayhow Yang³, Nadia A. Zatsepin², Yun Zhao³, Mengning Liang⁸, Andrew Aquila⁸, Mark S. Hunter⁸, Joseph S. Robinson⁸, Jason E. Koglin⁸, Sébastien Boutet⁸, Petra Fromme³, Anton Barty¹, Henry N. Chapman^{1,2,9}

1. Center for Free-Electron Laser Science, DESY, 22607 Hamburg, Germany
2. Department of Physics, University of Hamburg, 22761 Hamburg, Germany
3. Department of Chemistry and Biochemistry, Arizona State University, Tempe, Arizona, 85287 USA
4. Lawrence Livermore National Laboratory, Livermore, California 94550, USA
5. Department of Physics, Arizona State University, Tempe, Arizona 85287, USA
6. Physics Department, University of Wisconsin, Milwaukee, WI 53211, USA
7. Institute of Molecular Biology and Biotechnology (IMBB) Foundation for Research and Technology - Hellas (FORTH), Heraklion, Crete, Greece
8. Linac Coherent Light Source, Stanford Linear Accelerator Center (SLAC) National Accelerator Laboratory, 2575 Sand Hill Road, Menlo Park, California 94025, USA
9. Center for Ultrafast Imaging, 22607 Hamburg, Germany

email: kartik.ayyer@desy.de

In Serial Femtosecond Crystallography (SFX), the diffraction pattern from a series of small crystals streaming past the X-ray focus is recorded. For some samples, along with Bragg peaks and liquid background, additional scattering is observed at high resolution. We show that, with certain assumptions, this can be used to improve the resolution and quality of the final structure using iterative phasing techniques. With some real-world data collected at the Linac Coherent Light Source (LCLS), we demonstrate this method and show structural improvement, and discuss the general applicability of this method.

Keywords: serial femtosecond crystallography, XFEL

MS2-O4 Identification of rogue datasets in serial crystallography

Greta Aßmann¹, Kay Diederichs¹

1. Department of Biology, University of Konstanz, Box 647, 78457 Konstanz, Germany

email: greta.assmann@uni-konstanz.de

Advances in beamline optics, detectors and synchrotron sources allow new methods of crystallographic data collection. In serial crystallography, a large number of partial data sets from crystals with a small diffraction volume are measured. The general assumption underlying merging of data sets from different crystals in order to enhance x-ray data quality is only valid if the crystals are isomorphous, thus are structurally identical. Identification and exclusion of non-isomorphous data sets is therefore indispensable for merging and should be done by means of suitable data quality indicators. In our approach, CC1/2 [1], the correlation coefficient between two half-data sets composed of randomly assigned partial datasets is used as a quality indicator to identify rogue data sets. Remarkably, it was found that rejecting those data sets that reduce the overall CC1/2 significantly improved the PDB model obtained from the remaining datasets. This was verified by refinements of structures against the newly formed merged isomorphous data. Analysis of CC1/2 is therefore a sensible method to identify data sets containing systematic errors (displaying non-isomorphism) in comparison to conventional quality indicators such as Rmerge, which only accounts for the precision of the measurements and misleadingly discards weak data sets [1].

[1] Karplus P.A., Diederichs, K. (2012) Linking crystallographic model and data quality. *Science* 336, 1030-1033.

Keywords: Isomorphism, data quality, correlation coefficient, outlier rejection, serial crystallography

MS2-O5 Phase retrieval for randomly terminated finite crystals

Joe P.J. Chen¹, Rick A. Kirian¹, Richard J. Bean², Kenneth R. Beyerlein², Miriam Barthelmess², Chun Hong Yoon², Fenglin Wang², Flavio Capotondi³, Emanuele Pedersoli³, Anton Barty², Henry N. Chapman², Philip J. Bones⁴, Romain D. Arnal⁴, Rick P. Millane⁴, John C.H. Spence¹

1. Department of Physics, Arizona State University, Tempe, Arizona, USA

2. Center for Free-Electron Laser Science, DESY, Hamburg, Germany

3. Fermi, Elettra Sincrotrone Trieste, Trieste, Italy

4. Department of Electrical and Computer Engineering, University of Canterbury, Christchurch, New Zealand

email: jpchen1@mainex1.asu.edu

In serial femtosecond nanocrystallography with x-ray free-electron lasers, diffraction data can be obtained from crystals that have a small number of unit cells [1]. The fewer number of unit cells means that the diffraction patterns from these nanocrystals contain measurable information between the Bragg reflections courtesy of a lattice/shape transform that is no longer delta-like.

By separating the effect of the shape transform from the diffraction via its inherent periodicity about the reciprocal lattice [2], the averaged diffracted intensity from all crystals can be directly converted into the diffracted intensity of a single unit cell. The problem then becomes that of reconstructing a single, non-periodic object (the contents of the unit cell) from the amplitude of its Fourier transform, which is known to have a unique solution that can be found using iterative phase retrieval algorithms [3,4].

However, if there is more than one molecule per unit cell then the inter-Bragg diffraction from such crystals will depend on the particular configuration of the molecules on the crystal surface, as different unit cells can be defined for different surface terminations. To a first approximation, the diffraction of the unit cell recovered from the method described above is no longer that of a single kind of unit cell but is equal to the incoherent average over a set of unit cells that contain different arrangements of the molecule based on the space group at hand [5,6].

Following from the recent experimental success of shape transform phasing of synthetic crystals without randomly terminated edges [7], the applicability of direct iterative phase retrieval when multiple unit cells are present is explored using experimental data collected from synthetic crystals with random edge terminations at the FERMI free-electron laser in Trieste, Italy. Results so far indicate successful phase retrieval under this circumstance is still possible.

References

- [1] H.N. Chapman *et al.*, *Nature*, **470**, 73-78 (2011).
- [2] J.C.H. Spence *et al.*, *Opt. Express*, **19**, 2866-2873 (2011).
- [3] R.P. Millane, *J. Opt. Soc. Am. A*, **7**, 394-411 (1990).
- [4] S. Marchesini, *Rev. Sci. Instrum.*, **78**, 011301 (2007).
- [5] J.P.J. Chen and R.P. Millane, *J. Opt. Soc. Am. A*, **31**, 1730-1737 (2014).
- [6] R.A. Kirian *et al.*, *Phil. Trans. R. Soc. B*, **369**, 20130331 (2014).

[7] R.A. Kirian *et al.*, *Phys. Rev. X*, **5**, 011015 (2015).

Keywords: phase retrieval, shape transform, iterative projection algorithms, nanocrystal, edge effects

MS3. Structure solution on the fly (software) / Parallel data collection and structure analysis

Chairs: Manfred Weiss, Victor Lamzin

MS3-O1 DIMPLE: A difference map pipeline for the rapid screening of crystals on the beamline

Ronan Keegan¹, Marcin Wojdyr^{1,2}, Graeme Winter², Alun Ashton²

1. CCP4, Research Complex at Harwell, STFC Rutherford Appleton Laboratory, Didcot OX11 0FA, England

2. Diamond Light Source, Harwell Science and Innovation Campus, Didcot OX11 0DE, England

email: ronan.keegan@stfc.ac.uk

The ability to rapidly screen crystals is an essential requirement for efficient use of synchrotron beamlines when looking for potentially bound ligands. DIMPLE is an automated pipeline to make the process of screening crystals for bound ligands quick and efficient. It goes from a merged MTZ file and the known apo structure to a refined density map automatically and in a short space of time. The output presents the user with a set of images of the interesting pieces of density in the difference map unaccounted for by the apo structure. This allows a user to quickly decide if the crystal has a bound ligand present or not. When processing batches of crystals, such feedback allows the user to better decide what to measure next which leads to a more efficient use of the beam time. Recent developments have enhanced the pipeline to cover more complex cases, including changes in the space group and some changes in conformation. While the software is developed primarily for use at synchrotron beamlines during data acquisition, it is included in the CCP4 suite and can be used as well for in-house automation. Here we will also present a detailed analysis of the usage and success rate of DIMPLE on Diamond Light Source beamlines.

Keywords: Macromolecular Crystallography, Structure solution, ligands, CCP4, Diamond Light Source

MS3-O2 Automated structure solution from multiple data sets

Santosh Panjekar¹, Manfred Weiss², Victor Lamzin³

1. Australian Synchrotron, 800 Blackburn Road, Clayton, Melbourne

2. Helmholtz-Zentrum Berlin für Materialien und Energie, Berlin, Germany

3. EMBL-Hamburg, Germany

email: santosh.panjekar@synchrotron.org.au

Due to size and sensitivity of crystals and stronger X-ray source, it is often not possible to collect complete dataset and even if complete data set is collected from single crystal, it suffers from radiation damage (RD), which is detrimental for anomalous phasing. The advantage of combination of data sets has been well demonstrated and the combined datasets have been used from single or multiple crystals in order to improve multiplicity and anomalous signal (AS). The procedure requires time-consuming task to judge RD and isomorphism for selection of useful data sets for combination.

A number of python libraries have been used to design Auto-Rickshaw (AR) front and back-end engine for analysis, enabling users to choose dataset based on graphical plots from RD and AS along with input parameters necessary to invoke AR for SAD phasing. A graphical interface is generated on the fly for the beamline users. User can invoke AR job for combination of datasets on the local computer, resulting individual dataset are then uploaded along with the input parameters at the remote AR server for SAD phasing and link to the progress of each AR job is provided. This approach has been extended for MAD and SIRAS phasing.

In order to streamline, the above process has been automated that just requires directory path for the processed intensity data. Selection of the data is performed based on its unit cell and space group further followed by analysis of each dataset based on RD and AS. If the AS of individual dataset is above the threshold, then the dataset is pushed for post data analysis at the AR server otherwise the dataset is selected for clustering and scaling purpose. Similarly, each clustered and scaled data is analyzed and pushed further to AR server. In such automatic mode, in absence of sequence information, AR estimates input parameters on the fly. Complete data analysis is documented on the fly as PPTX file for readymade use for presentation.

The python based upfront AR module utilizes various crystallographic program such as XDSSTAT, XSCALE, POINTLESS, AIMLESS along with BLEND, which runs on a local beamline computer and evaluation of the dataset for experimental phasing using various crystallographic programs at the remote cluster (MASSIVE) or at the EMBL AR server.

AR development and workflow of the data analysis will be discussed along with long or short wavelength multiple datasets for S-SAD phasing.

Keywords: Auto-Rickshaw, experimental phasing, multiple data sets, S-SAD

MS3-O3 Analysis of multi-crystal datasets with xia2Richard J. Gildea¹, Graeme Winter¹, Gwyndaf Evans¹

1. Diamond Light Source

email: richard.gildea@diamond.ac.uk

Continued development of microfocus beamlines has enabled data collection from smaller crystals than ever before, with commensurate decrease in signal, whilst simultaneous advancements in beamline automation and detector technology permit ever faster and lower noise data collections. Consequently, automated data processing plays an essential part both during and after data collection. Furthermore, it is often necessary to merge together many partial datasets in order to obtain a complete dataset with sufficient signal-to-noise for subsequent structure solution and analysis. We present an overview of recent developments in xia2 [1] with an emphasis on automated processing of multi-crystal datasets and the incorporation of BLEND [2]. We will discuss improvements to parallel processing of multiple datasets in xia2, and highlight new tools for analysis of multi-crystal datasets, including clustering on unit cell parameters [2] and intensities [3, 4].

[1] G. Winter, *J. Appl. Cryst.* (2010). 43, 186-190[2] J. Foadi, P. Aller, Y. Alguel, A. Cameron, D. Axford, R. L. Owen, W. Armour, D. G. Waterman, S. Iwata and G. Evans, *Acta Cryst.* (2013). D69, 1617-1632.[3] R. Giordano, R. M. F. Leal, G. P. Bourenkov, S. McSweeney and A. N. Popov, *Acta Cryst.* (2012). D68, 649-658.[4] Q. Liu, T. Dahmane, Z. Zhang, Z. Assur, J. Brasch, L. Shapiro, F. Mancia, and W. A. Hendrickson, *Science* (2012). 336, 1033-1037.**Keywords:** xia2, blend, micro-crystal, multi-crystal, automation**MS3-O4 MoRDa, an automatic molecular replacement pipeline**Alexey Vagin¹, Andrey Lebedev²

1. Harwell, Didcot, OX11 0HX, UK

2. STFC Rutherford Appleton Laboratory, Didcot OX11 0FA, UK

email: vagin44@gmail.com

MoRDa is a pipeline for molecular replacement protein structure solution using x-ray data. The software package includes a database and a set of programs for the structure solution. The database (2G) is derived from the PDB and contains a compact description of non-redundant protein chains, domains, homo- and hetero-oligomers. The domain models are pre-processed to exclude flexible loops, which may hinder molecular replacement search. The automatic structure solution involves the search of the homologous chains and domains in the database, further modification of domain and chain models in accordance with the target sequence, composing oligomeric models if possible, and molecular replacement trials (Molrep) with the several search models. Accordingly, trials may include sequential searches for different domains or different chains, dependent on the target sequence and available models. In all cases, ensemble models are generated if there are several homologues of a particular domain or chain. Intermediate and final solutions are refined (Refmac), and selection of the most likely solution is done based on results of the refinements. User input consists of fasta-format file with one or more protein sequences and mtz- or cif-file with experimental structure amplitudes. The complete software package operates off-line. A smaller size package (0.9G) with coordinate files excluded requires Internet connection in order to download necessary files from the PDB.

Keywords: crystallography, pipeline

MS3-O5 Automated solutions for fragment screening at the HZB MX beamlines

Karine M. Sparta¹, Uwe Mueller¹, Manfred S. Weiss¹, Monika Ühle¹, Franziska Huschmann¹, Johannes Schiebel², Andreas Heine², Gerhard Klebe²

1. Helmholtz-Zentrum Berlin, Macromolecular Crystallography, Berlin, Germany
2. University of Marburg, Department of Pharmaceutical Chemistry, Marburg, Germany

email: karine.sparta@helmholtz-berlin.de

X-ray diffraction plays an essential role in fragment-based lead discovery and design to identify target hits, and determine the location and structure of fragments bound to a target protein. Recently, a second beamline at the HZB MX facility [1] has been upgraded with a Pilatus detector and sample changer and is dedicated for fragment screening campaigns, enabling fast high throughput experiments to be performed routinely.

In order to help users cope with the huge amount of data thus created and reliably interpret their results rapidly, we have developed the expert software XDSAPP [2] for the analysis of diffraction images during measurements with minimal effort and time. It mainly uses the diffraction data processing program XDS [3], along with additional software like POINTLESS from the CCP4 suite [4], XDSSTAT [5], SFCHECK [6] and PHENIX.XTRIAGE [7] for automated decision making. An independent refinement pipeline for automated ligand search based on PHENIX and COOT [8] has been developed and can also be used within XDSAPP. In the presentation, the workflow of the pipeline will be described and its application to an example will be discussed.

XDSAPP is available free of charge for academic users from www.helmholtz-berlin.de/bessy-mx.

References

- [1] Mueller, U. et al. (2012). *J. Synchrotron Rad.* **19**, 442-449.
- [2] Krug, M. et al. (2012). *J. Appl. Cryst.* **45**, 568-572.
- [3] Kabsch, W. (2012). *Acta Cryst. D* **66**, 125-132.
- [4] Collaborative Computational Project (1994). *Acta Cryst. D* **50**, 760-763.
- [5] Diederichs, K. (2006). *Acta Cryst. D* **62**, 96-101.
- [6] Vaguine, A. et al. (1999). *Acta Cryst. D* **55**, 191-205.
- [7] Adams, P.D. et al. (2010). *Acta Cryst. D* **66**, 213-221.
- [8] Emsley, P. et al. (2010). *Acta Cryst. D* **66**, 486-501.

Keywords: XDSAPP, fragment screening, automation, software, data processing, refinement

MS4. Advances in phasing, refinement, and autobuilding

Chairs: Navraj Pannu, Eleonor Dodson

MS4-O1 ARCIMBOLDO, an *ab initio* approach to MR phasing

Isabel Usón¹, Massimo Sammito², Claudia Millán², Rafael J. Borges²

1. Institutió Catalana de Recerca i Estudis Avançats (ICREA); Institut de Biologia Molecular de Barcelona (IBMB-CSIC)
2. Instituto de Biología Molecular de Barcelona (IBMB-CSIC)

email: uson@ibmb.csic.es

Ab Initio phasing of macromolecular structures, from the native intensities alone without need of derivatives or previous particular structural knowledge has been the object of a long quest. Currently, both experimental phasing and molecular replacement are going *ab initio*, as in the first case, inherent anomalous signal is succeeding with increasing generality[1] and in the second, the previous structural knowledge required is becoming unspecific[2,3,4]. Our own approach[5,6] relies on the combination of locating model fragments such as polyalanine alpha-helices, libraries of unspecific folds or portions of distant homologs with the program PHASER[7] and density modification with the program SHELXE[8]. Given the difficulties in discriminating correctly positioned fragments, many putative groups of fragments have to be tested in parallel, thus calculations are usually performed in a grid or supercomputer. The method has been called after the Italian painter Arcimboldo, who used to compose portraits out of fruits and vegetables. In the case of our program, most collections of fragments remain a “still-life”, but some are correct enough for density modification to reveal the protein's true portrait. Latest developments, such as the single machine implementation ARCIMBOLDO_LITE, advances on the supercomputer GORDON at the SDSC or the first case of a solution for an unknown all-beta structure will be described. (http://chango.ibmb.csic.es/ARCIMBOLDO_LITE).

- 1) Liu, Guo, Chang, Cai, Assur, Mancia, Greene and Hendrickson. (2014). *Acta Cryst. D* **70**, 2544-2557.
- 2) DiMaio, Terwilliger, Read, Wlodawer, Oberdorfer, Wagner, Valkov, Alon, Fass, Axelrod, Das, Vorobiev, Iwai, Pokkuluri & Baker. (2011). *Nature*, **473**, 540-543.
- 3) Bibby, Keegan, Mayans, Winn & Rigden. (2012). *Acta Cryst. D* **68**, 1622-1631.
- 4) Shrestha & Zhang. (2015). *Acta Cryst. D* **71**, 304-312.
- 5) Millán, Sammito & Usón. (2015). *IUCr J* **2**, 95-105.
- 6) Sammito, Millán, Rodríguez, de Ilarduya, Meindl, De Marino, Petrillo, Buey, de Pereda, Zeth, Sheldrick & Usón. (2013). *Nature Methods*, **10**, 1099-1101

7) McCoy, Grosse-Kunstleve, Adams, Winn, Storoni, Read. (2007). *J. Appl. Cryst.* **40**, 658–674

8) Thorn & Sheldrick. (2013). *Acta Crystallogr. D* **69**, 2251–2256.

Keywords: Phasing, ab initio, macromolecular crystallography, fragment search, ARCIMBOLDO, BORGES, SHREDDER, PHASER, SHELXE

MS4-O2 ARP/wARP 7.5 and beyond

Victor S. Lamzin¹, Philipp Heuser¹, Joana Pereira¹, Nils Petersen¹

¹. European Molecular Biology Laboratory, DESY, Notkestrasse 85, 22607, Hamburg, Germany

email: victor@embl-hamburg.de

The ARP/wARP software for macromolecular model building is being continuously developed. Its recent release 7.5 (www.arp-warp.org), jointly with the CCP4 6.5, comes complete with additional innovations targeting protein model building at medium-to-low resolution range; including improved polypeptide recognition, NCS-restraints, atom update, estimation of solvent content and model accuracy, and an option to carry out SAD-refinement. The process of identifying and fitting of bound ligands now incorporates the 84 most common ligands and is able to use cif files defining bond, torsion and plane restraints.

Additionally, currently under development is the novel method of validating built protein fragments (presented in a dedicated poster at this meeting), as well as approaches to accurately estimating the quality of electron density maps and thus the phases. For the latter, a comprehensive scoring function has been designed that makes use of the distributions of third-order moment invariants computed throughout the density map. The distributions of the invariants have been shown to depend on the quality of phases, and the central moments of the distributions can conveniently capture the phase changes. The application of this method to decision-making, protocol guiding or validation in automated macromolecular structure solution and model building will be presented. This method is capable of ranking electron density maps within a resolution range from 2 to 6 Å and up to 80° phase error.

Keywords: ARP/wARP, software

MS4-O3 Pitfalls of crystallographic reasoning, and linking crystallographic model and data quality

Kay Diederichs¹

1. University of Konstanz, D-78457 Konstanz, Germany

email: kay.diederichs@uni-konstanz.de

In the last decades, macromolecular crystallography has been extremely successful. But all that glitters is not gold: some of the concepts developed decades ago now need revision.

For example, analysis of crystallographic data quality is still somewhat fixated on values of R_{merge} (also called R_{sym}), and the distinction between accuracy and precision, as well as indicators of unmerged data precision and those of merged data precision still has to be realized in the crystallographic community. Furthermore, logical flaws and oversimplifications lead to inappropriate shortcuts that often reduce the quality of structures.

Recently we pointed out (Karplus and Diederichs [2012] *Science* **336**, 1030) that the high-resolution value of R_{merge} is not related to $R_{\text{work}}/R_{\text{free}}$ of a crystallographic model, and is therefore unsuitable to define a high-resolution cutoff of data to be included in refinement. A more meaningful indicator ($CC_{1/2}$) has been suggested and a derived quantity (CC^*) was shown to be limiting for $CC_{\text{work}}/CC_{\text{free}}$ of a crystallographic model.

This talk will demonstrate that as a consequence, crystallographers are now in a position to better understand the properties of their data, which may be used to obtain more accurate crystallographic models.

Keywords: refinement, high-resolution cutoff, precision, accuracy, data quality indicators

MS4-O4 Advances in synchrotron data collection protocols for experimental phasing

Aaron D. Finke¹, Tobias Weinert¹, Ezequiel Panepucci¹, Claus Fensburg², Clemens Vornheim², Gerard Bricogne², Vincent Olieric¹, Meitian Wang¹

1. Swiss Light Source, Paul Scherrer Institute, CH-5232 Villigen, Switzerland

2. Global Phasing Ltd., Sheraton House, Castle Park, Cambridge CB3 0AX, United Kingdom

email: aaron.finke@psi.ch

Experimental phasing by single- or multiple-wavelength anomalous diffraction (SAD or MAD) is the most popular method of *de novo* macromolecular structure determination. Recent overhauls at third-generation synchrotron light sources have dramatically sped up phasing data collection protocols. In particular, the reintroduction of multi-axis goniometers has enabled two major advances in anomalous data collection: the ability to collect “true” high-multiplicity, low-dose datasets on a single crystal entity, maximizing the anomalous signal output while minimizing both systematic and random measurement errors; and alignment of even-fold crystal symmetry axes along the spindle axis to collect Bijvoet pairs, thus reducing radiation damage-induced errors in measurement. We present our results in applying both strategies to challenging problems in experimental phasing.

Keywords: experimental phasing, SAD, MAD, multi-axis goniometer

MS4-O5 How well do we understand macromolecular crystals?Andrea Thorn¹, Rob Nicholls¹, Garib Murshudov¹

1. MRC Laboratory of Molecular Biology, Francis Crick Avenue, Cambridge Biomedical Campus, Cambridge CB2 0QH, UK.

email: andrea.thorn@web.de

In X-ray structure determination, the R-value reports how well a model agrees with the experimental data. In small molecule crystallography, R-values of 3% are routinely reached. However, for biological macromolecules, R-values are normally around 20% and even when the data extend to atomic resolution, the average R-value is 14%.

This is clear evidence that something is amiss; our current models of macromolecular crystal structures seem to be lacking. But what is this difference between our models and reality and how would we observe this difference, given that our assumptions about macromolecular structures are used to generate phases (and hence electron density) in the first place?

In this talk, some answers to these questions will be presented. It will also be shown how model deficiencies hamper in particular the structure determination of problematic structures, such as membrane proteins and large macromolecular complexes. In these cases, only low resolution data might be available and the poor phase estimates currently obtainable result in noisy electron density maps. A better understanding of the shortcomings in our current models (and methods) could be an important factor to solving the most difficult structures and to improving the others.

Keywords: macromolecules, refinement, phasing, macromolecular crystals

MS5. Structure and function of enzymes

Chairs: Joel Sussman, Ute Krengel

MS5-O2 New structures of *Thermotoga maritima* integral membrane pyrophosphatase suggest a conserved coupling mechanism for proton and sodium transportAdrian Goldman^{1,2,3}, Juho Kellosoalo², Craig Wilkinson¹, Tommi Kajander², Yu-Juh Sun⁴

1. Astbury Centre of Structural Molecular Biology, University of Leeds, Leeds, United Kingdom
2. University of Helsinki, Helsinki, Finland
3. Nankai University, Tianjin, China
4. National Tsing Hua University, Hsinchu, Taiwan

email: a.goldman@leeds.ac.uk

Membrane-bound pyrophosphatases couple transport of protons and/or sodium-ions through the biological membrane to pyrophosphate hydrolysis or synthesis (1). They occur in plants and in unicellular organisms and are crucial for abiotic stress tolerance (2). mPPases are dimeric, with both monomers having 16 trans-membrane helices (TMHs) and one continuous active site with distinctive regions for PP_i binding and ion transport (3). PP_i binding drives the closure of the cytoplasmic active site and thus mPPases utilize an alternate-access mechanism for ion pumping. PP_i hydrolysis is carried by an activated water molecule, which is coordinated between two conserved aspartates (4). Two new structures of different membrane-bound pyrophosphatases: a sodium-pump from *Thermotoga maritima* with bound sodium and competitive inhibitor, imidodiphosphate (IDP), and the *Vigna radiata* proton-pump with one phosphate bound reveal the movements of inner ring and outer ring TMHs and the corresponding opening and closing of the binding pocket. The structures reveal a hitherto unknown sodium-binding site and confirm our earlier hypothesis that the electrophilic phosphate group is released first from the active site (3, 5). Together with recent functional data, the structures also confirm our earlier hypothesis that TMH12 movement plays a role in ion pumping, likely by driving the formation of the periplasmic/luminal exposed conformation of the enzyme. The structures also suggest a model for how the coupling between ion pumping and PP_i hydrolysis is ensured by movement of TMHs 6 and 16, which brings the conserved aspartates into the correct position for catalytic water coordination only in the ion-bound state of the enzyme. These changes allow us to propose how proton-pumping evolved from sodium-pumping in mPPases.

References

1. Luoto, H. H., Baykov, A. A., Lahti, R. and Malinen, A. M. (2013) *Proc. Natl. Acad. Sci. U S A* **110**, 1255-1260.
2. Maeshima, M. (2000) *Biochim. Biophys. Acta* **1465**, 37-51.
3. Kellosalo, J., Kajander, T., Kogan, K., Pokharel, K. and Goldman, A. (2012) *Science* **337**, 473-476.
4. Lin, S. M., Tsai, J. Y., Hsiao, C. D., Huang, Y. T., Chiu, C. L., Liu, M. H., Tung, J. Y., Liu, T. H., Pan, R. L. and Sun, Y. J. (2012) *Nature* **484**, 399-403.
5. Tsai, J.-Y., Kellosalo, J., Sun, Y.-J. and Goldman, A. (2014) *Curr. Opin. Struct. Biol.* **27C**, 38-47.

Keywords: integral membrane proteins, pyrophosphatases, primary ion pumps, sodium pumping, evolution

MS5-O3 Effector proteins from pathogenic bacteria: focus on kinases

Mirosław Cygler¹, Andrey M. Grishin¹

¹. Department of Biochemistry, University of Saskatchewan, Saskatoon, Canada

email: miroslaw.cygler@usask.ca

Pathogens modify host cell responses through a ensemble of proteins ejected into the host through a syringe-like bacterial secretion system. One of the ways the cellular responses are modified to assure pathogen survival and proliferation inside the host is to hijack and redirect host signaling pathways. Bacterial effector kinases are among the tools to do just that. Kinases NleH1 and NleH2 from pathogenic *E. coli*, OspG from *Shigella*, SteC and SboH from *Salmonella*, LegK1-4 from *Legionella* and YspK and YpkA from *Yersinia* represent currently known effector kinases. Sequence analysis of these kinases indicates that some of them were derived from eukaryotes *via* horizontal gene transfer (SteC, LegK1-4, YpkA). Other kinases (NleH, OspG, SboH and YspK) have been so far identified only in the pathogenic bacteria. Structural investigations showed that NleH and OspG contain only a core kinase fold and lack the regulatory activation loop. While NleH is fully active on its own, OspG activity is stimulated by ubiquitin and even more by the ubiquitin-conjugating enzyme E2-ubiquitin complex. The structure of OspG:UbcH7-Ub complex and mutational analysis of OspG suggest the mechanism of OspG activation. Both NleH and OspG inhibit the NF- κ B pathway, however, their substrates are yet unknown.

Keywords: host-pathogen interactions; bacterial effector kinases; bacterial effectors, ubiquitination

MS5-O4 An integrative approach targeting phosphatase-substrate complexes for new cancer drug design strategy

Andrew H. Wang¹, Kai-En Chen¹, Shu-Yu Lin¹, Meng-Ru Ho¹, Chia-Cheng Chou¹, Tzu-Ching Meng¹

1. Institute of Biological Chemistry, Academia Sinica, Taipei 11581, Taiwan.

email: ahjwang@gate.sinica.edu.tw

Reversible phosphorylation is an essential post-translational modification in the regulation of numerous cellular activities. This fundamental mechanism is precisely controlled by protein kinases, protein phosphatases and thousands of their phosphoproteins in any given cells. Two examples will be presented on PTPN3 and two of its specific substrates, mitogen-activated protein kinase 12 (MAPK12/p38 γ) and epidermal growth factor (EGFR) pathway substrate 15 (Eps15).

The first study involves the structural elucidation of the PTPN3-p38 γ complex, which is known to be a novel target for Ras-dependent malignancies. We determined the molecular architecture of this phosphatase-kinase complex by employing a hybrid method combining X-ray crystallography, small-angle X-ray scattering and chemical cross-linking coupled with mass spectrometry. Our crystal structure of PTPN3 in complex with the p38 γ phosphopeptide presents a unique feature of the E-loop that defines the substrate specificity of PTPN3 towards fully activated p38 γ . The low resolution solution structure demonstrates the formation of an active-state complex between the phosphatase domain of PTPN3 and p38 γ . We show a regulatory function of PTPN3's PDZ domain, which stabilizes the active-state complex through interaction with the PDZ-binding motif of p38 γ . Binding of the PDZ domain to the PDZ-binding motif lifted the auto-inhibitory constraint of PTPN3, enabling efficient tyrosine dephosphorylation of p38 γ to occur. Our findings emphasize the potential of structure-based drug design to antagonize Ras transformation via intervention in PTPN3-p38 γ interaction.

In the second study, we have also determined the crystal structure of PTPN3 in complex with Eps15 phosphopeptide. Dephosphorylation of Eps15 by PTPN3 is important for the regulation of EGFR in non-small cell lung cancer. Binding of Eps15 phosphopeptide to the PTPN3 active site reveals a novel conformation, which is different to other PTP-phosphopeptide structures. Our phosphatase activity confirmed a high level of substrate specificity between PTPN3 and Eps15. Employing the biochemical approach, we have identified the key PTPN3 residue involved in the recognition of Eps15. (Chen KE et al, Science Signal. 2014 7(347):ra98, Structure, 2015, in press)

Keywords: phosphatase, synchrotron, cancer, drug discovery

MS5-O5 Towards a generalised approach for the time-resolved crystallographic study of enzymes

Diana C.F. Monteiro¹, Vijay Patel¹, Christopher P. Bartlett¹, Shingo Nozaki², Thomas D. Grant³, James A. Gowdy¹, Gary S. Thompson¹, Arnout P. Kalverda⁴, Edward H. Snell⁵, Hironori Niki², Arwen R. Pearson⁴, Michael E. Webb⁵

1. Astbury Centre for Structural Molecular Biology, University of Leeds, UK

2. Microbial Genetics Laboratory, Genetic Strains Research Center, National Institute of Genetics, Japan

3. Hauptmann-Woodward Medical Research Institute, Buffalo, NY, USA

4. Hamburg Centre for Ultrafast Imaging, Institute of Nanostructure and Solid State Physics, University of Hamburg, Germany

5. School of Chemistry, University of Leeds, UK

email: cm07dcfm@leeds.ac.uk

Protein motions and dynamics are essential for function. Static structural studies provide only very incomplete information about the active conformations adopted by proteins. In contrast, time-resolved crystallography enables the observation of both small-scale and large-scale protein conformational changes that occur during function.¹

To “watch” enzymes function in real-time, the enzymatic reaction must be triggered quickly and cleanly across the crystal. We have developed a new set of general photoactive reagents to trigger enzyme reactions using light. These reagents are designed such that they decouple photoactivation chemistry from the enzyme reaction and can be easily attached to strategically placed cysteines on the protein surface.

We are testing these new reagents using the protein aspartate α -decarboxylase (ADC) as a model system. This enzyme catalyses the conversion of aspartate to β -alanine, a precursor of coenzyme A. ADC is expressed as an inactive zymogen which cleaves post-translationally, yielding the catalytic pyruvoyl group. However, the cleavage requires an additional activating partner, PanZ.² To understand how ADC activation is catalysed by PanZ, we solved the structure of the ADC-PanZ protein-protein complex at high-resolution. With the aid of complementary techniques (SAXS, ITC, MS, NMR, *in cellulo* studies) we showed that not only does this protein-protein interaction promote ADC activation “mechanically” but that it is also involved in regulating CoA production in bacteria.³⁻⁴

1. Neutze, R.; Moffat, K., *Current Opinion in Structural Biology* **2012**, 22 (5), 651-659.

2. Nozaki, S.; Webb, M. E.; Niki, H., *MicrobiologyOpen* **2012**, 1 (3), 298-310.

3. Monteiro, D. C. F.; Rugen, M. D.; Shepherd, D.; Nozaki, S.; Niki, H.; Webb, M. E., *Biochemical and Biophysical Research Communications* **2012**, 426 (3), 350-355.

4. Monteiro, D. C. F.; Patel, V.; Bartlett, C. P.; Nozaki, S.; Grant, T. D.; Gowdy, J. A.; Thompson, G. S.; Kalverda, A. P.; Snell, E. H.; Niki, H.; Pearson, A. R.; Webb, M. E., **2015, manuscript accepted**.

Keywords: Time-resolved crystallography, post-translational modification, enzyme mechanisms

MS6. Membrane proteins and signal transduction pathways

Chairs: E. Yvonne Jones, Werner Kühlbrandt

MS6-O1 High-resolution structure and substrate and ion translocation mechanism of a di-carboxylate transporter

Oezkan Yildiz¹

1. Max-Planck-Institut für Biophysik, Germany

email: Oezkan.Yildiz@biophys.mpg.de

Membrane proteins are essential for transporting molecules across biological membranes, which makes them important drug targets. Secondary transporters, found in all kingdoms of life, transport substrates and ions across membranes and are therefore essential for many fundamental physiological processes. We have determined the crystal structure of a di-carboxylate transporter at 2.5 Å resolution to elucidate the transport mechanism. Uniquely, two different CitS homodimers are present simultaneously in the structure. In each dimer, one protomer is in the inward-facing and the other in the outward-facing conformation. Transport kinetics were determined by detailed substrate uptake measurements. Together, our data provide a complete six-step mechanism, which explains how the transporter binds the diracboxylate and substrate ions, translocates them across the membrane and the sequence in which they are released to the cytoplasm. Similar transport mechanisms may apply to a wide variety of related and unrelated secondary transporters.

Keywords: Membrane protein, X-ray structure, transporter, transport mechanism

MS6-O2 Structure, function, and inhibitors of the acid-gated *Helicobacter pylori* urea channel, an essential component for acid survival and chronic infectio

Hartmut Luecke^{1,2}

1. Unidad de Biofísica and Departamento de Bioquímica University of the Basque Country (UPV/EHU) and Spanish Science Research Council (CSIC)

2. University of California, Irvine

email: hudel@uci.edu

Half the world's population is chronically infected with *Helicobacter pylori*, causing gastritis, gastric ulcers and an increased incidence of gastric adenocarcinoma. Its proton-gated innermembrane urea channel, *HpUreI*, is essential for survival in the acidic environment of the stomach. The channel is closed at neutral pH and opens at acidic pH to allow the rapid access of urea to cytoplasmic urease. Urease produces NH_3 and CO_2 , neutralizing entering protons and thus buffering the periplasm to a pH of roughly 6.1 even in gastric juice at a pH below 2.0. Here we report the structure of *HpUreI*, revealing six protomers assembled in a hexameric ring surrounding a central bilayer plug of ordered lipids. Each protomer encloses a channel formed by a twisted bundle of six transmembrane helices. The bundle defines a previously unobserved fold comprising a two-helix hairpin motif repeated three times around the central axis of the channel, without the inverted repeat of mammalian-type urea transporters. Both the channel and the protomer interface contain residues conserved in the AmiS/UreI superfamily, suggesting the preservation of channel architecture and oligomeric state in this superfamily. Predominantly aromatic or aliphatic side chains line the entire channel and define two consecutive constriction sites in the middle of the channel. Mutation of Trp153 in the cytoplasmic constriction site to Ala or Phe decreases the selectivity for urea in comparison with thiourea, suggesting that solute interaction with Trp153 contributes specificity. The previously unobserved hexameric channel structure described here provides a new model for the permeation of urea and other small amide solutes in prokaryotes and archaea. Follow-up microsecond-scale unrestrained molecular dynamics studies now provide a detailed mechanism of urea and water transport by *HpUreI*.

References

- Strugatsky, D., McNulty, R.M., Munson, K., Chen, C.-K., Soltis, S.M., Sachs, G., Luecke H. "Structure of the proton-gated urea channel from the gastric pathogen *Helicobacter pylori*" (2013) *Nature* **493**, 255–258.
- Luecke, H. & Sachs, G. "*Helicobacter pylori*'s Achilles' Heel" (2013) *Immuno-Gastroenterology* **2**, 76.
- McNulty, R., Ulmschneider, J.P., Luecke, H., Ulmschneider, M.B. "Mechanisms of molecular transport through the urea channel of *Helicobacter pylori*" (2013) *Nature Communications* **4**, article number 2900.

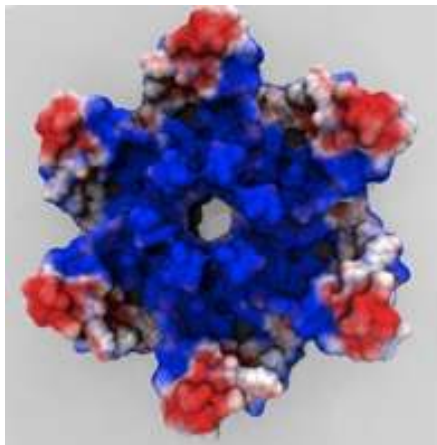


Figure 1.

Keywords: urea channel pH gating drug discovery

MS6-O3 Membrane-bound pyrophosphatase: A primary proton pump

Yuh-Ju Sun¹

1. Institute of Bioinformatics and Structural Biology, National Tsing Hua University, Hsinchu, Taiwan

email: yjsun@life.nthu.edu.tw

Membrane-embedded pyrophosphatases (M-PPases) couple the generation and utilization of membrane potentials to catalyze the hydrolysis of pyrophosphate (PPi) and pump ion across the membranes. M-PPases, the proton/sodium ion pumps occur in all three domains of life, including H⁺-PPases in prokaryotes, bacteria, and plant, Na⁺-PPases in prokaryotes and H⁺/Na⁺-PPases in bacteria. The *Vigna radiata* H⁺-PPase (VrH⁺-PPase) was isolated as a homodimeric form with 16 transmembrane helices each monomer. The crystal structure of VrH⁺-PPase in complex with a substrate analogue, imidodiphosphate (IDP), was determined by MAD and MIRAS methods. VrH⁺-PPase has a novel fold and pumping mechanism, different to the other primary pumps. The structural information of VrH⁺-PPase provides the basis for understanding a unique proton translocation pathway as well as the ion selection among various M-PPases.

Keywords: pyrophosphatases, proton/sodium ion pump, *Vigna radiata*,

MS6-O4 General mechanism of function of TIR domains

Bostjan Kobe¹, Thomas Ve¹, Simon Williams¹, Xiaoxiao Zhang¹,
Li Wan¹, Mohammed Alaidarous¹, Maud Bernoux², Kee Hoon
Sohn³, Jonathan Jones³, Michael Landsberg¹, Peter Dodds²

1. University of Queensland, Brisbane, Australia
2. CSIRO, Agriculture Flagship, Canberra, Australia
3. The Sainsbury Laboratory, Norwich, UK

email: b.kobe@uq.edu.au

TIR (Toll/interleukin-1 receptor, resistance protein) domains are key components of innate immunity signalling pathways. They are found in animals, plants and bacteria, for example in TLRs (Toll-like receptors) and TLR adaptors in animals, NLRs (nucleotide binding, leucine-rich repeat) in plants, and virulence factors interfering with immune responses in bacteria. While it has been well established that signalling depends on regulated self-association and homotypic association of TIR domains, every single TIR domain structure has revealed a different association mode [1]. In the search for common features, we have targeted a number of TIR domains from mammals, plants and bacteria to characterize structurally. We have determined the crystal structures of the TIR domains from the human TLR adaptor protein MAL [2], the bacterial protein TcpB from *Brucella melitensis* [3] and the plant immune proteins L6 from flax [4], RPS4 and RRS1 from *Arabidopsis* [5], SNC1 from *Arabidopsis* and MrRUN1 and MrRPV1 from grapevine (unpublished). In the case of the proteins RPS4 and RRS1, which work together as a protein complex to confer resistance to three different bacterial and fungal pathogens, we have determined, using linker-assisted crystallization, the first structure of a hetero-dimeric complex of TIR domains. The association interface in this complex is conserved in the crystals of the TIR domains of RPS4 and RRS1 on their own, as well as in those of SNC1, MrRUN1 and MrRPV1. Similarly, the dimerization interface observed in the structure of TcpB is conserved in the structure of the TIR domain-containing protein from *Paracoccus denitrificans*. We further observed that TLR4 TIR domains seed helical filament formation by MAL (cryo-electron microscopy reconstruction shown in Fig. 1), which in turn seeds a crystalline assembly of the TIR domain from TLR adaptor MyD88 (the crystals are currently being characterized by X-FEL). Jointly, these studies are yielding a general mechanism of function of TIR domains, which at least in some cases will involve signaling through higher-order assembly formation with prion-like features.[1] Ve T, Williams S, Kobe B (2015) Apoptosis 20: 250-61 [2] Valkov E et al, Proc Natl Acad Sci USA, 2011, 108, 14879-14884 [3] Alaidarous M et al, J Biol Chem, 2014, 289, 654-68 [4] Bernoux M et al, Cell Host Microbe, 2011, 9, 200-211 [5] Williams SJ et al, 2014, Science 344: 299-30

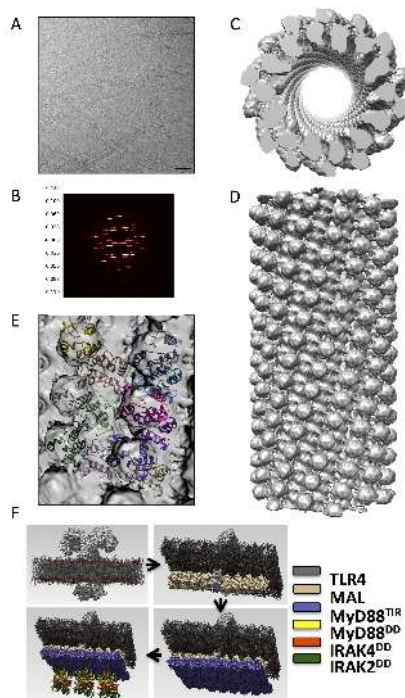


Figure 1. Structure of MAL filaments. A. Cryo-EM image. B. Power spectrum from a class average. The layer lines indicate helical symmetry. C/D. Cryo-EM reconstruction. E. Zoom-in showing MAL monomers fitted into electron density. F. Working model for signaling by TLR4/MAL/MyD88.

Keywords: Innate immunity, Bacterial pathogenesis, Linker-assisted crystallization, Cryo-electron microscopy, X-ray free-electron laser

MS6-O5 Covalent host-targeting by thioester domains of Gram-positive pathogens

Miriam Walden¹, John M. Edwards², Aleksandra M. Dziejulska²,
Rene Bergmann³, Gerhard Saalbach¹, Manfred Rohde³, Uli
Schwarz-Linek², Mark J. Banfield¹

1. John Innes Centre, Norwich, UK

2. University of St Andrews, UK

3. Helmholtz Centre for Infection Research, Germany

email: miriam.walden@jic.ac.uk

Gram-positive pathogens are a major health concern, with a lack of preventative therapeutics and the ever-increasing resistance to antimicrobials. One of the most crucial steps in infection is adhesion of the microbes to host tissues. Understanding the specific interactions at the host-microbe interface is vital in the development of novel strategies to combat disease. The discovery of complex cell-surface associated proteins, such as pili, has advanced our knowledge of this interaction, however the precise molecular mechanisms underlying the adhesion process remain unclear.

To date, these adhesins are only known to bind host cell receptors in a non-covalent manner. However, recent studies of a *Streptococcus pyogenes* pilus adhesin revealed the presence of an extremely rare internal thioester bond between the side chains of a Cys and a Gln residue. Mutation of this Cys to Ala results in a 75% reduction in adhesion to HaCaT cells, suggesting that this reactive internal linkage may mediate direct attachment.

We have now discovered that thioester domains (TEDs) are unexpectedly prevalent in cell-surface proteins of several clinically relevant Gram-positive pathogens. Using a combination of mass spectrometry and crystallography, we have confirmed the presence of the thioester bond within a selection of twelve TEDs. Furthermore, we show that for the streptococcal surface protein SfbI, this bond can be used as a 'chemical harpoon' to mediate covalent interaction with the host cell protein, Fibrinogen. This cross-linking reaction allows bacterial attachment to fibrin and SfbI binding to human epithelial cells. These findings support bacterial-encoded covalent binding as a new molecular principle in host-microbe interactions.

Keywords: Adhesion, pili, thioester bond, crystallography

MS7. Nucleic acids and their complexes and assemblies with proteins

Chairs: Miquel Coll, Christine Cardin

MS7-O1 Translational regulation of gene expression by Lin28 and Roquin

Udo Heinemann¹, Yasuhiro Murakawa¹, Markus Landthaler¹,
Florian Mayr¹, Anja Schütz¹

1. Max-Delbrück Center for Molecular Medicine,
Robert-Rössle-Str. 10, 13125 Berlin (Germany)

email: heinemann@mdc-berlin.de

RNA-binding proteins contribute to gene expression control by regulating the biogenesis of microRNAs and mRNA homeostasis. Recently, we have studied structural aspects of RNA binding of two important human RNA-binding proteins, Lin28 and Roquin.

Lin28 regulates the maturation of *let-7* microRNAs and binds to a large number of mRNAs (1). A Lin28-*let-7* regulatory axis is involved in mediating cell differentiation or pluripotency, and *LIN28* is overexpressed in a number of cancers. We have analyzed the binding of Lin28 to pre-*let-7* molecules by X-ray crystallography and biochemical approaches and provided evidence for an RNA binding model where the Lin28 cold-shock domain remodels the pre-*let-7* structure in order to allow subsequent and sequence-specific binding of the Lin28 zinc-knuckle domain (2). Combined with other studies of the Lin28-*let-7* interaction (3,4) this work provides a structural framework for the function of Lin28 in translation-level gene regulation.

Roquin proteins recognize a conserved class of stem-loop RNA degradation motifs, leading to mRNA deadenylation. We have determined the crystal structure of the ROQ domain of human Roquin1/RC3H1 and revealed a mostly helical fold bearing a winged helix-turn-helix (wHTH) motif (5). Through biochemical and mutational analyses we demonstrate that the wHTH motif is involved in binding stem-loop mRNAs that carry constitutive decay elements. Being part of a recent deluge of Roquin structural studies (5-8) our work contributes to putting the biological function of Roquin proteins on a solid mechanistic basis.

References

1. Mayr, F., Schütz, A., Döge, N. & Heinemann, U. (2012) *Nucleic Acids Res.* 40, 7492-7506.
2. Graf, R. et al. (2013) *RNA Biol.* 10, 1146-1159.
3. Nam, Y., Chen, C., Gregory, R.I., Chou, J.J. & Kim, V.N. (2011) *Cell* 147, 1080-1091.
4. Mayr, F. & Heinemann, U. (2013) *Int. J. Mol. Sci.* 14, 16532-16553.

5. Schuetz, A., Murakawa, Y., Rosenbaum, E., Landthaler, M. & Heinemann, U. (2014) *Nat. Commun.* 5:5701.

6. Schlundt, A. et al. (2014) *Nat. Struct. Mol. Biol.* 21, 671-678.

7. Tan, D., Zhou, M., Kiledjian, M. & Tong, L. (2014) *RNA. Nat. Struct. Mol. Biol.* 21, 679-685.

8. Srivastava, M. et al. (2015) *Nat. Commun.* 6:6253.

Keywords: Lin28, Roquin, RNA binding

MS7-O2 Recombinant multiprotein complex production: identification of a novel building block of the general transcription factor TFIID

Simon Trowitzsch¹

¹ Institute of Biochemistry, Goethe Universität Frankfurt

email: trowitzsch@biochem.uni-frankfurt.de

Multiprotein complexes are a cornerstone of biological activity, as many proteins appear to participate stably or transiently in large multisubunit assemblies. Analysis of the architecture of these assemblies and their manifold interactions is imperative for understanding their function at the molecular level. Powerful recombinant protein production technologies, e.g. MultiBac - a baculoviral expression vector system for multiprotein complex production, are constantly being developed to produce material in great enough quantities for structural and functional studies.

Here, I will present our recent work¹ on the general transcription factor IID (TFIID), which plays a key role in RNA polymerase II transcription initiation in eukaryotic cells. Human TFIID is a megadalton-sized multiprotein complex composed of the TATA-binding protein (TBP) and 13 TBP-associated factors (TAFs). How these individual proteins assemble into a functional transcription factor is poorly understood to date. We identified a heterotrimeric TFIID subcomplex consisting of the TAF2, TAF8 and TAF10 proteins, which assemble in the cytoplasm. This heterotrimeric TAF complex was produced recombinantly in insect cells using the MultiBac system. By means of native mass spectrometry, we defined the interactions between the TAFs and uncovered a central role for TAF8 in nucleating the complex. X-ray crystallography reveals a non-canonical arrangement of the TAF8-TAF10 histone fold domains. Binding assays including peptide arrays and surface plasmon resonance experiments showed that TAF2 binds to multiple motifs within the TAF8 C-terminal region. These interactions direct the incorporation of TAF2 into a core-TFIID complex that exists in the nucleus. Our results provide evidence for a stepwise assembly pathway of nuclear holo-TFIID, regulated by nuclear import of preformed cytoplasmic submodules.

1) Trowitzsch S, Viola C, Scheer E, Conic S, Chavant V, Fournier M, Papai G, Ebong IO, Schaffitzel C, Zou J, Haffke M, Rappsilber J, Robinson CV, Schultz P, Tora L, and Berger I. (2015) Cytoplasmic TAF2-TAF8-TAF10 complex provides evidence for nuclear holo-TFIID assembly from preformed submodules. *Nature Communications*. 6:6011.

Keywords: multiprotein complexes, transcription, TFIID, BEVS, MultiBac

MS7-O3 When RNP meets RNP: The signal recognition particle and the ribosome

Klemens Wild¹, Georg Kempf¹, Jan T. Grotwinkel¹, Bernd Segnitz¹, Irmgard Sinning¹

1. Heidelberg University Biochemistry Center (BZH), Germany

email: klemens.wild@bzh.uni-heidelberg.de

The signal recognition particle (SRP) is a ribonucleoprotein complex with a central role in co-translational targeting of membrane and secretory proteins. It is found in all three kingdoms of life and exhibits a conserved mode of action while composition and structure have undergone specific adaptations. In most organisms, SRP can be divided into two functional domains. The S domain mediates recognition and transport of ribosome – nascent chain complexes (RNCs) to the translocation channel via the interaction of SRP with the SRP receptor (SR), while the *Alu* domain stalls translation elongation on the ribosome until the nascent chain has been faithfully delivered.

Here we present crystal structures of a complete bacterial SRP *Alu* domain [1] and a ternary complex of human SRP S domain RNA, SRP19, and the SRP68-RBD [2, 3]. The structures reveal highly complex and unprecedented RNA folds and RNA-protein interactions and illustrate the principles of SRP RNA shaping for proper interaction with ribosomal RNA. The crystal structures are placed in high-resolution cryo-EM envelopes of SRP-RNC complexes explaining the modes of RNP-RNP interactions on an atomic level. Highlights of fold and function will be exemplified.

References:

- [1] Kempf, G., Wild, K. & Sinning, I. *Nucleic Acids Research* **42**, 12284-94 (2014).
- [2] Grotwinkel, J. T., Wild, K., Segnitz B. & Sinning, I. *Science* **344**, 101-4 (2014).
- [3] Wild, K. & Sinning, I. *RNA Biol* **11**, 1330-4 (2014).

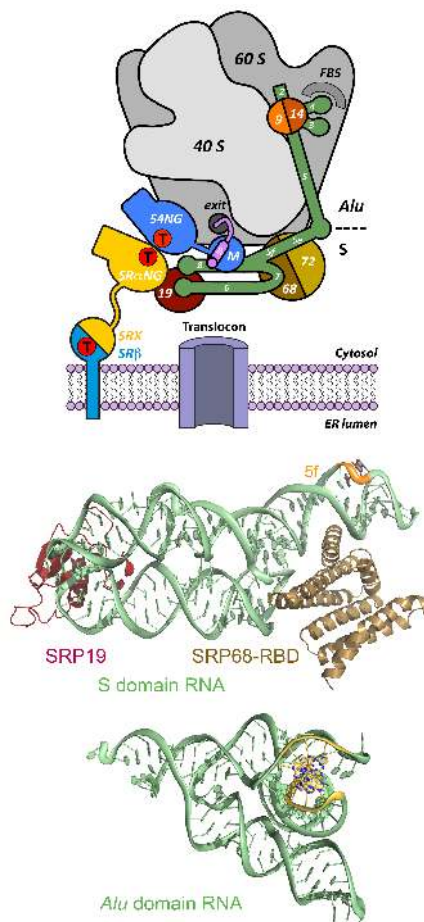


Figure 1. Co-translational targeting by SRP. Top panel: Scheme for the targeting of mammalian SRP-SR/RNC complexes to the translocation channel in the endoplasmic reticulum membrane. Structures are presented for the human S domain (middle) and a bacterial *Alu* domain (bottom).

Keywords: Signal Recognition Particle (SRP), protein targeting, protein-RNA and RNA-RNA interactions, X-ray crystallography

MS7-O4 From sequence to nanostructure: a critical base pair in RNA k-turns that confers folding and structural characteristics, and correlates with biological function

Lin Huang¹, Xuesong Shi², Daniel Herschlag², David Lilley¹

1. Nucleic Acid Structure Research Group, University of Dundee, Dundee, DD1 5EH, UK.

2. Department of Biochemistry, Stanford University, Stanford CA, 94305, USA.

email: huanglin2008@gmail.com

Kink turns (k-turns) are ubiquitous sequences that generate tight kinks within RNA helices that mediate tertiary interactions in the folding of large assemblies such as the ribosome, and often serve as targets for specific binding proteins. Because of this, k-turns play a key role in the assembly of ribosomes, the spliceosome and box C/D and H/ACA snoRNPs, as well as seven distinct riboswitch species.

Both tertiary contacts and protein binding can stabilize the kinked conformation, and some, but not all, sequences may fold in the presence of sufficient metal ion concentrations. These differential folding properties must be very important in the assembly and function of their RNA species. Another important structural characteristics is that most k-turns fall into one of two classes, depending on whether the acceptor of the H-bond donated by the -1n O2' is N3 or N1 of the conserved A2b (termed the N3 or N1 conformation). This changes the trajectory of the NC (Non-canonical) helix, thus potentially affecting tertiary contacts. Such conformational influences are likely to be very important in the biogenesis of large RNA protein assemblies.

By systematic analysis of Kt-7 variants we have identified the single base pair that follows the conserved A•G pairs (the 3b•3n basepair) as the critical determinant of ion-dependent folding, and we have enunciated rules for ion-induced folding together with a molecular explanation.

Here we determined more than 25 structures and found that 3b•3n basepair is the critical determinant of a k-turn's structure conformation (N3 or N1), and the results also agree with phylogenetic analysis. We also confirmed this observation by X-ray scattering interferometry (XSI), to probe the solution structural conformation of the k-turn.

The deduced sequence rules for k-turn folding and structure conformation have strong predictive value, and can be applied to many natural RNA sequences. To show those sequence rules are well understood and applicable to modeling and design, we successfully designed a nanostructure comprising six k-turns in a circular arrangement, the structure of which has been determined by X-ray crystallography at 3.0 Å resolution.

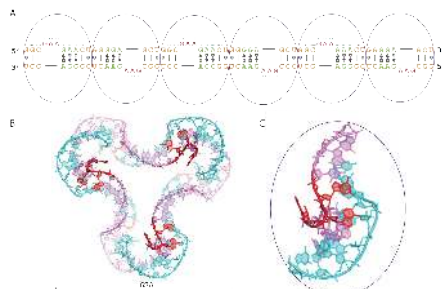


Figure 1. Design and structure of the RNA triangle. (A) Design of the RNA triangle with 6 Kt-7 sequences. (B) Structure of the RNA triangle. One strand colored blue, another strand colored violet, all the loop regions colored red. (C) One Kt-7 structure.

Keywords: RNA structure, kink-turn, X-ray crystallography, nanostructure

MS7-O5 Structure of the human 80S ribosome

S. Kundhavai Natchiar¹, Heena Khatter¹, Alexander G Myasnikov¹, Bruno P Klaholz¹

1. Centre for Integrative Biology (CBI), Department of Integrated Structural Biology, IGBMC (Institute of Genetics and of Molecular and Cellular Biology), 1 rue Laurent Fries, Illkirch, France

email: natchiar@igbmc.fr

Ribosomes are translational machineries in living cells that catalyse protein synthesis. Ribosome structures from various species are known to the atomic level, but that of the human ribosome has remained a challenge to address. We established a purification protocol to obtain homogenous 80S ribosomes from HeLa cells and characterized them biophysically. Here we report the near-atomic structure of the human ribosome derived from high-resolution single particle cryo electron microscopy using the in-house Titan Krios electron microscope, advanced image processing and dedicated computing resources, and atomic model building using new crystallography refinement procedures. The structure has an average resolution of 3.6 Å and reaches 2.9 Å resolution in the most stable regions and thus provides unprecedented insights into rRNA entities and amino acid side-chains. The final atomic model comprises ~220 000 atoms across the 5866 nucleotide residues and ~11590 amino acids of the 80 proteins, the 4 rRNA's and E-site tRNA. The structure reveals the specific molecular recognition of the exit site tRNA with rRNA and protein elements of the ribosome. It highlights atomic details of the molecular interactions at the ribosomal subunit interface which is seen to strongly remodel upon rotational movements of the ribosomal subunits. Moreover, the structure paves the way for studying various diseases associated with deregulated protein synthesis.

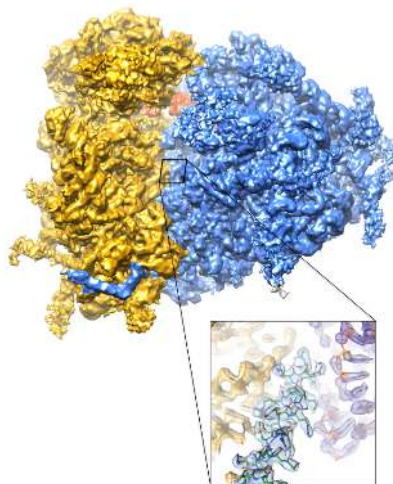


Figure 1. CryoEM towards atomic resolution

Keywords: Human 80S ribosome, E-site tRNA, Cryo electron microscopy

MS8. Molecular machines and motors

Chairs: Nenad Ban, Leonid Sazanov

MS8-O1 Transporting cargo over long distances: insight from dynein/dynactin structures

Andrew Carter¹

1. MRC Laboratory of Molecular Biology, Francis Crick Ave, Cambridge, CB2 0QH, UK

email: cartera@mrc-lmb.cam.ac.uk

Cells depend on components being moved to the correct place at the correct time. My group is interested in cytoplasmic dynein-1 (dynein-1), a motor which delivers many different cargos via the microtubule network. When dynein-1 is mutated it leads to neurodegeneration and it is susceptible to hijack by viruses which use it to travel into the cell. We have determined X-ray crystal structures of the dynein motor before and after it binds and hydrolyses ATP. We subsequently used single molecule fluorescence assays to show how a cofactor, dynactin, activates the full length 1.4MDa dynein complex to move long distances along microtubules. A high resolution (4.0Å) cryo-electron microscopy (cryo-EM) structure of dynactin explained how this 23 subunit complex is assembled. We also used a combination of cryo-EM and X-ray crystallography to show how dynactin binds to dynein. The two complexes are only brought together in the presence of an adaptor protein, Bicaudal-D2, that links them to the cargo they will carry. This suggests the large and intricate dynein/dynactin transport machine only assembles when a cargo is ready to move.

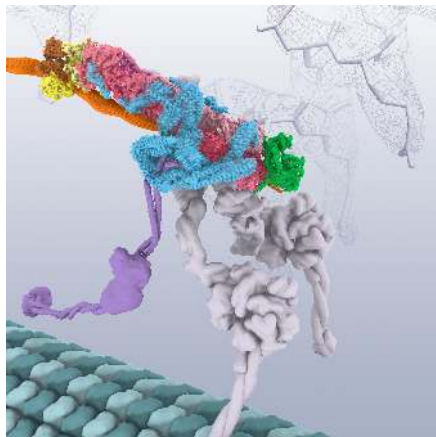


Figure 1. Model of the structure of cytoplasmic dynein (grey) bound to dynactin (multicolor) via the Golgi vesicle cargo adaptor BICD2 (orange). Dynein is reaching down towards its microtubule track.

Keywords: dynein, microtubule, motor, AAA+, machine, actin

MS8-O2 Crystal structure of the influenza A polymerase bound to the viral RNA promoter

Alexander Pflug¹, Delphine Guilligay¹, Stefan Reich¹, Stephen Cusack¹

1. EMBL Grenoble

email: apflug@embl.fr

According to the World Health Organization the influenza virus causes 250,000 to 500,000 deaths per year during its seasonal outbreak. Moreover the virus bears the potential to cause devastating pandemics with several million casualties when it evolves rapidly through reassortment between different strains; as happened with the 'Spanish flu' in 1918. During an infection influenza relies on its own polymerase to replicate its genome and transcribe mRNAs, encoding for the viral proteins that pack and wrap the viral genome copies to form new infectious virus particles. The influenza polymerase is a 250 kDa heterotrimeric protein-complex composed of the subunits PA, PB1 and PB2, with PB1 constituting the actual RNA-dependent RNA-polymerase (RdRp).

We present the crystal structure of the influenza A polymerase bound to its viral RNA promoter [1]. The structure depicts a molecule with a canonical viral RdRp in its core (protein PB1), closely intertwined with the proteins PA and PB2 (Figure 1). The novel structural information on the PB1 protein opens the door for a new era of structure-based drug development of RdRp-targeted anti-influenza agents. Homologous polymerases from other pathogenic viruses are used as drug targets successfully, as for instance the reverse transcriptase from HIV and the RNA polymerase from hepatitis C virus. It became now possible to apply this approach in case of influenza; not only because this is the first report of a structure of the influenza PB1 protein, but also because this is the first report of the recombinant production of enzymatically active PB1 protein in sufficient amounts for *in vitro* drug screenings. The structure of the polymerase complex gives important insight into the mechanism of this elaborate molecular machine. It depicts the binding to the RNA promoter, the conserved ends of the single-stranded genomic RNA segments, and it depicts how the PA endonuclease domain and PB2 cap-binding domain interact to achieve the so called cap-snatching of the host cell mRNA.

[1] Pflug A, Guilligay D, Reich S, Cusack S. (2014) *Nature*, 516, 355–360

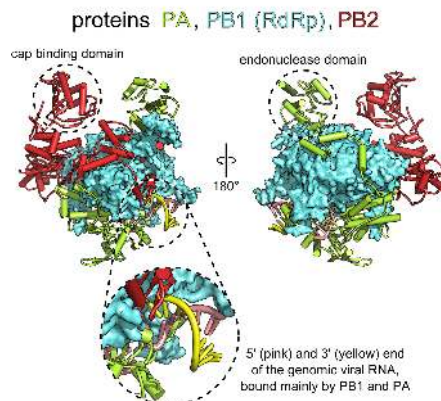


Figure 1. Overall architecture of the influenza polymerase complex. The RNA-dependent RNA-polymerase (RdRp) forms the core of the molecule, wrapped by the proteins PA and PB2 (PDB ID: 4WSB).

Keywords: influenza, polymerase, RNA, virus

MS8-O3 Fidelity of translation: structural viewAlexey Rozov¹, Natalia Demeshkina¹, Eric Westhof², Marat Yusupov¹, Gulnara Yusupova¹

1. Institut de Génétique et de Biologie Moléculaire et Cellulaire, Illkirch, France
 2. Institut de Biologie Moléculaire et Cellulaire, Université de Strasbourg, Strasbourg, France

email: rozov@igbmc.fr

mRNA translation by the ribosome is a complex and a highly error-prone process. The ribosome demonstrates very efficient discrimination to fit a right tRNA to mRNA codon. The discrimination of various near-cognate tRNA (with just one mismatch) presents a challenge, since the energy level differences are additionally influenced by the nature of the mismatch and its position in the codon-anticodon duplex. Therefore it is safe to presume that ribosome must utilize some kind of amplifying mechanism to bring the differences between tRNA to an easily discernable level.

First attempts to study the structure of ribosome decoding center were focused on the crystal structure of the 30S subunit soaked with short analogs of mRNA and tRNA (1). It was suggested that ribosome undergoes certain conformational changes induced strictly by the binding of cognate tRNA. Recently, our group has reported crystal structures of the 70S ribosome carrying cognate and near-cognate tRNAs in the A site (2). The conformational rearrangements of the 30S subunit appeared to be identical for all cases and, hence, non-discriminatory. The behavior of the introduced mismatches was, however, surprising. G•U base pairs, replacing the canonical G•C at either first or second position, adopted Watson-Crick geometry instead of usual wobble, implying involvement of rare tautomeric or ionic forms of the nitrogen bases. This finding led us to propose a new model of the decoding process. It appears that tRNA discrimination is mediated by the rigid mold of the ribosome decoding center which imposes the energy cost of fitting a mismatched base pair into the limits of the standard duplex geometry. Such cost will be high enough for the rejection of near-cognate tRNA in favor of cognate.

Here we present several structures of 70S ribosomes co-crystallized with mRNA and tRNAs featuring various mismatches in the first and second position of the A-site and P-site, modeling binding of near-cognate tRNA during decoding. The conclusions derived from our structural investigations are corroborated by the *in vivo* investigation of mistranslation events (3). Taken together, our data substantiate the proposed model of the rigid decoding center and provide an insight into explanation of variable protein mutation frequency.

1. Ogle JM, et al., *Cell*, **111**(5), 721-732 (2002)
2. Demeshkina N, et al., *Nature*, **484**(7393), 256-259 (2012)
3. Manickam N, et al., *RNA*, **20**(1), 9-15 (2014)

Keywords: translation, ribosome structure, X-ray crystallography**MS8-O4 Light-induced structural changes in a bacterial phytochrome**Heikki P. Takala¹

1. University of Jyväskylä, Finland

email: heikki.p.takala@jyu.fi

Phytochromes are light-sensing proteins found in plants and bacteria. They bind a linear tetrapyrrole chromophore (e.g. biliverdin) and cycle between a resting Pr and an activated Pfr state in response to the light environment. Canonical phytochromes contain a photosensory core region that includes a chromophore-binding domain (CBD) and a phytochrome-associated (PHY) domain. In bacterial phytochromes the photosensory region is followed by an output region that usually consists of a histidine kinase domain.

Our research aims to study the structural changes accompanying the phytochrome photocycle. Here we report light-induced changes in a bacterial phytochrome characterized by the means of X-ray-based methods [1]. SAXS and time-resolved WAXS indicate large light-driven structural changes in phytochrome dimer that occur in millisecond time scale. Most importantly, we have solved seminal crystal structures of phytochrome photosensory core region in its inactive and active states. The structures reveal light-induced refolding close to the chromophore, which leads to opening of the entire phytochrome dimer as the PHY domains move relative to each other (Figure 1). This large-scale opening is linked to the X-ray scattering (S/WAXS) data by molecular dynamics simulations.

These results can be considered as a breakthrough in the phytochrome field. The structural information helps us understand the how these light-driven molecular switches work, and it sets basis for a wealth of applications.

References: [1] Takala H, Björling A, Berntsson O, Lehtivuori H, Niebling S, Hoernke M, Kosheleva I, Henning R, Menzel A, Ihalaainen JA, Westenhoff S. (2014) Signal amplification and transduction in phytochrome photosensors. *Nature* 509(7499):245-8. doi: 10.1038/nature13310.

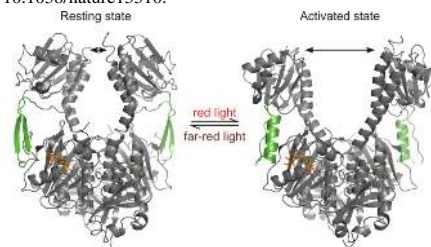


Figure 1. Crystal structures of the photosensory module dimer in the resting (left) and activated (right) states. Upon red light illumination the tongue of the PHY domain (green) changes its fold and the dimer opens up for several nanometers. Figure adapted from [1].

Keywords: phytochrome, photosensor, photocycle, light activation

MS8-O5 The crystal structure of the Na⁺-translocating NADH ubiquinone oxidoreductase from *Vibrio cholerae*

Gunter Fritz¹, Steuber Julia², Georg Vohl¹, Kay Diederichs³

1. University of Freiburg, Neurocenter

2. University of Hohenheim

3. University of Konstanz

email: guenter.fritz@uniklinik-freiburg.de

The human pathogen *Vibrio cholerae* maintains a Na⁺ gradient across the cytoplasmic membrane. The generated sodium motive force is essential for substrate uptake, motility, pathogenicity, or efflux of antibiotics. This gradient is generated by an integral membrane protein complex, the NADH:ubiquinone oxidoreductase (NQR). It catalyzes the same reaction like mitochondrial complex I but both respiratory enzymes exhibit a completely different architecture. NQR is closely related to the so-called RNF complex that is very common in bacteria and occurs as well as in archaea. The NQR complex consists of six different subunits, NqrA–NqrF. In order to get insights into the mechanism of redox driven Na⁺-transport we have isolated and crystallized the NQR of *Vibrio cholerae*. The crystals of the entire membrane complex diffract to 3.5 Å [1]. Moreover, we determined independently the structures of the major soluble domains of subunits NqrA, C and F at 1.9 Å, 1.6 Å and 1.7 Å, respectively, completing large parts of the structure of the respiratory complex at high resolution [1]. Altogether, the structural information gives a detailed picture of the NQR and allows also a close view on the core subunits of homologous RNF complex. The structural information available now allows for the first time the detailed analysis of the ion translocation pathway across the membrane and of the coupling between redox and translocation reactions. Moreover, recent structural information indicates that the pumping mechanism involves a large conformational change of the entire membrane protein complex.

References

[1] Steuber, J., Vohl, G., Casutt, M.S., Vorburger, T., Diederichs, K., and Fritz, G. (2014) Structure of the *V. cholerae* Na⁺-pumping NADH:quinone oxidoreductase. *Nature* 516: 62–67

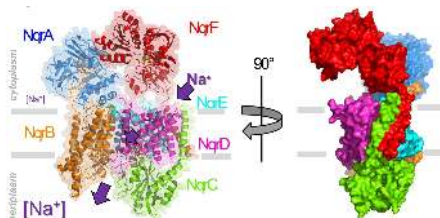


Figure 1. Structure of Na⁺-pumping NQR of *Vibrio cholerae*. The six subunits are shown in different colours, respectively. The membrane plane is indicated by grey bars.

Keywords: Membrane protein, Na⁺-pump, *Vibrio cholerae*,

MS9. Pharmaceutical crystallography and drug design

Chairs: David Brown, Andreas Heine

MS9-O1 Current perspectives in fragment-based ligand discovery

Roderick Hubbard¹

1. Vernalis (R&D) Ltd, Granta Park, Cambridge, CB21 6GB and YSBL, University of York, Heslington, York, YO10 5DD

email: roderick.hubbard@york.ac.uk

Over the past 15 years, fragment based discovery has become established as an important addition to the armoury of ligand discovery methods within the pharmaceutical industry. The methods are also very attractive for academic groups, as they require relatively low investment in compound libraries and can utilise biophysical screening methods available at most institutions.

In this presentation, I will briefly summarise the current approach to fragment based discovery used by most organisations. I will illustrate their application with some recent examples of drug discovery and then spend some time discussing the use of the methods for the identification of chemical tools for rapidly assessing features of proteins and their binding sites. I will conclude with a discussion of some of the current hot topics in fragments, to include 3D fragments and how to progress fragments in the absence of a crystal structure.

Keywords: fragment screening, structure-based discovery

MS9-O2 At play in the briar patch of epigenetics

Jim Kiefer¹, Patrick Trojer², Marie Classon¹, Maia Vinogradova¹, Victor Gehling², Shilpi Arora², Amy Gustafson¹, Brian Albrecht², Charles Tindell¹, Kaylyn Williamson², Catherine Wilson¹, Jennifer Busby², Yichin Liu¹, Pranoti Gangurde², David Arnott¹, Shane Buker², Tommy Cheung¹, Fei Lan², Erica Jackson¹, Megan Flynn¹, Andrea Cochran¹, Tobias Maille¹, Gulfem Guler¹, Christopher Bailey², Richard Cummings², Robert Pitti¹, Matthew Wongchenko¹, Yibing Yang¹, Ted Lau¹, Mike Costa¹, Jean-Christophe Harmange², Jeffrey Settleman¹

1. Genentech Inc., South San Francisco, California, USA

2. Constellation Pharmaceuticals, Cambridge, Massachusetts, USA

email: kiefer.james@gene.com

The understanding of non-genetic mechanisms in cancer biology and treatment resistance has steadily evolved over the last two decades. Several epigenetic modulator and monitoring proteins have been implicated in maintaining tumor cells in pluripotent – and often drug resistant – states. We have discovered a series of inhibitors that modulate epigenetic signaling and impact drug resistance. We used a multi-pronged approach to identify and optimize these molecules, including the determination of novel crystal structures of the target protein. In addition to aiding chemical design, these structures inform models for substrate recognition not previously possible in other systems.

Keywords: epigenetics, crystallography, inhibitor, cancer, structure based drug design

MS9-O3 Identification of novel allosteric inhibitors through Fragment-Based Drug Discovery and X-ray crystallography

Puja Pathuri¹, Susanne M. Saalau-Bethell¹, Andrew J. Woodhead¹, Valerio Berdini¹, Maria G. Carr¹, Gianni Chessari¹, Anne Cleasby¹, Miles Congreve¹, Joseph E. Coyle¹, Brent Graham¹, Steven D. Hiscock¹, Victoria Lock¹, Christopher W. Murray¹, M. Alistair O'Brien¹, Sharna J. Rich¹, Caroline J. Richardson¹, Tracey Sambrook¹, Mladen Vinkovic¹, Pamela A. Williams¹, Jeff R. Yon¹, Harren Jhota¹

1. Astex Pharmaceuticals, 436 Cambridge Science Park, Milton Road, Cambridge, United Kingdom

email: Puja.Pathuri@astx.com

X-ray crystallography provides a powerful and sensitive primary screening technique for fragment-based drug discovery with the potential to detect binding events not only at precedent active sites, but also in previously unexploited pockets. Fragment-based drug discovery at Astex uses a combination of X-ray crystallography and other biophysical techniques including NMR, ITC and thermal shift (T_m) to identify initial fragment hits at known binding sites and novel allosteric sites. Using our proprietary fragment screening platform, PyramidTM we have successfully discovered molecules that bind at novel allosteric sites in different enzyme families. During this presentation we will show how we used fragment based drug discovery in the identification of significant allosteric sites on the full length NS3 protein from the Hepatitis C Virus (HCV) and human soluble Adenylate Cyclase.

Keywords: Fragment-based drug discovery, crystallography, allosteric sites

MS9-O4 Crystallographic fragment-screening – Results from the HZB-Marburg collaboration

F. U. Huschmann^{1,2}, M. Gerlach², R. Foerster^{2,3}, A. Heine¹, M. Hellmig², G. Klebe¹, J. Linnik², P. H. Malecki^{2,4}, A. Metz¹, N. Radeva¹, J. Schiebel¹, K. Sparta², M. Steffien², M. Uehlein², P. Wilk^{2,5}, M. S. Weiss², U. Mueller²

1. Philipps Universitaet Marburg
2. Helmholtz-Zentrum Berlin
3. Freie Universitaet Berlin
4. Max Delbrueck Centrum
5. Humboldt Universitaet zu Berlin

email: franziska.huschmann@helmholtz-berlin.de

In the last decade, fragment-based lead discovery has evolved into a widely applied technique in drug development. While originally pre-screening fragment binding investigations by biophysical methods were mandatory, nowadays complete fragment libraries can be screened by X-ray crystallography, owing to the ever increasing level of automation in diffraction data collection using synchrotron radiation and processing. In this context, it is essential to use high throughput methods, to have good diffraction quality target protein crystals and to work with a high quality fragment library. Thorough crystallographic analysis of protein-fragment complexes and their binding modes reveal detailed structural knowledge to develop fragments (100-200 Da) into new potential lead structures (300-500 Da). Recently, we have started to establish an experimental facility optimized for high throughput fragment screening at the BESSY II storage ring [1]. We have validated our assembled library of 96 fragments against two target proteins. These initial results revealed that this library can identify binding partners at a hit rate of about 10%. In addition we are currently testing several novel techniques to simplify and accelerate sample preparation. The ultimate aim is to make our library in combination with a highly automated beamline [2] available for academic and industrial users. This unique facility for screening experiments and evaluation of bound fragments will enable efficient fragment screening on a much broader basis.

References:

- [1] U. Mueller, N. Darowski, M.R. Fuchs, R. Förster, M. Hellmig, K.S. Paithankar, S. Pühringer, M. Steffien, G. Zocher, M.S. Weiss, 2012, J. Syn. Rad., 19, 442
- [2] M. Krug, M. S. Weiss, U. Heinemann and U. Mueller, 2012, J. Appl. Cryst. 45, 568-572

Keywords: fragment screening, fragment libraries, X-ray crystallography

MS9-O5 Inhibition of human Aldehyde Dehydrogenase1 by the anti-tumor agent Duocarmycin

Sabine Schneider¹, Maximilian Koch¹, Sabrina Harteis¹, Lutz F. Tietze², Stephan A. Sieber¹, Sabine Schneider¹

1. TU Munich, Department of Chemistry and Centre for Integrated Protein Science CIPSM
2. Georg-August-Universitaet Goettingen

email: sabine.schneider@mytum.de

Inhibition of human Aldehyde Dehydrogenase1 by the anti-tumor agent DuocarmycinDuocarmycin SA an antibiotic metabolite isolated from Streptomyces, is one of the most potent anti-tumor agents known to date.^[1] This highly cytotoxic effect is currently exploited by conjugating duocarmycin to antibodies for specific tumor cell targeting. Two such antibody-drug conjugates (MDX-1203, SYD985) are now in phase I clinical trials against Non-Hodkins lymphoma, breast and kidney cancer.^[2] Previous studies revealed that duocarmycins and similar compounds exert their potent anti-tumor properties by DNA alkylation.^[3] However, recently an additional proteomic target, aldehyde dehydrogenase 1A1 (ALDH1A1), was identified in human lung cancer cell lines.^[4,5] ALDH1A1 is responsible for the oxidative formation of retinoic acid and therefore involved in gene regulation and cell differentiation.^[6] Moreover ALDH1A1 is highly expressed in several tumors^[7, 8, 9] where its expression is correlated with increased proliferation and poor prognosis. Dissection of the structure-activity relationship of duocarmycin showed that the alkylation subunit alone is sufficient for ALDH1A1 inhibition.^[5] Here we present biochemical data as well as the X-ray crystal structure of the ALDH1A1 without and in complex with a Duocarmycin analogue (sdb6). Sdb6 is covalently bound to one of the two active site cysteines, with the cyclopropabenzindole ring of the molecule forming pi-stacking with aromatic amino acid side chains. The structural and biochemical data shed light on the highly specific inhibitory mechanism of duocarmycine on ALDH1A1 and could aid the rational design of ALDH1A1 inhibitors.

References[1] L. F. Tietze, B. Krewer, *Chem Biol Drug*

- Des* 2009, 74, 205.[2]R. C. Elgersma, et al. *Mol Pharm.* 2015[3] D. L. Boger, D. S. Johnson, *Proc Natl Acad Sci U S A* 1995, 92, 3642.[4] T. Wirth, K. Schmuck, L. F. Tietze S. A. Sieber, *Angew Chem Int Ed Engl* 2012.[5] T. Wirth, G. F. Pestel, V. Ganai, T. Kirmeier, I. Schubert, T. Rein, L. F. Tietze, S. A. Sieber *Angew Chem Int Ed Engl* 2013, 52, 6921[6] A. Yoshida, A. Rzhetsky, L. C. Hsu, C. Chang, *Eur. J. Biochem.*1998, 251, 549.[7] C. Kahlert, F. Bergmann, J. Beck, T. Welsch, C. Mogler, E. Herpel, S. Dutta, T. Niemietz, M. Koch, J. Weitz, *BMC Cancer* 2011, 11, 275.[8] K. Morimoto, et. al. *Cancer Sci.* 2009, 100, 1062.[9] F. Jiang, et. al, *Mol. Cancer Res.* 2009, 7, 330.

Keywords: aldehyde dehydrogenase 1, antitumor agents, duocarmycin

MS10. Structural bioinformatics (SBI)

Chairs: Guido Capitani, Oliviero Italo Carugo

MS10-O1 Advances in PISA software for macromolecular assembly predictions from CCP4

Eugene Krissinel¹

1. Science and Technology Facilities Council, Rutherford Appleton
Laboratory, OX11 0FA, Oxford, UK

email: eugene.krissinel@stfc.ac.uk

PISA (Protein Interfaces, Surfaces and Assemblies) software from CCP4 remains a popular computational tool for the prediction of biological assemblies from crystallography data [1]. The method is based on the estimation of the dissociation free energy of predicted complexes, and reaches 90-95% correct results for the current content of the PDB.

It was found that the likelihood of wrong predictions grows exponentially with the decrease in the dissociation free energy, reaching over 50% for complexes bound as weakly as few kcal/mol [2]. Among few reasons for this behaviour [2] is the fact that oligomeric state of weakly bound complexes is expected to vary in dependence of chemical environment, in particular, protein concentration. It has been noticed that most disagreements between predicted and measured oligomeric states belong to situations where the relation between experimental conditions and protein's working environment in the cell is unclear.

Further advance in PISA software is reported, which allows a researcher to model concentration dependence of predicted oligomeric states, and by this to improve the interpretation of experimental results in the biologically interesting case of weakly bound macromolecular associations. The new PISA is based on the concept of assembly stock, or an equilibrated set of all complexes compatible with crystal packing. Graphical representation of concentration (or newly introduced aggregation index) profiles of stock's components allows a user to quickly identify the most probable oligomeric state. This is vastly superior over the previous way of analysis, based on the interpretation of bare figures for dissociation free energies. Other developments include advanced graphical interface and multi-parametric interaction radar, which indicates the likelihood for interface to represent a biologically relevant interaction.

The new PISA is available from CCP4 Software Suite [3] as a standalone (command-prompt) application, graphical interface QtPISA and web-server jsPISA at <http://www.ccp4.ac.uk/pisa>.

References

- [1] E. Krissinel, K. Henrick (2007) *J. Mol. Biol.* **372**, 774-797
- [2] E. Krissinel (2009) *J. Comp. Chem.* **31**, 133-143
- [3] M. D. Winn, C. C. Ballard, K. D. Cowtan, E. J. Dodson, P. Emsley, P. R. Evans, R. M. Keegan, E. B. Krissinel, A. G. W. Leslie, A. McCoy, S. J. McNicholas, G. N. Murshudov, N. S. Pannu, E. A. Potterton, H. R. Powell, R. J. Read, A. Vagin and K. S. Wilson (2011) *Acta Cryst.* **D67** 235-242.

Keywords: Protein Quaternary Structure, Crystal Packing Analysis, Macromolecular Crystallography, Crystal Interfaces

MS10-O2 *Proteopedia* - a scientific 'Wiki' bridging the rift between 3D structure and function of biomacromolecules

Joel L. Sussman¹, Jaime Prilusky¹

¹ Weizmann Institute of Science

email: Joel.Sussman@weizmann.ac.il

Scientists are now able to access 3D images of biomacromolecules underlying biological functions and disease. Rather than relying on text & 2D images to try to understand the function of biomacromolecular structures, a collaborative website called *Proteopedia*^{1,2} provides a new resource by linking written information & 3D structural information. This wiki web resource, <http://proteopedia.org>, displays protein structures & other biomacromolecules in an interactive format. The interactive images are surrounded by descriptive text containing hyperlinks that change the appearance (such as view, representations, colors or labels) of the adjacent 3D structure to reflect the concept discussed in the text. This makes the complex structural information readily accessible and comprehensible, even to non-structural biologists. Using *Proteopedia*, scientists & students can easily create descriptions of biomacromolecules linked to their 3D structure, e.g., a page on ribosome structure/function, <http://proteopedia.org/w/Ribosome>. Pages can be viewed on PCs, MACs, LINUX computers & even on iPads (that do not have JAVA), via the molecular viewer JSmol³, e.g., a page on HIV-1 protease, http://proteopedia.org/w/HIV-1_protease. Content is being added by *Proteopedia*'s ~2,900 users (in 60 different countries), in a dozen different languages, including Russian, Arabic & Chinese: [http://proteopedia.org/w/1vot_\(Chinese\)](http://proteopedia.org/w/1vot_(Chinese)). A number of journals & book publishers are using *Proteopedia* to complement their printed and web papers using *Proteopedia*'s "Interactive 3D Complements" (I3DCs) – see, e.g., <http://www.proteopedia.org/w/Journal:JBIC:6>. Pages for each of the >107,000 entries in the PDB have been automatically created with 'seed' information, and are both intrinsically useful and 'primed' for expansion by users. Scientists & students are invited to request a *Proteopedia* user account, **at no cost**, in order to edit existing pages & to create new ones, see: <http://proteopedia.org/w/Special:RequestAccount>.

References:

- Hodis, E., Prilusky, J., Martz, E., Silman, I., Moul, J. & Sussman, J. L. (2008). *Genome Biol* **9**, R121.
- Prilusky, J., Hodis, E., Canner, D., Decatur, W. A., Oberholser, K., Martz, E., Berchanski, A., Harel, M. & Sussman, J. L. (2011). *J Struct Biol* **175**, 244.
- Hanson, R. M., Prilusky, J., Renjian, Z., Nakane, T. & Sussman, J. L. (2013). *Israel J Chem* **53**, 207.



Figure 1. *Proteopedia* homepage: <http://proteopedia.org>

Keywords: Information Management, Wiki, education, structure/function

MS10-O3 AMPLE: exploiting structural bioinformatics developments to extend the reach of molecular replacement to difficult cases

Daniel J. Rigden¹, Jens Thomas¹, Ronan Keegan², Felix Simkovic¹, Martyn Winn³, Olga Mayans¹

1. Institute of Integrative Biology, University of Liverpool

2. STFC, Rutherford Appleton Laboratory

3. STFC, Daresbury Laboratories

email: drigden@liv.ac.uk

Molecular Replacement (MR) remains the most popular route to solution of protein crystal structures, accounting for over 70% of recent PDB submissions. Nevertheless, computational structure solution by MR is currently limited in scope by several factors. Most obviously, if the target has a novel fold then, by definition, no crystal structure is available to serve as a search model. This is a particular problem for membrane proteins which are poorly represented in the PDB due to their comparative experimental intractability. Even if the fold of the target can be recognised as familiar then the available structures may be too distantly related and so too structurally divergent to succeed. Coiled-coil proteins, a class with biomedical and biotechnological importance, have their own idiosyncratic difficulties due to promiscuous intra- and inter-chain interactions as well as unpredictable irregularities in secondary structure. AMPLE is a pipeline for unconventional MR which provides a framework to exploit innovations in structural bioinformatics to allow more difficult cases like those above to be addressed.

Novel folds have been successfully addressed by ab initio protein modelling with ROSETTA. We show here how a second program QUARK, importantly available as a server, solves a somewhat complementary set of targets [1]. The output from the QUARK server can be input seamlessly to our new AMPLE server. We further illustrate the potential of predicted contacts (evolutionary couplings) to raise the current size constraint on ab initio modelling: larger folds can now be predicted and the results used in MR. AMPLE also works very effectively for transmembrane proteins, solving cases as large as 223 residues. We report spectacular success in solving coiled-coil targets, reversing the previous perception of their being particularly difficult for MR [2]. AMPLE solved 80% of a large test set of diverse architectures without any requirement to predict oligomeric state. Successes included chain lengths up to 253 residues, cases that diffracted to only 2.9 Å and examples of complexes containing other protein chains or DNA. Finally, we report preliminary data employing AMPLE to generate structurally conserved core search models from computationally-derived flexibility-based ensembles. We suggest that this can enhance the success rate of MR when only distantly homologous structures are available.

1.Keegan et al (2015) Acta D71,338; 2.Thomas et al (2015) IUCR J 2,198

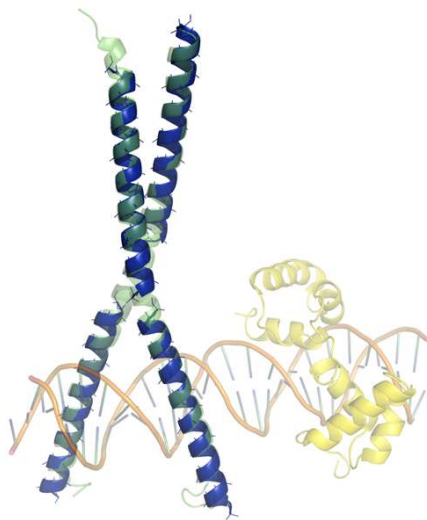


Figure 1. AMPLE solves a protein:DNA complex (1h8a) using the coiled-coil component. Four copies of a truncated search model (blue) allowed fully automated structure solution and required no knowledge of the coiled-coil association state.

Keywords: Molecular Replacement; Structural Bioinformatics; protein modelling; coiled-coil proteins; distant homology.

MS10-O4 From protein sequence to function and structure with BAR+Giuseppe Profiti¹, Rita Casadio¹, Francesco Aggazio¹, Pier Luigi Martelli¹, Piero Fariselli¹

1. Bologna Biocomputing Group, Bologna Computational Biology Network, University of Bologna, Italy

email: giuseppe.profiti2@unibo.it

We introduced a web server that allows functional and structural annotation of protein sequences. A previous version of our method was already described and validated, the Bologna Annotation Resource PLUS(+). BAR+ is a non hierarchical clustering method relying on a comparative large-scale genome analysis. The method relies on a non hierarchical clustering procedure characterized by a stringent metric that ensures a reliable transfer of features within clusters. The set includes 13,495,736 protein sequences that derive also from 988 whole genomes. BAR+ is constructed by performing an all-against-all pairwise alignment from all protein sequences available (collected from the entire UniProt). Each protein is then taken as a node and a graph is built allowing links among nodes only when the following similarity constrains are found among two proteins: their sequence identity (SI) is $\geq 40\%$ and the extent of the overlap after alignment (Coverage, CO) is $\geq 90\%$. By this clusters are simply the connected components of the graph. 70% of the whole data set of sequences fall into 913,962 clusters. Well annotated sequences are characterized by all the functional and structural annotations derived from UniProt entries. These include GO, PFAM, PDB and SCOP mapping (when available). Ligands are also listed when present in their PDB file/s. When a well annotated sequence falls into a cluster, it inherits the annotation/s that characterize the cluster. GO and PFAM features in the clusters are validated by computing a P-value. With this procedure, also distantly related homologs can inherit function and structure in a validated manner. This procedure increases the level of annotation when compared to that of UniProt. In BAR+ when PDB templates are present within a cluster (with or without their SCOP classification), profile HMMs are computed on the basis of sequence to structure alignment and are cluster-associated (Cluster-HMM). A library of 10,858 HMMs is available for aligning even distantly related sequences to a given PDB template/s. BAR+ is available at <http://bar.biocomp.unibo.it/bar2.0>. A recent new improvement relies on community detection techniques that allow the identification of groups of proteins relative to a specific ligand. By this, clusters are subdivided into smaller sets of closely related sequences, enhancing the specificity of the annotation in terms of different ligand binding to the same putative template.

Keywords: Protein structure prediction; protein function prediction**MS10-O5** New protein main-chain conformational descriptors on the validation and improvement of automatic protein model buildingJoana Pereira¹, Victor Lamzin¹

1. European Molecular Biology Laboratory (EMBL), c/o DESY, Notkestrasse 85, Hamburg 22607, Germany

email: joana.pereira@embl-hamburg.de

During the process of protein automated model building, ARP/wARP [1] represents the electron density map as a set of free atoms without any chemical identity and, through the use of density and distance checks, searches for free atoms on possible C α positions that could be forming a peptide unit. If two putative peptide units share a free atom, they are considered to be a dipeptide, the conformation of which is then evaluated against a two-parameter Ramachandran-like plot. We have found such an evaluation has proven to be very powerful with high-resolution data; however, more than two conformational degrees of freedom are required to properly account for experimental errors and to build models at 3.0 Å or lower resolution.

To address the problem, we utilised distance-geometry-based methods, which are often used in the NMR structure solution. We expanded on the premise that molecular conformation, represented by the relative three-dimensional location of atoms, can be calculated when the distances between all atoms in the molecule are known. We identified three independent parameters that describe dipeptide conformation; thereby enabling the separation of dipeptides corresponding to different secondary structural elements, from dipeptides in randomly generated conformation. By comparing the three-dimensional distribution of these parameters with the parameters calculated for random dipeptides, we were able to compute a scoring function for the evaluation of the likelihood of a dipeptide to be in a plausible conformation. Dipeptides with a score close to 1 are likely correct, while those with a score close to 0 should not be accepted.

Using this approach, we have been able to evaluate the quality of protein chain fragments built using ARP/wARP at different data resolutions. We have found that, at lower resolution, the constructed chain fragments have more dipeptide units which are likely in an incorrect conformation. We now plan to incorporate the newly developed method into the model building process and expect that this will increase the accuracy and completeness of the automatically constructed protein structures. Additionally, an overall score can also be calculated for the entire protein structure, providing the user with a general measure of the quality of the model.

[1] Langer G, Cohen SX, Lamzin VS, Perrakis A. *Nature Protocols*, 2008, 3(7), 1171-1179**Keywords:** automated model building, peptide conformation, structure validation, software, ARP/wARP

MS11. Hybrid approaches

Chairs: Guillermo Montoya, Jan Pieter Abrahams

MS11-O1 Two-dimensional membrane protein crystallography at X-FELs

Bill Pedrini¹

1. Paul Scherrer Institute, Switzerland

email: bill.pedrini@psi.ch

Compared to their three-dimensional counterparts, two-dimensional membrane protein crystals may offer the advantage of providing a more close-to-physiological environment for the protein molecules, in particular by reducing the risks of structural deformations due to non-native contacts. Moreover, quenching of possible structural motions, triggered by external stimuli, can be overcome. Unfortunately, the diffracting power of two-dimensional protein crystals is small, which makes radiation damage an insurmountable obstacle for X-ray diffraction at synchrotron sources. Free electron lasers now provide ultrashort and ultraintense X-ray pulses, which permit to acquire diffraction data before radiation damage has taken place. We report on the diffraction experiments performed at room temperature on bacteriorhodopsin two-dimensional crystals, using the submicrometer X-ray beam available at the CXI station of the LCLS free electron laser. The data demonstrate that the samples diffract to at least 4 Å of resolution. The results allow evaluating the potential and the limitations of two-dimensional crystallography at X-FEL, which emphasizes the role of the approach as a complementary technology to cryo electron microscopy.

Keywords: 2D crystals, membrane proteins, X-FEL, radiation damage

MS11-O2 Xen crystallography - choose your radiation

Tim Gruene¹, Hinrich W. Hahn¹, Anna V. Luebben¹, Flora Meilleur², George M. Sheldrick¹, David A. Köpfer³, Chen Song⁴, Ulrich Zachariae⁵, Bert L. de Groot³, Jens Luebben⁶

1. Department of Structural Chemistry, University of Göttingen, 37077 Göttingen, Germany

2. Oak Ridge National Laboratory, Oak Ridge, TN 37831-6142, USA

3. Biomolecular Dynamics Group, Max Planck Institute for Biophysical Chemistry, 37077 Göttingen, Germany

4. Department of Biochemistry, University of Oxford, Oxford OX1 3QU, UK

5. School of Engineering, Physics and Mathematics, University of Dundee, Dundee DD1 4HN, UK

6. Institute for Inorganic and Applied Chemistry, Martin-Luther-King-Platz 6, D-20146 Hamburg, Germany

email: tg@shelx.uni-ac.gwdg.de

Crystallographic structure determination can be carried out with X-rays, electrons, or neutrons as wave source. The number of 95,599 X-ray structures in the PDB [1] outnumbers 80 neutron structures and 47 electron structures by far. At present, however, the latter two technologies gain more and more interest, and this is for good reasons: they offer advantages over X-rays that make them complementary methods one should not forget to take into consideration when planning your experiment. In this talk I will relate to the specific choice of type of radiation with the presentation of two recent publications: The first one combines Molecular Dynamics with Anomalous X-ray dispersion in order to prove the K⁺ ions are transported through membrane channels by a "Knock-on" transport. This result knocks over a 60 year old dogma that assumed the co-transport of water molecules with K⁺ ions as shield to their electrostatic repulsion [2].

The second topic explains how to properly combine the results from X-ray data acquisition with neutron data. Common practise co-refines both data sets. I will argue that one should better treat separate experiments with separate refinement and explain how to combine both methods properly. Furthermore, hydrogen atoms, usually the focus of interest for macromolecular neutron data, should be refined rather than constrained. I will argue for separate refinement. Careful data interpretation is necessary at low data completeness often associated with neutron data, in order to soundly and reliably present your findings [3].

[1] www.wwpdb.org, H.M. Berman, K. Henrick, H. Nakamura (2003) "Announcing the worldwide Protein Data Bank" *Nature Structural Biology* 10 (12): 98.

[2] D. A. Köpfer, C. Song, T. Gruene, G. M. Sheldrick, U. Zachariae, B. L. de Groot "Ion Permeation in K⁺ Channels Occurs by Direct Coulomb Knock-On" *Science*, 2014, 346 (6207) 352-355

[3] T. Gruene, H.W. Hahn, A.V. Luebben, F. Meilleur, G.M. Sheldrick "Refinement of Macromolecular Structures against Neutron Data with SHELXL-2013" *J. Appl. Cryst.* 2014, 47, 462-466

Keywords: X-ray diffraction and Molecular Dynamics, Hydrogen Positions from Neutron Data, Assessment of Data Quality

MS11-O3 Analysis of flexible multidomain glycoproteins with SAXS, analytical ultracentrifugation, and torsion-angle molecular dynamics

Jordi Bella¹, Thomas A. Jowitt¹, Clair Baldock¹, David Garrod¹, Lydia Tabernero¹

1. Faculty of Life Sciences, University of Manchester, Manchester M13 9PT

email: jordi.bella@manchester.ac.uk

The extracellular regions of many cell-surface receptors and extracellular proteins are built from tandems of domains (immunoglobulin-like, cadherin, EGF-like, fibronectin type-III, etc) that are connected by inter-domain linkers of variable flexibility. This conformational flexibility, often combined with glycosylation, makes structural analysis of these multi-domain proteins particularly challenging. When high-resolution methods fail, biological small-angle X-ray scattering (SAXS) can provide at least some structural information about these molecules, mainly in terms of overall shape and dimensions. Drawbacks are the low resolution and limited amount of data, which can easily lead to overfitting or non-meaningful solutions that fit the data equally well. SAXS analysis of multi-domain proteins (or glycoproteins) often involves exploring their conformational space by generating a library of thousands of conformers, built from atomic models typically based on high-resolution crystal structures of homologous proteins. These conformers are then tested in turn against the SAXS data, and ensembles of best-fitting conformers are generated to describe the flexible states of these multi-domain proteins in solution (Tria *et al.*, 2015, IUCr, 2: 207-17). Torsion-angle molecular dynamics, as implemented in the popular crystallographic package CNS (Brunger *et al.*, 1998, *Acta Cryst.* D54: 905-21) offers an attractive route for exploring the conformational space of multi-domain proteins with much smaller libraries of conformers, thus requiring a smaller computational effort. In addition, it provides a more precise control of the flexibility between domains, allows for simultaneous sampling of the protein and sugar components of glycoproteins, and overcomes topological limitations for the definition of the flexible and rigid elements of the multidomain protein or glycoprotein being explored. Hydrodynamic data obtained from analytical ultracentrifugation can be combined with this conformational sampling to filter out conformers with unrealistic shapes and dimensions prior to their fitting to the SAXS data. This powerful combination increases the confidence in the SAXS analysis and produces more realistic models. Applications of this methodology will be illustrated with successful examples from our laboratory (Tariq *et al.*, 2015, *PNAS* in press).

Keywords: SAXS, molecular dynamics, analytical ultracentrifugation, hydrodynamic modeling

MS11-O4 Solving complex zeolite structures by combining electron crystallography, solid state NMR and powder X-ray diffraction

Xiaodong Zou¹, Tom Willhammar¹, Allen W. Burton², Yifeng Yun¹, Junliang Sun¹, Mobae Afeworki², Karl G. Strohmaier², Hilda Vroman²

1. Berzelii Centre EXSELENT on Porous Materials and Inorganic and Structural Chemistry, Department of Materials and Environmental Chemistry, Stockholm University, SE-106 91 Stockholm, Sweden

2. Corporate Strategic Research, ExxonMobil Research & Engineering Co. Inc, 1545 Route 22 East, Annandale, New Jersey 08801, USA

email: xzou@mmk.su.se

Zeolites are crystalline, microporous aluminosilicates that are used as catalysts or adsorbents in a wide array of industrial processes. Stable, multidimensional and extra-large pore zeolites are desirable by industry for catalysis and separation of bulky molecules. Here we report EMM-23, the first stable, three-dimensional extra-large pore aluminosilicate zeolite[1]. The structure of EMM-23 was determined from sub-micron sized crystals by combining electron crystallography, solid state NMR and powder X-ray diffraction.

The polycrystalline nature, the large unit cell and especially the presence of Q² and Q³ Si species make the structure determination of EMM-23 challenging. Electron crystallography has unique advantages for structure solution of nano- or micron-sized crystals[2]. We applied the recently developed the rotation electron diffraction (RED) method[3] and collected 252 ED frames covering a tilt range of 63.74° (Fig. 1). The crystallographic phase information from high resolution transmission electron microscopy (HRTEM) images has been used to facilitate the space group determination. The structure was solved from the RED data using direct methods, and refined by powder X-ray diffraction. Solid state NMR indicated that the zeolite possesses a high density of Q² and Q³ silicon species, which was not observed before in zeolites. The solid state NMR data provided important information about the possible disorders in the structure, which were used for the structure refinement. The framework contains highly unusual tri-lobe shaped pores that are bound by 21-24 Si/Al atoms. These extra-large pores are intersected perpendicularly by a 2D 10-ring channel system. EMM-23 is stable after calcination at 540°C.

References

- [1] T. Willhammar, A.W. Burton, Y. Yun, J. Sun, M. Afeworki, K.G. Strohmaier, H. Vroman, X. Zou. *J. Am. Chem. Soc.* 2014, 136, 13570.
- [2] X. Zou, S. Hovmöller, P. Oleynikov, *Electron Crystallography*, IUCr texts on crystallography, Oxford University Press, 2011.
- [3] W. Wan, J. Sun, J. Su, S. Hovmöller, X. Zou. *J. Appl. Cryst.* 2013, 46, 1863.

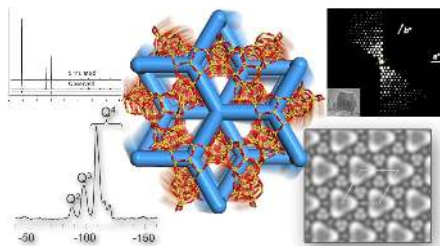


Figure 1. The structure of zeolite EMM-23 with the 3D channel system shown in blue (middle). The structure was solved by combining rotation electron diffraction (RED), HRTEM image, powder X-ray diffraction and solid state NMR.

Keywords: electron crystallography, electron diffraction, high resolution electron microscopy, crystallographic image processing, structure determination, space group determination, zeolite

MS11-O5 Structural insights into the conformation of the proline rich region of neuronal protein tau

Ondrej Cehlar^{1,2}, Rostislav Skrabana^{1,2}, Radovan Dvorsky³,
Michal Novak^{1,2}

1. Institute of Neuroimmunology, Slovak Academy of Sciences, Dubravská cesta 9, 845 10 Bratislava, Slovakia

2. Axon Neuroscience SE, Dvorakovo Nabrezie 10, 811 02 Bratislava, Slovakia

3. Molecular Biology II, Heinrich-Heine University, Düsseldorf, Germany

email: ondrej.cehlar@savba.sk

The Alzheimer's disease-associated protein tau is a typical representative of intrinsically disordered proteins (IDPs). Under physiological conditions, tau associates with microtubules and regulates their dynamics, whereas during the progression of neurodegeneration tau dissociates from microtubules, misfolds and deposits in brain tissue creating neurofibrillary tangles composed of paired helical filaments. The monoclonal antibody Tau5 was used as a surrogate tau protein binding partner to investigate the properties of the proline-rich region of tau molecule that contributes to its binding to microtubules. The Fab fragment of Tau5 has been crystallized alone and in complex with 30 amino acid long tau peptide ²⁰¹Gly-Arg²³⁰ [1] and both structures were solved to the 1.6 Å resolution [2]. The complex structure reveals the conformation of 16 residues long tau fragment and the comparison of both structures enables to observe the changes in the antibody paratope that occurred after binding of tau peptide. The kinetics of tau peptide binding to the tau5 Fab fragment was studied by the surface plasmon resonance analysis together with the evaluation of the impact of tau phosphorylation on sites T212, T217, T220 on the binding of tau peptide to the antibody. The molecular dynamics simulation was employed to evaluate the stability of the peptide conformation and the effects of phosphorylation. *Acknowledgement:* This work was supported by the Slovak Research and Development Agency under the contract Nos. LPP-0038-09, APVV-0677-12 and by VEGA No. 2/0163/13.

1. Cehlar, O.; Skrabana, R.; Kovac, A.; Kovacech, B.; Novak, M., Crystallization and preliminary X-ray diffraction analysis of tau protein microtubule-binding motifs in complex with Tau5 and DC25 antibody Fab fragments. *Acta Crystallogr F* **2012**, *68*, 1181-1185.

2. Cehlar, O.; Skrabana, R.; Dvorsky R.; Novak, M., Structure of tau peptide in complex with Tau5 antibody Fab fragment. *Acta Crystallogr D* (submitted 04/2015)

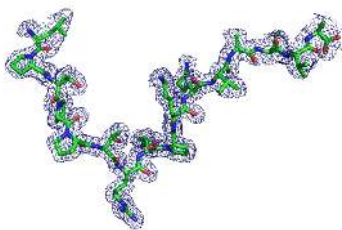


Figure 1. The structure of tau peptide 215-LPTPPTREPKKVAVVR²³⁰ with 2mF_o-DF_c electron density contoured at the level of 0.5σ. The sidechain of R230 has not been modeled due to the lack of sufficient electron density

Keywords: intrinsically disordered proteins, protein tau, Fab fragment, peptide conformation

MS12. Crystallization and crystal treatment

Chairs: Terese Bergfors, Matthew Bowler

MS12-O1 Successful crystal formation - the journey from idea to fruition

Naomi E. Chayen¹

1. Computational and Systems Medicine, Department of Surgery and Cancer, Imperial College London, Sir Alexander Fleming Building, Exhibition Road, London SW7 2AZ, UK

email: n.chayen@imperial.ac.uk

The availability of well-ordered crystals is essential to structure determination by X-ray crystallography. Nucleation is the first step that determines the crystallization process hence a search for the ultimate nucleating agent (nucleant) is ongoing. An ideal nucleant should induce efficient heterogeneous nucleation of crystals in a controlled manner and be effective in finding new crystallization condition and in improving crystal quality. It should be stable, easy to handle, and readily dispensed by robotics into numerous crystallization nano-droplets. This talk will discuss the strategies and the research of several years [1-4] resulting in our latest results [5] of the design, fabrication and validation of the first non-protein nucleating agents that can be used for the automated screening and optimization of any bio-macromolecule. These nucleants are dispensed using commercially available robots and their utilization bypasses the concerns associated with seeding, solid and viscous heterogeneous nucleants. The application of these materials is simple, quick, and 20 nanolitres is sufficient for each trial, thereby providing a potent tool for scientists in academia and industry endeavouring to increase their success. References [1] Chayen *et al.* (2001) *J. Molecular Biology* **312**, 591-595 [2] Chayen, N.E. *et al.* (2006) *Proc. Natl. Acad. Sci. U. S. A.* **103**, 597-601 [3] Saridakis *et al.* (2011) *Proc. Natl. Acad. Sci. U. S. A.* **108**, 11081-11086 [4] Khurshid *et al.* (2014) *Nature Protocols* **9**, Pages: 1621-1633 [5] Khurshid *et al.* (2015) *Acta Crystallographica D* **71**, 534-540. <http://www.iucr.org/news/research-news/smart-crystallization> <http://www.imperialinnovations.co.uk/CRMIP>

Keywords: crystallization, nucleation, proteins, macromolecules, automation, robotics

MS12-O2 Protein crystal transformation – new insights by new techniques

Reiner A. Kiefersauer^{1,2}, Breyan H. Ross^{1,2,3}, Robert Huber^{1,3,4,5}

1. Max-Planck-Institut für Biochemie, Am Klopferspitz 18, 82152 Martinsried, Germany

2. Proteros Biostructures GmbH, Bunsenstrasse 7a, 82152 Martinsried, Germany

3. Technische Universität München, Lichtenbergstrasse 4, 85747 Garching, Germany

4. Zentrum für Medizinische Biotechnologie, Universität Duisburg-Essen, 45117 Essen, Germany

5. School of Biosciences, Cardiff University, Cardiff CF10 3US, Wales

email: kiefersauer@proteros.de

Protein crystallography is the main technique to obtain structural information of biomolecules at atomic level, but requires crystals of sufficient quality and order. We designed and constantly developed a technical platform for post-growth crystal treatment based on a freely mounted crystal stabilized by a humidified gas stream combined with optical dimensional control of the crystal and analysis of its quality by X-rays (^{1,2}Free Mounting System).

In the presentation we will briefly introduce in this technique and describe the control of the crystal system during the process. Starting from the native crystal, disorder can be clearly addressed in the whole process (native crystal quality, crystal treatment, and freezing) and subsequently modulated and improved.

The addition of chemicals to the crystal by the deposition of small droplets (~ 30 picoliter) directly onto the crystal surface (Pico dropper) allows the systematic study of the influence of compounds as e.g. glycerol, polyethylene glycol, ³trimethylamine N-oxide, heavy metals to the crystal order. The increase of compound concentration in fine steps controlled by measuring the crystal extension and crystal order simultaneously allows to find the optimal concentration. After crystal treatment, the crystal can be readily frozen within a second by a mechanical switch from the humid gas stream to the cold gas stream for data collection.

We discovered that heating of the protein crystal by IR-Laser irradiation continuously or in pulses has the potential of inducing new physical ²processes. The speed of crystal shrinkage driven by light can play an important role in improving crystal order. Variation in the experimental setup (crystal in the cold gas stream, crystal under oil) combined with heat application offers new strategies for crystal annealing and improvement.

Overall, understanding of crystal transformation is a pre-condition for the evaluation of ideas about crystal optimization. Examples of crystal transformation on a macroscopic and microscopic scale will be shown in this presentation ending in an outlook for future work.

¹Kiefersauer R., Than M., Dobbek H., Gremer L., Melero M., Strobl S., Dias J., Soulimane T., Huber R. 2000. J. Appl. Cryst. 33, 1223-1230.

²Kiefersauer R., Grandl B., Krapp S., Huber R., 2014. Acta Cryst D. 70, 1224-1232.

³Marshall H., Venkat M., Seng N., Cahn J. & Juers D., 2012. Acta Cryst D. 68, 69-81.

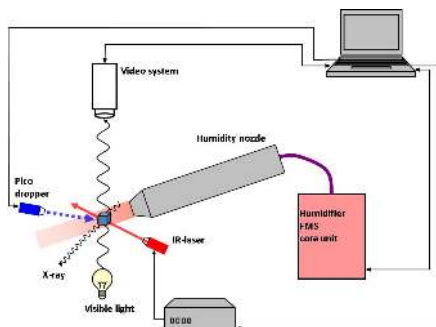


Figure 1. The protein crystal is held in the humidified gas stream and analyzed by X-rays (microscopic effects) and by a video system (macroscopic effects). The crystal is treated by heat (IR-laser) or / and by droplets of solution (Pico dropper). Optional combination of hardware for automation is possible.

Keywords: protein crystal, crystal transformation, dehydration, IR-laser, crystal improvement, crystal annealing

MS12-O3 The ins-and-out of a membrane protein; Structure-function through alternative crystallisation and harvesting approaches

Anna Polyakova¹, Scott Jackson², Alexander Cameron³, Peter J.F. Henderson¹, Arwen R. Pearson⁴

1. Astbury Centre for Structural Molecular Biology, University of Leeds, Woodhouse Lane, Leeds, LS2 9JT, United Kingdom

2. Institute of Molecular Biology and Biophysics, ETH Zurich, HPK G9.3, Otto-Stern-Weg 5, Zurich, 8093, Switzerland

3. Department of Life Sciences, University of Warwick, Gibbet Hill Road, Coventry, CV4 7AL, United Kingdom

4. Hamburg Centre for Ultrafast Imaging, Universität Hamburg, Luruper Chaussee 149, Hamburg, 22761, Germany

email: cm10ap@leeds.ac.uk

Secondary-active trans-membrane transporters couple the 'downhill' movement of ions with the 'uphill' movement of essential substrates, such as neurotransmitters or metabolites, across the cell membrane. Disruption of these vital processes is linked to some severe diseases in humans, for example Parkinson's disease. The aim of this project is to elucidate the structural basis of the transport mechanism of secondary-active transporters, using the bacterial sodium-hydantoin transporter Mhp1 as a model system. Currently, a number of static crystal structures of Mhp1 are available, representing snapshots of intermediate states along its transport cycle. However, they provide only limited insights into a highly dynamic process. In order to bridge the gaps between these snapshots, we are using a combination of X-ray crystallography and small-angle X-ray scattering (SAXS). We are using mainly X-ray crystallography to decipher the roles of individual residues in the transport mechanism and their interactions with ligands. A wide variety of strategies have been applied in the crystallisation, harvesting and cryo-protection steps to improve the data obtained from Mhp1 crystals. These include for example modifications to the crystal drop morphology (see figure) to improve crystal size and quality, as well as on-line crystal dehydration and contact-less harvesting by photoablation to minimise damage from cryo-protection and harvesting. In these studies a shrinking in the crystal a- and b-axes (which are parallel to the putative membrane normal) has been observed, giving less anisotropic data, improved electron density maps and has enabled us to solve crystal structures of Mhp1 mutants in complex with various ligands. Moreover, we are using SAXS to obtain information about the overall shape and detergent organisation around the protein in order to gain insight into crystallisation propensity and detergent packing in membrane protein crystals. We are overcoming the challenges imposed by the presence of the detergent molecules by combining SAXS with size-exclusion chromatography. The main goal of this project is to reveal structural and dynamic information that has not been observed before: what routes the substrates take through the protein; what conformational changes occur during substrate binding and release; how is the transport of ions and substrates coupled?

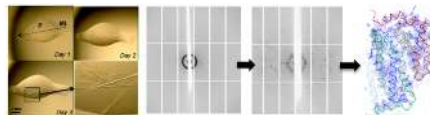


Figure 1. Illustration of how changing the drop morphology has improved crystal size and quality, enabling us to solve crystals of Mhp1 mutants in complex with various ligands.

Keywords: Membrane protein, crystallization

MS12-O4 Making the most out of screening experiments

Jia Tsing Ng¹, Carien Dekker², Markus Kroemer², Michael Osborne³, Frank von Delft^{1,4,5}

1. Structural Genomics Consortium, University of Oxford, Roosevelt Drive, Oxford OX3 7DQ, England
2. Novartis Institute for Biomedical Research, Novartis Campus, Postfach, CH-4056 Basel, Switzerland
3. Department of Engineering Science, University of Oxford, Parks Road, Oxford OX1 3PJ, England
4. Diamond Light Source Ltd, Harwell Science and Innovation Campus, Didcot OX11 0QX, England
5. Department of Biochemistry, University of Johannesburg, Auckland Park 2006, South Africa

email: jiatsing.ng@dtc.ox.ac.uk

We present computational tools that extract information from standard sparse-matrix screens, to help experimenters make informed decisions in subsequent crystallization effort, even if there were no crystals in the initial screen. Our method is based on the objective description of crystallization droplets using textons in Ng et al. (2014).

Firstly, we aid in the identification of crystals or microcrystals by ranking droplets according to their likelihood of containing crystalline behaviour. This allows users to view droplets in a more meaningful order and prioritise attention and time to what is likely to matter most.

Secondly, we describe screening experiments by the collective precipitation patterns across the screen. This enables us to cluster historical experiments at the Structural Genomics Consortium, Oxford by their precipitation behaviour. Each cluster has a different distribution of crystallization conditions that gave hits, which is then used to identify conditions for optimization for a new protein that falls into the same cluster.

Thirdly, based on the idea of Collins et al. (2005), we automatically generate an analysis of conditions that produced clear drops. These conditions can be used to design an alternative protein formulation buffer for further stabilization of the sample. A stable formulation allows for crystallization experiments at higher protein concentration. We present cases for each of these applications and how they have enabled the crystallization of difficult targets, and/or improved the crystal quality. A centralised software, TeXRRank, presents the above analysis of screening data and allows users to view and annotate their images.

References:

- Collins, B., Stevens, R. C., & Page, R. (2005). *Acta Crystallogr. Sect. F Struct. Biol. Cryst. Commun.* **61**, 1035–1038.
- Ng, J. T., Dekker, C., Kroemer, M., Osborne, M., & von Delft, F. (2014). *Acta Crystallogr. Sect. D Biol. Crystallogr.* **70**, 2702–2718.

Keywords: screening, machine vision, automated analysis

MS12-O5 Protein crystal nucleation induced by ionic liquid-functionalized mineral particles

Magdalena Kowacz¹, Mateusz Marchel¹, Lina Juknaite², Ana Luísa Carvalho², Maria João Romão², José M. S. S. Esperança¹, Luís Paulo N. Rebelo¹

1. Instituto de Tecnologia Química e Biológica - António Xavier, Universidade Nova de Lisboa, Av. da República, 2780-157 Oeiras, Portugal.
2. UCIBIO, REQUIMTE, Departamento de Química, Faculdade de Ciências e Tecnologia, Universidade Nova de Lisboa, 2829-516 Caparica, Portugal

email: magda@itqb.unl.pt

Nucleation is a critical step that determines the outcome of the entire crystallization process. Therefore, finding an effective nucleant for protein crystallization is of utmost importance for structural biology that relies on good quality crystals to solve the 3D structures of macromolecules. We show that crystalline barium sulfate (BaSO₄) with etched and/or ionic liquid (IL) functionalized surface can: (1) induce protein nucleation at protein concentrations well below the concentration needed to promote crystal growth at control conditions, (2) can shorten nucleation time, (3) increase growth rate and finally (4) can improve protein crystal morphology. These effects are shown for Hemoglobin, Myoglobin, Trypsin, Proteinase K, RNase A and Lysozyme.

Surface characteristics of our effective heterogeneous nucleant – porosity (dissolution pits), disorder (partially broken crystal contacts and liquid-like IL coating) and solid strain – support previously proposed surface-supported mechanisms of nucleation. These refer to protein entrapment and induction of supersaturation spikes inside of the pores, providing surface-protein binding sites at a right distance to match protein-protein spacing in the crystal or supporting of entropy-driven nucleation induced by strained mismatched solid support.

Moreover this work shows for the first time the effect of water-immiscible ionic liquids on crystallization of biomacromolecules from aqueous solution. This is enabled by the use of the hydrophobic ILs immobilized at the surface of a hydrophilic mineral. Our results indicate that partitioning of ionic liquid and of protein amphiphiles to solid surface is governed by the same mechanisms. Therefore ILs can serve as simple models giving some insight into protein-solid interactions. Both, ILs and biomacromolecules interact with the hydrophilic solid through their polar groups, while hydrophobic compartments determine their tendency to separate from aqueous solution and drive further hydrophobic association near the solid surface. ILs tune protein partitioning to the solid support by providing matching H-bonding sites as well as non-polar patches at hydrophilic surface.

Modification of the solid surface nanotopography and its functionalization are not restricted to the particular mineral-ILs system, so that their impact on protein conformational changes can be further explored.

The authors acknowledge financial support from Fundação para a Ciência e a Tecnologia (FCT).

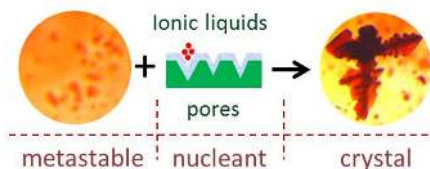


Figure 1. Mineral particles with porous surface and ionic liquid coating induce protein crystallization in a metastable zone.

Keywords: solid-supported crystallization, crystallization from metastable zone, heterogeneous nucleant

MS13. New instrumentation, methods and approaches in inorganic crystallography

Chairs: Anton Meden, Damien Jacob

MS13-O1 Complex metal hydrides: When powder diffraction needs help

Radovan Černý¹, Pascal Schouwink¹, Yolanda Sadikin¹, Matteo Brighi¹, Emilie Didelot¹

1. Laboratory of Crystallography, DQMP, University of Geneva, 24 Quai Ernest-Ansermet, CH-1211, Geneva Switzerland

email: Radovan.Cerny@unige.ch

'Real life' energy-related materials such as solid-state hydrogen storage compounds or components of electrochemical cells are usually polycrystalline, poorly crystallized, highly reactive and dynamic systems. Powder diffraction at modern high brilliance X-ray sources is the most useful tool to investigate such systems because it is easy, fast and extremely versatile with respect to measurement conditions as well as in situ setups. However, powder diffraction applied to these systems rapidly reaches its limits due to the bad crystallinity of samples prepared by mechanochemistry as well as due to the method itself. We will show how a complementary approach combining powder diffraction with non-diffraction methods such as vibrational spectroscopy, thermal analysis and supported by ab initio solid state calculations allows overcoming these limitations¹.

The investigation of samples containing several novel crystalline phases of uncertain chemical composition appears as a problem with no unique solution. We will show that a purposeful use of various samples of different nominal compositions, powder diffraction patterns measured while thermally decomposing each phase (T-ramping)², direct space methods for structure solution and refinement by ab initio solid state calculations does provide detailed structural information of novel compounds even for hydrogen atoms³.

The recently developed possibility of performing mechanochemistry, usually a "black box" approach, on reactive samples under the beam will also be discussed shortly. Ball milling mapped by in situ powder diffraction provides a means of "watching" the synthesis of novel materials, and it is the latest tool we have applied to follow the reactions of complex hydrides inside the reaction jars, capturing intermediate phases and tuning the milling conditions to selectively favour phase yields³.

References

1. Schouwink P. and Černý R. Complex hydrides: When powder diffraction needs help. *Chimia*, 68 (2014) nr. 1/2, 38-44, dx.doi.org/10.2533/chimia.2014.38

2 Cerny R. and Filinchuk Y. Complex inorganic structures from powder diffraction: case of tetrahydroborates of light metals. *Z. Kristallographie* 226(2011)882-891, dx.doi.org/10.1524/zkri.2011.1409

3 Schouwink P., Smrcok L. and Cerny R. The role of the Li⁺ node in the Li-BH₄ substructure of double-cation tetrahydroborates. *Acta Cryst. B*, 70 (2014) 871-878, dx.doi.org/10.1107/S2052520614017351

Keywords: powder diffraction, metal hydride

MS13-O2 Decomposing electron diffraction signals from multi-component microstructures

Alex Eggeman¹, Duncan Johnstone¹, Robert Krakow¹, Jing Hu², Sergio Lozano-Perez², Chris Grosvenor², Paul Midgley¹

1. University of Cambridge

2. University of Oxford

email: ase25@cam.ac.uk

Recent development of spatially resolved (scanning) diffraction in the TEM offers the capacity to study phase and crystallographic orientation with nanometre spatial resolution [1]. However despite the relatively small sample thickness in TEM there is still the possibility of two or more distinct phases contributing to a diffraction pattern in the dataset. One solution is to use multivariate statistical analysis [2] approaches to separate out the unique diffraction signals (or components) from the different phases in the system. This can provide useful information about the general diffraction signal from a phase by removing the small variations in diffraction patterns arising from local variations in the sample thickness or bending, allowing a more robust pattern match for regions of the same structure and orientation. It can also provide a robust method for localising phases within a scanned area allowing completely embedded phases to be separated from within the scanned diffraction data.

This approach will be shown through a number of different studies, starting with the analysis of twinning and epitaxial growth in semiconductor nanowires and continuing through to the separation of phases in partially oxidised zirconium, leading to confirmation of the existence of a proposed intermediate oxide [3] structure found at the metal-metal oxide interface.

The onward development of this approach is to isolate and track individual phases through a tilt-series of measurements, allowing tomographic reconstruction of the individual phases combined with understanding of the complete 3-D orientation relationships within the microstructure. This will be shown through a study on a nickel superalloy sample highlighting the coherent interface between matrix and precipitates within the microstructure.

[1] E. F. Rauch, *et al.*, *Microscopy and Analysis* **22**, (2008), S5-S8.

[2] F. de la Peña. *et al.* *Ultramicroscopy* **111**, (2011), 169-176.

[3] J Hu *et al.* *Micron* **69**, (2015), 35-42

Keywords: Scanning electron diffraction, principle component analysis, orientation tomography

MS13-O3 Accurate structure refinement from electron diffraction tomography data

Lukáš Palatinus¹, Cinthia A. Correa¹, Philippe Boullay², Gwladys Steciuk², Mauro Gemmi³, Damien Jacob⁴, Mariana Klementová¹, Pascal Roussel⁵

1. Institute of Physics of the AS CR, Na Slovance 2, 182 21 Prague, Czechia
2. CRISMAT - UMR6508 CNRS / ENSICAEN, 6 Bd du Maréchal JUIN, 14050 Caen, France
3. Center for Nanotechnology Innovation@NEST, Istituto Italiano di Tecnologia, Piazza San Silvestro 12, 56127 Pisa, Italy
4. UMET, UMR CNRS 8207-Université de Lille I, France
5. Ecole Nationale Supérieure de Chimie de Lille, Cité Scientifique, F-59652 Villeneuve d'Ascq, France

email: palat@fzu.cz

Structure analysis by electron diffraction has made an enormous progress in the last decade. From a status of a method deemed by many unsuitable for ab initio structure solution and very complicated for refinement it turned into an accepted tool of structure analysis, which can be used almost routinely to solve unknown structures. This is especially true for inorganic materials, which, in general, suffer less radiation damage under the electron beam than organic or organometallic compounds.

This progress was caused by the introduction of the electron diffraction tomography method (EDT) [1]. This method allows collecting complete diffraction information from a large part of reciprocal space. Such data can be processed in a way similar to single crystal x-ray data collection, and then used for structure solution and refinement. Unfortunately, the strong interaction between electrons and matter cause that the kinematical theory of diffraction is not valid for electrons to sufficient accuracy, the consequence being that the structures refined against EDT data lack accuracy and statistical reliability. The problem can be partially remedied by the combination of the EDT method with precession electron diffraction [2], but even then the dynamical character of diffraction has negative impact on the accuracy of the refinement results.

A solution to this problem is the method, which uses for structure refinement the full dynamical diffraction theory. Such method was developed recently [1] and implemented in the crystallographic computing system Jana2006 [2]. The method was tested on a range of inorganic materials. The comparison of the refined structures with the reference single crystal x-ray structures shows that the average distance between corresponding atoms in the refined and reference structure is typically less than 0.02 Å. With this accuracy, the method can be claimed to be comparable, if not superior to the Rietveld refinement from powder diffraction data, and allows an accurate single-crystal analysis from a single nano-sized crystal.

[1] Kolb, U., Gorelik, T., Kuebel, C., Otten, M. T., Hubert, D. (2007), *Ultramicroscopy*, **107**, 507-513.

[2] Vincent, R. & Midgley, P. A. (1994), *Ultramicroscopy*, **53**, 271-282.

[3] Palatinus, L., Petříček, L., Correa, C. A. (2015), *Acta Cryst. A*, **71**, 235-244.

[4] Petříček, V., Dušek, M., Palatinus, L. (2014), *Z. Krist.*, **229**, 345-352.

Keywords: electron diffraction, structure refinement

MS13-O4 Serial snapshot crystallography for materials science with SwissFEL

Catherine Dejoie¹, Stef Smeets¹, Christian Baerlocher¹, Nobumichi Tamura², Philip Pattison³, Rafael Abela⁴, Lynne McCusker¹

1. Laboratory of Crystallography, ETH Zurich, Zurich, Switzerland
2. Advanced Light Source, Lawrence Berkeley National Laboratory, Berkeley CA, USA
3. Swiss-Norwegian Beamline, European Synchrotron radiation Facility, Grenoble, France
4. Paul Scherrer Institut, Villigen PSI, Switzerland

email: c.dejoie@mat.ethz.ch

With the development of X-ray free-electron laser (X-FEL) sources that create ultra-fast X-ray pulses of unprecedented brilliance, a new option for the structural characterization of micro-crystalline inorganic materials is arising [1]. The SwissFEL facility (PSI, Switzerland), a new X-FEL source, is scheduled to come online in 2017 [2]. Any crystal placed in the extremely intense SwissFEL beam will be destroyed, but not before a diffraction pattern is generated. To get a full data set, therefore, many randomly oriented stationary crystals will have to be measured. One of the unique features of the SwissFEL facility will be that the bandwidth of the X-ray beam can be adjusted to give as much as a 4% wavelength spread. To evaluate the possibility of using the full energy range of the SwissFEL beam, we first simulated data for inorganic crystals. With the 4%-energy-bandpass mode, not only can more reflections be recorded per shot, but the intensities will also be measured more reliably [3]. To test the viability of this approach experimentally, the single-crystal diffractometer on the Swiss-Norwegian Beamlines at the ESRF was used to mimic the SwissFEL setup. The broad bandpass mode was achieved by collecting a diffraction pattern while the monochromator was scanned over a 4% energy range. Three test samples, with unit cells typical of small-molecule and inorganic structures were used: the zeolite ZSM-5, a hydrated cesium cyanoplatinate, and the mineral sanidine. In order to index the single-shot patterns of randomly oriented crystals of such materials, we have developed two indexing algorithms, one using Laue diffraction concepts and the other starting with a monochromatic approximation [4]. Both algorithms were optimized to index several orientations from a single pattern. We show that the individual patterns of up to 10 crystals measured simultaneously can be indexed, and the intensities extracted reliably for structure investigation. Even with a single shot, at least a partial analysis of the crystal structure will be possible, and this offers tantalizing possibilities for time-resolved studies. [1] H. N. Chapman, et al., *Nature*, 2011, **470**, 73-77. [2] B. D. Patterson, et al., *Chimia*, 2014, **68**, 73-78. [3] C. Dejoie, et al., *J. Appl. Cryst.*, 2013, **46**, 791-794. [4] C. Dejoie, et al., *IUCrJ*, 2015, accepted.

Keywords: SwissFEL, broad-bandpass beam, structure analysis, multi-crystal diffraction

MS13-O5 The nanocluster approach to elucidate complex intermetallics

Davide M. Proserpio^{1,2}, Vladislav A. Blatov², Gregory D. Ilyushin³

1. Dipartimento di Chimica, Università degli Studi di Milano, Via Golgi 19, 20133 Milano, Italy

2. Samara Center for Theoretical Materials Science, Samara State University, Ac. Pavlov St. 1, 443011 Samara, Russia,

3. Shubnikov Institute of Crystallography, Russian Academy of Sciences, Leninsky Prospect 59, 117333 Moscow, Russia

email: davide.proserpio@unimi.it

In the crystal chemistry of intermetallics, the classification in terms of atomic coordination polyhedra is traditionally used. However, the information about coordination of atoms does not determine the structure as a whole; therefore models that consider building blocks going beyond the first atomic coordination shell have been developed. The cluster model usually treats the structural fragments as nested polyhedra of a regular form that include atoms not necessarily connected to each other. The set of nested polyhedra does not always include all atoms and bonds of the structure; it usually describes only the general structural motif. In complicated and/or low-symmetrical (not only cubic) structures, the nested polyhedra cannot be selected unambiguously, and as a result, the same intermetallic compound can be described in several different ways. To resolve these problems, we have proposed the nanocluster method that implements a strict algorithm of searching for the structural units (nanoclusters) that model the entire crystal structure.[1] The method was realized in the program package ToposPro[2] and used to explore a number of complex intermetallics and the revealed nanoclusters were found in quite different compounds, even belonging to different structure types.[3,4] The work was supported by the Russian government (grant No. 14.B25.31.0005). [1] V.A. Blatov, G.D. Ilyushin, D.M. Proserpio., *Inorg. Chem.* 49 (2010) 1811-1818. [2] V.A. Blatov, A.P. Shevchenko, D.M. Proserpio, *Cryst. Growth Des.*, 14 (2014) 3576-3586. <http://topospro.com> [3] V.A. Blatov, G.D. Ilyushin, D.M. Proserpio., *Inorg. Chem.* 50 (2011) 5714-5724; [4] A.A. Pankova, V.A. Blatov, G.D. Ilyushin, D.M. Proserpio., *Inorg. Chem.* 55 (2013) 13094-13107.

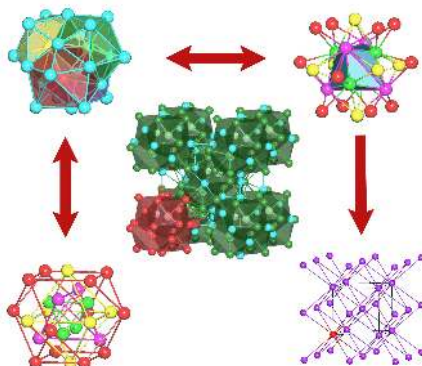


Figure 1.

Keywords: intermetallics, nanocluster

MS14. Mineralogical crystallography: Nature as a source of inspiration for new materials

applications in nanoelectronics, nanophotonics and energy and light harvesting. A second completely novel nanocomposite was prepared by the polymerization of carbon monoxide CO in silicalite. The polymer chains could be readily located on Fourier difference maps and the structure refinement shows that the isolated single polymer chains exhibit orientational and translational disorder. These polymer chains are, however, more stoichiometric and less branched than bulk polymers obtained by high pressure polymerization of this simple system. The polyCO/zeolite composite could be an interesting energetic material.

Keywords: zeolites, high-pressure, nanocomposites

Chairs: Nikolai Eremin, Rossella Arletti

MS14-O1 High pressure synthesis and structural studies of zeolite/polymer nanocomposites

Julien Haines¹, J. M. Thibaud¹, J. Rouquette¹, P. Hermet¹, O. Cambon¹, F. Di Renzo¹, A. van der Lee², D. Scelta³, M. Ceppatelli^{3,4}, K. Dziubek³, F. Gorelli^{3,5}, R. Bini^{3,6}, M. Santoro^{3,5}

1. ICGM-CNRS/Univ. Montpellier/ENSCM, Montpellier, France
2. IEM-CNRS/Univ. Montpellier, Montpellier, France
3. LENS, Sesto Fiorentino, Italy
4. ICCOM-CNR, Sesto Fiorentino, Italy
5. INO-CNR, Sesto Fiorentino, Italy
6. Dipartimento di Chimica, Univ. Firenze, Sesto Fiorentino, Italy

email: julien.haines@univ-montp2.fr

Zeolites represent an important family of porous materials based on corner sharing TO_4 ($T=Al, Si$) tetrahedra. The microporous nature of these materials allows insertion of a great variety of guest atoms, ions or molecules giving rise to a large number of technological applications in catalysis, molecular sieves and ion-exchange materials. Polymerization of simple organic molecules under high pressure in the subnanometric pores of pure SiO_2 zeolites can be used to produce novel nanocomposite materials, which can be recovered at ambient P and have remarkable mechanical, electrical or optical properties. Polymerization of ethylene in silicalite results in a nanocomposite with isolated chains of non-conducting polyethylene strongly confined in the pores based on single crystal x-ray diffraction data. Compared to the initial silicalite, the nanocomposite is much less compressible and has a positive rather than a negative thermal expansion coefficient. In order to target novel electrical and optical properties, isolated chains of conducting polymers can also be prepared in the pores of zeolite hosts at high pressure, such as polyacetylene, which was polymerized under pressure in the pores of the 1-D zeolite ZSM-22. The structure of this nanocomposite was determined by synchrotron x-ray powder diffraction data with complete pore filling corresponding to one planar polymer chain confined in each pore with a zig-zag configuration in the yz plane. This very strong confinement can be expected to strongly modify the electrical properties of polyacetylene. In this nanocomposite, our theoretical calculations indicate that the electronic density of states of polyacetylene exhibit van Hove singularities related to quantum 1D confinement, which could lead to future technological applications. This new material is susceptible to have

MS14-O2 Synthetic phases with mineral topology: crystal chemistry and physical properties

Olga V. Yakubovich¹, Ian M. Steele², Galina V. Kiriuichina¹, Olga V. Dimitrova¹, Larisa V. Shvanskaya¹, Olga S. Volkova¹, Aleksander N. Vasiliev¹

1. M.V. Lomonosov Moscow State University, Vorob'evy Gory, 119234, Moscow, Russia

2. Notre Dame Integrated Imaging Facility Stinson-Remick, B12 University of Notre Dame Notre Dame, IN 46556, USA

email: yakubol@geol.msu.ru

Novel phases prepared by hydrothermal synthesis are discussed in correlation with archetypes and derivative compounds. The $K_{2-x}Cu_xCl(PO_3)_4(OH)_{0.4}(VO_3)_x \cdot nH_2O$ microporous crystal structure determined at 100 K using synchrotron diffraction data, is based on a 3D anionic framework built from Cu- and V-centered five-vertex polyhedra and PO_4 tetrahedra, and includes channels with K atoms and H_2O molecules. It is a new structural representative of the topology shown by the lavendulan mineral group with structures formed by two types of alternating 2D slabs: one slab $[Cu_xX(TO_3)_4]_{\infty}$ ($X=Cl, O; T=As, P$) is common to all phases, whereas the slab content of the other set differs among the group members. This family of compounds is interpreted in terms of the modular concept as one polysomatic series.

The $Na_2Co_6(OH)_3[HPO_4][H_2PO_4]_3$ presents the first example of the ellenbergerite topology based on a 3D framework of octahedra and tetrahedra, with alkaline cations in the channels, usually occupied by transition metals. The reason for close unit-cell parameters of rather dense ellenbergerite-like and the microporous cancrinite-like Co phosphates is the nearly identical topology of their cation sublattices, where the same cations are set into diverse positions, thus providing a different distribution of the coordinating O atoms. It results in a formation of the cationic framework of Co octahedra in our case, while in the cancrinite-like phosphate Co forms a mixed anionic tetrahedral framework together with PO_4 groups. Magnetic susceptibility measurements revealed a strong antiferromagnetic interaction and magnetic transition to low temperature spin-canted phase at $T_N = 44$ K.

The $Rb_4[Na(H_2O)_2](H_2O)_4(HV_6O_{28})$ crystal structure established at 100 K is formed from monoprotonated decavanadate cages of ten sharing edges V-centered octahedra, which are joint together via hydrogen bonds in one-dimensional chains. Within these chains, protons are sandwiched between neighboring polyanions. Na and Rb atoms and H_2O molecules occupy interstices flanked by the anionic chains providing additional cross-linking in the structure. Two types of interactions ensure stability of the crystal structure, which may be treated as a combination of 3D cationic framework built by Rb and Na atoms, and 1D anionic chains of decavanadate units. Structural and genetic relations among protonated and deprotonated decavanadates with inorganic cations, including minerals of the pascoite group, are discussed.

Keywords: X-ray diffraction, 100 K, synchrotron radiation, crystal structure, topology, hydrothermal synthesis, vanadate, phosphate, vanadyl-phosphate, lavendulan, ellenbergerite, pascoite, polysomatic series

MS14-O3 Titanium and zirconium silicate ion-exchange materials for the treatment of nuclear waste

Jennifer E. Readman¹, Reece M. Hall¹, Hayley R. Green¹, Lauren M. Galligan¹

1. Centre for Materials Science, School of Forensic and Investigative Sciences, University of Central Lancashire, Preston, UK

email: jereadman@uclan.ac.uk

Zeolites are commonly used as ion-exchange materials for the remediation of nuclear waste, however, they have certain drawbacks. Unlike zeolites which contain SiO_4 and AlO_4 tetrahedra, microporous titanium silicates can contain SiO_4 tetrahedra and TiO_6 octahedra and therefore structures are possible which have no traditional aluminosilicate analogues^[1]. Microporous titanium silicates such as sitinakite $KNa_2Ti_3Si_3O_{13}(OH) \cdot 4H_2O$ and the synthetic niobium doped analogue are used as ion-exchange materials for the removal of Cs^+ and Sr^{2+} from nuclear waste^[2,3]. To date little work in this area has been carried out using microporous zirconium silicates. The work presented here will focus on the ion-exchange properties of umbite. Umbite is a naturally occurring small pore microporous zirconium titanium silicate. The mineral is found in northern Russia and synthetic analogues, $K_2ZrSi_3O_9 \cdot H_2O$, can be prepared in the laboratory^[4]. It has an orthorhombic cell with $a = 10.2977(2)$ Å, $b = 13.3207(3)$ Å and $c = 7.1956(1)$ Å. Ion-exchange studies have been carried out and have shown that umbite has a preference for common radionuclides, such as Cs^+ and Co^{2+} , even in the presence of competing ions. Natisite is another material which has interesting ion-exchange chemistry and is a layered titanium silicate with the ideal formula Na_2TiSiO_5 ^[5]. The structure consists of square pyramidal titanium, with the sodium cations located between the layers. This coordination environment is highly unusual for Ti. It crystallises in the tetragonal space group $P4/nmm$, with $a = b = 6.4967(8)$ Å and $c = 5.0845(11)$ Å. Inclusion of zirconium in the framework has a considerable effect on ion-exchange. It was found that increasing the levels of zirconium increased the affinity towards Cs and it was also found rate of exchange of Co was increased with increasing Zr content. The Zr doped materials take up Co from an aqueous solution within minutes whereas the undoped materials needing a contact time of several hours in order to reach the same level of exchange. A combination of techniques to probe long and short range order has been used to understand this behaviour. 1) P. A. Wright, *Microporous Framework Solids*, The Royal Society of Chemistry, Cambridge, 2008. 2) D. M. Poojary, *et al.*, *Chem. Mater.*, **6**, 2364 (1994). 3) A. Tripathi, *et al.*, *J. Solid State Chem.*, **175**, 72 (2003). 4) D. M. Poojary, *et al.*, *Inorg. Chem.*, **36**, 3072 (1997). 5) D.G. Medvedev *et al.*, *Chem. Mater.*, **16**, 3659 (2004).

MS14-O4 Naturally occurring metal-organic frameworksIgor Huskić¹, Tomislav Frišić¹¹. Department of Chemistry, McGill University, 801 Sherbrooke St. West, Montreal, Canada

email: igor.huskić@mail.mcgill.ca



Figure 1. Structural representations of umbite (left) and natisite (right). Water molecules and charge balancing cations have been removed for clarity.

Keywords: Zirconium silicate, Titanium silicate, Ion-exchange, XAS

Metal-organic frameworks (MOFs) are a class of artificial, man-made materials, composed of organic linkers coordinated to metal ions forming networks which often exhibit increased porosity.^[1] A pinnacle of modern materials science, various MOFs have been designed and made for use in catalysis, gas storage and separation, and as molecular sensors. In our work we examine two oxalate-based minerals, Stepanovite and Zhemchuzhnikovite, which were discovered in 1960s by Knipovich and co-workers in a coal deposit near the estuary of river Lena, in the former Soviet Union.^[2] The preliminary characterisation of these materials was conducted through available methods, namely elemental analysis and powder X-ray diffraction. The latter provided crystallographic characterization of these organic minerals in terms of crystallographic symmetry and unit cell parameters. We realized that the formulas of these minerals strongly resemble those of oxalate-based MOFs first developed by Descurtins^[3] in 1990s as novel magnetic materials. We now provide a full structural characterization of each mineral, obtained through synthetic means, which reveals two-dimensional hexagonal MOFs with honeycomb (6,3)-topology. Both minerals are made up of 2-dimensional layered networks with hexagonal cavities occupied by hexaaqua magnesium ions. While Stepanovite exhibits a rhombohedral lattice, Zhemchuzhnikovite adopts a different mode of layered stacking, leading to a hexagonal unit cell. The structures of Zhemchuzhnikovite and Stepanovite are, therefore, the first examples of open metal-organic frameworks found in nature. The herein presented structural analysis of these two minerals contrasts the established paradigm of MOFs as designed functional materials, and presents an unexpected new role for MOFs as naturally-occurring minerals. The presentation will also discuss the synthetic routes through which such minerals could form, e.g. by mineral weathering of oxides recently utilized for solvent-free “accelerated aging” synthesis of microporous.^[4]

[1] Kitagawa *et al.* *Angew. Chemie* **43** (2004) 2334 - 2375 [2] T. Echigo and M. Kimata *Canadian Mineralogist* **48** (2010) 1329 – 1357 [3] S. Descurtins *et al.* *Inorg. Chem.* **32** (1993) 1888–1892 [4] C. Mottillo *et al.* *Green Chemistry* **15** (2013) 2121-2131

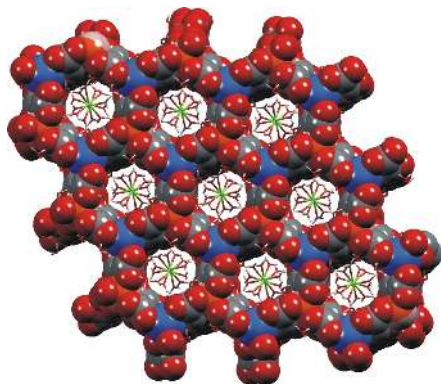


Figure 1. The structure of Zhemchuzhnikovite viewed down the crystallographic *c*-axis, demonstrating the overlap of neighboring sheets, which leads to the formation of channels occupied by $\text{Mg}(\text{H}_2\text{O})_6^{2+}$ ions.

Keywords: Metal-organic frameworks, minerals, mineral weathering

MS14-O5 A comprehensive analysis of the structure of imogolite nanotubes

Stéphan ROUZIERE¹, Mohamed-Salah AMARA¹, Erwan PAINEAU¹, Pascale LAUNOIS¹

¹. Laboratoire de Physique des Solides, UMR8502 Université Paris-Sud, Bât. 510, 91405 Orsay Cedex

email: stephan.rouziere@u-psud.fr

Imogolites, these 'tubular clays' with a diameter of the order of the nanometer, discovered in 1962 in volcanic soils [1], can now be synthesized through controllable pathways. They thus appear as most promising candidates for molecular recognition applications taking advantage of their one-dimensional porosity (catalysis, molecular sieves, sensors, etc) [2]. In 1972, natural imogolite nanotubes (INT) were proposed to have nominal composition $(\text{OH})_3\text{Al}_2\text{O}_3\text{SiOH}$, being formed of a curved gibbsite layer whose vacancies are bonded by isolated $[\text{Si}(\text{Ge})\text{O}_4]$ tetrahedra [3] (figure 1(a)). It was shown later that germanium can replace silicon [4]. Different studies corroborated the structural proposal of Cradwick and co-workers [3] but, to the best of our knowledge, more than forty years after their seminal article, no complete determination of INT structure has been achieved based on experimental data. We present here the first comprehensive X-ray scattering study, from small angles to wide angles, of three sorts of INT, in solution: natural and synthetic $(\text{OH})_3\text{Al}_2\text{O}_3\text{SiOH}$ nanotubes, with different diameters despite their similar composition, and synthetic $(\text{OH})_3\text{Al}_2\text{O}_3\text{GeOH}$ nanotubes [5]. We will explain the strategy we have developed to minimize interatomic distortions and to account for both small and wide angle X-ray scattering data (figure (b)). The refined atomic structures will be discussed with respect to energetical minimizations proposed recently [6]. It is of special interest since these numerical approaches are used as guides to predict new imogolite-like structures [7]. Our methodology should also be applied in the near future to newly-discovered imogolite-type nanotubes (double-walled nanotubes or functionalized nanotubes [2,8]).

[1] N. Yoshinaga, S. Aomine, *Soil Sci. Plant Nutr.* 8, 22 (1962), [2] D.Y. Kang et al, *Nat. Comm.* 5, 3342 (2014) ; M.S. Amara et al., *Chem. Mater.*, DOI: 10.1021/cm503428q. [3] P. Cradwick et al, *Nature* 240, 187 (1972), [4] S. Wada, K. Wada, *Clays and Clay Minerals* 30, 123 (1982), [5] M.S. Amara, S. Rouzière, E. Paineau, P. Launois, article in preparation, [6] K. Tamura, K. Kawamura, *J. Phys. Chem. B* 106, 271 (2002); S. Konduri et al, *Phys. Rev. B* 74, 033401 (2006); L. Guimarães et al, *ACS Nano* 1, 362 (2007); M. Zhao et al, *J. Phys. Chem. C* 113, 14834 (2009) ; M.P. Lourenço et al, *J. Phys. Chem. C* 118, 5945 (2014), [7] L. Guimarães et al, *Phys. Chem. Chem. Phys.* 15, 4303 (2013), [8] M.S. Amara et al, *Chem. Comm.* 49, 11284 (2013)

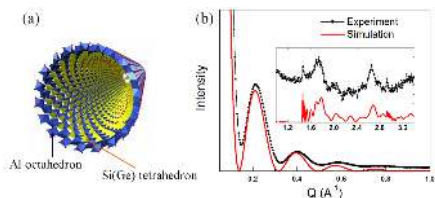


Figure 1. (a) Schematic representation of an imogolite nanotube; (b) X-ray scattering pattern of $(\text{OH})_2\text{Al}_2\text{O}_3\text{GeOH}$ nanotubes, together with its simulation for the refined structure, showing the good agreement between experiment and simulation.

Keywords: Crystallography, imogolite

MS15. Structure property relationships

Chairs: Kari Rissanen, Martin Bremholm

MS15-O1 Design and synthesis of molecular materials: mixed crystals for finer engineering

Matteo Lusi¹, Michael J. Zaworotko¹

¹. Chemical and Environmental Science, University of Limerick, Limerick, Ireland

email: matteo.lusi@ul.ie

The properties of a material depend on both the nature of its constituents (*chemistry*) and the way they are arranged in the space (*structure*). Crystal engineering is the discipline that investigates and exploits the relationship between structure and physical properties to produce tailor-made crystalline molecular materials. A limitation to such activity is represented by the finite (*discrete*) nature of the molecular components (*building blocks*) that prevent the material's fine tuning. By combining the functions and sterics of multiple, equivalent building blocks crystalline solid solutions (*mixed crystals*), whose composition can be varied in continuum, provide an extra degree of control over the material's properties. Hence, for this class of compounds the crystal engineering problem would coincide with the synthesis of the appropriate mixed crystal. Unfortunately, traditional crystallisation techniques are likely to result in molecule separation precluding the formation of mixed crystal. Therefore solvent-free alternatives must be developed and pursued. Solid-solid and solid-gas reactions represent a viable alternative to wet chemistry in the production of homogeneous solid solutions of organic, metalorganic and organometallic species. This strategy has proved successful in engineering reactivity, polymorphism, photoemission spectra and unit cell metrics of a number of materials including coordination polymers, molecular sieves, dyes and pharmaceuticals.

Keywords: crystal_engineering, solid_solutions, mixed_crystals, solid_state_reactions

MS15-02 Structure property relationships arising from anion order in solid oxynitridesJ. Paul Attfield¹¹. CSEC and School of Chemistry, University of Edinburgh UK

email: j.p.attfield@ed.ac.uk

Metal oxynitrides are an important class of emerging materials that in optimal cases may combine the advantages of oxides and nitrides. They generally have greater air and moisture stability than pure nitrides, but with smaller bandgaps than comparable oxides leading to useful electronic or optical properties. Anion order is important for controlling and tuning properties, and neutron diffraction provides good O/N contrast for experimental determinations of local or long range O/N order in solids. Differences in charge, size and covalent bonding between oxide and nitride are the important factors that drive anion order. For example, a robust partial anion order in SrMO_xN ($M = \text{Nb}, \text{Ta}$) and related oxynitride perovskites driven by covalency results in the disordered zig-zag MN chains that segregate into planes within the perovskite lattice [1,2,3,4]. This leads to unusual sub-extensive scaling of entropy, described as 'open order' [5]. Local anion order is important to optical materials. Size mismatch between host and dopant cations leads to local O/N clustering that tunes photoluminescence shifts systematically in $\text{M}_{1.95}\text{Eu}_{0.05}\text{Si}_3\text{Al}_2\text{N}_{8-x}\text{O}_x$ phosphors, leading to a red shift when the $M = \text{Ba}$ and Sr host cations are larger than the Eu^{2+} dopant, but a blue shift when the $M = \text{Ca}$ host is smaller [6].

[1] M. Yang et al. *Nature Chem.* **3**, 47 (2011). [2] Attfield, J.P. *Cryst. Growth. Des.* **13**, 4623 (2013). [3] L. Clark, J. Oró-Solé, K.S. Knight, A. Fuertes & J.P. Attfield, *Chem. Mat.* **25**, 5004 (2013). [4] J Oró-Solé, L Clark, N Kumar, W Bonin, A Sundaresan, JPAAttfield, C. N. R. Rao and A Fuertes. *Journal of Materials Chemistry C*, **2**, 2212-2220 (2014). [5] P.J. Camp et al. *JACS* **134**, 6762 (2012). [6] W-T Chen et al. *JACS* **134**, 8022 (2012).

Keywords: perovskite, oxynitride**MS15-03** Energy-related aspects of complex metal borohydrides and higher boranes: Beyond hydrogen storagePascal Schouwink¹, Yolanda Sadikin¹, Matteo Brighi¹, Emilie Didelot¹, Radovan Cerny¹¹. Laboratory of Crystallography, DQMP, University of Geneva, 24 Quai Ernest-Ansermet, CH-1211, Geneva

email: pascal.schouwink@unige.ch

Following the initial wave of interest driven by the extreme hydrogen densities and the potential to develop efficient on-board hydrogen storage, a deeper understanding of the building principles underlying borohydrides has allowed us to explore beyond hydrogen storage in the past years, making use of further specific properties related to the borohydride anion $[\text{BH}_4]^-$. In particular, a close structural relationship to metal oxides and halides provides us with a roadmap to a new class of materials, following the well-defined design concepts developed for garnets, spinels or perovskites, for instance. At the same time, the BH_4 group implements its own specific structural peculiarities, and is lighter in weight than most halide anions. With our contribution we wish to present new developments in the field of borohydride perovskites, targeting energy-related applications such as hydrogen-storage, solid state phosphors or magnetic refrigerants. While heteropolar di-hydrogen contacts facilitate H_2 elimination the homopolar contacts give rise to exotic mechanisms capable of stabilizing lattice instabilities at high temperatures in the perovskite lattice, breaking down the intuitive temperature behaviour of the lattice type that commonly leads to a decrease of polarization at high temperatures. Despite a rich spectrum of B-H vibrations, lanthanide luminescence does not suffer from vibrational quenching in $\text{AlLn}^{2+}(\text{BH}_4)_3$ or $\text{A}_2\text{Ln}^{3+}(\text{BH}_4)_6$. First results will also be discussed on the magnetocaloric effect of Gd^{3+} -containing borohydrides, lightweight paramagnetic materials lacking exchange interactions and potentially useful for magnetic refrigeration.

The vivid structural dynamics of the borohydride anion are exploited in the development of solid state electrolytes based on complex hydrides. The electrochemical stability of borohydrides is comparable to other material groups and cation mobility is promoted by the paddle wheel effect of BH_4^- . Very recently, larger anions such as $[\text{B}_{12}\text{H}_{12}]^{2-}$ or $[\text{B}_{10}\text{H}_{10}]^{2-}$ have emerged as improved "paddle wheels". Here, we extend this concept to mixed-anion compounds and will present topostructural analyses revealing possible 3D migration paths in $\text{Na}_2\text{BH}_2\text{B}_{12}\text{H}_{12}$. Electrical impedance spectroscopy shows that its ionic conductivity is in the order of 10^{-4} S/cm at 298 K, with an activation energy of 0.3-0.4 eV, evidencing the high mobility of Na^+ .

Keywords: powder diffraction, solid state electrolyte, disorder, borohydride

MS15-O4 Molecular rotors in nanoporous periodic architecturesAngiolina Comotti¹, Bracco Silvia¹, Donata Asnaghi¹, Piero Sozzani¹¹. University of Milano Bicocca, Department of Materials Science, Via R. Cozzi 55, 20125 Milano, Italy

email: angiolina.comotti@mater.unimib.it

New mesoporous hybrid covalent frameworks were prepared to realize a periodic architecture of fast molecular rotors containing dynamic C-F dipoles in their structure.[1] The mobile elements, designed on the basis of fluorinated p-divinylbenzene moieties, were integrated into the robust covalent structure through siloxane bonds, and showed not only the rapid dynamics of the aromatic rings (ca. 10^8 Hz at 325 K), as detected by solid-state NMR spectroscopy, but also a dielectric response typical of a fast dipole reorientation under the stimuli of an applied electric field. The nanochannels are open and accessible to diffusing-in gas molecules, and rotor mobility could be individually regulated by I_2 vapors. The iodine enters the channels of the periodic architecture and selectively reacts with the pivotal double bonds of the divinyl-fluoro-phenylene rotors without disrupting the structure, affecting their motion and the dielectric properties. The combination of porosity with rotor dynamics was also discovered in molecular crystals.

Disulfonated rotor-containing molecular rods were self-assembled with alkylammonium salts to fabricate porous supramolecular architectures held together by charge-assisted hydrogen bonds (Figure 1) [2]. The rotors, as fast as 10^8 Hz at 240 K, are exposed to the crystalline channels, which absorb CO_2 and I_2 vapors at low pressure. The rotor dynamics could be switched off and on by I_2 absorption/desorption, showing remarkable change of material dynamics by the interaction with gaseous species and suggesting the use of molecular crystals in sensing and pollutant management.

Moreover, porosity can be switched on/off in molecular crystals based on star-shaped azobenzene tetramers by photoirradiation[3]. Photoinduced trans-cis isomerization of molecules changes intermolecular interactions triggering the formation of a non porous material which can be reverted to porous crystals by visible light irradiation or thermal treatment.

Ref.: 1) Angew. Chemie Int. Ed. 2015, ASAP (VIP Article); 2) J. Am. Chem. Soc. 2014, 136, 618; 3) Nature Chem. 2015, accepted.

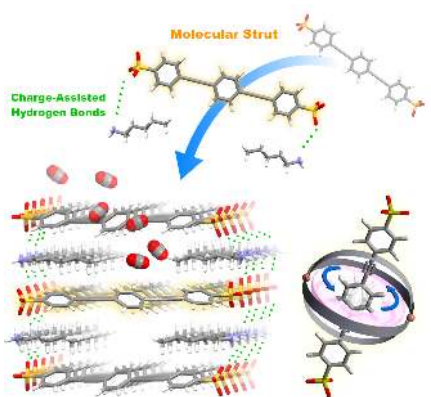
**Molecular Rotors in Organic Porous Architecture**

Figure 1.

Keywords: Porous Materials, Molecular Rotors

MS15-O5 Structure–property relationships in multiferroic metal–organic frameworks at high pressure

Ines E. Collings¹, Natalia Dubrovinskaja¹, Leonid Dubrovinsky²

1. Laboratory of Crystallography, University of Bayreuth, Bayreuth, Germany

2. Bayerisches Geoinstitut, University of Bayreuth, Bayreuth, Germany

email: ines.collings@uni-bayreuth.de

Dense metal–organic frameworks (MOFs) show promise for a new generation of multiferroic materials,^{1–3} which have technological importance in sophisticated multistate devices. MOFs present several advantages over already known multiferroic ceramic materials, such as increased framework flexibility, a vast chemical diversity, and numerous host–guest interactions. These characteristics could lead to increased ferroelectric responses and guest-tuned multiferroic properties. However, so far the study of multiferroic MOFs is in its infancy, and a much greater understanding of the structure–property relationships is needed in order to direct the design of functional multiferroic MOFs.

The dense MOF families of ammonium metal formates, $[\text{NH}_4][\text{M}(\text{HCOO})_3]$, and dimethylammonium metal formates, $[(\text{CH}_3)_2\text{NH}_2][\text{M}(\text{HCOO})_3]$, have shown great potential for multiferroic behaviour.^{1–4} The metal cations in the MOF—connected via organic ligands—provide the magnetic property, while the guest cation in the framework pore yields the ferroelectric response; host–guest interactions may then lead to coupling between the two ferroic parameters. Both these families of MOFs contain disordered A-site cations, which order in a preferential direction at low temperature (below 250 K) to create a switchable uniaxial electric dipole [Fig. 1]. Hydrogen bonding between the A-site cation and the formate linker, which connects the metal cations, provides a way to couple the electric and magnetic ordering.

In this study, we use high-pressure conditions in order to evoke electric and magnetic ordering in dense MOFs, which have already shown multiferroic behaviour at low temperature and ambient pressure. Investigating the structural evolution under pressure is important for determining the way chemical pressure (*i.e.* how different sizes of chemical components can mimic the effect of hydrostatic pressure) should be used in order to obtain desirable ferroelectric and ferromagnetic properties at ambient conditions.

References

- [1] W. Wang, L.-Q. Yan, J.-Z. Cong *et al.*, *Scientific reports*, 2013, **3**, 2024. [2] P. Jain, V. Ramachandran, R. J. Clark *et al.*, *J. Am. Chem. Soc.*, 2009, **131**, 13625–13627. [3] Y. Tian, A. Stroppa, Y. Chai *et al.*, *Sci. Rep.*, 2014, **4**, 6062. [4] G.-C. Xu, W. Zhang, X.-M. Ma *et al.*, *J. Am. Chem. Soc.*, 2011, **133**, 14948–14951. [5] M. Sánchez-Andújar, S. Presedo, S. Yáñez-Vilar *et al.*, *Inorg. Chem.*, 2010, **49**, 1510–1516.

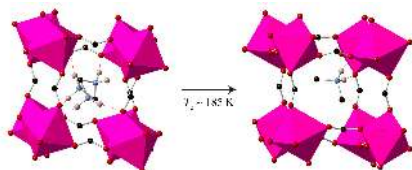


Figure 1. Ferroelectric phase transition of $[(\text{CH}_3)_2\text{NH}_2][\text{Mn}(\text{HCOO})_3]$ induced upon cooling from ambient temperature to below 185 K, creating a uniaxial electric dipole.⁵ Hydrogen bonds are shown in dotted red lines, and octahedral coordination about Mn^{2+} is represented by polyhedra.

Keywords: metal–organic framework, high pressure, multiferroic

MS16. Physical properties through lattice distortions: structure of perovskites & Co studied by electron microscopy and diffraction

[3] C. Suchomski, C. Reitz, D. Pajic, Z. Jaglicic, I. Djerdj, T. Brezesinski, *Chem. Mater.*, 2014, 26, 2337.

[4] C. Reitz, P. M. Leufke, H. Hahn, T. Brezesinski, *Chem. Mater.*, 2014, 26, 2195.

[5] C. Reitz, P. M. Leufke, R. Schneider, H. Hahn, T. Brezesinski, *Chem. Mater.*, 2014, 26, 5745.

Keywords: mesoporous, self-assembly, thin film, metal oxide, perovskite

Chairs: Jerome Rouquette, Artem Abakumov

MS16-O1 Synthesis and structure-property relationships of polymer-templated mesoporous mixed-metal oxide thin films

Torsten Brezesinski¹

1. Institute of Nanotechnology, Karlsruhe Institute of Technology,
Hermann-von-Helmholtz-Platz 1, 76344
Eggenstein-Leopoldshafen, Germany

email: torsten.brezesinski@kit.edu

In recent years, much attention has been devoted to solution-processed mesostructured metal oxide thin films with cubic and hexagonal pore symmetries. The primary reasons for this are their capability to outperform conventional bulk materials and the unprecedented properties because of the high surface-to-volume ratio resulting from the porous structure. Advances in polymer ("soft") templating have enabled the preparation of many important non-silicate mesostructured oxide thin films with different ordering lengths [1]. Their formation relies on the solution-phase coassembly of molecular inorganic building blocks with an amphiphilic polymer structure-directing agent (SDA) using an EISA process [2]. Despite the progress made over recent years, the synthesis of mixed-metal oxides remains challenging, mainly due to the difficulty of controlling the thermally induced crystallization. This process is often associated with the loss of nanoscale porosity and periodicity because of the mismatch between the stable grain size and pore wall thickness. In this talk, I will focus on the templating synthesis (and structure-property relationships) of some selected mixed-metal oxide thin films (perovskite-type $\text{PbZr}_{1-x}\text{Ti}_x\text{O}_3$, $\text{La}_{1-x}\text{A}_x\text{MnO}_3$, etc.) with both an ordered cubic network of ~20 nm pores and highly crystalline walls by using large poly(ethylene-co-butylene)-block-poly(ethylene oxide) and polyisobutylene-block-poly(ethylene oxide) diblock copolymer SDAs [3-5]. I will show that the integration of nanoscale porosity with texture-specific properties paves the way to broaden the scope of application of these materials.

[1] C. Sanchez, C. Boissiere, D. Grosso, C. Laberty, L. Nicole, *Chem. Mater.*, 2008, 20, 682.

[2] C. J. Brinker, Y. F. Lu, A. Sellinger, H. Y. Fan, *Adv. Mater.*, 1999, 11, 579.

MS16-O2 Exotic phases and strain in model perovskite under pressure

Bouvier Pierre¹

1. Institut Néel, CNRS/UJF, 25 rue des Martyrs BP166, Grenoble, 38042 France

email: pierre.bouvier@neel.cnrs.fr

Over the past 10 years, many efforts have been devoted to the (re-)examination of structural distortions in perovskites under high-pressure in order to identify general rules for their evolutions and interactions with reducing volume. I will present structural characterization of various model perovskites such as PbTiO_3 [1,2], SrTiO_3 [3], CaTiO_3 [4] and the multiferroic BiFeO_3 [5,6]. Through those example, I will show that the use of single crystal x-ray diffraction and Raman spectroscopy allows precise determination of symmetry adapted strains and order parameters and will discuss the appearance of either new kinds of large cells structures or the unusual emergence of a polar phase at high pressure.

1. Ferroelectricity of perovskite under pressure, I.A.Kornev, L.Bellaiche, P.Bouvier, P.-E.Janolin, B.Dkhil, J.Kreisel, Phys. Rev. Letters, **95** (2005) 196804/1-4.

2. High pressure effect on PbTiO_3 , P.E.Janolin, P.Bouvier, J.Kreisel, I.A.Kornev, L.Bellaiche, W.Crichton, M.Hanfland, B.Dkhil, Phys. Rev. Letters, **101** (2008) 237601/1-4.

3. Pressure-temperature phase diagram of SrTiO_3 up to 53 GPa, M.Guennou, P.Bouvier, J.Kreisel, D.Machon, Phys. Rev B **81**, 054115 (2010).

4. High-pressure investigations of CaTiO_3 up to 60 GPa, M.Guennou, P.Bouvier, B.Krikler, J.Kreisel, R.Haumont, G.Garbarino, Phys. Rev B, **82** (2010) 134101/1-10.

5. Effect of high pressure on the multiferroic BiFeO_3 , R. Haumont, P. Bouvier, A. Pashkin, K. Rabia, S. Frank, B. Dkhil, W. A. Crichton, C. A. Kuntscher, J. Kreisel, Phys. Rev. B **79**, 184110 (2009).

6. Multiple high-pressure phase transitions in BiFeO_3 , M.Guennou, P.Bouvier, G.S.Chen, B.Dkhil, R.Haumont, G.Garbarino, J.Kreisel, Phys. Rev. B **84**, 174107 (2011).

Keywords: perovskite, high-pressure, single crystal, structure, Raman

MS16-O3 Dynamics of oxygen vacancies in strontium titanate

M. Zschornak^{1,2}, J. Hanzig¹, H. Stöcker¹, C. Richter^{1,3}, M. Nentwich¹, E. Mehner¹, F. Hanzig¹, S. Jachalke¹, S. Gorfman⁴, B. Khanbabaee⁴, T. Leisegang¹, D. Novikov³, S. Gemming^{2,5}, D.C. Meyer¹

1. Institute of Experimental Physics, TU Bergakademie Freiberg, Germany.

2. Institute of Ion Beam Physics and Materials Research, HZ Dresden-Rossendorf, Germany.

3. Deutsches Elektronen-Synchrotron (DESY) Photon Science, Hamburg, Germany.

4. Department of Physics, University of Siegen, Germany.

5. Institute of Physics, TU Chemnitz, Germany.

email: matthias.zschornak@physik.tu-freiberg.de

Strontium titanate (SrTiO_3) is an oxide crystallizing with cubic perovskite-type of structure that exhibits a high tunability of electronic properties by means of defects. Apart from dopants, especially intrinsic defects and predominantly oxygen vacancies may severely alter the crystal's properties.

We have investigated the dynamics of oxygen vacancies in SrTiO_3 causing structural as well as symmetry changes under influence of an external electric field. Defect migration and separation in the crystal induce remarkable electronic modifications, accompanied with whole regions of a new metastable phase exhibiting repealed centrosymmetry, polar character and pyro- as well as piezoelectricity. These structural changes have been thoroughly studied by means of in-situ X-ray Diffraction, I-V characteristics, Raman, Sharp-Garn and Resonant X-ray Scattering. Structural dynamics in response to the electric field occur on two different time-scales, due to slow ionic transport on the one hand and rapid electronically driven atomic displacements on the other. Theoretical models have been developed to account for the experimental findings and will be presented in conjunction to the experimental results.

Keywords: oxides, perovskites, structural symmetry, defects, migration, electroformation, DFT

MS16-O4 Room temperature polarisation and magnetisation in a bulk layered perovskite by control of octahedral tilt distortions

Michael J. Pitcher¹, John B. Claridge¹, Matthew J. Rosseinsky¹

1. Department of Chemistry, University of Liverpool L69 7ZD, UK

email: michael.pitcher@liv.ac.uk

Combining spontaneous, switchable polarisation and magnetisation into a single phase “multiferroic” material is a major challenge in materials chemistry. Such materials, with strongly coupled electric and magnetic polarisation, could provide the basis for low-energy high-density information storage devices but are unlikely to be viable unless they can operate at (or close to) ambient temperatures. The design and synthesis of multiferroic materials is difficult because the typical electronic requirements of polarisation (P) and magnetisation (M) are antagonistic: *e.g.* proper ferroelectrics such as $\text{PbZr}_{1-x}\text{Ti}_x\text{O}_3$ require closed-shell s^2 and d^0 cations, while ferromagnetism at ambient temperatures requires a high concentration of open-shell cations.[1] Materials where both of these conditions are fulfilled above 300 K are very rare, and even in the leading example of BiFeO_3 – where P arising from the Bi^{3+} sublattice is combined with long-range antiferromagnetic order of the Fe^{3+} sublattice – the generation of an appreciable magnetisation and magnetoelectric coupling is challenging.[2] It is therefore important that new strategies for combining P and M at high temperatures are investigated. One basis for such a strategy is provided by recent theoretical work on “hybrid improper” ferroelectrics, which describes how specific combinations of octahedral tilt distortions in layered $(\text{AO})(\text{ABO}_3)_n$ perovskites may be used to break inversion symmetry.[3, 4] We have applied these structural principles to a carefully selected $(\text{AO})(\text{ABO}_3)_2$ parent phase with a strongly magnetic B-site sublattice, using chemical control to produce the desired polar distortion in a new series of compounds which order magnetically above room temperature.[5] In this series, electrical polarisation and spontaneous magnetisation are induced simultaneously by control of the same structural distortion (an octahedral tilt); these properties are therefore coupled (as demonstrated by a linear magnetoelectric response) and are shown to coexist at temperatures of up to 330 K across a range of compositions.[5]

1. N. A. Hill, *J. Phys. Chem. B*, **104**, 6694-6709 (2000)

2. G. L. Yuan and S. W. Or, *J. Appl. Phys.*, **100**, 024109 (2006)

3. N. A. Benedek and C. J. Fennie, *Phys. Rev. Lett.*, **106**, 107204 (2011)

4. J. M. Rondinelli and C. J. Fennie, *Adv. Mater.*, **24**, 1961-1968 (2012)

5. M. J. Pitcher *et al.*, *Science* **347**, 420-424 (2015)

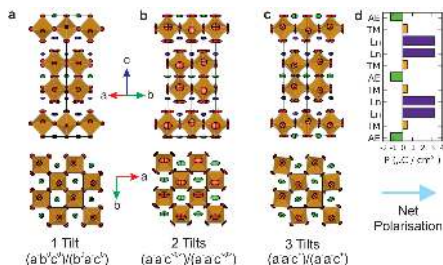


Figure 1. Successive octahedral tilt distortions imposed on a family of Fe-based $n = 2$ Ruddlesden-Popper phases by chemical substitution. (a – c) Refined crystal structures from neutron powder diffraction. (d) Layer-by-layer polarisation of the 3 tilt ($a^+a^-c^+$)/($a^-a^+c^-$) structure.

Keywords: perovskite, polar, weak ferromagnetism, magnetoelectric

MS16-O5 Imaging the dynamics of polar nanoregions in $\text{PbSc}_{0.5}\text{Ta}_{0.5}\text{O}_3$ using transmission electron microscopy and 'digital' electron diffraction

Ana M. Sanchez¹, R. Beanland¹, J. Peters¹, J. Jeffs¹, J. Edmondson¹, K. Evans¹, R. Römer^{1,2}

1. Department of Physics, University of Warwick, Coventry, West Midlands, CV4 7AL
2. Centre for Scientific Computing, University of Warwick, Coventry, West Midlands, CV4 7AL

email: a.m.sanchez@warwick.ac.uk

The existence of dynamically fluctuating regions with a dipole moment (polar nanoregions, or PNRs) in some relaxor materials is now generally accepted as necessary to explain their dielectric response. However little, if any, direct experimental observations of such regions have been made. Here, we show that fluctuating contrast can be observed under appropriate imaging conditions in $\text{PbSc}_{0.5}\text{Ta}_{0.5}\text{O}_3$ (PST) at room temperature using transmission electron microscopy. Its appearance is consistent with the existence of a domain or 'tweed' structure that is continuously altering on a time scale of milliseconds or less. We find that the domains become smaller and fluctuate more rapidly on heating as the Curie temperature is approached, while they enlarge and slow down upon cooling, switching over seconds or being completely frozen at liquid nitrogen temperature. They are linked to the presence of additional spots visible in electron diffraction patterns. We use 'digital' large angle convergent beam electron diffraction (D-LACBED) to obtain information about the symmetry of single frozen domains in PST.

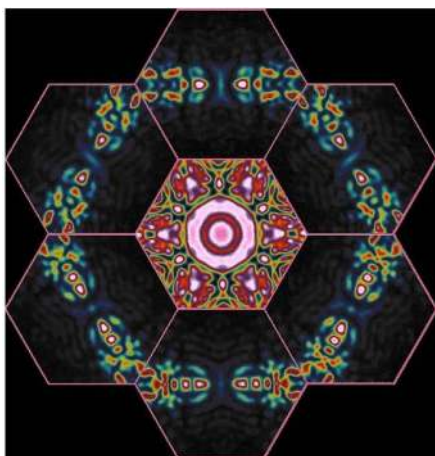


Figure 1. Digital large angle convergent beam electron diffraction (D-LACBED) pattern from a pseudo-cubic [111] zone axis from PST at 130K, showing mirror symmetry. This is incompatible with the nominal spacegroup of R3, but is consistent with R3m or R3c.

Keywords: Relaxor, ergodic, PNRs, tweed, digital diffraction

MS16-O6 Microstructural evolution of the ferroelectric solid solution $x\text{BiScO}_3$ -(1-x) PbTiO_3 throughout its morphotropic phase boundary

Kaustuv Datta^{1,2}, Andreas Richter³, Matthias Göbbels³, Reinhard Neder¹, Boriana Mihailova²

1. Department of Crystallography and Structure Physics, Friedrich-Alexander-Universität Erlangen-Nürnberg, Staudtstraße 3, Erlangen - 91058, Germany.
2. Department of Earth Sciences, Universität Hamburg, Hamburg - 20146, Germany
3. Department of Mineralogie, Friedrich-Alexander-Universität Erlangen-Nürnberg, Schlossgarten 5a, Erlangen - 91054, Germany.

email: kaustuv.phys@gmail.com

The structural state at the morphotropic phase boundary (MPB) is an important theme in the research of ferroelectric materials since ferroelectric solid solutions exhibit enhanced physical properties near MPB composition. Although an established understanding of creating MPB behaviour relies on invoking instability of average crystal structure or a low-symmetry monoclinic phase in the system driven by composition^[1], the actual mechanism is far more complex and heavily dependent on the local ordering of the cations as evidences found in recent diffuse scattering studies^[2] on either lead-free or lead-based based systems. We have studied an important and popular ferroelectric system $x\text{BiScO}_3$ -(1-x) PbTiO_3 , which was first reported in 2001^[1] with MPB characteristics^[3], using the total elastic scattering and Raman scattering methods to better understand its microstructural evolution as a function of composition and temperature in the vicinity of the MPB. Total scattering technique, which is essentially the analysis of the pair distribution function (PDF) of a system, provides crucial structural information at the microscopic level which are not easily available from conventional structural analysis like Rietveld refinement. Neutron powder diffraction experiments were carried out on six different compositions of $x\text{BiScO}_3$ -(1-x) PbTiO_3 in the range $0.30 < x < 0.40$ and neutron PDFs were analysed through RMC simulations to extract the behaviour of individual cations. It was observed that locally there was no abrupt change in any of the cation-cation correlations to assign the MPB unambiguously, however a trend was noticed in the distribution of directions of Ti cation including an ordering between Ti and Sc. These observations were corroborated by the Raman scattering data which further distinguish the roles different cations in terms of composition-induced and temperature-induced phase transitions for this system^[4].

Reference:

- [1] R. Guo, L. E. Cross, S-E. Park *et al* Phys. Rev. Lett. **84**, 5423-5426 (2000). [2] D. J. Goossens, ISRN Materials Science, **2013**, 107178/1-17 (2013). [3] R. E. Eitel, C. A. Randall, T. R. Shrout *et al*, Jpn. J. Appl. Phys. **40**, 5999 (2001). [4] K. Datta, A. Richter, M. Göbbels, R. B. Neder and B. Mihailova Phys. Rev. B **90**, 064112 (2014).

Keywords: ferroelectric materials, morphotropic phase boundary, pair distribution function, Raman scattering

MS17. In situ and in operando crystallography

[1] H. Ehrenberg, A. Senyshyn, M. Hinterstein, H. Fuess (2012). In Situ Diffraction Measurements: Challenges, Instrumentation, and Examples. In E.J. Mittermeier & U. Welzel (Eds.), *Modern Diffraction Methods* (528). Weinheim: Wiley-VCH.

Keywords: neutron scattering, Li-ion batteries

Chairs: Ivan Halasz, Nikolay Tumanov

MS17-O1 In-situ neutron scattering studies of Li-ion batteries

Anatoliy Senyshyn¹, Martin J. Mühlbauer², Oleksandr Dolotko¹,
Helmut Ehrenberg²

1. Heinz Maier-Leibnitz Zentrum, Technische Universität München, Germany

2. Institut für Angewandte Materialien - Energiespeichersysteme, Karlsruhe Institute of Technology, Germany

email: anatoliy.senyshyn@gmail.com

The energy storage media based on Li-ion technology have received a broad use in different applications ranging from supplying of portable devices to large electric vehicles. Despite its overall advantages and popularity, the Li-ion technology possess numerous drawbacks, which cannot be overcome and require systematic and detailed research, e.g. on issues concerning safety, stability of electrode materials, capacity improvements, temperature, homogeneity etc.

Modern Li-ion batteries are sophisticated electrochemical devices, possessing numerous degrees of freedom along with complicated geometries of the electrode integration, which change their state immediately after opening. This calls for new dedicated experimental techniques capable to reveal the information about processes occurring inside the cell "live". On the other hand the need for non-destructive battery testing eligible to minimize the risks for possible materials oxidation, electrolyte evaporation, cell charge changes *etc.* becomes of increasing importance in recent years.

In this sense neutron scattering has already been a well established tool for characterization of complex Li-containing systems [1], where the high penetration depths of thermal neutrons suits perfectly for non-destructive studies; the capability to localize light elements, e.g. hydrogen, lithium, provides excellent phase contrast; the neutron scattering lengths (not depending on $\sin(q)/\lambda$) give accurate structure factors leading to precise analysis of bond-length and Debye-Waller factor. In the current contribution the combination of two neutron-based experimental techniques, namely computed neutron tomography and neutron powder diffraction (both high-resolution and spatially-resolved), applied for studies on commercial Li-ion cells of the 18650-type (most common design with graphite and LiCoO_2 , used as anode and cathode, respectively) will be presented. Different aspects of lithium-ion battery organization on different length scales vs. chemical composition, fatigue, state-of-charge, temperature will be presented and discussed in brief.

MS17-O2 Analysis of complex phase transitions using time resolved XRPD data

Robert Dinnebier¹

1. Max-Planck-Institute für Solid State Research, Heisenbergstrasse 1, 70569 Stuttgart, Germany

email: r.dinnebier@fkf.mpg.de

Due to recent upgrades of synchrotron- and laboratory sources and the parallel development of new position sensitive detectors and reaction cells, it is now possible to collect a vast amount of powder diffraction patterns *in situ* in dependence on external variables (i.e. temperature or pressure) with a time resolution in the second or even sub-second regime thus allowing to track many complex structural changes in detail [1-6]. The real challenge is to get the maximum amount of information from these high quality data. In principal, the information content of a powder pattern is huge, but much effort is needed to reveal the often hidden information. In the last decade, many new ideas have been successfully applied to powder diffraction, like the method of maximum entropy (MEM), fundamental parameters, global optimization in direct space, parametric Rietveld refinement, kinetics, distortion mode amplitudes, to name just a few. It is the intention of this talk to discuss some hot topics in powder diffraction concerning methodology and application to various problems in solid state research. [1] Tomislav, F., Halasz, I. Beldon, P.J., Belenguer, A.M., Adams, F., Kimber, S.A.J., Honkimaäki, V., Dinnebier, R.E., *Nature Chem.*, **2013**, 5, 66–73. [2] Magdysyuk, O.V., Denysenko, D., Weinrauch, I., Volkmer, D., Hirscher, M., Dinnebier, R. E., *Chem. Commun.*, **2015**, 51, 714-717. [3] Magdysyuk, O.V., Müller, M., Dinnebier, R.E., Lipp, C., Schleid, T. J., *Appl. Crystallogr.*, **2014**, 47, 701-711. [4] Panda, M.K., Runčevski, T., Chandra, Sahoo, S., Belik, A.A., Nath, N.K., Dinnebier, R.E., Naumov, P., *Nat. Commun.*, **2014**, 5, 4811-4818. [5] Runčevski, T., Petrusevski, G., Makreski, P., Ugarkovic, S., Dinnebier, R.E., *Chem. Commun.*, **2014**, 50, 6970–6972. [6] Runčevski, T., Blanco-Lomas, M., Marazzi, M., Cejuela, M., Sampedro, D., Dinnebier, R.E., *Angew. Chem. Int. Ed.*, **2014**, 53, 6738-6742.

Keywords: *in situ* powder diffraction, parametric Rietveld refinement

MS17-O3 Kinetics of strain mechanisms in functional materials: Stroboscopic powder diffraction on piezoceramics

Manuel Hinterstein¹, Markus Hoelzel², Jérôme Rouquette³, Michael Knapp⁴, Helmut Ehrenberg⁴, Mark Hoffman¹

1. UNSW Australia, School of Materials Science and Engineering, 2052 Sydney, Australia

2. Research Reactor Heinz-Maier-Leibnitz (FRM II), Lichtenbergstr., Garching, Germany

3. Université Montpellier II, Institut Charles Gerhardt UMR CNRS 5253 Equipe C2M, Place Eu-gene Bataillon, Montpellier, France

4. Karlsruhe Institute of Technology, Institute for Applied Materials, 76344 Eggenstein-Leopoldshafen, Germany

email: m.hinterstein@unsw.edu.au

Piezoelectric ceramics exhibit the remarkable property to couple elastic strain and polarization under the influence of an applied electric field. Among the various types of ferroelectric devices only actuators rely on high electric fields to generate high strains and forces. Prominent examples for actuators are multilayer stack actuators used for nanopositioning or in modern combustion engines for automobiles to control injection cycles. Despite extensive studies and elaborated measurement techniques, the correlation between macroscopic strain and structural response is still not fully understood. Most of the relevant systems found up to now are compositions close to phase boundaries linking highly correlated phases. This results in major challenges for structural analyses due to overlapping reflections. Apart from the well-known field induced structural responses such as domain switching and the piezoelectric effect we recently identified field induced phase transitions in different systems as an additional poling mechanism [1,2]. In order to resolve all three involved poling mechanisms within only one experiment we developed a structural analysis technique with *in situ* X-ray and neutron powder diffraction data [3]. The results not only separately reveal the contributions of each poling mechanism to the macroscopic strain, but also different behaviours of the individual phases. In several studies on lead containing as well as lead free systems we found significant changes while crossing the phase boundaries. Additionally, the calculation of the elastic strain perfectly matches the macroscopic observations, confirming the accuracy of the applied models. With specially designed pump-probe stroboscopic data acquisition routines we recently were able to investigate these effects on time scales down to the microsecond regime. In this contribution we present the latest research on the elucidation of strain mechanisms in piezoceramics of different solid solution systems with perovskite structure. [1] M. Hinterstein, M. Knapp, M. Hoelzel, W. Jo, A. Cervellino, H. Ehrenberg and H. Fuess, *J. Appl. Phys.* **43**, 1314 (2010). [2] M. Hinterstein, J. Rouquette, J. Haines, Ph. Papet, M. Knapp, J. Glaum and H. Fuess, *Phys. Rev. Lett.* **107**, 077602 (2011). [3] M. Hinterstein, M. Hoelzel, J. Rouquette, J. Haines, J. Glaum, H. Kungl, M. Hoffman, *Acta Mater.* in revision (2015).

Keywords: piezoceramics, *in situ*, electric field, strain

MS17-O4 Real-time monitoring of the crystal / amorphous transformation in the β -trehalose molecular compound

William Pagnoux¹, Pierre Bordet¹, Pauline Martinetto¹, Aleksei Bychkov², Jean-François Willart¹, Emeline Dudognon¹, Marc Descamps³

1. Institut Néel, CNRS & Université Joseph Fourier, BP166, 38042 Grenoble, France

2. Institut Laue-Langevin, 6 rue Jules Horowitz, BP 156, F-38042 Grenoble, France

3. UMET, Univ. Lille 1, F-59655 Villeneuve d'Ascq, France

email: william.pagnoux@neel.cnrs.fr

A vast majority of “new” pharmaceutical compounds, in their crystalline form, are poorly soluble in water and need to be ground during the industrial fabrication process. These molecular crystals can undergo solid state transformations induced by the external stress, one of the most important being amorphization, known to generally improve bioavailability. Formulating drugs in the amorphous state is considered to be one of the most promising methods to improve dissolution properties. However, one main issue is the lack of understanding of the crystal-to-amorphous transformation mechanism.

Since now, the structural information on this transformation were obtained using *ex-situ* PXRD techniques. In this work, we have investigated *in situ* the evolution of the structure and microstructure of β -Trehalose during the milling itself. This provides a deeper insight into the amorphisation and recrystallization processes. This model molecular compound is well known to amorphize upon milling¹. We used Rietveld refinement and PDF analysis of high energy PXRD data. The former allows investigating the structure and microstructure but is limited to at least partly crystalline materials, while the latter can bring continuous information on particle size and internal arrangement whatever the crystallization state. Data were measured *ex situ* at the CRISTAL synchrotron beam line at SOLEIL and *in situ* as function of grinding time (ID15-ESRF) and temperature (ID11-ESRF). Samples were previously submitted to high energy milling for increasing times and characterized by DSC, Raman spectroscopy and laboratory PXRD. For the ID15 experiment, an oscillating milling device equipped with Perspex sample containing jars and zirconia balls was used².

Our study demonstrates that amorphization by energy milling is a 2 phase process, with immediate appearance of an amorphous fraction increasing with milling time, while the proportion and domain size of the remaining “crystalline” fraction decreases. High resolution data seem to indicate a modification of the local structure upon amorphisation, and temperature dependent data (figure) confirm a similar effect for the abrupt recrystallization occurring upon heating. The results of our investigations will be detailed during the conference.

This work is fund by the ANR project MiPhaSol.

[1] J. F. Willart, et al., Solid State Communications 119 (2001) 501

[2] T. Friščić, I. Halasz, W. Jones & al., Angew. Chemie - Int. Ed. 2013, 52 (44)

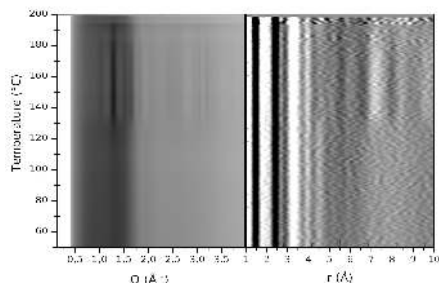


Figure 1. Temperature-dependent PXRD (left) and PDF (right) data of a 3h milled β -Trehalose sample, measured on heating at 3K/min on ID11-ESRF.

Keywords: Pharmaceuticals, X-Ray Diffraction, in-situ milling, in-situ recrystallization, Pair distribution function

MS17-O5 In situ synchrotron PXRD studies of the formation and growth of nanoparticles under solvothermal conditions

Peter Nørby¹, Martin Roelsgaard¹, Bo B. Iversen¹

¹. Department of Chemistry, Center of Materials Crystallography, Aarhus University, Denmark

email: noerby@chem.au.dk

It is well-known that the physical and chemical properties of nanoparticles can be modified by minor changes of either the morphology, size and/or crystal phase (ref. 1). Although, nanoparticles have been used for more than two decades in a range of different applications, such as photovoltaics, catalysis and sensing is the optimization of the properties based on empirical evidence. In situ crystallographic tools have proven useful in revealing the mechanism underlying the formation of nanoparticles. For the further progress in the development of tailored nanoparticles, understanding the mechanisms controlling formation and growth during solvothermal synthesis is of key importance.

We have used in situ synchrotron powder X-ray diffraction (PXRD) to study the formation and growth of different technological important materials such as colloidal monodisperse spherical Cu_{2-x}S nanoparticles synthesised in dodecanethiol (ref. 2), $\text{Y}_3\text{Al}_5\text{O}_{12}$ (ref. 3) and CoSb_2O_4 nanoparticles synthesised under hydrothermal supercritical conditions. It is vital for future improvements in properties that the extracted crystallographic information from in situ PXRD is translated into unique information about how to control the size and phase of nanoparticles. We have previous shown for Cu_{2-x}S nanoparticles how the crystalline precursor $[\text{CuSCl}_2\text{H}_{25}]$ decomposes upon heating and forms an isotropic liquid, which subsequently turns into colloidal β -chalcocite phase Cu_2S nanoparticles. In the present study on CoSb_2O_4 nanoparticles we show by in situ PXRD how the precursor stoichiometry influences the formation mechanism of the nanoparticles. The activation energy for the formation of phase pure CoSb_2O_4 is analysed and compared to similar oxides. Furthermore, we show how the crystallite size of CoSb_2O_4 nanoparticles varies as a function of synthesis temperature and time.

[1] Burda, C.; Chen, X. B.; Narayanan, R.; El-Sayed, M. A., *Chem. Rev.* 2005, 105, 1025

[2] Nørby, P.; Johnsen, S.; Iversen, B. B., *ACS Nano*, 2014, 8 (5), 4295

[3] Nørby, P.; Jensen, K. M. Ø.; Lock, N.; Christensen, M.; Iversen, B. B., *RSC Adv.* 2013, 3, 15368

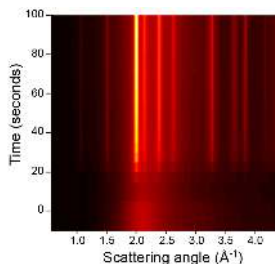


Figure 1. Sharpening of the Bragg peaks of CoSb_2O_4 as a function of synthesis time, resulting from the growth of the nanoparticles. The colour scale display the intensity of each peak.

Keywords: In situ PXRD, nanoparticles, formation, growth

MS18. Thermoelectric materials - from fundamental science to applications

Chairs: Oliver Oeckler, Sylvie Hébert

[1] Nolas, Sharp, Goldsmid, *Thermoelectrics Basic Principles and New Materials developments*, (Springer, 2001)

[2] G.J. Snyder & E.S. Toberer, *Nat. Mat.* **7**, 105 (2008)

[3] M. Christensen et al., *Dalton Transactions* **39**, 978 (2010)

[4] M.M. Koza et al., *Nat.Mat.* **7**, 805 (2008); *Phys. Rev. B* **81**, 174302; **84**, 014306; **89**, 014302; **91**, 014305; *J.Phys.Soc.Jpn.* **82**,114607 (2013)

[5] M.M. Koza et al., *Phys.Chem.Chem.Phys.* **16**, 27119 (2014)

Keywords: phonons, lattice thermal conductivity

MS18-O1 Structure dynamics relation of thermoelectric materials studied by neutron spectroscopy and *ab initio* calculations

Michael M. Koza¹

1. Institut Laue Langevin, B.P. 156, 38042 Grenoble, France

email: koza@ill.fr

Minimizing the lattice thermal conductivity k_l is one promising way of improving the figure of merit of thermoelectric materials [1,2]. Several mechanisms are known leading to a strong reduction of k_l . The most efficient mechanisms are due to complex structures resulting in a general diminishment of heat-carrying vibrational states and to scattering of the heat-carrying acoustic phonons. Phonon scattering can be accomplished in many ways. Imperfection of a structure in the form of site and chemical disorder, presence of voids, interfaces, surfaces and dislocations open up temperature independent scattering channels. In perfectly ordered, crystalline matter umklapp-scattering and multi-phonon events establish efficient scattering mechanisms at high temperatures.

In thermoelectric materials all those mechanisms are simultaneously present. Moreover, the interplay of disorder, anharmonicity and structure deformation on temperature and pressure changes can lead to new and non-stationary features in the dynamics of the compounds which can open up additional decay channels for acoustic phonons. The anharmonic off-center motion of cations in clathrates is one example of such complex dynamics [3].

A comprehensive characterization of the interplay of acoustic phonons with scattering centres requires their discrimination and the understanding of their effect on the collective dynamics on a microscopic scale. This prerequisite is met by Inelastic Neutron Scattering (INS) and neutron diffraction. INS is a spectroscopic technique sampling the 4-dimensional phase space of energy and momentum matching the energies of collective vibrational excitations and the interatomic distances in thermoelectric compounds. We present a characterization of the dynamics of filled skutterudites [4] and of the open-framework compounds AV₂Al₂₀ (A = Al, Ga, Sc, La) and AOs₂O₆ (A = K, Rb, Cs) [5]. We discuss the aspect of collective dynamics as well as the consequences of so called 'rattling' modes for the lattice thermal conductivity of these compounds.

References

MS18-O2 Inhomogeneity and anisotropy of chemical bonding in thermoelectric materials

Yuri Grin¹

1. Max-Planck-Institut für Chemische Physik fester Stoffe

email: Juri.Grin@cpfs.mpg.de

Two different strategies are employed to enhance the thermoelectric ability of materials in general and intermetallic compounds in particular. The electron-engineering approach deals with the effecting the electronic structure around the Fermi level in order to maximize the thermopower and/or to enhance the charge carrier mobility. The 'phonon engineering' utilizes the phonon glass-electron crystal concept creating centers scattering more strongly phonons than electrons. When the electron-engineering approach in the development of the thermoelectric materials is well established technique, the phonon-engineering part - the interconnection between the low thermal conductivity and crystal structures - is still offering a play yard for new chemical thoughts. Precise information about atomic ordering in the crystal structures of thermoelectrics allows better description and calculation of the electronic structure. The obtaining of this information requires often combination of spectroscopic techniques in addition to the diffraction ones. To get more insight into the thermoelectric behavior, the chemical bonding descriptors were found to be suitable analytical tool. Spatial separation of the regions with different atomic interactions in the crystal is an indicator for enhanced thermoelectric ability. For the compounds with the characteristic structural and bonding features, structural and bonding complexity opens an opportunity to influence more directly the thermal conductivity separating - at least partially - its lattice and electronic parts.

Keywords: Crystal structure; atomic ordering; chemical bonding

MS18-O3 Thermoelectric properties of Cu-doped germanium antimony tellurides

Stefan Schwarzmueller¹, Daniel Souchay¹, Gerald Wagner¹, Oliver Oeckler¹

1. Leipzig University, IMKM, Scharnhorststr. 20, 04275 Leipzig, Germany.

email: stefan.schwarzmueller@uni-leipzig.de

The high mobility of Cu atoms in thermoelectric materials like Cu_xSe ,^[1] Cu_{2-x}S ^[2] or Cu_xPSe_6 ^[3] leads to low thermal conductivities due to effective phonon scattering, as described by the phonon-liquid electron-crystal (PLEC) concept.^[1] However, these materials often lack high electrical conductivities, so that thermoelectric figures of merit (ZT) do not exceed 1 at temperatures up to 500 °C.

Inspired by thermoelectric chalcogenides with the group 11 element Ag (TAGS-materials),^[4,5] this issue was addressed by replacing Ag by Cu in samples with the compositions $\text{Cu}_x\text{Ge}_{1-x/2}\text{Sb}_2\text{Te}_{1.5}$ ($0 \leq x < 2$). For $1 \leq x$, homogeneous samples were obtained. They show phase transitions between metastable quenched pseudocubic and layered phases as well as NaCl-type high-temperature phases, similar to germanium antimony tellurides without Cu.^[6] Higher copper concentrations (e.g. $x = 0$) lead to a minority phase of Cu_2Te . HRTEM investigations reveal endotactically intergrown Cu_2Te precipitates ranging from 50 to 500 nm in a matrix which corresponding to $x \approx 1$. Temperature-dependent synchrotron powder diffraction (ID11, ESRF Grenoble) enables the detection of such precipitates and their structures, until they dissolve in the matrix at 425 °C during heating and reform at 350 °C during subsequent cooling. Samples with $x = 0$ show a lattice thermal conductivity of 0.35 $\text{W m}^{-1} \text{K}^{-1}$ at 500 °C, which is similar to that of Cu_xPSe_6 and thus below the theoretical glassy limit.^[3] The thermal conductivity as well as the Seebeck coefficient increase with increasing x . The maximum value for the electrical conductivity is similar for all compositions at around 650 S cm^{-1} but is shifted to lower temperatures with increasing x (500 °C for $x = 0$; 300 °C for $x = 1.66$). The materials show high figures of merit (ZT), approaching 2.0 for $x = 1.33$ at 480 °C.

[1] H. Liu, X. Shi, F. Xu, L. Zhang, W. Zhang, L. Chen, Q. Li, C. Uher, T. Day, G. J. Snyder, *Nat. Mater.* **2012**, *11*, 422.

[2] Y. He, T. Day, T. Zhang, H. Liu, X. Shi, L. Chen, G. J. Snyder, *Adv. Mater.* **2014**, *26*, 3974.

[3] K. S. Weldert, W. G. Zeier, T. W. Day, M. Panthöfer, G. J. Snyder, W. Tremel, *J. Am. Chem. Soc.* **2014**, *136*, 12035.

[4] F. D. Rosi, E. F. Hockings, N. E. Lindenblad, *RCA Rev.* **1961**, *22*, 82.

[5] T. Schröder, T. Rosenthal, N. Giesbrecht, M. Nentwig, S. Maier, H. Wang, G. J. Snyder, O. Oeckler, *Inorg. Chem.* **2014**, *53*, 7722.

[6] T. Rosenthal, M. N. Schneider, C. Stiewe, M. Döblinger, O. Oeckler, *Chem. Mater.* **2011**, *23*, 4349.

Keywords: heterostructures, ion-liquid-like thermoelectrics, germanium antimony tellurides, HRTEM

MS18-04 From tiny to tinier: combining techniques to reveal complex crystal intergrowths

Serena C. Tarantino^{1,2}, Alberto Zanetti¹, Nobuyoshi Miyajima³, Michele Zema^{2,4}, Florian Heidelbach³, Paolo Ghigna², Luca Olivi⁶, Maurizio Mazzucchelli⁷

1. CNR-IGG, Pavia, Italy
2. Dept. of Earth and Environmental Sciences, University of Pavia, Italy
3. Bayerisches Geoinstitut, University of Bayreuth, Germany
4. International Union of Crystallography, Chester, UK
5. Dept. of Chemistry, University of Pavia, Italy
6. Elettra, Sincrotrone Trieste S.C.p.A., Italy
7. Dept. of Chemical and Geological Sciences, University of Modena and Reggio Emilia, Italy.

email: tarser06@unipv.it

A combined approach which makes use of long- and short-range crystallographic tools, such as optical, scanning and transmission electron microscopies, electron backscatter diffraction (EBSD), X-ray Absorption Spectroscopy (XAS), together with X-ray and electron diffraction has been used to characterize the highly unusual tight alternation of diopside and titanian pargasite lamellae. These lamellae have been observed in samples from spinel dunitites belonging to the subcontinental mantle peridotite body of Balmuccia (Ivrea-Verbano Zone, Italy). The complicated multiphase arrangements displayed by most technological and geological materials on the one hand have dramatic effects on the physical properties of the material itself and, on the other hand, record its history. Microscopic inspections showed that in some grains, the thickness of the clinopyroxene lamellae (~20 µm) is around ten times that of amphibole, whereas in other cases the thicknesses of the two phases are comparable (2-5 µm). EBSD maps revealed an extremely ordered phase separation, in which amphibole lamellae, as well as the late crystals, are all parallel to (010) in the pyroxene, as expected on the basis of crystallographic considerations and in agreement with TEM observations. Diffraction contrast images showed the presence of finer (less than 100 nm) amphibole lamellae in the diopside, as well as the presence of semi-coherent interfaces giving rise to dislocations. Moreover, chain-width defects within the titanian pargasite have been revealed by HR-STEM images. STEM energy dispersive analyses revealed major element gradients across alternation of nm-scale lamellae, with diopside showing Al, Ti, Na and Fe increasing towards the contact with amphibole. Preliminary insights into the local structure of Ti⁴⁺, indicating a highly distorted octahedral coordination, have been obtained by means of XAS at the Ti-K edge performed on the same crystals. On the basis of these observations, hypotheses on the origin of the tight alternation of diopside and titanian pargasite lamellae in such magmatic systems will be discussed.

Keywords: crystal intergrowth, diffraction, electron microscopy

MS18-05 Transmission electron microscopy characterization of precipitate/matrix interfaces in doped Mn₄Si₇ thermoelectric crystal

Andrey Orekhov¹, Elena Suvorova¹

1. Shubnikov Institute of Crystallography of RAS, Moscow, Russia

email: andrey.orekhov@gmail.com

Higher manganese silicides (HMS) MnSi_{1.71-1.75} could attract more attention as potential middle-temperature thermoelectric materials that are cheap and non-toxic [1]. It was reported [2] that HMS crystals grown by Bridgman method with Ge, Mo and Al impurities had better properties (ZT~0.7) as well the amount of MnSi precipitates significantly reduced. Impurities in the HMS crystal lattice are believed can contribute to increasing the electrical conductivity and decreasing the thermal conductivity, and thus to the improvement of the thermoelectric performance. This paper reports the results of electron microscopy study of Al, Ge, Mo doped HMS crystals with general formula of ((Mn_{0.98}Mo_{0.02})(Si_{0.98}Ge_{0.02})_{1.75}Al_{0.01}) grown by the Bridgman technique at 1473 K in Ar atmosphere. Microstructures and phase analysis of as grown samples were examined by SEM, EBSD and by HRTEM/HRSTEM. Chemical composition was estimated by energy dispersive X-ray spectroscopy (EDS) in both SEM and TEM. Electron diffraction patterns and EDS data showed the formation of tetragonal Mn₄Si₇ single crystals. No other Mn-Si phases with the stoichiometry of MnSi_{1.71-1.75} were observed. The crystal matrix contains Al and Mo ~0.5 ± 0.3 at% and Ge ~1.5 ± 0.4 at%. No extra reflections on matrix crystal diffraction pattern were observed that means dopant elements occupy atom sites by substitution. Two types of nanosize precipitates in matrix crystal were found. Elliptical shape grains with 20x50 nm dimensions were arranged along [001]Mn₄Si₇. Another type precipitates were about 250 nm with strip-like structure. Nanodiffraction technique was applied for precipitates phase analysis. Hexagonal Mn₅Si₃ and cubic MnSi were observed for two types of precipitates. The structure of precipitates/matrix interface was examined by HRTEM. FFT filtering revealed extra planes at interfaces. The orientation relationships of precipitates/matrix were determined. The micro and nanostructure data of doped HMS may serve to optimize of crystal grows condition.

1. CRC Handbook of Thermoelectrics. Ed. D. M. Rowe (CRC Press, Boca Rayton, FL, 1995).

2. I. Aoyama, M.I. Fedorov, V.K. Zaitsev et al. // Jpn. J. Appl. Phys., 2005, V. 44, № 12 P. 8562-8570

Keywords: Structure of interfece, doped crystal, higher manganese silicide

MS19. Topology of crystal structures

Chairs: Davide Proserpio, Tonči Balić-Žunić

MS19-O1 Topological properties of crystal structures: from description to prediction

Vladislav A. Blatov¹

¹. Samara Center for Theoretical Materials Science, Samara State University, Samara, Russia

email: blatov@samsu.ru

Topological methods become more and more popular in crystal chemistry and materials science. At present, many topological descriptors are used to characterize and classify crystal structures. Here we consider the most important descriptors that feature local and overall architecture of the periodic networks. We mention the methods, software and databases that are used for the topological analysis and present some new ones.

However, the main purpose of the presentation is to show that the topological tools can be used not only to describe, but also to search for relations between crystal structures and to predict their topological motifs. With examples of molecular crystals, coordination polymers and intermetallic compounds we demonstrate how a knowledge database containing correlations 'chemical composition – local topology – overall topology' can be built from the initial experimental data. This database can then be used in an expert system to list possible local environments for a given structural unit (suprclusters) as well as possible extended architectures that can be assembled from the suprclusters. The probabilities of appearance of the corresponding topological motifs can be estimated that can essentially help in generation of trial structures for the subsequent evaluation by the DFT methods. Thus the topological tools being qualitative or semi-quantitative can be involved in the design of new crystalline materials in combination with the quantitative methods of mathematical modeling.

The work was supported by the Russian government (Grant 14.B25.31.0005).

Keywords: Topological methods, molecular crystals, coordination polymers, intermetallics, prediction

MS19-O2 Lanthanide-organic frameworks for optical sensing and nanothermometry

João Rocha¹

¹. University of Aveiro, CICECO, Department of Chemistry, Aveiro, Portugal

email: rocha@ua.pt

Ln^{3+} -organic frameworks (LnMOFs) are very promising materials for tackling the challenges in engineering of luminescent centres, also presenting much potential as multifunctional systems [1]. Very few other solid-state systems provide the unique opportunities of MOFs to establish relationships between structure, topology and optical properties.

Only 10% or so of MOFs are effectively microporous, exhibiting zeolite-type behaviour, and photoluminescence. The combination of porosity and light emission allows the design of intriguing new types of chemical species and temperature sensors, which I shall highlight here, namely: (i) nanoporous $\text{Eu}(\text{4,4'-(hexafluoroisopropylidene)bis(benzoic acid)})$ MOFs with anisotropic photoluminescence and magnetic properties and their application to sense ethanol in air [2]; (ii) miniaturized linear pH sensor based on a highly photoluminescent self-assembled $\text{Eu}/1,10\text{-phenanthroline-2,9-dicarboxylic acid}$ MOF [3]; (iii) aqueous suspensions of $\text{Tb}/\text{Eu}/1\text{-4-benzendicarboxylate}$ nanoparticles displaying an excellent performance as radiometric luminescent nanothermometers in the physiological-temperature (300-320 K) range [4]; (iv) one of the most sensitive cryogenic thermometers ($5.96\% \text{K}^{-1}$ at 25 K) reported so far, $[(\text{Tb}_{0.914}\text{Eu}_{0.086})_2(\text{PDA})_3(\text{H}_2\text{O})_2 \cdot 2\text{H}_2\text{O} (\text{PDA}=1,4\text{-phenylenediacetic acid})]$, consisting of LnMOFs nanoparticles [5]; (v) post-synthetic covalent modification of IRMOF-3 followed by the coordination to Nd/Yb affords unusual near-infrared light-emitting materials [6].

I acknowledge CICECO-Aveiro Institute of Materials (Ref. FCT UID/CTM/50011/2013), financed by national funds through the FCT/MEC and when applicable co-financed by FEDER under the PT2020 Partnership Agreement.

[1] Rocha J., Carlos L. D., Paz F. A. A., Ananias D., *Chem. Soc. Rev.*, **40**: 926 (2011).

[2] Harbuzaru B. V., Corma A., Rey F., Atienzar P., Jordá J. L., García H., Ananias D., Carlos L. D., Rocha J., *Angew. Chem. Int. Ed.*, **47**: 1080 (2008).

[3] Harbuzaru B. V., Corma A., Rey F., Jordá J. L., Ananias D., Carlos L. D., Rocha J., *Angew. Chem. Int. Ed.*, **48**: 6476 (2009).

[4] Cadiou A., Brites C. D. S., Costa P. M. F. J., Ferreira R. A. S., Rocha J., Carlos L. D., *ACS Nano*, **7**: 7213 (2013).

[5] Wang, Z., Ananias, D., Carminé-Sánchez, A., Brites, C. D. S., Imaz, I., MasPOCH, D., Rocha, J., Carlos, L.D., *Adv. Funct. Mater.*, in press.

[6] Abdelhameed R. M., Carlos L. D., Silva A., Rocha J., *Chem. Commun.*, **49**: 5019 (2013).

Keywords: MOFs, lanthanides, structure, photoluminescence, sensing, nanothermometry

MS19-O3 Space group of periodic cubic $\langle 110 \rangle$ six-way cylinder packing structures

Yoshinori Teshima¹, Takeo Matsumoto², Moreton Moore³

1. Chiba Institute of Technology, Department of Mechanical Science and Engineering, Narashino, Japan

2. Kanazawa University (Emeritus Professor), Department of Earth Sciences, Kanazawa, Japan

3. Royal Holloway University of London (Emeritus Professor), Department of Physics, Egham, UK

email: yoshinori.teshima@it-chiba.ac.jp

In the field of science, the complex structure of garnet has been explained on the basis of cylinder packing to be a periodic structure with a cubic $\langle 111 \rangle$ four-way cylinder packing [1]. Since then, cylinder packings have been extensively applied in the field of crystal chemistry. In particular, homogeneous cubic cylinder packings have been thoroughly investigated [2, 3]. In the field of engineering as well, cylinder packings are important for determining the fiber packings of composite materials [4, 5, 6]. The focus of our research is packing structure of equal cylinders having infinite length; specifically, the directions of these cylinders are restricted to six cubic $\langle 110 \rangle$ directions, namely, $A[1\ 1\ 0]$, $B[1\ -1\ 0]$, $C[1\ 0\ 1]$, $D[-1\ 0\ 1]$, $E[0\ 1\ 1]$, and $F[0\ 1\ -1]$. We refer to such a structure as a $\langle 110 \rangle$ six-way cylinder packing. There are several distinct $\langle 110 \rangle$ six-way cylinder packings [7, 8]. The known $\langle 110 \rangle$ six-way cylinder packings can be classified into three categories on the basis of packing density: $(\sqrt{2})\pi/9 \approx 0.494$ (Type-I), $(\sqrt{2})\pi/18 \approx 0.247$ (Type-II), and $(351\sqrt{2} + 108\sqrt{6})\pi/1936 \approx 0.376$ (Type-III). Recently, Teshima and Matsumoto studied the space group of the Type-III structure [9]. And Moore reported another type of periodic cubic $\langle 110 \rangle$ six-way cylinder packing structure (packing density ≈ 0.133) [10, 11]. In this study, authors will mention the space group of the Type-I and Type-II and consider a general description of periodic cubic $\langle 110 \rangle$ six-way cylinder packing structures.

[1] O’Keeffe, M. and Andersson, S. (1977) *Acta Cryst.*, **A33**, 914–923.

[2] O’Keeffe, M., Plévert, J., Teshima, Y., Watanabe, Y., and Ogawa, T. (2001) *Acta Cryst.*, **A57**, 110–111.

[3] O’Keeffe, M., Plévert, J., and Ogawa, T. (1992) *Acta Cryst.*, **A48**, 879–884.

[4] Hatta, H. (1988) *J. Japan Soc. Composite Materials*, **14**, 73–80.

[5] Hijikata, A. and Fukuta, K. (1992) *J. Japan Soc. Composite Materials*, **18**, 231–238.

[6] Parkhouse, J.G., and Kelly, A. (1998) *Proc. R. Soc. Lond.*, **A454**, 1889–1909.

[7] Teshima, Y. (1995) *Bussei Kenkyu*, **65**, 405–439 [in Japanese].

[8] Teshima, Y., Watanabe, Y., and Ogawa, T. (2001) *Springer-LNCS*, **2098**, 351–361.

[9] Teshima, Y. & Matsumoto, T. (2012) *Glass Phys. Chem.* **38**, 41–48.

[10] Moore, M. (1970) Laboratory notebook, 31 January 1970 (unpublished).

[11] Moore, M. & Teshima, Y. (2013) *Acta Cryst.* **A69**, s227 (ECM 28, 2013).

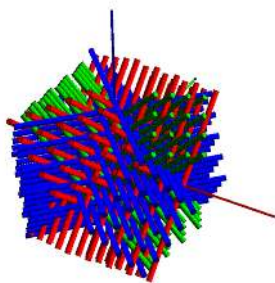


Figure 1. Overview of cylinder packing along six cubic $\langle 110 \rangle$ directions: Type-III

Keywords: cylinder packing, space group, symmetry

MS19-O4 Fluorite-related framework in the $\text{Pd}_{11}\text{As}_2\text{L}_2$ family of crystal structures

Oxana V. Karimova¹

1. Institute of Geology of Ore Deposits RAS, Staromonetny 35, Moscow, Russia

email: oxana.karimova@gmail.com

Recently, the crystal structures of palladium minerals with common formula $\text{Pd}_{11}\text{As}_2\text{L}_2$ ($\text{L}=\text{Sb, Te, Bi}$) were studied [1]. Isomertieite, $\text{Pd}_{11}\text{As}_2\text{Sb}_2$ (I), and törnroosite, $\text{Pd}_{11}\text{As}_2(\text{Te,Bi})_2$ (II), are cubic, sp.gr. $Fd-3m$, $Z=8$, unit-cell parameters for (I): a 12.297(5) Å, V 1859.3(2) Å³; for (II): $a=12.350(2)$ Å, $V=1883.6(4)$. Minerals are structurally isotype.

Isomertieite and törnroosite are intermetallic compounds, but their crystal structures can be described in terms Pauling polyhedrons. Palladium atom is considered as a center of a polyhedron, and As, Sb (or Te) atoms are considered as ligands. There are three types of Pd polyhedrons in the structure: PdAs_4 tetrahedra, PdSb_3As or PdTe_3As tetrahedra, and PdSb_3As_3 or PdTe_3As_3 octahedra. Pd polyhedrons share common edges forming three-dimensional framework.

Fluorite-related framework can be seen in the isomertieite crystal structure type. The framework of F-centered tetrahedra (FCa_4) is one of classic description of fluorite crystal structure. Kang and Eyring [2] used anion-centered tetrahedra for description of the rare earths oxides. Fluorite-related frameworks are made by four types “fluorite module” in the Kang-Eyring systematic. Krivovichev [3] extended Kang-Eyring system for the wide range of fluorite-related structures with vacancies in both anion and cation sites.

Fluorite modules of D_1 and U^3 types can be described in the structure of isomertieite and törnroosite. They are built up from seven tetrahedrons: six PdL_3As tetrahedra and one PdAs_4 tetrahedra. The supermodule in the $\text{Pd}_{11}\text{As}_2\text{L}_2$ structure is made by 8 fluorite modules. The supermodule has $p \times q \times r$ dimensions equal $2 \times 2 \times 2$ (accordance to Krivovichev system). Alternation of modules D_1 and U^3 types in the unit-cell is: layer 1 $\text{D}_1 \text{U}^3 \text{D}_1$ / layer 2 $\text{U}^3 \text{D}_1 \text{D}_1 \text{U}^3$. Four Pd-octahedra are joined together via common edges in a clusters. Pd-octahedra clusters located in a cavities of the tetrahedral framework.

This study is a part of IGEM RAS №72-3 basic research.

Acknowledgments. Author thanks Dr. T.L. Grokhovskaya, V.V. Gurzhiy and A.A. Zolotarev for their assistance in this scientific research. Single crystal study of isomertieite and törnroosite was made at the XRD Center SPbSU.

References

1. Kang Z. C., Eyring L. // J. Alloys Comp. 1998. V. 275, 30

2. Karimova O.V., Grokhovskay T.L., Gurzhiy V.V., Zolotarev A.A., Borisovskiy S.E. // 12 Platinum Symp. Yekaterinburg, Russia. 2014. Abstracts. 253.

3. Krivovichev S.V. // Solid State Sci. 1999. v.1, 211



Figure 1. Fluorite modules (a) and their alternation (b, c); and tetrahedral framework (d) in the isomertieite structure type.

Keywords: crystal structure, palladium arsenide, palladium telluride, fluorite-related framework

MS19-05 Templation effects and novel ZIF structures by solid state synthesisIvana Brekalo¹, Joseph R. Ramirez¹, Christopher M. Kane¹, K. Travis Holman¹¹. Department of Chemistry, Georgetown University, Washington, D.C. 20057, USA

email: ib308@georgetown.edu

In the last decade zeolitic imidazolate frameworks (ZIFs), a subclass of metalorganic frameworks (MOFs), have been rising in popularity due to their diverse topologies, good thermal and chemical stability, and large pore volumes, which could enable their use for gas-storage, separation of gases, and catalysis.¹ However, traditional solution synthesis methods are very energy demanding, they use large quantities of organic solvents and rather expensive inorganic nitrates as starting material, and, above all, are often irreproducible and hard to control, giving mixtures of different ZIF frameworks in often low yields. Mechanochemical alternatives have been proposed, including neat grinding², ion and liquid assisted grinding (ILAG)³, and most recently, accelerated aging⁴.

We explored several different methods for solid state ZIF synthesis, including neat and liquid-assisted grinding, slurring, as well as a modified accelerated aging procedure, giving rise to novel ZIF structures. We also show that we can direct the outcome of ZIF syntheses to frameworks containing a specific structural motif by employing an organic template using several different synthetic methods.

[1] Park, K.S.; Ni, Z.; Côté, A. P.; Choi, J. Y.; Huang, R.; Uribe-Romo, F. J.; Chae, H.H.; O’Keeffe, M.; Yaghi, O. M. *Proc. Natl. Acad. Sci. U. S. A.* **2006**, *103*, 10186–10191.

[2] Tanaka, S.; Kida, K.; Nagaoka, T.; Ota, T.; Miyake, Y.; *Chem. Commun.*, **2013**, *49*, 7884–7886.

[3] Beldon, P. J.; Fabian, L.; Stein, R. S.; Thirumurugan, A.; Cheetham, A. K.; Friščić, T. *Angew. Chem. Int. Ed.* **2010**, *46*, 9640–9643

[4] Cliffe, M. J.; Mottillo, C.; Stein, R. S.; Bučar, D.-K.; Friščić, T. *Chem. Sci.*, **2012**, *3*, 2495.

Keywords: zeolitic imidazolate frameworks, solid-state synthesis, templation

MS20. High pressure solid state chemistry

Chairs: Natalia Dubrovinskaya, Wilson Crichton

MS20-01 High-pressure high-temperature synthesis of new covalent metalsUlrich Schwarz¹¹. Max Planck Institute for Chemical Physics of Solids, Dresden, Germany

email: Ulrich.Schwarz@cpfs.mpg.de

In the last two decades, the advent of modern in-situ high-pressure x-ray diffraction techniques has markedly developed our knowledge of exotic structure patterns. The alteration of atomic configurations opens perspectives to substantially manipulate the electronic properties of solids. The increased number of neighbors in the atomic coordination sphere may give rise to an enlarged band dispersion and eventually metallization. Particularly in covalent framework assemblies, the combination of directed bonding with a significant density of states at the Fermi level creates the promising situation of covalent metals. This unique blend of properties has proven to be beneficial for phonon-mediated superconductivity.

This way, high-pressure studies have supplemented the map of high-temperature superconductors as much as they stimulated profound studies of the underlying principles. A straightforward method to access the useful effects of compression at ambient pressure is provided by synthesizing metastable compounds at extreme conditions. Recent preparation results and physical properties of selected binary compounds comprising covalent framework patterns will be discussed.

References

- A. Wosylus, Yu. Prots, U. Burkhardt, W. Schnelle, U. Schwarz, *STAM* **8**, 383 (2007). K. Meier, R. Cardoso-Gil, W. Schnelle, H. Rosner, U. Burkhardt, U. Schwarz, *ZAAC* **636**, 1466 (2010). K. Meier, L. Vasylychko, R. Cardoso-Gil, U. Burkhardt, W. Schnelle, M. Schmidt, Yu. Grin, U. Schwarz, *ZAAC* **636**, 1695 (2010). A. Wosylus, K. Meier, Yu. Prots, W. Schnelle, H. Rosner, U. Schwarz, Yu. Grin, *Angew. Chemie Int. Ed.* **49**, 9002 (2010). W. Schnelle, A. Ormeci, A. Wosylus, K. Meier, Yu. Grin, U. Schwarz, *Inorg. Chem.* **51**, 5509 (2012). K. Meier, A. Wosylus, R. Cardoso-Gil, U. Burkhardt, C. Curfs, M. Hanfland, Yu. Grin, U. Schwarz, *ZAAC* **638**, 1446 (2012). U. Schwarz, A. Wosylus, H.

Rosner, W. Schnelle, A. Ormeci, K. Meier, A. Baranov, M. Nicklas, S. Leipe, C. J. Müller, Yu. Grin, JACS 134, 13558 (2012). U. Schwarz, S. Tencé, O. Janson, C. Koz, C. Krellner, U. Burkhardt, H. Rosner, F. Steglich, Yu. Grin, Angew. Chemie Int. Ed. 52, 9853 (2013).

Keywords: high-pressure synthesis, binary compounds, metastable phases

MS20-O2 Crystal chemistry of postperovskite-type AMX_3 compounds

Yuichi Shirako^{1,2,3}, Youguo Shi^{4,5}, Jianshi Zhou², Kazunari Yamaura⁴, Masashi Hasegawa³, Masaki Akaogi¹

1. Department of Chemistry, Gakushuin University, Japan
2. Texas Materials Institute, Cockrell School of Engineering, University of Texas at Austin, USA
3. Department of Crystalline Materials Science, Nagoya University, Japan
4. Superconducting Properties Unit, National Institute for Materials Science, Japan
5. Institute of Physics, Chinese Academy of Science, P. R. China

email: shirako@numse.nagoya-u.ac.jp

Since the discovery of postperovskite type $MgSiO_3$, AMX_3 compounds with the postperovskite structure have attracted special attention for a recent decade in not only mineral physics but also condensed matter physics and materials science due to its alternative layered structure (ref. 1-6). Crystal chemistry of the postperovskite compounds has been quickly developed to seek for new postperovskite materials that are potentially useful in a variety of technology and science, regarding such as superconductivity and correlated electronics. It has been argued that ionic size and covalency are significant in stabilizing the postperovskite structure (ref. 7-10). Regarding ionic size, one can easily understand its effects on the tolerance factor and octahedral-site rotation of perovskite which may affect stability of the perovskite structure, leading to the perovskite to the postperovskite transition. However, in contrast, effects of bond covalency seem to be studied little over the perovskite-postperovskite transition. Therefore, no postperovskite compounds have been designed from a view point of covalent character except strong covalency in contrast to that of ionic size.

In this presentation, crystal chemistry of postperovskite materials in terms of nature of covalent bonds is discussed. These results indicate that the electron count of outermost shell of the cation which makes stronger covalent bond with anion than the other cation or total number of valence electrons of cluster ions is important as well as the electronegativity. It seems to be qualitatively similar with what was developed by Burdett et al for the other, some solid-state structures (ref. 11, 12). In addition, we will also report on a new material which was predicted based on these considerations.

- [1] Murakami et al., *Science*, **304**, 855 (2004).
- [2] Yamaura et al., *J. Am. Chem. Soc.*, **131**, 2722 (2009).
- [3] Cheng et al., *Phys. Rev. B*, **83**, 064401 (2011).
- [4] Shirako et al., *Phys. Rev. B*, **83**, 174411 (2011).
- [5] Ohgushi et al., *Phys. Rev. Lett.*, **110**, 217212 (2013).
- [6] Bernal et al., *Inorg. Chem.*, **53**, 12205 (2014).
- [7] Martin et al., *Am. Miner.*, **92**, 1912 (2007).
- [8] Ohgushi et al., *Phys. Chem. Miner.*, **35**, 189 (2008).

[9] Dobson et al., *Phys. Earth Planet. Int.*, **189**, 171 (2011).

[10] Akaogi et al., *Phys. Earth Planet. Int.*, **228**, 160 (2014).

[11] Burdett (1980), *Molecular Shapes*, Wiley-Int.

[12] Woodward, *Acta Cryst. B*, **53**, 44 (1997).

Keywords: perovskite, post-perovskite, nature of covalent bond, second-order Jahn-Teller distortion

MS20-O3 High pressure synthesis of bismuth disulfide, structural solution and its physical properties

Martin Bremholm¹, Simone M. Soendergaard-Pedersen¹, Morten B. Nielsen¹, Lars F. Lundegaard², Davide Ceresoli³, Yu-Sheng Chen⁴

1. Center for Materials Crystallography, Department of Chemistry and iNANO, Aarhus University, Denmark

2. Haldor Topsoe, Lyngby, Denmark

3. Center for Materials Crystallography and Institute of Molecular Science and Technology (CNR-ISTM), Milano, Italy

4. ChemMatCARS, The University of Chicago, Advanced Photon Source, Argonne, USA

email: bremholm@chem.au.dk

High pressure synthesis is an important method in the search for new compounds and in many cases pressure-stabilized compounds can be quenched to ambient conditions. Therefore high pressure syntheses push the boundaries of solid state chemistry. There is a large current interest in the metal dichalcogenides due to their crystal structures and electrical properties.^{1,2} The most sulfur rich phase in the Bi-S phase diagram is Bi₂S₃.³ Unlike the transition metal dichalcogenides, the Bi atoms in BiS₂ have anisotropic charge distribution and more complex structures are expected when comparing the layered structures of transition metal. The recent discovery of superconductivity in La(O,F)BiS₂ which consists of layers of insulating La(O,F) which donates electrons to superconducting layers of BiS₂, adds further motivation for studies of Bi dichalcogenides.⁴ Furthermore, bismuth chalcogenides, such the compound Bi₂S₃, are known to be good thermoelectric materials.⁵ The possibilities of using high pressure synthesis to discover new compounds in the Bi-S binary system were investigated as early as the 1960's.⁶ The research led to discovery of a compound with BiS₂ stoichiometry, but no structure solution of BiS₂ was reported. In this research the BiS₂ compound was synthesized by a high pressure and high temperature method using a multi-anvil large volume press and the structure was solved by single crystal x-ray diffraction. The structure contains Bi atoms in distorted square-based pyramidal coordination to five surrounding sulfur atoms. The structure, physical properties and theoretical calculations will be discussed and compared to other metal dichalcogenide compounds.

References

- [1] E. Selvi et al., *J. Phys. Chem Ref. Data*, 11(4), 1005, (1982).
- [2] M. Chhowalla et al., *Nature Chem.*, 5, 263, (2013).
- [3] J.-C. Lin et al., *J. Phase Equilib.*, 17(2), 132, (1996).
- [4] V. P. S. Awana et al., *Solid State Communications*, 157, 21, (2013).
- [5] Q. Yang et al., *J. Phys. Chem. C*, 117(11), 5515 (2013).
- [6] M. S. Silverman, *Inorg. Chem.*, 3(7), 1041 (1964).

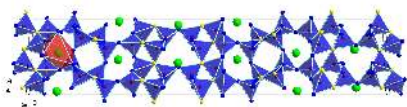
Keywords: High pressure, BiS₂, structure solution, metal dichalcogenides

MS20-O4 High-pressure synthesis of the new nickel borate $\text{HP-NiB}_4\text{O}_7$ Martin K. Schmitt¹, Hubert Huppertz¹

1. Institute of General, Inorganic and Theoretical Chemistry, Leopold-Franzens-University Innsbruck, A-6020 Innsbruck, Austria

email: martin.schmitt@uibk.ac.at

During the last decade, our research on the field of transition metal borates led to numerous new compounds like $\beta\text{-ZnB}_2\text{O}_7$ [1], $\text{M}_2\text{B}_{22}\text{O}_{39}\cdot\text{H}_2\text{O}$ ($\text{M} = \text{Fe}, \text{Co}$) [2], or $\text{HP-NiB}_2\text{O}_4$ [3], which is the first borate that shows exclusively BO_4 -tetrahedra sharing one common edge with a second BO_4 -tetrahedron. Here we present the new transition metal oxoborate $\text{HP-NiB}_4\text{O}_7$, which was synthesized starting from NiO and B_2O_3 under high-pressure/high-temperature conditions of 5 GPa and 900 °C in a Walker-type multianvil apparatus. Thus, this compound constitutes the low-pressure/low-temperature modification of the compound $\beta\text{-NiB}_2\text{O}_7$ [4], which was synthesized at 7.5 GPa and 1150 °C. $\text{HP-NiB}_4\text{O}_7$ crystallizes in the acentric, chiral space group P6_22 (No. 179) with $Z = 6$, $a = 4.258(6)$ Å, and $c = 34.882(7)$ Å. The structure consists of chains of BO_4 -tetrahedra, which are interconnected by B_2O_7 groups, thus forming a three-dimensional framework which contains the helically arranged nickel atoms (Fig. 1). This structure type is yet unknown in the field of borate chemistry underlining the importance of the parameter pressure in synthetic solid state chemistry. The characterization of the compound is complemented by magnetic and spectroscopic investigations.

Figure 1. Crystal structure of NiB_4O_7 **Keywords:** Borates, High-pressure, Synthesis**MS20-O5** Extreme-pressure loading of fuel related gases into nanoporous materials: unusual uptake behaviour in a Sc-based metal-organic frameworkJorge Sotelo^{1,2,3}, Christopher Woodall¹, Paul A. Wright², John Mowat³, Stephen A. Moggach^{1,2}

1. Centre for Science in Extreme Conditions, The University of Edinburgh, UK.

2. EaStChem School of Chemistry, The University of Edinburgh, UK.

3. EaStChem School of Chemistry, The University of St. Andrews, UK.

email: j.sotelo@ed.ac.uk

The development of new methods of storing, trapping or separating light gases, such as CO_2 or CH_4 has become of outmost importance from an environmental and energetic point of view. Porous materials such as zeolites and porous organic polymers have long been considered good candidates for this purpose. More recently, the ample spectrum of existing metal organic frameworks (MOFs) together with their functional and mechanical properties have attracted even further interest.¹ The channels found in these materials are ideal for the uptake of guests of different shapes and sizes, and with careful design they can show high selectivity. Adsorption properties of MOFs have been thoroughly studied,² however obtaining in depth structural insight into the adsorption/desorption mechanism of these materials is challenging, usually because the adsorbed species is hard to locate using crystallographic methods within the large porous cavities of a MOF, resulting in only partially occupied guests even at tens of bars of gas pressure and low temperatures.

Here we present high-pressure structural data on the microporous scandium framework, Sc_2BDC_3 ($\text{BDC} = \text{benzene-1,4-dicarboxylate}$) with included methane molecules from 2 to 25 kbar.³ Using a modified Merrill Bassett Diamond Anvil Cell (DAC) setup, CH_4 was cryoadsorbed into the DAC to 2 kbar. On initially loading the cell, it was possible to locate fully ordered adsorption sites for methane, in which previously only partially ordered sites were observed using an environmental gas-cell set-up (on the small molecule beamline I19, at the DIAMOND light source, UK), with methane loaded at much lower pressures (5 bar). Furthermore, increasing the pressure beyond 10 kbar resulted in a transition to a previously unobserved phase of Sc_2BDC_3 , where the b -axis of the ortho- F cell tripled. Although, the framework remains largely unaltered, the superfilling of the pores at high-pressures with methane translates into a re-ordering of the adsorption sites which permit a greater uptake of CH_4 . High-pressure cryoadsorption of gaseous molecules under ambient conditions may therefore provide a fruitful way in which to study much more easily the adsorption sites in porous MOFs via diffraction techniques, obtaining atomistic models which were previously unobtainable.

[1] T. D. Bennet, *et al.*, *CrystEngComm*, 17(2), 286 (2015)

[2] Special Issue on Metal-Organic Frameworks, *Chem Rev.*, 112, 673 (2012)

[3] S. R. Miller, *et al.*, *Chem. Commun.*, 30, 3850 (2005)

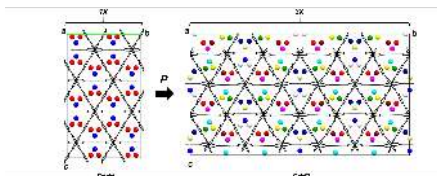


Figure 1. Upon application of pressure a transition to a previously unobserved phase of Sc_2BDC_4 is observed. The new phase has the b-axis of the ortho- F cell tripled and a rearrangement of the CH_4 adsorption sites.

Keywords: High-pressure crystallography, gas storage, nanoporous materials.

MS21. Advances in high-pressure methods

Chairs: Leonid Dubrovinsky, Ronald Miletich

MS21-O1 Extreme conditions beamline at Petra III, DESY: status and perspectives

Konstantin Glazyrin¹, Zuzana Konopkova¹, Wolfgang Morgenroth¹, Mario Wendt¹, Hanns-Peter Liermann¹

1. DESY

email: lorcat@gmail.com

Fast evolution of applied and fundamental sciences requires probing of material properties in the space of pressure, temperature and time. Application of X-ray diffraction to the matter subjected to extreme conditions can lead to new fascinating discoveries and improve our understanding of physical phenomena on macro- and micro-scale. Diamond Anvil Cell (DAC) high pressure technique has de facto become a standard, and its development has made it possible to perform direct experimental tests of old and new scientific concepts previously considered as extremely challenging or even impossible. The constantly growing strong demand from different scientific communities stimulates large scale facilities to provide more and more stations either dedicated or stations capable to conduct high pressure studies a part of their operation time.

Extreme Conditions Beamline (ECB - P02.2) of Petra III, DESY, Hamburg, Germany, is dedicated to micro X-ray diffraction studies of matter (powder or single crystal) at simultaneous high-pressure and high/low-temperatures.

We review current capabilities of the beamline and provide a description of sample environments available to users for high-pressure studies conducted in the DAC (e.g. laser heating, cryostat, resistive heating and etc.). As an overview of our capabilities we present case studies and demonstrate results obtained at the beamline (geoscience, material science, etc.). Then, we discuss future plans to upgrade the beamline. Here, we highlight developments of single crystal diffraction at simultaneous high-pressure and high/low temperatures employing laser/resistive heated DAC as well as cryogenically cooled DACs. Finally, we discuss the possibility to conduct time resolved single crystal diffraction studies using partial or 'pink' Laue diffraction - a technique under commission at the ECB at the moment.

Keywords: X-ray diffraction, static compression, Petra III large scale facility,

MS21-O2 Combined use of x-ray diffuse and inelastic scattering for the vibrational spectroscopy – and beyond

Alexei Bossak¹

1. European Synchrotron Radiation Facility, 71 avenue des Martyrs
Grenoble, France

email: bossak@esrf.fr

Since more than ten years the diffuse scattering studies re-gained their place in the domain of lattice dynamics investigations. The use of thermal diffuse scattering becomes particularly efficient, when coupled with the vibrational spectroscopy, i.e. inelastic x-ray scattering, and state-of-the-art *ab initio* calculations. Thermal diffuse scattering experiments can serve as a rigorous benchmark for parameter-free model calculations even for relatively complex structures, in particular if they are complemented with inelastic scattering techniques on powder, single crystals or both of them. Once the validity of the model is established, it then can be used to gain valuable insight into the dynamical properties of materials, often in a more meaningful way than from phonon dispersion curves or phonon-density-of-states alone. Acquisition of diffuse scattering roadmaps prior to the inelastic scattering experiment, particularly in the case of non-trivial (i.e. strongly correlated) systems is highly beneficial for choosing the experimental strategy, sometimes providing crucial information and always reducing the necessary measurement time. ID28 phonon spectroscopy beamline at ESRF has gained its place in the domain of high pressure studies thanks to versatile focusing scheme. Presently, dedicated side station for the diffuse scattering/diffraction studies is under construction. Being operational in parallel to the spectroscopic branch, it will not only improve the throughput of inelastic scattering experiments, but will be also productive for high-quality diffraction data collection under “medium” pressure, with further extension to 1 Mbar range upon ESRF machine upgrade.

Keywords: inelastic scattering, diffuse scattering, high pressure

MS21-O3 OrientXplot – a program to analyse and display relative crystal orientations

Ross J. Angel¹, Sula Milani¹, Matteo Alvaro², Fabrizio Nestola¹

1. University of Padova

2. University of Pavia

email: rossjohnangel@gmail.com

The correct determination of the relative orientations of single crystals has many applications. When single crystals undergo phase transitions, especially at high pressures, the relative orientations of the two phases yields insights into transition mechanisms. The orientations of olivines entrapped during diamond growth at extreme conditions within the Earth constrain the possible growth mechanisms of diamond (Nestola et al. 2014, *International Geology Review*). The crystallographic orientation of some inclusion minerals with respect to others in multi-phase inclusions found trapped inside minerals in rocks allows the crystallisation sequence of the inclusion to be deduced and thus further constraints to be placed upon the pressure-temperature history of the rock as a whole (Malaspina et al., 2015, *Contributions to Mineralogy & Petrology*).

Orientations of single crystals are usually determined by in-situ X-ray diffraction or ex-situ EBSD or electron diffraction. For a comparison between the orientations of guest crystals in different hosts, it is necessary to take into account the ambiguity in indexing the diffraction patterns that arises from the symmetry of both the guest and the host crystals. Failure to allow for this ambiguity can lead to errors in interpretation of orientation data, or failure to recognise systematics in the relative orientations of two phases. We have developed OrientXplot, a Windows™ program that reads all common types of orientation matrices and calculates and displays the relative orientations of pairs of crystals, such as twins or inclusion crystals trapped inside host crystals. OrientXplot can manipulate (under user control) the relative orientation matrices to apply the crystal symmetries and analyse the results. Relative orientation data can be displayed on a stereogram, or output in numerical form for plotting in external programs.

Although the program was originally written to analyse the orientations of single-crystal inclusions, it can be used to analyse and display in stereograms the relative orientations of any type of crystal pairs, including crystals deposited on substrates, twinned crystals, and domains arising from phase transitions. As such, it is both a research and a pedagogic tool.

OrientXplot is available free from www.rossangel.net. Development supported by ERC grant 307322 to F. Nestola.

Keywords: Software, single-crystal orientations, twinning

MS21-O4 Effect of various pressure media on the compressibility of the pressure standard quartz

Katharina S. Scheidl¹, Peter Kainzbauer², Alexander Kurnosov³,
Ronald Miletich¹

1. Department of Mineralogy and Crystallography, University of Vienna, Althanstraße 14, 1090 Vienna, Austria

2. Department of Inorganic Chemistry (Materials Chemistry), University of Vienna, Währinger Straße 42, 1090 Vienna, Austria

3. Bayerisches Geoinstitut, University of Bayreuth, Universitätsstraße 30, 95447 Bayreuth, Germany

email: katharina.sarah.scheidl@univie.ac.at

The diamond-anvil cell (DAC) technique has been successfully implemented to generate high pressures for *in situ* investigations. To compress material hydrostatically an appropriate pressure transmitting medium is required, which does not interact with the samples. Because of its simple loading, 4:1 methanol-ethanol mixture is most commonly used, but inert noble gases (such as argon, neon and helium) grow in popularity. However, helium is well known to interact with open framework structures like zeolites¹ as well as with compact structures like olivine² due to its ability to interpenetrate crystals as a consequence of its small atomic radius. In addition, helium atoms even diffuse into the diamond anvils and make them mechanically brittle³. The applied pressure in the chamber of the DAC is measured by means of pressure sensors; the most prominent materials are ruby⁴ and quartz⁵. Using the precisely determined equation-of-state (EoS) parameters of quartz, pressures can be derived. Compared to the dense structure of hcp-packed oxygen atoms in ruby, the structure of quartz represents a relatively open framework. Thus, the question arises to what extent noble-gas atoms intercalate and simultaneously stiffen the quartz structure relative to EoS parameters reported for quartz in non-penetrating pressure media⁵. The aim of this study is to determine the EoS parameters of quartz relative to volume and R-line shifts of ruby on compression in 4:1 methanol-ethanol, argon, neon and helium. Series of comparative compressibilities up to 10 GPa have been performed on a (10-10) orientated quartz crystal, which was loaded together with two different ruby crystals (each one in (11-20) and (0001) orientation). Apart from the positions of the R1 lines of both ruby crystals the unit-cell parameters of all sample crystals were measured in order to determine the EoS parameters through fitting the data to an appropriate Birch-Murnaghan equation. A comparison of the results obtained from the analogous experiments carried out in different pressure media will be presented.

References

[1] R.M. Hazen and L.W. Finger; Journal of Applied Crystallography, 14, 234-236 (1981).

[2] R.T. Downs et al.; Mineralogical Society of America, 81, 51-55 (1996).

[3] A. Dewaele et al.; Journal of Applied Physics, 99, 1-5 (2006).

[4] H.K. Mao et al.; Journal of Geophysical Research, 91, 4673-4676 (1986).

[5] R.J. Angel; Journal of Applied Crystallography, 30, 461-466 (1997).

Keywords: diamond anvil cell, pressure transmitting medium, pressure standard, quartz

MS21-O5 Development of a moderate pressure cell for the small molecule beamline I19 at Diamond Light Source

Charlie J. McMonagle¹, Scott C. McKellar¹, Jorge Sotelo¹, Mark R. Warren², Dave R. Allan², Stephen A. Moggach¹

1. EaStChem School of Chemistry, The University of Edinburgh, EH9 3JJ, UK
2. Diamond Light Source, Rutherford Appleton Laboratory, Didcot, UK.

email: c.j.mcmonagle@ed.ac.uk

Since the invention of diamond anvil cells (DACs), they have become the primary pressure cell design that has dominated high pressure science when kbar pressures are required. They have made data collection (both single-crystal and powder) routine, however they are not without their limitations. Fine control of pressure is difficult to achieve and measure accurately, particularly at lower pressures. For most molecular systems studied at pressure, this is not an issue, though often interesting phase behaviour or compressibility can occur even below 1 kbar. Currently there is relative paucity of pressure cell designs with cells capable of generating pressure from ambient pressure to several kbar.

Currently, gas cells have been made which allow 100's of bar of pressure to be applied to a crystal using a compressed gas, though these systems have primarily been built to study the uptake of gases into porous materials¹ or chemical reactions between the gas and the solid sample at elevated temperature and pressure.²⁻⁴ This falls somewhat short of the kbars of pressure required to close the gap on DACs.

Here we have begun to develop a static liquid cell capable of reaching 4 kbar that would not only close the pressure gap between current gas cell technology and DACs, but allow the investigation of materials from vacuum, to 4 kbar with the sample in a hydrostatic environment and as a function of very small pressure steps (ca 1 bar), allowing for the first time a high degree of crystallographic detail to be obtained without the usual limitations associated with modern DAC technology. This will allow us to observe structural changes, phase transitions and calculate with much greater precision the bulk moduli of soft molecular materials.

1 Yufit, D. S. & Howard, J. A. K. J. Appl. Crystallogr. 38, 583-586, (2005).

2 Chupas, P. J. et al. J. Appl. Crystallogr. 41, 822-824, (2008).

3 Jensen, T. R. et al. J. Appl. Crystallogr. 43, 1456-1463, (2010).

4 Andrieux, J. et al. J. Appl. Crystallogr. 47, 245-255, (2014).

Keywords: moderate pressure crystallography, new instrumentation

MS22. High response systems in practical and extreme conditions

Chairs: Yaroslav Filinchuk, Dmitry Chernyshov

MS22-O1 Time-resolved X-ray diffraction reveals the origins of high dielectric and electromechanical responses in ferroelectrics

Sem  n Gorfman¹, Hyeokmin Choe¹, Michael Ziolkowski¹, Thanakorn Iamsasti², Jacob Jones², Vladimir Shvartsman³, Jan Dec⁴, Ullrich Pietsch¹

1. Department of Physics, University of Siegen, D57072, Siegen, Germany

2. Department of Materials Science and Engineering, North Carolina State University, Raleigh, NC, 27695, USA

3. Institute for Materials Science, University of Duisburg-Essen, D-45141 Essen, Germany

4. Institute of Materials Science, University of Silesia, 12 Bankowa Street, PL-40-007 Katowice, Poland

email: gorfman@physik.uni-siegen.de

Ferroelectrics are the class of materials in which two or more equivalent states of spontaneous polarization are switchable by an external electric field. Ferroelectrics are interesting for their excellent dielectric and piezoelectric properties. Although the strong responses of ferroelectrics to an external electric field are clearly connected to the intense dynamics of a ferroelectric switching, the details of the accompanying processes remain unclear. For example, it is particularly difficult to separate intrinsic (atomic) and extrinsic (domain-wall motion) contributions. Both of them may be equally important for the materials properties, they could be activated by electric fields of different magnitudes and have different temporal dynamics.

This presentation explores the mechanisms of high dielectric and piezoelectric response in ferroelectrics and related (e.g. relaxor ferroelectric) systems using time-resolved X-ray diffraction [1]. We benefit from the capabilities of X-ray diffraction to sense the variation of atomic, mesoscopic, macroscopic and even disorder parameters at the same time. This way the dynamics of e.g. atomic positions, domain sizes and lattice parameters under electric field can be investigated and interconnected with one another. We will demonstrate how our recent X-ray diffraction studies of $\text{Sr}_{0.5}\text{Ba}_{0.5}\text{Nb}_2\text{O}_6$ single crystals revealed that electromechanical response of uniaxial ferroelectrics may express the correlation between the lattice parameter(s) and their domain size(s) [2]. We will further show how an anomalous X-ray scattering allows studying intrinsic dynamics of polarization reversal in the perovskite-based $\text{BaTiO}_3\text{-BiZn}_{0.5}\text{Ti}_{0.5}\text{O}_3$.

- [1] S. Gorfman. *Cryst Rev*, 20(3): 210–232, (2014).
 [2] S. Gorfman, H. Choe, V. V. Shvartsman, M. Ziolkowski, M. Vogt, J. Strempler, T. Lukasevic, U. Pietsch, *J. Dec. Phys. Rev. Lett* 114, 097601, (2015).

Keywords: ferroelectrics, electromechanical coupling, time-resolved X-ray diffraction

MS22-O2 Structural flexibility in prototypical zeolitic imidazolate frameworks

Michael T. Wharmby¹, Sebastian Henke², Thomas D. Bennett², Caroline Mellot-Draznieks³, Yuanzheng Yue⁴, Anthony K. Cheetham²

1. Diamond Light Source Ltd., UK
2. Department of Materials Science & Metallurgy, University of Cambridge, UK
3. CNRS UMR 8229, Sorbonne Universités, UPMC Univ Paris 06, Collège de France, France
4. Section of Chemistry, Aalborg University, Denmark

email: michael.wharmby@diamond.ac.uk

In recent years, it has become apparent that certain Metal-Organic Framework (MOF) compounds demonstrate remarkable structural flexibility. Understanding this behaviour is crucial to interpreting adsorption in porous compounds. MIL-53 provides the prototypical example, undergoing an anisotropic 'breathing' transition on exchange of adsorbate molecules, by cooling or by application of mechanical pressure.¹ Phase transitions also influence the gas adsorption behaviour of Zeolitic Imidazolate Frameworks (ZIFs), a significant subclass of MOFs. ZIF-8 demonstrates a gate-opening transition on adsorption of gas molecules and application of mechanical pressure,^{2,3} which is achieved by a rotation of the methylimidazolate linker units to open the windows of the sodalite cages. ZIF-7, also bearing a sodalite framework, demonstrates a slightly different gate-opening transition, achieved by a concomitant rotation of the benzimidazolate linkers and a distortion of the structure.⁴

We report new results in the understanding of the nature of the phase transitions in ZIF-7 and -8 and most significantly, the first example of extreme isotropic flexibility in ZIF compounds.⁵ Desolvated ZIF-4(Zn) undergoes an isotropic phase transition on cooling from 298 K to 80 K, leading to a 23 % reduction in pore volume and a closure of the pore space. This porous to non-porous phase transition was investigated by *in situ* synchrotron powder X-ray diffraction, which allowed the mechanism to be determined and also to confirm its discontinuous nature. The new low temperature structure is marginally less dense than that of the densest known ZIF phase, ZIF-zni. By combining structural results with DSC measurements and DFT calculations, the driving force for this new and unexpected transition was established. Using these results, it is now possible to understand the gas adsorption behaviour of this important framework compound.

References

- 1 Serre *et al.*, *Adv. Mater.*, 2007, 19, 2246–2251.
- 2 Moggach *et al.*, *Angew. Chem. Int. Ed.*, 2009, 48, 7087–7089.
- 3 Fairen-Jimenez *et al.*, *J. Am. Chem. Soc.*, 2011, 133, 8900–8902.
- 4 Zhao *et al.*, *Chem. Mater.*, 2014, 26, 1767–1769.
- 5 Wharmby *et al.*, *Angew. Chem. Int. Ed.*, 2015, (accepted).

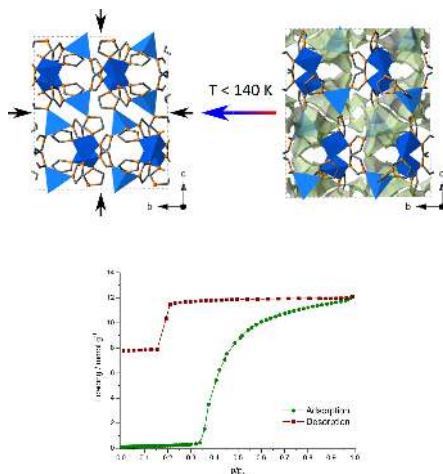


Figure 1. *Top:* Structural transition at 140 K in desolvated ZIF-4(Zn), showing the closure of the pore space (highlighted in green). Zn – blue; C – grey; N – orange. *Bottom:* N_2 adsorption isotherm at 77 K for ZIF-4(Zn). Large hysteresis is indicative of structural changes on adsorption.

Keywords: Porous/non-porous phase transition, zeolitic imidazolate framework, ZIF-4, ZIF-7, ZIF-8, low temperature, structure determination from powder data, breathing, gas adsorption, DFT

MS22-O3 Crystallographic features of the dehydration of samarium and yttrium oxalate decahydrates

Alexander Matvienko^{1,2}, Daniel Maslennikov³, Pavel Gribov², Stanislav Chizhik^{1,2}, Anatoly Sidelnikov¹, Boris Zakharov^{1,2}

1. Institute of Solid State Chemistry and Mechanochemistry, Kutateladze, 18, 630128, Novosibirsk, Russia

2. Novosibirsk State University, Pirogova, 2, 630090, Novosibirsk, Russia.

3. Université Montpellier 2, 34095, Montpellier cedex 5, France

email: matvienko67@gmail.com

The formation of solid product with new crystal structure usually occurs during solid state chemical reaction. The effects of this structural transformation on the morphology and kinetics of the reaction depend on the crystallographic features of a structural transformation. Hence, the ability to design and control the reaction product will depend on the ability to understand, and more importantly, to predict the crystallographic characteristics of a structural transformation. The analysis of the current knowledge and understanding of the crystallographic features of structural transformations is carried out in this work. Structural transformations during phase transformations are divided into two broad classes – the ‘reconstructive’ transformations and the ‘displacive’ transformations, exemplified by martensitic or shear transformations. This distinction is largely based on the mechanism of formation (nucleation and growth) of the product phase. The reconstructive transformations are thermally activated, involve migration of incoherent interface. The displacive transformations are associated with a glissile, coherent or partly coherent interface that migrates in a conservative fashion. There is always a correspondence between the matrix and product phase, together with a macroscopic change of shape of the transformed volume. We believe that this classification is valid for the structural transformation during solid state reactions. The comprehensive study of the structural and morphological changes during the dehydration reaction of samarium and yttrium oxalate decahydrates was carried out in this work. X-ray diffraction, TG-DTA methods, optical microscopy, TEM, SEM, Raman spectroscopy and N_2 sorption isotherm techniques were used. Basing on the analysis of structures, the orientation relations and shape deformations of crystals the mechanisms of the structural transformation were proposed. These transitions are similar to the displacive or martensitic transformations (Figure). However, the chemical reaction causes the transformation in this case. We used the crystallographic theories of martensitic transformation for the analysis of reaction-related deformation. Detailed analysis of atomic displacements was carried out and strain ellipsoids were obtained for each case. The reaction-related deformation determines the character of the fracture during the reaction.

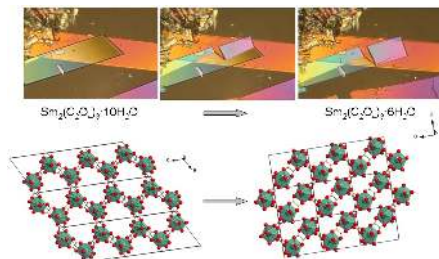


Figure 1. Changing crystal shape during dehydration of $\text{Sm}_2(\text{C}_2\text{O}_4)_3 \cdot 10\text{H}_2\text{O}$ in relation to crystal structure. Orientation relations: $[010]_{10} // [010]_6$, $[001]_{10} // [001]_6$, $(010)_{10} // (010)_6$

Keywords: dehydration reaction, structural transformation, displacive transformation, reaction-related deformation, fracture

MS22-O4 The solvent-dependent continuous breathing behaviour of a wine-rack MOF

Elliot J. Carrington¹, Craig McAnally², Ashleigh J. Fletcher²,
Stephen P. Thompson¹, Mark Warren³, Lee Brammer¹

1. University of Sheffield
2. University of Strathclyde
3. Diamond Light Source

email: dtp11ejc@sheffield.ac.uk

Metal-organic frameworks (MOFs) are a class of crystalline coordination polymers that are both highly porous and possess large internal surface areas. As a result of their structural diversity, chemical tunability and wide range of applications, these materials have gained popularity over the last couple of decades and a significant number of different framework structures are now known. Despite the large variety in the structures and in the building blocks, relatively few MOFs possess significant structural flexibility and even fewer exhibit continuous motions rather than defined phase transitions.

This talk will focus on the discovery of the novel flexibility exhibited by a previously reported wine-rack MOF. This MOF is a rare example that shows a large continuous breathing motion, which involves considerable changes in pore shape and size. These changes were not apparent from the originally published gravimetric adsorption isotherm, but have been identified by extensive crystallographic studies on the as-synthesised material. The breathing effect occurs in a single crystal-to-single crystal transformation with the change depending on the amount and type of contained solvent. These structural changes strongly affect the materials gas uptake. The selectivity has been monitored *in situ* using both single crystal and powder X-ray diffraction techniques



Figure 1. Representation of the changing pore shape upon loss of the as-synthesised solvent

Keywords: MOF, Flexible, Breathing

MS22-05 Pressure-induced phase transitions to non-superconducting polymorphs in the Wadsley-type bronzes $\beta\text{-A}_{0.33}\text{V}_2\text{O}_5$ (A = Li, Na)

Andrzej Grzechnik¹, Yutaka Ueda^{2,3}, Toru Yamauchi³, Michael Hanfland⁴, Paul Hering⁵, Vasily Potapkin⁵, Karen Fries⁵

1. Institute of Crystallography, RWTH Aachen University, 52066 Aachen, Germany

2. Toyota Chemical and Physical Research Institute, Nagakute, Aichi 480-1192, Japan

3. Institute for Solid State Physics, University of Tokyo, Kashiwa, Chiba 277-8581, Japan

4. European Synchrotron Radiation Facility, BP 220, 38043 Grenoble, France

5. Jülich Centre for Neutron Science, 52425 Jülich, Germany

email: grzechnik@xtal.rwth-aachen.de

$\beta\text{-A}_{0.33}\text{V}_2\text{O}_5$ bronzes (A = Li, Na, Ag) have a crystal structure (C2/m , $Z = 6$) [1] built of zigzag double strings of distorted VO_6 octahedra forming layers by joining corners. The adjacent layers are linked by chains of edge-sharing VO_5 tetragonal pyramids resulting in tunnels along the b axis. Each tunnel contains one symmetrically independent site that is partially occupied by the A^{1+} cations.

The low-dimensional $\beta\text{-A}_{0.33}\text{V}_2\text{O}_5$ bronzes exhibit metal-insulator phase transitions with successive charge-spin ordering at atmospheric conditions [2]. They are superconducting below about 8 K under high pressure, possibly due to a phase transition from the charge ordered to the superconducting phase [3]. The superconductivity occurs at about 7 GPa in $\beta\text{-Na}_{0.33}\text{V}_2\text{O}_5$ and $\beta\text{-Ag}_{0.33}\text{V}_2\text{O}_5$ and at about 9 GPa in $\beta\text{-Li}_{0.33}\text{V}_2\text{O}_5$. The exact mechanism of the superconductivity in these bronzes has not been presented so far. One of the most fundamental issues to be resolved is the determination of the underlying crystal structures. Here, we report on the high-pressure behaviour of $\beta\text{-Li}_{0.33}\text{V}_2\text{O}_5$ and $\beta\text{-Na}_{0.33}\text{V}_2\text{O}_5$ studied with synchrotron single-crystal diffraction in diamond anvil cells to 13 GPa and 20 GPa, respectively, at room temperature. $\beta\text{-Li}_{0.33}\text{V}_2\text{O}_5$ undergoes a series of transitions at about 9 and 11 GPa. $\beta\text{-Na}_{0.33}\text{V}_2\text{O}_5$ transforms to a new polymorph at about 12 GPa. Structure determinations and refinements reveal that the phase transitions in both materials are due to relative displacements of the adjacent octahedral layers. The relative position of the chains of edge-sharing VO_5 polyhedra with respect to the octahedral layers is changed. As a result, the tunnels populated by the A^{1+} cations collapse on compression. There is no evidence for the charge ordering of mixed-valence vanadium. Very strong one-dimensional diffuse scattering is observed in the intermediate high-pressure polymorphs indicating the presence of stacking faults.

Our observations strongly support the hypothesis that the underlying mechanism for superconductivity in the Wadsley-type $\beta\text{-A}_{0.33}\text{V}_2\text{O}_5$ vanadium bronzes is related to pressure-induced inter- and/or intra-ladder charge transfer or charge fluctuations in the two-leg ladder system present in the polymorphs with superconducting ground states [3].

References

1. A.D. Wadsley, *Acta Cryst.* 8, 695 (1955).
2. K. Ohwada et al., *Phys. Rev. B* 85, 134102 (2012).

3. T. Yamauchi, Y. Ueda, *Phys. Rev. B* 77, 104529 (2008).

Keywords: mixed-valence vanadates, crystal structure, high pressure

MS23-O2 Structure to property relations of single MBE grown GaAs and InAs nanowires onto silicon (111) studied by X-ray nanodiffraction

Ullrich Pietsch¹

1. Department of Physics, University of Siegen, 57068 Siegen, Germany

email: pietsch@physik.uni-siegen.de

Axial stacking faults separating zinc-blende and wurtzite entities are the major structural defects of MBE grown semiconductor nanowires (NWS). Structural composition, phase arrangement and residual strain of individual GaAs NWs grown on Si(111) can be investigated X-ray nano-diffraction employing a focused synchrotron. It is found that even neighbouring NWs grown on the same sample under the same growth conditions differ significantly in their phase structure. Moreover, the misfit strain at the substrate to NW interface releases within few monolayers due to relaxation towards the NW side planes [1]. The evolution of stacking faults is no constant but depends on growth time and the growth mode. In case of InAs NWs grown catalyst-free along the [111] we explored the dynamic relation between the growth conditions and the structural composition of the NWs using time-resolved X-ray scattering and diffraction measurements during the MBE growth. The spontaneous buildup of liquid indium droplet in the beginning of the growth process is accompanied by the simultaneous nucleation of InAs NWs predominantly grown in the wurtzite phase with low number of stacking faults. After nucleation the In droplets become consumed resulting in structural degradation of NWs due to the formation of densely spaced stacking faults [2]. For the first time the particular phase structure of single GaAs NWs could be correlated with their electrical properties. Here the V-I characteristics was measured in a dual Focused Ion Beam chamber the resistance and their effective charge carrier mobility was modeled in terms of thermo-ionic emission theory and space charge limited current model, respectively. Both resistance and inverse mobility show a qualitatively similar electric behavior comparing the inspected NWs. The same single NWs electrically measured have been inspected by X-ray nano-diffraction. The NWs were found to be composed by zinc-blende and twinned zinc-blende units separated by axial interfaces and a small plastic displacement. It turns out that the measured value of the extracted resistance and the inverse of effective mobility increases with the number of intrinsic axial interfaces, whereas the small plastic displacement has less influence on electrical properties [3]. We acknowledge support by BMBF and DFG.

[1] Biermanns et al. : J. Appl. Cryst. (2012). 45, 239–244

[2] Biermanns et al Nano Lett. 2014, 14, 6878–6883

[3] Bussone et al. Nano Lett. 2015, 15, 981–989

Keywords: nanodiffraction, nanowires, phases structure

MS23-O3 Exploring crystal structure, size and stoichiometry of lead chalcogenide QDs by x-ray total scattering and the Debye scattering equation

Antonietta Guagliardi¹, Federica Bertolotti², Dmitry Dirin³, Maria Ibáñez³, Maksym Kovalenko³, Antonio Cervellino⁴, Ruggero Frison¹, Norberto Masciocchi²

1. Istituto di Cristallografia, CNR, and To.Sca.Lab., I-22100 Como, Italy

2. Dipartimento di Scienza e Alta Tecnologia and To.Sca.Lab, Università dell'Insubria, I-22100 Como, Italy

3. Institute of Inorganic Chemistry, Department of Chemistry and Applied Bioscience, ETH Zürich, CH-8093 Zürich, Switzerland

4. The Swiss Light Source, Paul Scherrer Institut, CH-5232 Villigen, Switzerland

5. Istituto di Cristallografia, CNR, and To.Sca.Lab., I-22100 Como, Italy; University of Zurich, CH-8057 Zurich, Switzerland

email: antonella.guagliardi@ic.cnr.it

Colloidal lead chalcogenides Quantum Dots (QDs) are an increasingly important class of nanocrystalline materials. Due to strong quantum-size effects, they are very promising in fields of application as important as solar cells,[1] photodetectors[2] and thermoelectric devices.[3] Size-tunable QDs are typically synthesized using long organic ligands (controlling their growth and preventing from aggregation) providing metal-rich nanocrystals (NCs). Their complex functionality strongly depends on the structure and on the stoichiometry of the NCs. Many studies have concluded that they have a stoichiometric core and a Pb-terminated surface layer[4]. Using unconventional Wide-Angle X-ray Total Scattering techniques and a core-shell model relying on the Debye Scattering Equation, we characterized highly monodisperse PbS and PbSe – Oleate capped QDs (nominal sizes in the 3–8 nm range) in colloidal suspensions in terms of crystal structure, size and stoichiometry. Data were collected at the MS-XSA04 beamline of Swiss Light Source. Sample modeling was performed using the Debussy Suite[5]. The innovative approach enabled us to disclose novel and unexpected structural and compositional features, which will be presented in this communication.

[1] C. Piliego, L. Protesescu, S. Zulkarnaen Bisri, M.V. Kovalenko and M.A. Loi, *Energy Environ. Sci* (2013) **6**, 3054–3059.

[2] M. Böberl, M. V. Kovalenko, G. Pillwein, G. Brunthaler and W. Heiss, *Appl. Phys. Lett.* (2008), **92**, 261113–1–3.

[3] M. Ibáñez, R. J. Korkosz, Z. Luo, P. Riba, D. Cadavid, S. Ortega, A. Cabot, and M. G. Kanatzidis, *J. Am. Chem. Soc.* (2015) **133** (41), pp 16588–16597.

[4] I. Moreels, Y. Justo, B. De Geyter, K. Haustaete, C. Martins and Zeger Hens†, *ACS Nano* (2011), **5**, 2004–2012.

[5] a) A. Cervellino, C. Giannini and A. Guagliardi, *J. Appl. Cryst.* (2010), **43**, 1543–1547; b) A. Cervellino, R. Frison, F. Bertolotti and A. Guagliardi. (2015), in preparation.

Keywords: Lead chalcogenides, Quantum Dots, Total Scattering, Debye Scattering Equation

MS23-O4 X-ray nano-diffraction of semiconductor nano-structures for photonic and electronic applications

Vincent Favre-Nicolin^{1,2}, ELZO AIZARNA Marta^{1,2,3},
MANDULA Ondrej^{1,2,3,4}, MASTROPIETRO Francesca^{2,3,5},
CARBONE Gerardina^{3,6}, ANDRIEU François², CLAUDON
Julien^{1,2}, GERARD Jean-Michel^{1,2}

1. Univ. Grenoble Alpes, France
2. CEA, INAC-SP2M, Grenoble, France
3. ESRF, The European Synchrotron
4. Fondation Nanosciences, Grenoble, France
5. Université Aix-Marseille, Institut Fresnel, France
6. Max IV Laboratory, Lund University, Sweden
7. CEA-LETI, Minatec, Grenoble, France

email: Vincent.Favre-Nicolin@ujf-grenoble.fr

The last 20 years have seen a massive development of crystalline structures with sub-micrometer sizes, either with a simple miniaturization goal, or in order to exploit quantum confinement effects. The study of these objects is a challenge for crystallographers, as their size implies a weak, dif- fuse scattering rather than sharp Bragg peaks. Moreover, nano-structures, either due to the synthesis method or by design, are often heterogeneous and therefore present inhomogeneous strain and com- position 3D fields.

Thanks to the development of focused X-ray optics, it is now possible to measure the scattering from single nano-objects using X-ray Coherent Diffraction Imaging (XCDI) [1,2] and Ptychography. When used in the Bragg geometry, it allows not only to recover the shape (electronic density), but also the deformation field relatively to a perfect lattice, in the case of an inhomogeneous strain. We will illustrate the use of X-ray nanobeams on single homogeneous and heterogeneous nano- structures [3,4,5] used for photonic (single photon emission) and electronic (strained silicon-on- insulator) applications, and discuss the current performance, limits and prospects of the method.

[1] Miao J, Charalambous P, Kirz J & Sayre D (1999). *Nature* 400, 342

[2] Newton MC, Leake SC, Harder R & Robinson IK (2010) *Nat. Mater* 9, 120

[3] Favre-Nicolin V, Eymery J, Koester R & Gentile P (2009). *Phys Rev B* 79, 195401.

[4] Favre-Nicolin V et al. (2010) *New J. Phys.* 12, 35013.

[5] Mastropietro F, Eymery J, Carbone G, Baudot S, Andrieu F & Favre-Nicolin V (2013) *Phys. Rev. Lett.* 111, 215502

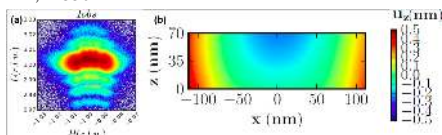


Figure 1. (a) Coherent diffraction pattern from a single strained Silicon-On-Insulator (sOI) line, with a 225x70 nm² cross-section. The curved shape is due to the bending of the strained line. (b) The displacement field refined for this line using the diffraction pattern.[5]

Keywords: Nanostructures, coherent diffraction, semiconductor

MS23-O5 Solvent-nanoparticle interfaces – source of solvent restructuring in solvation shells and disorder in nanoparticles

Mirijam Zobel¹, Simon A.J. Kimber², Reinhard B. Neder¹

1. Friedrich-Alexander-University Erlangen-Nürnberg, Erlangen, Germany
2. European Synchrotron Radiation Facility (ESRF), Grenoble, France

email: mirijam.zobel@fau.de

Pair distribution function (PDF) measurements have originally been used to study the structure of liquids and glasses. [1] Almost forgotten since, the method experienced a revival with increasing interest in nanoparticles and in situ studies of chemical reactions, where common x-ray diffraction fails. [2] To our knowledge, all previous in-situ PDF studies were undertaken in either aqueous or supercritical solvents [3], although manifold nanoparticle syntheses use organic solvents. The drawback to study nucleation in organic solvents are the direct implications of using them. Not only do they scatter x-rays stronger than water, but more importantly organic molecules possess several internal interatomic distances as well as feature pronounced intermolecular ordering within the bulk solvent. [1] In highly diluted systems as often found in nanoparticle nucleation, these intra- and intermolecular distances of the solvent molecules contribute to more than 99% of the overall signal in the experimental PDFs. The extraction of the nanoparticle signal hence requires understanding of the organic solvent. It has been theoretically predicted, that solvent molecules restructure at nanoparticle surfaces inside a nanoscopic solvation shell. [4] Within a well-chosen matrix of dispersed nanoparticles (ZnO, TiO₂, ZrO₂, Ag) in the primary alcohols methanol to 1-propanol as well as in nonpolar hexane, we could for the first time experimentally proof this restructuring effect at solvent-nanoparticle interfaces. The rearrangement of molecules reaches out as far as 2 nm into the bulk liquid and decays exponentially, see Fig. 1. [5] The interaction of the solvent molecules with the nanoparticle surface does, however, also influence the internal nanoparticle structure during nucleation. In reactions with high supersaturation, surface-bond ligand molecules trap the disorder within the particles before crystalline order is established. We show how different organic ligand molecules influence the crystallization process and that obviously gradual dynamic exchange processes of ligand and solvent molecules at the nanoparticle surface enable relaxation into a crystalline particle.

References:

- [1] Zachariasen, W. H., *J. Chem. Phys.* **3** (1935), 158
- [2] Borkiewicz, O. J., et al, *Phys. Chem. Chem. Phys.* **15** (2013) 8466
- [3] Jensen, K. M. O., et al, *J. Am. Chem. Soc.* **134** (2012), 6785
- [4] Spagnoli, D., et al, *Geochim. Cosmochim. Acta* **73** (2009), 4023
- [5] Zobel, M., et al, *Science* **347** (2015), 292

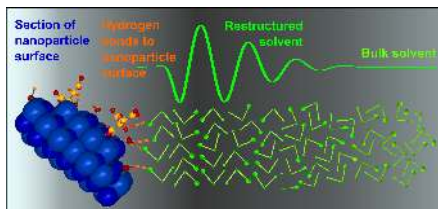


Figure 1. Solvent restructuring of ethanol at a ZnO nanoparticle interface (hydrogen atoms omitted for clarity) and resulting density oscillation observable by PDF. [5]

Keywords: nanoscopic solvation shell; nanoparticle; organic solvents;

MS24. Short range order and diffuse scattering

Chairs: Alexei Bosak, Thomas Weber

MS24-O1 Short-range order in cubic RbNbWO_6 and phase transition to tetragonal phase. Interpretation of X-ray diffuse scattering using group theory approach

Dorota Komornicka¹, Marek Wolczyr¹, Adam Pietraszko¹,
Wiesława Sikora², Andrzej Majchrowski³

1. Institute of Low Temperature and Structure Research, Polish Academy of Sciences, P.O. Box 1410, 50-950 Wrocław 2, Poland
2. Faculty of Physics and Applied Computer Science, AGH University of Science and Technology, Al. Mickiewicza 30, 30-059 Kraków, Poland
3. Institute of Applied Physics, Military University of Technology, 2 Kaliskiego St., 00-908 Warszawa, Poland

email: d.komornicka@int.pan.wroc.pl

A complex scheme of atomic displacements (modes; cf. Perez-Mato et al. [1]) that break the $Fd-3m$ symmetry of the high-temperature ($T_c > 395$ K) cubic phase of RbNbWO_6 and ultimately lead to a phase transition to the tetragonal phase was determined using the group theory approach (program MODY [2]). The resulting set of modes was used to construct a model of the disordered crystal that provides diffuse scattering (calculated with DISCUS program from DIFFUSE package [3]) that is consistent with the experimental results. Particularly characteristic extinctions are well reproduced (cf. Withers et al. [4]).

The resulting solution reveals a disordered structure of cubic RbNbWO_6 , which is a system of intersecting $\{111\}$ -type planes in which Nb/W atoms (statistically occupying centers of oxygen octahedra) are shifted along three symmetry-equivalent $[110]$ directions parallel to these planes. Oxygen atoms also move in a characteristic manner, but their shifts are considerably smaller and do not substantially affect the diffuse scattering pattern. The movements of Rb atoms are large but uncorrelated.

The obtained picture of the local structure of cubic RbNbWO_6 makes it necessary to change the interpretation of existing physical measurements, particularly dielectric measurement. Furthermore, the determined structure of the low-temperature tetragonal phase that exists below 395 K was found to be non-polar ($I-42d$ space group).

Group theory analysis provides a coherent picture of the phase transition from the disordered cubic phase to the ordered tetragonal phase. At T_c , in a multimodal crystal of the high-temperature phase, mode symmetry breaking occurs, and each of the four displacive modes is decomposed: only 1/4 of the atoms of every mode of $\mathbf{k} =$

(x, x, x) retain their $\square 110$ -type in-plane displacements; the displacements of the remaining atoms undergo reorientation to fulfill the conditions imposed by the $\mathbf{k} = (0, 0, 0)$ mode. The former group of displacements defines the direction of the appearing tetragonal axis.

[1] J. M. Perez-Mato, D. Orobengoa and M. I. Aroyo, 2010 *Acta Crystallogr. Sect. A* 66, 558. [2] W. Sikora, F. Bialas and L. Pytlík, 2004 *J. Appl. Crystallogr.* 37, 1015. [3] T. Proffen and R. B. Neder, 1997 *J. Appl. Crystallogr.* 30, 171. [4] R. L. Withers, M. I. Aroyo, J. M. Perez-Mato and D. Orobengoa, 2010 *Acta Crystallogr. Sect. B* 66, 315.

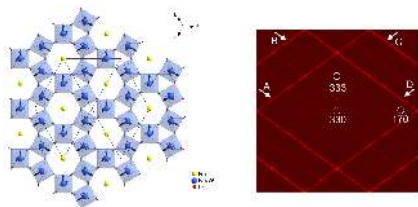


Figure 1. Scheme of atomic displacements in one of {111} RbNbWO₆ planes (left side) which reproduce the experimental diffuse scattering pattern. On the calculated section of the reciprocal space (right side) extinct diffuse streaks are marked with letters A – D and their directions are indicated by arrows.

Keywords: short-range order, X-ray diffuse scattering, phase transition, group theory

MS24-02 Diffuse scattering experiments with relaxor ferroelectrics: probing complexity of primitive cubic perovskite

Dmitry Chernyshov¹

¹ Swiss-Norwegian Beam Lines at the European Synchrotron Radiation Facility, Grenoble, France

email: dmitry.chernyshov@esrf.fr

Lead-based relaxors are puzzling ferroelectrics with centrosymmetric perovskite-like average structure and frequency dependent maximum of dielectric permittivity. The core of polar response in relaxors is local deviations from centrosymmetric structure due to a structural disorder; diffuse scattering is therefore expected to provide valuable information on the disorder. Here we focus on the experimentation and discuss diffuse scattering data for PMN relaxor collected as a function of temperature, pressure, and electric field. Different experimental problems and ways we present diffuse scattering are discussed. The anisotropy and shape of diffuse scattering can be successfully parameterized with a combination of two contributions. First term mimics thermal diffuse scattering, the corresponding microscopic glass-like realization corresponds to a fluctuation regime. The second term is located very near Bragg nodes and develops with cooling; it presumably represents frozen atomic displacements pinned by the static compositional disorder. The latter effect indicates an emergence of numerous long-lived states that is a hallmark of a dipole glass. The pressure does suppress polar correlations in a specific glass-like relaxor state, and above 40 kbar new non-polar phase becomes stable, while electric field leads to relatively small changes in the shape and intensity of diffuse scattering.

Keywords: diffuse scattering, relaxor, disorder, synchrotron radiation

MS24-O3 Diffuse X-ray scattering from ion-irradiated crystals: Monte Carlo simulations using multi-processing and GPU-accelerated computing

Jayanth Channagiri¹, Alexandre Boule¹, Aurélien Debelle²

1. SPCTS – CNRS UMR 7315, Centre Européen de la Céramique, 12 rue atlantis, 87068 Limoges Cedex, France
2. CSNSM, Université Paris-Sud, CNRS-IN2P3, 91405 Orsay Cedex, France

email: jayanth.channagiri@etu.unilim.fr

Ion irradiation/implantation techniques are widely employed in various field of materials science, for instance, in the processing of semiconductor materials, the synthesis of nanostructures, to simulate radiative environments. In all cases, the interaction of energetic ions with matter creates defects in the target material along the path of the incoming ions, which in turn affect the properties of the material. In some particular cases, e.g. when the crystals contain homogeneously distributed defects of the same type and size, it is known since several decades that simple models for the coherent and diffuse scattering intensity can be obtained. However, real-world materials often contain heterogeneous distributions of defects of different type, sizes, etc., which can only be analyzed using numerical methods that are often too resource-demanding (in terms of memory and CPU time) to be used on a regular basis.

In this work, we developed an innovative approach, where numerical crystals, containing up to $\sim 10^9$ unit cells, are computed and used to generate realistic two-dimensional diffuse scattering intensity distributions. The defect structures are generated within a Monte Carlo scheme using linear elasticity theory. High performance computing have been implemented using both multi-processing (i.e. distributing different computational tasks to the different cores of a multi-core central processing unit - CPU) and massively parallel computing on graphical processing units (GPUs). With this implementation, we were able to successfully compute, on a desktop workstation, reciprocal space maps (RSMs) from large crystals with an impressive speed-up of ~ 190 times when compared to the conventional single-processed computation (i.e. 5 minutes instead of ~ 15 hours) [1]. The efficiency of the method will be illustrated with some selected examples, in particular, ion-irradiated yttria stabilized zirconia which exhibits a complex defect structure that significantly evolves with increasing radiation dose, leading to dramatically different RSMs [2].

[1] J. Channagiri et. al., J. Appl. Cryst. (2015) 48, 252-261.

[2] A. Debelle et. al., J. Appl. Phys. (2014) 115, 183504.

Keywords: Irradiated materials, Diffuse scattering, Parallel computing

MS24-O4 Fit of organic crystal structures to PDF Data

Dragica Prill¹, Martin U. Schmidt¹, Pavol Juhás², Simon J.L. Billinge^{2,3}

1. Goethe University, Frankfurt am Main, Germany
2. Brookhaven National Laboratory, Upton, USA
3. Columbia University, New York, USA

email: prill@chemie.uni-frankfurt.de

Local structures in crystalline, nanocrystalline and amorphous organic compounds can be investigated using pair distribution functions (PDF). The experimental determination of the PDF curves of organic compounds is similar to that of inorganic compounds. However, the fit of a structural model to a given PDF curve is at present much more challenging, because the molecular geometry (bond lengths, bond angles, torsion angles) has to be taken into account. Such a fit has rarely been done [1].

We have developed a method to perform fits of organic structures to experimental PDF data using the new Python-driven program package DiffPy-CMI [2]. Bond lengths, bond angles and torsion angles were kept fixed. The molecular position and the spatial orientation of the molecules were fitted together with lattice parameters, scale factor and isotropic displacement parameters [3]. Our approach using two different isotropic displacement parameters for intramolecular and intermolecular vibrations was applied during all calculations [4].

Three examples were chosen: crystalline samples of naphthalene and allopurinol, and a nanocrystalline sample of quinacridone. Synchrotron powder patterns of the three samples were recorded at NSLS (Brookhaven, USA) with $\lambda = 0.18$ Å. From these data the experimental PDF curves were derived with PDFgetX3 [5].

Crystal structural models of the three compounds were fitted to the experimental PDF curves. In all cases a good fit of the crystal structural models to the experimental PDF curves could be achieved. Furthermore, the fit was successful as well, when random values for the molecular position and orientation were chosen as starting points. Hence, the procedure also allows the solution of crystal structures of crystalline and nanocrystalline organic compounds by using the PDF curves [3].

[1] M.T. Dove, M.G. Tucker, D.A. Keen, *Eur. J. Mineral.* **2002**, 14, 331-348

[2] C. L. Farrow, P. Juhás, S. J. L. Billinge, 2010, *SrFit*, unpublished.

[3] D. Prill, P. Juhás, S. J. L. Billinge, M. U. Schmidt, *to be published*.

[4] D. Prill, P. Juhás, M. U. Schmidt, S. J. L. Billinge, *J. Appl. Cryst.* **2015**, 48, 171-178.

[5] P. Juhás, T. Davis, C. L. Farrow, S. J. L. Billinge, *J. Appl. Cryst.* **2013**, 46, 560-566.

Keywords: Pair distribution function, PDF, organic compounds, nanocrystalline

MS24-O5 Electric ordering in metal-organic perovskites from total neutron scatteringHelen D. Duncan¹, Anthony E. Phillips¹, Martin T. Dove¹,
Matthew G. Tucker²

1. Queen Mary, University of London

2. ISIS facility, Rutherford Appleton Laboratory

email: h.duncan@qmul.ac.uk

Metal-organic frameworks (MOFs) have received significant attention over the past decades due to the wide range of structures and functionalities that can be elicited through the judicious choice of starting components. Of particular interest are MOFs which display magnetic and/or electrical ordering, with applications such as ferroelectric or multiple-state memory. A common motif for establishing electric ordering in MOFs is to place organic guest ions into charged frameworks. Here we consider two such MOFs; potassium imidazolium hexacyanoferrate (PIH) ($\text{H}_5\text{C}_3\text{N}_2\text{K}[\text{Fe}(\text{CN})_6]$) and multiferroic dimethylammonium manganese formate (DMMnF) ($(\text{CH}_3)_2\text{NH}_2[\text{Mn}(\text{HCOO})_3]$). Both have perovskite-like architecture, with the organic guest ions occupying the A site. In the high-temperature phase of these materials, the guest ion is free to rotate, and the local symmetry at the site is less than the crystallographic symmetry. Upon cooling, the guest ion freezes into place accompanied by subtle distortions of the framework. Even in the high-temperature phase, guest-framework interactions are expected to lead to local ordering, concealed by the spatial averaging implicit in Bragg crystallographic analysis. To reveal this order we have used the reverse Monte Carlo algorithm to refine structural models against total neutron scattering data, modelling the onset of ordering as the phase transition is approached. As well as giving data appropriate for pair distribution function analysis, neutrons have the advantage of revealing the positions of hydrogen atoms and distinguishing clearly between carbon and nitrogen, making them sensitive to the exact configuration of these hydrogen-bonded organic cations. These models are used to understand the local interactions that give rise to phase transitions. We model the interactions between neighbouring dipoles and the role of the framework in mediating these. We also compare the distortions of the covalent FeC_6 octahedra to those of the ionic KN_6 in PIH. The influences of a flexible formate framework compared to the rigid cyanide framework on guest ion dynamics are also compared. The structures of PIH and DMMnF are more complicated than materials previously reported using RMC, so these refinements and analysis demonstrate that RMC is suitable for more complex systems. It is hoped that an improved understanding of framework-guest interactions across phase transitions can be used to guide the design of future MOFs with desirable electric properties

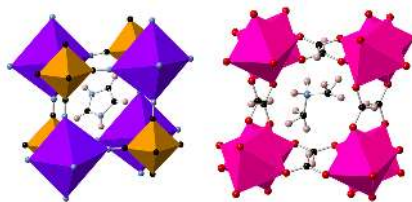


Figure 1. The perovskite-like MOFs: PIH (left) with two metal coordination environments and an imidazolium guest ion. DMMnF (right) with a more flexible formate framework and dimethylammonium guest ion

Keywords: Metal-organic framework, ferroelectric, multiferroic, RMC, neutron

MS25. Magnetic structures

Chairs: Oksana Zaharko, Wiesława Sikora

MS25-O1 Symmetry-based computational tools and databases for magnetic crystallography in the Bilbao Crystallographic Server

Luis Elcoro¹, J. Manuel Perez-Mato¹, Samuel V. Gallego¹, Emre S. Tasci², Gemma de la Flor¹, Moïse I. Aroyo¹

1. Dpto. De Física de la Materia Condensada. Facultad de Ciencia y Tecnología. Universidad del País Vasco, UPV/EHU, Apdo. 644 Bilbao 48080, Spain

2. Physics Department, Middle East Technical University, Ankara, Turkey

email: luis.elcoro@ehu.es

A deeper understanding of any magnetic ordering and its consequences requires a full characterization of the symmetry break involved. Thus, the assignment of a symmetry group (magnetic space or superspace group for a commensurate or incommensurate magnetic phase, respectively), is a basic step for the prediction and understanding of the magneto-structural properties of any magnetic phase. However, it was only in 2010 that the first computer readable listings of magnetic space groups were published, and about the same time the existing software for incommensurate structures, based in the superspace formalism, was extended to magnetic systems. These breakthroughs have been the basis for the development of novel computational tools that allow the systematic application of symmetry arguments in the study of magnetic structures. In this talk we present those recently made available in the Bilbao Crystallographic Server (www.cryst.ehu.es).

In general, the knowledge of the symmetry of the paramagnetic phase and the propagation **k**-vector(s) is sufficient to restrict the possible magnetic symmetries of a magnetic phase to a limited set. Generic magnetic structures complying with each of these symmetries can be constructed, and they can be taken as possible alternative models to be tested. The group-subgroup relations introduce an obvious hierarchy among them that can be exploited. These models can be retrieved and communicated for refinement, visualization, etc., through files in a format (magCIF), which is a direct extension of the CIF format. This is the framework of the magnetic section in the Bilbao Crystallographic Server. This approach complements and goes beyond the traditional representation method, and in this talk we present by means of various examples its capabilities. We show how the user can obtain online information about every magnetic space group (MGENPOS, MWYCKPOS, MAGNEXT), identify a magnetic space group from its symmetry operations given in an arbitrary setting (IDENTIFY MAGNETIC GROUP), derive the possible magnetic space groups for a given set of propagation

vectors (MAXMAGN, k-SUBGROUPSMAG) or generate a magnetic structure model complying with a chosen magnetic space group (MAXMAGN, MAGMODELIZE). We also present MAGNDATA, a freely available online database with more than 300 magnetic structures, both commensurate and incommensurate, which are described unambiguously using magnetic symmetry, and can be retrieved in the form of magCIF files.

Keywords: Bilbao Crystallographic Server, Magnetic Crystallography, Magnetic Structures Database, Magnetic Symmetry Software

MS25-O2 Escaping the quantum critical singularity; modulated magnetism in PrPtAlAndrew Huxley¹

1. The University of Edinburgh, UK

email: a.huxley@ed.ac.uk

The transition between ferromagnetism and paramagnetism is one of the simplest examples of a continuous phase transition. Interesting behaviour is expected when the transition temperature becomes small because incoherent fluctuations above the transition temperature then exist to low temperatures. Ultimately new forms of order must appear to satisfy the third law of thermodynamics or the transition must become first order.

The talk will explore how the fluctuations themselves drive order formation by a mechanism known as “order by disorder”. It will then focus on the application of this theory to the material PrPtAl where complex modulated states form at the interface between ferromagnetism and paramagnetism [1]. The origin of the magnetism will be described in PrPtAl as well as the identification of the complex magnetic states with neutron and X-ray diffraction.

[1] G. Abdul-Jabbar et al, *Nature Physics* **11**, 321–327 (2015).

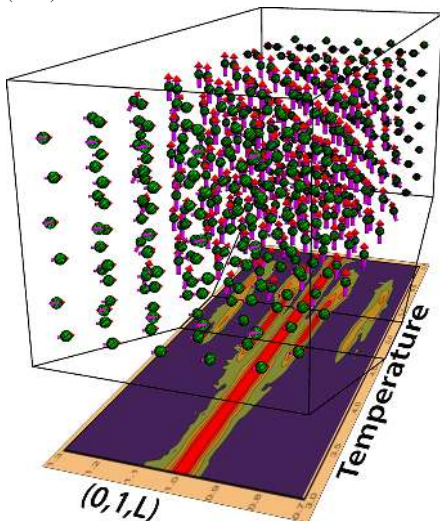


Figure 1. The horizontal plane shows neutron diffraction intensity (colour scale) plotted against reciprocal lattice position (0,1,L) and temperature. The 3 D image above is a magnetic structure consistent with the satellites and other data over the temperature range indicated.

Keywords: magnetism, modulated order, strongly correlated electrons.

MS25-O3 Multiferroic properties of GFO ferrite nanoparticles

Katarzyna Rečko¹, Ula Wolkowska², Françoise Damay³, Wojciech Olszowski^{1,4}, Anna Basa², Maria Biernacka¹, Dariusz Satula¹, Janusz Waliszewski¹, Krzysztof Szymański¹

1. Faculty of Physics University of Białystok, K. Ciołkowskiego 1L, 15-245 Białystok, Poland

2. Institute of Chemistry, University of Białystok, K. Ciołkowskiego 1K, 15-245 Białystok, Poland

3. Laboratoire Léon Brillouin, CEA-Saclay, 91191 Gif sur Yvette cedex

4. ALBA Synchrotron Light Source, Ctra. BP 1413 km. 3,3, 08290, Cerdanyola del Vallès, Barcelona, Spain

email: k.recko@uwb.edu.pl

Gallium iron oxide (GFO) nanoparticles were obtained by the sol-gel method in an environment of the different concentrated nitric acid and with different aging and heating temperatures. X-ray powder diffraction (XRD), neutron powder diffraction (ND), magnetization and Mössbauer spectroscopy (MS) measurements together with Transmission Electron Microscopy (TEM) and Scanning Electron Microscopy (SEM) techniques allowed to determine the chemical and physical properties of the samples. Results of these analyses confirmed a growing contribution of an extra hexagonal phase in direct proportion to the concentration of nitric acid and the lack of corundum-type precipitations at reduced temperatures of annealing steps. The structural and magnetic properties of GFO multiferroics have been intensively studied recently for its potential switch applications. The physical properties, especially magnetism in GaFeO_3 , depend strongly on the method of preparation. Therefore many efforts have been expended on fabrication of gallium iron oxide by Pechini modification of the sol-gel (SG) method. The gallium iron oxide (GFO) crystallizes in an orthorhombic crystal structure. The crystallographic unit cell contains 4 different cation sites and 6 oxygen anion sites all in general position (4a: x, y, z) of the Pc_{21n} space group (no. 33).

In the perfectly ordered structures sites labeled by Ga(1), Ga(2), and Fe(1), Fe(2) are entirely occupied by Ga^{3+} and by Fe^{3+} ions, respectively. In such a case, there are no chance to form uncompensated antiferromagnetism thanks to which spontaneous electric polarization could be steered. Such simple and effective mechanism works in so called switch materials with non-centrosymmetric chemical units, which can become an origin of ferroelectricity and simultaneously contain the magnetic ions.

The targeted preparation allows controlling the chemical order and, consequently, distribution of the magnetic ions.

Keywords: Multiferroics, nanoparticles, X-ray and neutron diffraction, Mössbauer spectroscopy

MS25-O4 Structural and magnetic properties of the low dimensional fluoride

β -FeF₃·3H₂O

Gwilherm Nenert¹, O Fabelo², K Forsberg³, C. V. Colin⁴, J. Rodriguez-Carvajal²

1. PANalytical B. V., Lelyweg 1, 7602 EA Almelo, The Netherlands

2. Institut Laue Langevin, 71 Avenue des Martyrs, 38000 Grenoble, France

3. School of Chemical Science and Engineering, Royal Institute of Technology, Teknikringen 42, SE 100 44 Stockholm, Sweden

4. Institut Néel, 25 rue des martyrs, BP 166, 38042 Grenoble, France

email: gwilherm.nenert@panalytical.com

The anisotropy inherent in low-dimensional (1-D) solid-state compounds leads to a variety of interesting magnetic, electronic, and optical properties, with applications including single-chain magnets for data storage, (1) multiferroics for bifunctional materials (2,3) and nonlinear optical materials for second harmonic generation (4,5). Certain types of 1-D materials containing isolated chains exhibit nearly ideal magnetic properties, acting as experimental models for Ising and Heisenberg spin chains, furthering our understanding of magnetic exchange in highly correlated systems (6). One of the strategies for building these 1-D magnetic materials is to incorporate small one- or three-atom linkers between magnetic centers to facilitate exchange along the chains or networks (7,8). Many of these compounds are known, but very few have been created using iron centers, and most rely on relatively large bridging ligands to separate the magnetically coupled components within the structure.

We report on the structural and magnetic properties of the low-dimensional fluoride β -FeF₃·3H₂O using SQUID magnetometry, X-ray and neutron diffraction. The structure consists of 1D-chains of corner-linked Fe[F₄(H₂O)₂] octahedra running parallel to [001] and isolated water molecules. A dense network of hydrogen bonds strongly connects the Fe-F chains. The structural formula is Fe[F₄(H₂O)_{0.5}]_{0.5}·H₂O. This material exhibits a very pronounced 1D character with a very broad maximum around 150 K in the magnetic susceptibility. Below T_N = 20 K, long range magnetic order appears characterized by **k** = (0 0 ½). From magnetic susceptibility, the intrachain magnetic coupling is estimated to be 18 K, while the interchain magnetic interaction is estimated to be about 3 K. We discuss this non negligible interchain coupling in light of the crystal structure of this material [9].

(1) Zhang, W.-X.; *et al.*, RSC Adv. 2013, 3, 3772–3798.

(2) Xu, G. C.; *et al.* J. Am. Chem. Soc. 2010, 132, 9588–9590.

(3) Xu, G. C.; *et al.* J. Am. Chem. Soc. 2011, 133, 14948–14951.

(4) Kandasamy, *et al.* Cryst. Growth Des. 2007, 7, 183–186.

(5) Anbuechzhiyan, M. *et al.* Mater. Res. Bull. 2010, 45, 897–904.

(6) Coulon, C.; *et al.* R. In Single-Molecule Magnets and Related Phenomena; Winpenny, R., Ed.; Springer-Verlag: Berlin, Germany, 2006

(7) Wang, X.-Y.; *et al.* Chem. Commun. 2008, 281–294.

(8) Sun, H.-L.; Wang, *et al.* Coord. Chem. Rev. 2010, 254, 1081–1100.

(9) G. Néner, *et al.*, in preparation

Keywords: magnetic structure, fluoride, low dimensional magnetism, x-ray diffraction, neutron

MS25-O5 Study of charge and spin ordering, lattice distortion, and magnetoresistance in $\text{SrFeO}_{3-\delta}$

Chao-Hung Du¹, S.-H. Lee¹, T. Frawley², P. D. Hatton², F. C. Chou³

1. Tamkang University
2. Durham University
3. National Taiwan University

email: chd0312@gmail.com

Using resonant x-ray scattering, magnetization, and conductivity measurements, we report the correlation between the giant magnetoresistance and the charge and spin ordering in an iron-based oxide $\text{SrFeO}_{3-\delta}$. SrFeO_3 (SFO) has a cubic structure with an isotropic metallic behavior. The cubic perovskite SrFeO_3 , in which iron is present as Fe^{4+} , exhibits the coexistence of metallic conductivity and screw-type antiferromagnetic ordering. However, the metallic state found in SrFeO_3 becomes unstable with respect to a charge disproportionation on Fe ions due to the oxygen deficient. In order to understand this oxidation effect on the magnetoresistance, crystals with different oxygen contents were grown by floating zone furnace. For this study, a crystal was characterized to have a $\delta \sim 0.19$ by transport measurements. From the conductivity and magnetization measurements, the crystal shows two unusual transport behavior at $T \sim 120$ K and 65 K. By the means of resonant x-ray scattering, including soft and hard x-rays, the former is in accord with the formation of charge disproportionation distortion of Fe ions, and the latter is the helical magnetic structure. The coupling of the helical magnetic structure and the lattice distortion results in a complicated phase transition and a giant magnetoresistance at 65 K. A thermal hysteresis transition is also observed, and can be understood as the consequence of the non-equilibrium thermal transition of the domain-like charge modulations.

Keywords: resonant x-ray scattering, charge ordering, spin ordering, magnetoresistance

MS26. Modulated, modular and composite materials

Chairs: Luis Elcoro, John Claridge

MS26-O1 Odd ones only - the systematic absences in Cu_3Sn and related structures

Carola J. Müller¹

1. Lund University, Sweden

email: carola.muller@chem.lu.se

The intermetallic compound Cu_3Sn has previously been described as a long-period³ antiphase boundary superstructure of the Cu_3Ti structure type. While the compound itself has been reported as a tenfold and an eightfold superstructure, ternary doped alloys show shorter repetitions. Interestingly, the diffraction patterns of these compounds show noncrystallographic absences that cannot be explained using the superstructure models. Since the compound exhibits phase broadening, these models are not satisfactory because the paucity of observed data does not allow for a refinement of the composition.

Here, an alternative, superspace model in the orthorhombic space group $Xmcm(0\beta 0)000$ is proposed, with the centering vectors $(0,0,0)$ and $(1/2,0,0,1/2)$. The presence of the non-crystallographic absences is explained as a result of a dominating occupational modulation that is accompanied by a weaker displacive modulation. Within this context, the triangle wave was tested as an alternative to the square wave for the modelling of structures whose diffraction images show odd order satellites only while the intensity of the satellites is decreasing dramatically. Additionally, it is demonstrated how varying the length and the direction of the modulation wavevector in the superspace model can be used to produce the crystal structures of the ternary Cu_3Sn compounds and other colored hexagonal close packing (h.c.p.) structures.

C.J. Müller, S. Lidin, *Acta Cryst. Sect. B*, **2014**, 70, 879-887.

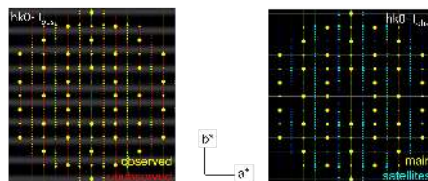


Figure 1. Treatment of the observed non-crystallographic absences in Cu_3Sn in a superstructure model in the 3D space group $Cmcm$ (left) and in an alternative $3+1$ D model in $Xmcm(0\beta 0)000$.

Keywords: modulated structure, intermetallic compound

MS26-O2 Frustrated octahedral tilting distortion in the incommensurately modulated perovskites

Artem M. Abakumov¹

1. EMAT, University of Antwerp, Groenenborgerlaan 171, B-2020, Antwerp, Belgium

email: artem.abakumov@uantwerpen.be

The 3D framework of corner-sharing octahedra in the perovskite ABO_3 structure is a very flexible construction. The ability of this framework to sustain distortions due to rotation/tilt of the octahedral units, or their deformations, or both together, without losing the corner-sharing connectivity, allows the perovskite structure to accommodate a very wide range of cations with diverse size, formal charge, and electronic properties. Crystallographic aspects of the distortions have been widely discussed in the literature and developed nowadays toward a rigorous group symmetry analysis for different types of distortions and their combinations. However, in some layered A-site ordered perovskites, such as $\text{Li}_{3x}\text{Nd}_{2/3-x}\text{TiO}_3$ and many others, substantially more complex pattern of the octahedral tilting distortion allegedly coupled to a compositional modulation at the A sublattice can be realized leading to incommensurability. Here we demonstrate a solution of the $\text{Li}_{0.15}\text{Nd}_{0.617}\text{TiO}_3$ incommensurate crystal structure using a combination of transmission electron microscopy, synchrotron X-ray and neutron powder diffraction [1, 2]. In contrast to earlier conjectures on the nanoscale compositional phase separation in the $\text{Li}_{3x}\text{Nd}_{2/3-x}\text{TiO}_3$ materials, all peculiarities of the incommensurate superstructure can be understood in terms of displacive modulations related to an intricate octahedral tilting pattern. It involves fragmenting the pattern of the out-of-phase tilted TiO_6 octahedra around the *a*- and *b*-axes into antiphase domains, superimposed on the pattern of domains with either pronounced or suppressed in-phase tilt component around the *c*-axis. The octahedral tilting competes with the second order Jahn–Teller distortion of the TiO_6 octahedra. This competition is considered as the primary driving force for the modulated structure. The A cations are suspected to play a role in this modulation affecting it mainly through the tolerance factor and the size variance. The reported crystal structure calls for a revision of the structure models proposed for the family of layered A-site ordered perovskites exhibiting a similar type of modulated structure.

1. A.M Abakumov, R. Erni, A.A Tsirlin, M.D Rossell, D. Batuk, G. Nenert, G. Van Tendeloo, *Chem. Mater.*, 25, 2670 (2013). 2. R. Erni, A.M. Abakumov, M.D. Rossell, D. Batuk, A.A. Tsirlin, G. Nénert, G. Van Tendeloo, *Nature Mater.*, 13, 216 (2014).

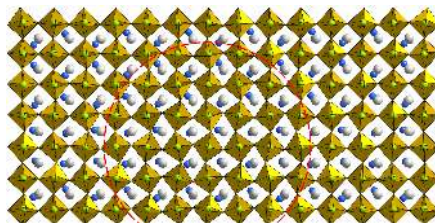


Figure 1. A part of the incommensurate $\text{Li}_{0.15}\text{Nd}_{0.617}\text{TiO}_3$ structure. The Ti atoms (green spheres) are in the oxygen octahedra. Nd and Li atoms are shown as gray and blue spheres, respectively. The dashed circle marks the region with a pronounced tilt of the TiO_6 octahedra around the *c*-axis.

Keywords: layered perovskite, incommensurately modulated structure, octahedral tilting, A-site ordering

MS26-O3 Phase transitions and critical phenomena in aperiodic composite crystalsCéline Mariette¹, Laurent Guérin², Philippe Rabiller², Bertrand Toudic²

1. Institut de Physique de Rennes, France

2. Institut de Physique de Rennes, UMR CNRS 6251, France

email: celine.mariette@u-psud.fr

These last decades, the concept of order has broadened to analyze materials which have long-range order with symmetries that are incompatible with periodicity. These aperiodic compounds are described in the frame of a higher-dimensional analogue of the physical space called crystallographic superspace, and these crystals are periodic structures in these superspaces [1]. Aperiodic crystals are usually classified into three categories: incommensurately modulated phases, quasicrystals and aperiodic composites. Aperiodicity in composite materials may appear rather naturally due to the possible misfit of the host and the guest parameters along their crystallographic directions. A prototype series is given by the alkane chains confined in honeycomb-like urea sublattices.

We will first present symmetry breakings in this prototype family and show the richness of phases appearing in higher dimension spaces [2]. We will report on pretransitional phenomena in such a high-dimensional space, generalizing the critical results previously reported at a lower dimensionality [3]. Very high-resolution diffraction data reveal anomalously large correlation lengths along the aperiodic direction, with all correlation lengths diverging at T_{cl} . This could be explained by low-frequency phason excitations that soften at T_{cl} at the critical wave vector, in accordance with an increase in the critical diffuse scattering intensity.

[1] T. Janssen, G. Chapuis, M. de Boissieu, *Aperiodic Crystals: From Modulated Phases to Quasicrystals*, (Oxford Univ. Press, Oxford, 2007). [2] B. Toudic et al., *Science* 319 (2008), 69-72. [3] C. Mariette et al., *PRB* 87 (2013) 104101.

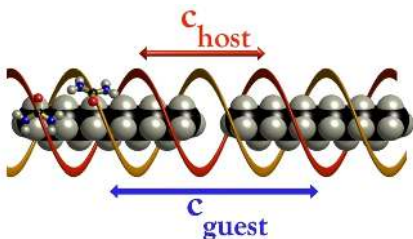


Figure 1. Aperiodic confinement of alkane in honeycomb-like urea sublattice

Keywords: composite crystal, phase transition, superspace crystallography

MS26-O4 Allotwinning: the overlooked form of twinningBerthold Stöger¹

1. Vienna University of Technology, Institute of Chemical Technologies and Analytics

email: bstoegeer@mail.tuwien.ac.at

Twinning is the association of equivalent macroscopic domains with a well-defined crystallographic orientation relationship [1]. A related, but often overlooked, phenomenon is allotwinning, the oriented association of *different* polytypes of the same compound [2]. Whereas the structural characterization of twinned crystals has become routine in the last years, only few structures of allotwins were published. Nevertheless, allotwinning is more common than expected and therefore needs to be addressed.

Two inorganic compounds ($K_2HAsO_4 \cdot 2.5H_2O$, $KAgCO_3$) and one metalorganic iron pincer-complex, crystallizing as allotwins are presented and the problems and pitfalls encountered during data reduction and structural characterization are discussed.

[1] Th. Hahn. *International Tables For Crystallography*, Vol. D (2006) pp. 393–448. Heidelberg: Springer.

[2] M. Nespolo, T. Kogure and G. Ferraris. *Z. Kristallogr.* (1999) **213**, 5–8.

Keywords: twinning, polytypism, data reduction, structure refinement

MS26-O5 The incommensurately modulated phase in (2-methylimidazolium) tetraiodobismuthate(III) thermochromic organic-inorganic hybrid

A. Gągor¹, M. Węclawik², B. Bądzior¹, R. Jakubas²

1. W. Trzebiatowski Institute of Low Temperature and Structure Research PAS, P.O. Box 1410, 50-950 Wrocław, Poland
2. Faculty of Chemistry, University of Wrocław, Joliot-Curie 14, 50-383 Wrocław, Poland

email: a.gagor@int.pan.wroc.pl

(2-methylimidazolium) tetraiodobismuthate(III) (abbreviated as (2-MIm)BiI₄) is a thermochromic, semiconducting hybrid. It undergoes structural first-order phase transition to incommensurately modulated phase at 308 K. The symmetry changes from *C2/c* to *C2/c*(0,β,0)0; the modulation wave vector $\mathbf{q}=0.575(2)\mathbf{b}^*$ [1]. The incommensurate phase is stable down to 100 K. The non-modulated structure consists of polymeric chains of [BiI₄]⁻ anions propagating in the *c* direction and stacks of 2-MIm⁺ counter-ions that couple to the anionic substructure via weak hydrogen bond interactions. The polymeric [BiI₄]⁻ anions comprise of distorted BiI₆ octahedra that form zig-zag chains by sharing the *cis* edges. The cations are dynamically disordered over two equivalent positions that are related by the two-fold axis. The transformation to incommensurate phase is triggered by a collective, sinusoidal displacement of bismuth and iodide atoms from their high-temperature positions. The intra-chain bonds in modulated phase do not differ considerably from their high temperature counterparts. Much significant deviations are observed between the chains which may be shifted up to ~0.4 Å relative to each other along the *c* direction. Substantial variations within the inter-chain Bi...Bi distances may have an impact on the semiconducting and thermochromic properties of this material. 2-MIm⁺ counter ions order in the incommensurate phase. In each cavity the 2-MIm⁺ adopts one of the two positions that were equivalent in the high-temperature phase. At 220 and 150 K the reorientation movements between the sites are blocked which is confirmed by dielectric response. DOS calculations together with asymmetric local environment of bismuth ions imply the presence of the stereochemically active bismuth lone pair 6s² electrons in both phases. The change of the lone pair activity may play the foreground role in the phase transition mechanism as far as the increased contribution of bismuth states in total DOS in the incommensurate phase is noted. This interpretation is consistent with structural data that show greater deformation of the bismuth coordination geometry in the modulated structure.

[1] A. Gągor et al. CrystEngComm, 2015, DOI: 10.1039/C5CE00046G

Acknowledgements. Part of the research (synthesis, DSC and dielectric measurements) was supported by the National Science Centre (Poland) under grant No. 2013/11/D/ST8/03297 and by the European Union under the European Social Fund.

Keywords: modulated structure, organic-inorganic hybrid, phase transition

MS27. Electron crystallography methods

Chairs: Alex Eggeman, Lukáš Palatinus

MS27-O1 Deformation mapping in the TEM by dark holography, nanobeam diffraction, geometrical phase analysis and precession electron diffraction. A comparison of the different techniques

David Cooper^{1,2}, Nicolas Bernier^{1,2}, Jean-Luc Rouviere^{2,3}

1. CEA LETI Minatéc
2. University Grenoble Alpes
3. CEA INAC Minatéc

email: daveycooper@gmail.com

In the last few years there has been an explosion in the number of transmission electron microscopy based (TEM) techniques that can be used for strain mapping with nm-scale resolution. These include dark field electron holography, the geometrical phase analysis of high-resolution images, nanobeam diffraction and more recently precession electron diffraction. In order to benchmark the different techniques a calibration specimen containing 10-nm-thick SiGe layers with different Ge concentrations has been grown by chemical vapour deposition. Due to the epitaxial growth, the lattice parameter of the SiGe will be expanded relative to the Si in the growth direction. Figure 1(a) shows a HAADF STEM image of the calibration specimen indicating the concentration of Ge present in each layer and deformation maps for the growth direction acquired by (b) GPA of HAADF STEM (c) dark field electron holography (d) precession electron diffraction and (e) finite element simulations are shown. The HAADF STEM deformation mapping has a spatial resolution of 1.5 nm which is imposed by the size of the mask used in Fourier space during the reconstruction and a measurement sensitivity of 0.25 % was determined by taking a standard deviation of the deformation measured in the unstrained silicon substrate. For the dark holography the spatial resolution imposed by the fringe spacing of the interference pattern is 6 nm with a measured sensitivity of 0.05 %. For precession diffraction, the spatial resolution imposed by the diameter of the electron probe is 2 nm and a sensitivity of 0.02% measured. While it is relatively straightforward to apply all of these techniques to simple calibration specimens where both large values of deformation are expected and the experiment is simplified due to the 1D nature of the strained layers. All of the techniques have been applied to a range of different specimens each with different complications, such as a 35-nm gate SiGe recessed source and drain pMOS device, a nMOS device tensile strained using a nitride film, to state of the art SOI-based semiconductors and a III/V superlattice. The advantages and disadvantages the

different strain mapping techniques are discussed.

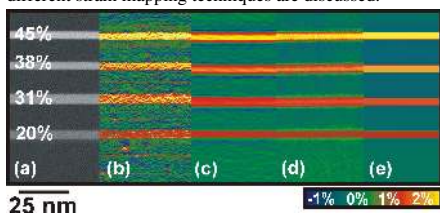


Figure 1. HAADF STEM image of the calibration specimens with deformation maps acquired by HAADF STEM, dark holography, precession diffraction and finite element simulations.

Keywords: Strain Mapping, TEM, Semiconductors.

MS27-O2 Electron diffraction and imaging of 3D nanocrystals of pharmaceuticals, peptides and proteins

Jan Pieter Abrahams^{1,2,3}, Eric van Genderen¹, Igor Nederlof⁴, Max Clabbers¹, Yaowang Li¹

1. LIC, Leiden University, Einsteinweg 55, 2333CC Leiden, The Netherlands

2. Biozentrum, University of Basel, Klingelbergstrasse 50/70 CH - 4056 Basel Switzerland

3. LBR, Paul Scherrer Institut, 5232 Villigen PSI, Switzerland

4. Amsterdam Scientific Instruments, Science Park 105 1098 XG Amsterdam The Netherlands

email: Abrahams@chem.leidenuniv.nl

High-energy electrons provide 1000 times more information per Gray (absorbed energy, i.e. radiation damage), compared to X-rays. Hence electrons outperform X-rays for structure determination when radiation damage is the limiting factor. Unlike X-rays, electrons can not only be diffracted, but also imaged. However, when imaging transparent samples, the *total number* of quanta per unit area determines the signal-to-noise ratio. When diffracting transparent samples, the *number of interacting* quanta per unit area determines the signal-to-noise ratio. Measuring electron diffraction accurately has only recently become possible with the advent of quantum area detectors. One of the challenges is that an electron microscope is flooded with photon radiation resulting from Bremsstrahlung generated by the high-energy electrons. Only an area detector that can discriminate between photon noise and electron signal is insensitive to this noise.

This difference in signal-to-noise ratio was demonstrated in practice for electrons using a Timepix quantum area detector. When imaging a 100 nm thick lysozyme protein crystal with electrons, typically one to two images of the same location could be measured with significant details up to 3.5 Å resolution. Subsequent images had suffered too much from radiation damage to show such detail. When diffracting similar crystals, hundreds of electron diffraction patterns with Bragg spots beyond 3 Å resolution could be measured from the same location. However, there is no such thing as a free lunch. Diffraction comes at a price: the structure factor phases are lost. They can only be retrieved using additional (prior) information, for instance obtained from (a few) electron images. We demonstrated this strategy by phasing the 3D structure factors of a nano-crystalline amyloid peptide.

Keywords: electron diffraction, phasing, detectors

MS27-O3 Structure refinement using 'digital' electron diffractionRichard Beanland¹

1. University of Warwick

email: r.beanland@warwick.ac.uk

Electron diffraction datasets that cover a large angular range can now be constructed from hundreds or thousands of convergent beam electron diffraction patterns using computer control of a transmission electron microscope. These 'digital' large angle convergent beam electron diffraction (D-LACBED) patterns contain a wealth of data that can in principle be used to refine structures and electron densities to unprecedented accuracy. We explore refinement strategies that match simulated D-LACBED patterns to experimental data, using the changing structure of Ca₃Mn₂O₇. This Ruddlesden-Popper compound exhibits a tilt of the oxygen octahedra about the long axis of the unit cell that appears to vary with temperature, as well as a second octahedral tilt, about an axis perpendicular to the first, that switches abruptly at a first order phase transformation around 350C. In order to obtain structural or electron density models that match experimental results, we have developed an open source Bloch-wave program, Felix. This software platform has been written clearly and concisely with a strong emphasis on architecture to aid further development. We show refinements based on atomic location and Debye-Waller factors and consider different approaches to find the best global fit to the data.



Figure 1. Sets of four 422-type D-LACBED patterns. At room temperature a horizontal mirror is present but no vertical one, indicating a spacegroup of Cmc21. The patterns become more symmetrical up to 300C, indicating Cmcn. Finally, intensities change abruptly when the material transforms to I4/mmm (400C).

Keywords: Structure refinement, Bloch wave, digital electron diffraction, Ca₃Mn₂O₇

MS27-O4 Fast electron diffraction tomographyMauro Gemmi¹, Mari Grazia Immacolata La Placa¹, Athanassios Galanis², Edgar F. Rauch³, Stavros Nicolopoulos²

1. Cener for Nanotechnology Innovation@NEST, Istituto Italiano di Tecnologia, Pisa, Italy

2. NanoMEGAS SPRL, Brussels, Belgium

3. SIMAP CNRS-Grenoble INP, Saint Martin d'Hères, France

email: mauro.gemmi@iit.it

Electron diffraction tomography (EDT) has completely changed the possibility of solving crystal structures using electron diffraction data. Electron diffraction tomography data, if collected in precession mode[1] or in rotation mode[2] are close enough to a kinematical approximation to be successfully used in ab-initio structure solution methods designed for kinematical scattering, like direct methods or charge flipping. In an EDT data collection the patterns are recorded while the crystal is tilted around the goniometric axis, therefore the crystal must be kept under the electron beam during rotation. The availability of a procedure for collecting automatic EDT on a nanocrystal without any recentring procedure would speed up the data collection, increase the number of crystals which could be analyzed for each TEM session, and reduce the electron dose suffered by the crystal. Thanks to the goniometer stability of a Zeiss Libra 120 electron microscope, we have developed an automatic data collection procedure which allows a 40° range data collection without any intervention of the operator in a total time of 2 minutes. Such a small angular range is suitable for unit cell determination and can be used as a phase screening method to identify new unknown phases on a multiphase sample. In some special cases, depending on the position in the sample grid, the dimension of the crystal and the sample holder type, the automatic procedure can collect a larger angular range, between 60° and 80°, suitable for structure solution. By playing on the tilt speed, the exposure time and the detector speed (increasing the readout by binning) the procedure can be adapted to collect precession assisted EDT (PEDT), rotation EDT (REDT) or a different EDT type, that we have called integrated EDT (IEDT), in which the reciprocal space between the patterns is sampled during the exposure, like what happens in x-ray single crystal diffraction with area detector. The method has been tested on a known crystal structure, MgMoO₄, which has been solved with data collected in the three data collection modes, PEDT, REDT and IEDT.

References.

- [1] Mugnaioli, E., Gorelik, T. E. & Kolb, U. (2009). *Ultramicroscopy*, 109, 758-765.
- [2] Zhang D., Oleynikov P., Hovmöller S., Zou X. D. (2010). *Z. Kristallogr.* 225 94.

Keywords: Electron diffraction tomography, precession electron diffraction

MS27-O5 Pair Distribution Function calculated from electron diffraction data

Tatiana E. Gorelik¹

1. Institute of Physical Chemistry Johannes Gutenberg-University
Mainz Welterweg 11, 55099 Mainz, Germany

email: gorelik@uni-mainz.de

Structure description through Pair Distribution Function (PDF) analysis has attracted particular interest in the last years with the declination of the technology towards nanocrystalline and amorphous materials. The structure of these materials cannot be described by a set of lattice basis vectors and atomic coordinates, but by a continuous function representing the probability to find atoms at a particular distance - PDF. Experimentally, the PDF is calculated from continuous scattering data, as a rule X-ray, or neutron diffraction. The employment of electron diffraction data for the PDF analysis, although not being completely new, survives a renaissance within the last years. Electron diffraction data for the PDF calculation is collected in a Transmission Electron Microscope (TEM), which has to be operated in a special way in order to collect optimal data for PDF. 2D electron diffraction patterns should be integrated into the 1D intensity profile, which then after a proper normalization will be transformed into a PDF. Specifics of electron diffraction data handling as well as the limitation of the method will be discussed. PDFs calculated from electron diffraction data for different materials will be presented and type of structural information extracted from the PDFs will be discussed.

Keywords: Electron Diffraction, PDF, nanostructure

MS28. Charge density studies

Chairs: Anders Madsen, Simon Coles

MS28-O1 Applications of hirshfeld surface analysis in crystal engineering and drug design

Simon Grabowsky¹

1. Universität Bremen

email: sgrabowsky@web.de

The tool of Hirshfeld Surface (HS) analysis for exploring intermolecular interactions in molecular crystals developed by Spackman and co-workers has become very popular in recent years.[1] It applies Hirshfeld's idea of stockholder partitioning to the procrystal electron density in order to construct meaningful molecular surfaces inside the crystal. Only coordinates and tabulated spherically symmetric atomic electron densities are needed. Hence, it is not an electron-density-analysis technique, however, properties such as theoretically calculated electron density, electrostatic potential and others can be plotted onto the HS to investigate interactions mediated through the surface.

In the context of applications of HS analysis, the following assumptions have to be discussed: To which extent can gas-phase calculated properties for isolated molecules explain crystal packing, and to which extent can crystal structures of small biologically active molecules simulate the situation of the same molecule within a biological environment?

Presented applications towards crystal engineering will include correlations of purely geometric HS mediated properties to melting points of compounds, and the use of HS analysis for isomorphism and polymorphism considerations.

Presented applications towards drug design will include discussions of the electrostatic potential on HS's in a pseudoreceptor modeling experiment, and will show how HS analysis contributes to the understanding of enhanced physiological effects of well-known drugs.

References:

[1] (a) M. A. Spackman, P. G. Byrom, *Chem. Phys. Lett.* 1997, 267, 215; (b) M. A. Spackman, J. J. McKinnon, D. Jayatilaka, *Cryst. Eng. Comm.* 2008, 10, 377; (c) M. A. Spackman, D. Jayatilaka, *Cryst. Eng. Comm.* 2009, 11, 19.

Keywords: Hirshfeld Surface Analysis

MS28-O2 XPAD, an hybrid pixel detector for charge density study on laboratory diffractometers

Wenger Emmanuel¹, Allé Paul², Dahaoui Slimane¹, Schaniel Dominik¹, Lecomte Claude¹

1. Université de Lorraine
2. CNRS

email: emmanuel.wenger@univ-lorraine.fr

The new generation of X-ray detectors, the hybrid pixel area detectors or 'pixel detectors', are based on direct detection and single-photon counting processes. Large linearity range, high dynamic and extremely low noise leading to unprecedented high signal-to-noise ratio, fast readout time (high frame rates) and electronic shutter are among their intrinsic characteristics which render them very attractive. First used on synchrotron beam lines, we will show that these detectors are also promising at laboratory sources, in particular for pump-probe or quasi-static experiments [1] and accurate electron density measurements [2]. An original laboratory diffractometer made from a Nonius Mach3 goniometer equipped with an Incoatec Mo micro source and an XPAD pixel area detector has been developed at the CRM2 laboratory. This diffractometer will be presented in the first part of the talk and the second part will be devoted to the first charge density analysis using an XPAD detector : Mo K α accurate charge density quality data up to 1.21 Å⁻¹ resolution have been collected on a sodium nitroprusside crystal using this prototype diffractometer. The multipolar electron density obtained will be compared to already published data (Pressprich et al., 1994, Nelyubina et al., 2008) In the third part of the talk, we will compare the measurements made with three different diffractometers (XPAD, Agilent Atlas CCD and PHOTON100 CMOS) on the same crystal of a relatively weakly scattering pure organic compound, 4-benzyloxy-3-methoxybenzaldehyde (C₁₅H₁₄O₃) to 0.96 Å⁻¹ resolution. The three charge density models obtained after multipolar refinements with identical strategies will be compared with unbiased criterions, like residual electron density maps and agreements factors.

[1] Diffraction studies under in-situ electric field using a 2D hybrid pixel XPAD detector : P. Fertey, P. Allé, E. Wenger, B. Dinkespiler, S. Hustache, K. Medjoubi, F. Picca, C. Lecomte and C. Mazzoli, *Journal of Applied Crystallography*, **46**, 1151-1161, 2013.

[2] XPAD X-ray hybrid pixel detector for charge density quality diffracted intensities on a laboratory equipment : E. Wenger, S. Dahaoui, P. Allé, P. Parois, C. Palin, C. Lecomte and D. Schaniel, *Acta Crystallographica B*, **70**, 5, 783-791, 2014.

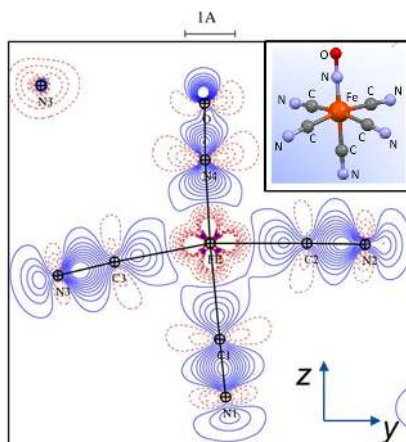


Figure 1. Deformation electron density after spherical atoms refinement in SNP and iron coordination polyhedron.

Keywords: Hybrid pixels detector, CCD X-ray detectors, CMOS X-ray detectors, charge density study, accurate X-ray diffraction data.

MS28-O3 Hirshfeld Atom Refinement for determining hydrogen positions in routine X-ray experiments

Magdalena Wońska¹, Simon Grabowsky², Paulina M. Dominiak¹,
Krzysztof Wozniak¹, Dylan Jayatilaka³

1. Faculty of Chemistry, University of Warsaw, ul. Pasteura 1, 02-093 Warsaw, Poland

2. Fachbereich 2 – Biologie/Chemie, Universität Bremen, Leobener Str. NW2, D-28359 Bremen, Germany

3. School of Chemistry and Biochemistry, University of Western Australia, 35 Stirling Highway, Crawley WA 6009, Australia

email: mwońska@chem.uw.edu.pl

Locating hydrogen is a crucial problem in chemistry as hydrogen atoms often constitute the outer layer of molecules and therefore mediate in many important interactions and take part in a variety of reactions and processes. Neutron diffraction experiments are considered the best source of information about coordinates and thermal motions of hydrogen atoms in crystals whereas X-ray diffraction is still believed to be a much less reliable method in this respect. The presented work shows that applying Hirshfeld Atom Refinement (HAR) [1][2] for X-ray data analysis constitutes a significant improvement in comparison to IAM in terms of positional parameters of hydrogen atoms. Furthermore, HAR enables refinement of hydrogen anisotropic displacement parameters (ADPs) based solely on X-ray data, which cannot be achieved with IAM.

The analyzed results are based on HAR carried out for 81 high resolution X-ray data sets collected for organic compounds at temperatures not higher than 140 K. In the applied method aspherical atomic scattering factors are obtained from Hirshfeld partition of molecular density calculated on the BLYP/cc-pVDZ level of theory for a molecule surrounded by a cluster of charges and dipoles simulating the influence of a crystal environment. The X-H bond lengths (C-H, N-H, O-H) present in the investigated compounds are grouped into bond types defined in the work by Bruno & Allen [3] and their averaged values are compared to the neutron results. The difference between both means for individual bond types is usually within two and often even within one X-ray standard deviation. Moreover, precision of bond lengths obtained in HAR of X-ray data is similar to the neutron one, except bond lengths in water molecules for which HAR values are significantly more precise. These results remain the same if HAR is performed for data trimmed to the standard resolution of 0.8 Å, which makes the method suitable for refinement of data from routine X-ray experiments for well scattering compounds. Additionally, a short analysis of ADPs obtained from HAR will be presented.

References

- [1] a) D. Jayatilaka, B. Dittrich, *Acta Cryst. A* 2008, 64, 383-393; b) S. C. Capelli, H.-B. Bürgi, B. Dittrich, S. Grabowsky, D. Jayatilaka, *IUCrJ* 2014, 1, 361-379.
- [2] D. Jayatilaka & D. J. Grimwood *Tonto: a Fortran-Based Object-Oriented System for Quantum Chemistry and Crystallography*. (New York: Springer, 2003).
- [3] F. H. Allen, I. J. Bruno, *Acta Cryst. B* 2010, 66, 380-386.

Keywords: Hirshfeld Atom Refinement, hydrogen positions, hydrogen ADPs, X-ray crystallography

MS28-O4 On precision and accuracy of X-ray results – How to get better quality results from different X-ray diffraction experiments

Krzysztof Wozniak¹, Fabiola Sanjuan-Szklarz¹, Magdalena Wońska¹, Sławomir Domagała¹, Paulina Dominiak¹

1. Biological and Chemical Research Centre, Chemistry Department, Warsaw University, Zwirki i Wigury 101, 02-089 Warszawa, Poland

email: kwozniak@chem.uw.edu.pl

Although everything seems to be already well known in the field of routine structural single crystal X-ray analysis and ca. 1.1 mln structures have been solved and refined so far, even commonly used approaches and models should be critically re-evaluated. It is incredible that the Independent Atom Model (IAM) of electron density effectively introduced a century ago is still the most common model of electron density used in structural analysis. One would even say that its success has dominated the whole field. When this model was introduced Max von Laue, the Braggs and their colleagues were using home-made pieces of equipment which could have hardly supplied qualitative information on diffraction spots. In consequence the errors associated with the model of electron density used were overshadowed by far larger diffraction hardware errors. However, within the past century there is an overwhelming progress in design and production of X-ray hardware which is made for needs of both small laboratories and large scale facilities. This progress in sophisticated X-ray hardware should also accelerate progress in the quality and complexity of models of electron density used to interpret experimental results. However, it is very surprising that although the quality of diffraction information collected in X-ray experiments in XXI century allows these days for far more thorough structural data quality, almost all crystallographers keep using 100 years old models of electron density effectively proving that even with the most modern scientific tools, one can step backward and do ca. 100 years old crystallography. In my presentation, I will discuss precision and accuracy of results as a function of resolution of X-ray data when IAM, experimental charge density studies, Hirshfeld Atom Refinement, and Transferable Aspherical Atom Model are applied. I will present a detailed comparison of structural, thermal and electronic parameters obtained for the same diffraction data sets when different models of electron density (IAM, TAAM, HAR, MM) are refined against collected intensities of reflections. Some practical suggestions will be presented how to estimate and improve the quality of single crystal X-ray diffraction structural results. The Authors acknowledge financial support within the Polish NCN MAESTRO grant, decision number DEC-2012/04/A/ST5/00609.



Figure 1. Symbolic consequences of application of the Independent Atom Model.

Keywords: Accuracy, precision, IAM, charge density, HAR, TAAM

MS28-O5 Improved thermal motion description for improved density models: towards Quantum Dynamic Crystallography

Anna A. Hoser^{1,2}, Anders O. Madsen²

1. Biological and Chemical Research Centre, Chemistry Department, University of Warsaw, Żwirki i Wigury 101, 02-089 Warszawa, Poland

2. University of Copenhagen, Chemistry Department, Copenhagen, Denmark

email: annahoser@gmail.com

Meaningful results from charge density studies can be obtained only when density is properly deconvoluted from thermal motion. Herein, we would like to present new approaches and models which improve thermal motion description. First approach is devoted to accurate estimation of hydrogen atoms ADPs. A major update of the frequently used in charge density studies SHADE server (<http://shade.ki.ku.dk>) will be presented. In addition to the options offered by SHADE2, the newest version offers two new methods. The first method combines the original TLS analysis with input from periodic *ab-initio* calculations. The second method utilizes input from experiment on related structures to evaluate ADPs of H atoms. In the second approach, we propose to utilize information obtained from harmonic frequency periodic *ab-initio* calculations at the Γ point, in the refinement of single crystal X-ray or neutron diffraction data. Our approach has many advantages. By refining frequencies for given normal modes we are obtaining lattice dynamical description, which is closer to reality than simple model with ADPs and we are obtaining better deconvolution of thermal motion from charge densities. The frequencies, which are obtained after the refinement, enable the calculation of thermodynamic properties. We also demonstrate that it is possible to significantly reduce the number of parameters used in refinement, with only a small increase of $wR2$. We will introduce the method and present some first results for four model systems including first applications of proposed model of thermal vibration to charge density studies.

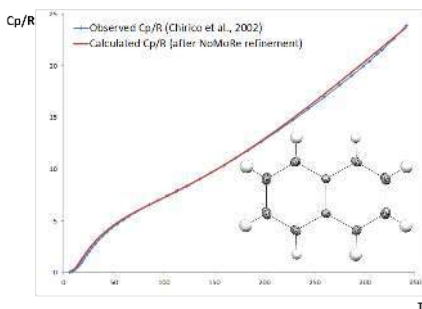


Figure 1. Estimated heat capacity for naphthalene after refinement compared with heat capacity from calorimetric measurements

Keywords: thermal motion, *ab-initio* calculations

MS29. Quasi crystals and aperiodic materials

Chairs: Andreas Schönleber, Janusz Wolny

MS29-O1 Statistical description of icosahedral quasicrystals

Radosław Strzalka¹, Ireneusz Buganski¹, Janusz Wolny¹

1. Faculty of Physics and Applied Computer Science, AGH University of Science and Technology, Krakow, Poland

email: strzalka@fis.agh.edu.pl

The atomic structure of icosahedral quasicrystals is modeled most frequently by using 6D description [1,2]. Within this approach, 3D polyhedra are considered as atoms stretched to multidimensional objects in perpendicular space. By projecting the objects (called atomic surfaces or occupation domains) on physical space, the real atomic structure is obtained. The refinement, however, is to be performed in real space. At the same time, it is rather difficult to adjust the 6D model during that process.

We show the alternative to the abovementioned method, *i.e.* the statistical description [3]. Here, the structure modeling can be done in physical space only with no need to lift the atomic structure to high dimensions. We replace atomic surfaces by statistical distribution of atomic positions with respect to the periodic reference lattice. The atomic structure is investigated by modeling this distribution. The statistical approach was already used for structure refinement of many decagonal phases [4]. It was also used to derive the structure factor of icosahedral quasicrystals based on 3D Penrose tiling [5].

In this talk, the details of structure modeling of icosahedral quasicrystals using the statistical description will be shown. The examples of atomic decoration of the Ammann rhombohedra will be considered and the application of the derived structure factor to the refinement procedure will be discussed.

[1] A. Katz, D. Gratias, *J. Non-cryst. Solids* **153&154** (1993) 187-195.

[2] H. Takakura, C. Pay-Gomez, A. Yamamoto, M. de Boissieu, *Nature Mater.* **6** (2007) 58-63.

[3] J. Wolny, *Philos. Mag.* **A77** (1998) 395-412.

[4] P. Kuczera, J. Wolny, W. Steurer, *Acta Cryst.* **B68** (2012) 578-589.

[5] R. Strzalka, I. Buganski, J. Wolny, *Acta Cryst.* **A71** (2015) DOI: 10.1107/S205327331500147

Keywords: icosahedral quasicrystal; structure modeling; statistical description; Average Unit Cell; diffraction pattern

MS29-O2 Long range ordered magnetic and atomic structures of the quasicrystal approximant in the Tb-Au-Si system

Girma Gebresenbut¹, Mikael Andersson², Přemysl Beran³, Pascal Manuel⁴, Per Nordblad², Martin Sahlberg¹, Cesar Gomez¹

1. Department of chemistry-Ångström laboratory, Uppsala university, 751 21 Uppsala, Sweden
2. Department of Engineering Sciences-Ångström laboratory, Uppsala university, 751 21 Uppsala, Sweden
3. Nuclear Physics Institute of the ASCR, v. v. i., Řež 130, 250 68 Řež, Czech Republic
4. ISIS Pulsed Neutron and Muon Facility, STFC Rutherford Appleton Laboratory, Chilton, Oxfordshire OX11 0QX, United Kingdom

email: girma.gebresenbut@kemi.uu.se

The atomic and magnetic structure of the 1/1 Tb(14)Au(70)Si(16) quasicrystal approximant has been solved by combining X-ray and neutron diffraction data. The atomic structure is classified as a Tsai-type 1/1 approximant with certain structural deviations from the prototype structures; there are additional atomic positions in the so-called cubic interstices as well as in the cluster centers. The magnetic property and neutron diffraction measurements indicate the magnetic structure to be ferrimagnetic-like below 9 K in contrast to the related Gd(14)Au(70)Si(16) structure that is reported to be purely ferromagnetic. This is to our knowledge the first reported magnetic structure determination of a quasicrystal approximant with magnetic long-range order

¹ Gebresenbut Girma, et. al, Journal of Physics: Condensed Matter 26 (32), 322202 (2014).

Keywords: Quasicrystal approximants, magnetic properties of quasicrystal approximants

MS29-O3 Three-dimensional eight-color structure

Shelomo I. BEN-ABRAHAM¹, Dvir FLOM¹

1. Department of Physics, Ben-Gurion University of the Negev, IL-8410501 Beer-Sheba, Israel

email: shelomo.benabraham@gmail.com

We present a three-dimensional generalization of the two-dimensional chair substitution tiling [R1999]. Our structure is a 3D substitution tiling based on eight cubic prototiles labeled 0, ..., 7, or equivalently by eight colors. The structure distinguishes between even and odd sites (labeled by even numbers or warm colors vs. odd numbers or cool colors, respectively). The structure is of the Toeplitz type and hence it has a pure point type Fourier spectrum [BG2013]. We discuss the symmetries of the structure. We also indicate how to generalize the structure to arbitrary dimension.

[BG2013] Baake M. and Grimm U., *Aperiodic Order, Volume 1: A Mathematical Invitation*, Cambridge University Press 2013.

[R1999] Robinson E.A., *Indag. Mathem. N.S.* **10** (1999) 581-599.

Keywords: aperiodic tilings, Toeplitz structure

MS29-O4 Quasiperiodic canonical-cell tiling with cubic symmetryNobuhisa Fujita¹¹. Institute of Multidisciplinary Research for Advanced Materials, Tohoku University, Sendai 980-8577, Japan

email: nobuhisa@tagen.tohoku.ac.jp

In canonical-cell tiling models [1] for icosahedral quasicrystals and their approximants, the atomic structure is presented as a packing of icosahedral clusters sitting on the vertices of a tiling composed of four standard polyhedra (A, B, C, and D), called the canonical cells. The canonical-cell geometry has indeed been observed in many approximants to icosahedral quasicrystals in different alloy systems. It is hence naturally expected that the same geometry holds also for icosahedral quasicrystals, and if so the canonical cells should be able to tile the space in a quasiperiodic manner so that icosahedral symmetry is globally retained. However, the existence of a tiling like the latter one has never been proved. In this work, an inflation rule for the canonical cells is worked out, and the existence of a quasiperiodic canonical-cell tiling has been confirmed for the first time. In the present inflation step, each canonical cell is expanded by a factor of τ^3 (τ : golden mean), and it is then divided into cells of the original sizes. Importantly, there are several different ways to divide expanded cells of the same shape (e.g. A) depending on their surrounding environment, still the division rules are determined locally. The atomic surface of this quasiperiodic canonical-cell tiling is studied by taking the perp-space images of the vertices. Interestingly, the atomic surface exhibits cubic symmetry rather than icosahedral symmetry.

[1] C. L. Henley, Phys. Rev. B 43, 993-1020 (1991).

Keywords: quasiperiodicity, canonical-cell tiling, inflation rule, icosahedral, cubic**MS29-O5 Unit-cell twinning in quasicrystals**Erik Zupanic¹, Albert Prodan¹, Herman J.P. Van Midden¹¹. Jožef Stefan Institute, Ljubljana, Slovenia

email: erik.zupanic@ijs.si

The discovery of quasicrystals [1] rose questions about some basic concepts of crystallography [2,3]. Their structure and the corresponding electron diffraction patterns are explained by means of unit-cell twinning. The twinning operation is applied onto primitive golden rhombohedra, obtained by a small deformation of a parent cubic close-packed structure. The deformation accounts for the required space filling and for the five-fold point symmetry. Stacking of the multiply twinned star polyhedra ("stellae dodecangulae") keeps the golden rhombohedra of adjacent nano-domains in-phase, regardless of their actual separation. The golden rhombohedra form a kind of an intergrown multiply twinned structure, with no obvious boundaries between individual twins.

By taking into account only low-index first order reflections it is shown that unit cell twinning enables a complete reconstruction of the quasicrystalline reciprocal space, with all remaining reflections being accounted for by strong dynamical scattering or belonging to weak higher-order reflections at the outskirts of the zero-Laue zone (Fig.1). Simulated diffraction patterns are in good accord with the published experimental ones of MnAl₆ [4].

Twinning and tiling are two fully compatible approaches and quasicrystals do not violate any of the existing crystallographic concepts. The golden rhombohedra, which represent the basic building elements, are small in comparison with the huge cubic cells, suggested in the past. No atoms, and the close packed ones in particular, can be ordered at distances of the order of a few nanometers, because there are no natural forces acting at such distances. When structures with huge unit cells indeed appear, they can only be a result of at least two competing periodicities, which lock-in after relatively large distances. That is also the case in quasicrystals, where the star polyhedra are a result and not the origin of multiple twinning, whose driving force is obviously the need to fill the space exactly with the slightly collapsed parent structure.

1. D. Shechtman et al., Phys. Rev. Lett., **53**, 1951 (1984).
2. D. Gratias, Europhysics news, **43/5**, 26 (2012).
3. <https://paulingblog.wordpress.com/tag/quasicrystals/>
4. J. Q. Guo et al., Phys. Rev. B, **62**, R14605 (2000).

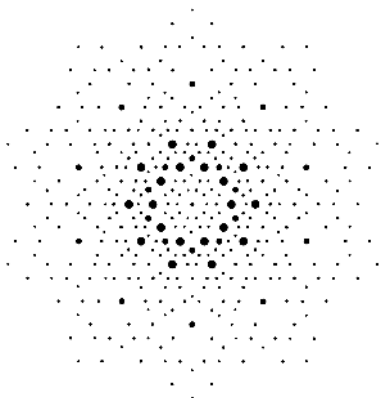


Figure 1. The simulated diffraction pattern along a quasicrystalline five-fold axis, composed of contributions from the multiply twinned golden rhombohedra and completed by dynamical scattering (the smallest radii).

Keywords: quasicrystals, unit-cell twinning, long-range order

MS30. Structure and function in coordination compounds

Chairs: Marijana Đaković, Janusz Lipkowski

MS30-O1 Hybrid porous materials

Michael J. Zaworotko¹

¹. Department of Chemical and Environmental Science, University of Limerick, Ireland

email: xtal@ul.ie

That composition and structure profoundly impact the properties of crystalline solids has provided impetus for exponential growth in the field of crystal engineering [1] over the past 25 years. This lecture will address how crystal engineering has evolved from structure design (form) to control over bulk properties (function) with particular emphasis upon an underexplored class of porous material: hybrid organic-inorganic compounds. Whereas porous crystalline materials such as purely inorganic materials (e.g. zeolites) and those based upon coordination chemistry (e.g. Metal-Organic Frameworks and Porous Coordination Polymers) are well studied and offer great promise for separations and catalysis, they can be handicapped by cost or performance (e.g. chemical stability, interference from water or low selectivity) limitations. Hybrid Porous Materials, HPMs, are much less studied. HPMs are built from metal or metal cluster “nodes” and combinations of organic and inorganic “linkers” and they represent an opportunity to overcome the weaknesses associated with existing classes of porous material. Two prototypal families of HPMs will be addressed: (i) Pillared square grids with pcu topology can afford exceptional control over pore chemistry, pore size and binding energy for CO₂. [2] Further, their performance is typically unaffected by moisture. (ii) mmo nets are based upon square grids linked by angular inorganic linkers such as chromate anions. [3] They also offer exceptional performance with respect to capture of CO₂ and other polarizable gases. New results related to the structure and properties of pcu and mmo HPMs will be presented. 1. (a) Desiraju, G.R. *Crystal engineering: The design of organic solids* Elsevier, 1989; (b) Moulton, B.; Zaworotko, M.J. *Chemical Reviews* 2001, 101, 1629-1658. 2. (a) Burd, S.D.; Ma, S.; Perman, J.A.; Sikora, B.J.; Snurr, R.Q.; Thallapally, P.K.; Tian, J.; Wojtas, L.; Zaworotko, M.J. *J. Amer. Chem. Soc.* 2012, 134, 3663-3666. (b) Nugent, P.; Belmabkhout, Y.; Burd, S.D.; Cairns, A.J.; Luebke, R.; Forrest, K.; Pham, T.; Ma, S.; Space, B.; Wojtas, L.; Eddaoudi, M.; Zaworotko, M.J. *Nature* 2013, 495, 80-84, 2013. 3. Mohamed, M.; Elsaïdi, S.; Wojtas, L.; Pham, T.; Forrest, K.A.; Tudor, B.; Space, B.; Zaworotko, M.J. *J. Amer. Chem. Soc.* 2012, 134, 19556-19559.

Keywords: crystal engineering, porous materials, carbon capture

MS30-O2 Structure and function of coordination compounds for radiopharmaceutical application

Andreas Roodt¹, Alice Brink¹, Marietjie Schutte-Smith¹, Hendrik G. Visser¹

1. Department of Chemistry, University of the Free State, Bloemfontein 9300, South Africa

email: roodta@ufs.ac.za

Many dynamic processes occur at the molecular level; thus fundamental understanding of structural behavior, and the associated influence on (kinetic) properties is still of prime importance. Herein we emphasize the continued relevance of small molecule crystallography in coordination chemistry in conjunction with an *integrated* mechanistic approach utilising spectroscopic techniques and specifically reaction kinetics, to counteract trivialized conclusions based on thermodynamic observations alone [1].

We highlight dynamics in small coordination compounds utilised as model radiopharmaceuticals and the importance of structure of the compounds on some functions thereof. The 4th and 5th row elements of the manganese triad, and in particular the ^{99m}Tc, ¹⁸⁸Re, ¹⁸⁶Re isotopes, find widespread application in nuclear medicine [2,3]. Thus, the *fac*-[M(CO)₃]⁺ core (M = ^{99m}Tc, ⁹⁹Tc, ¹⁸⁸Re, ¹⁸⁶Re) is of continued interest due to its potential in biomedical applications since it is a low-valent, low-spin, kinetically inert organometallic core with high *in vivo* stability. It coordinates many types of ligands which determine the hydro- and lipophilic properties.

Many overarching aspects of radiopharmaceuticals are imperative for its successful application; in particular, those associated with and directly influencing the kinetic stability and/or reactivity, and can be quite diverse. It is therefore important to consider these aspects in an overarching approach to enable better understanding and consequent potential more accurate prediction of *in vivo* behavior thereof [1, 3-6].

This presentation will underline some of the above mentioned aspects on small coordination compounds, and illustrate the importance of structure and concurrent different processes/ factors which significantly influence the *kinetics* in metal complexes and the structures thereof, including radiopharmaceutical models.

[1] Roodt, A.; Visser, H.G. & Brink, A. *Crystallogr. Rev.* 2011, **17**, 241.

[2] Alberto, R.; Schibli, R.; Waibel, R.; Abram, U. & Schubiger, A.P. *Coord. Chem. Rev.* 1999, 901.

[3] Schutte, M.; Kemp, G.; Visser, H.G. & Roodt, A. *Inorg. Chem.* 2011, **50**, 12486.

[4] Brink, A.; Visser, H.G. & Roodt, A. *Inorg. Chem.* 2013, **52**, 8950.

[5] Brink, A.; Visser, H.G. & Roodt, A. *Inorg. Chem.* 2014, **53**, 12480.

[6] Twala, T.N.; Schutte-Smith, M.; Roodt, A. & Visser, H.G. *Dalton Trans.* 2015, **44**, 3278.

Keywords: Coordination compounds, kinetics, structures, radiopharmaceuticals, rhenium.

MS30-O3 Guest-responsive metal-organic frameworks based on asymmetric bridging ligands

Susan A. Bourne¹, Gift Mehlana¹, Gaele Ramon¹

1. Centre for Supramolecular Chemistry Research, Department of Chemistry, University of Cape Town, Rondebosch 7701, South Africa

email: susan.bourne@uct.ac.za

Polymeric coordination compounds, and their subset metal-organic frameworks (MOFs) have provided a rich source of interest to researchers in solid state functional materials [1]. The inherent porosity achievable for 2D and 3D network structures generated from bridging ligands coordinated to metal ions allows for applications as diverse as catalysis, gas storage, separation and extraction [2]. While interpenetration can sometimes appear as a hindrance to engineering highly porous materials, it may hold some advantages in terms of thermal stability and increased functionality. Examples from our recent work will be presented, including MOFs incorporating Co(II) and Zn(II) with flexible pyridylcarboxylate ligands. These MOFs are robust to solvent loss. New crystalline phases result from the exposure of the empty frameworks to various solvents (Figure 1). The resulting solvatochromism has been correlated to solvent properties [3, 4].

References

1. Recent reviews: (a) A. Phan, C. J. Doonan, F. J. Uribe-Romo, C. B. Knobler, M. O'Keeffe, O. M. Yaghi, *Acc. Chem. Res.*, 2010, **43**, 58. (b) C. Janiak, J. K. Vieth, *New J. Chem.*, 2010, **34**, 2366. (c) J. J. Perry, J. A. Permana, M. J. Zaworotko, *Chem. Soc. Rev.*, 2009, **38**, 1400.

2. Recent examples include (a) O. K. Farha, Y. A. Oezguer, I. Eryazici, C. D. Malliakas, B. G. Hauser, M. C. Kanatzidis, S. T. Nguyen, R. Q. Snurr, J. T. Hupp, *Nat. Chem.*, 2010, **2**, 944. (b) S. Wang, J. Lin, X. Wang, *Phys. Chem. Chem. Phys.* 2014, **16**, 14656.

3. G. Mehlana, G. Ramon, S. A. Bourne. *CrystEngComm*, 2013, **15**, 9521.

4. G. Mehlana, G. Ramon, S. A. Bourne, *CrystEngComm*, 2014, **16**, 8160.

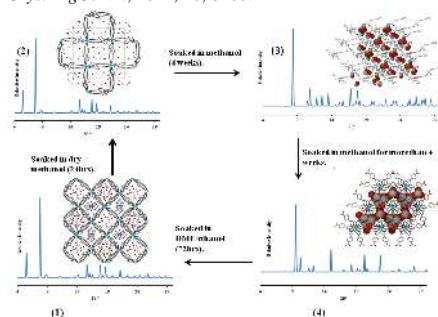


Figure 1. Phase transformations in a Co(II) MOF.

Keywords: MOF, solvatochromism, thermochromism, coordination compound

MS30-O4 Giant pentaphosphaferrocene-based supramolecules

Alexander V. Virovets^{1,2}, Eugenia V. Peresyphkina^{1,2}, Claudia Heindl¹, Manfred Scheer¹

1. University of Regensburg, Regensburg, Germany

2. Nikolaev Institute of Inorganic Chemistry SB RAS, Novosibirsk, Russia

email: avvirovets@yahoo.com

An intriguing inorganic analogue of ferrocene, pentaphosphaferrocene, $[\text{Cp}^{\text{R}}\text{Fe}(\eta^5\text{-P}_5)]$ ($\text{Cp}^{\text{R}} = \eta^5\text{-C}_5\text{R}_5$, $\text{R} = \text{Me}$ (Cp^{M}), CH_2Ph (Cp^{Bn})), has the ability to coordinate Cu^+ cations resulting in either coordination polymers or in giant supramolecules [1-4]. The quasi-spherical voids inside the latter can include various organic, inorganic and organometallic guest molecules and cations. This inclusion allowed us to stabilize such instable molecules as the paramagnetic 16 VE complex $[\text{CpCr}(\eta^5\text{-As}_5)]$ or light-sensitive yellow arsenic, As_4 , embedded as guests into $[\text{Cu}_{20}\text{Cl}_{20}(\text{Cp}^{\text{M}}\text{FeP}_5)_{12}]$ and $[\text{Cu}_{30}\text{I}_{30}(\text{Cp}^{\text{M}}\text{FeP}_5)_{10}(\text{MeCN})_6]$, respectively. Our recent solid state and solution study demonstrated the potential of $[\text{Cp}^{\text{Bn}}\text{Fe}(\eta^5\text{-P}_5)]$ in combination with CuX ($\text{X} = \text{Cl}, \text{Br}$) to switch between supramolecules of different porosity and shape [4]. With increasing amount of CuX the structures of the supramolecules change from spherical $[\text{Cu}_m\text{X}_m\{\text{Cp}^{\text{Bn}}\text{FeP}_5\}_{12}]$ ($m = 14\text{-}20$) to the tetrahedral aggregate $\{[\text{Cp}^{\text{Bn}}\text{FeP}_5]_{12}\}\{\text{CuBr}\}_{51}\{\text{MeCN}\}_8$ with an outer diameter of 3.56 nm. The use of Cp_2Co and $(\text{C}_6\text{H}_6)_2\text{Cr}$ as guests results in their partial oxidation and inclusion as cations into an anionic cage, e.g., $[\text{CoCp}_2^+ @ \{[\text{Cp}^{\text{M}}\text{FeP}_5]_8\text{Cu}_{24}\text{Br}_{28}(\text{CuBr})_{0.25}(\text{MeCN})_4(\text{MeCN})_2\}]^{3-}$ (Fig.).

Despite the objective obstacles like instability of crystals toward the loss of solvents, huge unit cells (up to $300\,000\text{ Å}^3$), disorder of the inorganic host scaffold and guest, our structural investigations revealed some unusual phenomena. Thus, we first discovered the π -stacking interaction involving the inorganic 6- e^- π -systems of the *cyclo-P*₅ forming the inner cavity of the supramolecule and Cp, *cyclo-P*₅ and *cyclo-As*₅ of the guest molecules that determine their orientation inside the void. Furthermore, the spherical supramolecules sometimes form, *contra-intuitively*, low-dense packings with huge intramolecular cavities [2].

This work was supported by ERC grant AdG339072-SELFPHOS.

[1] J. Bai et al (2003), *Science*, **300**, 781.

[2] E. V. Peresyphkina et al (2014), *Z. Krist. – Crystall. Mat.*, **229**, 735, and references therein.

[3] C. Schwarzmaier et al (2013), *Angew. Chem. Int. Ed.* (2013), **52**, 10896.

[4] F. Dielmann et al, *Chem.-A Eur. J.* (2015), Online, DOI: 10.1002/chem.201500692.

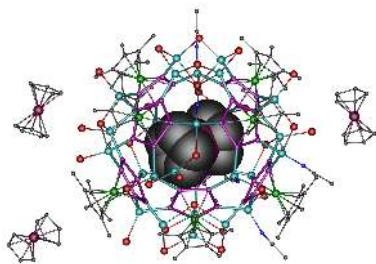


Figure 1. Inclusion of CoCp_2^+ into supramolecule (Fe green, Co purple, Cu cyan, Br brown)

Keywords: crystal structure and properties, pentaphosphaferrocene, host-guest compounds, supramolecular chemistry, disorder, intermolecular interactions

MS30-O5 Prohibited and allowed crystal-crystal transformations in phosphinate based coordination polymers

Annalisa Guerri¹, Andrea Ienco², Thierry Bataille³, Maria Caporali², Ferdinando Costantino⁴, Marco Taddei¹

1. Department of Chemistry "Ugo Schiff", University of Florence, via della Lastruccia 3 - 50019 Sesto Fiorentino (FI) - ITALY

2. Consiglio Nazionale delle Ricerche (CNR), Istituto di Chimica dei Composti Organometallici, Via Madonna del Piano 10, 50019 Sesto Fiorentino (FI), Italy

3. Sciences Chimiques de Rennes (UMR 6226) CNRS, Université de Rennes 1, Avenue du General Leclerc 35042 Rennes Cedex, France

4. Department of Chemistry, University of Perugia, Via Elce di Sotto 8, 06123 Perugia, Italy

email: annalisa.guerri@unifi.it

In the last years, several 1D, 2D and 3D coordination polymers based on diposphinic acid (pcp= P, P'-diphenylmethylenediphosphate or pc₂p= P, P'-diphenylethylenediphosphate) have been reported by our group.[1] We have described in several cases, crystal-crystal transformation induced by temperature and by water. For instance the 3D network of $[[\text{Cu}(\text{bipy})(\text{pc}_2\text{p})(\text{H}_2\text{O})][1]2.5\text{H}_2\text{O}]_n$ (bipy = 4,4'-bipyridine) rapidly transforms in the 2D slabs of $[[\text{Cu}(\text{bipy})(\text{pc}_2\text{p})(\text{H}_2\text{O})][1]3\text{H}_2\text{O}]_n$ [2]. We also found that the Metal Organic NanoTube (MONT) $[[\text{Cu}_2(\text{bpye})(\text{pc}_2\text{p})_2] 2.5\text{H}_2\text{O}]_n$ (bpye = 1,2-bis(4-pyridyl)ethane) is converted in the 1D slab $[\text{Cu}_2(\text{bpye})(\text{pc}_2\text{p})_2(\text{H}_2\text{O})_2]_n$ in water while the isostructural MONT $[[\text{Cu}_2(\text{bipy})(\text{pc}_2\text{p})_2] 5\text{H}_2\text{O}]_n$ remain unaltered.[3] Here we report the different behavior for the 1D iso-structural $[\text{Ni}(\text{H}_2\text{O})_4(\text{bipy})\text{pc}_2\text{p}]_n$, **1**, and $[\text{Ni}(\text{H}_2\text{O})_4(\text{bpye})\text{pc}_2\text{p}]_n$, **2** coordination compounds. Only an amorphous anhydrous phase was obtained in the case of **1**. For **2**, the monohydrated $[\text{Ni}(\text{H}_2\text{O})(\text{bpye})\text{pc}_2\text{p}]_n$ 3D phase, **3**, and the crystalline anhydrous $[\text{Ni}(\text{bpye})\text{pc}_2\text{p}]_n$ phase, **4**, have been isolated just varying the temperature. An interpretation based on supra-molecular interactions between the aromatic rings in competition with the other factors, like hydrogen bond, solvent and metal geometry will be discussed.

[1] F. Costantino, A. Ienco, M. Taddei in Tailored Organic-Inorganic Materials, Wiley 2015 in press

[2] T. Bataille, F. Costantino, A. Ienco, A. Guerri, F. Marmottini, S. Midollini. Chem. Commun., 6381 (2008)

[3] T. Bataille, S. Bracco, A. Comotti, F. Costantino, A. Guerri, A. Ienco, F. Marmottini. CrystEngComm, 14, 7170 (2012); M. Taddei, A. Ienco, F. Costantino, A. Guerri. RSC Adv., 3, 26177 (2013)

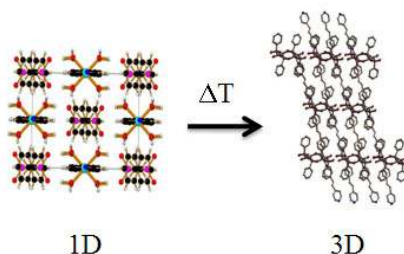


Figure 1. 1D to 3D transformation of the compound

Keywords: MONT, coordination polymers, transformation

MS31. Tailored physical properties in molecular crystals

Chairs: Sebastien Pillet, Pilar Gomez-Sal

MS31-O1 Quantification, systematics and modeling of mechanical effects in molecular crystals

Panče Naumov¹

1. New York University Abu Dhabi

email: pance.naumov@nyu.edu

Elastic materials that are capable of stimuli-responsive mechanical reconfiguration are indispensable for fabrication of mechanically tunable elements for actuation and energy harvesting, including flexible electronics, artificial muscles, and microfluidic elements. The advanced materials that will qualify for these applications in the future must fulfill an extended list of requirements including reversibility, rapid and controllable mechanical response that is proportional to the applied stimulus, and extended lifetime without fatigue.

Elastic properties are counter-intuitive for single crystals of molecular materials which are normally perceived as stiff and brittle entities. The growing realization that bending, curling, twisting, jumping and other mechanical effects of single crystals are surprisingly common has inspired researchers to control crystal motility for actuation. However, new mechanically responsive crystals are reported at a greater rate than their quantitative photophysical characterization; a quantitative identification of measurable parameters and molecular-scale factors that determine the mechanical response has yet to be established. We have recently developed an overarching model for the mechanical effects in crystals that aids our understanding of the macroscopic measurables that could be used for quantification and comparison of the performance of different mechanical effects. The results provide a basis for direct correlations with the molecular and crystal structure.

References:

- [1] M. Panda, S. Ghosh, N. Yasuda, T. Moriwaki, G. Dev Mukherjee, C. M. Reddy, P. Naumov, *Nature Chem.*, 2015, 7, 65.
- [2] M. Panda, T. Runčevski, S. C. Sahoo, A. Belik, N. K. Nath, R. Dinnebier, P. Naumov, *Nature Commun.*, 2014, 5, 4811.
- [3] N. K. Nath, M. Panda, S. Sahoo, P. Naumov, *CrystEngComm*, 2014, 16, 1850.
- [4] R. Medishetty, A. Husain, Z. Bai, T. Runčevski, R. E. Dinnebier, P. Naumov, J. J. Vittal, *Angew. Chem., Int. Ed.*, 2014, 53, 5907.

[5] N. K. Nath, L. Pejov, S. Nichols, C. Hu, N. Saleh, B. Kahr, P. Naumov, *J. Am. Chem. Soc.*, 2014, 136, 2757.

[6] S. C. Sahoo, M. K. Panda, N. K. Nath, P. Naumov, *J. Am. Chem. Soc.*, 2013, 135, 12241.

[7] P. Naumov, S. C. Sahoo, B. A. Zakharov, E. V. Boldyreva, *Angew. Chem., Int. Ed.*, 2013, 52, 9990.

[8] S. C. Sahoo, S. B. Sinha, M. S. R. N. Kiran, U. Ramamurty, A. Dericioglu, C. M. Reddy, P. Naumov, *J. Am. Chem. Soc.*, 2013, 135, 13843.

Keywords: actuators, molecular machines, mechanical effects, molecular crystals, photochemistry

MS31-O2 Intra- and inter-molecular interactions for the understanding of stereoselective catalytic properties of chiral metal complexes

Fernando J. Lahoz¹, Daniel Carmona¹, Pilar Lamata¹, Pilar García-Orduña¹, Ricardo Rodríguez¹, Luis A. Oro¹

1. Institute for Chemical Synthesis and Homogeneous Catalysis (ISQCH), University of Zaragoza-CSIC, C/ Pedro Cerbuna, 12, 50009 Zaragoza, Spain

email: lahocz@unizar.es

Most of the physical properties of molecular complexes depend on the *intramolecular bonding system* established in the discrete molecule, that could be ascertained through structural analysis. In the case of catalytic properties, even for homogeneous processes, the structural information emanated from X-ray studies could give significant information on *interatomic interactions*, in most cases a basic knowledge to understand activity and (stereo)selectivity.

The use of Lewis acids, based on metal complexes, as catalysts for the synthesis of highly demanded enantio pure compounds has been identified as one of the most versatile method, as their activity and selectivity could be well modulated through the modification of the metal center and its ancillary ligands. In the recent past, we have been studying a family of metal catalysts containing different P,P-, N,N- y P,O- donor ligands, for which we have established that their physical properties, in particular their stereoselectivity, are closely related to the presence of subtle intra-molecular interactions.

In fact, a systematic study of a family of complexes of the type $[(\eta^3\text{-ring})M(PP^*)(\text{substrate})]^{n+}$ ($(\eta^3\text{-ring})M^+ = (\eta^3\text{-C}_6\text{Me}_5)\text{Rh}$, $(\eta^3\text{-C}_6\text{Me}_5)\text{Ru}$ or $(\eta^3\text{-p-cymene})\text{Ru}$; substrate = methacrolein or α - β insaturated ketones) has been identified as active and selective catalysts in asymmetric Diels-Alder processes [1]. In these cases, weak intra-molecular interactions of the type CH/ π has been identified as responsible for the remarked obtained stereoselectivity. Furthermore, a related group of complexes $[(\eta^3\text{-ring})\text{Ru}(\text{POH})]^{n+}$ (POH: (S_{C1} , R_{C2})-Ph, PC)Ph HC(OH)-HCH, OMe) have also showed intrinsic catalytic properties both in Diels-Alder and Friedel-Crafts processes. For these species, the structural studies have shown how the different alternative coordination modes $\kappa^1\text{P}$, $\kappa^2\text{P,O}$ y $\kappa^3\text{P,O,O'}$ for the POH ligand increased the acid properties of the hydroxyl group and have given us clues to rationalize their different activities as Brønsted-acid catalyst through formation of inter-molecular hydrogen bonds. [2]

References

- [1] A. Becerra, R. Contreras, D. Carmona, F.J. Lahoz, P. García-Orduña, *Dalton Trans.*, **2013**, 42, 11640-11651; D. Carmona, F. Viguri, A. Asenjo, F.J. Lahoz, P. García-Orduña, L. A. Oro, *J. Mol. Cat. A*, **2014**, 385, 119-124 and references therein. [2] D. Carmona, M. P. Lamata, P. Pardo, R. Rodríguez, F.J. Lahoz, P. García-Orduña, I. Alkorta L.A. Oro, *Organometallics*, **2014**, 33, 616-619 and 6927-6936.

Keywords: Molecular Structure, Catalytic Properties, Interatomic Interactions, Enantioselectivity

MS31-O3 Novel 1-D rhodium polymeric chain systems *via* rhodium-rhodium interactions

Carla Pretorius¹, Alice Brink¹, Andreas Roodt¹

1. University of the Free State, Bloemfontein, South Africa, 9300

email: cpretorius87@gmail.com

Of interest to our research is the addition of metallophilic interactions to the arsenal library in the design of directionally orientated systems. The design of such systems has been highly motivated by the need for tuneable materials with unique magnetic, conducting, vapochromic and other properties that falls within a unique class of crystal engineering.

Metallophilic interactions occur when overlap arises between filled nd-orbitals, ns and np orbitals of transition metals such as gold, platinum, silver and rhodium. By facilitating these interactions metal centres are connected along one direction to form infinite 1-D metal chains. In our research, rhodium(I) complexes containing β -diketonato ligands were investigated for metallophilic interactions. A wide range of complexes were investigated with $[\text{Rh}(\text{acac})(\text{CO})_2]$ systems (acac= acetylacetone) displaying short Rh \cdots Rh interactions of 3.254(3) and 3.274(3) Å to complexes such as $[\text{Rh}(\text{4Cl-F}_3\text{bzac})(\text{CO})_2]$ (4Cl-F₃bzac= 1-(4-chlorophenyl)-4,4,4-trifluoro-1,3-butanedione) that contains ligands with greater steric bulk with Rh-Rh distances of 3.469(3) and 3.617(3) Å.

The tailoring of ligand systems by altering electronic and steric properties allowed the manipulation of the metallophilic interactions which in turn resulted in altered physical properties of the materials. Additionally, it was observed that different crystallization conditions could result in changes in the assembly of molecules as illustrated with the isolated polymorph of $[\text{Rh}(\text{4Cl-F}_3\text{bzac})(\text{CO})_2]$ that displayed less diverse Rh-Rh distances of 3.523(3) and 3.593(3) Å. Several novel rhodium complexes will be presented that displayed these unique metallophilic interactions. In addition, solution studies involving IR, UV/Vis and NMR that could evaluate induced stacking in solution by varying concentration and solvent choices will also be highlighted.

MS31-O4 Rational design of heterometallic molecular precursorsEvgeny V. Dikarev¹¹. Department of Chemistry, University at Albany, SUNY

email: edikarev@albany.edu

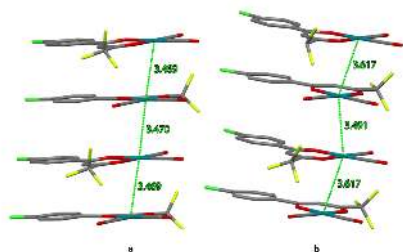


Figure 1. Rh...Rh interactions observed for [Rh(F₄Cibzac)(CO)]_n were found alternating between two pairs of molecules. a) Rh1²-Rh2 displayed interactions of 3.469(3) and 3.470(3) Å and b) Rh3-Rh4 have reported interactions of 3.491(3) and 3.617(3) Å.

Keywords: 1-D metal chains, metallophilic interactions, rhodium

The major focus of the title research is a design of heterometallic compounds that can be used as single-source precursors for the low-temperature synthesis of energy-related materials. The ultimate goal is to create heterometallic precursor with discrete molecular structure and with a proper metal:metal ratio for the target material. Several new strategies for a rational design of heterometallic compounds such as mixed-valent, mixed-ligand, and asymmetric ligand approaches will be discussed. These techniques were shown to effectively bring about changes in the connectivity pattern within heterometallic assembly and to yield molecular precursors with required stoichiometry, while avoiding the formation of coordination polymers. The applicability of the above approaches to the synthesis of single-source precursors for multiferroic oxides,¹ oxygen evolution reaction catalysts,² and prospective cathode materials of rechargeable batteries³ will be presented. X-ray crystallography serves as an efficient tool to rationalize the important features of heterometallic precursor structures such as oxidation states of transition metal atoms as well as the identities of elements with very close atomic numbers.

References

- 1) C. M. Lieberman, A. Navulla, H. Zhang, A. S. Filatov, E. V. Dikarev *Inorg. Chem.* **2014**, *53*, 4733–4738.
- 2) C. M. Lieberman, A. S. Filatov, Z. Wei, A. Yu. Rogachev, A. M. Abakumov, E. V. Dikarev *Chem. Sci.* **2015**, DOI: 10.1039/c4sc04002c.
- 3) Z. Wei, H. Han, A. S. Filatov, E. V. Dikarev *Chem. Sci.* **2014**, *5*, 813-818.

Keywords: heterometallic compounds, molecular precursors, mixed-metal materials

MS31-O5 Self-organization of the reaction-fracture coupled front on the mesoscopic scale caused by morphological instability at $\text{CuCl}_2 \cdot 2\text{H}_2\text{O}$ dehydration

Stanislav A. Chizhik^{1,2}

1. Novosibirsk State University; 630090 Pirogova, 2, Novosibirsk, Russia

2. Institute of Solid State Chemistry and Mechanochemistry, SB RAS; 630128 Kutateladze 18, Novosibirsk, Russia

email: csabox@yandex.ru

The kinetics of many heterogeneous solid state reactions can be described as propagation of the reaction-fracture coupled front appearing as a result of the feedback between the reaction and fracture [1].

Anisotropy of the mechanical properties of reagents results in that the rate of the reaction front depends on its crystallographic orientation. This can lead to a morphological instability of the front in some instances. If a reaction starts on a crystal face that corresponds to the orientation of slow movement then local perturbations of the front shape may result in formation of the front regions which move faster and so increasing initial disturbance. Initial flat front is partitioned to the pieces in which local crystallographic orientation differs from that of original front. On average the resulting reorganized front retains the initial front orientation but moves faster and produces different fracture morphology.

This picture was observed experimentally when studying dehydration of $\text{CuCl}_2 \cdot 2\text{H}_2\text{O}$. The front starting from faces (110) moves in deep of about 1 mkm retaining flat shape. Thereafter it partitions to sharp wedged pieces oriented as [010] and positioned in aperiodic manner distanced by 0.5 – 2 mkm from each other (Fig. 1). Average rate of the front increases several times.

With the single-crystal X-ray diffraction it was found out that the product consists of nano-sized twin crystallites of two orientations. Deformation tensor computed from these relations is characterized by strong anisotropy. In two directions there is shrinkage by 12% and 37% whereas in third an expansion occurs by 6%. We suggest that the product twins are formed in a ratio providing minimization of elastic strain energy. It is shown that the most significant decrease of the elastic strain energy can be achieved due to twinning on the initial (110) crystal face. According to the model this results in significant slowing down of the reaction front in this direction. At the same time the twinning can not provide a decrease of the stress for the front parallel to the face (100). Consequently such a front could be the fastest one. Thus the most likely perturbations of the initial flat front are the wedge-like formations directed along [010] which provide appearing of local front pieces slightly inclined to the fast direction (100). These theoretical results are fully confirmed by the experiments.

[1] S.A. Chizhik, A.A. Sidelnikov, *Solid State Ionics*, 178 (2007), 1487

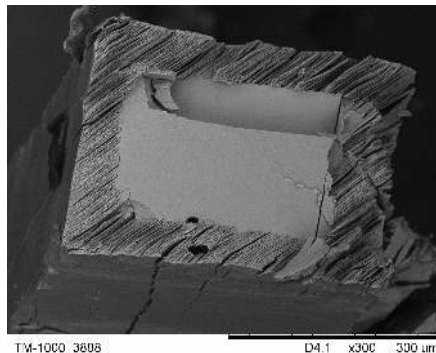


Figure 1. The crystal cut demonstrating the reaction-fracture front propagating from the faces (110)

Keywords: solid state reactions, fracture, feedback, morphology, self-organization

MS32. Halogen bonding in the solid state

Bushuyev et al. Chem. Sci. 2014, 5, 3158.

Keywords: halogen bonding, photo-mechanical effect, cocrystals, supramolecular, self-assembly, crystal-to-crystal

Chairs: Christer Aakeröy, Lee Brammer

MS32-O1 Perfluorinated azobenzenes for the design of new halogen-bonding molecules and photomechanical materials

Tomislav Friščić¹, Oleksandr S. Bushuyev¹, Christopher J. Barrett¹

1. McGill University

email: tomislav.friscic@mcgill.ca

Over the past decade, halogen bonding has developed from a laboratory curiosity to a powerful tool of crystal engineering, allowing the deliberate and controlled assembly of cocrystals, 1-, 2- or 3-dimensional supramolecular architectures and design of systems for molecular recognition and separation.¹ This presentation will focus on our recent exploration of solvent-free methodologies for the synthesis of multi-component materials based on halogen bonds, as well as the use of perfluorinated azobenzenes as building blocks for the synthesis of halogen-bonded cocrystals. In particular, we will describe how the extensive fluorination of the azobenzene moiety leads to new and attractive opportunities both in the design of photo-mechanical materials capable of mechanical response to visible light stimuli,² as well as in the synthesis of new molecular building blocks pre-designed for halogen-bonded self-assembly.³ The photo-mechanical properties of the herein described halogen-bonded materials are based on the previously never reported irreversible crystal-to-crystal cis-to-trans isomerization in the solid state. Whereas we find that this photo-mechanical effect is readily exhibited by several crystalline perfluorinated cis-azobenzenes, the use of halogen bond-driven cocrystallization allows, for the first time, the modulation and fine-tuning of their photo-mechanical behavior. The variation of different halogen bond acceptors in combination with a limited set of perfluorinated cis-azobenzene halogen bond donors as photo-mechanically active building blocks enabled the synthesis of a library of cocrystals with a range of photo- and thermo-chemical properties: from those that exhibit cis-trans isomerization without any change in crystal shape to those that undergo crystal-to-crystal isomerization accompanied by large scale bending. As an example of such tuning of photo-mechanical behavior of crystalline solids, the presentation will highlight a photo-mechanical halogen-bonded cocrystal that allows the *in situ* study of solid-state azobenzene isomerization by single crystal X-ray diffraction.⁴

1) Priimagi et al. Acc. Chem. Res. 2013, 46, 2686; 2) Bushuyev et al. J. Am. Chem. Soc. 2013, 135, 12556; 3) Bushuyev et al. CrystEngComm 2015, 17, 73; 4)

MS32-O2 Recent results with halogen bonds in crystal engineeringGautam R. Desiraju¹¹. Solid State and Structural Chemistry Unit, Indian Institute of Science, Bangalore 560 012, India

email: gautam_desiraju@yahoo.com

In a halogen bond, an electrophilic halogen atom makes an attractive contact with a negatively polarized species. Halogen bonds are somewhat similar and somewhat different from hydrogen bonds. They are similar because the protagonist atoms—halogen and hydrogen—are both electrophilic in nature. They are different because the size of a halogen atom is not negligible, unlike the small hydrogen atom in a hydrogen bond. In terms of crystal structure design, halogen bonds offer a unique opportunity in terms of the strength, size of halogens and a gradation of interactions. These gradations may be used in the design of ternary and possibly higher cocrystals. The specific directionality of the halogen bond makes it a good tool to achieve interaction orthogonality. Although halogen bonds have been mostly used in crystal engineering as if they were exactly like hydrogen bonds, this may be the right time to look at the *differences* between these two interaction types and exploit them in more subtle ways in crystal engineering. With a formal IUPAC definition in place and explosive growth in halogen bond research during the past few years, one may expect rapid growth in this area,

Keywords: crystal engineering**MS32-O3 Implication of halogen bonding in ligand substitution reactions: solid state studies**Marta E.G. Mosquera¹, Pilar Gomez-Sal¹, Francisco Fernández-Palacio¹, Lina M. Aguirre¹¹. Department of Organic Chemistry and Inorganic Chemistry, University of Alcalá

email: martaeg.mosquera@uah.es

The studies on the Halogen Bonding (XB) interaction have grown exponentially since the beginning of the century. Although XB interaction has been known for a long time, its importance has been particularly acknowledged in the last two decades.[1] In fact, the interest on XB keeps growing due to the broad array of areas where its influence has been observed, ranging from material science to biology.[2] In this context, one of our research areas is focused in the preparation of supramolecular organometallic networks, containing either main group or transition metal complexes using the versatility of the XB interaction.[3] In particular, the coordination compound $[\text{Ru}(\text{X})_2(\text{CNR})_4]$ is an interesting building block for the preparation of such networks and depending on the species involved in the interaction we can reach the formation of networks with different topology. As such, when the XB donor is ICl_4F it is observed the generation of the *synthon* $\text{M}-\text{Cl}^{\delta-}\cdots\text{X}^{\delta+}-\text{C}$ that renders the formation of a monodimensional zig-zag arrangement (figure 1 right). Changing the XB donor to X_2 it is possible to generate the bidimensional honey-comb network shown in figure 1 left. In the course of these studies we encountered an unexpected substitution reaction on the ruthenium coordination sphere where the chloride ligands are substituted by iodides. This is an unusual process since the only source of iodide in the reaction media was iodine. The isolation of several intermediates with different substitution degree and showing XB interactions in the solid state network gave us clues on the reaction mechanism and evidenced the clear influence of the XB species in this unusual reaction process.

References

- [1] N. Ramasubbu, R. Parthasarathy and P. Murray-Rust, *J. Am. Chem. Soc.* 1986, **108**, 4308; L. Brammer, E. A. Bruton and P. Sherwood, *Cryst. Growth Des.*, 2001, **1**, 277; C. B. Aakeröy, M. Baldrighi, J. Desper, P. Metrangolo and G. Resnati, *Chem. Eur. J.*, 2013, **19**, 16240
- [2] P. Metrangolo, G. Resnati, T. Pilati and S. Biella, *Halogen Bonding in Crystal Engineering*, Springer Berlin/Heidelberg, 2008, pp. 105-136; F. Zapata, A. Caballero, N. G. White, T. D. W. Claridge, P. J. Costa, V. Félix and P. D. Beer, *J. Am. Chem. Soc.*, 2012, **134**, 11533-11541.
- [3] F. Vidal, M^a A. Dávila, A. San Torcuato, P. Gómez-Sal, M. E. G. Mosquera, *Dalton Trans.*, 2013, **42**,

7074 - 7084

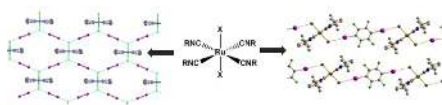


Figure 1.

Keywords: Halogen Bonding, Substitution Reactions

MS32-O4 Engineering ternary cocrystals by orthogonal hydrogen and halogen bonds

Filip Topić¹, Kari Rissanen¹

¹ University of Jyväskylä, Department of Chemistry, Nanoscience Center, P.O. Box 35, FI-40014 University of Jyväskylä, Finland

email: filip.f.topic@jyu.fi

In the still maturing field of halogen bonding, we have been especially interested in discovering new halogen bonding motifs [1,2] and applying them in crystal engineering [3].

The particular robustness of C–I...S halogen bond with thioureas has recently been highlighted, persisting even in solution [4]. In addition to that, the orthogonality of such interaction to hydrogen bonds has also been demonstrated [5], offering the possibility of constructing complex systems where the two can operate independently.

Also knowing that the crown ethers reliably cocrystallize with thioureas [6,7], this prompted us to combine thioureas with crown ethers and various (aromatic and non-aromatic) perfluorinated halogen bond donors, resulting in a large number of ternary cocrystals with high supramolecular yield. Besides the success of the strategy and the aesthetically appealing structures, these systems present other intriguing aspects, such as differing behavior of bromine- and iodine-based donors, tunable metrics and, finally, the possibility of constructing porous materials.

[1] Troff, R.W., Mäkelä, T., Topić, F., Valkonen, A., Raatikainen, K., Rissanen, K., *Eur. J. Org. Chem.* **2013**, 1617–1637. [2] Raatikainen, K., Rissanen, K., *CrystEngComm*, **2011**, *13*, 6972–6977. [3] Raatikainen, K., Rissanen, K., *Chem. Sci.*, **2012**, *3*, 1235–1239. [4] Robertson, C.C., Perutz, R.N., Brammer, L., Hunter, C., *Chem. Sci.*, **2014**, *5*, 4179–4183. [5] Arman, H.D., Gieseking, R.L., Hanks, T.W., Pennington, W.T., *Chem. Commun.*, **2010**, *46*, 1854–1856. [6] Drew, M.G.B., Nicholson, D.G., *Acta Cryst.*, **1985**, *C41*, 1358–1360. [7] Wishkerman, S., Bernstein, J., Hickey, M. B., *Cryst. Growth Des.*, **2009**, *9*, 3204–3210.

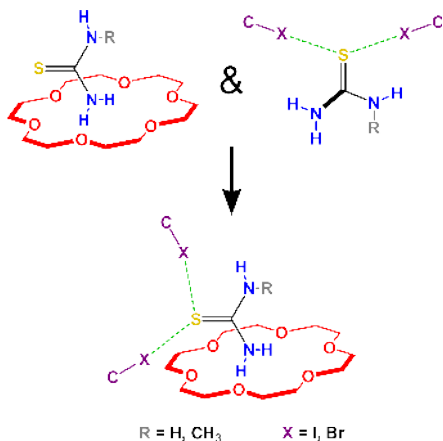


Figure 1. Hydrogen and halogen bonded motifs are combined in the studied ternary cocrystals.

Keywords: crystal engineering, ternary co-crystals, hydrogen bond, halogen bond, orthogonality

MS32-O5 Halogen bonding in host-guest compounds: Structures and kinetics of enclathration and desolvation

Francoise Mystere Amombo Noa¹, Susan Ann Bourne¹, Luigi Renzo Nassimbeni¹

¹. Centre for Supramolecular Chemistry, Department of Chemistry, University of Cape Town, Rondebosch 7701, South Africa.

email: noa.mystere@gmail.com

The host compounds tetrakis-(4-bromophenyl) ethylene and its iodo-analogue form inclusion compounds with a series of chloro- and iodo-methanes. Their structures have been elucidated and their non-bonded halogen···halogen contacts analysed and classified. Their kinetics of desolvation have been studied and the concomitant activation energies established. The velocity of the enclathration for the solid-methyl iodide vapour reactions and associate rate law have been established. Figure 1 shows halogen···halogen interactions between the host compound tetrakis-(4-bromophenyl) ethylene and the guest diiodomethane.

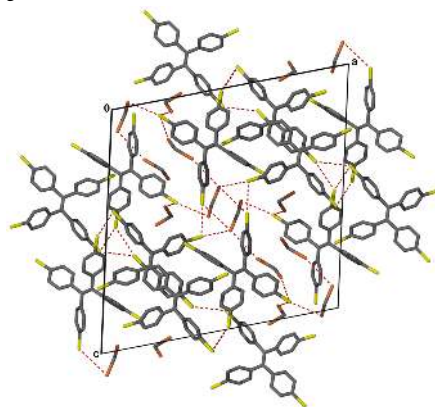


Figure 1. Packing diagram of tris diiodomethane bis tetrakis-(4-bromophenyl) ethylene along [010] showing halogen···halogen interactions.

Keywords: Halogen-halogen interactions, halogen bonding

MS33. Mechanical effects and properties of ordered matter

Chairs: Panče Naumov, Helena Shepherd

MS33-O1 Photomechanical effects in crystals: the role of temperature. A case study of linkage isomerization in $[\text{Co}(\text{NH}_3)_5\text{NO}_2]\text{Cl}(\text{NO}_3)$

Elena V. Boldyreva^{1,2}, Anatoly A. Sidelnikov², Stanislav A. Chizhik^{1,2}, Boris A. Zakharov^{1,2}, Elena V. Boldyreva^{1,2}

1. Novosibirsk State University, ul. Pirogova, 2, Novosibirsk 630090 Russian Federation, eboldyreva@yahoo.com

2. Institute of Solid State Chemistry and Mechanochemistry SB RAS, ul. Kutateladze, 18, Novosibirsk 630128

email: eboldyreva@yahoo.com

The research on mechanically responsive single crystals had developed and was very active back in the 1980s. Dating just back over a decade, this field was revived alongside the growing realization that the mechanical effects in crystals can be utilized as dynamic elements in macroscopic devices, and several research groups have been particularly prolific in this research field [1]. One of the issues when studying these transformations is to correlate the degree of nitro-nitrito phototransformation and the macroscopic mechanical response. In an early study of our group we have proposed to use the quantitative measurements of the elastic bending of needle-shaped crystals of $[\text{Co}(\text{NH}_3)_5\text{NO}_2]\text{Cl}(\text{NO}_3)$ on irradiation to follow the kinetics of the transformation and the effect of the elastic compression on the quantum yield [2-6]. We have now revisited this system and have modified the experiment design, in order to follow the effects of temperature in the range from 100 K to 400 K on the transformation. This made it possible to follow the role of temperature in the photomechanical effect, taking into account both the lattice strain related to the anisotropic thermal expansion and the reverse nitrito-nitro isomerization (studied by variable-temperature single-crystal X-ray diffraction). A direct experimental evidence of the feed-back arising on photochemical nitro-nitrito and on reverse thermal nitrito-nitro isomerization was obtained. The study can be considered as a case study, representative for any photoinduced transformation induced in needle-like crystals when irradiated from one side (i.e. with a gradient of transformation degree normal to the surface).

The research was supported by RFBR (project 14-03-00902).

1. Nath N.K., Panda M.K., Sahoo S.C., Naumov P. CrystEngComm, 2014, 16, 1850-1858.

2. Boldyreva E.V., Sidelnikov A.A., Chupakhin A.P., Lyakhov N.Z., Boldyrev V.V., Proceed. Acad. Sci. USSR 1984, 277, 893-896.

3. Boldyreva E.V., Sidelnikov A.A. Proceed. SB USSR, Chem. Sci., 1987, 5, 139-145.

4. Yakobson B.I., Boldyreva E.V., Sidelnikov A.A. Proceed. SB USSR, Chem. Sci., 1989, 1, 6-10.

5. Boldyreva E.V., Mol. Cryst. Liq. Cryst. Inc. Non-Lin. Opt. 1994, 242, 17-52.

6. Boldyreva E.V. Coord. Chem. Russ., 2001, 27(5), 323-350.

Keywords: bending crystals, photomechanical effects, thermal expansion, coordination compounds

MS33-O2 Photomechanical actuation in organic crystals: expansion, bending, coiling, twisting and peeling

Rabih O. Al-Kaysi¹

1. King Saud bin Abdulaziz University for Health Sciences/ King Abdullah International Medical Research Center/ Ministry of the National Guard Health Affairs

email: rabihalkaysi@gmail.com

In some organic crystals light can be absorbed to trigger a topologically controlled photochemical reaction. In general the photochemical reaction inside the crystal generates forces that can shatter a large single crystal and turn it to photoproduct powder. The shape, size and chemistry of the material making up the crystal have a drastic effect on the way these internal forces affect the crystal during a photochemical reaction. For molecular crystal nanowires made from *tert*-butyl anthracene-9 carboxylate photoreaction leads to an anisotropic expansion by up to 15% along the long axis of the wire. When single crystalline microribbons of fluorinated-9-anthracene carboxylic acid are irradiated with UV light, the ribbons twist then untwist after the light is switched off. Crystalline microblocks made from *cis*-dimethyl-2(3-(anthracen-9-yl)allylidene)malonate tend to peel off photoreacted layers after a brief exposure to visible light (405 nm).

Keywords: Photomechanics, Light, Molecular Crystals.

MS33-O3 Solid-state photodimerization of *o*-ethoxy-cinnamic acid

Demetrius C. Levendis¹, Manuel A. Fernandes²

1. Molecular Sciences Institute, School of Chemistry, University of the Witwatersrand, Johannesburg

2. Molecular Sciences Institute, School of Chemistry, University of the Witwatersrand, Johannesburg

email: demetrius.levendis@wits.ac.za

The complexity of this textbook example, where photodimerisation depends on the relative arrangement of molecules in each of the four polymorphs (α , β , γ and δ), has not yet been fully recognized. In this paper, we will discuss the intermolecular interactions that shape the polymorphs, crystal hopping, phase transformations and solid-state photodimerisation of *ortho*-ethoxy-cinnamic acid (*oetca*), all of which depend on the experimental conditions, crystallization method, and the history of the crystal.

On heating crystals of the α -form of *oetca* to 60 °C they hop, depending on the face that is in contact with the hot surface. Thereafter the crystals no longer hop, but undergo a reversible phase transformation from the α ($V = 499.5 \text{ \AA}^3$) to the δ (or α') form ($V = 1492.4 \text{ \AA}^3$). This is accompanied by a twisting of the molecules that may, at least in part, be the cause of the crystal hopping. The α and δ polymorphs undergo solid-state photodimerisation in different ways depending on whether it is carried out at room temperature or above 60 °C.

[1] Fernandes, M. A., Levendis, D. C., Schoening, F. R. L. (2004) A new polymorph of *ortho*-ethoxy-trans-cinnamic acid: single-to-single-crystal phase transformation and mechanism. *Acta Cryst. Section B-Structural Science*, **60**, 300-314.

[2] Fernandes, M. A., Levendis, D. C. (2004) Photodimerization of the α' -polymorph of *ortho*-ethoxy-trans-cinnamic acid in the solid state. 1. Monitoring the reaction at 293 K. *Acta Cryst. Section B-Structural Science*, **60**, 315-324.

[3] Fernandes, M. A., Levendis, D. C. (2015) Photodimerization of the α' Polymorph of *ortho*-Ethoxy-trans-cinnamic acid in the Solid State. Part2: Monitoring the Reaction at 343 K, *Acta Cryst. Section B (in preparation)*.

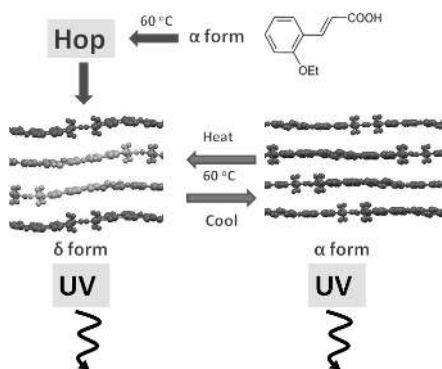


Figure 1. Schematic diagram showing the effect of heating and cooling the α and δ (or α') polymorphs of oetca

Keywords: solid-state reaction, photodimerisation, crystal hopping, thermosalt effect, single-crystal-to-single-crystal phase transformation, polymorph

MS33-O4 Identification of the cleavage planes in molecular crystals: topological and energetic aspects

Pavel N. Zolotarev¹, Massimo Moret², Davide M. Proserpio^{1,3}

1. Samara Center for Theoretical Materials Science, Samara State University, Samara, Russia

2. Dipartimento di Scienza dei Materiali, Università degli Studi di Milano Bicocca, Milano, Italy

3. Dipartimento di Chimica, Università degli Studi di Milano, Milano, Italy

email: paulzolotoff@gmail.com

Thin films of organic semiconductors have a wide application in modern electronic devices. Until now we have used substrate surfaces for organic molecular beam epitaxy (OMBE) [1] provided by β -alanine crystal primary cleavage plane (010). Having a stake in different types and symmetries of substrate surfaces, we searched through the Cambridge Structural Database (release 5.35 Nov 2013) by means of the ToposPro program package [2] modified with a specially tailored procedure that determines possibility of the crystal to cleave along a given surface. This procedure is based on the analysis of the share of intermolecular interaction energy of molecules within the layer compared to the total energy of interaction.

As a result, we have extracted 546 structures of amino acids derivatives with 2-periodic hydrogen bonded network as the most probable candidates for easily cleavable crystals. We discarded the structures of solvates and hydrates as inappropriate in order to guarantee stability to ultra-high vacuum conditions needed for OMBE. For some selected key structures we calculated intermolecular interaction energies by means of the PIXEL method [3] trying to establish the structural features that can lead to the ability of molecular crystals to cleave. In addition, we proposed a quantitative descriptor of intermolecular interaction anisotropy – the X parameter.

To prove the validity of the proposed scheme we crystallized five crystals and seven co-crystals of amino acids. Unit cell parameters as well as face indexing procedure were carried out on a diffractometer. Subsequently we tested the crystals on the cleavage. For β -alanine crystals, during the squeezing between two glass plates, secondary cleavage planes along {111} faces were found that is in full agreement with our prediction.

The work was supported by the Russian government (Grant 14.B25.31.0005).

References:

- [1] S. Trabattori, M. Moret, M. Campione, L. Raimondo, A. Sassella *Cryst. Growth Des.* **2013**, *13*, 4268.
- [2] V.A. Blatov, A.P. Shevchenko, D.M. Proserpio *Cryst. Growth Des.* **2014**, *14*, 3576.
- [3] A. Gavezzotti *J. Phys. Chem.* **2002**, *106*, 4145; A. Gavezzotti *J. Phys. Chem.* **2003**, *107*, 2344.

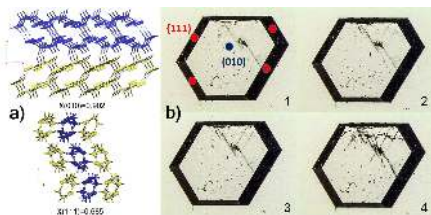


Figure 1. a) Computed values of X parameter for (010) and (111) layers in the structure of β -alanine; b) Sequential frames obtained during the squeezing of β -alanine crystal. Appearing secondary cleavage planes are parallel to {111}.

Keywords: Intermolecular interactions, mechanical properties of organic solids

MS33-O5 Solvent responsive 2D coordination networks: Breathing Materials

Gaëlle Ramon¹, Gift Mehlana¹, Susan Bourne¹

1. University of Cape Town

email: gaelle.ramon@uct.ac.za

The development of Metal Organic Frameworks (MOFs) was driven by the chemists' efforts to reproduce the microporosity observed in naturally occurring zeolites. By combining metal nodes and organic spacers, new crystalline compounds were obtained, displaying 3D porous structures and a certain robustness. Initially favoured, the 3D structures showed limitations with respect to some applications such as guest selectivity and separation. These were better achieved by another category of MOFs which were guest-responsive and dynamic: the breathing MOFs. These MOFs afforded added functionalities to that of the robust 3D materials through reversible structural transformations between large and small cavities. In this paper we will be presenting a novel 2D Breathing MOF^{1,2} assembled from mononuclear zinc(II) centres and 3-(4-pyridyl)benzoate ditopic linker. The novel material allows for the accommodation of large guest molecules with diameters larger than the original pores of their empty framework. The mechanism of the motion of the dynamic network will also be carefully described.

Keywords: MOF, sorption, crystalline structure

MS34. Growth, structure and application of multi-component crystals

Chairs: Christopher Frampton, Tomislav Friščić

MS34-O1 Form and function of co-crystals: From molecular dating to explosive interactions

Christ er B. Aakeröy¹

¹. Department of Chemistry, Kansas State University, Manhattan, KS, 66506, USA

email: aakeroy@ksu.edu

Our ability to imagine and synthesize molecular species has been developed and refined for over a century, and today we are capable of making extraordinary covalent entities that rival some of Nature's best efforts when it comes to structural complexity and chemical reactivity. However, some of the fundamental characteristics of chemistry, communication and change, are primarily initiated and controlled by reversible interactions between molecules, and intermolecular forces provide the conduits through which these interrelated process take place. In this contribution, several strategies for deliberate and directed supramolecular synthesis, based upon systematic structural studies are presented, and some practical applications thereof are also examined.

Keywords: hydrogen bonds, halogen bonds, molecular recognition, energetic materials

MS34-O2 Dynamics of porous metal-organic frameworks

Len Barbour¹

¹. Department of Chemistry and Polymer Science, University of Stellenbosch, Stellenbosch, South Africa

email: ljb@sun.ac.za

Metal-organic frameworks are favoured as porous materials owing to their supposed robust structures based on the principle of linking stable secondary-building unit nodes with suitable ligands. However, some frameworks are capable of a surprising level of dynamic behaviour upon activation, heating, guest uptake, and exposure to hydrostatic pressure. This phenomenon has important consequences for the possible utilisation of these materials for guest capture. This presentation will showcase a number of different metal-organic frameworks while discussing their dynamic behaviour in response to external stimuli.

Keywords: MOF, structural dynamics, thermal expansion, gas sorption

MS34-O3 Solvent dependence of competitive hydrogen vs halogen bonded self-assembly processes in multi-component crystal formation

Craig C. Robertson¹, James S. Wright¹, Elliot C. Carrington¹,
Robin N. Perutz², Christopher A. Hunter³, Lee Brammer¹

1. Department of Chemistry, University of Sheffield, Brook Hill, Sheffield, S3 7HF, U. K.

2. Department of Chemistry, University of York, Heslington, York, YO10 5DD, U. K.

3. Department of Chemistry, University of Cambridge, Lensfield Road, Cambridge, CB2 1EW, U.K.

email: craig.robertson@shef.ac.uk

A series of experiments were carried out which directly contrasted the ability of hydrogen and halogen bonding (HB & XB, respectively) to drive a self-assembly process and the effect that solvent has on this process. This was achieved in a competitive environment in which either a two-component HB network or a two-component XB network may co-crystallise from a system of three small organic molecules (HB donor, XB donor and acceptor). The experiments were carried out in seven solvents of different polarities, ranging from toluene to *i*-propanol. The identity and phase purity of the products was analysed by single crystal and powder X-ray diffraction. The investigation revealed that the network formed by co-crystallisation is indeed solvent dependent, with HB networks formed in lower polarity solvents, switching to XB networks in solvents of higher polarity. By adjusting the strength of the HB donor relative to the XB donor we were able to gain further solvent-dependent control and ultimately reverse the network selectivity in all solvents. These results reveal the solvent-dependent nature of Metrangolo and Resnati's original HB vs XB co-crystallisation experiment and demonstrate that the nature of the solvent is an important consideration and may offer a further level of control of the fidelity of self-assembly processes.

I. E. Corradi, S. V. Meille, M. T. Messini, P. Metrangolo and G. Resnati, *Angew. Chem. Int. Ed.*, **2000**, 39, 1782-1786

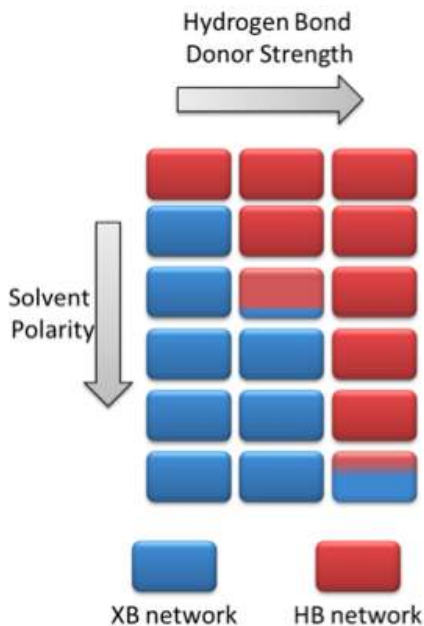


Figure 1. The outcome of a competitive co-crystallisation between a HB vs XB network in seven solvents is affected by both the nature of the solvent and the HB strength of the donor.

Keywords: Co-crystals, Halogen Bonding, Hydrogen Bonding, Solvent Effects

MS34-O4 Inclusion chemistry: Guest species determining properties of multi-component crystals

Gareth O. Lloyd¹

¹ Heriot-Watt University

email: g.o.lloyd@hw.ac.uk

The humble solvate has been a crystal form for as long as crystals have been recognised. Solvates, a type of multi-component crystal, have produced many scientific studies and important industrial materials. Examples include the hydrated “boiling stones” known as zeolites and the pharmaceutical solvates, their stability towards hydrate formation being incredibly important to modern lifestyles. Often banished to the supplementary information, the removal or exchange of solvents (guests) from multi-component crystals is a necessary step to produce a “porous” material and often is not as simple as just “boiling” the material. In this presentation we shall show how the use of different solvates can allow for the production of different desirable properties within a material. Even though you can remove most solvents from multi-component crystals leaving at least one component behind, this often leads to a non-porous “collapsed” phases [1]. Careful selection of the “right” solvent can lead to metastable porous materials as will be shown utilising solvates of metallocycles and metallocages (also known as metal-organic polyhedral, MOPs) in which the interplay between intrinsic and extrinsic cavities results in porosity [2]. When crystal engineering these molecular porous materials the “interactions” between the molecular building blocks can be overly focused on, but the guest can play a keystone role in determining the desired property [3]. The “solvation” of the molecular building blocks within the solid periodic structures means the inclusion of solvents in the solid is an important aspect of crystal engineering all porous materials. Finally, with porosity shown, inclusion chemistry is utilised to generate interesting physical properties in the form of gas storage and separation [4], fluorescence tuning [5] and paramagnetism from diamagnetic building blocks [6].

References

- [1] L. R. Nassimbeni, *Acc. Chem. Res.*, **2003**, *36*, 631.
- [2] C. Jones, J. C. Tan & G. O. Lloyd, *Chem. Commun.*, **2012**, *48*, 2110. [3] J. R. Holst & A. I. Cooper, *Adv. Mater.*, **2010**, *22*, 5212; L. J. Barbour, *Chem. Commun.*, **2006**, 1163. [4] T. Jacobs, G. O. Lloyd, J. A. Gertenbach, K. Mueller-Nederbock, C. Esterhuysen & L. J. Barbour, *Angew. Chem. Int. Ed.*, **2012**, *51*, 4913. [5] D. P. Yan, G. O. Lloyd, A. Delori, W. Jones & X. Duan, *ChemPlusChem*, **2012**, *77*, 1112. [6] S. V. Potts, L. J. Barbour, D. A. Haynes, J. M. Rawson & G. O. Lloyd, *J. Am. Chem. Soc.*, **2011**, *133*, 12948.



Figure 1. Solvent effects and solvent inclusion contribute to a large variety of phases, only some of which show porous properties and inclusion chemistry.

Keywords: Porous, Metallocycle, Molecular Cages, Solvates, Inclusion Chemistry

MS34-O5 Applications of density functional theory to crystal structure solution for multicomponent crystalsDavid S. Edgeley¹, Kenneth Shankland¹, Chris S. Frampton²1. University of Reading
2. Brunel University, London

email: d.s.edgeley@pgr.reading.ac.uk

Analysis of crystal structures in the Cambridge Structural Database (CSD) shows that there is an upwards trend in the number of structures being solved using X-ray powder diffraction, in spite of its limitations relative to single-crystal diffraction data. This trend can be attributed to the increasing quality of the diffraction data being collected, the ongoing development of techniques for solving structures, inherent interest in polycrystalline systems and ever-increasing computing power. Yet X-ray powder diffraction remains (in general) too information-poor in order to reliably determine hydrogen atom positions, and this affects conclusions that can be drawn from the crystal structure e.g. is a multicomponent system co-crystal or a salt¹?

The FDA defines pharmaceutical cocrystals and salts differently and regulatory schemes governing their production and identification differ significantly. Currently, cocrystals are defined as "crystalline materials composed of two or more molecules within the same crystal lattice" and generally classified by having a $\Delta pK_a < 1$, but they do not have a regulatory scheme. Pharmaceutical salts are highly regulated and defined as "Any of numerous compounds that result from replacement of part of all of the acid hydrogen of an acid by a metal or a radical acting like a metal: an ionic or electrovalent crystalline compound." Unfortunately the chemical difference between a salt and a cocrystal is far from distinct; a continuum of hydrogen atom transfer situations exists.

Pyrimethanil, a broad spectrum fungicide, has a tendency to form multicomponent crystal structures with lattices constructed from intermolecular bonds H-bonds lying along the cocrystal-salt continuum. Here we demonstrate that dispersion-corrected density functional theory (DFT-D)² can distinguish between pyrimethanil salts, cocrystals and intermediates by precisely determining hydrogen position. We then show how periodic DFT has been integrated into our structure determination workflows and demonstrate the advantage of this approach in accurately determining multicomponent crystal structures.

1. Chan, H.C.S., Kendrick, J., Neumann, M.A. & Leusen, F.J.J. *CrystEngComm* **15**, 3799–3807 (2013).
2. Giannozzi, P. et al. *Journal of Physics-Condensed Matter* **21** (2009).

Keywords: Salt, Cocrystal, DFT, H-bond**MS35.** Dynamics in nanoporous molecular crystals

Chairs: Angiolina Comotti, Len Barbour

MS35-O1 Breathing porous molecular crystalsKari Rissanen¹

1. Department of Chemistry, Nanoscience Center, University of Jyväskylä, Jyväskylä, 40014, Finland)

email: kari.t.rissanen@jyu.fi

An exciting research challenge in crystal engineering and supramolecular chemistry is to design, synthesize, and characterize porous architectures¹, topical example being the metallo-organic frameworks, MOF's, with applications in catalysis, separation, trapping of gases, etc.² The design of porous lattices normally relies on rigid 3-D lattices, which in some cases can undergo single-crystal-to-single-crystal transformations³ or exhibit porous behavior in a seemingly non-porous crystals.⁴

Our research interests over the last 25 years have been focused on the studies of weak non-covalent intermolecular, viz. supramolecular interactions as the driving force in self-assembly and molecular recognition, especially in the solid state by single crystal X-ray diffraction. Particularly the hierarchy and interplay of interactions, viz. concerted interactions, are becoming more and more important in the understanding of molecular self-assembly and crystal growth. Recently our work on halogen bonding⁵ revealed a halogen and hydrogen bonded (XB and HB) system based on an XB complex hexamethylenetetramine (HMTA) and N-iodosuccinimide (NIS)⁶ to result in a porous, yet breathing crystal lattice. The lecture will highlight the results and behavior of this intriguing system exhibiting concerted action of XB and HB.

References

1. L. J. Barbour, *Chem. Commun.* **2006**, 1163.
2. Thematic issue on MOF's, *Chem Soc. Rev.* **2014**, 43.
3. S. Sen, S. Neogi, K. Rissanen, P. K. Bharadwaj, *Chem. Commun.* **2015**, 51, 3173.
4. S. A. Herbert, A. Janiak, P. K. Thallapally, J. L. Atwood, L. J. Barbour, *Chem. Commun.* **2014**, 50, 15509.
5. G. R. Desiraju, P. S. Ho, L. Kloo, A. C. Legon, R. Marquardt, P. Metrangola, P. A. Politzer, G. Resnati and K. Rissanen, *Pure Appl. Chem.* **2013**, 85, 1711.
6. K. Raatikainen and Kari Rissanen, *CrystEngComm* **2011**, 13, 6972.
7. K. Raatikainen, K. Rissanen, *Chem. Sci.* **2012**, 2, 235.

Keywords: crystal structure, porosity, halogen bonding, hydrogen bonding

MS35-O2 Uptake and release of small molecules by flexible 1D coordination polymers that exhibit latent nanoporosity

Lee Brammer¹, Iñigo J. Vitórica-Yrezábal², James S. Wright¹

1. Department of Chemistry, University of Sheffield, Sheffield S3 7HF, UK

2. School of Chemistry, University of Manchester, Oxford Road, Manchester, M13 9PL, UK

email: lee.brammer@sheffield.ac.uk

Families of 1D coordination polymers have been developed in which flexibility of the polymer, arising from side-chain conformational changes and bond-breaking and reformation at labile metal centres, enables the uptake and release of a variety of small molecules by these materials in their crystalline form.^[1–4] These crystalline materials are not formally porous, but their flexibility results in latent porosity that facilitates the uptake and release processes. Transformations have been followed extensively by in situ diffraction studies, in some cases as single crystal-to-single crystal processes, but always also by XRPD. Diffraction studies are supported by TGA/DSC studies and use of gas-phase IR spectroscopy to establish equilibrium gas-solid behaviour where guest molecules are released into the vapour phase. The presentation will focus on using diffraction in combination with other techniques to investigate mechanism, and will provide examples that illustrate selectivity of guest entrapment.

[1] S. Libri, M. Mahler, G. Mínguez Espallargas, D. C. N. G. Singh, J. Soleimannejad, H. Adams, M. D. Burgard, N. P. Rath, M. Brunelli, L. Brammer, *Angew. Chem. Int. Ed.* **2008**, *47*, 1693–1697.

[2] I. J. Vitórica-Yrezábal, G. Mínguez Espallargas, J. Soleimannejad, A. J. Florence, A. J. Fletcher, L. Brammer, *Chem. Sci.* **2013**, *4*, 696–708.

[3] J. S. Wright, I. J. Vitórica-Yrezábal, H. Adams, S. P. Thompson, A. H. Hill, L. Brammer, *IUCrJ* **2015**, *2*, 188–197.

[4] I. J. Vitórica-Yrezábal, S. Libri, J. R. Loader, G. Mínguez Espallargas, M. Hippler, A. J. Fletcher, S. P. Thompson, J. E. Warren, D. Musumeci, M. D. Ward, L. Brammer, *Chem. Eur. J.* **2015**, in press.

Keywords: Flexible coordination polymer, molecular entrapment, latent porosity, guest uptake, guest release, in situ diffraction

MS35-O3 Coordination metallacycles assembled into microporous materials

Luciano Marchio¹, Irene Bassanetti¹, Corrado Atzeri¹, Matteo Tegoni¹, Vincent L. Pecoraro²

1. Dipartimento di Chimica, Università degli Studi di Parma, Parma, Italy

2. Department of Chemistry, University of Michigan, Ann Arbor, MI, USA

email: marchio@unipr.it

Porous solid materials represent one of the most intense areas of study for chemists, physicists, and materials scientists [1]. These systems have found a large number of applications in many fields, such as adsorption, separation and purification, as well as catalysis [2]. The construction of a reticular and porous architecture highly depends on the building units linked by means of different types of interactions. In particular, within the class of materials comprising covalent interactions the most notable examples are represented by covalent organic frameworks (COF) and porous aromatic frameworks (PAF). In the large and continuously growing class of metal organic framework (MOF) the main source of structural variability derives by the optimal match between an organic ligand bound to a metal center. Porous materials can also be obtained by the connections of oligomeric units by means of supramolecular interactions [1]. In the present contribution we show how two different oligomeric metallacycles, namely silver(I) hexamers [3] and copper (II) metallacrowns [4], can generate stable porous crystals. The role of the counteranion (BF_4^- , PF_6^- , NO_3^- , CF_3SO_3^- , CH_3CO_2^-) is of fundamental importance in defining the supramolecular interactions responsible in the way the metallacycles self-assembled into a diversity of 3D supramolecular architectures and cavities. The structural features and gas sorption properties will be presented.

[1] T. R. Cook, Y. R. Zheng, P. J. Stang *Chem. Rev.*, **2013**, *113*, 734–777. [2] C. Janiak, J. K. Vieth *New J. Chem.* **2010**, *34*, 2366–2388. [3] I. Bassanetti, A. Comotti, P. Sozzani, S. Bracco, G. Calestani, F. Mezzadri, L. Marchio *J. Am. Chem. Soc.*, **2014**, *136*, 14883–14895. [4] G. Mezei, C. M. Zaleski, V. L. Pecoraro *Chem. Rev.*, **2007**, *107*, 4933–5003.

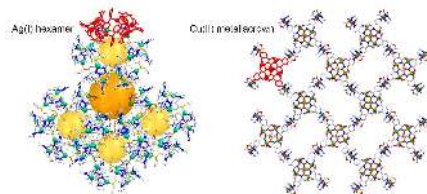


Figure 1. Crystal packing of the Ag(I) hexamers and of the Cu(II) metallacrown. In red are highlighted the building units.

Keywords: coordination polymers, metallacrowns, microporosity

MS35-O4 Structural behavior of highly hydrated cyclodextrin complexesJanusz Lipkowski¹, Iwona Justyniak²

1. Cardinal Stefan Wyszyński University in Warsaw, Faculty of Mathematical and Natural Sciences, Wojcieckiego 1/3, 01938 Warszawa, Poland
2. Institute of Physical Chemistry, Polish Academy of Sciences, Kasprzaka 44/52, 01-224 Warszawa, Poland

email: Janusz.lipkowski@wp.pl

Cyclodextrins are commonly known as materials having intra-molecular cavity able to accommodate guest species. This property, when combined with sorption in the inter-molecular space in the solid state structures of CDs leads to the very interesting structures and properties. When combined with complexation of metal ions by CDs, this area links to the very important, so-called- MOFs.

Cyclodextrins are hydrophilic in their outer part while more hydrophobic in the intramolecular space. Typical structural behavior is thus hydration in the outer sphere, or solvation, if water is mixed with other solvents, like alcohols. However, as we have recently discovered, hydration of the crystals while in mother solution may, in some cases, significantly differ quantitatively from the crystals picked-out in a drop of solution! Two novel crystal structures were found for such highly hydrated CDs and will be discussed in this paper. The structures can convert in a single crystal to single crystal transformation when partially dehydrated.

In general, such behavior may be observed only when CD moieties are at equilibrium with a solution of the respective guest and solvent species. The equilibria are quite sensitive to minor changes of solution chemical composition what may be observed microscopically as morphology changes of the crystalline phases. This phenomenon will be illustrated with short movies demonstrating crystal behavior on change of its environment

Additional information concerns the supramolecular aggregation of water in the samples. This will be discussed based on temperature dependence of lattice parameters of one of the highly hydrated structures. It shows a mixed hydrophilic/hydrophobic behavior. Hydrophobic hydration produces a reduction in density and an increase in the heat capacity. The expanded network causes the density decrease whereas the ordered bonds must be bent on increasing the temperature, so affecting the heat capacity. Thus, hydrophobic hydration behaves in an opposite manner to polar hydration, which increases the density and decreases heat capacity due to their associated disorganized hydrogen bonds being already bent or broken [1]. Experimental x-ray data will be presented to illustrate such a behaviour on CD complex structure

Reference:
Martin Chaplin, "Water – structure and science", www.lsbu.ac.uk/water
This work was supported by grant POIG.01.01.02-14-102/09

Keywords: cyclodextrin, organic zeolite, porous molecular structure, hydration, polymorphism

MS35-O5 Single-crystal-to-single-crystal transformations and porosity studies of mixed-ligand metal-organic frameworksClive L. Oliver¹

1. Centre for Supramolecular Chemistry Research, Department of Chemistry, University of Cape Town, Rondebosch, 7701, South Africa

email: clive.oliver@uct.ac.za

Metal-organic frameworks (MOFs), infinite systems built up of metal ions and organic ligands, have been extensively studied in materials and supramolecular chemistry due their structural diversity and application as porous materials, in catalysis, ion exchange, gas storage and purification. [1] We have investigated the construction of MOFs using transition metals (e.g., cadmium, copper, zinc) and mixed ligands (e.g., trimesic acid, 5-nitroisophthalic acid, 1,2-bis(4-pyridyl), 4,4'-bipyridine-N,N'-dioxide) with a view of producing porous materials which may be used for the sorption of gases or liquids. Several MOFs were produced which were characterized by single crystal X-ray diffraction, powder X-ray diffraction (PXRD), thermal analysis and sorption studies. At least three of these MOFs retained their crystallinity upon heating as indicated by variable-temperature PXRD. One of the MOFs is a 2-fold interpenetrated, pillared, cadmium metal-organic framework consisting of trimesic acid and 1,2-bis(4-pyridyl)ethane.[2] This compound exhibits a temperature-induced single-to-crystal-single-crystal (SC-SC) transformation upon the release of N,N'-dimethylformamide (stable up to 300 °C). SC-SC transformation was also observed when the desolvated form absorbed selected polar and non-polar organic solvents. In addition, gas (N₂, CO₂ and N₂O) sorption experiments were performed showing 2.5% N₂, 4.5% CO₂ and 3.4% N₂O absorption by mass at room temperature and moderate gas pressures (~10 bar). A second 2D network consisting of zinc, trimesate and 4,4'-bipyridine-N,N'-dioxide also remarkably showed a SC-SC transformation upon desolvation. In both structures no clear channels are present in the structure which indicate the occurrence of cooperative structural changes upon desolvation in order to retain their monocrystallinity.

Keywords: single-crystal-to-single-crystal transformation, porosity

MS36. Molecular crystals offering new insight into intermolecular interactions

Chairs: Paola Gilli, Carl Henrik Gørbitz

MS36-O1 Tailoring host-guest interactions for sensing with cavitands

Chiara Massera¹

1. Dipartimento di Chimica, Parco Area delle Scienze 17/A, 43124 Italy

email: chiara.massera@unipr.it

Cavitands, synthetic organic compounds with enforced cavities of molecular dimensions, represent a very important class of receptors for chemical and biochemical sensing [1]. Particularly attractive is the possibility of designing and decorating these receptors to tailor the supramolecular interactions responsible for the recognition of different analytes, thus tuning their selectivity towards desired classes of chemical species in presence of interferents [2]. In the case of aromatic guests, quinoxaline-bridged and linked quinoxaline-bridged cavitands have proved to be extremely effective receptors through the formation of π - π stacking and CH- π interactions, while the H-bond active tetraphosphonate cavitands are well-known for their ability to complex positively charged species and neutral molecules [3, 4].

We present our recent investigations in the field of supramolecular sensing with cavitands carried out by means of single-crystal X-ray analysis, studies in solution and theoretical calculations.

References

1. D. J. Cram, *Science*, **1983**, 219, 1177.
2. L. Pirondini, E. Dalcanale, *Chem. Soc. Rev.*, **2007**, 36, 695.
3. C. Massera, M. Melegari, E. Kalenius, F. Ugozzoli, E. Dalcanale, *Chem. Eur. J.*, **2011**, 3064.
4. E. Biavardi, F. Ugozzoli, C. Massera, *Chem. Commun.*, **2015**, 51, 3426.

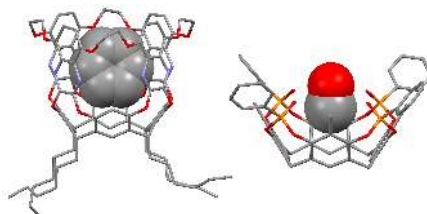


Figure 1. Molecular structure of the complex formed between a linked quinoxaline-bridged cavitand and benzene (left) and a tetraphosphonate cavitand and methanol (right).

Keywords: cavitands, molecular recognition, weak interactions

MS36-O2 Systematic investigations on molecular crystals of boronic acidsIzabela D. Madura¹, Karolina Czerwińska¹, Janusz Zachara¹¹. Warsaw University of Technology, Faculty of Chemistry

email: izamadura@gmail.com

Boronic acids of general formulae $R-B(OH)_2$ (R either aromatic or aliphatic) are the compounds of widespread applications starting from organic synthesis (including Suzuki-Miyaura cross-coupling reactions¹) through medicinal chemistry² to molecular recognition processes³ and crystal engineering⁴. The role in the latter will be discussed on the basis of systematic investigations on boronic acids crystals. Up-to-date there are around 300 boronic acids structurally characterized, thus comprising a valuable set for statistical survey.

The data will be analyzed using a bond-valence vector approach⁵ to ascribe the observed subtle molecular changes. Further, a hierarchical structure of these crystals will be presented with a discussion of a role of basic and large supramolecular synthons.^{6,7} It is important to note that in the case of boronic acids the basic synthons are mainly formed by O–H...O hydrogen bonds, which in combination with other interactions can form large synthons of variable dimensionality. In the case of fluoro-substituted phenylboronic acids the structure of the basic synthon was shown to interplay with the form of large synthons.⁸ In turn, the latter are said to act as intermediates between small synthons and crystal growth units, thus their investigation may comprise a preliminary studies on crystallization processes.⁹

The general rules will be illustrated with our own results of newly designed co-crystals and obtained polymorphic forms. The results of temperature dependant studies on the large synthons' structure will be also presented.

References:

- ¹ N. Miyaura, A. Suzuki *Chem. Rev.* 95 (1995) 2457.
- ² P.C. Trippier, C. McGuigan *Med. Chem. Commun.* 1 (2010) 183.
- ³ S.D. Bull, M.G. Davidson, J.M.H. van den Elsen, J.S. Fossey, A.T.A. Jenkins, Y.-B. Jiang, Y. Kubo, F. Marken, K. Sakurai, J. Zhao, T.D. James *Acc. Chem. Res.* 46 (2013) 312.
- ⁴ J. Hernández-Paredes, A.L. Olvera-Tapia, J.I. Arenas-García, H. Höpfl, H. Morales-Rojas, D. Herrera-Ruiz, A.I. Gonzaga-Morales, L. Rodríguez-Fragoso *CrystEngComm* (2015) DOI: 10.1039/C4CE01934B.
- ⁵ J. Zachara *Inorg. Chem.* 46 (2007) 9760.
- ⁶ G.R.Desiraju *J. Am. Chem. Soc.* 135 (2013) 9952.
- ⁷ P. Ganguly, G.R. Desiraju *CrystEngComm* 12 (2010) 817.
- ⁸ I.D. Madura, K. Czerwińska, D. Soldańska *Cryst. Growth. Des.* 14 (2014) 5912.
- ⁹ A. Mukherjee, K. Dixit, S.P. Sarma, G.R. Desiraju *IUCrJ* 1 (2014) 228.

Keywords: crystal engineering, co-crystals, molecular crystals, hierarchical structure, large supramolecular synthons, hydrogen bonding, boronic acids, weak interactions

MS36-O3 In situ visualisation & evaluation of intermolecular interactions in 3DPeter A. Wood¹, Ghazala Sadiq¹, Colin R. Groom¹, Suzanna C. Ward¹¹. Cambridge Crystallographic Data Centre

email: wood@ccdc.cam.ac.uk

The crystallographic community has now shared over 750,000 small molecule structures and these structures contain many millions of intermolecular interaction observations within them. By using this structural information to best effect we can both predict likely intermolecular interaction behaviour prior to crystallisation and also evaluate observed interactions in a new crystal compared to the structures that have been determined before.

Using the CSD interaction knowledge base IsoStar as the underlying data, Full Interaction Mapping in Mercury provides rapid visualisation of interaction preferences within a small molecule crystal structure. This approach provides a visual and intuitive way to understand and investigate intermolecular interactions in a crystal including hydrogen bonds, halogen bonds, stacking interactions and van der Waals contacts.

This presentation, timed to coincide with the 50th anniversary of the Cambridge Structural Database, will demonstrate the breadth of applicability of Full Interaction Mapping and the depth of insight that can be gained, using recently published structures as examples.



Figure 1. Full Interactions Maps displayed around the molecular conformation of sulfthiazole

Keywords: crystal engineering, intermolecular interaction, hydrogen bond, halogen bond

MS36-O4 Design and fine-tuning of magnetic properties in organic salts of semiquinone radical

Krešimir Molčanov¹, Vladimir Stilić², Nadica Maltar-Stirmečki¹, Ana Šantić¹, Biserka Kojić-Prodić², Lidija Androš Dubraja¹, Damir Pajić³

1. Rudjer Bošković Institute

2. Department of Chemistry, Faculty of Science, University of Zagreb

3. Department of Physics, Faculty of Science, University of Zagreb

email: kmolcano@irb.hr

Semiquinones are a class of stable organic radical anions; especially stable are ones with four electronegative substituents (Fig. 1a), which enhance delocalisation of the unpaired electron. Therefore, they are potential candidates for design of functional materials with fine-tuned magnetic properties.

Semiquinoid anions in crystals are usually stacked by π -interactions, and their magnetic properties depend on their interplanar distance. Most often, the radicals form closely bound dimers with coupled spins (type I, Fig. 1c) [1,2], resulting in diamagnetic properties. However, crystal engineering can be used to enlarge the ring separation distance with equidistant-ring stacks generating antiferromagnetic [3] or paramagnetic crystals (type II, Fig. 1c).

Our research has been aimed to obtain stable semiquinone systems with fine-tuned magnetic properties by crystal engineering: we varied size of substituents on the quinoid ring (Fig. 1a) and aromatic organic cations (Fig. 1b). Therefore, we varied substituents on the semiquinone ring: tetrachloro- (CA), tetrabromo- (BA) and 2,3-dicyano-5,6-dichlorosemiquinone (DDQ) were used as anions. Aromatic, approximately planar organic cations [pyridinium (py), N-methylpyridinium (N-MePy) and diquat] were used to check for possible π -interactions between cations and anions.

Crystallographic, magnetic (EPR, SQUID), electrical (impedance spectroscopy) and thermal (TG/DTA, DSC) methods were used to obtain data on structure, stability, magnetic and electrical properties of the crystalline compounds.

A pair of analogous salts, N-MePy•CA and N-MePy•BA is especially interesting: in CA salt closely bound radical dimers occur, similar to previously known K•CA•Me₂CO [1] and similar alkali salts of DDQ [2], and the crystals are diamagnetic due to spin pairing. In BA salt radicals are equidistant, similar to high-temperature polymorph of K•CA•MeCOEt [3]; due to larger interplanar distances, the crystals are paramagnetic.

To gain insight into spin coupling/decoupling and transport properties, impedance spectroscopy was done on single crystals with electrical contacts applied in the direction of stacking.

References

- [1] Molčanov, Kojić-Prodić, Babić, Žilić, Rakvin, *CrystEngComm*, 13 (2011), 5170.
- [2] Molčanov, Babić, Kojić-Prodić, Stare, Maltar-Stirmečki, Androš, *Acta Crystallogr. B*, 70 (2014), 181.
- [3] Molčanov, Kojić-Prodić, Babić, Pajić, Novosel, Zadro, *CrystEngComm*, 14 (2012), 7958.

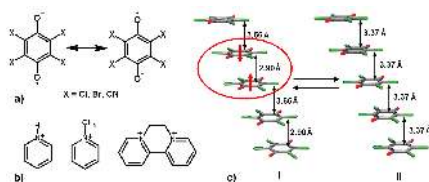


Figure 1. a) Electronic structure of semiquinone radical is between quinoid and aromatic due to an unpaired electron and negative charge delocalised throughout the ring. b) Used cations. c) Two types of stacks of quinoid rings: I dimers with coupled spins and II equidistant rings with no spin coupling.

Keywords: semiquinone radical, spin coupling, crystal engineering, magnetism, EPR spectroscopy, impedance spectroscopy

MS36-O5 Structural similarity in homologous families: the case of mandelic acids

Graham J. Tizzard¹, Simon J. Coles¹, Amy L. Ellis¹, Ka Leung¹,
Jonathan Sarson¹, Terence L. Threlfall¹

¹. Chemistry, Faculty of Natural and Environmental Sciences,
University of Southampton, UK

email: gjt1@soton.ac.uk

For several years we have been making detailed comparisons of the crystal structures of large sets of related compounds in an attempt to understand the factors determining the adoption of particular molecular arrangements within crystal structures [1-3].

As part of a larger crystallographic project to investigate the relationship between structure and chirality, we have synthesised and determined crystal structures of families of monosubstituted racemic mandelic acids (MAs) with fluoro, chloro, bromo, iodo, trifluoromethyl, methyl and methoxy substituents at the ortho, meta and para positions. Of these 21 permutations only four were previously described in the literature [4-7].

These have been investigated for structural similarity using the XPac software [8]. The results, presented pictorially as a structural relationship plot, show that rather more structures are built up from the carboxyl-chain hydroxyl hydrogen bonded dimer than from the conventional carboxylic acid dimer. The results show how all the structures are related and, based on the two types of dimer, the degree of similarity that they possess. Some structures with $Z > 1$ contain both sorts of dimers and there are many examples of isostructural sets. By analysing similarity in this related family of structures, both trends and gaps can be identified – for example a structure that should be present has been identified and subsequently synthesised and determined [9].

For the next stage of this study we are now investigating the co-crystallisation behaviour of the substituted racemic mandelic acids with enantiomerically pure phenylethylamine.

[1] Hursthouse, M. B., Montis, R., Tizzard, G. J., (2010), *CrystEngComm*, 12, 953-959

[2] Hursthouse, M. B., Montis, R., Tizzard, G. J., (2011), *CrystEngComm*, 13, 3390-3401

[3] Gelbrich, T., Threlfall, T. L., Hursthouse, M. B., (2012), *Acta Cryst. C* 10, O421-U299

[4] Larsen, S. and Marthi, K., (1994), *Acta Cryst. B*, 50, 373-381

[5] Larsen, S. and Marthi, K. (1997), *Acta Cryst. B*, 53, 280-292

[6] He, Q., Zhu, J., Gomaa, H., Jennings, M., Rohani, S., (2009), *J. Pharm. Sci.*, 98 1835-1844

[7] He, Q., Rohani, S., Zhu, J., Gomaa, H., (2010), *Cryst.Growth Des.*, 10 5136-5145

[8] Gelbrich, T., Hursthouse M. B. (2005), *CrystEngComm*, 7, 324-336

[9] Coles, S. J., Ellis, A. L., Leung, K., Sarson, J., Threlfall, T. L., Tizzard, G. J., (2014), *CrystEngComm*, 16, 10816-10823.

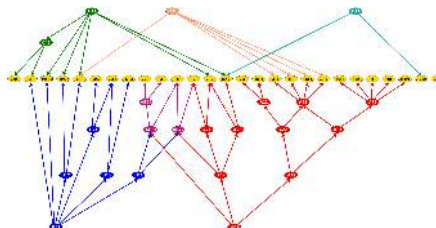


Figure 1. Structural relationship diagram for substituted racemic MAs. Yellow nodes are crystal structures. Blue and red nodes show packing similarities based on 8- and 10- membered H-bonded dimer rings respectively and purple nodes are based on both. Other colour nodes show non-dimeric similarities

Keywords: Mandelic acid, structural similarity

MS37. Molecular crystalline processes at ambient and non-ambient conditions

Chairs: Elena Boldyreva, Gareth Lloyd

MS37-O1 Structural changes induced in crystals by photochemical reactions at ambient and high pressure

Julia Bąkiewicz¹, Krzysztof Konieczny¹, Ilona Turowska-Tyrk¹

1. Faculty of Chemistry, Wrocław University of Technology, Wybrzeże Wyspiańskiego 27, 50-370 Wrocław, Poland

email: julia.bakowicz@pwr.edu.pl

The main subject of our interest is monitoring the paths of photo-induced structural transformations in single crystals by means of X-ray structure analysis (for instance [1-6]). In particular, we analyze structural changes brought about by photochemical reactions in ambient and extreme conditions. The studies facilitate gaining the knowledge of influence of pressure on the course of photochemical processes in crystals.

Studies of this type require data collection and structure determination for many partly reacted crystals, *i.e.* containing reactant and product molecules in different proportions. In the case of high-pressure experiments this is a big challenge for researchers.

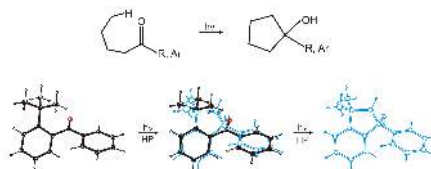
The results on monitoring the structural changes in crystals of 2-*tert*-butylphenylphenylmethanone (I) [6] and benzylammonium 4-(2,4,6-triisopropylbenzoyl)benzoate (II) brought about by the photocyclization reactions at different pressures will be presented (Figure 1).

Variations in the unit cell parameters, molecular geometry and molecular orientation brought about by the photochemical reactions at various pressures will be shown. Additionally, changes in a reaction rate and crystal structure caused by only high pressure, *i.e.* without photo-induction, will be discussed.

References

- [1] I. Turowska-Tyrk, J. Bąkiewicz, J.R. Scheffer, *Acta Cryst.*, 2007, B63, 933-940.
- [2] E. Trzop, I. Turowska-Tyrk, *Acta Cryst.*, 2008, B64, 375-382.
- [3] J. Bąkiewicz, J. Skarżewski, I. Turowska-Tyrk, *CrystEngComm*, 2011, 13, 4332-4338.
- [4] J. Bąkiewicz, I. Turowska-Tyrk, *J. Photochem. Photobiol. A*, 2012, 232, 41-43.
- [5] J. Bąkiewicz, J. Olejarz, I. Turowska-Tyrk, *J. Photochem. Photobiol. A*, 2014, 273, 34-42.
- [6] J. Bąkiewicz, I. Turowska-Tyrk, *CrystEngComm*, 2014, 16, 6039-6048.

compound (I):



compound (II):

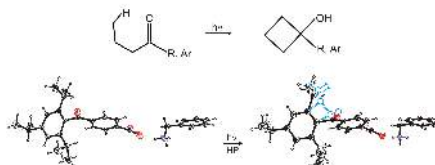


Figure 1. The equations of the studied photochemical reactions and the molecular structures in pure reactant, partly reacted and pure product crystals.

Keywords: single-crystal X-ray structure analysis, photochemical reactions, high pressure

MS37-O2 Spin crossover materials: from molecular motion to switchable mechanical propertiesHelena J. Shepherd¹, Paul Raithby¹

1. University of Bath, UK

email: H.J.Shepherd@bath.ac.uk

The spin crossover (SCO) phenomenon involves the switching of a transition metal complex between high spin (HS) and low spin (LS) states as a result of some perturbation to the species (for example changes in temperature or pressure, or as a result of light irradiation). Molecular species in the HS and LS states are distinguished by differences in their colour, magnetic moment and structure [1].

The strain associated with SCO has recently been demonstrated as an active component in actuating devices [2] and it is clear that mechanical properties play pivotal role in the switching phenomenon. Thus it is surprising that while the volumetric and morphological changes associated with the switching event are usually well characterised by traditional crystallographic methods, elastic moduli and their correlation with molecular structure have never been thoroughly analysed.

Single crystal X-ray diffraction techniques at elevated pressure and variable temperatures, complimented by spectroscopic and magnetic studies, have been used to probe the structure-properties relationship of a series of molecular Fe^{II} derivatives. A range of fascinating pressure-induced behaviours has been observed providing unprecedented insight into the driving forces behind the dynamic solid state processes. Examples include negative linear compression that is structurally antagonistic to the requirements of SCO [3] and pressure-induced stepped SCO accompanied by symmetry breaking [4]. More importantly, these studies have for the first time allowed a systematic investigation into the relationship between crystal structure and mechanical properties for a family molecular SCO complexes.

[1] M. A. Halcrow (Ed.) *Spin-Crossover Materials: Properties and Applications*, Wiley, 2013.

[2] H. J. Shepherd *et al.*, *Nature Commun.*, 2013, **4**, 2607

[3] H. J. Shepherd *et al.*, *Angew. Chem.*, 2012, **59**, 3910

[4] H. J. Shepherd *et al.*, *Phys. Rev. B.*, 2011, **84**, 144107

Keywords: Molecular Materials, Mechanical Properties, Spin Crossover, Structure Property Correlations

MS37-O3 Understanding polymorph stability and phase transformations by combining ab-initio lattice dynamics, multi-temperature elastic scattering and inelastic scattering measurementsAnders O. Madsen¹, Anna A. Hoser¹, Monika Kovacic¹, Ioana Sovago¹

1. Department of Chemistry, University of Copenhagen, Copenhagen, Denmark.

email: madsen@chem.ku.dk

The relative stability of polymorphic molecular crystals is not easy to assess, neither from experiment nor from ab-initio approaches. Despite recent advances in periodic DFT calculations, which have helped crystal structure prediction tremendously, it is still not possible to predict the relative stabilities at ambient conditions. In this contribution, we use models of thermal motion derived from ab-initio lattice dynamical calculations in refinements against X-ray diffraction data [1], and show how this can lead to an understanding of the different contributions of entropy and enthalpy to the free energies of the different polymorphic structures. We use the tetramorphic anti-tuberculosis drug pyrazinamide [2] as test case. Pyrazinamide undergoes several solid-state phase transformations as a function of temperature, and it is thus possible to construct a tentative phase diagram of the relative stabilities [3–4], which compare favourably to our modeling efforts. Additionally, inelastic X-ray and neutron diffraction measurements have been performed in order to further validate the resulting models.

References:

1. Hoser, A. A. and Madsen, A. Ø. Dynamic Quantum Crystallography: Lattice dynamical models refined against diffraction data. *Acta Cryst. A, Advances*, 2015. Submitted.
2. Wahlberg, N., Ciochon, P., Petricek, V. & Madsen, A. Ø. Polymorph Stability Prediction: On the Importance of Accurate Structures: A Case Study of Pyrazinamide. *Crystal Growth & Design* 14, 381–388 (2014).
3. Castro, R. A. et al. A new insight into pyrazinamide polymorphic forms and their thermodynamic relationships. *Crystal Growth & Design* 10, 274–282 (2009).
4. Cherukuvada, S., Thakuria, R. & Nangia, A. Pyrazinamide Polymorphs: Relative Stability and Vibrational Spectroscopy. *Crystal Growth & Design* 10, 3931–3941 (2010).

Keywords: Polymorphism, Lattice Dynamics, Density Functional Theory, Debye-Waller factors

MS37-O4 Thermodynamics and kinetics of polymorphic transitions in amino acid crystals

Joost A. van den Ende¹, Mireille M.H. Smets¹, Daniël T. de Jong¹, Sander J.T. Brugman¹, Bernd Ensing², Paul T. Tinnemans¹, Hugo Meekes¹, Herma M. Cuppen¹

1. Institute for Molecules and Materials, Radboud University, Heyendaalseweg 135, 6525 AJ Nijmegen, The Netherlands

2. Van 't Hoff Institute for Molecular Sciences, University of Amsterdam, Science Park 904, 1098 XH Amsterdam, The Netherlands

email: j.vandenende@science.ru.nl

Polymorphism in molecular crystals can effect bioavailability of pharmaceuticals through a difference in solubility or dissolution rate between the polymorphic forms. To achieve optimal control of polymorphism it is essential to fully understand both the thermodynamics and kinetics of transitions between the different polymorphic forms. We will present a combined experimental and computational study of these relations for DL-norleucine and some preliminary computational results for L-phenylalanine. Both compounds crystallize in forms that exhibit hydrogen-bonded bilayers. The mechanism of solid-to-solid polymorphic transitions in these crystals is likely to be governed by cooperative movement of full bilayers.

For the α and β polymorphic forms of DL-norleucine the temperature dependence of the lattice parameters and the energetic properties in Molecular Dynamics (MD) simulations is remarkably similar.[1,2] These results are confirmed by single-crystal X-ray diffraction and Differential Scanning Calorimetry (DSC) measurements.[2] The absence of any discontinuities in the properties opens the possibility of a second-order solid-to-solid polymorphic transition between these two enantiotropically related polymorphs. Nudged Elastic Band (NEB) calculations[2], however, show the existence of relatively large energy barriers upon transforming the β polymorphic form towards the α form, which indicates a first-order transition.

References:

[1] J. A. van den Ende and H. M. Cuppen, *Cryst. Growth Des.*, 2014, 14, 3343-3351, dx.doi.org/10.1021/cg5002804

[2] J. A. van den Ende, M. M. H. Smets, D. T. de Jong, S. J. T. Brugman, B. Ensing, P. T. Tinnemans, H. Meekes, and H. M. Cuppen, *Faraday Discuss.*, accepted for publication, DOI: 10.1039/c4fd00214h

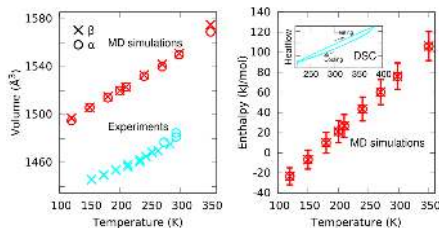


Figure 1. The temperature dependence of the volume and energetic properties of the α and β polymorphic forms of DL-norleucine is remarkably similar, both in MD-simulations and experiments.

Keywords: polymorphism, solid-to-solid phase transitions, Molecular Dynamics simulations, amino acids

MS37-O5 Photo-induced NO linkage isomerism in nitrosyl complexes : A photocrystallographic and infrared analysis

Nicolas CASARETTO¹, PILLET Sébastien¹, BENDEIF El-Eulmi¹, SCHANIEL Dominik¹, GALLIEN K.E. Anna², KLUFERS Peter², WOIKE Theo³

1. University of Lorraine, CRM2, UMR 7036, Vandoeuvre-les-Nancy, F-54506, France

2. Department Chemie der Ludwig-Maximilians-Universität, 81377 Munich, Germany

3. Institut für Strukturphysik, TU Dresden, Dresden, Germany

email: nicolas.casaretto@univ-lorraine.fr

Photoinduced metastable linkage NO isomers have been known for a long time in mono-nitrosyl transition metal complexes. The NO ligand can adopt three bonding modes: the linear (or bent) geometry of the ground state (GS), the metastable (MS1) isonitrosyl, as well as the metastable (MS2) side-on configuration. Each metastable state can be populated, up to 100% in some compounds, using laser illumination with the suitable wavelength.

The discovery of photoinduced linkage NO isomers in the complex $[\text{Fe}(\text{CO})_2(\text{NO})_2]$, which exhibits two NO ligands, raises the question whether two different NO ligands on the same metal center can form linkage isomers jointly or independently, opening up for a combination of several metastable states for the dinitrosyl complex.

Light-induced reversible metastable NO linkage isomers are explored in the dinitrosyl compounds $[\text{RuCl}(\text{NO})_2(\text{PPh}_3)_2]\text{BF}_4$ and $[\text{RuBr}(\text{NO})_2(\text{PCy}_3)_2]\text{BF}_4$ by a combination of photocrystallographic and infrared analysis.

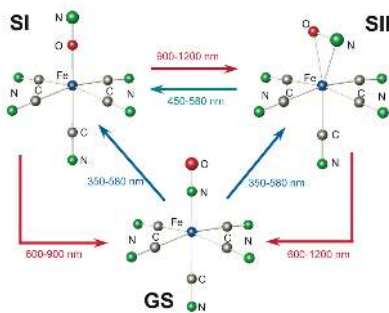


Figure 1. Photo-isomerism of the nitrosyl ligand in $\text{Fe}(\text{NO})(\text{CN})_5$

Keywords: Photo-isomerism, Nitrosyl complexes, Photo-crystallography, Infrared spectroscopy

MS38. Combining crystallographic information with other methods

Chairs: Marco Milanese, Poul Norby

MS38-O1 *In crystallo* optical spectroscopy at synchrotron beamlines - where we are at?

Florian Dworkowski^{1,2}

1. Paul Scherrer Institut

2. Swiss Light Source

email: florian.dworkowski@psi.ch

While a powerful tool for structure determination, the depth of information yielded by X-ray diffraction techniques is somewhat limited. Especially when it comes to verification of chemical characteristics of the sample, a means of gaining additional, complementary data is invaluable. For macromolecular crystallography, for example, this additional information might include, but is not limited to, redox states of metal cofactors, identification of bound ligands and onset and strength of undesired photochemistry. A particular useful approach to harvest this data is the integration of optical spectroscopies, including UV-visible absorption, fluorescence or Raman spectroscopy, into synchrotron beamlines, allowing for (quasi) simultaneous collection of spectroscopic information and diffraction data. Several synchrotron teams, from various fields and all over the world, have thus taken great effort to integrate the necessary instrumentation into their (typically already crowded) beamline stations. This integrated approach results in the possibility to gain the complementary information under identical experimental conditions, using the same sample, thus minimizing any systematic errors that might result from sequential measurements. However, *in crystallo* spectroscopy, especially when performance has to be compromised to allow *in situ* measurements, poses a very special set of challenges, even to the experienced spectroscopist. Here we will present the current state of some instruments, and showcase some of the challenges and success along the way, both in the area of hard- and software development as well as scientific achievements.

Keywords: in crystallo, in situ, Raman, UV/Vis, spectroscopy, synchrotron instrumentation, macromolecular crystallography

MS38-O2 Methods for extracting and combining information from different datasets of crystalline samples

Rocco Caliendo¹

I. CNR - Institute of Crystallography, Bari, Italy

email: rocco.caliandro@ic.cnr.it

Statistical methods can be applied for the analysis of multiple measurements to extract relevant information. Principal component analysis (PCA), for example, has been recently used for achieving enhanced selectivity in the framework of the Modulated Enhanced Diffraction technique [1-2], to identify the time-dependence of structural changes and to classify samples according to their X-ray powder diffraction (XRPD) profiles [3]. Statistical methods can be as well applied for the joint analysis of measurements from different techniques. Recent examples concern the use of PCA for comparing information from XRPD and infrared spectroscopy [4], and of the covariance matrix to combine XRPD with mass-spectrometry and NMR measurements [5]. Such multivariate analysis methods have been recently implemented a computer program devoted to crystallographic applications [6]. The statistical methods used and their implementation will be described, and examples of their applications will be given.

References

- [1] Caliendo R, Chernyshov D, Emerich H, Milanese M, Palin L, Urakawa A, van Beek W, Viterbo D (2012). Patterson selectivity by modulation-enhanced diffraction. *J. Appl. Cryst.*, 45, 458-470.
- [2] M. Milanese, L. Palin, D. Viterbo, R. Caliendo, A. Urakawa, W. van Beek and D. Chernyshov (2014) Chemical Selectivity in Diffraction by Statistical Analysis of in situ XRPD Data *Acta Cryst.*, A 70, C1471.
- [3] R. Caliendo, A. Libutti, B. D. Belviso, G. Chita, M. Monteleone (2014) Characterization of plant biomass derived black carbon (biochar) as soil amendment by X-ray powder diffraction European Biomass Conference and Exhibition proceedings, ISBN 978-88-89407-52-3 pag. 951-957.
- [4] R Caliendo, G Di Profio, O Nicolotti (2013) Multivariate analysis of quaternary carbamazepine-saccharin mixtures by X-ray diffraction and infrared spectroscopy *J. Pharm. Biomed. Anal.* 48-79, 269-279.
- [5] A Rizzuti, R Caliendo, V Gallo, P Mastrorilli, G Chita, M Latronico (2013) A combined approach for characterization of fresh and brined vine leaves by X-ray powder diffraction, NMR spectroscopy and direct infusion High Resolution Mass Spectrometry *Food Chemistry*, 141, 1908-1915.
- [6] R. Caliendo and D. B. Belviso (2014) RootProf: software for multivariate analysis of unidimensional profiles *J. Appl. Cryst.*, 47, 1087-1096.

Keywords: Multivariate analysis, Covariance matrix, Chemical selectivity, Qualitative analysis.

MS38-O3 Solid State – Solutions to the Solution and *vice versa*

Dietmar Stalke¹

I. Georg-August-Universität Göttingen, Institut für Anorganische Chemie, Göttingen, Germany

email: dstalke@chemie.uni-goettingen.de

In his seminal case study on the relationships between solvation, aggregation and reactivity in organolithium chemistry Collum stated “X-ray crystallography provides little insight into the thermodynamics of aggregation and solvation.”^[i] This is right for most chemical substances as the crystal structure is commonly believed to represent the least soluble derivative in the pot and not necessarily the most abundant, let alone the most reactive species. Moreover, the least populated species might represent the eye of the needle in the equilibrium the whole reaction goes through anyway on the course towards the overall product. The talk will elucidate the interaction of X-ray structure analysis, spectroscopy and computational chemistry. We synthesised, crystallized and structurally characterized various thermolabile s-block organometallic aggregates and studied their behaviour in solution by 1/2-D heteronuclear NMR experiments^[ii] and computational chemistry^[iii] to start from firm ground and explore their constitution and behaviour in solution. Unequivocally in this canon of methods X-ray structure analysis plays a leading role but all can learn from another: There are more beasts in the pot than those giving the nicest single crystals.^[iv] Without structural information it is impossible to get the intermediates.^[v] Structural plausibility, i. e. information from the CCDC provides new insights into solution.^[vi]

- [i] D. B. Collum, *Acc. Chem. Res.* **1992**, 25, 448-454.
- [ii] M. Granitzka, A.-C. Pöppler, E. K. Schwarze, D. Stern, T. Schulz, M. John, R. Herbst-Irmer, S. K. Pandey, D. Stalke, *J. Am. Chem. Soc.* **2012**, 134, 1344-1351. [iii] J. Hey, D. M. Andrada, R. Michel, R. A. Mata, D. Stalke, *Angew. Chem.* **2013**, 125, 10555–10559; *Angew. Chem. Int. Ed.* **2013**, 52, 10365–10369. [iv] A.-C. Pöppler, M. Granitzka, R. Herbst-Irmer, Y.-S. Chen, B. Iversen, M. John, R. A. Mata, D. Stalke, *Angew. Chem.* **2014**, 126, 13498-13503; *Angew. Chem. Int. Ed.* **2014**, 53, 13282-13287. [v] T. Niklas, D. Stalke, M. John, *Chem. Commun.* **2015**, 51, 1275-1277. [vi] R. Neufeld, D. Stalke, submitted.

Keywords: interaction of X-ray structure analysis, spectroscopy and computational chemistry

MS38-O4 Charging fragments of fullerenes with multiple electrons: remarkable structural transformations and metal binding records from X-ray crystallography and ⁷Li NMR

Marina A. Petrukhina¹

1. Department of Chemistry, University at Albany

email: mpetrukhina@albany.edu

Non-planar carbon allotropes, such as fullerenes and nanotubes, attract significant interest due to their outstanding properties and potential applications as lightweight carbonaceous materials for microelectronics and energy storage. Open geodesic polyarenes, representing fragments of fullerenes and caps of nanotubes, are broadly used for theoretical and experimental studies of curved π -surfaces. Their excellent electron accepting abilities have been the focus of our attention in the last several years. We investigate redox properties of the bowl-shaped corannulene (C₂₀H₁₀) that is able to accept up to 4 electrons in step-wise reduction reactions. We isolated crystalline products of various reduced states of corannulene and accomplished their first X-ray crystallographic characterization. This allowed us to reveal remarkable structural transformations of π -bowl upon addition of multiple electrons. Moreover, the resulting carbanions were shown to serve as unique bowl-shaped aromatic ligands for metal coordination. The highly reduced corannulene was confirmed to form fascinating supramolecular aggregates with multiple lithium ions encapsulated between non-planar decks.^[1] The use of single crystal X-ray diffraction was crucial for this work as previous NMR investigations failed to provide correct structural assignments. Next, we pushed further the coordination limit of the tetra-reduced bowl having one electron per five C-atoms and being more electron rich than the fullerene-hexaanion. We used the concomitant alkali metal reduction reactions that resulted in the isolation of a new class of triple-decker sandwich structures with a record number of alkali metals encapsulated. A synergistic use of X-ray crystallography, NMR spectroscopy and DFT calculations was required in order to rationalize the electronic structures and dramatic ⁷Li NMR shifts shown by these unprecedented mixed alkali metal supramolecular aggregates.^[2,3] These novel results establish a new paradigm in alkali metal binding for curved polyaromatic surfaces, allowing to further advance carbon-based materials for energy-storage applications.

References

- [1] A. V. Zabula, A. S. Filatov, S. N. Spisak, A. Yu. Rogachev, M. A. Petrukhina. *Science* **2011**, 333, 1008.
- [2] A. S. Filatov, A. V. Zabula, S. N. Spisak, A. Yu. Rogachev, M. A. Petrukhina. *Angew. Chem. Int. Ed.* **2014**, 53, 140.
- [3] A. S. Filatov, S. N. Spisak, A. V. Zabula, J. McNeely, A. Yu. Rogachev, M. A. Petrukhina. *Chem. Sci.* **2015**, 6, 1959.

Keywords: curved polyarenes, stepwise reduction, crystal structures, NMR spectroscopy, DFT calculations

MS38-O5 Crystallisation in-situ - and much more - at the ESRF BioSAXS BM29 beamline

P. Pernot¹, F. Bonnet², S. Teychené³, N. V. Pham³, D. Radajewski⁴, B. Biscans², P. Guillet², M. Brennich¹, A. Round⁴

1. ESRF-The European Synchrotron, 71 Avenue des Martyrs, Grenoble, France
2. Institut des Biomolécules Max-Mousseron, 33 rue Louis Pasteur, Avignon, France
3. Laboratoire de Génie Chimique, 4 allée Emile Monso, Toulouse, France
4. EMBL, Grenoble Outstation, 71 Avenue des Martyrs, Grenoble, France

email: rejma@esrf.fr

BioSAXS, or macromolecular solution scattering, plays an ever-increasing role in structural evaluation in biology since the introduction of dedicated synchrotron beamlines. A number of robots have been developed to offer high throughput and automation. The combination of SAXS with size exclusion chromatography (SEC), where the eluted sample is exposed to X-rays immediately after separation, is also explored. The ESRF BioSAXS beamline BM29 provides routinely two experimental modes: i) STATIC mode using a sample changer and ii) HPLC mode with SEC on line. Automatic switching between these two modes is done by remote control allowing optimal use of available beamtime. Dedicated beamline control and data acquisition software allows sample-changer control and real-time data display (two-dimensional and one-dimensional). It is connected to a data processing pipeline, providing automatic data processing up to *ab initio* models for both modes. Data collection parameters and results are logged and stored in the modified ISPyB database (a laboratory information management system that combines sample tracking and experiment reporting).

Recently, within a Long Term Project cooperation, droplet microfluidics devices were introduced to the beamline. The figure shows the current set-up on the beamline with the inset photograph of droplet generation in the microfluidics chip. The droplets (containing buffer, protein in solution and crystallisation agent) are driven by an oil phase and exposed to X-rays in a fused silica capillary of 300 μ m diameter in vacuum. The capillary is connected directly to the exit of the microfluidic chip and sealed into BM29 standard sample holder. Thanks to an external trigger signal, data are recorded only when droplets cross the X-ray beam to avoid radiation damage of oil and total reflection on droplet walls. With help of such a device crystallisation studies in situ of *glucose isomerase* were carried out.

In the presentation, an overview of macromolecules in solution experiments and possibilities at BM29 will be given, together with the description of latest results with digital microfluidic devices.

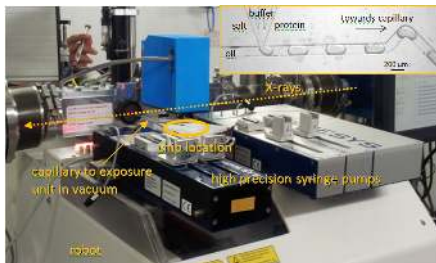


Figure 1. Photograph of microfluidics set-up at BM29 beamline. Inset represents a screen snapshot of droplet generation during crystallisation experiment. Small black dots appearing in droplets on right side are first crystals.

Keywords: small angle X-ray scattering, microfluidics, proteins in solution

MS39. Recent advances in diffraction instruments, detectors and data processing

Chairs: Trevor Forsyth, Rosanna Rizzi

MS39-O1 Updates in single-crystal neutron diffraction

Silvia C. Capelli¹

1. ISIS neutron and muon source, STFC-RAL, Harwell Science Campus, Didcot, UK

email: silvia.capelli@stfc.ac.uk

Single-crystal neutron diffraction is represented all over the world by a small set of instruments operated by specialists at large-scale facilities. In addition, very often every neutron diffraction instrument has a unique setup with dedicated hardware and software and, most of the time, an in-house made detector with in-house software for both data collection and data treatment. This situation has relegated neutron diffraction in a niche of experimental techniques to be used only when unavoidable. New materials combining inorganic and organic moieties, especially developed for exhibiting multiple physical properties, present nowadays a challenge to structural analysis, requiring more and more to combine x-rays and neutron data in order to obtain a more thorough description of the systems under study. In this talk, a survey on the actual possibilities and some outlooks in single-crystal neutron diffraction will be given, in particular touching upon 2D detectors, data collection and data processing software.

Keywords: neutron diffraction, single-crystal, 2D detectors

MS39-O2 Hierarchical description of the structural disorder in doped ceria compounds via real and reciprocal space analysis

Michela Brunelli¹, Mauro Coduri², Marco Scavini^{3,4}, Mattia Allietta³, Paolo Masala³, Claudio Ferrero⁵

1. Swiss-Norwegian Beamlines, ESRF, BP 220, Grenoble, 38043, France
2. National Research Council, Institute for Energetics and Interphases, Corso Promessi Sposi 29, 23900 Lecco, Italy
3. Università degli Studi di Milano, via Golgi 19, 20133 Milano, Italy
4. CNR-ISTM, via Golgi 19, 20133 Milano, Italy
5. European Synchrotron Radiation Facility, 6 av. J. Horowitz, BP 220, 38043 Grenoble, France

email: brunelli@esrf.fr

In this work, a hierarchical approach for elucidating the structural disorder in doped ceria compounds at different scale lengths is presented.

In doped ceria compounds ($\text{Ce}_{1-x}\text{RE}_x\text{O}_{2-x/2}$, with $\text{RE} = \text{La}, \text{Nd}, \text{Sm}, \text{Gd}, \text{Y}, \text{Yb}$) ionic conductivity occurs by migration through the oxygen vacancies introduced for charge balance, after doping with lower valent cations. Oxygen diffusion is though impeded above a critical dopant concentration which is likely to originate from defects aggregations.

The aim of this investigation is to describe the structure of such defect aggregations, by following the structural evolution of these materials at different length scales: from the short to the long-range via the analysis of the disorder at the mesoscopic scale. This is achieved by combining real space (Pair Distribution Function) and reciprocal space (Rietveld refinement and the line profile analysis) analysis of powder diffraction data.

The relationships between the fluorite structure of ceria (CeO_2) and the C-type structure of the dopant oxides was exploited: the structure of doped samples is described with the structure of the C-type using one structural disorder parameter (the positional degree of freedom of cations). The reciprocal space analysis showed that doped samples undergo a phase transition from fluorite to C-type at ~ 0.3 doping concentration, while at the local scale a continuum of structural evolution is evident: dopant-rich- and Ce-rich *droplets*, (i.e. small regions, few Ångstroms wide) form and coexist, exhibiting either a distorted fluorite or a C-type structure in the entire compositional range. At larger length scale these *droplets* average into C-type nanodomains embedded in the fluorite matrix, whose extension increases with doping. The forced connection of these nanodomains led to the formation of *antiphase boundaries*, observed as peak broadening in the *Q*-space patterns of superstructure peaks only¹.

Furthermore, we introduce a more general crystallographic rationale to describe the fluorite to C-type phase transformation mechanism, which is based

on the percolation of hierarchical defect structures. The approach could be generally applied for the analysis of disorder in other highly doped materials.

Reference:

¹ M. Coduri, M. Scavini, M. Allietta, M. Brunelli and C. Ferrero, *Chem. Mater.* **25**, 4278-4289 (2013)

Keywords: Doped Ceria, Disorder, Pair Distribution Function; Powder Diffraction, Hierarchy

MS39-O3 The EIGER detector for macromolecular crystallography

Arnau Casanas¹, Marcus Mueller², Clemens Schulze-Briese²,
Meitian Wang¹

1. Swiss Light Source at Paul Scherrer Institut, Switzerland
2. DECTRIS Ltd., Switzerland

email: arnau.casanas@psi.ch

Single photon-counting devices developed in recent years have represented a major breakthrough in detector technology enabling noise-free detection and novel acquisition modes. The Dectris EIGER detector offers a pixel size of $75 \times 75 \mu\text{m}^2$, frame rates up to 3 kHz and a dead-time of 3.8 μs . An EIGER 1M prototype was tested at the Swiss Light Source beamline X10SA for its application in macromolecular crystallography. The combination of the fast frame-rate and the very short dead-time enables finer data collection plus the numerous advantages associated to higher rotation speeds. A careful analysis of the image summation of extremely fine phi-sliced images yields the best overall statistics/data and can also be used to optimize the dose by finding the best the balance between diffraction and radiation damage. Data collected on both test and challenging crystals will be presented. In addition, the latest results obtained with an EIGER 16M will also be reported.

Keywords: Hybrid pixel detectors

MS39-O4 Neutron macromolecular crystallography at the Institut Laue-Langevin

Matthew P. Blakeley¹, Estelle Mossou¹

1. Institut Laue-Langevin

email: blakeleym@ill.fr

Neutron crystallography allows direct determination of the hydrogen and/or deuterium atom positions of a macromolecule, providing complementary information to that gained via X-ray crystallography. Knowledge of the protonation states of amino-acid residues, along with the positions and orientations of individual water molecules, can often be crucial towards understanding the macromolecule's specific function and behaviour. At the Institut Laue-Langevin, recent improvements to instrumentation for neutron macromolecular crystallography (*i.e.* the quasi-Laue cold neutron diffractometer LADI-III and the monochromatic thermal neutron diffractometer D19) are extending the limits of the field. Sub-mm³ crystals are now regularly being used for data collection, structures have been determined to atomic resolution, and much larger unit-cell systems (cell edges >100 Å) are being studied. Data collection at cryogenic temperatures is also possible, allowing a wider array of experiments, including studies of cryo-trapped enzymatic intermediates. To illustrate the improved performance and capabilities, examples of recent studies [1-6] from the two complementary neutron diffractometers will be presented.

- [1] Weber *et al.*, (2013) *J. Med. Chem.*, **345**, 193-197.
- [2] Cuypers *et al.*, (2013) *Angew. Chem. Int. Ed. Engl.* **52**, 1022-1025. [3] Casadei *et al.*, (2014) *Science*, **345**, 193-197. [4] Langan *et al.*, (2014) *Structure* **22**, 1287-1300. [5] Haupt *et al.*, (2014) *IUCrJ*, **1**, 429-438.
- [6] Howard *et al.*, (2015) *Proc. Natl. Acad. Sci. U.S.A.*, submitted.

Keywords: Neutron, crystallography, hydrogen, deuterium, protonation, perdeuteration, enzyme mechanism, drug design

MS39-O5 Indexing of multi-crystal snapshots collected with a broad bandpass beam

Stef Smeets¹, Catherine Dejoie¹, Christian Baerlocher¹, Lynne B. McCusker¹

1. Laboratory of Crystallography, ETH Zurich, Switzerland

email: stef.smeets@mat.ethz.ch

X-FEL sources provide new opportunities for analyzing difficult crystal structures. Our interest is in organic/inorganic materials with unit cells much smaller than those of the macromolecular crystals that have been the focus of most X-FEL studies to date. We are developing a strategy for the collection and processing of such data [1], based on the broad-bandpass mode (4% energy bandwidth) that will be provided at SwissFEL [2]. The crystals are destroyed by the extremely intense X-ray pulse, so only single snapshots of the sparse data can be recorded, and this makes indexing a challenge. The problems to be overcome are four-fold: (1) accurate orientations have to be retrieved from a single frame, (2) the wavelength associated with each diffraction spot is indeterminate, (3) the unit cells are small, so the number of observations per frame is limited, and (4) the orientations of multiple crystals should be determined from a single frame.

Experiments mimicking a 4%-energy-bandpass mode were performed on SNBL at the ESRF on samples of the zeolite ZSM-5 (up to 15 crystals measured simultaneously), the mineral sanidine, and a cesium cyanoplatinate. We examined several existing methods for indexing these data, assuming the unit cell to be known *a priori*, but most of them proved to be ill-suited. Only a modified Laue-based approach could be applied successfully, but computation times became a limitation in the multi-crystal experiments. Therefore, a new strategy was developed to deal specifically with the data at hand. Candidate crystal orientations are generated either by searching for the indices that match the d-spacings and angles of two low-resolution non-collinear reflections, or with a brute force approach that tries 1.5 million roughly equally distributed rotation matrices that cover all possible crystal orientations. The idea is that only a good solution will index a large number of reflections. To index multiple patterns, the smallest subset of orientation matrices that indexed the largest number of reflections are to be identified. For each sample, the indexing routine performed admirably, and the orientations of up to 11 crystals could be determined from a single frame. While our algorithms were developed with SwissFEL in mind, they can be applied to any data collected in single snapshot mode with either monochromatic or broad-bandpass radiation.

[1] C. Dejoie *et al.*, *IUCr*, 2015, accepted.

[2] B. D. Patterson *et al.*, *Chimia*, 2014, **68**, 73-78.

Keywords: X-FEL, indexing, broad bandpass beam, multi-crystal diffraction

MS40. X-ray diffraction from microsecond to femtosecond time range (including FELs)

Chairs: Christian Betzel, Anton Barty

MS40-O1 Sample preparation and delivery for serial and time-resolved crystallography

Dominik Oberthuer^{1,2}

1. University of Hamburg, Luruper Chaussee 149, 22607 Hamburg, Germany

2. Center for Free-Electron Laser Science, Deutsches Elektronen-Synchrotron DESY, Notkestraße 85, 22607 Hamburg, Germany

email: dominik.oberthuer@desy.de

Serial crystallography methods at both X-ray free-electron lasers (Chapman, 2011) and third generation synchrotron sources (Gati, 2014; Stellato, 2014) are now well established, making it possible to determine the structures of proteins that only form very small crystals or that are extremely radiation sensitive. Serial crystallography methods are also very well suited for time-resolved experiments (Tenboer, 2014), making it possible to reveal the dynamic nature of biological macromolecules and their interactions at near-atomic resolution and on ultrafast timescales. In case of such experiments one deliberately strives to grow micro or sub-micron sized crystals of proteins that would otherwise form larger crystals as well. Small crystals not only allow for uniform laser excitation of all unit-cells in the X-ray beam, but possibly for future mix-and-diffuse studies of reactions that cannot be photo-induced. Size homogeneity of the crystals and, since the amount of sample is limited, a high yield of crystals and optimized sample delivery methods are very important in this regard. Here promising new crystallization methods will be shown, as well as a pipeline for crystal characterization prior to the crystallographic experiment and an overview on strategies to reduce sample consumption. Chapman, H. N., (2011) Femtosecond X-ray protein nanocrystallography. *Nature* 470, 73-77. Gati, C., (2014) Serial crystallography on in vivo grown microcrystals using synchrotron radiation. *IUCr* 1. Stellato, F., (2014) Room-temperature macromolecular serial crystallography using synchrotron radiation. *IUCr* 1, 204-212. Tenboer, J., (2014) Time-resolved serial crystallography captures high-resolution intermediates of photoactive yellow protein. *Science* 346, 1242-1246.

Keywords: Serial Crystallography, FEL, Crystallization, Methods

MS40-O2 Microsecond-resolved in-situ
SAXS/WAXS experiments on the
nucleation and growth of CdS quantum dots
along a free liquid jet

Andreas Magerl¹, Andreas Schiener¹

1. Friedrich-Alexander University of Erlangen-Nuremberg;
Crystallography and Structural Physics; Staudtstr. 3; 91058
Erlangen; Germany

email: andreas.magerl@fau.de

The tremendously growing scientific and industrial interest on semiconducting nanoparticles (quantum dots) relates to the change of the physical and chemical properties of a semiconductor, when its size becomes smaller than the exciton diameter of the bulk material. This so called quantum confinement effect allows tailoring particles properties by controlling its size. To manufacture suitable particles, it is important to get a detailed understanding of the underlying nucleation and growth mechanisms. With the present study we pioneer a novel method to measure both the morphology (SAXS) and the crystalline structure (WAXS) during the early stages of particle formation via fast in-situ experiments along a free liquid jet. Diluted chemicals are brought together in a Y-shaped micro mixer and ejected as a continuous free jet after mixing. The nanoparticle formation takes place in the free jet and different formation stages are addressed by targeting a monochromatic synchrotron X-ray beam on different positions along the jet. This allows to access reaction times between 10 μ s and 10 ms, while illuminating these stages for exposure times up to several seconds in order to obtain a high quality scattering signal. We have investigated the nucleation and early growth of CdS without disturbing the reaction by the addition of stabilizers. These experiments give for the first time a detailed insight into the nucleation and growth process of nanoparticles by precipitation reaction on a time scale which is three orders of magnitude smaller than in earlier studies. The results indicate that the nucleation of CdS prenucleation clusters already takes place on the sub-ms time scale. Furthermore, the temperature and time-dependence of the quantum dot formation proof a diffusion limited growth mechanism for larger particles, which appears to be a very fundamental formation mechanism for these type of fast precipitation reactions.

Keywords: In-Situ; SAXS/WAXS; CdS; Quantum Dots

MS40-O3 Serial femtosecond
crystallography on *in vivo* grown crystals at
SACLA - developments and results

Leonard M.G. Chavas¹, Sasa Bajt², Lars Gumprecht¹, Henry N.
Chapman^{1,3,4}

1. Center for Free-Electron Laser Science, Deutsches
Elektronen-Synchrotron DESY, Notkestraße 85, 22607 Hamburg,
Germany

2. Photon Science, Deutsches Elektronen-Synchrotron DESY,
Notkestraße 85, 22607 Hamburg, Germany

3. Department of Physics, University of Hamburg, Luruper
Chaussee 149, 22607 Hamburg, Germany

4. Centre for Ultrafast Imaging, Luruper Chaussee 149, 22607
Hamburg, Germany

email: leonard.chavas@desy.de

Serial femtosecond crystallography (SFX) uses x-ray pulses from free-electron laser (FEL) sources to outrun radiation damages and thereby overcome long-standing limits in the structure determination of macromolecular crystals. Intense x-ray FEL pulses allow the collection of damage-free data at room temperature, and give the opportunity to study highly time-resolved reactions including irreversible events. By taking full advantage of high repetition rate x-ray pulse delivery schemes, protein structures could be determined in just minutes of measurement time. Automation in sample delivery during SFX experiments could therefore induce a turnover of samples much higher than at today's third generation synchrotrons and automated macromolecular crystallography beamlines, as no crystal alignment or complex robotic motions are required.

Challenges exist at various levels of the experiments, going from the vast nature of the samples to be screened at FELs, handling a large number of samples with minimum human intervention, but also fully characterising the overall injection and sample environment system. The Centre for Free-Electron Laser science has developed a scientific unit that concentrates on breaking down these various milestones and prepares ways for the SFX scientific community to experiment in a user friendly and reliable environment. The presentation will introduce the latest tools that were engineered for high-throughput SFX, emphasising on the developments for automated replenishment of samples and sample injection devices. Early results of SFX experiments on *in vivo* grown crystals performed at the Japanese XFEL SACLA will be highlighted.

Keywords: SFX, XFEL, *in vivo* crystals, high-throughput

MS40-O4 Direct observation of the excited state structure of a Ag(I)-Cu(I) complex

Radosław Kamiński^{1,2}, Katarzyna N. Jarzemska^{1,2}, Bertrand Fournier², Elżbieta Trzop², Jesse D. Sokolow², Yang Chen², Robert Henning³, Philip Coppens²

1. Czochralski Laboratory of Advanced Crystal Engineering, Biological and Chemical Research Centre, Department of Chemistry, University of Warsaw, Żwirki i Wigury 101, 02-089 Warsaw, Poland
2. Department of Chemistry, University at Buffalo, The State University of New York, Buffalo, NY 14260-3000, USA
3. The Consortium for Advanced Radiation Sources, University of Chicago, Chicago, IL 60637, USA

email: rkaminski@chem.uw.edu.pl

Heterodentate coordination complexes have been extensively studied because of their rich electronic and luminescent properties, which are of importance in the design of molecular devices. The short metal-metal contacts found in such complexes determine the nature of the lowest lying emissive states, and must be explored in order to understand their physical properties. Recent advances in time-resolved (TR) synchrotron techniques supported by specific data collection strategies and data processing procedures¹ allow for elucidation of molecular excited state geometries in the solid state. The approach has been so far successfully applied to several high-quality Laue-data sets collected at the 14-ID BioCars beamline at the Advanced Photon Source.²

In this contribution we present synchrotron TR experiment results obtained for a new solvent-free crystal form of a model complex containing Ag(I) and Cu(I) ($\text{Ag}_2\text{Cu}_2\text{L}_4$, $\text{L} = 2$ -diphenylphosphino-3-methylindole ligand). This system exhibits red solid-state luminescence with a lifetime of about 1 μs . This is one of the shortest-lived excited states we have studied so far with the Laue technique. The relatively short lifetime goes along with significant structural changes observed upon irradiation, such as, the Ag...Ag distance shortening of about 0.26 Å for the excited state. The results clearly show strengthening of the Ag...Ag interactions suggesting a bond formation upon excitation.⁴ The photocrystallographic findings are supported by spectroscopic measurements and quantum computations. The results confirm the triplet nature of the emissive state originating mainly from a ligand-to-metal charge transfer.

Research was funded by the NSF (CHE1213223). BioCARS Sector 14 is supported by the NIH, National Center for Research Resources (RR007707). The APS is funded by the U.S. DoE, Office of Basic Energy Sciences (W-31-109-ENG-38). KNJ is supported by the Polish Ministry of Science and Higher Education through the "Mobility Plus" program.

[1] (a) P. Coppens, M. Pitak, M. Gembicki, et al., *J. Synchrotron Rad.* **2009**, 16, 226 (b) J. Kalinowski, B. Fournier, A. Makal, et al. *J. Synchrotron Rad.* **2012**, 19, 637. [2] T. Graber, S. Anderson, H. Brewer, et al. *J. Synchrotron Rad.* **2011**, 18, 658-670. [3] I. O. Koshevoy, J. R. Shakirova, A. S. Melnikova et al. *Dalton Trans.* **2011**, 40, 7927. [4] K. N. Jarzemska, R. Kamiński, et al., *Inorg. Chem.* **2014**, 53, 10594.

Keywords: photocrystallography, time-resolved Laue diffraction, argentophilic interactions

MS40-O5 Investigation of ultrafast dynamics of a molecular diode (PyDMA) using time-resolved Laue diffraction

Sreevidya Thekku Veedu^{1,2}, Simone Techert^{1,2}

1. Deutsches Elektronen Synchrotron (DESY), Hasylab, Notkestr. 85, Hamburg, Germany.
2. Max-Planck Institute for Biophysical Chemistry, Am Fassberg 11, Göttingen, Germany.

email: sreevidya.thekku.veedu@desy.de

Inspired by the electron transfer (ET) reactions as fundamental processes in chemistry and also in biology, we focussed on a promising model i.e. donor-acceptor (D-A) systems which are synthetic molecules to understand the mechanism of photo induced electron transfer process. Light harvesting complexes are functional centers in plants where sunlight is converted into chemical energy. However, due to the complexity of the biological photo-reaction center, research has been focused on a smaller chemical model which share characteristic with their biological counter parts. Pyrene-N,N-dimethylaniline (PyDMA), a compound in which the electron donor N,N-dimethylaniline is covalently linked to the electron acceptor pyrene. Due to the small distance between the donor and the acceptor in PyDMA, a strong electronic interaction exists which manifests itself through femtosecond electron transfer processes. Knowledge of the geometry or mechanism of molecular excited states at atomic resolution is crucial for a full understanding of photo-induced chemical processes. Time-resolved X-ray diffraction (TR-XRD) using polychromatic synchrotron radiation allows a detailed study of the time evolution of structural intermediates and short living states of chemical systems at wide range of time-scales, drawing a complete picture of the photo-induced charge transfer process. Investigation of photo-excitation processes in molecular single crystals, where the initial photo-excitation processes occur on extremely short time-scales (femto-picosecond time domain) have been in the focus of scientific investigations due to their possible applications, e.g. as optical switches. We investigated photo-induced structural changes of our system at 100 ps temporal resolution and will be discussed.

Keywords: Photo-induced electron transfer, PyDMA, Laue diffraction

MS41. Advanced powder diffraction

Chairs: Radovan Černý, Michela Brunelli

MS41-O1 Multidimensional studies of heterogeneous working devices

Gavin Vaughan¹

1. ESRF, CS40220 38043 Grenoble Cedex 9 France

email: vaughan@esrf.fr

Real working systems for chemical applications are typically highly heterogeneous, and the isolated characterization of their constituent elements, ex-situ, is typically not sufficient to understand their operation under real working conditions. Likewise, studies of model systems may capture the essential operation of these devices, but not the interaction between atomic structure and nano- and microscopic engineering which may in fact be of crucial importance in the actual functioning of these devices.

For this reason, methods have been developed to carry out three dimensional diffraction characterization, often coupled with ancillary probes or simultaneous absorption tomography, of real devices under real operational conditions. In order to understand fully the functioning of devices key to the energy economy, such as batteries, fuel cells, solar cells and hydrogen storage materials, or of reactions crucial the chemical industry, such as catalysis or large-scale syntheses, simultaneous characterization on multiple length scales is a requirement.

We will discuss the experimental means to probe via synchrotron X-ray diffraction methods the multi-dimensional space spanned by the properties of interest to understand the chemical functioning of such systems. Examples will be given, in particular for poorly crystalline or amorphous materials, for which three-dimensional volumes have been reconstructed, with each voxel characterized with respect to its atomic, microstructural and temporal evolution.

Keywords: diffraction tomography, synchrotron, in operando

MS41-O2 Femtosecond X-ray powder diffraction

Michael Woerner¹

1. Max Born Institute for Nonlinear Optics and Short Pulse Spectroscopy Max-Born-Strasse 2A, 12489 Berlin, Germany

email: woerner@mbi-berlin.de

The spatial arrangement of valence electrons determines structural and functional properties of crystalline matter. While equilibrium electron distributions have been derived with high precision from stationary x-ray diffraction experiments, their transient changes during optically induced functional and/or relaxation processes have remained mainly unexplored. Femtosecond x-ray powder diffraction allows for determining transient electron density maps in crystals with a spatial resolution of 0.03 nm and a temporal resolution of 100 fs. Using a tabletop, laser driven, femtosecond hard x-ray source in combination with a setup for x-ray powder diffraction to record diffraction patterns consisting of several tens of reflections we study in a pump-probe approach, photo-induced structure changes in the femtosecond time domain by diffracting ultrashort hard X-ray pulses from the excited sample. Both changes of atomic arrangements, i.e. lattice geometries, and of electronic charge density are addressed. In the talk I shall discuss our measurements of transient electron density maps in a variety of ionic crystals [1-6].

[1] M. Woerner, F. Zamponi, Z. Ansari, J. Dreyer, B. Freyer, M. Prémont-Schwarz, T. Elsaesser, *Journal of Chemical Physics* **133** (2010) 064509/1-8 (see also perspective by J. Miller, *Physics Today*, Vol. **63** (2010), 13-15)

[2] F. Zamponi, P. Rothhardt, J. Stingl, M. Woerner, T. Elsaesser, *Proceedings of the National Academy of Sciences of the United States of America* **109** (2012) 5207-5212

[3] J. Stingl, F. Zamponi, B. Freyer, M. Woerner, T. Elsaesser, A. Borgschulte, *Physical Review Letters* **109** (2012) 147402/1-5

[4] B. Freyer, F. Zamponi, V. Juvé, J. Stingl, M. Woerner, T. Elsaesser, M. Chergui, *Journal of Chemical Physics* **138** (2013) 144504/1-8

[5] V. Juvé, M. Holtz, F. Zamponi, M. Woerner, T. Elsaesser, A. Borgschulte, *Physical Review Letters* **111** (2013) 217401/1-5

[6] M. Woerner, M. Holtz, V. Juvé, T. Elsaesser, A. Borgschulte, *Faraday Discussions* **171** (2014) 373-392

[7] J. Weisshaupt, V. Juvé, M. Holtz, S.A. Ku, M. Woerner, T. Elsaesser, S. Ališauskas, A. Pugžlys, A. Baltuška, *Nature Photonics* **8** (2014) 927-930 [8] J. Weisshaupt, V. Juvé, M. Holtz, M. Woerner, T. Elsaesser, *Structural Dynamics* **2** (2015) 024102/1-19

Keywords: Femtosecond X-ray powder diffraction, powder diffraction

MS41-O3 Proving relaxor-type ferroelectricity in Pr-doped SrTiO₃ by XRPD

Stefano Checchia¹, Mauro Coduri², Marco Scavini¹, Michela Brunelli³, Claudio Ferrero³, Mattia Allietta¹

1. Università Degli Studi di Milano - Dipartimento di Chimica, via C. Golgi 19, 20133 Milano (Italy)

2. IENI-CNR, corso Promessi Sposi 29, 23900 Lecco (Italy)

3. ESRF - The European Synchrotron, 6 rue Jules Horowitz B.P 220 F, 38043 Grenoble (France)

email: stefano.checchia@unimi.it

Chemical doping at both the Sr and Ti sites is a feasible way to break the quantum paraelectric state of SrTiO₃. Room temperature ferroelectricity has been detected in Pr-doped SrTiO₃, but the mechanism leading to ferroelectric response is controversial. Recently, the dielectric permittivity behavior of doped SrTiO₃ was attributed to relaxor-type ferroelectricity, generally associated with the formation of Polar Nanoregions (PNRs). From a structural point of view, PNRs are the outcome of a nanoscale phase separation of regions in which cations are off-centered with respect to the long-range phase.

We present a thorough x-ray powder diffraction study performed at ID22 (ESRF) on Sr_{1-x}Pr_xTiO₃ (SPTO) samples with 1% to 15% Pr in a wide range of T. In view of the smaller ionic radius of Pr³⁺ (0.99 Å) and Pr⁴⁺ (0.85 Å) with respect to Sr²⁺ (1.44 Å), the relaxor FE state could be supported by an off-centred position of Pr ions in their oxygen cage, that would give rise to dielectric dipoles around which PNRs can form.

Rietveld analysis evidenced a second-order structural phase transition from *Pm-3m* to *I4/mcm* with a critical temperature T_c strongly dependent on Pr doping. Temperature dependence of the superstructure reflections, of the FWHM of cubic reflections, and of the *a*³*a*³*c*² type tilting of TiO₆ octahedra were sensible parameters of the transition (Figure 1-A,B).

PDF analysis of XRPD data for *x*=0.150 showed that the local structure of SPTO is consistent with *I4/mcm* even at T > T_c (Figure 1-B,C), suggesting tetragonal domains of 30 Å size within a cubic long range structure. The evidence of centrosymmetry is not consistent at any T with a BaTiO₃-like FE state in SPTO, thus, a displacive phase transition can be ruled out.

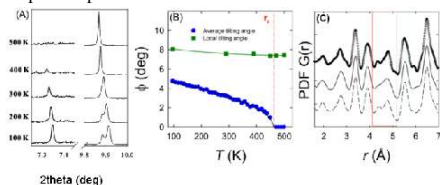


Figure 1. For the *x*=0.150 sample: (A) T-evolution of 211 superstructure reflection and of a structure peak. (B) Tilting angle vs T (blue), tilting angle from local PDF refinement (green). (C) PDF at T=500 K. Observed (circles) and calculated PDF (lines) obtained from cubic and tetragonal structural models.

Keywords: ferroelectrics, total scattering, strontium titanate, polar nanoregions

MS41-O4 Clean and energy-efficient syntheses of M-MOF-74 materials by mechanochemistry and accelerated ageing, monitored through *in-situ* powder x-ray diffraction

Patrick A. Julien¹, Krunoslav Užarević², Athanasios Katsenisi¹, Ivan Halasz², Tomislav Friščić^{*1}

1. McGill University, Montreal, Qc, Canada

2. Institut Ruder Bošković, Zagreb, Croatia

email: patrick.julien@mail.mcgill.ca

Microporous metal organic frameworks (MOFs) based on 2,5-dihydroxyterephthalic acid, generally known as M-MOF-74 have emerged as promising class of materials for a wide variety of applications including gas storage and separation¹, catalysis², and sensors³. "Accelerated ageing" and mechanochemical syntheses are environmentally friendly and economical techniques which allow the reaction of abundant, stable, and inexpensive metal oxides with MOF linker precursors to provide synthesis which avoids the use of bulk solvents and reduce the energy cost when compared to traditional solvothermal synthesis⁴. This work discusses how mechanistic insights from *in-situ* synchrotron powder X-ray diffraction of these milling reactions⁵ were used to optimize the synthesis of various M-MOF-74 analogues in very high yields, using both accelerated ageing and milling techniques.

(1) Queen, W. L.; Hudson, M. R.; Bloch, E. D.; Mason, J. A.; Gonzalez, M. I.; Lee, J. S.; Gygi, D.; Howe, J. D.; Lee, K.; Darwish, T. A.; James, M.; Peterson, V. K.; Teat, S. J.; Smit, B.; Neaton, J. B.; Long, J. R.; Brown, C. M. *Chemical Science* **2014**, 5, 4569. (2) Xiao, D. J.; Bloch, E. D.; Mason, J. A.; Queen, W. L.; Hudson, M. R.; Planas, N.; Borycz, J.; Dzubak, A. L.; Verma, P.; Lee, K.; Bonino, F.; Crocellà, V.; Yano, J.; Bordiga, S.; Truhlar, D. G.; Gagliardi, L.; Brown, C. M.; Long, J. R. *Nat Chem* **2014**, 6, 590. (3) Liu, G.-l.; Qin, Y.-j.; Jing, L.; Wei, G.-y.; Li, H. *Chemical Communications* **2013**, 49, 1699. (4) Cliffe, M. J.; Mottillo, C.; Stein, R. S.; Bucar, D.-K.; Friščić, T. *Chemical Science* **2012**, 3, 2495. (5) Friščić, T.; Halasz, I.; Beldon, P. J.; Belenguer, A. M.; Adams, F.; Kimber, S. A. J.; Honkima, V.; Dinnebier, R. E. *Nat Chem* **2013**, 5, 66.

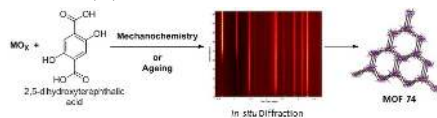


Figure 1. Monitoring the synthesis of M-MOF-74 by milling or "accelerated ageing" through *In-situ* Synchrotron Powder X-Ray Diffraction

Keywords: Metal Organic Frameworks, Powder X-ray Diffraction, Synchrotron, Mechanochemistry

MS41-05 The crystal structure and decomposition properties of the first Al-based amidoborane from *in situ* x-ray powder diffraction

Iurii Dovgaliuk¹, Damir A. Safin¹, Lars H. Jepsen², Zbigniew Łodziański³, Vadim Dyadkin⁴, Torben R. Jensen², Michel Devillers¹, Yaroslav Filinchuk¹

1. Institute of Condensed Matter and Nanosciences Université catholique de Louvain Place L. Pasteur 1, 1348 Louvain-la-Neuve, Belgium E-mail: yaroslav.filinchuk@uclouvain.be

2. Center for Materials Crystallography, Interdisciplinary Nanoscience Center and Department of Chemistry, Aarhus University Langelandsgade 140, DK-8000 Aarhus C, Denmark

3. Department of Structural Research INP Polish Academy of Sciences ul. Radzikowskiego 152, 31-342 Kraków, Poland

4. Swiss-Norwegian Beam Lines European Synchrotron Radiation Facility rue Horowitz 6, 38043 Grenoble, France

email: iurii.dovgaliuk@uclouvain.be

Complex hydrides, such as NaAlH_4 , are reversible hydrogen stores operating only at elevated temperatures, even in the presence of catalysts. Chemical hydrides, such as NH_2BH_3 (AB), release a number of by-products upon thermolysis and are often non-reversible. Here we show that ball milling of NaAlH_4 -4AB mixture or heating it to $\sim 70^\circ\text{C}$ produces the first Al-based amidoborane $\text{Na}[\text{Al}(\text{NH}_2\text{BH}_3)_4]$ and 4.5 wt% of pure hydrogen. The structure was solved from synchrotron X-ray powder diffraction and confirmed through DFT and spectroscopic studies, contains previously unknown tetrahedral $[\text{Al}(\text{NH}_2\text{BH}_3)_4]^-$ anions, where NH_2BH_3^- ligands are coordinated to Al via N atoms. Upon heating, this complex yields in two steps 9 wt% of hydrogen with traces of ammonia, NaBH_4 , and amorphous products.

The structure of $\text{Na}[\text{Al}(\text{NH}_2\text{BH}_3)_4]$ (space group *P*-1, $a = 9.4352(2)$, $b = 7.7198(1)$, $c = 7.6252(1)$ Å; $\alpha = 97.211(1)$, $\beta = 109.223(2)$, $\gamma = 89.728(2)^\circ$, $R_p = 5.7\%$) is the second amidoborane with a triclinic structure, after the bimetallic $\text{Na}[\text{Li}(\text{NH}_2\text{BH}_3)_2]$.^[1] The central Al atom adopts tetrahedral coordination exclusively via nitrogen atoms from four NH_2BH_3^- , making it a new member of Al complex hydrides with tetrahedral coordination, after alanes AlH_3 , complex amides $[\text{Al}(\text{NH}_2)_4]^-$ and borohydrides $[\text{Al}(\text{BH}_4)_4]^-$. The structure consists of $[\text{Al}(\text{NH}_2\text{BH}_3)_4]^-$ anions and Na^+ cations, the latter are being octahedrally coordinated by six BH_3 groups, similar to Na^+ in $\text{Na}_2[\text{Mg}(\text{NH}_2\text{BH}_3)_4]$.^[2] The $\text{Na}(\text{NH}_2\text{BH}_3)_6$ octahedra are linked via edges into infinite zig-zag chains. The dehydrogenation of the complex is partially reversible: $\sim 27\%$ of the released hydrogen can be reabsorbed at 250°C and 150 bar of hydrogen. Hydrogen reabsorption does not regenerate NaAlH_4 or $\text{Na}[\text{Al}(\text{NH}_2\text{BH}_3)_4]$, but occurs between amorphous products and intermediates of the dehydrogenation. Further study of the Al-B-N-H products may open a way to a new family of reversible hydrogen storage materials. The combination of complex and chemical hydrides is made possible thanks to the lower stability of Al-H bonds compared to B-H and due to the strong Lewis acidity of the complex-forming Al^{3+} . This system opens a way to a series of aluminium tetraamidoboranes with improved hydrogen storage properties such as hydrogen storage density, hydrogen purity and the reversibility.

1. K. J. Fijalkowski, R. V. Genova, Y. Filinchuk et al. *Dalton Trans.* **2011**, 40, 4407-4413.

2. H. Wu, W. Zhou, F. E. Pinkerton et al. *Chem. Commun.* **2011**, 47, 4102-4204.

Keywords: X-ray powder diffraction, complex hydrides, hydrogen storage

MS42. Imaging and tomography techniques by neutrons and X-rays

imaging providing a 3D investigation of whole specimens and quasi-histological information of tissues at clinically compatible doses. In addition, PCI may represent a powerful tool in animal models investigations allowing for the longitudinal follow up of cancer evolution or therapeutical effects.

Keywords: phase contrast imaging, low dose computed tomography, high resolution imaging

Chairs: Vincent Favre-Nicolin, Alessia Cedola

MS42-O1 Frontiers of phase-contrast computed tomography

Paola Coan¹

¹. Department of Clinical Radiology and Department of Physics, Ludwig-Maximilians University, Munich, Germany

email: Paola.Coan@physik.uni-muenchen.de

Background: X-ray imaging has been the most important and widespread diagnostic tool in Medicine over the last century. Despite its huge success, for example in imaging bone structure, X-ray diagnostics ultimately reaches its limits in the examination of soft tissues, such as small tumours in healthy tissues, lungs or articular cartilage. Moreover, medical diagnostic imaging requires high contrast at low radiation dose: a condition that often limits the sensitivity of the method. In this scenario, the application to biomedical imaging of coherent X-ray phase-contrast imaging (PCI) methods, which explicitly utilise the wave character of X-ray light, has attracted a vivid interest in medical imaging.

Material and methods: PCI employs the dual property of X-rays of being simultaneously absorbed and refracted while passing through a tissue. Different PCI modalities have been developed (based on X-ray interference or diffraction mechanisms). The produced image contrast is a combination of X-ray absorption, refraction and ultra-small angle scattering. Whole or portions of human tissues such tumour-bearing breasts, pathological livers and osteoarthritic joints provided by the Ludwig Maximilians University (LMU, Pathology and Forensic medicine departments) were imaged in computed tomography (CT) mode. Blinded radiologists quantitatively evaluated the visual aspects of the PCI-CT images with respect to sharpness, contrast and the discrimination of different structures/tissues. IRB-approval for this study was granted by the ethics committee of the LMU.

Results: Low dose, high resolution PCI-CT images of clinically interesting specimens were obtained. Comparative studies in which PCI images were correlated to results produced with clinical diagnostic imaging tools (i.e. CT scans, magnetic resonance imaging, histology). The radiological blinded evaluation showed a statistically relevant difference in image quality in PCI-CT against conventional diagnostic images.

Conclusions: PCI-CT enables depiction of fine tissue changes previously not detectable by conventional diagnostics techniques. Results suggest that PCI-CT has the potential of becoming a valuable method in clinical

MS42-O2 "Stop-and-go" in-situ tomography of dynamic processes – gas hydrate formation in sedimentary matrices

Andrzej Falenty¹, Marwen Chaouachi¹, Sigmund H. Neher¹,
Kathleen Sell², Jens-Oliver Schwarz², Martin Wolf², Frieder
Enzmann², Michael Kersten², David Haberhür³, Werner F. Kuhs¹

1. GZG Abt. Kristallographie, Universität Göttingen, Goldschmidtstr. 1, 37077 Göttingen, GERMANY
2. Institut für Geowissenschaften, Johannes Gutenberg-Universität Mainz, Becherweg 21, 55099 Mainz, GERMANY
3. Swiss Light Source, Paul Scherrer Institut, 5232 Villigen, SWITZERLAND

email: afaletn@uni-goettingen.de

Investigations of dynamic processes followed with in-situ tomography methods have proven to be challenging due to a typical tradeoff between the quality and resolution of reconstructions and acquisitions time. This ill compromise is particularly troublesome for rapid processes like crystallization, dissolution and coarsening where sub- μm pixel resolution details are frequently of crucial importance for physical properties or reactivity kinetics. Here, we report on a well-working solution to this issue in form of a "stop-and-go" synchrotron-based X-ray CT method that combines benefits of sub- μm resolution with complex environments of in-situ experimental cells under elevated gas pressure. The method has been successfully used to mimic the nucleation and growth processes of natural hydrate in various sedimentary matrices at simulated marine conditions (Figure 1). Xenon gas was employed to enhance the density contrast between gas hydrate and the fluid phases involved. The nucleation sites are easily identified with a sub- μm pixel resolution and the various growth patterns are clearly established. These micro-structural findings are highly relevant for future efforts of quantitative rock physics modeling of gas hydrates and ultimately correct detection and quantification of this new source of hydrocarbons. The "stop-and-go" CT method is complemented by a newly developed synchrotron-based method [1] which allowed us to determine the crystallite size distributions (CSD) during the growth and post-formation coarsening of the gas hydrate using the identical pressure cell. Understanding the complex morphologic changes may eventually permit the determination of the formation age of gas hydrates deposits [2, 3], which are largely unknown at present.

[1] Neher et al., A new fast method to derive Crystallite Size Distributions (CSD) from 2D X-ray diffraction data (this conference) [2] Klapp et al., (2007), GRL, 34 : L13608, DOI:10.1029/2006GL029134 [3] Chaouachi et al., In-situ determination of the evolution of the crystallite size distributions of GH-bearing sediments using two-dimensional X-ray diffraction (this conference)

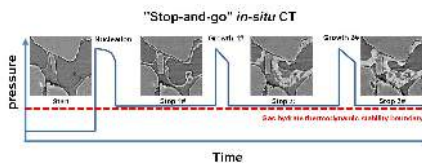


Figure 1. The "stop-and-go" experimental procedure: (1) The initial micro structure (start). (2) The reaction starts by pressurizing the cell (nucleation). (3) The reaction is "paused" by lowering pressure (Stop#1). The procedure can be repeated to study the further stages of the growth.

Keywords: in-situ tomography, gas hydrate

MS42-O3 Water window ptychographic imaging with characterized coherent X-rays

Max Rose¹, Petr Skopintsev^{1,2}, Dmitry Dzhigaev^{1,3}, Oleg Gorobtsov^{1,4}, Tobias Senkbeil^{5,6,7}, Andreas von Gundlach^{5,6,7}, Thomas Gorniak^{5,6,7}, Anatoly Shabalin¹, Jens Viehhaus¹, Axel Rosenhahn^{5,6,7}, Ivan Vartanyants^{1,3}

1. Deutsches Elektronen-Synchrotron DESY, Notkestrasse 85, 22607 Hamburg, Germany
2. Moscow Institute of Physics and Technology (State University), Dolgoprudny, Moscow Region 141700 Russia
3. National Research Nuclear University 'MEPhI' (Moscow Engineering Physics Institute), Kashirskoe shosse 31, 115409 Moscow, Russia
4. National Research Center, 'Kurchatov Institute', Kurchatov Square 1, 123182 Moscow, Russia
5. Analytical Chemistry - Biointerfaces, Ruhr-University Bochum, Universitätsstraße 150, 44780 Bochum, Germany
6. Applied Physical Chemistry, University of Heidelberg, Im Neuenheimer Feld 253, 69120 Heidelberg, Germany
7. Institute of Functional Interfaces, Karlsruhe Institute of Technology, Eggenstein-Leopoldshafen, Germany

email: max.rose@desy.de

We report on a ptychographical coherent diffractive imaging experiment in the water window with focused soft X-rays at 500 eV. A X-ray beam with high degree of coherence was selected for ptychography at the P04 beamline of the PETRA III synchrotron radiation source. We measured the beam coherence with the newly developed nonredundant array method and determined a coherence length of 4.1 μm and a global degree of coherence of 35% at 100 μm exit slit opening in vertical direction. A pinhole, 2.6 μm in size, selected the coherent part of the beam that was used to obtain ptychographic reconstruction results of a lithographically manufactured test sample and a fossil diatom. The achieved resolution was 53 nm for the test sample and only limited by the size of the detector. The diatom was imaged at a resolution better than 90 nm.

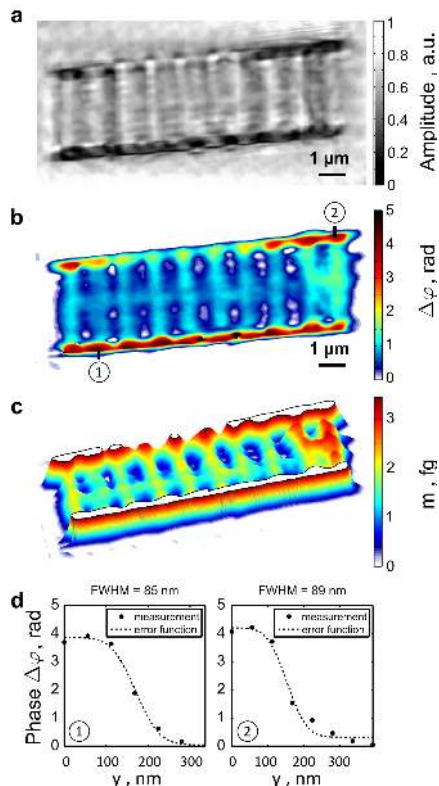


Figure 1. Ptychographic reconstruction of the amplitude (a) and the phase (b) of the fossil diatom. (c) Integrated SiO_2 mass along the depth of the diatom and (d) FWHM values of two error function fits along the black lines indicated in the phase reconstruction in (b).

Keywords: ptychography, water window, non-redundant array, soft x-ray, diatom, coherent diffractive imaging, coherence

MS42-O4 *In situ* visualisation of dendritic growth in solidifying Ga – In alloys

Natalia Shevchenko¹, Olga Roshchupkina¹, Joerg Grenzer¹,
Carsten Baecht¹, Sven Eckert¹

1. Helmholtz-Zentrum Dresden-Rossendorf, P.O. Box 510119,
01314 Dresden, Germany

email: n.shevchenko@hzdr.de

X-ray absorption contrast techniques are an effective tool for investigating solidification processes in opaque metallic alloys. This work is devoted to the *in situ* visualization of the dendritic growth during the bottom-up solidification of a Ga-25wt%In alloy under natural and forced convections. Many effects of melt flow on the mushy zone structure were observed by standard X-ray radiography with a spatial resolution of 5-10 microns [1, 2]. The flow-induced variations of the local solute concentration result in an unsteady development of the primary dendrites and trigger or inhibit the development of secondary and tertiary arms (Fig. 1). Variations of the vertical and lateral temperature gradients induce modifications of the melt flow pattern, which lead to different segregation structures and dendrite morphology. A more detailed analysis of the particular processes (a detachment of side branches and growth of a dendrite tip) were carried out using synchrotron X-ray radiography with a spatial resolution of less than 1 μm . The synchrotron experiments were performed at the ROBL beam line (BM20, European Synchrotron Radiation Facility, Grenoble) at an energy of 28.5 keV. The combination of synchrotron X-ray radiography and synchrotron X-ray diffraction shows a big potential for orientation analysis of the growing grains and lattice parameter determination of the solid phase.

References:

[1] Shevchenko N., Boden S., Gerbeth G. and Eckert S.,
Metall. and Mat. Trans. A 44 (2013) 3797-3808

[2] Shevchenko N., Roshchupkina O., Sokolova O.,
Eckert S., Journal of Crystal Growth 417 (2015) 1-8

Acknowledgments: The research is supported by the German Helmholtz Association in form of the Helmholtz-Alliance "LIMTECH".

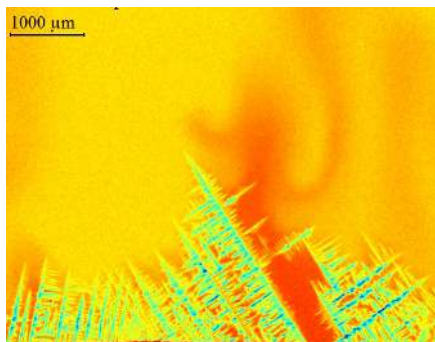


Figure 1. Snapshot of the dendritic structure and gallium plumes in the solidifying Ga – In alloy.

Keywords: Directional solidification, melt flows, X-ray radiography, Ga–In alloys

MS42-O5 Random arrangement of the phase domains in single nanowires

Arman Davtyan¹, Andreas Biermanns¹, Otmar Loffeld¹, Ullrich Pietsch¹

1. Faculty of Science and Technology, University of Siegen, Siegen, Germany

email: davtyan@physik.uni-siegen.de

The distribution of rotational twins within single semiconductor nanowires (NWs) has been studied using the nanobeam x-ray diffraction setup at ID1 beamline at ESRF [1]. Stacking faults, and twins are the major defects in NWs. Coherent x-ray diffraction imaging (CDI) using a nano-beam synchrotron radiation provides a non destructive method to investigate the defect structures in NWs. However, as x-rays probe intensity distributions in reciprocal space, and the phase information is lost during the experiment and can be retrieved using phase retrieval algorithms [2]. In case of a highly defective NW structure, this approach is challenging as the planar defects lead to a complex speckle pattern along certain directions in reciprocal space (fig 1a), whose inversion has up to now not been shown. Here, we present a novel approach how to retrieve the arrangement of twin domains within single GaAs nanowires along the NW growth axis. A combination of the phase retrieval algorithms and methods such as Error-Reduction (ER), Hybrid Input-Output (HIO) and Shrink Wrap (SW) [3] have been used to retrieve the lost phase information. Probing about 10^4 different trial phases the arrangement and the length of particular phase segments is different but the average number of phase changes is rather constant. This leads to the conclusion that one can determine the defect density by CDI but still not the detailed phase arrangement. In present case the calculated defect density is 0.240 defects/nm. Moreover, we have studied the effect of the certain range chosen in reciprocal space along the speckle rod pattern (by cutting a number of sub regions from Fig.1a) on the final result of the PR analysis, and found a correlation in between Δq_z , density of the speckles and number of phase switches. Finally we support the PR analysis by numerically simulating the NW with different possibilities of having ZB / TZB phase segments of completely random arrangement or in an arrangement of possible defect free segment length. These simulations come to confirm the PR result showing that in the case of random arrangement of the ZB and TZB simulated speckle patterns shows similar features compare to measured one.

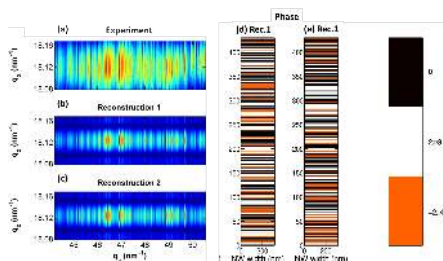


Figure 1. (a) Experimentally recorded (CDI) speckle pattern of the single GaAs NW. (b,c) Fourier transform of the reconstructed NW after the phase retrieval. (d,e) Retrieved phase of the NW for two different random phases as a starting phase in phase retrieval algorithm.

Keywords: Coherent X-Ray Diffraction Imaging, Phase Retrieval

MS43. Thin films, stresses and textures

Chairs: Fabiola Liscio, Magali Morales

MS43-O1 Thiophene based molecules on solid surfaces: the appearance of polymorphs

Roland Resel¹

¹, Institute of Solid State Physics, Graz University of Technology

email: roland.resel@tugraz.at

The origins of specific polymorph phases within thin films are still not well understood. Based on a set of similar molecules – mainly thiophene based molecules with conjugated cores and flexible side chains at the terminal ends – the appearance of polymorph crystal structures at solid surfaces will be discussed. The crystallisation is studied starting from the first monolayer up to device relevant film thicknesses. Variation of the thin film deposition method and deposition parameters lead to different phases. Some of the phases (surface induced phases) are observed only within thin films and the other phases (single crystal phases) are stable as macroscopic single crystals. For some molecules a quite rich appearance of different phases is observed, while for other cases only the single crystal phase is observed. Solution of the crystal structures reveal that the molecular packing as well as the conformation of the molecules can be quite different. The appearance of surface induced crystal structures, their characteristic features and their stability will be discussed.

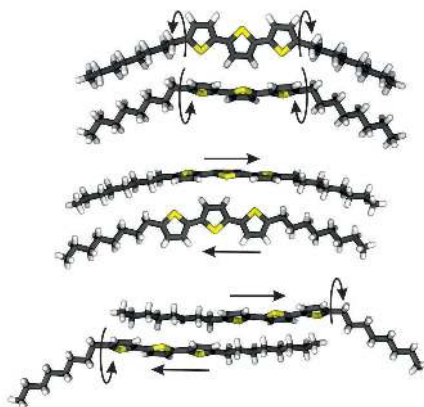


Figure 1. Packing of two neighbouring dioctyl-terthiophene molecules as found in the different phases observed within thin films (top), within the single crystal phases at $T = 100$ K (middle) and $T = 296$ K (below). Arrows mark the differences in the conformation (top, below) and in the packing (middle, below).

Keywords: surface induced crystal structures

MS43-O2 Depth-dependent evolution of texture and stress in thin films

Mario Birkholz¹

1. IHP, Im Technologiepark 25, 15236 Frankfurt/Oder, Germany

email: birkholz@ihp-microelectronics.com

Modern technological devices to a large extent rely on polycrystalline thin films [1]. This holds for instance for integrated circuits from the semiconductor industry, sensoric and optical layers to mention only a few examples. Often, polycrystalline films exhibit pronounced gradients, i.e. depth-dependent evolutions of fiber texture and residual stress [2]. These phenomena are, for instance, highly relevant for wurtzite-structured thin films composed of ZnO or AlN that are currently under development for fully CMOS integrated surface acoustic wave (SAW) devices for biomolecular sensing applications, see Fig. 1 from Ref. [3]. It will be shown how a fiber texture gradient may be modeled in kinematical x-ray diffraction and which effect it has on the intensity mapping of the fiber Bragg reflection I_{HKL} in tilt angle γ scans [4]. The formalism presented makes use of the μ product from the linear attenuation coefficient μ and film thickness t . If the increase of fiber texture degree per unit thickness is given by n_1 it is found that the measured intensity distributions $I_{HKL}(\gamma)$ sensitively depend on the n_1/μ ratio. The formalism is demonstrated by synchrotron-based investigations of ZnO layers, for which the texture gradient was determined by a technique that relies on the variation of the x-ray wavelength [5]. As an example for the significance of residual stresses the preparation of 50 nm thin TiN layers is presented that are intended for mechanical applications in microelectromechanical systems (MEMS) [6]. In this case, tensile strains had to be introduced into suspended layers in order to operate them as bendable beam excited in a quasi-electrostatic operation mode.

1. M. Birkholz with contributions by P. F. Fewster and C. Genzel: *Thin Film Analysis by X-Ray Scattering*, Wiley-VCH, Weinberg (2005)

2. M. Birkholz, C. Genzel, T. Jung, *J. Appl. Phys.* **96** (2004) 7202

3. F. Fenske, B. Selle, M. Birkholz, *Jap. J. Appl. Phys. Lett.* **44** (2005) L662

4. M. Birkholz, *J. Appl. Cryst.* **40** (2007) 735

5. M. Birkholz, N. Darowski, I. Zizak, *Z. Kristall.* **27** (2008) 263

6. M. Birkholz, K.-E. Ehwald, P. Kulse, J. Drews, M. Fröhlich, U. Haak, M. Kaynak, E. Matthus, K. Schulz, D. Wolansky, *Adv. Func. Mat.* **21** (2011) 1652

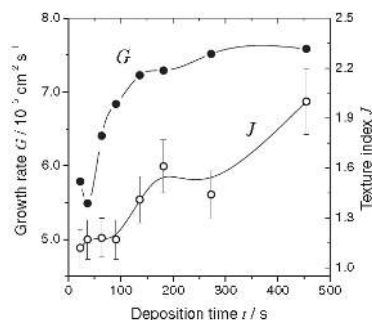


Fig. 1. Growth rate G derived from atomic areal density measurements (left ordinate) and texture index J (right ordinate) for a set of ZnO:Al samples as a function of deposition time t . Growth rate G and texture index J are seen to increase concomitantly.

Figure 1.

Keywords: thin film, texture, residual stress, depth gradients

MS43-O3 Interplay of microstructure defects in GaN layers

David Rafaja¹, David Rafaja¹, Mikhailo Barchuk¹, Christian Roeder², Jens Kortus²

1. Freiberg University of Technology, Institute of Materials Science
2. Freiberg University of Technology, Institute of Theoretical Physics

email: rafaja@ww.tu-freiberg.de

Because of its large energy gap, gallium nitride is regarded as prospective electronic material for LEDs emitting in the ultra-violet spectral range. Due to the lack of appropriate native substrates, GaN is typically grown on foreign wafers. Consequently, the production of large perfect GaN crystal is impeded by the lattice misfit between the substrate material and GaN, which is nearly 15 % for GaN grown on sapphire with the surface orientation (0001). Due to the slightly different thermal expansion coefficients of GaN and Al₂O₃, the lattice misfit is reduced at the growth temperature, but the reduction of the lattice misfit is only 0.1 %. As the corresponding interatomic distances, i.e. the distances between Ga atoms in GaN and between Al atoms in Al₂O₃, are larger in GaN than in Al₂O₃, compressive stress in GaN is expected, but not always observed. The lattice misfit and the resulting lattice strain are compensated by misfit dislocations in GaN. The dislocations act as recombination centres for charge carriers, thus they are unwanted in the GaN crystals. Still, many deposition techniques facilitate dislocation bunching during the growth of GaN and consequently the formation of GaN domains with a greatly reduced local dislocation density. In this contribution, the effect of the dislocation bunching is illustrated on the correlation between the residual stress and the density of threading dislocations in GaN layers grown by hydride vapour phase epitaxy. The residual stresses were determined by using two complementary methods – X-ray diffraction and micro-Raman spectroscopy. The later method revealed not only the average residual stress but also its depth gradient. The dislocation densities were concluded from the broadening of X-ray diffraction lines, the dislocation bunching from the transmission electron micrographs. In this context, the reliability of two competing X-ray diffraction methods were compared, which are alternatively utilized for determination of the density of threading dislocations. The first method is based on the analysis of the dislocation-controlled crystal mosaicity from the azimuthal scans in the reciprocal space, the second one on the analysis of the local strain fields around the threading dislocations from the two-dimensional mapping of the reciprocal space. Finally, the effect of the dislocation bunching on the dislocation density determined by using the respective method is discussed.

Keywords: Gallium nitride, X-ray diffraction, micro-Raman spectroscopy, residual stress, dislocation density, dislocation bunching

MS43-O4 Unravelling the mechanisms of and controlling molecular thin film growth

Stefan M. Kowarik¹, Sebastian Bommel^{1,2}, Linus Pithan¹, Peter Schäfer¹, Christopher Weber¹

1. Humboldt Universität zu Berlin
2. DESY Hamburg

email: stefan.kowarik@physik.hu-berlin.de

Molecular, crystalline thin films are relevant in many technological applications but their thin film morphology is complicated to quantify as growth inherently is a non-equilibrium process. This means that the route to the final film structure is determined not simply by a minimization of the free energy, but by a non-trivial competition between thermodynamics and kinetics. For a quantitative understanding one therefore needs information on the nanoscopic surface processes such as molecular binding as well as surface diffusion and step-edge crossing. *In situ* real-time X-ray scattering is ideally suited for such measurements as it can be used to monitor temporal changes on the atomic scale.

We show how two types X-ray growth oscillations can be used to unravel growth of the molecule C60. Real-time Grazing Incidence Small Angle Scattering (GISAXS) can be combined with simultaneous X-ray reflectivity measurements to characterize both in-plane and out-of-plane film structure as a function of time. From this we determine diffusion barrier, step edge barrier and binding energy for C60 for a detailed, quantitative description of the thin film growth in dependence of growth rate and temperature. Beyond those two control parameters of rate and temperature, we report that light can act as a third, distinct parameter to control growth. We show that even at moderate intensities of ~1 W/cm² a direct influence of light on the molecular crystal structure in thin films is visible. For the example of alpha-sexithiophene (6T) bimodal growth with two coexisting crystal phases can be suppressed and phase purity increased.

S. Bommel, S. Kowarik, et al. "Unravelling the multilayer growth of the fullerene C₆₀ in real-time", *Nature Communications*, **5**, 5388 (2014)

L. Pithan, S. Kowarik, et al. "Light control of polymorphism in thin films of Sexithiophene", *Crystal Growth and Design*, **15** (3), 1319-1324, (2015)

Keywords: growth, growth oscillations, XRR, GISAXS, optical control

MS43-O5 Growth and structural characterization of thin oriented Co_3O_4 (111) films prepared by decomposition of layered cobaltates

Radomir Kuzel¹, Josef Bursik², Miroslav Soroka², Filip Mika³

1. Charles University in Prague, Faculty of Mathematics and Physics, Ke Karlovu 5, 121 16 Prague 2, Czech Republic
2. Institute of Inorganic Chemistry of the Academy of Sciences of the Czech Republic, v.v.i., 250 68 Husinec-Rez 1001, Czech Republic
3. Institute of Scientific Instruments, Academy of Sciences of the Czech Republic, v.v.i., Kralovopolska 147, 612 64 Brno, Czech Republic

email: kuzel@karlov.mff.cuni.cz

The formation and structure of highly (111)-oriented Co_3O_4 films prepared by a novel procedure from weakly (001)-oriented NaCoO_2 were studied by XRD. We have found that (111)-oriented Co_3O_4 thin films with (pseudo) epitaxial relation to $\alpha\text{-Al}_2\text{O}_3$ (001) substrate can be successfully prepared by chemical solution deposition method through the transformation of (001)-oriented NaCoO_2 thin films under optimised annealing conditions. The best results were obtained with the first annealing done at 700 °C for 60 minutes (crystallization of $\gamma\text{-Na}_x\text{CoO}_2$) and the second annealing at 900 °C enabling the transformation of NaCoO_2 into Co_3O_4 phase. The degree of preferred orientation in Co_3O_4 as determined by φ -scans and pole figure measurements depended on the Na content in the starting NaCoO_2 phase. The content should fall within the region where thermodynamically stable Na_xCoO_2 phases exist (i.e., $0.3 \leq x \leq 1$). The highest volume fraction of well-oriented spinel phase was found for the films prepared from precursor solution with $x \sim 0.5$. The number of maxima observed in φ scans of spinel phase indicated the existence of in-plane twins since twice more maxima were detected than it would correspond to the multiplicities of the measured lattice planes. Hence the scans suggest the occurrence of two types of growth domains with the same out-of-plane [111] orientation, but with their <011> and <110> axes rotated by 180° into mirror directions. Such twinning is observed for other (hhh)-oriented spinel films on substrates with dissimilar structures. Relatively higher spread (10 °) of in-plane orientation may be a consequence of weaker interfacial bond between film and substrate because the annealing temperatures used were not sufficient to evoke high crystallization and densification of oxidic network. Surface morphology of the films was investigated using electron microscopy and atomic force microscopy. The microstructure of NaCoO_2 film was formed by platelet-like grains with the longitudinal size of approximately 500-700 nm. The grains piled up into assembly with pronounced longitudinal texture parallel to the interface. The transformation of (001) oriented NaCoO_2 structure into (111)-oriented Co_3O_4 structure manifested itself in change to microstructure of coarse equiaxed grains with the average size comparable to the film thickness and forming near-columnar microstructure. Supported by the Grant Agency of the Czech Republic no. 14-18392S.

Keywords: thin films, chemical solution deposition, cobalt oxides

MS44. New applications of old algorithms in crystallography

Chairs: George Sheldrick, Isabel Uson

MS44-O1 R_{free} : a dinosaur marked for extinction?

Dusan Turk^{1,2}, Jure Praznikar^{1,2,3}

1. Department of Biochemistry and Molecular and Structural Biology, Jozef Stefan Institute, Jamova 39, 1000 Ljubljana, Slovenia
2. Centre of excellence for Integrated Approaches in Chemistry and Biology of Proteins, Jamova 39, 1000 Ljubljana, Slovenia
3. Faculty of Mathematics, Natural Sciences and Information Technologies, University of Primorska, Glagoljaska 8, 6000 Koper, Slovenia.

email: dusan.turk@ijs.si

In the early 90s in the absence of rigorous geometric restraints the structure validation was first introduced in the reciprocal space with R_{free} . Nowadays, however, over fitting can be controlled in real space by the rigorous use of geometric restraints and validation tools. In refinement the practice was established that the deviations from ideal geometry are defined as a target used to scale crystallographic energy terms. Hence, over fitting of models which leads to severe deviations from ideal geometry is not really possible anymore. Hand in hand with the progress of tools delivering better models also the amount of data used for the TEST set was gradually decreasing from the initial 10% and more to 5% and less. Its portion is now practically limited by the request for statistical reliability of the Maximum Likelihood (ML) Cross Validation parameters. The use of the TEST set concept has its limitations: it does not allow the use of all data in refinement and map calculations, the presence of NCS makes it impossible to decouple the independence of TEST set reflections from the rest of the data, and the exchange of the TEST set can result in a considerably different gap between R_{work} and R_{free} . To overcome the limitations of the R_{free} concept we developed an approach that uses the WORK set to calculate the phase error estimates in the ML refinement from simulating the model errors via the random displacement of atomic coordinates. We call it ML Free Kick refinement as it uses the ML formulation of target function and is based on the idea to free the model from the model bias imposed by the chemical energy restraints used in refinement. This approach of calculation of error estimates is superior to the cross validation approach: it reduces the phase error and increases the accuracy of

molecular models, is more robust, provides clearer maps, and may use a smaller portion of data for the TEST set for calculation of the Rfree or leave it out completely.

Praznikar, J. & Turk, D. (2014) Free kick instead of cross-validation in maximum-likelihood refinement of macromolecular crystal structures. *Acta Cryst. D70*, 3124-3134.

Keywords: refinement, maximum likelihood, Rfree, macromolecule, structure accuracy

MS44-02 MoPro software: a continuous evolution and extension of algorithms from "MOLly for PROteins" to "MOlecular PROperties"

Christian Jelsch^{1,2}

1. CNRS

2. Université de Lorraine. France

email: christian.jelsch@univ-lorraine.fr

There have been an increasing number of biological macromolecule structures solved at ultra-high resolution. The refinement program MoPro [1,2] dedicated to the charge density refinement at (sub)atomic resolution of structures ranging from small molecules to biological macromolecules, was therefore developed starting from MOLLY software of Hansen & Coppens [3] written in Fortran language. The program uses the multipolar pseudo-atom model [3] for the electron-density refinement. Alternative methods are also proposed later, such as modelling bonding and lone-pair electron density by virtual spherical atoms.

A charge-density database ELMAM2 [4] was constructed to enable the transfer of multipolar parameters to proteins and was later extended to model common chemical group in organic molecules. The program allows with time more and more complex refinement strategies to be written and has numerous restraints, constraints applying on the charge density or the stereochemistry. Analysis tools to compute the static electron-density and electrostatic potential are derived from the initial MOLLY secondary programs and are available in VMoPro visualisation program. Fourier electron density maps and topological charge integration were programmed from scratch while an existing FFT was incorporated. Some automation tools were programmed to spare the user's time such as local axes definition, importation, exportation, restraints and constraints preparation as well as an automatic charge density refinement strategy.

A graphical user interface MoProGUI was developed in JAVA over the years in order to guide the MoPro user and show him, by exploring the menus, the numerous options and tools available.

The last stage is the development of MoProViewer [5] written in C++, a molecular viewer which is also a Graphical User Interface of VMoPro. MoProViewer enables, in addition, to compute some properties such as the atomic charge in atomic basins from a 3D grid. Some recent tools available are the solvent accessible surface and Hirshfeld surface.

[1] Guillot B., Viry L., Guillot R., Lecomte C. & Jelsch C. J. *App. Cryst.* (2001). 34, 214-223.

[2] Jelsch, C.*, Guillot, B., Lagoutte, A. & Lecomte, C., (2005). *J. Appl. Cryst.* 38, 38-54

[3] Hansen & Coppens, *Acta Cryst.* (1978), A34, 909-921.

[4] Domagala et al., *Acta Cryst.* (2012). A68, 337-351.

[5] Guillot, B., Espinosa, E., Huder, L., Jelsch, C. *Acta Cryst.* (2014). A70, C279

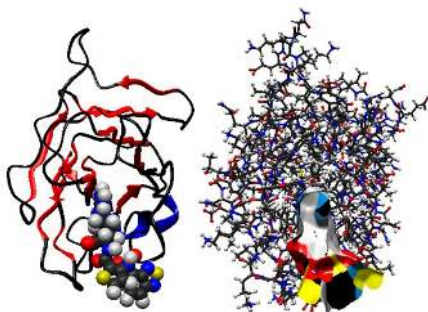


Figure 1. Left: Ribbon view of neuropilin 1, fragment b1 3D structure with bound inhibitor EG00229. Right: Hirshfeld surface of the protein/ligand interface coloured according to protein atom species.

Keywords: Charge density refinement, Restraints, Constraints, Molecular Properties, Molecular Viewer, Hirshfeld surface.

MS44-O3 Likelihood based molecular replacement model pruning in Phaser

Robert D. Oeffner¹, Airlie J. McCoy¹, Randy J. Read¹

¹. Cambridge Institute for Medical Research, University of Cambridge, Hills Road, Cambridge, CB2 0XY, United Kingdom

email: rdo20@cam.ac.uk

The use of likelihood as a target for molecular replacement (MR) calculations in *Phaser* [1] has increased sensitivity over traditional Patterson-based methods, allowing structures to be solved with smaller fragments or models derived from more distant homologues. Both the likelihood score and the probability of success are enhanced if the MR model is pruned *a priori* using tools such as Sculptor [2] or Chainsaw [3] to remove domains, loops or side chains that are predicted from the sequence alignment to be poorly conserved. However, the optimal sequence alignment and optimal pruning become more ambiguous as the sequence relationship becomes more distant, and there can be unexpected domain motions even in close relatives. In these circumstances, potential solutions can be lost because of poor signal or failure in packing tests.

A new likelihood-based *a posteriori* MR model pruning feature has been added to *Phaser* to deal with such problems, thereby improving clear MR solutions as well as rescuing potential solutions with poor signal-to-noise. Smoothly varying occupancies are refined along the protein chain, and then a threshold occupancy is chosen to decide which parts of the starting model should be retained. The residues discarded are typically from poorly-conserved surface loops or domains that have undergone a rigid-body motion. Removing these parts of the structure can rescue MR solutions that would otherwise be discarded by the packing test. In addition, the likelihood-based model pruning also clarifies which domains still need to be placed in multi-component structure solutions.

[1] A. J. McCoy, R. W. G. Grosse-Kunstleve, P. D. Adams, M. D. Winn, L. C. Storoni and R. J. Read, "Phaser crystallographic software," *Acta Cryst D*, vol. 40, pp. 658–674, 2007.

[2] G. Bunkoczi and R. J. Read, "Improvement of molecular-replacement models," *Acta Cryst. D*, vol. 67, pp. 303–312, 2011.

[3] N. Stein, "CHAINSaw: a program for mutating pdb files used as templates in molecular replacement," *Journal of Applied Crystallography*, vol. 41, pp. 641–643, 2008.

Keywords: Phaser, molecular replacement, maximum likelihood, pruning

MS44-O4 Structure solution of nanocrystalline organic compounds from non-indexed powder data using cross-correlation functions

Martin U. Schmidt¹, Stefan Habermehl¹, Lea Totzauer¹

¹ Goethe-Universität, Institut für Anorganische und Analytische Chemie, Max-von-Laue-Str. 7, D-60438 Frankfurt am Main, Germany

email: m.schmidt@chemie.uni-frankfurt.de

Nanocrystalline organic compounds frequently show powder diffractograms with only 10 to 30, generally very broad reflections, which resist a reliable indexing. In such cases the crystal structure can, nevertheless, be solved by a direct fit of crystal structural models to the powder pattern using cross-correlation functions [1]. The cross-correlation function allows a fit of a simulated powder pattern to an experimental one, even if the lattice parameters considerably deviate and the calculated peaks do not overlap with the experimental ones. In the past, cross-correlation functions were used, e.g., for NMR spectra [2] or for assessment of the similarity between powder diagrams of different structures [3]. We use the cross-correlation functions for structure solution by global optimisation and developed a corresponding program called FIDEL (FI with DEviating Lattice parameters) [1]. The procedure resembles the real-space methods used for structure solution from indexed powder data. The crystal structure is described by lattice parameters, space group, molecular geometry, molecular position and spatial orientation. Starting from random values, the lattice parameters, the molecular position and orientation are varied. In each step the powder diffractogram is calculated and compared with the experimental one, and the structure is optimised until a good fit is achieved. In contrast to the real-space methods, lattice parameters are not given beforehand, but are optimised simultaneously with all other variables, starting from random values. This global optimisation is performed in all statistically frequent space groups. Subsequently the best structures are subjected to a Rietveld refinement with TOPAS, using a self-written automated refinement procedure. The best structure is finally post-refined by a user-controlled Rietveld refinement using TOPAS. The whole procedure is demonstrated on nanocrystalline samples of 2,9-dichloroquinacridone (R2=R9=Cl, R4=R11=H) and 4,11-difluoroquinacridone (R4=R11=F, R2=R9=H).

[1] S. Habermehl, P. Mörschel, P. Eisenbrandt, S.M. Hammer, M.U. Schmidt, *Acta Cryst* **2014**, B70, 347-359.

[2] D.S. Stephenson, G. Binsch, *J. Magn. Reson.* **1980**, 37, 395-407. [3] R. de Gelder, R. Wehrens, J.A. Hageman, *J. Computat. Chem.* **2001**, 22, 273-289.

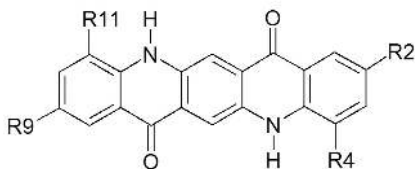


Figure 1.

Keywords: cross-correlation functions, structure determination from powder data, powder diffraction, organic compounds, nanocrystalline compounds

MS44-O5 Use of clustering algorithms to combine partial solutions in reciprocal spaceClaudia Millán¹, Massimo Sammito¹, Rafael J. Borges^{1,2}, Isabel Uson^{1,3}

1. Dept. of Structural Biology, Institute of Molecular Biology of Barcelona (IBMB), Spanish National Research Council (CSIC), Barcelona, Spain
2. Dept. of Physics and Biophysics, Biosciences Institute (IBB), São Paulo State University (UNESP), Botucatu, São Paulo, Braz
3. Catalan Institution for Research and Advanced Studies (ICREA), Barcelona, Spain

email: cmncrri@ibmb.csic.es

Molecular replacement (MR) is the most frequent approach to solve the phase problem in macromolecular crystallography, but depends on the availability of a good enough starting model. Recently, MR is going ab initio in a number of approaches and as a consequence, its previous limits are being overcome through extremely sophisticated methods, targeting the area between purely ab initio and traditional MR, like AMPLE^{1,2}, MR-Rosetta³, or the method proposed by Zhang⁴. ARCIMBOLDO⁵ and BORGES⁶ methods take the approach of using very small ideal models or libraries of local folds. Clustering methods had previous application in low resolution phasing approaches such as the Few Atoms Method⁷. More recently, Buehler et al. proposed the application of cluster analysis to MR phasing⁸, pointing out that in cases in which partial or poor models are used, discrimination of the optimal position is not straightforward, and often, a number of weak peaks with partially correct orientations are found. Comparison of coordinates of partial solutions is not an easy task, as search models may fit the electron density in different ways. Instead, maps can be generated and its mean phase difference measured, producing a phase-combined map that may model differences and result in a better estimate of the atomic coordinates. We have applied phase combination to ARCIMBOLDO partial solutions and proof of principle has been established by studying optimal strategies starting with test cases. We have evaluated the reliability of possible figures of merit and how to best characterize differences (using mean phase differences or map correlation coefficients). These results, just submitted for publication, have been implemented to increase the radius of convergence and efficiency of the ARCIMBOLDO methods. The approach developed has been essential to solve a previously unknown structure with 430 aminoacids in the asymmetric unit and data to 1.5Å where classical MR methods had failed.

- Bibby, J. *et al.* (2013). *Acta Cryst.* D69, 2194-2201
 Bibby, J. *et al.* (2012). *Acta Cryst.* D68, 1622-1631
 DiMaio, F. *et al.* (2011). *Nature*, 473(7348), 540-543
 Shrestha, R. *et al.* (2015). *Acta Cryst.* D71, 304-312
 Millán, C. *et al.* (2015). *IUCrJ* 2, 95-105
 Sammito, *et al.* (2013). *Nature Methods*, 10, 1099-1101
 Lunin, V.Yu. *et al.* (1995). *Acta Cryst.*, D51, 896-903.
 Buehler, A. *et al.* (2009). *Acta Cryst.* D65, 644-650

Keywords: Phasing, Clustering, Ab initio, Molecular Replacement**MS45. Chemical information as prior knowledge in crystallography**

Chairs: Anthony Linden, Rob Nicholls

MS45-O1 Fitting ensemble models of disorder using a priori chemical structure informationRichard I. Cooper¹

1. Department of Chemistry, University of Oxford, UK

email: richard.cooper@chem.ox.ac.uk

Finding and refining suitable crystallographic models of highly disordered regions of a structure is often a time consuming and thankless task: the improvement in fit and model phases gained by carefully fitting molecules to disordered regions of scattering density makes little difference to the interpretation of the 'important' parts of a crystal structure. Difficult cases can include: partially occupied solvent in voids, unidentified mixtures of disordered solvents, and solvent which is not constrained by the space group symmetry of the parent structure.

A more convenient option is to apply the bypass algorithm, implemented in PLATON as Squeeze.¹ The method adds a reciprocal space correction to the calculated structure factors based on the Fourier transform of the difference scattering density in the void regions of the crystal structure. Iterative improvement of phases using this scattering contribution can converge on a solution which gives a reliable correction to the data. Additional checks, such as the approximate number of scattering electrons in the solvent volume can help to rationalise the correction. The form of the scattering density used in the correction is not constrained, except that it must lie in the unoccupied regions (solvent accessible voids) of the structure. The results usually show an improvement in expected geometry and standard uncertainties of the remaining structure.²

An alternative approach is to make use of computing power to find a disordered model which gives the best fit to the data. Such a model can be constructed using an ensemble of partially occupied molecules placed in the solvent accessible regions of the structure and optimised using random sampling of different occupancies, conformations and positions. The sampling is optimised by using observed distributions of geometry and interaction from known structures.

The application of this method to some disordered structures is presented and shown to give a physically interpretable description of the scattering from a disordered solvent (Figure 1). Additional a priori real-space information, such as satisfying weak intermolecular interactions can also be used to guide solutions.

[1] P. van der Sluis and A. L. Spek (1990) *Acta Cryst* A46, 194–201.

[2] A. L. Spek (2015) *Acta Cryst* C71, 9–18

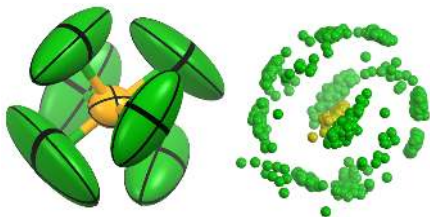


Figure 1. Conventional a.d.p. model of disordered PF_6^- anion (left); ensemble of partially occupied molecular models (right) revealing more detailed orientational disorder.

Keywords: disorder, a priori chemical information, solvent

MS45-O2 Use of chemical restraints in Phenix

Nigel W. Moriarty¹

¹ Physical Biosciences Division, Lawrence Berkeley National Laboratory, Berkeley, CA 94720

email: NWMoriarty@lbl.gov

The models obtained from crystallography can be improved by the use of prior chemical knowledge. Phenix (Adams, 2010) makes use of previously obtained experimental data and also predictive methods such as quantum chemistry (QC) to improve the accuracy of crystallographic models.

The electronic Ligand Builder & Optimization Workbench (eLBOW) (Moriarty, 2009) is used in Phenix to generate geometries and restraints for use in structure refinement. These can be determined by the using built-in semi-empirical QC methods, including RM1 and AM1, or via third party QC packages. It can also interface with the experimental geometries available via the Mogul program (Bruno, 2004). Libraries of restraints can be generated automatically, however, validation is essential to ensure accurate results. These range from simple checks to ensure topological correctness to detailed checks that highlight limitations of the generation method.

The Phenix structure refinement program, phenix.refine (Afonine, 2012), can make use of prior and predictive chemical methods in multiple ways to improve molecular models. The geometry of the protein can be improved using the Conformation Dependent Library (Moriarty, 2014) to adjust the main chain geometry based on the conformation of the backbone. Macromolecular geometry can also be improved by using more physically realistic potentials from molecular mechanics, such as Amber (Case, 2014). Finally, ligand geometries can be improved by the application of molecular modeling force fields (MMFF) or semi empirical QC (PM6) gradients from the AFTTT program (Wlodek, 2006), or the use of QC methods from the DivCon library (Borbulevych, 2014).

References

- Adams, P.D., P.V. Afonine, G. Bunkoczi, V.B. Chen, I.W. Davis, N. Echols, J.J. Headd, et al. 2010. *Acta Cryst. D* 66:213–21
- Afonine, P.V., R.W. Grosse-Kunstleve, N. Echols, J.J. Headd, N.W. Moriarty, et al. 2012. *Acta Cryst. D* 68:352–67
- Borbulevych, O.Y., N.W. Moriarty, P.D. Adams & L.M. Westerhoff. 2014. *Comput. Cryst. Newsl.* 5:26–30
- Bruno, I.J., J.C. Cole, M. Kessler, J. Luo, W.D.S. Motherwell, L.H. Purkis, et al. 2004. *J. Chem. Inf. Comput. Sci.* 44:2133–44
- Case, D.A., V. Babin, J.T. Berryman, R.M. Betz, D.S. Cai, et al. 2014. *AMBER 14*. UCSF
- Moriarty, N.W., R.W. Grosse-Kunstleve & P.D. Adams. 2009. *Acta Cryst. D* 65:1074–80
- Moriarty, N.W., D.E. Tronrud, P.D. Adams & P.A. Karplus. 2014. *FEBS J.* 281:4061–71
- Wlodek, S., A.G. Skillman, and A. Nicholls. 2006. *Acta Cryst. D* 62:741–49

Keywords: ligands, restraints, quantum chemistry, force fields, ligand libraries, validation

MS45-O3 SEQUENCE SLIDER: a multi sequence evaluator and its application in venomics

Rafael J. Borges^{1,2}, Massimo Sammito¹, Claudia Millán¹, Marcos R.M. Fontes², Isabel Usón^{1,3}

1. Dept. of Structural Molecular, Institute of Molecular Biology of Barcelona (IBMB), Spanish National Research Council (CSIC), Barcelona, Spain

2. Dept. of Physics and Biophysics, Biosciences Institute (IBB), São Paulo State University (UNESP), Bocuatu, São Paulo, Brazil

3. Dept. of Structural Biology, Catalan Institution for Research and Advanced Studies (ICREA), Barcelona, Spain

email: rjborges@ibb.unesp.br

Structural biology has been an invaluable tool in the biomedical field of venomics with drug design, comprehension of physiological mechanisms and improvement of antivenom therapy (Calvete et al., 2009). Venom extraction is a common procedure as it is stored in an accessible gland. Thus, often, snake toxins are directly obtained from natural venom purification, rather than through recombinant protein production. Characterized by one of the most rapid evolutionary divergence and variability in any category of proteins, venoms are composed by a cocktail of toxins (Calvete et al., 2009). With such complex composition, it is a challenge to obtain high purity toxins, since physico-chemical properties may be shared among different proteins. Thus, the obtained samples from final steps of purification can be a mixture of isoforms and/or different protein. In such cases, the sequence may not be clearly determined by mass spectrometry and even after protein isolation through crystallization, determining side chain composition in the crystallographic model may not be trivial. SEQUENCE SLIDER aims to address such scenario integrating other sources of experimental data. Starting from a partial or complete model assigning and evaluating different sequence possibilities against diffraction data. The side chains are modeled combining hypotheses assembled with SCWRL4 (Krivov et al., 2009) and/or COOT (Emsley et al., 2010) and refinement through REFMAC (Murshudov et al., 2011) and/or BUSTER (Bricogne et al., 2011). The varied sequences are generated using a probability distribution based on experimental results of mass spectrometer or on phylogenetic statistics. Correct model discrimination is evaluated through proposition of a Figure of Merit integrating global and local crystallographic indicators, energy and complementary experimental knowledge. SEQUENCE SLIDER is being applied to determine unsolved snake venom toxin crystallography datasets and revisit toxins deposited in the protein databank.

References

- Bricogne, G. et al. (2011). BUSTER Cambridge, United Kingdom: Global Phasing Ltd.
- Calvete, J. J. et al. (2009). FEBS Lett. 583, 1736–1743.
- Emsley, P. et al. (2010). Acta Crystallogr. D Biol. Crystallogr. 66, 486–501.
- Krivov, G. G. et al. (2009). Proteins. 77, 778–795.
- Murshudov, G. N. et al. (2011). Acta Crystallogr. D Biol. Crystallogr. 67, 355–367.

Keywords: Venomics, Crystallography, protein sequencing, refinement, modeling, phasing, ARCIMBOLDO, mass spectrometry

MS45-O4 DSR – Enhanced modelling and refinement of disordered structures with SHELXL

Daniel Kratzert¹, Ingo Krossing¹

1. Albert-Ludwigs-Universität Freiburg

email: dkratzert@gmx.de

One of the remaining challenges in single-crystal structure refinement is the proper description of disorder in crystal structures. DSR performs semi-automatic modelling of disordered moieties in SHELXL^[1]. It contains a database that includes molecular fragments and their corresponding stereochemical restraints and a fitting procedure to place these fragments on the desired position in the unit cell. The program is also suitable for speeding up model building of well-ordered crystal structures.

Writing a special DSR command into the SHELXL .res file of the target structure instructs DSR on where to place and how to orient a molecular fragment from the fragment database in the unit cell (Figure 1). In addition, it is possible to define the occupancy, residue or part number of the fitting fragment. The fragment can be inverted, e.g. to fit the other conformer of twisted tetrahydrofuran.

Molecular fragments can be either imported directly from the GRADE server of Globalphasing Ltd.^[2], from existing crystal structures or from ab initio calculations. DSR offers several more options available to make disorder modelling a convenient process.

[1] G. M. Sheldrick, *Acta Cryst.* **2015**, C71, 3–8.

[2] Grade Web Server, *Global Phasing Ltd.*
<http://grade.globalphasing.org>.

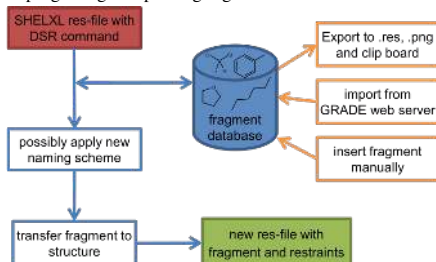


Figure 1. General work flow of the DSR program.

Keywords: X-ray structure, refinement, disorder, SHELXL, molecular fragments.

MS45-O5 Deriving a chemical context for protein-bound monosaccharides

Jon Agirre¹, Kevin Cowtan¹

¹. York Structural Biology Laboratory, Department of Chemistry, The University of York, England

email: jon.agirre@york.ac.uk

Any attempt at gaining chemical information from a public structural biology repository such as the Protein Data Bank (PDB) should deal with the fact that many deposited structures contain errors. Remediation efforts to date have, with the exception of PDB-REDO [1], focused on the correction of naming problems, while the atomic coordinates remain untouched until a new entry supersedes them. Therefore, scientists are encouraged to use as many validation tools as possible in order to arrive at meaningful conclusions.

Structural fingerprinting is a process that, starting from a set of deposited atomic models, extracts a chemical context for a target non-protein compound. The resulting fingerprint can be used for detecting the compound's features and context in an electron density map, thus allowing for its interpretation in terms of atomic positions. The approach, which is already an integral part of the Nautilus software for the automated detection and modelling of nucleic acid [2], has recently been extended to work with cyclic carbohydrates. However, the prerequisite systematic analysis of the monosaccharide-containing entries in the PDB archive has uncovered new issues involving ring conformation, to be added to the already known nomenclature problems [3]. A curated set of structures suitable for fingerprinting has been produced after combining prior chemical knowledge into a list of validation criteria, implemented in the Privateer package [4]. The impact of chemical validation on the fingerprinting method and its practical applications will be discussed.

[1] R.P. Joosten et al, IUCrJ, 2014, 1:213-220.

[2] K. Cowtan, IUCrJ, Vol. 1, No. 6, 2014, p. 387-392.

[3] T. Lütke, Acta Cryst., 2009, D65, 156-168.

[4] J. Agirre and K. Cowtan, Computational Crystallography Newsletter, Jan 2015, p. 10-12.

Keywords: carbohydrates, model building, conformation,

MS46. The use of resonant scattering and diffraction for the analysis of materials

Chairs: Jean-Louis Hodeau, Eugen Weschke

MS46-O1 Application of resonant X-ray scattering to thermoelectric materials that contain elements with similar electron counts

Oliver Oeckler¹

¹. Leipzig University, Faculty of Chemistry and Mineralogy, IMKM, Scharnhorststr. 20, 04275 Leipzig

email: oliver.oeckler@uni-leipzig.de

Layered compounds derived from Sb₂Te₃ and substituted variants thereof constitute one of the most important classes of efficient thermoelectric materials. They contain distorted rocksalt-type slabs separated by van der Waals gaps. In germanium antimony tellurides, for example, the thermoelectric properties can be enhanced by substituting Ge with Sn or Cd or by partially replacing Sb by In. In addition, doping with Ag approaches other efficient materials like AgSbTe₂. Precise structural data are essential for the understanding of structure-property relationships. In such compounds, elements with similar electron counts such as Ag, Cd, In, Sn, Sb and possibly Te share the same Wyckoff positions which may additionally contain vacancies. Whereas vacancies tend to order, the other elements (often several of them) are usually mixed in different ratios on different positions. In some cases, periodic concentration gradients were observed.

In contrast to conventional structure analyses, resonant X-ray diffraction is an excellent tool to differentiate elements with usually low scattering contrast [1] and to reveal such partial ordering phenomena. Synchrotron data collected near the absorption edges are affected by dispersion correction terms $\Delta f'$ of up to 10 electrons. Joint refinements with multiple datasets collected at all K edges involved and at wavelengths far from edges are the most suitable strategy and avoid many shortcomings of "traditional" δ syntheses (which thus appear obsolete). A number of practical aspects were analyzed in detail [2] so that questions like "which is the optimal wavelength?" or "how is beamtime used most efficiently?" can unequivocally be answered. Various sources for $\Delta f'$ values were evaluated, the best being experimental values obtained from fluorescence data via the Kramers-Kronig transform and values that are refined using comparable "calibration compounds". The talk aims at giving practical guidelines rather than theoretical considerations and addresses both single-crystal and powder techniques. How can state-of-the-art precision be combined with "high throughput"?

[1] J. L. Hodeau, V. Favre-Nicolin, S. Bos, H. Renevier, E. Lorenzo, J. F. Berar, *Chem. Rev.*, **2001**, *101*, 1843.

[2] S. Welzmler, P. Urban, F. Fahrnbauer, L. Erra, O. Oeckler, *J. Appl. Crystallogr.* **2013**, *46*, 769.

Keywords: thermoelectrics, resonant scattering, element distribution

MS46-O2 Electronic depth profiles with atomic layer resolution from Resonant X-ray Reflectivity

Jochen Geck^{1,2}, M. Zwiebler¹, B. Gray³, J. Chakhalian³, J. Freeland⁴, F. He⁵, A. Koitzsch¹, P. Komissinskiy⁶, E. Schierle⁷, S. Sutarto³, U. Treske¹, M. Vafaee⁶, E. Weschke⁷, G. A. Sawatzky⁸, L. Alff⁹, S. Macke^{9,10}, J. E. Hamann-Borrero¹

1. Leibniz Institute for Solid State and Materials Research, IFW-Dresden, Helmholtzstr. 20, 01069 Dresden, Germany
2. Institut für Strukturphysik, Technische Universität Dresden, D-01062 Dresden, Germany
3. Department of Physics, University of Arkansas, Fayetteville, Arkansas 70701, USA
4. Advanced Photon Source, Argonne National Laboratory, Argonne, Illinois 60439, USA
5. Canadian Light Source, University of Saskatchewan, Saskatoon, Saskatchewan, S7N0X4, Canada
6. Institute of Materials Science, Technische Universität Darmstadt, 64287 Darmstadt, Germany
7. Helmholtz-Zentrum Berlin für Materialien und Energie, Albert-Einstein-Str. 15, D-12489 Berlin, Germany
8. Department of Physics and Astronomy, University of British Columbia, Vancouver, V6T1Z1, Canada
9. Max Planck-UBC Centre for Quantum Materials, Vancouver, V6T1Z1, Canada
10. Max Planck Institute for Solid State Research, Heisenbergstr. 1, 70569 Stuttgart, Germany

email: J.Geck@ifw-dresden.de

Resonant x-ray reflectivity (RXR) provides a unique experimental tool to study the surface and buried interfaces of oxide heterostructures. The analysis of reflectivity data usually assumes homogeneous properties throughout the volume of the constituent materials, i.e., the internal atomic structure of these materials is usually neglected. However, when the x-ray energy is tuned to an absorption edge, this approximation can cease to provide a good description of the experiment, because lattice planes with and without the elements at resonance will interact with the photons very differently. As a result, RXR can also provide important and very useful information about a heterostructure at the atomic level. We have therefore developed a scheme for analyzing RXR-data, which takes the atomic structure of a material into account by “slicing” it into atomic planes with characteristic optical properties. Using LaSrMnO_4 and $\text{YBa}_2\text{Cu}_3\text{O}_{7-\delta}$ as examples, we discuss the implications of this approach. Our analysis not only allows to determine structural information such as interface terminations and stacking of atomic layers, but also enables to extract depth-resolved spectroscopic information with atomic resolution, thus further enhancing the capability of the technique to study emergent phenomena at surfaces and interfaces.

Keywords: oxide heterostructures, resonant soft x-ray scattering

MS46-O3 Towards to control the Dzyaloshinskii-Moriya interaction in chiral magnets with $P2_13$ crystal structure

Vadim Dyadkin¹, Sergey Grigoriev², Dmitry Chernyshov¹

1. Swiss-Norwegian Beamlines at the ESRF

2. Petersburg Nuclear Physics Institute

email: diadkin@esrf.fr

The sense of chiral magnetic ordering, observed in compounds with chiral crystal structure, depends on the sign of the Dzyaloshinskii-Moriya interaction (DMI). We have probed structural and magnetic chiralities for a series of monogermanides and monosilicides of 3d-metals as well as for Cu_2OSeO_3 single crystals. Scattering of polarized neutrons on chiral magnetic structures was used to determine the absolute magnetic configuration. The absolute crystal structure was established by the X-ray single crystal diffraction data providing that resonant contribution enables to observe violation of the Friedel law.

We show that the chiral magneto-lattice coupling mapped phenomenologically as the DMI could be applied to control magnetic chirality as needed for spintronics applications. The sign of the Dzyaloshinskii constant D defines the chirality of magnetic helix γ_m relative the structural chirality Γ_c . The product $\text{sgn}(D) \times \Gamma_c \times \gamma_m$ is an invariant with respect to inversion and time-reversal operations ensuring that left-handed and right-handed polymorphs have the same energy. For monosilicides and monogermanides the sign of D depends on 3d-element that results in a number of interesting phenomena for the solid solutions.

Keywords: chirality, absolute structure, Dzyaloshinskii-Moriya interaction

MS46-O4 The use of resonant X-ray diffraction to tune destructive interference as a highly sensitive probe for structural distortions

Carsten Richter^{1,2}, Erik Mehner¹, Melanie Nentwich¹, Juliane Hanzig¹, Matthias Zschornak¹, Dmitri V. Novikov², Dirk C. Meyer¹

1. Institute of Experimental Physics, TU Bergakademie Freiberg, Germany

2. Deutsches Elektronen-Synchrotron (DESY) Photon Science, Hamburg, Germany

email: carsten.richter@desy.de

Resonant X-ray diffraction was used to study site-specific deviations from the ideal perovskite-type structure of strontium titanate (SrTiO_3). Varying the X-ray wavelength close to the absorption edge of a resonant atom allows to precisely tune its scattering amplitude. For an ideal crystal structure and Bragg reflections where atoms scatter out of phase, this effect can be used to nullify the structure factor due to destructive interference. Tiny deviations of the atom positions from the average structure and the resulting change of scattering phase can, after averaging, be expressed as an extra factor to the scattering amplitude. In the case where the displacement is due to temperature, this parameter is well known as the Debye-Waller factor. In general, this factor is different for each atom which results in a change of the conditions for destructive interference and has a strong effect on the resonant diffraction spectra of the above mentioned reflections. The choice of reflection within this set defines the resolution and the direction probed by the method. We used this effect to characterize the displacement of atoms in SrTiO_3 caused by temperature, defects and external electric field. The measurements were performed in the region of the Sr-K absorption edge on $\{00l, l=2n+1\}$ reflections. In the focus of our investigations was the strained phase of SrTiO_3 which forms during application of a 1 MV/m DC electric field as reported in literature [1]. It could be validated that the new phase is polar which is expressed as a displacement of titanium from the center position in field direction. The method has proven a high sensitivity already for displacements in the 0.001 Å regime.

[1] J. Hanzig, M. Zschornak, et al., Phys. Rev. B 88, 024104 (2013), doi:10.1103/PhysRevB.88.024104

Keywords: resonant diffraction, destructive interference, atomic displacement, perovskites, symmetry breaking

MS46-O5 Atomic structure of nanoalloy catalysts by resonant high-energy XRD and atomic PDFs analysis

Valeri Petkov¹

¹. Dept. Physics, Central Michigan University, Mt. Pleasant, MI 48859 USA

email: petko1vg@cmich.edu

With current technology moving rapidly toward smaller scales nanometer-size alloys are being produced in increasing numbers and explored for various applications, in particular catalytic ones. To understand better and so gain more control over the performance of nanoalloy catalysts, precise knowledge of their atomic-scale structure is needed. With bulk alloys such knowledge is almost straightforward to obtain by Bragg x-ray diffraction (XRD). Unfortunately, Bragg XRD is inapplicable to nanoalloys since their XRD patterns show a limited number of distinct Bragg peaks, if any, and a very pronounced diffuse component. The problem can be solved by employing a non-traditional approach involving high-energy XRD and atomic pair distribution functions (PDF)s analysis [1]. However, for a nanoalloy comprising n atomic species a single XRD experiment yields a total atomic PDF which is a weighted sum of $n(n+1)/2$ partial PDFs. This could make the interpretation of PDF data for nanoalloys ambiguous. Using resonant high-energy XRD allows particular partial PDFs to be highlighted and others dimmed thus giving very much needed chemical specificity [2-4]. In the talk we will briefly introduce resonant high-energy XRD as applied to atomic PDFs analysis and give examples from several recent studies on nanoalloy catalysts of Au-Pt, Au-Cu, Pt-Pd and Pt-Ru families, including building 3D structure models on the basis of total and partial atomic PDFs and using the models for rational consideration of nanoalloy structure-catalytic properties relationships.

[1]. V. Petkov, *Materials Today* 11 (2008) 28.

[2]. V. Petkov and S. Shastri, *Phys. Rev. B* 81 (2010) 165428.

[3]. V. Petkov et al., *Nano Lett.* 12 (2012) 4289.

[4]. V. Petkov et al., *J. Phys. Chem. C* 117 (2013) 22131.

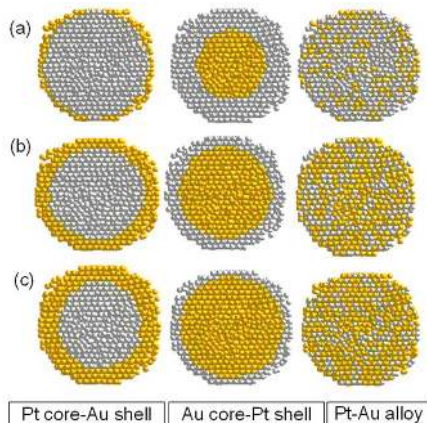


Figure 1. 3D structure models of 5 nm Au-Pt nanoalloy particles tested and refined against resonant high-energy XRD data as explained in ref. [3].

Keywords: Nanoalloys high-energy resonant XRD atomic PDFs analysis 3D structure modeling

MS47. History of crystallography and ECA

crystallographic association brings together experts in the field who develop and promote crystallography.

Keywords: history of crystallography in Croatia

Chairs: Sine Larsen, Howard Flack

MS47-O1 History of crystallography in Croatia

Biserka Kojić-Prodić¹

1. Rudjer Bošković Institute, Zagreb, Croatia

email: kojic@irb.hr

The international Year of Crystallography 2014 has also marked the 140th anniversary of crystallography in Croatia. That was closely associated with mineralogy. The Department of Mineralogy and Geology was established in 1874 at the Faculty of Philosophy, the University of Zagreb, and prof. Gj. Pilar in 1875 started to teach crystal morphology and optics. The first exhibition of minerals was organised 1846 in Zagreb. The Balkan Peninsula, geodynamically one of the most active in Europe, is abundant with minerals and has been examined intensively by generations of our earth scientists.

X-ray crystallography in Croatia started by M. Paić (1905-1997) who applied powder diffraction in characterization of mercury compounds and in 1933 defended his PhD thesis at Sorbonne. After 2nd world war he returned to Zagreb to be the head of the Physics Dept. at the Faculty of Science, where S. Hondl already established X-ray laboratory (1925-1937). In 1946 D. Grdenić went in Moscow to A. N. Nesmeyanov to study organomercury compounds for his PhD that brought him into contact with A. I. Kitaigorodskii. He returned to Zagreb 1948 and started X-ray structure analysis; in 1952 he founded Laboratory of General and Inorganic Chemistry, Dept. of Chemistry, Faculty of Science. In 1955 he went for two-year postdoctoral studies to D. Hodgkin in Oxford. The experience of these two pioneers in X-ray diffraction and the very elementary equipment gave a chance to establish the first crystallographic groups oriented to physics, structural chemistry, and mineralogy in Zagreb. Š. Ščavničar, a mineralogist, used that very equipment to carry out his PhD on the structure of mercury oxochloride under mentorship of Grdenić; his postdoctoral studies followed at Sorbonne. Katarina Kranjc introduced small angle scattering and in 1954, under supervision of M. Paić, she became the first lady who won PhD in physics.

Rudjer Bošković Institute was founded in 1950; in collaboration with the University of Zagreb new scientific disciplines were introduced. X-ray laboratory was founded by Grdenić and new generation came into crystallography. Collaboration with the prominent international crystallographers has enabled us to adopt contemporary methods and develop new ideas. Some of the highlights will be presented in the lecture. National

MS47-O2 Close encounters with crystallographers who made historyDavide L.M. Viterbo¹¹. Di SIT, Università del Piemonte Orientale, Viale T. Michel 11, 15121 Alessandria, Italyemail: davide.viterbo@mfn.unipmn.it

I started research in Crystallography in 1962 and during my long career I had the invaluable chance of meeting several crystallographers who are well known for their important contributions to our science. From my first experience in Oxford in 1968, when Dorothy Hodgkin and her group were still fighting with insulin, to my three years in York working with Michael Woolfson and my freindly meetings with Herbert Hauptman, Jerome and Isabella Karle, David Sayre and all the most important contributors to the early developments of direct methods, I could profit from their open attitude not only to enlarge my knowledge of crystallography, but also to acquire a more positive view of human relations. I also had the unique experience of listening to the fascinating lectures on diffraction theory delivered by Paul Ewald, one of the Founding Fathers of X-ray crystallography. Last but not least was my Italian adventure with Carmelo Giacovazzo and the SIR team and my lasting friendship with all of them.

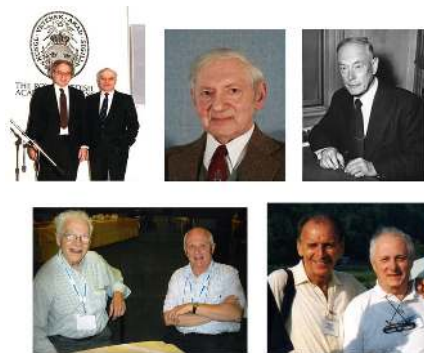


Figure 1. H. Hauptman, J. Karle, M. Woolfson, P. Ewald, D. Sayre, C. Giacovazzo.

Keywords: History of crystallography, important crystallographers

MS47-O3 A (very brief) history of macromolecular crystallographyAlexander Wlodawer¹¹. Macromolecular Crystallography Laboratory, National Cancer Institute, Frederick, MD, USAemail: wlodawer@nih.gov

X-ray crystallography is just over 100 years old as a scientific discipline. Successful determination of the first macromolecular structures (of oxygen carrier proteins, myoglobin and hemoglobin) was first reported about 55 years ago. To celebrate the achievements of crystallographers, the United Nations declared the year 2014 to be "The International Year of Crystallography". Whereas the celebrations are now over, progress in the field is not slowing down, and close to 100,000 crystal structures of proteins and nucleic acids are now available in the Protein Data Bank. This success was due to many important, often iconic, achievements of crystallographers that led to major advances in our understanding of the structure and function of biological macromolecules. At least 42 scientists received Nobel Prizes in Physics, Chemistry, or Medicine for their contributions that included the use of X-rays or neutrons and crystallography, including 24 who made seminal discoveries in macromolecular sciences. Thus the history of crystallography may be illustrated by the achievements of the recipients of this most prestigious scientific honor. Many technical advances, such as the use of synchrotron radiation and the recent introduction of free electron lasers as X-ray sources, also contributed to making this success possible.

Keywords: crystallography, history, Nobel Prizes

MS47-O4 Nikola Tesla, scientist and inventor – discovery of X-rays

Stanko Popović^{1,2}

1. Croatian Academy of Sciences and Arts, Zagreb, Croatia
2. Department of Physics, Faculty of Science, University of Zagreb, Croatia

email: spopovic@phy.hr

Miraculous inventions and scientific achievements have made Nikola Tesla, *the Croatian inventor* (*The New Yorker* 2013), world-famous. There are hundreds of books and papers dealing with the life and work of Tesla that confirm the above statement. In 1960 the term *tesla*, T, was given to the SI unit of the magnetic field. Starting in 1894 Tesla experimented with mysterious *shadowgraphs* similar to those that *later* were studied by W. C. Röntgen (L. I. Anderson, *21st Century Books*, 1994). Tesla was aware of an unknown *very special radiation* that had damaged film in his laboratory, later identified as *Röntgen rays* or *X-rays*. Unfortunately, much of his early research was lost when his laboratory in New York was burnt down on March 13, 1895. Röntgen published his discovery on November 8, 1895. In the beginning of 1896 Tesla proceeded with experiments in X-ray imaging, designing a high energy unipolar vacuum tube that had no target electrode. The electrons were accelerated by peaks of the electric field produced by the high-voltage Tesla coil. Tesla realized that the source of X-rays was the site of the first impact of electrons within the tube. Tesla devised several experimental set-ups to produce X-rays, that were of much greater power than obtainable with ordinary apparatus. He stated that the cathodic stream was composed of small particles, and that the produced X-rays were transverse waves possessing many properties of light. Tesla described his experiments in a series of papers in *Electrical Review New York*, the first paper appearing in March 11, 1896. Tesla gave Röntgen full credit for his discovery. Röntgen congratulated Tesla on his sophisticated images, wondering how he had achieved such impressive results. Tesla commented on physiological hazards in working with X-rays and gave recommendations for protection. Therefore, there is much evidence that confirm the legacy of Tesla in the discovery of X-rays. His lecture before the New York Academy of Sciences in 1897 validated to some degree his primacy in research of X-rays. One will never know who would have won the Nobel prize for the discovery of X-rays if Tesla's work had not been lost by fire. The least one can do is to appreciate his pioneer work in this field (Hrabak, M. *et al.* (2008). *RadioGraphics* 28, 1189).

Keywords: discovery of X-rays, Nikola Tesla

MS47-O5 European crystallography before the discovery of X-rays

Jean-Louis Hodeau¹, Rene Guinebreteire²

1. Univ. Grenoble Alpes, Institut Neel - CNRS, 38042 Grenoble, France
2. ENSCI, SPCTS, 87068 Limoges, France

email: hodeau@neel.cnrs.fr

The origins of crystallography started with humanity's interrogation with crystals. From the end of the 16th century, scientists found that minerals like quartz regularly display angular shapes that are unlikely to be random. De Boodt, Kepler, Hooke, Huygens and Steno considered the cause to be related to the internal nature of the crystal. In the 17th century Steno first suggested that the hexagonal form of quartz crystals was preserved during growth. The term "*Crystallography*" was first used in 1723 by Cappeller.

Crystallographers in the 18th century managed to form a picture of crystal's internal structure on the basis of their external geometry. Romé de l'Isle was inspired by Linnaeus's biological classification system and proposed using the shape of the crystal as a mean of classification. From his observations of scraps of broken calcite, Haüy constructed models of crystals by stacking small bricks together, bricks which he called "*molécules intégrantes*". All these investigations gave rise to this new science of "*crystallography*", one of the oldest of the "*physical*" sciences, together with astronomy, mechanics and optics.

In the 19th century, German and French researchers introduced the concepts of lattice, axis, centre, and mirror plane of symmetry as criteria to classify crystals. Weiss rejected Haüy's "*molécules intégrantes*" theory and led a German school advocating the use of symmetry in crystals. Hessel and Frankenheim showed that there are only 32 ways of combining these symmetries. In 1840, Delafosse replaced Haüy's solid little bricks with the notion of volumes formed of space and molecules. Bravais described the sum of the volumes as a lattice system repeating itself, with an identical motif at each lattice point, and showed that there are only 14 types of lattice system. At the end of the 19th century, the hypothetical molecules were replaced by more complex wallpaper-like patterns containing atoms and new symmetries. These symmetry patterns were hypothesised by Sohncke and then recorded by Schoenflies and Fedorov. This classification of crystals based on their symmetry and lattice structure is still with us today. It is invaluable for studying the physical properties of crystals (optical, mechanical and thermal).

We can see that in the early 20th century, before the first X-ray diffraction experiments allowed to "*see inside*" crystals, crystallographers had already established a body of experimental and theoretical knowledge of them.

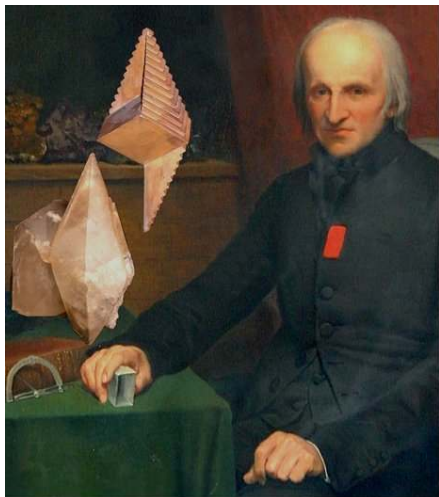


Figure 1. Calcite crystal in scalahedron form and a wooden model made by Haüy to illustrate his "stacked bricks" theory of crystal shape. Haüy with a calcite crystal and a Carangeot contact goniometer. © Muséum de Grenoble; © Collection des Minéraux – UPMC Paris; © Musée de Minéralogie – Mines Paris.

Keywords: Crystallography, History, Education

MS48. Teaching and outreach of crystallography

Chairs: Krešimir Molčanov, Bart Kahr

MS48-O1 Passing the baton of knowledge: The Zurich School of Crystallography

Anthony Linden¹

1. Department of Chemistry, University of Zurich, Winterthurerstrasse 190, CH-8057 Zurich, Switzerland

email: anthony.linden@chem.uzh.ch

Universities have largely dropped formal crystallography courses from their curricula, even though the technique is important in so many fields of research and Nobel Prizes are regularly awarded to scientists who have used crystallography or diffraction techniques at some point in their ground-breaking work. In the absence of the availability of formal training or access to an expert within an institution, how does a young person doing a PhD, for example, in chemistry, acquire the knowledge to competently carry out crystallographic analyses on the synthesised compounds? Hand-me-down knowledge from more senior group members can be one way, but often leads to partial basic knowledge that only covers the cases encountered, or the person learns how to get results by pushing buttons without really understanding what happens behind those buttons and how to get the best possible data or recognise when things are not going according to expectation.

A number of successful crystallography schools have sprung up over the years with the aim of offering courses and training for those who do not have access to such courses at their home institutions. The Zurich School of Crystallography, inaugurated in 2007, is one such school. The school focuses on teaching the essential theory and hands-on practical aspects of small-molecule crystallography over 13 days. Two special features of the school are that there is one tutor dedicated to every two participants for the duration of the course, and we encourage participants to send us crystals of a compound of current interest in their own research, so that they go home with a completed structure ready to publish. The participants also visit the Swiss Light Source synchrotron and the neutron spallation facility of the Paul Scherrer Institute to get a taste of "big science".

This presentation will describe the philosophy and strategy behind The Zurich School of Crystallography with examples of our experiences of what works well, what sometimes does not work quite as well, and the organisational challenges and successes. The close-knit collegiate atmosphere of the school leads to a convivial learning environment and some participants of earlier schools are still active and even leaders in crystallography today.

Keywords: Crystallographic teaching, schools, education, teaching

MS48-O2 History as a tool for a crystallographic storyteller

Vladimir Stilić¹

1. Department of Chemistry, Faculty of Science, University of Zagreb

email: vstilić@chem.pmf.hr

One of the crucial problems in communicating science to non-scientists is making the scientific contents interesting. The general way of achieving this goal is to arrange the science which is to be communicated into an interesting and engaging narrative – in other words to tell a story. The storyline has a double function: it captures the attention of the readers / listeners, and at the same time it provides a framework in which the scientific content is arranged. The audience thus learns about science almost without realising that they are learning, and, in the ideal case, will at the end desire to learn even more. History of science provides a natural source of narratives which can be used in science communication. Not only that a well presented historic account of a given subject can by itself be an engaging *story*, but also the knowledge of the earlier stages of the development of a scientific area, often enables the presenter to introduce the given area to their audience in a simpler, more understandable, and sometimes more amusing way. Many basic notions of modern crystallography can be introduced through historic accounts. These include not only the areas which have been (fully) developed in the past centuries (e.g. crystal morphology and symmetry), but also the ‘more modern’ notions of crystal structure have their origins in models and ideas which were present considerably earlier than the 20th century. The purpose of this talk is to present some of the ways in which the history of crystallography can be an inspiration for presentations an activities aimed at communication of crystallography to wide audiences, as well as to share some experiences accumulated over the past several years of communicating and popularising crystallography in Croatia.

Keywords: history of crystallography, science communication

MS48-O3 Outreach of IYCr: an example of an hybrid approach in crystallography teaching

Martin Fark¹, Dubravka Šišak Jung², Peter Høghøj³

1. STOE & Cie GmbH

2. DECTRIS

3. Xenocs

email: fark@stoe.com

Traditionally, crystallography was defined as a mathematical description of crystalline matter that exhibits three-dimensional periodicity. Nowadays, with the arrival of new materials and advances of instrumentation, crystallography is taken under the umbrella of material science. Synchrotrons are widely accessible, computing power is cheap, laboratory diffractometers are automated, and the conventional crystallography definition is no longer valid: samples are “structurally challenged”, have two-dimensional periodicity, or even non-existent (structure prediction). Without any doubt, this multitude of samples, techniques and methods broadened the scope and outreach of crystallography. However, this outreach appears to be restrained. While in the modern world these automated processes cause basic crystallographic knowledge to be neglected, developing and less-privileged countries are lagging even more behind, having only limited access to both modern equipment and traditional crystallographic education. In the scope of the International Year of Crystallography (IYCr), joint forces of academia, equipment manufacturers and large-scale facilities proposed an initiative to overcome these differences. By organizing a series of admission-free Schools and Workshops worldwide, the initiative aimed to adjust crystallography teaching to the needs of a specific region (developed, developing and less-privileged) or a particular interest group. By taking these factors into account, these programs allowed students and researchers to increase their knowledge in crystallography, and gain insights into specific aspects of material science. Outcomes of this hybrid approach in crystallography teaching will be illustrated on the example of OpenFactory, a crystallography school organized by IUCr, IYCr, STOE, DECTRIS and Xenocs. This international school gathered participants from various fields of research. After being introduced to basics of crystallography, diffraction and scattering, this theoretical knowledge was put into practice at STOE’s and Xenocs’ application laboratories. Such a hands-on experience with hardware and software enabled a solid foundation for further research of the participants. International environment, variety of research fields, scientific backgrounds and interests served as an overview of crystallographic activities worldwide, and opened up possibilities for future projects and collaborations.



Figure 1. STOE DECTRIS Xenocs OpenFactory

Keywords: OpenFactory, IYCr 2014, Workshop, Crystallography Teaching

MS48-O4 The IUCr-UNESCO OpenLab project

Michele Zema^{1,2}, Claude Lecomte³

1. International Union of Crystallography, 5 Abbey Square, Chester, UK

2. Università degli Studi di Pavia, via Ferrata 1, Pavia, Italy

3. CRM2, Université de Lorraine and CNRS, Nancy, France

email: mz@iucr.org

The worldwide nature of the UN International Year of Crystallography has provided new opportunities to develop educational activities at all levels in parts of the world where crystallography is as yet a poorly developed science, and to set in motion new initiatives in capacity building and international cooperation. In this regard and to stimulate curriculum development, the IUCr and UNESCO have set up the OpenLab project, a network of operational crystallographic laboratories in selected universities in Africa, Latin America and South-East Asia, as a practical start in addressing such training requirements.

During 2014 and the first months of 2015, a total of 15 OpenLabs have been organized, which provided high-level educational opportunities to local students and young professors, taking advantage of the scientific and educational expertise of the IUCr, the diplomatic and educational channels of UNESCO, and the partnership of crystallographic instrumentation manufacturers. In the OpenLabs, about 20 to 30 selected participants were taught an experimental crystallography class and were able to collect and interpret single crystal or powder X-ray diffraction data. Some other companies also collaborated in an OpenFactory, an intensive training workshop at their European headquarters where some 20 selected early-career scientists travelled from many countries to gain hands-on experience of the latest equipment. More details and reports about these events are at <http://www.iycr2014.org/openlabs>.

Part of this project is closely connected with the “*Crystallography in Africa*” initiative of the IUCr, thanks to which crystallographic equipment has been recently installed or is being installed in some sub-Saharan African countries (e.g. Cameroon, Cote d’Ivoire, Senegal). The IUCr is willing to continue the OpenLab project and transform it into a long-term sustainable initiative in the following years. The involvement of the crystallographic community with established tradition and expertise is the key to the success of the initiative.

Keywords: IYCr2014, education, crystallography schools

MS48-O5 Interesting crystallography for young schoolkids: methodical receptions of teaching

Tatiana A. Eremina¹, Nikolay N. Eremin¹

¹. Moscow State University, Geological Faculty, Department of crystallography and crystal chemistry

email: t_eremina@list.ru

It is not a secret that the professional orientation of every young person is formed in childhood. In this respect, crystallographers are in a losing position. Despite to the fact that 2014 was proclaimed by UNESCO as the International Year of Crystallography, "Crystallography" as the subject is not included into the school program practically in any country. One can only superficially at the lessons of geometry, physics and chemistry relates to this wonderful science about crystals. But crystals have always attracted the attention of both children and adults for its beauty and perfection of forms. Popular books on crystallography in Russia (their number is very small) disappeared from the market at once because of great interest to the subject. And the training manuals, addressed to teachers working with children, are practically absent. Of course, in some centers of additional children's education in Russia there are very good geological classes, but, unfortunately, even inside them crystallography being taught unsystematically, classes are not equipped with textbooks, materials and posters; sometimes crystallography in such circles is simply no one to teach. This circumstance prompted the authors to create a textbook «Entertaining crystallography» <http://biblio.mccme.ru/node/2823> (150 pages, ISBN: 978-5-4439-0081-0, MCCME: Moscow Center for Continuous Mathematical Education publishing) (fig 1). This book may be useful for students who decided to learn the basics of crystallography in amount sufficient for successful participation in school subject competitions such as at (<http://geoschool.web.ru/olympiad/>). . We tried a lot to present a new difficult for children material in simple language as much as possible. However, the book is not intended for easy reading. The reader will have to show some patience to master some labor-intensive sections of the manual. The authors hope that the reward of patience is the satisfaction of further study crystallography - a wonderful science of the most beautiful creations of inorganic nature. Also, this guide may be useful for crystallographic classes' teachers in the preparation of the discipline lesson plans. Each lesson in the textbook is supplemented by control questions and practical exercises in order to help in consolidation of the material. Additionally, there are sweeps for self-making some crystal 3D-models.



Figure 1. The book "Entertaining crystallography" focused on school children of different ages (left); at Moscow Open Geology Olympiad (right).

Keywords: crystallography for children, popular textbook

MS49. How to?

Chairs: Sofiane Saouane, Wulf Depmeier

MS49-O1 Careers in industry following a PhD in crystallography

Rachel Macmaster¹

1. Molecular Dimensions

email: Rachel@moleculardimensions.com

A crystallography PhD can open many doors. A career in industry can be wide and varied. This talk will focus on the types of positions and career paths available, with some examples from personal experience.

Keywords: Protein Crystallography, Careers, Biotechnology, Life Sciences

MS49-O2 How to start a career in industry as a crystallographer

Alessia Bacchi¹

1. University of Parma

email: alessia.bacchi@unipr.it

It could happen that finishing one's PhD feels like facing a journey to an unknown world outside., with different rules and different expectations compared to the safe nest of student life. What skills do industries require from crystallographers? Are crystallographers needed in this outside world? According to the American Chemical Society, crystallography specialists may look for opportunities in instrument and software development and customer support for instrument manufacturing companies, in positions as user support at national laboratories, or working in crystal-growing laboratories. Crystallographers have also been associated with the geosciences, metallurgy, and ceramics engineering, but areas of demand in the medical and life sciences are growing exceptionally today. An overview of careers opportunities, and some real examples will be discussed.



Figure 1. Journey to the center of the Earth, 1959

Keywords: job opportunity, PhD, post-doc

MS49-O3 PhD in crystallography: report on 20 years work in industry

Mathias Meyer¹

1. Agilent Technologies Poland Sp. z o.o., Ul. Szarskiego 3, PL-54-609 Wrocław

email: drmathiasmeyer@gmail.com

There are quite different roots which end up in crystallography. The missing good perspectives for an academic career made a career in industry an alternative. Over the last 20 years I was able to apply and expand my crystallographic 'know-how' in a way I was not imagining at the time of PhD. Language and communication skills are good assets, likewise interest in computing and technology. The work in industry can be very creative and is - for sure - mainly result driven.

The talk will highlight pivot points, challenges and mentors which helped on the way. There is never a straight trajectory.

Keywords: industry, career, PhD

MS49-O4 Early career steps as a crystallographer in academia

Simon J. Coles¹

1. University of Southampton, UK

email: s.j.coles@soton.ac.uk

This talk will explore the options facing an early career academic in the field of crystallography. It will be cast from the perspective of a chemical crystallographer but also touch on all other areas of the discipline. The discipline is very diverse and therefore the options are numerous! I will sketch out different career pathways and their key requirements whilst highlighting some of the opportunities that may lead to them being realised.

Keywords: career pathways

MS49-O5 How to survive as a crystallographer in academia?

Sine Larsen¹

1. University of Copenhagen, Denmark

email: sine@chem.ku.dk

Crystallography penetrates a waste range of scientific disciplines from mathematics, physics over chemistry to biology. This is the strength of our science but at the University level it also makes it difficult to identify the “departmental home” of crystallography. The days are gone when a Department of Crystallography could be found at several universities in Europe and the US. So how does a young crystallographer pursue her or his career in academia? In the presentation I shall give an overview of my own academic career as a crystallographer, which started around 50 years ago, and use this in a comparison of the conditions the young crystallographers are facing to-day with the hope of initiating some animating discussions with the audience.

Keywords: University, academia, crystallography

MS50. Cultural and historical aspects of crystallography

Chairs: Aleksandar Višnjevac, Petr Bezdička

MS50-O1 Unveiling ancestral practices in the procurement and treatment of raw materials through mineralogical analysis

Giovanni Cavallo¹

1. Institute for Materials and Constructions, Via Trevano, 6952 Canobbio, CH

email: giovanni.cavallo@supsi.ch

The fortune of ochre since Prehistory is due to its great versatility in several fields and availability in many geological environments. Archaeologists use the term “ochre” in a broad sense for the designation of iron oxides and hydroxides, treated and untreated, natural and artificial, often associated with accompanying minerals. Studies on ochre provenance are generally based on geochemical analysis. Here a mineralogical approach is proposed as preliminary step to differentiate potential sources and establish possible routes at a local scale.

Keywords: ochre, provenance, processing, thermal treatment, Prehistory

MS50-O2 Symmetry, light, materials: the crystallography of cultural heritage

Gilberto Artioli¹

1. Dipartimento di Geoscienze, Università di Padova

email: gilberto.artioli@unipd.it

Crystallography greatly contributes to our understanding and management of cultural heritage. The most immediate connection is the popular relationship between art, architecture, and symmetry: from the graphical perception of symmetry in M.C. Escher's drawings, which most of us borrow during crystallography classes, to the higher-dimensions symmetry found both in quasicrystals and in the intricate decorations developed in the Arabic world. However, being at the forefront of the investigation of matter, crystallography embraces most of the techniques and the methodologies routinely employed for the characterization of materials in archaeometry and art conservation. A number of examples will be discussed showing the application of crystallographic techniques to cultural heritage problems and issues. Specifically, the combination of imaging techniques (2D and 3D mapping, tomography) with diffraction and spectroscopy is developing as a powerful tool for the non-invasive investigation of valuable and unique objects.



Figure 1. Symmetry point groups help decoding the Etruscan numerals: read the story in *Archaeometry* 53, 1031-1043, 2011.

Keywords: cultural heritage, conservation, archaeometry, symmetry

MS50-O3 Frank Allen: creating and using the Cambridge Structural Database System

Colin R. Groom¹

1. Cambridge Crystallographic Data Centre

email: groom@ccdc.cam.ac.uk

For 45 of the 50 years of the Cambridge Structural Database, Frank Allen contributed not only to its development; he also led the way in showing the value of this tremendous community resource.

Frank helped make crystallography unique in science, in that the output of every experiment, in the form of atomic coordinates, is available to everyone. From the inception of the technique, to structures determined this morning – we can all see them. This presentation will review what Frank saw, covering his contribution to the first fifty years of scientific research using the CSD.

Frank took the stories told by each individual structure and turned them into an anthology. This presentation will show how he then helped us to enjoy this *Opera Omnia*.

Keywords: small molecule

Poster presentations

OTSSP167, which is an orally administrative MELK selective inhibitor, conferring an IC_{50} of 0.41 nM. OTSSP167 effectively fits into the active site of MPK38, thus offering an opportunity for structure-based development and optimization of MELK inhibitors.

Keywords: MPK38, UBA Linker, Protein crystal structure

MS1. Recent experimental developments in synchrotron macromolecular crystallography

Chairs: Gordon Leonard, Marjolein Thunnissen

MS1-P1 The structures of the kinase domain and UBA domain of MPK38 suggest the activation mechanism for kinase activity

Youngje Cha¹, Yong-Soon Cho¹, YingJin Kang¹, Kuglae Kim¹,
Youngje Cha¹, Hyun-Soo Cho¹

1. Yonsei University

email: azzogoory@gmail.com

Murine protein serine/threonine kinase 38 (MPK38) is the murine ortholog of human maternal embryonic leucine zipper kinase (MELK), which belongs to the SNF1/AMPK family. MELK is considered as a promising drug target for anticancer therapy, because MELK overexpression and hyper-activation correlate with several human cancers. Activation of MPK38 requires the extended sequence (ExS) containing the ubiquitin-associated (UBA) linker and UBA domain, and phosphorylation of the activation loop. However, the activation mechanism of MPK38 is unknown. This paper reports the crystal structure of MPK38 (T167E), which mimics a phosphorylation state of the activation loop in complex with AMP-PNP. In the MPK38 structure, the UBA linker forces the inward movement of the α C helix into an intermediate conformation, in which the activation loop might not be stabilized. Then, phosphorylation of the activation loop induces movement of the activation loop toward the C-lobe and results in closing of interlobar cleft. These processes generate a fully active state of MPK38. This structure suggests that MPK38 has a similar molecular activation mechanism as that of other kinases of the SNF1/AMPK family. Recently, we also reported the structure of MPK38 in complex with

MS1-P2 Current status of sample exchange robots at the photon factory macromolecular crystallography beamlines

Masahiko Hiraki^{1,2}, Yusuke Yamada^{2,3}, Naohiro Matsugaki^{2,3},
Toshiya Senda^{2,3}

1. Mechanical Engineering Center, Applied Research Laboratory, KEK (High Energy Accelerator Research Organization)
2. School of High Energy Accelerator Science, SOKENDAI (the Graduate University for Advanced Studies)
3. Structural Biology Research Center and Photon Factory, Institute of Materials Structure Science, KEK (High Energy Accelerator Research Organization)

email: masahiko.hiraki@kek.jp

The Structural Biology Research Center at the Photon Factory (PF) has developed sample exchange robots PAM (PF Automated Mounter) to achieve fully automated data collection in high-throughput X-ray experiments and/or remote experiments. The PAM was based on the robots SAM developed by SSRL macromolecular crystallography group, but the PAM has double tongs for rapid sample exchanging. The PAM has been installed at the PF macromolecular crystallography beamlines BL-5A, BL-17A, AR-NW12A and AR-NE3A. A beamline BL-1A was built for low energy experiments and operated since 2010. We have firstly installed the PAM modified to fit the BL-1A. For effective lower energy experiments, we covered whole diffractometer with a helium chamber recently. In parallel with development of the helium chamber, we developed a new sample exchange robot in order to minimize a leak of helium gas, named PAM-HC (PAM for Helium Chamber). Cryo-pins are grasped by a collet chuck that is placed on a tip of a slim robot arm. The PAM-HC can access a sample rotation axis of the diffractometer in the helium chamber through a tunnel in a side of the chamber. In addition, we are now developing an offline sample storing system based on PAM, which can automatically store the flash-cooled samples into the cassettes. Current status of the PAM and the PAM-HC will be presented.

Keywords: Robot, Automation, Macromolecular crystallography

MS1-P3 The crystallography endstation at beamline P11 at PETRA III

Anja Burkhardt¹, Saravanan Panneerselvam¹, Bernd Reime¹, Tim Pakendorf¹, Nicolas Stuebe¹, Pontus Fischer¹, Jan Meyer¹, Dennis Goeries¹, Martin Warmer¹, Alke Meents¹

1. Deutsches Elektronen-Synchrotron DESY

email: anja.burkhardt@desy.de

The "Bio-Imaging and Diffraction Beamline" P11 at PETRA III is dedicated to structure determinations from periodic (crystalline) and aperiodic biological samples (*e.g.* entire cells). For this purpose two state-of-the-art experiments are available: an X-ray microscope utilizing tender X-rays between 2.4 and 10 keV [1] and a crystallography endstation operated between 5.5 and 30 keV.

The flexible P11 X-ray optics allow to tailor the beam properties to the needs of the experiment: A large parallel beam is available for investigations of large unit cell systems, such as viruses and large molecular complexes. For structure determinations from microcrystals a highly intense microbeam can be generated. With this serial crystallography experiments using liquid delivery systems [2] or silicon chips [3] can be realized.

The X-ray optics comprise an LN₂ cooled double crystal monochromator, followed by a first Kirkpatrick-Baez (KB) mirror system which consists of two horizontal and one vertical deflecting mirror and is located in the P11 optics hut. A second KB system is installed very close to the crystallography endstation at 73 m. All KB mirrors are dynamically bendable. The first KB system can be used to generate a secondary source at 65.5 m. With this beam sizes down to 300 × 300 μm² FWHM (*v* × *h*) can be realized at the sample position. The second KB system allows for further refocusing the X-ray beam into a spot of 4 × 9 μm² FWHM (*v* × *h*) with full flux from the source (2 × 10¹³ ph/s at 12 keV). Smaller beam sizes down to 1 × 1 μm² with more than 2 × 10¹¹ ph/s in the focus can be obtained by slitting down the secondary source at the cost of flux.

At P11, all experiments are installed on an 8 m long granite support which provides an extremely stable setup for vibration sensitive experiments. The crystallography endstation is equipped with a high precision single axis goniostat with a combined sphere of confusion of less than 100 nm.

In addition, P11 is ideally suited for high-throughput crystallography and fast crystal screening. A Pilatus 6M-F detector allows for fast data collection with frame rates of up to 25 Hz. Crystals can be mounted in less than 10 s using an automatic sample changer and a large storage dewar provides space for 368 samples.

[1] A. Meents, B. Reime, N. Stuebe, N. *et al.*, Proceedings of SPIE 8851, 88510K (2014).

[2] F. Stellato, D. Oberthuer, M. Liang *et al.*, IUCr J, 204 (2014).

[3] P. Roedig, I. Vartiainen, R. Duman *et al.*, submitted.

Keywords: Macromolecular crystallography, synchrotron, beamline

MS1-P4 SONICC implementation at GM/CA-beamline 23IDB at the Advanced Photon Source

Michael Becker¹, Sergey Stepanov¹, Justin A. Newman², Shane Sullivan², Robert M. Everly², Christopher M. Dettmar², Scott J. Toth², Paul D. Schmitt², Stephen Corcoran¹, Dale Ferguson¹, Robert F. Fischetti¹, Garth J. Simpson²

1. GM/CA@APS, Argonne National Laboratory, Argonne, IL, USA

2. Dept. of Chemistry, Purdue University, West Lafayette, IN, USA

email: mbecker@anl.gov

Second order nonlinear optical imaging of chiral crystals (SONICC), based on femtosecond laser scanning microscopy, has been implemented at GM/CA@APS undulator beamline 23ID-B for rapid protein crystal localization and centering. The technique is based on infrared laser light impinging on non-centrosymmetric crystals of proteins, which may selectively yield a frequency-doubled, visible signal generated by the anharmonic response of the electron cloud of the protein in response to the laser field. One aim of this method is to locate small crystals grown in opaque crystallization media for centering in X-ray beams of only a few microns or less in cross-section, such as for membrane-protein crystals grown in mesophase [1]. The optical system implemented for generation and detection of Second Harmonic Generation (SHG) signals at beamline 23IDB has been described [2]. The system also provides the capability to scan visible laser light across the sample and detect two-photon excited UV fluorescence (TPE-UVF), which provides complementary contrast based on the native fluorescence of proteins. Recent efforts towards providing user-friendly capabilities include: increasing rates of data acquisition, providing bright-field laser imaging capabilities, and incorporation of laser-safety interlocks suitable for a user program. SHG imaging has also enabled direct experimental visualization of electric fields generated by photoelectrons that are produced as a result of X-ray absorption, which provides insight on X-ray damage in samples [3]. Recent advances will be presented.

[1] D. Kissick, C. Dettmar, M. Becker, A. Mulichak, V. Cherezov, S. Ginell, K. Bataille, L. Keefe, R. Fischetti, G. Simpson, *Acta Cryst.*, 2013, D69, 843–851.

[2] J.T. Madden, S. Toth, C. Dettmar, J. Newman, R. Oglesbee, H. Hedderich, R. Everly, M. Becker, J. Ronau, S. Buchanan, V. Cherezov, M. Morrow, S. Xu, D. Ferguson, O. Makarov, C. Das, R. Fischetti, G. Simpson, *J Synchrotron Rad.*, 2013, 20, 531–540.

[3] C.M. Dettmar, J.A. Newman, S.J. Toth, M. Becker, R.F. Fischetti, G.J. Simpson. *Proc.Nat. Acad. Sci.USA*, 2015, 112, 696–701.

Keywords: SONICC, synchrotron, imaging, microcrystals

MS1-P5 Multicrystal analysis with DIALS and BLEND

Pierre Aller¹, David Waterman², James Foadi³, James Parkhurst¹, Luis Fuentes-Montero¹, Richard Gildea¹, Graeme Winter¹, Gwyndaf Evans¹

1. Diamond Light Source, Harwell Science and Innovation Campus, OX11 0DE Didcot, UK

2. STFC Rutherford Appleton Laboratory, OX11 0DE Didcot, UK

3. Membrane Protein Laboratory, Diamond Light Source, Harwell Science and Innovation Campus, OX11 0DE Didcot, UK

email: pierre.aller@diamond.ac.uk

The recent developments of micro-focus beamlines¹ and *in situ* data collection^{2,3} have led to a renewed interest in multiple crystal dataset analysis⁴. Although the availability of smaller beams is instrumental to the data collection of microcrystals, the impact of the radiation damage prevents the collection of a complete dataset from a single crystal. For a typical experiment on a micro-focus or sub micro-focus beamline we should expect to merge small wedges of data collected on multiple crystals in order to get a complete set. However, processing and merging small wedges of data from multiple crystals is not trivial and typically requires some analysis to establish isomorphous groups of data for merging.

Programs such as BLEND⁵ have been developed to help and guide users to merge data from the isomorphous crystals together using cluster analysis. BLEND's cell dimension analysis can be improved by simultaneously analysing multiple crystals with DIALS (dials.diamond.ac.uk) to produce a more accurate set of unit cell dimensions. In this work we detail these recent developments and provide several examples of their application.

1 Evans, G., Axford, D., Waterman, D. G. & Owen, R. L. Macromolecular microcrystallography. *Crystallography Reviews* **17**, 105–142 (2011).

2 Aller, P. *et al.* Application of *in situ* diffraction in high-throughput structure determination platforms. *Methods in molecular biology* **1261**, 233–253, doi:10.1007/978-1-4939-2230-7_13 (2015).

3 Axford, D. *et al.* *In situ* macromolecular crystallography using microbeams. *Acta crystallographica. Section D, Biological crystallography* **68**, 592–600, doi:10.1107/S0907444912006749 (2012).

4 Smith, J. L., Fischetti, R. F. & Yamamoto, M. Micro-crystallography comes of age. *Current opinion in structural biology* **22**, 602–612, doi:10.1016/j.sbi.2012.09.001 (2012).

5 Foadi, J. *et al.* Clustering procedures for the optimal selection of data sets from multiple crystals in macromolecular crystallography. *Acta crystallographica. Section D, Biological crystallography* **69**, 1617–1632, doi:10.1107/S0907444913012274 (2013).

Keywords: Multicrystals, datasets merging, BLEND, DIALS

MS1-P6 From crystal to structure with the versatile macromolecular crystallography beamline I04 at Diamond Light Source

Ralf Flaig¹, Jonathan Blakes¹, Graham Duller¹, Richard Fearn¹, Pierpaolo Romano¹, Irakli Sikharulidze¹, Graeme Winter¹, David R. Hall¹

1. Diamond Light Source, Harwell Science and Innovation Campus, Didcot, OX11 0DE, United Kingdom

email: ralf.flraig@diamond.ac.uk

Diamond Light Source currently operates five beamlines for macromolecular crystallography (MX) and soon seven beamlines will serve the MX user community. I04, a widely tuneable (5-25 keV, core range 6-14 keV) SAD/MAD station [1] started with the user programme in early 2007 and is in continuous development in order to improve the experimental capabilities, especially to enable structure solution from increasingly problematic and difficult samples. We have now installed a focusing system using compound refractive lenses allowing the user to change the beam size from 10 (h) x 5 (v) up to 110 (h) x 100 (v) microns over a wide energy range and thus be better able to match the beam size to the crystal size or be able to select more precisely the best part of the crystal. To improve signal to noise, beam defining apertures can be used and the data are recorded on a large area pixel array detector. Multi-axis goniometry is used for optimising crystal orientation for phasing experiments, getting more complete and higher multiplicity data or optimizing data collection protocols for radiation sensitive samples. The flexible beamline design also allows for an easy change between standard cryo or room temperature experiments as well as experiments under humidity control and it also enables the beamline to be controlled remotely. We have projects to improve the beamline hardware but are also developing the beamline software further. Data collection strategies (EDNA [2]) for optimised anomalous data collection are provided alongside optimal crystal orientations (XOAlign [3]). GDA [4], the data collection GUI, allows an easy setup of inverse beam or interleaved MAD data sets. Data are automatically processed using various pipelines including FAST_DP [5] and XIA2 [6] and the analysis of the anomalous signal can trigger an automated pipeline (FAST_EP) that provides a quick analysis of the phasing potential of the collected data using no prior information. More complex pipelines are being developed which will use prior information to enable structure solution with the aim to provide crystal to structure capability automatically at the beamline.

References

- [1] <http://www.diamond.ac.uk/Beamlines/Mx/I04.html>
- [2] Incardona, M.-F., Bourenkov, G. P., Levik, K., Pieritz, R. A., Popov, A. N. & Svensson, O. (2009). *J. Synchrotron Rad.* **16**, 872
- [3] <https://code.google.com/p/xdsme/>
- [4] <http://www.opengda.org/>
- [5] <https://zenodo.org/record/13039>
- [6] <http://xia2.sourceforge.net>

Keywords: Diamond Light Source, macromolecular crystallography, beamlines, experimental phasing, data collection

MS1-P7 Radiation induced non-isomorphism in protein crystals: a systematic study

Gianluca Santoni¹, Alexander Popov¹, Gleb Bourenkov²

1. European Synchrotron Radiation Facility, F38043Grenoble, France

2. EMBL Hamburg Outstation c/o DESY, D-22607 Hamburg, Germany

email: gianluca.santoni@esrf.fr

Increase in the systematic intensity measurements errors under progressing radiation dose is only partly compensated by scaling and radiation-damage corrections (as zero-dose extrapolation [1]). These errors are typically attributed to the variation in the unit cell dimensions and associated small changes in the crystal molecular packing, and to the localized chemical changes known as site-specific radiation damage [2]. We are attempting to understand quantitatively describe these errors on the basis of the structures refined against series of complete data sets collected in massive dose-dependent series. For a number of model systems, specialized data collection protocols were designed which deliver individual high resolution data sets at low doses of 0.1 to 0.2 MGy, ensure sufficient signal-to-noise up to the high doses 10-20 MGy and minimize the influence of other factors as structural inhomogeneity across the crystal volumes or uneven dose deposition. The results indicate that intensity changes are predominantly due to the variation in individual atomic temperature factors. The dependence of isotropic temperature factors on the absorbed dose follows linear relation for most individual atoms, exceptions are the atoms affected by site-specific damage. The slopes of these linear evolutions are distributed according to an inverse gamma function. B-factors variation has been used to determine a mathematical model to describe the decays of intensities and will be presented. [1] Diederichs, K., McSweeney, S., & Ravelli, R. B. G. (2003). *Acta Crystallographica Section D Biological Crystallography*, 59, 903-909. [2] Garman, E. F. (2010). *Acta Crystallographica. Section D, Biological Crystallography*, 66, 339-51

Keywords: Radiation damage, non-isomorphism, B-factor

MS1-P8 EMBL P13 beamline and derivative laboratory at PETRA III

@DESY: phasing of biological macromolecules with softer X-rays and heavy atom derivatives

Michele Cianci¹, Gleb Bourenkov¹, Johanna Kallio¹, Guillaume Pompidor¹, Stefan Fiedler¹, Thomas Schneider¹

1. EMBL, Hamburg, Germany

email: michele.cianci@embl-hamburg.de

For many heavy atom compounds the anomalous signal is enhanced when collecting data at low energies (>2 Å wavelength) compared to standard data collections at 1 Å wavelength. The macromolecular crystallography beamline P13 is in operation since late 2012 and it is part of the European Molecular Biology Laboratory Integrated Facility for Structural Biology at PETRA III (DESY, Hamburg, Germany). P13 is tunable across the energy range from 4 to 17.5 keV to support crystallographic data acquisition exploiting a wide range of elemental absorption edges for experimental phase determination. Data collections at energies as low as 4 keV (3.1 Å) are possible due to the optimized beam line design, the high photon flux of up to 2×10^{10} ph/sec at 4 keV, the custom calibration applied to the PILATUS 6MF detector, and the availability of a partial Helium-path. This set-up allows exploiting very long wavelengths to harness the anomalous signal from heavy atoms for phase determination. Using adaptive X-ray mirrors and a set of apertures the beam size can be easily adjusted to the crystal size. The beam line offers rapid access to a heavy atom derivative laboratory equipped for solution preparation, soaking and crystal manipulation. The heavy atom library includes more than 150 compounds from more than forty elements, including Xenon gas and Uranyl compounds. We will present the results of the structure solution from test models, the related methods and the instrumentation.

Keywords: Phasing, Heavy atoms, Softer X-rays**MS1-P9** Automated system for data collection and data processing using microcrystalsKeitaro Yamashita¹, Kunio Hirata¹, Yoshiaki Kawano¹, Go Ueno¹, Kazuya Hasegawa², Takashi Kumasaka¹, Masaki Yamamoto¹

1. RIKEN SPring-8 Center, Advanced Photon Technology Division, Sayo, Japan

2. JASRI/SPring-8, Research & Utilization Division, Sayo, Japan

email: k.yamashita@spring8.or.jp

On BL32XU, a micro-beam beamline at SPring-8, diffraction data are collected with typical horizontal beam size of 1 µm. This micro-beam has enabled data collection using small crystals, especially LCP crystals of membrane proteins that are important targets on the beamline. For crystals of 10 µm or larger, a complete data-set could be obtained from a single crystal. However, for smaller crystals or weakly diffracting crystals, only small fraction of a complete data-set could be obtained from a single crystal, and therefore more crystals are required.

In order to facilitate crystal structure analysis using many microcrystals, we are developing an automated system for data collection and data processing from small crystals. Multiple data of small wedges can be collected using a single loop where many crystals are mounted. To find crystal positions accurately, raster diffraction scan using low-dose X-rays is performed in advance of data collection. We have developed a crystal alignment tool *SHIKA* based on the raster diffraction scan, which shows possible crystal position on 2D spot population map. *SHIKA* automatically processes new images in accordance with each raster diffraction scan. Found crystal positions are transferred to *KUMA* (a tool suggesting data collection strategy with predicted radiation damage) to start data collection immediately. Typical oscillation range of very small crystals is 10° or 20° for each crystal.

The datasets are processed automatically using *XDS* (Kabsch, 2010). Images that have few or no spots in low resolution area are discarded prior to data processing. After data processing, the datasets are hierarchically clustered based on unit cell dimensions using *BLEND* (Foadi, 2013). The clusters with large completeness are subjected to merging using *XSCALE* or *Aimless* (Evans, 2011). Outliers are detected based on pairwise correlation. This automated system has greatly reduced time and effort spent on beamline or at home.

Keywords: microbeam beamline, microcrystal, merging

MS1-P10 Application of on-chip room-temperature protein crystallography to visualize the dynamics of structural changes

Svetlana Kapis¹, Michael Heymann², Markus Perbandt¹, Guoqing Chang², Franz Kärtner², Christian Betzel¹

1. Institute of Biochemistry and Molecular Biology, University of Hamburg, Laboratory of Structural Biology of Infection and Inflammation, c/o DESY, Notkestr. 85, Build. 22a, 22603 Hamburg, Germany

2. Center for Free-Electron Laser Science, DESY, Notkestrasse 85, 22607 Hamburg, Germany

email: kapis@chemie.uni-hamburg.de

The visualization of conformational changes at high spatial and temporal resolution still remains an experimental challenge in structural biology. The time dimension is incorporated by triggering the reaction of interest in the crystal prior to X-ray exposure, and then collecting the diffraction patterns at different time delays. Serial crystallography is a powerful approach to collect complete diffraction data sets by measuring single diffraction pattern from single non-frozen crystals and a breakthrough for Time-resolved X-ray crystallography (TRX) experiments. However, very high crystal quantities are needed. Recent advances in diffraction compatible microfluidic systems offer new opportunities to position single microcrystals into the beam. Therefore only several hundreds of crystals are required to collect complete datasets. A semi-transparent microfluidic chip has been developed to conduct *in situ* pump-probe X-ray diffraction to experiments at time scales between 50 milliseconds to 1 second. We are applying this approach using a highly promising drug target candidate Thioredoxin from *Wuchereria bancrofti* (WbTrx-1). The parasite *Wuchereria bancrofti* causes human lymphatic filariasis, a disease that affects approximately 130 million people worldwide. WbTrx-1 has a molecular weight of 16 kDa, contains one disulphide bridge and acts as an antioxidant by ensuring the supply of reducing equivalents for many biological functions via thiol-disulphide exchange cycle. In a first step the time resolved S-S bond cleavage of WbTrx-1 induced by UV radiation will be studied. This approach may be also convenient for solving the phase problem using Radiation Damage Induced Phasing (RIP) method. Details will be presented.

Keywords: Time-resolved X-ray crystallography (TRX), reaction kinetics, Radiation Damage Induced Phasing (RIP)

MS1-P11 The analysis of the mesh scan data for macromolecular data collection

Igor Melnikov¹, Gleb P. Bourenkov², Olof Svensson¹, Alexander N. Popov¹

1. European Synchrotron Radiation Facility, F-38043 Grenoble, France

2. EMBL Hamburg Outstation c/o DESY, D-22607 Hamburg, Germany

email: igor.melnikov@esrf.fr

Developments in microfocus X-ray beamlines and fast shutterless data acquisition with a pixel-array detectors have enabled diffraction data collection from crystals exhibiting strong variation in diffraction quality, as well as from multiple very small crystals mounted in one sample holder. One of the core features of the protocol of such complex diffraction experiments is the ability to automatically recognise and rank protein diffraction on images collected during the low-dose 2D mesh scans. We will present novel methods and software programs which can score the quality of diffraction and identify positions and shapes of individual single crystals. Using a complex statistical analysis the program compares diffraction patterns measured at different spots of the mesh and detects whether they correspond to one or different crystal lattice, or to an overlap of multiple crystal lattices. Further, this information together with the estimates of diffraction quality is used by the program BEST^[1] to design the optimal protocol of multi-crystal/multi-position data collection, considering radiation damage effects. The program can be also useful in the evaluation of synchrotron serial crystallography data^[2]. The details of algorithm and results of the first test applications will be discussed.

References:

1. G.P. Bourenkov & A.N. Popov Acta Crystallogr. (2010). D66, 409-419
2. Gati C, Bourenkov G, Klinge M, Rehders D, Stellato F, Oberthur D, Yefanov O, Sommer BP, Mogk S, Duszko M, Betzel C, Schneider TR, Chapman HN, Redecke L. (2014) IUCrJ 1(Pt 2):87-94.

Keywords: Crystallography, 2D Mesh Scan, Diffraction analysis

MS1-P12 Development of serial crystallography at ESRF, ID13Anastasiia Shilova¹, Britta Weinhausen¹, Manfred Burghammer^{1,2}

1. European Synchrotron Radiation Facility (ESRF), Grenoble, France

2. Department of analytical chemistry, Ghent University, Belgium

email: anastasiya.shilova@esrf.fr

Development of serial diffraction methods, which are complementary to efforts currently taken at hard x-ray free electron laser (XFEL) facilities have an extremely high impact on structural biology. Where single molecule and nano-crystal diffraction is out of reach at conventional synchrotron sources, fast room temperature experiments on large ensembles of micron sized crystals could benefit from certain advantages over the XFEL approach.

First approach to develop serial crystallography of membrane proteins is to perform lipidic cubic phase (LCP) microjet-based serial millisecond crystallography at synchrotrons[1], similar to XFELs[2]. The main advantages of this method are: crystal injection using LCP-jet combined with a micro-beam allows diffraction data to be collected at room temperature, without crystal freezing and difficult crystal handling steps; thousands of crystals can be screened in a short time with less than a milligram of protein and the method is well suited for time-resolved diffraction studies. The LCP-jet method has been recently demonstrated by solving a structure of the bacteriorhodopsin at a resolution of 2.4 Å[3].

Second approach is based on scanning micro-crystals, which are deposited on solid supports. First successful results have already been obtained using lysozyme micro-crystals[4]. This approach, relying rather on controlled spatial distribution and subsequent scanning, allows to overcome severe limitations of available sample volumes (in particular for membrane proteins) and also it has further opportunities for optimization.

The other approach is to use special crystallization plates[5]. This system is based on a new crystallization plate that allows growing crystals on very thin films that can then be excised with a laser beam to recover the crystalline material. Due to their design, plates allow to collect diffraction data in-situ with very low background and to reduce mechanical stress for the crystals.

References

- [1] - collaboration with U. Weierstall (ASU, USA), R. Neutze, J. Standfuss, I. Moraes Marie-Curie ITN 'NanoMem'
- [2] - U. Weierstall, D. James, C. Wang, et al., *Nature Communications* **5**, 3309 (2014)
- [3] - P. Nogly, et al. (2015). *IUCrJ* **2**, doi:10.1107/S2052252514026487, in press
- [4] - N. Coquelle et al., Raster-scanning protein crystallography using micro and nano-focused synchrotron beams, accepted, *Acta Cryst. Section D*
- [5] - Marquez & Cipriani. *Methods Mol Biol.* **2014**, **1091**: 189-95. PMID:23695565

Keywords: serial crystallography, membrane proteins, nanobeam, microbeam, LCP-injector

MS1-P13 Akt-mediated phosphorylation increases the binding affinity of hTERT for importin α to promote efficient nuclear translocationJeong Seok Cha¹, Kuglae Kim¹, Sun-Ah Jung¹, Jeong Seok Cha¹, Hoyoung Kim¹, In-Kwon Chung¹, Hyun-Soo Cho¹

1. Yonsei University

email: pickcha1121@yonsei.ac.kr

hTERT is a catalytic component of telomerase that can extend the telomere end of genomic DNA. This protein has been shown to highly express in tumor cell. Residue S227 of hTERT is phosphorylated by Akt kinase [1] and hTERT is strongly localized to the nucleus. hTERT has a nuclear localization signal (NLS) from G220 to A242 containing two basic regions which might interact with hImportin α with bipartite binding mode. We used isothermal titration calorimetry (ITC) to determine the specificity of hImportin $\alpha 5$ confirming the effect of phosphorylation on binding affinity. As a result, Phosphorylated hTERT S227 is higher affinity than un-phosphorylated hTERT. To see the molecular mechanism in detail, the complex structure of hTERT_NLS peptide and hImportin $\alpha 5$ has been solved at a resolution at 2.4Å. As might be expected, hTERT_NLS is shown to interact with hImportin $\alpha 5$ with bipartite binding mode. Phosphorylated S227 of hTERT interacts with R395 of hImportin $\alpha 5$ by hydrogen bond, which explains increased affinity by phosphorylation resulting in more efficient nuclear localization of telomerase. This result suggests that phosphorylation of TERT is a regulation strategy of localization for telomerase activity control.

[1] Sang Sun Kang, Taegun Kwon, Do Yoon Kwon, and Su Il Do, *The Journal of Biological Chemistry*, **274**(19), 1999, 13085.

Keywords: hTERT, hImportin α , Protein crystal structure

MS1-P14 The macromolecular crystallography beamlines BioMAX and MicroMAX at the MAX IV laboratory

Marjolein Thunnissen¹, Roberto Appio¹, Johan Unge¹, Jie Nan¹, Mikel Equirua¹, Alberto Nardella¹, Derek T. Logan^{1,2}, Christopher Ward¹, Thomas Ursby¹

1. The MAX IV Laboratory, Box 118, SE-221 00, Lund Sweden
2. Dept. of Biochemistry & Structural Biology, Lund University, Box 124, SE-221 00, Lund, Sweden

email: marjolein.thunnissen@maxlab.lu.se

The MAX IV storage ring facility at the MAX IV Laboratory, Lund, Sweden, will come in operation in mid 2016. Due to a multibend achromats approach, the 3 GeV ring will have exceptionally low emittance which will lead to an unprecedented brilliance for a synchrotron radiation source. The BioMAX beamline is one of the first phase beamlines and is dedicated to macromolecular crystallography. Thanks to the low emittance of the storage ring, the focused beam will both be small, $20 \times 5 \mu\text{m}^2$, have a low divergence, $0.1 \times 0.1 \text{ mrad}^2$ with a flux at the sample $>10^{13}$ photons/s. The optics of the beamline are relatively simple with a fixed offset double crystal monochromator and a pair of KB mirrors. This design allows work with both small crystals and large biomolecular complexes with concomitantly large unit cells. BioMAX is designed to be flexible and serve a broad range of needs for the life science community. The experimental setup will be equipped with an MD3 diffractometer with a vertical main rotation axis and two additional axes in a mini-kappa geometry. The setup will include state-of-the-art area detector, sample changer, beam conditioning equipment and auxiliary equipment such as sample cryo and fluorescence detector. The beamline will be controlled using MXCuBE version 3 being developed in collaboration with six other facilities in Europe. The beamline will offer remote access and will use ISPyB for sample management.

A second station, MicroMAX, a microfocus macromolecular crystallography beamline, is proposed as a state-of-the-art exploratory beam line. MicroMAX will deliver a $0.7 \mu\text{m}^2$ focal spot beam diameter with an X-ray flux $>10^{13}$ photons/sec in monochromatic mode, and approaching 10^{15} photons/sec in polychromatic mode. Because of these state-of-the-art specifications, MicroMAX will allow very large data sets to be rapidly collected from thousands of micron sized macromolecular crystals cooled to cryogenic temperatures using sample mounting and freezing technologies familiar to any protein crystallographer. In parallel, MicroMAX will develop novel sample delivery environments that will allow the pursuit of serial data collection strategies both at room temperature and using cryo-technologies. This beamline will allow new structures to be solved from very small crystals; and will accelerate the rate of progress towards structures of extremely challenging crystallization targets.

Keywords: Synchrotrons, protein crystallography, automation, serial crystallography

MS1-P15 Facilities for macromolecular crystallography at the HZB

Manfred S. Weiss¹, Ronald Förster¹, Martin Gerlach¹, Michael Hellmig¹, Franziska U. Huchmann¹, Alexandra Kastner¹, Eric Kolibacz¹, Piotr Malecki¹, Karine Sparta¹, Michael Steffien¹, Monika Uhlein¹, Piotr Wilk¹, Uwe Mueller¹

1. Helmholtz-Zentrum Berlin

email: manfred.weiss@helmholtz-berlin.de

The Macromolecular Crystallography (MX) group at the Helmholtz-Zentrum Berlin (HZB) has been in operation since 2003. Since then, three state-of-the-art synchrotron beam lines (BL14.1-3) for MX have been built up on a 77-wavelength shifter source [1,2]. Currently, the three beam lines represent the most productive MX-stations in Germany, with close to 1400 PDB depositions (Status 03/2015). BLs14.1 and 14.2 are energy tuneable in the range 5.5-15.5 keV, while beam line 14.3 is a fixed-energy side station operated at 13.8 keV. All beam lines are equipped with state-of-the-art detectors: BL14.1 with a PILATUS 6M detector and BL14.3 with a large CCD-detector. The HZB-MX beamlines are in regular user operation providing close to 200 beam days per year and about 600 user shifts to approximately 70 research groups across Europe. During the first half of 2015 the endstation of BL14.2 is completely rebuilt. After the re-opening it will feature a DESY-type nanodiffractometer, a G-ROB sample changer and a PILATUS 2M detector. BL14.3 has been equipped with a HCl crystal dehydration device since 2011. In addition to serving the user community mainly as a screening beam line, it is currently the only MX beamline in Europe with a HCl device permanently installed [3]. Additional user facilities include office space adjacent to the beam lines, a sample preparation laboratory, a biology laboratory (safety level 1) and high-end computing resources. On the poster, a summary on the experimental possibilities of the beam lines and the ancillary equipment provided to the user community will be given.

[1] U. Heinemann, K. Büsow, U. Mueller & P. Umbach (2003). *Acc. Chem. Res.* **36**, 157-163.

[2] U. Mueller, N. Darowski, M. R. Fuchs, R. Förster, M. Hellmig, K. S. Pathankar, S. Pühringer, M. Steffien, G. Zocher & M. S. Weiss (2012). *J. Synchr. Rad.* **19**, 442-449.

[3] M. W. Bowler, U. Mueller, M. S. Weiss, J. Sanchez-Weatherby, T. L.-M. Sorensen, M. M. G. M. Thunnissen, T. Ursby, A. Gobbo, S. Russi, M. G. Bowler, S. Brockhauser, O. Svensson & F. Cipriani (2015). *Cryst. Growth Des.* **15**, 1043-1054.

Keywords: Macromolecular Crystallography, Synchrotron, HCl

MS1-P16 Recent results and developments on PROXIMA 2A

William Shepard¹, Denis Duran¹, Sebastian Le Couster¹, Frederic Blache¹, Aurelien Delmotte¹, Roger Fourme¹, Gavin Fox¹, Rob Meijers¹, Thierry Moreno¹, Sandra Pierre-Joseph¹, Martin Savko¹

1. Synchrotron SOLEIL

email: william.shepard@synchrotron-soleil.fr

PROXIMA 2A is an energy tunable (6 – 15 keV) micro-focus beamline at Synchrotron SOLEIL dedicated to macromolecular crystallography (MX). Since opening in March 2013, many users have benefited from its fine focus (10 $\mu\text{m} \times 5 \mu\text{m}$, H \times V FWHM) and high flux ($>10^{12}$ ph/s), and with such a high flux density, they have discovered that their micro-crystals diffract beyond their expectations. The experiments are controlled via the MXCuBE_V2 interface [1], which not only launches standard and MAD data collections, but also records and manages multiple positions on the sample. The micro-focused X-rays are frequently exploited in order to select out the best diffracting zone of a crystal. With this mind, grid and line scans are currently automated via command line, and these functionalities will be soon incorporated within the MXCuBE interface. Helical scans are already available, implemented within MXCuBE and frequently employed by the users. The data quality from helical scans is comparable to standard data collection strategies. The beamline is also equipped with a CATS robotic sample changer, which consists of a 9-unipuck dewar (total 144 pins). Up to 200 samples have been screened in a 24-hour period. The CATS robot is also capable of screening crystallization plates, and although this functionality is still being commissioned, the preliminary results are very encouraging. Developments are also underway with other *in situ* data collection strategies. In particular, the beamline is equipped with a Plugmaker, which is a device that can perform crystallization experiments on micro-fluidic chips. These chips can be mounted directly on to the goniometer and the crystals tested under X-rays. Finally, the current area detector (ADSC Q315r) will be soon upgraded to an EIGER 9M, which will offer a faster readout and lower noise level. Coupled with its high flux density and multiple functionalities, PROXIMA 2A has become a versatile instrument for the MX community.

[1] Gabadinho *et al.*, *J. Synchrotron Rad.* **2010**, *17*, 700-707.

Keywords: beamline, microcrystallography, macromolecular crystallography, synchrotron

MS1-P17 VMXm: a new sub-micron beamline for macromolecular crystallography at Diamond Light Source

Jose Trincão¹, Anna Warren¹, Pierre Aller¹, Graham Duller¹, Kevin Wilkinson¹, Andy Stallwood¹, David Laundy¹, Lucia Allianelli¹, Kawal Sawhney¹, Guenther Rehm¹, Gwyndaf Evans¹

1. Diamond Light Source, Diamond House, Harwell Science and Innovation Campus, Didcot, Oxfordshire, OX11 0DE, UK

email: jose.trincao@diamond.ac.uk

The increasing complexity of currently studied biological targets has pushed the demand for microfocus MX beamlines with ever smaller beam sizes and higher intensities. Serial Femtosecond Crystallography at XFELs is one approach to sub-micron crystals, but is still largely inaccessible to most users and far from ready for mainstream usage. VMXm is a new beamline being built at Diamond Light Source aiming to bridge the gap between current microfocus beamlines and XFELs. It is being designed to optimize the *data to protein-material ratio* in microcrystallography targeting crystal sizes down to 0.5 microns. The beamline optics will deliver a beamsize of 0.5 - $>5 \mu\text{m}$ vertically, using a single custom-profiled fixed focal length mirror [1], and 0.5 - 5 μm horizontally *via* a two stage demagnification scheme and a variable secondary source aperture. The beamline will operate at wavelengths between 7 and 25 keV delivering between 10^{12} and 10^{13} ph/s to the sample (at 12 keV) depending on the optical configuration. The source, optics and end-station designs for VMXm will be presented together with novel solutions to the problem of sample visualisation and alignment for submicron crystals.

References

[1] Laundy, D., Allianelli, L., Sutter, J., Evans, G. & Sawhney, K. Surface profiling of X-ray mirrors for shaping focused beams. *Optics Express* **23**, 1576-1584 (2015).

Keywords: micro-focus, VMXm, beamline, sub-micron, serial crystallography

MS3. Structure solution on the fly (software) / Parallel data collection and structure analysis

Chairs: Manfred Weiss, Victor Lamzin

MS3-P1 Correcting for radiation damage in macromolecular crystallography

Jonathan C. Brooks-Bartlett¹, Garib Murshudov², Elspeth F. Garman¹

1. Laboratory of Molecular Biophysics, Department of Biochemistry, University of Oxford, South Parks Road, Oxford OX1 3QU, UK

2. Structural Studies Division, MRC Laboratory of Molecular Biology, Francis Crick Avenue, Cambridge CB2 0HQ, UK

email: jonathan.brooks-bartlett@dtc.ox.ac.uk

Radiation damage is an unavoidable phenomenon that occurs during macromolecular crystallography (MX) experiments. It manifests itself in several ways including an overall decrease in reflection intensity of the diffraction pattern. Often these effects can be so severe that structure determination is not possible.

When data were routinely collected at room temperature, mathematical correction of reflection intensities to account for radiation damage was a common procedure [e.g. ref 1]. Radiation doses absorbed by cryocooled crystals are now much greater than they were previously, and the true behaviour of the reflection intensities is too complex to be described by a simple zero order correction.

Here we present two reflection intensity correction models. The first is a redundancy based model that extends previous models [2]. This model relies on portions of the data being highly multiplicitous so that the parameters of the model can be found by a weighted least squares fit. The remaining portions of low multiplicity can then be extrapolated later, by following the trends of the high multiplicity data. The extensions to the previous model include explicit dose parameterisation using RADDOSE-3D [3] and a new dose decay model [4] that captures the nonlinear behaviour of reflection intensities empirically.

The second model treats the crystal degradation and the reflection intensity observations as a stochastic (random) process. Explicitly we use a hidden Markov model to describe the data collection process. The model parameters that correspond to the maximum likelihood of observing the data can then be determined. This in turn allows for the reflection intensities to be determined from any given crystal state. The advantage of this model is that it does not rely on having high multiplicity data.

Both models have been used to correct highly damaged data collected from crystals of bovine pancreatic insulin. The resulting data reduction and refinement statistics will be compared.

References

1. Abrahams SC, Marsh P (1987), *Acta Cryst. A*, **43**, 265-269.
2. Diederichs K (2006), *Acta Cryst. D*, **62**, 96-101
3. Zeldin OB, Gerstel M, Garman EF (2013), *J. Appl. Cryst.* **46**, 1225-1230
4. Leal RMF *et al.*, Popov AN (2012), *J. Synch. Radiat.* **20**, 14-22

Keywords: Radiation Damage, Zero Dose Extrapolation, Reflection Intensity Correction, Macromolecular crystallography

MS3-P2 Decision making in automated structure solution pipelinesMelanie Vollmar¹, David Waterman², Irakli Sikharulidze¹, Graeme Winter¹, Dave Hall¹, Gwyndaf Evans¹¹. Diamond Light Source Ltd, Harwell Science and Innovation Campus, Didcot, Oxfordshire, OX11 0DE, United Kingdom². Science and Technology Facilities Council, Rutherford-Appleton Laboratory, Harwell Science and Innovation Campus, Didcot, OX11 0FA, United Kingdom

email: melanie.vollmar@diamond.ac.uk

In recent years data collection, especially at third generation synchrotrons, has become so fast that in many cases scientists choose to shoot first and then ask the question later. This approach may not always be the most efficient and the resulting data set may be insufficient for structure determination due to a number of reasons, e.g. radiation damage leading to incomplete data or insufficient anomalous signal. Additionally, especially when using remote access, data collection is not always carried out by scientists with appropriate training and experiments may not be planned well enough.

Many tools and pipelines already employed at Diamond or within CCP4 help scientists to analyse their data and assist in decision-making while still having access to the crystal at the beamline. Databases such as ISPyB or beamline control software like GDA allow the user to provide additional information like protein sequence, crystallisation condition and atomic scatterer for derivative crystals prior to the experiment or while at the beamline. In the past two decades a multitude of quality metrics (e.g. R_{merge} , R_{int} , $I/\sigma I$, CC_0 , CC_{ano} , CC_{map}) have been proposed, accepted, declined and modified to assist scientists in decision-making through the entire structure solution process.

Here we present how structure determination pipelines at Diamond will change over the next few years. In collaboration with CCP4 the existing pipeline infrastructure is to be transferred into a complex network for structure solution. Currently existing user data has been analysed with established software and pipelines and judged based on known quality metrics. In the long run this will serve as the basis to train a structure solution network in decision-making, which may involve defining additional new quality metrics or even allow scientists to provide biological data, results from mutation studies and sequence analysis, to increase the chances of solvability of a protein structure.

Weiss (2001) *J Appl Cryst* 34 130-135Mueller-Dieckmann *et al.* (2005) *Acta Cryst. D* 61 1263-1272Mueller-Dieckmann *et al.* (2004) *Acta Cryst. D* 60 28-38Cianci *et al.* (2008) *Acta Cryst. D* 64 1196-1209Diederichs/Karpuls; (2013) *Acta Cryst. D* 69 1215-1222Delageniere, S. *et al.* (2011). *Bioinformatics*, 27, 3186-3192Beteva, A. *et al.* (2006). *Acta Cryst. D* 62, 1162-1169**Keywords:** structure solution, automated pipelines, decision making**MS3-P3** New metrics for anomalous data qualitySelina L.S. Storm¹, Guillaume Pompidor¹, Fabio Dall'Antonia¹, Gleb Bourenkov¹, Thomas R. Schneider¹¹. European Molecular Biology Laboratory, Notkestr. 85, 22607 Hamburg, Germany

email: selina.storm@embl-hamburg.de

Experimental phasing is oftentimes hindered by radiation damage. Several metrics are available to judge data quality and the anomalous signal by taking all measured data into account¹⁻⁴.

For application in practice, it would be useful to have metrics with which one can easily identify a subset of data which are least radiation damaged and thereby increase then chance of successful phasing.

In absence of radiation damage, all Bijvoet differences would be the same. With increasing radiation damage, subsequently recorded Bijvoet mates and anomalous differences vary. By monitoring the behavior of subsequently recorded Bijvoet pairs, it should be possible to identify the point at which adding the next measurement, more noise than signal is introduced into a resulting data set.

We will present an evaluation of different metrics in terms of their ability to estimate the usefulness of Bijvoet differences as a function of dose deposited in a crystal.

References: ¹ M. Weiss, *J. Appl. Cryst.* (2001): 130-135² C. Mueller-Dieckmann *et al.*, *Acta Cryst. D* (2005): 1263-1272³ P. Karplus, & K. Diederichs, *Science* (2012): 1030-1033⁴ G. Bunkóczi *et al.*, *Nature methods* (2014): 126-130**Keywords:** radiation damage, experimental phasing

MS3-P4 Reaching a new highpoint with crystallography software - APEX3

Martin Adam¹, Eric Hovestreydt¹, Michael Ruf², Joerg Kaercher²

1. Bruker AXS GmbH, Oestliche Rheinbrueckenstrasse 49, 76187 Karlsruhe, GERMANY, info@bruker-axs.com

2. Bruker AXS Inc., 5465 E. Cheryl Parkway, Madison, WI 53711, USA, info@bruker-axs.com

email: martin.adam@bruker.com

In 2004, the APEX2 single crystal suite was first launched and deemed a huge leap forward in terms of functionality and design, compared to previously available software. This suite allowed for complete crystal structure determination, from data collection on the instrument to finalization of a publishable structure, to be completed within one program. Since its launch, the performance of the APEX2 suite has been continuously enhanced by the addition of various features. Today it is one of the most popular software suites used in chemical crystallography. Now, the most extensive revision is available: APEX3. This major new release takes full advantage of important developments in computer hardware and operating systems. Improvements to the new package include a state-of-the-art graphical user interface built with the modern QT4 development framework, updates to faster versions of Python and the PostgreSQL database as well as multi-CPU support for faster data processing, structure solution and reporting. The updated AUTOSTRUCTURE plug-in makes full use of the revolutionary Intrinsic Phasing structure solution engine, increasing the out-of-the-box success rate of structure determinations far beyond 90%. The new Structure Determination plug-in incorporates various structure solution modules, including SHELXT, while ShelXle is fully incorporated as the new default option for fast and convenient structure refinement. Moreover, the efficient twin handling routines known from the APEX2 suite are now fully integrated into the GUI for a new level of seamless twin support. APEX3 extends the ease of use of APEX2, and is readily learned by new users and students alike, keeping the focus on learning the science of crystallography.



Figure 1. APEX3 Splash screen

Keywords: comprehensive crystallography software, easy-to-use, most popular suite, automated structure solution, SHELXTL

MS4. Advances in phasing, refinement, and autobuilding

Chairs: Navraj Pannu, Eleonor Dodson

MS4-P1 BRICKWORX builds recurrent rna and dna structural motifs into medium and low-resolution electron density maps

Grzegorz Chojnowski^{1,2}, Tomasz Walen^{1,3}, Pawel Piatkowski¹, Wojciech Potrzebowski¹, Janusz M. Bujnicki^{1,4}

1. International Institute of Molecular and Cell Biology, Warsaw, Poland

2. Present address: European Molecular Biology Laboratory, Hamburg, Germany

3. Faculty of Mathematics, Informatics, and Mechanics, University of Warsaw, Warsaw, Poland

4. Institute of Molecular Biology and Biotechnology, Faculty of Biology, Adam Mickiewicz University, Poznań, Poland

email: gchojnowski@gmail.com

BrickworX is a computer program that builds crystal structure models of nucleic acid molecules using recurrent RNA motifs extracted from RNA Bricks database (<http://iimcb.genesilico.pl/mabricks>) or B-DNA double helices. In a first step, phosphate groups are detected in a user-provided electron-density map. Subsequently, comparing the three-dimensional patterns of the P atoms with a database of nucleic acid fragments, matching positions of the motifs in the unit cell are found. Finally, the matched motifs are merged and refined in real space to find the most likely conformations, including a fit of the sequence to the electron-density map.

The Brickworx program is available for download and as a web server at <http://iimcb.genesilico.pl/brickworx>.

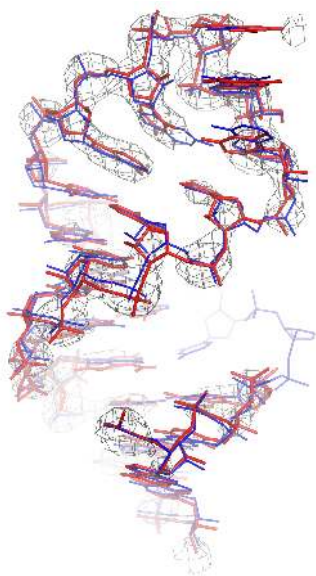


Figure 1. Comparison of published coordinates of the GCGA tetraloop from the group II intron IC subdomain (blue, PDB code 3bwp) and crystal structure model built using Brickworx (red). The model was fitted into the experimentally phased map (3.1 Å resolution) shown contoured at 3.0 σ .

Keywords: model building, nucleic acids, macromolecular models

MS4-P2 Advances in CCP4 software suite for macromolecular crystallography

Andrey Lebedev¹, Eugene Krissinel¹, Charles Ballard¹, Ronan Keegan¹, Ville Uski¹, David Waterman¹, Marcin Wojdyr²

1. CCP4, STFC, Research Complex at Harwell, Oxford, OX11 0FA, United Kingdom

2. Diamond Light Source Ltd, Harwell Campus, Oxford, OX11 0DE, United Kingdom

email: andrey.lebedev@stfc.ac.uk

The Collaborative Computational Project Number 4 (CCP4) was set up in the late 1970's in the UK to bring together developers of software for macromolecular crystallography. During the past years many leading software developers in the field of protein crystallography contributed to the CCP4, and the current CCP4 Software Suite provides tools and packages covering all aspects from data collection through to structure deposition [1]. Here we will present details of the latest release series of the Suite, version 6.5.

Release 6.5 brings a few new elements as well as updates and bug fixes to many of the components in the Suite. In particular, this release enforces ligand-related functionalities in CCP4 by introducing new structure and restraint generator Acedrg and carbohydrate validator Privateer-validate. In addition, the new tools enabled to curate and expand the monomer library. Advances in the processing part of the suite comprise processing multi-crystal datasets processing with Blend and multi-lattice datasets with Feckless software. Experimental phasing module has been significantly enforced with new automatic pipeline Crank-2.

In recent years, CCP4 Software Suite has undergone a considerable modernization, which made software building, testing, distribution and updating an automated routine. Yet new challenges arise owing to changing computing environments and concepts, OS updates, thirst for automation, increasing role of graphical front-ends and trends toward remote, web-based computations and hosting projects in the Cloud. We discuss these challenges and general directions for CCP4 development in middle-term perspective.

[1] M. D. Winn, C. C. Ballard, K. D. Cowtan, E. J. Dodson, P. Emsley, P. R. Evans, R. M. Keegan, E. B. Krissinel, A. G. W. Leslie, A. McCoy, S. J. McNicholas, G. N. Murshudov, N. S. Pannu, E. A. Potterton, H. R. Powell, R. J. Read, A. Vagin and K. S. Wilson (2011) Overview of the CCP4 suite and current developments, *Acta Cryst.* **D67** 235-242.

Keywords: Biological Macromolecular X-ray Crystallography, Software for Crystallography, Crystal Structure Determination

MS4-P3 Latest developments in HKL2MAP 0.4

Fabio Dall'Antonia¹, Thomas R. Schneider¹

1. European Molecular Biology Laboratory, Hamburg Outstation, Notkestrasse 85, 22607 Hamburg, Germany.

email: fabio.dallantonia@embl-hamburg.de

HKL2MAP [1] is a graphical user interface (GUI) for the semi-automatic operation of the command-line-driven programs SHELXC/D/E [2]. These programs in combination with the GUI are widely used for macromolecular crystallographic phasing, not the least due to their runtime speed, and suited for on-the-fly assessment of diffraction data at synchrotron sources.

HKL2MAP allows for the selection of input files with diffraction data in various formats and automatically extracts unit cell parameters and space group for FA data preparation with SHELXC. Most importantly, it now supports input commands and result visualization regarding the latest SHELXC feature for multi-crystal SAD, where several data sets, also partial ones, can be merged for a maximization of multiplicity. Concerning substructure determination, HKL2MAP works with the multi-CPU version of SHELXD, where the achieved speed benefit is relevant for difficult cases that require a large number of solution trials. The program SHELXE for phase calculation and density modification (DM) underwent significant feature extensions during the last years, most prominently substructure site refinement for optimization of initial heavy-atom phases and peptide backbone auto-tracing for the iterative improvement of the DM steps. HKL2MAP renders the numerical SHELXE results graphically and thus facilitates the monitoring of phase quality. The line graphs for sequential progress visualization are now complemented by 3d ribbon graphs for the SHELXE poly-ala models. This automatically updated 3d view with continuous mouse rotation and zoom provides further information on phasing success by supporting the discrimination of map interpretability with respect to the two enantiomorph substructures. Furthermore, HKL2MAP employs COOT [3] as the graphical display program, so that the final poly-ala model and electron density map can be readily inspected post phasing.

The usage of HKL2MAP is demonstrated by means of practical examples, with a focus on multi-crystal SAD phasing scenarios. HKL2MAP is freely available for academic usage and can be downloaded from <http://webapps.embl-hamburg.de>.

References:

- [1] T. Pape & T. R. Schneider (2004). *J. Appl. Cryst.* **37**, 843-4.
- [2] G. M. Sheldrick (2010). *Acta Cryst.* **D66**, 479-85.
- [3] P. Emsley et al. (2010). *Acta Cryst.* **D66**, 486-501.

Keywords: MX-Phasing, GUI, SHELXC/D/E

MS4-P4 Direct phase selection of initial phases from single-wavelength anomalous dispersion (SAD) for the improvement of electron density and *ab initio* structure determination

Chun-Jung Chen^{1,2,3}

1. Life Science Group, Scientific Research Division, National Synchrotron Radiation Research Center

2. Institute of Biotechnology, National Cheng Kung University

3. Department of Physics, National Tsing Hua University

email: cjchen@nsrrc.org.tw

The optimization of the initial phasing has been a decisive factor in the success of the subsequent electron density modification, model building and structure determination of biological macromolecules with the single-wavelength anomalous dispersion (SAD) method. Two possible phase solutions (Φ_1 and Φ_2) generated from two symmetric phase triangles in the Harker construction for the SAD method cause the well-known phase ambiguity. We have developed a novel *Direct phase selection method* utilizing the θ_{DS} list as a criterion to select optimized phases from Φ_1 or Φ_2 of a subset of reflections with the high *percentage of correct* phases to replace the corresponding initial SAD phases $\Phi_{SAD}^{[1]}$. Based on our work, the reflections with angle θ_{DS} in a range $35 - 145^\circ$ are selected for an optimized improvement; θ_{DS} is the angle between the initial Φ_{SAD} phase and a preliminary density-modification (DM) phase Φ_{DM} . The results show that utilizing the additional direct phase selection step prior to simple solvent flattening without phase combination using the existing DM programs, such as *RESOLVE* or *CCP4 DM*, improves significantly the final phases, in terms of the increased correlation coefficient of electron-density maps and diminished mean phase errors. With the improved phases and density maps from our developed method of direct phase selection, the completeness of built residues with main chains and side chains of protein molecules is enhanced for efficient structure determination.

[1] Chen, C.-D., Huang, Y.-C., Chiang, H.-L., Hsieh, Y.-C., Chuankhayan, P., Chen, C.-J. "Direct phase selection of initial phases from single-wavelength anomalous dispersion (SAD) for the improvement of electron density and *ab initio* structure determination" *Acta Cryst.* (2014). **D70**, 2331-2343.

Keywords: SAD phasing, direct phase selection

MS4-P5 The end point of model refinement in macromolecules; what are the coordinate errors?John R. Helliwell¹, Manickam Gurusaran², Kanagaraj Sekar²¹. School of Chemistry, University of Manchester, Brunswick Street, Manchester, M13 9PL, UK². Supercomputer Education and Research Centre, Indian Institute of Science, Bangalore, Karnataka, 560012, India

email: john.helliwell@manchester.ac.uk

The end point of model refinement obviously requires a knowledge of the individual atomic position errors. The provision of such 'metadata' for the individual atomic coordinates has not been routinely done. As G Murshudov and E J Dodson state "without giving some estimate of the reliability of the model parameters the refinement procedure cannot be complete" [1]. The only refinement program which has an option to do this is the full matrix inversion option in SHELXL of G Sheldrick [2], usually applied at atomic resolution. We have adopted the Diffraction Precision Index (DPI) average for coordinate errors in macromolecules [3] to characterize the positional errors of individual atoms involved in non-covalent interactions [4] based on the sqrt (individual atomic B factor / the average B factor). It is used where restraints of a protein model refinement are not applied eg ion pairs or for metal ligands or protonation state determinations when a bond distance restraint is removed. As a web accessible tool we provide an ion pairs knowledgebase (<http://cluster.physics.iisc.ernet.in/sbps>). Now we also provide a webtool to calculate the error on any protein PDB file atom [described in detail with examples in ref 5]. A modified PDB file can be saved (<http://cluster.physics.iisc.ernet.in/dpi/>). In the preparation of structures for PDB deposition the distance errors for solvent molecules to their binding partners can now be used in evaluating clashes [5], where atomic position restraints have not been used. In cases where non-crystallographic symmetry has been used in a model refinement an appropriate user guidance message is provided by our webtool.

REFERENCES

1. G Murshudov and E J Dodson Simplified error estimation a la Cruickshank in macromolecular crystallography CCP4 Newsletter - January 1997.
2. Sheldrick, G.M. (1995) SHELXL-93 Institut fuer Anorg.Chemie, Goettingen, Germany.
3. D. W. J. Cruickshank (1999). Acta. Cryst. D 55, 583–601.
4. M. Gurusaran, M. Shankar, R. Nagarajan, J. R. Helliwell and K. Sekar (2014). IUCrJ 1, 74–81.
5. K. S. Dinesh Kumar, M. Gurusaran, S.N. Sathesh, P. Radha, S. Pavithra, K.P.S. Thulaa Tharshan, J R Helliwell and K. Sekar Online_DPI: A web server to Calculate the Diffraction Precision Index for a Protein Structure (2015) J Appl Cryst in press.

Keywords: Macromolecular atomic coordinate errors; Ion pairs; Metal ligand; Solvent clashes; DPI.

MS4-P6 A nuclease cut three ways: phasing from distant homologues, an ideal α -helix and Zn-SADHuw T. Jenkins¹, Alfred A. Antson¹¹. York Structural Biology Laboratory, Department of Chemistry, University of York, York, YO10 5DD, UK

email: huw.jenkins@york.ac.uk

An in-situ proteolytic fragment of the large terminase from bacteriophage G20C produced crystals that diffracted to 1.45 Å resolution. The structure was initially solved by molecular replacement using an ensemble of the five available structures of nuclease domains from homologues with between 13 and 20% sequence identity. The MR solution was autobuilt to an almost complete poly-alanine trace with SHELXE and completed with ARP/wARP.

The structure contained five α -helices including a 13-residue long unbent α -helix so an attempt was made to solve the structure starting from a single ideal α -helix. Phaser successfully placed a 14-residue ideal α -helix and density modification by ACORN using phases calculated from this α -helix combined with artificially extended data to 1.0 Å enabled the structure to be automatically built using ARP/wARP. Unexpectedly, the placed α -helix corresponded not to the straightest α -helix of the nuclease domain but to the third longest α -helix of 11 amino acids.

It was clear from the maps that the active site of the nuclease domain contained a metal ion with reasonable anomalous signal at the wavelength used for data collection (0.9763 Å). Subsequent XRF revealed the presence of zinc (from the crystallisation conditions) and structure solution by Zn-SAD using SHELX from a dataset collected at 1.2824 Å was extremely straightforward.

These three approaches will be discussed together with some recent experiences with using low identity models for molecular replacement and also fragment-based MR approaches.

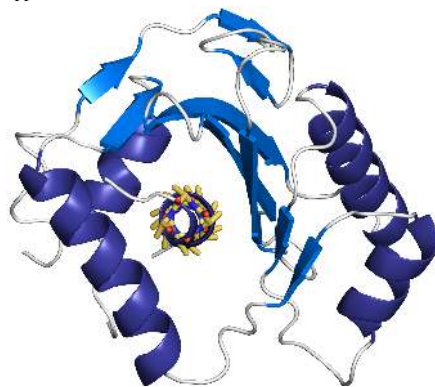


Figure 1. Structure of proteolytic fragment of G20C large terminase with 14-residue ideal α -helix used to solve the structure shown as yellow sticks.

Keywords: phasing, MR, fragments, SAD

MS4-P7 Automated refinement of low-resolution macromolecular structures using prior information

Oleg Kovalevskiy¹, Robert A. Nicholls¹, Garib N. Murshudov¹

1. MRC Laboratory of Molecular Biology, Cambridge, UK

email: okovalev@mrc-lmb.cam.ac.uk

Due to poor observation to parameter ratios at resolutions below 3 Å, using additional information can improve and stabilise the refinement process. ProSMART [1] generates external restraints for protein and nucleic acid chains based on known structures of homologous molecules, idealised fragment geometries, and hydrogen bonds detected in the refined structure. These restraints are used by REFMAC5 [2] to stabilise refinement of a model. However, the optimal refinement protocol varies from case to case, and it is not always obvious how to select appropriate homologous structure(s), or other sources of prior information, for restraint generation. After running extensive tests on a large dataset of low-resolution models, we identified the best performing refinement protocols and strategies for selection of homologous structures used for restraint generation. These strategies and protocols are implemented in the Low-resolution Structure Refinement Pipeline.

The pipeline performs auto-detection of twinning and selects the optimal scaling method and solvent parameters. The pipeline can work with manually-supplied homologous structures, or run an automated BLAST search and download homologues. The pipeline tests a number of refinement protocols in order to find the best protocol for a target model, including: simple jelly-body refinement; refinement using external restraints generated from single and multiple homologues followed by relaxation with jelly-body refinement; and hydrogen bonds restraints.

We observed a strong correlation between the success of refinement using external restraints and the global RMSD between the target and homologous structures. Substantial model improvement was observed with homologues sharing as low as 75% sequence similarity. Restraints based on hydrogen bonds were found to improve refinement when no homologues were available for a particular chain. The automated pipeline improved Rfree values, geometry and Ramachandran statistics for 84% of the test cases.

The automated pipeline presented facilitates hassle-free automated selection of the optimal set of external restraints for low-resolution structure refinement and allows subsequent use of the optimal protocol in latter refinement runs.

References:

1. R.A. Nicholls, F. Long and G.N. Murshudov (2012) *Acta Cryst.* D68, 404-417.
2. G.N. Murshudov, P. Skubak, A.A. Lebedev, N.S. Pannu, R.A. Steiner, R.A. Nicholls, M.D. Winn, F. Long and A.A. Vagin (2011) *Acta Cryst.* D67, 355-367.

Keywords: ProSMART, Refmac5, Refinement of protein structures, Low resolution

MS4-P8 Pushing the boundaries of crystallography: Debye-Waller factor redefined

Janusz Wolny¹, Ireneusz Buganski¹, Pawel Kuczerka^{1,2}, Radoslaw Strzalka¹

1. Faculty of Physics and Applied Computer Science, AGH University of Science and Technology, Krakow, Poland

2. Laboratory of Crystallography, ETH Zurich, Switzerland

email: Janusz.Wolny@fis.agh.edu.pl

The main purpose of crystallography is to solve and refine crystal structures based on measured diffraction data. Complex crystals structures require big datasets consisting also of weak peaks. By using synchrotron facilities and modern detectors it is possible to collect diffraction patterns with a very high dynamic range. It is, however, a big challenge to properly process the measured data. One of many corrections applied during structure refinement process is the Debye-Waller (D-W) factor correction. It compensates for the perturbations arising from thermal vibrations (phononic term) or flips (phasonic term) of atoms. The D-W factor can be also generalized to a statistical interpretation [1,2]. The general formula for D-W factor is $\exp[-k^2\sigma^2]$, where k is the scattering vector and σ is a variance of the distribution of atomic arrangement (both in physical or perpendicular space).

In our presentation we discuss the limitations of the D-W factor in terms of structure refinement and propose a way to improve the results of such analysis. We prove that the D-W factor substantially limits the range of diffraction data possible to use in a refinement process. It works correctly only for small values of the exponential in the formula above. For real crystals (including quasicrystals), satisfactorily good results are only obtained for strong reflections with intensities higher than 1% in relative scale. Peaks with intensities 10^{-4} - 10^{-3} are refined rather incidentally (see e.g.[3]). This means that including weak reflections in a refinement procedure frequently makes the results worse.

We show how to improve the use of D-W factor. Our calculations are performed for a simple 1D model quasicrystal – the Fibonacci chain. Both the model choice and its low dimensionality do not affect our concluding remarks. We modeled the fluctuations in physical and perpendicular space. We claim, that redefinition of the D-W factor by either including higher-order moments of the statistical distribution or replacing the Gauss function with more appropriate functions essentially allows also weak peaks to be included in the refinement. Our results are general and can be applied for structural investigations of perfect crystals, including quasicrystals, but also any systems with defects or highly disordered.

1. J. Wolny, *Acta Cryst.* A48 (1992) 918-921
2. J. Wolny, S. Kapral, L. Pytlík, *Phil. Mag. A* 81 (2001) 301-310
3. P. Kuczerka, J. Wolny, W. Steurer, *Acta Cryst.* B68 (2012) 578-589

Keywords: Debye-Waller factor; refinement; statistical approach; Fibonacci chain

MS5. Structure and function of enzymes

Chairs: Joel Sussman, Ute Krenkel

MS5-P1 A leucine residue in the L2 loop is critical for caspases 3 and 7 active site formation

Moonil Kim¹

1. Medical Genomis Research Center, Korea Research Institute of Bioscience and Biotechnology (KRIBB), South Korea

email: kimm@kribb.re.kr

Various apoptotic signals can activate caspases 3 and 7 by triggering the L2 loop cleavage of their proenzymes. These two enzymes have highly similar structures and functions, and serve as apoptotic executioners. The structures of caspase 7 and procaspase 7 differ significantly in the conformation of the loops constituting the active site, indicating that the enzyme undergoes a large structural change during activation. To define the role of the leucine residue on the L2 loop, which shows the largest movement during enzyme activation but has not yet been studied, Leu168 of caspase 3 and Leu191 of caspase 7 were mutated. Kinetic analysis indicated that the mutation of the leucine residues sometimes improved the K_m but also greatly decreased the k_{cat} , resulting in an overall decrease in enzyme activity. The tryptophan fluorescence change at excitation/emission = 280/350 nm upon L2-L2' loop cleavage was found to be higher in catalytically active mutants, including the corresponding wild-type caspase, than in the inactive mutants. The crystal structures of the caspase 3 mutants were solved and compared with that of wild-type. Significant alterations in the conformations of the L1 and L4 loops were found. These results indicate that the leucine residue on the L2 loop has an important role in maintaining the catalytic activity of caspases 3 and 7.

Keywords: Leucine, L2 loop, caspase-3, caspase-7

MS5-P2 Structure-based engineering of Methionyl tRNA Synthetase for expression of photoactivatable proteins with photomethionine in *E. coli*.

Myung Kyu Lee¹, Myung Kyu Lee¹

1. Bionanotechnology Research Center, KRIBB, 125 Gwahak-ro, Yuseong-gu, Daejeon 305-806, Korea

email: mklee@kribb.re.kr

Photo-methionine (pM; L-2-amino-5,5-azido-hexanoic acid) with a diazirine group has a structural similarity with methionine (Met). In this work, we tried *in vivo* expression of pM containing proteins in *E. coli*. Expressions of proteins cloned into the pET-28a vector in *E. coli* B834 Met auxotroph were failed in the minimal medium with pM, but successful in that with Met. Engineering of *E. coli* methionyl-tRNA synthetase (MRS) for three residues interacting with the Met sulfur moiety (PNAS, 106: 15282, 2009) was not effective for expression of photoactivatable proteins with pM incorporation. Here we report that a MRS variant with mutations of five residues (two additional residues plus three reported residues) successfully allow the expression of various photoactivatable proteins. The side group of Met is accessible to its binding site of the wild type MRS through a narrow cavity (J Mol Biol, 306: 446, 2001), and the additional residues are possibly acting as a gate of the cavity. In this aspect, the side chain of pM with a bulky diazirine group may not access to the binding site of MRSwt, and therefore widening of the gate by mutation is considered to enable protein biosynthesis in the presence of pM. Indeed, co-transformation of MRS5m was allowed expression of various proteins in the presence of pM. The photoactivatable proteins were found to induce photocrosslinking with the specifically interacting proteins upon UV irradiation. The engineered MRS5m will be also useful for incorporation of noncanonical amino acids with the similar side chain of pM.

Keywords: Methionyl tRNA synthetase, protein engineering, photomethionine, photoactivatable protein expression in *E. coli*

MS5-P3 Structural characterization of *Helicobacter Pylori* pathogenic proteins. The case of α -carbonic anhydrase

Maria Elena M.E. Compostella¹, Giuseppe Zanotti¹

1. Department of Biomedical Sciences, University of Padova

email: elena.compostella@gmail.com

Helicobacter Pylori is a gram-negative, flagellated, spiral-shaped bacterium, able to colonize the human stomach, a very peculiar niche. It affects more than half of world's population. Its infection can lead to severe gastroduodenal diseases, like chronic gastritis, gastric and duodenal ulcer, gastric adenocarcinoma and mucosa-associated lymphoma. Therefore, *H. Pylori* contagion is a worldwide problem. Several bacterial species are able to transit the human stomach, but only one, *H. Pylori*, survives intragastric acidity long enough to establish a chronic colonization. There are several mechanisms involved in the acidic acclimation; particularly important in this aspect are the enzymes urease and carbonic anhydrase. Two different carbonic anhydrases (CA) are coded by *Helicobacter Pylori*: the α -CA, with periplasmic localization, and the β -CA, with cytoplasmic localization. Carbonic anhydrases are metalloenzymes that catalyze the hydration of carbon dioxide to bicarbonate, crucial for the neutralization of the pH and the consequent survival of bacterium in the acidic environment of the stomach. The active site of the α -CA consists of a Zn^{2+} ion coordinated by three histidine residues. This enzyme is inhibited by many sulfonamide/sulfamate compounds and the growth of the pathogen can be blocked; thus α -CA represent a promising drug target for the treatment of patients infected by drug-resistant strains. *H. Pylori* α -CA was cloned as fusion protein with 6-His-tag in the pETit C-His vector, without the signal peptide at the N-terminus. The plasmid was transformed in the recombinant *Escherichia Coli* strain BL21(D3). The protein was purified by IMAC chromatography and gel-filtration. The His-tag was removed by incubation with TEV protease. Crystals were grown by vapor diffusion sitting drop technique. The diffraction data were collected at 1.5 Å resolution and the three-dimensional structure was solved by molecular replacement.

Keywords: *Helicobacter Pylori*, carbonic anhydrase, metalloenzyme, acidic acclimation

MS5-P4 NowGFP: a green fluorescent protein with an anionic tryptophan-based chromophore

Sergei Pletnev^{1,2}, Nadya V. Pletneva³, Karen S. Sarkisyan³, Alexander S. Mishin³, Konstantin A. Lukyanov³, Ekaterina A. Goryacheva³, Zbigniew Dauter¹, Vladimir Z. Pletnev³

1. Macromolecular Crystallography Laboratory, National Cancer Institute, Argonne IL, USA

2. Basic Research Program, Leidos Biomedical Research, Inc., Argonne IL, USA

3. Shemyakin-Ovchinnikov Institute of Bioorganic Chemistry, Russian Academy of Sciences, Moscow, Russia

email: pletnevs@mail.nih.gov

A green-emitting fluorescent variant NowGFP with the tryptophan-based chromophore (Thr65-Trp66-Gly67) was recently developed from cyan mCerulean by introducing 18 point mutations. NowGFP is characterized by bright green fluorescence at physiological and higher pH and by weak cyan fluorescence at low pH. Illumination with blue light induces irreversible photoconversion of NowGFP from a green to cyan-emitting form. We report here the X-ray structures of the intact NowGFP at pH 9.0 and pH 4.8, and of its photoconverted variant, NowGFP_{conv}, at 1.35, 1.18, and 2.5 Å resolution, respectively. The structure of NowGFP at pH 9.0 suggests the anionic state of Trp66 of the chromophore to be the primary cause of its green fluorescence. At both examined pH, Trp66 predominantly adopts *cis* conformation; only ~20% of *trans* conformation was observed at pH 4.8. It was shown that Lys61 is a key residue, playing a central role in the chromophore ionization; it adopts two distinct pH-dependent conformations. At high pH, the side chain of Lys61 forms two H-bonds, one with the indole nitrogen of Trp66 and the other with the carboxyl group of the catalytic Glu222, enabling an indirect non-covalent connection between them that promotes Trp66 deprotonation. At low pH, the side chain of Lys61 is directed away from Trp66 and forms an H-bond with Gln207. Here we observe that photoconversion of NowGFP is accompanied by decomposition of the Lys61 side chain. The residues Lys61, Glu222, Thr203, and Ser205 form a local H-bond network connected with the indole ring of the chromophore Trp66; replacement of any of these residues dramatically affects the spectral characteristics of NowGFP.

Keywords: fluorescent proteins, photoconversion

MS5-P5 Structure function studies of a catechol oxidase from *Aspergillus oryzae*Leena Penttinen¹, C. Gasparetti¹, J. Rouvinen¹, K. Kruus², N. Hakulinen¹

1. University of Eastern Finland, Department of Chemistry, P. O. BOX 111 80101 Joensuu, Finland
 2. VTT Technical Research Centre of Finland, PO Box 1000, FIN-02044 VTT, Finland

email: leena.penttinen@uef.fi

Catechol oxidase (EC. 1.10.3.1) belongs to a family of coupled binuclear copper oxidoreductases together with tyrosinase (1.14.18.1) and *o*-aminophenol oxidase (1.10.3.4). Catechol oxidase oxidizes *p*-substituted *o*-diphenols to corresponding *o*-quinones. Tyrosinase has an additional monophenolase activity *i.e.* it can catalyze the *o*-hydroxylation of *p*-substituted monophenols to *o*-diphenols, which then subsequently oxidizes to corresponding *o*-quinones. *o*-Aminophenol oxidases catalyze the mono-oxygenation of *p*-substituted *o*-aminophenols into the corresponding *o*-nitrosophenols. Several crystal structures of tyrosinases have been solved, but catechol oxidases are much less studied.

The first crystal structure of a fungal catechol oxidase from *Aspergillus oryzae* (AoCO4) was recently solved [1]. In addition, a crystal structure of a plant catechol oxidase from *Ipomoea batatas* is known. Now we want to determine the complex structures of AoCO4 to understand the structural determinants for different substrate specificities among coupled binuclear copper enzymes and to elucidate the reaction mechanisms. At the moment, we are optimizing the recombinant overexpression of AoCO4.

[1] Hakulinen, N., Gasparetti, C., Kaljunen, H., Kruus, K., Rouvinen, J., 2013 *J.Biol.Inorg.Chem.*, 18, 917-929

Keywords: Type 3 copper enzymes, Catechol oxidase, Tyrosinase, Binuclear copper site

MS5-P6 Structural insight into the phytoene desaturase of riceAnton Brausemann¹, Sandra Gemmecker², Peter Beyer², Oliver Einsle¹

1. Institut für Biochemie, Albert-Ludwigs-Universität Freiburg, Albertstr. 21, 79104 Freiburg im Breisgau, Germany
 2. Institut für Biologie, Zellbiologie, Albert-Ludwigs-Universität Freiburg, Schänzlestr. 1, 79104 Freiburg im Breisgau, Germany

email: brausemann@bio.chemie.uni-freiburg.de

Vitamin A deficiency is a major health problem in developing countries resulting in blindness in children, increased risk of infection or death that has to be tackled via drugs or dietary supplementation. The biosynthesis of β -carotene, one of its precursors, has been extensively researched. So far a structural insight into involved proteins lacked however. In plants and cyanobacteria two desaturases, two *cis-trans* isomerases and a cyclase are involved in the biosynthesis of β -carotene starting with the isoprenoid 15-*cis*-phytoene.[1] The first enzyme in this biochemical pathway is the FAD containing phytoene desaturase (PDS) that is located at the stromal side of plastid membranes and catalyzes the insertion of two *trans* double bonds in 15-*cis*-phytoene. We have successfully crystallized PDS of *Oryza sativa* in complex with its herbicidal inhibitor norflurazon. The structure was solved using the weak anomalous signal of the soaked mercuric compound thiomersal and refined to a resolution of 2.77 Å. PDS shows a kinked arrangement of two globular domains linked by a single FAD moiety. A highly hydrophobic channel leads the substrate to the putative quinone binding site that is blocked by norflurazon in our model thus showing competitive binding of substrate and electron acceptor.

[1] Beyer P, Al-Babili S, Ye X, Lucca P, Schaub P, Welsch R, et al. Golden Rice: introducing the beta-carotene biosynthesis pathway into rice endosperm by genetic engineering to defeat vitamin A deficiency. *J Nutr.* 2002;132:506S-10S.

Keywords: beta-carotene, phytoene desaturase, rice, plant biochemistry, flavin

MS5-P7 Structural insights into malonyl-CoA reductase of 3-hydroxypropionate cycle

Burak V. Kabasakal¹, Burak V. Kabasakal¹, Charles Cotton¹, James W. Murray¹

1. Department of Life Sciences, Wolfson Biochemistry Building, Imperial College London, Exhibition Road, London SW7 2AZ, U.K

email: burak.kabasakal11@imperial.ac.uk

The novel crystal structures of C-terminal part of Malonyl CoA reductase (MCR) from *Chloroflexus aurantiacus* and its NADPH bound form have been determined in 2.05 Å and 2.11 Å, respectively. NADPH bound structure has a considerable conformational change compared to the native MCR. It forms an unusual hairpin structure near the NADPH binding site at the interface between the enzyme and solvent. The residues forming the hairpin structure are disordered at the native MCR. Furthermore, there is no significant difference between these two structures. NADPH binding site involves many consecutive hydrophobic residues which are necessary for nucleotide binding. Moreover, NADPH interacts with the polar residues which may play a crucial role in catalytic activity. These novel structures will elucidate the catalytic mechanism of MCR.

Keywords: protein crystallography, 3-HP cycle, carbon fixation, Malonyl CoA reductase

MS5-P8 The first X-ray structure of prokaryotic dipeptidyl peptidase III

Igor Sabljic¹, Karl Gruber², Peter Macheroux³, Manja Luić¹

1. Division of Physical Chemistry, Ruđer Bošković Institute, Zagreb, Croatia

2. Institute of Molecular Biosciences, University of Graz, Graz, Austria

3. Institute of Biochemistry, Graz University of Technology, Graz, Austria

email: isabljic@irb.hr

Dipeptidyl peptidase III (DPP III) is a widely distributed cytosolic zinc peptidase from the M49 family, which hydrolyses dipeptides from the N-termini of its peptide substrates. Until now, most studies on DPP III were done on orthologs from eukaryotic organisms, showing that DPP III participates in the intracellular protein catabolism and oxidative stress response. The knowledge about prokaryotic DPP III is very scarce, particularly data on its catalytic mechanism, physiological function and structural characteristics are lacking. We have been studying two bacterial orthologs: DPP III from the human gut symbiont *Bacteroides thetaiotaomicron* (*Bt*) and from *Caldithrix abyssii* (*Ca*), which inhabits hydrothermal vents. Both proteins were produced in *Escherichia coli* and then purified. Diverse crystallization screens were applied and wild-type *Ca*DPP III crystals were obtained. Crystallization experiments with wild-type *Bt*DPP III failed probably due to charge heterogeneity. In order to overcome this problem, specific amino acid replacements (all cysteines were replaced by serines) were introduced and crystals of the variant protein were grown. Datasets for both DPP III proteins were collected at BESY II, Germany. Up to date, all efforts to solve the structures of the two proteins using molecular replacement method and anomalous dispersion of the zinc ions, were unsuccessful. Therefore, selenomethionine labeled *Bt*DPP III, non-cysteine variant, was prepared and the crystals were obtained in the same crystallization condition as the non-labelled protein. Diffraction data up to 1.8 Å resolution were collected at Elettra Trieste, Italy, and the first prokaryotic DPP III structure was solved using single-wavelength anomalous dispersion of the selenium atoms. *Bt*DPP III crystallized in space group *P*3₁21 with unit cell dimensions *a*=103.5 Å and *c*=141.6 Å and one molecule per asymmetric unit. The overall fold is typical for a member of the M49 family with two domains separated by a wide cleft. The upper domain is mostly helical with a tetracoordinated zinc ion, while the lower domain contains mixed secondary structure elements with a five-stranded β-barrel core. The main structural difference between *Bt*DPP III and eukaryotic DPP III is the absence of a 30 amino acid loop in upper domain. In human DPP III this loop contains the ETGE motif which is supposed to be responsible for binding KEAP1, a repressor protein from the Keap1-Nrf2 signaling pathway.

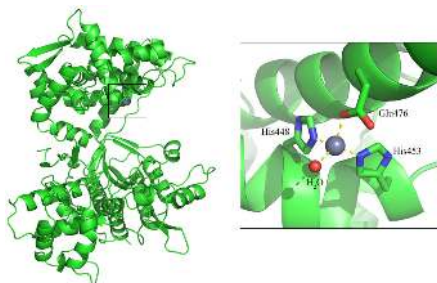


Figure 1. Overview of the BtDPP III structure. A two domains protein with characteristic M49 fold. The active site is located in the upper domain, containing a zinc ion coordinated by two histidines from the characteristic HECLGH motive, one glutamic acid from the EEARAD motive, and a water molecule.

Keywords: Dipeptidyl peptidase III, metallopeptidase, M49 family, *Bacteroides thetaiotaomicron*, *Caldithrix abyssi*

MS5-P9 The cell-shape determining Csd6 protein from *Helicobacter pylori* constitutes a new family of L,D-carboxypeptidase

Hyoun Soek Kim^{1,2}, Byung Woo Han¹, Se Won Suh²

1. Research Institute of Pharmaceutical Sciences, College of Pharmacy, Seoul National University, Seoul 151 742, Republic of Korea

2. Department of Chemistry, College of Natural Sciences, Seoul National University, Seoul 151 742, Republic of Korea

email: kobooks@gmail.com

Helicobacter pylori causes gastrointestinal diseases, including gastric cancer. Its high motility in the viscous gastric mucosa facilitates colonization of the human stomach, and depends on the helical cell shape and the flagella. In *H. pylori*, Csd6 is one of the cell shape-determining proteins that play key roles in determining the cell shape by alteration of cross-linking or by trimming of peptidoglycan mucopeptides. Csd6 is also involved in deglycosylation of the flagellar protein FlaA. To better understand its function, we have carried out biochemical, biophysical, and structural characterizations. We show that Csd6 has three-domain architecture and exists as dimers in solution. The N-terminal domain plays a key role in dimerization. The middle catalytic domain resembles those of L,D-transpeptidases and its pocket-shaped active-site is uniquely defined by the four loops I–IV, among which the loops I and III show the most distinct variations from the known L,D-transpeptidases. Our mass analyses confirm that Csd6 functions only as L,D-carboxypeptidase but not as L,D-transpeptidase. Our D-Ala-complexed structure reveals binding modes of both the substrate and product to the catalytic domain. The C-terminal nuclear transport factor 2-like domain possesses a deep pocket for possible binding of pseudaminic acid and our *in silico* docking supports its role in deglycosylation of flagellin. On the basis of our findings, we propose that *H. pylori* Csd6 and its homologs constitute a new family of L,D-carboxypeptidase. This work provides insights into the function of Csd6 in regulating the helical cell shape and motility of *H. pylori*.

Keywords: Csd6, cell shape, L,D-carboxypeptidase, *Helicobacter pylori*, HP0518, flagellin, peptidoglycan

MS5-P10 Structural investigations of purine nucleoside phosphorylase from *Helicobacter pylori* II

Marija Luić¹, Karolina Gucunski¹, Ivana Lešić Ašler¹, Zoran Štefanić¹

1. Ruder Bošković Institute, Bijenčka c. 54, 10000 Zagreb, Croatia

email: marija.lucic@irb.hr

Helicobacter pylori is a well-known human pathogen involved in the development of many diseases. Due to the ever-growing infection rate and increase of *H. pylori* antibiotic resistance, it is of utmost importance to find a new way to attack and eradicate *H. pylori*. The purine metabolism in *H. pylori* is solely dependent on the salvage pathway and one of the key enzymes in this pathway is purine nucleoside phosphorylase (PNP). Therefore, PNP could be a promising drug target for inhibiting *H. pylori* growth. Like most bacterial PNPs, *H. pylori* PNP is a homohexameric protein that can be regarded as a trimer of dimers. The active site conformation of each monomer can be either open or closed (Koellner et al., 2002). In accordance with our hypothesis, substrate binding takes place in open, and catalytic action occurs in the closed conformation. In the crystal structures of the very similar *E. coli* PNP complexed with its ligands we have found the following distributions of the closed and open active sites: 3 open + 3 closed (Koellner et al., 2002), 4 open + 2 closed sites (Miklešević et al., 2011). In the frame of this meeting in the presentation "Structural investigations of purine nucleoside phosphorylase from *Helicobacter pylori*, two crystal structures of the PNP from the *H. pylori* clinical isolate in complex with ligands will be described. To our surprise, in both crystal structures 5 open + 1 closed conformations were found. To the best of our knowledge, this is first such case among homohexameric PNP enzymes. Very recently, we have obtained also first crystals of the PNP from a referent strain of this bacterium, *Helicobacter pylori* 26695 in complex with ligands and data collection as well as crystal structure determination is under way. It is important to stress out that in the clinical isolate very important catalytic amino acid Asp204 is mutated in Asn, which, very likely, has implications to the catalytic mechanism. Differences in the active site conformations between PNP enzymes from two different *H. pylori* strains will be discussed, as well as possible implications on the PNP mechanism of action.

Koellner, G., Bzowska, A., Wielgus-Kutrowska, B., Luić, M., Steiner, T., Saenger, W., & Štepiński, J. (2002). *J. Mol. Biol.* **315**, 351–371.

Miklešević, G., Štefanić, Z., Narczyk, M., Wielgus-Kutrowska, B., Bzowska, A., & Luić, M. (2011). *Biochimie*. **93**, 1610–1622.

Keywords: Purine nucleoside phosphorylase, *Helicobacter pylori* 26695

MS5-P11 Structural insights into fatty acid metabolism in *Bacillus subtilis* sporulation

Genevieve E. Baker¹, Paul R. Race¹

1. School of Biochemistry, University of Bristol, Bristol, UK

email: genevieve.baker@bristol.ac.uk

Bacillus subtilis is the model Gram-positive bacterium. Its genetic and physiological characterisation is of value not only for elucidating its basic biology, but also that of related pathogenic microorganisms. Similarly to other *Bacilli*, *B. subtilis* undergoes sporulation, a process of cellular differentiation producing metabolically dormant endospores. Studies of this process have important implications for understanding the life cycle and infectivity of related pathogenic *Bacilli* e.g. *B. anthracis*, responsible for anthrax. Despite the medical importance of sporulation questions still remain regarding the metabolic pathways involved in this process. As well as being integral components of phospholipid membranes fatty acids can also be metabolised and used as a source of energy by microorganisms. The mother cell metabolic operon (*mmg*) consists of genes with sequence similarity to those involved in fatty acid metabolism. Although exact roles for the enzymes encoded for by the *mmg* genes remain cryptic, they appear to play an important role in energy production during sporulation. Here I present recent progress in the structural and functional characterisation of the Mmg proteins, and explore their ability to form a single functional enzymatic complex. I highlight the implications of these findings for our understanding of *B. subtilis* sporulation.

Keywords: Multiprotein Complex, Metabolism, Structure.

MS5-P12 Structural analysis of HD-PTP phosphatase and complexes with ESCRTsLydia Tabernero¹, Deepanker Ghaloth¹, Colin Levy¹, Paul Mould¹, Thomas Jowitt¹, Clair Baldock¹, Phil Woodman¹¹. Faculty of Life Sciences, University of Manchester, Manchester, UK

email: lydia.tabernero@manchester.ac.uk

HD-PTP/PTPN23 is a tumour suppressor phosphatase that sits at the crossroads of three essential processes; endocytosis, down-regulation of mitogenic receptors, and cell migration. HD-PTP is essential for down-regulation of activated EGFR by coordinating its trafficking to the lysosome for degradation. This role involves the specific recruitment of three different endosomal sorting multi-protein complexes, ESCRTs, that control the formation of the intraluminal vesicles to which EGFR is sorted. However, the molecular mechanism that regulates the exchange between ESCRTs is still unknown. HD-PTP is a 180KDa multidomain protein that contains a **Bro1** domain, a **coiled-coil** domain, a Pro-rich region (**PRR**), and a C-terminal **PTP** domain. Bro1 binds STAM2 and CHMP4, subunits of ESCRT-0 and -III respectively. The coiled-coil domain interacts with UBAP1 of the ESCRT-I complex. Bro1 and coiled-coil domains are also found in Alix, a protein involved in cytokinesis and viral budding. Binding to STAM2 and UBAP1 is unique to HD-PTP, but CHMP4 binds also to the Bro1 domains of human Brox (unknown function) and Alix. To understand the basis for this specific binding we have determined high resolution structures of the Bro1 and coiled-coil domains of HD-PTP in complex with several subunits of the ESCRT machinery.

The structure of the HD-PTP coiled-coil domain reveals an unexpected extended fold, different from the coiled-coil domain (V domain) in Alix, that explains the selective binding to UBAP1. The structures of the Bro1 and coiled-coil complexes revealed the details of the binding interfaces in HD-PTP at the atomic level. This data, together with biochemical binding analysis and mutagenesis have established the molecular determinants for specific interactions and selectivity between Bro1-containing proteins.

The results invoke a model in which HD-PTP, via its N-terminal domains, plays a role as a major scaffold binding platform to regulate ESCRT-dependent trafficking as well as co-localisation of other important signalling pathways.

Keywords: phosphatase, EGFR signalling, scaffold protein, ESCRT complexes

MS5-P13 Structures of ferredoxin/flavodoxin-NADP(H) oxidoreductases in *Bacillus cereus*Ingvild Gudim¹, Hans-Petter Hersleth¹¹. The Department of Biosciences, Section for Biochemistry and Molecular Biology, University of Oslo. P.O Box 1066 Blindern, 0316 Oslo, Norway.

email: ingvild.gudim@ibv.uio.no

Ferredoxin/flavodoxin-NADP(H) oxidoreductases (FNRs) catalyse the NADPH dependent reduction of the electron transfer mediators ferredoxin (Fd) and/or flavodoxin (Fld). FNR and Fd/Fld hence form an electron transfer network for efficient shuttling of electrons to different Fd/Fld-dependent enzyme systems.

Three flavodoxins, two ferredoxins and three ferredoxin/flavodoxin reductases have been identified in *Bacillus cereus*, but it is so far not known how they interact. We have previously, using a tag-free purification procedure, purified and crystallised several of these electron transfer proteins and also some of their redox partner enzymes. Here we present the structures of two of the ferredoxin/flavodoxin-NADP(H) oxidoreductases from *Bacillus cereus*.

Further investigations will focus on protein-protein complexes of the electron transfer proteins. The aim is to establish whether there are any specific interactions between the proteins, *i.e.* whether any one protein preferably interacts with any of its redox partners, and if so, what the structural basis is for this interaction.

Acknowledgements. Financial support by the Norwegian Research Council through projects 231669/F20.

Keywords: protein crystallography, redox enzymes, flavoproteins

MS5-P14 Elucidation of the structure and mechanism of CouO, a small molecule C-methyltransferase from *Streptomyces rishiriensis*

Tea Pavkov-Keller^{1,2}, Kerstin Steiner¹, Mario Faber³, Martin Tengg³, Helmut Schwab³, Karl Gruber², Mandana Gruber-Khadjawi¹

1. Austrian Centre of Industrial Biotechnology GmbH, Graz, Austria
2. University of Graz, Institute of Molecular Biosciences, Graz, Austria
3. Technical University, Graz, Austria

email: tea.pavkov@uni-graz.at

The addition of a methyl group to biologically active molecules such as hormones, proteins, lipids and nucleic acids causes a change in the physico-chemical properties of the molecules. The methyltransferase (MT) enzymes catalyze this methylation reaction. The biological functions of methylation include biosynthesis, detoxification, metabolism, signal transduction, and nucleic acid processing. Although several classes of MT enzymes are known, the great majority of methylation reactions are catalyzed by the S-adenosylmethionine-dependent MTs (SAM-MTs).

The small-molecule C-methyltransferase CouO from *Streptomyces rishiriensis* is involved in the biosynthesis of the antibiotic coumermycin A1 [1]. The enzyme was cloned and expressed in *Escherichia coli*, crystallized [2] and enzymatically characterized in our group [3]. Here we report the high-resolution crystal structure of CouO. The overall structure exhibits a core with a Rossmann-like α/β -fold typical of Type I SAM-dependent methyltransferases [4]. CouO is present as a dimer in the asymmetric unit and S-adenosyl-L-homocysteine (SAH) is bound in the cofactor binding site. Based on the crystal structure of CouO and docking experiments, the mutagenesis studies of active site amino acids were performed. As a result, we propose a mechanism for the alkyl transfer reaction.

[1] Pacholec M, Tao J, Walsh C T. CouO and NovO: C-Methyltransferases for Tailoring the Aminocoumarin Scaffold in Coumermycin and Novobiocin Antibiotic Biosynthesis. *Biochemistry* 2005; 44:14969–14976.

[2] J Lyskowski A, Tengg M, Steinkellner G, Schwab H, Gruber-Khadjawi M, Gruber K. Crystallization of the novel S-adenosyl-L-methionine-dependent C-methyltransferase CouO from *Streptomyces rishiriensis* and preliminary diffraction data analysis. *Acta Cryst.* 2012; F68:698–700.

[3] Stecher H, Tengg M, Ueberbacher BJ, Remler P, Schwab H, Griengl H, Gruber-Khadjawi M. Biocatalytic Friedel-Crafts alkylation using non-natural cofactors. *Angew Chem Int Ed Engl.* 2009; 48(50):9546–8.

[4] Schubert H L, Blumenthal R M, Cheng X. Many paths to methyltransfer: a chronicle of convergence. *Trends Biochem. Sci.* 2003; 28(6):329–335.

Keywords: C-methyltransferase, S-adenosyl-L-homocysteine

MS5-P15 Crystal structure of *Streptomyces rimosus* extracellular lipase

Ivana Lešćić Ašler¹, Ivana Lešćić Ašler¹, Zoran Štefanić¹, Marija Luić¹, Biserka Kojić-Prodić¹

1. Ruđer Bošković Institute, Bijenička c. 54, 10000 Zagreb, Croatia

email: ilesic@irb.hr

Upton & Buckley (1995) recognized a new family of lipolytic enzymes, which they originally named GDS(L) lipolytic enzymes after the conserved motif containing the catalytic serine. A new name, SGNH hydrolases, was proposed after the four amino acids that are conserved in the active site (Mølgaard et al., 2000). This particular group comprises lipases, proteases, thioesterases, arylesterases, lysophospholipases, carbohydrate esterases and acyltransferases. Some of the SGNH hydrolases display high flexibility in the active site which enables them to accept a wide range of different types of substrates, but it is as yet unclear whether this property of promiscuity is common to all enzymes of this family.

We have recently discovered that the extracellular lipase from *Streptomyces rimosus* (SrLip) exhibits substrate and catalytic promiscuity (Lešćić Ašler et al., 2010). In order to gain better insight into the structural and mechanistic basis of enzyme catalysis, we investigated the interactions of this enzyme with several inhibitors. The general mechanism-based serine protease inhibitor 3,4-dichloroisocoumarin (DCI) was shown to be the most effective and covalently bound to the active-site serine (Zehl et al., 2004).

Purified SrLip was incubated with 600-fold molar excess of DCI and crystallisation screens were set. Only one crystal grew from 0.1 M MES pH 6.5, 25% PEG 2000 MME. This crystal was used for data collection on the XRD beamline of the Elettra synchrotron, Trieste, Italy. A 98.4% complete data set was collected to a resolution of 1.7 Å at 100 K. The protein crystallized in the monoclinic space group P2₁, with unit-cell parameters a = 38.1, b = 78.7, c = 56.6 Å, β = 104.5°. The starting model for the molecular-replacement procedure was built using the Phyre server, based on Phospholipase A1 from *Streptomyces albidoflavus* NA297.

Crystal structure of SrLip will be discussed in detail, with special emphasis on active site shape and topology, considering this enzyme's broad substrate specificity.

Lešćić Ašler, I., Ivić, N., Kovačić, F., Schell, S., Knorr, J., Krauss, U., Wilhelm, S., Kojić-Prodić, B. & Jaeger, K. E. (2010). *ChemBiochem* **11**, 2158–2167.

Mølgaard, A., Kauppinen, S. & Larsen, S. (2000). *Structure* **8**, 373–383.

Upton, C. & Buckley, J. T. (1995). *Trends Biochem. Sci.* **20**, 178–179.

Zehl, M., Lešćić, I., Abramić, M., Rizzi, A., Kojić-Prodić, B. & Allmaier, G. (2004). *J. Mass Spectrom.* **39**, 1474–1483.

Keywords: SGNH hydrolase, *Streptomyces rimosus*, catalytic promiscuity, 3,4-dichloroisocoumarin, crystal structure

MS5-P16 Structural insight into magnetochrome-mediated biomineralization

Marina I. Siponen¹, Arnoux Pascal¹, Faivre Damien², Pignol David¹

1. Laboratoire de bioenergetique cellulaire, CEA Cadarache, IBEB/UMR7265, F-13108, Saint-Paul-les-Durance, France

2. Department of Biomaterials, Max Planck Institute of Colloids and Interfaces, Research Campus Golm, 14424 Potsdam, Germany

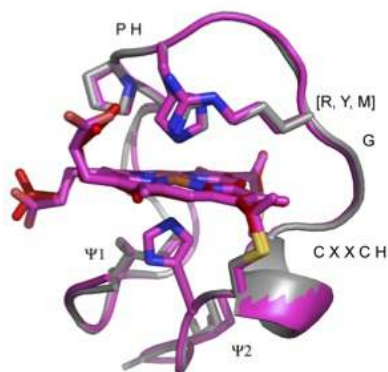
email: misiponen@gmail.com

Biomining is the process by which organisms produce minerals from environmental elements. The minerals produced often result in materials, which have superior properties than similar man-made materials, making them of significant interest in understanding the mechanisms of biomineralization. Magnetotactic bacteria (MTB) are a group of microorganisms which biomineralise nano-sized crystal of magnetite. These crystals present in a prokaryotic organelle, the magnetosome, allow them to swim along Earth's magnetic field lines. Magnetosomes are proteolipidic vesicles filled by a 35-120 nm magnetite crystal. Since magnetite is a mix of iron(III) and iron(II), iron redox state management within the magnetosome is a key issue. In this respect, we have recently started pointing out the importance of a MTB-specific c-type cytochrome domain (magnetochrome; MCR), found in several magnetosome-associated proteins (MamE, P, T and X). In order to understand the mechanistic importance of this domain in the biomineralization process, we have elucidated the structure of the MCR-containing MamP protein. Our results demonstrate that MamP is an iron oxidase that contributes to the formation of iron(III) ferrihydrite eventually required for magnetite crystal growth *in vivo*, demonstrating the molecular mechanisms of iron management taking place inside the magnetosome, emphasizing the role of the MCR in iron biomineralization.

Reference:

Siponen MI, et al (2013) Structural insight into magnetochrome-mediated magnetite biomineralization. *Nature* **502(7473)**: 681-4

Siponen MI, Adryanczyk G, Ginot N, Arnoux P, Pignol D (2012) Magnetochrome: a c-type cytochrome domain specific to magnetotactic bacteria. *Biochem Soc Trans.* **40(6)**:1319-23



MCR motif : Ψ1 X₅₅ PHXX [R, Y, M] GX CXXCHX Ψ2

Figure 1. The magnetochrome domain is one of the smallest C-type cytochrome domains identified thus far. This domain has shown to be specific to magnetotactic bacteria and required for electron transfer in the ferrous oxidase activity of the MamP protein.

Keywords: Biomineralization, magnetotactic bacteria, magnetochrome protein domain

MS5-P17 The effects of electrostatic interactions and side-chain stabilization during chorismate mutase-catalyzed Claisen rearrangements

Daniel Burschowsky¹, David Balcells¹, Einar Uggerud¹, Peter Kast², Ute Kregel¹

1. Department of Chemistry, University of Oslo

2. Laboratory of Organic Chemistry, ETH Zurich

email: danielbu@kjemi.uio.no

The chorismate mutase (CM) of *Bacillus subtilis* is a well-characterized model enzyme that catalyzes the pericyclic rearrangement of chorismate to prephenate. However, the relative contributions of transition-state stabilization and geometry to its catalytic efficiency (10^6 -fold) were debated during the last decade. An almost inactive variant of CM, where the charged catalytic residue Arg90 was replaced by a neutral citrulline, was supposed to resolve the debate, but the disagreement still persisted. Specifically, it was unclear if the observed changes in reaction energies for the inactive variant stemmed from large-scale structural changes or electrostatic effects. With a series of high-resolution crystallographic snapshots along its reaction coordinate we showed that the enzyme variant is structurally identical to wild-type CM and that the electrostatic stabilizing effect is therefore almost entirely responsible for catalysis.

The detailed experimental structural information of the main reaction states also allowed us to examine the active sites of the CM wild type and variant with quantum chemical simulations, without introducing conformational artifacts. Instead of using molecular dynamics to relax our structures beforehand, we were able to use the amino acid structures that comprise the active site environment directly. We optimized the geometries of truncated active site models in the presence of substrate, transition state and product for a range of dielectric constants and at different levels of density functional theory, which enabled us to confirm the electrostatic nature of CM catalysis. In addition, by following the intrinsic reaction coordinate of this model system, we were able to describe mechanistic details for this enzyme. Most prominently, a 13° rotation of the catalytic side chain serves as an induced fit for a selective electrostatic stabilization of the transition state, which plausibly explains the catalytic proficiency of this enzyme.

1. Burschowsky D, *et al.* (2014) Electrostatic transition state stabilization rather than reactant destabilization provides the chemical basis for efficient chorismate mutase catalysis. *Proc Natl Acad Sci U S A* 111(49):17516-17521.

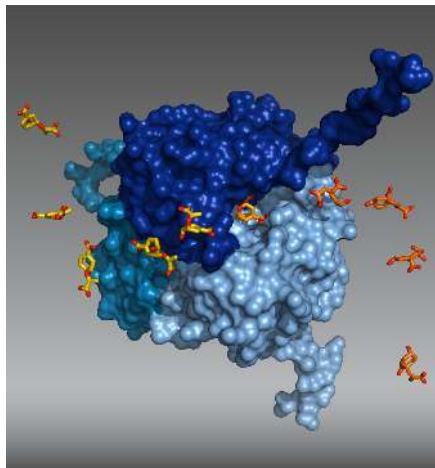


Figure 1. An artistic impression of the model enzyme chorismate mutase in action. Yellow colored chorismate molecules coming in from the left are transmuted via a bicyclic transition state (here depicted with a light orange transition state analog) to prephenate, shown in orange.

Keywords: enzyme mechanism, chorismate mutase, pericyclic reaction

MS5-P18 Crystal structures of amidase Cwp6 and related cell wall protein Cwp8 from *Clostridium difficile*

Aleksandra Usenik¹, Miha Renko^{1,2}, Marko Mihelič^{1,2}, Gregor Pretnar², Dušan Turk^{1,2}

1. Jožef Stefan Institute, Ljubljana, Slovenia

2. Centre of Excellence for Integrated Approaches in Chemistry and Biology of Proteins (CIPKeBiP), Ljubljana, Slovenia

email: aleksandra.usenik@ijs.si

The cell wall of Gram-positive bacteria is a surface, exoskeletal organelle composed of peptidoglycan, secondary polymers and a wide variety of proteins providing its unique structural and functional properties. Apart from covalently anchored LPXTG-like cell wall proteins Gram-positive bacteria also harbour several types of cell wall proteins non-covalently attached via cell wall binding domains in some cases forming surface protein layers (S-layers). In *Clostridium difficile* 630, one of the most important nosocomial pathogens causing antibiotic-associated diarrhea that can lead to potentially lethal pseudomembranous colitis, there are 29 cell wall proteins (CWPs), including the major S-layer precursor, SlpA, sharing three tandem CWB2 repeats. While it was recently shown that CWB2 repeats mediate non-covalent binding to the anionic polymer PSII, we report here the crystal structures of *C. difficile* cell wall proteins Cwp8 and Cwp6 revealing the structure of the cell wall-anchoring module of CWB2 domains. It consist of three tandem, ~ 100 residues long, compact CWB2 domains. Additional structural insight into the molecular organization of *C. difficile* cell wall is provided by showing partial structural similarity of the N-terminal part of Cwp8 to the LMW-SLP truncated derivative. Based on biochemical characterization of Cwp6 and its C-terminal domain structural alignment with PDB deposits, we also conclude that Cwp6 is a zinc-dependent N-acetylmuramoyl-L-alanine amidase belonging to an Amidase_3 (PF01520) family.

Keywords: Gram-positive bacteria, *Clostridium difficile*, cell wall proteins, S-layer, CWB2 domain, amidase

MS5-P19 Conformational study of *Bacteroides thetaiotaomicron* dipeptidyl peptidase III

Marko Tomin¹, Sanja Tomić¹, Igor Sabljic¹

1. Ruđer Bošković Institute

email: marko.tomin@irb.hr

Dipeptidyl peptidase III isolated from *Bacteroides thetaiotaomicron*, Bt-DPP3, is a two-domain zinc exopeptidase from M49 family. Members of this family, characterized by their HEXXGH motive, cleave dipeptidyl residues from the N-terminus of their substrates. The crystallographically determined Bt-DPP3 structure¹, consisting of two domains separated by a wide cleft, strongly resembles 3D structure of the human ortholog despite their low sequence identity (~23%).

Our earlier computational study clearly showed that human DPP3 experiences long-range conformational changes in solution². We showed that, among a number of different forms that it can adopt, the compact form is the most stable and enzymatically active. In this work we used classical and accelerated MD to examine the conformational landscape of Bt-DPP3 as well as influence of ligand binding on the protein structure and dynamics. Special emphasis has been placed on the zinc ion coordination flexibility, since the existing data for human DPP3 suggests the high plasticity of the Zn²⁺ coordination³.

1. I. Sabljic, private communication
2. A. Tomić, M. González, S. Tomić, *J Chem Inf Model*, 52 (2012) 1583-94.
3. A. Tomić, S. Tomić, *Dalton trans.*, 43 (2014) 15503-14.

Keywords: dipeptidyl peptidase III, computational

MS5-P20 The active site structure of manganese-containing *Brassica rapa* auxin-amidohydrolase BrILL2

Marina Grabar Branilović¹, Ana Smolko², Filip Šupljika³, Branka Salopek-Sondi², Ivo Piantanida³, Sanja Tomić¹

1. Ruder Bošković Institute, Division of Physical Chemistry, Bijenička 54, Zagreb, Croatia
2. Ruder Bošković Institute, Division of Molecular Biology, Bijenička 54, Zagreb, Croatia
3. Ruder Bošković Institute, Division of Organic Chemistry and Biochemistry, Bijenička 54, Zagreb, Croatia

email: mgrabar@irb.hr

Auxin-amidohydrolase from *Brassica rapa* (*Br*), BrILL2, belongs to the M20D metallopeptidase subfamily, related to the amidohydrolase superfamily (M20) of enzymes which hydrolyze a number of different substrates, including amino acids, sugars, nucleic acids, and organophosphate esters.¹ BrILL2 is catalytically the most efficient auxin-amidohydrolase from *Br*, playing a key role in homeostasis of the plant hormone auxin in a way to hydrolases amino acid conjugates (AACs) of auxins (IAA, IBA, IPA). A large concentration of free auxins, of which the most common is indole-3-acetic acid (IAA), is toxic for plants, so only about 5% of the total concentration of auxin molecules in plants is in the free (active) form, while the rest is stored in inactive forms, mostly as amino acid and sugar conjugates.² In order to hydrolyze the amide bond of amino acid conjugated auxins (inactive, storage forms), and release the free auxin, BrILL needs manganese.³ The aim of our research was to determine number of the manganese ions, Mn²⁺, in the enzyme active site, and the influence of Cys to Ser mutations on the protein structure and activity. In order to fulfil this aim we conducted an interdisciplinary study combining different experimental and computational approaches: biochemical, spectroscopic, calorimetric and computational.

¹ Seibert, C. M., Raushel, F. M. (2005). *Biochemistry*, 44, 6383–6391.

² Ludwig-Müller, J. (2011). *Journal of Experimental Botany*, 62(6), 1757–1773.

³ Savić, B., Tomić, S., Magnus, V., Gruden, K., Barle, K., Grenković, R., Ludwig-Müller, J., Salopek-Sondi, B. (2009). *Plant & Cell Physiology*, 50(9), 1587–1599.

Keywords: auxin-amidohydrolase, *Brassica rapa*, manganese ions, Cys, interdisciplinary study

MS5-P21 The active center and beyond: towards new selective inhibitors of *S*-adenosyl-L-homocysteine hydrolase from *Pseudomonas aeruginosa*

Krzysztof Brzezinski¹, Justyna Czyrko¹, Monika Imierska¹, Patrycja Olszyska¹

1. Institute of Chemistry, University of Białystok, Hurtowa 1, 15-399 Białystok, Poland

email: k.brzezinski@uwb.edu.pl

Drug-resistant bacteria are an important healthy issue, as many human pathogens have gained resistance to a wide range of commercially available pharmaceuticals. *Pseudomonas aeruginosa* has a natural resistance to many antibiotics and disinfectants. This opportunistic pathogen causes a myriad of infection to immunosuppressed patients, including endocarditis, microbial keratitis of eye, pneumonia, urinary tract infections and chronic lung infection in patient with cystic fibrosis or cancer. Numerous virulence factors, the large number of multi-drug efflux systems, as well as the low permeability of the outer membrane are key factors in pathogenesis of *P. aeruginosa*. Moreover, *P. aeruginosa* is capable of growing in complex bacterial communities, called biofilms, which makes them more resistant to antibiotics than single-grown cells.

S-adenosyl-L-homocysteine hydrolase (SAHase) is an essential enzyme involved in the regulation of methylation reactions. This applies to both, healthy host cells and their invading pathogens form. Therefore, selective inhibition of SAHases in targeted cells is an excellent possibility for a drug intervention at the molecular level of cell metabolism. SAHases are highly-conserved enzymes with almost identical organization of the active site. This fact practically precludes design of highly selective inhibitors against the enzymes of pathogenic origin that would not affect the human cells. Therefore, the aim of this study is not to focus on the active site but to elucidate mechanisms of substrate and inhibitor delivery to the substrate-binding pocket of *P. aeruginosa* SAHase. The premises about various mechanisms which regulate the accessibility of the substrate binding pocket are based on crystallographic studies of SAHases from various organisms. However, the chemical nature of the different regulation mechanisms has not yet been explained. Additionally, apart from the active site, a role of a non-conservative entrance to the substrate-binding pocket in substrate delivery to the active site is proposed.

This project is supported by a grant from the Polish National Science Center (No. UMO-2013/09/B/NZ1/01880).

Keywords: *S*-adenosyl-L-homocysteine, *S*-adenosyl-L-homocysteine hydrolase, *S*-adenosyl-L-methionine, methyltransferases

MS5-P22 Crystal Structure of the cytoplasmic portion of histidine kinase SrrB from *Staphylococcus aureus*

Wen-Yih Jeng^{1,2,3,4}, Ya-Jin Jheng^{2,3}, Chia-I Liu^{1,4,5}, Chieh-Shan Lee^{2,3}, Te-Jung Lu⁶, Yueh-Hao Chen⁶, Chuan Liu⁶

1. Core Facilities for Protein Structural Analysis, Academia Sinica, Taipei 115, Taiwan
2. University Center for Bioscience and Biotechnology, National Cheng Kung University, Tainan 70101, Taiwan
3. Department of Biochemistry and Molecular Biology, National Cheng Kung University, Tainan 701, Taiwan
4. Institute of Biological Chemistry, Academia Sinica, Taipei 11529, Taiwan
5. School of Medical Laboratory Science and Biotechnology, Taipei Medical University, Taipei 110, Taiwan
6. Department of Medical Laboratory Science and Biotechnology, Chung Hua University of Medical Technology, Tainan 717, Taiwan

email: wyjeng@mail.ncku.edu.tw

Staphylococcus aureus is a major cause of nosocomial infections today. *S. aureus* infection is considered to be the reason for the increasing number of antibiotic-resistant strains. Furthermore, *S. aureus* can produce slime layer or multilayered biofilm embedded with the glycocalyx on the surface of various biomaterials. *S. aureus* can persist in clinical settings and increase resistance to antimicrobial agents through biofilm formation. SrrB is a histidine kinase which responds to environmental stimuli by regulating its cognate response regulator SrrA. Under low-oxygen growth conditions, the staphylococcal regulator SrrAB induces *ica* locus transcription and polysaccharide intercellular adhesion (PIA) production, known as a major component of biofilm.

Here, we report the crystal structure of cytoplasmic portion of SrrB (SrrBc) from *S. aureus* in a dimeric form at 1.78 Å resolution. The overall structure of SrrBc forms a unique homodimer which is mediated by two pairs of long dimerization α -helices. To the rear of dimerization helices is the ATP binding domain of SrrB which consists of three parallel α -helices, one short anti-parallel β -sheet, one core mixed type β -sheet and a disordered ATP-lid region. Moreover, one disulfide bond (Cys469 and Cys506) is located within the core β -sheet to stable the structure. We propose that the redox state of this disulfide bond in the ATP binding domain of SrrB might play a key role to mediate the interaction between SrrB and SrrA, thus alter the target gene of SrrAB in transcription level in *S. aureus*.

Keywords: biofilm, multiple antibiotic resistant, two-component system

MS5-P23 Insight into recognition between aminoacyl carrier protein and its binding partner

Aleksandra Maršavelski¹, Marko Močibob², Ita Gruić-Sovulj², Robert Vianello¹

1. Quantum Organic Chemistry Group, Ruder Bošković Institute, Bijenička cesta 54, HR-10000 Zagreb, Croatia.
2. Department of Chemistry, Faculty of Science, University of Zagreb, Horvátovac 102a, HR-Zagreb, Croatia.

email: aleksandra.marsavelski@irb.hr

Acyl carrier-protein (ACP) is one of the most promiscuous protein in terms of protein-protein interactions within the cell. Common to both, primary and secondary cell metabolic pathways, ACP acts as a central acceptor of various intermediate products of fatty acid, polyketide and nonribosomal peptide synthesis pathways. Thus, it's quite puzzling how ACP selects correct protein partner among many possible upstream and downstream binding partners. To address this question we choose recently described protein-protein complex formed between aminoacyl carrier protein from *Bradyrhizobium japonicum* (Bj CP) and Bj Gly:CP ligase 1. We performed molecular dynamics simulations, MM-GBSA binding free energy calculations, alanine scanning mutagenesis, and multiple sequence alignment to get deeper insight into relevant protein-protein interactions between three forms of the aminoacyl carrier protein and their partner protein Bj Gly:CP ligase 1 (Figure 1). Our result are in line with experimental findings and indicate that correct protein-protein communication is regulated through specific non-polar contribution of the interacting amino acid residues placed at the interface between aminoacyl carrier protein and partner Bj Gly:CP ligase 1. *In silico* alanine scanning mutagenesis along with multiple sequence alignment aided in classifying interacting residues as universally required for aminoacyl carrier protein binding and those that determine the selectivity.

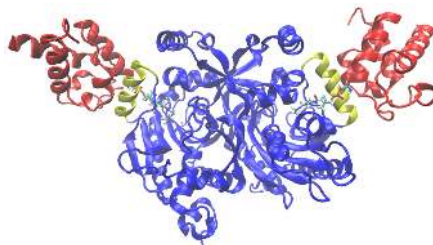


Figure 1. Bj CP - Bj Gly:CP ligase 1 2:1 complex given in the cartoon representation. Both Bj CPs are given in red, while Bj Gly:CP ligase 1 is shown in blue with CP-binding helices given in yellow.

Keywords: molecular recognition; molecular dynamics simulations; protein-protein interactions; acyl carrier proteins

MS5-P24 Structural studies of AggC, an novel O-GlcNAc transferase involved in protection of virulence-associated cell proteins in *Staphylococcus aureus*

Chia-I Liu¹, Tzu-Ping Ko², Wen-Yih Jeng^{3,4}, Wei-Jung Chang^{2,3}, Jhih-Tong Ge¹, Andrew H.-J. Wang^{2,3,5}

1. School of Medical Laboratory Science and Biotechnology, College of Medical Science and Technology, Taipei Medical University, Taipei 10031, Taiwan
2. Institute of Biological Chemistry, Academia Sinica, Taipei 11529, Taiwan
3. Core Facilities for Protein Structural Analysis, Academia Sinica, Taipei 11529, Taiwan
4. University Center for Bioscience and Biotechnology, National Cheng Kung University, Tainan 70101, Taiwan
5. Graduate Institute of Translational Medicine, College of Medical Science and Technology, Taipei Medical University, Taipei 10031, Taiwan

email: ponpiqq@gmail.com

Glycosylation of bacterial cell wall proteins play a critical role in bacterial pathophysiology. Two novel O-linked glycosyltransferases (OGTs), AggB and AggC, decorate all SD (serine-aspartate) repeats of adhesins with N-acetylglucosamine (GlcNAc) moieties, which containing the virulence factors ClfA (a fibrinogen-binding clumping factor A), ClfB, SdrC (SD repeats C), SdrD, SdrE of *S. aureus* and SdrF, SdrG SdrH of *S. epidermidis*. Recently, it has been demonstrated that glycosylated SD repeats proteins can facilitate bacterial adhesion, immune evasion, colonization, persistence and invasion of host tissue. This specific modification also promotes *S. aureus* replication in the bloodstream of mammalian hosts. AggB and AggC modify all SD repeats proteins by an ordered mechanism, with AggC appending the sugar residues proximal to the target SD repeats, followed by additional modification by AggB. Here we report two crystal structures of *S. aureus* AggC, as a binary complex with citrate (2.8 Å) and as a ternary complex with UDP and GlcNAc (2.2 Å). The structures provide clues to the enzyme catalytic mechanism, implying how AggC recognizes target peptide sequences, and reveal the fold of the unique β -meander domain and a core catalytic domain with GT-B fold. Structure-based mutagenesis of AggC was also performed to explore the roles of amino acids involved in substrate binding. In summary, this information will accelerate the rational design of biological experiments to investigate AggC functions and also help the design of inhibitors as a therapeutic target.

Keywords: glycosyltransferase, adhesion, *Staphylococcus aureus*

MS5-P25 Crystal structure of a novel *Caulobacter crescentus* oxidoreductase and its complexes

Helena Taberman¹, Martina Andberg², Anu Koivula², Juha Rouvinen¹, Tarja Parkkinen¹

1. Department of Chemistry, University of Eastern Finland, P.O. Box 111, 80101 Joensuu, Finland
2. VTT Technical Research Centre of Finland Ltd, P.O. Box 1000, 02044 VTT, Finland

email: helena.taberman@uef.fi

Using biocatalysts in producing chemicals from renewable raw materials is an emerging industrial sector and a scope of active research. Further development in this field is required to help fuel the next generation of biorefineries and contribute to the bioeconomy. We have been interested to find novel D-xylose converting enzymes for the exploitation of hemicellulose containing biomasses. Some D-xylose dehydrogenases belong to the Gfo/Idh/MocA enzyme family, including the glucose-fructose oxidoreductase (GFOR) of *Zymomonas mobilis*. During studies on D-xylose dehydrogenases, we encountered an open reading frame (ORF) from fresh water bacterium *Caulobacter crescentus* automatically annotated as a GFOR or as a D-xylose dehydrogenase. To evaluate whether this ORF is involved in D-xylose conversion, it was cloned, expressed and purified from *Saccharomyces cerevisiae*.

The *C. crescentus* oxidoreductase has a high sequence identity (49%) with the Zn GFOR (2, PDB ID: 1H6A). Zn GFOR enzyme uses a tightly bound NADP⁺ cofactor, which is regenerated in the oxidation/reduction cycle, presumably through a ping-pong reaction mechanism (1). The main substrates of GFOR are D-glucose and D-fructose, the former oxidized to D-gluconolactone whereas the latter is reduced to D-sorbitol. The characterisation of the *C. crescentus* oxidoreductase demonstrated that it can catalyse both the oxidation and reduction of several different saccharides to corresponding aldonolactones and alditols, respectively.

In this study, the crystal structures of the holo-form of Cc oxidoreductase and its complexes with different sugars and sugar polyols have been determined. The structures demonstrate a two-domain structure composed of the classical N-terminal Rossmann fold for dinucleotide binding (3) and of a β -sheet formed of seven, mostly antiparallel, β -strands, separated by three α -helices. Two Cc oxidoreductase monomers form a dimer by packing their open-faced β -sheets together. The structures are currently under refinement. The results provide insight into the cofactor and ligand binding, and help us to elucidate the exact reaction mechanisms of the enzyme.

The work was part of the Finnish Centre of Excellence in White Biotechnology-Green Chemistry (Academy of

Finland decision no. 118573).

References

1. Cleland, W. W. (1963) *Biochem. Biophys. Acta* **67**, 104-137.
2. Nurizzo, D. et al. (2001) *Biochemistry* **40**, 13857-13867.
3. Rao, S. T. & Rossmann, M. G. (1973) *J. Mol. Biol.* **76**, 241-156.

Keywords: oxidation/reduction cycle, biomass, crystal structure, enzyme mechanism

MS5-P26 The *cis*-peptide conformation at loop I of the Hypoxanthine phosphoribosyltransferases is not essential for the binding of substrates

Francisco J. Medrano¹, Francisco J. Medrano¹, Antonio Romero¹

1. Centro de Investigaciones Biológicas; Ramiro de Maeztu, 9; 28040-Madrid; Spain

email: fjmedrano@cib.csic.es

Hypoxanthine phosphoribosyltransferases (HPRT; EC 2.4.2.8) catalyze the transfer of a phosphoribosyl group from 5-phospho-a-D-ribosyl-1-pyrophosphate (PRPP) to a purine base (hypoxanthine, guanine or xanthine) to form pyrophosphate (PPi) and a purine nucleotide, inosine monophosphate (IMP), guanosine monophosphate (GMP), or xanthosine monophosphate (XMP), respectively. At the active site one of the loops involved in the binding of the substrates (loop I) all the HPRT structures known up to now have a peptide bond in a *cis* conformation allowing the binding of one phosphate group. We have solved the structure of the HPRT from *Chromobacterium violaceum* in the presence of the substrates PRPP, IMP and GMP; and in all of these structures we have not observed the presence of the *cis* conformation at loop I. This protein presents a glycine at the second position of this three residue loop, while the usual amino acid present at this position are lysine or arginine that are involved in the ability or inability to carry out the pyrophosphorolysis (reverse) reaction, respectively.

Keywords: HPRT, Loop I, *cis*-peptide conformation

MS5-P27 Purine nucleoside phosphorylase from bacterium *Helicobacter pylori* strain 26695: cloning, expression, purification, characterisation and crystallisation

Karolina Gucunski¹, Ivana Lešćić Asler¹, Marija Luić¹

1. Laboratory for Chemical and Biological Crystallography, Division of Physical Chemistry

email: karolina.gucunski@gmail.com

Purine nucleoside phosphorylase (PNP) is the key enzyme in the purine salvage pathway. It catalyses the reversible phosphorolytic cleavage of the glycosidic bond of ribo- and deoxyribonucleosides, in the presence of inorganic orthophosphate as a second substrate to generate the purine base and ribose(deoxyribose)-1-phosphate.

Helicobacter pylori is a Gram-negative, microaerophilic bacterium, human pathogen involved in development of many diseases as gastric ulcers and stomach cancer, and therefore known for its ability to colonize human stomach. Study of the *H. pylori*, due to the ever growing infection rate and increase of *H. pylori* antibiotic resistance, is centred on understanding pathogenesis and finding a way to attack and eradicate *H. pylori*.

H. pylori PNP represents potential drug target as this bacterium cannot synthesize purine rings through *de novo* pathway and has to rely on purine production through purine salvage pathway. It belongs to the class of bacterial high-molecular-mass homohexamers with specificity for both 6-oxo- and/or 6-aminopurines.

Purine nucleoside phosphorylase gene *deoD* was isolated from genomic DNA of *Helicobacter pylori* (strain 26695) and amplified using Phusion High-Fidelity PCR kit with the set of specific DNA primers for both 5' and 3' ends of the gene. Resulting plasmid pET21b-HP26695*deoD*, with ampicillin resistance and without purification tag, was transformed into *E. coli* strain BL21-CodonPlus(DE3)RIL. Induction conditions for PNP expression in *E. coli* were optimised and evaluated by SDS-PAGE electrophoresis of bacterial culture filtrate.

Purification of overexpressed PNP from the bacterial culture filtrate was performed by anion exchange chromatography on Q-Sepharose FF column. Next step, which gave single protein band on SDS-PAGE was affinity chromatography, performed on Sepharose-FormycinA column.

Biochemical characterisation involves kinetic studies, as well as temperature and pH effects on stability and activity of PNP. Crystallisation experiments with purified purine nucleoside phosphorylase from *H. pylori* are under way.

Keywords: *Helicobacter pylori*, purine nucleoside phosphorylase, biochemical characterisation, enzyme kinetics, crystallisation

MS5-P28 A sequence-specific DNA glycosylase mediates restriction-modification in *Pyrococcus abyssi*

Masaru Tanokura¹, Ken-ichi Miyazono¹, Yoshikazu Furuta^{2,3}, Miki Watanabe-Matsui³, Takuya Miyakawa⁴, Tomoko Ito⁴, Ichizo Kobayashi^{1,2,3}

1. Department of Applied Biological Chemistry, Graduate School of Agricultural and Life Sciences, The University of Tokyo

2. Department of Medical Genome Sciences, Graduate School of Frontier Science, The University of Tokyo

3. Institute of Medical Science, The University of Tokyo

4. Graduate Program in Biophysics and Biochemistry, Graduate School of Science, The University of Tokyo

email: amtanok@mail.ecc.u-tokyo.ac.jp

Restriction-modification systems consist of genes that encode a restriction enzyme and a cognate modification methyltransferase. It was believed that restriction enzymes are sequence-specific endonucleases that cleave double-stranded DNAs at specific sites by catalyzing the hydrolysis of phosphodiester bonds. R.PabI is a type II restriction enzyme from a hyperthermophilic archaea *Pyrococcus abyssi* that recognizes 5'-GTAC-3' sequence and cleaves double-stranded DNAs without the addition of a divalent cation, although most restriction enzymes require divalent cations for their activity. The structural and mutational analyses of R.PabI in our previous work showed that R.PabI forms a homodimer and has a novel DNA-binding fold called a "half-pipe," which consists of a highly curved anti-parallel β -sheet. Because the structure of R.PabI shares no structural similarity to any other protein with a known function, the structural basis for the sequence-recognition and DNA-cleavage mechanisms of R.PabI remained unclear. In this study, we report the crystal structure of R.PabI in complex with a double-stranded DNA containing the R.PabI recognition site. The structure of the R.PabI-DNA complex shows that R.PabI unwinds a double-stranded DNA at the 5'-GTAC-3' site and flips the guanine and adenine bases out of the DNA helix to recognize the sequence (Figure). The electron-density map of the R.PabI-DNA complex shows that R.PabI releases adenine bases from the R.PabI recognition site. This suggests that R.PabI catalyzed the cleavage of the *N*-glycosidic bond of adenine nucleotide in the same way as DNA glycosylases. Biochemical assays using HPLC and MALDI-TOF MS spectrometry also support the observation that R.PabI catalyzes the hydrolysis of the *N*-glycosidic bond of adenine nucleotide. These results show that R.PabI is not an endonuclease but a sequence-specific adenine DNA glycosylase. R.PabI is the first example of a restriction enzyme that shows DNA glycosylase activity. Mutational analyses reveal the active site of the adenine DNA glycosylase activity of R.PabI. The two opposing apurinic/aprimidinic (AP) sites generated by R.PabI are cleaved by heat promoted β elimination and/or by endogenous AP endonucleases of

host cells to introduce a double-strand break.

References: K Miyazono, Y Furuta, M Watanabe-Matsui, T Miyakawa, T Ito, I Kobayashi, M Tanokura. Nat Commun. 2014 5:3178.

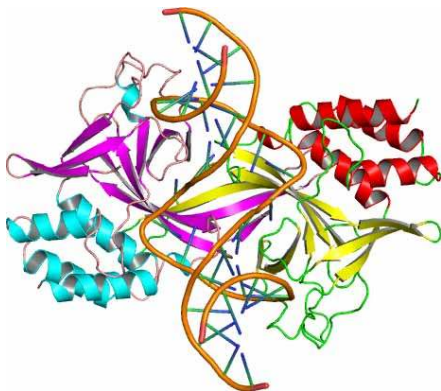


Figure 1. Crystal structure of the R.PabI-DNA complex.

Keywords: restriction enzyme, DNA glycosylase

MS5-P29 Structure-function relationship of zinc-dependent 3' nucleotidases/endonucleases

Jan Dohnalek¹, Tomáš Koval^{1,2}, Mária Trundová¹, Jan Stránský¹, Karla Fajfarová^{1,2}, Petr Kolenko^{1,2}, Jarmila Dušková¹, Tereza Skálová¹, Jindřich Hašek¹

1. Institute of Biotechnology AS CR, Vídeňská 1083, 14220 Prague, Czech Republic

2. Institute of Macromolecular Chemistry AS CR, Heyrovského nám. 2, 16206 Prague, Czech Republic

email: dohnalek007@gmail.com

Our earlier structure-function studies of tomato bifunctional nuclease 1 (TBN1) showed several key characteristics of this nuclease capable of cleaving single strand and double strand DNA, RNA and structured RNA and also capable of 3' nucleotidase activity (Koval *et al.*, 2013). TBN1 belongs to a wider group of zinc dependent nucleases from plants, bacteria and eukaryotic pathogens. Their natural role is in scavenging of nutrients, specific apoptotic processes and senescence in plants or in pathogen – host interactions. Our x-ray structure of the TBN1 enzyme provided a detailed view of the active site and rather unusual and repeated occlusion of the active site in crystal structures by a surface loop of a neighbouring enzyme molecule (Koval *et al.*, 2013). Other structural studies were performed by other groups for *Penicillium citrinum* DNase P1 (Romier *et al.*, 1998) and for an *Arabidopsis thaliana* endonuclease (Yu *et al.*, 2014). The known structures and functional data for all these nucleases prove presence of more or less identical active centre (trinuclear zinc cluster) but show different substrate specificity and modulation of the active site around the catalytic centre, together with varied pH optima and substrate preference/specificity. Attempts were made to describe in detail the catalytic mechanism of this enzyme but our recent data show that our understanding of substrate binding, cleavage and product release is limited and further experiments and analysis are necessary. Here we undertake the task of mapping known structural data onto other known sequences of nucleases of the same type. The main questions include the variability of the role of glycosylation, formation of stabilizing disulfide bridges, presence and nature of the first and second base-binding site, enzyme maturation and especially substrate specificity and inhibition. Our project is focused on structural characterization of *Legionella pneumophila* 3' nucleotidase and its inhibition and related enzymes from trypanosomatids. Recently, we have successfully cloned and expressed this enzyme which under normal conditions is toxic for the producing bacterium.

The project is supported by BIOCEV CZ.1.05/1.1.00/02.0109 ERDF, and MSMT projects EE2.3.30.0029 and LG14009.

1. Koval, T., Lipovova, P., Podzimek, T., *et al.* (2013) Acta Cryst. D69, 213–226.

2. Romier, C., Dominguez, R., Lahm, *et al.* (1998) Proteins, 32, 414–424.

3. Yu T-F., Maestre-Reyna M, Ko, C-Y., *et al.* (2014) PLoS ONE 9(8): e105821.

Keywords: 3' nucleotidase, endonuclease, zinc cluster, substrate specificity, human pathogens, *Legionella*

MS5-P30 A novel *p*-nitrophenyl butyrate-specific esterase from *Photobacterium* sp. 6M7-44 : gene cloning and characterization

Young-Ok Kim¹, In-Suk Park¹, Bo-Hye Nam¹, Dong-Gyun Kim¹, Cheul-Min An¹

1. National Fisheries Research and Development Institute

email: yobest12@korea.kr

A bacterial strain that produced an esterase was isolated from the whole body of arkshell, *Scapharca broughtonii* and identified as *Photobacterium* sp. 6M7-44. In the present study, the corresponding gene was cloned using the shotgun method. The amino acid sequence deduced from the nucleotide sequence (918bp) corresponded to a protein of 305 amino acid residues with a calculated molecular weight of 34,299 Da. The esterase showed 43–45% identities with the putative esterases of *Photobacterium halotolerans*, *Photobacterium angustum* and *Vibrio* sp. N418, respectively. The esterase contained a putative leader sequence, as well as the conserved catalytic triad (Ser, His, Asp), consensus pentapeptide GXSG, and oxyanion hole sequence (HG). The protein 6M7-44 was produced in both soluble and insoluble forms when *Escherichia coli* cells harboring the gene were cultured at 18°C. The enzyme showed specificity for C4 (butyrate) as a substrate, with little activity toward the other *p*-nitrophenyl esters tested. The optimum pH and temperature for enzyme activity were pH 9.0 and 30°C, respectively. Relative activity remained up to 90% even at 5°C with an activation energy of 6.29 kcal/mol, which indicated that it was a cold-adapted enzyme. Enzyme activity was inhibited by Cd²⁺, Cu²⁺, and Hg²⁺ ions. As expected for a serine-esterase, activity was inhibited by phenylmethylsulfonyl fluoride. It was remarkably active and very stable in the presence of commercial detergents and organic solvents. This cold adapted esterase has potentials for use as a biocatalyst and detergent additive for use at low temperature.

Keywords: *Photobacterium* sp., cold-adapted esterase, gene expression, substrate specificity

MS5-P31 Structural studies of a novel type of chitinase from archaea

Yuichi Nishitani¹, Ayumi Horiuchi², Tamotsu Kanai^{2,3}, Haruyuki Atomi^{2,3}, Kunio Miki^{1,3}

1. Graduate School of Science, Kyoto University, Japan.

2. Graduate School of Engineering, Kyoto University, Japan.

3. CREST, Japan.

email: ynishi@kuchem.kyoto-u.ac.jp

Thermococcus chitonophagus is a hyperthermophilic archaeon, isolated from media containing only chitin as carbon source. It is the first hyperthermophile which can grow in such media. To elucidate its ability to degrade and assimilate chitin, we performed genome analysis and found “Tc-ChiX”, a putative novel chitinase. Tc-ChiX has a secretion signal peptide and two regions having high sequence identity with chitin binding domain of chitinase from a hyperthermophilic archaeon *T. kodakarensis* in the N-terminal domain. On the other hand, the C-terminal domain contains no DXDXE motif conserved in the GH18-type chitinase family and even shares no sequence similarity. We have performed X-ray structure analysis of Tc-ChiX to clarify the reaction mechanism of this chitinase.

As the overexpression of Tc-ChiX in full-length was not straightforward, we constructed Tc-ChiX(ABD), only consisting of a putative chitinase domain. This truncated mutant could be sufficiently overexpressed and retained its enzymatic activity. We initially crystallized the sample of this mutant at 20°C, and obtained crystals of the substrate complex diffracting X-rays to 2.55 Å resolution. Moreover, when the crystallization temperature was changed to 35°C, crystals with a different shape were obtained. Diffraction experiments revealed that the maximum resolution of new crystals was improved to 1.95 Å and the space group was also changed from P2₁2₁2₁ to P6₃. Finally, we determined both crystal structures. These structures are different in crystal packing, and substrate-binding modes are also remarkably different. We will discuss the reaction mechanism and the substrate selectivity of Tc-ChiX based on obtained structural and biochemical information.

Keywords: archaea, chitinase, crystal structure

MS5-P32 pH-profile analysis of β -amylase/maltose complex crystal measured at room temperature

Bunzo Mikami¹, Hirokazu Kawamura¹, Kimihiko Mizutani¹, Nobuyuki Takahashi¹

¹. Laboratory of Applied Structural Biology, Graduate School of Agriculture, Kyoto University, Japan

email: mikami@kais.kyoto-u.ac.jp

β -amylase catalyzes the liberation of maltose from the non-reducing ends of α -1, 4-glucan such as starch and glycogen. In contrast to α -amylase, β -amylase produces β -anomeric maltose, and is classified as an inverting enzyme. Though the structural features of β -amylases have been clarified, the detailed enzymatic mechanism of β -amylase action has not been well understood especially in the hydrolytic process including the activation of glycoside linkage to be cleaved. In soybean β -amylase (SBA), the hydrolysis of the α -1, 4-glucosyl linkage is proceeded by two catalytic residues, Glu186 (acid) and Glu380 (base). The enzyme has two mobile loops, flexible loop (residue 96-103) and inner loop (residue 341-345) near the active site. The conformation of these loops change during enzyme action. In this paper, we are intended to determine the structural changes of SBA/maltose complex in a different pH media. In order to control pH correctly, we have determined the crystal structure at room temperature to avoid the undesirable effect of freezing and cryo-protectant such as glycerol. SBA was crystallized by a hanging-drop vapor diffusion (10 ml of 10mg/ml enzyme) against 1 ml of the bottom solution containing 45% saturated ammonium sulfate. The obtained crystals larger than 0.3 mm length were packed in glass capillaries after soaked with 200mM maltose in the different pH buffer, containing 45% saturated ammonium sulfate for 30min at 20°C. More than ten diffraction data sets were collected at room temperature with a CCD detector at BL26B1 beam-line at SPring-8. The crystal of SBA belonged to a space group of $P3_121$. The crystal data were collected with 98-100 % completeness and R_{merge} of 0.04-0.05 up to 1.58-1.68 Å resolution. The models were refined with SHELXL program including protein anisotropic B-factors. The refined models contains one molecules of SBA comprising 492 amino acid residues, 3-7 sulfate ions and 403-450 water molecules with $R = 0.12$ -0.13 and $R_{\text{free}} = 0.14$ -0.16. At pH 4.9-7.8, two maltose molecules were located at the subsites -2~-1 and +1~+2 with α -anomer boat form at subsite -1, whereas α/β -anomer chair forms were clearly found at pH below 4.4 (Fig. 1). This indicates that the glucose residue at subsite -1 is distorted to boat form by the deprotonation of a protein residue in the active site. The elucidation of the structure significance of the distorted sugar form on the catalytic process of this enzyme is now in progress.

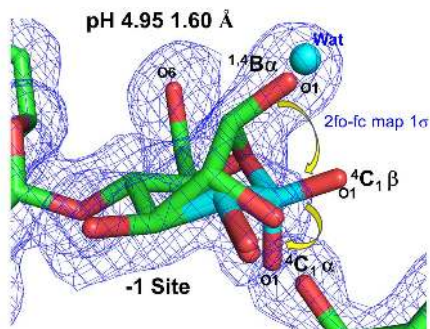


Figure 1. The effect of pH on the binding mode of maltose in the active site of SBA.

Keywords: beta-amylase, enzyme/substrate complex, enzyme catalytic mechanism

MS5-P33 Structure-functional relationships of a novel haloalkane dehalogenase with two halide-binding sites

Tatyana Prudnikova^{1,2}, Radka Chaloupkova³, Pavlina Rezacova^{4,5}, Jiri Damborsky³, Ivana Kuta-Smatanova^{1,2}

1. Faculty of Science, University of South Bohemia in Ceske Budejovice, Ceske Budejovice, Czech Republic
2. Institute of Nanobiology and Structural Biology, Academy of Sciences of the Czech Republic, Nove Hradky, Czech Republic
3. Loschmidt Laboratories, Department of Experimental Biology and Research Centre for Toxic Compounds in the Environment RECETOX, Masaryk University, Brno, Czech Republic
4. Institute of Molecular Genetics, Academy of Sciences of the Czech Republic, Prague, Czech Republic
5. Institute of Organic Chemistry and Biochemistry, Academy of Sciences of the Czech Republic, Prague, Czech Republic

email: talianensis@gmail.com

Haloalkane dehalogenases (EC 3.8.1.5) are bacterial enzymes cleaving a carbon-halogen bond by a hydrolytic mechanism in a broad range of halogenated aliphatic compounds [1]. Novel haloalkane dehalogenase DbeA from *Bradyrhizobium elkanii* USDA94 was structurally and biochemically characterized in this study. The crystal structure of DbeA was solved to 2.2 Å resolution and revealed the presence of two halide-binding sites. The first chloride-binding site was located in the active site in between two halide-stabilizing residues. The second chloride-binding site was buried deeply in the protein core and was approximately 10 Å from the first binding site. This second halide-binding site is unique to DbeA and has not been previously reported in any other crystal structure of this enzyme family. To elucidate the role of the second halide-binding site in enzyme functionality, a two-point mutant (I44L+Q102H) lacking this site was constructed, purified and biochemically characterized. Its comparison with the wild type enzyme revealed that elimination of the second halide-binding site decreased stability of the enzyme in the presence of chloride salt and decreased its catalytic activity by an order of magnitude. Moreover, the two-point substitution resulted in a shift of the substrate-specificity class, which is the first time this has been demonstrated for the haloalkane dehalogenase enzyme family. Changes in the catalytic activity of the variant were attributed to deceleration of the rate-limiting hydrolytic step, mediated by lower basicity of the catalytic histidine [2].

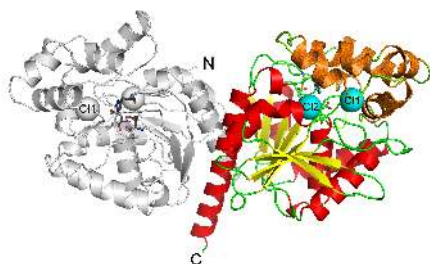


Figure 1. Overall structure of the haloalkane dehalogenase DbeA.

Keywords: Haloalkane dehalogenase, halide-binding site,

MS5-P34 Structure-functional studies of selected haloalkane dehalogenases

Ivana Kuta-Smatanova^{1,2}

1. Faculty of Science, University of South Bohemia in Ceske Budejovice, Branisovska 31, 370 05 Ceske Budejovice, Czech Republic
2. Institute of Nanobiology and Structural Biology, Academy of Sciences of the Czech Republic, 142 20 Prague, Czech Republic

email: ivanaks@seznam.cz

X-ray crystallography is the major technique to get the structure of biological macromolecules at atomic resolution. Protein structures are central to understand the detailed mechanisms of biological processes and to discover novel therapeutics, biosensors, etc. using a structure-based approach. Several non-membrane and membrane protein complexes, which are important for living on the earth, have been crystallized using different crystallization techniques such as standard, advanced and alternative methods.

At this time several haloalkane dehalogenases, their mutant variants and complexes with substrates are systematically studied in our laboratory. Developed methods, obtained crystallization and crystallographic data were compiled and results were published in scientific journals [1]. This presentation will be focused on description and comparison of crystallization conditions and crystallographic results of selected proteins such as DhaA from *Rhodococcus rhodochrous* NCIMB 13064, DbeA of *Bradyrhizobium elkanii* USDA94, LinB of *Sphingobium japonicum* UT26, DpcA from *Psychrobacter cryohalolentis* K5, and DmxA from *Marynabacter sp* ELB 17.

This research is supported by the GACR (P207/12/0775).

1. Chaloupkova R, et al., *Acta Crystallogr. D Biol. Crystallogr.* **70**, 1884–1897 (2014)

Keywords: haloalkane dehalogenases, crystallization, structure

MS5-P35 Solution studies of human dipeptidyl peptidase III (hDPPIII) reveals dynamic equilibrium between different substates

Prashant Kumar¹, Henning Seidel², Young-Hwa Song², Christian Hübner², Peter Macherox³, Karl Gruber¹

1. Institute of Molecular Biosciences, University of Graz, Graz - 8010, Austria
2. Institute of Physics, University of Lübeck, Lübeck, Germany
3. Institute of Biochemistry, Graz University of Technology, Graz, Austria

email: prashant.kumar@uni-graz.at

Dipeptidyl peptidase III (DPPIII) is one of the most important enkephalin degrading enzymes associated with mammalian pain modulatory system. DPP III is also known to degrade several opioid peptides apart from enkephalin and endomorphin. Since the opioid peptides modulate a large number of physiological processes, therefore DPP III is an important molecule to study. The crystal structure of the free form of the enzyme shows an open, extended conformation, whereas the crystal structure of the complex reveals a large conformational change upon peptide binding (Bezerra et al., PNAS, 2012). To investigate the behaviour of human DPPIII (hDPPIII) in solution we performed SAXS measurements which shows that this substrate triggered conformational change also occurs in solution. For the unbound form, however, the SAXS data indicate that the protein exists in either a mixture of fully open, fully closed or of other, different intermediate conformations. This conformational plasticity revealed by crystal structure and SAXS led us to perform single molecule fluorescence resonance energy transfer (smFRET) with hDPPIII. SmFRET results show a broad range of energy transfer distribution between the two labels for the unbound form of the enzyme, with one maxima at low energy transfer corresponding to fully open conformation and another maxima at an intermediate closed conformation. For the bound form of the enzyme, two main maxima are observed, one at high energy transfer efficiency corresponding to the fully closed conformation and the other at a similar energy distribution as the intermediate closed conformation. These observations suggest the existence of equilibrium between different substates within the conformational space of the enzyme. Recently we were able to capture the crystal structure of the closed form of the enzyme in the absence of any ligand, however the crystal structure of the intermediate state still eludes us. The role of the intermediate state is unclear at the moment but this might just explain the promiscuity displayed by the enzyme. Our MD simulation data of 1.5 μ sec also indicates the existence of intermediate state which is in agreement with our experimental data. The insights gained by our structure determination and solution studies on hDPPIII provide valuable information about a common thread between structural and functional properties of enzymes and also the relation between the conformational dynamics and chemistry in enzyme catalysis.

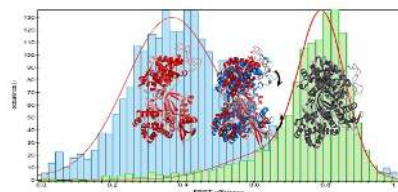


Figure1: Energy transfer histogram of human DPP III from smFRET. Energy transfer efficiency histogram of unbound (in blue) and bound (green). Crystal structure of fully open (blue), fully closed (black) and intermediate structure obtained from MD simulation (blue) superimposed with fully open structure (red). All three structures placed roughly according to their energy transfer efficiency.

Figure 1. Energy transfer efficiency histogram of hDPP III from smFRET and structures corresponding to their energy transfer efficiency

Keywords: Conformational plasticity, Opioid peptides, Peptidase, Single molecule, SAXS

MS5-P36 High-density transfection is superior for production of readily crystallizable glycoproteins in suspension adapted HEK293S GnTI⁻ cells: a case study of human lymphocyte receptor LLT1

Ondřej Vaněk¹, Jan Bláha¹, Petr Pachl², Petr Novák^{1,3}

1. Department of Biochemistry, Faculty of Science, Charles University in Prague, Hlavova 8, Prague, 12840, Czech Republic

2. Institute of Organic Chemistry and Biochemistry, Academy of Sciences of the Czech Republic, Flemingovo nám. 2, Prague, 16610, Czech Republic

3. Institute of Microbiology, Academy of Sciences of the Czech Republic, Vídeňská 1083, Prague, 14220, Czech Republic

email: ondrej.vanek@natur.cuni.cz

Human embryonic kidney 293 cell line deficient in N-acetylglucosaminyltransferase I (HEK293S GnTI⁻) is well known tool for recombinant expression of proteins with homogeneous and deglycosylatable N-glycosylation, a feature crucial especially within protein crystallography [1]. So far production protocols using this cell line were based either on lengthy stable cell line generation or transient transfection of adherent cell culture that is costly to scale-up and has reportedly lower expression yields [2].

In this work we have adapted HEK293S GnTI⁻ cell line to growth in suspension and optimized its transient transfection. While transfection at standard cultivation cell density proved very little success we have found out that concentrating the cells to high cell density substantially increases transfection efficiency, greatly enhancing protein yields and creating fast and scalable production process.

We demonstrate this on the production of soluble lectin-like transcript 1 (LLT1, gene *lec2d*) receptor naturally present on natural killer and T-lymphocytes, but upregulated in glioblastoma cells, one of the most lethal tumors, where it acts as a mediator of immune escape. Furthermore, we show that His176Cys mutation is critical for LLT1 stability, leading to reconstruction of disulfide bridge and that LLT1 forms non-covalent homodimer whose dimerization does not depend on presence of its N-glycans [3].

The prepared soluble domain of LLT1 with homogeneous glycosylation was readily crystallized and following optimization of crystal conditions this protein preparation ultimately led to the first structure determination of this receptor described so far [4].

This study was supported by BIOCEV CZ.1.05/1.1.00/02.0109 from the ERDF, by the Czech Science Foundation (project 15-15181S), by the Ministry of Education, Youth and Sports of the Czech Republic (grant LG14009), by Charles University (UNCE 204025/2012, SVV 260079/2014), High Education Development Fund (FRVS 669/2013), BioStruct-X (EC FP7 project 283570) and Instruct, part of the European Strategy Forum on Research Infrastructures (ESFRI) supported by national member subscriptions.

[1] Reeves *et al.*, *Proc. Natl. Acad. Sci. USA* 99, 2002, 13419-13424. [2] Aricescu *et al.*, *Acta Cryst. D62*, 2006, 1243-1250. [3] Bláha *et al.*, *Protein Expres. Purif.* 109, 2015, 7-13. [4] Skálová *et al.*, *Acta Cryst. D71*, 2015, 578-591.

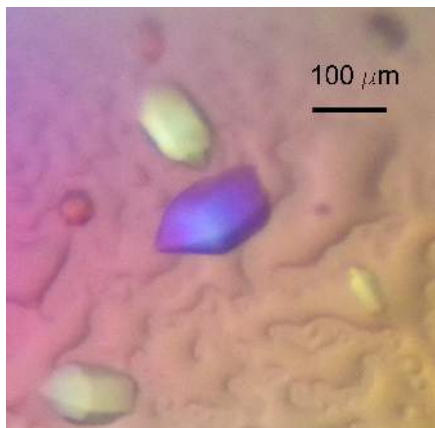


Figure 1. First observed crystals of glycosylated LLT1(H176C) receptor soluble domain produced in HEK293S GnTI⁻ cell line.

Keywords: LLT1; HEK293S GnTI⁻; C-type lectin-like; NK cell; N-glycosylation; transient transfection; lymphocyte receptor

MS5-P37 Structural investigation of the small GTPase ARL4DSasa Petrovic¹, Yvette Roske¹, Udo Heinemann¹

1. Max Delbrück Center for Molecular Medicine, Robert-Rössle-Strasse 10, 13125 Berlin, Germany

email: sasa.petrovic@mdc-berlin.de

ARL4D (ADP-ribosylation factor-like protein 4D) is a small GTPase which cycles from the membrane-attached GTP-bound form and the cytosolic GDP-bound form (1). It is a member of the ADP-ribosylation factor/ARF-like protein (ARF/ARL) family of Ras-related GTPases. ARL4D contains a nuclear localization signal on the C-terminus, thus can be found in the nucleus (2), as well as at the cytoplasm and plasma membrane (1). The membrane binding of ARL4D is mediated by both an N-terminal myristoyl group and an N-terminal amphipathic helix (3). *ARL4D* expression is developmentally regulated during embryogenesis (2), and its overexpression has been shown to suppress adipogenesis (4). ARL4D has the ability to recruit ARNO (Arf nucleotide-binding site opener) to the plasma membrane through interaction with its pleckstrin homology (PH) domain (1). Subsequently, ARNO acts as a nucleotide exchange factor and activator of Arf6, a small GTPase that regulates endocytosis, actin dynamics and cell adhesion (5, 6). Our aim is to characterize, structurally and biochemically, ARL4D alone, and in complex with its interaction partner ARNO. This will provide an insight into the mode of function of this GTPase, and a possibility to explain specific features compared to other members of the ARF/ARL family.

(1) Hofmann E, *et al.* (2007). "The Arl4 family of small G proteins can recruit the cytohesin Arf6 exchange factors to the plasma membrane". *Current Biology*, 17: 711–716.

(2) Lin CY, *et al.* (2000). "ARL4, an ARF-like protein that is developmentally regulated and localized to nuclei and nucleoli". *Journal of Biological Chemistry*, 275: 37815–37823.

(3) Pasqualato S, *et al.* (2002). "Arf, Arl, Arp and Sar proteins: A family of GTP-binding proteins with a structural device for 'front-back' communication". *EMBO Reports*, 3: 1035–1041.

(4) Yu J, *et al.* (2011). "Overexpression of the small GTPase Arl4D suppresses adipogenesis". *International Journal of Molecular Medicine*, 28: 793–798.

(5) Chardin P, *et al.* (1996). "A human exchange factor for ARF contains Sec7- and pleckstrin-homology domains". *Nature*, 384: 481–484.

(6) Li C, *et al.* (2007). "ARL4D recruits cytohesin-2/ARNO to modulate actin". *Molecular Biology of the Cell*, 18: 4420–4437.

Keywords: crystallography, GTPase**MS5-P38** Characterization of electrostatic interactions in active sites of caspasesUrszula A. Budniak¹, Paulina M. Dominiak¹

1. Department of Chemistry, University of Warsaw, Pasteura 1, 02-093 Warsaw, Poland

email: ubudniak@chem.uw.edu.pl

Apoptosis (programmed cell death) is an intensely examined cell process because its failure can trigger a tumor development. Enzymes that play crucial role in apoptosis, but also in necrosis and inflammation, are called caspases and belong to the family of cysteine proteases. Initiator caspases receive a signal, get activated and cleave effector caspases, which cleave other proteins leading to cell death. This chain reaction is known as "caspase cascade".

For the purpose of this project various caspases interacting with inhibitors were examined. The Protein Data Bank [1,2] was utilized to find the highest quality structures of caspases bounded up with ligands. After structure validation, all missing hydrogen atoms were added. Electron density distribution of protein complexes was reconstructed using the Transferred Aspherical Atom Model approach based on the University at Buffalo Databank [3,4]. This database contains multipolar parameters describing electron density of pseudoatoms obtained via theoretical calculations. On the basis of electron density distribution, energy of electrostatic interactions was calculated. Characterization of intermolecular interactions was possible thanks to calculations in the Mopro [5] or XD [6] program.

Investigations of energetic properties of caspases may contribute to our knowledge about protein properties in general and, more importantly, gives an opportunity to find novel ligands binding more effectively to their active sites, what is essential for drug design.

References:

1. RCSB PDB www.rcsb.org/pdb.
2. Berman, H.M et al. (2000) *Nucl. Acids Res.*, 28: 235–242.
3. Volkov, A., Li, X., Koritsanszky, T. S., Coppens, P. (2004) *J. Phys. Chem. A*, 108: 4283–4300.
4. Jarzemska, K. N., Dominiak, P. M. (2010) *Acta Cryst A*, 68: 139–147.
5. Guillot B., Viry L., Guillot R., Lecomte C. & Jelsch C. (2001) *J. Appl. crystallogr.*, 34: 214–223.
6. Volkov, A.; Macchi, P.; Farrugia, L. J.; Gatti, C.; Mallinson, P.; Richter, T.; Koritsanszky, T. (2006) XD2006 - a computer program package for multipole refinement, topological analysis of charge densities and evaluation of intermolecular energies from experimental and theoretical structure factors.
7. DOI: 10.2210/pdb4ps1/pdb.

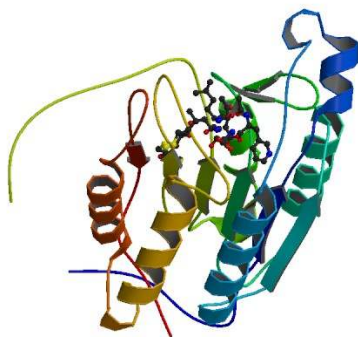


Figure 1. An example of caspase with a ligand (PDB ID: 4PS1) [7]

Keywords: caspases, ligands, electrostatic interactions, UBDB, TAAM

MS5-P39 Crystallization and structural characterization of glyceraldehyde dehydrogenase from *Thermoplasma acidophilum*

Iuliia Iermak¹, Jeroen R. Mesters², Oksana Degtjarik¹, Fabian Steffler³, Volker Sieber³, Ivana Kuta Smatanova^{1,4}

1. Faculty of Science, University of South Bohemia, Branišovska 31, CZ-37005 České Budejovice, Czech Republic

2. Institute of Biochemistry, University of Lübeck, Ratzeburger Allee 160, 23538 Lübeck, Germany

3. Chemistry of Biogenic Resources, Straubing Centre of Science, Technische Universität München, Schulgasse 16, 94315 Straubing, Germany

4. Institute of Nanobiology and Structural Biology GCRC, Academy of Sciences of the Czech Republic, Zamek 136, 373 33 Nove Hrad, Czech Republic

email: julia.ermak90@gmail.com

Biotechnological production of chemical compounds is an environmentally more gentle process compared to their fabrication from natural fossil resources. In terms of bio-production, cell-free processes are more effective than microbial production techniques since the enzymes can tolerate higher concentrations of final product than the cells. The glyceraldehyde dehydrogenase from *Thermoplasma acidophilum* (TaAIDH) is a part of an artificial cell-free enzyme cascade for production of isobutanol and ethanol from glucose. TaAIDH catalyzes the oxidation of D-glyceraldehyde to D-glycerate in this synthetic pathway. Various mutants of TaAIDH were constructed by random approach followed by site-directed and saturation mutagenesis in order to improve the enzymes' properties essential for its functioning within the cascade. Further optimization of TaAIDH requires structural information about the enzyme for which crystallization followed by X-ray diffraction analysis was employed.

Different types of TaAIDH wild-type crystals grew within one to two weeks after initial screening in 30 diverse conditions. In order to obtain the best quality crystals, optimization was carried out considering the following parameters: (a) already known diffraction quality of crystals; (b) size and shape of crystals (big single crystals with sharp edges preferred); (c) different crystal forms. Optimization, including variation of pH, protein and precipitant concentrations and ratios, resulted in adequate crystal quality only for condition H6 of the Morpheus screen (Molecular Dimensions Ltd., UK). These crystals diffracted X-rays to 1.95 Å resolution and belonged to space group $P2_1$ with 8 molecules per asymmetric unit and unit cell parameters of $a = 95.29$ Å, $b = 152.35$ Å, $c = 149.90$ Å, $\alpha = \gamma = 90.0^\circ$, $\beta = 92.19^\circ$.

The structure of TaAIDHwt was solved by molecular replacement using the coordinates of betaine-aldehyde dehydrogenase from *Pseudoalteromonas atlantica* T6c (sequence identity 38%, PDB ID 3K2W). The final model contains two tetramers in the asymmetric unit that are related by non-crystallographic symmetry with

differences observed in regions participating in crystal contacts. The *TaAldHwt* homotetramer consists of two homodimers that display a very tight connection through the formation of an extended beta-sheet between monomers of the dimer. The structure refinement of *TaAldHwt* is in progress.

Keywords: glyceraldehyde dehydrogenase, cell-free enzyme cascade, bioproduction

MS5-P40 Structural and biochemical characterization of dipeptidyl peptidase III from *Porphyromonas gingivalis*

Altijana Hromic¹, Nina Jajcanin-Jozic², Prashant Kumar¹, Silvia Wallner³, Peter Macheroux³, Marija Abramic², Karl Gruber¹

1. Institute of Molecular Biosciences, University of Graz, Graz, Austria

2. Institute Rudjer Boskovic, Zagreb, Croatia

3. Institut of Biochemistry, Graz University of Technology, Graz, Austria

email: altijana.hromic@uni-graz.at

Porphyromonas gingivalis is gram-negative, human pathogenic bacterium. It is found in the oral cavity and it is known to cause periodontal disease by invading human gingival fibroblasts. It also contains an enzyme which belongs to the DPP III family. Dipeptidyl peptidase III (DPP III), also known as enkephalinase B, is an enkephalin-degrading enzyme that cleaves dipeptides sequentially from the N-termini of substrates. All DPPs III described thus far contain the unique zinc binding motif HEXXGH characteristic for metallopeptidase family M49. An important role of DPP III in the mammalian pain modulatory system is supported by several recent findings: low levels of DPP III activity were detected in the cerebrospinal fluid of individuals suffering from acute pain; DPP III exhibits high in vitro affinity towards the important neuropeptides endomorphin-1 and endomorphin-2. The exact function of DPP III from *Porphyromonas gingivalis* is still unknown. It could possibly be involved in pathogenicity. With the human DPP III shares 20,3 % sequence identity. According to homology model, it was possible to obtain two domains: one is DPP III domain also observable in humans and additional alpha-alpha superhelix domain which is not recognized as transmembrane domain. We aim at determining the potential substrates and also to solve the structure of the enzyme in order to get insight into the potential function of the protein. Here we represent the ITC- and SAXS- data as well as crystallization experiments as first important steps towards this goal.

Keywords: DPP III, SAXS, ITC, Crystallization

MS5-P41 Structure and function of microcystin and CP12-CBS in toxic cyanobacteria

Claudia Hackenberg¹, Elke Dittmann², Victor Lamzin¹

1. European Molecular Biology Laboratory, c/o Desy, Hamburg, Germany
2. Institute for Biochemistry and Biology, University of Potsdam, Germany

email: hackenberg@embl-hamburg.de

Microcystins (MC) are the most common and notorious toxins produced by harmful cyanobacterial blooms in marine, brackish and fresh water habitats. They strongly inhibit protein phosphatases type 1 and 2A in the liver by covalently binding to cysteines in the active site [1,2], causing severe and often lethal hepatic necrosis. It is assumed that MC increase the resistance of toxic cyanobacteria towards various environmental stresses [3,4], enabling the toxic species to become dominant. Detailed knowledge about the actual molecular function of MC is, however, still fairly limited.

We aim to follow up on the hypothesis that MC binds to the cysteine pairs of proteins and acts as protein-modulating metabolite [4] by investigating its effect on two known target proteins: the small regulatory Calvin cycle protein 12 (CP12) and the photosynthetic protein phosphoribulokinase (PRK) of *Microcystis*. These proteins are of particular interest, because: 1) the activity of PRK is regulated by CP12 in a redox-dependent manner [5]; 2) cyanobacteria possess a variety of several CP12-variants, a.o. curiously being fused to a CBS domain (Bateman domain) [6]. The CBS domain is found in various organisms, where it is fused to a wide range of proteins regulating their activity. Mutations of the CBS domain are implicated in several hereditary human diseases [7]. Its function in cyanobacteria, particularly as fusion protein with CP12, is so far unknown.

The fusion of CP12 with CBS suggests a functional connection as well as different, multiple roles of CP12 in cyanobacteria. The interaction of CP12 and PRK with microcystin may even add a further layer of complexity in the regulation, stability and activity of these proteins in harmful cyanobacteria. Using interaction studies and macromolecular crystallisation we aim to explore: 1) the role of the CBS domain in CP12; 2) whether CP12-CBS is still regulating PRK; 3) the binding site of microcystin on PRK and CP12; and 4) if microcystin is affecting the stability, conformation and activity of CP12-CBS and PRK.

- [1] Goldberg et al., Nature 376:745-753 (1995)
- [2] Xing et al., Cell 127:341-353 (2006)
- [3] Dzailas & Grossart, PLoS ONE 6:e25569 (2011)
- [4] Zilliges et al., PLoS ONE 6:e17615 (2011)
- [5] Tamoi et al., Proc. Natl. Acad. Sci. USA, 42:504-513 (2005)
- [6] Stanley et al., Plant J., 161:824-835 (2013)
- [7] Scott et al., J. Clin. Invest. 113:274-284 (2004)

Keywords: Microcystin, CP12, Phosphoribulokinase

MS5-P42 Biochemical and structural studies of substrate recognition and reaction mechanism of M23 metallopeptidases

Izabela Sabala¹, Elżbieta Jagielska¹, Maja Grabowska¹, Honorata Czapinska¹, Matthias Bochtler^{1,2}

1. International Institute of Molecular and Cell Biology, Warsaw, Poland
2. Institute of Biochemistry and Biophysics, Polish Academy of Sciences, Warsaw, Poland

email: izabela@iimcb.gov.pl

Peptidoglycans build a thick layer around each cell providing a solid envelop around the cell and securing its integrity. They have to be rigid to stand the internal pressure and at the same time flexible to allow cell expansion and division. The rigidity of the cell wall is provided by the thick network of peptidoglycans while its flexibility by orchestrated action of peptidoglycan hydrolases. Each bond in peptidoglycans is believed to be cut by a specific hydrolase. Many of them have been biochemically and structurally characterized but despite enormous efforts a basic questions on their mechanism of action or determination of specificity remains unanswered. Composition and structure of peptidoglycan is species specific and in the case of *Staphylococcus* is characterized by presence of pentaglycine cross-bridges, which are cleaved by endopeptidases belonging to M23 family of metallopeptidases, like an autolysin LytM and a bacteriocine lysostaphin. These two enzymes have the same specificity and catalytic domains of over 50% of aa identity but they differ in their role and activity regulation. By combining biochemical and structural methods we have gained new insights into structural bases of peptidoglycan recognition and mechanism of action of M23 family represented by lysostaphin and LytM. We have crystallized and analyzed structures of (1) full length lysostaphin, (3) catalytic domain of lysostaphin and the (3) LytM catalytic domain in complex with transition state analogue. These analysis supported by biochemical tests allow us to propose and discuss the possible mechanism of hydrolysis for M23 peptidases and defined some of the structural features determining substrate specificity. This information is important not only for our deeper understanding of basic biological processes but might also have a great impact on application of these enzymes in combating staphylococcal infections. Lysostaphin has been successfully tested in various biomedical applications but the main limitation of its use is naturally occurring resistance caused by incorporation of serine into the pentaglycine bridges. The same applies to LytM demonstrating effectiveness as antibacterial agent. Our research might provide information necessary for engineering enzyme specificity overcoming the existing resistance mechanism.

Keywords: M23 peptidases, peptidoglycan hydrolases, lysostaphin, LytM, staphylococcus

MS5-P43 Structure and function of lytic polysaccharide monoxygenasesSaioa Urresti¹, Glyn R. Hemsworth¹, Hannah C. Screeton¹, Paul H. Walton¹, Gideon J. Davies¹¹. York Structural Biology Laboratory, Department of Chemistry, The University of York, YO10 5DD, York, UK

email: saioa.urresti@york.ac.uk

The drive for energy security and environmental sustainability has led to the development of biofuels derived from waste biomass such as lignocellulose, chitin etc., generically known as second generation biofuels. However, the degradation of these substrates is difficult due to their high complexity and recalcitrance. Classic glycoside hydrolases (GHs) can achieve this degradation, but their efficiency is limited. A major recent breakthrough has been the discovery of novel mononuclear Cu oxygenases termed "lytic polysaccharide monoxygenases" (LPMOs)¹ that oxidatively open-up the crystalline biomass rendering it accessible to GH action. LPMOs are found in a number of sequence-based families (www.cazy.org) where they generically termed "Auxiliary Activities" and are classified into families AA9, AA10, AA11 and AA13. Recent structural insight has revealed that the majority of structures present a flat surface, where catalysis takes place at the Cu centre. I shall present details of new LPMO structures, demonstrate how these enzymes produce aldonic acid products and show how photo-reduction in the synchrotron X-ray beam complicates electron density interpretation.

¹Hemsworth *et al.*: Recent insights into copper-containing lytic polysaccharide mono-oxygenases. Curr. Opin. Struct. Biol. 2013, 23, 660–668.

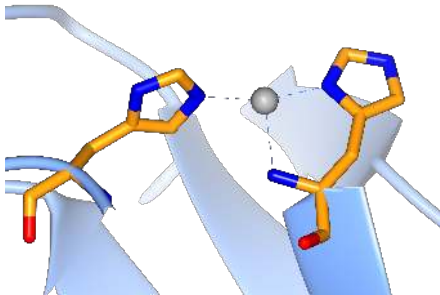


Figure 1. Histidine brace. The copper is coordinated by the imidazole and main-chain amino group of the N-terminal histidine and a further histidine imidazole group. The metal displays a Cu (I) coordination in the crystal structure (in contrast with the EPR results), due to radiation damage.

Keywords: Lytic polysaccharide monoxygenases, LPMO, copper-dependent oxygenase

MS5-P44 Structural basis of the peptidoglycan binding to LytA, the major pneumococcal autolysinTatyana Sandalova¹, Birgitta Henriques-Normark^{2,3}, Dusan Heseck⁴, Mijoon Lee⁴, Shahriar Mobashery⁴, Alexey Kikhney⁵, Dmitri Svergun³, Peter Mellroth^{2,3}, Adnane Achour¹

1. Karolinska Institutet, Science Life Lab, Stockholm, Sweden
2. Department of Microbiology, Tumor and Cell Biology (MTC), Karolinska Institutet, 171 77 Stockholm, Sweden
3. Department of Laboratory Medicine, Division of Clinical Microbiology, Karolinska University Hospital, 17176 Stockholm, Sweden
4. Departments of Chemistry and Biochemistry, University of Notre Dame, Notre Dame, 46556 Indiana, USA
5. European Molecular Biology Laboratory (EMBL), Hamburg Outstation, Notkestrasse 85, 22603 Hamburg, Germany

email: Tatyana.Sandalova@ki.se

Autolysins are bacterial cell wall hydrolytic enzymes that mediate antibiotic induced lysis and may function as important virulence factors for bacterial pathogens. The cell wall of *S.pneumoniae* is a complex three-dimensional network of peptidoglycan (PG) and teichoic acids which protect the cells against mechanical stress and internal osmotic pressure and serves as a scaffold for many associated proteins that modulate the cell wall activity or interacts with the environment. The major autolysin of *S.pneumoniae*, LytA breaks the PG by hydrolyzing the amide bond between glycan chains and peptide stems. LytA associates with the cell wall through its C-terminal choline-binding domain by non-covalent interactions with phosphocholine moieties of the pneumococcal teichoic acids.

We present the three-dimensional structure of the major autolysin LytA of *Streptococcus pneumoniae*. The crystal structure of two separate LytA domains combined with small angle X-ray scattering of the full length protein reveal that LytA homodimer adopts a cherry-like conformation with two catalytic domains located far from each other, in trans configuration relatively to the plane of the two C-terminal choline-binding domains.

The 1.05Å crystal structure of the catalytic domain exhibits a prominent Y-shaped binding crevice that can accommodate a peptidoglycan fragment of four/five saccharides and a stem pentapeptide. The active site contains a zinc ion bound to two histidine residues and one aspartate, located at the bottom of the branch point of the crevice. Co-crystallization of the inactive mutant of the LytA catalytic domain and a peptidoglycan fragment produced crystals of the complex diffracting to the same resolution as substrate-free LytA. This allowed us to model more than 100 atoms of the peptidoglycan fragment. The structure displays the specific conformation of four sugars in the active site of autolysin different from any other peptidoglycan fragment. The importance of protein-sugar interactions far from the catalytic site was confirmed by mutational studies. We hypothesize that substrate requirements restrict LytA to the sites on the cell wall where nascent peptidoglycan synthesis occurs.

Keywords: Peptidoglycan, autolysis

MS5-P45 Structure and mechanism studies of human tyrosinase

Xuelei Lai^{1,2}, Montserrat Soler-López², Harry J. Wichers³, Bauke W. Dijkstra¹

1. Laboratory of Biophysical Chemistry, University of Groningen, Groningen, The Netherlands
2. ESRF-The European Synchrotron
3. Wageningen University and Research Center, Wageningen, The Netherlands

email: lai@esrf.fr

Tyrosinase (EC 1.14.18.1) is a binuclear copper-containing enzyme that is widely distributed throughout bacteria, fungi, plants and animals. The enzyme catalyzes the *o*-hydroxylation of monophenols to the corresponding *o*-diphenols and the subsequent conversion of the *o*-diphenols to the corresponding *o*-quinones. Tyrosinases have been implicated in a variety of biological functions. In plants, tyrosinases have been suggested to participate in wound healing, defense reactions and in the synthesis of flower pigments. In fungi, tyrosinases have been postulated to participate in spore formation, defense reactions, and pigmentation. In mammals, including humans, the enzyme is responsible for skin pigmentation abnormalities, such as albinism, vitiligo and other melanin-related syndromes.

Human tyrosinase is a type I trans-membrane glycoenzyme that is found specifically in neural crest-derived pigment-producing cells (melanocytes) of the skin, choroid and iris and in the neuroectoderm-derived RPE (Retinal Pigment Epithelium) of the eye. It catalyzes the initial and rate-limiting steps of melanin pigment production. Mutations in the human tyrosinase gene directly cause oculocutaneous albinism type 1 (OCA1), an autosomal recessive disorder characterized by reduced melanin pigment in the hair, skin and eyes.

The aim of this project is to solve the crystal structure of human tyrosinase and its substrate/inhibitor bound structures using crystallography, and characterize some of the most novel mutants that cause OCA1. These information will help us to understand the structure basis for the oculocutaneous albinism type 1 and provide valuable information for drug design. We have successfully expressed human tyrosinase in insect cells as secreted protein and is fully active. We also crystallized it under several different conditions and the crystals diffracted up to 4 Å in the first diffraction test.

Keywords: enzyme, crystallography

MS5-P46 *Helicobacter pylori* protein function assignment through the 3D structure

Giuseppe Zanotti¹

1. Department of Biomedical Sciences, University of Padua, Via Ugo Bassi 58/B, 35131 Padua, Italy

email: giuseppe.zanotti@unipd.it

Despite the identification of *H. pylori* dating back to 1984, its pathogenesis remains poorly understood at the molecular level. In our laboratory we are working on the structural characterization of proteins of the bacterium relevant for pathogenesis or host colonization. In this communication we will focus on four secreted proteins, whose function was unknown or undefined, and we will show how the crystal structure, combined with other experimental evidences, can provide clues about the physiological function of the protein.

HP1561. Its high-resolution structure reveals a bi-lobed fold with a narrow cleft between the N- and C-terminal domains. CeuE shares a common architecture typical of Class III periplasmic binding proteins. Crystal structure and solution data demonstrate that it binds Ni²⁺ through a metallophore.

HP1028. It is a protein relevant for colonization and for the survival of the bacterium in the stomach. The three-dimensional structure of the protein reveals that it belongs to the family of lipocalins, a group of proteins that bind and transport small molecules. Its structure, along with the localization of the mature protein in the bacterial periplasm and the position of *hp1028* gene in the bacterial genome, points to a role in *H. pylori* chemotaxis.

HP1029. This protein has a sequence identity (around 35%) with a putative β -D-galactosidase and with members of the YhcH/YjgK/YiaL protein family. Its structure is very similar to that of the only member of the DUF386m family whose three-dimensional structure is known, YhcH from *H. influenza*, but a Zn²⁺ ion is present in the active site.

HP1454. It is a protein of 303 amino acids found in the extracellular milieu. Its structure presents an elongated bent shape, composed by three distinct domains that possess folds already present in other structures. The crystal structure does not allow a clear identification of the function.

Keywords: *Helicobacter pylori*; pathogens; gastritis

MS5-P47 Characterisation of a phosphinothricin N-acetyltransferase from *Pseudomonas syringae*

Anna M. Davies¹, Renée Tata¹, David R. Trentham¹, Brian J. Sutton¹, Paul R. Brown¹

¹. King's College London, Randall Division of Cell and Molecular Biophysics, London, United Kingdom

email: anna.davies@kcl.ac.uk

The herbicide glufosinate contains the glutamate analog phosphinothricin, which inactivates glutamine synthetase. Protection of crops against the herbicide is conferred by the *bar* gene, first isolated from *Streptomyces*, the product of which N-acetylates phosphinothricin [1,2]. A putative phosphinothricin N-acetyl transferase from *Pseudomonas aeruginosa* PAC1, termed pita, displayed activity with methionine-sulfoximine but not phosphinothricin, although both compounds are glutamate analogs [3]. We cloned and expressed a putative phosphinothricin N-acetyltransferase with 41% sequence identity to pita, from *Pseudomonas syringae* pv. tomato DC3000, a strain responsible for bacterial speck in tomato and *Arabidopsis thaliana* [4]. Kinetic characterisation of this enzyme, termed syr_bar, demonstrated specificity for phosphinothricin, and not methionine sulfoximine. The structure of syr_bar was solved to 1.6Å resolution, revealing a dimeric arrangement, with a similar overall fold and active site structure to pita. We also solved the structure for syr_bar in complex with phosphinothricin to 2.6Å resolution, in a second crystal form. Comparison with pita from *P. aeruginosa*, and kinetic and crystallographic characterisation of syr_bar active site mutants, has provided insight into the determinants governing specificity for methionine-sulfoximine and phosphinothricin.

[1] Thompson, C.J. (1987) EMBO J. 6,2519

[2] Wohlleben, W. (1988) Gene 70,25

[3] Davies, A.M. et al. (2007) Biochemistry 46,1829

[4] Zhao, Y. et al. (2003) The Plant Journal 36,485

Keywords: GNAT, N-acetyltransferase, enzyme

MS5-P48 Dragonfly[®] screen optimizer helps researchers tackle tuberculosis

Paul Thaw¹

¹. TTP Labtech

email: paul.thaw@ttplabtech.com

The ability to crystallise proteins, nucleic acids or macromolecular complexes pose significant challenges to the protein crystallography community, from large scale screening assays for the determination of initial crystallization conditions, screen optimization and final screen set-up. Protein crystal optimization is vital to ensure high quality X-ray diffraction data for the solving of high resolution structure. This process involves the set-up of a series of complex screening combinations where the ratios of the individual components identified from primary crystallization studies are varied. In order to reduce the effort and tedium of this process, TTP Labtech have designed dragonfly[®] for crystallization screening as an addition to their successful mosquito liquid handling portfolio. This poster will describe an example of how the dragonfly has benefited drug discovery. Dr. Michal Blaszczyk at Cambridge University, UK has optimised the conditions for the crystallization of a target enzyme involved in the growth of the mycobacteria that causes tuberculosis (*Mycobacterium tuberculosis*). Extensive screening using TTP Labtech's mosquito Crystal produced the initial hits which went on to be optimised. Using dragonfly optimization of 20 conditions took 1 week rather than a more usual time of several weeks. This high throughput optimization screening method also reduced the volume of condition media required by nearly two thirds, mainly due to the ability to perform the screen in 96-well rather than 24-well, plates. The highly reproducible results have led to optimised crystals that diffract well. Dr Blaszczyk plans to use dragonfly to develop high throughput methods that have not been possible previously, for example, *in situ* screening for crystallization. This poster demonstrates that "dragonfly" is a valuable, compact, low cost addition to the crystallographer's bench. It eliminates lengthy and complicated plate set-up at the optimization stage of crystallization.

Keywords: mycobacteria, optimisation

MS5-P49 Crystal structures of RSEGFP and RSGREEN0.7 reveal photoswitching in EGFP-derived fluorescent proteins

Elke De Zitter¹, Sam Duwé², Peter Dedecker², Luc Van Meervelt¹

1. Biomolecular Architecture, KU Leuven, Celestijnenlaan 200F, 3001 Leuven
2. Molecular Imaging and Photonics, KU Leuven, Celestijnenlaan 200F, 3001 Leuven

email: elke.dezitter@chem.kuleuven.be

Reversible photoswitchable fluorescent proteins (PS-FPs) play a key role in superresolution fluorescence microscopy such as PALM (1) and pcSOFI (2). Although several examples of these PS-FPs are well known, we developed the rsGreen series, a palette of PS-FPs, based on the frequently used Enhanced Green Fluorescent Protein (EGFP, 3,4). In comparison to rsEGFP (5), another EGFP-based PS-FP, the rsGreens show an enhanced maturation efficiency at 37°C and faster photoswitching behavior, which makes them suitable for subcellular and superresolution visualization studies.

One of these new FPs, rsGreen0.7 has been crystallized, both in its green-emitting (green-on) and dim (green-off) state. They have the typical β -barrel fold as seen in other FPs. These crystal structures give a first glance at the photoswitching mechanism of EGFP-based PS-FPs. Comparison of the green-on and green-off state shows that photoswitching is accompanied by a *cis-trans* isomerization of the chromophore, which is situated in the center of the barrel. Surprisingly, this isomerization is different when compared with Dronpa (6,7) and other well-known PS-FPs. Both in Dronpa and rsGreen0.7, the *p*-hydroxyphenyl moiety of the green-off state chromophore is out of plane compared with the green-on state. However, in rsGreen0.7, this effect is more pronounced. Moreover, the orientation of this moiety is completely different between both proteins.

During the design of rsGreen0.7, residues that could influence the photoswitching behavior and/or the barrel-stability were mutated. As we also determined the crystal structure of its parent, rsEGFP, we were able to elucidate the effect of these mutations and to get a better understanding of the relationship between structure and function in this family of PS-FPs.

References

1. Betzig, E., et al., Science, 2006. 313(5793): p. 1642-5.
2. Dedecker, P., et al., Proc Natl Acad Sci U S A, 2012. 109(27): p. 10909-14.
3. Cormack, B.P., et al., Gene, 1996. 173(1 Spec No): p.33-8.
4. Yang, T.T., et al., Nucleic Acids Res., 1996. 24(22): p.4592-3.
5. Grotjohann, T., et al., Nature, 2011. 478(7368): p.204-8.
6. Ando, R., et al., Science, 2004. 306(5700): p.1370-3.
7. Andresen, M. et al., Proc. Natl. Acad. Sci. USA, 2007. 104(32): p.13005-9.

Keywords: Fluorescent proteins, Photoswitchability, Structure analysis

MS5-P50 The structural basis for an essential subunit interaction in influenza virus RNA polymerase

Sam-Yong Park¹, Hisashi Yoshida¹, Mio Ohki¹, Kanako Sugiyama²

1. Drug Design Laboratory, Graduate School of Medical Life Science, Yokohama City University, 1-7-29 Suehiro, Tsurumi, Yokohama, 230-0045, Japan,
2. Drug Design Group, Kanagawa Academy of Science and Technology (KAST), 3-2-1 Sakado, Takatsu, Kawasaki 213-0012, Japan

email: park@tsurumi.yokohama-cu.ac.jp

Influenza A virus is a major human and animal pathogen with the potential to cause catastrophic loss of life. Influenza virus reproduces rapidly, mutates frequently, and occasionally crosses species barriers. The recent emergence of swine-origin influenza H1N1 and avian influenza related to highly pathogenic forms of the human virus has highlighted the urgent need for new effective treatments. Here we demonstrate the importance to viral replication of a subunit interface in the viral RNA polymerase which presents a new set of potential drug binding sites entirely independent of surface antigen type. No current medication targets the heterotrimeric RNA polymerase complex. All three subunits, PB1, PB2, and PA are required for both transcription and replication. PB1 carries the polymerase active site, PB2 includes the capped-RNA recognition domain, and PA is involved in assembly of the functional complex, but so far very little structural information has been reported for any of them. We describe two crystal structures of complexes made by fragments of PA and PB1, and PB1 and PB2^{1,2}. These novel interfaces are surprisingly small, yet they play a crucial role in regulating the 250 kDa. polymerase complex, and are completely conserved among swine, avian and human influenza viruses. Given their importance to viral replication and strict conservation, the PA/PB1 and PB1/PB2 interfaces appear to be promising targets for novel anti-influenza drugs of use against all strains of influenza A virus. It is hoped that the structures presented here will assist the search for such compounds.

References

1. Obayashi E, Yoshida H, Kawai F, Shibayama N, Kawaguchi A, Nagata K, Tame JR, Park SY. *Nature*. 454, 1127-1231. 2008.
2. Sugiyama K, Obayashi E, Kawaguchi A, Suzuki Y, Tame JR, Nagata K, Park SY. *EMBO J*. 28, 1803-1811. 2009.

Keywords: Influenza Virus, RNA Polymerase, Structure

MS5-P51 Crystal structure of *M. tuberculosis*' toxin in complex with its neutralizing antitoxin

Do-Hwan Ahn¹, Bong-Jin Lee¹

1. The Research Institute of Pharmaceutical Sciences, College of Pharmacy, Seoul National University, Gwanak-gu, Seoul 151-742, Republic of Korea

email: kerronn@snu.ac.kr

As most of bacteria and archaea, *Mycobacterium tuberculosis* (the causative agent for tuberculosis in human) possesses toxin-antitoxin systems on its chromosome. Studies tracking the systems' role in bacterial and archaeal physiology found evidences support that the system is related to dormant formation. Given the fact that dormancy is the key tactic *Mycobacterium tuberculosis* adopts to evade host's immune response and to obtain tolerance against antibiotics, toxin-antitoxin systems are believed to be an attractive target for new antibiotics development. Here, we present crystal structure of MazE(Antitoxin)-MazF(Toxin) pair from *Mycobacterium tuberculosis* determined at 2.3Å. It shows two C-terminal α -helices of MazE lie on the crevice at the center of MazF dimer and this MazE₂-MazF₂ heterotrimer dimerizes to form MazE₂-MazF₄ heterohexamer.

Keywords: M. tuberculosis, Toxin-antitoxin system, MazEF

MS5-P52 Elucidating the role of Esterase-6 from *Drosophila melanogaster* in the olfactory response

Nicholas J. Fraser¹, Faisal Younus², Jian-Wei Liu², Chris Coppin², Gunjan Pandey², John G. Oakeshott², Colin J. Jackson¹

1. Research School of Chemistry, Australian National University, Canberra, ACT, 2601, Australia

2. CSIRO Ecosystems Science, Canberra, ACT 2601, Australia

email: nicholas.fraser@anu.edu.au

Carboxylesterases are abundant in the genomes of insects and have been investigated for their diverse roles in insecticide resistance, lipid metabolism and reproduction. They can be subdivided into eight subfamilies which include α -esterases, β -esterases, juvenile hormone esterases, acetylcholinesterases and four other proteins with an esterase like fold. There is little known at a structural level about the β -esterases despite the key role they have in the reproductive success of *Drosophila melanogaster*. Low expression hampers studies into insect carboxylesterases including the β -esterase, esterase-6. In this work esterase-6 was successfully heterologously expressed in *Escherichia coli* and crystals were obtained following lysine methylation. The structure of esterase-6 shows a unique entry to the active site compared to other carboxylesterases, which is a result of a loop insertion. In comparison to the closest homologs, the change of entry to the active site results in a smaller binding site. Enzyme kinetics, docking experiments and molecular dynamics showed that short chains esters are preferred substrates for the enzyme and the proposed substrate for 30 years, 11-cis- vaccenyl acetate is not the substrate for esterase-6. The successful recombinant expression of esterase-6 opens up a route for expression of other carboxylesterases and the first structure of a β -esterase has been solved giving a possible target for insecticides, an indication of the substrate specificity of β -esterases, and elucidating the mode of action of an enzyme that has been a mystery for over 30 years.



Figure 1. Structure of the first insect β -esterase solved, esterase-6

Keywords: Carboxylesterase, Protein Structure, Docking, Molecular Dynamics,

MS5-P53 Structural investigation of streptococcal collagen-like protein ScI2 from invasive M3-type group *A Streptococcus pyogenes*

Flavia Squeglia¹, Maria Romano¹, Beth Bachert², Alfonso De Simone³, Slawomir Lukomski², Rita Barisio¹

1. Institute of Biostructure and Bioimaging (IBB) of the Italian National Research Council (CNR)

2. Department of Microbiology, Immunology, and Cell Biology, West Virginia University School of Medicine 2095 Health Sciences North, WV 26506, Morgantown, USA

3. Imperial College London, South Kensington, London SW7 2AZ, UK

email: squegliaflavia@gmail.com

The arsenal of virulence factors deployed by streptococci includes streptococcal collagen-like (ScI) proteins. These proteins, which are characterized by a globular domain and a collagen-like domain, play key roles in streptococcal pathogenesis, like establishing host-adhesion, evade the host immune defenses, or mediate biofilm formation [1,2]. However, no three-dimensional structural information is available so far for any of the ScI proteins. In this work, we proved that the ScI2 protein is expressed by invasive M3-type strain MGAS315 of *Streptococcus pyogenes* and is found on the bacterial cell surface. We solved the x-ray crystallographic structure of the globular domain of ScI2.3, the first of any ScI, and used modeling and molecular dynamics techniques to gather structural information on the entire ScI2.3. This structure shows a novel fold among collagen trimerization domains of either bacterial or human origin. Despite there being low sequence identity, we observed that ScI2.3 globular domain structurally resembles the gp41 subunit of the envelope glycoprotein from human immunodeficiency virus type 1, an essential subunit for viral fusion to human T cells. Molecular dynamics data evidence a high flexibility of ScI2.3 with remarkable inter-domain motions that are likely instrumental to its biological function [3,4]. Our results provide molecular tools for the understanding of ScI-mediated streptococcal pathogenesis and important structural insights for the future design of small molecular inhibitors of streptococcal invasion.

References:

1. Humtsoe J.O. *et al.*, (2005), *J Biol Chem*, 280(14):13848-57;
2. Rasmussen M. & Bjorck L., (2001), *Mol Microbiol.*, 40(6):1427-38;
3. Squeglia *et al.*, (2013), *Acta Crystallogr Sect F Biol Cryst Commun.*, 69(Pt 9):1023-5;
4. Squeglia *et al.*, (2014), *J Biol Chem.*, 289(8):5122-33;

Keywords: Collagen-like protein, Crystal Structure, Molecular Dynamics

MS5-P54 Crystal structure of PhoU from *Pseudomonas aeruginosa*, a negative regulator of the Pho regulon

Sang Jae Lee¹, Bong-Jin Lee¹, Se Won Suh²

1. The Research Institute of Pharmaceutical Sciences, College of Pharmacy, Seoul National University, Gwanak-gu, Seoul 151-742, Republic of Korea

2. Department of Chemistry, College of Natural Sciences, Seoul National University, Seoul 151-742, Republic of Korea

email: sjlee33@snu.ac.kr

In *Escherichia coli*, seven genes (*pstS*, *pstC*, *pstA*, *pstB*, *phoU*, *phoR*, and *phoB*) are involved in sensing environmental phosphate (Pi) and controlling the expression of the Pho regulon. PhoU is a negative regulator of the Pi-signaling pathway and modulates Pi transport through P_i transporter proteins (PstS, PstC, PstA, and PstB) through the two-component system PhoR and PhoB. Inactivation of PhoY2, one of the two PhoU homologs in *Mycobacterium tuberculosis*, causes defects in persistence phenotypes and increased susceptibility to antibiotics and stresses. Despite the important biological role, the mechanism of PhoU function is still unknown. Here we have determined the crystal structure of PhoU enzyme from *Pseudomonas aeruginosa*. It exists as a dimer in both the crystal and solution, with each monomer consisting of two structurally similar three-helix bundles. The overall structure of *P. aeruginosa* PhoU dimer resembles those of *Aquifex aeolicus* PhoU and *Thermotoga maritima* PhoU2. However, it shows distinct structural features in some loops and the dimerization pattern.

Keywords: PhoU, PA5365, Pho regulon, phosphate homeostasis, drug tolerance

MS5-P55 What can we learn about nucleotide metabolism from a thermophilic anaerobic ribonucleotide reductase?

Oskar Aurelius¹, Renzo Johansson¹, Viktoria Bågenholm¹, Daniel Lundin², Fredrik Tholander³, Alexander Balhuizen¹, Tobias Beck⁴, Margareta Sahlin², Cecilia Emanuelsson¹, Britt-Marie Sjöberg², Etienne Mulliez⁵, Derek T. Logan¹

1. Dept. of Biochemistry and Structural Biology, Lund University, Lund, Sweden

2. Dept. of Biochemistry and Biophysics, Stockholm University, Stockholm, Sweden

3. Dept. of Medical Biochemistry and Biophysics, Karolinska Institute, Stockholm, Sweden

4. Dept. of Inorganic Chemistry, Göttingen University, Göttingen, Germany

5. Chimie et Biologie des Métaux, CEA Grenoble, Grenoble, France

email: oskar.aurelius@biochemistry.lu.se

The first time that radical species were characterised in enzyme mechanisms was upon the discovery of ribonucleotide reductases (RNRs) more than 50 years ago. Radical chemistry in enzymology has later been found to take place in a wide range of enzymes in which challenging chemistry is carried out. RNRs catalyse the reduction of ribonucleotides to deoxyribonucleotides. This is a key step in the *de novo* synthesis of building blocks for DNA and is found in the vast majority of known organisms.

Here we present the anaerobic RNR from the thermophile *Thermotoga maritima* studied by X-ray crystallography, small-angle X-ray scattering, enzyme assays and complementary biophysical methods. In many regards the *T. maritima* system appears to be a typical anaerobic RNR. However, its (catalytic subunit, tmNrdD) active site stands out greatly by lacking a pre-positioned cysteine residue, expected to take part in radical delivery to the substrate. This has not been seen in any other structurally studied RNR of any type. In contrast, it still maintains a glycy radical site in a conserved position for Gly* radical enzymes. This radical site can be activated by introducing the reduced radical SAM activase, in presence of its cosubstrate S-adenosyl methionine. The highly unexpected structural arrangement found in the active site and its implications upon the biochemistry and structural biology of RNRs will be discussed.

RNRs are not only fascinating enzyme systems to study because of the above mentioned chemistry or their significance in nucleotide metabolism, but also because of their intricate allosteric regulation to maintain balanced dNTP pools. RNRs contain allosteric sites to regulate substrate specificity and in some cases separate sites for overall activity regulation. By the use of X-ray crystallography the structural changes induced by different combinations of effectors and effector/substrate complexes has been studied in the *T. maritima* anaerobic RNR. These changes in hydrogen bonding networks between the specificity and active site, upon nucleotide binding, allows for a better understanding of the cooperativity between the sites.

Many things can be learned about RNRs from the anaerobic *T. maritima* system and an overview highlighting its biochemistry, active site, allosteric regulation and further puzzle pieces from complementary methods will be presented.

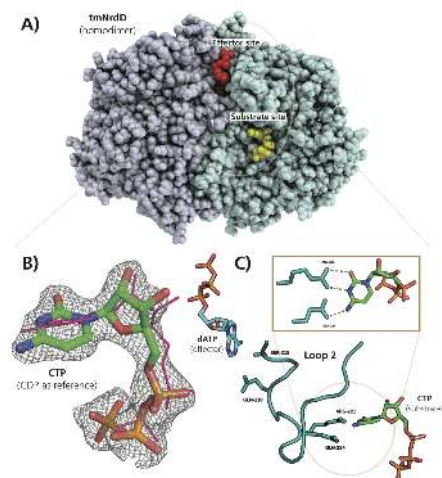


Figure 1. A) The homodimer of tmNrdD in complex with dATP (effector) and CTP (substrate) from X-ray crystallography. B) CTP shown with a 2F_o-F_c mesh contoured at 1.2 σ (CDP when in complex with tmNrdD shown in magenta as a reference). C) Overview of key amino acids in loop 2 for nucleotide recognition.

Keywords: Glycyl radical enzymes, radical SAM, metalloproteins, anaerobic enzymology, allosteric regulation, nucleotide metabolism, X-ray macromolecular crystallography, small-angle X-ray scattering

MS5-P56 Sulfur shuttling across a chaperone during molybdenum cofactor maturation

Pascal Arnoux^{1,2,3}, Christian Ruppel⁴, Flore Oudouhou⁵, Jérôme Lavergne^{1,2,3}, Marina I. Siponen^{1,2,3}, René Toci³, Ralf R. Mendel⁴, Florian Bittner⁴, David Pignol^{1,2,3}, Axel Magalon³, Anne Walburger⁵

1. Laboratoire de Bioénergétique Cellulaire, CEA, DSV, IBEB, Saint-Paul-lez-Durance, France
2. CNRS, UMR 7265 Biologie Végétale et Microbiologie Environnementales, Saint-Paul-lez-Durance, France
3. Aix Marseille Université, CEA, CNRS, BVME UMR 7265, 13108, Saint Paul-Lez-Durance, France
4. Department of Plant Biology, Technical University, Braunschweig, D-38106, Germany
5. Aix Marseille Université, CNRS, LCB UMR 7283, 13402, Marseille, France

email: pascal.arnoux@cea.fr

Formate dehydrogenases (FDHs) are of great interest for being natural catalysts able to sequester atmospheric CO₂ used for generating reduced carbon compounds with possible uses as fuel. Most FDHs are metalloenzymes harboring a molybdenum or tungsten cofactor in their active site. Activity of FDHs in *Escherichia coli* strictly requires the sulfurtransferase *EcFdhD* which likely transfers sulfur from *IscS* (a general sulfur transfer platform) to the molybdenum cofactor (*Mo-bisPGD*, see Figure 1) of FDHs. Here we show that *EcFdhD* binds the molybdenum cofactor *in vivo*. Additionally, *EcFdhD* has sub-micromolar affinity for GDP used as a surrogate of the molybdenum cofactor's nucleotide moieties. The *EcFdhD* crystal structure was solved in complex with GDP showing the symmetrical binding of two GDPs on the same protein dimer face, a dynamic loop harboring two functionally important cysteine residues on the opposite face and a tunnel connecting these two faces at the center of the dimer. Strikingly, the distance between the two GDP moieties of the *Mo-bisPGD* present at the active site of FDHs, allowing us to propose a model for the sulfuration mechanism of *Mo-bisPGD* where the sulfur atom is shuttled across the chaperone's dimer. This model is supported by structure-guided mutagenesis and functional studies with distinct variants either affected on catalysis/sulfur transfer or GDP binding. Overall, our results provide a first molecular basis for sulfuration of *Mo-bisPGD* prior to its insertion into FDHs. Additionally, it provides a nice example of how the symmetry of an enzyme can mirror the symmetry of its substrate.

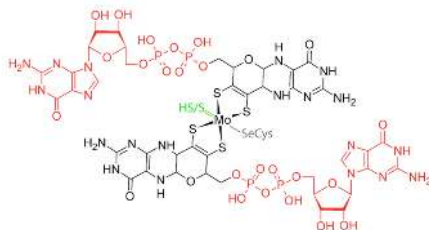


Figure 1. Structure of the Mo-bisPGD substrate of FdhD, or how to transfer a sulfur to the molybdenum atom at the center of the substrate. The GDP moiety of Mo-bisPGD is highlighted in red.

Keywords: Enzyme, symmetry, sulfur transfer

MS5-P57 Crystal structure of Csd3 from *Helicobacter pylori*, a cell-shape determining metallopeptidase

Hye Jin Yoon¹, Doo Ri An², Hyoun Sook Kim³, Se Won Suh^{1,2}

1. Department of Chemistry, Seoul National University, Korea
2. Department of Biophysics and Chemical Biology, Seoul National University, Korea
3. College of Pharmacy, Seoul National University, Korea

email: yoonhj@snu.ac.kr

Helicobacter pylori is associated with various gastrointestinal diseases such as gastritis, ulcer, and gastric cancer. Its colonization of the human gastric mucosa requires high motility, which depends on the helical cell shape. Seven cell shape-determining genes (*csd1*, *csd2*, *csd3/hdpA*, *ccmA*, *csd4*, *csd5*, and *csd6*) have been identified in *H. pylori*. These proteins play key roles in determining the cell shape through modifications of the cell-wall peptidoglycan by alteration of crosslinking or by trimming of peptidoglycan muropeptides. Among them, Csd3 (also known as HdpA) is a bi-functional enzyme. Its d,d-endopeptidase activity cleaves the d-Ala⁴-mDAP³ peptide bond between crosslinked muramyl tetra- and penta-peptides. It is also a d,d-carboxypeptidase that cleaves off the terminal d-Ala⁵ from the muramyl pentapeptide. Here we have determined the crystal structure for this protein, revealing the organization of its three domains in a latent and inactive state. The N-terminal domain 1 and the core of domain 2 share the same fold despite a very low level of sequence identity and their surface charge distributions are different. The C-terminal LytM domain contains the catalytic site with a Zn²⁺ ion, like similar domains of other M23 metallopeptidases. Domain 1 occludes the active site of the LytM domain. The core of domain 2 is held against the LytM domain by the C-terminal tail region that protrudes from the LytM domain. This work could serve as the foundation in discovery of novel inhibitors that would prove helpful in fighting infections by the major human pathogen *H. pylori*.

[1] An, D.R. *et al.* (2015) *Acta Cryst D* **71**, 675-686.

[2] Sycuro, L.K. *et al.* (2010) *Cell* **141**, 822-833.

Keywords: *Helicobacter pylori*, csd3, cell shape determinant, M23B metallopeptidase

MS5-P58 Structural investigations of purine nucleoside phosphorylase from *Helicobacter pylori* I

Zoran Štefanić¹, Ivana Leščić Ašler¹, Goran Miklešević¹, Marija Luić¹

1. Division of Physical Chemistry, Ruder Bošković Institute, Bijenička 54, 10000 Zagreb, Croatia

email: zoran.stefanic@irb.hr

Helicobacter pylori is bacterial pathogen known for its ability to colonize and persist in human stomach (Makola et al., 2007). It is estimated that today *H. pylori* infects more than half of the world's population. Severe impact that *H. pylori* has on human health, makes the search for effective drugs to fight this pathogen of the utmost importance.

Purine nucleoside phosphorylase (PNP) represents one promising drug target for this pathogen, as it is the key enzyme in the purine salvage pathway. *H. pylori* PNP is a homo-hexameric protein, and can be regarded as a trimer of dimers (Fig. 1a). The active site of each monomer can be in either open or closed conformation. Although the first solved crystal structure of very similar *E. coli* PNP, complexed with its ligands showed 3 open + 3 closed conformations (Koellner et al., 2002) we have recently determined several structures of *E. coli* PNP with 4 open + 2 closed sites conformations (Miklešević et al., 2011).

Two crystal structures of the PNP from the clinical isolate of *H. pylori* have been determined. Both belong to the orthorhombic crystal system and space group $P2_12_12_1$. The crystal cells are different though: unit cell axes are 74, 129, 155 Å (crystal grown at pH 7) and 104, 120, 139 Å (crystal grown at pH 4.5). Interestingly, it was found in both structures, that the protein has 5 open + 1 closed conformations, which is the first such case, to the best of our knowledge. In the structure from pH 7 crystallization conditions, the closed active site is occupied with one phosphate ion (substrate) and one hypoxanthine molecule (product) in the so-called *dead-end complex*, while all five open sites are empty. The structure at pH 4.5 has the closed active site fully occupied (Fig. 1b), while the open sites are partially occupied with hypoxanthine and phosphate. Differences in active site conformations between *H. pylori* and *E. coli* PNP structures will be discussed as well as possible implications on the PNP mechanism of action.

Koellner, G., Bzowska, A., Wielgus-Kutrowska, B., Luić, M., Steiner, T., Saenger, W., & Stepniński, J. (2002). *J. Mol. Biol.* **315**, 351–371.

Makola, D., Peura, D. a., & Crowe, S. E. (2007). *J. Clin. Gastroenterol.* **41**, 548–558.

Miklešević, G., Štefanić, Z., Narczyk, M., Wielgus-Kutrowska, B., Bzowska, A., & Luić, M. (2011). *Biochimie.* **93**, 1610–1622.

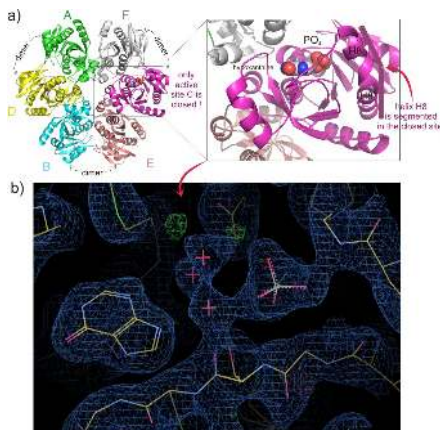


Figure 1. a) Hexameric structure of *H. pylori* PNP b) closed active site of the *H. pylori* PNP containing one hypoxanthine molecule, and one phosphate ion, forming a *dead-end complex*.

Keywords: Purine nucleoside phosphorylase, *Helicobacter pylori*, dead-end complex

MS5-P59 Structural and enzymatic kinetic studies of the chloroplast gamma-ketol reductase from *Arabidopsis thaliana*

Sarah Mas y mas¹, Curien Gilles², Giustini Cécile², Ferrer Jean-Luc¹, Rolland Norbert², Cobessi David¹

1. Institut de Biologie Structurale, Université Grenoble Alpes, CNRS, CEA, 71 Avenue des Martyrs, 38044 Grenoble, France
2. Laboratoire de Physiologie Cellulaire et Végétale, CNRS, Université Grenoble Alpes, CEA, INRA, 17 Rue des Martyrs, 38054 Grenoble, France

email: sarah.mas-y-mas@ibs.fr

In the course of the production of the signaling hormone jasmonate in chloroplast, gamma-ketol is released in the 13-LOX pathway. This highly reactive compound can damage lipids, proteins and DNA. Therefore it must be reduced. The chloroplast envelope Quinone OxidoReductase Homolog (ceQORH) from *Arabidopsis thaliana* represents 1 to 2 % of the protein envelope. It binds NADPH, lacks a classical *N*-terminal and cleavable chloroplast transit peptide. It is transported through the chloroplast envelope by an unknown alternative pathway without cleavage of its internal chloroplast targeting sequence [1], [2]. We showed that this enzyme binds NADPH and reduces gamma-ketol [3]. Therefore, it has been renamed gamma-ketol reductase. It is inhibited by the ketodien 13-KOTE and 13-KODE [3]. Using X-ray crystallography and analytical ultracentrifugation, we showed that the gamma-ketol reductase displays several oligomerization states [4]: the apo enzyme is a dimer, holoenzyme is a monomer and the enzyme bound to inhibitor is a tetramer. Structure analysis also revealed that the ligand binding site is large and hydrophobic allowing the enzyme to bind a broad range of ligands with a high affinity for gamma-ketol. By contrast with the other quinone oxydoreductases which dimerize by making a 12 stranded beta-sheet, the gamma-ketol reductase dimerizes through interaction of 2 alpha-helices from the Rossmann fold. These structural characteristics and the enzyme properties make ceQORH a new class distinct from the quinone oxydoreductases.

[1] Miras et al.,(2002) . J. Biol. Chem. 227 : 47770-47778

[2] Miras et al., (2007) . J. Biol. Chem. 282 : 29482-29492

[3] Curien et al.,(2015) (submitted)

[4] Mas y Mas et al., (2015) . Acta Cryst F. 71 : 455-458

Keywords: ceQORH, Chloroplast, gamma-ketol, X-ray crystallograph, analytical ultracentrifugation, oligomerization states

MS5-P60 Characterization of enzymes involved in biosynthesis and modification of sialic acids and their derivatives

Ronny Helland¹

1. The Arctic University of Norway, Norway

email: ronny.helland@uit.no

Sialic acids play important roles in biological, pathological, and immunological processes, but they may also be building blocks for development of new drugs, nutraceuticals or high-value components in cosmetics. Sugar-modifying enzymes can therefore be utilized in many different areas of molecular biology and medicine, and a combination of chemical and enzymatic synthesis has the potential to produce new saccharides with useful properties.

The project aims to identify and characterize sugar-modifying enzymes from marine cold adapted species in order to improve the fundamental understanding of their role in bacterial pathogenesis and to identify targets for pharmaceutical and commercial exploitation. The project further aims at identifying enzymes which can be utilized in biomass conversion, i.e. from chitin or cellulose to high value products in medicine, cosmetics and food industry.

N-acetylneuraminidase (Nal), catalyzing the reversible cleavage of N-acetylneuraminic acid (Neu5Ac, also often called sialic acid) to N-acetylmannosamine (ManNAc) and pyruvate, is used as model system for exploring the catalytic mechanism and substrate/product modulation.

Keywords: sialic acids, carbohydrate chemistry, protein crystallography

MS5-P61 Molecular analysis of a G-actin sensor

Stephane Mouilleron¹

1. Francis Crick Institute, London, UK

email: stephane.mouilleron@crick.ac.uk

Actin dynamics control many aspects of cell shape and cell motility through regulatory interactions with a large variety of actin-binding proteins. Signalling to these actin regulators frequently involves a Rho GTPase-stimulated pathway that leads to a dramatic fluctuation in the levels of monomeric actin (G-actin) following polymerisation to F-actin. Recent studies have identified a molecular G-actin sensor called the RPEL domain that links RPEL-containing proteins and their subcellular localisation to actin dynamics. The RPEL domain contains a tandem array of typically three RPEL motifs, each of which is competent to bind a G-actin molecule (1). The domain is present in two otherwise unrelated protein families; the MRTF family of serum response factor (SRF) transcriptional co-activator proteins and the Phactr family of actin and PP1 phosphatase-binding proteins. We have begun to investigate how the RPEL domain operates in both of these protein contexts and how it modulates subcellular localisation, transcriptional regulation and actomyosin contractility. To define the molecular basis for the sensor we have reconstituted pentameric and trimeric G-actin complexes with the RPEL domain from both MRTF-A and Phactr and used crystallography to reveal discrete supramolecular assemblies with repetitive arrangements of the G-actin subunits around the “crankshaft”-shaped RPEL domain (2). These arrangements are quite different from F-actin intermolecular contacts and are quite unexpected. Our crystal structures reveal cooperative loading of G-actin onto the RPEL domain that we show by several cell-based reporter assays to be of functional importance. These structures explain how G-actin interaction alters the subcellular localisation of both MRTF-A and Phactr by inhibiting nuclear import through competing with importin α -binding (2).

Keywords: actin, RPEL, RhoGAP, NLS, Phactr,

MS5-P62 Structural insights into the pathology of *Erwinia amylovora*, the causative agent of Fire Blight

Joseph D. Bartho^{1,2}, Marco Salomone-Stagni¹, Dominico Bellini², Jochen Wuerges¹, Mirco Toccafondi¹, Armin Schmitt¹, Nicola Demitri³, Martin A. Walsh², Stefano Benini¹

1. Faculty of Science and Technology, Free University of Bolzano, Piazza Università 5, Bolzano, Italy

2. Diamond Light Source, Harwell Science and Innovation Campus, Didcot, Oxfordshire, OX110DE, United Kingdom

3. ELETTRA Sincrotrone Trieste S.C.p.A., Basovizza, Italy

email: josephdale.bartho@natec.unibz.it

Erwinia amylovora is a gram negative bacterial pathogen of *Rosaceae* plants, known to infect over 100 species, but most devastating to cultivated apple and pear. Current control measures can reduce the rate of new infections, but the only effective control of existing infections is destruction of the infected plants, resulting in significant economic losses to pome fruit industries. As antibiotic spraying is banned in Europe, and antibiotic resistance is becoming more prevalent in other areas, there is increasing demand for new control measures.

Studying the molecular basis of infection is essential for identifying and understanding which genes are important for infection and their mechanisms of overcoming host resistance, and can provide a platform for the development of new targeted control measures to effectively manage this disease.

Infection associated proteins have been investigated based on their importance to the multiple molecular pathways required for successful infection. These include proteins involved in protein secretion, sugar metabolism, siderophore synthesis, exopolysaccharide synthesis, and pathogenic effector proteins. The structural analysis of these proteins by X-ray crystallography have revealed new insights into their roles in infection and plant resistance, along with further potential applications in industry. A selection of these results relating to the various infection pathways will be presented.

Keywords: Protein structure, effector protein, pathogenicity, *Erwinia*

MS6. Membrane proteins and signal transduction pathways

2. Mayerhofer, H., Panneerselvam, S., and Mueller-Dieckmann, J. (2012). *J. Mol. Biol.* **415**, 768–779.

3. Mayerhofer, H., Panneerselvam, S., Kaljunen, H., Tuukkanen, A., Mertens, HD., and Mueller-Dieckmann, J. (2015). *Journal of Biological Chemistry*. **290**, 2644–58.

Keywords: histidine kinase, plant signalling, ethylene, two component system, ETR1, protein phosphorylation

Chairs: E. Yvonne Jones, Werner Kühlbrandt

MS6-P1 Crystal structure of the catalytic domain of the ethylene receptor ETR1 from *Arabidopsis thaliana*

Saravanan Panneerselvam¹, Jochen Mueller Dieckmann²

1. PETRA III, DESY, Hamburg, Germany

2. University of Hamburg, Biozentrum, Hamburg, Germany

email: saravanan.panneerselvam@desy.de

Plants employ ethylene to regulate many developmental processes such as seed germination, root growth, fruit ripening, and senescence (1). *Arabidopsis thaliana* perceives ethylene by a group of five partly redundant, membrane bound receptors (ETR1, ETR2, ERS1, ERS2, EIN4). Ethylene binds at the N-terminal hydrophobic domain of the receptors and initiate the signalling events via its cytosolic domain. The receptor cytosolic domain contains several different domain which are triggering the signalling events by interacting with different proteins such CTR-1 kinase (2). In case of ETR1, the cytosolic domain is made of a GAF domain followed by a histidine kinase dimerization (dHp) and catalytic domain (CA) and a receiver domain (RD).

Sequence analysis of ethylene receptors indicated similarity to bacterial two-component systems (TCS) by their C-terminal cytosolic histidine kinase (HK) and receiver domains. Based on the integrity of signature motifs in the catalytic domain of the HK, the receptors are further assigned to two subfamilies. Members of subfamily 1 (ETR1 and ERS1) possess all sequence motifs of canonical HK domains and also histidine kinase activity. Subfamily 2 receptors (ETR2, ERS2 and EIN4) have incomplete motifs and lack histidine kinase activity. While all receptors participate in ethylene signal transduction, members of subfamily 1 seem to play a predominant role.

To understand the kinetic and regulatory mechanism of ethylene receptors, we have successfully crystallized and solved the structure of catalytic domain of ETR1. The protein was crystallized with various nucleotides. Crystals obtained in the presence of ADP belong to space group $I2_12_1$ with one molecule per asymmetric unit and diffract x-ray radiation to beyond 1.85 Å resolution. The overall structure assumes an α/β sandwich fold and closely resembles the CA domain of HK853. The crystal structure reveals the flexibility of ATP lid and the metal specificity of subfamily 1 receptors through the unusual binding of an metal ion with adenine moiety of ADP and residue C573 from G3 motif (3).

References:

1. Bleeker, A.B. & Kende, H. (2000). *Annu. Rev. Cell Dev. Biol.* **16**, 1–18

Acta Cryst. (2015). **A71**, s237

s237

MS6-P2 Crystal structure of *Plasmodium falciparum* calmodulin / peptide complex

Veronika Harmat^{1,2}, Zsolt Dürvanger¹, Tünde Juhász³, Károly Lilioni³

1. Institute of Chemistry, Eötvös Loránd University, Budapest, Hungary
2. MTA-ELTE Protein Modelling Research Group, Budapest, Hungary
3. Institute of Enzymology, Research Centre for Natural Sciences, Hungarian Academy of Sciences, Budapest, Hungary

email: veronika@chem.elte.hu

Calmodulin, a ubiquitous calcium binding protein is present in all eukaryotic cells. It regulates the action of more than 100 proteins by interacting with them in a calcium dependent way. Both of its lobes contain two calcium binding EF-hand motifs. Ca²⁺ binding of the protein causes a global conformational change and exposure of hydrophobic patches on both domains capable for binding target proteins. Though the bound segments of the target possess basic amphiphilic helix conformation, the target orientation, distances of their anchoring residues and orientations of the calmodulin lobes varies within the complexes. Some calmodulin antagonist compounds were reported to inhibit *Plasmodium falciparum*, suggesting *P. falciparum* calmodulin could be a possible target of anti-malarial treatment. Structures of calmodulin and apocalmodulin from several species are known, but that of *P. falciparum* has not been published. Though calmodulin is a highly conserved protein, its structure explores differences between vertebrate and *P. falciparum* calmodulin.

We solved the structure of calmodulin from *P. falciparum* in complex with a model target peptide (melittin, a component of bee venom) and refined the structure to 2.4 Å resolution. The structure contains four calmodulin/melittin complex units showing two main binding modes of the peptide: there are some differences in the orientations of calmodulin lobes and binding patterns for the peptide. It is the flexibility of the middle short coil segment within the melittin helix that facilitates different binding modes to calmodulin. The structure suggests that interactions with the two calmodulin lobes are formed independently.

This study was supported by the MedInProt program of the Hungarian Academy of Sciences; OTKA grants NK101072 to V.H., PD104344 to T.J. and K82092 to K.L. We acknowledge Paul Scherrer Institut, Villigen, Switzerland for providing synchrotron radiation beamtime, and Gergő Gögl and Péter Ecsédi for collecting data. The research leading to these results has received funding from the European Community's 7th Framework Programme (FP7/2007-2013) under BioStruct-X (grant agreement No.283570).

Keywords: calcium signalling, protein/peptide complex, flexible binding, *Plasmodium falciparum*

MS6-P3 The molecular bases of $\delta\beta$ T-cell mediated antigen recognition

Stephanie Gras^{1,2}, Eric Chabrol¹, Sidonia B.G. Eckle³, Renate de Boer⁴, James McCluskey³, Jamie Rossjohn^{1,2,5}, Mirjam H.M. Heemskerk⁴

1. Department of Biochemistry and Molecular Biology, School of Biomedical Sciences, Monash University, Clayton, Victoria 3800, Australia
2. Australian Research Council Centre of Excellence for Advanced Molecular Imaging, Monash University, Clayton, Victoria 3800, Australia
3. Department of Microbiology and Immunology, Peter Doherty Institute for Infection and Immunity, University of Melbourne, Parkville, Victoria 3010, Australia
4. Leiden University Medical Center, Department of Hematology, C2-R, P.O. Box 9600, 2300 RC Leiden, The Netherlands
5. Institute of Infection and Immunity, Cardiff University, School of Medicine, Heath Park, Cardiff CF14 4XN, UK

email: stephanie.gras@monash.edu

$\alpha\beta$ and $\gamma\delta$ T-cells are disparate T-cell lineages that, via their use of either $\alpha\beta$ or $\gamma\delta$ T-cell antigen receptors (TCRs) respectively, can respond to distinct antigens. Here we characterise a new population of human T-cells, term $\delta\beta$ T-cells, that express TCRs comprising a TCR- δ variable gene fused to a Joining- α /Constant- α domain, paired with an array of TCR- β chains. We characterised the cellular, functional, biophysical and structural characteristic feature of this new T-cells population that reveal some new insight into TCR diversity. We provide molecular bases of how $\delta\beta$ T-cells can recognise viral peptide presented by Human Leukocyte Antigen (HLA) molecule. Our findings highlight how components from $\alpha\beta$ and $\gamma\delta$ TCR gene *loci* can recombine to confer antigen specificity thus expanding our understanding of T-cell biology and TCR diversity.

Keywords: immunology, new T cell receptor, HLA

MS6-P4 Porcine CD21 molecule is expressed on mature B cells in two different forms CD21^a and CD21^b

Marek Sinkora¹, Jana Sinkorova¹

1. Laboratory of Gnotobiology, Institute of Microbiology of the Czech Academy of Science, v.v.i., Nový Hrádek, Czech Republic

email: marek.sinkora@tiscali.cz

Monoclonal antibodies IAH-CC51, BB6-11C9.6 and B-Ly4 are routinely used to detect CD21 orthologue on the surface of porcine B lymphocytes. Cross-reactive studies show that IAH-CC51 and B-Ly4 recognize only a portion of B cells that are positive for pan-specific BB6-11C9.6. This indicates that CD21 is always present on all mature B cells but can be expressed in at least two differential forms, and these were assigned as CD21^a and CD21^b. Detection of CD21^b by IAH-CC51 or B-Ly4 together with anti-CD2 antibodies can be used to define four subpopulations of B cells. Ontogenetic and *in vitro* culture studies, analysis of cell size, expression of CD11b and class-switched phenotype together with measurement of proliferation and cell death, revealed that these subsets represent distinct populations. Phenotypic and functional features collectively suggest that CD21⁺ B cells are less mature than CD21⁺. Moreover, different CD21 forms are expressed differentially during B cell development in the bone marrow. Recent results indicate that CD21^a is expressed earlier in development than in humans and mice whereas expression of porcine CD21^b follows the established paradigm of humans. Unfortunately, western-blot and mass spectrometry studies that would show that all three antibodies recognize proteins with the same molecular weight and sequence could not be done. Specifically, we were unable to precipitate antigen from cell lysates, purify antigen from cell lysates by affinity chromatography or isolate antigen from reversible cross-linked antigen directly on cell surface. For that reason, a new approaches for isolation of porcine CD21 forms have to be introduced to characterize different forms that should have also different function and perhaps binding capacity for C3 and/or IFN- α . By our knowledge, this is the first indication that end-stage B lymphocytes can express differential forms of CD21, which can be significant not only for swine but also for other species including man. This work was supported by Czech Science Foundation grant P502/12/0110 and 15-02274S.

Keywords: B lymphocytes, Development of immune system

MS6-P5 Towards understanding phosphoinositide 3-kinase γ (PI3K γ)-dependent signaling network

Andreja Vujcic Zagar¹, Leonardo Scapozza¹, Oscar Vadas¹

1. Pharmaceutical Biochemistry/Chemistry, School of Pharmaceutical Sciences, University of Geneva, Quai Ernest-Ansermet 30, 1211 Geneva, Switzerland

email: andreja.vujciczagar@unige.ch

Phosphoinositide 3-kinases (PI3K) play a crucial role in PI3K/Akt signaling pathway, involved in cell proliferation, differentiation, survival and migration. The PI3K/Akt signaling is one of the most commonly deregulated pathways in cancer. PI3Ks are lipid kinases activated downstream of receptor tyrosine kinases, G protein-coupled receptors and small GTPases of the Ras superfamily. They phosphorylate the 3'-hydroxyl group of the inositol ring of phosphatidylinositol lipid substrates, which act as second messenger molecules by recruiting and activating effector proteins to cellular membranes, *e.g.* Akt kinase (1). The aim of our work is to understand the role and mechanism of action of phosphoinositide 3-kinase γ (PI3K γ) by its crystal structure elucidation and functional characterization (both *in vitro* and *in vivo* assays). PI3K γ is a PI3K isoform expressed mostly in hematopoietic cells and in the heart. It has been linked to tumor formation and metastasis, chronic inflammation, autoimmune and heart disease. It is a heterodimer, which consists of a p110 γ catalytic subunit that associates with either p87 or p101 regulatory subunit (1-3). Here we present overproduction in insect cells using the MultiBac expression system (4) purification and crystallization strategy for the wild type p110 γ /p101 complex as well as p110 γ in complex with p101 deletion mutants. The p101 deletion mutants were designed based on hydrogen-deuterium exchange mass spectrometry experiments (5).

1. Vanhaesebroeck B, *et al.* (2010) *Nat Rev Mol Cell Biol* 11:329-341.
2. Fritsch R, *et al.* (2013) *Cell* 153:1050-1063.
3. Shymanets A, *et al.* (2013) *J Biol Chem* 288:31059-31068.
4. Bieniossek C, *et al.* (2008) *Current protocols in protein science / editorial board, John E. Coligan ... [et al.]* Chapter 5:Unit 5 20.
5. Vadas O, *et al.* (2013) *Proc Natl Acad Sci U S A* 110:18862-18867.

Keywords: PI3K γ , signaling, cancer, inflammation

MS6-P6 The role of active humidity control in successful membrane protein crystallization with mosquito[®] Crystal and mosquito[®] LCP

Joby Jenkins¹, David Smith¹

1. TTP Labtech, Melbourn Science Park, Melbourn, Royston, Herts, SG8 6EE, UK

email: marketing@ttplabtech.com

Membrane proteins are involved in a wide range of physiological functions and abnormalities in the structures of these proteins can lead to many known diseases such as heart disease, depression, cancer and many others. However, growing crystals of membrane proteins which are suitable for x-ray diffraction remains a challenge for crystallographers. The use of liquid handling robots such as TTP labtech's mosquito[®] Crystal and mosquito[®] LCP has increased throughput and repeatability allowing for many more conditions to be easily screened. They also offer the ability to accurately dispense nanolitre volumes of both protein and screen solutions, which saves valuable protein and reduces reagent costs. The mosquito LCP is capable of automating both microbatch and vapour diffusion methods of protein crystallography (sitting drop, hanging drop) as well as crystallisation of membrane proteins using the bicelle and the highly viscous lipidic cubic phase (LCP) methods. This can be achieved without instrument configuration changes and provides significant flexibility in the crystallisation workflow. This poster describes the features of mosquito Crystal and mosquito LCP, showing their ability to successfully overcome inherent issues in the automated set-up of membrane protein crystallisation screen trials. It also demonstrates the effective use of an active humidity chamber with mosquito LCP to crystallise a GPCR, the b₁-adrenoceptor (b₁AR). Interestingly, a 12% increased yield of crystals was observed when using the mosquito active humidity chamber compared to the same cubic-phase experiment set up in its absence. In summary, whilst mosquito LCP can rapidly set up a crystallisation screen, the use of TTP Labtech's active humidity chamber ensures there is minimal evaporation of the LCP drops which ultimately yields significant increases in both reproducibility and success rate.

Keywords: membrane protein, humidity control, crystallisation drop set-up

MS6-P7 Structural and functional characterization of Ybr137wp implicate its involvement in the targeting of tail-anchored proteins to membranes

Chwan-Deng Hsiao¹

1. Institute of Molecular Biology, Academia Sinica, Nankang, Taipei 115 Taiwan

email: hsiao@gate.sinica.edu.tw

Nearly 5% of membrane proteins are guided to nuclear, endoplasmic reticulum, mitochondrial, Golgi, or peroxisome membranes by their C-terminal transmembrane domain and are classified as tail-anchored (TA) membrane proteins. In *Saccharomyces cerevisiae*, the Guided Entry of TA-protein (GET) pathway has been shown to function in delivery of TA proteins to the ER. The sorting complex for this pathway is comprised of Sgt2, Get4, and Get5 and facilitates the loading of nascent tail-anchored proteins onto the Get3 ATPase. Multiple pull-down assays also indicated that Ybr137wp associates with this complex *in vivo*. Herein, we report a 2.8-Å resolution crystal structure for Ybr137wp from *Saccharomyces cerevisiae*. The protein is a decamer in the crystal and also in solution as observed by size-exclusion chromatography and analytical ultracentrifugation. In addition, isothermal titration calorimetry indicated that the C-terminal acidic motif of Ybr137wp interacts with the tetratricopeptide repeat (TPR) domain of Sgt2. Moreover, an *in vivo* study demonstrated that Ybr137wp is induced in yeast exiting the log-phase culture and ameliorates the defect of TA-protein delivery and cell viability derived by the impaired GET system under starvation condition. Therefore, this study might suggest a possible role for Ybr137wp related to targeting of tail-anchored proteins.

Keywords: endoplasmic reticulum, tail-anchored membrane proteins, Ybr137wp

MS6-P8 PR-10: one fold for many phytohormones?Mariusz Jaskolski^{1,2}, Milosz Ruszkowski¹, Joanna Sliwiak¹

1. Center for Biocrystallographic Research, Institute of Bioorganic Chemistry, Polish Academy of Sciences, Poznań, Poland

2. Department of Crystallography, Faculty of Chemistry, A. Mickiewicz University, Poznań, Poland

email: mariuszj@amu.edu.pl

Plant Pathogenesis-Related proteins of class 10 (PR-10) are abundant multigene proteins differentially expressed in various organs in stressful conditions, such as pathogen invasion. They have a canonical fold consisting of a seven-stranded antiparallel β -sheet gripped over a long C-terminal helix α 3, whose free end rests on a V-shaped support formed by two shorter helices. A bizarre feature of the PR-10 fold is a huge hydrophobic cavity enclosed by helix α 3 and the β -sheet. Amazingly, this internal void does not lead to instability, as in biochemical and mechanical studies the PR-10 proteins appear to be even more stable and robust than typical globular proteins. In a number of crystallographic and biophysical studies, the PR-10 proteins have been shown to bind plant hormones from entirely disjointed chemical groups. So far, proteins with PR-10 fold have been studied in complexes with cytokinins, brassinosteroids, gibberellins, abscisic acid and melatonin. The emerging picture is, however, extremely puzzling because not only can the same PR-10 protein bind phytohormones from entirely different groups, but the same ligands are often found in different binding modes and with variable stoichiometry. These perplexing observations seem to contradict our notion of specificity of protein-ligand recognition but may hold the key to the puzzle of the biological function of PR-10 proteins.

Keywords: pathogenesis-related proteins, phytohormones, plant signal transduction

MS6-P9 Structural basis for protein translocation and insertion in the outer membrane by Omp85 proteinsFabian Gruss¹, Roman P. Jakob¹, Bernard Clantin^{2,3}, Vincent Villere^{2,3}, Sebastian Hiller¹, Timm Maier¹

1. Biozentrum, University of Basel, Switzerland

2. CNRS UMR8576, Unité Glycobiologie Structurale et Fonctionnelle, Villeneuve d'Ascq, France

3. Univ. Lille Nord de France, Lille, France

email: fabian.gruss@unibas.ch

Omp85 proteins transport protein substrates across or insert them into the outer membrane of Gram-negative bacteria. Their general architecture comprises a C-terminal 16-stranded transmembrane β -barrel pore and one or more periplasmic N-terminal POTRA domains, which mediate initial substrate interactions.

We determined the crystal structure of the Omp85 insertase TamA, which is involved in autotransporter biogenesis in *E. coli* (1). The TamA barrel shows reduced interactions between the first and last strand and a lipid-occupied lateral gate, which together suggest hybrid-barrel formation and lateral release as a plausible membrane insertion mechanism. Two highly conserved signature motifs in Omp85 proteins, located in the extracellular L6 loop and the inner barrel wall, respectively, interact and stabilize the closed barrel. Equivalent features were also observed in the crystal structure of the Omp85 protein BamA, the general outer membrane insertase (2). The requirement for lateral barrel opening between strands 1 and 16 was confirmed by crosslinking (3). Contrasting observations were made for the Omp85 translocase FhaC from *B. pertussis*, which secretes filamentous hemagglutinin to the extracellular space and is involved in bacterial virulence. Here, a crystal structure visualized loop L6 in a different conformation, without interaction of the two signature motifs (4).

To analyze the differences between Omp85 translocases and insertases, we determined the crystal structure of an FhaC variant defective in substrate recognition. In this structure the L6 loop conformation is equivalent to the one of TamA and BamA (5). Re-analysis of the original wt-FhaC crystal structure revealed that the L6 loop was affected by mismodeling and adopts identical conformations in all Omp85 structures. This conformation is thus a structural characteristic of the entire Omp85 family and provides a common structural basis for both protein translocation and insertion. Furthermore, the structure of the FhaC variant reveals a mechanism for substrate selection based on FhaC plug-helix release and linker competition, which may well be relevant for other Omp85 translocases involved in two-partner secretion.

1) Gruss F. et al., Nat. Struct. Mol. Biol. 20, 1318–1320 (2013).

2) Noinaj N. et al., Nature 501, 385–390 (2013).

3) Noinaj N. et al., Structure 22, 1055–1062 (2014).

4) Clantin B. et al., Science 317, 957–961 (2007).

5) Maier T. et al., Nat. Commun. 6, 10.1038/Ncomms8452 (2015).

Keywords: Omp85, TamA, FhaC, TPS, two-partner secretion, autotransporter, outer membrane

MS6-P10 Crystal structure of the human IL-17AF heterodimer

Arnaud Goepfert¹, Sylvie Lehmann¹, Jean-Michel Rondeau¹

1. Novartis Institutes for BioMedical Research, Basel, Switzerland

email: arnaud.goepfert@novartis.com

IL-17A and IL-17F are the best characterized and most closely-related members of the IL-17 family which also includes IL-17B, C, D, and E. These pro-inflammatory cytokines bind to a heteromeric receptor complex composed of the IL-17 receptor A (IL-17RA) and the IL-17 receptor C (IL-17RC) to mediate host protection against infections, while also contributing to the pathogenesis of various autoimmune diseases.¹ IL-17A and IL-17F share 50% sequence identity and are known to function as homodimers. Nevertheless, they can also form a biologically active heterodimer, IL-17AF,^{2,4} which also signals through the IL-17RA/IL-17RC receptor complex,³ but whose physiological role is still largely unknown. We have determined the crystal structure of human IL-17AF at 2.3 Å resolution. Like IL-17A and F, IL-17AF is a disulfide-linked dimer, with the two protein chains associated in a parallel manner. Both subunits show the expected cystine-knot fold with two intrachain disulfide bridges. The core of the dimer interface is mainly defined by one pair of anti-parallel β -strands from each chain and involves many hydrophobic residues conserved across IL-17A and F. Additionally, the N-terminal segments of each protein chain reach the other subunit across the dimer interface, thus providing extensive additional contacts. Besides their similar overall topology, the IL-17RA receptor binding sites are highly conserved between the hetero- and homo-dimeric forms.^{6–8} In human IL-17AF, however, a hydrophobic pocket that is essential for IL-17RA recognition is occluded in the IL-17F subunit by a phenylalanine residue (Phe18) of the N-terminal region of IL-17A. Interestingly, while this binding site is also occupied by two phenylalanine residues (Phe10 and Phe11) in the IL-17F homodimer it is freely accessible in the IL-17A homodimer.^{6,8} This hydrophobic lock may thus be an important structural element in modulating IL-17RA receptor binding and may contribute to the distinct binding affinities of this receptor for the different IL-17A/F isoforms.⁵

References 1. Wei J & Chen D (2013) *Emerging Microbes & Infections* 2, e60. 2. Chang SH, Dong C (2007) *Cell Res*; 17(5): 435–40. 3. Liang SC et al (2007) *J Immunol*; 179: 7791–7799. 4. Wright JF et al (2007) *J Biol Chem*; 282: 13447–13455. 5. Wright JF et al (2008) *J Immunol*; 181: 2799–2805. 6. Hymowitz SG et al (2001) *EMBO J*; 20(19): 5332–41. 7. Ely LK et al (2009) *Nat Immunol*; 10(12): 1245–51. 8. Liu S et al (2013) *Nat Commun*; 4: 1888.

Keywords: IL-17, cytokine, structure

MS7. Nucleic acids and their complexes and assemblies with proteins

Chairs: Miquel Coll, Christine Cardin

MS7-P1 Structural basis for the inhibition of CCL2-signaling by a mirror-image aptamer

Christian Betzel¹, Oberthuer Dominik^{1,2}

1. Laboratory for Structural Biology of Infection and Inflammation, University of Hamburg, c/o DESY Building 22a, Notkestrasse 85, 22607 Hamburg, Germany

2. Center for Free-Electron Laser Science, Deutsches Elektronen Synchrotron-DESY, Notkestrasse 85, 22607 Hamburg, Germany

email: Christian.Betzel@uni-hamburg.de

The crystal structure of a 40mer mirror-image RNA oligonucleotide completely built from nucleotides of the non-natural L-chirality in complex with the pro-inflammatory chemokine L-CLL2 (monocyte chemoattractant protein 1), a natural protein composed of regular L-amino acids, will be reported (Oberthuer, 2014). The L-oligonucleotide is an L-aptamer (a Spiegelmer®) identified to bind L-CCL2 with high affinity, thereby neutralizing the chemokine's activity. CCL2 plays a key role in attracting and positioning monocytes; its overexpression in several inflammatory diseases makes CCL2 an interesting pharmacological target. The PEGylated form of the L-aptamer, NOX-E36 (emapticap pegol), already showed promising efficacy in clinical Phase II studies conducted in diabetic nephropathy patients. The structure of the L-oligonucleotide•L-protein complex was solved and refined to 2.05 Å. It unveils the L-aptamer's intramolecular contacts and permits, in combination with binding studies, a detailed analysis of its structure-function relationship. Furthermore, the analysis of the intermolecular drug-target interactions reveals insight into the selectivity of the L-aptamer for certain related chemokines. Oberthuer, D. et al. Crystal structure of a mirror-image L-RNA aptamer (Spiegelmer) in complex with the natural L-protein target CCL2. *Nat Commun* 6, 6923 (2015).

Keywords: CCL2, aptamers, L-RNA, chemokines, drug-target interactions

MS7-P2 Structural and biochemical insights into grainyhead-like 1 and its homolog grainyhead-like 3

Qianqian Ming¹, Yvette Roske¹, Anja Schuetz¹, Udo Heinemann¹

1. Max-Delbrück Center for Molecular Medicine Berlin-Buch, Germany

email: Qianqian.Ming@mdc-berlin.de

Grainyhead is one of the best studied genes encoding transcription factors of the CP2 family (TFCP2) which contribute to the regulation of gene expression from early embryonic development to terminal cell differentiation in *Drosophila*. It has been established that there are three Grainyhead homologs in the human genome, encoding transcription factors Grainyhead-like 1, 2, and 3 (Grhl1, Grhl2, Grhl3). They are expressed in the surface ectoderm and in other epithelial tissues. By regulating genes involved in cell junction formation and proliferation, they can control the development and differentiation of multicellular epithelia. Molecular mechanisms of Grhl function have been ascribed in three ways. Grhl genes can be regulated at the transcriptional level or by alternative splicing. Following post-translational modification, Grhl proteins can compete with an activator or repressor for DNA binding or associate with other transcription factors, cooperatively regulating common downstream genes. Despite the experimental studies already been published, the knowledge on the structural mechanism of activity of this transcription factors remains sparse. There is no structure report about any CP2 family member as yet of. In our current work we employ X-ray crystallography to analyze the three-dimensional structure of human Grhl1 and Grhl3. Like all members of the Grhl family the proteins Grhl1-3 are composed of three domains, a N-terminal transactivation domain (TAD), a central DNA-binding domain (DBD) and a C-terminal dimerization domain (DD). We have obtained soluble Grhl1 and Grhl3 protein with several constructs varying in length, and we obtained crystals for truncated Grhl1. The crystal optimization and structure determination is ongoing, and we hope to present a first glimpse of the 3D structure at the conference. Meanwhile we used electrophoretic mobility shift assays (EMSA) and isothermal titration calorimetry (ITC) to investigate the DNA binding behavior of the soluble Grhl constructs. In the future, upon structural determination of the Grhl1 DBD by itself and in complex with DNA response elements, as well as by comparison of the Grhl1 and Grhl3 DNA-binding network, we aim to explain the structural basis of the Grhl proteins' DNA sequence recognition and binding to the response elements.

Keywords: cp2,grhl,transcription factor,crystal

MS7-P3 Fascinating novel coordination chemistry of copper(II) bound to d(CGCGCG) and explored by single crystal X-ray analysis

Bernhard Spingler¹, Melanie Rohner¹, Alfredo Medina-Molner¹

1. University of Zurich, Switzerland

email: spingler@chem.uzh.ch

Generating supramolecular *n*-dimensional arrays by combining metals with DNA building blocks that are modified in order to include metal binding sites is a very active field of research⁽¹⁾. Using unmodified nucleobases avoids a potentially difficult synthesis with the disadvantage of a less defined coordination mode of the metal. In the following, we will concentrate on copper(II) as a linking metal and guanine as the natural ligand for metals in unmodified DNA. In this context, it is interesting to explore the binding of two guanines, that are part of two different oligonucleotides, to one copper center as a simple way in order to build up supramolecular structures.

Previously, we were exploring the ability of mono- and dinuclear metal complexes to induce Z-DNA⁽²⁾. In this presentation, we will report about our X-ray studies of copper(II) ions with DNA hexamers⁽³⁾ of the general sequence d(CG)₃ that form 3 different packing modes as observed in 3 crystal structures with resolutions ranging from 2.15 Å to 1.45 Å. Dependent upon other factors being present and/or crystallization conditions, different packing motives were observed. Excitingly, we observed the first intramolecular O6,N7-chelate of a neutral purine nucleobase to copper as well as the first meridional N,N,O coordination of 2 guanines to copper. The fascinating coordination chemistry of copper(II) imposed by the Z-DNA oligonucleotides and its differences to simple nucleobases as ligands for copper(II)⁽⁴⁾ will be discussed as well.

(1) Burns, J. R.; Zekonyte, J.; Siligardi, G.; Hussain, R.; Stulz, E. *Molecules* **2011**, *16*, 4912; McLaughlin, C. K.; Hamblin, G. D.; Sleiman, H. F. *Chem. Soc. Rev.* **2011**, *40*, 5647; Kalachova, L.; Pohl, R.; Bednarova, L.; Fanfrlik, J.; Hock, M. *Org. Biomol. Chem.* **2013**, *11*, 78.

(2) Medina-Molner, A.; Spingler, B. *Chem. Commun.* **2012**, *48*, 1961; Medina-Molner, A.; Rohner, M.; Pandiarajan, D.; Spingler, B. *Dalton Trans.* **2015**, *44*, 3664.

(3) Kagawa, T. F.; Geierstanger, B. H.; Wang, A. H.-J.; Ho, P. S. *J. Biol. Chem.* **1991**, *266*, 20175; Geierstanger, B. H.; Kagawa, T. F.; Chen, S.-L.; Quigley, G. J.; Ho, P. S. *J. Biol. Chem.* **1991**, *266*, 20185; Rohner, M.; Medina-Molner, A.; Spingler, B. **2015**, submitted.

(4) Sletten, E.; Flogstad, N. *Acta Cryst.* **1976**, *B32*, 461; Sheldrick, W. S. *Acta Cryst.* **1981**, *B37*, 1820; Zhou, P.; Li, H. *Dalton Trans.* **2011**, *40*, 4834; Nagapradeep, N.; Venkatesh, V.; Tripathi, S. K.; Verma, S. *Dalton Trans.* **2014**, *43*, 1744.

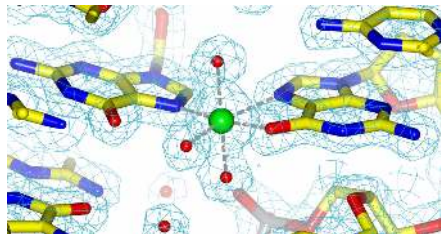


Figure 1. Intramolecular O6,N7-chelate of guanine (right) to copper (green) and meridional N,N,O coordination of 2 guanines to copper.

Keywords: DNA, metal, supramolecular arrangement, copper(II)

MS7-P4 Signal sequence binding to the archaeal signal recognition particle

Elisabeth Sauer-Eriksson¹, Tobias Hainzl¹

¹, Department of Chemistry, Umea University, Sweden

email: elisabeth.sauer-eriksson@umu.se

The signal recognition particle (SRP) co-translationally targets proteins to the endoplasmic reticulum in eukaryotes or to the plasma membrane in prokaryotes. As the initiating step, SRP binds to the N-terminal signal sequence of nascent secretory or membrane proteins as they emerge from the ribosome. The SRP-ribosome nascent chain complex is then targeted to the membrane through a GTP-dependent interaction with the SRP receptor (SR). The signal sequence is released from SRP and inserted into the translocon channel. Finally, GTP hydrolysis triggers the dissociation of SRP from SR, and SRP can start another cycle of protein targeting.

SRP composition varies in the three domains of life. However, the evolutionary conserved SRP core only comprises the SRP54 protein bound to the coaxial stacked helices 5 and 8 of SRP RNA. SRP54 comprises an N-terminal NG domain that interacts with SR and a C-terminal methionine-rich M domain that binds to the signal sequence. Signal-sequence binding in the SRP54 M domain must therefore be effectively communicated to the SRP54 NG domain for receptor interaction. We have determined the 2.9 Å crystal structure of unbound- and signal-sequence bound SRP forms, both present in the asymmetric unit. The structures provide evidence for a coupled binding and folding mechanism in which signal-sequence binding induces the concerted folding of the GM linker helix, the finger loop, and the C-terminal alpha helix α M6. This mechanism allows for a high degree of structural adaptability of the binding site and suggests how signal-sequence binding in the M domain is coupled to repositioning of the NG domain for accelerated receptor interaction. We propose that signal-sequence recognition via a disorder-to-order transition of multiple structural elements facilitates specific recognition of widely diverse signal sequences.

Keywords: signal recognition particle, SRP, crystal structure, signal peptide, archaea

MS7-P5 Application structures of nucleotide-protein complexes to study RNA recognition by bacterial and archaeal Lsm proteins

Alexey D. Nikulin¹, Natalia V. Lekontseva¹, Victoria N. Murina¹, Ekaterina Y. Nikonova¹, Alice O. Mikhaylina¹, Svetlana V. Tishchenko¹

1. Institute of Protein Research, Russia Academy of Sciences

email: nikulin@vega.protres.ru

Sm-like proteins (Lsm) exist in all three domains of life and are defined by the so-called Sm fold, which is comprised of an N-terminal α -helix and five anti-parallel β -strands. Bacterial Lsm proteins Hfq is a post-translational regulator of gene expression that binds small non-coding RNAs (sRNA) and promotes their interaction with mRNAs. Eukaryotic Lsm proteins act as chaperone for mRNAs and non-coding RNAs through various steps in metabolism. Function of the archaeal Lsm proteins have studied poor but it is known they bound archaeal sRNA.

Structures of Lsm proteins in complexes with short oligo-RNAs promote understanding involvement of the proteins in the RNA metabolism greatly. Recently we have used complexes of proteins with single ribonucleotides to determine the RNA-binding sites on the protein surface [1]. The complexes can be obtained before crystallization or by soaking of the protein crystals in the ribonucleotides solution. Typically, preparation of nucleotide-protein crystals is easier than the crystallization of large RNA-protein complexes. Using this technique we have identified three different RNA-binding sites on the Hfq surface, one of them have been located for the first time. Now we are using this technique to study archaeal Lsm proteins from *Methanococcus jannaschii* and *Sulfolobus solfataricus* and our last results will be demonstrated. This method can be used to study any RNA-binding protein interacting with single-stranded RNA.

This work was supported by the Russian Scientific Foundation (grant # 14-14-00496) and by the Russian Foundation for Basic Research (grant #13-04-00783).

[1] V. Murina, N. Lekontseva, A. Nikulin, Hfq binds ribonucleotides in three different RNA-binding sites, Acta Crystallogr, D69 (2013) 1504-1513.

Keywords: Lsm, Hfq, archaea, RNA-protein interaction, single-stranded RNA, ribonucleotide-protein complexes

MS7-P6 Structural biology of 5hmC-specific endonuclease PvuRtsII

Asgar Abbas Kazrani¹, Monika Kowalska¹, Honorata Czapinska¹, Matthias Bochtler^{1,2}

1. International Institute of Molecular and Cell Biology, Trojdena 4, 02109 Warsaw, Poland

2. Institute of Biochemistry and Biophysics, Polish Academy of Sciences, Pawinskiego 5a, 02106 Warsaw, Poland

email: abbas@iimcb.gov.pl

PvuRtsII is a prototype for a larger family of restriction endonucleases that cleave DNA containing 5-hydroxymethylcytosine (5hmC) or 5-glucosylhydroxymethylcytosine (5ghmC), but not 5-methylcytosine (5mC) or cytosine. Here, we report a crystal structure of the enzyme at 2.35 Å resolution. Although the protein has been crystallized in the absence of DNA, the structure is very informative. It shows that PvuRtsII consists of an N-terminal, atypical PD-(D/E)XK catalytic domain and a C-terminal SRA domain that might accommodate a flipped 5hmC or 5ghmC base. Changes to predicted catalytic residues of the PD-(D/E)XK domain or to the putative pocket for a flipped base abolish catalytic activity. Surprisingly, fluorescence changes indicative of base flipping are not observed when PvuRtsII is added to DNA substrates containing pyrrolocytosine in place of 5hmC (5ghmC). Despite this caveat, the structure suggests a model for PvuRtsII activity and presents opportunities for protein engineering to alter the enzyme properties for biotechnological applications.



Figure 1. Model for PvuRtsII dimer binding to 5hmC containing DNA

Keywords: PvuRtsII, endonuclease, SRA, PD-(D/E)XK, 5-hydroxymethylcytosine

MS7-P7 X-ray crystallographic and photophysical studies of DNA i-motifs

Sarah P. Gurung¹, James P. Hall^{1,2}, Graeme Winter¹, John A. Brazier³, Rohanah Hussain¹, Giuliano Siligardi¹, Thomas Sorensen¹, Christine J. Cardin^{2,4}

1. Diamond Light Source, Harwell Science and Innovation Campus, Didcot, UK

2. Department of Chemistry, University of Reading, Reading, UK

3. School of Pharmacy, University of Reading, Reading, UK

4. Dynamic Structural Sciences, Research Complex at Harwell, Harwell Science and Innovation Campus, Didcot, UK

email: sarah.gurung@diamond.ac.uk

An i-motif is a four stranded structure made of cytosine-rich DNA sequences. Its sequence is usually in the format of $C_{2-5}L_{1-9}C_{2-5}L_{1-9}C_{2-5}L_{1-9}C_{2-5}$, where C is cytosine and L represents any other base. The conformational change from the C-rich single strand DNA to i-motif takes place between pH 5 and 6.7. These acidic conditions help two parallel i-motif duplexes “zip” together in an antiparallel orientation by protonating N3 in cytosines to create hemiprotonated C-C⁺ base pairs (fig. 1).¹

The i-motif can form as either an inter- or an intramolecular structure. However, only six i-motif crystal structures have been reported on the NDB; all of which are tetramolecular, even though i-motifs *in vivo* would exist as unimolecular. The c-Myc, Bcl-2 and hTERT i-motifs are all unimolecular and are present in the promoter regions of their respective oncogenes.² Like the guanine rich G-quadruplex, the presence of a cytosine rich sequence has also been detected within the promoter region of the human telomeric and centromeric DNA, making i-motifs an attractive subject for gene transcription modulation.

UV and synchrotron radiation CD (srCD; beamline B23 at Diamond Light Source) spectroscopy were used to study the structural stability of intramolecular i-motifs. Our results showed that i-motifs with shorter loop lengths exhibit the highest stability.³ Crystallisation trials based on these initial results will be discussed along with previously recorded i-motif crystals grown in new conditions. We will also be reporting the diffraction of d(CCCT)₄ crystals at 0.68 Å at beamline I02, illustrating the advances in modern-day DNA crystallography via synchrotron radiation. Combination of results from the mentioned instrumental approaches shows that these methods are actually complementary.

References

1. Gehring, K., Leroy, J. L. & Gueron, M. A tetrameric DNA structure with protonated cytosine-cytosine base pairs. *Nature* **363**, 561–565 (1993).
2. Phan, A. T. & Mergny, J.-L. Human telomeric DNA: G-quadruplex, i-motif and Watson-Crick double helix. *Nucleic acids research* **30**, 4618–25 (2002).
3. Gurung, S. P., Schwarz, C., Hall, J. P., Cardin C. J. & Brazier, J. A. The importance of loop length in the stability of i-motif structures. *Chem. Commun.* **51**, 5630–32 (2015).

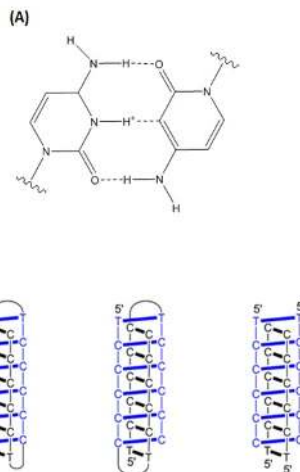


Figure 1. (A) C-C⁺ base pairing in i-motifs. (B) Schematic diagrams of unimolecular (left) bimolecular (middle) and tetramolecular (right) i-motifs.

Keywords: i-motif, DNA, srCD

MS7-P8 New G-quadruplex DNA structures

Boris L. Shivachev¹, Louiza T. Dimova², Rosica P. Nikolova²,
Hristina I. Shirkova², Lilia Tzvetanova², Peter Hristoff¹, Georgi
Radoslavov¹, Doukov I. Tzanko³

1. Institute of Biodiversity and Ecosystem Research, Bulgarian Academy of Sciences 2 Gagarin Street, 1113 Sofia, Bulgaria
2. Institute of mineralogy and crystallography "Acad. Ivan Kostov"
3. Macromolecular Crystallographic Group, Stanford Synchrotron Radiation Lightsource, SLAC National Accelerator Laboratory, Stanford University, Stanford, CA 94309

email: blshivachev@gmail.com

The selection of potential new G-quadruplex DNA sequences has been performed using bioinformatics. The possible formation of G-quadruplex by the selected sequences has been assessed by PCR and fluorescence methods. Attempts for growing suitable single crystals of the selected DNA sequences has been performed in parallel. The results for G-quadruplex formation obtained by the molecular biology method and from crystallization results have been compared in order to verify the viability of the methods.

Keywords: Nucleic acid, G-quadruplex, DNA

MS7-P9 Radiation damage in protein-nucleic acid complexes

Charles S. Bury¹, John E. McGeehan², Mikhail B. Shevtsov³,
Alfred A. Antson¹, Elspeth F. Garman¹

1. Department of Biochemistry, University of Oxford, South Parks Road, Oxford, OX1 3QU
2. Biophysics Laboratories, Institute of Biomedical and Biomolecular Sciences, University of Portsmouth, King Henry I Street, Portsmouth, Hampshire PO1 2DY, UK
3. Laboratory of Structural Biology of GPCRs, Moscow Institute of Physics and Technology, Dolgoprudny 141700, Russia
4. York Structural Biology Laboratory, Department of Chemistry, University of York, York YO10 5DD, UK

email: charles.bury@dtc.ox.ac.uk

Significant progress has been made over recent years in understanding how radiation damage mechanisms affect crystalline protein structure determination. Despite an active field studying the radiation chemistry of nucleic acids interacting with ionising radiation, few MX investigations exist on specific damage manifestations for crystalline DNA/RNA in their complexes with protein. Quantitative controlled comparisons between crystallised protein and nucleic acid damage mechanisms separately remain inherently difficult, but such challenges can be circumvented through investigating naturally forming nucleoprotein complexes. A recent study (1) utilised a model protein-DNA complex C.Esp1396I (2) to quantitatively investigate specific damage mechanisms for protein and DNA in a biologically relevant complex over a large dose range (2.07–44.63 MGy). A computational approach was developed to systematically locate damage sites, identifying typical specific damage sites on the complex. Strikingly the DNA component was determined to be far more resistant to specific damage than the protein for the investigated dose range.

For such complexes, the protein may be simply more susceptible to radiation damage, or may act as an electron/radical scavenger to protect DNA constituents. To address this issue, our previous computational strategy has been extended to statistically investigate damage dynamics in crystals of a large protein-RNA complex: TRAP (tryptophan-binding RNA attenuation protein) bound to 53 base RNA (3). The TRAP-RNA complex naturally crystallises in a 1:1 ratio with its RNA-unbound form, making it an ideal controlled experiment. RNA binding has been observed to stabilise susceptible protein residues, providing direct protection from electron density loss and disorder. Damage-susceptible acidic residues located far from the RNA-binding interface have increased decarboxylation rates upon RNA binding; the direct mechanisms behind this damage heterogeneity, and the implications of scavenging effects within crystalline nucleoprotein complexes are yet to be established.

References

1. Bury C, *et al.*, McGeehan, JE (2015). *J. Synchrotron Radiat.* 22, 213–224
2. McGeehan JE, *et al.*, Kneale GG (2008). *Nucleic Acids Res.* 36(14), 4778–87
3. Hopcroft NH, *et al.*, Antson AA (2002). *Nature* 58(4), 615–621

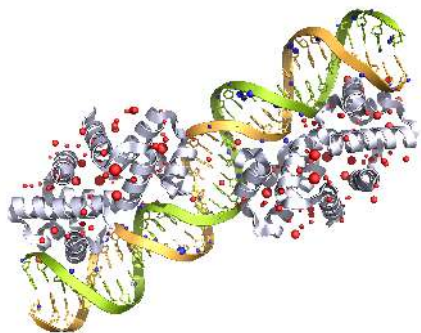


Figure 1. Representation of specific damage distribution throughout the C.Esp1396I complex at 44.63 MGy (1). Specific damage sites are represented as spheres, with radii proportional to electron density loss. Spheres closer/ further than 2 Å to/from the DNA strands are coloured blue/red.

Keywords: macromolecular X-ray crystallography, radiation damage, protein-nucleic acid complexes

MS7-P10 Structural studies on DNA cleavage-and-ligation nucleases of mobile genetic elements involved in spread of antibiotic resistance

Radosław Pluta^{1,2}, D Roeland Boer¹, Alicia Guasch¹, Silvia Russi¹, José Ruiz-Maso³, Cris Fernandez-Lopez³, Fabian Lorenzo-Diaz³, Maria Lucas⁴, Gloria del Solar³, Fernando de la Cruz⁴, Manuel Espinosa³, Miquel Coll¹

1. Institute for Research in Biomedicine (IRB Barcelona), Spain and Institut de Biologia Molecular de Barcelona (CSIC), Spain
2. International Institute of Molecular and Cell Biology in Warsaw (IMCB Warsaw), Poland
3. Centro de Investigaciones Biológicas (CSIC), Madrid, Spain
4. Instituto de Biomedicina y Biotecnología de Cantabria (IBBTec), Santander, Spain

email: rpluta@genesilico.pl

Plasmids and integrative and conjugative elements (ICEs) are major mobile genetic elements (MGEs) that provide routes for rapid acquisition of new genetic information in bacteria and therefore contribute to the spread of antibiotics resistance. Essential for their action are plasmid/ICE-encoded site- and strand-specific one-metal-ion endonucleases called relaxases. Conjugative relaxases cleave a single strand of the DNA substrate by formation of an intermediate covalent adduct with the scissile phosphate of the DNA nic site. After the ssDNA-relaxase molecule is transferred to the recipient cell, relaxases ensure re-ligation of their DNA cargo. Additionally, plasmids and some ICEs encode for DNA replication relaxases, crucial for their maintenance. Understanding plasmid/ICEs conjugal transfer and replication may aid in combating the spread of antibiotics resistance as well as contribute to the development of new tools for DNA delivery into human cells. Structures of replicative and conjugative relaxases RepB, MobM and TrwC that were solved in our lab are compared herein.

Keywords: relaxases, endonucleases, bacterial conjugation, plasmid replication, antibiotic resistance

MS7-P11 Structural similarity between the N-terminal domain of LonA proteases and the highly conserved RNA-binding PUA domainsAlla Gustchina¹, Alexander Wlodawer¹, Tatyana Rotanova²

1. Macromolecular Crystallography Laboratory, National Cancer

Institute, Frederick, MD, USA

2. Shemyakin-Ovchinnikov Institute of Bioorganic Chemistry, Russian Academy of Sciences, Moscow, Russia

email: gustchia@mail.nih.gov

Homooligomeric LonA proteases are the key components of the protein quality control system in bacteria and eukaryotes. Proteolytic activity of LonA is coupled to ATP hydrolysis. Pioneering studies in the 1980s have shown that members of this family of proteases/ATPases are also nucleic acid-binding proteins, and their proteolytic and ATPase activities are stimulated by DNA binding. Such studies indicated that a number of different DNA species increased the rate of degradation of target proteins by the protease, and suggested that association with DNA might be involved in regulation of protein breakdown in cells. In particular, studies of the mitochondrial LonA demonstrated that this enzyme binds to DNA and RNA, and that the binding affinity is affected by the presence of a nucleotide and a protein substrate.

Structural data for the individual domains and/or their combinations have recently become available for several representative LonA proteins. Crystal structure of the N-terminal fragment of *E. coli* LonA comprising residues 1–117 revealed structural similarity to the PUA domain, a highly conserved RNA-binding motif found in a wide range of archaeal, bacterial, and eukaryotic proteins. Here we compare the structure of the N-terminal domain of LonA to the structures of the PUA domains from several protein complexes with RNA, with the aim to reveal possible epitopes for the interactions with nucleic acids.

Keywords: ATP-dependent protease, structure comparison**MS7-P12** Structural investigation of importin β :importin7:histone1 complexNives Ivic¹, Silvija Bilokapic Halic¹, Mario Halic¹

1. Gene Center, Ludwig-Maximilians University, Munich

email: nivic@irb.hr

During DNA replication, histones synthesised in the cytoplasm must be imported into the nucleus for the formation of nucleosomes on newly replicated DNA. In spite of their small size, histones are transported by active transport requiring import receptors. The core histones are transported in the nucleus by monomeric import receptors, members of the importin β superfamily. Exceptions are linker histones, which require a formation of a heterodimeric receptor consisting of two importin β family members, importin β (Imp β) and importin7 (Imp7). Up to date, there is no detailed structural information about the interaction network and recognition mode between importin β , importin7 and histone1. Biochemical data indicate that both, histone1 core and tail, are important for the interaction with Imp β :Imp7, which should result with defined histone tail structure. Each of the proteins is individually overexpressed in bacterial cells and for all of them a successful purification protocol has been established. The importin β :importin7:histone1 complex was prepared by mixing the three proteins in a molar ratio 1:1:1 in assembly buffer. Currently crystallization trials are underway. With molecular size of around 250 kDa, the trimeric complex is at the limits of cryo electron microscopy, which makes it a very good model for pushing cryoEM to new frontiers. Initial negative stain grids have been prepared for each component of the complex, as well as the complex itself. The grids have been inspected using the electron microscope Morgagni. Complex particles can be clearly distinguished from the single particles found on the grids. Negative stain data collection for initial 3D reconstruction will be performed; as well the samples for cryo-electron microscopy (cryoEM) are being prepared.

Keywords: protein crystallography, histones, importins, nucleosome

MS7-P13 Structure and mechanism of reverse transcriptases

Elzbieta Nowak¹, Jennifer T. Miller², Marion K. Bona², Justyna Studnicka¹, Petr V. Konarev³, Roman H. Szczepanowski⁴, Wojciech Potrzebowski⁵, Dmitri I. Svergun³, Jakub Jurkowski¹, Janusz Bujnicki⁵, Stuart F. Le Grice², Marcin Nowotny¹

1. Laboratory of Protein Structure, International Institute of Molecular and Cell Biology, Warsaw, Poland
2. Reverse Transcriptase Biochemistry Section, HIV Drug Resistance Program, Frederick National Laboratory, Frederick, MD, USA
3. European Molecular Biology Laboratory, Hamburg Outstation, Hamburg, Germany
4. Biophysics Core Facility, International Institute of Molecular and Cell Biology, Warsaw, Poland
5. Laboratory of Bioinformatics and Protein Engineering, International Institute of Molecular and Cell Biology, Warsaw, Poland

email: enowak@iimcb.gov.pl

Reverse transcription is a complex process in which single stranded RNA is converted into integration competent double-stranded DNA. This process is exclusively performed by enzyme called reverse transcriptase (RT). The RT-s are a multidomain proteins which consist of N-terminal polymerase domain and a C-terminal RNaseH domain. The multifunctional RTs possess two active sites, first is placed in polymerase domain, where all DNA elongation steps occur and the second is within RNaseH domain which is responsible for RNA hydrolysis within DNA/RNA hybrid. All of the structural information available for RTs concern the retroviral enzymes (1,2). In contrast there is paucity in equivalent studies on counterpart enzymes of LTR-containing retrotransposons, from which they are evolutionarily derived. We recently solved the first crystal structure of Ty3 RT in complex with its RNA/DNA substrate (3). In contrast to its retroviral counterparts, Ty3 RT adopts an asymmetric homodimeric architecture, whose assembly is substrate-dependent. More strikingly, our structure and biochemical data suggest that the RNase H and DNA polymerase activities are contributed by individual subunits of the homodimer.

(1) Huang H et al. "Structure of a covalently trapped catalytic complex of HIV-1 reverse transcriptase: implications for drug resistance" 1998, *Science*, 282, 1669-75.

(2) Nowak E et al. "Structural analysis of monomeric retroviral reverse transcriptase in complex with an RNA/DNA hybrid" 2013, *Nucl. Acids Res.* 41, 3874-87.

(3) Nowak E et al. "Ty3 reverse transcriptase complexed with an RNA-DNA hybrid shows structural and functional asymmetry" 2014, *NSMB*, 21 (4), 389-396.

Keywords: reverse transcription, protein DNA/RNA complex

MS7-P14 Viral RNA binding by the human IFIT1-IFIT3 protein complex in the innate immune response.

Maria W. Górna¹, Gregory I. Vladimer², Yazan M. Abbas³, Anna Gebhardt⁴, Matthias Habjan⁴, Beatrice T. Laudenschach⁴, Christina Dimech³, Irene Y. Xie⁴, Keiryn L. Bennett⁴, Bhushan Nagar⁴, Andreas Pichlmair⁴, Giulio Superti-Furga²

1. Faculty of Chemistry, University of Warsaw, 02-093 Warsaw, Poland
2. CeMM Research Center for Molecular Medicine of the Austrian Academy of Sciences, 1090 Vienna, Austria
3. Department of Biochemistry, and Groupe de Recherche Axé sur la Structure des Protéines, McGill University, Montreal, Quebec H3G 0B1, Canada
4. Innate Immunity Laboratory, Max-Planck Institute of Biochemistry, 82152 Martinsried/Munich, Germany

email: mgorna@chem.uw.edu.pl

The interferon-induced proteins with tetratricopeptide repeats (IFITs) have recently emerged as a potent innate immune effectors that bind non-self RNA, which results in the inhibition of translation of viral transcripts. The structure of IFIT5 reveals the mode of recognition of the 5' triphosphate (PPP) group on RNA, whereas IFIT1 can recognize both 5'-PPP or cap 0 groups. IFIT1 interacts with IFIT3, which has no known RNA binding capability on its own, and for which the role in the larger multi-IFIT complex is elusive. Here, we begin the dissection of the role of the higher-order IFIT complexes and demonstrate that the IFIT1-IFIT3 complex binds RNA with a higher affinity than IFIT1 alone. The IFIT1-IFIT3 interaction, which is mediated by the last tetratricopeptide repeat motifs in both proteins, is necessary for the full antiviral effect of IFIT1 against VSV. In cells, IFIT1 and IFIT3 associated together, and re-distributed and co-localized together with PPP-RNA. We propose a new role for IFIT3 as an enhancer of IFIT1 activity. Regulation of the IFIT1-IFIT3 complex may provide additional possibility for signal integration in the antiviral response.

Keywords: tetratricopeptide repeats, RNA binding, IFIT

MS7-P15 Studies of the conformational changes on the ribosomal GTPase EFL1 using SAXS

Dritan Siliqi¹, Nuria Sanchez-Puig², Eugenio de la Mora², Alfonso Méndez-Godoy², Davide Altamura¹, Cinzia Giannini¹, Teresa Sibillano¹, Michele Saviano¹

1. Institute of Crystallography-CNR, Via G. Amendola, 122/O. 70126, Bari, Italy

2. Instituto de Química, Universidad Nacional Autónoma de México, Circuito Exterior, Ciudad Universitaria, México D.F., México.

email: dritan.siliqi@ic.cnr.it

Ribosome biogenesis is closely linked to the cell growth and proliferation. Dysregulation of this process causes several diseases collectively known as ribosomopathies. One of them is the Shwachman-Diamond Syndrome, and the SBDS protein mutated in this disease participates with EFL1 in the cytoplasmic maturation of the 60S subunit. Recently, we have shown that the interaction of EFL1 with SBDS resulted in a decrease of the Michaelis-Menten constant (K_M) for GTP and thus SBDS acts as a GEF for EFL1 (1). Subsequent studies demonstrated that SBDS greatly debilitates the interaction of EFL1 with GDP without altering that for GTP. The interaction of EFL1 alone or in complex with SBDS to guanine nucleotides is followed by a conformational rearrangement. Understanding the molecular strategy used by SBDS to disrupt the binding of EFL1 for GDP and the associated conformational changes will be key to understand their mode of action and alterations occurring in the disease. The structure of the GTPase EFL1 is not known and its crystallization has been unsuccessful at least in our hands. In this study, we aim to show the conformational changes resulting from the interactions between EFL1 and its binding partners, the SBDS protein and the guanine nucleotides using SAXS technique (2,3). SAXS will provide structural information of the proteins and their conformational changes (4). For the SAXS data analysis we have built models of EFL1 using by EF-2 as homology template and of SBDS using the crystal structures of the archaea orthologues.

The authors acknowledge financial support PGR2015 "Con il contributo del Ministero degli Affari Esteri e dalla Cooperazione Internazionale, Direzione Generale per la Promozione del Sistema Paese".

References

1. Gijsbers, A., Garcia-Marquez, A., Luviano, A., and Sanchez-Puig, N. (2013). *Biochem. Biophys. Res. Commun.* **437**, 349-354.
2. Altamura, D., Lassandro, R., De Caro, L., Siliqi, D., Ladisa M. & Giannini, C. (2012). *J. Appl. Cryst.* **45**, 869-873.
3. Svergun, D., Koch, Michel H.J., Timmins, P.A. and May, R.P. (2013). *Small Angle X-Ray and Neutron Scattering from Solutions of Biological Macromolecules*. Oxford University Press.
4. Petoukhov, M.V., Franke, D., Shkumatov, A.V., Tria, G., Kikhney, A.G., Gajda, M., Gorba, C., Mertens, H.D.T., Konarev, P.V. and Svergun, D.I. (2012). *J. Appl. Cryst.* **45**, 342-350.

Keywords: Elongation factor-like 1, Shwachman-Diamond Syndrome, BIOSAXS

MS7-P16 The structural basis of asymmetry in DNA recognition and catalysis: binding and cleavage by the I-SmaMI meganuclease

Betty W. Shen¹, Bradley Walker², Abigail Lambert¹, Barry L. Stoddard¹, Brett K. Kaiser²

1. Division of Basic Sciences, Fred Hutchinson Cancer Research Center, Seattle, WA, U.S.A.

2. Department of Biology, Seattle University, Seattle WA, U.S.A

email: bshen@fhcrc.org

LAGLIDAG homing endonucleases (LHEs) are highly specific DNA cleaving enzymes, also termed 'meganucleases', that are used for genome engineering. These proteins are found both as homo-dimers and as pseudo-symmetric single-chain monomers. Like many other enzymes that act on DNA targets, meganucleases often display highly asymmetric DNA recognition properties, with the overall binding affinity and cleavage activity dominated by interactions between one protein domain and a corresponding DNA half-site. While the importance of asymmetric target recognition, binding and cleavage by meganucleases is important both with respect to their natural function and to their engineering in the lab, the structural basis for that behavior has not been well understood. Here we describe a systematic biochemical and structural analysis for a single-chain meganuclease, I-SmaMI, in which we determined the structure of the wild-type enzyme in the absence of bound DNA, in a complex with uncleaved DNA, and in a complex with cleaved DNA product. Structural comparisons of these structures, combined with binding and cleavage analysis of the wild-type and mutated variants of both the enzyme and substrate, demonstrated the asymmetric 'dominance' by one protein domain over the other during DNA recognition, binding and cleavage of the pseudo-symmetric target site. Information gained from the current study of the I-SmaMI is expected to contribute significantly toward the understanding and reengineering of other meganucleases.

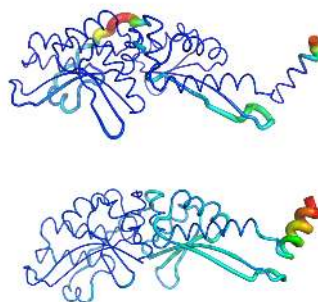


Figure 1. Putty cartoon representations of Apo I-SmaMI model. Top: colored according to B-factor of individual C α atoms. Bottom: colored according to normalized RMSD between the C α atoms of unbound and un-cleaved DNA bound I-SmaMI structures.

Keywords: LAGLIDAG, homing endonuclease, meganuclease

MS8. Molecular machines and motors

STAS domain in SLC26/SulP anion transporters. J Mol Biol. 16, 448.

Keywords: SLC26 anion transporters, prestin, piezoelectric molecular motor, STAS domain

Chairs: Nenad Ban, Leonid Sazanov

MS8-P1 Structural characterization of the STAS domain of prestin

Elisa Costanzi¹, Graziano Lolli¹, Elisa Pasqualetto¹, Greta Bonetto¹, Roberto Battistutta¹

1. Department of Chemical Sciences, University of Padua, via Marzolo 1, 35131 Padova, Italy

email: elisa.costanzi@studenti.unipd.it

Prestin is the anion-dependent motor protein responsible for the outer hair cells (OHCs) electromotility, at the basis of the increased sensitivity and frequency selectivity of the hearing process in mammals. Electromotility is the ability to convert changes in the membrane potential into variations in the OHCs cell length, with an amplification of the auditory stimulus. Prestin, member of the SulP/SLC26 family of anion transporters, is an ATP- and Ca²⁺-independent molecular motor with piezoelectric properties. Prestin function relies on the presence of different monovalent anions. Physiologically the most relevant is chloride that has been proposed to be the extrinsic voltage sensor. While in non-mammals prestin has been shown to be an electrogenic anion transporter, in mammals prestin is considered an incomplete transporter. Topologically, prestin is divided into a large transmembrane domain, a short cytosolic N-term tail and a long cytosolic C-term portion mainly composed by a so-called STAS (Sulphate Transporters and Anti-Sigma factor antagonist) domain, essential for function. The 3D structure of the STAS domain from rat prestin consists of a central β -sheet, composed of 6 β -strands, surrounded by 5 α -helices, a fold conserved from bacteria to mammals (Pasqualetto et al, 2010). Recently, the experimentally validated 3D model of the mammalian TM domain of prestin identified the central anion-binding site in the middle of the domain, along as a possible pathway leading anions from the cytosol (Gorbunov et al, 2014). However, the cytosolic recruitment site for anions has not been identified yet. Here we present crystallographic data revealing the presence of an anion-binding site in the STAS domain of an incomplete-transporter prestin that is absent in a non-mammalian homologue with exchangers properties. This anion-binding site is important for the fine regulation of the electromotile properties of this molecular motor.

Gorbunov D, Sturlese M, Nies F, Kluge M, Bellanda M, Battistutta R, Oliver D (2014) Molecular architecture and the structural basis for anion interaction in prestin and SLC26 transporters. *Nat Comm*, 5, 3622.

Pasqualetto E, Aiello R, Gesiot L, Bonetto G, Bellanda M, Battistutta R (2010) Structure of the cytosolic portion of the motor protein prestin and functional role of the

MS8-P2 Crystal structure of truncated FlgD from the human pathogen *Helicobacter pylori*

Ivana Pulić^{1,2}, Laura Cendron², Marco Salamina², Dubravka Matković-Čalogović¹, Giuseppe Zanotti²

1. University of Zagreb, Faculty of Science, Department of Chemistry, Zagreb, Croatia

2. University of Padua, Department of Biomedical Sciences, Padua, Italy

email: ipulic@chem.pmf.hr

Helicobacter pylori is a Gram-negative pathogen able to colonize the human stomach and is responsible for several gastric pathologies, including gastritis, peptic ulcer, gastric adenocarcinoma and MALT lymphoma.¹ In order to survive in the hard stomach environment and to permanently settle in it, *H. pylori* has to move through the mucous layer and adhere to gastric epithelial cells, especially during the initial phases of the infection. In doing so it has to rely on the flagella, a rotatory nano-machine. Major sections that define the flagellum are: the filament, the hook and the basal body.² In this bacterium FlgD is absolutely needed for the assembly of the flagellar hook, but it has not been detected in the mature flagellum.³ In order to clarify the structural and functional properties of this *H. pylori* virulence factor we performed cloning, purification, crystallization and X-ray analysis studies. The HP0907 gene was cloned from two different *H. pylori* strains, 26695 and G27. Single crystals were prepared by the sitting drop vapor diffusion method using an automated crystallization platform (Oryx 8 robot). Two different crystal forms were obtained. Diffraction data of native FlgD_G27 (*HpFlgD_m*) were measured at the ID14-4 beamline (ESRF, Grenoble, France) and they belong to the monoclinic system, space group *P*2. Crystals of both native and seleno-methionine FlgD_26695 (*HpFlgD_t*) belong to the tetragonal space group *I*422 and the diffraction data of this second crystal form were measured at the PXIII beamline (SLS, Villigen, Switzerland). The quaternary structure in both crystal forms is a tetramer. Four monomers are present in the asymmetric unit of *HpFlgD_m*, corresponding to a V_M of 2.63 Å³ Da⁻¹ and an approximate solvent content of 53%. In the structure of *HpFlgD_t* there is one monomer in the asymmetric unit, with a V_M of 3.26 Å³ Da⁻¹ and an approximate solvent content of 62%. The tetramer is generated by the four-fold symmetry axis. Although crystallization of the full length proteins of both strains, FlgD_G27 and FlgD_26695 was attempted (316 and 301 amino acids residues, respectively) the structures revealed the truncated form with the monomers comprising residues Asn127 - Lys272.

[1] Rothenbacher, D. and Brenner H., *Microbes Infect*, **5** (2003) 693-703.

[2] Soutourina O.A. and Bertin P.N., *FEMS Microbiol Rev* **27** (2003) 505-523.

[3] Ohnishi, K., Fan F., Schoenhalz G.J., Kihara M. and Macnab R.M., *J Bacteriol*, **179** (1997) 6092-6099.

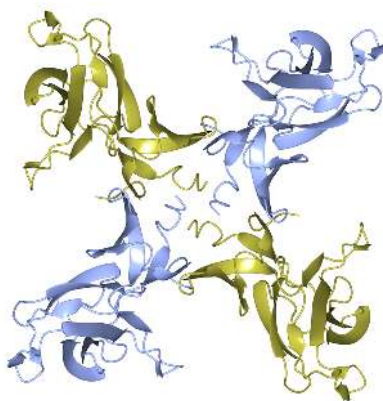


Figure 1. The quaternary structure of the monoclinic form of *HpFlgD* (two independent monomers are shown in blue and gold color)

Keywords: *H. pylori*, FlgD, X-ray diffraction

MS8-P3 Structural and Biochemical Characterization of Sjögren syndrome/scleroderma autoantigen 1 (SSSCA1)

Harmonie J.G. Perdreau-Dahl^{1,2}, Hanne Guldsten², Cinzia Progidà³, Magnus Arntzen⁴, Bernd Thiede⁴, Oddmund Bakke³, J. Preben Morth^{1,2}

1. Institute for Experimental Medical Research (IEMR), Oslo University Hospital, Ullevål PB 4956 Nydalen, NO-0424 Oslo, Norway

2. Centre for Molecular Medicine Norway (NCMM), Nordic EMBL Partnership, University of Oslo, P.O. Box 1137 Blindern, 0318 Oslo, Norway

3. Centre for Immune Regulation, Department of Molecular Biosciences, University of Oslo, Blindernveien 31, 0371 Oslo, Norway

4. The Biotechnology Centre of Oslo, University of Oslo, P.O. Box 1137 Blindern, 0318 Oslo, Norway

email: harmonie.perdreau@ncmm.uio.no

Sjögren syndrome/scleroderma autoantigen 1 (SSSCA1) was discovered in the late 1990's as a novel auto-antigen over-expressed in Sjögren's syndrome and/or scleroderma patients [1]. Functionally, SSSCA1 is largely uncharacterized although it has been linked to mitosis and centromere association [1; 2]. In the past five years, it has been reported in a number of studies for its possible implication in: (i) The Wnt signaling pathway [3; 4], (ii) the cellular proliferation or stroma activation of several cancer cells [5] and (iii) identified as a key gene for pathway activity in colorectal adenoma-to-carcinoma progression [6]. In order to verify these hypotheses and to characterize SSSCA1, we have combined results from structural biology, cellular imaging techniques and proteomics.

Human SSSCA1 is a small protein of 21.5 kDa composed of three domains: An N-terminal zinc finger domain, an intermediate proline-rich region and a C-terminal helical domain. A phylogenetic tree revealed that SSSCA1's domains architecture is evolutionary conserved. We have recently determined the crystal structure of the highly conserved zinc binding domain at a resolution of 2.8 Å and showed that SSSCA1 forms a homodimer. This domain possesses a unique architecture and represents a new Pfam family of clan Zn-binding ribbon domain.

The primary structure of the C-terminus has been predicted as highly disordered [7]. SSSCA1 therefore belongs to the very large protein family of intrinsically disordered proteins (IDP's), whose function is coupled to the folding/binding with a specific partner. We have thus developed a tandem affinity purification (TAP) method coupled to cell imaging and mass spectrometry [8] to identify SSSCA1's binding partners in different cancer cell lines. We are now working on the confirmation and characterization of the five best hits using different approaches (cellular assays, human cells, yeast and *E. coli* expression, purification, crystallization, drug screening ...).

References:

- [1] Muro, *et al.*, Clin Exp Immunol 111 (1998) 372-6.
- [2] Zhou, *et al.*, J Immunol 167 (2001) 7126-33.
- [3] Voronkov, *et al.*, J Med Chem 56 (2013) 3012-23.

- [4] Huang, *et al.*, Nature 461 (2009) 614-20.
- [5] Sillars-Hardebol, *et al.*, J Pathol 226 (2012) 1-6.
- [6] Sillars-Hardebol, *et al.*, Tumour Biol 31 (2010) 89-96.
- [7] Ward, *et al.*, Bioinformatics 20 (2004) 2138-9.
- [8] Gingras, *et al.*, Nat Rev Mol Cell Biol 8 (2007) 645-54.

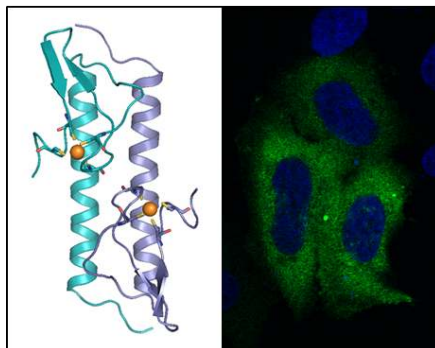


Figure 1. Crystal structure of SSSCA1's Zn-binding domain and subcellular localization in human cells.

Keywords: Crystallography, zinc binding, mitosis

MS9. Pharmaceutical crystallography and drug design

Chairs: David Brown, Andreas Heine

MS9-P1 Understanding nanoscale order in amorphous pharmaceuticals

Konstantin B. Borisenko¹, Wanjing Li², Graham Buckton²,
Andrew Stewart³, Angus I. Kirkland¹

1. Department of Materials, University of Oxford, Parks Road, Oxford OX1 3PH, UK.

2. School of Pharmacy, Faculty of Life Sciences, University College London, 29-39 Brunswick Square, London, WC1N 1AX, UK.

3. Department of Physics and Energy, University of Limerick, Limerick, Ireland.

email: konstantin.borisenko@materials.ox.ac.uk

According to differential scanning calorimetry spray-dried pharmaceutical formulations of indomethacin and polyvinylpyrrolidone form amorphous solid solution. These formulations also appear amorphous when examined by X-ray diffraction. However, these materials still possess nanocrystalline order as revealed by nanoscale electron diffraction. The structure of the nanocrystals of indomethacin appear to represent a range of the known bulk crystalline structures as well as new phases. We discuss implications of nanoscale organisation in amorphous pharmaceuticals for building reliable structure – properties correlations in such materials.

Keywords: amorphous pharmaceuticals, electron diffraction, nanoscale order

MS9-P2 Pharmaceutical drug discovery at the IMCA-CAT Advanced Photon Source user facility

Anne Mulichak¹, Anne Mulichak¹, Kevin P. Bataille¹, Joe Digilio¹, J. Lewis Muir¹, Eric Zoellner¹, Lisa J. Keefe¹

1. IMCA-CAT/Hauptman-Woodward Medical Research Institute, Argonne National Laboratory, Argonne IL 60439

email: mulichak@anl.gov

Regular and rapid cycles of crystallographic information are now an integral part of the pharmaceutical structure-based drug design process. The Industrial Macromolecular Crystallography Association Collaborative Access Team (IMCA-CAT) operates a macromolecular crystallography facility at the Advanced Photon Source that was founded to meet the demands of IMCA member pharmaceutical companies for reliable, high-quality, high-throughput data collection, while ensuring a secure environment for proprietary research. The 17ID micro-focused high-flux insertion device beamline, equipped with a Pilatus 6M pixel array detector, allows for very fast data collection times. The beam size can be easily optimized for each sample using a mini-beam quad collimator with user-selectable beam sizes of 50, 20, 10 and 5 mm. An Alio goniometer has a small (1.2 µm) sphere of confusion, providing stable sample positioning, and X-ray beam position is maintained within 2 µm by custom software in real time. Automated sample mounting is performed with a Rigaku ACTOR robot compatible with both Rigaku and ALS/Unipuck style magazines, providing fast yet reliable sample exchanges, and enabling remote access and unattended data collection. Mail-in is now offered as an optional access mode for IMCA members and subscribing companies, utilizing fully automated data collection for routine sample systems and manual collection by beamline staff for systems requiring more attention. A secure website provides a convenient mechanism for companies to communicate data collection requests, as well as monitor status and results for their samples. Mail-in eliminates the burden of data collection for companies and allows beamtime to be used most efficiently and flexibly. While targeting the needs of industrial research, the automation and rapid data collection times at IMCA-CAT are also well suited for structural genomics and other research efforts requiring high-throughput experiments. Access is available through subscription memberships for industrial users needing regular and guaranteed proprietary beamtime, and to academic researchers through the APS General User Program.

Keywords: synchrotron, pharmaceutical, high-throughput

MS9-P3 Investigating nanocrystalline drugs embedded in a polymeric matrix by Debye Function Analysis

Carlotta Giacobbe¹, Dritan Hasa², Dario Voinovich², Antonio Cervellino³, Norberto Masciocchi⁴, Antonietta Guagliardi⁵

1. European Synchrotron Radiation Facility CS 40220 - 38043 Grenoble Cedex 9, France
2. Department of Pharmaceutical Sciences, University of Trieste, P. le Europa 1, I-34127 Trieste, Italy
3. Paul Scherrer Institut, 5232 Villigen PSI, Switzerland
4. Dipartimento di Scienza e Alta Tecnologia, Università dell'Insubria, I-22100 Como, Italy
5. Istituto di Cristallografia, CNR, I-22100 Como, Italy

email: giacobbe@esrf.fr

The release rate of a solid drug is directly related to particle size; smaller crystals have, in fact, an enhanced ability to reach their physiological target^[1]. To this goal, the use of mechanical energy, inducing size/morphological modifications, represents a straightforward, green, and innovative approach. The process takes the name of *mechano-chemical activation*, and has recently been introduced as an efficient pharmaceutical processing technique.^[2] The release rate of a solid drug is directly related to particle size; smaller crystals have, in fact, an enhanced ability to reach their physiological target^[1]. To this goal, the use of mechanical energy, inducing size/morphological modifications, represents a straightforward, green, and innovative approach. The process takes the name of *mechanochemical activation*, and has recently been introduced as an efficient pharmaceutical processing technique.^[2] In our work, cocrystal mixtures of Vinpocetine (VIN) (C₂₂H₂₆N₂O₂), a poorly soluble drug used for the treatment of cognitive disorders and related symptoms^[3], and Cross-Linked Polyvinylpyrrolidone (C₄H₅NO)_n (PVP-CL), have been investigated at variable milling time and 1:4 and 1:7 VIN:PVP weight ratios. The Debye Function Analysis (DFA) of several mixtures is applied for the first time to extract information about structure, size and size distribution, morphology and amorphization of drug nanoparticles. To this aim, we used high resolution data collected at the Material Science beamline MS-X04SA of the Swiss Light Source, and the DEBUSSY suite of programs^[4] modeling the total (Bragg and diffuse) sample scattering. Quantitative results on the diverse microstructure modifications controlled by the milling time and the drug-to-polymer ratio will be presented. They show a clear trend between time, size distribution and weight ratio. Moreover, investigations on the biopharmaceutical performance of the most activated systems are in progress to be correlated to the previous results. Significantly, while other methods are commonly used to characterize nanocrystalline drugs, especially in terms of size and morphology (TEM, HRTEM – at the expenses of sample deterioration), the DFA method here discussed offers a novel, exhaustive (and statistically sound) characterization tool^[5,6].

Keywords: drugs, debye function analysis, particle size

MS9-P4 Understanding packing interactions and physicochemical properties of novel multicomponent crystal forms of azelaic acid-based anti-inflammatory drugs combining X-ray and NMR

M. Teresa Duarte¹, Inês C. B. Martins¹, Mariana Sardo², Luís Mafra²

1. Centro de Química Estrutural, Instituto Superior Técnico, Universidade de Lisboa, Av. Rovisco Pais 1, 1049-001 Lisboa, Portugal,
2. CICECO, Universidade de Aveiro, 3010-193 Aveiro, Portugal

email: teresa.duarte@tecnico.ulisboa.pt

In this work we are presenting complementary studies of X-ray single crystal and powder diffraction as well as SSMNR crystallography in the understanding of packing interactions in multicomponent crystal forms. This approach presents a new insight into the understanding of the new physicochemical properties of this new pharmaceutical entities. Our aim is to optimize crystal engineering methods for the structural elucidation of pharmaceuticals, following an X-ray and NMR Crystallography approach where NMR techniques sensitive to crystal packing arrangement are used in tandem with diffraction and computer modeling Structure-activity relationship and solid-state analysis, in particular X-ray diffraction and solid-state NMR spectroscopy, are particularly relevant in pharmaceutical industry where the majority of active pharmaceutical ingredients (APIs) occur as solids. [1, 2] Multicomponent crystal forms of APIs (co-crystals, molecular salts, solvates, hydrates and salts) have been extensively studied over the last years. [2, 3] These new forms proved to be an efficient method of improving physicochemical properties of drugs without changing the biological activity, resulting in the improvement of important characteristics such as solubility, dissolution rate, stability under variable RH conditions and bioavailability. [2] Azelaic acid (AA) is an antibacterial product used to treat acne and other skin disorders. This API exhibit low solubility and its performance would benefit from a solubility enhancement. [4] We developed new crystalline solid forms structural, chemical and thermal characterizations will be presented.

Acknowledgments The authors acknowledge funding of the projects POCL/QUI/58791/2004, PEst-OE/QUI/UI0100/2013, PTDC/CTM-BPC/122447/2010, RECI/REQ-QIN/0189/2012 and post-doc grant SFRH/BPD/78854/2011 by Fundação para a Ciência e a Tecnologia

References [1] André, V.; Piedade, M. F. M.; Duarte, M. T., *CrystEngComm* **2012**, 14, 5005-5014. [2] Braga, D.; Maini, L.; Sanctis, G.; Rubini, K.; Grepioni, F.; Chierotti, M. R.; Gobetto, R., *Chem.Eur.J.* **2003**, 9, 5538. [3] Martins, I.; Martins, M.; Fernandes, A.; André, V.; Duarte, M. T., *CrystEngComm* **2013**, 15, 8173. [4] Hebert, R. F., Therapeutically improved salts of azelaic acid. U.S. Patent 6,734,210. May 11, **2004**.

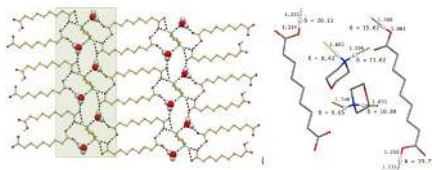


Figure 1. Crystal packing of Azelaic acid:piperazine cocrystal from SCXRD; molecular salt of Azelaic acid:morpholine from SSNMR crystallography

Keywords: Pharmaceutical cocrystals; X-ray Crystallography ; NMR Crystallography; Physicochemical properties

MS9-P5 Envisaging ZMOFs towards improved drug delivery and release

Vania Andre¹, M. Teresa Duarte¹

1. Centro de Química Estrutural, Instituto Superior Técnico, Universidade de Lisboa, Av Rovisco Pais, 1049-001 Lisbon, Portugal

email: vaniandre@ist.utl.pt

The continuous quest for efficient and cost-effective novel alternatives to improve drugs' performance assumes a key role in pharmaceutical industry. One of the topics that has received great attention in this quest is the development of systems that facilitate the controlled delivery and release of drugs. Over the past 7 years, the application of metal organic frameworks (MOFs) for controlled delivery of drug molecules has emerged. These supramolecular chemistry-based structures display several properties that transform them into promising drug carriers: remarkable high surface areas and large pore sizes for drug encapsulation; intrinsic biodegradability; versatile functionality for post-synthesis grafting of drug molecules; scalability to the nanoregime. [1,2]

Among MOFs, zeolite-like metal-organic frameworks (ZMOFs) and zeolitic imidazolate frameworks (ZIFs), MOFs with zeolitic architectures, exhibit particularly interesting properties that make them powerful platforms for drug delivery and/or controlled release of drug molecules. ZIFs are comprised of tetrahedral transition metal ions connected by imidazolate units arranged in topologies with large cages and small apertures, while in ZMOFs the scope of ligands connected to the metal ions is not limited to imidazolate compounds. ZIFs exhibit high thermal and chemical stability, overcoming two of the main issues when considering the use of MOFs in biomedical applications. [3,4]

We have been exploring this type of materials for controlled drug delivery and release of psychoactive drugs and several promising results have been already obtained.

References:

1. Allendorf MD, Stavila V: **Crystal engineering, structure-function relationships, and the future of metal-organic frameworks.** *CrystEngComm* (2015) 17(2):229-246.
2. Horcajada P, Gref R, Baati T, Allan PK, Maurin G, Couvreur P, Ferey G, Morris RE, Serre C: **Metal-organic frameworks in biomedicine.** *Chemical Reviews* (2012) 112(2):1232-1268.
3. Eddaoudi M, Sava DF, Eubank JF, Adil K, Guillerme V: **Zeolite-like metal-organic frameworks (zmoFs): Design, synthesis, and properties.** *Chemical Society reviews* (2015) 44(1):228-249.
4. Guillerme V, Kim D, Eubank JF, Luebke R, Liu X, Adil K, Lah MS, Eddaoudi M: **A supermolecular building approach for the design and construction of metal-organic frameworks.** *Chemical Society Reviews* (2014) 43(16):6141-6172.

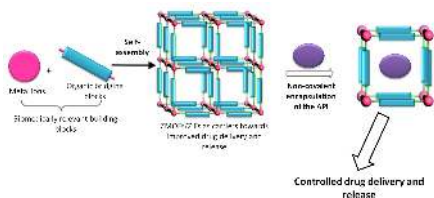


Figure 1. ZMOFs design towards controlled drug delivery (adapted from Rocca et al, *Acc.Chem.Res.*, 44(2011), 957)

Keywords: BioMOFs, pharmaceuticals, drug delivery

MS9-P6 PANDDA: multi-dataset methods for finding hits from fragment screening by X-ray crystallography

Nicholas M. Pearce¹, Sebastian Kelm², Jiye Shi², Charlotte M. Deane¹, Frank von Delft^{1,3}

1. University of Oxford
2. UCB Pharma
3. Diamond Light Source

email: nicholas.pearce@stx.ox.ac.uk

We present novel PAN-Dataset Density Analysis (PANDDA) methods for processing the data obtained from Crystallographic Fragment Screen (CFS) campaigns.

CFS experiments are ideal for identifying small “fragment” molecules that bind to a protein, but historically this method has been disfavoured due to low throughput and high complexity. With increasing automation and other technical advances, it is now a streamlined, routine experiment at beamline I04-1 at Diamond Light Source.

However, bottlenecks remain in the processing of the resulting data. The small compounds frequently bind with low occupancy, leading to subtle or ambiguous signal in the observed electron density. Datasets must be inspected manually to ensure that binding fragments are not missed. Manual inspection is time consuming and inaccurate, in particular when there are many binding sites, or when fragments bind outside of known binding sites.

CFS experiments using soaking protocols lead to datasets that are broadly isomorphous (near-identical). In this case, the interpretation of CFS data requires the examination of hundreds of similar datasets to identify binding events. Rather than processing and inspecting each dataset separately - the current state-of-the-art - there is a scientific opportunity to analyse these datasets simultaneously.

The nature of the screening experiment results in most of the datasets displaying no evidence of the fragment binding – ‘empty’ datasets. Rather than discarding these datasets, we instead average them to generate a very accurate picture of the fragment-free crystal electron density. The variation in the electron density at each point in the aligned datasets is then analysed to identify outliers in individual datasets. This characterization of the fragment-free crystal creates a reliable baseline with which we can identify the areas of individual datasets where a fragment binds, or where a structural shift is observed.

Preliminary results show the PANDDA approach is capable of accurately identifying bound fragments in CFSs. On a training set of 200 structures, all 3 known hits are identified by the method, whilst 80% of datasets are correctly rejected as empty (false negative rate = 0). The PANDDA method also increased the number of hits: 3 extra hits were identified that were missed in the manual analysis.

The PANDDA method provides an objective indication of the presence of bound fragments, and can detect the binding of fragments with weak affinities.

Keywords: Fragment Screening, Crystallographic Methods

MS9-P7 Novel inhibitors of beta-lactamase

Daria Beshnova¹, Ciaran Carolan¹, Johanna Kallio¹, Claudia Hackenberg¹, Victor Lamzin¹, Vitaly Grigorenko², Maya Rubtsova¹, Alexander Majouga², Alexey Egorov²

1. European Molecular Biology Laboratory, c/o DESY, Notkestrasse 85, 22607 Hamburg, Germany
2. Department of Chemistry, Lomonosov Moscow State University, GSP-1, Leninskie Gory, Moscow, 119991, Russia

email: beshnova@embl-hamburg.de

Beta-lactam antibiotics represent the most widely used group of antibacterial agents with broad-spectrum activity. However, bacteria can develop antibiotic resistance, often mediated by beta-lactamases. These enzymes render antibiotics inactive through the hydrolysis of the beta-lactam ring, resulting in the degradation of the drug. This process can be inhibited, but due to frequent mutations in the active site of the enzyme, inhibitors become ineffective at an accelerating rate. Thus, the identification of alternative means of beta-lactamase inhibition and the development of improved inhibitors is a priority.

To address this challenge, we used a computational approach specifically developed for this purpose, ViCi (<http://www.embl-hamburg.de/vici>), which uses a number of mathematical descriptors of molecular shape and charge distribution in a search for compounds that are similar to a template inhibitor. We screened a database of eight million compounds using four known low-affinity beta-lactamase inhibitors as a starting point. Recombinant TEM-171 beta-lactamase was expressed and used to kinetically assay the top 500 compounds from the ViCi screening. The best lead inhibitor, targeted to the allosteric site of TEM-171, had an order of magnitude higher *in vitro* affinity compared to the known inhibitors.

Using these potential novel inhibitors, we synthesised a number of chemically modified compounds; aiming for their higher activity, solubility and reduced toxicity compared to the known inhibitors. We have identified several new derivative compounds with promising characteristics.

Moreover, we have initiated X-ray crystal structure determination and have determined the structure of recombinant TEM-171 to a resolution of 2.0 Å. A series of inhibitor soaks have been initiated to decipher the mode of ligand binding.

Keywords: non-covalent inhibitors, beta-lactamase, computational drug design

MS9-P8 The crystal structure of a common allergen in complex with its specific patient-derived antibody

Alkistis N. Mitropoulou^{1,2}, Anna M. Davies^{1,2}, Tihomir S. Dodev^{1,3}, Louisa K. James^{1,2}, Rebecca L. Beavil¹, Hannah J. Gould^{1,2}, James M. McDonnell^{1,2}, Andrew J. Beavil^{1,2}, Brian J. Sutton^{1,2}

1. King's College London, Randall Division of Cell and Molecular Biophysics, London, UK
2. Medical Research Council & Asthma UK Centre in Allergic Mechanisms of Asthma, London, UK
3. NIHR Biomedical Research Centre at Guy's and St. Thomas's Hospitals and King's College London, London, UK

email: alkistis.mitropoulou@kcl.ac.uk

In recent decades, the incidence of allergy, an immune disorder mediated by immunoglobulin E (IgE), has become more common¹. According to the European Federation of Allergy (EFA), the incidence of allergy in Europe has rapidly increased, with allergic rhinitis affecting approximately 20% of the population². More than 50% of these cases are associated with allergy to grass pollen³. The symptoms of this disease not only cause discomfort to patients, but may also lead to fatal anaphylaxis. The aetiology of allergy is debated, but it is widely accepted that the initiation of the allergic response involves the crosslinking of IgE with its high affinity receptor complexes on mast cells by allergens, which requires at least two epitopes on the allergen. This triggers the early phase of the allergic reaction, involving mast cell degranulation and the release of mediators. Interactions between IgE and allergens are poorly understood, mainly due to insufficient structural information on IgE-allergen complexes. A structure-based strategy provides insights into the nature of allergens and promotes engineering of new hypoallergenic proteins for therapeutic intervention in allergic disease. To that end, we present here the crystal structure of a grass pollen allergen *Phl p 7* and its complex with a specific Fab. The allergen has undergone conformational changes, which did not allow for a straightforward molecular replacement structure determination, making the project crystallographically challenging.

[1] Gould and Sutton, 2008. *Nat. Rev. Immunol.* 8, 205–17.

[2] Valovirta E., 2011. EFA report

[3] Normansell et al., 2014. *Cochrane Database Syst. Rev.*, 1, CD003559

Keywords: therapeutic intervention, allergy, challenging phasing, antibody complex

MS9-P9 Crystal structure comparison methods

Jan Rohlíček¹, Michal Hušák²

1. Institute of Physics of the ASCR, v.v.i., Na Slovance 2, 182 21 Prague 8, Czech Republic

2. Department of solid state chemistry, University of Chemistry and Technology Prague, Technická 5, Prague 6, Czech Republic

email: rohlícek@fzu.cz

Crystal structures can be compared by many ways – by chemical composition, unit cell parameters, atomic positions, by positions of fragments or by other properties or values describing the crystal structure. Comparison of different properties give us a different results. The basic question is, what we would like to compare? We developed several crystal structure comparison methods, which can be divided into two basic approaches - (i) comparing of fingerprints and (ii) comparing of atomic positions. In the first case we selected pair-distribution function and powder diffraction pattern as fingerprints and we tested their sensitivity for small (e.g. change of one atom) and large (e.g. change of several atoms) changes. In the case of the second approach, it is obvious, that crystal structures has to be overlapped before comparing of atomic positions. This is the most difficult task of these methods. The success or failure of these methods depends on success or failure of the overlapping algorithm. In general, the situation is complicated by different atom labelling and, in the case of different space group, it is also complicated by different content of the asymmetric part of the unit cell and the situation can be also complicated by presence of special positions. We developed two algorithms for crystal structure overlapping - one of them is slow but it finds the overlay automatically and the second one is much faster but it needs the user definition of the similar fragment. We developed a testing code for this purpose, which we called CrystalCMP and which can be freely downloaded from [this link](http://sourceforge.net/projects/crystalcmp/) (<http://sourceforge.net/projects/crystalcmp/>). We will show success or failures and also strengths and weakness of suggested methods.

Financial support from Grant Agency of the Czech Republic, the project number is 14-03276S.

Keywords: Comparison, packing, similarity, crystal structure

MS9-P10 Light-atom structures: absolute configuration determination and beyond

Jürgen Graf¹, Michael Ruf², Holger Ott², Bruce Noll², Séverine Freisz², Alexander Gerisch², Birger Dittrich³, Andreas Kleine¹, Carsten Michaelsen¹

1. Incoatec GmbH

2. Bruker AXS

3. Georg-August-Universität Göttingen

email: graf@incoatec.de

The determination of the absolute configuration of light-atom structures is central to research in pharmaceuticals and natural-product synthesis [1]. In the absence of elements heavier than silicon, it is often problematic to make a significant assignment of absolute configuration. Traditionally, heavy-atom derivatives were prepared which have a stronger anomalous signal compared to the native compound. However, this is not always feasible.

The assignment of the absolute structure of pure organic compounds has become somewhat easier with the advent of high-intensity microfocus sources [2], as the increased flux density improves the anomalous signal through improvements in counting statistics. In order to maximize the anomalous signal, X-ray sources with Cu anodes are usually used for the absolute structure determination. However, these data are usually limited to a maximum resolution of about 0.80 Å. High-brilliance microfocus X-ray sources with Mo targets enable the collection of high quality data beyond 0.40 Å within a reasonable amount of time. This allows not only a more accurate modelling of the electron density by using aspherical scattering factors, but also enables a reliable determination of the absolute structure, despite the significantly lower anomalous signal obtained with Mo-K_α radiation.

With the recently introduced liquid-Gallium-jet X-ray source unprecedented beam intensities can be achieved [3]. The shorter wavelength of Ga-K_α compared to Cu-K_α slightly weakens the anomalous signal of a typical light-atom structure. However, due to the shorter wavelength, the highest resolution for the liquid metal-jet source is typically at about 0.70 Å, compared to about 0.80 Å for Cu-K_α. Hence, about 50% more unique reflections can be recorded. This clearly improves the structural model and the quality of the Flack parameter.

Selected results on the absolute structure and charge density determinations for light-atom structures will be presented.

[1] H. D. Flack, G. Bernardinelli, Chirality, 2008, 20, 681 – 690.

[2] T. Schulz, K. Meindl, D. Leusser et al., J. Appl. Cryst., 2009, 42, 885 – 891.

[3] M. Otendal, T. Tuohimaa, H. M. Hertz et al., Rev. Sci. Instrum., 2008, 79, 016102.

Keywords: Absolute Structure Determination, Charge Density Studies, Instrumentation

MS9-P11 Structure-Function-Analysis of proteins involved in the metabolic pathway of vitamin K acting as major pathogenic factors in *Staphylococcus aureus* infection

Aline Melro Murad^{1,2}, Carsten Wrenger³, Christian Betzel^{1,2}

1. Institute for Biochemistry and Molecular Biology, University of Hamburg, Martin-Luther-King-Platz 6, 20146 Hamburg, Germany
2. Laboratory for Structural Biology of Infection and Inflammation c/o DESY, Build. 22A, Notkestraße 85, 22603 Hamburg, Germany
3. Unit for Drug Discovery, Department of Parasitology Institute of Biomedical Science, University of São Paulo, Av. Prof. Lineu Prestes 1374, 05508-000 São Paulo-SP, Brazil

email: aline.melro.murad@chemie.uni-hamburg.de

In recent years the level of infections caused by human bacterial pathogens is rising. In Europe, attention has been drawn on infections acquired during hospitalization, specially caused by the methicillin-resistant *Staphylococcus aureus* (MRSA). Therefore, novel chemotherapeutic agents are urgently required, which solely target the bacteria and not the human host. Genome analyses indicated the presence of a functional vitamin K biosynthetic pathway consisting of the gene products MenA-F. Vitamin biosynthetic pathways are not present in humans and therefore inference with the host organism is not expected. In order to discover selective pro-drugs high resolution structural information about the respective enzymes participating in the biosynthetic pathway is required. In terms of structure based pro-drug design we target the proteins MenF, MenH and DHNA of the vitamin K metabolism in *S. aureus*, in order to obtain high-resolution structure information. Thus, genes of these proteins were cloned into pAKS-IBA-3 vector and expressed in *Escherichia coli*. Proteins were purified on affinity column containing the Strep-Tactin resin and impurities were removed using size exclusion and ion exchange columns. To investigate stability, homogeneity and secondary structure prior to crystallization experiments, dynamic light scattering (DLS) and circular dichroism (CD) were performed. Once verified the stability and homogeneity, initial crystallization trials were performed with DHNA using sitting drop vapor-diffusion mixing 1 μ L of protein (10 mg/ml) with 1 μ L of reservoir solution (100 mM HEPES-Na pH 7.0, 1 M lithium sulphate) in MRC Maxi 48-well plates at 20 °C. Protein crystals were observed after 2-3 days, reaching maximum dimensions within a week. The crystals were transferred to a cryo-protective solution (reservoir solution added 15% glycerol), flash-cooled in liquid nitrogen and initial diffraction data were collected applying a conventional rotating anode X-ray source. Preliminary CD and structural results show that 4-hydroxybenzoyl-CoA thioesterase (DHNA) consists of four repeating units (homo-tetramer) with approx. 22% of alpha helices, 49 % beta sheets, 4 % loops and 24.5 % random coil. The protein crystal diffracted to 2.6 Å resolution, belonging to the space group P2₁. Initial crystallization experiments for MenF and MenH are ongoing as well as the incorporation of selenomethionine for DHNA to solve the Phase problem. Up to date details will be presented.

Keywords: methicillin-resistant *Staphylococcus aureus* (MRSA), Vitamin K biosynthesis, Pro-drugs, Drug design, Crystallography

MS9-P12 Structural studies of β -lactoglobulin from various species

Krzysztof Lewinski¹, Joanna I. Loch¹, Piotr Bonarek², Agnieszka Polić², Mateusz Czub¹, Magdalena Kopec¹, Mira Ludwikowska¹

1. Faculty of Chemistry, Jagiellonian University in Kraków, Poland
2. Faculty of Biochemistry, Biophysics and Biotechnology, Jagiellonian University in Kraków, Poland

email: lewinski@chemia.uj.edu.pl

β -Lactoglobulin (LG) is a small globular protein of m.w. 18-20 kDa, belonging to the lipocalin family. Lipocalins share fold in which a core element is 8-stranded β -barrel. Four flexible loops surround entrance to the binding pocket located in the interior of beta-barrel. Reversible opening and closing of EF loop attributed to pH changes regulates access to the binding pocket. At physiological conditions LG forms dimers with subunits related by 2-fold symmetry.

LG has been found in the whey fraction of milk of more than 30 species, but not in human milk. The physiological function of LG is not well recognized, probably it is a molecular transporter of hydrophobic compounds. Recently, increased attention is focused on lipocalins due to their potential utilization in clinical applications as molecular transporters. Such an application of lactoglobulins requires numerous modifications influencing their binding properties. Therefore, to gain better understanding of individual residues role in ligand binding, we have undertaken systematic structural and thermodynamic studies of LG from various species being natural modifications to this protein.

Most thoroughly studied LG is a bovine protein (BLG) isolated from cow milk, for which crystal structures of several complexes with various ligands are available. The most abundant BLG isoforms are A and B that differ at two positions: D64G and V118A. The milk of sheep contains three isoforms of LG (A, B and C) that compared to isoform B of BLG have six substitutions. Only one isoform of LG has been found to date in goat milk, it also differs from BLG-B at six positions.

In this work we present crystal structures of bovine, sheep and goat LG. It was found that in BLG substitutions of polar residues in positions 64 and 118 affected thermodynamic of ligand binding but not influence overall structure of complexes. Systematic distortion of the β -barrel was observed in sheep protein in comparison to BLG. Also, differences in distribution of electrostatic potentials on the molecular surface in the dimer interface and entrance to the binding pocket region have been observed. In crystal structures of goat LG unusual conformation of flexible EF loop has been found, indicating that opening and closing access to the binding pockets in LG dimer might be sequential and cooperative.

This study was partially supported by the Polish National Science Centre, grant DEC-2012/05/B/ST/5/00278.

Keywords: lactoglobulin, lipocalin

MS9-P13 Structural studies of new β -lactoglobulin variants possessing modifications introduced to the binding site

Joanna I. Loch¹, Magdalena Tworzydło², Piotr Bonarek², Agnieszka Polić¹, Kinga Kaczor¹, Monika Siuda¹, Mateusz Gotkowski¹, Krzysztof Lewinski¹

1. Faculty of Chemistry, Jagiellonian University in Kraków, Poland
2. Faculty of Biochemistry, Biophysics and Biotechnology, Jagiellonian University in Kraków, Poland

email: loch@chemia.uj.edu.pl

Bovine β -lactoglobulin (BlgB) is a small lipocalin (18.3 kDa) that has ability to bind wide range of hydrophobic ligands. BlgB could be re-engineered to gain high specificity towards selected compounds. A series of new BlgB variants were design utilizing analysis of substitutions occurrence in structurally related lipocalins. Mutations were introduced to the protein binding site to investigate their impact on BlgB binding properties and structural stability.

All lactoglobulin variants were produced in *E.coli Origami B(DE3)* and purified to homogeneity by ion-exchange and size-exclusion chromatography. New mutants and their complexes with ligands were crystallized by hanging-drop vapour diffusion method. X-ray diffraction data were collected on *SuperNova* diffractometer. Structures were solved by molecular replacement.

Crystal structures of new BlgB variants revealed that some amino acid replacements in the binding site especially in positions 56, 58, 92, 105 and 107 stabilize protein structure. It was also observed that mutations in position 56 and 105 affect mode of binding of aromatic or aliphatic compounds by altering the shape of the hydrophobic β -barrel interior. Modifications introduced at the binding site entrance where most of polar residues are located, did not affect significantly ligand binding mode but seem to destabilize protein structure and alter interactions in the crystalline phase.

Results of structural and in-solution studies of new lactoglobulin variants revealed that BlgB affinity to compounds possessing aliphatic and aromatic fragments can be modified mostly by modelling the shape of binding pocket. Additional polar residues introduced to the region of binding, that act as hydrogen bond donors and acceptors, play a secondary role in increasing lactoglobulin affinity to selected ligands.

This study was supported by the Polish National Science Centre, grant number 2012/05/B/ST5/00278.

Keywords: lipocalin, lactoglobulin, mutations

MS9-P14 Crystallographic fragment screening: challenges, opportunities and lessons learned

Andreas Heine¹, Johannes Schiebel¹, Nedyalka Radeva¹, Alexander Metz¹, Franziska U. Huschmann^{1,2}, Monika Uhlein², Karine Sparta², Manfred S. Weiss², Uwe Mueller², Gerhard Klebe¹

1. Institute of Pharmaceutical Chemistry, Philipps-University Marburg, Marburg, Germany
2. Helmholtz-Zentrum Berlin für Materialien und Energie, Macromolecular Crystallography, Berlin, Germany

email: heine@staff.uni-marburg.de

Nowadays, fragment screening is an established method for lead development in pharmaceutical drug research. Library design and applied screening methods are critical for successful hit identification. We generated a small library, consisting of 364 compounds, which does not strictly adhere to the Astex rule of three often applied for library design.¹ The pepsin-like aspartyl protease endothiapepsin (EP) was selected for library validation. EP is a model system for proteins involved in serious diseases such as malaria (plasmeprins), hypertension (renin) and Alzheimer's disease (β -secretase) and, therefore, can aid in further drug development. Fragments tend to exhibit only low affinity toward their target protein due to their limited size. This hampers hit identification and, therefore, often multiple screening methods are applied. We used a biochemical as well as various biophysical assays as pre-screening methods. Surprisingly, the results of the different screening methods showed only limited overlap. Thus, we decided that crystallographic screening of the entire library is ultimately required to identify all fragments that bind to EP. In any case, the resulting structural information is the basis for further synthesis by medicinal chemists. Crystallographic screening of an entire library requires a steady supply of crystals, reproducible soaking conditions and a sufficient amount of beamtime. The latter was provided by the HZB BESSY II MX beamlines,² in combination with automation in initial data processing and refinement. More than 60 fragment complex structures were obtained which will be compared to results from other screening methods. The binding modes of the resulting fragments will be discussed and provide an ideal basis for further development of endothiapepsin inhibitors.

1. H. Köster, T. Craan, S. Brass, C. Herhaus, M. Zentgraf, L. Neumann, A. Heine, G. Klebe; A Small Nonrule of 3 Compatible Fragment Library Provides High Hit Rate of Endothiapepsin Crystal Structures with Various Fragment Chemotypes, *J. Med. Chem.* 54, 2011, 7784-7796.

2. U. Mueller, N. Darowski, M. R. Fuchs, R. Forster, M. Hellmig, K. S. Paithankar, S. Pühringer, M. Steffien, G. Zocher, M. S. Weiss; Facilities for macromolecular crystallography at the Helmholtz-Zentrum Berlin, *J. Synchrotron Radiat.* 19, 2012, 442-449.

Keywords: fragment-based drug design

MS9-P15 Polymorphism and phase stability of ketoprofen saltsM. Ben Nasr¹, A. Doudouh¹, P. Durand¹, A. Gansmuller¹, E. Aubert¹, E. Espinosa¹

1. Laboratoire CRM2 Université de Lorraine

email: mahjouba.ben-nasr@univ-lorraine.fr

Ketoprofen is a Non-Steroidal Anti-Inflammatory Drug (NSAID) of propionic acid class having analgesic and antipyretic effects [1]. It exhibits poor water solubility and dissolution rate [2]. To enhance its solubility, ketoprofen has been formulated and marketed as a trometamol salt [3].

Up to now the structures of ketoprofen salts were unknown. Recently, we have succeeded to obtain single crystals of a salt of racemic ketoprofen with trometamol, as well as two polymorphs of S-ketoprofen-trometamol salts (Fig.1). The prepared salts were characterized by using single-crystal and powder X-ray diffraction, DSC, FT-IR and ¹³C CP-MAS NMR, coupled with Density Functional Theory calculations. The structures and properties of these salts, which show enhanced aqueous solubility as compared to pure ketoprofen, will be discussed.

References:

- [1] M., Dixit, P., Kulkarni, R., Vaghela, *Trop. J. Pharm. Res.* 12, 317–322 (2013).
- [2] P. S. Yadav, V. Kumar, U. P. Singh, H. R. Bhat, B. I. Mazumder, *Saudi Pharm. J.* 21, 77– 84 (2013).
- [3] B. J. Sweetman, *Acute Pain*, 4, 109–115 (2003).

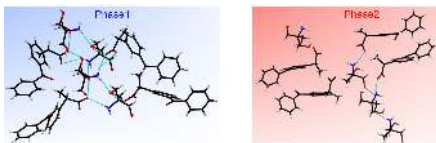


Figure 1. Crystal structures of two polymorphs of S-ketoprofen-trometamol salts. N-H...O and O-H...O hydrogen bonds are shown as blue lines

Keywords: Crystallization, ketoprofen, trometamol, salt, hydrogen bonding, solubility.

MS9-P16 Conserved hydrogen bonding in tetrahydrocarbazolone derivatives: Influence of solution-state assembly on crystal form nucleationKatharina Fücke¹, Robert M. Edkins^{2,3}, Elliott Hayden¹

1. School of Medicine, Pharmacy and Health, Durham University Queen's Campus, University Boulevard, Stockton-on-Tees, TS17 6BH, United Kingdom

2. Institut fuer Anorganische Chemie, Julius-Maximilians-Universitaet Wuerzburg, Am Hubland, 97074 Wuerzburg, Germany

3. Department of Chemistry, Durham University, South Road, Durham, DH1 3LE, United Kingdom

email: katharina.fuecke@durham.ac.uk

Different crystal forms (polymorphs) may vary substantially in their physico-chemical characteristics, including melting point, chemical and physical stability, solubility and dissolution rate, the latter of which represents both a challenge and an opportunity for the pharmaceutical industry.¹ Bioactive molecules typically have multiple functional groups, enabling them to interact with receptors and thus show pharmacological action. Furthermore, as drug molecules become ever larger, they tend to show increased flexibility. These two factors make investigations and predictions of the crystallisation behaviour of most drug molecules inherently difficult.² In this study, we investigate two tetrahydrocarbazolone derivatives, as they represent core fragments of many antibacterial and antiviral drugs and prodrugs,³ whilst having a rigid core with only one hydrogen-bond (HB) donor and one HB acceptor functionality, enabling us to deconvolute the influence of specific functional groups. In addition, the influence of the position of methylation on the existence of supramolecular synthons is probed. *Ortho*-methylated tetrahydrocarbazolone (OCB) can exist in four polymorphs, three of which show the anticipated dimer formation, a synthon proved to exist in the pre-crystallisation solution. The thermodynamically stable polymorph, however, crystallises in a catemer motif but has a considerably longer nucleation time. When moving the methyl group from the *ortho*- to the *para*-position (PCB), only dimer formation was observed, while the different polymorphs become very close in energy and concomitant crystallisation occurred. Thus, subtle changes in molecular structure can have profound influences on crystallisation behaviour. It is also predicted that a bio-isosteric replacement of the CH₃ group of OCB with CF₃ will further stabilise the catemer, highlighting a potential problem for the design and subsequent formulation of new drugs.

¹ D. J. W. Grant, in *Polymorphism in Pharmaceutical Solids*, ed. H. G. Brittain, Marcel Dekker Inc., New York, 1999, pp. 1–33.

² S. L. Price, *Chem. Soc. Rev.*, 2014, **43**, 2098.

³ (a) X. Li and R. Vince, *Bioorg. Med. Chem.*, 2006, **14**, 2942; (b) G. Periyasami, R. Raghunathan, G. Surendiran and N. Mathivanan, *Bioorg. Med. Chem. Lett.*, 2008, **18**, 2342; (c) K. S. Gudmundsson, P. R. Sebahar, L. D. A. Richardson, J. G. Catalano, S. D. Boggs, A. Spaltenstein, P. B. Sethna, K. W. Brown, R. Harvey and K. R. Romines, *Bioorg. Med. Chem. Lett.*, 2009, **19**, 3489.

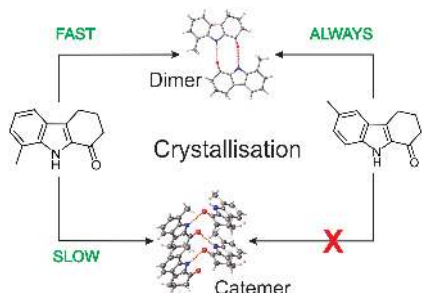


Figure 1. How subtle changes in substitution pattern can effect massive changes in crystallisation behaviour.

Keywords: pharmaceuticals, polymorphism, aggregation in solution

MS9-P17 Structural analysis and molecular docking studies of nitrogen containing steroidal compounds as potential antitumor agents

Olivera R. Klisurić¹, Edward T. Petri², Anelka S. Čelić², Katarina M. Penov Gašić³, Marija N. Sakač³, Jovana J. Ajduković³, Andrea R. Nikolić³, Aleksandar M. Oklješa³, Marina P. Savić³, Dimitar S. Jakimov⁴, Evgenija A. Đurendić²

1. Department of Physics, Faculty of Sciences, University of Novi Sad, Trg Dositeja Obradovića 4, 21000 Novi Sad, Serbia

2. Department of Biology and Ecology, Faculty of Sciences, University of Novi Sad, Trg Dositeja Obradovića 4, 21000 Novi Sad, Serbia

3. Department of Chemistry, Biochemistry and Environmental Protection, Faculty of Sciences, University of Novi Sad, Trg Dositeja Obradovića 3, 21000 Novi Sad, Serbia

4. Oncology Institute of Vojvodina, Institutski put 4, 21204 Novi Sad, Serbia

email: olivera.klisuric@df.uns.ac.rs

Nitrogen containing steroidal compounds target a variety of biological processes, and are potential candidates for the treatment of a wide-range of diseases, including breast and prostate cancer. Prostate cancer is the second most common cancer among men worldwide, while among women, breast cancer is the second leading cause of cancer deaths today. Breast tumors with a relatively high concentration of estrogen receptors can often be treated successfully with steroid-based anti-hormonal therapy. Similarly, several nitrogen containing steroidal compounds have been developed for the treatment of prostate cancer, including Abiraterone, VN/124-1 (galeterone) and VN/85-1 which reduce circulating androgen levels through inhibition of 17 α -hydroxylase/17,20-lyase (CYP17).

Building on our previous work [1-3], in the present study we present more than 20 nitrogen containing androstane derivatives. Synthesized products were validated by spectroscopy and X-ray crystallography, and screened for antitumor potential by *in silico* molecular docking and anti-proliferation studies. Molecular docking simulations were performed against known clinical targets of steroidal chemotherapeutic drugs currently used in the treatment of breast and prostate cancer: estrogen receptor α (ER α), androgen receptor (AR), Aromatase (CYP19A1) and 17,20-lyase/17 α -hydroxylase (CYP17A1). Virtual screening and *in vitro* anti-proliferation studies suggest that A-modified 17(E)-picolinylidene androstane derivatives represent promising candidates for the development of a new series of steroid-based compounds for the treatment of prostate cancer, indicating the need for more detailed future studies.

Acknowledgement:

The authors would like to thank the Ministry of Education, Science and Technological Development of the Republic of Serbia (Grant No. 172021) and Provincial Secretariat for Science and Technological Development of Vojvodina (Grant No. 114-451-3600/2013-03) for financial support.

References:

1. Ajduković, J.; Gašić, K. P.; Jakimov, D.; Klisurić, O.; Šanta, S. J.; Sakač, M.; Aleksić, L.; Đurendić, E. *Bioorganic & Medicinal Chemistry* 2015, 23, 1557–1568

2. Ajduković, J.; Đurendić, E.; Petri, E.; Klisurić, O.; Čelić, A.; Sakač, M.; Jakimov, D.; Gaši, K. P. *Bioorganic & Medicinal Chemistry* 2013, 21, 7257–7266

3. Gaši, K. P.; Oklješa, A.; Petri, E.; Čelić, A.; Đurendić, E.; Klisurić, O.; Csanadi, J.; Batta, G.; Nikolić, A.; Jakimov, D.; Sakač, M. *Med. Chem. Commun.* 2013, 4, 317–323

Keywords: androstane derivatives, X-ray crystallography, molecular docking, antiproliferative activity, antitumor

MS9-P18 Human LLT1, a ligand for NKR-P1, and its variability under various conditions

Tereza Skálová¹, Jan Bláha², Karl Harlos³, Jarmila Dušková¹, Tomáš Koval⁴, Jan Stránský¹, Jindřich Hašek¹, Ondřej Vaněk², Jan Dohnálek^{1,4}

1. Institute of Biotechnology, Academy of Sciences of the Czech Republic, v.v.i., Vídeňská 1083, 142 20 Praha 4, Czech Republic

2. Department of Biochemistry, Faculty of Science, Charles University Prague, Hlavova 8, 128 40 Praha 2, Czech Republic

3. Division of Structural Biology, The Wellcome Trust Centre for Human Genetics, University of Oxford, Roosevelt Drive, Oxford OX3 7BN, United Kingdom

4. Institute of Macromolecular Chemistry, Academy of Sciences of the Czech Republic, v.v.i., Heyrovského nám. 2, 162 06 Praha 6, Czech Republic

email: t.skalova@gmail.com

Natural killer cells (NK cells) are large granular lymphocytes able to kill virally infected, stressed or tumor cells. Unlike T-cells, the activity of NK cells is innate.

NKR-P1 (CD161) is a receptor on a surface of human NK cells. LLT1 is a ligand for NKR-P1 receptor, expressed primarily on activated lymphocytes and antigen presenting cells. The interaction of the ligand with the receptor inhibits NK cell cytotoxicity; however, it may have also activation effects in some cases. Extracellular domains of both binding partners, NKR-P1 and LLT1, have C-type lectin like (CTL) fold.

Using X-ray diffraction, we determined four structures of LLT1 [1] from protein produced in HEK293S GnTI-cells [2]. The protein with GlcNAc₅ glycosylation packs into hexamers (consisting of three dimers) in crystals. The protein deglycosylated after the first N-acetylglucosamine was found in our crystal structures in forms of dimers (in pH 7.0) and monomers (in pH 3.5).

The LLT1 structures show that LLT1 follows the “classical” mode of dimerization known from other structures with the same fold (CD69 [3], CLR-g [4]). The series of the LLT1 structures (PDB codes 4QKG, 4QKH, 4QKI, 4QKJ) bring insight into variability of the dimerization interface, flexibility of the outer long loop of the CTL domain and influence of glycosylation on the structure.

This study was supported by BIOCEV CZ.1.05/1.1.00/02.0109 from the ERDF, by the Czech Science Foundation (project 15-15181S), by the Ministry of Education, Youth and Sports of the Czech Republic (grant LG14009), by Charles University (UNCE 204025/2012, SVV 260079/2014), High Education Development Fund (FRVS 669/2013), BioStruct-X (EC FP7 project 283570) and Instruct, part of the European Strategy Forum on Research Infrastructures (ESFRI) supported by national member subscriptions.

[1] Skálová et al., *Acta Cryst.* 2015, D71, 578–591. [2] Bláha et al., *Protein Express. Purif.* 2015, 109, 7–13. [3] Natarajan et al., *Biochemistry* 2000, 39, 14779–14786. [4] Skálová et al., *J. Immunology* 2012, 189, 4881–4889.

MS9-P19 MASSIF1: fully automated macromolecular crystallography

Matthew W. Bowler¹, Didier Nurizzo¹

¹. European Molecular Biology Laboratory, Grenoble Outstation, Grenoble, France

email: Bowler@esrf.fr

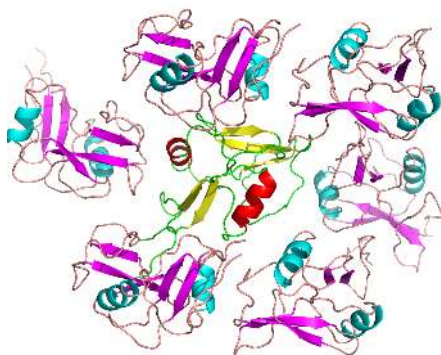


Figure 1. Monomeric form of LLT1 (PDB code 4QKG) and its crystal contacts.

Keywords: LLT1, NK receptor, C-type lectin like

MASSIF1 is a unique facility for the high throughput, fully automatic characterisation and data collection of crystals of macromolecules. The new service is not designed to replace user visits to the synchrotron but rather to do the hard work of screening crystals or collecting data sets through the night, freeing researchers to spend time on more challenging data collection problems and study the underlying biology. Beam time is booked flexibly and samples then enter a queuing system, users interact with the beamline by describing experimental requirements, that are used by the beamline software to set data collection parameters, in a database, ISPyB, where results are also viewed and downloaded. The service is made possible by RoboDiff – a new ESRF-developed sample changer that also acts as a goniometer –, a highly intense X-ray beam (3×10^{12} ph/sec in $100 \times 50 \mu\text{m}^2$) and complex workflows that fully evaluate samples, centre the best volumes and collect diffraction data sets optimised for maximum resolution with minimised radiation damage. As MASSIF1 is fully automatic, data are collected for the first time in a consistent manner and should allow the accumulation and comparison of a large amount of information that was previously unknown, including the exact dimensions of crystals and deeper information about their quality. Once the beamline has been running for an extended period, it will provide a treasure trove of additional information to feed back into crystallisation experiments and the software used to collect the data. In less than three months of operation more than 6 million diffraction images have been collected from 4272 samples ranging from initial hits from crystallisation experiments to large-scale data collection for drug discovery programmes. The automatic routines developed are often able to locate crystals more effectively than the human eye and in many cases have obtained higher resolution data sets as all positions within a sample can be evaluated for diffraction quality. The routines used on MASSIF-1 have been developed using a workflow tool that is also used to provide a wide variety of complex data acquisition protocols available on all ESRF MX beamlines.

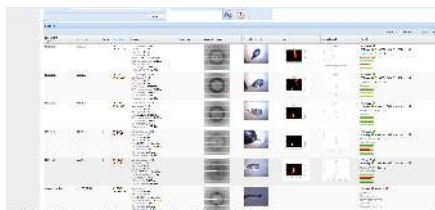


Figure 1. Summary page of data collections performed on MASSIF1 as seen in ISPyB showing diffraction quality maps, snapshots and the results of processed data.

Keywords: Automation, fragment screening, robotics, workflows

MS9-P20 Designed Armadillo repeat proteins serve as scaffolds for the rational assembly of peptide binders with picomolar affinities

Peer Mittl¹, Simon Hansen¹, Patrick Ernst¹, Andreas Plückthun¹

1. Department of Biochemistry, University of Zürich, Winterthurer Str. 190, 8057 Zürich

email: mittl@bioc.uzh.ch

Background: The specific recognition of macromolecules is key for many applications in biochemical research, medical diagnostics and disease treatment. Currently the development of new recognition molecules depends on the immunization of lab animals or combinatorial biochemistry techniques. Since both approaches are elaborate and require the availability of sufficient amounts of stable target molecules we are developing a modular system that should allow the rational design of sequence-specific peptide binding proteins. This system is based on the armadillo repeat scaffold, because natural armadillo repeat proteins bind their targets in extended anti-parallel conformations with very regular binding topologies.

Results: Although dArmRP with 2nd generation capping repeats were predominantly monomeric in solution, crystal structures of dArmRP with different numbers of internal repeats revealed domain-swapped N-caps. Redesign of the N-cap significantly improved thermodynamic stability and abrogated swapping of N-caps. These 3rd generation dArmRP recognize full-consensus peptides with very high affinities. Dissociation constants decrease exponentially with the number of internal repeats of the dArmRP and the lengths of the target peptides. Several crystal structures of complexes between dArmRPs with five or six internal repeats and full-consensus (KR)₅ peptides (either free or fused to the N- and C-termini of globular proteins) confirm that the binding mode fulfills the expected regular topology. Further crystal structures of complexes between dArmRPs and the mismatch (RR)₅ peptide revealed that dArmRPs recognize their target peptides in a side-chain specific manner.

Conclusion: Several crystal structures confirm that 3rd generation dArmRPs behave as stable and monomeric molecules that allow the selective recognition of targeted peptides with the expected topology. The logarithmic relationship between dissociation constant and target peptide length suggests a linear relationship between free energy of binding and number of dipeptide-binding modules. Therefore, the rational design of sequence-specific binders with picomolar affinities from a pool of dipeptide-specific armadillo repeats should indeed be possible.

Keywords: protein engineering, structure/activity relationship, binding proteins, armadillo repeat, solenoid protein

MS10. Structural bioinformatics (SBI)

Chairs: Guido Capitani, Oliviero Italo Carugo

MS10-P1 Archaeal species evolved contemporaneously with fungi

William L. Duax¹

1. Hauptman Woodward MRI

email: duax@hwi.buffalo.edu

We are currently analyzing the evolution of proteins of the ribosome that have conserved their 3-dimensional fold in all living species for approximately 3 billion years. We have found that although less than 10% of the residues in aligned ribosomal proteins are conserved at 95% or greater identity these immutable residues are responsible for the three-dimensional fold of the conserved core of each ribosomal protein. We find that the ribosomal proteins of archaeal species and cytosolic eukaryota share sequence and structural features that distinguish them from those of all bacteria and eukaryotic mitochondria and chloroplasts. This indicates contemporaneous emergence of eukaryota and archaea. This is clearly illustrated in the analysis of ribosomal protein S19 presented here. These studies permit accurate annotation of thousands of gene products that are ambiguously annotated in the TrEMBL database, and indicate that ribosomal proteins can be used to define a rooted evolutionary tree of all cellular species.

Keywords: Evolution, Archaea, Ribosome

MS10-P2 Transferable aspherical atom model refinement of protein and DNA structures against ultra-high-resolution X-ray data

Maura Malinska¹, Zbigniew Dauter¹

1. Synchrotron Radiation Research Section, MCL, National Cancer Institute, Argonne National Laboratory, Argonne, IL 60439, USA

email: mmalinska@anl.gov

In contrast to the independent atom model (IAM), in which all atoms are assumed to be spherical and neutral, transferable aspherical atom model (TAAM) takes into account charge transfer and deformation of the valence charge density resulting from the chemical bond formation, the presence of lone electron pairs, or intra- and intermolecular interactions. Both models can be used for refinement of small and large molecules e.g. proteins and nucleic acids, against ultra-high-resolution X-ray diffraction data. The University at Buffalo theoretical databank of aspherical pseudoatoms has been tested in the refinement of the tripeptide Phe-Val-Phe, Z-DNA hexamer duplex, Z-DNA dodecamer and aldose reductase. Application of the TAAM to these data improves quality of density maps and visibility of hydrogen atoms. It also slightly lowers the conventional R factor, improves the atomic displacement parameters and the results of the Hirshfeld rigid-bond test. Additional advantage is that the transferred charge density permits to estimate Coulombic interaction energy and electrostatic potential.

Keywords: structure, precision and accuracy, interaction

MS10-P3 Purification, structural characterization and homology modeling of a novel neurotoxic peptide (Acra3) from the scorpion *Androctonus crassicauda*

Suheyra Ozbey¹, Damla Koçak¹, Filiz Betül Kaynak¹, Figen Çalışkan²

1. Department of Engineering Physics, Hacettepe University, 06800 Beytepe, Ankara, Turkey

2. Department of Biology, Faculty of Science and Art, Eskisehir Osmangazi University, 26480 Eskisehir, Turkey

email: sozbey@hacettepe.edu.tr

Androctonus crassicauda is one of the Southeastern Anatolia scorpions of Turkey with ethnomedical and toxicological importance. Information on the biochemistry, pharmacology, active principles and mechanism of action of the venom is crucial for the development of specific antivenoms. The venom group in the Biology Department of Eskisehir Osmangazi University is focused at the characterization of the main components of this scorpion venom, due to the fact that very little is known thus far on this species.

The isolation of neurotoxic peptide Acra3 by chromatographic separations (HPLC and TSK-gel sulfopropyl) and its chemical and functional characterization were also performed and recently reported (Caliskan et al. 2012, Peptides 37: 106-112). Acra3 is a 7620 Da molecular weight peptide, with 66 amino acid residues and has eight cysteine residues, crosslinked by four disulfide bridges.

We have currently carried out the structural characterization of Acra3 peptide by using the small angle x-ray solution scattering. From the small angle scattering data overall structural parameters of the protein e.g. molecular radius of gyration (Rg), maximum particle diameter (Dmax) were derived.

Furthermore, three-dimensional structure modeling of Acra3 was also predicted by amino acid sequence alignment and then homology modeling by using FASTA and CLUSTALW EBI and Swiss Model servers. These models will be used as the starting point for nanosecond-duration molecular dynamics simulations.

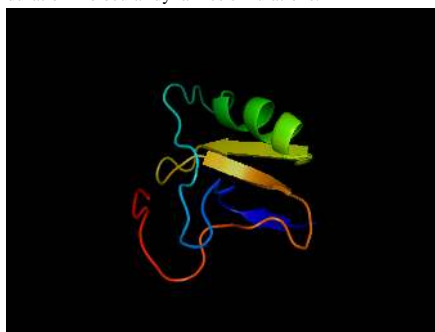


Figure 1. Homology structure of Acra3

Keywords: scorpion peptide, Acra3, *Androctonus Crassicauda*, homology modeling

MS10-P4 Molecular modelling studies of protein-ligand interactions on haloalkane dehalogenases

Michal Kutý^{1,2,3}, Pavel Malcher³, Ivana Kuta Smatanova^{1,2}

1. Faculty of Science, University of South Bohemia in Ceske Budejovice, Branisovska 31, 370 05 Ceske Budejovice, Czech Republic

2. Institute of Nanobiology and Structural Biology, Academy of Sciences of the Czech Republic, 142 20 Prague, Czech Republic

3. Fac Fisheries & Protect Waters, Univ South Bohemia Ceske Budejovice, Zátíší 728/II, 389 25 Vodnany, Czech Republic

email: kutym@seznam.cz

Haloalkane dehalogenases (EC 3.8.1.5) are enzymes belong to the α/β -hydrolase superfamily [1] of enzymes that catalyze the hydrolytic cleavage of carbon-halogen bonds in halogenated hydrocarbons to yield the corresponding alcohol, a proton and a halide [2]. Therefore, haloalkane dehalogenases (HLDs) catalyze reactions of great environmental and biotechnological significance. This work is focused on the protein-ligand interactions in a recently constructed stable and solvent-resistant haloalkane dehalogenase DhaA from *Rhodococcus rhodochrous* NCIMB 13064 and its variants with mutations in the residues that form the access tunnel connecting the enzyme's buried active site to the surrounding solvent. In the previous study [3] crystallographic analysis followed by classical molecular dynamics revealed that enhanced catalytic activity of mutant DhaA106 is due to an increase in the diameter of the access tunnel and the mobility of the adjacent secondary structure elements. In this work we study the interactions and different binding sites between a protein and a ligand by using molecular dynamics method GROMACS [4] and PELE [5,6] (an acronym Protein Energy Landscape Exploration) that combines a Monte Carlo stochastic approach with protein structure prediction and is capable of accurately reproducing long time scale processes.

This research is supported by the GACR (P207/12/0775).

References:

1. Ollis, D. L., Cheah, E., Cygler, M., Dijkstra, B., Frolova, F., Franken, S. M., Harel, M., Remington, S. J., Silman, I., Schrag, J., Sussman, J. L., Verschuere, K. H. G. & Goldman, A. (1992), *Protein Eng.* 5, 197–211.
2. Damborský J., Rorije E., Jesenská A., Nagata Y., Klopman G., Peijnenburg W. J. (2001), *Environ. Toxicol. Chem.*, 20, 2681–2689.
3. Liskova V., Bednar D., Prudnikova T., Rezacova P., Koudelakova T., Sebestova E., Kuta Smatanova I., Brezovsky J., Chaloupkova R., Damborsky J. (2015), Balancing the stability-activity trade-off by fine-tuning dehalogenase access tunnels. *ChemCatChem* 7, 648–659.
4. Van Der Spoel D, Lindahl E, Hess B, Groenhof G, Mark AE, Berendsen HJ (2005). "GROMACS: fast, flexible, and free". *J Comput Chem* 26 (16): 1701–18.
5. PELE: Protein energy landscape exploration. A novel Monte Carlo based technique (2005), *J. Chem. Theo. Comput.*, 1(6):1304–1311.
6. PELE web server: atomistic study of biomolecular systems at your fingertips (2013), *Nucleic Acids Research*, 41(W1):W322–W328.

Keywords: haloalkane dehalogenases, structure, molecular modeling, PELE, Gromacs

MS10-P5 Detection of *trans* – *cis* flips and peptide plane flips in protein structures

Wouter G. Touw¹, Robbie P. Joosten², Gert Vriend¹

1. Centre for Molecular and Biomolecular Informatics, Radboud university medical center, Geert Grooteplein-Zuid 26-28 6525 GA Nijmegen, The Netherlands

2. Department of Biochemistry, Netherlands Cancer Institute, Plesmanlaan 121 1066 CX Amsterdam, The Netherlands

email: wouter.touw@radboudumc.nl

Peptide bonds connect adjacent amino acids in proteins. The partial double bond character of the peptide bond restricts its torsion and the dihedral angle ω ($C\alpha_{i-1} - C_{i-1} - N_i - C\alpha_i$) only has values around 180° (*trans*) or 0° (*cis*). Many *cis* peptide bonds have been incorrectly modelled in the PDB (Protein Data Bank) as *trans* peptides or *vice versa*. A coordinate-based Random Forest classifier is presented to detect peptide bonds that need either a *trans* – *cis* flip or a 180° flip of the entire peptide plane. Like the method developed by Weiss & Hilgenfeld (1999), the prediction is based on the distorted local geometry of the local protein backbone when it is forced to adopt an incorrect conformation. The prediction performance on 1088 independent manually validated test cases was excellent for all flip types and for all amino acid types. The method predicts thousands of corrections in the PDB. Several examples were found in which the necessary flip causes our understanding of the structure function relation of the molecule to radically change.

Keywords: peptide flip, *cis* peptide bond, structure validation

MS10-P6 Novel network perspective on the structure, function and dynamics of proteins

Mario Albrecht¹, Doncheva T. Nadezhda²

1. Graz University of Technology

2. Max Planck Institute for Informatics

email: mario.albrecht@tugraz.at

In recent years, a new interdisciplinary area of research that combines network science and structural biology in the context of visual analytics has emerged. By representing protein structures as networks of interacting residues and applying network visualization and analysis techniques, we facilitate the analysis of structure-function relationships and gaining more insight into complex molecular mechanisms such as protein-protein and protein-ligand interactions. To this end, we offer a software suite (including our tools RINalyzer and RINerator) that supports interactive, multi-layered visual analysis of protein structures and their molecular function in protein binding, allostery, drug resistance and other interaction mechanisms. In particular, our integrative approach can be applied to visually analyze the impact of sequence mutations on protein structure.

To capture the dynamic nature of protein structures and interactions, we also developed a special approach to visualizing and analyzing ensembles of protein structures as generated by MD simulations or NMR. We use dynamic, weighted residue interaction networks (dRINs) that account for the different protein conformations within the ensemble. Possible applications of this approach include the identification of structurally and functionally important residue interactions, the comparison of ligand-binding modes in protein interactions, as well as the characterization of protein mutations and their effect on structure and function (see Figure).

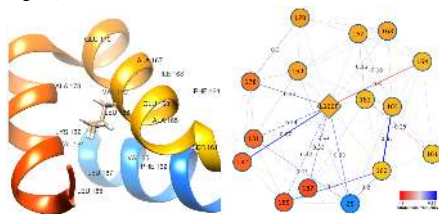


Figure 1. Close-up on the mutation L166P in the DJ-1 wild-type structure with PDB identifier 1PDV (left) and in the comparison dRIN (right). Network edges correspond to non-covalent residue interactions that are more frequent in the wild-type (blue lines) or mutant (red lines) structures.

Keywords: protein structure, protein function, residue network, molecular dynamics, NMR, visual analytics

MS10-P7 Comparing electrostatic potentials from experiment, point charges and theoryClaudia M. Wandtke¹, Jens Luebben^{1,2}, Birger Dittich^{1,2}1. Georg-August University Göttingen
2. Hamburg University

email: claudia.wandtke@chemie.uni-goettingen.de

A popular analysis for protein structures is the investigation of the electrostatic potential (ESP). It can yield information about possible drug receptor interactions. Therefore, it is also helpful to look at the ESP of a drug molecule. Except for proteins and nucleic acids, charges are not always easily accessible.

This is why we have developed a new, rapid way to a molecular ESP making use of the model compounds in the invariom database [1], for structures of organic molecules. Automatic parameter assignment relies on the local-atomic bonding environment, in this case invariom classification. ESP computation just requires atomic point charges and bond distances to hydrogen atoms from quantum chemistry, and both are provided by the invariom database [1]. These point charges are derived by the RESP [2] procedure for the invariom model compounds and transferred according to invariom name. Hence we call them invariom point charges.

A complementary approach is an ESP from an experimental charge density study, which requires high resolution single crystal X-ray data. Since programs for aspherical scattering factors are complex, we want to assess how well simplified approaches with point charges from different sources can reproduce such an experimental ESP.

A suitable tool for the comparison of ESPs is presented. It is based on MOLISO [3] code and a relative root-mean-square (RRMS) formula known from computational chemistry [4]. Procedures and comparisons will be applied to a series of biologically active organic molecules. ESPs from different methods, including theoretical and experimental charge density, will be compared.

[1] B. Dittich, C. B. Hübschle, K. Pröpper, F. Dietrich, T. Stolper, J. J. Holstein, *Acta Cryst.* B69 (2013) 91.

[2] C. I. Bayly, P. Cieplak, W. D. Cornell, P. A. Kollman, *J. Phys. Chem.* 97 (1993) 10269.

[3] C. B. Hübschle, P. Luger, *J. Appl. Cryst.* 39 (2006) 901.

[4] D. E. Williams, *Rev. In Comp. Chem.* 2 (1991) 219.

Keywords: Electrostatic potential, invarioms, point charges, charge density.

MS10-P8 BORGES libraries: from phasing to structural bioinformaticsMassimo Sammito¹, Claudia Millán¹, Rafael J. Borges^{1,2}, Lynn T. Eyck³, Isabel Usón^{1,4}1. Dept. of Structural Biology, Institute of Molecular Biology of Barcelona (IBMB), Spanish National Research Council (CSIC), Barcelona, Spain
2. Dept. of Physics and Biophysics, Biosciences Institute (IBB), São Paulo State University (UNESP), Botucatu, São Paulo, Brazil
3. Dept. of Chemistry and Biochemistry, University of California, San Diego, CA, USA
4. Dept. of Structural Biology, Catalan Institution for Research and Advanced Studies (ICREA), Barcelona, Spain

email: massimo.sammito@ibmb.csic.es

Despite their differences, *de novo* structure prediction in bioinformatics and *ab initio* phasing methods in crystallography share a common baseline: the use of previous structural knowledge to reveal the tertiary structure of unknown proteins. In phasing, the ubiquitous alpha helices have been widely used as structural building blocks in ARCIMBOLDO_LITE^[1]. Nevertheless, some cases require going a step further and moving from secondary to tertiary structure. The emergent strategy, based on fragment libraries as set of initial phases for experimental data, is being the key to success in a number of methods located between Molecular Replacement and pure *ab initio*^[2,3,4,5]. Our approach relies on characterization of nonspecific Local Folds^[5] as small discontinuous composites of secondary structure elements. Due to their sequence variability, LF can only be evaluated through geometrical descriptors, such as Characteristic Vectors^[5], and their spatial constraints. BORGES^[5] program implements this idea combining CV geometry, clustering and optimized structural superposition to build user customized LF libraries. The extraction of this kind of libraries requires data mining over more than 100,000 structures deposited in the Protein Data Bank and the design of a specialized database collecting CVs and relations among them. Statistical analysis of LF distribution and pattern recognition studies can only be afforded with the power of a supercomputer, as the one provided by the San Diego Supercomputer Center in California (US)^[6], and may reveal interesting features which could augment our structural expertise.

[1] Millán, C., et al. (2015) Macromolecular *ab initio* phasing enforcing secondary and tertiary structure. *IUCrJ*, 2(1), 95–105.

[2] Bibby, J., et al. (2012) AMPLE: a cluster-and-truncate approach to solve the crystal structures of small proteins using rapidly computed *ab initio* models. *Acta Crystallogr. D Biol. Crystallogr.*, 68(Pt 12), 1622–3

[3] Keegan, R. M., et al., (2015) Exploring the speed and performance of molecular replacement with AMPLE using QUARK *ab initio* protein models, *Acta Crystallogr. D Biol. Crystallogr.*, 71(2), 338–343.

[4] DiMaio, F, et al. (2011) Improved molecular replacement by density- and energy-guided protein structure optimization. *Nature*. 26:473 (7348), 540-3.

[5] Sammito, M., et al. (2013) Exploiting tertiary structure through local folds for crystallographic phasing. *Nat Methods*. 10(11), 1099-101.

[6] <http://www.sdsc.edu>

Keywords: Fragment libraries, Local Folds, Supercomputing

MS10-P9 Identification and structural modeling of a novel virulence factor from *H.pylori*

Burcu Kaplan-Türköz¹

1. Ege University, Faculty of Engineering, Department of Food Engineering, Bornova, Izmir, Turkey

email: bkaplan@sabanciuniv.edu

Pathogens produce virulence factors, which help bacteria to invade the host, cause disease and evade host defenses. Recently a class of bacterial proteins which share homology with the Toll/IL-1 receptor (TIR) domain was identified. Those from pathogens; *Brucella* (BtpA and BtpB), uropathogenic *E. coli* (TcpC), *Salmonella* (TlpA) and *Yersinia* (YpTIR) were characterized and their effects on the immune system especially targeting TLR signaling was documented. (1-5) BtpA was shown to be directly involved in the virulence of *Brucella* (5) and the crystal structure of BtpA confirmed the presence of the TIR domain fold. (6). It is yet to be proven if other bacterial proteins with putative TIR domains also function in bacterial pathogenesis. *H. pylori* is a Gram-negative bacteria that colonizes the human stomach and associates with most gastric pathologies, including gastric cancer. *H.pylori* is known for its ability to achieve persistent infection with minimal immune response (7). *H.pylori* might possess a TIR domain containing virulence factor, which can play a role in suppressing TLR signaling analogous to BtpA. In order to identify a putative *H.pylori* TIR domain protein, database were searched and HP1437 was found. HP1437, a 239 amino acid protein has a predicted C terminal TIR domain similar to BtpA/TlpA/TcpC and it contains the conserved TIR domain regions. In this study, HP1437 will be characterized using bioinformatic approaches in order to understand its possible role as a bacterial TIR domain protein. The tertiary structure of HP1437 and that of the C terminal TIR domain will be modelled using homology modeling. The structural models with the highest scores will be searched in protein structure database. The structural alignments will reveal the level of similarity of HP1437 to BtpA or other TIR domain protein structures. The results might contribute to our understanding of the reduced immune response to *H.pylori*.

Acknowledgements: This work is supported by TÜBİTAK-BİDEB (grant number: 114C095).

References: 1:Rana R.R. et al 2011, Microb Pathog, 51,89-95. 2: Salcedo, S.P. et al; 2008, PloS Pathog, 4, e21. 3: Cirl, C. et al., 2008, Nat Med, 14, 399-406. 4:Newman, R.M. et al.,2006, Infect Immun, 74, 594-601. 5:Salcedo, S.P. et al., 2013, Front Cell Infect Microbiol, 3,28. 6: Kaplan-Türköz, B. et al., FEBS Lett, 587 (21) 3412-16. 7: Salama, N. R. et al., 2013, Nat Rev Microbiol, 11(6)385-99.

Keywords: *H.pylori*, homology modeling, virulence factor

MS10-P10 Crystal structure of YwpF from *Staphylococcus aureus* reveals its architecture comprised of a β -barrel core domain resembling type VI secretion system proteins and a two-helix pair

Kyu-Yeon Lee¹, Sang Jae Lee¹, Dong-Gyun Kim¹, Bong-Jin Lee¹

1. The Research Institute of Pharmaceutical Sciences, College of Pharmacy, Seoul National University, Gwanak-gu, Seoul 151-742, Republic of Korea

email: purple290@snu.ac.kr

The *ywpF* gene (SAV2097) of the *Staphylococcus aureus* strain Mu50 encodes the YwpF protein, which may play a role in antibiotic resistance. Here, we report the first crystal structure of the YwpF superfamily from *S. aureus* at 2.5 Å resolution. The YwpF structure consists of two regions: an N-terminal core β -barrel domain that shows structural similarity to type VI secretion system (T6SS) proteins (e.g. Hcp1, Hcp3, and EvpC) and a C-terminal two-helix pair. Although the monomer structure of *S. aureus* YwpF resembles those of T6SS proteins, the dimer/tetramer model of *S. aureus* YwpF is distinct from the functionally important hexameric ring of T6SS proteins. We therefore suggest that the *S. aureus* YwpF may have a different function compared to T6SS proteins.

Keywords: *Staphylococcus aureus*, YwpF, SAV2097, type VI secretion system (T6SS) proteins

MS10-P11 PDB2INS - an interface to SHELXL refinements of macromolecules

Anna V. Luebben¹, Jens Luebben¹, George M. Sheldrick¹

1. Georg-August University Goettingen

email: annavera.luebben@stud.uni-goettingen.de

PDB2INS is an Open Source Python program that reads a PDB file and prepares an .ins file for macromolecular refinement with SHELXL. The necessary restraints for the refinement are taken from the CCP4 reftmac monomer library, provided by the GRADE or PRODRG servers or extracted from a reference structure. The latter approach is particularly useful for refinement against neutron data where the reference structure has been refined already against higher resolution X-ray data. It may also be useful for mutants or protein complexes when a higher resolution structure is available for a wild-type or component protein. PDB2INS takes advantage of recent developments in SHELXL, e.g. for restrained anisotropic refinement or refinement against neutron data [1-3].

[1] Sheldrick, G.M. Acta Cryst. C71 (2015) 3-8. [2] Gruene, T., Hahn, H.W., Luebben, A.V., Meilleur F. and Sheldrick, G.M. J. Appl. Cryst. 47 (2014) 462-466. [3] Thorn, A., Dittrich, B. and Sheldrick G.M. Acta Cryst. A68 (2012) 448-451.

Keywords: SHELXL, Macromolecular Refinement

MS10-P12 Analyzing protein-protein contacts at the PDB-wide level

Guido Capitani¹, Jose Duarte^{1,2}, Kumaran Baskaran¹, Nikhil Biyani¹, Spencer Bliven^{1,3}

1. Paul Scherrer Institute, Villigen, Switzerland
2. ETH Zurich, Switzerland

3. University of California San Diego, USA

email: guido.capitani@psi.ch

As of March 2015, the Protein Data Bank [1] contains more than 105'000 entries: it reached this size largely thanks to the technical advances of macromolecular crystallography in the last 10-15 years. The complexity and diversity of macromolecular crystal structures, however, often make it challenging to establish which of the protein-protein contacts observed in a crystal do bear biological relevance and which ones are lattice contacts. We tackled this problem by creating a general protein interface classification method (EPPIC, Evolutionary Protein-Protein Interface Classifier, www.eppic-web.org [2]). EPPIC analyzes all interfaces in a crystal and classifies them as biological or as crystal contacts by analyzing their evolutionary footprint (or lack thereof). It also uses a geometric interface classification criterion based on our definition of interface core residue [3]. We are now using EPPIC to analyze protein-protein contacts on a PDB-wide scale. To that end, we assembled an automated computational pipeline to run our program on the entire PDB and store the results in a relational database [4], containing about 880'000 interfaces to date. The EPPIC approach, PDB-wide computational pipeline and selected results will be presented.

[1] Berman HM, Henrick K & Nakamura H, *Nature Structural Biology*, 2003, 10, 98

[2] Duarte JM, Srebnik A, Schärer M & Capitani G, *BMC Bioinformatics*, 2012, 13, 334

[3] Schärer, MA, Grütter MG & Capitani G, *Proteins*, 2010, 78, 2707-13

[4] Baskaran K, Duarte JM, Biyani N, Bliven S & Capitani G, 2014, *BMC Structural Biology*, 14, 22

Keywords: Structural bioinformatics, EPPIC, protein-protein interfaces, crystal contacts

MS11. Hybrid approaches

Chairs: Guillermo Montoya, Jan Pieter Abrahams

MS11-P1 Application of magnetically oriented microcrystal array to X-ray and neutron crystallography

Shu Tsukui¹, Fumiko Kimura¹, Tsunehisa Kimura¹

1. Division of Forest and Biomaterials Science, Graduate School of Agriculture, Kyoto University, Kitashirakawa, Sakyo-ku, Kyoto 606-8502, Japan

email: tsukui.shu.52w@st.kyoto-u.ac.jp

The diffraction method is powerful to elucidate the crystal structure of substances at atomic resolution. It is a prerequisite to prepare single crystals large enough for the acquisition of single crystal data. Owing to the synchrotron facilities, the sizes required for X-ray crystallography are getting smaller and smaller, as small as several tens micrometers in size, but yet it is difficult for many substances to crystallize to this size. Size restriction is much severer in neutron crystallography; for example, single crystals of millimeter sizes or more are required in case of proteins.

We have proposed a new technique that enables to convert microcrystals to pseudo-single crystals. Microcrystals are biaxially aligned by using magnetic fields to obtain a magnetically oriented microcrystal array (MOMA). The magnetic susceptibility of biaxial crystals (triclinic, orthorhombic and monoclinic crystal systems) has susceptibility tensor with three different principal values, χ_1 , χ_2 , and χ_3 (we assume $\chi_1 > \chi_2 > \chi_3$). The principal axes corresponding to χ_1 and χ_2 are referred to as easy and hard magnetization axes, respectively. The easy axis aligns parallel to the applied static field, while the hard axis aligns parallel to the z axis when a magnetic field rotation in the xy plane is applied. Combination of these two magnetic fields (referred to as modulated rotating magnetic field) causes three-dimensional alignment of microcrystals.

Orthorhombic hen egg-white lysozyme (HEWL) microcrystals (5-10 μm) were chosen for a model study. The HEWL microcrystals were suspended in a suspension liquid medium (whether ultra-violet curable resin or hydrosol). A capillary containing the microcrystal suspension was subjected to a modulated rotation in the center of 8 T superconducting magnet to achieve 3D alignment. The 3D alignments were consolidated by photo-polymerization of the UV-curable resin or gelation of the hydrosol to obtain MOMAs. X-ray diffraction measurements were carried out at SPring-8. The diffraction images shown in **FIG. 1** were obtained, from which the crystal structure at resolutions higher than 2.0 Å was obtained. Neutron diffraction measurements were carried out on deuterated MOMA prepared in a similar way. Diffraction spots were observed.

These results show that a combination of MOMAs with X-ray and neutron diffraction measurement is of great use for single crystal analyses of protein crystals that do not grow to required sizes.

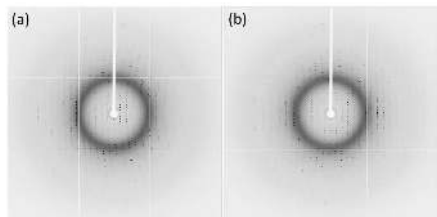


Figure 1. X-ray diffraction images, (a) and (b), taken at two different angles 90° apart. The edges of the images correspond to resolution of 1.79 Å. The averaged full width of half maximum (FWHM) of the diffraction spots are 2.14 and 2.77° for (a) and (b), respectively.

Keywords: X-ray crystallography, Neutron crystallography, Micro-crystallography, Magnetic orientation

MS11-P2 Adsorption of hydrocarbons in the porous borohydride framework $\gamma\text{-Mg}(\text{BH}_4)_2$

Maria G. Babashkina¹, Nikolay A. Tumanov¹, Damir A. Safin¹, Vorakmsy Ban¹, Bo Richter², Torben R. Jensen², Matthew R. Hudson³, Craig M. Brown³, Gail N. Iles⁴, Scott W. Jorgensen⁵, Yaroslav Filinchuk^{*1}

1. Institute of Condensed Matter and Nanosciences, Université catholique de Louvain, Place L. Pasteur 1, 1348 Louvain-la-Neuve, Belgium

2. Center for Materials Crystallography, Interdisciplinary Nanoscience Center and Department of Chemistry, Aarhus University, Langelandsgade 140, 8000 Aarhus C, Denmark

3. Center for Neutron Research, National Institute of Standards and Technology, Gaithersburg, MD 20899, USA

4. Department of Crystallography, Helmholtz-Zentrum Berlin, 14109 Berlin, Germany

5. Chemical and Environmental Sciences Lab General Motors R&D Center, 30500 Mount Rd, Warren, MI 48090, USA

email: maria.babashkina@gmail.com

*yaroslav.filinchuk@uclouvain.be

The first porous hydride, $\gamma\text{-Mg}(\text{BH}_4)_2$, was discovered recently [1]. It has about 1/3 of space in a form of small pores available to guest molecules, such as H_2 , N_2 or CH_4 , [1]. It is expected that the hydridic nature of the borohydride ligands, exposed by H^- into the pores, gives rise to specific guest-host interactions and thus to a selectivity of adsorption. In this work we study adsorption of methane, ethane, propane and butane into $\gamma\text{-Mg}(\text{BH}_4)_2$.

In situ X-ray diffraction data show that only methane and ethane are adsorbed into the pores, while propane and butane are too large to enter. Variable temperature diffraction under different gas pressures allowed us not only to localize the guests, but also to extract the isosteric heats of adsorption directly from the diffraction data [1, 2]. Neutron powder diffraction was done on doubly isotopically substituted $\gamma\text{-Mg}({}^{11}\text{BD})_2$, loaded with CD_4 (NIST) and C_2H_6 (HZB). Accurate localization of the guest molecules allows to determine the nature and the role of the guest-host interactions.

On saturation, 2/3 of methane and ethane molecules are adsorbed per Mg atom. The isosteric heats of adsorption, 22 (CH_4) and 32 (C_2H_6) kJ/mol of gas, allow to store 15–30 weight % of fuel gases at room temperature. This work will be complemented by volumetric studies of the adsorption enthalpies, as well as by theoretical calculations aiming to understand perfectly clear the nature of the intermolecular interactions.

[1] Y. Filinchuk, B. Richter, T.R. Jensen, V. Dmitriev, D. Chernyshov, H. Hagemann, *Angew. Chem. Int. Ed.*, 50, 2011, 11162.

[2] Y. Filinchuk, Get more for your porous system: heats of adsorption from powder diffraction data. ECM-27, Bergen, 2012.

Keywords: adsorption, *in situ* powder diffraction, porous hydride, thermodynamics

MS11-P3 Structure resolution of the complex γ -La₆W₂O₁₅

Stéphanie Kodjikian^{1,2}, Christophe Lepoittevin^{1,2}, Holger Klein^{1,2},
Thomas Schönenberger^{1,2}, Olivier Leynaud^{1,2}, Marie-Hélène
Chambrier³, François Goutenoire⁴

1. CNRS, Institut NEEL, F-38042 Grenoble, France

2. Univ. Grenoble Alpes, Institut NEEL, F-38042 Grenoble, France

3. Univ. d'Alsace, Unité de Catalyse et de Chimie du Solide, F-62307 Lens, France

4. Univ. du Maine, Institut des Molécules et Matériaux du Mans, F-72085 Le Mans, France

email: stephanie.kodjikian@neel.cnrs.fr

Oxides in the La₂O₃-MO₃ (M = Mo and W) system are of significant technological interest for their laser applications [1], ionic conduction [2], catalytic [3] and ferroelectric [4] properties. The La₂O₃-WO₃ phase diagram has been studied by a number of groups [5-7], but little detailed crystallographic information was reported due to the lack of good single crystals. Some of the reported compositions have not been appropriately characterized. Recently, the structures of La₂WO₆, La₁₈W₁₀O₅₇ and La₁₀W₂O₂₁ were solved using X-ray powder diffraction (XRPD) [8-10]. For the La₆W₂O₁₅ compound phase transitions at 630 and 930°C have been reported [1-3]. The structure of the high temperature phase α -La₆W₂O₁₅ was determined ab-initio by XRPD using direct methods [11]. The lower-temperature forms β and γ , however, couldn't be determined due to the large number of reflections in the X-ray powder diffraction pattern and the relatively low symmetry of the system. The existing literature on γ -La₆W₂O₁₅ only relates two sets of unit cell parameters [5-6], that almost match the XRPD pattern of γ -La₆W₂O₁₅, but some weak peaks remain without indexation and can't be explained by the presence of any impurity.

Here we present the combination of XRPD and electron diffraction studies to solve the complex structure of γ -La₆W₂O₁₅. From standard selected area electron diffraction the unit cell was determined to be monoclinic with cell parameters a=1.56 nm, b=1.21 nm, c=1.47 nm, β =110°. Due to the low symmetry of the crystal system and the large unit cell, a huge number of reflections needed to be acquired, so that electron diffraction tomography was used to record the intensities. The structure of γ -La₆W₂O₁₅ was successfully solved.

[1] Kumaran et al, J Cryst Growth 292 (2006) 368-372

[2] Lacorre et al, Nature 404 (2000), 856-858

[3] Alonso et al, J Solid State Chem 177 (2004) 2470-2476

[4] Brixner et al, J Solid State Chem 5 (1972) 186-190

[5] Yoshimura et al, Mater Res Bull. 11 (1976) 151-158

[6] Yanoskii et al, Sov Phys Crystallogr 20(3), 354-355

[7] Ivanova et al, Inorg Mater (1970) 803-805

[8] Chambrier et al, J Solid State Chem 183 (2009) 209-214

[9] Chambrier et al, Inorganic Chemistry 48 (2009) 6566-6572

[10] Chambrier et al, Inorganic Chemistry 53 (2014) 147-159

[11] Chambrier et al, J Solid State Chem 183 (2010) 1297-1302

Keywords: structure determination, electron crystallography, X-ray powder diffraction

MS11-P4 Exploring molecular recognition mechanisms in the multistep phosphorelay signaling in plants: crystal structure of His phosphotransmitter AHP2 and modeling of its interaction with sensor histidine kinase CKII

Oksana Degtjarik¹, Radka Dopitová², David Reha^{1,3}, Sandra Puehringer⁴, Blanka Pekarová², Olga Otrusínová², Michal Kutý^{1,3}, Manfred S. Weiss⁵, Lukáš Zidek², Lubomír Janda², Ivana Kutá Smanetová^{1,3}, Jan Hejábek²

1. University of South Bohemia, Faculty of Science, Ceske Budejovice, Czech Republic
2. Central European Institute of Technology (CEITEC), Masaryk University, Brno, Czech Republic
3. Academy of Sciences of the Czech Republic, Institute of Nanobiology and Structural Biology GCRC, Nové Hrad, Czech Republic
4. University of Salzburg, Department of Molecular Biology, Salzburg, Austria
5. Helmholtz-Zentrum Berlin for Materials und Energy BESSY-II, Berlin, Germany

email: degtjarik648@gmail.com

In plants, histidine phosphotransfer proteins (HPTs) transmit the signal between diverse sensor histidine kinases (HKs) and response regulators within multistep phosphorelay (MSP) pathway. The ability of HPTs to interact with the receiver domains of sensor histidine kinases with different affinities indicates the certain specificity of the interaction between two partners. In order to explore the structural determinants of the interaction specificity between AHP2 and the receiver domain of histidine kinase CKII (CKII_{RD}) from model plant *Arabidopsis thaliana*, we determined the crystal structure of AHP2 by SIRAS protocol at 2.53 Å resolution. Molecular dynamics simulations for 100 ns were applied to identify the key residues responsible for the AHP2-CKII_{RD} interaction. The AHP2-CKII_{RD} interaction was confirmed by NMR measurements – resulting chemical shifts partially overlap with the model. AHP2-CKII_{RD} model reveal strong protein-protein complex; the comparison of the model with recently published crystal structure of AHP1-AHK5_{RD} suggests significant differences in binding interface between both complexes, mostly in the amino acid residues mediating hydrophilic interactions. Due to the fact that the vast majority of interacting residues in AHP1 and AHP2 are represented by highly conserved residues, small structural differences of both AHPs and AHK_{RD}s seem to be sufficient for determination of specific molecular recognition as could be seen by our bioinformatical and structural comparisons.

Keywords: protein crystallography, MD simulations, NMR, Arabidopsis, signal transduction, multistep phosphorelay, molecular recognition

MS11-P5 The keratin-10 binding region of the pneumococcal serine rich repeat protein (PsrP) forms a domain-swapped dimer and intermolecular β-sheets – implications for biofilm formation of *Streptococcus pneumoniae*

Tim Schulte¹, Jonas Löfling², Cecilia Mikaelsson¹, Alexey Kikhney³, Karina Hentrich⁴, Aurora Diamante¹, Christine Ebel⁴, Staffan Normark², Dmitri Svergun³, Birgitta Henriques-Normark², Adnane Achour¹

1. Science for Life Laboratory, Department of Medicine Solna, Karolinska Karolinska Institutet, Stockholm, Sweden
2. Department of Microbiology, Tumor and Cell Biology (MTC), Karolinska Institutet, Stockholm, Sweden
3. European Molecular Biology Laboratory (EMBL), Hamburg Outstation, Notkestrasse 85, 22603 Hamburg, Germany
4. Institut de Biologie Structurale, CEA-CNRS-Université Grenoble, France

email: Tim.Schulte@ki.se

The commensal bacterial pathogen *Streptococcus pneumoniae* colonizes the upper respiratory tract of humans and can cause pneumonia, sepsis and meningitis. The role of the pneumococcal serine-rich repeat protein (PsrP) is to present the basic region (BR) domain for interaction with keratin 10 (KRT10) on the extracellular surface of host lung cells through its MSCRAMM-related globular binding region domain [1,2] as well as for biofilm formation through self-oligomerization [3]. PsrP belongs to the family of serine-rich repeat (SRR) proteins with a long, putatively glycosylated serine rich repeat domain that is covalently anchored to the cell wall and extends the functional domain out of the capsule [3,4].

Biophysical analysis of the BR domain by small-angle X-ray scattering (SAXS), analytical ultracentrifugation and X-ray crystallography reveals the formation of a domain-swapped dimer and an intermolecular β-sheet that could be relevant for the function of PsrP in biofilm formation. Furthermore, SAXS and circular dichroism experiments revealed the N-terminal BR₁₂₂₋₁₆₆ region as a non-globular and probably disordered structure. We also demonstrate that this disordered N-terminal fragment is cleaved off by the human furin protease, a known activator of other toxins and virulence factors, potentially promoting pneumococcal biofilm formation.

References

- [1] P. Shivshankar *et al.*, Mol. Microbiol 73 (2009) 663.
- [2] T. Schulte *et al.*, Open Biol. 4 (2014) 130090.
- [3] C.J. Sanchez *et al.*, PLoS Pathog 6 (2010).
- [4] S. Ramboarina *et al.*, J. Biol. Chem 285 (2010) 32446.

Keywords: structural biology

MS11-P6 Mechanistic basis for site-specific functions of focal adhesion kinase

Stefan T. Arold¹, Karen Brami-Cherrier², Nicolas Gervasi², Katarzyna W. Walkiewicz¹, Gress Kadarec², Jean-Antoine Girault²

1. King Abdullah University of Science and Technology (KAUST), Saudi Arabia
2. Institut du Fer à Moulin, Paris, France

email: stefan.arold@kaust.edu.sa

Focal adhesion kinase (FAK) controls adhesion-dependent cell motility, survival, and proliferation, and plays a major role in development and cancer. Interestingly, FAK has different functions in different cellular compartments. For example at focal adhesions, FAK regulates integrin signalling in a kinase-dependent manner, whereas in the nucleus it exerts kinase-independent anti-apoptotic effects. We have combined SAXS with data from x-ray crystallography, NMR, bioinformatics, biochemical and functional analyses, to provide first structural insights into full-length FAK. Through specifically affecting the structural dynamics of FAK, we show that low-probability conformational transitions are of biological importance. Collectively, our data show how the dynamics and allosteric interplay between ligands and FAK's several domains controls site-specific activity of FAK. Our results reveal how FAK detects the coincidence of multiple signals to generate an environment-specific outcome.

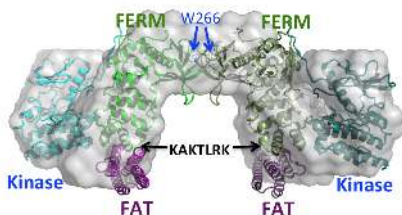


Figure 1. Structure of full-length focal adhesion kinase, obtained by hybrid methods.

Keywords: focal adhesion, kinase, SAXS, NMR, confocal microscopy, x-ray crystallography

MS11-P7 Structural studies of the human Nuclear EXosome Targeting complex

Nicholas Sofos¹, Mikael B. Winkler¹, Ditlev E. Brodersen¹

1. Centre for mRNP Biogenesis and Metabolism, Department of Molecular Biology and Genetics, Aarhus University, DK-8000 Aarhus C

email: sofos@mbg.au.dk

RNA decay is an important process in all domains of life as it is essential for maturation of nuclear RNAs, regulates the abundance of transcripts, and prevents the accumulation of spurious transcripts. The main machinery responsible for 3'-5' decay in eukaryotes is the RNA exosome; a multi-component protein complex consisting of a 9-subunit inactive core and the associated nucleases Rrp44 and Rrp6[1]. In addition, the exosome utilizes a number of different cofactors that stimulate enzymatic activity and serve as adapters for its many substrates. A chief activator of the nuclear exosome is the MTR4 helicase, which mainly functions in the context of the TRAMP complex in human nucleoli, and in the context of the NEXT (Nuclear EXosome Targeting) complex in the nucleoplasm.

The NEXT complex consists of the RNA DexH-box helicase MTR4, the Zn-knuckle protein ZCCHC8, and the putative RNA binding protein RBM7 – with the latter two being highly conserved in vertebrates only. Consistent with its residence in the nucleoplasm, NEXT is required for degradation of promoter upstream transcripts (PROMPTs) and other non-coding RNA PolII transcripts[2][3].

Individual fragments of the NEXT subunits have been purified for crystallization trials and interaction profiling of core fragments. A fragment of the RBM7 protein has been crystallized and diffraction data has been collected. So far, the data quality is too low and optimization is ongoing.

In a parallel approach, the endogenously expressed NEXT complex has been extracted and purified for negative stain EM. Data processing is ongoing.

[1] Chlebowski, A., Lubas, M., Jensen, T.H., and Dziembowski, A. (2013). RNA decay machines: the exosome. *Biochim. Biophys. Acta* 1829, 552–560. [2] Lubas, M., Christensen, M.S., Kristiansen, M.S., Domanski, M., Falkenby, L.G., Lykke-Andersen, S., Andersen, J.S., Dziembowski, A., and Jensen, T.H. (2011). Interaction profiling identifies the human nuclear exosome targeting complex. *Mol. Cell* 43, 624–637. [3] Lubas, M., Andersen, P., Schein, A., Dziembowski, A., Kudla, G., and Jensen, T. (2015). The Human Nuclear Exosome Targeting Complex Is Loaded onto Newly Synthesized RNA to Direct Early Ribonucleolysis. *Cell Reports*.

Keywords: crystallography, electron microscopy, NEXT complex

MS12. Crystallization and crystal treatment

Chairs: Terese Bergfors, Matthew Bowler

MS12-P1 Crowning proteins: modulating the protein properties using crown ethers

Cheng-Chung Lee^{1,2}, Manuel Maestre-Reyna¹, Andrew H.-J. Wang^{1,2}

1. Institute of Biological Chemistry, Academia Sinica, Taipei 115, Taiwan.

2. Core Facilities for Protein Structural Analysis, Academia Sinica, Taipei 115, Taiwan.

email: chengung@gate.sinica.edu.tw

Protein crystallization is a main bottleneck in protein X-ray crystallography analysis. Crystallization optimization is often achieved only on a case-by-case, trial-and-error basis. By first identifying a ring-shaped binding mode for low-molecular weight polyethylene glycol (lmwPEG) in a number of protein crystal structures, we established crown-ether (18-Crown-6; CR) as reliable crystallization additives as a powerful crystallization tool. Our studies showed that crown ethers can modify protein surface behavior dramatically by stabilizing either intra- or inter-molecular interactions. Crown ethers can also be used to modulate a wide variety of protein surface behaviors beyond crystallization, such as oligomerization, domain-domain interactions, or stabilization in organic solvents. By solving the structures of several crystals obtained in the presence of CRs, we observed direct interactions in crystals. In some cases, CR improved crystal quality and resolution, making it possible to solve the complex structure. CRs were found to modify protein surface properties by yielding complexes, which resulted in alternative tertiary and quaternary structures. There are three distinct CR interaction modes, namely the K-crown, the C-crown and the KC-crown modes (Figure). CRs also increased protein rigidity and, by CR–CR stacking, mediated direct interactions between hydrophobic patches and charged amino acids. We therefore propose that CRs, by their ability to modify protein surfaces, can be used as: 1) powerful additives in protein crystallography; 2) molecular probes to search for potential binding pockets; and 3) reporters of protein conformational changes.

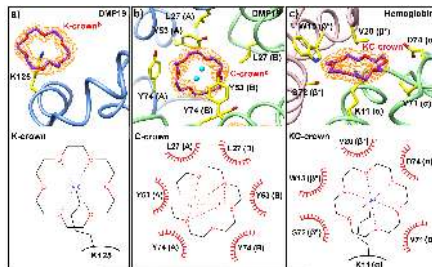


Figure 1. CR binding modes. a) K-crown, a single Lys binds the CR axially. b) C-crown, hydrophobic and p-orbital containing side-chains interact laterally with CR. c) KC-crown, the CR is coordinated axially by a Lys, while hydrophobic and p-orbital containing side-chains interact with it laterally.

Keywords: crystallography, crown ether, protein modulating, additive

MS12-P2 Crystallization of transcriptional metalloregulator protein CueR in complex with Hg²⁺

Valeria Bugris¹, Ria K. Balogh², Veronika Harmath¹, Zsolt Flákóvics¹, Sándor Brockhauser¹, Áttila Jancsó²

1. Biological Research Center, Hungarian Academy of Sciences, Temesvári krt. 62, H-67 26 Szeged, Hungary

2. University of Szeged, Dóm tér 7, H-67 20 Szeged, Hungary

email: bugris.valeria@brc.mta.hu

The optimal concentration of metal ions in bacteria is controlled by transcriptional metalloregulators. MerR proteins operate by an activation mechanism based on a conformational change of the DNA-bound protein upon metal ion coordination. This also affects the structure of the DNA and therefore, RNA polymerase can initiate the transcription of the regulated genes leading to the formation of proteins the role of which is the removal of metal ion from the cell. The MerR family member CueR (Cu efflux Regulator) protein regulates the intracellular amount of Cu-ion in several strains of bacteria. The CueR protein gives a transcriptional response only for singly charged transition metal ions (Cu^I, Ag^I and Au^I). Our aim is to solve the structure of the CueR protein in complex with an unfavoured divalent metal ion, the strong binder Hg^{II}. From these studies we will learn about the structural differences compared with the already available protein structures containing monovalent metal ions [Changela et al, Science, 2003, 301: 1383]. The main goal of these studies is to understand the structural details of bacterial metal ion regulatory mechanisms on molecular basis. For this purpose we have optimized the conditions of the CueR protein expression and purification in *E. coli*, and set up a crystallization screen with similar conditions as described in the literature. The results of these experiments will be presented.

*R.K. Balogh and V. Bugris contributed equally to this work.

Keywords: crystallization, CueR, complex with Hg(II)

MS12-P3 The latest developments of detecting and sorting protein micro- and nano-crystals

Lars Thormann¹, Robin Schubert¹, Arne Meyer², Karsten Dierks², Markus Perbandt¹, Christian Betzel¹

1. University of Hamburg, Center of Ultrafast Imaging, Laboratory for Structural Biology of Infection and Inflammation, c/o DESY, Build. 22a Notkestr. 85 22607 Hamburg / Germany

2. Xtal Concepts GmbH, Marlowring 19, 22525 Hamburg / Germany

email: lars.thormann@chemie.uni-hamburg.de

Applying high brilliant Synchrotron Radiation X-ray free-electron laser (XFELs) radiation in combination with Serial Femto Second Crystallography (SFX) offers today the possibility to collect diffraction data from micro- and nano-sized protein crystals at room temperature before radiation damage will be effective. Due to the superior intensity of FEL radiation the required size of the protein crystals to be used for SFX is significantly smaller compared to those used for conventional diffraction data collection. However, in comparison to conventional protein crystallography a high number of these crystals is required ($> 10^5$), delivered in concentrated suspensions via a particular sample delivery jet technology. Exceptionally some large crystals or particles in the suspension can unfortunately block the sample delivery jet and can cause problems along the SFX data collection. Therefore in different approaches crystal scoring techniques are presently under development. We designed and developed a reliable approach combining latest multi-channel *in situ* DLS techniques and micro-pump technology to score and sort in high throughput mode crystal suspensions for SFX applications. The present sorting hardware and microfluidics carrier is designed to be combined also with other detection methods, e.g. second harmonic generation (SHG); (confocal) depolarized dynamic light scattering (DDLS) and UV light fluorescence detection. Details will be presented.

Keywords: Crystal Sorting, XFEL, SFX, DLS

MS12-P4 Structural basis for sensitivity of fluorescent proteins to molecular Oxygen investigated by high-pressure crystallography

Bénédicte Lafumat¹, Royant Antoine^{1,2}, de Rosny Eve², Van der Linden Peter¹, Leonard Gordon¹, Carpentier Philippe¹

1. ESRF, 6 Rue Jules Horowitz, Grenoble, France

2. IBS, 6 rue Jules Horowitz, Grenoble, France

email: benedictelafumat@esrf.fr

Since the successful cloning of the green fluorescent protein (GFP) from the jellyfish *Aequorea victoria* in 1992, fluorescent proteins (FPs) have revolutionized Life Science [1]. A FP 3-dimensional structure is basically that of a β -barrel protecting the chromophore responsible for the fluorescence. FPs show scales of sensitivity to molecular Oxygen (O_2) that is most likely related to the porosity of the β -barrel combined with the reactivity of the chromophore. In particular, photosensitizing FPs [2] consume O_2 and generate cytotoxic reactive oxygen species (ROS) upon photobleaching and are thus of interest for light-induced cell killing methods [3]. Our project aims at studying the flexibility/porosity of β -barrels and the reactivity of chromophores, and thus at comprehending the mechanism that govern the sensitivity of FPs to O_2 . We are exploiting pressure and high-pressure crystallography to explore the conformational sub-states and reveal the dynamic motions of β -barrel strands of FPs, and secondly to identify O_2 pathway and specific binding site in FPs. Specific cells have been designed to cryo-cool protein crystals under pressure or high-pressure of Helium (He) [4], Krypton (Kr), and O_2 gas. Indeed, it has been shown that high-pressure crystallography with the He cryo-cells allows exploring the energy landscapes of proteins, providing access to their conformational sub-states and their dynamics [2]. O_2 and Kr cryo-cells allow populating channels and potential sites of affinity for O_2 in FPs. In complement to X-ray crystallography, pressure induced modifications of PFs are characterized by in-crystallo UV-visible and Raman spectroscopy. For these studies, a set of FPs have been produced and crystallized including the efficient photosensitizer KillerRed. During this presentation, we will introduce the different methodologies and present the pressure-induced structural changes of some FPs, which already allows us to identify flexible weakness in β -barrels and potential entrance/exit gates for O_2 in FPs. The ultimate purpose of this work will be to provide the structural basis that allows identifying efficient photosensitizers that could have important applications in cancer photodynamic therapy.

[1] Shimomura et al (1962) J Cell Comp Physiol. **59**, 223-39; [2] Carpentier et al (2012) J. Am. Chem. Soc. **134**, 18015-21; [3] Jacobson et al (2009), Trends in Cell Biology, **18** (9), 443-50; [4] Van der Linden et al (2014) J. Appl. Cryst. **47**, 584-92

Keywords: Fluorescent proteins, molecular Oxygen, Photosensitizer, High pressure, X-ray crystallography

MS12-P5 The feasibility of crystallization of flexible proteins using maltose-binding protein

Yuya Hanazono¹, Kazuki Takeda¹, Kunio Miki¹

1. Graduate School of Science, Kyoto University

email: yuya-h@kuchem.kyoto-u.ac.jp

Sufficient quality crystals of proteins are indispensable to determination of the whole protein structures including the side chains by using X-ray crystallography. It has been reported that protein tags, such as maltose-binding protein (MBP), glutathione S-transferase, thioredoxin are useful to get better crystals. Though previous crystallographic studies through the use of fusion protein were carried out to reveal the structure for rigid proteins or domains, there are many flexible proteins or peptides, which are required further researches. In order to examine the feasibility of crystallization of flexible proteins or peptides using rigid protein tags, we studied about the two such examples where flexible peptides are fused with MBP.

We determined two structures of flexible peptides fused with MBP. Crystals of the peptides with MBP diffracted X-rays at 2 Å. In their crystal structures, these peptides whose electron densities are well defined have secondary structures. CD spectroscopic analysis indicated that the secondary structure contents in the crystals are comparable with those in the 30% TFE solution, which simulates *in vivo* conditions. These results show that the crystal structures represent the structures of the peptides in the cells. Therefore, crystallographic approach fusing with rigid protein tags could be a promising tool to determine the structure of the flexible peptides.

Keywords: maltose-binding protein, flexible peptide, circular dichroism

MS12-P6 Multicomponent mixtures for ligand solubilization and cryoprotection

Enrico A. Stura¹, Lidia Ciccone², Livia Tepshi¹

1. CEA, iBiTec-S, Service d'Ingénierie Moléculaire des Protéines, Laboratoire de Toxinologie Moléculaire et Biotechnologies, Gif-sur-Yvette, F-91191, France.

2. Dipartimento di Farmacia, Università di Pisa, Via Bonanno 6, 56126 Pisa, Italy.

email: estura@cea.fr

Ligand solubilization can prove problematic when crystallizing protein-ligand complexes. We have investigated the use of mixed compounds both for soaking of ligands into crystals and in crystallization complexes. The mixed solubilizing compounds achieves complete solubilization of a large variety of hydrophobic ligands resulting in the first crystal structure of a protein in complex with curcumin (Ciccone, Tepshi, Nencetti, & Stura, 2015). The set of mixed solubilizers, that include DMSO, 1,4-dioxane, 2,3-butanediol, 1,2-propanediol, glycerol, ethylene glycol and diethylene glycol, are also effective as a cryoprotectant when formulated together with a precipitant and buffer in the same ratio as previously reported (Vera & Stura, 2014). We have compared the resolution to which crystals diffract using these compounds with those previously formulated with equivalent results (Ciccone, Vera, Tepshi, & Stura, 2015). The main differences in the new development is the introduction of dioxane for ligand solubilization and butanediol for cryoprotection. The latter may be responsible for increased crystal stability in the soaking solutions. In the presentation we will report on ongoing tests on new compound for ligand solubilization, for use as an additive in crystallization and for cryoprotection. The compound appear to be highly effective and has been evidenced in the electron density of crystals grown or soaked in solutions containing it. Initial tests with the mixed and ligands for heavy atom derivatization are ongoing as well as the development of new detergents for protein crystallization. Preliminary results with the new detergents suggests that they can be used to obtain polymorphs (Vera et al., 2013) never obtained before.

Ciccone, L., Tepshi, L., Nencetti, S., & Stura, E. A. (2015). Transthyretin complexes with curcumin and bromo-estradiol: evaluation of solubilizing multicomponent mixtures. *New Biotechnology*, 32, 54–64.

Ciccone, L., Vera, L., Tepshi, L., & Stura, E. A. (2015). Multicomponent mixtures for cryoprotection and ligand solubilization. *Biotechnology Reports*, accepted.

Vera, L., Antoni, C., Devel, L., Czarny, B., Cassar-Lajeunesse, E., Rossello, A., ... Stura, E. A. (2013). Screening Using Polymorphs for the Crystallization of Protein-Ligand Complexes. *Crystal Growth & Design*, 13: 1878–1888.

Vera, L., & Stura, E. A. (2014). Strategies for Protein Cryocrystallography. *Crystal Growth & Design*, 14, 427–435.

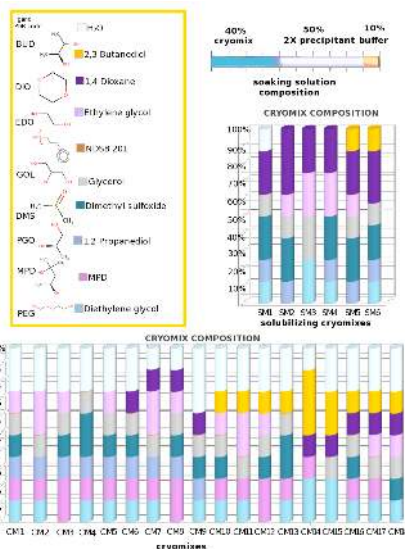


Figure 1.

Keywords: Ligand solubilization, cryoprotection, additives for protein crystallization

MS12-P7 Crystal transformation using IR laser radiation

Breyan H. Ross^{1,2,3}, Evi Stahl³, Stephan Krapp², Robert Huber^{1,3,4,5}, Reiner A. Kiefersauer^{1,2}

1. Max-Planck-Institut für Biochemie, Am Klopferspitz 18, 82152 Martinsried, Germany
2. Proteros Biostructures GmbH, Bunsenstrasse 7a, 82152 Martinsried, Germany
3. Technische Universität München, Lichtenbergstrasse 4, 85747 Garching, Germany
4. Zentrum für Medizinische Biotechnologie, Universität Duisburg-Essen, 45117 Essen, Germany
5. School of Biosciences, Cardiff University, Cardiff CF10 3US, Wales

email: breyanross@gmail.com

For solving crystallographic biomolecular structures sometimes crystals simply do not diffract good enough. Post-crystallization treatments aim to overcome this situation by adjusting the environmental variables of the crystal in order to improve the diffraction quality. One strategy used in our laboratory is crystal dehydration by Free Mounting System (FMS) technique (1). Using CO dehydrogenase (CODH) crystals as a model of improvement by dehydration we characterized the use of a novel device to control relative humidity (rh) based on Infra-red laser (2). Interestingly the dehydration process of CODH shows two stages, with the last one, the more stable and well diffracting state (3). On the other side, depending on the crystal system, dehydration could cause loss of diffraction, one example is tetragonal crystals of lysozyme. We compare the different states to explain how the transformation occurs. Not just protein crystals can be dehydrated, but also DNA crystals can be subject of this approach. We used origami DNA crystals to study crystal transformation, analyzing several variations of the constructs like different ending of the strands. We found that crystal transformation in the case of improvement is accompanied by a cell dimension contraction and the formation of new crystal contacts. In the case of deterioration, there is also a contraction of unit cell dimension but there is a reorganization of crystal contacts keeping the symmetry. Using the laser we can evaluate transformation in terms of kinetics or diffraction quality. Evaluating these crystal systems we aim to explore the structural basis of crystal transformation and also to develop the laser technique to control water content in crystal systems exploring possible advantages over the current relative humidity control techniques.

1.- Kiefersauer R., Than M., Dobbek H., Gremer L., Melero M., Strobl S., Dias J., Soulimane T., Huber R. 2000. *J. Appl. Cryst.* 33, pp. 1223-1230.

2.- Kiefersauer R., Grandl B., Krapp S., Huber R., 2014. *Acta Cryst D*, 2014, 70, pp. 1224-1232.

3.- Dobbek H., Gremer L., Kiefersauer R., Huber R., Meyer O. 2002. *PNAS Vol.99*, pp. 15971-15976

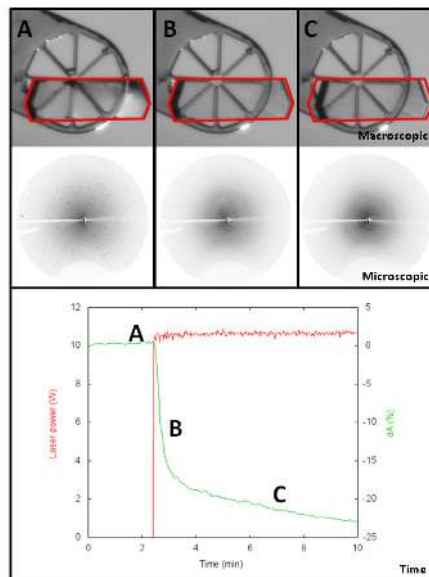


Figure 1. Lysozyme transformation. A, correspond to 96% rh. B, first intermediate state at 91% rh. C, final state, below 91% rh. Lower panel, shows the curve of dehydration measured by back projections of the red square in the upper panel. Constant laser power of 5W and increasing frequency up to 1000 Hz.

Keywords: Crystal transformation, infrared laser, dehydration, crystal contacts, crystal improvement, annealing

MS12-P8 Applying robust statistical methods to assess the effect of excess solvent in long wavelength data collection

Sam Horrell¹, Ramona Duman¹, Juan Sanchez-Weatherby¹,
Richard Strange², Armin Wagner¹

1. Diamond Light Source, Harwell Science and Innovation Campus, Chilton, Didcot, Oxfordshire, OX11 0DE, UK

2. Molecular Biophysics Group, School of Biological Sciences, University of Liverpool, Crown Street, Liverpool, Merseyside, L69 7ZB, UK

email: sam.horrell@liv.ac.uk

As modern macromolecular crystallography (MX) is addressing increasingly challenging projects, there is a greater need to improve the quality of diffraction data. Amongst the most limiting factors affecting data quality are crystal quality, radiation damage and the signal-to-noise ratio. This study focuses on improving the signal-to-noise ratio by removing surrounding solvent to reduce background scatter and absorption. Although not considered critical for standard MX experiments, in the light of long-wavelength and microcrystal MX, it becomes a limiting factor. This is evident from the variety of sample handling and mounting systems developed to reduce these effects; including the loopless mounting method (Kitago *et al.* 2010), the use of adhesive materials for harvesting (Kitatani *et al.* 2008), coating samples with atomically thin graphene sheets (Wierman *et al.* 2013), shaping macromolecular crystals with PULSA (Kitano *et al.* 2005) and excising crystals grown on ultrathin films with a femtosecond laser (Marquez & Cipriani. 2014).

Here (Horrell *et al.* 2015) we use robust statistical analysis to show manipulation of macromolecular crystals and removal of excess solvent in a humid air stream can be done at no cost to crystal integrity. To test this, we transferred large populations of macromolecular crystals from nylon loops to Kapton MicroMounts, using micromanipulators for precise movement, and a humidity control device (Sanchez-Weatherby *et al.* 2009), to preserve crystals during the process. Diffraction data collected at $\lambda = 1 \text{ \AA}$ from lysozyme, thaumatin, insulin and ferritin show no significant difference between test and control samples, emphasising this methods potential. Similar tests with data collected at longer wavelengths ($\leq 2 \text{ \AA}$) on protein crystals from *P. aeruginosa*, *P. carotovorum* and *P. syringae* have revealed protein dependent effects on data quality based on exposure to the humid air stream and data collection around $\lambda = 2 \text{ \AA}$.

Horrell, S. *et al.*, (2015). To be Submitted to *Acta crystallographica. Section D*

Kitago, Y. *et al.*, (2010). *Journal of Applied Crystallography* **43**, 341-346

Kitano, H. *et al.*, (2005). *Journal of bioscience and bioengineering* **100**, 50-53

Kitatani, T. *et al.*, (2008). *Applied Physics Express* **1**, 1-3

Sanchez-Weatherby, J. *et al.*, (2009). *Acta crystallographica* **D65**, 1237-1246

Wierman, J. L. *et al.*, (2013). *J Appl Crystallogr* **46**, 1501-1507

Marquez, J. A. & Cipriani, F. (2014). *Methods in molecular biology* **1091**, 197-203

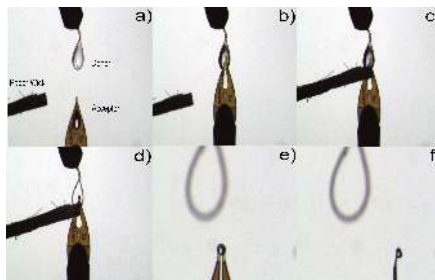


Figure 1. A microscope view of the step wise transfer (a-f) of a 50 μm insulin crystal from a nylon CryoLoop to a Kapton MicroMount in a humidity controlled stream by removing excess solvent.

Keywords: Humidity Control, Sample Handling, Long Wavelength X-ray Crystallography, Data Quality.

MS12-P9 Innovative protein crystallization screensFabrice GORREC¹

1. MRC Laboratory of Molecular Biology, Francis Crick Avenue, Cambridge Biomedical Campus Cambridge, CB2 0QH, UK

email: fgorrec@mrc-lmb.cam.ac.uk

At the MRC-LMB, despite using a set of commercially available conditions considered as very large (≥ 1440 conditions), the yield of experiments containing protein crystals with sufficient quality to solve structures is regularly below 1%. In addition to sample properties, an underlying reason for such low yield is the very large number of combinations of variables associated with protein crystallization.

We argue that our approach to initial crystallization screening is yet under-sampled and hence an even larger set of conditions should be preferred whenever possible. Protein crystallization screen formulations should evolve in parallel with the increasing complexity of the samples and the technical difficulties encountered during the process of structure determination. Notably, demands of cryo-crystallography, as well as solutions to the phase problem should be taken into account more. In this context, developed the Pi and MORPHEUS approaches to formulation and the corresponding screens.

The formulation of a Pi screen is derived from the incomplete factorial approach. Combinations of 3 reagents are produced following the modular distribution of a given set of up to 36 stock solutions. Maximally diverse conditions can be produced by taking into account the properties and the concentrations of the chemicals used to formulate a 96-condition screen. The Pi sampling method is intended to help laboratories on a day-to-day basis to test new crystallization screen formulations based on the properties of the macromolecules investigated.

A MORPHEUS screen (also consisting of 96 conditions) integrates several innovative approaches developed elsewhere, such as mixes of potential ligands, convenient buffer systems and precipitant mixes that also act as cryoprotectants. Molecules frequently observed in the PDB to co-crystallize with proteins have been selected to formulate MORPHEUS I and II. The aim was to increase yield of quality crystals with molecules acting as protein stabilizers, crystal packing bridges, or any other role beneficial to protein crystallization.

Increasing the initial yield of quality crystals is key for the determination of novel protein structures by X-ray diffraction. Ideally, demanding optimizations and issues with reproducibility will be bypassed.

Keywords: crystallography; proteins; crystallization; screen; formulation; additives

MS12-P10 Protein surface modifying agents in protein crystallizationJindřich Hašek¹, Tereza Skálková¹, Petr Kolenko¹, Jarmila Dušková¹, Tomáš Koval¹, Karla Fejfarová¹, Jan Stránský¹, Jan Dohnálek¹

1. Institute of Biotechnology, Academy of Sciences of the CR, Vídeňská 1083, 142 20 Prague 4, Czech Republic

email: hasekj@seznam.cz

Uniform stacking of protein molecules into the growing crystal requires a dominance of a single protein-protein adhesion mode. Existence of mutually **incompatible protein-protein adhesion modes** in the same crystal leads to stacking faults, to low quality crystals, or to crystallization failure. The substances balancing kinetics of the protein-protein adhesion in different adhesion modes are called **"Protein Surface Active Molecules" (PSAM)** [1]. The PSAM binding selectively and temporarily to the protein surface compete with protein-protein adhesion modes, or sometimes can form the protein-protein crosslinks built-in permanently into the growing crystals.

The **theory of PSAM** describes protein crystallization as a regular deposition of **short-life protein-PSAM adducts** and stresses a role of these "sticking molecules" with highly specific adhesion to different protein-surface patches active in crystallization processes. The PSAM-protein adducts decompose after the protein is fixed on crystal surface or when the other protein adducts try fix in correct position and orientation nearby on the growing crystal surface. Proper choice of PSAM eliminates deposition of protein molecules in the **crystallographically incompatible protein-protein adhesion modes**. It is decisive for a success of protein crystallization in many cases.

The concept of crystallization as a regular deposition of naked protein molecules on the growing crystal surface is here replaced by the concept of regular deposition of the PSAM-protein adducts. It is more difficult for imagination, but provides explanations of many enigmatic crystallization phenomena. It increases the **number of crystallizable proteins**, allows preparation of crystals with **protein-protein complexes**, and leads to higher quality diffraction data by **minimizing probability of stacking faults** in crystal. It explains why **combination of several "successful additives"** can lead to crystallization failure. It allows also a preparation of polymorphs allowing study of **protein conformation in different environments** with different pH, different water content, etc. One can also choose the **polymorph ensuring the highest accuracy** of structure determination.

The study supported by ERDF CZ.1.05/1.1.00/02.0109 BIOCEV, LG14009, CSF 15-15181S, MSMT EE2.3.30.29, SGS13/219/OHK4/3T/14

[1] Hašek, J. (2006) Z. Kristallogr. 23, 613-619; Hašek, J. (2011) J. Synchr. Radiation 18, 50-52; Hašek, J. et al (2011) Z. Kristallogr. 28, 475-480.

Keywords: Keywords: protein crystallization, protein-protein adhesion, protein surface, hydrophilic polymers

MS13. New instrumentation, methods and approaches in inorganic crystallography

Chairs: Anton Meden, Damien Jacob

MS13-P1 Nano-diffraction in STEM and fluctuation electron microscopy of phase-change material

Manuel Bornhöft^{1,2}, Tobias Saltzmann³, Julia Benke⁴, Paul M. Voyles⁵, Ulrich Simon^{3,6}, Matthias Wuttig^{4,6}, Joachim Mayer^{1,2,6}

1. Central Facility for Electron Microscopy, RWTH Aachen University, Germany
2. Ernst Ruska-Centre, Forschungszentrum Jülich GmbH, Germany
3. Institut für Anorganische Chemie, RWTH Aachen University, Germany
4. I. Physikalisches Institut (IA), RWTH Aachen University, Germany
5. Department of Materials Science and Engineering, University of Wisconsin, USA
6. JARA - Fundamentals of Future Information Technologies, RWTH Aachen University, Germany

email: bornhoeft@gfe.rwth-aachen.de

We investigated the phase-change materials Sb_2Te_3 by nano beam diffraction in a scanning transmission electron microscope (nano-diffraction in STEM) and $\text{Ag}_4\text{In}_3\text{Sb}_{67}\text{Te}_{26}$ by fluctuation electron microscopy (FEM). Both methods rely on illuminating the areas of interest of the sample by a small (probe size is around 2 nm) and almost parallel (convergence angle of 0.54 mrad) electron probe. This creates nano diffraction patterns with the spatial resolution of the probe size. We also extract information about the nanometer scale medium range atomic order (MRO) of amorphous materials by calculating the variance out of 500-1000 nano-diffraction patterns of amorphous material. This technique is called STEM-FEM [1]. The nano diffraction in STEM is used to identify crystalline regions of Sb_2Te_3 samples. The FEM is used to gather information about the MRO of $\text{Ag}_4\text{In}_3\text{Sb}_{67}\text{Te}_{26}$ samples. To help to understand the reaction mechanism of the wet chemical synthesis of hexagonal Sb_2Te_3 platelets, we investigated Sb_2Te_3 intermediates of the reaction with nano diffraction in STEM. By scanning the intermediates with the electron probe and collecting nano diffraction patterns at the same time, it is possible to identify the crystalline areas of the intermediate. The investigation by nano diffraction helped to reveal part of the reaction mechanism of Sb_2Te_3 platelets in the wet chemical synthesis [2]. These platelets would have promising application in memory applications or as model systems. A deeper understanding of the crystallization kinetics of $\text{Ag}_4\text{In}_3\text{Sb}_{67}\text{Te}_{26}$ is needed, because the crystallization speed is the limiting factor of the writing speed of possible phase change memory devices using $\text{Ag}_4\text{In}_3\text{Sb}_{67}\text{Te}_{26}$ [3]. The MRO of

the amorphous phase of $\text{Ag}_4\text{In}_3\text{Sb}_{67}\text{Te}_{26}$ could play an important role in the difference of crystallization speeds of as-deposited and melt-quenched $\text{Ag}_4\text{In}_3\text{Sb}_{67}\text{Te}_{26}$. The normalized variance is calculated by doing FEM in STEM in a STEM dedicated Titan.

References:

- [1] Voyles, P.M. and D.A. Muller, Fluctuation microscopy in the STEM, in Ultramicroscopy. 2002. p. 147-159.
- [2] Saltzmann, T., et al., Shape without Structure: An Intriguing Formation Mechanism in the Solvothermal Synthesis of the Phase-Change Material Sb_2Te_3 . *Angewandte Chemie International Edition*, 2015.
- [3] Salinga, M., et al., Measurement of crystal growth velocity in a melt-quenched phase-change material. *Nature Communications*, 2013. 4.

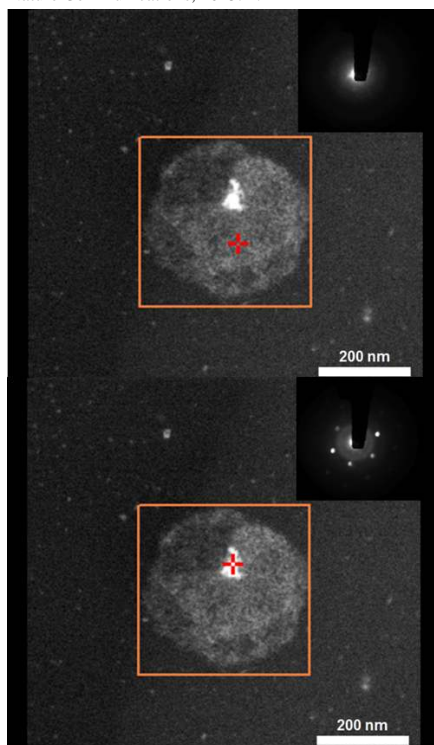


Figure 1. The boxes are marking the region scanned by nano-diffraction. The crosses are marking the actual positions of the electron probe. The nano-diffraction patterns shows, that the main body of the intermediate is amorphous. Only a small part of the bright core part of the intermediate is crystalline.

Keywords: Nano-diffraction, TEM, STEM, phase-change, FEM

MS13-P2 A new cubic phase in the Li-Mn-Ge-O system solved by 3D electron diffraction methods

Holger Klein^{1,2}, Christophe Lepoitevin^{1,2}, Stéphanie Kodjikian^{1,2}, Lei Ding^{1,2}, Claire V. Colin^{1,2}, Céline Darie^{1,2}, Pierre Bordet^{1,2}

1. Univ. Grenoble Alpes, Inst NEEL, F-38042 Grenoble, France
2. CNRS, Inst NEEL, F-38042 Grenoble, France

email: holger.klein@neel.cnrs.fr

Recently, research on quasi-one-dimensional magnetic and multiferroic materials has renewed the interest in pyroxenes of the stoichiometry AMX_2O_6 (A = alkali metal, M = transition metal, X = Si or Ge). In these phases the magnetic M^{3+} ions form chains and chemical substitution on the A and M sites can change the magnetic coupling along these chains making this system a rich field for the exploration of new phases of interesting magnetic properties [1]. In this work we report the discovery of a new phase in the Li-Mn-Ge-O system. A HP-HT solid state reaction was performed on a mixture of nominal stoichiometry $\text{LiMnGe}_2\text{O}_6$ during 1 h at a temperature of 850°C and a pressure of 3 GPa in a belt press. Powder X-ray diffraction yielded a diffractogram that could not be indexed by known phases of this system. An electron diffraction study in a transmission electron microscope was conducted in order to identify any unknown phases. In the case of structures that promise interesting properties a more targeted synthesis can then be undertaken. For the purpose of this work, we studied one of several unknown phases in the powder in more detail. From standard selected area electron diffraction the unit cell was determined to be cubic with cell parameter $a = 1.17$ nm. Precession electron diffraction, eliminating critical multiple diffraction effects, allowed determining the extinction conditions leading to space group $la\bar{3}d$. EDX analysis in the TEM showed a Mn/Ge ratio of 1/1, while the Li and O content could not be quantified. Intensities were recorded by in-zone axis precession electron diffraction and by electron diffraction tomography. Combining the data from both methods yielded the structure which we will present here with special attention to the determination of the Li in this phase.

[1] J. Cheng, W. Tian, J. Zhou et al., 2013, J. American Chem. Soc., 135, 2776-2786

Keywords: electron crystallography, structure determination, pyroxene

MS13-P3 A new fast method to derive Crystallite Size Distributions (CSD) from 2D X-ray diffraction data.

Sigmund H. Neher¹, Chaouachi Marwen¹, Falenty Andrzej¹, Klein Helmut¹, Werner F. Kuhs¹

1. Georg-August-University Göttingen

email: sneher@gwdg.de

We present our new method *fast diffraction CSD analysis* for deriving CSDs of polycrystalline materials or powders from 2D diffraction data. This analysis can be carried out with standard lab equipment as well as on synchrotron instruments equipped with a 2D detector. The typical range of application covers crystallite sizes from sub- μm (on synchrotron sources) to hundreds of μm .

We will present details of the measurement technique (1), the data reduction (2), the calibration and scaling (3) and (4) a generalized approach to the Lorentz correction, the beam profile correction and the absorption correction.

(1) For the CSD analysis an image sequence of a stepwise rotation measurement (ϕ or ω rotation) with a "spotty" diffraction patterns is needed. The rotational range is commonly a few degrees with a step size chosen as a fraction of the rocking curve. The appearance of each spot needs to be resolved in a sufficient number of images to evaluate its rocking curve. (2) Data reduction is done by a computer Program written in Python. Every spot is detected, isolated from other overlapping spots (if needed) and assigned to its appearance in consecutive frames. All integrated intensities form the Intensity Distribution (ID) of the sample. (3) For each analysis a standard material with known CSD needs to be measured under exactly the same conditions as the sample. With an established scaling factor between the known standard CSD and the measured standard ID and by using the ratio between the structure factors of sample and standard, the sample CSD can be calculated (see fig.). (4) To both, the sample ID and the standard ID, the Lorentz correction and a absorption correction are applied. In addition the IDs are deconvoluted with the lateral beam profile.

So far the method has been successfully tested with a Bruker APEX II CCD-detector using a laboratory X-ray source, at ESRF ID 15 in Grenoble using the PIXIUM 4700 and with the Perkin Elmer XRD 1622 at DESY Hamburg. For testing we use several well defined single crystal Corundum powder grain size fractions characterized with SEM imagery. A very satisfactory performance was achieved. Due to its speed, the method holds considerable promise also for in-situ studies of crystal growth, recrystallization and coarsening processes [1].

[1] M. Chaouachi et al., *In-situ* determination of the evolution of the crystallite size distributions of GH-bearing sediments using two-dimensional X-ray diffraction, this conference.

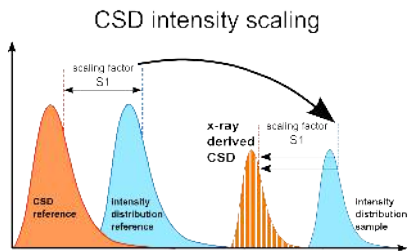


Figure 1. CSD intensity scaling: The scaling factor, S_1 , between the measured Intensity Distribution (ID) and the volume distribution (CSD) of the reference is used to derive the sample CSD from the measured sample ID.

Keywords: CSD, X-Ray, Crystallite Size Distribution

MS13-P4 Is it possible to collect reliable data on a laboratory diffractometer for a single crystal containing giant disordered supramolecules?

Eugenia V. Peresypkina^{1,2}, Alexander V. Virovets^{1,2}

1. University of Regensburg, Regensburg, Germany

2. Nikolaev Institute of Inorganic Chemistry SB RAS, Novosibirsk, Russia

email: peresyp@niic.nsc.ru

The advantages of the synchrotron radiation sources in diffraction studies are well-known. But laboratory diffractometers equipped with modern micro-focus X-ray tubes have their advantages, first of all, full-time availability that provides structure determination keeping pace with the ongoing chemical study, and enough space for laboratory equipment to manipulate samples. During last decade we systematically investigate structural chemistry of the compounds based on pentaphosphaferrocene, $[\text{Cp}^R\text{Fe}(\eta^5\text{-P}_5)]$ ($\text{Cp}^R = \eta^5\text{-C}_5\text{R}_5$, $\text{R} = \text{Me}, \text{CH}_2\text{Ph}$), and Cu^+ , Ag^+ (M^+) salts. Coordination of M^+ to P atoms of *cyclo*- P_5 rings results in various giant supramolecules containing dozens of heavy atoms confined by Cp^R ligands (Fig. 1) [1,2]. At that, inorganic core is often disordered resulting in weak high-angle reflections. The crystals usually demonstrate strong tendency for twinning and quick losing of solvent and, therefore, cannot be pre-selected in the lab before transporting to the synchrotron.

Our equipment allows us to keep a sample in the argon atmosphere and select the crystals at about -100°C . Using Agilent Technologies SuperNova diffractometer (CuK α micro-focus source, Titan^{S2} CCD detector) and single crystals with $V \sim 30\,000\text{ \AA}^3$ we systematically investigate how to measure weak intensities avoiding reflections overlap and how to improve the quality of diffraction data, the reliability of the structural model and quality factors by optimization of such factors as scan width, crystal-to-detector distance and detector mode, exposure time and redundancy. We use the results to tune the data collection strategies originally designed for small molecules and succeeded, for example, in the refinement of the crystal structures with following characteristics:

1: $a=61.88$, $b=68.87$, $c=69.66\text{ \AA}$, $V=296829\text{ \AA}^3$, $Fddd$, 370 unique non-H positions, $d>0.83\text{ \AA}$, $R_1=0.15$

2: $a=43.12$, $b=42.13$, $c=43.28\text{ \AA}$, $\beta=92.31^\circ$, $V=78555\text{ \AA}^3$, $C2/c$, 585 non-H's, $d>0.83\text{ \AA}$, $R_1=0.08$

3: $a=46.4$, $b=31.92$, $c=91.33\text{ \AA}$, $\beta=97.44^\circ$, $V=134142\text{ \AA}^3$, $C2/c$, 762 non-H's, $d>0.98\text{ \AA}$, $R_1=0.13$

[1] E. V. Peresypkina et al (2014), *Z. Kristallogr.*, **229**, 735, and references therein.

[2] F. Dielmann et al (2015), *Chem.-A Eur. J.*, DOI: 10.1002/chem.201500692.

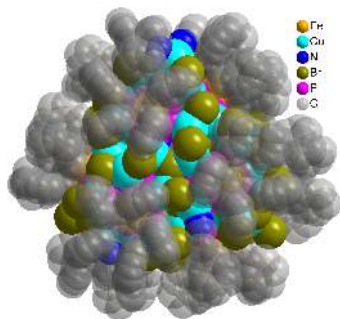


Figure 1. Supramolecule $[(\text{Cp}^{\text{Bn}}\text{Fe}(\eta^5\text{-P}_5))_{12}(\text{CuBr})_{51}(\text{MeCN})_8]$ in 1, H atoms are omitted for clarity.

Keywords: X-ray single-crystal diffraction, data collection strategies, model refinement, disorder, unstable crystals

MS13-P5 Automated data analysis for X-ray diffraction experiments in chemical crystallography

Markus Gerstel¹, David R. Allan¹, Alun W. Ashton¹, Paul V. Hathaway¹, Harriott Nowell¹, Sarah A. Barnett¹, Mark R. Warren¹, Graeme Winter¹

¹. Diamond Light Source, Harwell Science and Innovation Campus, Didcot, Oxfordshire OX11 0DE, England

email: markus.gerstel@diamond.ac.uk

In chemical crystallography the routine use of fully automated data reduction (Winter & McAuley, 2011) is not as widespread as in the closely related field of macromolecular crystallography (MX). Data processing times are not crucial for data collection on laboratory sources and did not constitute the rate-limiting step for collections at the two dedicated small-molecule synchrotron beamlines worldwide. As data collection times decrease through advances in detector technology, processing times become more important.

Here we present the current progress in adapting and extending MX data analysis and reduction software to chemical crystallography applications, and implementing these in an automated data processing pipeline at the dedicated chemical crystallography beamline I19 at the Diamond Light Source (Nowell *et al.*, 2012). The beamline will, following an extensive hardware and software upgrade later this year, be equipped with a Pilatus 2M pixel-array detector. The concomitant reduction in data collection time and the expected increase in the volume of data collected necessitates a greater level of automation in terms of data processing and reduction. To achieve this goal MX software, such as GDA (General Data Acquisition framework; Gibbons *et al.*, 2011) used for data collection at DLS, the data reduction expert system xia2 (Winter, 2010) and the Diffraction Integration for Advanced Light Sources (DIALS) software suite, are modified and extended to accommodate chemical crystallography requirements.

In chemical crystallography data are commonly collected using spherical or hemispherical data collection strategies, which are comprised of multiple sweeps based on the rotation method. In the proposed setup the auto-indexing solutions are continually refined throughout data acquisition, and, based on the relevant current indexing solution and hitherto collected data, further data collection strategies are evaluated using DIALS, and subsequently proposed to the experimenter.

Diffraction data are processed in the background using xia2 and DIALS, which both run as modules in the Computational Crystallography Toolbox (cctbx; Grosse-Kunstleve *et al.*, 2002).

Gibbons, E.P., *et al.*, *Proceedings of the ICALEPCS* (2011). 529–532.

Grosse-Kunstleve, Ralf W., *et al.*, *J. Appl. Cryst.* (2002). **35**.1, 126–136.

Nowell, H., *et al.*, *J. Synchrotron Rad.* (2012). **19**, 435–441.

Winter, G., *J. Appl. Cryst.* (2010). **43**, 186–190.

Winter, G. and McAuley, K.E., *Methods* (2011). **55**, 81–93.

Keywords: chemical crystallography, data reduction, automation

MS13-P6 Measuring the magnitude and sign of the effective piezoelectric coefficient by mechanical impact method

Svetlana Roshchenko¹, Konstantin Zakutailov²

1. PhD student, National University of Science and Technology "Moscow Institute of Steel and Alloys"

2. Docent, National University of Science and Technology "MISIS"

email: rsn33@bk.ru

Method of impact action allows determining magnitude and sign of the effective piezoelectric coefficient not only for thin films [1], but for the bulk piezoelectric materials too. Feature of the method is the possibility of its use in technological terms, which allows sorting piezoelectric plates and greatly reduce production costs in the manufacture of piezoelectric devices.

This new express method consists in the application of shock pulse exposure to the sample and removing the piezoelectric response signal using an oscilloscope. Sign of the effective piezoelectric coefficient is determined with the polarity of the signal electric response, and its amplitude and impact force allow calculating the value of the effective piezoelectric coefficient of mechanical impact. Vertical impact is controlled with a calibration system using the value of acceleration in the plane perpendicular to the direction of impact.

In practice, the value of the effective piezoelectric coefficient is required, i.e. the superposition of piezoelectric coefficients of the material taken in a definite relation to each other, depending on the orientation of the crystal. Mean values of the effective piezoelectric coefficients most commonly used crystals and the size of their standard deviations were calculated, which are the basic parameters in obtaining reliable experimental values by the method of mechanical impact.

For testing the method, X-cut quartz, Y-cut LiNbO₃ and a 127.86°Y- LiNbO₃ plate samples with the well-known theoretical values were taken. Measurements were conducted in a experimental setup several times for each sample.

Dependence of the effective piezoelectric coefficient on the ratio of Li to Nb is theoretically calculated for 127.86°Y-LiNbO₃ plate. Measurement of the effective piezoelectric coefficient and its theoretical dependence on the composition of lithium niobate enables to estimate the ratio of Li to Nb, that is equal to 49.5 mol. % of Li₂O for our specimen. Measurements of the effective piezoelectric coefficients proposed method and its calculation results showed good agreement with the calculated values of measurements according to the literature.

[1] Guo Q., Cao G.Z., Shen I.Y. "Measurements of piezoelectric coefficient d_{33} of Lead Zirconate Titanate thin films Using a Mini Force Hammer." Journal of Vibration and Acoustics 135 (2013): n. pag. Print.

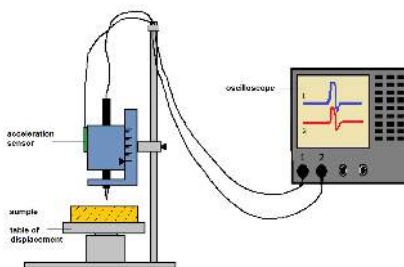


Figure 1. Scheme of setup for measuring the effective piezoelectric coefficient by mechanical impact method

Keywords: effective piezoelectric coefficient, piezoelectricity, impact force, lithium niobate, quartz

MS14. Mineralogical crystallography: Nature as a source of inspiration for new materials

Chairs: Nikolai Eremin, Rossella Arletti

MS14-P1 Crystal branching phenomena in calcite as a consequence of anisotropic impurity incorporation at nonequivalent step type geometries?

Felix Wiethoff¹, Jürgen Schreuer¹

¹ Ruhr-University Bochum, Institute of Geology, Mineralogy and Geophysics

email: felix.wiethoff@rub.de

The growth behavior of calcite at different physico-chemical conditions is due to its abundance in natural (biogenic and abiogenic) and artificial (e.g. hot water pipelines) systems of general interest. Since the first AFM investigations on {104} calcite growth hillocks it is known that incorporation of Mg^{2+} as an impurity in the $CaCO_3$ system is distributed unequally at different step type geometries (obtuse and acute) of the growth spiral [1]. This results in different sectors of Mg^{2+} enrichment known as sector zoning [2].

Due to the high resolution and short observation period in AFM experiments only the starting conditions of impurity influenced crystal growth behavior was studied in detail but long term consequences on the macroscopic scale were neglected.

We observed in Mg^{2+} containing gel based calcite growth experiments (duration of 2 months) pronounced crystal branching phenomena and complex pathological morphologies. From optical microscopy and EBSD pole-figures we derived that the branched sub-units are not parallel to their substrate resulting in systematic undulous extinction behavior in cross polarized light. We assume that impurity incorporation is the principal cause for the establishment of an ordered dislocation network which is responsible for this tilted sub-units.

Beside growth striation due to diffusion controlled transport mechanism in the porous medium and the negative distribution coefficient of Mg^{2+} in calcite [3] we suggest that the kink type selective incorporation at nonequivalent steps is responsible for such a strain induced branching process.

These observations explain potentially the long known undulous optical extinction behavior of Mg-Calclites known as radiaxial fibrous calcites (RFC) and fascicular optic fibrous calcites (FOFC), respectively [4].

References:

- [1] Davis, K.J., Dove, P.M., Wasylenki, L.E., de Yoreo, J.J.: *Morphological consequences of differential Mg^{2+} incorporation at structural distinct steps on calcite*. Am. Min. **89** (2004) 714-720
- [2] Reeder, R.J., Paquette, J.: Sector zoning in natural and synthetic calcites. Sediment. Geol. **65** (1989) 239-247
- [3] Rimstidt, J.D., Balog, A. and Webb, J.: *Distribution of trace elements between carbonate minerals and aqueous solutions*. Geochim. Cosmochim. Ac. **62** (1998) 1851-1863
- [4] Richter, D. K., Neuser, R. D., Schreuer, J., Gies, H. and Immenhauser, A.: *Radial-fibrous calcites: A new look at an old problem*. Sediment. Geol. **239** (2011) 23-36

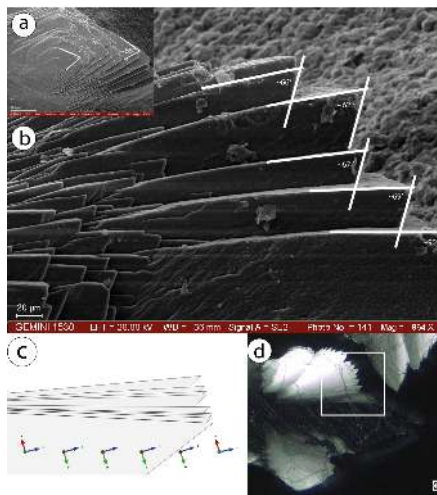


Figure 1. a) Crystal branching phenomenon of an in gel grown calcite crystal. b) Same crystal-type tilted by 90°. c) Set of slightly tilted {102} rhombohedra resemble the observed growth morphology as in b). d) Thin section seen with crossed polarizers. Note the distinct growth segments and undulosity.

Keywords: Calcite, Crystal branching, Undulosity, Dislocations

MS14-P2 The crystal structure of a davidite related ternary oxide $\text{La}_{1.78}\text{Mn}_{6.6}\text{Ti}_{13.62}\text{O}_{38}$ Amalija Golobič¹, Maja Vidmar¹, Srečo D. Skopin², Danilo Suvorov², Anton Meden¹¹ University of Ljubljana, Faculty of Chemistry and Chemical Technology, Večna pot 113, 1000 Ljubljana, Slovenia² Jožef Stefan Institute, Jamova 39, 1000 Ljubljana, Slovenia

email: amalija.golobic@fkkt.uni-lj.si

The title compound is a new ternary oxide in the $\text{La}_2\text{O}_3\text{-Mn}_2\text{O}_3\text{-TiO}_2$ pseudo-ternary system. It was synthesized by wet precipitation technique using manganese (III) oxide and lanthanum nitrate diluted in citric acid and the water solution of titanium (IV) isopropoxide. The product was calcined at 750°C in air and sintered at 1100°C for 20 h. After the heat treatment, the sample was cooled by quenching to room temperature. The formula of the obtained single phase product is $\text{La}_{1.78}\text{Mn}_{6.6}\text{Ti}_{13.62}\text{O}_{38}$, which is in accordance to the synthetic ratio of metals and supported by scanning electron microscopy (SEM) using wavelength-dispersive (WDS) and energy-dispersive spectroscopy (EDS). The compound is isostructural with naturally occurring crichtonite group minerals, which crystallize in trigonal system in $R\bar{3}$ space group. It conforms to the general formulae AM_2O_{38} , where A is occupied by a large cation: Ca, Sr, xRb, K, Na and rare-earth elements – RE. The minerals with RE on A site are called davidites.

The X-ray powder diffraction pattern was collected on a PANalytical X'Pert PRO MPD diffractometer in reflection geometry using $\text{CuK}\alpha_1$ in range from 10° to 120° 2 θ . Crystal structure was determined using Rietveld method incorporated in TOPAS-Academic program taking a structure of $\text{Ca}_2\text{Zn}_2\text{Ti}_2\text{O}_{38}$ [1] as a starting model. The Ca^{2+} on cuboctahedral site A, surrounded by 12 O^{2-} anions, is replaced by La^{3+} . The Ca^{2+} on octahedral M(1) site is replaced by La^{3+} and Mn^{2+} (La/Mn)2. Mn^{2+} is additionally disposed over tetrahedral site M(2) (instead of Zn^{2+} , Mn3), while the rest of Mn^{2+} is sharing the octahedral M(3) site with Mn^{2+} and Ti^{4+} (Ti/Mn)1. Sites M(4) and M(5) are fully occupied by Ti^{4+} (Ti2, Ti3). Sites A and M(1) lie on 3-fold rotoinversion axis, M(2) lies on 3-fold axis, M(3), M(4) and M(5) lie on general positions. $a=9.28107(7)$ Å, $c=68.4560(5)$ Å, $V=666.237(15)$ Å³, 34 structural and 9 profile parameters, $R=2.82$, $R_p=3.56$, $R_w=16.80$, $R_{wp}=12.75$.

[1] Gatehouse, B. & Grey, I. J. *Solid State Chem.* **46**, 151–155 (1983).

Financial support of the Ministry of Education, Science and Sport of the Republic of Slovenia is gratefully acknowledged (grants P1-0175, P2-0091, MR-33158).

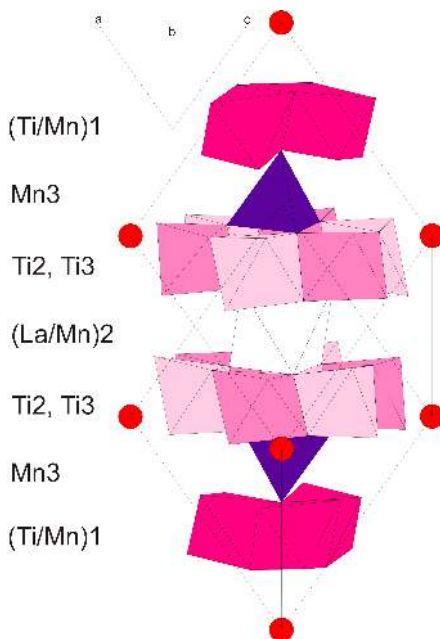


Figure 1. Unit cell of title compound extended to complete polyhedra.

Keywords: powder diffraction, ternary oxide, ceramics, davidite, Rietveld refinement.

MS14-P3 High-temperature behaviour of astrophyllite and magnesioastrophyllite from Khibiny massif (Kola peninsula, Russia)Elena S. Zhitova¹, Maria G. Krzhizhanovskaya¹, Sergey V. Krivovichev^{1,2}, Victor N. Yakovenchuk²1. Saint Petersburg State University
2. Nanomaterials research Centre, KSC, RAS

email: zhitova_es@mail.ru

The thermal behaviour of natural astrophyllite and magnesioastrophyllite (Khibiny massif, Kola peninsula, Russia) was studied using in situ high-temperature XRD in the range 25-1000 °C by means of Rigaku Ultima IV powder X-ray diffractometer (CuK α) with a high-temperature camera. The first reflections of new high-temperature phase were detected at 500 °C and 550 °C for astrophyllite and magnesioastrophyllite, respectively. Peaks of new phase were shifted in the high-angle region. Reflections of both, initial minerals and its high-temperature phase presented in the diffraction pattern at the temperature of the phase transition. In the temperature range 525- 775 °C only high-temperature phase remained. Both minerals decompose at 775 °C. Single crystal X-ray diffraction of astrophyllite was carried out for both phases using single-crystal diffractometer Bruker APEX II, MoK α . Unit cell parameters of original astrophyllite are $a = 5.3752(1)$, $b = 11.8956(3)$, $c = 11.6554(3)$ Å, $\alpha = 113.157(2)$, $\beta = 94.530(2)$, $\gamma = 103.112(2)$ °, $V = 655.47(3)$ Å³. Unit cell parameters of high-temperature phase are $a = 5.3287(4)$, $b = 11.790(1)$, $c = 11.4332(9)$ Å, $\alpha = 112.530(8)$, $\beta = 94.539(6)$, $\gamma = 103.683(7)$ °, $V = 633.01(9)$ Å³. Thermal behaviour of studied material changes from thermal expansion for initial phases to contraction for high-temperature phases. The decrease of the unit-cell parameters is probably the result of change of oxidation of iron that leads to the shortening of the Fe-O bond lengths.

The XRD studies have been performed at the X-ray Diffraction Centre of St. Petersburg State University.

This work was supported by the Russian Foundation for Basic Research (project no.14-05-31229), StSPbU internal grant № 3.37.222.2015 and the President of Russian Federation Grant for Young Candidates of Sciences (to AAZ, grant MK-3296.2015.5).

Keywords: thermal behaviour of natural layered titanosilicates, Kola alkaline massifs, astrophyllite

MS14-P4 Synthesis, structure and low temperature behaviour of Sidorenkite/Bonshtedtite-like sodium carbonophosphates containing Ni(II), Fe(II) and Mn(II)Sephira Riva¹, Serena Margadonna¹

1. College of Engineering, Swansea University, SA2 8PP Swansea, UK

email: 839245@swansea.ac.uk

Recent predictions highlighted the promising features of sidorenkite ($Na,Mn(PO_3)(CO_3)$)- and bonshtedtite ($Na,Fe(PO_3)(CO_3)$)-like compounds for the development of new, low cost, Na-based batteries. These materials are characterized by high theoretical specific energy and stability at air exposure; moreover, they can undergo reversible Na-ion intercalation/de-intercalation by changing the oxidation state of the central transition metal.

$Na_3M(PO_3)(CO_3)$ [$M=Ni, Mn, Fe$] were synthesised via hydrothermal synthesis. Temperature, starting concentrations, reaction time and stirring were modulated to obtain pure samples.

Compounds were characterised using synchrotron radiation (ID31 at the ESRF), with temperature ranging from 10K to 290K. Data were collected in transmission mode by using 0.5mm glass capillaries and scanning from 0 to 30 2 θ ($\lambda=0.39992$ Å).

Crystals were found to have monoclinic sidorenkite structure (P2₁/m). Each cell unit consists of a transition metal octahedron sharing four vertices with the tetrahedral PO_4 group and an edge with the CO_3 group. The connection of transition metal octahedra, PO_4 tetrahedra and planar CO_3 groups create a two-dimensional subunit, which extends along the [1 0 0] plane. Sodium ions occupy two distinct interstitial positions between the double layers formed by tetrahedral PO_4 groups and MO_6 octahedra. These sites are coordinated by 7 (multiplicity 2) and 6 (multiplicity 4) oxygen atoms.

The dependence of cell volume and interatomic distances from temperature was quantified from cell parameters variations (a , b and c lattice parameters; β angle). The carbonophosphates structure was proven extremely stable, with no phase transitions occurring in the selected temperature region.

Magnetic properties tests highlighted the anti-ferromagnetic behaviour of Ni, Mn, and Fe carbonophosphates; as well as the existence of several magnetic transitions at temperatures lower than 10K.

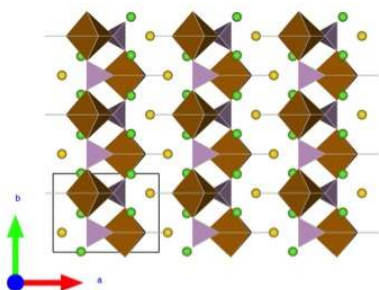


Figure 1. Structure of $\text{Na}_4\text{Fe}(\text{PO}_3)_4(\text{CO}_3)$ (bonshtedtite) viewed along $[0\ 0\ 1]$ plane. Fe^{3+} octahedra and PO_4 tetrahedra are highlighted in brown and purple respectively. Na atoms occupying sites of multiplicity 2 (green) and 4 (yellow) are displayed. Oxygen atoms are hidden for clarity.

Keywords: Carbonophosphates, Low-temperature crystallography, SQUID

MS14-P5 Temperature and pressure induced phase transitions in chevkinite group. A joint XRD, XPS and EPMA structural studies

Marcin Stachowicz¹, Krzysztof Woźniak¹, Bogusław Bagiński², Ray Macdonald²

1. Biological and Chemical Research Centre, Chemistry Department, University of Warsaw, Żwirki i Wigury 101, 02-089 Warsaw, Poland

2. Institute of Mineralogy, Geochemistry and Petrology, University of Warsaw, 02-089, al. Żwirki i Wigury 93, Warsaw, Poland

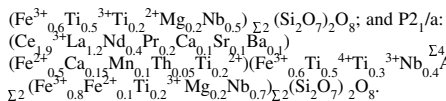
email: marcin.stachowicz@chem.uw.edu.pl

The chevkinite group of minerals (chevkinites and perrierites) are increasingly being recognized as accessory phases in a wide range of igneous and metamorphic rocks. The general formula for the most common members of the group, is $\text{A}_4\text{BC}_2\text{D}_2(\text{Si}_2\text{O}_7)_2\text{O}_8$, where the most common cations are $\text{A} = \text{Ca}^{2+}$, REE^{3+} , Sr^{2+} , Th^{4+} ; B , C , $\text{D} = \text{Fe}^{2+}$, Fe^{3+} , Ti^{4+} , Al^{3+} , Mn^{2+} , Mg^{2+} . Annealing at 750°C of niobian chevkinite-(Ce) single crystal from the Biraya rare-metal deposit (Russia) resulted in a phase transition from the space group C2/m to $\text{P2}_1/\text{a}$. This may be of particular interest for researchers dealing with metamict minerals because annealing may lead to a slightly different crystal structure from the initial one, additionally a migration of cations to different crystallographic sites was observed during annealing. To confirm the new findings, next X-ray measurements on different unannealed and annealed crystals were performed.

A reversed effect of a phase transition was monitored on a single crystal of perrierite from Nettuno, Italy loaded into the diamond anvil cell. The compressibility of this mineral was analysed on the basis of fourteen X-ray diffraction (XRD) experiments from ambient pressure up to 6.4 GPa.

X-ray photoelectron spectroscopy (XPS) can give valuable results in the investigation of element valency especially when the amount of sample is insufficient for Mössbauer spectroscopy. This method can give information on any element and oxidation state, as long as the characteristic spectra for different ions are separated. This could provide crucial independent information allowing the establishment of the correct crystal structures of complex minerals. In Nb-bearing chevkinite-(Ce) iron is present as Fe^{2+} and Fe^{3+} and Ti is present as Ti^{4+} , Ti^{3+} and possibly Ti^{2+} . With this information the volumes of the first coordination spheres could be matched with the ionic radii of elements and their masses with site scattering factors in the analyzed crystal structures to obtain the most probable allocation of cations.

Empirical formulae for niobian chevkinite-(Ce) was established by joined XRD, XPS and EPMA analyses for C2/m : $(\text{Ce}_{1.9}^{3+}\text{La}_{1.2}\text{Nd}_{0.4}\text{Pr}_{0.2}\text{Ca}_{0.1}\text{Sr}_{0.1}\text{Ba}_{0.1})_{\Sigma 4}(\text{Fe}_{2.0}^{2+}\text{Ca}_{0.15}\text{Mn}_{0.1}\text{Th}_{0.05})_{\Sigma 2}(\text{Fe}_{0.7}^{3+}\text{Ti}_{0.5}^{4+}\text{Nb}_{0.6}\text{Al}_{0.1}\text{V}_{0.1})_{\Sigma 2}$



Keywords: Chevkinite group, composition, phase transition, oxidation state, high pressure, annealing

MS14-P6 Characterization of Mn octahedral molecular sieves by electron diffraction and Rietveld refinement

Enrico Mugnaioli¹, Enrico Mugnaioli¹, Michael Gregorkiewicz¹, Mauro Gemmi², Marco Merlini³

1. Dipartimento di Scienze Fisiche, della Terra e dell'Ambiente, Università degli Studi di Siena, Siena, Italy
2. Center for Nanotechnology Innovation@NEST, Istituto Italiano di Tecnologia, Pisa, Italy
3. Dipartimento di Scienze della Terra 'A. Desi o', Università degli Studi di Milano, Milan, Italy

email: enrico.mugnaioli@unisi.it

Manganese is an extremely versatile element due to its multiple oxidation states. Tunneled octahedral manganese oxides are found in nature as alteration products in mineralized rocks. Their structures are characterized by channels walled by edge-sharing MnO_6 octahedra and hosting different ionic species (Na, K, Ba...). Small differences in manganese oxidation state are associated with a wide structural variety of framework connectivity and pore sizes [1].

Tunneled manganese oxides belong to the group of octahedral molecular sieves (OMS), due to their open framework structures recalling the better-known tetrahedral molecular sieves, i.e. zeolites. In the last years OMS raised an increasing interest for their electronic properties. While tetrahedral frameworks are typically electronic insulators, OMS are mixed electronic/ionic conductors. The octahedrally coordinated elements in OMS frameworks have easily accessible $3d$ orbitals. Oxidation state and band gap are structurally related and depend on position and coordination of the extra-framework ions. Manganese tunneled oxides find advanced applications in gas sensing, heterogeneous catalysis, batteries and supercapacitors [2]. Moreover, manganese OMS exhibit electric and magnetic transitions at relatively high temperatures and show a superconductive behavior connected with charge-ordering of framework and extra-framework atoms [3].

A systematic structure characterization of manganese OMS is hampered by difficulty in growing single crystals and achieving pure synthetic products. In this contribution we present the structure investigation of several natural and synthetic manganese OMS, combining X-ray powder diffraction, transmission electron microscopy and electron diffraction tomography [4]. The frameworks of unknown structures were determined ab-initio by direct methods, and extra-framework ion positions were identified during structure refinement. Intermediate phases occurring during the synthesis were tracked by thermal analysis and structurally characterized. Finally, order-disorder transitions of extra-framework atoms, eventually associated with superstructure modulations, were investigated by cryo-controlled experiments.

[1] Pasero, M. (2005). *Rev. Mineral. Geochem.* **57**, 291–305.

[2] Wei, W. *et al.* (2011). *Chem. Soc. Rev.* **40**, 1697–1721.

[3] Sato, H. *et al.* (1999). *Phys. Rev. B* **20**, 12836–12841.

[4] Mugnaioli, E. *et al.* (2009). *Ultramicroscopy* **109**, 758–765.

Keywords: manganese oxide, Rietveld refinement, electron diffraction, phase transition

MS14-P7 Size-controlled synthesis of a mordenite type zeolite from organic template free initial gel

Yuri A. Kalvachev¹, Totka D. Todorova¹

¹. Institute of Mineralogy and Crystallography, Bulgarian Academy of Sciences

email: kalvachev@clmc.bas.bg

One of the widely used zeolite minerals mordenite has chemical formula $\text{Na}_2(\text{H}_2\text{O})_{24}[\text{Al}_8\text{Si}_{40}\text{O}_{96}]$. Its structure is characterized by 12-membered and 8-membered rings running along the c axis, and another 8-membered rings running along the b axis; these channels accommodate extraframework cations and water molecules. The mineral, especially synthetic varieties, has many industrial applications such as isomerization catalysts. The structure has an orthorhombic unit cell ($a = 18.1 \text{ \AA}$, $b = 20.5 \text{ \AA}$, and $c = 7.5 \text{ \AA}$) with topological space group symmetry Cmcn.

This study reports on the hydrothermal synthesis of mordenite crystals without an organic template and on the characterization of resulting crystals, as the ultimate goal has been to decrease the crystal size. Two synthesis approaches have been applied. The first one involved subjecting a standard initial gel $18\text{SiO}_2 : \text{Al}_2\text{O}_3 : 1.24\text{K}_2\text{O} : 1.21\text{Na}_2\text{O} : x\text{H}_2\text{O}$ to hydrothermal crystallization for a period of 2 to 7 days ($x=600, 280$ and 22.5). The second approach included the usage of seeds employing the same initial gel composition. The crystals growth kinetics of mordenite at a different seed content (1, 2 and 5 wt. %) has been studied. The seed-assisted process enabled us to synthesize mordenite crystals of submicrometric range. Particle size distribution of the resulting products strongly depends on the water content in the initial gel and on the amount of added seed. It has been found that seed concentration and water content in the initial gel are the key factors influencing the crystallization time and the physicochemical properties of crystalline products. Six hours is the shortest time in which zeolite mordenite with high crystallinity is obtained.

Acknowledgments. The authors acknowledge the financial support from the operational programme ‘Human Resources Development’ within project BG051PO001-3.3-06-0027.

Keywords: Nanozeolites, Mordenite, Hydrothermal synthesis, Seed-mediated synthesis

MS14-P8 Seed-mediated synthesis of nanosized crystals of Beta zeoliteBorislav Z. Barbov¹, Yuri A. Kalvachev¹

1. Institute of Mineralogy and Crystallography, Bulgarian Academy of Sciences

email: barbov@imc.bas.bg

The high industrial interest to zeolite Beta originates from the broad Si/Al range in zeolite Beta ($5 - \infty$) and its particular structure, being an intergrowth of different polymorphs and therefore being disordered in one dimension. The combination of three-dimensional pore architecture composed of intersecting 12-ring channels with strong acid sites makes this zeolite useful catalyst in a number of processes - such as catalytic cracking, hydroisomerisation, alkylation of aromatics, and esterification reactions, *etc.* In order to obtain nanosized crystals of zeolite Beta hydrothermal seed-induced synthesis is performed. Nanosized zeolites are important in catalytic and adsorptive applications. Smaller crystals of zeolites have larger surface areas and less diffusion limitations compared to zeolites with micrometer-sized crystals. During the synthesis two types of seeds are used - crystal seeds and mother liquor. Seed-induced synthesis by using of mother liquor as seeds leads to high yield of zeolite crystals. Crystal growth kinetics of the material as a function of seed content, type of seeds and Si/Al ratio of the initial gel are studied. After the optimization of crystallization conditions a highly crystalline material with crystal size 100–200 nm is synthesized. The obtained crystals were characterized by X-ray diffraction, scanning electron microscope, thermogravimetric analysis, and infrared spectroscopy.

Acknowledgments. The authors acknowledge the financial support from the operational programme “Human Resources Development” within project BG051PO001-3.3-06 - 0027.

Keywords: Nanozoelites, Zeolite Beta, Seed-assisted synthesis

MS14-P9 RbMnPO₄ Zeolite-ABW-Type Material: a new multiferroic mineral related materialS. Prugovecki¹, G. Nénert¹, L. Lin², R. Kremer³, H. Ben Yahia⁴, C. Ritter⁵, E. Gaudin⁴, O. Isnard⁶

1. PANalytical B. V., Lelyweg 1, 7602 EA Almelo, The Netherlands

2. Department of Physics, Southeast University, Nanjing 211189, China

3. Max Planck Institut für Festkörperforschung, Heisenbergstrasse 1, D-70569 Stuttgart, Germany

4. Institut de Chimie de la Matière Condensée de Bordeaux (ICMCB), UPR 9048-CNRS, Université, Bordeaux 1, 87, Av Dr. Schweitzer, 33608 Pessac Cedex, France

5. Institut Laue Langevin, Diffraction Group BP 156, 6 rue Jules Horowitz, F-38042 Grenoble Cedex 9, France

6. Institut Néel, CNRS/Université Joseph Fourier, 25 rue des martyrs, BP 166, 38042 Grenoble, France

email: stjepan.prugovecki@panalytical.com

The relation between crystal structure and properties of minerals and mineral-related materials is the key for technological benefit. A revival of the investigation of minerals related materials by the physicists and chemists took place in the recent years due to raising interest in multiferroic and magnetoelectric materials. Magnetoelectric materials are particularly of interest as one can control their magnetic properties by the application of an electric field and vice-versa. On the other hand, minerals have been a large source of materials for magnetoelectric compounds. Families like triphylite (LiMPO₄, M = Co, Fe, Ni) [1], boracites (M₃B₃O₁₃X, M = transition metal ion, Mg, Cd; X = halogen, OH, F or NO₃) [2] or pyroxenes AMX₂O₆ (A = Li, Na, Ca; M = transition metal ion; X = Si, Ge) have been widely investigated due to their magnetoelectric and multiferroic properties [3]. Here, we report on the magnetic and dielectric properties of a zeolite-ABW-type material, namely RbMnPO₄ [4,5]. This material exhibits a complex and rich phase diagram as function of temperature as illustrated in Figure 1. This system exhibits 5 different phases as function of temperature ($T_1 = 4.7$ K, $T_2 = 5.1$ K, $T_3 = 175^\circ\text{C}$, $T_4 = 260^\circ\text{C}$) with complex interplay between physical and crystallographic properties.

[1] I. Kornev, et al., Phys. Rev. B 62, 12247 (2000); Jiying Li, et al., Phys. Rev. B 79, 144410 (2009); J.-P. Rivera, Ferroelectrics 161, 147 (1994); D. Vaknin, et al., Phys. Rev. B 65, 224414 (2002); D. Vaknin, J. L. Zarestky, J.-P. Rivera, and H. Schmid, Phys. Rev. Lett. 92, 207201 (2004); A. Scaramucci, E. Bousquet, M. Fechner, M. Mostovoy, and N. A. Spaldin, Phys. Rev. Lett. 109, 197203 (2012).

[2] R. Nelmès; J. Phys. C: Solid State Phys., 7, 3840-3854 (1974).

[3] S. Jodlauk, et al., J. Phys.: Condens. Matter 19 432201 (2007); G. Nénert, et al., Phys. Rev. B 79, 064416 (2009); G. Nénert, et al., Phys. Rev. B 81, 184408 (2010); G. Nénert, et al., Phys. Rev. B. 82, 024429 (2010).

[4] G. Nénert et al., Inorg. Chem. 2013, 52, 9627–9635

[5] G. Nénert et al., in preparation

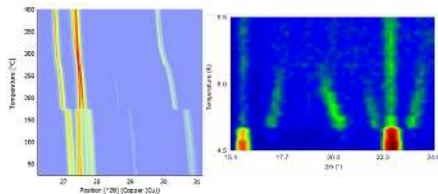


Figure 1. Temperature dependence above room temperature (left) and at low temperature (right) of RbMnPO₄, demonstrating the existence of 5 different phases in the explored temperature range.

Keywords: multiferroic, phase transition, magnetoelectric

MS14-P10 Enamel microstructure and tooth embryonic development

Anna Kallistová^{1,2}, Ivan Horáček³, Petr Čejchan², Roman Skála^{1,2}

1. Institute of Geochemistry, Mineralogy and Mineral Resources, Faculty of Science, Charles University, Albertov 2, Prague 2, Czech Republic.

2. Institute of Geology, Czech Academy of Sciences, v.v.i., Rozvojová 269, Prague 6, Czech Republic.

3. Department of Zoology, Faculty of Science, Charles University, Viničná 7, Prague 2, Czech Republic.

email: kallistova@gli.cas.cz

INTRODUCTION

Tooth enamel is one of the most resistant inorganic components in the mammalian bodies that significantly affect both quality and life expectancy of an individual; it depends on the mutual arrangement of aggregates of the hydroxyapatite crystallites (Koenigswald & Clemens, 1992) and their characteristic properties. While the organization of aggregates is controlled by cooperation of cellular activity (ameloblasts) and pre-existing organic matrix (Boskey, 2007), the influence of Hap crystallites properties on the enamel quality has not been studied in detail up to now. In the present study we focus on the microstructure (i.e. crystallite size, micro-strain) of Hap of the laboratory minipig molars with different lengths of embryonic development stage and its implications for the final quality of the enamel.

MATERIALS, METHODS

Samples from 20 minipigs (aged 16 - 108 mths) were studied. First, second and third molar of each individual were used to obtain teeth with the same dental function but with different length of embryonic development.

RESULTS

While the crystallite size at 1₁₁/1₁ direction increases from M₁ to M₃ for all samples studied, the micro-strain shows an opposite trend (Fig. 1). The prolonged period of M₃ molar formation leads to enamel with lowest degree of lattice imperfection and, hence, arguably yields tooth with highest resistance to both mechanical and chemical damage and can perform its function for a long time period to ensure an adequate nutrition. Moreover, by comparing the young and old individuals, we showed that the enamel microstructure of individual molar types is time invariant.

CONCLUSIONS

In the present study we showed that the effect of mechanical abrasion and/or the chemical degradation caused by the oral environment (hence the subject's age) on the microstructure can be excluded. We also demonstrated that the length of the tooth's embryonic development stage has a positive effect on the quality of its enamel.

REFERENCES

Boskey, A. L. (2007). Mineralization of bones and teeth. *Elements*, 3, 385-391. Koenigswald, W. von and Clemens, W. A. (1992). Levels of complexity in the microstructure of mammalian enamel and their application in studies of systematics. *Scan. Micr.*, 6, 195-218.

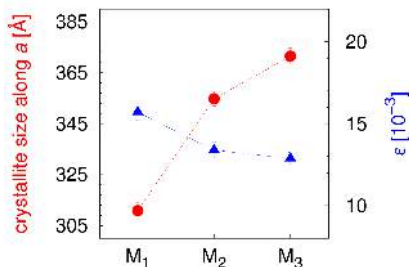


Figure 1. Crystallite size along *a* axis (red circles, left ordinate) and micro-strain (blue triangles, right ordinate) of various molar types. Crystallite size along the direction of *c* axis shows analogues behavior.

Keywords: crystallite size, micro-strain, enamel development

MS14-P11 High-temperature, high-pressure hydrothermal synthesis of uranium silicates and germanates

Kwang-Hwa Lii¹

¹. Department of Chemistry, National Central University, Zhongli, Taiwan

email: liikh@cc.ncu.edu.tw

Most uranium minerals can be classified as oxidized species in which U is fully oxidized to U⁶⁺, and reduced species, in which U occurs primarily as U⁴⁺. Uranyl silicates are an important group of U(VI) minerals in the altered zones of many uranium deposits.¹ One naturally occurring U(IV) silicate exists, namely coffinite (USiO₄), which is an important ore mineral for uranium. Numerous synthetic U(VI) silicates and germanates containing organic amines or alkali metals as counterions have also been reported.² In contrast to the U(VI) compounds, the chemistry of materials containing U(V) is considerably less developed owing to the tendency of U⁵⁺ to either oxidize to U⁶⁺ or disproportionate to U⁴⁺ and U⁶⁺. We have synthesized a U(V) silicate and a germanate by a high-T, high-P hydrothermal method in gold ampoules contained in a high-pressure reaction vessel at ca. 600 °C and 170 MPa.^{3a,3b} Following the synthesis of the U(V) compound, a number of mixed-valence uranium silicates and germanates have been synthesized, for example, a mixed-valence U(IV,V) silicate, Cs₃K(UO)₂Si₃O₁₀^{3c} U(IV,V) germanate, Cs₃U(UO₂)(Ge₂O₇)₃H₂O^{3d} U(V,V) germanates, A₃(U₂O₄)Ge₂O₇ (A³⁺ = Rb, Cs),^{3e} and a U(IV,V,V) silicate, Na₂U^{IV}O₂(U^VO₂)₂(U^{V/VI}O₂)₂Si₄O₁₆,^{3f} in which three oxidation states of uranium co-exist in one compound. In addition, tetravalent-uranium compounds, Cs₃USi₃O₁₅ and Cs₃UGe₈O₃₀^{3g,3h} were also synthesized. All members in the family of uranium silicates and germanates with the oxidation states of uranium from +4 to +6 have been observed.

References

- (a) Burns, P. C. *Rev. Mineral.* 1999, 38, 23-90. (b) Finch, R. J.; Murakami, T. *Rev. Mineral.* 1999, 38, 24-179.
- (a) Wang, X.; Huang, J.; Jacobson, A. J. *J. Am. Chem. Soc.* 2002, 124, 15190-15191. (b) Lin, C.-H.; Chiang, R.-K.; Lii, K.-H. *J. Am. Chem. Soc.* 2009, 131, 2068-2069.
- (a) Chen, C.-S.; Lee, S.-F.; Lii, K.-H. *J. Am. Chem. Soc.* 2005, 127, 12208-12209. (b) Nguyen, Q. B.; Chen, C.-L.; Chiang, Y.-W.; Lii, K.-H. *Inorg. Chem.* 2012, 51, 3879-3882. (c) Lee, C.-S.; Wang, S.-L.; Lii, K.-H. *J. Am. Chem. Soc.* 2009, 131, 15116-15117. (d) Nguyen, Q. B.; Liu, H.-K.; Chang, W.-J.; Lii, K.-H. *Inorg. Chem.* 2011, 50, 4241-4243. (e) Lin, C.-H.; Lii, K.-H. *Angew. Chem. Int. Ed.* 2008, 47, 8711-8713. (f) Lee, C.-S.; Lin, C.-H.; Wang, S.-L.; Lii, K.-H. *Angew. Chem. Int. Ed.* 2010, 49, 4254-4256. (g) Liu, H.-K.; Lii, K.-H. *Inorg. Chem.* 2011, 50, 5870-5872. (h) Nguyen, Q. B.; Lii, K.-H. *Inorg. Chem.* 2011, 50, 9936-9938.

Keywords: uranium, silicate, germanate, hydrothermal

MS14-P12 Effective transport of electronic excitation energy through zeolite channels : a structural study

Lara Gigli¹, Rossella Arletti¹, Jenny G. Vitillo², Gianmarco Martra³, Gabriele Alberto³, Gloria Tabacchi², Ettore Fois², Simona Quartieri⁴, Giovanna Vezzalini⁵

4 Gigli L., Arletti R.; Tabacchi G.; Fois E.; Vitillo J. G.; Martra G.; Agostini G.; Quartieri S. and Vezzalini G., J. Phys. Chem. C 2014, 118, 15732–15743

Keywords: Artificial antenna systems, zeolite L, X-ray structural refinements, energy transfer

1. Dipartimento di Scienze della Terra, Università degli Studi di Torino, Via Valperga Caluso 35, 10125-Torino, Italy
2. Dipartimento di Scienza ed Alta Tecnologia, Università degli Studi dell'Insubria, Via Lucini 3, 22100-Como, Italy
3. Dipartimento di Chimica, Università degli Studi di Torino, Via Pietro Giuria 7, 10125-Torino, Italy
4. Dipartimento di Fisica e Scienze della Terra, Università degli Studi di Messina, Viale Ferdinando Stagno d'Alcontres 3, 98166-Messina S.Agata, Italy
5. Dipartimento di Scienze Chimiche e Geologiche, Università degli Studi di Modena e Reggio Emilia, Via Campi 183, 41125-Modena, Italy

email: lara.gigli@unito.it

The development of an artificial system able to mimic the green plants (natural photosynthesis) has been a long-standing challenge. Artificial antenna systems can be realized once several organized chromophores are able to absorb the incident light and to channel the excitation energy to a common acceptor component [1-3]. The properties of the systems depend on the molecular packing inside the channels. Artificial antenna can be built by incorporating suitable guests into the one-dimensional channels of zeolite L (ZL). In this work we present a detailed structural study of two hybrid systems in which dyes (fluorenone and thionine) are encapsulated in zeolite L channels. These two molecules were chosen since it has been demonstrated that a “two-dyes antenna system” - in which fluorenone (FL) (donor molecule) and thionine (Th) (acceptor molecule) are organized in Zeolite L porosities - shows remarkable optical properties. Due to the impossibility of studying, from the structural point of view a “two-dyes systems”, two “one-dye” hybrids (ZL/fluorenone and ZL/thionine) were firstly synthesized and characterized [4]. The results of thermogravimetric, IR, and X-ray structural refinements carried out for the one-dye ZL/FL and ZL/Th systems established that 1.5 molecules of FL and 0.3 molecules of Th per unit cell is the maximum loading, respectively. The FL carbonyl group strong interact with a K⁺ of the ZL. On the other hand, short distances between the carbon, sulfur and nitrogen atoms of Th and two water molecule sites, in turn at bond distance from the oxygen atoms of the main channel, suggested a water-mediated Th-ZL interactions. The energy transfer from excited FL molecules, forming the non-covalent nanoladder in the ZL channel, and Th, deposited on the external surface of ZL particles, is currently under investigation.

The authors acknowledge the Italian Ministry of Education, MIUR-Project: “Futuro in Ricerca 2012 - ImPACT- RBFR12CLQD”.

References

- 1 Calzaferri G.; Huber S.; Maas H., Angew. Chem. Int. Ed., 2003, 42, 3732-3758.
- 2 Calzaferri G.; Lutkouskaya K., Photochem. Photobiol. Sci., 2008, 7, 879 – 910.
- 3 Calzaferri G.; Méallet-Renault R.; Brühwiler D.; Pansu R.; Dolamic I.; Dienel T.; Adler P.; Li H.; Kunzmann A., ChemPhysChem. 2011, 12, 580-594.

MS14-P13 Cronstedtite-1M, occurrence and structure

Jiří Hybler¹, Mariana Klementová¹, Isabella Pignatelli², Régine Mosser-Ruck³

1. Institute of Physics, Academy of Science of Czech Republic, Na Slovance 2, CZ-18224 Prague 8, Czech Republic

2. Laboratory for the Chemistry of Construction Materials (LC2) 2517 Boelter Hall, 420 Westwood Plaza Department of Civil & Environmental Engineering University of California Los Angeles, CA 90095

3. GeoRessources, UMR 7359, Université de Lorraine, France

email: hybler@fzu.cz

Cronstedtite is trioctahedral 1:1 phyllosilicate of general formula $(\text{Fe}^{2+}_{3-x}\text{Fe}^{3+}_x)(\text{Si}_{2-x}\text{Fe}^{3+}_x)\text{O}_5(\text{OH})_4$, where $0 < x < 0.8$. Polytypes refined to date are: 3T, (Šmrček *et al.*, 1994); 1T, (Hybler *et al.*, 2000); 2H₂, (Hybler *et al.*, 2002). Other polytypes including 1M are rare.

Pignatelli *et al.* (2013) prepared small (1-5 µm) cronstedtite crystals by reacting a claystone with iron at 60-90 °C. The TEM studies and SAED images revealed prevailing 1M polytype accompanied by less abundant 3T, and 2M₁.

A rare crystal of cronstedtite-1M from Eisleben (Saxony-Anhalt, Germany) was identified by Mikloš (1975). This crystal was long time regarded as inappropriate for data collection because it provided diffusely streaked characteristic reflections due to the partial stacking disorder. Nevertheless, its recent re-investigation allowed data collection and structure refinement (Hybler, 2014).

Lattice parameters are: $a = 5.5033(3)$, $b = 9.5289(6)$, $c = 7.3328(5)$ Å, $\beta = 104.493(7)^\circ$, space group *Cm*, formula $(\text{Fe}^{2+}_{2.461}\text{Fe}^{3+}_{0.539})(\text{Si}_{1.461}\text{Fe}^{3+}_{0.539})\text{O}_5(\text{OH})_4$, $Z = 2$, $R_{\text{obs}} = 2.42\%$. The structure is built of octahedral (*Oc*), and tetrahedral (*Tet*) sheets forming the 1:1 layer by sharing apical corners of *Tet* sheet. The polytype is generated by a monotonous repetition of $-(\mathbf{a} + \mathbf{a}_2)/3$ layer shifts (\mathbf{a} , \mathbf{a}_2 are vectors of the hexagonal protocell), and it belongs to the Bailey's group A. There are two octahedral Fe sites *M1* (at *m*), *M2* (in a general position). The *M2* octahedron is larger than *M1*, the *Oc* sheet is thus *meso-octahedral*. Only one tetrahedral position, *T1*, is occupied by Si/Fe in the ratio 0.731:0.269(9). The *Tet* sheet is ditrigonalized, $\alpha = +12.7^\circ$. Hydrogen atoms were localised, two of them are involved in hydrogen bonds, linking OH groups of the *Oc* sheet with basal oxygen atoms of the *Tet* sheet.

The study was partially supported by the grant 15-0204S of the Czech Science Foundation.

References:

Hybler, J., Petříček, V., Ďurovič, S. & Šmrček, L. (2000). *Clays Clay Miner.* 48, 331-338.

Hybler, J., Petříček, V., Fábry, J. & Ďurovič, S. (2002). *Clays Clay Miner.* 50, 601-613.

Hybler, J. (2014). *Acta Cryst.* B70, 963-972.

Mikloš, D. (1975). Ph.D. Thesis. Institute of Inorganic Chemistry of Slovak Acad. Sci., Bratislava.

Pignatelli, I., Mugnaioli, E., Hybler, J., Mosser-Ruck, R., Cathelineau, M. & Michau, N. (2013). *Clays Clay Miner.* 61, 277-289.

Šmrček, L., Ďurovič, S., Petříček, V. & Weiss, Z. (1994). *Clays Clay Miner.* 42, 544-551.

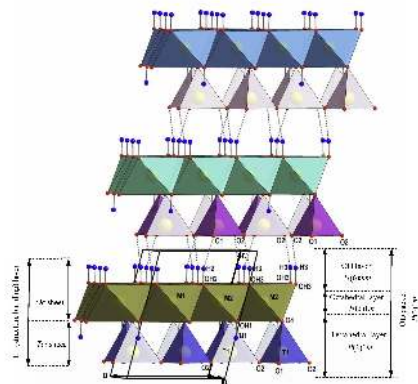


Figure 1. Structure of cronstedtite-1M, model of coordination polyhedra, side view (close to monoclinic b). Delimitation of structure building and OD layers, as well as atom labels and hydrogen bonds are indicated. Note shifts of consecutive layers due to the stacking mode of the polytype.

Keywords: Cronstedtite, polytypism, OD structure

MS14-P14 The crystal structure of symplecite

Gligor Jovanovski¹, Tomče Runčevski², Petre Makreski³, Robert E. Dinnebier²

1. Research Center for Environment and Materials, Macedonian Academy of Sciences and Arts, Bul. Krste Misirkov 2, 1000 Skopje, Macedonia

2. Max Planck Institute for Solid State Research, Heisenbergstrasse 1, 70569 Stuttgart, Germany

3. Institute of Chemistry, Faculty of Natural Sciences and Mathematics, Ss. Cyril and Methodius University, Arhimedova 5, 1000 Skopje, Macedonia

email: gligor@pmf.ukim.mk

Even after half a century of the discovery of the mineral symplecite there is no detailed report on its crystal structure. There is no deposited atomic coordinates and displacement parameters for symplecite in the ICSD and the only known crystallographic information is its unit cell symmetry and parameters.^[1,2] As a response on this lack of structural knowledge, we revisited the system and performed thorough crystallographic study on a natural sample from the Laubach Mine (Germany). Symplecite is a secondary mineral and often occurs with impurities. However, a careful selection of microcrystals provided a phase-pure sample. The crystal structure of symplecite was solved *ab initio* from high-resolution, laboratory X-ray powder diffraction data and refined with the Rietveld method. The refinement of converged quickly giving unit cell parameters of $a = 4.752(3)$ Å, $b = 7.786(5)$ Å, $c = 9.260(6)$ Å, $\alpha = 106.38(3)^\circ$, $\beta = 93.05(4)^\circ$, $\gamma = 98.14(4)^\circ$, and the symmetry was confirmed to be triclinic (with the space group $P\bar{1}$). It was shown that its crystal structure (Figure 1) is indeed isostructural to metavivianite. In this contribution, we present the crystal structure of symplecite, and we relate it to the crystal structures of the minerals metavivianite^[3] and parasymplecite.^[1,4] In addition, we complemented the crystallographic study with infrared and Raman vibrational spectroscopy,^[5] drawing spectra–structure correlations.

References

- [1] T. Ito, Acta Crystallogr. 7 (1954) 630c.
- [2] K. Schmetzer, G. Tremmel, W. Bartelke, Neues Jahrb. Mineral., Abh. 138 (1980) 94–108.
- [3] N.V. Chukanov, R. Scholz, S.M. Aksenov, R.K. Rastsvetaeva, I.V. Pekov, D.I. Belakovskiy, K. Krambrock, R.M. Paniago, A. Righi, R.F. Martins, F.M. Belotti, V. Bermanec, Mineral. Mag. 7683 (2012) 725–741.
- [4] H. Mori, T. Ito, Acta Crystallogr. 3 (1950) 1–6.
- [5] Makreski, S. Stefov, L. Pejov, G. Jovanovski, Spectrochim. Acta Part A 144 (2015) 155–162.

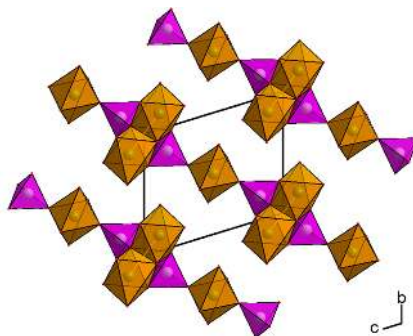


Figure 1. Crystal packing diagram of symplecite viewed perpendicular to the *a*-crystallographic axis.

Keywords: symplecite, mineral, crystal structure

MS14-P15 Mineral-like phases in the MO–CdO–As₂O₅–H₂O system (M^{2+} = Mg, Mn, Fe, Co, Ni, Cu, Zn)

Tamara Đorđević¹, Sabrina Gerger¹, Ljiljana Karanović²

1. Institut für Mineralogie und Kristallographie Universität Wien Althanstr. 14 1090 Wien Austria
2. Faculty of Mining and Geology, Laboratory for Crystallography, Dušina 7, 11000 Belgrade, Serbia

email: tamara.djordjevic@univie.ac.at

In order to understand the mobility of the As⁵⁺ in the environment, one has to investigate structural features and stabilities of arsenic compounds that occur as the result of natural and technological processes. The synthesis of mineral analogues that are stable over geological time scales could lead to increased stability of waste bearing phases. Having this in mind, the arsenates in the MO–CdO–As₂O₅–H₂O (M^{2+} = Mg, Mn, Fe, Co, Ni, Cu, Zn) system have been studied by means of the single-crystal X-ray diffraction and vibrational spectroscopy. Up to now only four arsenates from this system have been observed and structurally investigated [1-3]. The low temperature hydrothermal reactions of Cd(OH)₂, As₂O₅ and metal-bearing salts has revealed three new compounds: Cd₄⁷⁵Ni_{0.25}(AsO₄)₂(AsO₄OH)·4H₂O (1), Cd₄⁷⁵Co_{0.25}(AsO₄)₂(HAsO₄)₂(H₂AsO₄)_{0.5} (2) and Cd₄⁷⁵Zn_{0.25}(AsO₄)₂(AsO₄OH)₂·2H₂O (3). Their structures were determined by single-crystal X-ray diffraction. 1 is a cadmium analogue of the mineral miguelromeroite, Mn₄H₂(AsO₄)₂·4H₂O [4]. It crystallises monoclinic (s.g. C2/c, *a* = 18.375(4), *b* = 9.5395(19), *c* = 9.977(2) Å, *b* = 96.19(3)°, *V* = 1738.6(6) Å³, *Z* = 4. 2 is isotopic to the alluaudite-like Cd-arsenates described in [3] (s.g. C2, *a* = 11.981(2), *b* = 12.485(3), *c* = 6.7661(14) Å, *b* = 113.23(3)°, *V* = 930.1(3) Å³, *Z* = 4). 3 represents previously unknown structure type. It is triclinic (s.g. P1, *a* = 6.8700(10), *b* = 7.513(2), *c* = 8.275(2) Å, *a* = 84.68(3)°, *b* = 82.48(3)°, *g* = 82.79(3)°, *V* = 418.82(16) Å³, *Z* = 2) and is composed of edge-linked octahedral chains running parallel to [101]. The chains contain Cd₁O₆(H₂O)₂ and (Zn₂/Cd₂)₂O₆(H₂O)₂ octahedral pairs sharing opposite edges, which are further interconnected via AsO₄OH²⁻ tetrahedra sharing common vertices and intralayer hydrogen bonds. The layers are positioned parallel to the (010) plane and connected only by interlayer hydrogen bonds. The infrared spectra were measured for all three compounds. The OH stretching frequency is in good agreement with the observed O–O distances. *Financial support of the Austrian Science Foundation (FWF) (Grant V203-N19) is gratefully acknowledged.* References: [1] Cooper, M.A. & Hawthorne, F.C. (1996) Can. Mineral. 34, 623-630 [2] Effenberger, H. (2002) Z. Kristallogr. Suppl. Iss. 19, 85 [3] Stojanović, J., Đorđević, T., Karanović, Lj. (2012) J. Alloy. Compd. 520, 180-189 [4] Kampf, A.R. (2009) Am. Mineral. 94, 1535-1540.

Keywords: cadmium arsenates, hydrothermal synthesis, crystal structure, infrared spectroscopy

MS14-P16 MD study of radiation damage in zircon in connection with the problem of utilization of high-level waste

Oleksii Hrechanivskyi¹, Vadim Urusov²

1. Institute of Geochemistry, Mineralogy and Ore Formation of NAS of Ukraine
2. Moscow State University, Moscow, Russia

email: hrechanovsky@gmail.com

Vitrification, or immobilization of nuclear wastes into glass, is the most widespread method of their treatment. However, the service life of such matrices is no longer than 30–40 years. An alternative to vitrification of nuclear wastes is utilization of high-level waste (HLW) in ceramic matrices and materials.

Many authors have considered zircon as a matrix for the disposal of nuclear fuel and weapons-grade plutonium. However, over the geological time, the alpha-decay of uranium and thorium atoms has brought about a damage of the structure of zircon and its transition from the crystalline state to the X-ray amorphous (metamict) state.

The **purpose** of the present work was to investigate the mechanisms of formation of a cascade of atomic displacements in the structure of zircon due to the alpha-decay under the action of recoil nuclei.

The radiation damage in zircon was investigated by the method of molecular dynamics (MD). This method consists in calculating trajectories of the motion of all atoms involved in a system on the basis of Newton's second law. As a recoil nucleus for a zircon nanofragment of 400 × 400 × 400 Å³ in size containing about 5 million atoms, we used the knock-on atom of thorium (analogue of the recoil atom) with the energy of 20 keV. As the program for the MD modeling, we used the program complex DL_POLY. The computer calculations were fulfilled on the supercomputer SKIF MSU CHEBYSHEV.

The calculations carried out showed that the motion of the knocked-on thorium atom with the energy of 20 keV results in its impact with other atoms of the system. These atoms are displaced from the equilibrium positions, begin to move, and, in turn, displace other atoms. This process results in the formation of the atomic displacement cascade (fig. 1).

Close overlap of three atomic displacement cascades was also studied using the MD simulation method. Results show that the number of Frenkel pairs increases nearly linearly with number of such cascades. The number of formed Frenkel pairs of Zr and O (taking into account their content in zircon) less, than in the case of Si atoms.

In whole obtained results show that in zircon every alpha-decay of radioactive elements results in the origin of amorphous area. These results also indicate that most correct model of zircon amorphization is the direct impact model of amorphization.

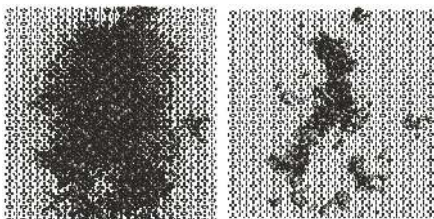


Figure 1. Radiation damage, produced by 20 keV Th recoil in zircon at the peak of the damage (left column) and after structure relaxation (right column).

Keywords: radiation resistance of minerals, semiempirical interatomic potential method, molecular dynamics method, computer simulation of the structure and properties of the crystal, Frenkel defects

MS14-P17 Nanoscale structure refinement of pyroxenes using precession electron diffraction tomography

Damien Jacob¹, Pascal Roussel², Lukas Palatinus³, Yvan Ngassa Tankeu⁴, Chiara Domeneghetti⁴, Fernando Camara⁵

1. UMET, UMR 8207 CNRS-Université Lille 1, 59 655 Villeneuve d'Ascq, France

2. UCCS, UMR 8181 CNRS-Université Lille 1, Ecole Nationale Supérieure de Chimie de Lille, 59655 Villeneuve d'Ascq, France

3. Institute of Physics of the Academy of Sciences of the Czech Republic, 182 21 Prague, Czech Republic

4. Dipartimento di Scienze della Terra, Università di Torino, 10125-Torino, Italy

5. Dipartimento di Scienze della Terra e dell'Ambiente, Università di Pavia, 27100-Pavia, Italy

email: damien.jacob@univ-lille1.fr

The precession electron diffraction (PED) technique [1] has been originally developed for structure determination at a submicrometer scale in a transmission electron microscope (TEM). The resulting intensities keep dynamical in nature, due to electron multiple scattering, but are more closely correlated with the structure factor values with respect to the non-precessed intensities, which is crucial for structure solution and refinement [2]. Since, many structures have been solved using PED, recently combined with the tomographic acquisition of 3D electron diffraction data (PEDT) [3]. Even more recently, a full structure refinement method based on PEDT data and dynamical calculations of diffracted intensities has been successfully proposed [4].

In the field of mineralogy, the sensitivity of PED data to structure factors can be used to refine cations fractionation on specific sites with mixed occupancies. This gives access to the ordering parameter of structures such as Fe²⁺ and Mg bearing pyroxenes. Ordering phenomena being time and temperature dependent, we get quantitative information concerning the thermal history and closure temperature of diffusion processes in the hosting rocks. The present study concerns the application of the full structure dynamical refinement method on natural pyroxenes from various origin, including (Fe²⁺,Mg)SiO₃ orthopyroxene (already studied thanks to a 2D zone-axis approach [5]) and (Fe²⁺,Mg,Ca)SiO₃ clinopyroxene. The refinement of 3D electron diffraction data against dynamical calculations enables the estimation of the (Fe,Mg) occupancies on M1 and M2 sites of the structures with a good precision, the refined values being closed to those deduced from XRD experiments at the grain scale. We will discuss on the accuracy and sensitivity of the method and on its potential application in the field of geothermometry using local analysis of terrestrial or extra-terrestrial pyroxene bearing rocks.

[1] Vincent, R., and Midgley, P.A. (1994) *Ultramicroscopy*, 53(3), 271-282.

[2] Sinkler, W., and Marks, L.D. (2010) *Zeitschrift Fur Kristallographie*, 225(2-3), 47-55.

[3] Mugnaioli, E., Gorelik, T. E. & Kolb, U. (2009). *Ultramicroscopy* 109, 758-765

[4] Palatinus, L., Petricek, V., and Correa, C.A. (2015). *Acta Crystallographica Section A*, 71(2), 1-10.

[5] Jacob, D., Palatinus, L., Cuvillier, P., Leroux, H., Domeneghetti, C., and Camara, F. (2013) *American Mineralogist*, 98(8-9), 1526-1534.

Keywords: electron crystallography, structure refinement, pyroxene, cooling history

MS14-P18 Structural distortion of biogenic aragonite in *Ranella Oleria* mollusc shell layers

Salim Ouhenia¹, Daniel Chateigner², Stéphanie Gascoin²

1. Equipe de cristallographie et de simulation des matériaux, Laboratoire de physique des matériaux et catalyse, Université de Bejaia, Bejaia 06000, Algérie.

2. Laboratoire CRISMAT-ENSICAEN (CNRS UMR 6508), Université de Caen Basse-Normandie, 6 bd M. Juin, 14050 Caen, France.

email: ouhenia@yahoo.fr

Mollusc shells, mainly made of calcite and aragonite crystalline polymorphs of calcium carbonate, are fascinating organic-mineral biocomposites with high mechanical performances, as they attain a fascinating increase in both strength and toughness compared to the geological mineral. The major part of organic materials is intercrystalline, and in a minor way intracrystalline (Pokroy et al., 2006). The organic represents less than 5% in volume, is a biopolymer dispersed in inorganic crystal of calcium carbonate (Barthelat and Espinosa, 2007). This organic part behaves as nanometer growth-control of the inorganic crystals and also plays an important role in stopping crack propagation in nacre (Cortie et al., 2006). This has stimulated chemists and materials scientists to design and synthesize high performance materials with a microstructure similar to that of nacre (Wang et al., 2013). In the present work we made use of Combined Analysis to determine the structure and unit-cell distortions of constituting aragonite crystallites of the shell layers (figure 1) of the gastropod *Ranella oleria*. This approach was chosen because it allows working on real samples, without grinding operation (Ouhenia et al., 2008). SEM analyses show the presence of three distinct layers; an inner layer composed of Radial Lamellar, an intermediate comarginal crossed lamellar layer and an outer crossed lamellar layer. The refinement of X-ray diffraction diagrams, gives quantitatively the structure of the three layers and their respective aragonite unit-cell distortions. An anisotropic unit-cell distortion is quantified for the three layers which is attributed to the combined effects of inter- and intra-crystalline macromolecules.

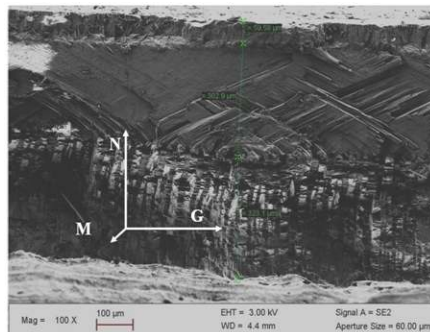


Figure 1. figure 1: Cross-section SEM image of the fractured shell at the location indicated in G, M and N indicate the Growth, Margin and Normal directions, respectively.

Keywords: Ranelle Olerea , mollusc shell, combined analysis.

MS15. Structure property relationships

Chairs: Kari Rissanen, Martin Bremholm

MS15-P1 Crystal Math – When numerical algorithms meet black magic

Max Pillong¹, Ekkehard Görlach¹, Gregory A. Landrum¹, Philippe Piechon¹, Jerome G.P. Wicker², Richard I. Cooper², Trixie Wagner¹

1. Novartis Institutes for BioMedical Research, Basel, Switzerland

2. Department of Chemistry, University of Oxford, Oxford, United Kingdom

email: max.pillong@novartis.com

Determining the three-dimensional structure of small drug-like molecules is an inevitable process in the design of novel potential drugs in both the industrial as well as the academic domain. The most commonly used method is structure determination by X-ray diffraction, which requires either crystalline powder or a tightly packed single crystal of a compound. When it comes to growing the latter, the optimal conditions differ from case to case and are usually determined by a chemist's experience combined with a practical trial-and-error approach. For our in-house structure elucidation service, we have devised a standard procedure of subsequent crystallization experiments that every compound undergoes. The results from these standardized experiments are stored in an Oracle database accessible via a graphical user interface and have been recorded for the past four years.

In order to further increase our understanding of the conditions and the process of crystallization by solvent evaporation, we conducted several statistical analyses on the abovementioned crystallization database. This includes a first assessment and substitutions of the solvents used in the standard experiments, as well as statistical correlation analysis of compound similarity, solubility and crystallinity, based on molecular fingerprints. Identified correlations in the database were then used to guide rational machine learning approaches.

Machine learning is a collective term for numerous algorithmic approaches that can be used to find regularities and correlations in multi-dimensional data, premised on mathematical models¹. These models can subsequently be used for classification or predicting properties of previously unknown data points. Applications in pharmaceutical research divisions worldwide include the prediction of a drug's activity, side effects, metabolism and physicochemical properties such as solubility, melting points or transmembrane permeability. However, only few approaches have attempted to amalgamate machine learning techniques with predicting small molecule crystallization^{2,3}.

We present here preliminary results of our efforts to build a machine learning model that is able to distinguish whether a compound will form a crystal under certain conditions. Our aim is to train this model on our in-house data and then use it to predict optimal crystallization conditions for previously unseen compounds.

Keywords: crystallisation, statistical analysis, crystallisation database, machine learning

MS15-P2 Substituent effects in nitro derivatives of carbazole investigated by XRD studies and DFT calculations

Krzysztof Ejmont¹, Krzysztof Ejmont¹, Katarzyna Gajda¹, Bartosz Zarychta¹, Katarzyna Kopka¹, Zdzisław Daszkiewicz¹

¹. Faculty of Chemistry, University of Opole, Oleska 48, 45-052 Opole, Poland

email: ejmont@uni.opole.pl

Carbazole and its derivatives have attracted significant attention owing to their applications in pharmacy. These compounds are considered also to be potential candidates for electronic applications such as colour displays, organic semiconductors, laser and solar cells as they demonstrate electroactivity and luminescence. In the last years, cross-linked polycarbazole have been widely employed as electron donors in materials for organo-electronic applications as organic light emitting diodes (OLEDs) [1]. The crystal structure of 9*H*-carbazole (I, Fig. 1a), has been re-determined at low temperature for use as a reference structure in a comparative study with the structures of 1-nitro-9*H*-carbazole (II, Fig. 1b), and 9-nitrocarbazole (III, Fig. 1c). All three solid-state structures are slightly nonplanar, the dihedral angles between the planes of the arene and pyrrole rings ranking from 0.40(7)° in (III) to 1.8(2)° in (II). Nevertheless, a density functional theory (DFT) study predicts completely planar conformations for the isolated molecules. To estimate the influence of nitro-group substitution on aromaticity, the HOMA (Harmonic Oscillator Model of Aromaticity) [2,3] descriptor of π -electron delocalization has been calculated. The HOMA indices for the isolated and solid-state molecules are relatively consistent and decrease in value for aromatic rings that are substituted with a π -electron-withdrawing nitro group. Substitution of the arene ring influences the π -electron delocalization in the ring only weakly, showing strong resistance to a perturbation of its geometry, contrary to what is observed for nitro substitution of the five-membered heterocyclic pyrrole ring. In (II), the molecules are arranged in near-planar dimers connected to each other by strong N-HO hydrogen bonds that stack parallel to the crystallographic *b* axis. A similar stacking arrangement is observed in (III), although here the stacked structure is formed by stand-alone molecules [4]. References: [1] Shirota Y, Kageyama H, (2007) Chem. Rev. 107, 953–1010 [2] Krygowski TM (1993) J. Chem. Inf. Comput. Sci. 33, 70–78 [3] Krygowski TM, Cyranski MK (1996) Tetrahedron 52, 10255–10264 [4] Gajda K, Zarychta B, Kopka K, Daszkiewicz Z, Ejmont K (2014) Acta Cryst. C70, 987–991.

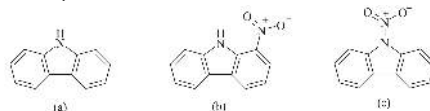


Figure 1. The chemical schemes of nitro derivatives of carbazole

Keywords: carbazole, substituent effect, DFT calculations, HOMA index

MS15-P3 Hydrogen bonds in supramolecular crystals of carboxylic acid salts with aliphatic amines

Paulina Sołtysiak¹, Paulina Sołtysiak¹, Błażej Dziuk¹, Bartosz Zarychta¹, Krzysztof Ejsmont¹

1. Faculty of Chemistry, University of Opole, Oleska 48, 45-052 Opole, Poland

email: paulinkaaa_88@interia.pl

Design of new materials with interesting structure and properties is a very important area of research in materials science. This strategy is based on the formation of hydrogen bonds between molecules and/or ions in the crystal.¹⁻⁵ The salts composed of carboxylic acids and amines serve as a perfect example of compounds which crystal structures are stabilized by ionic interactions along with strong N-H...O hydrogen bonds.⁴ In the salts of oxalic acid with amines there are many characteristic structural motifs i.e.: isolated oxalate monoanions or dianion units, linear chains of carboxylate monoanions formed by strong O-H...O hydrogen bonds or dimers of carboxylate monoanions.^{5,6} In present study we have analyzed supramolecular structures of four salts: allylammmonium hydrogen oxalate hemihydrates⁷ (I), allylammmonium hydrogen succinate⁸ (II), bis(allylammmonium) oxalate⁹ (III) and isobutylammmonium hydrogen oxalate hemihydrates¹⁰ (IV) (Fig. 1). In the crystal structures of (I), (II) and (IV) the anionic sublattices are stabilized by strong O-H...O hydrogen bonds, while in (III) where anions are unprotonated only N-H...O hydrogen bonds are observed. The anionic and cationic substructures are linked to each other by N-H...O bonds accompanied by electrostatic interactions. The molecules form different structural patterns i.e.: chains (I), helical-like chains (II), layers (II) (III) or channels (IV), depending on the hydrogen bonds arrangement. References: [1] G. R. Desiraju, *Acc. Chem. Res.*, 37 (2002) 565-573. [2] G. R. Desiraju, *J. Chem. Sci.*, 122, (2010) 667-675. [3] G. R. Desiraju, *J. Am. Chem. Soc.*, 135, (2013) 9952-9967. [4] K. Ejsmont, J. Zaleski, *Acta Cryst. E62* (2006) o2512-o2513. [5] R. Vaidhyanathan, S. Natarajan, C. N. R. Rao, *J. Chem. Soc. Dalton Trans.*, (2001) 699-706. [6] J. C. MacDonald, C. P. Doeewstein, M.M. Pilley, *Cryst. Growth Des.* 1, (2001) 29-38. [7] B. Dziuk, B. Zarychta, K. Ejsmont, *Acta Cryst. E70*, (2014) o852. [8] B. Dziuk, B. Zarychta, K. Ejsmont, *Acta Cryst. E70*, (2014), o917-o918. [9] B. Dziuk, B. Zarychta, K. Ejsmont, *Acta Cryst. E70*, (2014), o1229-o1230. [10] B. Dziuk, B. Zarychta, K. Ejsmont, *Acta Cryst. E70*, (2014), o1175.

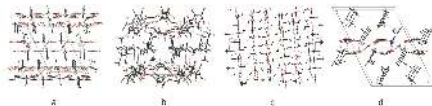


Figure 1. Crystal structure of (a) allylammmonium hydrogen oxalate hemihydrate, (b) allylammmonium hydrogen succinate, (c) bis(allylammmonium) oxalate and (d) isobutylammmonium hydrogen oxalate hemihydrate

Keywords: carboxylic acid salts, hydrogen bonds, supramolecules

MS15-P4 Atomic nature of the high anisotropy of borate thermal expansion

Stanislav K. Filatov¹, Rimma S. Bubnova^{1,2}

1. Department of Crystallography, St. Petersburg State University, University Emb., 7/9, St. Petersburg, 199034, Russia

2. Institute of Silicate Chemistry of the Russian Academy of Sciences, Makarova Emb., 2, St. Petersburg, 199034, Russia

email: filatov.stanislav@gmail.com

The oxygen compounds are the excellent objects for thermal studies due to their wide occurrence. The actual data were taken preferably from the crystal chemistry of borates as one of the most representative class of oxygen compounds: in borates the boron atom could be located in BO_4 tetrahedra same as Si in SiO_4 tetrahedra as well as in BO_3 triangles like the carbon in carbonate ion CO_3 . The borates are the champions in strongly anisotropic thermal deformations due to presence of the rigid B-O groups, BO_3 triangles and symmetrically non-fixed angles in the unit cells. A question can arise, why such anisotropy of thermal deformations characteristic for borates is not characteristic to the same extent, for example, for silicates? Answer is simple – there are no unalterable atomic groups in silicates, such as rigid boron-oxygen groups, and there are no TO_3 triangles. In their turn, these planar anionic groups, like TO_3 triangles, form the basis of crystal structures of carbonates and nitrates, thereby compounds of these classes exhibit a strong anisotropy of thermal vibrations of oxygen atoms O and central atoms T (C, N) and, as a consequence, a strong anisotropy of thermal deformations of a compound in general is characteristic for them. Thus, mass manifestation of strong anisotropy of thermal deformation of crystals has at least three main reasons: (1) shears which are characterised by changes of angular lattice parameters; (2) strong anisotropy of atomic thermal vibrations in planar anionic groups (TO_3 triangles); (3) hinges, or deformations of an assembly of corner-sharing rigid groups, having no own (internal) degrees of freedom to adjust themselves to varying thermodynamic conditions (T , p , X). The first of the listed reasons can be realized in silicates and their structural analogues, the first and the second in carbonates, and all the three reasons are realized in borates. That is why borates demonstrate strongly anisotropic thermal expansion most often. It can be assumed that this is characteristic not only for thermal deformations, but also for pressure, compositional and other types of crystal structure deformations.

Acknowledgements. The work is supported by RFBR 15-03-06354.

[1] Bubnova R. S. & Filatov, S. K. Z. *Kristallogr.*, 2013, 228 (9), 395-428. [2] Filatov, S. K. & Bubnova, R. S. *Phys. Chem. Glasses: Eur. J. Sci. Technol. B*, 2015, 56 (1), 24-35.

Keywords: anisotropy of thermal expansion, low- and high-temperature diffraction

MS15-P5 Approach to determination the thermal expansion tensor and its interpretationRimma S. Bubnova^{1,2}, Vera A. Firsova¹, Sergey N. Volkov¹, Stanislav K. Filatov²

1. Grebenshchikov Institute of Silicate Chemistry, Russian Academy of Sciences, Makarov Emb. 2, St. Petersburg, 199034 Russia
2. St. Petersburg State University, University Emb. 7/9, St. Petersburg, 199034 Russia

email: rimma_bubnova@mail.ru

Presently, there is a growing interest in studying the thermal behavior of a substance by the diffraction methods. Thermal expansion is caused by the anharmonicity of the atomic thermal vibrations. Thermal expansion of a crystal lattice is described by a symmetric tensor of the second rank: in the crystalline substances, in accordance with their symmetry, the expansion anisotropy is manifested. In the general case of triclinic crystals, all axes of the expansion tensor are situated arbitrarily with respect to the crystallographic axes, the tensor is characterized by six parameters: the coefficients along three principal mutually orthogonal axes of the tensor (α_1 , α_2 , α_3) and three angles, determining the orientation of these axes in the space of the crystal. There is presented a program (Riet_to_Tensor) for determining the thermal expansion tensor of the crystals of any system by a set of experimental diffraction data received using X-ray, synchrotron and other radiations at different temperatures. An algorithm is implemented, which allows carrying out all calculations from the experimental determination of the reflection angles 2θ hkl to the calculation of the principle values of the thermal extension tensor. The drawing of the 3D-surface of the tensor and its 2D-sections, including the orientation of the tensor axes with respect to the crystallographic axes is provided. The Rietveld method is used to refine cell dimensions and other structure and peak parameters received from *.cif files. Temperature dependence of the cell parameters can be approximated by several types of functions: polynomials, power, Debye and Einstein thermal models. The program has a subprogram to calculate and investigate the temperature dependence of refined parameters, atomic distances and valence angles. As an example the tensor coefficients of borates, silicates and sulphates are presented and results are discussed from high-temperature crystal chemistry.

Acknowledgements. The work is supported by Russian Foundation for Basic Research 15-03-06354. XRD study is performed at X-ray Diffraction Centre of Saint Petersburg State University.

Keywords: In situ study, anisotropy of thermal expansion, low- and high-temperature diffraction, phase transitions, Rietveld refinement

MS15-P6 Structure and electrical properties of Cr_2O_3 - Fe_2O_3 - P_2O_5 and Cr_2O_3 - PbO - Fe_2O_3 - P_2O_5 glasses and glass-ceramicsAna Šantić¹, Andrea Moguš-Milanković¹, Željko Skoko², Delbert E. Day³

1. Ruđer Bošković Institute, Zagreb, Croatia
2. Faculty of Science, University of Zagreb, Croatia
3. Missouri University of Science and Technology, Rolla, USA

email: asantic@irb.hr

Iron phosphate glasses are electronically conducting glasses with polaronic conduction mechanism where conduction takes place by electrons hopping from Fe^{2+} to Fe^{3+} . Consequently, polaron transport directly depends on $\text{Fe}^{2+}/\text{Fe}^{3+}$ ratio and overall Fe_2O_3 content. On the other hand, electronic conduction in iron phosphate glass-ceramics depends on (micro)structure, size, shape, distribution and nature of the crystalline phase(s).

The aim of the present study was to investigate structure and electrical properties of iron phosphate glasses and glass-ceramics containing PbO and Cr_2O_3 as a nucleating agent. For that purpose two series of glasses, $(43.3-x)\text{PbO}$ - $(13.7+x)\text{Fe}_2\text{O}_3$ - $43.0\text{P}_2\text{O}_5$ ($0 \leq x \leq 30$ mol%) and $x\text{Cr}_2\text{O}_3$ -($28.3-x$) PbO - $28.7\text{Fe}_2\text{O}_3$ - $43.0\text{P}_2\text{O}_5$ ($0 \leq x \leq 10$ mol%), were prepared by melt quenching technique. The structural changes in glasses were investigated using X-ray diffraction analysis (XRD), Raman and Mössbauer spectroscopies and scanning electron microscopy whereas electrical properties were investigated by impedance spectroscopy.

The Raman spectra and XRD of PbO - Fe_2O_3 - P_2O_5 compositions showed that melt underwent partial crystallization when Fe_2O_3 content is ≥ 33.7 mol%. With increasing molar O/P ratio and fraction of Fe^{2+} ions, the length of phosphate units decreases which causes a higher crystallization tendency of the melt. For fully amorphous glasses with < 33.7 mol% Fe_2O_3 , electrical conductivity increases with the increase of $\text{Fe}^{2+}/\text{Fe}^{3+}$ indicating polaronic transport. On the other hand, the electrical conductivity of the partially crystallized samples decreases despite the increase in Fe^{2+} fraction which can be attributed to a massive crystallization of several crystalline phases: $\text{Fe}_3(\text{PO}_4)_6$, $\text{Fe}_3(\text{P}_2\text{O}_7)_2$, $\text{Fe}_2\text{Pb}_3(\text{PO}_4)_4$ and FePO_4 . However, the electrical conductivity of partially crystallized sample with 33.7 mol% Fe_2O_3 is still considerably high which is related to the fast conduction at the interfaces between crystallites and glassy phase.

The structural studies on the Cr_2O_3 - PbO - Fe_2O_3 - P_2O_5 glasses showed that the compositions containing up to 4 mol% Cr_2O_3 formed fully amorphous samples while compositions containing 8 and 10 mol% Cr_2O_3 partially crystallized during cooling to $\text{Fe}_3(\text{PO}_4)_6$, $\text{Fe}_2\text{Pb}_3(\text{PO}_4)_4$ and $\text{Cr}_2\text{Pb}_3(\text{PO}_4)_4$. The electrical conductivity within this series is a function of the $\text{Fe}^{2+}/\text{Fe}^{3+}$ ratio and passes through a maximum at 0.48 which indicates that the conduction process is controlled entirely by the polaron transfer between iron sites.

Keywords: glass-ceramics, electrical conductivity

MS15-P7 Synthesis, molecular structure and spectroscopic characterization of N-(4-nitrophenyl)-2, 2-dibenzoylacetamide (NPDBA): with experimental (X-Ray, FT-IR, ¹H and ¹³C-NMR and UV-Vis) techniques and theoretical calculations

Serife Yalcin¹, Serife P. YALCIN¹, Umit Ceylan², Ahmet O. Sanoglu³, Mehmet Sönmez², Muhittin Aygün⁴

1. Central Laboratory, Osmanbey Campus, Harran University, 63190 Şanlıurfa, TURKEY
2. Department of Physics, Faculty of Arts and Sciences, Ondokuz Mayıs University, 55139 Samsun, Turkey
3. Department of Chemistry, Faculty of arts and Sciences, Gaziantep University, 27310, Gaziantep, TURKEY
4. Department of Physics, Faculty of arts and Sciences, Dokuz Eylül University, Buca, 35150, Izmir, TURKEY

email: serifyalcin@harran.edu.tr

The title compound, C₂₂H₁₆N₂O₅, was synthesized and characterized by experimental techniques (FT-IR, ¹H-NMR, ¹³C-NMR, UV-Vis and X-Ray single crystal determination) and theoretical calculations. According to X-Ray diffraction results, the title compound crystallizes in the monoclinic space group P12₁/c1 with *a* = 10.023 (2) Å, *b* = 21.587 (5) Å, *c* = 9.401 (2) Å and β = 110.29 (3)°, and *Z* = 4 in the unit cell. The molecular geometry, vibrational frequencies, molecular electrostatic potential (MEP), thermodynamic properties, the dipole moments, HOMO-LUMO energy has been calculated by using the Density Functional Theory (DFT) method with 6-311G(d,p) and 6-311++G(d,p) basis sets. ¹H and ¹³C-NMR chemical shifts show good agreement with experimental values.

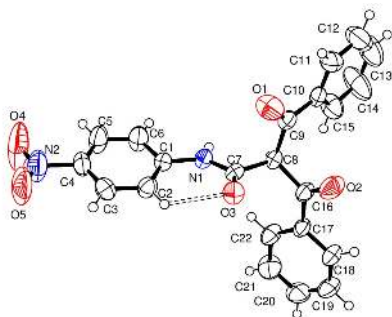


Figure 1. The molecular structure of the title compound.

Keywords: X-ray diffraction; Density functional theory; Quantum chemical calculations; Carboxamide; Characterization.

MS15-P8 Unusual thermal polymorphic transformation $I\text{-}43d \leftrightarrow P2_1/a \leftrightarrow I\text{-}a3d$ of KBSi_2O_6

Maria G. Krzhizhanovskaya¹, Rimma S. Bubnova^{1,2}, Elena S. Derkacheva², Wulf Depmeier³, Stanislav K. Filatov¹

1. Saint Petersburg State University, University Emb., 7/9, St. Petersburg, 190034, Russia
2. Grebenshchikov Institute of Silicate Chemistry of the Russian Academy of Sciences, Adm. Makarov Emb., 2, St. Petersburg, 190034, Russia
3. Dept. of Earth Sciences, University of Kiel, Germany

email: krzhizhanovskaya@mail.ru

Up to now three topologically identical modifications of KBSi_2O_6 with the 3D tetrahedral framework of the ANA type [Zeolite DATABASE] are known: cubic $I\text{-}43d$ [Ihara, Kamei 1980; Miklos et al 1992], cubic $I\text{-}a3d$ [Martucci et al 2011] and monoclinic $P2_1/a$ [Belokoneva et al 2010]. In present study the polycrystalline sample of cubic KBSi_2O_6 was obtained by solid-state reaction from stoichiometric mixture. The monoclinic modification of KBSi_2O_6 ($P2_1/a$) was prepared by hydrothermal synthesis at 600 °C and 5 kBar. The thermal behavior of both modifications upon heating in air was studied by high-temperature X-ray powder diffractometry (HTXRD) and differential scanning calorimetry (DSC) in the temperature range 25–1100 °C. In accord to both HTXRD and DSC results the cubic modification undergoes reversible thermal transformations: $I\text{-}43d \leftrightarrow P2_1/a \leftrightarrow I\text{-}a3d$. The temperature dependence looks complicated. The jumps of values of cell parameters are registered near the point of both $I\text{-}43d \leftrightarrow P2_1/a$ and $P2_1/a \leftrightarrow I\text{-}a3d$ transformations. The volume thermal expansion coefficients are about 70, 50 and $30 \times 10^{-6} \text{ °C}^{-1}$ for $I\text{-}43d$, $P2_1/a$ and $I\text{-}a3d$ phases, respectively. The HTXRD data on the transition temperatures are in a good agreement with DSC data both on heating and cooling. Taking into account well known tendency of substances to increase their symmetry on heating, polymorphic transformation cubic-monoclinic-cubic looks unusual. $P2_1/a$ hydrothermal phase transforms reversibly into $I\text{-}a3d$ polymorph. Both modifications decompose above 1000 °C with SiO_2 formation. In [Martucci et al 2011] the direct reversible transformation $I\text{-}43d \leftrightarrow I\text{-}a3d$ of slightly hydrated KBSi_2O_6 has been studied by Rietveld refinement from synchrotron data. Our experiment showed that the addition of Na or Rb to KBSi_2O_6 stabilized the direct transformation $I\text{-}43d \leftrightarrow I\text{-}a3d$ as well. In [Millini et al 1993] non-stoichiometrical KBSi_2O_6 enriched in SiO_2 was obtained by hydrothermal synthesis with $I\text{-}a3d$ symmetry. It seems that even insignificant variations in composition could lead to stabilization of different modifications of boroleucite structure.

Acknowledgements. The work is supported by Russian Foundation for Basic Research 15-03-06354. XRD study is performed at X-ray Diffraction Centre of Saint Petersburg State University.

Keywords: borosilicate, leucite, high-temperature transformation

MS15-P9 A new structural type in alkaline rare-earth sulfides MRES₂ and TRES₂

Jan Fábry¹, Lubomír Havlák¹, Margarita Henriques², Michal Dušek², Jan Rohlíček², Marek Pasciak¹, Miloš Kopecný¹, Jiří Kub¹

1. Institute of Physics of the Academy of Sciences of the Czech Republic a Na Slovance 2, 182 21 Praha 8, Czech Republic
2. Institute of Physics of the Academy of Sciences of the Czech Republic, Cukrovarnická 10, 162 00 Praha 6, Czech Republic

email: fabry@fzu.cz

Some of the rhombohedral structures of the title compounds (see Fig. 1) are promising class of luminophors (e.g. Havlák *et al.*, 2011). The present analysis was undertaken in order to improve crystal data which are necessary for crystal engineering. Single-crystal X-ray analysis of NaNdS₂, NaSmS₂ and NaEuS₂ revealed a new structural type among Na rare-earth sulfides. This structural type has already been described for NaPrTe₂ (*Fd-3m*; Lissner & Schleid, 2003). However, the symmetry of NaNdS₂, NaSmS₂ and NaEuS₂ may be slightly distorted from the symmetry of *Fd \bar{m}* as it is indicated by the Rietveld refinement. This structural type can be considered as a transitory state between the cubic phase which corresponds to NaCl with disordered cations and the rhombohedral one of - NaFeO₂ structural type – see Fig. 1. The structures of NaCl type show diffuse scattering which is most intense in NaLaS₂ and which corresponds to that observed by Guymont *et al.* (1990) in $\text{Li}_{1-x}\text{Eu}^{2+}_{2x}\text{Eu}^{3+}_{1-x}\text{S}_2$. Moreover, another new structural type has been discovered for NaTbS₂. For other structures of MRES₂ see Fábry *et al.*, 2014a,b and Havlák *et al.*, 2015 (RE means a rare-earth element).

Acknowledgements: The support by the grant 15-12653S "Validation and Interpretation of Modulated Structures" of GA CR is gratefully acknowledged.

Fábry, J., Havlák, L., Dušek, M., Vaněk, P., Dražákoupil, J. & Jurek, K. *Acta Cryst.* (2014a). **B70**, 360-371.

Fábry, J., Havlák, L., Kučeráková, M. & Dušek, M. *Acta Cryst.* (2014b). **C70**, 533-535.

Guymont, M., Tomas, A. & Palazzi, M. (1990). *Phys. Status Solidi*, **118**, 29-40.

Havlák, L., Jarý, V., Nikl M., Boháček, P. & Bárta J. (2011). *Acta Mater.* **59**, 6219-6227.

Havlák, L., Jarý, V., Rejman, M., Miháková, E. Bárta J. & Nikl, M. (2015). *Optical Materials*, **41**, 94-97.

Lissner, F. & Schleid, T. (2003). *Zeitschrift f. Anorganische u. Allg. Chem.* **629**, 1895-1897.

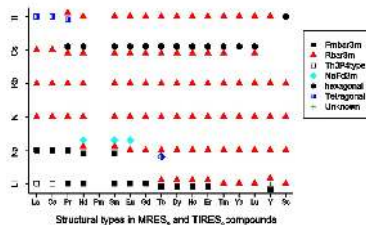


Figure 1. The overview of known structural types in MRES₂ and TRES₂.

Keywords: Alkaline and thallium rare-earth sulfides, crystal chemistry, luminophors, structure analysis, diffuse scattering.

MS15-P10 A kaleidoscope of hypercoordinated alkali metal imidazolates: single source precursors for hybrid borohydrides

Damir A. Safin¹, Koen Robeyns¹, Nikolay A. Tumanov¹,
Voraksmay Ban¹, Yaroslav Filinchuk^{*1}

¹. Institute of Condensed Matter and Nanosciences, Université catholique de Louvain, Place L. Pasteur 1, 1348 Louvain-la-Neuve, Belgium

email: damir.a.safin@gmail.com

Zeolitic imidazolate frameworks (ZIFs) are an outstanding class of MOFs, constructed from tetrahedrally configured transition metal cations linked through bridging imidazolate (Im) spacers. ZIFs are structurally isomorphic to zeolites since the metal-Im-metal angle is similar to the Si-O-Si angle (145°) in the latter compounds. This feature was exploited to produce a huge variety of porous transition metal-based ZIFs. Our initial goal was to combine Im and alkali metal borohydrides in the same structure with the formation of porous borohydride compounds, where Im serves as a structural unit of the framework, while borohydride anions provide with functionality. Surprisingly, we found that alkali metal-based imidazolates are not structurally characterized so far. This might be explained both by their general unavailability and by efficient hydrolysis. Thus, the coordination chemistry of Im towards alkali metal cations (Li⁺, Na⁺ and K⁺) remains a challenge. With this in mind and inspired by the storage properties of ZIFs, we have turned our attention to Im-based coordination compounds with Li⁺, Na⁺ and K⁺ as well as determination of their structures.

Homoleptic 3D MOF-like structures [Na(Im)]_n and [K(Im)]_n (Figure 1) were obtained by the direct reaction of the corresponding hydroxide and ImH, while [Li(Im)]_n was produced using a stepwise synthetic approach through the formation of heteroleptic compounds [Li(ImH)(Im)]_n and [Li(DMSO)(Im)]_n each exhibiting a 2D sheet-like structure. Using an equimolar mixture of two or three alkali metal hydroxides yielded heteronuclear homoleptic 3D MOF-like structures [LiK(Im)₂]_n, [NaK(Im)₂]_n, [Na₂K(Im)₃]_n and [Li_{0.89}Na_{1.12}(ImH)₃(Im)₃]_n or a heteroleptic complex [Li_{1.84}Na_{1.16}(ImH)₂(Im)₃]_n constructed from 2D sheets. Thus, the presence of the parent ligand ImH in the structure of reported compounds decreases the dimensionality of the framework from 3D to 2D. The coordinative demand of the metal cation in is increasing with an increase of the ionic radii. The Li⁺ cation exhibits a strong propensity to form heteroleptic structures, while the K⁺ cation allows to coordinate the Im ring through the π -system. While the alkali metal cations found in the CSD show preferred coordination to the nitrogen atom in the plane of Im, the alkali metal sites in this work are distributed over a larger range from 0 to 90°, and show even a wider distribution than for non-alkali metal cations found in the CSD (Figure 1).

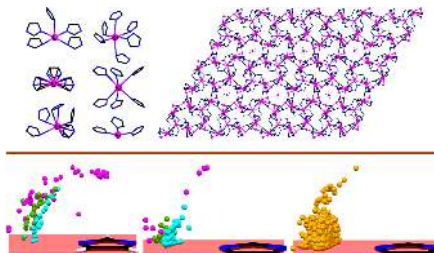


Figure 1. Coordination of the metal cations (top left) and packing (top right) in [K(Im)]_n. Distribution of the metal sites around Im for the structures reported herein (bottom left), for the structures of substituted Im with alkali (bottom middle) and with other metal cations (bottom right).

Keywords: alkali metal cations, crystal structure, imidazole, metal organic frameworks, zeolitic imidazolate frameworks

MS15-P11 A crystallographic characterization of pseudo single crystal Ni-base superalloy - thermal expansion and lattice misfit

Kathrin Demtröder¹, Gunther Eggeler², Jürgen Schreuer¹

1. Ruhr-University Bochum, Institute for Geology, Mineralogy and Geophysics
2. Ruhr-University Bochum, Institute for Materials

email: kathrin.demtroeder@rub.de

Today composite pseudo-single crystals of nickel-base superalloys are widely used for turbine blades in gas turbines and jet engines. These critical components have to operate in the creep range, where they have to withstand mechanical loads at temperatures exceeding by far half of the melting point in K. The favorable mechanical properties of these superalloys are related to their characteristic microstructure [1] which consists of cuboid-like γ' -precipitates with ordered Ni_3Al -structure embedded in a fcc-type γ -matrix [2,3]. The evolution of this microstructure during alloy processing and high temperature deformation, however, depends on the alloy composition, the temperature and the thermo mechanical history of the material. In order to study the evolution of the microstructure at high temperatures under high mechanical loads, a superalloy of type ERBO/1 [4] was investigated. The distributions of γ/γ' lattice constants of as-cast, thermally treated and mechanically treated (creep parameters: 1320 K / 36 h / 160 MPa, $\epsilon \approx 1\%$) samples were measured using X-ray diffraction techniques. Moreover, atomic force microscopy, optical microscopy, electron microprobe analysis and scanning electron microscopy were applied to characterize the microstructure. Our results indicate that the lattice constant measurements cannot be directly interpreted merely on the basis of a lattice misfit between the two phases, because the dislocation density in the γ -channels clearly affects the results. Moreover, creep experiments with an uniaxial mechanical load lead not only to the well-known directional coarsening of the γ' -precipitates (rafting), but also to an anisotropic distribution of the dislocations in the γ -channels. An effort was made to determine the temperature dependence of elastic constants [5] as well as the thermal expansion coefficient of ERBO/1 using dilatometry. Anomalies were observed above about 900 K. These anomalies are probably related to the gradual dissolution of γ' -particles at higher temperatures.

References:

- [1] S. Kaculis *et al.*, *Surf. Interface Anal.*, **2012**, 44, 982-985
- [2] R. C. Reed, *The Superalloys*, 2006.
- [3] T. M. Pollock, *et al.*, *Acta Metall. Mater.*, **1992**, 40, 1-30.
- [4] A. B. Parsa *et al.*, *Advanced Eng. Materials*, **2015**, 17, 216-230
- [5] K. Demtröder *et al.*, Influence of microstructure on macroscopic elastic properties and thermal expansion of nickel-base superalloys ERBO/1 and LEK94, accepted for publication in *Matwiss. & Werkstofftechn.*

Keywords: Superalloys, single-crystal X-ray diffraction, thermal expansion, microstructure

MS15-P12 Combining X-ray diffraction and pyroelectric measurements for phase transition investigations

Erik Mehner¹, Sven Jachalke¹, Juliane Hanzig¹, Hartmut Stöcker¹, Carsten Richter^{1,2}, Matthias Zschornak¹, Dirk C. Meyer¹

1. Institute of Experimental Physics, TU Bergakademie Freiberg, Germany.
2. Deutsches Elektronen-Synchrotron (DESY), Photon Science, Hamburg, Germany.

email: erik.mehner@physik.tu-freiberg.de

Near morphotropic phase boundaries differences in structures may be too subtle to be resolved via single crystal diffraction. In semi-crystalline polymers structural and thermodynamic parameters may be broadly distributed, thus limiting access to these parameters. Therefore, additional information from the symmetry constraints of pyroelectricity provides otherwise unavailable insight into the nature of these phase transitions.

As cases in point we present combined X-ray diffraction and pyroelectric studies on SrTiO_3 and $\text{P(VDF}_{70}\text{-TrFE}_{30})$. Studying the migration-induced field-stabilised polar phase (MFP-phase) of SrTiO_3 yields not only the pyroelectric coefficient but allows a space group prediction $P4mm$ for the MFP-phase. Besides, the electric signature of the forming process corroborates the hypothesis of oxygen migration. The temperature-dependent pyroelectric characterisation of the polyvinylidene fluoride copolymer with trifluoroethylene $\text{P(VDF}_{70}\text{-TrFE}_{30})$ shows pyroelectricity also in the phase assumed paraelectric in literature. Combined with the field reversibility of the pyroelectric effect we postulate a phase transition from ferroelectric to ferroelectric. Implicitly, these data contradict the established orthorhombic to hexagonal cell change in the transition and help to construct an improved structure model.

Keywords: pyroelectricity, polymer, perovskite, phase transition, symmetry breaking, SrTiO_3 , PVDF

MS15-P13 Effect of pristine nanostructure on first cycle electrochemical characteristics in Lithium-excess cathode ceramics

Lars Riekehr¹, Jinlong Liu², Björn Schwarz³, Florian Sigel³,
Yongyao Xia², Helmut Ehrenberg³

1. Technical University Darmstadt, Material Science Department
2. Fudan University Shanghai, Institute of New Energy
3. Karlsruhe Institute of Technology, Institute for Applied Materials - Energy Storage Systems

email: lriekehr@st.tu-darmstadt.de

The rechargeable Lithium ion battery is a very important energy storage technology today. Layered transition metal oxides that are mainly based on LiCoO_2 or LiNiO_2 are currently used as cathode ceramic due to their high operating voltage and high specific capacity of 140-160 mAh/g. In order to obtain even higher energy densities, materials such as the "Li-excess" layered oxides, a composite structure of $\text{Li}[\text{Li}_{1/3}\text{Mn}_{2/3}]\text{O}_2$ (LIR) and LiMO_2 ($\text{M} = \text{Ni, Co, Mn}$) (NCM) are promising candidates, because of their high specific capacity (> 250 mAh/g), higher safety and reduced cost [1-4]. Conventional NCM layered oxides with alternating Li- and TM-layers exhibit R-3m space group symmetry, while the honey comb like ordering of Li and Mn ions within the transition metal (TM) layer of LIR and their characteristic stacking sequences reduce space group symmetry to C2/m. In Li-excess layered materials, NCM and LIR form a nanocomposite embedded in a coherent cubic closed packed oxygen lattice. Concerning application as cathode material, size and distribution of domains with C2/m like cation ordering in the composite structure are of great importance. Cathode materials with a certain ratio of LIR:NCM have been prepared by different synthesis routes as well as two other ratios of composition. The complex nano structures of the pristine material has been extensively characterized by detailed (HR)/TEM investigations and a profound evaluation of the synchrotron XRD patterns by conventional Rietveld refinement and by DIFFaX simulations to estimate C2/m domain sizes by modelling the Warren shaped C2/m superstructure reflections. The nanocomposite structure is correlated with first electrochemical cycle characteristics including a complex activation process, initial irreversible capacity loss, anomalous capacity etc.

References:

- [1] B. Xu, C. R. Fell, M. Chic and Y. S. Meng, *Energy Environ. Sci.* (2011) **4** 2223.
- [2] Z. Lu, D. D. MacNeil and J. R. Dahn, *Electrochem. Solid-State Lett.* (2001) **4** A191.
- [3] C. P. Grey, W. S. Yoon, J. Reed and G. Ceder, *Electrochem. Solid-State Lett.* (2004) **7** A290.
- [4] M. M. Thackeray, S.-H. Kang, C. S. Johnson, J. T. Vaughey, R. Benedek and S. A. Hackney, *J. Mater. Chem.* (2007) **17** 3112.

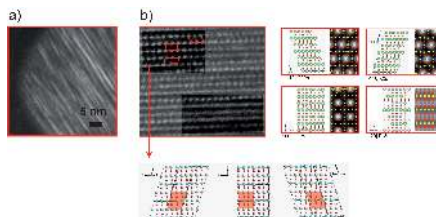


Figure 1. a) TEM dark-field image using C2/m related reflections. The bright regions correspond to C2/m 'domains' in agreement with results from XRD data analysis. b) HRTEM image showing individual 'double TM metal' columns of C2/m 'domains' with high density of different crystallographic orientations.

Keywords: HRTEM, synchrotron XRD, DIFFaX, Lithium Ion Battery, Li-rich layered structures

MS15-P14 Structure, dielectric and electric properties of diisobutylammonium hydrogensulfate crystals

Tamara J. Lukianova¹, Vasyi Kinzhybal¹, Ewa Markiewicz²,
Bożena Hilez², Adam Pietraszko¹

1. Institute of Low Temperature and Structure Research PAS, Wrocław, Poland

2. Institute of Molecular Physics PAS, Poznań, Poland

email: t.lukianova@int.pan.wroc.pl

The $[(\text{CH}_3)_2\text{CHCH}_2\text{NH}_2][\text{HSO}_4]$ (abbreviated as **dibahs**) salt was obtained from 1:1 mixture of diisobutylamine (99%, Sigma-Aldrich) and 30% aqueous solution of sulfuric acid (purum, Sigma-Aldrich). Single crystals were grown by slow evaporation of water at room temperature. DSC studies have revealed two high-temperature reversible phase transitions at 336/319 K (**III**→**II**) and 339/337 K (**II**→**I**), respectively for heating/cooling cycles. Single-crystal X-ray diffraction data were collected at room temperature (phase **III**), after heating to 360 K (phase **I**) and after cooling to 335 K (phase **II**). At room temperature **dibahs** crystallizes in the triclinic symmetry (space group *P*-1). Its crystal structure is built of isolated ordered diisobutylammonium cations (**diba**) and hydrogensulfate anions (**hs**) arranged into layered crystal packing. On heating **dibahs** transforms into monoclinic space group *P*2₁/*c* and the transition (**III**→**II**) may be classified as both of “order–disorder” and of “displacive” one and related to a disorder of the **diba** cations and a reorientation of the inorganic sublattice. The second transition (**II**→**I**) is followed by a change in the symmetry to orthorhombic space group *Cmce* and caused by an increase in the disorder in organic sublattice and a small deformation. As-grown single crystals of **dibahs** are usually single domain and ferroelastic domains were found to appear at room temperature due to application of a small mechanical stress. Evolution of the ferroelastic domain pattern was measured on heating and on cooling. Dielectric response and ac conductivity were measured for pellets (powder pressed at 600 MPa) with gold evaporated electrodes using an Alpha-A High Performance Frequency Analyzer (Novocontrol GmbH) combined with Quatro Cryosystem for the temperature control. The Figure below shows temperature variation in dielectric permittivity ϵ' and electric conductivity s' at various frequencies. The dielectric anomalies are related to changes in the electric conductivity. The activation energy E_a was calculated for dc conductivity (1 Hz) and in the range: 413 K < T < 435 K → $E_a = 1.78$ eV, 356 K < T < 395 K → $E_a = 0.23$ eV, 335 K < T < 341 K → $E_a = 1.51$ eV. The low activation energy of 0.23 eV in the temperature range between ~356 K and ~395 K can be ascribed to fast transport of the acid proton in the lattice of **dibahs** crystals.

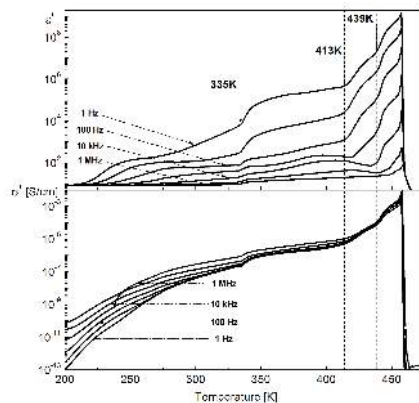


Figure 1.

Keywords: crystal structure, phase transitions, ferroelastic, dielectric and electric properties

MS15-P15 Anomalous thermal expansion in α -titaniumBoris N. Kodess¹, Hakon Hope²

1. ICS&E-VNIIMS

2. Department of Chemistry, Univesity of California

email: kodess@mail.ru

The unit cell parameters of single crystals of Ti were determined in the range 10 to 295 K. For several samples of two single crystals, experiments were also carried out at room temperature in full Ewald sphere. Results showed homogeneity of the characteristics in different parts of the single crystals. A comparison of the lattice parameters of Ti determined on different diffractometers showed very good reproducibility when used for calculations in the high-angle region (the difference is not more 0.00002 nm). The values of the cell parameters correspond to high-purity powders of Ti in the JCPDS database [1]. For the sample with the best micro-structures were constructed temperature dependencies from of the axial ratios of the unit cell parameters, c/a , and the thermal expansion coefficient, TEC. At low temperatures we found negative value of TEC, attributed to c only. It is important that in the same range of temperatures from 10 to 50 K have been found anomalies in the elastic constants [2] and the temperature dependence of paramagnetic susceptibility [3]. We consider two complementary hypotheses. First - the anomalous TEC can be connected with an electronic topological phase transition. The possibility of this type phase transition for Ti is described in [4]. Second - in the low-temperature range occurs the possibility of appearance precursors of the low-temperature phase transition to the ω phase. Note that this ω phase for Ti occurs after low pressures at room temperature [5]. Extrapolation of the transition temperature of hcp - ω -phase, which depends on pressure and temperature [5, etc.], is the reason for suggesting that this ω phase may occur due to compression of the lattice when the temperature is lowered to the range 10-30 K, under normal pressure. It is an interesting fact that the ω phase of elemental Ti corresponds to structural type A1B2 (C32), which favors the appearance of the superconducting state. [1] JCPDS (Joint Committee on Powder Diffraction Standards), No. 44-1294, [2] Fisher, E. S., Renken, C. J. Phys. Rev. (1964) 135, Issue 2A, pp. 482-494 [3] Collings E.W. & Ho, J. C. (1971) Phys. Rev. B, 4(2), 349 [4] Souvatzis P., Eriksson O., Kaznelson M.I. Phys. Rev. Lett. (2007), v.99, 015901 [5] Zhang J., Zhao Y., Hixson RS, Gray III GT, Wang L, Utsumi, W. Hiroyaki S., Takanori H. Phys. Rev. (2008), B78, p. 054119

Keywords: Titanium, thermal expansion, low temperature, ω -phase

MS15-P16 Structure and multiferroic properties of a new Sr-based pyroxene familyPierre Bordet¹, Lei Ding¹, Claire V. Colin¹, Céline Darie¹

1. Institut Néel, CNRS & Université Grenoble Alpes, BP166, 38042 Grenoble Cedex 9, France

email: pierre.bordet@neel.cnrs.fr

Compounds belonging to the Pyroxene family are well known as rock-forming minerals, and have thus drawn substantial interest by mineralogists. In this family of general chemical formula $AM(Si, Ge)_2O_6$, A is usually an alkali metal monovalent cation or a divalent alkaline earth cation, and B may be a trivalent or divalent transition metal cation. Among pyroxene compounds, the monoclinic clinopyroxenes are characterized by isolated one-dimensional chains of MO_6 octahedra linked by edge-sharing. Due to this specific arrangement, clinopyroxene compounds where M is a magnetic transition metal cation have attracted considerable attention in recent years. Investigations revealed that these compounds present a rich diversity of intriguing low-dimensional magnetic properties. The existence and possible interplay of low dimensionality and magnetic frustration may result in multiferroic and/or magneto-electric (ME) properties.

We have undertaken the study of pyroxene compounds where A and M are divalent cations. Among these, Sr-based pyroxenes were not reported up to now. Here we present the synthesis of the new compounds $SrCoGe_2O_6$ and $SrMnGe_2O_6$ which both display the high clinopyroxene structure with space group $C2/c$. We will show their structure determination using single crystal and powder x-ray diffraction and neutron powder diffraction (NPD, D1B-ILL) and compare their structures to those of their Ca-based analogues. The magneto-electric properties of both compounds were investigated by polarization measurements vs applied magnetic field and NPD. $SrMnGe_2O_6$ displays multiferroic properties with a cycloid-type incommensurate spin structure, while $SrCoGe_2O_6$ is an antiferromagnet with a similar magnetic structure as the $CaCoGe_2O_6$ compound. These results will be detailed at the conference.

Keywords: Multiferroics, Pyroxene, magnetic structure

MS15-P17 The structure directing role of Al and Cs in design of novel 3D open-framework compounds, Cs₂CuAl₄O₈ and CsAl₂BP₆O₂₀

Larisa V. Shvanskaya^{1,2}, Olga V. Yakubovich¹

1. Lomonosov Moscow State University, GSP-1, Leninskie Gory, 119991 Moscow, Russia
2. National University of Science and Technology "MISIS", Leninsky Prospekt 4, 119049 Moscow, Russia

email: lshvanskaya@mail.ru

Of special interest in searching for new materials is the design of stable phases with open microporous structures based on mixed type frameworks. These kind of zeolite-like materials are promising not only as catalysts, sorbents, molecular sieves etc, but also as materials with magnetic, electronic, photoluminescence properties, to name a few. Two new compounds, Cs₂CuAl₄O₈ ($a=8.4551(7)$, $b=10.0118(9)$, $c=17.073(1)$ Å, $\beta=101.64(2)^\circ$, $V=1415.5(3)$ Å³, $P2_1/c$, $Z=4$) and CsAl₂BP₆O₂₀ ($a=11.815(2)$, $b=10.042(1)$, $c=26.630(4)$, $V=3159.6(3)$ Å³, $Pbca$, $Z=8$) have been obtained by the high temperature crystallization method in the phosphate system at the 1050° and 950°C, accordingly. Their crystal structures, determined by single-crystal X-ray diffraction, both are based on mixed anionic frameworks with caesium cations in the channels and cavities. The copper aluminate structure is built by double layers of corner-sharing AlO₄ tetrahedra interconnected by chains of edge-sharing CuO₄ square planes. The topology of a 2D aluminate layer is similar to those found in the ATT-type zeolites and isostructural silicate minerals armstrongite, davanite, and dalyite. A 3D mixed anionic framework of the borophosphate structure is assembled by based on BO₄⁺, PO₄[−] tetrahedra and AlO₆ octahedra, sharing oxygen vertices. The Cs⁺ cations play the templating role in the structure formation of both compounds. The aluminum atoms stabilize the mixed anionic framework in the CsAl₂BP₆O₂₀, and play the key role in the design of 2D layers in the Cs₂CuAl₄O₈ structure. A complex of physical characteristics for different future applications is possible in connection with new synthesized compounds.

Keywords: X-ray diffraction, crystal structure, properties, microporous, flux method

MS15-P18 H...H clashes in published carboxylic acid structures

Carl H. Schwalbe^{1,2}

1. Cambridge Crystallographic Data Centre, 12 Union Road, Cambridge CB2 1EZ
2. School of Life & Health Sciences, Aston University, Birmingham B4 7ET, U.K.

email: carlschwalbe@hotmail.com

Being difficult to locate accurately from X-ray diffraction data, hydrogen atoms are often placed in calculated positions. However, the SHEXL manual warns about the possibility that “the automatic placing of hydrogen atoms has assigned the hydrogens of two different O-H or N-H groups to the same hydrogen bond” [1], and CheckCIF includes a test [2] of D-H...H-D contacts that gives a PLAT417 Class A alert if the H...H distance is less than 1.8 Å. Wood et al. [3] showed that even under high pressure, H atoms come no closer than 1.7 Å. The Cambridge Structural Database (version 5.35 updated to February 2014) was surveyed for structures with clashing carboxyl H atoms subject to the filters $R \leq 0.1$ and no gross (non-hydrogen) disorder. Initially the O=C-OH...HO-C=O arrangement was considered. Violations of the CheckCIF criterion were found in 32 such structures (one corrected in a subsequent redetermination). Making the sites partially occupied or substituting O---H---O interactions with the H atom at the midpoint eliminates the clashes. As a criterion for the latter situation a separate search for accurate and trouble-free structures in the CSD with this feature gave 89 observations with mean O...O distance 2.456 Å and standard deviation of the mean 0.017 Å; 24 of the above 31 structures fall within the range 2.40 to 2.51 Å. Making H atom sites partially occupied or placing a single H atom between O atoms reduces the hydrogen count. In most cases it is possible, based on geometric criteria, to suggest locations where the missing H atoms could be replaced. Of course, these remain hypothetical until they can be confirmed with structure factors. Clashing H atoms in a pair-bonded dimer can be resolved by exchanging one C=O for C-OH. Five dimers with CheckCIF violations had C-O distances identical within 0.027 Å, suggesting partially occupied H sites or 180° rotation of entire COOH groups. Two structures seem to have one C=O inappropriately protonated. It is evident that, even in this era of validation software, authors, referees and readers must be on guard against COOH...HOOC clashes.

[1] <http://shelx.uni-ac.gwdg.de/SHELX/shelx97.pdf>, page 2-7. Accessed 11 December 2014.

[2] <http://journals.iucr.org/services/cif/datavalidation.html>. Accessed 11 December 2014.

[3] P. A. Wood, J. J. McKinnon, S. Parsons, E. Pidcock & M. A. Spackman (2008) *CrystEngComm*, 10, 368–376.

Keywords: Hydrogen atom clashes, CheckCIF violations, carboxylic acids

MS15-P19 Two polymorphic nanoribbon structures with near-white light photoluminescence

Sue-Lein Wang¹

1. Department of Chemistry, National Tsing Hua University

email: slwang@mx.nthu.edu.tw

Two polymorphic nanoribbon structures in the zincphosphite system (NTHU-14) were prepared and discovered to exhibit interesting photoluminescence (PL) properties. They are the first neutral organo-zinc phosphites in which the 2.8 nm-wide and S-shaped ribbons are arranged into R- and L- arrays, resulting in RLR and RRR stackings, thus creating two polymorphic phases: 14- α and 14- β . Although both can display near-white light under the excitation of 320 nm UV-light, the two polymorphs reveal distinctly different emissions in the visible region. However, the major differences observed in optical property could not be ascribed to the difference in their structural as usually expected. We noted that for either R-arrays or L-arrays, π - π bonding is the only intra-array interaction force and hydrogen bonds is the only inter-array force, existing between a pair of adjacent ribbon arrays. Therefore, the two polymorphic structures are considered identical in terms of intra- and inter-ribbon-bonding interactions. In this presentation, descriptions and discussions on the synthetic strategy, the unique structures, characterizations, and the origin of emissions and the resultant photoluminescence properties for the two polymorphs of NTHU-14 are presented in detail.

Keywords: polymorph, photoluminescence, organo-zinc phosphite

MS15-P20 Novel ammonium manganese hydrate phosphate – a possible precursor for Li-ion batteries

Galina V. Kiriukhina¹, Olga V. Yakubovich^{1,2}, Olga V. Dimitrova¹

1. Lomonosov Moscow State University, Moscow, Russia

2. Institute of Geology of Ore Deposits, Petrography, Mineralogy, and Geochemistry, Russian Academy of Sciences, Moscow, Russia

email: g-biralo@yandex.ru

The crystal structure of a new modification of the niahite mineral $\text{NH}_4\text{MnPO}_4 \cdot \text{H}_2\text{O}$, obtained in the form of single crystals under hydrothermal conditions, is determined by X-ray diffraction (Xcalibur-S-CCD diffractometer, $R = 0.0259$): $a = 17.582$, $b = 4.909$, and $c = 5.731$ Å; space group = $Pnam$, $Z = 4$, $D_x = 2.497$ g/cm³ [1].

A new modification of the niahite is centrosymmetric. Both structures are based on chess-board type layers built from MnO_6 octahedra sharing O vertices. PO_4 tetrahedra are attached to the free cages from both sides of these layers; the “hanging” vertex of the phosphate tetrahedra, which is unshared with other polyhedra, protrudes to the adjacent layer. NH_4 groups are situated between the layers and form hydrogen bonds connecting the layers together.

As we showed earlier [2, 3], the niahite, $\text{NH}_4\text{MnPO}_4 \cdot \text{H}_2\text{O}$ structure type can be obtained by the transformation of the crystal structure of lithiophilite LiMnPO_4 (Fig. 1). The Mn/P layers of the same topology are repetitive polysomes of both crystal structures. These layers are directly connected into a 3D framework by sharing oxygen vertices of octahedra and tetrahedra. Small octahedral voids of the lithiophilite crystal structure are populated by Li atoms.

Olivine-type LiMPO_4 ($M = \text{Fe, Mn, Co, Ni}$) phosphates are currently among the most efficient cathode materials for lithium batteries [4–6]. In [4] it was shown that the LiFePO_4/C , which was synthesized, using the $\text{NH}_4\text{FePO}_4 \cdot \text{H}_2\text{O}$ precursor, exhibits high rate capability at different current rate values. The LiMnPO_4/C , synthesized by the same procedure with the $\text{NH}_4\text{MnPO}_4 \cdot \text{H}_2\text{O}$ precursor, exhibits sound, but lower with respect to the LiFePO_4/C , electrochemical properties [4–6]. This way of LiMPO_4 phases' preparation is targeted to increase the capacity of the material. It was shown that synthesis of LiMnPO_4 by ion exchange in the $\text{NH}_4\text{MnPO}_4 \cdot \text{H}_2\text{O}$ precursor retains the morphology of precursor crystals. It is highly probable that the new centrosymmetric modification of “niahite” will be even more efficient for this purpose.

[1] G. Kiriukhina, O. Yakubovich, O. Dimitrova, *Cryst. Rep.* 60 (2), 198 (2015).

[2] O. Yakubovich, O. Karimova *et al.*, *Acta Cryst. C* 55, 151 (1999).

[3] O. Yakubovich, O. Karimova *et al.*, Dokl. Akad. Nauk. 342 (1), 40 (1995).

[4] Ch. Wu, J. Xie *et al.*, Cryst. Eng. Commun. 16, 2239 (2014).

[5] G. Li, H. Azuma & M. Tohda, Electrochem. Solid State Lett. 5 (6), A135 (2002).

[6] N. Bramnik & H. Ehrenberg, J. Alloys Compd. 464, 259 (2008).

Keywords: Niahite, crystal structure, lithium ion batteries, lithiophilite

MS15-P21 Shape and confinement effects of various terminal siloxane groups and C₆₀ on supramolecular interactions of hydrogen-bonded bent-core liquid crystals

Hong-Cheu Lin¹, I-Hung Chiang¹, Wei-Tsung Chuang², Chia-Lin Lu¹, Chun-Yen Liao¹

1. Department of Materials Science and Engineering, National Chiao Tung University, Hsinchu, Taiwan.

2. National Synchrotron Radiation Research Center, Hsinchu, Taiwan

email: linhc@mail.nctu.edu.tw

To investigate the shape and confinement effects of the terminal siloxane groups and C₆₀ on the self-assembled behavior of molecular arrangements in hydrogen-bonded (H-bonded) bent-core liquid crystal (LC) complexes, several H-bonded bent-core complexes with string-, ring-, ball-, and cage-like siloxane termini (i.e., linear siloxane unit -Si-O-Si-O-Si-, cyclic siloxane unit (Si-O)₄, ball-shaped C₆₀, and silsesquioxane unit POSS₄, respectively) were synthesized and investigated. By X-ray diffraction measurements, different types of mesophases were controlled by the shape effect of the string- and cage-like siloxane termini, respectively. In addition, the confinement effect of various terminal siloxane groups and C₆₀ (accompanied by increasing the numbers of attached H-bonded bent-core arms) resulted in higher transition temperatures and the diminishing of mesophasic ranges (even the disappearance of mesophase). Moreover, AFM images showed the bilayer smectic phases were aligned to reveal highly ordered thread-like structures by a DC field. By spontaneous polarization measurements within the mesophasic ranges, different ferroelectric and anti-ferroelectric behavior were observed, which can be manipulated by the molar ratios of these binary mixtures. Finally, the electro-optical performance of these H-bonded bent-core LC complexes could be optimized through binary mixtures of proton donors and acceptors with various molar ratios.

Keywords: hydrogen-bonded, bent-core, liquid crystal, ferroelectric, anti-ferroelectric

MS15-P22 Synthesis and structural characterization of off-stoichiometric $\text{Cu}_2\text{ZnSnSe}_4$

Laura E. Valle Rios¹, Galina Gurieva², Susan Schorr^{1,2}

1. Freie Universität Berlin, Germany
2. Helmholtz-Zentrum Berlin, Germany

email: laura.valle-rios@helmholtz-berlin.de

$\text{Cu}_2\text{ZnSnSe}_4$ is a low cost alternative absorber material for solar cells. Record efficiency of 12.6% was reported for a CZTSSe based thin film solar cell [1]. The polycrystalline absorber layer exhibits an off-stoichiometric composition which causes intrinsic point defects (vacancies, anti-sites, interstitials) which determine the electronic properties of the material significantly.

This work focuses on the synthesis and characterization of off-stoichiometric CZTSe. In literature [2] off-stoichiometric types have been suggested, amongst them: A-type Cu-poor/Zn-rich; B-type Cu-poor/Sn-poor. We have synthesized powder samples by solid state reaction from pure elements in sealed evacuated silica tubes. The first reaction took place at 750°C with several temperature steps in between. After reaction samples were ground, pressed in pellets and annealed again.

To determine phase content and chemical composition of the obtained samples, an electron microprobe system equipped with wavelength dispersive X-ray analysis was used. The measurements proved the presence of CZTSe as main phase within all the different off-stoichiometric synthesized samples. The lattice parameters of the CZTSe main phase were determined by Rietveld analysis from XRD data. Refinements were performed by FullProf [3] with the kesterite structure model, because stoichiometric CZTSe crystallizes in the kesterite type structure [4].

Moreover, neutron powder diffraction experiments were performed at the Spallation Neutron Source in Oak Ridge/US as well as at the Berlin Research Reactor BERII in HZB/Germany. The neutron scattering length of Cu and Zn is different, therefore is possible to distinguish between Cu^+ and Zn^{2+} site occupation in the crystal structure. Further Rietveld refinements of neutron diffraction data additionally with the average neutron scattering length analysis method lead the determination of cation distribution, the Cu/Zn order-disorder in the 2c and 2d site and the formation of intrinsic point defects related to the according off-stoichiometric cation substitution type.

A study of the cation distribution and point defects formation in the crystal structure of the CZTSe phase concerning the different off-stoichiometry types will be presented.

Acknowledgments: KESTCELLS 316488.

[1] Wang, et al., *Adv. Energy materials* (2013). [2] Lafond, et al., *ZAAC* 638, (2012) 2571-2577. [3] Carvajal, et al., www.ill.eu/sites/fullprof. [4] Schorr, *Sol. Energ. Mat. Sol. Cells* 95 (2011) 1482-1488.

Keywords: kesterite, crystal structure

MS15-P23 Intermolecular interactions and second-harmonic generation properties of 1,5-diarylpentenynes

Anna V. Vologzhanina¹, Kyrill Y. Suponitsky¹, Evgeniya D. Voronova¹

1. A.N.Nesmeyanov Institute of Organoelement Compounds RAS

email: vologzhanina@mail.ru

The chalcone family (e.g. 1,3-diarylprop-2-en-1-ones) is well known to exhibit second-harmonic generation (SHG) properties [1] being crystallized in acentric crystals. To reveal factors responsible for crystallization of their quasi-planar derivatives in acentric space groups and the effect of $\text{C}\equiv\text{C}$ bond on SHG properties, fourteen quasi-planar 1,5-diarylpentenynes were synthesized and their crystal structures were investigated. Seven of these compounds crystallize in acentric and chiral space groups. Intermolecular bonding was studied by means of periodic DFT calculations followed by the topological analysis of charge density within framework of the quantum theory of 'Atoms in Molecules' [2]. The role of the $\text{C}-\text{H}\cdots\text{O}$ interactions as driving force for supramolecular synthon formation has been demonstrated. Three types of $\text{C}-\text{H}\cdots\text{O}$ bonded synthons were revealed for this family (Figure). Those synthons are in accord with the charge distribution along the conjugated system that allows direct synthesis of acentric crystals of 1,5-diarylpentenynes. SHG properties for seven compounds crystallizing in chiral space groups have been investigated both theoretically and experimentally and confirmed prominent crystalline nonlinear optical susceptibility of this family. The crystal packing effects on calculated SHG properties have been estimated based on the recently proposed Charge Model. SHG measurements confirmed a validity of the Charge Model and demonstrated an efficiency of this family for potential application as materials for nonlinear optics.

We acknowledge the Russian Science Foundation for financial support (Grant 14-13-00884).

[1] *Nonlinear Optics of Organic Molecules and Polymers*. Ed. Nalwa, H. S. & Miyata, S. 1996. CRC Press, Boca Raton, Florida. [2] Bader, R. F. W. *Atoms in Molecules: A Quantum Theory*. 1994. USA: Oxford University Press.

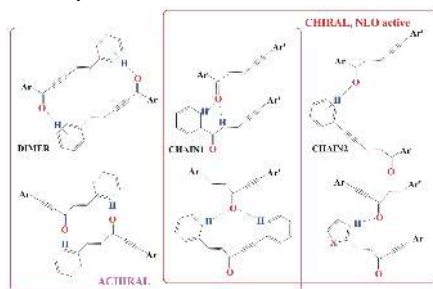


Figure 1. Schematic view of supramolecular synthons in crystals of 1,5-diarylpentenynes.

Keywords: 1,5-diarylpentenynes, second-harmonic generation properties, $\text{C}-\text{H}\cdots\text{O}$ interactions, charge density

MS15-P24 Large guest-dependent anisotropic thermal expansion in a series of organic inclusion compounds

Emile R. Engel¹, Vincent J. Smith¹, Charl X. Bezuidenhout¹,
Leonard J. Barbour¹

1. Department of Chemistry and Polymer Science, Stellenbosch University

email: ere@sun.ac.za

Most studies of extreme anisotropic thermal expansion have involved inorganic compounds.¹ In recent years, however, various examples have come to light of large anisotropic thermal expansion in organic crystals.² We recently reported on a nitromethane solvate of 18-crown-6 that undergoes large uniaxial negative thermal expansion with large positive expansion along the other two principal axes.³ The present study investigated the thermal expansion behaviour of two inclusion compounds (**2** and **3**) that are analogous to the nitromethane solvate described above (**1**). The three compounds have isoskeletal crystal structures but, curiously, they exhibit drastically different thermal expansion profiles over a common temperature range of 180–273K.

Linear coefficients of thermal expansion (Figure 1) were determined using PASCAL.⁴ The overall trends for **1** and **2** are similar in that the expansion is negative along one axis and positive along the other two, however, the magnitude of thermal expansion is lower for **2** in all respects. Compound **3** exhibits only positive thermal expansion along two principal axes and near-zero thermal expansion along the third. The overall volumetric expansion for all three compounds is nevertheless exceptionally large for organic inclusion compounds.

The underlying mechanism of anisotropic thermal expansion in each case involves a combination of relatively weak intermolecular interactions. These were investigated computationally by calculating single-point energies and mapping electrostatic potentials.

Evidently, guest replacement is a potential strategy for greatly modifying the thermal expansion behaviour of an organic inclusion compound, even where the overall molecular packing in the crystal is unaffected.

References

- [1] G.D. Barrera, J.A.O. Bruno, T. H. K. Barron, N.L. Allan, *J. Phys.: Condens. Matter*, 2005, 17, R217; W. Miller, C.W. Smith, D.S. Mackenzie, K.E. Evans, *J. Mater. Sci.*, 2009, 44, 5441.
- [2] D. Das, T. Jacobs, L.J. Barbour, *Nat. Mater.*, 2010, 9, 36; S. Bhattacharya, B.K. Saha, *Cryst. Growth Des.* 2012, 12, 4716; S. Bhattacharya, B.K. Saha, *CrystEngComm*, 2014, 16, 2340.
- [3] E.R. Engel, V.J. Smith, C.X. Bezuidenhout, L.J. Barbour, *Chem.Comm.*, 2014, 50, 423.
- [4] J. Cliffe, A. L. Goodwin, *J. Appl. Crystallogr.*, 2012, 45, 1321.

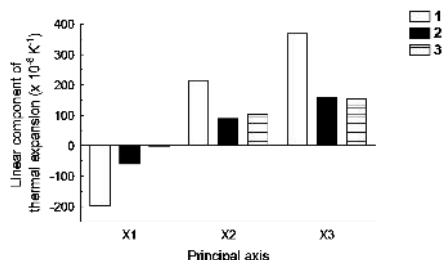


Figure 1. Linear coefficients of thermal expansion for **1**, **2** and **3** over the temperature range 180–273K.

Keywords: thermal expansion, inclusion compound, 18-crown-6

MS15-P25 B3 and B20 compounds: pseudosymmetry and nonlinear optical properties

Anastasia P. Gazhulina¹, Mikhail O. Marychev¹

¹ N.I. Lobachevsky State University of Nizhni Novgorod, Nizhni Novgorod, Russia

email: asyagazhulina@yandex.ru

In the present work, we have studied 111 crystals of AB type compounds belonging to two non-centrosymmetric structural types with cubic symmetry, namely, zinc blende (B3) and FeSi (B20) [1]. For selected crystals we have quantitatively estimated the degree of invariance with respect to the operation of inversion η (pseudoinversion) with a view to tracing the possible relationships between the nonlinear optical properties of these crystals and this symmetry characteristic. The second-order susceptibility of crystal determines the intensity of generation of the second optical harmonic and is a structure- and symmetry-sensitive property of crystal. For centrosymmetric crystals, the second-order susceptibility should be zero. One might suggest that reduction of symmetry will lead to some dependence of the second-order susceptibility of crystal on the degree of invariance of crystal structure with respect to inversion. In this context, the main goals of our investigation were first-principles calculations of the electronic structure and nonlinear optical properties of crystals of B3 and B20 types, calculation of the pseudoinversion values for these crystal structures, and comparison of the obtained computational data.

Calculations of the electron structure and nonlinear optical properties of crystals were based on the density-functional theory and employed three approximations for exchange-correlation potential, while the degrees of pseudoinversion of these structures were calculated using program package Pseudosymmetry [2]. The results obtained for some crystals are in agreement with the well-known experimental and computational data. For example Fig. shows $\eta-|\chi_{123}|$ diagrams for B3 type crystals by the results of calculations using the LDA potential, together with a histogram of the distribution of these crystals with respect to the degree of pseudoinversion, and a map of the values of a polynomial approximating the empirical function of the density of points on the $\eta-|\chi_{123}|$ plane.

It is demonstrated that the degree of pseudosymmetry as a quantitative characteristic of crystal structures can be useful for establishing correlations between the structural features of crystals and their physical properties. The results of this work can be useful for researchers engaged in the development of materials with preset properties.

[1] A.P. Gazhulina, M.O. Marychev, J. Alloy. Compd. 623 (2015) 413

[2] N.V. Somov, E.V. Chuprunov, Crystallogr. Rep 59 (2014) 37

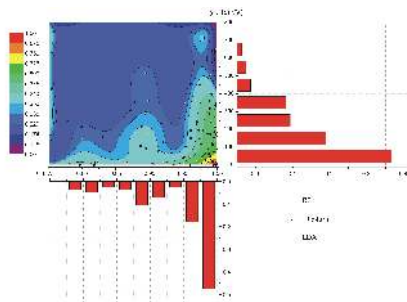


Figure 1. Diagrams $\eta-|\chi_{123}|$ for B3 type crystals calculated in the framework of LDA and histograms of distributions with respect to η (horizontal axis) and $|\chi_{123}|$ (vertical axis)

Keywords: pseudosymmetry, nonlinear optical properties, density functional theory

MS15-P26 Fluorous low-dielectric-constant materials: non-porous coordination polymers vs. metal-organic frameworks

Simona Galli¹, Alessandro Cimino^{1,2}, Carlotta Giacobbe^{1,3},
Giovanni Palmisano¹, Angelo Maspero¹, Joshua F. Ivy², Chi
Yang², Sammer Tekarli², Mohammad A. Omary²

1. Dipartimento di Scienza e Alta Tecnologia, Università dell'Insubria

2. Department of Chemistry, University of North Texas

3. ESRF, Grenoble, France.

email: simona.galli@uninsubria.it

Identifying novel low-dielectric-constant (low- κ) materials for integrated circuit (IC) use is a main concern for the microelectronics industry.

Metal-organic frameworks (MOFs) and functional non-porous coordination polymers (FN-PCPs) are studied as alternatives to currently applied low- κ dielectrics: their properties can be modulated through a sensible choice of nodes and spacers, with the added value of the high thermal stability imparted by *N*-donor struts. Compared to MOFs, FN-PCPs possess *i*) higher material density, granting a higher density of functionally-active centers; and *ii*) lower sensitivity to high- κ species, such as water ($\kappa \sim 80$), due to lack of porosity. Nevertheless, few reports, regarding exclusively MOFs, have appeared to date on dielectric properties.

Here we report on two classes of related CPs:

1. Tetrazolate-based CPs: These include FN-PCP-1 ($\text{Ag}_2(\text{FBTB})$, $\text{FBTB} = 1,4\text{-bis}-(\text{tetrazol-5-ate})\text{tetrafluorobenzene}$) and FMOF-3 ($\text{Cu}(\text{FBTB})$), which are isostructural to $\text{Ag}_2(\text{BTB})$ [1] and $\text{Cu}(\text{BTB})$ [2], respectively. As demonstrated by VT-PXRD, fluorination enhances thermal stability: FN-PCP-1 and FMOF-3 decompose in air at 260 and 400 °C, respectively (vs. 380 °C T_{dec} for $\text{Ag}_2(\text{BTB})$; 100 °C $T_{\text{phase change}}$ for $\text{Cu}(\text{BTB})$). Fluorination and lack of porosity favour water stability: contact angles up to $\sim 75^\circ$ were measured for FN-PCP-1 (vs. $\sim 50^\circ$ for $\text{Ag}_2(\text{BTB})$); FN-PCP-1 is recovered intact after 1 month exposure to water vapours while FMOF-3 undergoes a phase change after 24 h. Fluorination reduces κ_{RT} values to 2.59(3) for FN-PCP-1 and 2.44(5) for FMOF-3 (vs. 3.79(4) for $\text{Ag}_2(\text{BTB})$). After 72 h exposure to water vapours FN-PCP-1 κ increases to only 2.63(5).

2. Triazolate-based CPs: These include FMOF-1 ($\text{Ag}_2(\text{Ag}_4\text{Tz}_6)$, $\text{Tz} = 3,5\text{-bis}(\text{trifluoromethyl})\text{-1,2,4-triazolate}$) [3] and its polymorph FN-PCP-2 ($\text{Ag}_7(\text{Tz}_7)$). FMOF-1 is stable, under N_2 , up to 380 °C. DFT simulations show that both FMOF-1 and FN-PCP2 possess non-polar building blocks. Measured contact angles up to $\sim 160^\circ$ for FMOF-1 suggest superhydrophobicity. A record low- κ_{RT} is obtained from preliminary studies that remain ongoing.

Work is in progress to complete this case study and exploit other metal-ligand combinations, maintaining the

above promising properties yet increasing the thermal stability up to the ~ 450 °C needed for practical IC application.

References

- [1] A.Maspero *et al.* Inorg.Chim.Acta 2009, 362, 4340.
- [2] M.Dincă *et al.* J.Am.Chem.Soc. 2006, 128, 8904.
- [3] C.Yang *et al.* J.Am.Chem.Soc. 2007, 129, 15454.

Keywords: Powder X-ray diffraction, coordination polymers, metal-organic frameworks, low- κ dielectrics, thermal stability, hydrophobicity

MS15-P27 Prediction of isostructural series of solvatesIva Koupilová¹, Michal Hušák¹, Jan Rohlíček¹

1. Department of solid state chemistry, UCT Prague, Prague, Czech Republic

email: iva.koupilova@vscht.cz

Organic molecules can usually form crystal solvated structures with a multiple different solvents. In general, there are two possible situations how the solvate can be formed: (i) the solvate creates a new crystal structure in a new structural type by changing the space group and/or lattice parameters, or (ii) the solvate creates a crystal structure in the same space group and similar unit cell where only the molecule of solvent is changed. We call this second case as a series of isostructural solvates. Bromocriptine mesylate (BCM) forms two series of isostructural solvates. 21 new solvates of BCM were prepared in the space group $P2_1$, and three more solvates were prepared in the space group $P2_12_12_1$. In BCM's case, we found a correlation between the volume of the unit cell and the volume of the solvent's molecule. We inspired by this BCM case and we have created a general algorithm to identify more isostructural series of solvates from the Cambridge structural database (CSD). The algorithm works on the basis of similarity evaluation by comparing reduced unit cell parameters, reduced unit cell volume and space group of actualized list of solvates' groups from work van de Streek¹. The aim of this work is to confirm correlation between the change of the volume of the unit cell and the volume of the solvent's molecule and also to find a predictive model of new series of isostructural solvates.

Financial support from specific university research: MSMT No 20/2015.

- (1) van de Streek, J. *Crystengcomm* **2007**, 9, 350.

Keywords: isostructural solvates, prediction, bromocriptine mesylate

MS15-P28 Using time-resolved X-ray diffraction to test the piezoelectricity of the field-stabilized polar phase in SrTiO₃Behnam Khanbabaee¹, Carsten Richter², Erik Mehner², Juliane Hanzig², Semen Gorfman¹, Dirk C. Meyer², Ullrich Pietsch¹

1. Solid State Physics, Department of Physics, University of Siegen, Germany

2. Institute of Experimental Physics TU Bergakademie Freiberg, Germany

email: khababaee@physik.uni-siegen.de

The aim of this contribution is to test the piezoelectricity of a SrTiO₃ single crystal using stroboscopic time-resolved X-ray diffraction. Although the cubic perovskite and, hence, centrosymmetric structure of SrTiO₃ at room temperature prohibits the appearance of piezoelectricity, it is known that application of a static electric field for extended period of time (~12 hours) breaks this symmetry and creates the migration induced field stabilized polar (MFP) phase [1]. In the present work, we used time-resolved X-ray diffraction to test piezoelectricity of this phase. We started the measurements by applying a static voltage of $U_0 = 100$ V (corresponding to the electric field of 1 kV/mm) for around 12 h in order to form the MFP phase followed by changing the voltage to dynamical mode by adding a time dependent, triangular shaped AC component to the above mentioned static voltage. Then, various symmetrical and asymmetrical Bragg reflections of SrTiO₃ were scanned under applied 1 kHz triangular shape electric field. The results for the 002 reflection (see Fig. 1) clearly show the electric field induced angular shift of the Bragg peak corresponding to the MFP phase, while the position of the bulk peak was always fixed. This result indicated that the MFP is indeed piezoelectric. The variation of the Bragg position with applied periodic electric field allows estimating the piezoelectric coefficient (d_{33}), describing the longitudinal elongation in response to field applied along the crystallographic c axis (polar axis of the MFP phase). From the observed shifts of the 0 0 2 reflection, we estimated that the $d_{33} > 27.3$ pC/N which is ~10 higher than e.g. such of quartz.

[1] J. Hanzig, M. Zschornak, et al., *Phys. Rev. B* **88**, 024104 (2013), doi:10.1103/PhysRevB.88.024104

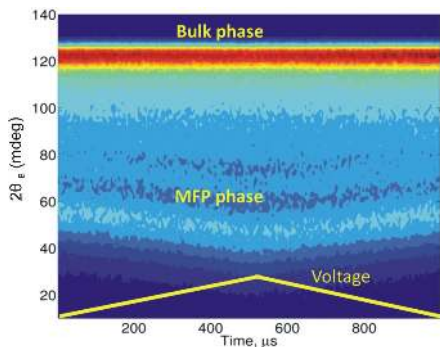


Figure 1. Time resolved X-ray diffraction 002 reflection under triangular shape 1 kHz electric field (yellow curve). The top sharp peak corresponds to the bulk and deviated weak bottom peak corresponds to MFP phase

Keywords: time-resolved X-ray diffraction, SrTiO₃, piezoelectricity

MS15-P29 Synthesis, crystal structure, spectroscopic characterization and theoretical study of Nicotinaldehyde N-phenylsemicarbazone

Rafael Mendoza-Meroño¹, Rubén Soria-Martínez¹, Santiago García-Granda¹

¹. Facultad de Química. Departamento de Química-Física y Analítica. Universidad de Oviedo

email: rafam80@gmail.com

Semicarbazones are derivative of imines compounds, which could be obtained by the condensation reaction between a ketones or aldehydes and semicarbazides. Semicarbazones exist in two tautomeric forms, keto (A) and enol (B) forms. The *keto* form acts as bidentate neutral ligand and the *enol* form can deprotonates acting as anionic ligand, making the semicarbazones versatile ligands in both neutral and anionic forms [1,2]. The coordination mode is influenced by the number and type of substituents groups; this is because the active donor sites of the ligand vary depending upon the substituents. In view of the importance of these compounds, the synthesis, crystal structure, spectroscopic characterization and theoretical study of Nicotinaldehyde N-phenylsemicarbazone have been carried out. In the first part of this study the semicarbazone molecule was synthesized and characterized by FT-IR, FT-Raman and NMR. The crystal structure was determined by X-ray single-crystal diffraction. The molecules crystallize in a P2₁/c space group and form in the crystal packing N-H...O and N-H...N hydrogen bonds forming a centrosymmetric *synthon*. Other interactions like C-H... π and π ... π stacking helps to stabilize the crystals. In the second part, the molecular geometry was optimized using DFT method and compared with the experimental data obtained from X-ray single-crystal experiment. The experimental (FT-IR) and calculated vibrational frequencies (using DFT) have been compared. The stability and charge delocalization was studied by natural bond orbital (NBO) analysis as well as the potential energy distribution (PED). Milliken population analysis on atomic charges is also calculated.

Acknowledgments: Spanish Ministerio de Economía y Competitividad (MAT2013-40950-R) and ERDF funding is acknowledged.

[1] R.Pavan, P. Maia, S.Leite, S. Defflon, V. Batista, A. (2010). *Eur J Med Chem.* **2010** 45, 1898–1905.
[2] P.Yogeeswari,P.,D. Sriram , V. Veena,, R.Kavya, R., K.Rakhra., J.Ragavendran, S.Mehta, R.Thirumugan, *Biomedicine & Pharmacotherapy.* **2005** 59, 51–55.

Keywords: Semicarbazone, single-crystal X-ray diffraction, DFT studies.

MS15-P30 Thiolate halide copper(I) 2D coordination polymers with thermochromic luminescent properties

Josefina Perles¹, Javier Troyano², Carlos Zaldo³, Félix Zamora², Salomé Delgado²

1. Laboratorio de Difracción de Rayos X de Monocristal, Servicio Interdepartamental de Investigación, Universidad Autónoma de Madrid, 28049 Madrid, Spain

2. Departamento de Química Inorgánica, Facultad de Ciencias, Universidad Autónoma de Madrid, 28049 Madrid, Spain

3. Departamento de Materiales Fotónicos, Instituto de Ciencia de Materiales de Madrid (CSIC), 28049 Madrid, Spain

email: josefina.perles@uam.es

The design of coordination compounds and, particularly, coordination polymers^{1,2} as advanced materials is one of the most exciting and promising topics in materials science. The physical properties of this type of compounds are strongly dependent on the nature of the constituents, both the metal center and the ligands used to construct the polymer in the solid state. However, the structure itself in the solid state also plays a crucial role. In the case of coordination polymers, the obtention of a flexible framework can lead to small changes in the crystal packing under different experimental conditions, which may in turn affect the properties.

Three new 2D polymeric copper(I) thiolates with formula $[\text{Cu}_2\text{X}(\text{HT})_2]_n$ (X= Cl, Br, I; HT= 4-mercaptophenol) have been synthesised by solvothermal procedures. The crystal structures of these coordination polymers have been solved by single crystal X-ray diffraction. They display a similar layered structure with the hydroxyl groups from the HT ligands joining the polymeric sheets by hydrogen bonds.

These compounds present a strong orange emission at room temperature. A reversible thermochromic effect is observed on cooling, stronger in the iodine derivative. The emission changes from orange, at room temperature, to green at lower values. Photoluminescence in these coordination polymers has been studied at different temperatures, and the disappearance of the lower energy band is observed with decreasing temperature, together with an increase in the intensity of the more energetic band. Changes in the luminescent properties are associated with the structural modifications observed in the crystal structures solved both at room temperature and at 110 K.

1-Kitagawa, S.; Noro, S.: *Comprehensive Coordination Chemistry*, 2004; Vol. 7.

2-Batten, S. R.; Neville, S. M.; Turner, D. R.: *Coordination polymers: Design, analysis and application*; Royal Society of Chemistry, 2008.

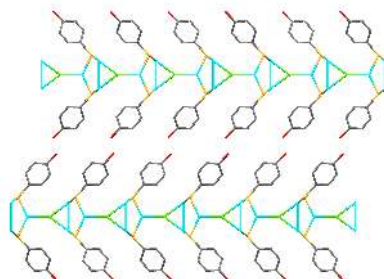


Figure 1. Layered structure of $[\text{Cu}_2\text{Cl}(\text{HT})_2]_n$ at room temperature viewed along the c axis. Hydrogen atoms have been omitted for clarity.

Keywords: coordination compounds, photoluminescence, framework flexibility

MS15-P31 High-temperature synthesis of the new strontium borogermanate $\text{Sr}_{3-x/2}\text{B}_{2-x}\text{Ge}_{4+x}\text{O}_{14}$ ($x = 0.32$)

Benedikt Petermueller¹, Huppertz Hubert¹

¹ Institute of General, Inorganic and Theoretical Chemistry, Leopold-Franzens-University Innsbruck, A-6020 Innsbruck, Austria

email: Benedikt.Petermueller@student.uibk.ac.at

Benedikt Petermüller^{a}, Hubert Huppertz^a*

^aInstitute of General, Inorganic and Theoretical Chemistry, Leopold-Franzens-University Innsbruck, A-6020 Innsbruck, Austria

The strontium borogermanate $\text{Sr}_{3-x/2}\text{B}_{2-x}\text{Ge}_{4+x}\text{O}_{14}$ ($x = 0.32$) [1] (Figure 1) was synthesized by high-temperature solid-state reaction of SrO , GeO_2 , and H_2BO_3 in a NaF/KF flux system using platinum crucibles. The structure determination revealed that $\text{Sr}_{3-x/2}\text{B}_{2-x}\text{Ge}_{4+x}\text{O}_{14}$ ($x = 0.32$) crystallizes in the trigonal space group $P321$ (No. 150) with the parameters $a = 800.7(2)$ and $c = 488.8(2)$ pm, with $R1 = 0.0281$, $wR2 = 0.0671$ (all data), and $Z = 1$. The crystal structure of $\text{Sr}_{3-x/2}\text{B}_{2-x}\text{Ge}_{4+x}\text{O}_{14}$ ($x = 0.32$) consists of distorted SrO_8 cubes, GeO_4 octahedra, GeO_4 tetrahedra, and BO_4 tetrahedra. In addition to the structural investigations, Raman and IR-spectroscopic investigations were carried out. Taking into account that $\text{Sr}_{3-x/2}\text{B}_{2-x}\text{Ge}_{4+x}\text{O}_{14}$ ($x = 0.32$) is isotypic to $\text{Ca}_3\text{Ga}_2\text{Ge}_2\text{O}_{14}$ [2,4] this compound represents the first boron-containing member of the family of langasites ($\text{La}_3\text{Ga}_2\text{SiO}_{14}$) possessing the general composition $\text{A}_3\text{XY}_2\text{Z}_2\text{O}_{14}$ [4]. This class of compounds is highly interesting concerning their piezoelectric properties because nearly all 140 known member crystallize in the trigonal noncentrosymmetric space group $P321$. [5, 6] As several members of the langasite family are already promising piezoelectric materials, the herein reported compound leads to a wider range of compositions which might lead to better piezoelectric properties of potential materials.

[1] B. Petermüller, L. L. Petschnig, K. Wurst, G. Heymann, H. Huppertz, *Inorg. Chem.* 53, 9722 (2014)

[2] E. L. Belokoneva, M. A. Simonov, A. V. Butashin, B. V. Mill, N. V. Belov, *Dokl. Akad. Nauk SSSR* 255, 1099 (1980)

[3] E. L. Belokoneva, N. V. Belov, *Dokl. Akad. Nauk SSSR* 260, 1363 (1981)

[4] B. V. Mill, E. L. Belokoneva, T. Fukuda, *Russ. J. Inorg. Chem.* 43, 1168 (1998)

[5] B. V. Mill, B. A. Maksimov, Yu. V. Pisarevskii, N. P. Danilova, A. Pavlovskaya, S. Werner, J. Schneider, *Kristallografiya* 49, 60 (2004)

[6] H. Ohsato, T. Iwataki, H. Morikoshi, *Trans. Electr. Electron Mater.* 13, 51 (2012)

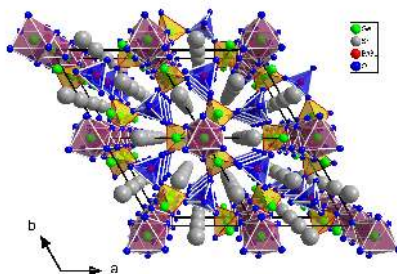


Figure 1. Crystal structure of $\text{Sr}_{3-x/2}\text{B}_{2-x}\text{Ge}_{4+x}\text{O}_{14}$ ($x = 0.32$) down $[001]$ exhibiting channels created through the GeO_4 -B/ GeO_4 network an occupied by Sr atoms (grey)

Keywords: Piezoelectricity, Langasite, Synthesis

MS15-P32 A high-temperature molecular ferroelectric Zn/Dy complex exhibiting single-ion magnet behavior and lanthanide luminescence

Jerome Rouquette¹, Long Jerome¹, Thibaud Jean Marc¹, Ferreira A.S. Rute², Donnadieu Bruno¹, Carlos D. Luis², Vieru Veaceslav³, Chibotaru F. Liviu³, Konczewicz Leszek⁴, Haines Julien¹, Guari Yannick¹, Larionova Joulia¹

1. ICGM-CNRS/Univ. Montpellier/ENSCM, Montpellier, France
2. Physics Department and CICECO, University of Aveiro, 3810-193, Aveiro
3. Theory of Nanomaterials Group and INPAC, Katholieke Universiteit Leuven, Celestijnenlaan, 200F, Heverlee, B-3001, Belgium
4. Laboratoire Charles Coulomb, UMR 5221, Univ. Montpellier, France

email: jerome.rouquette@um2.fr

Multifunctional molecular ferroelectrics are exciting materials synthesized using molecular chemistry concepts, which may combine a spontaneous electrical polarization, switched upon applying an electric field, with another physical property. Herein we report an example of a high temperature ferroelectric material based on a chiral Zn²⁺/Dy³⁺ complex exhibiting Dy³⁺ luminescence, optical activity and magnetism. We investigate the correlations between the electric polarization and the crystal structure and between the low temperature magnetic slow relaxation and the optical properties [1].

[1] J. Long, J. Rouquette, J.-M. Thibaud, R.A.S. Ferreira, L.D. Carlos, B. Donnadieu, V. Vieru, L.F. Chibotaru, L. Konczewicz, J. Haines, Y. Guari, J. Larionova, A high-temperature molecular ferroelectric zn/dy complex exhibiting single-ion-magnet behavior and lanthanide luminescence, *Angewandte Chemie* (International ed. in English), 54 (2015) 2236-2240.

Keywords: Keywords: molecular ferroelectric, single ion magnet, structure/properties relationships

MS15-P33 Structural characterisation of stoichiometric and off-stoichiometric Cu₂ZnSn(S_xSe_{1-x})₄ by neutron diffraction

Galina Gurieva¹, Laura Elisa Valle-Rios², Kai Neldner¹, Daniel M. Többen¹, Stefan Zander¹, Alexandra Franz¹, Susan Schorr^{1,2}

1. Helmholtz-Zentrum Berlin für Materialien und Energie, Department of Crystallography
2. Freie Universitaet Berlin, Institute of Geological Sciences, Berlin, Germany

email: galina.gurieva@helmholtz-berlin.de

Quaternary Cu₂ZnSn(S_xSe_{1-x})₄ compounds are promising semiconductor materials for absorber layer in thin film solar cells due to direct band gap in the range 1-1.5 eV and high absorption coefficient (>10⁴ cm⁻¹) [1,2]. All constituents of these films are abundant, low cost and non-toxic. The highest conversion efficiency of Cu₂ZnSn(S_xSe_{1-x})₄ solar cell is till now 12.6% [3]. In spite of previously reported stannite type structure for CZTSe, CZTS and CZTSe crystallize both in the kesterite type structure (space group) [4,5]. A differentiation between the isoelectronic cations Cu⁺ and Zn²⁺ and consequently kesterite and stannite type structures is not possible using X-ray diffraction due to their similar scattering factors. But neutrons diffraction can solve this problem; the coherent scattering lengths are sufficiently different for these cations. It was shown by this method that both Cu₂ZnSnS₄ and Cu₂ZnSnSe₄ occur in the kesterite structure [6]. A "detailed" structural analysis of stoichiometric as well as off-stoichiometric Cu₂ZnSn(S_xSe_{1-x})₄ powder samples grown by solid state reaction, was performed by neutron diffraction. Rietveld refinement of neutron diffraction data using the FullProf suite software [7] lead to accurate values of lattice constants and site occupancy factors. From the latter the average neutron scattering length was derived which has given insights into the cation distribution within the crystal structure of stoichiometric as well as off-stoichiometric samples from Cu₂ZnSn(S_{1-x}Se_x)₄ solid solution with different x values. The correlated information about changes in lattice parameters and cation site occupancies, details on the existing intrinsic point defects and their amounts obtained by neutron diffraction will be discussed. Acknowledgments: Financial supports from IRSES PVICEKEST 269167 and KESTCELLS 316488, FP7-PEOPLE-2012 ITN, Multi-ITN is highly appreciated. [1] J.M. Raulot, et al., *J. Phys. Chem. Solids* **66** (2005) 2019. [2] P.A. Fernandes et al., *Phys. Status Solidi C* **7** (2010) 901. [3] Wang, et al., *Adv. Energy Mater.* (2014), **4**, 1301465. [4] S.Schorr, *Solar Energy Materials and Solar Cells*, **95** (2011)1482. [5] S. Schorr, H.-J. Hoebler, and M. Tovar, *Eur. J. Mineral.* **19**, 1 (2007). [6] Siebentritt, S. and Schorr, S. *Prog. Photovolt: Res. Appl.*, **20**, 512 (2012) [7] Juan Rodriguez-Carvajal and Thierry Roisnel, www.ill.eu/sites/fullprof/

Keywords: CZTSSe, neutron diffraction, kesterite

MS15-P34 Solid state molecular packing and photoluminescence of platinum complexes based on 1,5-naphthyridin-4-olate ligands

Chin-Ti Chen^{1,2}, Anurack Poloek^{1,3,4}, Chieh Wang², Chiao-Wen Lin¹, Chao-Tsen Chen⁴

1. Institute of Chemistry, Academia Sinica

2. Department of Applied Chemistry, National Chiao Tung University

3. Nano Science and Technology Program, TIGP, Academia Sinica

4. Department of Chemistry, National Taiwan University

email: chintchen@gate.sinica.edu.tw

Four heteroleptic platinum complexes, FPtdmaND, FPtOPhND, FPtCzND, and FPtpxzND, have different molecular packing patterns, which affect their photoluminescence (PL) in solution and in solid state or doped thin film (of PS, CBP, 4P-NPB). Interestingly, these platinum complexes exhibited varied emission from greenish yellow to orange red wavelengths due to their monomeric and aggregate/excimeric emission, which is either substituent of 1,5-Naphthyridin-4-olate ligand (ND), concentration of dopant, or host material dependent.

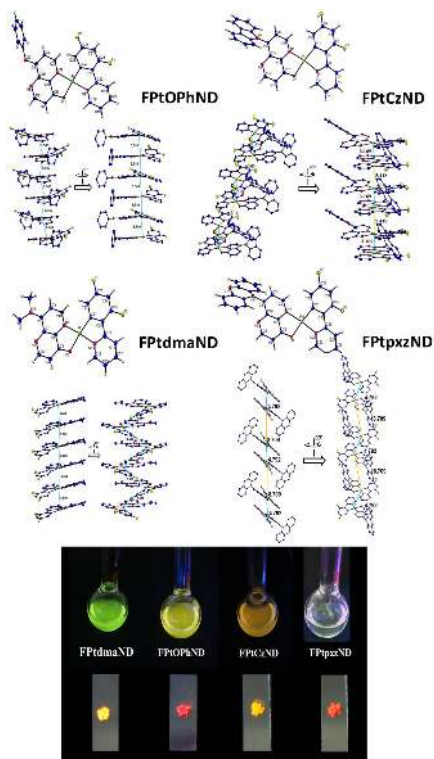


Figure 1. X-ray crystal molecular packing structure and photoluminescence image of four platinum complexes

Keywords: Molecular packing, Photoluminescence, Platinum complexes

MS15-P35 Relationship between the composition, structural parameters and properties of single-crystal KDP with nano-titania

Galina M. Kuzmicheva¹, Olesya I. Timaeva¹, Elena N. Domoroshchina¹, Vadim V. Grebeney², Anna V. Kosinova³

1. Department of Materials Science and Technology of Functional Materials and Structures, State University of Fine Chemical Technologies of M. V. Lomonosov, 119571, Moscow, Russia
2. Institute of Crystallography, Russian Academy of Sciences, 119333, Moscow, Russia
3. Institute for Single Crystals NAS of Ukraine, 61001, 60 Lenin Ave. Kharkov, Ukraine

email: galina_kuzmicheva@list.ru

Development perspectives for new nonlinear optical elements (NLO) based on combinations of inorganic matrix with various inorganic functional nanoparticles are discussed now. The presence of nano-TiO₂ in a crystalline matrix of KDP (KH₂PO₄) leads to increase the magnitude of cubic nonlinear susceptibility, changes the sign of the nonlinear refractive response and increases the efficiency of second harmonic generation of composite system KDP:TiO₂ (V.Ya. Gayvoronsky et al. 2013). The aim of this paper is to establish the relationship between composition, structural parameters and dielectric properties of composites KDP:TiO₂.

X-ray diffraction study of the initial samples with nano-TiO₂ (phase analysis, the sizes of coherent scattering regions - *D*) indicated the presence of anatase (sample 1; *D* = 50 (4) Å) and η-TiO₂ (sample 3; *D* = 38 (2) Å) (sulfate method) and anatase (sample 2; *D* = 150 (8) Å) (chloride method) at them. Pure KDP crystals and KDP:TiO₂ (composites I, II, III with incorporated TiO₂ nanoparticles from the samples 1, 2 and 3, correspondingly) were grown by the temperature reduction method onto point seed. According to X-ray microanalysis, the sulfur content is greater in the sample 3 (4.37–7.58 wt %) and composite III (11.99 wt %) as compared with sample 1 (2.17–3.73 wt %) and composite I (4.54 wt %). The samples from growth sectors {100} and {101} of KDP and KDP:TiO₂ crystals were cut for the investigation.

Analysis of the results of X-ray single crystal study revealed the most significant structural changes in the composite III ({100}): a very small value of O–H distance and a short distance P–O compared with the same distances in the structures of KDP and composites I, II, vacancies in the K¹⁺ sites and located ions Ti⁴⁺ in the vicinity of the K¹⁺ positions. It was established that the general composition of the composite III ({100}) can be described as (K_{0.950(1)}l_{0.050})(Ti_{0.052(2)})(H¹⁺_{2–x}l_x)(PO₄)_{3–y}(SO₄)_{1–y}l_y (l – vacancy).

It was established that the magnitude of dielectric permittivity (ε') for KDP and KDP:TiO₂ is different depending on the growth sectors (ε' {101} > ε' {100}). It is greater for composite II in comparison with composite I and composite III ({100}) has the smallest value of ε', which correlates with the interatomic distance O–H.

This work was carried out as a part of a state task of the Ministry of Education and Science of Russian Federation (№ 4.745.2014/K; 2014–2016).

Keywords: KDP: nano-TiO₂, structure, dielectric properties

MS15-P36 Absolute structure of (E)-2,2'-[3-(2-Nitrophenyl)prop-2-ene-1,1-diyl]bis (3-hydroxy-5,5-dimethylcyclohex-2-en-1-one)

Joo Hwan Cha¹, Jae Kyun Lee², Yong Seo Cho²

1. Advanced Analysis Center, Korea Institute of Science & Technology, Hwarangro 14-gil, Seongbuk-gu, Seoul, South Korea
2. Center for Neuro-Medicine, Korea Institute of Science & Technology, Hwarangro 14-gil, Seongbuk-gu, Seoul, South Korea

email: jhcha@kist.re.kr

Herewith we present the crystal structure of (E)-2,2'-[3-(2-nitrophenyl)prop-2-ene-1,1-diyl]bis(3-hydroxy-5,5-dimethylcyclohex-2-en-1-one) (**A**) [1], (E)-2,2'-[3-(4-nitrophenyl)prop-2-ene-1,1-diyl]bis(3-hydroxy-5,5-dimethylcyclohex-2-en-1-one) (**B**) [2]. In the compound (**A**), C₂₅H₂₉N₂O₆, each of the cyclohexenone rings adopts a half-chair conformation. Each of the pairs of hydroxy and carbonyl O atoms are oriented to allow for the formation of intramolecular O—H...O hydrogen bonds, which are typical of xanthene derivatives. The nitro group is rotationally disordered over two orientations in a 0.544 (6):0.456 (6) ratio. In the crystal, weak intermolecular C—H...O hydrogen bonds link molecules into layers parallel to the *ab* plane. The compound (**B**), each of the cyclohexenone rings adopts a half-chair conformation. The hydroxy and carbonyl O atoms face each other and are oriented to allow for the formation of two intramolecular O—H...O hydrogen bonds. In the crystal, weak C—H...O hydrogen bonds are formed between molecules, generating a two-dimensional supramolecular structure.

[1] Cha, J. H., Kim, Y. H., Min, S. J., Cho, Y. S. & Lee, J. K. (2011). *Acta Cryst.* **E67**, o3153.

[2] Cha, J. H., Cho, Y. S., Lee, J. K., Park, J. H. & Sato, H. (2012). *Acta Cryst.* **E68**, o2510.

Keywords: X-ray crystallography of organic compounds; xanthene; absolute structure determination

MS15-P37 Pressure and temperature dependence of charge transfer behaviour of the κ -(BEDT-TTF)₂Cu₂(CN)₃ organic conductor.

Alexey V. Kuzmin¹, Khasanov S. Salavat¹, Shibaeva P. Rimma¹

¹ Institute of Solid State Physics, Chernogolovka, Russia

email: kuzminav@issp.ac.ru

Since 1982 when the first metallic compound based on adjusted π -conjugated donor BEDT-TTF (ET) molecules has been found the interest to organic complexes with quasi-2D electronic structure has been only increasing. The κ -type ET_xX salts with polymer-like inorganic anions X=Cu₂(CN)₃ deserved a great attention due to their superconducting properties and spin-frustration possibilities within the anisotropic triangular sublattice of the face-to-face pair of ET molecules. The origin of this superconductivity can be found in quantum spin liquid and caused by spin interaction in half-filled triangular lattice in this type Mott insulator. In the pressure-temperature phase diagram of the κ -(BEDT-TTF)₂Cu₂(CN)₃ crystals, a Mott insulator (spin liquid), metal (Fermi liquid) and superconducting states converge near 3.5kbar-4K point [1]. We investigated the structure of the untwinned crystal samples at low temperatures and elevated pressures. X-ray diffraction data were collected in the 90K - 300K temperature region at ambient pressure and from ambient to 8 kbars pressure at room temperature using Oxford Diffraction Gemini-R diffractometer with Atlas CCD detector (MoK α_1 =0.71073Å, graphite monochromator, ω -scan method), Diacell Bragg-(S) Plus diamond anvil cell for high pressure experiments and Oxford CryoJet Systems to provide the temperature control during experiments. In this report we analyze the crystal structure transformations and modifications of the triangular spin lattice parameters due to high pressure in comparison with the temperature changes. The values of transfer integrals t' and t were calculated by site-energy correction and band-fitting methods within density functional theory. The difference between results of these two approaches is discussed.

The reported study was supported by RFBR, grant No14-02-01150

References

[1] Y. Kurosaki, Y. Shimizu, K. Miyagawa, K. Kanoda, and G. Saito, Phys. Rev. Lett. 95, 177001 (2005).

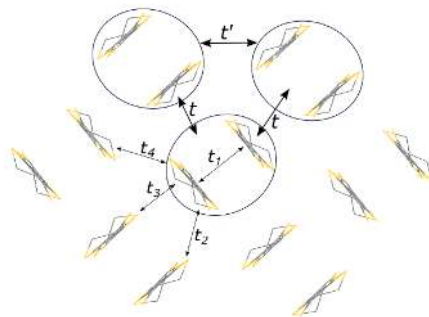


Figure 1. Dimer of ET molecules as an unit of κ -type salts arrangement and transfer integrals.

Keywords: crystallography, high pressure, organic conductive materials

MS15-P38 Influencing Rh(I) dicarbonyl and phosphine complexes with substituted enaminoketonesGertruida J.S. Venter¹, Gideon Steyl², Andreas Roodt¹

1. Department of Chemistry, University of the Free State, Bloemfontein, South Africa 9301
2. Golder Associates Pty. Ltd., Milton, Queensland, Australia 4064

email: VenterGJS@ufs.ac.za

X-PhonyH (X = aromatic substituents; PhonyH = 4-(phenyl-amino)pent-3-en-2-one) compounds belong to the group of enaminoketones. These compounds contain nitrogen and oxygen donor atoms as well as an alkene functionality (see Figure 1), and as such these electron-rich compounds are of interest in various areas, including application as liquid crystals [1], in fluorescence studies [2], the medical field [3,4] and with significant potential in homogeneous catalysis [5].

This study is therefore concerned with the synthesis of PhonyH derivatives as ligand system and the influence of halide and aryl substitution on such ligands with regard to rhodium(I) complex formation. A range of crystal structures of the (i) free ligands, (ii) complexes of the type $[\text{Rh}(\text{X-Phony})(\text{CO})_2]$ (X-Phony = 4-(phenyl-amino)pent-3-en-2-onato derivatives) [6], and (iii) $[\text{Rh}(\text{X-Phony})(\text{CO})(\text{PPh}_3)]$ (substitution of a CO group in (ii) by PPh_3) complexes [7,8] as catalyst precursors will be discussed. Furthermore, the exchange between free and coordinated phosphine as indicated through nuclear magnetic spin transfer techniques will be highlighted.

References

- [1] W. Pyżuk, A. Krówczyński and E. Górecka, *Mol. Cryst. Liq. Cryst.* **237** (1993), 75–84.
- [2] M. Xia, B. Wu and G. Xiang, *J. Flu. Chem.* **129** (2008), 402–408. [3] H.Y. Tan, W.K. Loke, Y.T. and Tan, N.-T. Nguyen, *Lab Chip* **8** (2008), 885–891.
- [4] W.J. Fanshawe, L.S. Crawley, S.R. Safir, G.E. Wiegand and E.C. Cooley, Substituted enaminoketones (1974), US3997530 (Patent).
- [5] V.A. Nair, M.M. Suni and K. Sreekumar Proc. *Indian Acad. Sci. (Chem. Sci.)* **114** (2002), 481–486.
- [6] G.J.S. Venter, G. Steyl and A. Roodt, *J. Coord. Chem.* **67** (2014), 176–193.
- [7] G.J.S. Venter, G. Steyl and A. Roodt, *Z. Kristallogr.* **228** (2013), 410–412.
- [8] G.J.S. Venter, G. Steyl and A. Roodt, *Acta Cryst. E* **65** (2009), m1606–m1607.

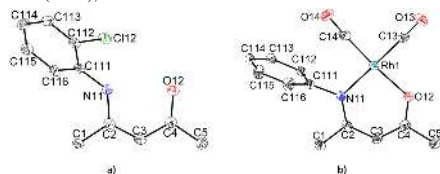


Figure 1. Illustration of a) 4-(2-chloro-phenyl-amino)pent-3-en-2-one (2-Cl-PhonyH) and b) dicarbonyl-[4-(phenylamino)pent-3-en-2-onato]-rhodium(I) $[\text{Rh}(\text{Phony})(\text{CO})_2]$.

Keywords: rhodium, enaminoketone, catalysis, exchange

MS15-P39 High-temperature behavior of lithium peroxide Li_2O_2 Yoshitaka Matsushita¹, Motoharu Imai², Satoshi Kawada¹

1. Chemical Analysis & X-ray Diffraction, Materials Analysis Station, National Institute for Materials Science
2. Materials Development Group, Superconducting Properties Unit, Environment and Energy Materials Division, National Institute for Materials Science

email: MATSUSHITA.Yoshitaka@nims.go.jp

Lithium peroxide Li_2O_2 is one of the well-known classic compound. And also, Li_2O_2 is very important compound for Li-air batteries,² because the overall reaction in a Li– O_2 cell is the oxidation of lithium metal to Li_2O_2 upon discharge and its subsequent reduction upon charge. Even so, the accurate crystal structure of this compound had not been solved. Recently, we solved its crystal structure using powder synchrotron x-ray diffraction data, and its space group was $\text{P6}_3/\text{mmc}$.

For the application, we must know the details of thermal behavior of this compound to avoid any troubles on the battery. Therefore, in this study, we examined this compound using TG-DTA and high-temperature XRD in our lab.

Keywords: Lithium battery compound, Li_2O_2

MS15-P40 New luminescent materials based on ortho-phenylenediboronic acid – from crystal engineering to spectroscopic properties

Katarzyna N. Jarzemska¹, Radosław Kamiński¹, Krzysztof Durka², Marcin Kubiś³, Krzysztof Nawara⁴

1. Czocharński Laboratory of Advanced Crystal Engineering, Biological and Chemical Research Centre, Department of Chemistry, University of Warsaw, Żwirki i Wigury 101, 02-089 Warsaw, Poland

2. Department of Chemistry, Warsaw University of Technology, Noakowskiego 3, 00-664 Warsaw, Poland

3. Department of Chemistry, University of Warsaw, Pasteura 1, 02-093 Warsaw, Poland

4. Institute of Physical Chemistry, Polish Academy of Sciences, Kasprzaka 44/52, 01-224 Warsaw, Poland

email: katarzyna.jarzemska@gmail.com

Arylboronic acids have already found many applications in diverse areas of chemical science, such as organic synthesis, catalysis or crystal engineering. Quite recently we have worked on para- and ortho-phenylenediboronic acids.^{1,2} In the present study, we focus our attention on a new class of adducts based on the latter compound.

It occurred that a simple one-pot reaction of ortho-phenylenediboronic acid with 8-hydroxyquinoline results in a new photoactive species. The reaction proceeds smoothly even in solvent-free conditions (mechanochemistry) and allows obtaining many modifications of such complexes (regarding both the acid and N-donor compound) in high yield. It was possible to crystallize and structurally characterize many of these systems, including several fluorinated derivatives and various solvatomorphs.

Additionally, luminescent properties of the studied complexes were investigated using the time-resolved spectroscopy, both in solution and in the solid state. The recorded emission spectra indicate the possibility of tuning the colour of the emitted light in the visible regime (from blue to orange). The determined lifetimes are of nanosecond order (9 – 15 ns), which suggests that the main contribution to the emitted light comes from the fluorescence process (singlet-to-singlet transition) what is further supported by the DFT calculations. Theoretical results show also that the charge transfer processes occur mostly in the quinoline ring fragment. The emission quantum yields determined in solution are in the range of 10 to 30%. The lifetimes and quantum yield values are highly dependent on the number of fluorine substituents in the acidic part of the molecule. The more the F-substituents present, the lower the corresponding values.

[1] K. Durka, K. N. Jarzemska, R. Kamiński, S. Luliński, J. Serwatowski, K. Woźniak *Cryst. Growth Des.* **2012**, *12*, 3720.

[2] K. Durka, K. N. Jarzemska, R. Kamiński, S. Luliński, J. Serwatowski, K. Woźniak, *Cryst. Growth Des.* **2013**, *13*, 4181.

Keywords: phenylenediboronic acids, quinoline derivatives, crystal engineering, fluorescence

MS16. Physical properties through lattice distortions: structure of perovskites & Co studied by electron microscopy and diffraction

Chairs: Jerome Rouquette, Artem Abakumov

MS16-P1 Molecular dynamics modeling of radiation stability of Ca(Zr,Ti,Sn)O₃ perovskites

Nikolai N. Eremin¹, Nikolai Protasov¹, Oleksii Hrehchanivskyi²

1. Moscow State University, Geological Faculty

2. Institute of Geochemistry, Mineralogy, and Ore Formation, National Academy of Sciences of Ukraine

email: neremin@mail.ru

The aim of this work was to investigate the relation between the radiation stability and the composition of Ca(Zr,Ti,Sn)O₃ solid solution using method of molecular dynamics (MD). This compound with perovskite structure (space group *Pbnm*) is one of the promising matrices for utilization of high level radioactive waste. Note that a new mineral *lakargiite*, which represents the Ca(Zr,Ti,Sn)O₃ solid solution with the maximal molar fraction $x(\text{CaZrO}_3) = 0.93$ and maximal fractions $x(\text{CaTiO}_3) = 0.22$ and $x(\text{CaSnO}_3) = 0.20$, was registered in 2007. Our original approach, described in [1] makes it possible to simulate the solid solutions using representative supercell of limited size with optimal atomic distribution. Thus, for MD simulation we used a supercell with different compositions with sizes 310×210×315 Å, which contains 1.4 million atoms with a maximally disordered distribution of Zr, Ti, and Sn. As an analog of the recoil atom the knocked out Th atom with energy of 20 keV was used. After the formation of the atomic displacement cascade at instant $t=0.71$ ps the structure starts to be "restored" and displaced atoms partially return to their sites or equivalent crystallographic sites. At the end of the simulation ($t=20$ ps), the total number of Frenkel pairs is minimal (figure 1). In contrast to some other tested materials defects in Ca(Zr,Ti,Sn)O₃ are mainly of the point character, which indicates the high stability of this solid solution to the radioactive effect. We evaluated parameter a , which characterized susceptibility to amorphization of material under radiation damage. This parameter numerically equal to a part of the energy of Th atom, which is consumed for the formation of Frenkel pairs in a cascade of displaced atoms. It was shown that the dependence of a -parameter on the solid solution composition is lowest for Sn-Zr compositions, whereas Ti-riched compositions exhibit poorer performance. Thus the radiation stability of Sn-Zr-riches matrices can be of unquestionable interest

Acta Cryst. (2015). **A71**, s334

Keywords: CaO–La₂O₃–TiO₂ ternary system, Structure relations, Perovskites, X-Ray powder diffraction, Rietveld refinement

MS16-P3 Sol–gel synthesis of double perovskite quaternary tellurium-containing metal oxides: Ba₂NiTeO₆, Ba₂CoTeO₆

Marko Nuskol¹, Mirjana Bijelić², Suraj Mal¹, Jasminka Popović¹, Željko Skoko², Igor Đerd¹

1. Division of Materials Physics, Ruđer Bošković Institute, Bijenička cesta 54, 10 000 Zagreb

2. Department of Physics, Faculty of Science, University of Zagreb, Bijenička cesta 32, 10 000 Zagreb, Croatia.

email: mnuskol@gmail.com

Interest in double perovskite A₂B'B''O₆ structures comes from the discovery of its colossal magnetoresistance properties exhibited at room temperature by Sr₂FeMoO₆.¹ Later it was discovered that perovskites can also act as electrode materials in solid oxide fuel cells (SOFCs),^{2,3} and transducers and memories,^{4,5} indicating why it is important to invest time to fully understand the nature of their physical and chemical characteristics.

Highly crystalline double perovskite Ba₂NiTeO₆ and Ba₂CoTeO₆ have been prepared via novel sol-gel route using citric acid as chelating agent. Both materials have been studied by X-ray diffraction (XRD), scanning electron microscope (SEM), transmission electron microscopy (TEM), and SQUID magnetic measurements. As obtained XRD patterns are carefully analyzed by the Rietveld method using programs X'Pert Highscore Plus and FULLPROF.^{6,7}

It was found that at room temperature Ba₂NiTeO₆ crystallizes in space group *R*-3*m* with *a* = 5.7965(4) Å, *c* = 28.600(3) Å. Ba₂CoTeO₆ has been refined in the space group *R*-3*m*; *a* = 5.8003(2) Å, *c* = 14.2672(5) Å are showing trigonal perovskite structure. Average crystallite size is 44 nm for Ba₂NiTeO₆ and 104 nm for Ba₂CoTeO₆, respectively.

We acknowledge financial support from the Unity through Knowledge Fund (www.ukf.hr) of the Croatian Ministry of Science, Education and Sports (Grant Agreement No. 7/13).

1. K. I. Kobayashi, T. Kimura, H. Sawada, K. Terakura and Y. Tokura, *Nature*, 1998, **395**, 677.

2. B. C. H. Steele, A. Heinzel, *Nature*, 2001, **414**, 345.

3. A. J. Jacobson, *Chem. Mater.*, 2010, **22**, 660-674.

4. M. E. Lines and A. M. Glass, *Oxford University Press*, 1977.

5. Y. Tokura, *Journal of Magnetism and Magnetic Materials*, 2007, **310**, 1145-1150.

6. HighScore Plus, X-ray diffraction software for phase identification, semi-quantitative phase analysis, pattern treatment, profile fitting and more, PANalytical Company.

7. J. Rodriguez-Carvajal, "FULLPROF: A Program for Rietveld Refinement and Pattern Matching Analysis", *Abstracts of the Satellite Meeting on Powder Diffraction of the XV Congress of the IUCr*, France, 1990, p. 127.

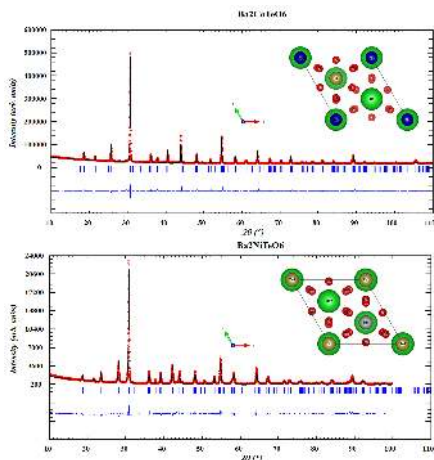


Figure 1. XRD Refinement for a) $\text{Ba}_{0.5}\text{CoTeO}_6$ and b) $\text{Ba}_{0.5}\text{NiTeO}_6$ made by FULLPROF program. Inset is 3D visualization program for structural models made by Vesta software.

Keywords: double perovskite, sol-gel synthesis, XRD refinement

MS16-P4 Phase transitions in relaxor ferroelectric materials with tungsten bronze type structures

Siegbert Schmid¹, Thomas A. Whittle¹

¹. School of Chemistry, The University of Sydney, Sydney NSW 2006, Australia

email: siegbert.schmid@sydney.edu.au

Ferroelectric materials are essential for modern electronic applications, from consumer electronics to sophisticated technical instruments. Relaxor ferroelectric materials provide the advantage of high dielectric constants over broad temperature ranges not seen in traditional ferroelectrics. Tungsten bronze type compounds have been shown to display a variety of industrially relevant optical and electronic properties amongst others. There is a fundamental relationship between the physical properties displayed by ferroelectrics and the crystal structures in which they form. Of particular interest are compositions and temperatures near phase transition. These are important because near phase transitions, particularly morphotropic phase transitions, physical properties are often dramatically enhanced.^{1,2} This work focuses on the structural investigation of tungsten bronze type relaxor ferroelectric materials in the system $\text{Ba}_{1-x}\text{Sr}_x\text{Ti}_{1-y}\text{Zr}_y\text{Nb}_y\text{O}_{15}$ ($0 \leq x \leq 3$; $0 \leq y \leq 1$). A combination of X-ray, neutron (ToF and constant wavelength) and electron diffraction were employed to map the room temperature phase diagram. In addition, morphotropic phase boundary compositions were determined accurately. Variable temperature synchrotron X-ray diffraction studies were utilised to further explore the phase diagram for non-ambient conditions. Temperature dependent phase transitions were determined and the relationship between composition and transition temperature analysed. Structural models used in this work resulted from Rietveld refinements against powder diffraction data. This work will shed light on new lead free relaxor ferroelectric materials.

1. Ahart, M.; Somayazulu, M.; Cohen, R. E.; Ganesh, P.; Dera, P.; Mao, H.-k.; Hemley, R. J.; Ren, Y.; Liermann, P.; Wu, Z. *Nature* **2008**, *451*, 545.

2. Pandey, D.; Singh, A. K.; Baik, S. *Acta Crystallogr A* **2008**, *64*, 192.

Keywords: tungsten bronze type structures, phase transitions, relaxor ferroelectrics

MS16-P5 Synthesis and structural chemistry
of cation ordered double perovskite
Ba₃Fe₂TeO₉ and Sr₃Fe₂TeO₉ via novel sol
– gel route

Suraj Mal¹, Jasminka Popović¹, Marko Nuskol¹, Željko Skoko²,
Mirjana Bijelić², Gordana Duković³, Igor Djerđ¹

1. Division of Materials Physics, Ruder Bošković Institute, Bijenička 54, 10000 Zagreb, Croatia
2. Department of Physics, Faculty of Science, University of Zagreb, Bijenička 32, 10000 Zagreb, Croatia
3. Department of Chemistry and Biochemistry, University of Colorado Boulder, 215 UCB Boulder, CO 80309, USA

email: kaswan.suraj@gmail.com

The term “perovskite” having general formula ABX₃, can accommodate a wide variety of elements with the advantage of manipulation in stoichiometry for advanced technologies including magnetism, dielectric behavior, conductivity or even multiferroic behavior. The stoichiometric changes can lead to obtain double perovskite with general formula A₂B'B''O₆ which are widely studied so far [1-3], where six coordinate sites are occupied by B' and B'', while 12-coordinate sites are occupied by A cation. Additionally another interesting class of multiferroic compounds with more complex geometry (A₃B'2B''O₉) have been investigated (Sr₃Fe₂MoO₉ and Sr₃Fe₂UO₉) and reported with strong ferromagnetic properties with TC well above room temperature [4-5]. The major drawback while synthesizing above mentioned metal oxides is the tedious solid state synthesis which require high temperature calcination and more time for phase purity. Here we report a successful synthesis of double perovskite Ba₃Fe₂TeO₉ and Sr₃Fe₂TeO₉ by novel environmental friendly ‘sol-gel’ process using citric acid as complexing medium followed by calcination step. Both compounds have been studied by powder X-ray diffraction (Rietveld), transmission electron microscopy (TEM), scanning electron microscopy (SEM) and magnetic measurements. At room temperature, the crystal structure of Ba₃Fe₂TeO₉ is hexagonal, space group P6₃/mmc (194), with *a* = 5.7665, *c* = 14.2024 Å; while Sr₃Fe₂TeO₉ the crystal structure is cubic, with space group Pm-3m (221), and *a* = 3.9353 Å. Ideally, Ba₃Fe₂TeO₉ and Sr₃Fe₂TeO₉ double perovskite contains Fe³⁺ and Te⁶⁺ cations, ordered in a way that superexchange interactions between neighboring Fe³⁺ spins are the nominal mechanism accounts for the magnetism of these materials. We acknowledge financial support from the Unity through Knowledge Fund (www.ukf.hr) of the Croatian Ministry of Science, Education and Sports (Grant Agreement No. 71/13). 1. Y. D. Li, C. C. Wang, R. L. Cheng, Q. L. Lu, S. G. Huang and C. S. Liu, *Journal of Alloys and Compounds*, 2014, 598, 1-5. 2. A. Sasaki, Y. Doi and Y. Hinatsu, *Journal of Alloys and Compounds*, 2009, 477, 900-904. 3. M. P. Singh, K. D. Truong, S. Jandl and P. Fournier, *Journal of Applied Physics*, 2010, V107, 4. M. C. Viola, J. A. Alonso, J. C. Pedregosa and R. E. Carbonio, *Eur. J. Inorg. Chem.*, 2005, 1559. 5. R. M. Pinacca, M. C. Viola, J. C. Pedregosa, R. E. Carbonio and J. A. Alonso, *J. Mater. Chem.*, 2005, 15, 4648.

Keywords: Multiferroic, Double perovskite, sol-gel

MS16-P6 Structural complexity in
non-stoichiometric oxides: From
fundamental aspects to application

Jürg Schefer¹, Werner Paulus², Monica Ceretti², Matthias Frontzek¹, Lukas Keller¹

1. Laboratory for Neutron Scattering and Imaging, Paul Scherrer Institute, CH-5232 Villigen PSI, Switzerland
2. Institute Charles Gerhardt, UMR 5253, Université de Montpellier, 5 Pl Eugène Bataillon, CC1504, FR-34095 Montpellier Cedex 5, France

email: jurg.schefer@psi.ch

Certain oxides with the composition $R_xM_yO_4$ (*R* = rare earth, *M* = transition metal) crystallizing in the K₂NiF₄ structure have been found to intercalate oxygen at ambient temperatures through a topotactic reaction. The intercalated oxygen strongly influences the oxygen mobility [1] and the electronic properties presumably both through structural order and change of valence for the transition metal ions. In La₂CuO_{4+d} (*d* = 0 ... 0.07) oxygen intercalation changes the electronic properties from an antiferromagnetic semiconductor to a high-temperature superconductor [2]. In Pr₂NiO_{4+d} (*d* = 0 ... 0.25) small amounts of intercalated oxygen suppresses the antiferromagnetic order of the Ni-sublattice [3,4]. Further oxygenation leads to defined, long-range ordered superstructures over the full crystal volume with unit cells up to cell volumes of 3,000,000 Å³. In Pr₂NiO_{4+d} these oxygen-rich phases can be electrochemically prepared at room temperature leading to kinetically stabilized phases which are inaccessible through high temperature synthesis. Moreover, the electrochemical process allows varying the oxygen content with precision thus allowing tuning electronic state and resulting superstructure. Therefore, Pr₂NiO_{4+d} is especially suited to study the correlation between structural, charge and orbital order and the resulting electronic properties. In our contribution we will present a detailed single crystal study on electrochemically prepared Pr₂NiO_{4+d} using single crystal neutron and x-ray diffraction data. Exemplarily shown in Fig. 1 these data show the complex oxygen superstructures as a function of the oxygen content *d*. With the complementary use of neutrons and x-ray we are able to distinguish charge, spin and orbital order. Apparently the presence of intercalated oxygen implies valence order of Ni²⁺/Ni³⁺ stemming from orbital ordering. Further, the long-range oxygen order points to the presence of an organizing interaction. Based on neutron spectroscopic measurements we will show that in the oxygen rich phases additional phonon modes are present. These modes are the fundamental interaction leading to the structural order and also to the room temperature mobility of the intercalated oxygen ions. This phonon-assisted transport would be new phenomenon of oxygen transport and its understanding could lead to solid oxide fuel cells application at room temperature.

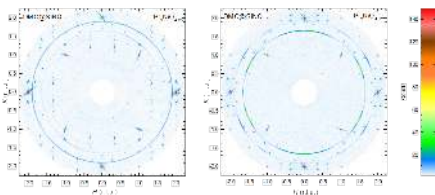


Figure 1. HK0 maps of $\text{Pr}_{0.12}\text{Ni}_{0.88}$ single crystals with $d=0.25$ (left) and $.12$ (right) at $T=100\text{K}$ collected at DMC@SINQ ($a=b=3.8\text{\AA}$, $c=12.3\text{\AA}$). Additional peaks originate from the oxygen superstructure which in the case of $d=0.12$ partly vanish at room temperature.

Keywords: oxygen diffusion, perovskites, functional structures, sustainable materials

MS16-P7 On the tetragonal phase of sodium bismuth titanate, $\text{Na}_{0.5}\text{Bi}_{0.5}\text{TiO}_3$ (NBT)

David Walker¹, Dean S. Keeble², Christopher J. Howard³, Kevin S. Knight⁴, Pam A. Thomas¹

1. Department of Physics, University of Warwick, Coventry, UK
2. Diamond Light Source Ltd, Rutherford Appleton Laboratory, Oxfordshire, UK
3. School of Engineering, The University of Newcastle, Callaghan, NSW, 2308, Australia
4. ISIS Science Division, Rutherford Appleton Laboratory, Oxfordshire, UK

email: d.walker.2@warwick.ac.uk

Sodium bismuth titanate, $\text{Na}_{0.5}\text{Bi}_{0.5}\text{TiO}_3$ (NBT), has attracted attention as a potential component of lead-free piezoelectrics with the ultimate aim of replacing the industrial standard material lead zirconate titanate (PZT). At room temperature the crystal structure is monoclinic pseudo-rhombohedral on average (space group Cc or disordered $R3c$). Above $\sim 573\text{K}$ on heating, the structure is tetragonal, solved by Jones & Thomas [1] in $P4bm$. Above $\sim 833\text{K}$ it becomes cubic ($Pm\bar{3}m$).

NBT can be combined with BaTiO_3 (BT) amongst other useful perovskites, to make the solid-solution $\text{NBT}_{1-x}\text{BT}_x$ (NBT-BT). BT is tetragonal ($P4mm$) at room temperature and its solid-solution with NBT can be described by $R3c$ up to $x \sim 0.06$. At $x = 0.06$, it was thought that the structure changed abruptly from rhombohedral to tetragonal in an analogous fashion to the so-called morphotropic phase boundary in PZT. However, subsequent works showed that the transition is rather more gradual and that a fully tetragonal polar structure described by $P4mm$ is not established until $x > 0.1-0.15$ [2]. Ma & Tan reported that the transition between the ferroelectric rhombohedral and tetragonal phases in NBT-BT takes place via a pseudo-cubic weakly polar region of composition space assigned as $P4bm$. This phase can be prompted into a more strongly polar phase by application of an electric field [3], referred to as an E-field induced phase transition if the new state persists after the E-field is removed. The understanding of this E-field induced behaviour and the favourable physical properties that accompany it are predicated on understanding the structure and nature of the $P4bm$ phase itself.

New detailed parametric structural data for NBT are presented in the temperature range from 573-943K. The tetragonal phase region is bounded by metrically cubic phases at both high and low temperatures, with the high temperature phase being the cubic aristotype. The tetragonal strain is maximum at $670(\pm 5)\text{K}$. New structural refinements in key regions of the temperature phase diagram are presented and correlated with physical property data, particularly optical birefringence measurements from single crystals [4] and results of pair distribution function (PDF) analysis.

[1] G. O. Jones & P. A. Thomas, *Acta Cryst. B* 56, 426-430 (2000)

[2] C. Ma & X. Tan, *Solid State Comms.* 150, 1497-1500 (2010)

[3] C. Ma et al, *Phys. Rev. Lett.* 109 (2012)

[4] S. Gorfman et al *J. Appl. Cryst.* 45, 444-452 (2012)

Keywords: Ferroelectrics, X-ray Diffraction, Non-ambient Diffraction, NBT

MS16-P8 Structural phase transitions in
(Ce,La)Pd₂Al_(2-x)Ga_x seriesPetr Doležal¹, Milan Klicpera¹, Dominik Kriegner¹, Zdeněk Matěj¹, Jiří Prchal¹, Pavel Javorský¹¹. Charles University in Prague, Faculty of Mathematics and Physics, (DCMP), Ke Karlovu 5, 121 16 Prague 2, Czech Republic

email: petr284@seznam.cz

Tetragonal CeT₂X₂ compounds (T: d-block element and X: p-block element) exhibit interesting physical properties such as pressure-induced superconductivity, valence fluctuating phenomena or strong crystal field exciton-phonon coupling leading to the formation of a new quantum state in CePd₂Al₂ [1]. The CeT₂X₂ compounds generally crystallize in centrosymmetric ThCr₂Si₂- or CaBe₂Ge₂-types with tetragonal crystal structure. Compounds crystallizing in the CaBe₂Ge₂ structure are frequently reported to undergo transition to structures with lower-symmetry at low temperatures. CePd₂Al₂ and CePd₂Ga₂ compounds exhibit such a structural transition from tetragonal CaBe₂Ge₂-type structure to an orthorhombic structure at 13.5 K [1] and to a triclinic structure at 125 K [2], respectively. Moreover the same structural phase transition was observed also in their non-magnetic La analogues [1,2].

The present study focusses on the examination of lattice distortion in (Ce,La)Pd₂Al_(2-x)Ga_x compounds with Ga doping at low temperature. The type of transition and transition temperature within the series were investigated by low-temperature powder X-ray diffraction. Complementary the measurements of temperature dependent magnetization, specific heat, electrical resistivity and electrical resistivity under hydrostatic pressure were performed on selected compounds, including CePd₂Al₂ single crystal, and are discussed from the thermodynamic point of view. The structural transition temperature in the CePd₂Al_(2-x)Ga_x compounds increases with Ga content (more steeply for x > 0.8), whereas the opposite development is observed for La counterparts. The low-temperature orthorhombic crystal structure (Cmma 67) has been found in the whole series. The evolution of the crystal structure in the studied composition series is discussed in the context of other tetragonal CeT₂X₂ compounds.

[1] L.C. Chapon, E.A. Goremychkin, et al., *Physica B* 378-380, 819 (2006)[2] J. Kitagawa, M. Ishikawa, *Journal of the Physical Society of Japan*, 2380-2383, 68 (1999)**Keywords:** (Ce,La)Pd₂Al_(2-x)Ga_x, structural phase transition, CaBe₂Ge₂ structure, low temperature powder diffraction**MS16-P9** SUBGROUPS: A novel program
in the Bilbao Crystallographic Server for the
analysis of distorted structuresJ. Manuel Perez-Mato¹, Luis Elcoro¹, Mois I. Aroyo¹, Samuel V. Gascó¹, Emre S. Tasci², Gemma de la Flor¹¹. Univ. del Pais Vasco (UPV/EHU), Facultad de Ciencia y Tecnología, Dept. Física de la Materia Condensada, Apdo 644, 48080 Bilbao, Spain². Department of Physics Engineering, Hacettepe University, 06800 Ankara, Turkey

email: jm.perez-mato@ehu.es

A new program has been added to the Bilbao Crystallographic Server (www.cryst.ehu.es), which greatly extends its capabilities concerning the analysis of group-subgroup relations of space groups and the symmetry characterization of distorted structures. The main task of this online freely available tool is to derive all the symmetries that are possible for a distorted phase, provided that the relation of its lattice with respect to the one of the parent undistorted structure is known. For a given parent space group and a supercell defining the lattice maintained by the distortion, SUBGROUPS generates all possible subgroups of the parent space group whose translational symmetry corresponds to the observed lattice. The group-subgroup hierarchy among all the calculated possible symmetry breaks is visualized through group-subgroup trees, and their physical equivalence is monitored by their classification according to conjugacy classes. The program can work with parent symmetries described in non-standard settings and the supercell input can be substituted by the introduction of the (commensurate) modulation wave vectors (one or more) involved in the distortion. The search can be truncated up to some specific subgroup, or filtered according to the crystal system, point group, etc. A much more interesting filter is also available, which permits to identify the subgroups that can be realized if the primary distortion corresponding to the transition order parameter transforms according to one irreducible representation (irrep) of the parent space group. Thus, the so-called irrep isotropy subgroups (or irrep epikernels and kernels) for any space group and any irrep (and their group-subgroup hierarchy) can be obtained. Some examples of application of this computational tool to the characterization of distorted structures will be presented.

By default SUBGROUPS only provides the space groups that are possible for the observed lattice of the distorted phase, but optionally all intermediate subgroups can also be derived. In this way the program can be applied to obtain the full hierarchical tree of intermediate subgroups relating any group-subgroup pair of space groups.

Keywords: Bilbao Crystallographic Server, distorted structures, group-subgroup relations, isotropy subgroups, epikernels, irreducible representations

MS16-P10 Electron tomography and HAADF-STEM imaging to solve the collapsed structure $\text{Pb}_4\text{Sr}_{13}\text{Fe}_{24}\text{O}_{53}$

Christophe Lepoitevin¹, Pierre Bordet¹, Oleg Lebedev²,
Stéphanie Kodjikian¹, Holger Klein¹

1. Univ. Grenoble Alpes, Institut NEEL, F-38042 Grenoble, France
2. CNRS, Institut NEEL, F-38042 Grenoble, France
2. Laboratoire CRISMAT, UMR6508, CNRS ENSICAEN, Caen, France

email: christophe.lepoitevin@neel.cnrs.fr

The strontium ferrites and cobaltites $(\text{Sr}_{4-x}\text{Ca}_x)(\text{Fe}_{1-x}\text{Co}_x)\text{O}_{13\pm\delta}$ exhibit mixed-conducting behaviour [1], [2] and thermoelectric power [3], which are governed by the oxygen non-stoichiometry. The refinement in 4D formalism, from single crystal X-ray diffraction data [4] of the incommensurate modulated structure of $\text{Sr}_4\text{Fe}_6\text{O}_{13\pm\delta}$, allowed its accurate description. The structure is described in an orthorhombic system and consists basically of an intergrowth of one perovskite-type layer $[\text{SrFeO}_3]$ with a complex $[\text{SrFe}_3\text{O}_{3.5\pm\delta/2}]$ layer, related to a rock salt-type block, where Fe can be found in three different environments: tetrahedron, trigonal bipyramids and tetragonal pyramid. To create distortions in $\text{Sr}_4\text{Fe}_6\text{O}_{13\pm\delta}$ as shearing mechanisms, we decided to substitute Sr^{2+} by the isovalent cation Pb^{2+} , and investigate the $\text{Sr}_{4-x}\text{Pb}_x\text{Fe}_6\text{O}_{13\pm\delta}$ system. Although its ionic radius is very close to the one of Sr^{2+} , distortions can easily be induced by the presence of the $6s^2$ lone pair. For $x > 0.7$, a new phase has then been isolated with a chemical formula $\text{Pb}_4\text{Sr}_{13}\text{Fe}_{24}\text{O}_{53}$ [5], and its complex structure has been solved using a combination of electron diffraction tomography with HAADF-STEM imaging. Selected area electron diffraction revealed a commensurately modulated structure, with the supercell parameters: $a = 3.5$ nm, $b = 0.56$ nm, $c = 2.57$ nm and $\beta = 98^\circ$. Due to the low symmetry of the crystal system and the big unit cell, a huge number of independent reflections needed to be recorded to solve this structure, that is why electron diffraction tomography was perfectly suitable for this work. The data collection was carried out by tilting the sample holder from -50° to $+50^\circ$, and to obtain the reflections of the missing cone and improve the completeness, a new collection was realized after having rotated the support grid of 90° . HAADF-STEM imaging was very complementary since it allowed the accurate determination of Pb positions. Finally the structure consists of a terrace structure derived from $\text{Sr}_4\text{Fe}_6\text{O}_{13\pm\delta}$ with a collapse of the layers $[\text{SrFeO}_3]_\infty$ and $[\text{SrFe}_3\text{O}_{3.5\pm\delta/2}]_\infty$.

[1] B.C.H. Steele, Mater. Sci. Eng. B, 13 (1992), 79 [2] N.Q. Minh, J. Am. Ceram. Soc., 76 (1993), 563 [3] S. Guggilla, T. Armstrong, A. Manthiram, J. Solid State Chem., 145 (1999), 260 [4] O. Pérez, B. Mellenne, R. Retoux, B. Raveau, M. Hervieu, Solid State Sci., 8 (2006), 431 [5] C. Lepoitevin, S. Malo, O. Pérez, N. Nguyen, A. Maignan, M. Hervieu, Solid State Sci., 8 (2006), 1294

Keywords: structure resolution, electron diffraction tomography, collapsed structure

MS17. In situ and in operando crystallography

Chairs: Ivan Halasz, Nikolay Tumanov

MS17-P1 In-situ determination of the evolution of the crystallite size distributions of GH-bearing sediments using two-dimensional X-ray diffraction

Marwen Chaouachi¹, Sigmund H. Neher¹, Andrzej Falenty¹,
Werner F. Kuhs¹

1. University of Göttingen, GZG, Department of Crystallography, Goldschmidtstr. 1, 37077 Göttingen, Germany.

email: mchaoua@gwdg.de

Natural gas hydrates are found worldwide in marine sediments and permafrost regions. The detection and quantification of GH present in marine sediments is crucial for safe oil and gas extraction, seafloor stability assessments and for quantifying the impact of GH in climatic change. Hence, there is a considerable interest in studying the microstructure of GH-bearing sediments. Although a large amount of research on GH has been carried out over the years, the micro-structural aspects of GH growth and the crystallite sizes of hydrate in sediments are still poorly known and understood.

The present study was undertaken to determine for the first time the evolution of the crystallite sizes of GH-bearing sediments in order to better understand the formation process of GH in porous media and its impact on the resulting aggregates. For that, a custom-build pressure cell operating up to several MPa was used to form *in-situ* xenon hydrate at 276 K in undersaturated sediments made of natural quartz sand. The evolution of GH CSD's was studied using synchrotron X-ray diffraction at the ID15B beamline (ESRF - France). The evolution of the crystallite sizes was investigated with a time resolution from seconds to several days in order to follow the initial growth and coarsening processes of GH. The size of crystallites was directly determined from the diffracted intensities using our newly developed method called "*fast diffraction CSD analysis*" [1] here applied for the first time to *in-situ* work.

Our results show that the sizes of GH crystallites increase with time (see Figure): the evolution of crystallites sizes is rapid at the beginning of the formation than slows down with time which suggests diffusion limited reaction and a decrease of the rate of formation by depletion of one GH constituent (water in this case). A coarsening process converting hydrate crystals into larger masses takes place and continues to time-scales beyond our study. Our findings are in good agreement with visual observations using X-ray tomography [2].

[1] S. H. Neher et al., A new fast method to derive Crystallite Size Distributions (CSD) from 2D X-ray

diffraction data, this conference.

[2] A.Falenty et al., Stop-and-go *in-situ* tomography of dynamic processes –gas hydrate formation in sedimentary matrices, this conference

[3] Klapp et al. (2010), *Earth Planet. Sci. Lett.*, 299(1-2), 207-217, doi: 10.1016/j.epsl.2010.09.001.

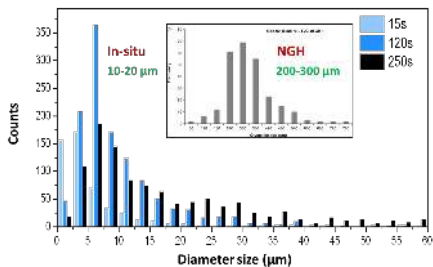


Figure 1. CSD of growing xenon hydrates after 15, 120 and 150 s. Insert shows the considerably larger CSD of a natural GH from Gulf of Mexico [3] indicative of appreciable coarsening of natural samples.

Keywords: In-situ, Crystallite Size Distribution, X-ray Diffraction, Gas Hydrates

MS17-P2 In-situ single crystal XRD study of absorption and desorption of CO₂ in zeolite Y

Eleonora Conterosito¹, Marco Milanesio¹, Luca Palin¹, Davide Viterbo¹

¹. Università del Piemonte Orientale Dipartimento di Scienze e Innovazione Tecnologica Viale T. Michel 11, I-15121 Alessandria, Italy

email: eleonora.conterosito@unipmn.it

X-ray diffraction methods in general allow only a limited chemical selectivity. Structural information on a subset of atoms is here obtained by modulating the stimulus supplied in situ on a crystal thus extracting structural information from the changing part of the scattering density within the overall crystal structure. Single crystal XRD data were collected in situ on a zeolite Y, in which CO₂, acting as active species, is desorbed upon heating. After out gassing the single crystal sample, anchored in a capillary, CO₂ was introduced in the capillary and the temperature modulated to obtain adsorption and desorption of the CO₂. In this way it has been possible to determine the sites where CO₂ is absorbed, its variations in occupancy and the motions between the sites. The cell parameter of the zeolite was found to decrease while increasing the temperature as CO₂ was desorbing, leaving the channels. It was then possible to determine the overall diminution in the occupancy of CO₂ while increasing the temperature and the shift of CO₂ moieties between the sites upon absorption and desorption.

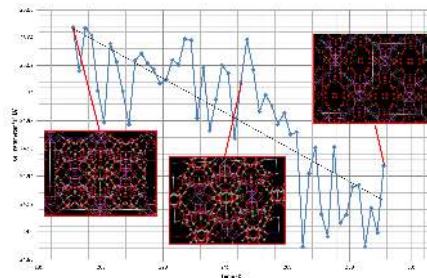


Figure 1. Cell parameter of Zeolite Y versus temperature and structures at selected temperatures.

Keywords: X-ray Single Crystal Diffraction, Chemical Selectivity, Substructure refinement, Modulation Enhanced Techniques, Fourier Filtering, Zeolites, Gas Adsorption.

MS17-P3 Defect fluorite vs pyrochlore: the $M_2M'_2O_7$ caseDavid G. Billing¹, Stuart F. Miller¹¹. DST-NRF Centre of Excellence in Strong Material, School Of Chemistry, University of the Witwatersrand, Johannesburg

email: dave.billing@wits.ac.za

In recent times we have prepared a considerable number of mixed metal oxides with the $M_2M'_2O_7$ stoichiometry. Our interest principally being to investigate the thermoresponsive behaviour of these materials via VT-PXRD methods and to assess their potential as energy materials in Solid Oxide Fuel Cells (SOFC's).

Crystallographically, the defect fluorite structure with space group $Fm\bar{3}m$ (No 225) and pyrochlore structures with space group $Fd\bar{3}m$ (No 227) are isometric. In the defect fluorite (DF) phase, the M and M' cations are completely disordered and oxygen atoms are evenly distributed into all the tetrahedral sites formed by cations. Each oxygen position having a 7/8 occupancy, and hence the description as a 'defect fluorite' phase. The pyrochlore (P) phase is a superstructure of the DF phase with the *a*-axis doubled. Upon heating the DF phase converts to the P phase and although there are a number of reports in the literature reporting on this phase transition, the detailed phase behaviour of most of these materials remain relatively unexplored. Further heating in our experience has occasionally resulted into the decomposition of the mixed metal oxide into simpler, primary oxides. We have focused our studies on materials prepared via the sol-gel method. Typically materials are prepared as the DF phase and then subsequently converted to the P phase by heating. The materials produced have been extensively characterised via VT-PXRD, COXA, Rietveld, Raman, TGA and EIS. Our over aim being to comprehensively understand the phase property relationships of these materials, and to use this to determine ideal candidate materials for making proof of concept SOFC's

Selected results of the study are to be presented. Including thermal expansion coefficients of materials studied and a COXA study of the phase transition.

Keywords: Defect Fluorite, Pyrochlore, VT-PXRD, SOFC's

MS17-P4 Phase behaviour and thermal transformations within the $Cu^{II}X_2(PO_4)_3$ [$X = Ti, Zr, Hf \& Sn$] seriesRoy P. Forbes¹, Dave G. Billing¹¹. University of the Witwatersrand

email: roy.forbes@wits.ac.za

The sodium zirconium phosphate (NZP) family is of academic and industrial importance. The $[Zr_2(PO_4)_3]^-$ is composed of a rigid framework containing channels that are suitable for occupation by numerous cations.[1] This structure is unique and a large number of elemental substitutions are possible.[2] A further consequence thereof is that NZP and many of its analogues possess a number of commercially useful physical properties, for example, low thermal expansion behaviour, fast alkali transportation as well as exhibiting mild oxidative catalytic behaviour. In the present study substitutions at the tetrahedral site were investigated for a series of $Cu^{II}X_2(PO_4)_3$ [$X = Ti, Zr, Hf \& Sn$] compounds. It has previously been shown that $CuZr_2(PO_4)_3$ and several of its analogues may be unstable to thermal treatment in air.[3] This is attributed to the migration of Cu(I) cations from the framework structure.[4] The chemical, catalytic and ionic properties of the $CuX_2(PO_4)_3$ type phases have previously been reported.[5] Citing a lack of structural data in the literature there is as a consequence no quantitative description of the phenomena that occur during thermal treatment. The purpose of this study was thus to examine possible structural and compositional changes and their relation to the thermal stability of these compounds. Transformations that were achieved with the $Cu^{II}X_2(PO_4)_3$ series are displayed below in Figure 1. Significant results will be presented.

References

- [1] Hong HYP; Crystal structure and crystal chemistry in the system $Na^{1+}_xZr_2Si_{x-3}O_{12}$; Materials Research Bulletin; 1976; **11**:173
- [2] Roy R, Agrawal DK, McKinstry HA; Very Low Thermal Expansion Coefficient Materials; Annual Reviews Materials Science; 1989;19:59
- [3] El Jazouli A, Alami M, Brochu R, Dance JM, Le Flem G, Hagenmuller P; The Nasicon-like copper(II) zirconium phosphate $Cu_{0.5}Zr_2(PO_4)_3$ and related compounds; Journal of Solid State Chemistry; 1987;**71**:444
- [4] El Jazouli A, Soubeyroux JL, Dance JM, Le Flem G; The Nasicon-like copper(II) titanium phosphate $Cu_{0.5}Ti_2(PO_4)_3$; Journal of Solid State Chemistry; 1988; **74**:584
- [5] Anantharamulu N, Koteswara Rao K, Rambabu G, Vijaya Kumar B, Velchuri Radha, Vithal M; A wide-ranging review on Nasicon type materials; Journal of Materials Science; 2011; 46:2821

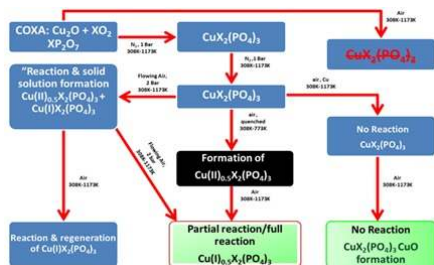


Figure 1. Structural and chemical transformations observed within the $\text{Cu}^{II}\text{X}_2(\text{PO}_4)_3$ [X = Ti, Zr, Hf & Sn] series

Keywords: framework materials, thermal stability

MS17-P5 Real-time XRD and XAS investigation on the influences of vanadium additives to the structural chemical state evolutions of LiFePO_4 of a lithium-ion

Chih-Hao Lee¹, Chih-Wei Hu^{1,2}, Tsan-Yao Chen¹, Hui-Chia Su², Ching-Yu Chiang², Bor-Yuan Shew²

1. Department of Engineering and System Science, National Tsing Hua University

2. National Synchrotron Radiation Research Center

email: chlee@mx.nthu.edu.tw

The influence of adding vanadium on the structure evolution and electrochemical performance of LiFePO_4 were systematically investigated by *in-situ* x-ray powder diffraction and x-ray absorption near edge structure spectroscopy. Our results indicate that the addition of a small amount of vanadium (less than at 1%) significantly reduces the formation of non-crystalline (highly disordered) triphylite and remnant heterosite phases in the cathode of battery especially at higher C rates. By adding vanadium, the cycle stability of LiFePO_4 cathode is improved by 14.9% compared to that of pristine LiFePO_4 cathode in the batteries. Such an enhancement could be attributed to the improved ion diffusion kinetics and reduced inactive LiFePO_4 in cathode by the reversible excess charge – vacancy effects of supervalent-vanadium additive in cathode during electrochemical redox cycles. The most interesting point is the difference between diffraction intensity ratio determined by XRD and ratio of oxidation state of Fe ion determined XAS. Without V additives, this difference is much larger after cycling, which implies the disorder irreversible phase persists.

Keywords: lithium ion battery, XRD, XAS, phase transition

MS17-P6 In situ studies of materials for high-temperature CO₂ capture and storage

Matthew T. Dunstan¹, Wen Liu², Adriano F. Pavan³, Serena Maugeri⁴, Martin Dove⁴, Dami Taiwo⁵, Paul Shearing³, Chris D. Ling³, Stuart A. Scott⁶, John S. Dennis², Clare P. Grey¹

1. Department of Chemistry, University of Cambridge
2. Department of Chemical Engineering and Biotechnology, University of Cambridge
3. School of Chemistry, University of Sydney
4. School of Physics and Astronomy, Queen Mary, University of London
5. Department of Chemical Engineering, University College London
6. Department of Engineering, University of Cambridge

email: mtd33@cam.ac.uk

In order to combat the climate change owing to the ever-increasing concentration of CO₂ in the atmosphere due to anthropogenic emissions, we must change the way by which energy is primarily generated, that is by combustion of fossil fuels. The carbon capture and storage (CCS) scheme offers a plausible solution to the urgent need for a carbon neutral energy source from stationary sources, including power plants and industrial processes, since energy generated from renewable sources such as wind, solar and biomass are unlikely to meet the demand over the next two decades. The most mature technology for post-combustion capture uses a liquid sorbent, amine scrubbing. However, with the existing technology, a large amount of heat is required for the regeneration of the liquid sorbent, which introduces a substantial energy penalty [1]. The use of alternative sorbents for CO₂ capture, such as CaO, has been investigated extensively in recent years [2]. However there are significant problems associated with the use of CaO based sorbents, the most challenging one being the deactivation of the sorbent material. When almost pure CaO sorbents such as limestone are used, the capture capacity of the solid sorbent could fall by as much as 90 mol % after the first few carbonation-regeneration cycles. In this study a variety of *in situ* techniques were employed to better understand the cause of this deterioration from both a structural and morphological standpoint, and to compare its performance with that of recently developed sorbents incorporating Al-based additives [3, 4]. *In situ* synchrotron x-ray diffraction experiments found no bulk structural changes to occur upon reaction for the different materials, with the added phase remaining inert. Further x-ray and neutron PDF studies were employed to better understand the local surface and interfacial structures formed upon reaction, and how the reaction front proceeds through the individual sorbent particles. Finally, *in situ* x-ray tomography experiments were employed to track the morphological changes in the sorbents during carbonation, including the changes in porosity and tortuosity of the particles over different reaction times.

[1] Rao, A.B.; Rubin, E.S. *Environ. Sci. Technol.* 2002, 36, 4467–4475.

[2] Anthony, E. J. *Ind. Eng. Chem. Res.* 2008, 47, 1747–1754.

[3] Dennis, J.S., Pacciani, R., 2009. *Chem. Eng. Sci.*, 64(9), 2147–2157.

[4] Li, Z.S., *et al.*, 2005. *Energy and Fuels*, 19(4), 1447–1452.

Keywords: Gas-solid interactions, diffraction, tomography, carbon capture

MS17-P7 A controlled pressure/temperature set-up for synchrotron in situ studies of solid-gas processes and reactions: Case of the structural deformation of ZIF-8

Santiago Garcia-Granda¹, Jose Montejó-Bernardo¹, Germán Castro², Conchi O. Ania³

1. Physical and Analytical Chemistry Department, Faculty of Chemistry, University of Oviedo-CINN, 33006-Oviedo, Spain
2. Spanish CRG BM25 Beamline at the ESRF, SpLine, Synchrotron Radiation Facility, BP 220, 38043 Grenoble, France
3. National Coal Institute (INCAR, CSIC), 33080-Oviedo, Spain

email: sgg@uniovi.es

A novel set-up has been designed and used for synchrotron radiation X-ray high-resolution powder diffraction (SR-HRPD) in transmission geometry for in situ solid–gas reactions and processes in an isobaric and isothermal environment. The pressure and temperature of the sample are controlled from 10–3 to 1000 mbar and from 80 to 1000 K, respectively. To test the capacities of this novel experimental set-up, structure deformation in the porous material zeolitic imidazole framework (ZIF-8) by gas adsorption at cryogenic temperature. The adsorption properties of ZIF-8 for a variety of strategic gases, shows unusual multi-stepped adsorption features for the adsorption of various gas probes (i.e., N₂, CO, Ar, O₂) [1–3]. There seems yet to be a dearth in the understanding of the gas adsorption properties of flexible materials [3,4]. X-ray diffraction experiments were conducted at the Spanish CRG BM25 SpLine at ESRF in a controlled environment chamber with fine control of the gas dosage, sample outgassing under vacuum, temperature control and simultaneous SR-HRPD recording [4]. Figure 1 shows the nitrogen adsorption/desorption isotherm of ZIF-8 at 85K and the SR-HRPD diffractograms (inset) corresponding to various gas loadings. Measurements were fast enough to observe the evolution of the crystallographic phases of the material, making possible to determine structural changes in the solid at in operando conditions [4].

The real time monitoring of the SR-HRPD patterns of ZIF-8 indicate that the gas-induced structural flexibility is linked to the organization of the adsorbed gas molecules in the adsorption sites, as well as the polarizability and molecular size and shape of the gases.

REFERENCES

- [1] D. Fairen-Jimenez, S.A. Moggach, M.T. Wharmby, P.A. Wright, S. Parsons, T. Duren, J. Am. Chem. Soc. 133 (2011) 8900.
- [2] S.A. Moggach, T.D. Bennett, A.K. Cheetham Angew. Chem., Int. Ed. 48 (2009) 7087.
- [3] C.O. Ania, E. García-Pérez, M. Haro, J.J. Gutiérrez-Sevillano, T. Valdés-Solís, J.B. Parra, S. Calero, J. Phys. Chem. Lett. 3 (2012) 1159.
- [4] Salas-Colera E, Muñoz-Noval A, Heyman C, Ania CO, Parra JB, García-Granda S, Calero S, Rubio-Zuazo J, Castro GR, J. Synchr. Rad. 22 (2015) 1.

Acknowledgments

We thank financial support from Spanish MINECO (MAT2013-40950-R) and ERDF.

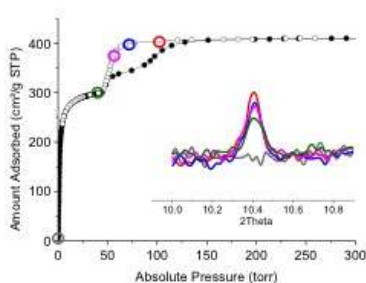


Figure 1. Equilibrium N₂ adsorption/desorption isotherm 85 K of ZIF-8 and (inset) real time SR-HRPD during gas release (desorption branch).

Keywords: XRPD; isobaric/isothermal environment, ZIF-8, adsorption, solid-gas reactions

MS17-P8 Garnet inclusions in diamond: The role of elastic properties

Lorenzo Scandolo¹, Sula Milani², Gabriele Zaffiro¹, Matteo Di Prima¹, Mattia L. Mazzucchelli¹, Matteo Alvaro¹, Chiara M. Domeneghetti¹, Fabrizio Nestola²

1. Department of Earth and Environmental Sciences, University of Pavia, Italy
2. Department of Geosciences, University of Padua, Italy

email: lorenzo.scandolo01@universitadipavia.it

Although inclusion-bearing diamonds are so rare (about 1% of the diamond retrieved), they are geologically relevant because they are the only direct and unaltered samples that we have from the Earth's mantle. Investigation of mineral inclusions still trapped in diamond allows retrieving several pieces of information about the Earth's interior and its active geodynamics (e.g. providing the definition of the initiation of subduction processes, capturing the redox state of the mantle etc... [1]). Therefore it is clear that the determination of the entrapment pressure (i.e. depth of formation) of these mineral inclusions is a fundamental tile for the understanding of the Earth's mantle dynamic as it allows constraining the chemico-physical environment in which diamond and their inclusions formed. The recently developed 'elastic geobarometer' method [2] allows retrieving the entrapment pressure for a diamond-inclusion pair provided the knowledge of the thermoelastic parameters for both diamond and inclusion. Since mineral inclusions in diamonds from the subcratonic lithospheric mantle are mostly represented by garnet (38%) together with olivine (18%), clinopyroxene (16%), orthopyroxene (8%), Mg-chromite (18%) and sulphides (2%) our study has been focused on the determination of reliable elastic properties for endmember garnets (e.g. pyrope, almandine, grossular and uvarovite). Knowledge of the thermoelastic properties for endmember garnets should in principle allow calculating thermoelastic parameters for potentially any garnet composition commonly found in diamond. In particular, here we present the investigation of endmember garnets thermal expansion by in situ single crystal X-ray diffraction at high-temperature conditions. The measurements have been performed on the same crystals used by [3] for their high-P investigation adopting the same methods for the unit-cell parameters determination (e.g. 8-position centring using SINGLE software, [e.g. 4, 5]). Further details on the high temperature apparatus and measurements method here adopted are reported in [6]. The thermal expansion so calculated allowed retrieving the entrapment pressure 5.67 GPa at 1500K for an eclogitic garnet with composition Py51Al22Gr27.

References [1] Shirey et al. (2013) *RiMG*, 75, 355. [2] Angel et al. (2014) *Am Mineral*, 99, 2146. [3] Milani et al. (2015) *Lithos*, in press [4] King and Finger (1979) *JAC*, 12, 374. [5] Angel and Finger (2011) *JAC*, 44, 247. [6] Alvaro et al (2015) *JAC*, submit.

Keywords: Diamond, Inclusion, Diffraction, Mantle, Garnet

MS17-P9 Quantitative in situ study of salbutamol crystallization as a function of relative humidity and temperature

Olga Narygina¹, Sarah Zellnitz², Christian Resch³, Hartmuth Schroettner⁴, Nora Anne Urbanetz²

1. PANalytical B.V., Almelo, the Netherlands
2. Research Center Pharmaceutical Engineering GmbH, Graz, Austria
3. Anton Paar GmbH, Graz, Austria
4. Austrian Centre for Electron Microscopy and Nanoanalysis, Graz, Austria,

email: olga.narygina@panalytical.com

Salbutamol, a β_2 -adrenoreceptor agonist, is a common drug used for the treatment of bronchial asthma via inhalation. Spray dried salbutamol sulphate and salbutamol base particles intended for the use as active pharmaceutical ingredient in dry powder inhalers are amorphous as a result of spray drying (Littringer et al., 2013). However, the crystallization of the amorphous salbutamol particles may be triggered by exposure to humid air or by heating of the sample (Columbano et al., 2002). Knowing the critical conditions of salbutamol crystallization is essential for the correct handling and storage of the drug. In order to quantitatively characterize the process of salbutamol crystallization we performed a series of time- resolved powder X-ray diffraction experiments at variable temperature (25 and 35 °C) and relative humidity (60 %, 70 %, 80 %, 90 %). Quantification of amorphous-to-crystalline ratio as a function of time at variable temperature and relative humidity was performed using the Partial Least Squares Regression, PLSR (Degen et al., 2014; Zellnitz et al., submitted). We show that the crystallization speed of salbutamol sulphate and salbutamol base is a non-linear function of both temperature and relative humidity (Figure 1).

Littringer, E. M., Zellnitz, S., Hammernik, K., Adamer, V., Friedl, H., and Urbanetz, N. A. (2013) "Spray Drying of Aqueous Salbutamol Sulfate Solutions Using the Nano Spray Dryer B-90—The Impact of Process Parameters on Particle Size," *Drying Tech.*, **31**, 1346-1353.

Columbano, A., Buckton, G., and Wikeley, P. (2002) "A study of the crystallisation of amorphous salbutamol sulphate using water vapor sorption and near infrared spectroscopy," *Int. J. Pharm.* **237**, 171-178.

Degen, T., Sadki, M., Bron, E., König, U., and Nénert, G. (2014) "The HighScore Suite," *Powder Diff.*, **29**(S2), S13-S18

Zellnitz, S., Narygina, O., Resch, C., Schroettner, H., and Urbanetz, N. A., "Crystallization speed of salbutamol as a function of relative humidity and temperature," submitted to *Int. J. Pharm.*

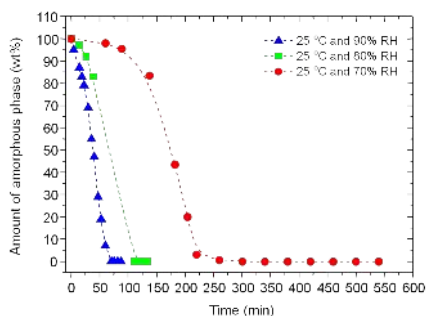


Figure 1. Amorphous-to-crystalline ratio for spray dried salbutamol plotted as a function of time at relative humidity of 70 %, 80 % and 90 %.

Keywords: Pharmaceuticals, crystallization process, X-ray diffraction, partial least square regression

MS17-P10 In situ XRD study of reduction of $\text{Mn}_x\text{Zr}_{1-x}\text{O}_2$ solid solutions

Olga A. Bulavchenko^{1,2}, Sergey V. Tsybulya^{1,2}, Andrey A. Saraev^{1,2}, Vasily V. Kaichev^{1,2}, Tatyana N. Afonassenko³, Pavel G. Tsyrl'nikov³

1. Borekov Institute of Catalysis SB RAS
2. Novosibirsk State University
3. Institute of Hydrocarbon Processing SB RAS

email: isizy@catalysis.ru

Solid solutions based on ZrO_2 exhibit high catalytic activity in a number of practically important reactions. Mn-Zn mixed oxides can effectively catalyze the gas-phase oxidation of hydrocarbons or chlorocarbons. Mn cations can enter the lattice of ZrO_2 with the formation of solid solutions $\text{Mn}_x\text{Zr}_{1-x}\text{O}_2$, in which lattice oxygen possesses sufficiently high mobility and hence high reactivity.

A series of mixed Mn-Zr oxides with different molar ratios Mn/Zr (0.1-9) have been prepared by coprecipitation of manganese and zirconium nitrates and characterized by XRD and N_2 adsorption techniques. It has been found that at low Mn/Zr ratios, when the Mn content is below 30 atom %, the catalysts are single-phase solid solutions ($\text{Mn}_x\text{Zr}_{1-x}\text{O}_2$) based on a ZrO_2 structure. According to XPS data, manganese in these solutions exists mainly in the Mn^{4+} state. An increase in the Mn content mostly leads to an increase in the number of Mn cations in the structure of the solid solutions, but a part of manganese form Mn_2O_3 and Mn_3O_4 in crystalline and amorphous states.

Reduction of solid solutions in hydrogen was studied by a TPR, in situ XPS and XRD, at temperature range 100 to 700 °C. Figure 1 shows a series of diffraction patterns recorded during the reduction of the sample with Mn/Zr=1. At room temperature, the sample contains two phases: a solid solution $\text{Mn}_x\text{Zr}_{1-x}\text{O}_2$ and Mn_2O_3 . The reduction of this sample leads to a change in the lattice parameter of the solid solution $\text{Mn}_x\text{Zr}_{1-x}\text{O}_2$, which is indicated by the shift of corresponding peaks to larger angles. Besides, the reduction leads to transformations of manganese oxides. The reduction of the solid solutions proceeds in a wide temperature range 100-700 °C via two steps. In the first stage, at temperatures of 100-500°C, manganese cations undergo partial reduction to Mn^{2+} , whose presence is confirmed by XPS measurements. The lattice parameter of $\text{Mn}_x\text{Zr}_{1-x}\text{O}_2$ in this case varies because of changes in the oxidation state of manganese cations in the bulk of solid solution. In the second stage, at temperatures of 500-700°C, manganese cations exit from the bulk of the solid solution and segregate on its surface. The lattice parameter at this stage increases because of the decrease in the number of Mn cations in the oxide.

This work was supported by the RSCF project №14-23-00037.

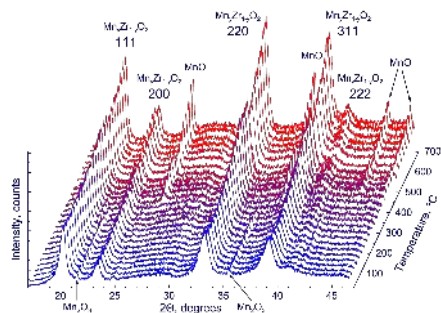


Figure 1. Series of diffraction patterns ($\lambda = 1.0157 \text{ \AA}$) recorded in situ during reduction with hydrogen in the temperature ranges from 30 to 700 °C

Keywords: in situ XRD, solid solution, reduction

MS17-P11 A new micro-furnace for “in situ” high-temperature single crystal X-ray diffraction measurements

Matteo Alvaro¹, Ross J. Angel², Claudio Marciano¹, Sula Milani², Lorenzo Scandolo¹, Mattia L. Mazzucchelli¹, Gabriele Zaffiro¹, Greta Rustioni¹, Matteo Briccola³, Chiara M. Domeneghetti¹, Fabrizio Nestola²

1. Department of Earth and Environmental Sciences, University of Pavia, Pavia, Italy.

2. Department of Geosciences, University of Padua, Italy

3. Department of Design, Polytechnic University of Milan, Italy

email: matteo.alvaro@gmail.com

Elastic properties reflect the nature of atomic bonding and allow the retrieval of crucial information about physical, chemical and mechanical behavior of materials. This explains the strong and increasing interest in quantifying elastic properties of materials in several scientific fields. To this aim several devices and methods have been developed so far. In particular, for high temperature devices for “in-situ” measurements, even if the small isothermal volume required for single-crystal X-ray diffraction experiments, the design of a furnace should also aim to reduce thermal gradients by including a large thermal mass that encloses the sample. However, this solution often leads to complex design that results in a restricted access to reciprocal space or attenuation of the incident or diffracted intensity.

Here we present a newly-developed H-shaped Pt-Pt/Rh resistance micro-furnace for in-situ high-temperature single-crystal X-ray diffraction measurements. The compact design of the furnace together with the long collimator-sample-detector distance allows us to perform measurements up to $2\theta = 70^\circ$. The microfurnace is equipped with a water cooling system that allows a constant thermal gradient to be maintained that in turn guarantees thermal stability with oscillations smaller than 5°C in the whole range of operating T of room-T to 1200°C. The furnace has been built for use with a conventional 4-circle Eulerian geometry diffractometer equipped with point detector and automated with the SINGLE software (Angel and Finger 2011) that allows the effects of crystal offsets and diffractometer aberrations to be eliminated from the refined peak positions by the 8-position method (King and Finger 1979), and thus maximize precision in unit-cell measurements. The software has been modified to reduce chimney effects in the furnace and thus improve the stability by (i) restricting the χ circle movements to between -90° and $+90^\circ$; (ii) optimizing the order of measurements to minimize χ circle movements (iii) imposing a waiting time after large angular movements on χ .

Temperature calibration has been performed iteratively by combining measurements with a standard small diameter thermocouple mounted in the same conditions as the sample together with the lattice parameter determination of materials with known thermal expansion behavior (i.e. quartz and pure silicon).

References

- Angel RJ, Finger LW (2011) JAppCryst, 44:247.
- King HE, Finger LW (1979) JAppCryst, 12:374.

Keywords: X-Ray diffraction, single crystal, high temperature, thermal expansion

MS17-P12 Neutron diffraction study of piezoelectric material under electric field

Takuro Kawasaki¹, Takayoshi Ito², Yasuhiro Inamura¹, Takeshi Nakatani¹, Stefanus Harjo¹, Wu Gong¹, Kazuya Aizawa¹, Takaaki Iwahashi¹

1. J-PARC Center, Japan Atomic Energy Agency
2. Technical Support Group, CROSS-Tokai

email: takuro.kawasaki@j-parc.jp

Piezoelectric material is widely used as an actuator and other various devices because the size of the material can be controlled by the applied electric field. Two types of microscopic deformation, lattice strain and domain switching, produces this macroscopic deformation. On the other hand, time-resolved measurement is attracting great interest in order to observe transient phenomena of materials under external fields. The behaviors of the lattice and the domain under the cyclic electric field can be studied by time-resolved *in-situ* diffraction experiment. In this study, the lattice strain and the domain characteristic of piezoelectric material under static and cyclic electric fields were studied by time-of-flight neutron diffraction. The diffraction intensities from PZT-based ceramics were measured at Engineering Materials Diffractometer TAKUMI in J-PARC. The intensities in the parallel direction and the vertical direction to the field were measured simultaneously by $\pm 90^\circ$ detector banks. The collected data were divided based on the voltage and the phase conditions of applied electric field and were converted to diffraction patterns using the data reduction software developed in J-PARC. The variation of the position and the intensity of the diffraction peaks according to the applied field were found in the patterns. The responses of the lattice and the domain to the field were successfully observed.

Keywords: neutron diffraction, piezoelectric material, lattice strain

MS17-P13 High-pressure study of $\text{Mn}(\text{BH}_4)_2$: a new polymorphs with high hydrogen density

Nikolay Tumanov¹, Elsa Roedern², Dorrit B. Nielsen², Torben R. Jensen², Alexander V. Talyzin³, Radovan Černý⁴, Dmitry Chernyshov⁵, Vladimir Dmitriev³, Zbigniew Łodziana⁶, Yaroslav Filinchuk¹

1. Institute of Condensed Matter and Nanosciences, Université catholique de Louvain, place L. Pasteur 1, 1348 Louvain-la-Neuve, Belgium
2. Center for Materials Crystallography, Interdisciplinary Nanoscience Center (iNANO) and Department of Chemistry, University of Aarhus, Langelandsgade 140, DK-8000 Aarhus C, Denmark
3. Department of Physics, Linnaeus väg 24, Umeå University, Umeå S-90187, Sweden
4. Laboratory of Crystallography, DPMC-MaNEP, University of Geneva, quai Ernest-Ansermet 24, 1211 Geneva, Switzerland
5. Swiss Norwegian Beam Lines (SNBL) at the European Synchrotron Radiation Facility (ESRF), rue Jules Horowitz, 38043 Grenoble, France
6. INP Polish Academy of Sciences, Department of Structural Research, ul. Radzikowskiego 152, 31-342 Kraków, Poland

email: nikolay.tumanov@uclouvain.be

Hydrogen economy is one of the perspective trends in the future of renewable energy, but hydrogen storage is still a limiting factor. A possible way is to chemically bound hydrogen in light-weight compounds. In this context, metal borohydrides have been studied intensively in recent years. One of the problems in the practical application of borohydrides as hydrogen storage materials is often a too high or a too low decomposition temperature, but manganese borohydride is one of the borohydrides with moderate temperature of decomposition (160 °C). The structure and properties of metal borohydrides are usually studied at ambient conditions, but applying high hydrostatic pressure to the compounds not only adds an additional dimension to the phase diagram, revealing new high-pressure polymorphs of borohydrides, but may also allow to discover new high-pressure phases that are stable upon decompression. Such compounds are not only denser than those known to form at ambient conditions, but may also provide new or improved properties to a system, *e.g.* regarding, stability, decomposition and melting temperatures, etc. For instance, $\delta\text{-Mg}(\text{BH}_4)_2$, obtained by compression of $\text{Mg}(\text{BH}_4)_2$ to ~ 1 GPa, is more stable in air [1], than its ambient pressure phases.

The high-pressure behavior of $\text{Mn}(\text{BH}_4)_2$ was studied up to 15 GPa using diamond anvil cells and powder X-ray diffraction and Raman spectroscopy and two new polymorphs was discovered using combination of diffraction and DFT calculations. The first polymorph, $\delta\text{-Mn}(\text{BH}_4)_2$, forms near 1 GPa and is isostructural to a magnesium analog, $\delta\text{-Mg}(\text{BH}_4)_2$. This polymorph is stable upon decompression to ambient conditions. The same polymorph was obtained by compression of $\alpha\text{-Mn}(\text{BH}_4)_2$ in a large-volume steel press, as well as by high-energy ball milling. The thermal stability was studied by *in situ* powder X-ray diffraction and thermal analysis coupled with mass-spectroscopy. $\delta\text{-Mn}(\text{BH}_4)_2$ transforms back to $\alpha\text{-Mn}(\text{BH}_4)_2$ upon heating (67-109 °C) and decomposition is initiated at 130 °C, releasing hydrogen and some diborane. The high-pressure polymorph, $\delta'\text{-Mn}(\text{BH}_4)_2$, transforms into a second, $\delta''\text{-Mn}(\text{BH}_4)_2$, in the pressure range of 8.6-11.8 GPa, with

BH₄⁻ groups ordered in a superstructure. δ'-Mn(BH₄)₂ is not isostructural to the second high-pressure phase of Mg(BH₄)₂. Equations of state were determined for α- and δ-Mn(BH₄)₂.

Y. Filinchuk, B. Richter, T. R. Jensen, V. Dmitriev, D. Chernyshov, and H. Hagemann, *Angew. Chem. Int. Ed.*, 2011, **50**, 11162.

Keywords: hydrogen storage, borohydrides

MS17-P14 In situ X-ray crystallography of colloidal crystals under sintering conditions

Alexey V. Zozulya¹, Elena A. Sulyanova², Anatoly Shabalin¹, Janne-Mieke Meijer³, Dmitry Dzhigaev^{1,4}, Oleg Gorobtsov^{1,5}, Ruslan P. Kurta⁶, Sergey Lazarev¹, Ivan Zaluzhnyi^{1,4}, Ulf Lorenz⁷, Andrej Singer⁸, Olexandr Yefanov⁹, Ilya Besedin^{1,4}, Michael Sprung¹, Andrei V. Petukhov³, Ivan A. Vartanyants¹

1. Deutsches Elektronen-Synchrotron DESY Hamburg
2. Shubnikov Institute of Crystallography RAS, Leninskii pr. 59, 119333 Moscow, Russia
3. van 't Hoff laboratory for Physical and Colloid Chemistry, Debye Institute for Nanomaterials Science, University of Utrecht, Padualaan 8, 3508 TB Utrecht, The Netherlands
4. National Research Nuclear University MEPhI (Moscow Engineering Physics Institute), Kashirskoye ch. 31, 115409 Moscow, Russia
5. NRC Kurchatov Institute, Akademika Kurchatova pl. 1, 123182 Moscow, Russia
6. European XFEL GmbH, Notkestraße 85, D-22607 Hamburg, Germany
7. Department of Chemistry, University of Potsdam, D-14476 Potsdam, Germany
8. University of California, 9500 Gilman Dr., La Jolla, San Diego, California 92093, USA
9. Center for Free-Electron Laser Science, DESY, Notkestraße 85, D-22607 Hamburg, Germany

email: alexey.zozulya@desy.de

Periodic photonic nanostructures enable to manipulate and control light emission and propagation due to existence of band gaps [1, 2]. Photonic crystals represent a new class of nanomaterials with promising applications in optical communication lines, sensor technology and data storage. Colloidal crystals formed by self-assembly of sub-micrometer colloidal spherical particles [3] are especially attractive due to their large area, low fabrication costs and a wide range of particle size and shape. Investigation of a real structure of these materials and its temperature dependence is of utmost importance for the future development of photonic devices.

Band gap properties of colloidal crystals can be altered by thermal treatment (dry sintering) [4]. The physical reason for this phenomenon is not well understood. The behavior of low-order spin-coated polystyrene (PS) colloidal films under annealing treatment provides only rough picture of structural evolution [5]. Our recent studies of high-quality PS colloidal crystals upon incremental heating conditions have revealed detailed scenario of colloidal crystal melting [6, 7]. X-ray diffraction studies of PS colloidal crystals have been carried out in transmission and reflection geometries using high resolution X-ray scattering setup at the Coherence Beamline P10 of the PETRA III light source. Diffraction peak parameters, such as q-values, integrated peak intensities, the radial and azimuthal widths, were analyzed as a function of temperature [7]. Temperature dependencies of lattice distortions, mosaic spread and a size of coherently scattering domain were evaluated by Williamson-Hall method. As a result we identified four stages of structural evolution in PS crystals upon sintering: steady-state, pre-melting, shape transformation and crystal melting. The observed peculiarities of lattice distortions indicate that the evolution of in-plane and out-of-plane order plays a central role in the process of colloidal crystal melting.

References

[1] S. G. Johnson, J. D. Joannopoulos, Photonic crystals: The road from theory to practice. Springer, USA, 2001.

[2] Y. A. Vlasov, *et al. Phys. Rev. E* **61**, 5784–5793 (2000).

[3] J.-M. Meijer, *et al. Langmuir* **28**, 7631–7638 (2012).

[4] H. Miguez, *et al. Adv. Mater.* **10**, 480–483 (1998).

[5] G. Herzog, *et al. Langmuir* **28**, 8230–8237 (2012).

[6] A.V. Zozulya, *et al. J. Appl. Cryst.* **46**, 903–907 (2013).

[7] E.A. Sulyanova, *et al. Langmuir*, published online (2015).

Keywords: In situ crystallography, colloidal crystals, thermal treatment, small-angle X-ray scattering

MS17-P15 How do zeolite capture CO₂? in-situ synchrotron XRPD investigation of gas adsorption in FAU systems

Rossella Arletti¹, Lara Gigli¹, Francesco Di Renzo², Simona Quartieri³

1. Department of Earth Sciences - University of Torino (Italy)

2. Institut Charles Gerhardt Montpellier (France)

3. Department of Physics and Earth Sciences - University of Messina (Italy)

email: rossella.arletti@unito.it

The separation of CO₂ from other light gases has been largely practiced in the past. In particular, much of the work concerned the separation of CO₂ for the purification of natural gas¹. More recently, great emphasis has been given to CO₂ separation from the flue gases associated with combustion processes^{2,3}. This interest is directly linked to the importance of CO₂ as a key anthropogenic greenhouse gas, strictly linked to global climate changes⁴. In this work we describe the positions and the interactions of the CO₂ molecules adsorbed in zeolite cavities, on the basis of *in situ* synchrotron X-Ray Powder Diffraction (XRPD) experiments performed at the MCX beamline at Elettra Sincrotrone Trieste source. Three different zeolite samples were investigated: NaX, NaY and CaLSX. They share the same FAU framework type, but have different Si/Al ratios and cation contents. After a HT treatment, carried out to remove the water molecules hosted in the channels, the samples were saturated with CO₂ at 1 bar for 30 minutes and XRPD patterns were collected on an image plate at a fixed wavelength. In order to study the CO₂ desorption behavior, a series of patterns was collected upon heating from room T to 600°C. The experiments show that CO₂ was successfully adsorbed in the zeolite channels of all the samples. Forty-eight and forty CO₂ molecules were localized in Na-Y and Ca-LSX supercage, respectively. In the sodic sample the molecules-cation interactions are water mediated, while in the Ca phase the CO₂ molecules directly interact with the cation sited in the supercage. In the Na-X sample five Na-coordinated CO₂ molecules were localized in the sodalitic cage, while carbonate-like species were found near the supercage. Due to the low number of CO₂ molecules found by this structure refinement, we can not exclude that further molecules are present in the cages with a disordered distribution. Upon heating up to 600°C, NaX and NaY underwent a complete release of all the previously adsorbed CO₂ molecules. On the contrary, Ca-LSX retained 25 CO₂ molecules, suggesting a stronger bonding interaction with Ca cations in the channels.

References: ¹ S. Sridhar, B. Smjitha, T. M. Aminabhavi, Sep. Purif. Rev. 2007, 36, 113. ² D. Aaron, C. Tsouris, Sep. Purif. Rev. 2005, 40, 321. ³ H. Balat, C. Oz, Energy Explor. Exploit. 2007, 25, 357. ⁴ H. Yang, et al., J. Environ. Sci. (Beijing, China) 2008, 20, 14.

Keywords: zeolite, CO₂, XRPD, structure

MS17-P16 Using *in situ* X-ray diffraction to observe solvent exchange during MOF synthesis

Yue Wu¹, Matthew I. Breeze², Guy J. Clarkson², Franck Millange³, Dermot O'Hare¹, Richard I. Walton²

1. Department of Chemistry University of Oxford, Oxford, OX1 3TA, U.K.

2. Department of Chemistry, University of Warwick, Coventry, CV4 7AL, U.K.

3. Département de Chimie, Université de Versailles-St-Quentin-en-Yvelines, France

email: yue.wu.mail@gmail.com

Metal-organic frameworks (MOF) materials are most commonly synthesised using solvothermal methods. Very often, MOFs contain solvent molecules coordinated to metal atoms in the framework skeleton; this solvent can then exchange with other species - for example, H₂O and DMF. To date, it has been impossible to quantify whether a framework is initially formed with one solvent that can be exchanged with another to reach the final product, or if the final product is the only species formed. Using time-resolved monochromatic high energy X-ray diffraction with a custom IR furnace cell ('ODISC', the Oxford-Diamond *In-Situ* Cell, Fig. 1, left),¹ we have been able to understand this behaviour in a laboratory-scale reaction at an unprecedented level of detail.

We present an *in situ* study of the solvothermal crystallisation of a new ytterbium MOF from a water/DMF mixture under solvothermal conditions. Analysis of high resolution powder patterns using Rietveld refinement reveals an evolution of lattice parameters and electron density during the crystallisation process. Quenching studies confirm that this is due to a gradual topochemical replacement of coordinated solvent molecules: the water initially coordinated to Yb³⁺ is replaced by DMF as the reaction progresses (Fig. 1, right). This study shows the possibility of studying very subtle changes in laboratory-scale reactions, which would be relevant not only to solvent exchange studies but also in the investigation of e.g. the preferential incorporation of different species mixed-metal and mixed-ligand frameworks.

Rev. Sci. Instrum. **2012**, 83 (8), 084101.

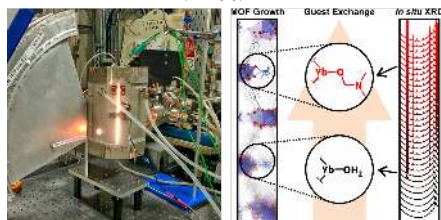


Figure 1. (left) ODISC furnace; (right) *In situ* guest exchange occurs during MOF growth

Keywords: *in situ* diffraction, MOF

MS17-P17 *In situ* investigation of the mechanochemical syntheses of new cadmium phenylphosphonates

Manuel Wilke^{1,2}, Lisa Batzdorf^{1,2}, Franziska Fischer^{1,2}, Klaus Rademann², Franziska Emmerling¹

1. BAM Federal Institute for Materials Research and Testing, Berlin, Germany

2. Department of Chemistry, Humboldt-University of Berlin, Berlin, Germany

email: manuel.wilke@bam.de

Metal phosphonates are metal organic compounds consisting of a metal ion and an organic phosphonic acid, usually deprotonated. Typically, metal phosphonates crystallize in layer structures where the organic part points into the interlayer space and can be classified as porous coordination polymers (PCP)^[1]. The research on this topic is of great interest because of their high potential of applications for gas storage^[2], catalyses^[3], proton conductors^[4], and surface modification^[5]. Usually, metal phosphonates are synthesized from solution, often under hydrothermal conditions for a reasonable crystallinity. Against this background, the syntheses of the crystalline cadmium phenylphosphonates Cd(O₃PPh)₂·H₂O (1), Cd(HO₂PPh)₂ (2), and Cd(HO₂PPh)₂·(H₂O)₃PPH (3) from solid state reactions by grinding together cadmium acetate with respective equivalents of phenylphosphonic acid is presented. (2) and (3) can not be synthesized by any other synthesis method so far. The milling reactions were investigated *in situ* using synchrotron PXRD. The setup was developed by our group^[6]. Based on these data, the identification of intermediates is possible and the reactions mechanisms can be analyzed in detail.

[1] K. Maeda, *Microporous Mesoporous Mat.* **2004**, 73, 47-55.

[2] T. Y. Ma, X. Z. Lin, X. J. Zhang, Z. Y. Yuan, *New J. Chem.* **2010**, 34, 1209-1216.

[3] R. Sen, D. Saha, D. Mal, P. Brandao, G. Rogez, Z. Lin, *European Journal of Inorganic Chemistry* **2013**, 2013, 5020-5026.

[4] R. M. P. Colodrero, P. Olivera-Pastor, A. Cabeza, M. Papadaki, K. D. Demadis, M. A. G. Aranda, *Inorg. Chem.* **2010**, 49, 761-768.

[5] P. H. Mutin, G. Guerrero, A. Vioux, C. R. Chim. **2003**, 6, 1153-1164.

[6] L. Batzdorf, F. Fischer, M. Wilke, K. J. Wenzel, F. Emmerling, *Angew. Chem.-Int. Edit.* **2015**, 54, 1799-1802.

Keywords: *in situ*, metal phosphonate, XRD

MS18. Thermoelectric materials - from fundamental science to applications

Chairs: Oliver Oeckler, Sylvie Hébert

MS18-P1 Interplay between structural transitions and thermoelectric properties in a Mn hollandite

Sylvie Hébert¹, Jesus Prado Gonjal¹, Hidefumi Takahashi¹, Denis Pelloquin¹, Antoine Maignan¹

1. Laboratoire CRISMAT, UMR6508 CNRS et ENSICAEN, 6 Bd du Maréchal Juin, 14050 Caen Cedex, France

email: sylvie.hebert@ensicaen.fr

NaCoO_2 and misfits are still the best p type thermoelectric oxides, with the combination of a large Seebeck coefficient, together with a metallic behaviour at 300K, and small values of thermal conductivities [1-3]. Their unique thermoelectric properties come from the presence of CoO_6 layers made of edge shared CoO_6 octahedra, with Co^{3+} and Co^{4+} in low spin states. New families of oxides have since then been investigated to find new potential thermoelectric materials. Among them, hollandites present an interesting crystallographic structure with (i) ribbons made of edge shared octahedra, and (ii) the presence of tunnels, in which large cations can be inserted. Several hollandites have been investigated, with both p and n type doping, and large power factors have been observed [4-5]. In this poster, the results obtained in the case of $\text{BaMn}_2\text{O}_{16}$ hollandite will be presented, with the evidence of a structural transition at high T. The impact of this structural transition on the transport properties will be discussed.

[1]: I. Terasaki, Y. Sasago and K. Uchinokura, Phys. Rev. B56, R 12685(1997).

[2]: K. Takahata, Y. Iguchi, D. Tanaka, and T. Itoh, I. Terasaki, Phys. Rev. B61, 12551 (2000).

[3]: S. Hébert, W. Kobayashi, H. Muguerra, Y. Bréard, N. Raghavendra, F. Gascoin, E. Guilmeau, A. Maignan, Physica Status Solidi A210, 69 (2013).

[4]: W. Kobayashi, S. Hébert, O. Pérez, D. Pelloquin, A. Maignan, Phys. Rev. B79, 085207 (2009).

[5]: A. Maignan, O. I. Lebedev, G. Van Tendeloo, C. Martin, S. Hébert, Phys. Rev. B82, 035122 (2010).

J. Prado Gonjal, Present address : University of Reading
H. Takahashi, Present address : Nagoya University

Keywords: Oxides, hollandites

MS19. Topology of crystal structures

Chairs: Davide Proserpio, Tonči Balić-Žunić

MS19-P1 Crystal chemistry of Al-phosphate minerals with complex H-bond networks

Francesco Capitelli¹, Giancarlo Della Ventura², Fabio Bellatreccia², Maria Rosaria Ghiara³, Manuela Rossi³, Emanuela Schingaro³, Gennaro Ventruti⁴, Angela Altomare⁵, Michele Saviano⁵

1. Istituto di Cristallografia – CNR Monterotondo (Rome, Italy)

2. Dipartimento di Scienze, Università Roma Tre (Rome, Italy)

3. Real Museo Mineralogico and Dipartimento di Scienze della Terra dell'Ambiente e delle Risorse, Università Federico II Naples (Naples, Italy)

4. Dipartimento di Scienze della Terra e Geoambientali, Università di Bari (Bari, Italy)

5. Istituto di Cristallografia – CNR Bari (Bari, Italy)

email: francesco.capitelli@ic.cnr.it

The $(\text{PO}_4)_x$ oxyanion combines with over 30 elements to form natural phosphates, which are among the most complex and variegated compounds in all the mineral world, displaying a large number of recognized phases (about 300), most of them featuring hydrogen as hydroxyl groups and water molecules. Thus, hydrogen bond displays a crucial role in stabilizing the hydroxy-hydrated phosphate frameworks, providing the additional bond-valence contribution to the anions. Hence, the oxygen atoms of $(\text{PO}_4)_x$ groups easily interact with neighbor cationic environments in the structure. For this reason, many phosphates are characterized by the presence of an intricate network of O-H...O interactions, joining the polyhedral units and making up the three dimensional framework (Huminicki & Hawthorne, 2002). In this sense, the study of such complex structures is achieved by means of Single-Crystal X-Ray Diffraction, with the contribute of powder FTIR spectroscopy, being the latter a powerful tool for the study of hydrogen in minerals, especially in presence of high OH/H₂O contents.

In this work, we present the structure investigations of selected aluminum phosphates: vauxite $\text{FeAl}_2(\text{PO}_4)_2(\text{OH})_2 \cdot 6\text{H}_2\text{O}$, wardite $\text{NaAl}_2(\text{PO}_4)_2(\text{OH})_2 \cdot 2\text{H}_2\text{O}$, wavellite $\text{Al}_2(\text{PO}_4)_3(\text{OH},\text{F}) \cdot 5\text{H}_2\text{O}$, augelite $\text{Al}_2(\text{PO}_4)_2(\text{OH})_2$, whiteite $\text{CaFeMgAl}_2(\text{PO}_4)_4(\text{OH})_2 \cdot 8\text{H}_2\text{O}$ (Ventruti *et al.*, 2015, and references therein). Main crystallographic features (bonds, angles, interactions) were examined and compared with those obtained from phosphate literature, and the networks of hydrogen bonds were further analyzed according to the Libowitzky (1999) relationship, for the range of D-H...A bond systems in the structure, in order to compare results of OH frequencies from FTIR spectra with those observed by X-ray refinement.

References

Huminicki, D.M.C. & Hawthorne, F.C. (2002): The crystal chemistry of phosphate minerals. *Reviews in Mineralogy and Geochemistry* **48**, 123-253.

Venturi G., Monno A., Schingaro E., Lacalamita M., Della Ventura G., Bellatreccia F., Cuocci C., Capitelli F. Structure refinement and vibrational spectroscopy of vauxite from the type locality, Lallagua (Bolivia). *Canadian Mineralogist*, in press.

Libowitzky, E. (1999): Correlation of O-H stretching frequencies and O-H...O hydrogen bond lengths in minerals. *Monatshefte für Chemie* **130**, 1047-1059.

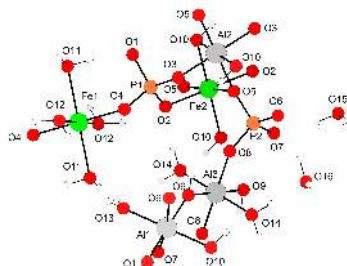


Figure 1. Cationic and anionic environments for vauxite.

Keywords: phosphates; structure refinement; hydrogen bonds; FTIR

MS19-P2 Constructing new porous materials based on polymeric cage metallosiloxanes

Alexander A. Korlyukov¹, Anna V. Volozhanina¹, Olga I. Shchegolikina¹, Alexei N. Bilyachenko¹, Boris G. Zavin¹, Nataliya V. Sergienko¹

¹ I. A.N. Nesmeyanov Institute of Organoelement Compounds, 119991, Russian Federation, Moscow, Vavilova Str., 28

email: alex@xrlab.ineos.ac.ru

We report on structural features and electronic properties of polymeric metallosiloxanes obtained by X-ray studies, magnetic measurements and theoretical calculations. Polymer structure of metallosiloxanes (MOS) under discussion composed from cage monomeric units containing various number of transition metals (Cu, Ni, Mn, Fe) interconnected by alkali-metal ions and weak interatomic interactions (hydrogen bonds or staking interactions). The type of supramolecular architecture (1D, 2D or 3D, see Figure 1) can be controlled by variation of ionic radii of alkali metal, the nature of solvent used for crystallization and addition of chelating ligands. These factors also affect the size of MOS monomeric units which can include 2-11 transition metal atoms forming metaloxide core partially coated by cyclic and acyclic siloxanolate ligands. Magnetic measurements have shown the pronounced ferro- and antiferromagnetic properties depending on number and the nature of transition metal in MOS core.

It was demonstrated by powder X-ray diffraction (XRD) and XAFS studies that polymer structure established at low temperature by single crystal XRD in the most of cases retained at room temperature. The role of metallosiloxanes as structure building units, the topology of resulting nets and accessibility of the voids were analyzed. In addition, the strength of coordination bonds and weak interatomic interactions responsible for the stabilization of polymer structures were estimated in terms of R. Bader's QTAIM theory.

Authors are grateful to Prof. Yan Zubavichus (Kurchatov Center for Synchrotron Radiation and Nanotechnology) for help with XAFS and single-crystal synchrotron studies. The work was supported by Russian Science Foundation (grant 14-23-00231).

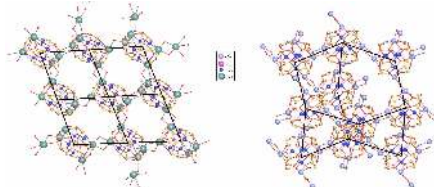


Figure 1. Fragments of the sql and dia nets in the structures of sodium (left) and cesium (right) coppersiloxanes

Keywords: metallosiloxanes, coordination polymers, structure building unit, magnetic properties, QTAIM studies.

MS19-P3 Polyoxometalates as structurally diverse and efficient catalysts for artificial photosynthesis

Kim D. von Allmen¹, René Moré¹, Greta R. Patzke*¹

¹. University of Zurich, Department of Chemistry B, Winterthurerstrasse 190, CH-8057 Zurich, Switzerland

email: kim.vonallmen@chem.uzh.ch

Polyoxometalates (POMs) are metal oxo clusters which are preferably formed by W, Mo and V in their high oxidation states. They emerge from complex self-assembly processes and excel through an exceptionally wide range of applications. An impressive multitude of POM structure types has been reported to date, ranging from low nuclearity to nanoscale clusters. POMs are furthermore applied as highly active catalysts, e.g. for organic transformations and artificial photosynthesis, and their magnetic properties and biomedical applications are of current interest. [1]

The controlled preparation and precise crystallographic characterization of new POMs is crucial to generate libraries for screening their potential applications. We have studied the reaction of the lacunary precursor material $\text{Na}_{10}[\alpha\text{-SiW}_9\text{O}_{34}]\cdot 15\text{H}_2\text{O}$ (SiW_9) with Ga(III) ions in aqueous solution. The emerging new crystal structures of $\text{K}_{10}[\text{Ga}(\text{H}_2\text{O})_2(\alpha\text{-SiW}_9\text{O}_{35}(\text{OH})_2)_2]\cdot 35.5\text{H}_2\text{O}$ (**Ga-1**) and $\text{K}_{12}[\text{Ga}_2(\text{H}_2\text{O})_2(\alpha\text{-SiW}_{10}\text{O}_{36})_2]\cdot 30\text{H}_2\text{O}$ (**Ga-2**) have been described in detail. Both compounds could be isolated in phase pure form and were characterized with a wide range of additional spectroscopic and electrochemical methods. [2]

While our structural chemistry work highlights the preparation and isolation of new Ga-containing polyoxometalates, our most recent studies are focused on POM catalyst development. Ni-substituted POMs have been investigated as water reduction catalysts (WRC) for visible-light driven H_2 evolution. [3] In order to establish structure-activity relationships (SAR), Ni-based Keggin-type POMs of the general type $[\text{Ni}(\text{H}_2\text{O})\text{XW}_9\text{O}_{39}]^n$ ($\text{X} = \text{P}, \text{Ge}, \text{Si}$) have been crystallized and characterized by X-ray crystallographic methods. All three compounds have been tested as WRCs in an established photochemical assay for visible-light driven H_2 evolution, and the heteroatom was found to have an important influence on their H_2 evolution activity. In order to understand and explain the observed trends, electrochemical experiments and DFT calculations have been performed.

[1] J. R. Poeppelmeier, *Comprehensive Inorganic Chemistry 5116*, Second Edition ed., Elsevier, Amsterdam, 2013. [2] K. von Allmen, P.-E. Car, O. Blaque, T. Fox, R. Müller, G. R. Patzke, *Z. Anorg. Allg. Chem.* **2014**, 640, 781–789. [3] K. von Allmen, R. Moré, R. Müller, J. Soriano-López, A. Linden, G. R. Patzke, in revision.

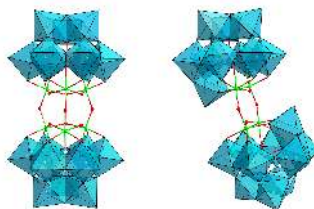


Figure 1. Polyhedral ball-and stick representation of Ga-1 (left), Ga-2 (right).

Keywords: Polyoxometalates, Artificial photosynthesis, Nickel, Gallium, Catalysis

MS19-P4 SACADA-the database of three periodic carbon allotropes

Andrey A. Golov^{1,2}, Artem A. Kabanov¹, Davide M. Proserpio^{1,3},
Vladislav A. Blatov^{1,2}

1. Samara Center for Theoretical Materials Science, Samara State University, Samara, Russia
2. Chemistry Department, Samara State University, Samara, Russia
3. Dipartimento di Chimica, Università degli Studi di Milano, Milano, Italy

email: angolov1990@mail.ru

Nowadays the modeling of new carbon allotropes is very popular. There are more than 400 articles on the topic of hypothetical carbon allotropes by the data of Scopus database [1]. Mistakes in classification and naming of carbon allotropes are almost inevitable due to vast amount of unsystematized data. For example, the (RL3)2 structure was described for the first time in 1997 [2] and then rediscovered in 2013 [3] under the name of oC32. Another example of typical mistake is an assigning the same name to several different structures. For instance, Y-carbon corresponds to different structures in articles [4, 5]. The main purpose of the work is accumulation and systematization of the data on all three periodic carbon allotropes. We have extracted the data of crystal structures and physical properties for 260 unique carbon allotropes (corresponding to 236 topological types) from 195 articles. The topological characteristics of the structures were calculated by ADS program implemented in ToposPro [6]. The maximal symmetry embeddings of the nets corresponding to 236 topological types were obtained by Systre program [7]. The all results of the study are presented in Samara Carbon Allotrope Database (Fig.1) [8].

The work was supported by the Russian government (Grant 14.B25.31.0005).

References

1. R.D.H. Tobing, ARPN Journal of Engineering and Applied Sciences, 2015, **10**, 1238-1243.
2. R.H. Baughman, A.Y. Liu, C. Cui, and P.J. Shields, Synthetic Metals, 1997, **86**, 2371-2374.
3. M. Zhang, H. Liu, Y. Du, X. Zhang, Y. Wang and Q. Li, Phys.Chem.Chem. Phys., 2013, **15**, 14120-14125.
4. Q. Zhu, Q. Zeng and A. R. Oganov, Phys. Rev. B, 2012, **85**, 201407.
5. J.Y. Jo and B.G. Kim, Phys. Rev. B, 2012, **86**, 075151.
6. V.A. Blatov, A.P. Shevchenko and D.M. Proserpio, Cryst. Growth Des., 2014, **14**, 3576–3586.
7. O. Delgado-Friedrichs, The Gavrog Project, <http://gavrog.org>.
8. D.M. Proserpio, A.A. Kabanov and A.A. Golov, Samara Carbon Allotrope Database, <http://sacada.sctms.ru/>.



Figure 1. Image of SACADA.

Keywords: New carbon allotropes, topology of crystal structure, SACADA database.

MS19-P5 Syntheses and crystal structures of novel $\text{Zr}(\text{SeO}_3)(\text{SeO}_4)$ and $\text{Zr}(\text{SeO}_4)_2 \cdot \text{H}_2\text{O}$

Gerald Giester¹, Manfred Wildner¹

1. Institut für Mineralogie und Kristallographie, Universität Wien, Althanstr. 14, 1090 Wien, Austria

email: gerald.giester@univie.ac.at

Two new compounds, a) $\text{Zr}(\text{SeO}_3)(\text{SeO}_4)$ and b) $\text{Zr}(\text{SeO}_4)_2 \cdot \text{H}_2\text{O}$, were obtained in the course of a long-term project focusing on the crystal chemistry of Se^{4+} , $6+$ - M^{4+} oxyanions with $\text{M}^{4+} = \text{Ti}$, Zr , Hf , as well as Mn , Ge , Sn and Pb [1,2].

Both phases were synthesized at low-hydrothermal conditions (Teflon-lined steel vessels, 220°C) from mixtures of $\text{Zr}_2\text{O}_3(\text{CO}_3)(\text{OH})_2$, H_2SeO_4 and minor contents of water. Colorless single crystals up to 0.2 mm in length were obtained within a period of one week and were studied by single crystal X-ray techniques (Bruker APEXII diffractometer, MoK α Incoatec Microfocus Source, 293 K). The crystal structures were solved and refined by a package of SHELX programs [3]. $\text{Zr}(\text{SeO}_3)(\text{SeO}_4)$ crystallizes in the orthorhombic space group *Pbca* (No. 61), with $a = 8.295(2)$, $b = 9.476(2)$ $c = 15.370(3)$ Å, $V = 1208.1(5)$ Å³, $Z = 8$, $R1 = 0.0316$; $\text{Zr}(\text{SeO}_4)_2 \cdot \text{H}_2\text{O}$ is monoclinic, space group *P2₁/n* (No. 14), with $a = 5.332(1)$, $b = 7.962(2)$, $c = 16.256(3)$ Å, $\beta = 92.19(1)^\circ$, $V = 689.6(3)$ Å³, $Z = 4$, $R1 = 0.0195$.

$\text{Zr}(\text{SeO}_3)(\text{SeO}_4)$ and $\text{Zr}(\text{SeO}_4)_2 \cdot \text{H}_2\text{O}$ represent new structure types built from isolated a) ZrO_6 octahedra or b) ZrO_5 pentagonal dipyramids, further cornerlinked via a) SeO_4 tetrahedra and trigonal SeO_3 pyramids or b) only SeO_4 groups to three-dimensional frameworks. Mean cation-oxygen bond lengths, a) Zr^{4+} : 2.063 Å, Se^{4+} : 1.679 Å, Se^{6+} : 1.623 Å and b) Zr^{4+} : 2.137 Å, Se^{4+} : 1.631 Å, Se^{6+} : 1.635 Å, are in accordance with literature. In case of b) one H_2O group is ligand of the ZrO_7 coordination forming hydrogen bonds with 2.65 and 2.76 Å donor-acceptor distances.

Literature:

- [1] Giester, G., Wildner, M. (1991): Hydrothermal synthesis and crystal structure of $\text{Mn}(\text{SeO}_3)_2$. Journal of Solid State Chemistry 91, 370-374.
- [2] Steinhauser, G., Luef, C., Wildner, M., Giester, G. (2006): Syntheses and crystal structures of $\text{Pb}(\text{SeO}_3)_2$ and two modifications of $\text{Sn}(\text{SeO}_3)_2$. Journal of Alloys and Compounds 419, 45-49.
- [3] Sheldrick, G.M. (2008): A short history of SHELX. Acta Crystallogr. A 64, 112-122.

Keywords: $\text{Zr}(\text{SeO}_3)(\text{SeO}_4)$, $\text{Zr}(\text{SeO}_4)_2 \cdot \text{H}_2\text{O}$, crystal structure

MS19-P6 A knowledge database for intermetallics: the collection of Topological Types of Nanoclusters

Tatiana G. Akhmetshina¹, Arina A. Pankova¹, Vladislav A. Blatov¹, Davide M. Proserpio^{1,2}

1. Samara Center for Theoretical Materials Science, Samara State University, Ac. Pavlov St. 1, 443011 Samara, Russia

2. Dipartimento di Chimica, Università degli Studi di Milano, Via Golgi 19, 20133 Milano, Italy

email: akhmetshina.tanya@yandex.ru

The main goal of our work was to develop a database containing information on structural building units in intermetallics. We have applied a universal method based on the strict algorithm of searching for the multi-shell onion-like primary nanoclusters that assemble the intermetallic compounds [1]. This “Nanoclustering” procedure was implemented in the program package ToposPro [2]. Using the information on more than 27,000 crystal structures of intermetallics from the ICSD and Pearson’s Crystal Data, we have created the *Topological Types of Nanoclusters* (TTN) collection. The TTN collection contains 1006 polyhedral and 1016 multishell nanoclusters as local configurations of atoms and as primary nanoclusters in intermetallics. To illustrate the possibility of the TTN collection we have considered icosahedron-based intermetallics. Altogether, 319 ordered intermetallic compounds with centered icosahedra as primary nanoclusters were fully investigated. As a result, we have found correlations between topological parameters and chemical composition of those intermetallics. In particular, the A@M12 composition is realized in 87 compounds of which 84 assemble into **bcc-x** (body-centered cubic) motif. We have collected the distributions on chemical composition, symmetry and topological parameters in a knowledge database. It is shown that the knowledge database can be used to find possible motifs of assembling building units in intermetallics, and further, to predict new possible intermetallic compounds.

[1] Vladislav A. Blatov *Struct. Chem.* **2012**, *23*, 955–963.

[2] Vladislav A. Blatov, Alexander P. Shevchenko, and Davide M. Proserpio *Cryst. Growth Des.* **2014**, *14*, 3576–3586 <http://topospro.com>

Keywords: intermetallics, topology

MS19-P7 Rod packing nets in 3-periodic metal-organic frameworks

Andrey V. Goltsev¹, Evgeny V. Alexandrov¹, Vladislav A. Blatov¹, Davide M. Proserpio^{1,2}

1. Samara Center for Theoretical Materials Science (SCTMS), Samara State University, Ac. Pavlov St. 1, Samara 443011, Russia

2. Dipartimento di Chimica, Università degli Studi di Milano, Via Golgi 19, 20133 Milano, Italy

email: andregoltsev@gmail.com

The main goal of our work is creating the strict and useful taxonomy for packings of rods into metal-organic frameworks. The classification of rod-packings by the set of robust descriptors and establishing the correlations between their crystal structure and composition is very important task for design of new MOFs and prediction of their properties [1]. Using ToposPro [2] we found rod packings in 5132 coordination polymers (26.9% from the overall list of 3D coordination polymers). These structures analyzed with cluster representation gives 4805 simplified chains that consist of one set of parallel rods (only in one direction); 309 contain two sets of rods in two different directions; 16 - three directions; 2 - four directions. Classification is carried out in according with 14 types of packings described by O’Keeffe and coworkers [1, 3]. For more detailed classification we used topological type of underlying net of the structure to characterize the global topology, as well composition and coordination of ligands and bridging groups in rods to describe the local topology. The values of these descriptors will be stored in the “Knowledge database” of MOFs and can efficiently be used by “Expert system” for prediction of new MOFs with the specified set of properties and crystal structure composition [4].

[1] N.L. Rosi, J. Kim, M. Eddaoudi, B. Chen, M. O’Keeffe, O.M. Yaghi, *JACS*, **2005**, *127*, 1504–1518

[2] V.A. Blatov, A. P. Shevchenko, D. M. Proserpio, *Cryst. Growth Des.* **2014**, *14*, 3576–3586 <http://topospro.com>.

[3] M. O’Keeffe, S. Andersson, *Acta Cryst.*, **1977**, *A33*, 914–923

[4] E.V. Alexandrov, A.P. Shevchenko, A.A. Asiri, V.A. Blatov, *CrystEngComm*, **2015**, DOI: 10.1039/C4CE02418D

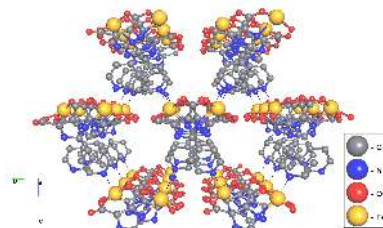


Figure 1. The parallel 1-periodic rods in 3-periodic crystal structure of $\{[\text{Fe}(\text{HPIDC})(\text{H}_2\text{O})_2] \cdot 2\text{H}_2\text{O}\}_n$ (some valence bond changed to hydrogen bonds).
*2-(pyridin-4-yl)-1H-imidazole-4,5-dicarboxylate

Keywords: Metal-organic frameworks, topological classification, rod packings, topology of crystal structure

MS20. High pressure solid state chemistry

Chairs: Natalia Dubrovinskaia, Wilson Crichton

MS20-P1 Dynamic compression and time-resolved XRD across the phase boundaries of the high-P polymorphs of CaCO_3

Ronald Miletich¹, Huijeong HWANG², Yongjae LEE², Diego GATTA³, Thomas PIPPIINGER⁴

1. Department for Mineralogy and Crystallography, University of Vienna, Althanstrasse 14, A-1090 Wien, Austria
2. Department of Earth System Sciences, Yonsei University, Shinchon 134, Seoul 120749, Republic of Korea
3. Dipartimento di Scienze della Terra, Università degli Studi di Milano, Via Botticelli 23, I-20133 Milano, Italy
4. Department for Mineralogy and Crystallography, University of Vienna, Althanstrasse 14, A-1090 Wien, Austria; STOE & Cie GmbH, Hilpertstrasse 10, D-64295 Darmstadt, Germany

email: ronald.miletich-pawliczek@univie.ac.at

Calcium carbonate, CaCO_3 , shows a rich polymorphism with in total 7 phases at ambient and non-ambient pressure and temperature conditions. Compression of calcite, the trigonal low-P form (space group R-3c), results in the transformation to a monoclinic structure ("calcite-II", space group P2₁/c) at P > 1.4 GPa and hereafter into two triclinic structures (phases III and IIIb, space group P-1) [1-3]. Phase IIIb is considered to be either metastable or have a stability field at high-P low-T conditions [3]. One of the speculations about the existence of the phases III and IIIb was the fact that compression rates appear to determine the structural stability [1]. Therefore, a time-resolved XRD in-situ study under controlled compression rates using a dynamic diamond-anvil cell (dDAC) was accomplished at SSRL (Stanford Synchrotron Radiation Lightsource) BL 10-2 beamline on a polycrystalline CaCO_3 sample compressed under rates of 0.0052 to 0.017 GPa/frame for 1 second exposure time per frame using a Dectris Pilatus 300k detector. The I-II transition was found to reveal a smooth shift of the XRD Bragg peaks corresponding to the splitting, which follows the trigonal-to-monoclinic distortion within a pressure interval between 1.57 and 1.77 GPa. The transition from II to III starting at 2.67 GPa is characterized by the coexistence of III and IIIb, while at 2.98 GPa the XRD pattern only consists of the lines of phase III. The field of III+IIIb coexistence slightly varies with the compression rate (2.67-2.98 GPa at 0.0052 GPa/sec; 2.89-3.04 GPa at 0.017 GPa/sec), and corresponds to the pressure range for IIIb as recently reported [3]. Nevertheless, the XRD patterns recorded with the dDAC reveal a further change at P > 4.68 GPa, which has not been yet identified but might be considered as a new phase. The results of this dynamic compression are also compared to the findings of the Raman

investigations under non-hydrostatic conditions, which have been carried out in order to identify the influence of stress on shifting phase boundaries.

[1] Merlini, M., Hanfland, M., Crichton, W.A. (2012) *Earth Planet Sci Lett* 333-334, 265-271

[2] Merlini, M., Crichton, W.A., Chantel, J., Guignard, J., Poli, S. (2014): *Min. Mag.* 78, 225-233

[3] Pippinger, T., Miletich, R., Merlini, M., Lotti, P., Schouwink, P., Yagi, T., Crichton, W.A., Hanfland, M. (2015): *Phys. Chem. Min.* 42, 29-43

Keywords: high pressure, phase transition, calcium carbonate, polymorphism

MS20-P2 High-pressure phase transitions in ordered and disordered ternary tetradymite $\text{Bi}_2\text{Te}_2\text{Se}$

Morten B. Nielsen¹, Paraskevas Parisiades², Solveig R. Madsen¹, Martin Bremholm¹

1. Center for Materials Crystallography (CMC), Department of Chemistry and iNANO, Aarhus University, Aarhus, Denmark

2. European Synchrotron Radiation Facility (ESRF), Beamline ID27, Grenoble, France

email: mbnielsen@chem.au.dk

We report studies of pressure-induced phase transitions of ordered and disordered ternary tetradymite $\text{Bi}_2\text{Te}_2\text{Se}$ by synchrotron powder x-ray diffraction in diamond anvil cells for pressures up to 57 and 48 GPa, respectively. The first sample (SB) was prepared from a single crystal with ordered Se/Te sites (fig. 1a) while the second sample (Q) was prepared from a quenched melt resulting in tetradymite with disordered Se/Te. This allowed for an investigation of the effect of disorder on the phase transitions and the equation of states (EoS) of the tetradymite α -phase.

Fitting the 3rd order Birch-Murnaghan EoS to the tetradymite α -phases yielded bulk moduli K_0 of 36.7(9) and 40.3(19) GPa and K'_0 of 6.0(3) and 4.8(6) for the SB and Q samples, respectively. An electronic topological transition was observed in both samples at pressures of 3.8 and 2.6 GPa, respectively. This was followed by a transition near 10 GPa to a phase that is isostructural with the β -phase of Bi_2Te_3 (fig. 1b).¹ The Se/Te ordering only affected the transition pressure to a small extent.

A cubic phase that resembles the δ -phase observed in high-pressure studies of Bi_2Te_3 (fig. 1c)^{1,2} appeared at 16-19 GPa, but the ternary composition lead to a more complex structure. The presence of a low angle diffraction peak in the δ -phase demonstrated that the true structure is not simply body-centered cubic. In this way the samples resemble Bi_2Se_3 where Bi and Se show a high degree of ordering, but the proposed structures in literature³⁻⁵ of $\delta\text{-Bi}_2\text{Se}_3$ did not fully describe the data for $\delta\text{-Bi}_2\text{Te}_2\text{Se}$. The nature of the partial ordering of the Se/Te in the high-pressure $\delta\text{-Bi}_2\text{Te}_2\text{Se}$ is discussed through various short-range ordering models.

References:

- [1] L. Zhu *et al.*, *Phys. Rev. Lett.* **106** (14), 145501 (2011)
- [2] M. Einaga *et al.*, *Phys. Rev. B*, **83** (9), 092102 (2011); S. J. Zhang *et al.*, *J. Appl. Phys.* **111** (11), 112630 (2012)
- [3] J. G. Zhao *et al.*, *J. Phys.: Condens. Matter* **25** (12), 125602 (2013)
- [4] G. T. Liu *et al.*, *J. Phys. Chem. C* **117** (19), 10045 (2013)
- [5] R. Vilaplana *et al.*, *Phys. Rev. B* **84** (18), 184110 (2011)

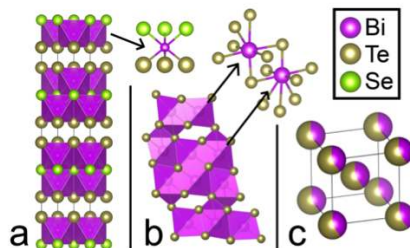


Figure 1. a) α -phase tetradymite $\text{Bi}_2\text{Te}_2\text{Se}$, b) β -phase Bi_2Te_3 , c) δ -phase Bi_2Te_3 .

Keywords: Tetradymite, $\text{Bi}_2\text{Te}_2\text{Se}$, Substitutional Alloy

MS20-P3 $\text{Mg}_2\text{Fe}_3\text{O}_5$ a novel breakdown product of MgFe_2O_4 at high pressureTiziana BOFFA BALLARAN¹, UENVER-THIELE Laura², WOODLAND B. Alan²

1. Bayerisches Geoinstitut, Universität Bayreuth, D - 95440 Bayreuth, Germany
2. Institut für Geowissenschaften, Goethe-Universität Frankfurt, Altenhöferallee 1, D – 60438 Frankfurt am Main, Germany

email: tiziana.boffa-ballaran@uni-bayreuth.de

Since the recent discovery of the novel oxide Fe_3O_5 resulting as a breakdown product of siderite or magnetite [1,2], investigations on the possible substitutions of Mg and Cr for Fe^{2+} and Fe^{3+} and their implication for the Earth's mantle have been undertaken [3]. Fe_3O_5 crystallises in the *Cmcm* space group and has a structure similar to that of $\text{Sr}_2\text{Ti}_2\text{O}_7$ and CaFe_2O_7 , consisting of layers of edge-sharing FeO_6 octahedra and layers of trigonal prisms alternating along the *c*-axis. In the present study the structure of a novel $\text{Mg}_2\text{Fe}_3\text{O}_5$ oxide, synthesized at 15 GPa and 1550 °C from a mixture of MgFe_2O_4 and MgO , has been determined by means of single-crystal X-ray diffraction. This compound is isostructural with Fe_3O_5 and it can be considered as the other end-member of a binary system between these two oxides involving the complete substitution of Fe^{2+} for Mg. The Mg and Fe^{3+} cations are disordered among the three crystallographic sites of the $\text{Mg}_2\text{Fe}_3\text{O}_5$ structure, although preference of Mg for the trigonal prism coordination is observed. Substitution of Mg into the Fe_3O_5 structure reduces the octahedral distortion of both octahedral sites. It also has been reported that FeCr_2O_4 dissociates into $\text{Fe}_2\text{Cr}_2\text{O}_5$ and Cr_2O_3 at high pressure [4]. However, such compound appears to be isostructural with $\text{Mg}_2\text{Al}_2\text{O}_5$, having space group *Pham* and a different stacking of the octahedral units that, in this case, form long chains surrounding the trigonal prisms. This is quite puzzling given that samples belonging to the Fe-Cr solid solution with up to 50% of the $\text{Fe}_2\text{Cr}_2\text{O}_5$ component [3] appear instead to crystallise in the *Cmcm* space group. A possible explanation of such difference may reside in the different Jahn-Teller distortions of the two compounds, since in $\text{Fe}_2\text{Cr}_2\text{O}_5$ only Cr^{3+} is present while in $\text{Mg}_2\text{Fe}_3\text{O}_5$ the transition cation is exclusively Fe^{3+} . M_4O_5 phases can now be considered a new addition to the phase relations of a number of simple oxide systems at pressures and temperatures at which the spinel-structured phase becomes unstable. These phases may form complex solid solutions; moreover, our results indicate that cation order-disorder phenomena may help to stabilize the M_4O_5 phase, particularly at higher temperatures.

References:

- [1] Lavina, B. et al. (2011). PNAS, 108, 17281-17285.
- [2] Woodland, A.B. et al. (2012). Am Mineral, 97, 1808-1811.
- [3] Woodland, A.B. et al. (2013). Contrib Mineral Petrol, 166, 1677-1686.
- [4] Ishii, T. et al. (2014). Am Mineral, 99, 1788-1797.

Keywords: $\text{Mg}_2\text{Fe}_2\text{O}_5$, Fe_4O_5 , high-pressure, crystal structure**MS20-P4** High pressure synthesis and characterization of hydrogenated nitrogen-rich carbonaceous polymerKamil F. Dziubek^{1,2}, Margherita Citroni^{1,3}, Samuele Fanetti¹, Carla Bazzicalupi¹, Marco Pagliai^{1,3}, Mohamed Mezouar⁴, Roberto Bini^{1,3}

1. LENS - European Laboratory for Non-Linear Spectroscopy, Sesto Fiorentino, Italy
2. Faculty of Chemistry, Adam Mickiewicz University, Poznań, Poland
3. Department of Chemistry "Ugo Schiff", University of Florence, Sesto Fiorentino, Italy
4. European Synchrotron Radiation Facility ESRF, Grenoble, France

email: rumianek@amu.edu.pl

High pressure synthesis and recovery of new materials based on the C-N-H system have gained remarkable interest fueled by their potential use as high energy density materials, layered graphitic structures for nanoelectronics, metal-free photocatalysts or intermediates for the production of superhard carbon nitrides. Due to its highly symmetric molecule with C and N atoms alternating in an aromatic ring and equal contents of all three elements, 1,3,5-triazine (*s*-triazine, $\text{C}_3\text{N}_3\text{H}_3$) is a promising candidate for the synthesis of novel extended compounds.

We have thoroughly studied pressure and temperature induced reaction in solid *s*-triazine and characterized its phase diagram and *P-T* stability boundaries of the crystalline molecular phases by the means of IR spectroscopy. The reaction kinetics was analyzed as well. Powder diffraction patterns measured as a function of pressure allowed us to obtain atomic coordinates for the high pressure phase II of *s*-triazine and to confirm the previously described low temperature crystal form of *C2/c* space group symmetry, existing at atmospheric pressure below 198.07 K. Following the pressure evolution of short C...N contacts we determined the critical minimum distance, which marks the threshold of the chemical reaction. In addition, the stable amorphous product of the reaction was recovered to ambient conditions and analyzed by IR spectroscopy and pair distribution function analysis. Depending on the reaction conditions different products are formed.

Kamil F. Dziubek gratefully acknowledges the Polish Ministry of Science and Higher Education for financial support through the "Mobilność Plus" program.

Keywords: high pressure chemistry, synthesis, functional materials

MS20-P5 Pressure induced structural collapse of the hydroquinone – formic acid clathrate; a pressure medium dependent non-linear optical phase transition

Espen Eikeland¹, Maja K. Thomsen¹, Solveig R. Madsen¹, Jacob Overgaard¹, Mark Spackman², Bo B. Iversen¹

1. Center for Materials Crystallography, Department of Chemistry and iNANO, Aarhus University, DK-8000 Aarhus C, Denmark
2. School of Chemistry and Biochemistry, M310, University of Western Australia, 35 Stirling Hwy, Crawley, 6009, Western Australia

email: eikeland@chem.au.dk

As of the beginning of the 21st century supramolecular chemistry and crystal engineering have become central areas for the development of organic materials, with applications as diverse as targeted drug delivery, chemical separation, sensors and catalysis. Yet, it is striking that the fundamental chemistry governing even simple self-assembly processes are not well understood.^[1] The challenge of studying molecular aggregates are their inherent complexity, with even the simplest molecular crystal having numerous superimposed intermolecular interactions, all of which contribute to the cohesive energy of the solid. To better understand self-assembly processes, one needs to quantitatively determine the different intermolecular interactions energies. Spackman and coworkers have developed a computational approach to calculate accurate intermolecular interactions energies called *energy frameworks*. In this study *energy frameworks* are used to look at changes in host-guest interaction energies for the hydroquinone-formic acid clathrate system (HQ-HCOOH) when subjected to external pressure. Single crystal high-pressure crystallography is the perfect experimental method for probing intermolecular interactions by forcing the host and guest molecules together. Furthermore a new phase transition is found in which the host structure collapses and the guest molecules migrate out of the cavities. The high-pressure phase is a non-linear optical material, interesting in it's own right for developing photonic and optoelectric devices. The *energy frameworks* can here be used to explain the phase transition and why it only takes place when using a hydrostatic pressure medium.

Altogether this work presents a method for gaining quantitative information about different intermolecular interaction energies as a function of pressure, which will enable us to better understand the formation of complex supramolecular aggregates.

S.I. Stupp and L.C. Palmer. *Chemistry of Materials*, **2014**, 26, 507-518.

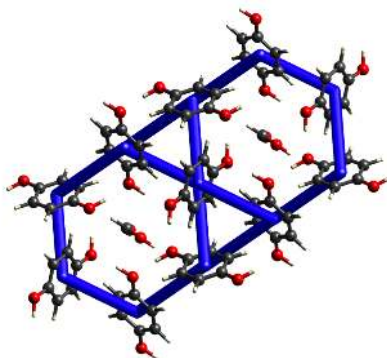


Figure 1. Energy framework of the host structure before the phase transition in the hydroquinone - formic acid clathrate. The pillars connecting host molecules correspond to total interaction energies of 34 kJ/mol.

Keywords: energy frameworks, intermolecular energies, high-pressure crystallography, host-guest interactions, organic clathrates.

MS20-P6 Quasiparticle band structure, spectral weights and degree of d-electron localization in Iron Silicides

Igor S. Sandalov^{1,2}, Natalia Zamkova^{2,3}, Vyacheslav Zhandun², Sergei G. Ovchinnikov^{2,3}

1. KTH Royal Institute of Technology, SE 100 44 Stockholm, Sweden

2. L.V.Kirensky Institute of physics, Siberian Branch of Russian Academy Sciences, 660036 Krasnoyarsk, Russia

3. Siberian Federal University, 660041 Krasnoyarsk, Russia

email: sandalov@kth.se

The degree of quasiparticle (QP) localization as well as QP spectral weights (SWs) determine the cohesive energy and, hence, the degree of stability of a crystal under pressure. Both QP band structure and their SWs can be measured by angle-resolved photoemission spectroscopy (ARPES). SWs also manifest themselves in Compton-scattering experiments and in the effective mass of QPs at the Fermi surface. We report results of our *ab initio* calculations of the QP spectra and SWs quasiparticle for Fe_3Si and α - $FeSi_2$, performed within Hedin's GW approximation (GWA) by means of Vienna Ab initio Simulation Package (VASP). Comparison of the GGA-to-DFT and GWA band structures shows that both theories reflect peculiarities of the crystal structures in similar shape of the bands in certain *k*-directions, however, i) Fermi energies for GGR bands are lower by ~0.5 eV than the one for GWA for both compounds; ii) GWA density of electron states smoother than the GGR one and existing peaks in the density of QP states are shifted with respect to each other; iii) while the spectral weights of QPs for GGA calculation are equal to unity by definition, the GWA ones are decreased almost by half in both compounds and show non-monotonic behavior (see figure) only in those parts of bands where the delocalized states contribute to their formation. Both methods give *d*-electrons localized and large magnetic moment in Fe_3Si of iron ion is surrounded iron ions, whereas the *Si*-atom nearest neighbors lead to delocalization of *d*-electrons and quenched magnetic moments. The α - $FeSi_2$, where all iron ions have the *Si* ions in nearest neighbors, is Pauli paramagnet. Estimation of diagrams responsible for the screening of Coulomb interaction within simplified model shows that GW approximation, even with inclusion of the standard vertex corrections, cannot describe the contribution from quasilocated electrons to the spectral weights and, correspondingly, to the correlation mechanism of d(f)-electron delocalization, considered earlier within the periodical Anderson model (Phys. Rev. B 62, 16370 (2000-II)). Thus, the *ab initio* methods for systems with strongly correlated electrons are needed where different approximations for *d(f)* - and delocalized electrons will be used from the very beginning. The ARPES measurements for these compounds would be of great help for further understanding of underlying physics.

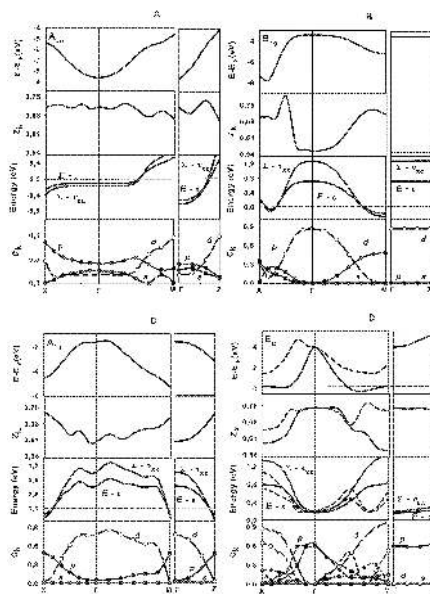


Figure 1. The α - $FeSi_2$ bands. QP filled bands, spectral weights Z_i , the *k*-dispersion of numerator and denominator of Eq.(4) in arXiv:1501.05898v3[cond-mat.mtrl-sci] and the character coefficients C_i ; d- and p- characters are denoted by empty and filled circles, the black squares stand for s character.

Keywords: strongly correlated electrons, delocalization

MS20-P7 Glycine co-crystals at low temperature and high pressure: X-ray diffraction and spectroscopic study

Evgeniy A. Losev¹, Boris A. Zakharov^{1,2}, Elena V. Boldyreva^{1,2}

1. Institute of Solid State Chemistry and Mechanochemistry SB RAS, Kutateladze, 18, Novosibirsk, 630128, Russia

2. REC-008, Novosibirsk State University, Pirogova, 2, Novosibirsk, 630090, Russia

email: losev.88@mail.ru

There are three “true” co-crystals of glycine with carboxylic acids (with no proton transfer from acidic component to basic one) reported up to now: those with glutaric (GG), DL-tartaric (GT) and phthalic (GP) acids. The co-crystal of glycine with glutaric acid was obtained in two research groups independently [1, 2]. The behaviour of this co-crystal at low temperature and high pressure was investigated in our laboratory previously and first order phase transition was discovered [3, 4].

The present study was focused on the effect of variations in temperature and pressure on two other co-crystals of glycine - with DL-tartaric and phthalic acids. Both co-crystals were stable on cooling down up to 100 K. The changes of unit cell parameters and in the geometry of the hydrogen bonds were followed. No phase transitions were detected, in contrast to GG co-crystal.

The effect of pressure on selected co-crystals was much more significant. The two molecular co-crystals underwent reversible phase transformations at quite low pressures. The phase transitions were accompanied by fracture (Fig. 1). Despite this, the crystal structure of the high-pressure phase of GT co-crystal could be solved by single crystal X-ray diffraction. The changes in the structure as compared with the low-pressure phase were analysed in terms of molecular conformations and hydrogen bonded motifs. However, it was impossible to solve the structure of GP co-crystal after the high-pressure phase transition, due to a complete fracture of the single crystal, although Raman spectra could be measured for the new phase. The crystal structures of high-pressure phases of glycine co-crystals were compared with each other. The features of structural rearrangement and changes in hydrogen bond network were analysed using X-ray diffraction and spectroscopic data.

The work was supported by the Russian Foundation for Basic Research (RFBR) (Grant No. 14-03-31866 mol-a).

[1]Losev, E.A., Zakharov, B.A., Drebuschak, T.N., Boldyreva, E.V. *Acta Crystallogr., Sect. C: Cryst. Struct. Commun.*, 2011, 67 (8), pp. o297-o300. [2]Riscob, B., Shakir, M., Kalyana Sundar, J., Natarajan, S., Wahab, M.A., Bhagavannarayana, G. *Spectrochim. Acta, Part A*, 2011, 78 (1), pp. 543-548. [3]Zakharov, B.A., Losev, E.A., Kolesov, B.A., Drebuschak, V.A., Boldyreva, E.V. *Acta Crystallogr., Sect. B: Struct. Sci.*, 2012 68 (3), pp. 287-296. [4]Zakharov, B.A., Losev, E.A., Boldyreva, E.V. *CrystEngComm*, 2013, 15 (9), pp. 1693-1697.

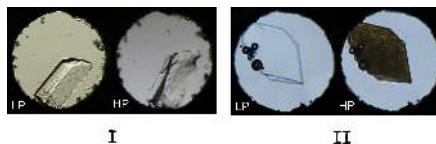


Figure 1. The destruction of glycine co-crystals under high pressure. I – glycine-DL-tartaric acid co-crystal, II – glycine-phthalic acid co-crystal. LP – low-pressure phase, HP – high-pressure phase

Keywords: high-pressure, glycine, co-crystal, hydrogen bond

MS20-P8 Structural complexity of dense lithium: electronic originValentina F. Degtyareva¹¹. Institute of Solid State Physics Russian Academy of Sciences, Chernogolovka, Russia

email: degtyar@issp.ac.ru

Lithium – the lightest alkali metal – exhibits unexpected structures and electronic behavior at high pressures [1,2]. As the heavier alkalis, Li is bcc at ambient pressure and transformed first to fcc (at 7.5 GPa). The high-pressure form Li-*c16* (at 40-60 GPa) is similar to Na-*c16*. The other high pressure phases found for Li (*hR1*, *oC88*, *oC40*, *oC24*) at pressures up to 130 GPa are specific to Li, whereas for heavier alkali metals there are several sheared forms. The different route of Li high-pressure structures correlates with its special electronic configuration containing the only 3 electrons (at 1s and 2s levels). Complex structures for Li are analyzed within the model of Fermi sphere – Brillouin zone interactions [3,4]. Stability of *post*-fcc structures for Li can be supported by Hume-Rothery arguments when new diffraction planes appear close to the Fermi level and characterized by pseudogap formation near the Fermi level decreasing the crystal energy. The filling of Brillouin-Jones zones by electron states for a given structure defines the physical properties as optical reflectivity, electrical resistivity and others. Recently found Li transformations metal-semiconductor-metal [2] are related to the Fermi surface – Brillouin zone configurations for corresponding structural states.

[1] Guillaume C.L. et al., *Nature Physics* 2011, 7, 211. [2] Matsuoka T. et al., *Phys. Rev. B* 2014, 89, 144103. [3] Degtyareva V.F., *Phys. Usp.* 2006, 49, 369. [4] Degtyareva V.F., Smirnova I.S., *Z. Kristallogr.* 2007, 222, 718.

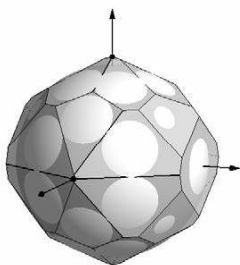


Figure 1. The Brillouin-Jones zone constructed for Li-*oC40* at 75 GPa is almost filled by electron states consisting with the experimentally found semiconducting properties of this Li phase.

Keywords: alkali metals, high pressure, crystal structures, Hume-Rothery effects

MS20-P9 Compressibility and pressure-induced deformation mechanisms in Si-FerrieriteGiovanna Vezzalini¹, Paolo Lotti², Diego G. Gatta², Rossella Arletti³, Giovanna Vezzalini¹, Simona Quartieri⁴

1. Dipartimento di Scienze Chimiche e Geologiche, Università di Modena e Reggio Emilia, Via S. Eufemia 19, 41100 Modena, Italy
2. Dipartimento di Scienze della Terra, Università degli Studi di Milano Via Botticelli 23, 20133 Milano, Italy
3. Dipartimento di Scienze della Terra, Università di Torino, Via Valperga Caluso 35, 10125 Torino, Italy
4. Dipartimento di Fisica e Scienze della Terra, Università di Messina, Viale Ferdinando Stagno d'Alcontres 31, 98166 Messina S. Agata, Italy

email: mariagiovanna.vezzalini@unimore.it

Several experimental and theoretical studies have recently been performed in order to describe the compressibility and the pressure-induced deformation mechanisms (at the atomic scale) of nominally hydrophobic all-silica zeolites, compressed in penetrating or non-penetrating media (PTM) (i.e. [1-5]). In this paper, we explore - using penetrating and non-penetrating *P*-transmitting media - the crystal-fluid interaction upon pressure of an all-silica ferrierite-type zeolite [Si-FER: Si₃₆O₇₂]. Compression of Si-FER in silicon oil (as a non-penetrating medium) showed a remarkable flexibility of this framework in response to the applied pressure. A first displacive *Pmnn* to *P12₁/n1* phase transition was observed at ~ 0.7 GPa, followed by a second displacive transition to the *P2₁/n11* space group (via the intermediate *P-1* structure) at ~ 1.24 GPa. All the three observed polymorphs show a virtually identical bulk compressibility: the average β_V being 0.051(4), 0.056(9) and 0.055(3) GPa⁻¹, respectively. The structural deformation of the framework is mainly accommodated by the compression and the distortion of the 10- and the 8-ring channels running along *c* and *b*, respectively. The compression of Si-FER in three potentially penetrating media [i.e., methanol:ethanol:H₂O = 16:3:1 (mew), ethylene glycol (egl) and 2metil-2-propen-1ol (mpo)] showed evidence of crystal-fluid interactions at high pressure. Common features among the three experiments are: 1) the *Pmnn* to *P12₁/n1* phase transition at ~ 0.7 GPa (except for mew, where it occurs at ~ 1.5 GPa) and 2) the absence of the *P2₁/n11* polymorph (previously observed in silicon oil), coupled with a less pronounced compressibility compared to that in silicon oil, suggesting penetration of PTM molecules. For all the *in situ* experiments, the orthorhombic symmetry was restored after decompression.

The authors acknowledge the Italian Ministry of Education, MIUR-Project: "Futuro in Ricerca 2012 - ImPACT- RBFR12CLQD".

References [1] Gatta, G.D. (2008) *Z. Kristallogr.*, 223, 160-170. [2] Gatta, G.D. and Lee, Y. (2014) *Min. Mag.*, 78, 267–291 [3] Arletti, R., Vezzalini, G., Quartieri, S., Di Renzo, F., Dmitriev, V. (2014) *Micr. Mesop. Mat.* 191, 27–37. [4] Quartieri, S., Leardini, L., Arletti, R., Vezzalini, G. (2014) *Acta Cryst.* A(70), C1255. [5] Vezzalini, G., Arletti, R., Quartieri, S. (2014) *Acta Cryst.* B70, 444–451

Keywords: Zeolite, high-silica ferrierite, compressibility, phase transition, penetrating PTM, non penetrating PTM, fluid penetration

MS20-P10 The structure of 10 Å phase formed by talc hydration at 450°C and 4 GPa: *in situ* diffraction study

Anna Y. Likhacheva¹, Sergey V. Rashchenko¹, Konstantin D. Litasov¹, Aleksey I. Ancharov²

1. Sobolev Institute of geology and mineralogy SB RAS

2. Budker Institute of Nuclear Physics SB RAS

email: alih@igm.nsc.ru

The interest to high-pressure hydrous silicates is related with the problem of water recycling within subducting lithosphere [1]. The 10 Å phase $\text{Mg}_3\text{Si}_4\text{O}_{10}(\text{OH}) \cdot x\text{H}_2\text{O}$ is of special significance because its stability is intermediate between the minerals of oceanic peridotites (serpentine, talc, chlorite) and deep-seated silicates [2]. Previous structural studies of 10 Å phase were performed on quenched samples, whereas the analysis of *in-situ* structure could specify the equilibrium water content in it, which is still debatable [3].

The structure of 10 Å phase formed from the reaction of talc plus water at 450°C and 4 GPa was studied by powder diffraction using DAC with resistive heating. The diffraction experiments were performed at 4th beamline of VEPP-3 storage ring of SSTRC, Novosibirsk ($1 = 0.3685$ Å). Rietveld method [4] was applied to refine the lattice parameters, atomic coordinates and the occupancy of interlayer H_2O site in the structure of 10 Å phase. The lattice parameters of 10 Å phase at 450°C / 4 GPa are $a = 5.234(1)$, $b = 9.053(2)$, $c = 10.87(1)$ Å, $b = 99.2(1)^\circ$, $V = 508.5(6)$ Å³ ($C2/m$). The best fit was obtained for the structure model with split position Ow of interlayer H_2O molecule (Fig. 1). The Ow site has three short (2.6 Å) $\text{Ow}-\text{O}_{\text{tet}}$ distances with corresponding angles $\angle \text{O}_{\text{tet}}-\text{Ow}-\text{O}_{\text{tet}}$ of 101-108°, favorable for the orientation of $\text{protons}^{\text{tet}}$ towards tetrahedral O atoms. The half occupancy of the Ow site corresponds to one H_2O molecule per formula unit, which agrees with the recent estimations performed on quenched samples [3] and shows no significant change of water content during quenching.

This work is supported by RFBR (grant #13-05-00185) and Ministry of Education and Science of Russian Federation (project No 14.B25.31.0032). The work was carried out involving the equipment belonging to the SSTRC.

[1] Schmidt M.W. & Poli S. (1998) Earth Planet. Sci. Lett. **163**, 361. [2] Fumagalli P., Stixrude L., Poli S. et al. (2001) Earth. Planet. Sci. Lett. **186**, 125. [3] Comodi P. (2005) Am. Miner. **90**, 1012. [4] Larson A.C. & Von Dreele R.B. General structure analysis system (GSAS). Report LAUR, Los Alamos National Lab, New Mexico, 2000.

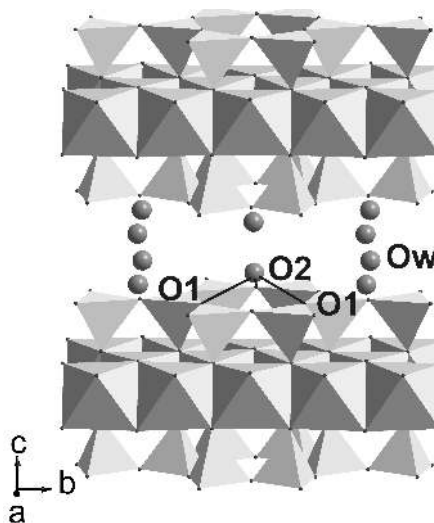


Figure 1. The crystal structure of 10 Å phase at 450°C and 4 GPa. The lines mark the short $\text{Ow}-\text{O}_{\text{tet}}$ distances.

Keywords: talc, 10 Å phase, powder diffraction, high pressure, high temperature.

MS20-P11 Crystallographic study of layered MS_2 compounds under pressure

Mette O. Filso¹, Simone M. Søndergaard-Pedersen¹, Martin Bremholm¹, Bo B. Iversen¹

¹. Center for Materials Crystallography, Dept. of Chemistry and iNANO, Aarhus University (DK)

email: filsoe@chem.au.dk

The applications of layered disulfides are vast and range from lubricants [1] and electrode materials [2] to optoelectronic devices and transistors [3]. The structure is built from stacks of sulfur-metal-sulfur 'sandwich' layers, and the difference in bonding within and between these layers is of great importance for the properties of the materials.

The interesting electronic properties can be altered either by reducing the single crystal to a mono- or a bilayer, by intercalation, or by pressure - all effects which affect the interlayer S-S interaction [4,5]. However, in spite of the many analyses already performed on these compounds, surprisingly little is known about the true nature of this interaction, and about the crystal structures of high-pressure phases.

In this study, a diamond anvil cell setup has been utilized in a detailed crystallographic investigation of the high-pressure structures of TiS_2 and SnS_2 .

It is the goal of this analysis to expand the knowledge of the S-S interlayer interaction and its impact on the structural changes caused by pressure. Elaborate structural knowledge can in turn lead to a more thorough explanation of the interesting properties of this group of compounds.

[1] Martin, J.; Donnet, C.; Le Mogne, T.; Epicier, T., *Phys. Rev. B* **48** (1993), 10583-10586

[2] Scrosati, B., *Nature* **373** (1995), 557-558

[3] Radislavljevic, B.; Radenovic, A.; Brivio, J.; Giacometti, V.; Kis, A., *Nat. Nanotechnol.* **6**, 3 (2011), 147-150

[4] Peelaers, H.; Van de Walle, C. G., *J. Phys. Chem. C* **118** (2014), 12073-12076

[5] Allan, D. R.; Kelsey, A. A.; Clark, S. J.; Angel, R. J.; Ackland, G. J., *Phys. Rev. B* **57**, 9 (1998), 5106-5110

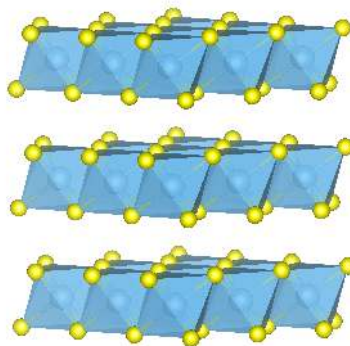


Figure 1. Structure of TiS_2 , space group P-3m1

Keywords: Metal Sulfides, High-pressure Crystallography, Layered Structures, Diamond Anvil Cell

MS20-P12 I_7^- : from stoichiometry to structural unitAlexander J. Blake¹, Jeremiah P. Tidey¹, Amy E. Lisle¹, Martin Schröder¹¹. The University of Nottingham

email: a.j.blake@nottingham.ac.uk

High pressure studies of metal coordination complexes have been reported for almost 30 years, but it is only recently these have appeared in significant numbers: in fact, of a total of around 50 studies, approximately two-thirds have appeared in the last five years [1]. One consequence of this limited number is that much of the coverage comprises isolated studies of very different materials and properties, with systematic comparative studies such as [2] being rare.

As part of a broader programme searching for new phenomena in metal coordination complexes, we turned our attention to the iodide salt of the complex cation $[\text{Ag}(\text{[18]aneS}_6)]^+$: this crystallises with the stoichiometry $[\text{Ag}(\text{[18]aneS}_6)]\text{I}_7$ and adopts a highly unusual and visually striking structure (see Figure 1) whereby the cation templates the formation of a distorted cubic cage consisting of iodine molecules (I_2) and iodide ions (I^-) with iodine-iodine separations of 2.7519(14) Å for $\text{I}-\text{I}$ and 3.3564(15) Å for $\text{I}^-\cdots\text{I}$ [3]. The iodines and iodides form an extended polymeric matrix in which the cations reside.

In response to compression to a maximum pressure of 46 kbar, $[\text{Ag}(\text{[18]aneS}_6)]\text{I}_7$ undergoes two distinct phase changes and increasing desymmetrisation of the cubic cage, the details and consequences of which will be explored.

References:

1. J. P. Tidey, H. L.S. Wong, M. Schröder & A. J. Blake, "Structural Chemistry of Metal Coordination Complexes at High Pressure", *Coord. Chem. Rev.* 2014, **277–278**, 187–207.
2. D. R. Allan, D. Bailey, N. Bird, A. J. Blake, N. R. Champness, D. Huang, C. P. Keane, J. McMaster, T. J. Prior, J. P. Tidey & M. Schröder, "High pressure studies of six palladium and platinum thioether dihalide complexes", *Acta Crystallogr., Sect. B* 2014, **70**, 469–486.
3. A. J. Blake, R. O. Gould, S. Parsons, C. Radek and M. Schröder, "Self-Assembly of Polyanions at a Metal Cation Template: Synthesis and Structures of $\{[\text{Ag}(\text{[18]aneS}_6)]\text{I}_7\}_n$ and $[\text{Ag}(\text{[18]aneS}_6)]\text{I}_3$ ", *Angew. Chem. Int. Ed. Engl.* 1995, **34**, 2374–2376.

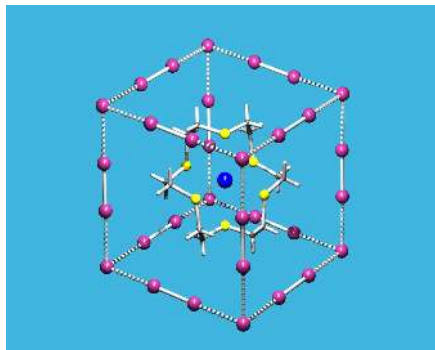


Figure 1. A section of the extended structure of $\{[\text{Ag}(\text{[18]aneS}_6)]\text{I}_7\}_n$.

Keywords: high pressure, coordination complex, phase change, desymmetrisation, polyiodide

MS20-P13 *In situ* crystallographic evidence to isolate pore forms under gas pressure in a flexible Zn(II)-MOF

Prem Lama¹, Leonard J. Barbour¹¹. Department of Chemistry and Polymer Science, University of Stellenbosch, Stellenbosch 7600, South Africa

email: plama@sun.ac.za

A variety of rigid porous metal organic frameworks (MOFs) have been synthesized which have shown potential application in terms of catalysis and gas separations due to high porosity and pore volumes.^[1] As compared to rigid porous MOFs, due to the tunability of size, shape and pores by using desired metal ions and the organic linkers, a number of flexible MOFs have been reported.^[2] As a result of this flexibility, MOFs can undergo expansion or contraction of the pores in the presence or absence of the guest molecules to produce structural change.^[3] The flexible MOFs have better affinity to offer variety of pores on adsorption of different molecules which can be stabilized by non covalent interactions such as H-bonding, $\pi \cdots \pi$ interaction or van der Waals interactions etc. If these different pore forms can be isolated without losing single crystallinity, the exact interaction of the guest molecules with the host framework can be easily understood. We report a flexible Zn(II)-MOF that displays different pore forms (PF1→PF3) under ethane gas pressure. These systems have been characterized by single-crystal X-ray diffraction using an environmental gas cell.^[4] The pore forms were further verified by gas sorption analysis and high pressure differential scanning calorimetry.

[1] (a) McDonald, T. M.; Lee, W. R.; Mason, J. A.; Wiers, B. M.; Hong, C. S.; Long, J. R. *J. Am. Chem. Soc.* **2012**, 134, 7056-7065. (b) Lama, P.; Aijaz, A.; Neogi, S.; Barbour, L. J.; Bharadwaj, P. K. *Cryst. Growth Des.* **2010**, 10, 3410-3417. (c) Eddaoudi, M.; Li, H.; Yaghi, O. M. *J. Am. Chem. Soc.* **2000**, 122, 1391-1397. (d) Zhang, Z.; Zaworotko, M. J. *Chem. Soc. Rev.* **2014**, 43, 5444-5455. (e) Aggarwal, H.; Bhatt, P. M.; Bezuidenhout, C. X.; Barbour, L. J. *J. Am. Chem. Soc.* **2014**, 136, 3776-3779. [2] (a) Henke, S.; Schneemann, A.; Fischer, R. A. *Adv. Funct. Mater.* **2013**, 23, 5990-5996. [3] (a) Nijem, N.; Wu, H.; Canepa, P.; Marti, A.; Balkus, Jr. K. J.; Thonhauser, T.; Li, J.; Chabal, Y. J. *J. Am. Chem. Soc.* **2012**, 134, 15201-15204. (b) Coudert, F.-X.; Mellot-Draznieks, C.; Fuchs, A. H.; Boutin, A. *J. Am. Chem. Soc.* **2009**, 131, 11329-11331. (c) Alhamami, M.; Doan, H.; Cheng, C.-H. *Materials*, **2014**, 7, 3198-3250. [4] T.; Jacobs, G. O.; Lloyd, J.-A.; Gertenbach, K. K.; Müller-Nedebock, C.; Esterhuysen, L. J. Barbour, *Angew. Chem., Int. Ed.* **2012**, 51, 4913-4916.

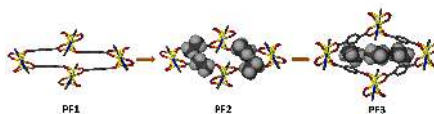


Figure 1. Diagram showing different pore forms of Zn(II)-MOF under ethane gas pressure

Keywords: Flexible MOFs, High Pressure Differential Scanning Calorimetry, In Situ Gas Modelling, Gas sorption

MS20-P14 High-pressure study of
R,S-ibuprofenKinga Ostrowska¹, Magdalena Kropidłowska¹, Andrzej
Katrusiak¹1. Department of Materials Chemistry, Faculty of Chemistry,
Adam Mickiewicz University Umultowska 89b, 61-614 Poznań,
Poland

email: kinga.ostrowska@poczta.fm

R,S-Ibuprofen is an important non-steroidal anti-inflammatory drug used for relieving pain, helping with fever and reducing inflammation.¹ It crystallizes at varied pressure (0.1 MPa – 4.00 GPa) in the monoclinic, space group $P2_1/c$.² It is an optically active compound with both *s* and *r*-isomers. The *S*-ibuprofen is more active and hence desired for pharmaceutical applications. Its structure is monoclinic, space group $P2_1$.³ Single crystals of *r,s*-ibuprofen have been grown *in situ* at isothermal and isochoric conditions in a modified Merrill-Bassett⁴ diamond-anvil cell (DAC) from different achiral and chiral solutions. Their structures were determined by X-ray diffraction. High-pressure crystallizations of *R,S*-ibuprofen lead to the same crystal phase as the one at ambient conditions. It is a carboxylic acid with molecules linked by double OH•••O bridges into dimers. At 4.0 GPa the crystal is compressed to about 80% of its ambient-pressure volume. *r,s*-Ibuprofen crystal structure is stabilized by C-H•••O contacts. The crystal compression and thermal expansion as well as shortest H•••O distances comply with the inverse-relationship rule of pressure and temperature changes.

REFERENCES

- [1] Van Esch, A.; Van Steensel-Moll, H. A.; Steyerberg, E. W.; Offringa, M.; Habbema, J. D.; Derksen-Lubsen, G. *Arch. Pediatr. Adolesc. Med.* **1995**, *149*, 632–637.
- [2] (a) McConnell, J. F. *Cryst. Struct. Commun.* **1974**, *3*, 73–75. (b) Shankland, N.; Wilson, C. C.; Florence, A. J.; Cox, P. J. *Acta Cryst. Sect. C* **1997**, *53*, 951–954.
- [3] Freer, A. A.; Bunyan, J. M.; Shankland, N.; Sheen, D. B. *Acta Cryst. Sect. C* **1993**, *49*, 1378–1380.
- [4] Merrill, L.; Bassett, W. A. *Rev. Sci. Instrum.* **1975**, *45*, 290–294.

Keywords: High-pressure; crystallization; crystal compression; hydrogen bond; intermolecular interactions

MS20-P15 High-pressure polymorphism of
 α -D-glucoseEwa Patyk¹, Andrzej Katrusiak¹1. Department of Materials Chemistry, Faculty of Chemistry,
Adam Mickiewicz University, Umultowska 89b, 61-614 Poznań,
Poland

email: ewapatyk@amu.edu.pl

Carbohydrates create group of compounds most important for all living organisms. They are widely used in food, pharmaceutical, construction and other industries. One of the most significant representative of sugars is glucose. It is main energy carrier in human organism and takes part in many important biochemical processes. Processing and recognition of glucose is based on the unique structural pattern of hydroxyl groups that allows creation of multiple hydrogen bonds and intermolecular contacts. Recently we have shown how pressure can influence the solid-state preferences of bonding pattern of other well-known sugar, (+)-sucrose.[1] Compression of crystalline sucrose leads to its isostructural phase transition, and thorough reorganization of O-H•••O hydrogen bonds and C-H•••O contacts. Herein we present study of α -D-glucose crystals behavior at high-pressure and the first high-pressure monosaccharide polymorph ever reported.[2]

Crystals of α -D-glucose were either mounted in the Merrill-Bassett diamond-anvil cell (DAC)[3] and compressed or recrystallized isochorically at high-pressure. Obtained crystals were measured using 4-circle X-ray diffractometer in the 0.2–6.2 GPa pressure range.

Collected data shown discontinuity of α -D-glucose unit-cell volume and parameters at 5.40 GPa which was later proven to be an evidence of its isostructural phase transition. α -D-Glucose preserves its orthorhombic symmetry, space group $P2_12_12_1$ ($Z=1$) on transformation from phase I to phase II. During the transition, its molecules rearrange their aggregation due to compression which in turn leads to modification of intermolecular interactions. Role of strong O-H•••O hydrogen-bonds diminish, their number decrease after phase transition, and weaker interactions such as C-H•••O contacts increase their number and therefore importance in phase II.

Structural modification observed for α -D-glucose coincide to some point with those reported for (+)-sucrose. It makes us believe that structural similarities of carbohydrates can be reflected in their high-pressure behavior.

References:

1. E. Patyk, J. Skumiel, M. Podsiadlo, A. Katrusiak, *Angew. Chem. Int. Ed.* **51** (2012) 2146–2150.
2. E. Patyk, A. Katrusiak, *Chem. Sci.* **6** (2015) 1991–1995.
3. L. Merrill, W. A. Bassett, *Rev. Sci. Instrum.* **45** (1974) 290–294.

Keywords: glucose, high-pressure, polymorphism

MS20-P16 Pressure-induced penetration of organic molecules in Si-Ferrierite

Simona Quartieri¹, Rossella Arletti², Paolo Lotti³, Diego Gatta³,
Maria Giovanna Vezzalini⁴

1. Dipartimento di Fisica e Scienze della Terra, Università di Messina, Viale Ferdinando Stagno d'Alcontres 31, 98166 Messina S. Agata, Italy.
2. Dipartimento di Scienze della Terra, Università di Torino, Via Valperga Caluso 35, 10125 Torino, Italy.
3. Dipartimento di Scienze della Terra, Università degli Studi di Milano Via Botticelli 23, 20133 Milano, Italy
4. Dipartimento di Scienze Chimiche e Geologiche, Università di Modena e Reggio Emilia, Via S. Eufemia 19, 41100 Modena, Italy.

email: squartieri@unime.it

In the last 10-15 years, the behavior of natural and synthetic zeolites under pressure has attracted great attention (i.e. [1,2]). These porous materials respond to pressure in a large variety of modes and the effects of applied pressure and molecular spatial confinements of the pressure transmitting media can open extremely interesting applicative scenarios. For instance, owing to their open framework with cages and channels of molecular dimensions, zeolites could be considered as a negative-image of nanomaterials: the relevant nanosized portion is the open space which can be accessed or filled by suitable guest chemicals, intruded in the zeolite pores upon compression. Moreover, pressure can play an important role also in increasing the efficiency of zeolites as "nano-reactors" in the field of heterogeneous catalysis, favoring the access of reactants and products to/from the catalytically active sites and the aggregation of molecules of proper shape in the microporous cavities. In this study we explore - by both single-crystal and synchrotron X-ray powder diffraction and using a number of penetrating and non-penetrating pressure transmitting media - the crystal-fluid interaction upon pressure of a siliceous matrix with ferrierite-type topology [Si-FER: Si₃₆O₇₂], expected to favor the penetration of liophilic/hydrophobic guest species. The following aspects are investigated: *i*) the structural deformations induced by compression on the framework; *ii*) the elastic parameters and the unit-cell variations in response to pressure; *iii*) the penetration of extraframework H₂O and/or organic guest molecules (methanol, ethanol, ethylene glycol, 2methyl-2propen-1-ol); *iv*) the reversibility extents of the observed phenomena; *v*) the comparison between the overall elastic behavior of Si-FER and those of other siliceous zeolites.

The authors acknowledge the Italian Ministry of Education, MIUR-Project: "Futuro in Ricerca 2012 - ImPACT- RBFR12CLQD".

References: [1] Gatta, G. D. and Lee, Y. (2014) Zeolites at high pressure: A review. *Min. Mag.*, 78, 267–291. [2] Vezzalini, G., Arletti, R., Quartieri, S. (2014) HP-induced structural changes, amorphization and molecule penetration in MFI microporous materials: a review. *Acta Cryst.* B70, 444–451

Keywords: zeolite, siliceous ferrierite, high pressure, synchrotron X-ray powder diffraction, organic molecules intrusion

MS20-P17 Crystal structure mechanism of the hydrostatic compression in Mg-rich orthopyroxene

Tonči Balić-Zunić¹, Fabrizio Nestola², Tiziana Boffa Ballaran³,
Roland Stalder⁴

1. Natural History Museum, University of Copenhagen, Oster Voldgade 5-7, 1350 Copenhagen, Denmark
2. Dipartimento di Geoscienze, Università degli Studi di Padova, Padova 35131, Italy
3. Bayerisches Geoinstitut, University of Bayreuth, Universitaetsstrasse 37, D-95447 Bayreuth, Germany
4. Institute of Mineralogy and Petrography, University of Innsbruck, Innrain 52, 6020 Innsbruck, Austria

email: toncib@snm.ku.dk

Orthopyroxene is supposed to make 10 – 20% of the Earth's material under the Lithosphere and thus represent one of the major minerals of the uppermost Mantle. Its high-pressure stability is rather limited compared to other mantle minerals and terminates at around 300 km depth. That orthopyroxene might be one of the crucial factors in the formation of Asthenosphere (magma-generating layer at the bottom of Lithosphere) was suggested from a study of water solubility in this mineral [1]. Recent accurate studies of the crystal structure of pure enstatite [2] and of the Al+H-rich enstatite (this work) contribute high-pressure crystal structure data which, in combination with previous accurate studies of Ca-rich [3] and Fe+Al-rich [4] enstatite give possibility to investigate influences of various expected natural substitutions in the Mg end-member of the orthopyroxene solid solution. All studies were made with the use of improved diamond-anvil cells on laboratory diffractometers with area detectors. Details of the development of crystal structures under hydrostatic compression explain the destabilization of Ca-substituted orthopyroxene on high pressures and the opposite effect of the Fe+Al or Al+H substitution. They are illustrated through detailed analysis of the bond lengths, polyhedral volumes and polyhedral distortions of the four distinct coordination polyhedra in this crystal structure. [1] Mierdel, K., Keppler, H., Smyth, J.R., and Langenhorst, F.: *Science*, 315, 364–368 (2007). [2] Periotto, B., Balić-Zunić, T., Nestola, F., Katerinopoulou, A., Angel, R.J.: *American Mineralogist*, 97, 1741–1748 (2012). [3] Nestola, F., Gatta, G.D., and Boffa Ballaran, T.: *American Mineralogist*, 91, 809–815 (2006). [4] Nestola, F., Boffa Ballaran, T., Balić-Zunić, T., Secco, L., and Dal Negro, A.: *American Mineralogist*, 93, 644–652 (2008).

Keywords: orthopyroxene, crystal structure, high pressure, crystal chemistry

MS20-P18 Urea and thiourea: similar compounds – different resultHanna Tomkowiak¹, Kinga Ostrowska¹, Andrzej Katrusiak¹

1. Department of Materials Chemistry, Faculty of Chemistry, Adam Mickiewicz University, Umultowska 89b, 61-649 Poznań, Poland

email: hannat@amu.edu.pl

Urea, (NH₂)₂CO, and thiourea, (NH₂)₂CS, are two of the most common chemical compounds, widely used in chemical practice and industry, mainly for the production of fertilizers, but also pharmaceuticals, insecticides, dyes, plant protection agents, pesticides, corrosion inhibitors, fungicides and as a component explosives.

The single crystals of both compounds have been *in situ* grown from aqueous solution in a diamond-anvil cell [1] and their structure have been determined by X-ray diffraction. Urea and thiourea crystallize as anhydrides at 0.10 GPa. Both these compounds have been intensely studied at normal conditions and in the function of temperature and pressure, while only thiourea hydrates have been obtained from aqueous solution under high pressure.

For urea, three pressure-induced phases: I (tetragonal space group $P-4_2m$), III (orthorhombic space group $P2_12_12_1$) and IV (orthorhombic space group $P2_12_12$) have been reported with increasing pressure at room temperature; the phase transitions I – III at 0.48 GPa, III – IV at 2.80 GPa. No hydrates have been obtained of urea crystallized at high pressure of aqueous solution. The thermodynamic phase transitions in urea have been rationalized by a microstructural mechanism involving the interplay of pressure-induced molecular reorientations, with hydrogen bonds competing for access to lone-electron pairs of carbonyl oxygen, and by the increasing role of van der Waals interactions [2].

For thiourea, at high-pressure the hydrated or anhydrous crystals can be obtained. Above 0.55 GPa thiourea crystallizes as monohydrate (NH₂)₂CS·H₂O. At 0.70 GPa another hydrate, 3(NH₂)₂CS·2H₂O, ² is formed, but above 1.20 GPa anhydrous thiourea becomes stable again. The structural factors favoring the formation of hydrates above 0.55 GPa involve new types of hydrogen bonds involving water molecules and the more efficient molecular packing [3].

References:

- [1] Merrill L.; Bassett W. A. *Rev. Sci. Instrum.* **45** (1974) 290-294.
- [2] Olejniczak, A.; Ostrowska, K.; Katrusiak, A. J. *Phys. Chem. C* **113** (2009) 15761-15767.
- [3] Tomkowiak H., Olejniczak A., Katrusiak A. *Cryst. Growth Des.* **13** (2013) 121-125.

Keywords: thiourea, urea, high pressure

MS20-P19 Study of magnetite, franklinite and gahnite at high pressure and high temperatureChristian Lathe¹, Michael Wehber¹, Hans J. Mueller¹, Joern Lauterjung¹

1. GFZ German Research Centre for Geosciences, Telegrafenberg, 14473 Potsdam, Germany

email: christian.lathe@gfz-potsdam.de

Magnetite (FeFe₂O₄), Franklinite (ZnFe₂O₄), and Gahnite (ZnAl₂O₄) are Spinel and crystallize in the cubic crystal structure $Fd-3m$ with eight formula units per elementary cell and with the general formula AB₂O₄ (where A represents divalent and B trivalent cations, respectively). In the spinel structure, oxygen ions form a cubic-closest packing with 16 octahedral and 8 tetrahedral sites. All three examined Minerals crystallize in the normal spinel structure. This means the tetrahedral sites are occupied by A cations and the octahedral sites are occupied by B cations (⁴A⁶B₂O₄).

For the systematic study of the thermo-elastic properties at elevated conditions, Spinel with different iron content are used. The thermal expansion as a function of pressure is deduced from *in-situ* X-ray diffraction analyses at elevated pressures and temperatures. The interrelation of thermal expansion, compression behavior and iron content is the focus of the study.

The experiments were carried out at HASYLAB (Hamburg, Germany) on two beamlines (F2.1, W2) at DORIS III ring, with a single stage (MAX80) and a double stage (MAX200x) multi-anvil press, respectively. XRD-Spectra at both presses were collected using energy-dispersive mode.

Isothermal experiments were performed at the MAX200x up to 15 GPa at ambient temperature. To obtain the bulk moduli, the data points were fitted to a 3rd order Birch-Murnaghan equation of state yielding to $KT = 184(3)$ GPa and $K' = 4.5(2)$ for Magnetite, $KT = 178(3)$ GPa and $K' = 4.6(4)$ for Franklinite, and $KT = 204(4)$ GPa and $K' = 4.9(6)$ for Gahnite, respectively.

The temperature and pressure dependent volume change were derived from compression experiments using MAX80 apparatus up to 5 GPa at temperatures of 298, 500, 700, 900 and 1100 K.

Keywords: Spinel, equation of state, elastic properties, thermal properties

MS20-P20 Irreversible pressure induced phase transformation in blossomite, α -Cu₂V₂O₇, mineral

Neven Strukan¹, Gwilherm Nénert², Alexei Belik³, Boris V. Slobodin⁴

1. RENACON d.o.o., Vrbik 20, 10000 Zagreb, Croatia
2. PANalytical B. V. Lelyweg 1, 7602 EA Almelo, The Netherlands
3. International Center for Materials Nanoarchitectonic, National Institute for Materials Science (NIMS), 1-1 Namiki, Tsukuba, Ibaraki 305-0044, Japan
4. Institute of Solid State Chemistry, Russian Academy of Sciences, Yekaterinburg, 620041, Russia

email: neven.strukan@renacon.hr

Anhydrous copper vanadates are characteristic minerals of high-temperature volcanic fumaroles [1]. Among the list of fumarolic mineral species containing Cu and V, Cu₂V₂O₇ appears in the form of either blossomite, α -Cu₂V₂O₇ [2], or ziesite, β -Cu₂V₂O₇ [3]. An additional polymorph modification as a γ form has been also reported which is related to the β -A2P2O7 structure-type [4]. These 3 polymorphs, which are similar in structure but differ markedly in the kinetics of their formation and reversibility of their transformations [5]. Cu₂V₂O₇ material has been attracted a lot of attention, not only in mineralogy but also due to its importance as cathode material for rechargeable lithium batteries [6]. Recently, this material received further attention from the physics community. Cu₂V₂O₇ exhibits low dimensional magnetic properties [7] and due to the polar structure of blossomite (α -Cu₂V₂O₇ phase, space group Fdd2), it has been shown to be a promising new multiferroic material [8]. Despite all these investigations, yet very little is known about the pressure dependence of this material. In order to gain further understanding of Cu₂V₂O₇, we have investigated the effect of pressure at room temperature on the crystal structure of blossomite up to 6 GPa. We report on a new δ -Cu₂V₂O₇ polymorph arising from an irreversible phase induced transition at room temperature. Using high resolution x-ray powder diffraction, we were able to solve the structure of this new polymorph. It exhibits symmetry P21/c with cell parameters $a = 9.4547(3)$ Å, $b = 11.4168(3)$ Å, $c = 5.0652(1)$ Å, and $\beta = 97.12^\circ$. We discuss this new phase in relation to the previously reported polymorphs. [1] J. M. Hughes, R. E. Stoiber, J. Volcanol. Geotherm. Res. 24, 283-291.. (1985) [2] P. D. Robinson, et al., Am. Mineral. 72, 397-400 (1987). [3] J. M. Hughes, et al., Am. Mineral. 65, 1146-1149 (1980). [4] S. V. Krivovichev, et al., Can Mineral 43, 671-677 (2005) [5] B. V. Slobodin et al., Inorganic Materials, 2010, Vol. 46, pp. 196-200 [6] Tranchant, et al., J. Electroanal. Chem., 1988, vol. 242, pp. 181-190. [7] O. Janson et al., Phys. Rev. B 83, 094435 (2011). A. A. Tsirlin et al., Phys. Rev. B, 82, 144416 (2010) [8] J. Sannigrahi, et al., arXiv:1501.00809

Keywords: phase transformation, high pressure, blossomite

MS21. Advances in high-pressure methods

Chairs: Leonid Dubrovinsky, Ronald Miletich

MS21-P1 Kinetic control on high-pressures solid-state phase transitions

Arianna Lanza^{1,2}, Martin Fisch^{1,2}, Elena Boldyreva^{3,4}, Piero Macchi¹, Nicola Casati²

1. Department of Chemistry and Biochemistry, University of Bern, Freiestrasse 3, 3012 Bern, Switzerland
2. Swiss Light Source, Paul Scherrer Institute, 5232 Villigen, Switzerland
3. Institute of Solid State Chemistry and Mechanochemistry, Russian Academy of Sciences, Siberian Branch, Novosibirsk, Russia 630128
4. Novosibirsk State University, Novosibirsk, Russia 630090

email: arianna.lanza@dcb.unibe.ch

Applying high pressure is a powerful method to induce transformations in the solid state. As a matter of fact, compression alters the thermodynamic state of a solid and can induce lattice strain, phase transitions or even chemical reactions. However, as in every physico-chemical transformation, an important role is played by the kinetic aspect of the process. Despite the increasing popularity of high-pressure investigations of solid state materials, kinetic effects are seldomly taken into account during experiments and data interpretation. We found that the compression rate adds a new perspective to phase diagrams of solids, which can even provide the key to explain complex polymorphic systems. Not only can the onset pressure of each transition and the ranges of coexistence of polymorphs be modified by controlling the compression rate, but also a particular pressure increase rate may trigger unexpected solid state transformations, producing otherwise inaccessible phases. These phenomena were initially observed and investigated for the system [CuF₂(H₂O)₂(pyz)]_n (pyz=pyrazine) which showed coexistence of two phases above ca. 3 GPa.¹ A new, even richer example is L-serine, characterized by a complex high pressure behavior with three known polymorphs, for which the critical pressure of each transition and the ranges of coexistence of the phases have been controversially reported.² In addition to this, the existence of an elusive fourth phase² has so far remained an open question. The puzzle could be solved by high pressure synchrotron powder X-ray diffraction, under controlled pressure increase rates.²

REFERENCES:

- (1) Lanza, A.; Fiolka, C.; Fisch, M.; Casati, N.; Skoulatos, M.; Rüegg, C.; Krämer, K. W.; Macchi, P. Chem. Commun. 2014, 50 (93), 14504; and references therein.

(2) Fisch, M.; Lanza, A.; Boldyreva, E.; Macchi, P.; Casati, N. J. Phys. Chem. C 2015, [Online early access], DOI: 10.1021/acs.jpcc.5b05838; and references therein.

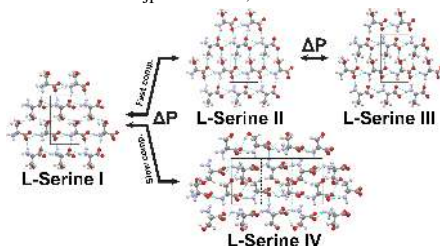


Figure 1. Two parallel pathways were found for L-serine in response to high pressure, evidencing that the compression rate can significantly affect the high pressure behaviour of solid state materials.

Keywords: Polymorphism, high-pressure crystallography, amino acids, synchrotron X-ray powder diffraction, solid-state kinetics, kinetic control

MS22. High response systems in practical and extreme conditions

Chairs: Yaroslav Filinchuk, Dmitry Chernyshov

MS22-P1 Engineering second and third generation MOFs and elucidating their structure property relationships

Varavara I. Nikolayenko¹, Leonard J. Barbour¹

¹. University of Stellenbosch

email: vin@sun.ac.za

A cursory glance of the literature reveals many reviews illustrating the enormity of the field of crystal engineering.^{1,2,3,4,5,6} The practically infinite number of combinations of organic bridging ligands with metals possessing different coordination geometries for the construction of functional MOF materials ensure that this field will continue to evolve and prosper for many years to come. Using a selection of carefully chosen components (two symmetrical N donor ligands, a flexible acid and either zinc or cadmium) under solvothermal conditions, several interesting materials have been obtained. These materials are all porous, possess varying degrees of interpenetration and show interesting SC SC transformations, guest sequestration and guest storage capabilities.

Although crystal engineering has not yet reached the point where one can reliably predict the outcome of a set of crystallisation components, work such as this, is intended to widen the general knowledge such that guidelines may eventually be established that will enable target directed MOF design.

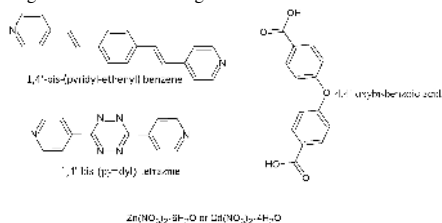


Figure 1. Synthetic components required for the formation of several interesting second and third generation MOFs.

Keywords: MOFs, Third generation, transformations, Single Crystal-Single Crystal

MS23. Nanoscale structures

Chairs: Joke Hadermann, Rainer Timm

MS23-P1 Nanocrystalline CoMn_2O_4 as anode material for lithium ion batteries: Effect of structure and microstructure

Mirjana Bijelić¹, X. Liu², Christian Suchomski³, Aleksandra B. Djurišić², Alan M.C. Ng^{2,4}, M. H. Xie², Zora Popović⁵, Q. Sun², Jasminka Popović⁶, Igor Djerđ⁶, Željko Skoko¹

1. Department of Physics, Faculty of Science, University of Zagreb, Bijenička c. 32, Zagreb, Croatia
2. Department of Physics, University of Hong Kong, Pokfulam Road, Hong Kong
3. Institute of Physical Chemistry, Justus-Liebig-University Gießen, Heinrich-Buff-Ring 58, D-35392 Gießen, Germany
4. Department of Physics, South University of Science and Technology of China, Shenzhen, China
5. Chemistry Department, Faculty of Science, University of Zagreb, Horvatovac 102a, 10000 Zagreb, Croatia
6. Division for Materials Physics, Ruder Bošković Institute, Bijenička c. 54, Zagreb, Croatia

email: mali@phy.hr

Rechargeable lithium-ion batteries (LIBs) have found applications in wide range of devices e.g. mobile phones and notebooks but LIBs also possess great potential for utilization in high power applications, such as hybrid electric vehicles¹. The performance of LIBs is greatly determined by the composition, structure and microstructural features of anode and cathode materials. Recent papers point to CoMn_2O_4 as an attractive candidate for alternative LIBs anode material²⁻⁵. The majority of the existing work on battery performance appears to focus on complex morphologies while the studies on the effect of crystal structure on battery performance have been scarce. As-prepared cobalt-dimanganate was prepared by precipitation route. Additionally, samples were thermally treated at $T=300$, 400 and 500°C . Structural investigation using XRPD and Raman spectroscopy have been carried out in order to correlate specific structural features with preparation conditions and furthermore with electrochemical properties. Changes in unit-cell as function of temperature were calculated; observed decrease is inconsistent with simple spinel-type exchange of Co^{2+} by Mn^{3+} on the tetrahedral site, and vice versa on the octahedral site. Based on the Raman spectroscopy an alternative structural model: $^{IV}[\text{Co}^{2+}_{1-x}\text{Mn}^{2+}_x]^{VI}[\text{Co}^{3+}_{2-2x}\text{Mn}^{3+}_{2x}]\text{O}_4$ has been proposed. Rietveld refinement showed increase of M-O distances within tetrahedra, caused by thermally enhanced substitution of Co^{2+} by larger Mn^{3+} cations at A-site. Consequently, octahedral B-site becomes partially occupied by Co^{3+} on the account of the transferred Mn cations. In all samples, initial capacity drops as commonly observed in high capacity metal oxide materials. However, after a certain number of cycles

specific capacity increases again. Among all samples, thermally treated from 100 - 500°C , highest specific capacities are observed for sample treated at highest temperature (500°C) despite its large particle size. In terms of the particle size, it has been shown that in some metal oxides better capacity retention is obtained for larger particle sizes and it was proposed that there is an optimal size for improved capacity retention⁶.

1. A. R. Armstrong et al., Nat Mater, 10, 223-229, 2011.
2. L. Hu et al., Sci. Rep., 2, 217-226, 2012.
3. Y. Li et al., Nanoscale, 5, 2045-2054, 2013.
4. L. Wang et al., J. Mater. Chem. A, 1, 2139-2143, 2013.
5. L. Zhou et al., Adv. Mater., 24, 745-748, 2012b.
6. P. Poizot et al., Nature, 407, 496-499, 2000.

Keywords: LiBs, Raman spectroscopy, temperature, specific capacity

MS23-P2 Local structure of semicrystalline P3HT films probed by nanofocused diffraction

Ruslan Kurta^{1,2}, Linda Grodd³, Eduard Mikayelyan³, Oleg Gorobtsov^{2,4}, Ivan Zaluzhnyy^{2,5}, Ilaria Fratoddi^{6,7}, Iole Venditti⁷, Maria Vittoria Russo⁷, Michael Sprung², Souren Grigorian³, Ivan Vartanyants^{2,5}

1. European XFEL GmbH, Albert-Einstein-Ring 19, D-22761 Hamburg, Germany
2. Deutsches Elektronen-Synchrotron DESY, Notkestraße 85, D-22607 Hamburg, Germany
3. Department of Physics, University of Siegen, Walter-Flex-Straße 3, D-57072 Siegen, Germany
4. National Research Center "Kurchatov Institute", Kurchatov Square 1, 123182 Moscow, Russia
5. National Research Nuclear University, "MEPhI", 115409 Moscow, Russia
6. CNIS, University of Rome Sapienza, P.le A. Moro 5, I-00185 Rome, Italy
7. Department of Chemistry, University of Rome Sapienza, P.le A. Moro 5, I-00185 Rome, Italy

email: ruslan.kurta@xfel.eu

Semicrystalline conjugated polymers are promising cost-effective candidates for organic electronic devices, in particular, for organic field-effect transistors and solar cells [1]. One of the most studied compounds is poly(3-hexylthiophene) (P3HT) and its blends. Typical feature of this polymer is a mixture of poor and well organized domains, the latter are addressed to be crystalline and assumed to strongly improve device performance [2]. Our study aims to improve understanding of the role of nanoparticle additives in the structure formation and nanomorphology of P3HT in order to enhance functional properties of optoelectronic devices.

We present results of nanofocused x-ray studies of structural properties of P3HT blends with gold nanoparticles (AuNPs) [3-5]. The hidden structural features of semicrystalline polymer films are revealed by applying the novel x-ray cross-correlation analysis (XCCA) technique [6-8]. In comparison with radial intensity curves usually analyzed in scattering experiments, the Fourier spectra of the cross-correlation functions provide extended information about the structural order in the system. Spatially resolved maps of orientational distribution of crystalline domains allow us to distinguish sample regions of predominant face-on morphology, with a continuous transition to edge-on morphology. As compared to a pristine P3HT film, the P3HT/AuNPs blend is characterized by substantial ordering of crystalline domains, which can be induced by Au nanoparticles. We also observed stronger structural variations of the P3HT matrix in the film regions with higher concentration of gold nanoparticles.

[1] Salleo A, Kline R J, Delongchamp D M, Chabynck M L (2010). *Adv. Mater.* 22, 3812.

[2] Sirringhaus H et al. (1999). *Nature* 401, 685.

[3] Kurta R P et al. (2014). *J. Phys.: Conf. Series* 499, 012021.

[4] Quintiliani M et al. (2014). *J. Mater. Chem. C* 2, 2517.

[5] Kurta R P et al. (2014). *Phys. Chem. Chem. Phys.* 17, 7404.

[6] Wochner P et al. (2009). *Proc. Natl. Acad. Sci. USA* 106, 11511.

[7] Altarelli M, Kurta R P, Vartanyants I A (2010). *Phys. Rev. B* 82, 104207.

[8] Kurta R P, Altarelli M, Vartanyants I A (2013). *Adv. Cond. Matt. Phys.* 2013, 959835.

Keywords: Semicrystalline polymers, nanofocused diffraction, x-ray cross-correlation analysis

MS23-P3 Crystal orientation mapping on metallic nanoparticles by electron diffraction methods

Arturo Ponce¹, Muriel Veron², Francisco Ruiz-Zepeda¹, John E. Sanchez², Ulises Santiago¹, Fernando Mendoza-Santoyo¹, Jesus Velazquez-Salazar¹, Miguel Jose-Yacamán¹

1. Department of Physics and Astronomy, University of Texas at San Antonio, One UTSA Circle, San Antonio, Texas 78249, USA.

2. Laboratoire SIMaP, Grenoble INP – CNRS – UJF, Saint Martin D'Hères Cedex, France

email: arturo.ponce@utsa.edu

Electron diffraction in transmission electron microscopy (TEM) provides crystallographic information of the specimens. Lately, new methodologies in electron diffraction such as diffraction in scanning modes, the use of aberration correctors to sharpen the probe size and precession electron diffraction (PED) among others have been becoming more frequent for the characterization of nanostructured materials. On the other hand, for data collection new detectors have been also developed with high sensitivity and high speed to collect intensities from the electron diffraction patterns in nanometric sized and sensitive materials like in metallic nanoparticles. In the present work we determine the geometry of modified gold decahedra nanoparticles by using crystalline orientation mapping and coherent electron diffraction. In both cases, nanoarea electron diffraction (NED) and small condenser aperture have been used, which reduce the diameter of the electron beam to a few nanometers. Coherent electron diffraction shows streaks lines, which have been measured and related to high index crystallographic planes in multiple faceted nanoparticles. The analysis of the geometry of these nanoparticles has been performed from the indexing of multiple electron diffraction patterns collected through PED and then raster the electron beam through the area of interest on the sample. The patterns are recorded in an external ultrafast CCD camera attached to the viewing screen of the microscope and every electron diffraction pattern is registered at each step of the scanned and stored in a computer for a subsequent indexing process. The result can then be displayed as a phase or an orientation map of the scanned area as can be observed in the color map of the Figure 1. The pattern recognition is done by calculating a cross correlation and a reliability value for each experimental pattern with crystallography open database. The particle has been oriented in the five-fold symmetry and lateral view. The maps obtained are analyzed and correlated with the projection of the different orientations of the crystals within the nanoparticle.

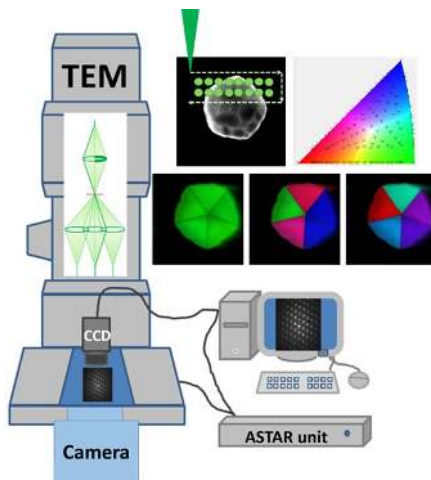


Figure 1. Schematic representation the ASTAR-precession electron diffraction system attached to a transmission electron microscope and the orientation maps of a decahedral gold nanoparticle oriented in the five-fold symmetry and its pole figure color chart.

Keywords: decahedral nanoparticles, electron diffraction, crystal orientation maps, precession electron diffraction

MS23-P4 The fabrication of ZnO microrods on monolayer graphene and their photocatalytic application

Jincheng Fan¹

1. School of Materials Science and Engineering, Anhui University of Technology, Maanshan 243002, China

email: fanjincheng2009@163.com

ZnO microrods were fabricated on graphene/SiO₂/Si substrate by a simple hydrothermal method. The products were characterized using X-ray powder diffraction, scanning electron microscopy, energy dispersive x-ray spectrometry, photoluminescence and UV–visible spectrometry. ZnO microrods were exhibited hexagonal wurzite structure. Some ZnO clusters and twinned ZnO structures were spreaded on the microrod array layer. The formation mechanism of ZnO microrods was discussed, emphasizing the formation mechanism of ZnO clusters and twinned ZnO structures. Furthermore, ZnO nanorods demonstrated good photocatalytic performances and O vacancies and O interstitials were considered to be the active sites of the ZnO photocatalyst.

Keywords: ZnO microrods□Monolayer graphene□Photocatalytic application

MS23-P5 Progress in microstructure analysis by diffraction

Matteo Leoni^{1,2}

1. International Centre for Diffraction Data - ICDD, 12 Campus Blvd, Newtown Square, PA 19073 (USA)

2. DICAM – University of Trento, via Mesiano, 77 – 38123 Trento (Italy)

email: matteo.leoni@unitn.it

Most scientists still believe that Scherrer equation [1] and the Williamson-Hall plot [2] are the only tools available to extract microstructure data from any diffraction pattern. Terms such as “average crystallite size” and “microstrain” are common, but their true physical meaning is often ignored. The consequence is that qualitative results are often mistaken as fully quantitative ones.

In the past decades, a set of full pattern methods has been proposed to extract quantitative microstructure data from the diffraction patterns by considering physical modes for the material [3-5]. In this way, distributions (of size and shape) and defects can be quantified together with the more traditional structural data.

The recent advancements in the field are shown, leading to the possibility of extracting quantitative data from the diffraction pattern of materials that are no longer fully 3D periodic, extending down to the 2D periodic case.

[1] P. Scherrer, Nachr. Ges. Wiss. Goettingen, Math.-Phys. Kl. (1918) 98–100.

[2] G. K. Williamson, W. H. Hall, Acta Metall. 1 (1953) 22–31.

[3] P. Scardi, M. Leoni, Acta Crystallogr. A 58 (2002) 190–200.

[4] M. Leoni, A. F. Gualtieri, N. Roveri, J. Appl. Cryst. 37 (2004) 166–173.

[5] R. J. Koch, M. Leoni, Scientific Reports (2015). Submitted.

Keywords: nanostructured materials, XRD, Line Profile Analysis, defects, stacking faults, 2D materials

MS23-P6 Structural characterization of quantum dot lattices by GISAXS: models and software package *GisaxStudio*

Maja Buljan¹, Igor Mekterović², Marko Karlušić¹, Iva Bogdanović-Radović³, Darko Mekterović³, Marko Jerčinić⁴, Sigrid Bernstorff⁵, Nikola Radić¹, Vlastislav Holy⁵

1. Ruder Bošković Institute, Bijenička cesta 54, 10000 Zagreb, Croatia
2. Faculty of Electrical Engineering and Computing, 10000 Zagreb, Croatia
3. University of Rijeka, Department of Physics, Radmile Matejević 2, 51000 Rijeka, Croatia
4. Elettra-Sincrotrone Trieste, SS 14 km 163.5, 34149 Basovizza, Italy
5. Charles University in Prague, Prague, Czech Republic

email: mbuljan@irb.hr

We present models for structural characterization of nanostructured materials consisting of different quantum dot lattices by GISAXS (grazing incidence small angle x-ray scattering). They enable the determination of the shape and arrangement properties of the formed nano-objects as well as their statistical distributions. The developed models are incorporated in a new program *GisaxStudio*. It contains two families of models: *-3dLattice* for the analysis of three-dimensional quantum dot lattices formed by different self-assembly processes and *-iBeam* which is suitable for the analysis of GISAXS intensity distributions measured on ion-beam modified materials.

GisaxStudio is a modular, multi-platform program for GISAXS analysis of various nanostructured materials. It is written in Java programming language, featuring a graphical user interface, built-in optimization algorithms and visualization. It stores all data in the relational database which facilitates data exchange and reproducibility. It is free for non-commercial use and can be downloaded from the <http://homer.zpr.fer.hr/gisaxstudio>.

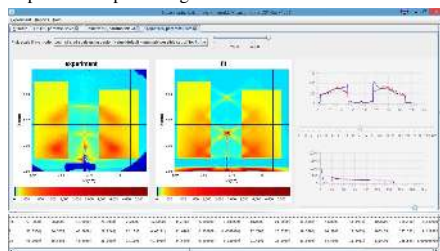


Figure 1. One of the windows of the program *GisaxStudio* showing the experimental and simulated GISAXS maps.

Keywords: GISAXS, *GisaxStudio*, Program, Quantum dot lattices

MS23-P7 Synthesis of carbon nano-onion/nickel hydroxide/oxide composites for electrochemical supercapacitor electrode applications

Marta E. Plonska-Brzezinska¹, Diana Brus¹, Krzysztof Brzezinski¹, Luis Echegoyen²

1. Institute of Chemistry, University of Białystok, Hurtowa 1, 15-399 Białystok, Poland
2. Department of Chemistry, University of Texas at El Paso, 500 W. University Ave., El Paso, TX 79968, USA

email: mplonska@uwb.edu.pl

The high temperature annealing of ultra-dispersed nanodiamonds (5 nm, average size) leads to their transformation into CNO structures (5–6 nm in diameter, 6–8 shells), that can be also described as multi-shelled fullerenes. The interest in carbon nano-onions is driven by their unusual physico-chemical properties as well as by promising applications in electronics, optics, and in energy conversion and storage. In electrical double layer capacitors (EDLCs) the energy can be stored via ion adsorption and the capacitance is associated with an electrode-potential-dependent accumulation of charge at the electrode interface through polarization. During the charging/discharging process of carbon-based EDLCs, the electrode material is not electrochemically active. In pseudocapacitors the electrode material is electrochemically active and faradaic reactions take place. The type of charge storage mechanism determines the electrochemical performance of EDLCs and the electrode materials are also crucial. New types of supercapacitors which combine the advantages of both double layer capacitors and pseudocapacitors are the subject of this work. Carbon nano-onion (CNO) and Ni(OH)₂ or NiO composites were prepared by a simple method, which is based on chemical loading of Ni(OH)₂ on the carbon surface. The electrochemical properties of the resulting composites were studied to investigate their potential as supercapacitors. The samples were characterized by transmission and scanning electron microscopic methods, powder diffraction techniques and by differential-thermogravimetric analyses. Textural properties were characterized using nitrogen gas adsorption analyses. Pristine inorganic samples of NiO and Ni(OH)₂ revealed different morphologies and porous characteristics when compared to those of the CNO composites, which showed unique electrochemical properties. The electrochemical performance of the CNO/Ni(OH)₂ or CNO/NiO composites is largely affected by the mass, the morphology and distribution of the Ni(OH)₂/NiO phase. The electrochemical properties of these electrodes were investigated using cyclic voltammetric and electrochemical impedance spectroscopic analyses. Compared with pristine CNOs (40 F/g), modified CNOs with the inorganic components show improved electrochemical performance (ca. 1125 F/g for CNOs/Ni(OH)₂ and ca. 370 F/g for CNOs/NiO).

We gratefully acknowledge the financial support of the National Science Centre, Poland, grant #2012/05/E/ST/03800

Keywords: carbon nano-onion, composite, supercapacitor, capacitance

MS23-P8 TEM characterization of hydroxyapatite nanocrystals grown on the bacterial cellulose fibrils

Natalya A. Arkharova¹, Alexander V. Severin², Albert K. Khripunov³, Andrey S. Orekhov¹, Vera V. Klechkovskaya¹

1. Institute of Crystallography, RAS, 119333, Leninskii pr. 59, Moscow, Russia

2. Department of chemistry, Moscow State University, 119991, 1-3 Leninskiye Gory, Moscow, Russia

3. Institute of Macromolecular Compounds, RAS, 199004, Bol'shoi pr. 31, St. Petersburg, Russia

email: natalya.arkharova@gmail.com

Hydroxyapatite (HAP) nanocrystals were synthesized by the biomimetic approach (simulation of the biosynthesis in natural bone): synthesis of HAP nanocrystals occurred in the presence of bacterial cellulose fibrils. Due to its properties (biocompatibility, elasticity, high wet strength, conformability, high modulus value) and crystalline structure bacterial cellulose (BC) is promising collagen substitute material. Composites were prepared with the different BC/HAP mass ratios by gradual increasing of BC portion up to maximum possible: BC/HAP_1 - 0,04/1 g, BC/HAP_2 - 0,24/1 g, BC/HAP_3 - 0,79/1g, BC/HAP_4 - 1/1g. Microstructure of the samples was investigated with transmission electron microscopy (TEM) and electron diffraction. High-resolution TEM (HRTEM) and HRTEM simulation by the Bloch wave method were used to determine the thickness of the HAP nanocrystals. In all prepared samples HAP nanoparticles are textured along [0001] direction to the BC fibril direction similarly to alignment of mineral nanocrystals on collagen fibrils in natural bone (Fig.1.). It was determined that the more mass proportion of the BC is in the solution than there are less big HAP nanoparticles in the sample and their sizes are close to sizes of mineral crystals in bone.

This work was supported by grant RFBR № 14-02-31258.

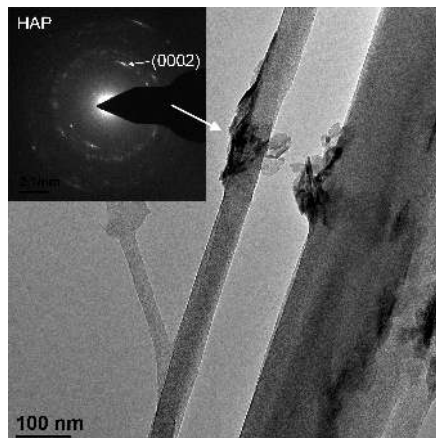


Figure 1. TEM image of HAP agglomerate grown on the bacterial cellulose fibril and its diffraction pattern.

Keywords: bacterial cellulose, hydroxyapatite nanoparticles, electron microscopy, electron diffraction

MS23-P9 Structural study of ceria-doped TiO₂ prepared at different conditions

Tereza Brunatova¹, Lenka Matejova², Zdenek Matej¹, Stanislav Danis¹

1. Charles University, Faculty of Mathematics and Physics, Dept. of Condensed Matter Physics, Prague, Czech Republic
2. CNT – Nanotechnology Center, Technical University of Ostrava, 17. listopadu 15/2172, 708 33 Ostrava - Poruba, Czech Republic

email: brunatovat@centrum.cz

In our contribution we will present structural studies of titania oxide doped by ceria by means of X-ray diffraction at room and at elevated temperatures. Doping of Ce atoms in TiO₂ structure affects the photocatalytic properties. Sample have been prepared by hydrothermal synthesis at different temperatures and pressures. Using software package MStruct the real structure of investigated samples has been examined as well.

Keywords: X-Ray diffraction, nanostructured TiO₂-Ce

MS23-P10 XRD characterization of structural evolution and morphology properties of silica-doped alumina aerogels

Vera P. Pakharukova^{1,2}, Dmiry A. Yatsenko^{1,2}, Anton S. Shalygin^{1,2}, Evgeny Y. Gerasimov^{1,2}, Sergey V. Tsybulya^{1,2}, Oleg N. Martyanov^{1,2}

1. Borekov Institute of Catalysis, SB RAS, Pr. Lavrentieva 5, 630090 Novosibirsk, Russia
2. Novosibirsk State University, Pirogova Street 2, 630090 Novosibirsk, Russia

email: verapakharukova@yandex.ru

Nanocrystalline aluminas are widely used as catalyst supports. A major advantage of aerogels compared to conventional alumina supports is their high specific surface area, high mesoporosity. Silica-doped alumina aerogels have a potential for high-temperature catalytic applications due to resistance to thermal coarsening and phase transformations. Structure and particle morphology are known to affect material properties. Thus, several studies revealed impact of morphology parameters on a thermal behavior of the alumina aerogels.

The objective of this work was study of phase transformations, morphology parameters of the silica-doped alumina aerogels by X-Ray Diffraction (XRD) analysis. To obtain information on the structure, dispersion, and morphology modeling XRD patterns was performed using the Debye Scattering Equation. The method allows calculating the XRD pattern from systems of nanoparticles with any structure, shape, and size. The aerogels with various molar Al:Si ratios were synthesized by the sol-gel method followed by supercritical drying. The pseudoboehmite phase was identified in the aluminium-rich aerogels calcined at 300°C. The XRD patterns featured anisotropic broadening of peaks. Modeling XRD patterns evidenced a plate shape of crystallites. The crystallites in the alumina aerogel were rectangular plates with average dimensions of 20x6.5x25 nm. The anisotropy was more pronounced in silica-doped alumina aerogel with Al:Si ratio of 9:1 (fig.1). Material consisted of pseudoboehmite plate-like crystallites with a thickness of one lattice constant in the [010] direction (14.0x1.2x14.5 nm in size). The pseudoboehmite structure is composed of octahedral oxygen layers packed in [010] direction. Formation of two-dimensional packets proceeded organization three-dimensional crystal structure. The results were supported by transmission electron microscopy.

It was shown that the silica dopant retarded the pseudoboehmite crystallization and its further transformation to γ -alumina phase upon calcination. The aerogels with high silica loading were X-ray amorphous within a wide temperature range. The morphology parameters were expected to be preserved at topotactic transition of the pseudoboehmite to alumina phase.

The work was performed in the framework of the Research and Educational Center for Energy Efficient Catalysis (Novosibirsk State University, Borekov Institute of Catalysis). The structural studies were supported by the RSCF project №14-23-00037.

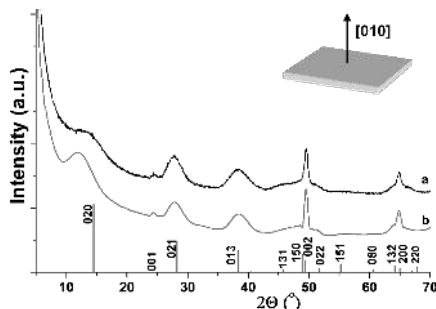


Figure 1. (a) - experimental XRD pattern of the aerogel sample (Al:Si=9:1); (b) - calculated diffraction pattern for AlO(OH) crystallites with dimensions of 14.0x1.2x14.5 nm (49x1x39 unit cells)

Keywords: nanostructure, alumina, pseudoboehmite, XRD, DSE

MS23-P11 Strain-relaxation in GaAs / InGaAs core-shell nanowire heterostructures grown by MBE onto Si(111)

Ali Al Hassan¹, Ryan B. Lewis², Andreas Biermanns¹, Emmanouil Dimakis², Lutz Geelhaar², Ullrich Pietsch¹

1. Naturwissenschaftlich-Technische Fakultät der Universität Siegen, 57068 Siegen, Germany

2. Paul-Drude-Institute für Festkörperelektronik, Hausvogteiplatz 5-7, 10117 Berlin, Germany

email: ali_al_hassan@live.com

Semiconductor core-shell nanowires (NW) with different shell thickness can be grown onto [111] oriented silicon substrates without major structural defects due to the strain release towards the NW side planes [1]. This approach offers the possibility to form radial hetero-structures (HS) between highly lattice-mismatched materials but the process of strain relaxation is not fully understood.

We report on detailed investigations of anisotropic strain and strain relaxation mechanism in GaAs/In_{0.25}Ga_{0.75}As/GaAs NWHS grown by MBE onto Silicon (111) substrate. Independent from core-shell thickness ratio, x-ray diffraction measurements with scattering vector along the 111 growth direction shows no Bragg peak splitting but a single out-of plane lattice parameter explained by the strain balance between slightly expanded GaAs and compressed InGaAs shell. On the other hand, X-ray measurements along the NW side planes and edges show peak splitting between core and shell material confirming the appearance of in-plane lattice mismatch. The mismatch is different measuring along the (1-10) or the (2-1-1) directions that can be explained by a nominal In content of 22.5% and 18.5%, respectively. The difference can be related to strain induced segregation along the NW edges as it has been observed in AlGaAs/GaAs core-shell NWs [2]. Our data are interpreted in terms of finite element calculations revealing an insight into the complexity of strain relaxation mechanism in MBE grown core-shell nanowires.

Related publications

[1] A Biermanns, S Breuer, A Trampert, A Davydok, L. Geelhaar and U Pietsch, *Lattice parameters and strain accomodation in Ga-assisted grown GaAs nanowires on Silicon (111)*, Nanotechnology 23, 2012, 305703.

[2] M. Heiss, Y. Fontana, A. Gustafsson, G. Wüst, C. Magen, D. D. O'Regan, J.W. Luo, B. Ketterer, S. Conesa-Boj, A. V. Kuhlmann, J. Houel, E. Russo-Averchi, J. R. Morante, M. Cantoni, N. Marzari, J. Arbiol, A. Zunger, R. J. Warburton and A. Fontcuberta i Morral, *Self-assembled quantum dots in a nanowire system for quantum photonics*, Nature Materials 12 (5), 439-444, 2013.

Keywords: Strain relaxation, core-shell nanowires, finite element method, hetero-structures, x-ray diffraction.

MS23-P12 Structural studies of MoS₂ intercalation compounds with aromatic molecules

Alexander S. Goloveshkin¹, Alexander A. Korlyukov¹, Natalia D. Lenenko¹, Alexandre S. Golub¹, Ivan S. Bushmarinov¹

1. A.N. Nesmeyanov Institute of Organoelement Compounds, Russia

email: golov-1@mail.ru

Molybdenum disulfide is an important graphene analog demonstrating semiconducting properties. The unique feature of the MoS₂ layers is the susceptibility of their atomic structure and properties to negative charge transferred onto layers. The crystalline MoS₂ can be exfoliated into single-layer dispersion of MoS₂ crystals by reduction of starting material to LiMoS₂ followed by detachment of its layers in aqueous solvents [1]. This dispersion reacts with organic salts in solution, producing precipitates of layered MoS₂ intercalated with their cations [2].

Recently [3], we have found that the powder X-ray diffraction patterns of (R_nN) MoS₂ (R= H, alkyl) can be modeled using the “supercell approach” [4,5] developed by C. Ufer for full-pattern modeling of turbostratically disordered clays. This method allowed direct refinement of both MoS₂ layer geometry and the cation positions.

In the current work, we investigate the applicability of this approach to intercalation compounds of MoS₂ with aromatic moieties. Initially, the difference between the calculated and experimental patterns was unacceptable due to intense symmetric peaks unexplained by purely turbostratic disorder. We found that these peaks correspond to short-range correlations between MoS₂ layer positions, and successfully modeled them assuming that the turbostratic disorder is actually exhibited by stable bilayer fragments (Fig. 1).

This new “bilayer-supercell” model allowed us to refine the powder patterns of new intercalation compounds. We obtained the preferred geometry and relative positions of MoS₂ layers, as well as the orientation of aromatic molecules in the interlayer space. The PW-DFT-d calculations based on this model confirm our results.

[1] P. Joensen, R.F. Frindt, S.R. Morrison, *Mat. Res. Bull.* 21 (1986) 457.

[2] A.S. Golub, I.B. Shumilova, Yu.N. Novikov, J.L. Mansot M. Danot. Phenanthroline intercalation into molybdenum disulfide. *Solid State Ionics*, 1996, v.91, N 3-4, p.307-314.

[3] A.S. Goloveshkin, N.D. Lenenko, V.I. Zaikovskii, A.S. Golub, A.A. Korlyukov, I.S. Bushmarinov, *RSC Adv.*, 2015, 5, 19206-19212.

[4] K. Ufer, G. Roth, R. Kleeberg, H. Stanjek, R. Dohrmann, J. Bergmann, *Z. Krist.* 219 (2004) 519.

[5] X. Wang, J. Li, R.D. Hart, A. van Riessen, R. McDonald, *J. Appl. Cryst.* 44 (2011) 902.

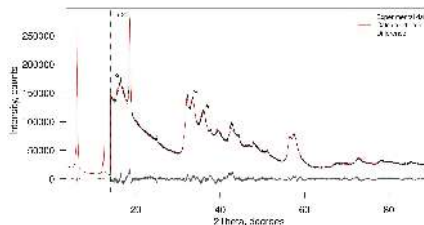


Figure 1. The powder pattern of intercalation compound of MoS₂ with 1,8-bis(dimethylamino)naphthalene. Asterisks (*) denote the peaks caused by correlation between the MoS₂ layers.

Keywords: powder diffraction, layered systems, molybdenum disulfide

MS23-P13 Simulation of X-ray diffraction scattering for nanostructured aluminum oxides

Dmitriy A. Yatsenko^{1,2}, Sergey V. Tsybulya^{1,2}

1. Borekov Institute of Catalysis, SB RAS, Pr. Lavrentieva 5, 630090 Novosibirsk, Russia

2. Novosibirsk State University, Pirogova Street 2, 630090 Novosibirsk, Russia

email: d.a.yatsenko@gmail.com

The metastable g-, h-, c-Al₂O₃ polymorphs prepared by low-temperature decomposition of the various aluminum hydroxides are the nanocrystalline systems with complex hierarchical nanostructure [1]. They are widely used as catalysts and supports. Therefore, the investigation of the relationship between physicochemical properties, atomic structure and nanostructure of materials is an actual problem.

However, the structure determination of alumina by the powder scattering data is a significant challenge due to the complexity of the diffraction patterns. Specific shape of primary nanocrystallites and their type of coherent ordering in the nanostructure are cause of significant and, moreover, anisotropic broadening of the diffraction peaks. The purpose of this report is the illustration of possibilities of the method associated with the creation of an nanostructured systems and the subsequent calculation of the diffraction pattern.

The method is based on the Debye equation and known in the literature as Debye Function Analysis (DFA) [2]. It is full-profile method which is applicable for any an arbitrary atoms collection, and therefore can be used for crystalline materials or nano-structured objects. The calculations were performed on the DIANNA program [3], which is public-domain software and available on the website: www.sourceforge.net/projects/dianna.

This work is supported by Russian Science Foundation project N 14-23-00037.

1. Tsybulya S.V., Kryukova G.N. Nanocrystalline transition aluminas: Nanostructure and features of x-ray diffraction patterns of low-temperature Al₂O₃ polymorphs // Phys.Rev. 2008. B77. 024112.

2. Tsybulya S.V., Yatsenko D.A. X-ray diffraction analysis of ultradisperse systems: The Debye formula. Journal of Structural Chemistry. 2012. Volume: 53. P. S150-S165.

3. Yatsenko D.A., Tsybulya S.V. DIANNA (Diffraction Analysis of Nanopowders): software for structural analysis of ultradisperse systems by x-ray methods. Bulletin of the Russian Academy of Sciences: Physics. 2012. T. 76(3). P. 382-384.

Keywords: X-ray analysis, XRD, modeling, nanostructure, Debye scattering equation, DFA

MS23-P14 Structure determination of molecular nanocomposites by combining pair distribution function analysis and solid-state NMR

Dominik Schaniel^{1,2}, El-Eulmi Bendeif^{1,2}, Axel Gansmüller^{1,2}, Kuan-Ying Hsieh^{1,2}, Sebastien Pillet^{1,2}, Theo Woike³, Mirjam Zobel⁴, Reinhard Neder⁴, Mohamed Bouazaoui⁵, Hicham El Hamzaoui⁵

1. Université de Lorraine, CRM2, UMR 7036, Vandoeuvre-les-Nancy, F-54506, France

2. CNRS, CRM2, UMR 7036, Vandoeuvre-les-Nancy, F-54506, France

3. Institut für Strukturphysik, TU Dresden, Zellescher Weg 16, Dresden, Germany

4. Crystallography and Structural Physics, University of Erlangen-Nürnberg, Staudtstr. 3, D-91058 Erlangen, Germany

5. Laboratoire de Physique des Lasers, Atomes et Molécules (PhLAM), CNRS (UMR 8523), IRCICA (CNRS, USR 3380), Bâtiment P5, Université Lille 1-Sciences et Technologies, F-59655 Villeneuve d'Ascq Cedex, Fr

email: dominik.schaniel@univ-lorraine.fr

Transparent mesoporous silica monoliths of well controlled porosity and a narrow pore size distribution around 6 nm have been used to elaborate sodium nitroprusside (SNP) nanocomposites. The obtained nanomaterials could be characterised using X-ray total scattering coupled to atomic pair distribution function analysis (PDF) and solid-state NMR spectroscopy. The PDF analysis allows for a structural description of the confined species as well as for the identification of various existing phases: SNP isolated molecules and SNP crystalline nanoparticles. The model obtained suggests that the nanocrystals have the same molecular structure as the bulk crystalline material and measure about 6 nm in diameter. This result is quite exceptional since the space available inside the pores is only about ten times the size of the molecules. The multi-nuclei Solid State NMR investigation confirms the structural model proposed by the PDF analysis and assigns the isolated molecules to dynamic disorder of a solvated phase. The latter approach additionally provides quantitative information on the relative ratio between the dynamic molecules and the rigid nanocrystals. This result is exploited to study the evolution of the two confined SNP phases with respect to solvating water molecules. We show that the confined SNP nanocrystals can be easily dissolved when storing the nanocomposites at increasing atmospheric relative humidity.

[1] Sanchez *et al.*, *Adv. Mater.* **2003**, *15*, 1669 ; Vinu *et al.*, *J. Nanosci. Nanotec.* **2005**, *5*, 347. [2] Deniz *et al.*, *Chem. Eur. J.* **2012**, *18*, 15782. [3] Blecher *et al.*, *Nanomedicine : Nanotechnology, Biology, and Medicine* **2012**, *8*, 1364. [4] T.-W. Sung, Y.-L. Lo, *Sensors and Actuators B : Chemical* **2012**, *173*, 406. [5] Hsieh *et al.*, *RSC Adv.* **2013**, *3*, 26132. [6] Bendeif *et al.*, *RSC Adv.* **2015**, *5*, 8895.

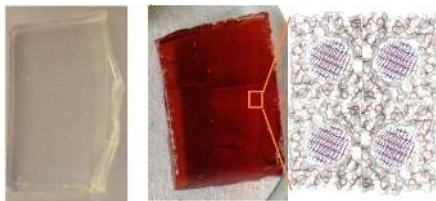


Figure 1. Photographs of transparent empty silica monolith (left) and SNP-silica nanocomposite (right) and schematic representation of encapsulated nanoparticles.

Keywords: total scattering, NMR, nanocrystalline material, molecular compounds

MS23-P15 Tailoring phase composition and microstructural features of $\text{Ba}_4\text{Nb}_2\text{O}_9$ polymorphs *via* thermal decomposition route

Martina Vrankić¹, Jasminka Popović¹, Marijana Jurić¹

¹. Ruder Bošković Institute, Bijenička cesta 54, 10000 Zagreb, Croatia

email: mvrankic@irb.hr

Synthesis of nanoparticles with a controlled size has been found to be crucial for tailoring desired material properties since thermal, electric, optical, catalytic, and magnetic properties are strongly composition-, structure-, but also, size- and shape-dependent.^{1,2} It is well known that $\text{Ba}_4\text{Nb}_2\text{O}_9$ exhibits mixed electronic, oxide ion, and proton conductivity, which makes it especially attractive in the field of fuel cells, steam electrolyzers, and humidity sensors.³ Especially, the γ - $\text{Ba}_4\text{Nb}_2\text{O}_9$ phase exhibits several orders higher conductivity than α - $\text{Ba}_4\text{Nb}_2\text{O}_9$ due to a faster protonic and oxide ionic transport.³ Up to now, the γ polymorph was metastable at room temperature (RT) and so could be isolated only by quenching the sample from high temperatures, because slow cooling led to a transformation to α phase.³ In the present study the mixed $\text{Ba}^{\text{II}}\text{--Nb}^{\text{V}}$ containing oxides were prepared using $\{\text{Ba}_2(\text{H}_2\text{O})_2[\text{NbO}(\text{C}_2\text{O}_4)_2]\text{H}_2\text{C}_2\text{O}_4\} \cdot \text{H}_2\text{O}$ as a single-molecular precursor.² A systematic study of preparation conditions was carried out, namely, tuning the final structural and microstructural parameters by (i) the holding time (2, 1 and 0.5 h) at 1175 °C and (ii) the cooling rate (3, 7 and 12 °C min⁻¹) from 1175 °C back to RT. Nanocrystalline products obtained by thermal decomposition of the precursor were investigated by X-ray powder diffraction at RT. Size and strain analysis were obtained in the course of the Rietveld refinement. Since all samples prepared by a cooling rate of 12 °C min⁻¹ contained only the γ - $\text{Ba}_4\text{Nb}_2\text{O}_9$ polymorph, it was evident that faster cooling prevented the $\gamma \rightarrow \alpha$ phase transition, which resulted in the retention of the high-temperature γ - $\text{Ba}_4\text{Nb}_2\text{O}_9$ phase at RT. Shortening of the time period for which γ - $\text{Ba}_4\text{Nb}_2\text{O}_9$ containing samples were held at 1175 °C had no impact on their phase composition. All samples were found to be strain free. Crystallite sizes were ~20 nm for γ - $\text{Ba}_4\text{Nb}_2\text{O}_9$ prepared with a holding time of 2 h while it decreased to ~5 nm with shortening of the holding time to 0.5 h.

References:

- (1) Fernández-García, M.; Martínez-Arias, A.; Hanson, J. C.; Rodríguez, J. A. *Chem. Rev.* **2004**, 104, 4063–4104.
- (2) Burda, C.; Chen, X.; Narayanan, R.; El-Sayed, M. A. *Chem. Rev.* **2005**, 105, 1025–1102.
- (3) Ling, C. D.; Avdeev, M.; Kutteh, R.; Kharton, V. V.; Yaremchenko, A. A.; Fialkova, S.; Sharma, N.; Macquart, R. B.; Hoelzel, M.; Gutmann, M. *Chem. Mater.* **2009**, 21, 3853–3864.

Keywords: phase composition, size and strain analysis, Rietveld refinement

MS23-P16 Facile route for preparation of nanocrystalline ZnMn_2O_4 : effect of preparation conditions on structure and microstructure

Sanja Brkić¹, Jasminka Popović¹, Mirjana Bijelić², Christian Suchomski³, Zora Popović⁴

1. Division for Materials Physics, Ruder Bošković Institute, Bijenička c. 54, Zagreb, Croatia
2. Department of Physics, Faculty of Science, University of Zagreb, Bijenička c. 32, Zagreb, Croatia
3. Institute of Nanotechnology, Karlsruhe Institute of Technology, Hermann-von-Helmholtz-Platz 1, Eggenstein-Leopoldshafen, Germany
4. Department of Chemistry, Faculty of Science, University of Zagreb, Horvátovac 102A, Zagreb, Croatia

email: sbrkic@irb.hr

Traditional synthesis of spinel materials such as solid-state route involving grinding and firing of a mixture of oxides, nitrates or carbonates which requires elevated temperatures and prolonged process times have been abandoned. Indeed, majority of papers on manganese spinels are focused on low cost preparation methods which proceed at moderate temperatures (600 °C) with enhanced reaction kinetics [1,2]. Interestingly, Liu *et al.* reported a room temperature route for preparation of AMn_2O_4 (A=Zn, Co, Cd) from metal acetates [3]. Although synthetic route proposed by Liu *et al.* represents a facile and very efficient route for low temperature synthesis of spinel materials, in order to utilize this route for the targeted design of nanomaterials it is necessary to establish, very precisely, correlations between specific preparation conditions (concentration of NaOH, aging period, and temperature of additional heat treatments), structure, microstructure and properties. Detailed structural investigation using X-ray powder diffraction (XRPD) and Raman spectroscopy have been carried out in order to correlate specific structural and microstructural features with changes in preparation conditions. ZnMn_2O_4 was prepared by precipitation with NaOH ($c=0.25\text{--}0.8$ M) from solution of Zn and Mn acetates. Also, sample obtained by 0.8 M NaOH was additionally heat treated at $T=300, 400$ and 500 °C. Pronounced difference in crystallinity was observed with increase in concentration of NaOH. Based on the results of Raman spectroscopy a model described by the formula: $[\text{Zn}^{2+}, \text{Mn}^{2+}]_{\text{tet}}[\text{Zn}^{2+}, \text{Mn}^{3+}, \text{Mn}^{4+}]_{\text{oct}}\text{O}_4$ has been proposed and tested upon structural data. It was shown, based on Rietveld structure refinement, that unit-cell constants as well as the inversion parameter of spinel lattice increase with the increase in temperature of thermal treatment.

1. L. Hu *et al.*, *Sci. Rep.*, **2**, 217-226, 2012. Y. 2. Li *et al.*, *Nanoscale*, **5**, 2045-2054, 2013. 3. Y. Liu *et al.* *RSC Advances*, **4**, 4727-4731, 2014.

Keywords: manganese spinels, XRPD, microstructure

MS23-P17 Synthesis and characterization of ultrasmall zirconia particles prepared via nonhydrolytic route

Jess E. Gambe¹, Fabien Remondière¹, Olivier Masson¹, Jenny Jouin¹, Abid Berghout¹, Philippe Thomas¹

1. Science des Procédés Céramiques et de Traitements de Surface (SPCTS), CNRS UMR 7315, Centre Européen de la Céramique, 12 Rue Atlantis, 87068 Limoges Cedex, France

email: jess.gambe@etu.unilim.fr

Zirconia has been applied to various fields in materials science due to its noteworthy electronic, mechanical and thermal properties. These properties become distinctive for ultrasmall particles which are neither that of atomic nor bulk characteristics¹. Structure determination of ultrasmall nanoparticles is at the forefront of modelling their properties and is still at its infancy². In order to help in getting their structural models it is crucial that we synthesize quality ultrasmall particles. However, synthesis of ultrasmall particles with good control over the size and phase purity is not easily done. One way is to use nonhydrolytic route which is advantageous in terms of purity and homogeneity³. In this work, we were able to synthesize well crystallized ultrasmall particles using a modified nonhydrolytic route without surfactants. Average structural and morphological characterizations via classical X-ray diffraction and transmission electron microscopy were done on the samples. Results show that we were able to manipulate the phase purity of our samples from dual phase to single phase. Also, we observed a good control over the size of our particles which are in the nanoscale range from ~5.0 to ~1.0 nm and appear to have a spherical shape. Furthermore, the modified nonhydrolytic approach allowed us to produce nanoparticles at low temperatures from ~210 down to ~100°C with good compositional purity. One of the reasons why we were able to achieve these results is due to the fine tuning of the ratio of precursors to adjust the alkalinity of the solution. Whereas the average structure of our ultrasmall particles is consistent to that of a tetragonal phase zirconia, the atomic-pair distribution function analysis reveal that the particles demonstrate local structural distortions to that of the ideal tetragonal phase zirconia.

References

- [1] M.L. Steigerwald, *et al.*, *Annu.Rev.Mater.Sci.*(1989), 19, 471-495
- [2] S.J.L. Billinge, *Phys.*(2010) 3, 25
- [3] P. H. Mutin, *et al.*, *Chem. Mat.*(2009), 21, 582–596

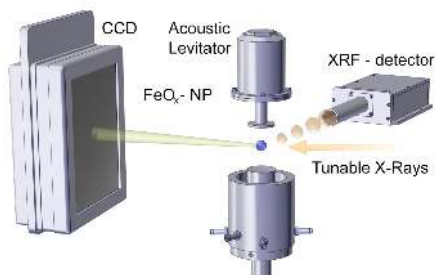


Figure 1. Experimental setup of coupling XANES and SAXS using an acoustic levitator as sample holder. XANES spectra were collected using an XRF-detector.

Keywords: Iron oxide nanoparticles, XANES, SAXS, time-resolved

MS24. Short range order and diffuse scattering

Chairs: Alexei Bosak, Thomas Weber

MS24-P1 Modeling charge density variations in molecular crystals

Michael Wall¹

1. Los Alamos National Laboratory, Los Alamos, USA

email: mewall@lanl.gov

I will describe our efforts to accurately model charge density variations in molecular crystals. A key goal is to fill a gap in traditional crystallography by providing more detailed information about molecular motions. Our approach integrates molecular dynamics simulations, fast quantum mechanical computations, and information from diffuse X-ray scattering. It is timely as the necessary computations are becoming increasingly feasible, and as traditional structure determination methods are approaching the limits of their achievable accuracy. Elements of our approach have been applied to protein and small molecule systems, yielding new insights. Computational methods are being made available in publicly available software (<https://github.com/mewall/lunus>).

Keywords: diffuse X-ray scattering, molecular notions, charge density variations

MS24-P2 Monitoring packing changes in planar molecules

Dean S. Keeble¹, Luke A. Rochford², Helen Y. Playford³, Matt G. Tucker^{1,3}

1. Diamond Light Source, Harwell Science and Innovation Campus, UK.
2. Department of Chemistry, University of Warwick, UK.
3. ISIS Facility, Rutherford Appleton Laboratory, Harwell Science and Innovation Campus, UK

email: dean.keeble@diamond.ac.uk

The way that small molecules pack together can have substantial ramifications on observed physical properties, optical adsorption, and device characteristics, even if the molecular structure is identical. Small pi-conjugated molecular semiconductors such as phthalocyanines, subphthalocyanines, and squaraines demonstrate great potential in organic photovoltaics, field effect transistors and light emitting diodes. Their properties are readily tuneable due to their ability to accommodate a variety of metal centres, and structures can be further modified by substitution of outer-skeleton hydrogen atoms for a huge number of other atoms or small chemical moieties. However, whilst the effects of these substitutions on physical properties are measured routinely, it is much more uncommon to study the underlying influence on intra- and inter-molecular bonding. Since many physical properties depend critically on chemical bonding, increased understanding of the influence of substitution could pave the way for the targeted design of new materials. We will present a pair distribution function (PDF) study of some exemplar molecular semiconductors, in order to demonstrate the ability of the PDF technique to directly study how metal and hydrogen substitution are structurally accommodated in these systems. In particular, we will look at how it is possible to observe changes in molecular packing using the PDF.

Keywords: pair distribution function, organic semiconductors, molecular packing, short-range order

MS24-P3 Phase transitions in $\text{PbZr}_{1-x}\text{Ti}_x\text{O}_3$ with low Ti concentrations studied by X-ray scattering

Daria A. Andronikova^{1,2}, Alexei Bosak³, Yurii Bronwald^{1,2}, Roman Burkovsky^{2,3}, Dmitry Chernyshov^{2,3}, N. G. Leontyev⁴, I.N. Leontyev⁵, Sergey Vakhrushev^{1,2}

1. Ioffe Institute, St. Petersburg, Russia
2. St.Petersburg Polytechnical University, St. Petersburg, Russia
3. ESRF, Grenoble, France
4. Azov-Black Sea State AgroEngineering Academy, Russia
5. Southern Federal University, Russia

email: andronikova.daria@gmail.com

$\text{PbZr}_{1-x}\text{Ti}_x\text{O}_3$ (PZT) is a solid solution of lead titanate PbTiO_3 and lead zirconate PbZrO_3 . PZT is the famous and the most practically used ferroelectric. The reason of this popularity is that PZT possesses exceptionally good piezoelectric properties, has the high value of dielectric constant and the high phase transition's temperature. Phase diagram of PZT demonstrates complexity. The area of our study is located at region of low concentration of Ti. There are two phases, namely ferroelectric and antiferroelectric one. Paraelectric-ferroelectric phase transition is accompanied by the appearance of the superlattice M-type reflections $\frac{1}{2}(h\ k\ 0)$. Electron diffraction studies of ferroelectric phase have revealed the existence of the M-reflections splitting for PZT with high concentration of Zr [1]. At the moment corresponding structure modulation is not understood completely.

PZT single crystals X-ray diffraction at Ti concentrations 0,7%, 1,5% and 3,3% has been studied on Swiss-Norwegian beamline of European synchrotron radiation source. Diffraction measurements revealed the appearance of strong anisotropic diffuse scattering around Bragg spots. The splitting of M-superstructure was observed. The details are presented in the poster.

[1] J Ricote, D L Corker, R W Whatmore, A M Glazer, J Dec and K Roleder, *Phys.: Condens. Matter* 10, 1767–1786 (1998)

Keywords: phase transition, lead zirconate, X-ray scattering, diffuse scattering, antiferroelectric

MS24-P4 Interpretation of single crystal diffuse scattering augmented by density functional theory and spectroscopyMatthias J. Gutmann¹¹. Rutherford Appleton Laboratory, ISIS Facility, Chilton Didcot, Oxfordshire OX11 0QX, United Kingdom

email: matthias.gutmann@stfc.ac.uk

Ever since the pioneering works of the Braggs which started crystallography and Born and von Karman which started the field of vibrational spectroscopy, the two disciplines were seen as being separate.

Born's insight into the nature of thermal diffuse scattering (TDS) arising in crystallographic experiments established a link between the two [1]. When using X-ray diffraction, the TDS is integrated in energy but resolved in momentum. Interesting effects can occur in a time-of-flight single crystal neutron diffraction experiment, when some neutrons can accidentally match the wave-vector and energy of phonons, as has been noted by Willis [2].

The complementarity of using spectroscopy, TDS and density functional theory will be illustrated in a series of Alanine compounds.

In addition, we have devised a method of simulating the diffuse scattering arising from one-phonon inelastic excitations in a neutron time-of-flight Laue single crystal experiment. These effects are illustrated experimentally using NaCl, the first crystal structure solved by the Braggs. In addition they are simulated using DFPT phonons obtained from CASTEP first principles code.

[1] M. Born and K. Lonsdale, *Nature* 150, 490 (1942).

[2] B. T. M. Willis, *Acta Cryst.* A42, 514 (1986).

Keywords: diffuse scattering**MS24-P5** Disordered structure of the Mg-Al and Ni-Al oxides prepared by the thermal decomposition of layered double hydroxidesSvetlana V. Cherepanova^{1,2}, Natalya N. Leont'eva³¹. Borekov Institute of Catalysis². Novosibirsk State University³. Institute of Hydrocarbons, Omsk, Russia

email: svch@catalysis.ru

The structures of the mixed oxides prepared by the decomposition of Mg-Al and Ni-Al layered double hydroxides (LDH) at the moderate temperatures (400 – 800 °C) have not been completely investigated up to now. It is related with the presence of a diffuse scattering along with the peaks inherent to MgO- or NiO-like structure on the XRD patterns. The HRTEM evidences that the structures of the mixed oxides are different. The Mg-Al oxide structure is disordered in three directions. The Ni-Al oxide has the 1D disordered sandwich-like structure. These data were used for the simulation of the XRD patterns on the base of the models of 1D and 3D disordered crystals with use of the DIFFaX software and the self-developed Debye equation scattering program.

By means of the Debye simulation it was confirmed that structure of the Mg-Al oxide is very defective and consists of the layers of octahedrally (O) coordinated cations as in the MgO structure in [111] direction and mixed octahedral-tetrahedral (OT) layers as in a spinel structure. Layers contain row-ordered cation vacancies. On the Figure one can see that the presence of the OT layers results in decrease in the intensity of the 200 diffraction peak of MgO-like structure and appearance of the two peaks of diffuse scattering. Ordering of cation vacancies leads to the stacking faults (SFs) in the plane of layers that broadens the first peak of diffuse scattering. At the definite concentrations of defects a good correspondence between the experimental and calculated XRD patterns is achieved.

Such disordered structure can be formed as a result of a migration of Al³⁺ ions from LDH's Mg-Al brucite-like layers to the interlayer during thermal removing of water molecules, hydroxyl- and carbonate-ions. Reconstruction of the LDH's hydrotalcite structure from the mixed Mg-Al oxide upon contact with water can be explained by the reverse migration of cations during the filling of interlayers by water and hydroxyl-ions. This model is not suitable for the non-rehydratable Ni-Al oxide. It was shown that the one part of Al³⁺ ions keeps in octahedral layers and the other part migrates to the surface forming amorphous alumina. By means of the simulation it was shown that possible presence of spinel-like surface layers epitaxially connected with NiO-like core can lead to the appearance of the diffuse scattering observed on the experimental XRD patterns.

This work was supported by the Russian Science Foundation (Grant 14-23-00037).

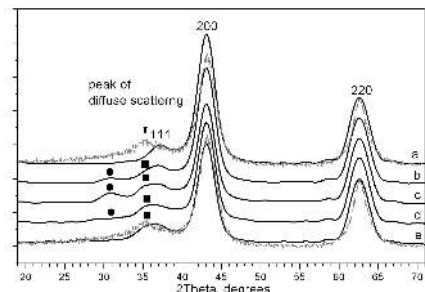


Figure 1. The XRD patterns: experimental (grey) and simulated (black) using structural models containing O layers (MgO) and OT ones (spinel) with OT concentration: a) 0, b) 0.1, c) 0.2 and additional SFs with probability: d) 0.15, e) 0.30. Squares and circles show first and second peaks of diffuse scattering.

Keywords: diffuse scattering, disorder

MS24-P6 Analysis of short range phenomena in two novel materials using the PDF-method

Philipp Hans¹, Berthold Stöger¹, Nastaran Hayati-Roodbari², Paul Kautny³, Klaudia Hradil¹

1. X-ray center, Vienna UT

2. Materials science and physics, University of Salzburg

3. Institute for applied synthetic chemistry, Vienna UT

email: philipp.hans@tuwien.ac.at

In the present contribution the results of our radial distribution (RDF) studies on partial crystalline or amorphous materials will be presented. Radial distribution functions give information on the occurrence of all atom-to-atom distances in the substance. Out of the intensity of their maxima one can read out details on the number of distances, out of their widths their distance variations.

In one case the modelling of the structural disorder in silicon-nano-particles with intended application as novel battery anode materials is covered. As these studies are performed on powders, simulations have to take into consideration all effects originating from the particle-ensemble like the distribution of particle size and shape. Together with the data of small angle scattering (SAXS) measurements, models of those materials are presented.

The second class of compounds are host-materials for organic-light-emitting-diodes (OLEDs). Host materials are applied as amorphous films and a comparison of the PDFs of crystalline and amorphous structure gives insight into the structural changes due to amorphisation. It is assumed that torsions induced by sterically demanding groups are correlated with electronic properties.

Keywords: short range analysis, models of disorder, partially amorphous materials, diffuse scattering

MS24-P7 Investigating short-range order in transition-metal-bearing aluminosilicate garnets with ^{27}Al and ^{29}Si MAS-NMR spectroscopy: Using paramagnetic interactions to directly measure local atomic configurations

Aaron C. Palke¹, Charles A. Geiger², Jonathan F. Stebbins³

1. Gemological Institute of America, Carlsbad, CA 92008, USA
2. Department of Materials Science and Physics, Section Mineralogy, Salzburg University, A-5020 Salzburg, Austria
3. Department of Geological and Environmental Sciences, Stanford University, Stanford, CA 94305, USA

email: aaron.palke@gia.edu

The rich crystal chemistry of the garnet group is related to the presence of three crystallographic cation sites with different coordination environments into which a wide range of elements can substitute. Most natural silicate garnets with the general formula $\text{X}_3\text{Y}_2\text{Si}_3\text{O}_{12}$ are solid solutions and they are important phases in Earth's crust and upper mantle. Thus, an understanding of their thermodynamic properties is important for petrogenetic modeling, but very little is known about one of the key thermodynamic terms, the configurational entropy. This term is determined by cation order-disorder, which can be both long and short-range in nature.

We present ^{27}Al and ^{29}Si Magic Angle Spinning Nuclear Magnetic Resonance (MAS-NMR) spectra for a suite of natural and synthetic pyrope-rich ($\text{Mg}_3\text{Al}_2\text{Si}_3\text{O}_{12}$) and grossular-rich ($\text{Ca}_3\text{Al}_2\text{Si}_3\text{O}_{12}$) solid solutions containing the paramagnetic transition metals Fe^{2+} , Fe^{3+} , Cr^{3+} , and V^{3+} . The divalent cations can substitute at the X site and the trivalent cations at the Y site. The possibility of short-range order in the respective solid solutions is investigated.

The spectra show that paramagnetic interactions involving the unpaired electrons from Fe^{3+} and Cr^{3+} only lead to peak broadening and loss of resolution of the ^{27}Al and ^{29}Si resonances. On the other hand, peak broadening from paramagnetic Fe^{2+} and V^{3+} is less severe, but for these species new paramagnetically shifted peaks having relatively large frequency shifts from the central resonances can be observed. These peaks are caused by Fe^{2+} or V^{3+} located at X or Y sites, respectively, that are greater than 5 Å away from the ^{27}Al or ^{29}Si nucleus. Taken together, such paramagnetically shifted peaks can provide a greater level of information concerning local structure (order/disorder) due to the fact that these peaks are sensitive to variations in site occupancy up to four atomic bonds away from the NMR active nucleus. NMR measurements, therefore, have the potential to measure the presence/absence of short-range ordering in transition-metal-bearing garnets and also a wide range of other materials. The spectroscopic results could complement structural information obtained from diffuse scattering measured in diffraction experiments.

Keywords: short-range order, NMR spectroscopy, mineralogy, garnet

MS24-P8 Nanoparticle crystal formation by the solvent-assisted nanoparticle self-assembly probed *in situ* by the grazing-incidence small-angle X-ray scattering

Matej Jergel¹, Karol Vegso¹, Peter Šiffalovič¹, Eva Majková¹, Adeline Buffet², Stephan V. Roth²

1. Institute of Physics, Slovak Academy of Sciences, Dúbravská cesta 9, 845 11 Bratislava, Slovakia
2. HASYLAB, DESY, Notkestrasse 86, 22603 Hamburg, Germany

email: matej.jergel@savba.sk

The self-assembled two- and three-dimensional arrays of colloidal nanoparticles have been extensively studied in the last decade as promising structures for applications in nanophotonics, plasmonics, photovoltaics, biotechnology, sensors and other fields. As these arrays may be viewed as nanoparticle crystals, usual crystallographic concepts may be adopted for their analyses. The solvent-assisted self-assembly is a very attractive method for preparation of nanoparticle crystals because of its simplicity and possibility to obtain various symmetries such as hexagonal, rhombohedral, face-centered cubic or body-centered cubic depending on the external drying parameters. However, little is known about the self-assembly kinetics itself that gives a key to tailoring the structure and thereby properties of the nanoparticle crystal. We report on a time-resolved study of the nanoparticle self-assembly into a high-quality nanoparticle crystal with the face-centered cubic crystallographic symmetry. The grazing-incidence small-angle X-ray scattering (GISAXS) at MINAXS beamline of the high-brilliance synchrotron radiation source Petra III (DESY) was employed to track kinetics of the solvent evaporation driven self-assembly on casting a colloidal drop of plasmonic silver nanoparticles of 6 nm diameter on a silicon substrate. The short-range (cumulative) disorder typical for paracrystal structures before the complete solvent evaporation at 300-350 s after the drop casting was found with the exception of a time window of 125-150 s where a highly regular transient phase with the long-range order was observed. It is attributed to interaction between the organic surfactant shells of the neighboring nanoparticles (oleic acid and oleylamine) getting into contact in presence of the solvent residua (toluene) to the end of the solvent evaporation. This results in a larger nanoparticle hydrodynamic diameter with a smaller dispersion and thus temporary improvement of the crystallization. Such a behavior, that has never been observed before, has direct impact on the quality of the resulting nanoparticle crystal and tailoring its properties. The support of the projects APVV-0308-11 and VEGA 2/0004/15 is acknowledged.

Keywords: colloidal nanoparticles, nanoparticle self-assembly, nanoparticle crystal, paracrystal model, GISAXS

MS24-P9 Combined 3D- Δ PDF and Monte Carlo analysis of disorder in NaLaF₄

Ruggero Frison¹, Thomas Weber², Tara Michels-Clark³, Michal Chodkiewicz⁴, Anthony Linden¹, Hans-Beat Bürgi^{1,5}

1. Department of Chemistry, University of Zurich, CH-8057 Zurich Switzerland
2. Laboratory of Crystallography, Department of Materials, ETH Zurich, CH-8093 Zurich Switzerland
3. Lawrence Berkeley National Laboratory, Berkeley, CA 94720, USA
4. Biological and Chemical Research Centre, Department of Chemistry, University of Warsaw, Zwirki i Wigury 101, 02-089 Warszawa, Poland.
5. Department of Chemistry and Biochemistry, University of Bern, CH-3012 Bern Switzerland

email: ruggero.frison@uzh.ch

Many crystalline materials of scientific and technological interest possess disordered local structure arrangements that give rise to distinct diffuse scattering intensity. With the availability of high quality 3-D diffraction data and high performance computing infrastructures, detailed investigations of diffuse scattering data that were not possible only a few years ago are now within reach. From the 3-D data, the 3D-Difference Pair Distribution Function (3D- Δ PDF) can be calculated and the various types of disorder present in the structure identified and quantified in terms of an abstract model of interatomic vectors [1,2]. These results are extended by building and optimizing large Monte Carlo (MC) model crystals using parallelized algorithms [3,4]. Such MC simulations lead to a specific (and possibly improved) atomistic disorder model. NaLaF₄ was chosen for a case study; it is an efficient up-conversion phosphor [5] belonging to the family of rare earth-doped (Er³⁺, Yb³⁺) sodium lanthanide tetra fluorides [6]. Its distinctive, planar X-ray diffuse scattering was remeasured with synchrotron radiation at SNBL@ESRF, analyzed with the dual 3D- Δ PDF / MC approach and modeled in terms of occupational and positional disorder of the La, Na and F atoms. The final model along with possible alternative models will be discussed on the basis of our modeling strategy. We conclude that the dual modeling strategy provides an efficient procedure for the quantitative analysis of diffuse scattering data.

We thank Dr. Dmitry Chernyshov and the technical staff of SNBL@ESRF for their help during measurement.

[1] T. Weber and A. Simonov, *Zeit. für Krist.*, (2012) 227, 238-247.

[2] A. Simonov, T. Weber, and W. Steurer, *J. App. Cryst.* (2014) 47, 1146-1152.

[3] T. Weber and H.-B. Bürgi, *Acta Cryst. A*, (2002) 58, 526-540.

[4] T. M. Michels-Clark, V. E. Lynch, C. M. Hoffmann, J. Hauser, T. Weber, R. Harrison and H. B. Bürgi, *J. Appl. Cryst.* (2013) 46, 1616-1625.

[5] T. Kano, H. Yamamoto, Y. Otomo, *J. Electrochem. Soc.* (1972) 119, 1561-1564. J.F. Suyver, J. Grimm, K.W. Krämer, H.U. Güdel, *J. Lumin.* (2005) 114, 53-59. A.Sarakovskis, J. Grube, A. Mishnev, M. Springis, *Opt. Mat.* (2009) 31, 1517-1534.

[6] A. Aebischer, M. Hostettler, J. Hauser, K. Krämer, T. Weber, H.U. Güdel, H.B. Bürgi, *Angew. Chem. Int. Ed.* (2006) 45, 2802-2806.

Keywords: 3D-PDF, Monte Carlo modelling, Diffuse scattering, Computing

MS25. Magnetic structures

Chairs: Oksana Zaharko, Wiesława Sikora

MS25-P1 Tuning a cation distribution and microstructure of CoMn_2O_4 nanoparticles: structural and magnetic studies

Jasminka Popović¹, Marijana Jurić¹, Damir Pajić², Jelena Habjanić¹

1. Ruder Bošković Institute, Bijenička 54, 10000 Zagreb, Croatia
2. Department of Physics, Faculty of Science, University of Zagreb, Bijenička 32, 10000 Zagreb, Croatia

email: jpopovic@irb.hr

Complex metal oxides, especially one crystallizing in the spinel-type family AB_2O_4 , represent an important class of functional materials. Their unique chemical, electric, magnetic and mechanical properties have found versatile applications ranging from energy storage and conversion to magnetism, electronics and catalysis.¹⁻³ Majority of recent work on spinels appears to be strongly focused on electrochemical properties, while the structural and magnetic studies have been scarce in spite of few papers reporting on very intriguing and complex but still poorly understood magnetic behaviour.^{4,5}

In this study we have exploited the possibility of novel synthetic route to tune the structural and microstructural properties by simple alternations in preparation conditions,^{6,7} and to, furthermore, correlate these effects to magnetic behaviour. The samples were prepared by thermal decomposition of a heterometallic single-molecular precursor $\{[\text{Co}(\text{bpy})][\text{Mn}_2(\text{C}_2\text{O}_4)_2]\cdot\text{H}_2\text{O}\}$ (1) ($\text{bpy} = 2,2'$ -bipyridine) at $T = 500, 700, 800$ and 1000°C . The X-ray powder diffraction revealed increase in the unit-cell parameters of CoMn_2O_4 with the increase of formation temperature. This indicated on thermally induced increase of the inversion parameter within spinel lattice. Pronounced changes in the cation distribution, i.e. substitution of Co^{2+} by Mn^{3+} on the tetrahedral A site, and vice versa on the octahedral B site, were confirmed by the increase of octahedral $^{55}\text{Mn}-\text{O}$ and decrease of tetrahedral $^{59}\text{Co}-\text{O}$ bond distances. Crystal structure and graphical result of the final Rietveld refinement for the CoMn_2O_4 phase, heat treated at 800°C , is shown in Fig. 1. Increase of the applied decomposition temperature was reflected greatly on the magnetic behavior of CoMn_2O_4 , including the increase of hysteresis width, increase of blocking temperature and raised expression of the low temperature antiferromagnetic-like transition. Those effects could originate from the nano-particle growth and increased anisotropy due to change of the inversion, as well as from the rearrangement of interactions between the spins.

References: 1. Hemberger, J. et al., *Nature*, 2005, 434, 364. 2. Fan, H. J. et al., *Nature Mater.*, 2006, 5, 627. 3. Matsuda, M. et al., *Nature Phys.*, 2008, 3, 397. 4. Bordeneuve H. et al., *Solid State Sci.*, 2010, 12, 379. 5.

Zhang, H. T., Chen, X. H., *Nanotechnology*, 2006, 17, 1384. 6. Habjanić, J. et al., *Inorg. Chem.*, 2014, 53, 9633. 7. Popović, J. et al., *Cryst. Growth Des.*, 2013, 3, 2161.

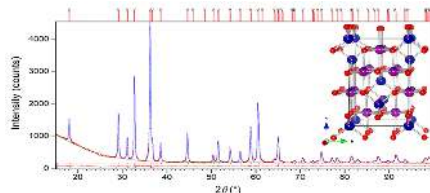


Figure 1. Graphical result of the final Rietveld refinement for the CoMn_2O_4 phase, obtained by heating compound 1 at 800°C . Inset: Crystal structure of CoMn_2O_4 .

Keywords: spinel structure, inversion parameter, magnetic properties

MS25-P2 Magnetic order and crystal structure of FeOCl described in superspace

Andreas Schönleber¹, Jian Zhang¹, Sander van Smaalen¹, Patrick G. Reuvekamp², Reinhard K. Kremer², Anatoliy Senyshyn³

1. Laboratory of Crystallography, University of Bayreuth, Bayreuth, Germany
2. Max Planck Institute for Solid State Research, Stuttgart, Germany
3. Forschungs-Neutronenquelle Heinz Maier-Leibnitz, FRM-II, Garching, Germany

email: andreas.schoenleber@uni-bayreuth.de

The metal(III) oxyhalide FeOCl crystallizes at room temperature in orthorhombic space group symmetry Pmmn. The structure is built by slabs consisting of Fe₂O₂ bilayers enclosed by layers of Cl atoms; the interaction between the slabs is of van der Waals type [1,2]. An antiferromagnetic phase transition was first observed by means of Mössbauer spectroscopy [3] and then confirmed by other techniques [4–6] while the reported values for TN are in the range of 80 – 92 K. Two different models for the magnetic superstructure are proposed, an incommensurate cycloidal one [4] and a commensurate spiral one [6]. Both models are based on orthorhombic symmetry.

We have performed low-temperature neutron powder diffraction experiments at instrument SPODI (FRM2, Garching, Germany) and low-temperature single crystal X-ray diffraction at beamline D3 (Hasylab/DESY, Hamburg, Germany) to explore and describe the magnetic and nuclear superstructures.

The analysis of our experiments shows that the magnetic phase transition occurs at TN = 82.0(2) K and is of second order, that the magnetic and structural modulation wave vector varies in an intermediate temperature range with temperature and that this transition is accompanied by the development of a monoclinic lattice distortion at low temperatures [5], indicating a strong magnetoelastic coupling. Those findings have been also reported for the other MOCl compounds VOCl and CrOCl [7,8]. In our contribution we will propose models for the magnetic and nuclear structures applying magnetic superspacegroup symmetry [9,10]

[1] S. Goldsztaub: C. R. Hebd. Seances Acad. Sci. 198 (1934) 667–669. [2] M. D. Lind: Acta Crystallogr. B 26 (1970) 1058–1062. [3] R. W. Grant: J. Appl. Phys. 42 (1971) 1619–1620. [4] A. Adam & G. Buisson: Phys. Stat. Sol. A 30 (1975) 323–329. [5] J. Zhang et al.: Phys. Rev. B 86 (2012) 134428. [6] S. R. Hwang et al.: Phys. Rev. B 62 (2000) 14157–14163. [7] A. Schönleber et al.: Phys. Rev. B 80 (2009) 064426. [8] J. Angelkort et al.: Phys. Rev. B 80 (2009) 144416. [9] V. Petříček, J. Fuksa & M. Dušek: Acta Crystallogr. A 66 (2010) 649–655. [10] J. M. Perez-Mato et al.: J. Phys.: Condens. Matter 24 (2012) 163201.

Keywords: magnetic order, modulated crystal; magnetoelastic coupling

MS25-P3 Occupation disorder in Mn₂Co_{1-x}Rh_xSn compounds

Vaclav Holy¹

1. Charles University in Prague

email: holy@mag.mff.cuni.cz

The structure of Mn₂CoSn is the Heusler cubic lattice A₂BC. Since Mn is more electropositive than Co, the basic structure of this compound is inverted, i.e. the Mn ions occur in both fcc lattices mutually shifted by one fourth of the body diagonal. We have investigated a series of Mn₂Co_{1-x}Rh_xSn polycrystalline samples by powder diffraction using CoK_α and CuK_α lines, and by EXAFS. From powder diffraction it follows that the structure undergoes a tetragonal distortion at approx. x=0.3. Several types of the occupation disorder in Heusler alloys exist in the literature; however some types can be excluded a-priori due to the absence of specific peaks in the powder diffraction patterns. We have determined the disorder type by fitting of the integrated diffraction intensities and of the EXAFS data to particular disorder models. The comparison of the measured and simulated EXAFS spectra demonstrated that the occupational disorder is a necessary feature, which must be considered in the analysis of EXAFS data, otherwise the fitting results are not physically feasible.

Keywords: Heusler alloys, occupation disorder, x-ray diffraction, EXAFS

MS25-P4 Thermal and magnetic anomalies of $\text{Mn}_{1-x}\text{Co}_x\text{Ge}$

Gleb A. Valkovskiy¹, Evgeniy V. Altynbaev^{1,2}, Maria D. Kuchugura^{1,2}, Ekaterina G. Yashina^{1,2}, Vadim A. Dyadkin³, Anatoly V. Tsvyashchenko⁴, Dmitry Chernyshov³, Sergey V. Grigoriev^{1,2}

1. Faculty of Physics, Saint Petersburg State University, 198504 Saint Petersburg, Russia

2. Petersburg Nuclear Physics Institute, Gatchina, 188300 Saint Petersburg, Russia

3. Swiss-Norwegian Beamlines at the ESRF, Grenoble 38000, France

4. Institute for High Pressure Physics, 142190, Troitsk, Moscow Region, Russia

email: Valkovskiy_Gleb@mail.ru

The helimagnets with chiral spin structure are interesting because of a wide range of unusual phenomena related to their magnetic ordering. An incomplete but representative list includes skyrmion structures, magnetostriction and magnetoresistance, coupling of structural and magnetic chiralities [1-5]; some of them may find application in the next generation spintronic devices. Besides well-known MnSi, this family includes MnGe, possessing a number of advantages, such as high transition temperature T_N of about 170 K (instead of ≈ 29 K in MnSi) and a large ordered Mn moment of about $1.8 \mu_B$ at 2 K (compared to $0.4 \mu_B$ at 2 K in MnSi) [6 - 8]. It was shown that MnGe has additional specific feature, namely a broad transition region from ordered helical phase to a disordered paramagnetic one, from T_N to $T_C \approx 270$ K [6 - 8]. The nature of the region is not yet entirely clear, in particular ferromagnetic nanoregions (~ 1 nm) were suggested to exist between T_N and T_C based on small angle neutron scattering data [6]. Here we report an anomaly in thermal expansion in the same region for MnGe and follow the evolution of thermal properties as a function of x in the series of $\text{Mn}_{1-x}\text{Co}_x\text{Ge}$ solid solutions, i.e. from the helimagnet MnGe to the diamagnet CoGe. Thermal expansion was studied by fitting the lattice parameter dependence on temperature based on synchrotron powder diffraction data in terms of the Debye model. The deviation from the Debye model increases with decreasing cobalt concentration, with the largest deviation for MnGe in the region between T_N and T_C . In particular, a negative increment to the linear thermal expansion coefficient was observed for MnGe in this temperature range. The reason for this effect is considered to be anomalous magnetic behavior.

Keywords: magnetostriction, powder diffraction

MS25-P5 Magnetic-crystallographic p , T -phase diagram of Fe_{1+x}Te : A high-pressure neutron diffraction study

Jens-Erik Jørgensen¹

1. Dept. of Chemistry, Aarhus University, DK-8000 Aarhus C, Denmark

email: jenserik@chem.au.dk

The crystal and magnetic structures of Fe_{1+x}Te for $x = 0.087$ and 0.141 have been studied by neutron powder diffraction in the temperature range from 5 to 170 K at pressures in the range from ≈ 0.8 to ≈ 7 GPa. The p , T -phase diagrams of the two Fe_{1+x}Te compounds contain three phases with monoclinic, orthorhombic and tetragonal symmetry. The tetragonal phase with space group $P4/nmm$ is stable at ambient conditions as well as at pressures. In the case of $\text{Fe}_{1.087}\text{Te}$ the monoclinic and orthorhombic phases are both antiferromagnetically ordered and stable at temperatures below ≈ 69 K while the non-magnetic tetragonal phase is stable above this temperature. The monoclinic phase is stable for $p \leq 1.2$ GPa while the orthorhombic phase is stable for $1.2 \leq p \leq 1.7$ GPa and the tetragonal phase becomes stable at higher pressures at the lowest measured temperatures. The p , T -phase diagrams of $\text{Fe}_{1.087}\text{Te}$ are shown in Fig. 1. $\text{Fe}_{1.141}\text{Te}$ shows the same type of p , T -phase diagram as $\text{Fe}_{1.087}\text{Te}$ although the stability range of the orthorhombic is larger, $0.8 \leq p \leq 2.3$ GPa. The magnetic ordering is antiferromagnetic bicollinear and commensurate with propagation vector $\mathbf{k} = (\frac{1}{2} \ 0 \ \frac{1}{2})$ in the monoclinic phase while it is incommensurate with propagation vector $\mathbf{k} = (\frac{1}{2} - \delta \ 0 \ \frac{1}{2})$ in the orthorhombic phase. The wave-length of the modulation of the magnetic structure of the orthorhombic phases was found to increase with pressure. The pressure-induced collapse of magnetic order at ≈ 1.7 GPa in the case of $\text{Fe}_{1.087}\text{Te}$ is accompanied by an abrupt change in volume and compressibility, suggestive of a spin state change of the Fe^{2+} ions in the FeTe layers. The observed abrupt change in volume and compressibility is presumably related to the earlier observed transition from the tetragonal to a collapsed tetragonal phase at ≈ 4 GPa at ambient temperature [1].

References: [1] J.-E. Jørgensen, J. Staun Olsen, L. Gerward, High Pressure Research 31, 603 (2011), [2] J.-E. Jørgensen, D. Sheptyakov, EPJB 86:18 (2013)

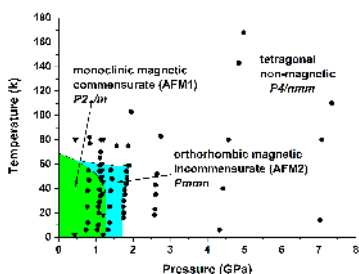


Figure 1. p,T -phase diagram of $\text{Fe}_{1.087}\text{Te}$. The tetragonal $P4/nmm$ phase is paramagnetic while the monoclinic $P2_1/m$ and the orthorhombic $Pmmn$ phases are magnetically ordered. Experimental data points are marked with ● (this work) and ▼ (Ref. 2).

Keywords: Magnetic structure, high-pressure, neutron diffraction

MS25-P6 Magnetic structures in complex materials revealed by resonant soft X-ray diffraction

Eugen Weschke¹, Schierle Enrico¹, Frano Alex², Keimer Bernhard²

1. Helmholtz-Zentrum für Materialien und Energie, Albert-Einstein-Str. 15, D-12489 Berlin, Germany

2. Max-Planck-Institut für Festkörperforschung, Heisenbergstrasse 1, D-70569 Stuttgart, Germany

email: eugen.weschke@helmholtz-berlin.de

With magnetic scattering factors as large as $200 r_0$ (classical electron radius) [1], x-ray diffraction using resonant photon energies in the soft x-ray regime provides particular sensitivity to magnetic ordering in transition metals by directly addressing the 3d or 4f electronic states. The corresponding wavelengths are of the order of 1 nm, yielding a rather small Ewald sphere. Notwithstanding, there are a number of important materials that can hardly be studied by other methods. From only one accessible magnetic Bragg peak detailed information about magnetic structures can be obtained, as discussed for a few examples.

Applied to a thin epitaxial film of the simple antiferromagnet EuTe, the method yields magnetic diffraction peaks that exhibit detailed Laue oscillations (Fig. 1). The temperature dependence of these profiles can be analyzed to obtain layer-resolved magnetization profiles [2].

Nickelate superlattices composed of layers of LaNiO_3 (LNO) and LaAlO_3 (LAO) or DyScO_3 (DSO) can be grown with excellent structural quality with varying substrate-induced strain. While bulk LNO is nonmagnetic, dimensionality-driven magnetic order was observed in the superlattices for nickelate layers of 2 unit cells thickness. In addition, by exploiting the polarization dependence of resonant magnetic scattering, strain-dependent spin-moment directions could be determined, paving a way for controlling magnetic order [3].

For bulk crystals of multiferroic DyMnO_3 , the availability of circular polarized x-rays in combination with the magnetic sensitivity at resonance could be used to determine the chirality of the magnetic structures that are intimately linked to the ferroelectric properties of the material [4].

References

- [1] J. Fink et al., *Resonant elastic soft x-ray diffraction*. Rep. Prog. Phys. **76**, 056502 (2013).
- [2] E. Schierle et al., *Antiferromagnetic Order with Atomic Layer Resolution in EuTe(111) Films*. Phys. Rev. Lett. **101**, 267202 (2008).
- [3] A. Frano et al., *Orbital Control of Non-collinear Magnetic Order in Nickel Oxide Heterostructures*. Phys. Rev. Lett. **111**, 106804 (2013).
- [4] E. Schierle et al., *Cycloidal order of 4f moments as a probe of chiral domains in DyMnO₃*. Phys. Rev. Lett. **105**, 167207 (2010).

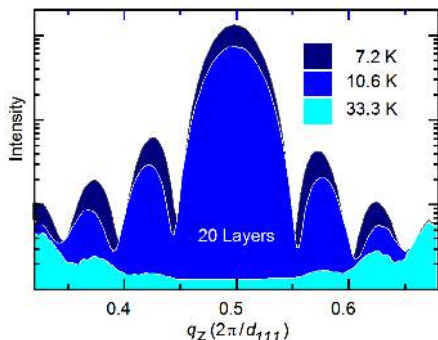


Figure 1. ($\frac{1}{2} \frac{1}{2} \frac{1}{2}$) magnetic diffraction peak recorded from 20 layers of EuTe at the Eu- M_2 resonance. The temperature-dependent Laue oscillations can be analyzed to provide the layer-resolved magnetizations of the film.

Keywords: Resonant x-ray scattering, transition metal oxides, thin films, heterostructures, multiferroics

MS25-P7 Antiferromagnetic ordering in selected TmTX (T = transition metal; X – p-electron element) intermetallics

Stanislaw Baran¹, Andrzej Szytula¹, Dariusz Kaczorowski², Anthony Arulraj³, Françoise Damay⁴, Andreas Hoser³, Boguslaw Penc¹

1. Marian Smoluchowski Institute of Physics, Jagiellonian University, ul. prof. Stanisława Łojasiewicza 11, PL-30-348 Kraków, Poland
2. Institute of Low Temperature and Structure Research, Polish Academy of Sciences, P. O. Box 1410, PL-50-950 Wrocław, Poland
3. Helmholtz-Zentrum Berlin für Materialien und Energie GmbH, Hahn-Meitner Platz 1, D-14-109 Berlin, Germany
4. Laboratoire Leon Brillouin, UMR 12, CEA-Saclay, CEA-CNRS, F-91191 Gif-sur-Yvette Cedex, France

email: stanislaw.baran@uj.edu.pl

Ternary intermetallics of general composition RTX (R – rare earth element; T = transition metal; X – p-electron element) are interesting group of compounds which draws researchers' interest for several decades. Among these compounds special concern is attracted to those crystallizing in the ZrNiAl-type structure. This hexagonal structure (space group P-62m) consists of layers containing rare earth atoms separated by layers consisting of two remaining elements. Within one layer the rare earth atoms form a distorted kagome lattice. Such a triangular arrangement of atoms having localized magnetic moments may lead to magnetic frustration in case of antiferromagnetic interactions.

In this study we report on physical properties of six thulium intermetallics crystallizing in the ZrNiAl-type structure, namely: TmTIn (T = Ni, Pt, Pd) and TmAgX (X = Si, Ge, Sn). The compounds have been investigated by means of magnetometric, heat capacity and electrical resistivity measurements. Their magnetic structures were derived from neutron diffraction data. All investigated compounds show antiferromagnetic ordering with Néel temperatures not exceeding 4.2 K. Among magnetic structures both the commensurate ones as well as incommensurate with crystal structure are found. Especially interesting is the case of magnetic structure in TmAgX (X = Si, Ge) where to each of three magnetic moments, present in the crystal unit cell, a different propagation vector is applied. Magnetic structure determination has been supported by a symmetry analysis.

Keywords: magnetic structure, neutron diffraction, rare earth intermetallics

MS25-P8 The substitution effect of chromium on the physicalproperties $\text{La}_{0.65}\text{Eu}_{0.05}\text{Sr}_{0.3}\text{Mn}_{1-x}\text{Cr}_x\text{O}_3$ nanocrystalline properties study of $\text{SrFe}_{12}\text{O}_{19}/\text{CoFe}_2\text{O}_4$ compositeMarwène Oumezzine¹, Mar García Hernández², Federico Mompeán², Mohamed Oumezzine¹

1. Laboratoire de Physico-chimie des Matériaux, Département de Physique, Faculté des Sciences de Monastir, Université de Monastir, 5019, Tunisia.

2. Instituto de Ciencia de Materiales, CSIC, Sor Juana Inés de la Cruz s/n, 28049 Madrid (Spain).

email: umezzine@hotmail.co.uk

Nanocrystalline powders of $\text{La}_{0.65}\text{Ba}_{0.33}\text{Mn}_{1-x}\text{Cr}_x\text{O}_3$ perovskites have been synthesized by the sol-gel method. X-ray diffraction along with the Rietveld-refinement shows the formation of pure crystalline phase with rhombohedral symmetry (space group R-3C, no. 167). Magnetic measurements indicate that the ferromagnetic double exchange interaction is weakened with increasing Cr concentration, resulting in a shift in T_C from 342K to 285K as x varied between 0 and 0.15. Furthermore, all samples undergo a paramagnetic (PM) - ferromagnetic (FM) phase transition at $T = T_C$. Based on the idea that doped manganites consist of ferromagnetic-metallic and paramagnetic-semiconducting (M-SC) regions coexisting in the same specimen, a good fit of the resistivity with the phenomenological percolation model, may be obtained by combining the contributions of the resistivity above and below T_{M-SC} by a single expression in the temperature region between 20 and 400K. We found that the estimated results are in good agreement with the obtained experimental data. The maximum magnetic entropy change (ΔS_M) and the relative cooling power (RCP) for the composition x=0.1 are found to be, respectively, 4.20 J kg⁻¹ K⁻¹ and 238 J kg⁻¹ for a 5-T field change, making of this material a promising candidate for magnetic refrigeration near room temperature. Arrott plot analyses and a universal curve method were applied to study the order of the magnetic transition in this system.

Keywords: Nanocrystalline manganites, Rietveld refinement, magnetic properties, modified sol-gel Pechini method

MS25-P9 Synthesis, structural characterisation, magnetic and dielectric

characterisation, magnetic and dielectric

characterisation, magnetic and dielectric

characterisation, magnetic and dielectric

characterisation, magnetic and dielectric

characterisation, magnetic and dielectric

characterisation, magnetic and dielectric

characterisation, magnetic and dielectric

characterisation, magnetic and dielectric

characterisation, magnetic and dielectric

characterisation, magnetic and dielectric

characterisation, magnetic and dielectric

characterisation, magnetic and dielectric

characterisation, magnetic and dielectric

characterisation, magnetic and dielectric

characterisation, magnetic and dielectric

characterisation, magnetic and dielectric

characterisation, magnetic and dielectric

characterisation, magnetic and dielectric

characterisation, magnetic and dielectric

characterisation, magnetic and dielectric

characterisation, magnetic and dielectric

characterisation, magnetic and dielectric

characterisation, magnetic and dielectric

characterisation, magnetic and dielectric

characterisation, magnetic and dielectric

characterisation, magnetic and dielectric

characterisation, magnetic and dielectric

characterisation, magnetic and dielectric

characterisation, magnetic and dielectric

characterisation, magnetic and dielectric

characterisation, magnetic and dielectric

characterisation, magnetic and dielectric

characterisation, magnetic and dielectric

characterisation, magnetic and dielectric

characterisation, magnetic and dielectric

characterisation, magnetic and dielectric

characterisation, magnetic and dielectric

characterisation, magnetic and dielectric

characterisation, magnetic and dielectric

characterisation, magnetic and dielectric

characterisation, magnetic and dielectric

characterisation, magnetic and dielectric

characterisation, magnetic and dielectric

characterisation, magnetic and dielectric

characterisation, magnetic and dielectric

characterisation, magnetic and dielectric

characterisation, magnetic and dielectric

characterisation, magnetic and dielectric

characterisation, magnetic and dielectric

characterisation, magnetic and dielectric

characterisation, magnetic and dielectric

characterisation, magnetic and dielectric

characterisation, magnetic and dielectric

characterisation, magnetic and dielectric

characterisation, magnetic and dielectric

characterisation, magnetic and dielectric

characterisation, magnetic and dielectric

characterisation, magnetic and dielectric

characterisation, magnetic and dielectric

characterisation, magnetic and dielectric

characterisation, magnetic and dielectric

characterisation, magnetic and dielectric

characterisation, magnetic and dielectric

characterisation, magnetic and dielectric

characterisation, magnetic and dielectric

characterisation, magnetic and dielectric

characterisation, magnetic and dielectric

characterisation, magnetic and dielectric

characterisation, magnetic and dielectric

characterisation, magnetic and dielectric

characterisation, magnetic and dielectric

characterisation, magnetic and dielectric

characterisation, magnetic and dielectric

characterisation, magnetic and dielectric

characterisation, magnetic and dielectric

characterisation, magnetic and dielectric

characterisation, magnetic and dielectric

characterisation, magnetic and dielectric

characterisation, magnetic and dielectric

characterisation, magnetic and dielectric

characterisation, magnetic and dielectric

characterisation, magnetic and dielectric

characterisation, magnetic and dielectric

characterisation, magnetic and dielectric

characterisation, magnetic and dielectric

characterisation, magnetic and dielectric

characterisation, magnetic and dielectric

characterisation, magnetic and dielectric

characterisation, magnetic and dielectric

characterisation, magnetic and dielectric

characterisation, magnetic and dielectric

characterisation, magnetic and dielectric

characterisation, magnetic and dielectric

characterisation, magnetic and dielectric

characterisation, magnetic and dielectric

characterisation, magnetic and dielectric

characterisation, magnetic and dielectric

characterisation, magnetic and dielectric

characterisation, magnetic and dielectric

characterisation, magnetic and dielectric

characterisation, magnetic and dielectric

characterisation, magnetic and dielectric

characterisation, magnetic and dielectric

characterisation, magnetic and dielectric

characterisation, magnetic and dielectric

characterisation, magnetic and dielectric

characterisation, magnetic and dielectric

characterisation, magnetic and dielectric

characterisation, magnetic and dielectric

characterisation, magnetic and dielectric

characterisation, magnetic and dielectric

characterisation, magnetic and dielectric

characterisation, magnetic and dielectric

characterisation, magnetic and dielectric

characterisation, magnetic and dielectric

characterisation, magnetic and dielectric

characterisation, magnetic and dielectric

characterisation, magnetic and dielectric

characterisation, magnetic and dielectric

characterisation, magnetic and dielectric

characterisation, magnetic and dielectric

characterisation, magnetic and dielectric

characterisation, magnetic and dielectric

characterisation, magnetic and dielectric

characterisation, magnetic and dielectric

characterisation, magnetic and dielectric

characterisation, magnetic and dielectric

characterisation, magnetic and dielectric

characterisation, magnetic and dielectric

characterisation, magnetic and dielectric

characterisation, magnetic and dielectric

characterisation, magnetic and dielectric

characterisation, magnetic and dielectric

characterisation, magnetic and dielectric

characterisation, magnetic and dielectric

characterisation, magnetic and dielectric

characterisation, magnetic and dielectric

characterisation, magnetic and dielectric

characterisation, magnetic and dielectric

characterisation, magnetic and dielectric

characterisation, magnetic and dielectric

characterisation, magnetic and dielectric

characterisation, magnetic and dielectric

characterisation, magnetic and dielectric

characterisation, magnetic and dielectric

characterisation, magnetic and dielectric

characterisation, magnetic and dielectric

characterisation, magnetic and dielectric

characterisation, magnetic and dielectric

characterisation, magnetic and dielectric

characterisation, magnetic and dielectric

characterisation, magnetic and dielectric

characterisation, magnetic and dielectric

characterisation, magnetic and dielectric

characterisation, magnetic and dielectric

characterisation, magnetic and dielectric

characterisation, magnetic and dielectric

characterisation, magnetic and dielectric

characterisation, magnetic and dielectric

characterisation, magnetic and dielectric

characterisation, magnetic and dielectric

characterisation, magnetic and dielectric

characterisation, magnetic and dielectric

characterisation, magnetic and dielectric

characterisation, magnetic and dielectric

characterisation, magnetic and dielectric

characterisation, magnetic and dielectric

characterisation, magnetic and dielectric

characterisation, magnetic and dielectric

characterisation, magnetic and dielectric

characterisation, magnetic and dielectric

characterisation, magnetic and dielectric

characterisation, magnetic and dielectric

characterisation, magnetic and dielectric

characterisation, magnetic and dielectric

characterisation, magnetic and dielectric

characterisation, magnetic and dielectric

characterisation, magnetic and dielectric

characterisation, magnetic and dielectric

characterisation, magnetic and dielectric

characterisation, magnetic and dielectric

characterisation, magnetic and dielectric

characterisation, magnetic and dielectric

characterisation, magnetic and dielectric

characterisation, magnetic and dielectric

characterisation, magnetic and dielectric

characterisation, magnetic and dielectric

characterisation, magnetic and dielectric

characterisation, magnetic and dielectric

characterisation, magnetic and dielectric

characterisation, magnetic and dielectric

characterisation, magnetic and dielectric

characterisation, magnetic and dielectric

characterisation, magnetic and dielectric

characterisation, magnetic and dielectric

characterisation, magnetic and dielectric

characterisation, magnetic and dielectric

characterisation, magnetic and dielectric

characterisation, magnetic and dielectric

characterisation, magnetic and dielectric

characterisation, magnetic and dielectric

characterisation, magnetic and dielectric

characterisation, magnetic and dielectric

characterisation, magnetic and dielectric

characterisation, magnetic and dielectric

characterisation, magnetic and dielectric

characterisation, magnetic and dielectric

characterisation, magnetic and dielectric

characterisation, magnetic and dielectric

characterisation, magnetic and dielectric

characterisation, magnetic and dielectric

characterisation, magnetic and dielectric

characterisation, magnetic and dielectric

characterisation, magnetic and dielectric

characterisation, magnetic and dielectric

characterisation, magnetic and dielectric

characterisation, magnetic and dielectric

characterisation, magnetic and dielectric

characterisation, magnetic and dielectric

characterisation, magnetic and dielectric

characterisation, magnetic and dielectric

characterisation, magnetic and dielectric

characterisation, magnetic and dielectric

characterisation, magnetic and dielectric

characterisation, magnetic and dielectric

characterisation, magnetic and dielectric

characterisation, magnetic and dielectric

characterisation, magnetic and dielectric

characterisation, magnetic and dielectric

characterisation, magnetic and dielectric

characterisation, magnetic and dielectric

characterisation, magnetic and dielectric

characterisation, magnetic and dielectric

characterisation, magnetic and dielectric

characterisation, magnetic and dielectric

characterisation, magnetic and dielectric

characterisation, magnetic and dielectric

characterisation, magnetic and dielectric

characterisation, magnetic and dielectric

characterisation, magnetic and dielectric

characterisation, magnetic and dielectric

characterisation, magnetic and dielectric

characterisation, magnetic and dielectric

characterisation, magnetic and dielectric

characterisation, magnetic and dielectric

characterisation, magnetic and dielectric

characterisation, magnetic and dielectric

characterisation, magnetic and dielectric

characterisation, magnetic and dielectric

characterisation, magnetic and dielectric

characterisation, magnetic and dielectric

characterisation, magnetic and dielectric

characterisation, magnetic and dielectric

characterisation, magnetic and dielectric

characterisation, magnetic and dielectric

characterisation, magnetic and dielectric

characterisation, magnetic and dielectric

characterisation, magnetic and dielectric

characterisation, magnetic and dielectric

characterisation, magnetic and dielectric

characterisation, magnetic and dielectric

characterisation, magnetic and dielectric

characterisation, magnetic and dielectric

characterisation, magnetic and dielectric

characterisation, magnetic and dielectric

characterisation, magnetic and dielectric

characterisation, magnetic and dielectric

characterisation, magnetic and dielectric

characterisation, magnetic and dielectric

characterisation, magnetic and dielectric

characterisation, magnetic and dielectric

characterisation, magnetic and dielectric

characterisation, magnetic and dielectric

characterisation, magnetic and dielectric

characterisation, magnetic and dielectric

characterisation, magnetic and dielectric

characterisation, magnetic and dielectric

characterisation, magnetic and dielectric

characterisation, magnetic and dielectric

characterisation, magnetic and dielectric

characterisation, magnetic and dielectric

characterisation, magnetic and dielectric

characterisation, magnetic and dielectric

characterisation, magnetic and dielectric

characterisation, magnetic and dielectric

characterisation, magnetic and dielectric

characterisation, magnetic and dielectric

characterisation, magnetic and dielectric

characterisation, magnetic and dielectric

MS25-P10 Magnetic and crystal structures of the multiferroic $\text{Ca}_2\text{CoSi}_2\text{O}_7$ melilite at low temperatures

Andrew Sazonov^{1,2}, Vladimir Hutanu^{1,2}, Martin Meven^{1,2}, Bálint Náfrádi³, István Kézsmárki⁴, Hiroshi Murakawa⁵, Yoshinori Tokura^{5,6,7}

1. Institute of Crystallography, RWTH Aachen University, Aachen, Germany
2. JCNS Outstation at MLZ, Garching, Germany
3. École Polytechnique Fédérale de Lausanne, Laboratory of Nanostructures and Novel Electronic Materials, Lausanne, Switzerland
4. Department of Physics, Budapest University of Technology and Economics and Condensed Matter Research Group of the Hungarian Academy of Sciences, Budapest, Hungary
5. Multiferroics Project, ERATO, Japan Science and Technology Agency (JST), University of Tokyo, Tokyo, Japan
6. Cross-Correlated Materials Research Group (CMRG) and Correlated Electron Research Group (CERG), RIKEN Advanced Science Institute, Wako, Japan
7. Department of Applied Physics and Quantum Phase Electronics Center (QPEC), University of Tokyo, Tokyo, Japan

email: mail@sazonov.org

The magnetic properties of $\text{Ca}_2\text{CoSi}_2\text{O}_7$ are often compared with those of other multiferroic compounds from the same family, such as $\text{Ba}_2\text{CoGe}_2\text{O}_7$. However, in contrast to $\text{Ba}_2\text{CoGe}_2\text{O}_7$, the crystal structure of $\text{Ca}_2\text{CoSi}_2\text{O}_7$ is described as a commensurate lock-in phase below approx. 150 K with a supercell tripled along the *a* and *b* axes related to the normal state above approx. 480 K. Thus, the magnetic structure of $\text{Ca}_2\text{CoSi}_2\text{O}_7$ is not necessarily the same as in other melilites. In order to characterise the magnetic order of $\text{Ca}_2\text{CoSi}_2\text{O}_7$, we performed a detailed crystallographic study at temperatures just above (10 K) and below (2.2 K) the antiferromagnetic phase transition (5.7 K) by neutron diffraction on single crystals. The results of the magnetic structure refinement are discussed and compared with those from $\text{Ba}_2\text{CoGe}_2\text{O}_7$.

Keywords: melilites, multiferroics, magnetic structure

MS25-P11 Theoretical study of complex relationships among chemical disorder, crystal stability, electronic and magnetic properties in Fe-based α -phases and high entropy alloys

Janusz Tobola¹, Jakub Cieslak¹, Stanislaw Kaprzyk¹

1. AGH University of Science and Technology, Faculty of Physics and Applied Computer Science, Al. Mickiewicza 30, 30-059 Krakow, Poland

email: tobola@ftj.agh.edu.pl

Nowadays, *ab initio* calculations are well-adapted tools to investigate microscopic reasons for appearance of specific physical behaviours in ordered compounds and disordered alloys. The charge- and spin-selfconsistent Green function Korringa-Kohn-Rostoker method belongs to the well-established techniques to determine electronic band structure and relevant physical quantities such as density of states, magnetic moments, magnetic structure, hyperfine fields and total energy. Besides, the KKR combined with the coherent potential approximation (CPA) [1] allows for reliable treatment of chemical disorder in complex multicomponent systems [2].

In this work, the KKR-CPA methodology is applied to study two different groups of materials:

(i) Fe-based σ -compounds (space group P42/mnm), which belongs to the famous Frank-Kasper phases, are characterised by high coordination numbers and lack of stoichiometry. Their topological and chemical complexity appears to determine particular relations among crystal stability, electronic structure features as well as magnetic properties and hyperfine interactions. Recent results of KKR-CPA calculations on Fe-*M* (*M*= V, Cr, Mo, W) [2-4] σ -phases will be presented in view of magnetisation, neutron diffraction and Mossbauer data.

(ii) High entropy alloys (HEA), which consist of at least five transition metal elements (sometimes also s, p element) with almost equal concentrations, crystallize in surprisingly simple structures (bcc, fcc or hcp). On the whole, the crystal stability of these highly disordered systems appear to be driven essentially by configuration entropy, but also by the magnetic entropy. Besides, the chemical disorder strongly affects the electronic and magnetic properties of HEA as well as the preference of the crystal structure (bcc vs. fcc). The KKR-CPA results obtained for the $\text{Al}_x\text{CrFeNiCo}$ [5] and PdCrFeNiCo HEA will be discussed in view of XRD and magnetisation data.

This work is supported by the National Science Center (NCN) in Poland (Grant DEC-2012/05/B/ST3/03241).

References:

- [1] A. Bansil, S. Kaprzyk, P. E. Mijnenarens, and J. Tobola, *Phys. Rev. B* 60, 13396 (1999).
- [2] J. Cieslak, J. Tobola, S. M. Dubiel, and W. Sikora, *Phys. Rev. B* 82, 224407 (2010).

[3] J. Cieslak, S. M. Dubiel, J. Tobola, *J. Phys. Chem. Sol.* 74, 1303 (2013).

[4] J. Cieslak, S. M. Dubiel, M. Reissner, J. Tobola, *J. App. Phys.* 116, 183902 (2014).

[5] K. Jasiewicz, J. Cieslak, J. Tobola, submitted to *J. Alloys Comps.* (2015).

Keywords: ab initio calculation, electronic structure, phase stability, magnetic properties, chemical disorder

MS26. Modulated, modular and composite materials

Chairs: Luis Elcoro, John Claridge

MS26-P1 Systematical study of the structure of Ni₂MnGa single crystals by high-resolution x-ray diffraction reciprocal space mapping

Petr Cejpek¹, Václav Holý¹, Oleg Heczko²

1. Charles University in Prague, Faculty of Mathematics and Physics, Ke Karlovu 3, 121 16, Prague 2

2. Institute of Physics of the Academy of Sciences in Prague, Na Slovance 1999/2, 182 21, Prague 8

email: petr.cejpek@centrum.cz

Ni₂MnGa is nominally cubic, however small deviations from exact 2:1:1 stoichiometry give rise to structural changes, leading to tetragonal or even monoclinic lattices. Up to now, the structure of Ni₂MnGa has been studied mostly by means of powder diffraction; in our work we performed a detailed study of the structure of Ni₂MnGa single crystals using high-resolution x-ray diffraction and reciprocal space mapping. Our samples were found monoclinic at room temperature and they exhibit large twinning domains detected from splitting of diffraction peaks in reciprocal space. Moreover, we found distinct satellite peaks at non-integer HKL positions demonstrating that the lattice structure is self-modulated along [110]. This modulation can be described by a harmonic displacement wave, the coefficients of which have been obtained from a numerical analysis of the integrated intensities of the satellite peaks. We performed an annealing study and found martensitic (monoclinic)/austenitic(cubic) phase transition at approx. 60°C with the hysteresis of about 10°C; the twinning and modulation peaks disappeared in the cubic (high-temperature) phase.

Keywords: shape memory alloy, reciprocal space mapping, twinning, modulated structure, high-temperature diffraction

MS27. Electron crystallography methods

Chairs: Alex Eggeman, Lukáš Palatinus

MS27-P1 Pair distribution function analysis of amorphous compounds using TEM electron diffraction

Partha P. Das^{1,2}, Mauro Gemmi³, Chaoren Liu⁴, Jorge E. Velasco⁴, Daniel Crespo⁴, Stavros Nicolopoulos¹

1. NanoMEGAS SPRL, Brussels, Belgium

2. Electron Crystallography Solutions, Madrid, Spain

3. Center for Nanotechnology Innovation @NEST, Istituto Italiano di Tecnologia, Pisa, Italy

4. Department of Physics & CRNE, Universitat Politècnica de Catalunya-BarcelonaTECH, Spain

email: partha@ecrystalsolutions.com

It is known that in amorphous materials crystalline order exists only at short range and conventional X-Ray diffraction does not bring immediate structural information as no diffraction Bragg peaks or sharp rings are present. Pair distribution function analysis (PDF) from total scattering experiments can be used to understand the type short range order present in these types of compounds; this can be done usually with conventional Mo/Ag X-Ray diffraction (however is time consuming as it may take up to 24 hours per sample) or using Synchrotron facilities. As an alternative, PDF analysis based on electron diffraction (ED) in any transmission electron microscope (TEM) can be used to study local order. The main advantages of using ED for PDF analysis is the very quick data acquisition time (from few msec to 2-3 minutes per ED pattern) and possibility of probing small nm size areas.

In this work two different types of samples were studied: 1) a metallic glass material with composition Pd_{42.5}Ni_{7.5}Cu₃₀P₂₀ to understand possible non-homogeneity in the material by scanning different areas of the sample 2) Honduras Opal amorphous sample to understand local ordering.

Data were collected using a 120 kV Zeiss Libra TEM microscope with 2k x 2k TMS CCD camera. Since it is important for reliable PDF analysis to have good quality data at high Q range, in order to increase the dynamic range of the experimental ED data and to increase counting statistics, several ED patterns were collected from the same area and were further summed up. PDF patterns were obtained after normalization and Fourier transformation using the software PDFGetEGui.

For the amorphous glass Pd_{42.5}Ni_{7.5}Cu₃₀P₂₀ sample, after collecting several ED PDF patterns at different positions intervals (every 200 nm) a change of individual PDF peak positions was observed, which could be possibly ascribed to inhomogeneity of the sample.

For the Honduras Opal mineral sample, ED PDF analysis reveals clearly the existence of short range order (up to 7 Å). Distances (which correspond to different atom bondings) of main PDF peak positions are very close to characteristic interatomic distances of SiO₂ structure.

For both cases structure modeling is underway to fully describe the structural environment in short range.

References:

Anstis, G. R., Liu, Z., Lake, M., Ultramicroscopy 1988, 26, 65-70

Abeykoon, M., Malliakas, C. D., Juhás, P., Božin, E. S., Kanatzidis, M. G., Billinge, S. J. L., Z Krist 2012, 227, 248-256

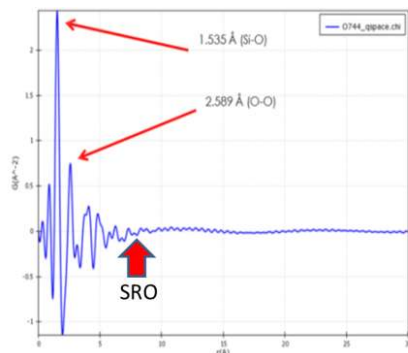


Figure 1. Pair distribution function as obtained from honduras opal data

Keywords: Electron Diffraction, Transmission Electron Microscopy, Amorphous Material, Pair Distribution Function

MS27-P2 Indexing electron diffraction patterns from randomly-oriented crystals

Yunchen Wang¹, Wei Wan¹, Xiaodong Zou¹

¹. Berzelii Center EXSELENT on Porous Materials and Inorganic and Structural Chemistry, Department of Materials and Environmental Chemistry, Stockholm University, SE-106 91 Stockholm

email: yunchen.wang@mmk.su.se

Electron diffraction (ED) can be used to study nanometre-sized crystals and provides information about the unit cell, space group and even intensities for a complete structure solution. With a known unit cell, ED patterns can be indexed. The reflection indices are found after indexing and the reflection conditions can be used to derive the space group. Indexing is usually done with in-zone ED patterns from aligned crystals. Alignment of the crystal can be time consuming and for many electron beam sensitive materials it is very difficult, even impossible. Indexing ED patterns from randomly orientated crystals is thus necessary and it gives valuable information about the phase of the material and the space group. The orientation of the crystal can be determined and quantitative intensities of the reflections extracted for structure solution. Similar problem has been studied in femtosecond X-ray crystallography using X-ray free electron laser [1]. However the algorithms cannot be adopted for electron data due to the differences in wavelengths. Here we propose a fast and robust approach for indexing ED patterns from randomly orientated crystals, given the unit cell parameters. Rather than measuring the d^* values and mutual angles of the reflection vectors and matching them to the calculated values, we use instead the “difference vectors”, which are obtained by subtracting the 2D coordinates of pairs of diffraction spots. Difference vectors typically have shorter d^* values than the original reflection vectors and are thus easier to index (less ambiguity). Zone axes given by the difference vectors are close to the actual zone axes along which the ED patterns are taken. They can be used to quickly narrow down the solution for indexing all the reflections in the ED pattern. The algorithm has been tested with the frames of a 3D ED dataset from zeolite silicalite-1 (unit cell: $a = 20.090 \text{ \AA}$, $b = 19.738 \text{ \AA}$, $c = 13.142 \text{ \AA}$, space group: $Pnma$).

[1] H. N. Chapman, et al., Nature **470**, 73(2011)

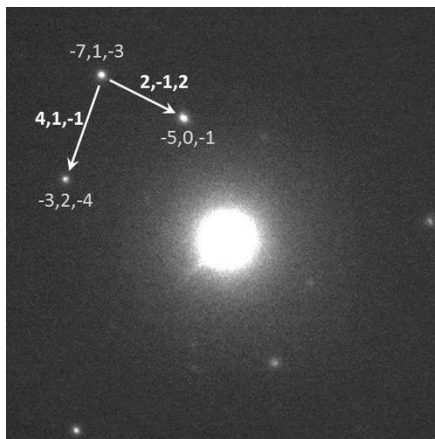


Figure 1. Illustration of the “difference vector” approach for indexing ED patterns from randomly orientated crystals. The ED pattern was taken from a zeolite silicalite-1 crystal in a random orientation. Three reflections generate difference vectors which are of lower resolution and easier to index.

Keywords: electron diffraction, indexing, random, crystallography

MS27-P3 Phase identification and structure determination of crystallites in multiphase powder samples by rotation electron diffraction

Wei Wan^{1,2}, Yifeng Yun^{1,2}, Faiz Rabbani², Jie Su^{1,2}, Hongyi Xu^{1,2},
Sven Hovmöller^{1,2}, Mats Johansson², Xiaodong Zou^{1,2}

1. Berzelii Center EXSELENT on Porous Materials, Stockholm University, SE-10691 Stockholm, Sweden
2. Inorganic and Structural Chemistry, Department of Materials and Environmental Chemistry, Stockholm University, SE-10691 Stockholm, Sweden

email: wei.wan@mmk.su.se

Phase identification and structure determination of submicrometre-sized crystals are important in materials science and crystallography. The most widely used technique for these purposes is powder X-ray diffraction (PXRD). However, the use of PXRD is limited in multiphase samples, especially those containing unknown phases. Electron crystallography has proven a promising alternative for studying individual phases in multiphase crystalline samples containing submicrometre-sized particles. The recently developed rotation electron diffraction (RED) method can be used to collect complete three-dimensional electron diffraction (ED) data from single crystals of submicrometre-sizes in a transmission electron microscope [1,2]. The unit cells and space groups of the crystals can be easily determined and the atomic structures can be solved *ab initio* and refined against the ED data or PXRD data. Here we show a case where RED made it possible to identify as many as four distinct compounds within one sample containing submicrometre-sized crystals in a Ni–Se–O–Cl system [3].

PXRD patterns of the sample could not be indexed using existing known phases (Fig. 1a). Four RED datasets were collected from four crystals with different morphologies and processed using the RED data processing software [2] (Fig. 1b–e). The unit cells were determined and the reflections were indexed. The reflection intensities were extracted and could be used to solve the structures of all four compounds by direct methods using SHELX [4] (Fig. 1f–i). One of the structures was later found in the ICSD database. One of the unknown compound was iso-structural to a known Co–Se–Cl–O phase. The other two structures were new. Nearly all peaks in the PXRD pattern could be indexed using the four phases and the structure models obtained from the RED data were confirmed by Rietveld refinement against the PXRD data.

References

- [1] Zhang, D., Oleynikov, P., Hovmöller, S. & Zou, X.D. (2010). *Z. Kristallogr.* 225, 94.
- [2] Wan, W., Sun, J., Su, J., Hovmöller, S. & Zou, X.D. (2013). *J. Appl. Cryst.* 46, 1863.
- [3] Yun, Y.F., Wan, W., Rabbani, F., Su, J., Xu, H.Y., Hovmöller, S., Johansson, M. & Zou, X.D. (2014). *J. Appl. Cryst.* 47, 2048.
- [4] Sheldrick, G. M. (2008). *Acta Cryst.* A64, 112.

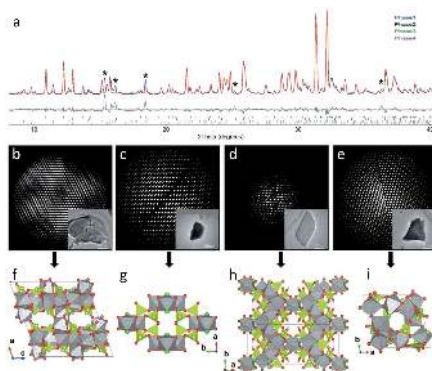


Figure 1. (a) Rietveld refinement against the PXRD pattern using the four phases determined from the RED data. (b)–(e) Reconstructed 3D reciprocal lattices of the four phases with the TEM images inserted. Scale bar = 200 nm. (f)–(i) Structure models of the four phases.

Keywords: electron diffraction, phase identification, structure solution

MS27-P4 Optimization of rotation electron diffraction data collection and data processing

Magdalena O. Cichocka¹, Jie Su¹, Wei Wan¹, Xiaodong Zou¹

¹. Inorganic and Structural Chemistry and Berzelii Centre EXSELENT on Porous Materials, Department of Materials and Environmental Chemistry, Stockholm University, SE-106 91 Stockholm, Sweden

email: magdalena.cichocka@mmk.su.se

Electron crystallography is a very powerful technique for structural analysis of nano- and micron-sized crystals [1]. We have developed rotation electron diffraction (RED) for automated collection and processing of 3D ED data [2]. More than 1000 ED frames can be collected from an arbitrarily oriented crystal in less than an hour by RED (Fig. 1). The unit cell, possible space groups and ED intensities can be obtained. The 3D ED methods have shown to be very powerful and efficient for phase identification and structure determination [3,4]. Now an unknown structure can be solved in less than 8 h, from the data collection to structure solution. Although it is possible to solve the structures from the RED data, the R-values are still very high (20-50%). The ED intensities are affected by absorption and multiple scattering. Radiation damage is also a limiting factor [5], which may lead to low resolution and incomplete data, as well as inaccurate intensities.

Here we show how different data collection parameters of the RED method can affect the determination of unit cell, space group, and the accuracy of the atomic positions. The calcined zeolite silicalite-1, which is a pure silica form of the MFI framework family, was chosen as an example to optimize the parameters of RED method on structure analysis of zeolites [6].

Accurate unit cell parameters could be obtained with a large tilt range. For normal unit cell determination, a large tilt step can be applied. On the other hand, for structure determination a small tilt step is preferred, as the intensities would be more accurate due to the fine sampling. The tilt step can affect intensities of the reflections, which cause inaccurate atomic positions and high R-values in the refinement. The resolution of RED data can also affect the refinement result and atomic positions. We will present how to optimize the data processing to obtain better ED intensities.

[1] X. Zou, S. Hovmöller, P. Oleynikov, *Electron Crystallography*, IUCr texts on crystallography, Oxford University Press, 2011.

[2] W. Wan, J. Sun, J. Su, S. Hovmöller, X. Zou, *J. Appl. Cryst.* 2013, 46, 1863.

[3] J. Su, W. Wan, J. Sun, S. Hovmöller, X. Zou, *Micropor. Mesopor. Mater.* 2014, 189, 115.

[4] T. Willhammar, X. Zou, et al., *J. Am. Chem. Soc.* 2014, 136, 13570.

[5] R. Martinez-Franco et al., *Proc. Natl. Acad. Sci. U. S. A.* 2013, 110, 3749.

[6] C. Nave, *Radiat. Phys. Chem.* 1995, 45, 483.

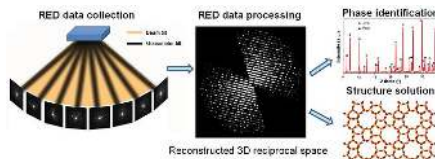


Figure 1. Illustration of a complete structure solution from Rotation Electron Diffraction (RED) data.

Keywords: 3D electron diffraction, structure determination, structure solution, zeolite

MS27-P5 Accurate structure refinement of thin films using 3D electron diffraction data

Gwladys Steciuk¹, Lukas Palatinus², Philippe Boullay¹, Adrian David¹, Morgane Lacotte¹, Olivier Copie¹, Wilfrid Prellier¹,
Hélène Rotella¹

1. CRISMAT, CNRS UMR 6508, 6 Bd du Maréchal JUIN 14050 CAEN Cedex, France
2. Institute of Physics of the AS CR, v.v.i. Na Slovance 2, 182 21 Prague, Czechia

email: gwladys.steciuk@ensicaen.fr

2D nanostructures emerge as one leading topic in fundamental materials science where transition metal oxides appear as promising candidates because of their strong interplay between charge, spin, orbital and lattice. Low distortions or size effects due to substrate strain and reduced dimension of the film could induce drastic changes in the observed properties between a thin film material and its bulk analogous. In most cases, the challenge for thin film materials is not to solve the structure, which is generally known, but the structure analysis should be accurate enough to account for these small variations.

Regarding the data collection, Precession Electron Diffraction Tomography (PEDT) aims to collect a series of randomly oriented diffraction patterns at a fixed angular interval. It is similar to the phi-scan data collection used in single crystal X-ray diffraction (XRD) but applicable to objects of a few tens of nanometers. Not limited by the geometry of the sample, the PEDT data collection allowed to access a much larger number of reflections than one would ever obtain using reciprocal space maps acquired with a high-resolution diffractometer [1]. Still, unlike the case of XRD, the kinematical theory of diffraction is not valid for electrons. By limiting the paths for multiple scattering, PEDT allows to reduce dynamical effects but not enough to consider PEDT data as kinematical. To tackle this problem, the recent implementation of refinements based on the dynamical diffraction theory in JANA2006 [2] is very promising.

In this contribution, we will present our first results on the use of the dynamical diffraction theory for the accurate structure refinement of perovskite related compounds from PEDT data. First, the result of the structure refinement considering the kinematical approximation and the dynamical theory will be presented for PrVO_3 , a compound with a distorted perovskite structure. The results obtained for bulk- PrVO_3 will be compared against the solution from neutron diffraction illustrating the gain of reliability achieved using the dynamical theory. Second, we will use and discuss the interest and limitation of this new crystallographic tool to refine the structure of perovskite related thin films.

[1] H. Rotella, et al, *J. Phys.: Condens. Matter* 27 (2015) 175001.

[2] L. Palatinus et al, *Acta Cryst. A* 71 (2015) 235.

Keywords: precession electron diffraction tomography, structure refinement, thin film

MS27-P6 Electron crystallography of 3D nano-crystals

Max T.B. Clabbers¹, Eric van Genderen¹, Igor Nederlof^{1,2},
Yao-Wang Li¹, Jan Pieter Abrahams¹

1. Leiden University, Biophysical Structural Chemistry, Einsteinweg 55, 2333CC Leiden, The Netherlands
2. Amsterdam Scientific Instruments, Science Park 105, 1098XG Amsterdam, The Netherlands

email: clabbersm@gmail.com

Many proteins do not form crystals large enough and of sufficient quality for 3D structure determination by X-ray crystallography. For such sub-micron sized 3D crystals there are several alternatives: intense XFEL sources, electron imaging and electron diffraction. Solving new structures using these approaches remains a problem as ab-initio crystal phasing is hampered by experimental constraints that severely compromise data quality. These constraints include incomplete sampling of Bragg spots and (for electron diffraction), dynamic and inelastic scattering.

In case of electron diffraction, complete sampling of Bragg spacings can be achieved with a fast Timepix quantum area detector. This detector is of unprecedented sensitivity and combined with continuous crystal rotation electron diffraction data can be collected under low dose conditions. From a single frozen lysozyme nano-crystal of only 200 nm thin a rotation series of 40 degrees was collected with very fine slicing showing diffraction up to 2 Å resolution. Furthermore, in case of small pharmaceutical compounds, a complete dataset could be collected at room temperature from nano-crystals of only 200 nm thin showing Bragg spots up to 0.8 Å resolution. Phasing and structure solution for these pharmaceuticals was possible using direct methods yielding a structural model at atomic resolution.

Ab-initio phase information can be measured directly by electron imaging of protein nano-crystals. This experimental approach allows enhancing the resolution of electron images of 3D nano-crystals to beyond 2 Å including crystal phases, by separating mosaic blocks within nano-crystals through image processing.

Keywords: Electron crystallography, nano-crystals, quantum area detector

MS27-P7 Dynamically refined PEDT of Ni₂Si compared to XRD

Cinthia A. Corrêa^{1,2}, Mariana Klementová², Lukáš Palatinus²

1. Department of Physics of Materials, Charles University Prague
2. Institute of Physics, Academy of Sciences of the Czech Republic

email: cinthiac@gmail.com

Electron diffraction tomography (EDT) [1] combined with the precession electron diffraction (PED) [2] are ideal techniques for structural analysis of single nanocrystals. The strong interaction between electrons and matter, compared to X-ray, allows structural analysis of nanocrystals as small as tens of nanometers. During the EDT experiment, the crystal is tilted in small steps and a diffraction pattern is collected for each position, giving three-dimensional information of the reciprocal space. However, the strong interaction between the electron beam and matter generates multiple scattering of the beam and the accurate structure refinement requires the use of the dynamical diffraction theory for the calculation of model intensities. The dynamical character of the reflections can be suppressed by using PED. The technique consists of precessing the beam around the optical axis of the microscope, where the resulting intensities are integrated for each angular position of the beam. These integrated intensities are more sensitive to structure parameters and less sensitive to crystal imperfections. Despite of the damping of the dynamical effects, the refinement against precession EDT (PEDT) data using kinematical diffraction theory gives low accuracy of the structure parameters and high residual factors. The dynamical refinement for EDT data sets was implemented recently [3] and has been shown to be superior to the kinematical refinement, giving lower figures of merit and higher accuracy of the structure parameters. In this work, the dynamical refinement is used for the structure analysis of a nanowire of Ni₂Si with the diameter of 16 nm. The dynamical refinement against a data set collected by PEDT is compared to kinematical refinement and to a reference structure, obtained by single crystal X-ray diffraction. The structure has orthorhombic *Pnma* symmetry with 3 independent atoms. It is shown that the single crystal X-ray structure and the PEDT structure match very well with an average distance of atomic positions less than 0.015 Å.

[1] Kolb, U., Gorelik, T., Kuebel, C., Otten, M.T., Hubert, D. (2007). *Ultramicroscopy* **107** (6-7), 507-513

[2] Vincent, R., Midgley, P.A. (1994). *Ultramicroscopy* **53** (3), 271-282. Mugnaioli, E., Gorelik, T., Kolb, U. (2009). *Ultramicroscopy* **109** (6), 758-765

[3] Palatinus, L., Petříček, V., Corrêa, C.A. (2015). *Acta Crystallographica A* **71**, 235-244

This work is financially supported by the Czech Science Foundation, project 13-25747S.

Keywords: Nanocrystal, precession electron diffraction tomography, dynamical refinement, X-ray.

MS27-P8 Machine learning decomposition of scanning precession electron diffraction data

Duncan N. Johnstone¹, Alexander S. Eggeman¹, Paul A. Midgley¹

1. Department of Materials Science & Metallurgy, University of Cambridge, UK

email: dnj23@cam.ac.uk

Scanning precession electron diffraction (SPED) is being developed to map the crystalline phases in materials with nm resolution and across micron sized regions. Precession electron diffraction (PED) patterns are recorded using a double conical rocking beam system [1] as the electron beam is scanned across the sample [2]. The 4-dimensional (two real & two reciprocal) data set can be analysed in a number of ways. Most simply, 'virtual' dark-field images can be formed by plotting the intensity of a diffracted beam (sub-set of pixels) as a function of beam position. Each PED pattern can also be matched to a library of simulated patterns, determining the orientation and producing orientation images, typically as Euler angle maps [2]. This analysis is hindered by 'artefacts' such as specimen bending and thickness variations, the effect of which can be reduced by utilising larger precession angles. The remaining challenge that we address is the appropriate treatment of diffraction patterns that comprise signals from overlapping crystals.

We apply machine learning approaches based on non-negative matrix factorisation (NMF) and principal component analysis (PCA) combined with independent component analysis (ICA) in order to learn the underlying 'component patterns', that make up the data, together with their associated 'loadings' at each real space pixel. An example of such decomposition is shown in the figure below. Loading maps indicate the region where the component pattern is significant and resembles a simplified dark-field image. Loading maps corresponding to different component patterns may have overlapping regions of intensity where mixed diffraction patterns have been separated into individual components. This decomposition is the key to performing 3D volume reconstructions with crystallographic information at each voxel [3]. Here we report on the development of this approach by evaluating the decomposition of PED data systematically using a number of algorithms. In particular, results are presented demonstrating the merits of sparsity and non-negativity constraints imposed on the aforementioned decompositions. Twin boundaries in GaAs nanowires were used as a test case to validate the methods, which have then been applied to a number of more complex cases.

[1] R Vincent, and P A Midgley, *Ultramicroscopy*, 1994, 53, 271-282

[2] E Rauch et al, *Zeitschrift für Kristallographie* 2010, 225, 103-109

[3] A S Eggeman, R Krakow, and P A Midgley, submitted

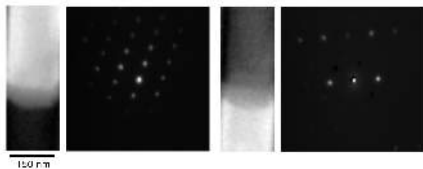


Figure 1. Component patterns with their spatial loadings across an inclined twin boundary in a GaAs nanowire decomposed from scanning precession electron diffraction data by using non-negative matrix factorisation. Overlapping bright regions in loading maps indicate where mixed patterns were separated.

Keywords: Orientation Imaging, Crystallographic Mapping, Precession Electron Diffraction, Machine Learning, Multivariate Statistical Analysis

MS27-P9 Enhanced technique for characterization of strain distribution in crystal from EBSD patterns

Vadym Khomenko¹

1. Yuriy Fedkovych Chernivtsi National University, Chernivtsi, Ukraine

email: primaldarkness@mail.ru

Electron backscattering diffraction method (Kikuchi method) is used for determination of crystal orientation, phase, strain and stress state of crystals. Elastic strains caused by the distortion of crystal structure change the interplanar distances [1]. The last ones reveal themselves in the changing of intensity distribution onto the Kikuchi pattern to have been measured. Due to the high spatial resolution and high locality the EBSD method can be used for studying of highly inhomogeneous samples. Weld joints of NiCrFe and artificial diamond crystals are these kinds of materials. Kikuchi patterns were obtained by using scanning electron microscope "Zeiss" Evo-50 with CCD detector

The enhanced technique which combines two-dimensional Fourier transformation of Kikuchi pattern as whole and analysis of intensity profiles of separate Kikuchi bands was developed. The strain tensor determination was performed using the new approach which is based onto the local cross-correlation of intensity peaks of multi-beam areas.

Approbation of developed technique was carried out on two diamonds samples: one of them was obtained by temperature gradient method in Fe–Al–C system and second – in Mg–C+bor system by growth method on diamond single crystal synthesized in Ni–Mn–C system. As a result characteristic surfaces of strain tensor were constructed for local areas, which correspond to different crystalline blocks (Fig. 1).

Next, the samples of weld joint of NiCrFe nickel alloy with crack have been researched for the purpose of establishment of probable causes of crack formation. In addition to Kikuchi patterns the distribution of chemical composition was obtained by means of X-ray microanalysis. The features of strain distribution around crack were established. Particularly, it was demonstrated that maximal strain values are spreaded along the low angle boundaries of subgrains.

1. Fodchuk I. Determination of structural inhomogeneity of synthesized diamonds by backscattering electron diffraction / I.Fodchuk, S. Balovskyak, M. Borch, Ya. Garabazhiv, V. Tkach // Phys. Status Solidi A. – 2011. – Vol. 208, № 11. – P. 2591–2596.

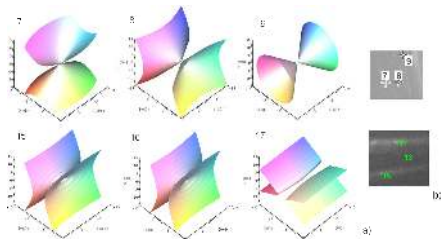


Figure 1. Characteristic surfaces of strain tensor (a), which corresponds to different local areas (labeled by numbers) of diamond crystal (b)

Keywords: EBSD, strain measurement, strain tensor, diamond crystals, weld joints

MS28. Charge density studies

Chairs: Anders Madsen, Simon Coles

MS28-P1 Lone electron pair dispersion - experimental charge density study of cubic arsenic(III) oxide

Piotr A. Gunka¹, Zygmunt Gontarz¹, Janusz Zachara¹

¹. Warsaw University of Technology, Faculty of Chemistry

email: piogun@ch.pw.edu.pl

The first experimental charge density study of arsenolite, cubic polymorph of arsenic(III) oxide, extended by periodic DFT calculations is reported. The presence of weak As...O interactions is confirmed and their topological characterization based on experimental electron density is provided utilizing both the Quantum Theory of Atoms in Molecules (QTAIM) and non-covalent interactions descriptor based on reduced density gradient (NCI-RDG). Spatial dispersion of arsenic lone electron pair (LEP) into three domains is observed in the Laplacian of electron density as well as in electron localization function (ELF) for the first time. The domains are located *trans* with respect to the primary As-O bonds as evidenced by the analysis of ELF. This could be related to the formation of these chemical bonds and/or to the tetrahedral clustering of arsenic atoms. Similar clustering has been observed in Sb(III) and Bi(III) oxyalts, suggesting LEPs may play significant role in this phenomenon. The dispersion of LEPs may be a more general effect for heavy elements and the issue should be investigated thoroughly to understand its origin and structural consequences.

Authors thank National Science Centre for financial support of this work (DEC2012/05/N/ST5/00283).

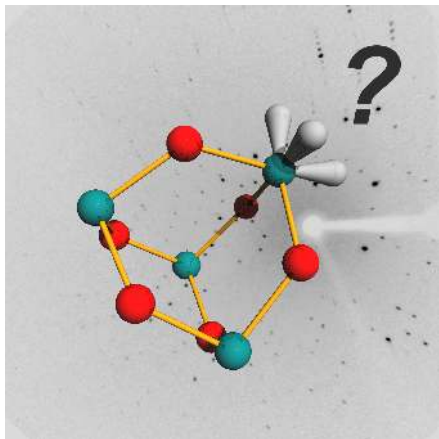


Figure 1. Dispersion of arsenic lone electron pair into three domains located *trans* with respect to the primary As–O bonds.

Keywords: charge density, arsenic(III) oxide, lone electron pair, stereoactivity

MS28-P2 Experimental charge density analysis for doxycycline

Anna M. Makal¹

¹. University of Warsaw, Biological and Chemical Research Centre, ul. Żwirki i Wigury 101, 02-089 Warsaw, POLAND

email: amakal@chem.uw.edu.pl

Doxycycline is a well established wide-spectrum antibiotic, known for its antibacterial and anti-protozoal activity and included in the WHO Model List of Essential Medicines. The drug is commercially available in the hyclate (hydrochloride hemiethanolate hemihydrate) or monohydrate form. Since in the crystal structures of both doxycycline presents the same tautomeric form as that observed in the antibiotic-protein complexes, both crystal forms are interesting in terms of modeling antibiotic-protein interactions.

Presented here are the results of the experimental charge density analysis for both doxycycline monohydrate and doxycycline hydrochloride. The network of intra- and intermolecular interactions of the doxycycline in both crystal forms is analyzed and classified in terms of topological analysis, interaction energies and source function contributions. Interaction energies are also compared with the results of theoretical periodic calculations.

The additional proton bound to the O3 oxygen in the case of doxycycline hydrochloride does not change the global conformation of the antibiotic molecule, but it significantly influences the distribution of charges and the resulting electrostatic potential of the molecule. As the oxygen atom O3 is directly involved in the intermolecular interactions of doxycycline with the host proteins, availability of the electron density distribution for both protonated and deprotonated variant enables more exact prediction of the antibiotic-protein interactions at different host protein protonation states.

The conformation of the antibiotic in the crystal lattice of both forms is compared with the conformation known for the antibiotic-target protein complexes deposited in PDB. The major difference is the breaking of the intramolecular hydrogen bond network in order to form two protein-ligand contacts. The differences are also explored by means of Hirshfeld surface analysis of the doxycycline in the crystal network and doxycycline in the protein environment.

AM and KW acknowledge financial support within the Polish NCN MAESTRO grant, decision number DEC-2012/04/A/ST5/00609.

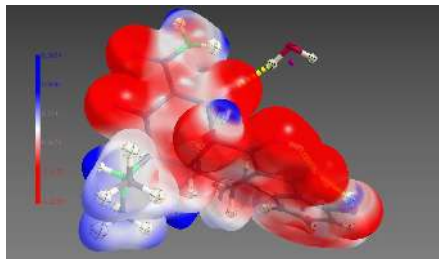


Figure 1. The electrostatic potential around doxycycline moiety in doxycycline monohydrate.

Keywords: doxycycline, antibiotic, protein-ligand interactions

MS28-P3 Dithiadiazolyl radicals - structures and charge densities of their crystals and cocrystals

Sławomir Domagała¹, Krzysztof Kościł¹, Sean W. Robinson², Delia A. Haynes², Krzysztof Woźniak¹

1. Department of Chemistry, University of Warsaw, Warszawa, Poland

2. Department of Chemistry and Polymer Science, Stellenbosch University, Republic of South Africa

email: slawdom@chem.uw.edu.pl

Purely organic systems can exhibit conductivity, superconductivity or magnetically ordered phases - properties usually thought as restricted only for crystals containing metallic centres (Cu, Mn, etc.). One of the most intriguing groups of such systems is a family of dithiadiazolyl radicals.[1] These radicals are chemically stable, so they can be arranged in closely packed structures. Relatively high electrostatic polarization allows for inter- and intramolecular S...N interactions. In the crystal phase, the dithiadiazolyl group often co-exists with a phenyl molecular fragment, which further stabilizes the crystal lattice by introducing an intermolecular $\pi\cdots\pi$ aromatic interactions (e.g. phenyl...perfluorophenyl stack interaction). The spin structure of these compounds is strongly coupled to the crystal structure. One can then try to adjust the magnetic properties (e.g. FM-AFM ordering) of such systems by small changes of structural parameters (e.g. distances between molecules in stack). This and other intriguing properties suggest that the dithiadiazolyl radicals are promising candidates for the construction of molecular devices.

The scope of the work was to determine the quantitative electron density distribution and its parameters (ρ and $\Delta\rho$ in critical points, integrated charges, etc.) for the series of model crystals of radicals belonging to dithiadiazolyl family.[2] The Hansen-Coppens multipole expansion of electron density model was refined against the high resolution ($\sin\theta / \lambda > 0.7\text{\AA}^{-1}$). X-ray diffraction data to obtain the best models of the electron density distribution in given crystals. These models were then used to calculate quantitative electron density properties using the Bader's Quantum Theory of Atoms in Molecules (QTAIM) such as critical points parameters (ρ_{CP} , $\Delta\rho_{\text{CP}}$, bond paths), atomic basins or integrated electron density parameters (integrated charges, atomic multipoles and volumes, etc). The obtained results and detailed analysis of dithiadiazolyl radicals should hopefully help in a better understanding of the magnetic phenomena in organic systems.

[1] Rawson, J. M., Alberola, A., Whalley, A., J. Mater. Chem. 16, (2006), 2560-2575. [2] C. Allen, D.A. Haynes, C.M. Pask, J.M. Rawson, CrystEngComm 11, (2009), 2048-2050.

Keywords: electron charge density, radicals, cocrystals

MS28-P4 Crystal structure and DFT calculations of 2-naphthalenecarboxamide ,3 hydroxy-N(2-methylphenyl)

Ahmet Erdönmez¹, Sibel A. Baba², Erbil Ağar³, Ufuk Çoruh⁴

1. ondokuzmayis university, faculty of art and science, department of physics 55139 Atakum/Samsun, TURKEY
2. ondokuzmayis university, institute of science 55139 Atakum/Samsun, TURKEY
3. ondokuzmayis university, faculty of art and science, department of chemistry 55139 Atakum/Samsun, TURKEY
4. ondokuzmayis university, faculty of education, department of physics 55139 Atakum/Samsun, TURKEY

email: erdonmez@omu.edu.tr

The structure of title compound 2-Naphthalenecarboxamide ,3 Hydroxy-N(2-methylphenyl) $C_{18}H_{15}NO_2$, has been synthesized. The Schiff base compound has been characterized by single-crystal X-ray diffraction technique. The compound crystallizes in the monoclinic space group P2₁/c with the following unit-cell dimensions $a=15.1334(13)\text{Å}$, $b=7.0994(4)\text{Å}$, $c=12.7712(12)\text{Å}$, $\alpha=90.000(0)^\circ$, $\beta=97.221(7)^\circ$, $\gamma=90.000(0)^\circ$, $V=1361.23(19)\text{Å}^3$, $Z=4$. The crystal structure contains intramolecular N-H...N hydrogen bond. X-ray measurements was carried out on a STOE IPDS II diffractometer with MoK α radiation. The molecular structure was solved by direct method using SHELXS97 and refinement by full-matrix least-squares on F² using SHELXL97 program. An Ortep-3 view of the molecule of title compound is shown in Fig. 1.



Figure 1. Ortep-3 diagram of the title compound

Keywords: Schiff base, tautomeric effect, DFT Calculations

MS28-P5 Free energy determination applied for gallic acid monohydrate polymorphs

Ioana Sovago¹, Anna Hoser¹, Anders Madsen¹

1. Department of Chemistry, University of Copenhagen, Universitetsparken 5, Copenhagen, 2100

email: ioana.sovago@chem.ku.dk

The contribution of both entropy and enthalpy in crystal structure relative stability determination play an important role in understanding the formation and behaviour of a specific polymorph. Investigating the effects of vibrational entropy is a key factor in achieving a better understanding the relative stability of polymorphic materials. Due to low-frequency molecular vibrations, it is rather difficult to estimate vibrational entropy accurately. Therefore, the thermodynamic contribution should be extracted by combining the calculated vibration entropy with temperature-controlled crystallographic measurements. The kinetic contribution will be as well estimated by combining the calculated vibrational energies with crystallographic measurements. Gallic acid monohydrate has been shown to crystallise into five different polymorphs and it was rather difficult to obtain meaningful crystal structure prediction.¹ Hence, we considered is a good candidate for free energy investigation. Single crystal X-ray diffraction experiments were carried out at four different temperatures (10 K, 95 K, 123 K, and 175K) at a relatively high diffraction angle. The data obtained was then used in an aspherical atom refinement implemented in XD software² in order to obtain accurate atomic and anisotropic displacement parameters (adps). In a subsequent step the aspherical atom refinement data together with periodic ab-initio calculations were used in a normal mode refinement for gaining the vibrational entropy. The entropy was calculated using the periodic ab-initio calculations for each form. The 10K data collection for form III reveal a change in the unit cell parameters with $Z'=3$ for the asymmetric unit. The volume is three times expanded and the molecules in the asymmetric unit show *pseudo* symmetry. Therefore, the structure can be defined from only one molecule with *pseudo*- $Z'=1$ as in case of the room temperature data of this form. Some of the H atoms involved in the (8) ring were found to show disorder. This is a possible explanation of the lack in H atom positions determination in the previous crystal structure prediction of gallic acid monohydrate polymorphs.¹

Reference:

1. D. Braun, R. Bhardwaj, A. Florence, D. Tocher, S. L. Price, *CrystGrowthDes*, 2012, **13**,19-23.
2. A. Volkov, P. Macchi, L. Farrugia.; C. Gatti, P. Mallinson, T. Richter, T. Koritsanszky, *XD-2006*

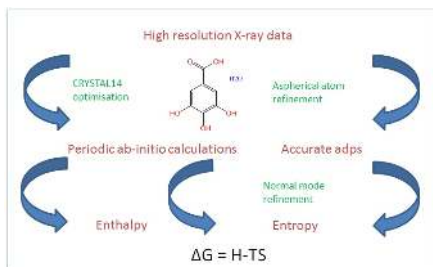


Figure 1.

Keywords: high resolution X-ray diffraction, periodic ab-initio calculations, gallic acid

MS28-P6 Experimental electron density of cytosinium chloride in crystalline state

Małgorzata K. Cabaj¹, Paulina M. Dominiak¹

¹. Faculty of Chemistry, University of Warsaw, Pasteura 1, 02-093 Warsaw, Poland

email: mcabaj@chem.uw.edu.pl

Comprehensive goal of my work is to analyze charge density distribution and intermolecular interactions between nucleobases in crystalline state. It is crucial to know precisely potential of this molecules to form particular type of interactions, especially in the context of RNA structure predictions. Presented work is focused on cytosinium chloride.

Single crystals of cytosinium chloride were obtained by slow evaporation of solvent from mixture of cytosine and 4-thiouracil dissolved in water with small amount of hydrochloric acid. High resolution (0.5 Å) X-ray diffraction data were collected on monocrystal diffractometer at 90 K. The data were next subject to data reduction, structure solution, independent atom model refinement and finally multipolar refinement procedures. Several strategies of data reduction and multipolar refinement were tested to obtain the best model of crystal electron density.

Cytosine chloride crystallizes in P2₁/n group in monoclinic system. Unit cell consists of one protonated cytosine molecule and one chloride ion located almost in the same plane. Cytosine forms dimers through double hydrogen bond between O2 and N3 atoms (see Figure 1). Hydrogen bonds, besides cation – anion interactions, play important role in building the crystal structure and determination of crystal lattice energy.

I will present comparison of chosen data reduction and refinement strategy with others and discuss which parameters decided on its superiority. The second part will be dedicated to more profound description of cytosine chloride structure and evaluation of intermolecular interactions based on charge density.

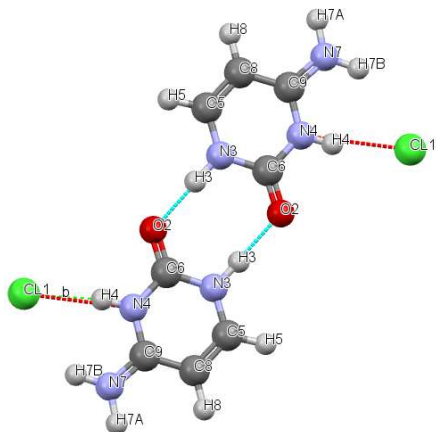


Figure 1. Cytosine dimer

Keywords: charge density, cytosine, hydrogen bonds

MS28-P7 Experimental deformation electron density studies of (-)-cytosine and its simply salts

Maciej Kubicki¹, Agata Owczarzak¹

¹ Faculty of Chemistry, Adam Mickiewicz University in Poznan, Poland

email: mkubicki@amu.edu.pl

The interest in cytosine, a naturally occurring alkaloid, and related compounds has been growing recently, stimulated by the realization of their biological activity. (-)-Cytosine (Scheme 1) is an alkaloid, naturally occurring in plants of the *Leguminosae* family, which interacts with nicotine-acetylcholine receptors and has been applied in investigation of the central nervous system and in anti-nicotine therapy. This alkaloid has been found to moderately increase the concentration of dopamine alleviating the symptoms of nicotine deprivation (the so-called nicotine hunger). Therefore, cytosine has been employed in nicotine withdrawal therapy in the form of Tabex® (Eastern and Central Europe), Chantix® (USA) or Champix® (Canada and Europe) formulations. According to literature data, cytosine derivatives have been tested also for their use in the treatment of Alzheimer's and Parkinson's diseases. In this communication we will present the details of electron density distribution in the cytosine and some of its salts (chloride, nitrate etc.), determined by means of high-resolution X-ray diffraction and described within Hansen-Coppens multipolar model. The deformation electron density of the alkaloid and its salts will be compared and the changes occurring upon protonation will be discussed. Additionally, the topological analysis of the electron density distribution will be applied to describe and analyze the details of the bonds and intermolecular interactions in the crystal structures. This is a part of the wider project which is supposed to compare the biological activity (defined by the ability of making complexes with the DNA fragments) of the known and newly synthesized cytosine derivatives, with the details of the electron density distribution, determined by means of high resolution X-ray diffraction. The result should be the library of the multipolar expansion coefficients for cytosine neutral molecule and cytosinium cations, applicable in similar studies of more complicated derivatives, dimers etc., for which the complexation studies will be also performed. This work is supported by a grant from the Polish National Science Center, 2013/11/B/ST5/01681 (to MK).

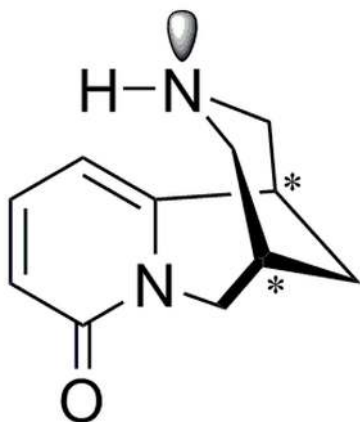


Figure 1. Scheme of (-)Cytisine

Keywords: cytisine, salts, electron density, topological analysis

MS28-P8 The influence of data collection quality on the multipolar parameters of sulfur and chlorine atoms in 5-chloro-2-mercaptobenzimidazole (CMBZT)

Anita M. Owczarzak¹, Maciej Kubiak¹

¹ Adam Mickiewicz University

email: aniwow@amu.edu.pl

During our studies of charge density distribution in thioamide compounds, we very often were faced with the evidence of electron density depletion around the nuclei of sulfur atoms, which can be observed as a certain ring in the deformation charge density maps (fig 1.). As such a “ring effect” is observed regularly in charge density studies not only for sulfur but also for other heavier atoms (chlorine, bromine ect.) we decided to look more closely at this subject.

The high resolution data has been collected using Xcalibur diffractometer with Eos detector at 100K for two 5-chloro-2-mercaptobenzimidazole (CMBZT) crystals of deliberately different quality.. The structures have been refined using Hansen-Coppens multipolar model [1] implemented in MoPro software [2], using (almost) exactly the same procedure for both cases. In a communication we will focus on a comparison of the multipole parameters and topological analyses of CMBZT compound. In addition, the influence of cutting off the data on the results of refinement has been also studied.

[1]Hansen, Coppens, *P.Acta Crystallographica Section A* **34**, 909–921 (1978).

[2]Jelsch,Guillot, Lagoutte, Lecomte, *J. Appl. Cryst.* **38**,38-54

Keywords: charge density, thioamide, sulfur

[3] R. F. W. Bader, *Atoms in Molecules: A Quantum Theory*, Clarendon: Oxford, UK, 1990

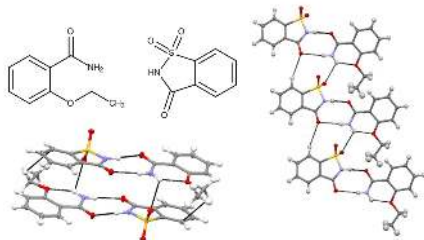


Figure 1. Top left: Structure of EA:SAC co-crystal, right: linear ID tape motif in form I, bottom left: tetrameric motif in form II.

Keywords: charge density, polymorphism, co-crystal, structure, interactions

MS28-P10 Non-Innocent role of ligands in some Ni organometallic complexes as viewed through the Spin Density Source Function

Ahmed M. Orlando^{1,2}, Carlo Gatti^{1,3}, Leonardo Lo Presti^{1,2,3}

1. Center for Materials Crystallography, Aarhus University, Langelandsgade 140, 8000 Aarhus, Denmark
2. Dipartimento di Chimica, Università degli Studi di Milano, Via Golgi 19, 20133 Milano, Italy
3. CNR-ISTM, Istituto di Scienze e Tecnologie Molecolari, Via Golgi 19, 20133 Milano, Italy

email: ahmed.orlando@unimi.it

A key feature of the non innocent metal ligand complexes is that the oxidation state of the central metal atom and the electronic structure of the ligands can not be *a priori* and unambiguously determined.^[1] In this work we apply the recently introduced Spin Density Source Function^[2] to a series of Ni metal complexes to get insight on the factors that lead to ferro- or anti-ferro magnetic coupling behaviour and to quantitatively distinguish whether the ligands play a innocent or non-innocent role. Three neutral Ni radical organometallic complexes, of general formula $[\text{CpNi}(\text{dithiolene})]^{\bullet}$, are investigated, namely $[\text{CpNi}(\text{tfd})]^{\bullet}$ (tfd=1,2-bis(trifluoromethyl) ethene-1,2-dithiolate) (1), $[\text{CpNi}(\text{mnt})]^{\bullet}$ (mnt=maleonitriledithiolate) (2) and $[\text{CpNi}(\text{adt})]^{\bullet}$ (adt=acrylonitrile-2,3-dithiolate) (3). They are all known to exist in doublet state ($S = 1/2$) and to show, in their dimeric forms, a strong anti-ferromagnetic coupling that can not be explained solely by short S...S intermolecular contacts^[3]. In fact DFT calculations showed that spin density is strongly delocalized on the NiS_2 moiety and, more importantly, up to 20% of $s(r)$ is delocalized on the Cp ring. As a result, the intermolecular Cp...Cp and Cp...dithiolene overlap interactions lead to anti-ferromagnetic couplings mediated by ligands that are commonly classified as innocent. The Source function enables to quantify to which extent the spin density is delocalized over the metal center and the Cp and dithiolene ligands, and to assess the role played by the π -stacking in the exchange interaction between molecules in their dimers. Finally, with the help of solid state quantum mechanical simulations it allows to detect quantitatively the effect of crystal packing on the spin density delocalization mechanism and on the resulting magnetic coupling in the solid state.

References: [1] Kim P Butin, Elena K Beloglazkina and Nikolai V Zyk, *Russ. Chem. Rev.* **2005**, 74, 531 [2] C. Gatti, A. M. Orlando and L. Lo Presti, *Chemical Science*, under revision. [3] T. Cauchy, E. Ruiz, O. Jeannin, M. Nomura, M. Formiguè, *Chem. Eur. J.* **2007**, 13, 8858

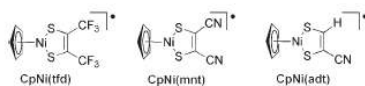


Figure 1.

Keywords: Non Innocent Ligands, Source Function, Spin Density, Magnetic Interactions

MS28-P11 Anharmonic thermal motion in glutathion investigated by the Maximum-Entropy-Method (MEM)

Christian B. Hübschle¹, Birger Dittrich², Charlotte Ruhmlieb², Sander van Smaalen¹

1. University of Bayreuth, Laboratory of Crystallography, Bayreuth

2. University of Hamburg, Institute of Inorganic and Applied Chemistry, Hamburg

email: chuebsch@moliso.de

γ -L-Glutamyl-L-cysteinyl-glycine (Glutathion) was measured at 100K using MoK α radiation. A dynamic electron density map was calculated by the PRIOR[1] program of the BayMEM[2] suite and used for the Maximum-Entropy-Method calculation. As a model for this prior density Invarioms[3] with harmonic ADP's were applied. In the Invariom refinement for the prior model coordinates and harmonic ADP's were refined and multipole parameters were taken from the data-base.

A previous Invariom refinement refining Gram-Charlier parameters up to 3rd order on the carboxyl oxygen atoms of the glycine part of the molecule led to probability density function with significant negative values. The MEM can not produce such artefacts. We show the effect of the anharmonic motion on the dynamic electron density.

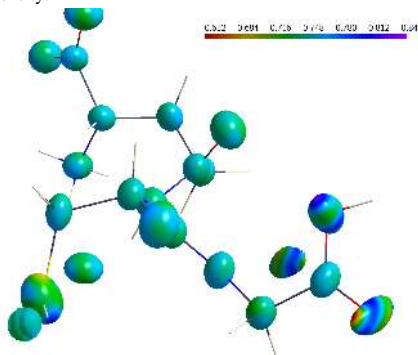


Figure 1. Isosurface of the MEM-electron density of Glutathion at 5 eÅ⁻³ mapped with the electron density value of the harmonic prior density. Atoms in green show almost no anharmonic effect.

Keywords: anharmonic motion, maximum-entropy-method, Glutathion

MS29. Quasi crystals and aperiodic materials

Chairs: Andreas Schönleber, Janusz Wolny

MS29-P1 An Icosahedral Quasicrystal as a golden modification of the icosagrid and its connection to the E8 lattice

Fang Fang¹

1. Quantum Gravity Research, Los Angeles, CA, U.S.A.

email: fang@QuantumGravityResearch.org

We present an icosahedral quasicrystal as a modification of the icosagrid, a multigrid with 10 plane sets that arranged with icosahedral symmetry. We use the Fibonacci chain to space the planes obtaining a quasicrystal with icosahedral symmetry. It has a surprising correlation to the Elser-Sloane quasicrystal [4], a 4D cut-and-project of the E8 lattice. We call this quasicrystal the Fibonacci modified icosgrid quasicrystal(FMIQ). We found that the FMQC totally imbeds another quasicrystal that is a compound of 20 3D slices of the Elser-Sloane quasicrystal. The slices, which contains only regular tetrahedra, are put together by a certain 'golden rotation' [5]. Interesting 20Gs (20-tetrahedron clusters arranged with the 'golden rotation') appear repetitively in the FMQC and are arranged with icosahedral symmetry. It turns out that this 'golden rotation' is the dihedral angle of the 600-cell (the super-cell of the Elser-Sloane quasicrystal) and the angel between the tetrahedral facets in the E8 polytope known as the Gosset polytope. We suggest that the FMIQ is an alternative result of releasing the transdimensional "geometric frustration" while maintaining the regularity of the tetrahedra.

Keywords: icosagrid, Fibonacci, Elser-Sloane quasicrystal, E8, 600-cell

MS29-P2 Complex cubic structures: mixed zincides/cadmides/mercurides CaM_{16} and SrM_{16}

Caroline Röhr¹, Marco Wendorff¹, Michael Schwarz¹¹ Universität Freiburg, Institut für Anorganische und Analytische Chemie

email: caroline@ruby.chemie.uni-freiburg.de

In a systematic synthetic, crystallographic and bond theoretical study, the stability ranges as well as the distribution of the isoelectronic late *p*-block elements Zn, Cd and Hg in the polyanions ('coloring') of the recently reported new mercurides (Sr/BaHg_6 [1]) and the prominent YCd_6 -type phases (Ca/SrCd_6 [2]) have been investigated.

The stability range of the YCd_6 -type structure of CaCd_6 and SrCd_6 ($Im-3$, $a \approx 1500\text{--}1600$ pm) could be continuously extended to considerable high Hg contents of $\text{CaCd}_{0.89}\text{Hg}_{5.11}$ and $\text{SrCd}_{0.83}\text{Hg}_{5.17}$, respectively. All Ca compounds of this series form the original stoichiometric YCd_6 -type structure with a type 2 triple split disorder (d2) of the $[M(2)_4]$ tetrahedra in the pentagondodecahedra (cf. figure top right).

For SrCd_6Hg_6 a cubic $2 \times 2 \times 2$ superstructure of the YCd_6 -type ($Fd-3$, $a \approx 3200$ pm, $\text{Eu}_4\text{Cd}_{25}$ -type [3]) appears. Herein, the $[M(2)_4]$ tetrahedra are no longer disordered, but $\frac{3}{4}$ of the cubes, which are not occupied in the aristotype and partially occupied in the new Hg-rich ternary Ca-Zn mercurides like e.g. $\text{CaZn}_{1.7}\text{Hg}_{4.40}$, are filled in an ordered fashion. The shape and filling of the cubes is evidentially connected with the orientation of the $[M(2)_4]$ tetrahedra inside the pentagondodecahedra (cf. figure).

At the section $\text{CaZn}_{0.5}\text{Cd}_5$, larger amounts of smaller Zn atoms cause the formation of ternary variants of the cubic $\text{Mg}_7\text{Zn}_{11}$ -type structure [4] ($\text{Ca}_5\text{Zn}_5\text{Cd}_5$; $Pm-3$ $a=918.1$ pm, $R1=0.035$). For Ca-Zn-Hg , the new likewise complex cubic 1:5 (20:100) phase $\text{CaZn}_{1.7}\text{Hg}_{3.7}$ ($F-43m$, $a=2145.4$ pm, $R1=0.0704$), which is closely related to $\text{Ba}_{20}\text{Hg}_{103}$ and its ternary Zn/Cd derivatives [5], is formed in addition.

The results of the FP-LAPW DFT bandstructure calculations like the *Bader* charges and volumes are used to rationalize the Zn/Cd/Hg distribution in the new mixed metallides. For the calculation of an YCd_6 -type representative, a model compound ' CaHg_6 ' was set up using the crystal data of $\text{CaCd}_{0.89}\text{Hg}_{5.11}$, which has been transformed into the subgroup $I23$ to resolve the disorder of the $[M(2)_4]$ tetrahedra (fig. bottom right).

[1] M. Wendorff, C. Röhr, *J. Alloys Compd.* **546**, 320 (2013).

[2] G. Bruzzone, *Gazz. Chim. Ital.* **102**, 234 (1972).

[3] C. P. Gomez, S. Lidin, *Chem. Eur. J.* **10**, 3279 (2004).

[4] V. Mihajlov, C. Röhr, *Z. Anorg. Allg. Chem.* **636**, 1792 (2010).

[5] M. Wendorff, C. Röhr, *Z. Naturforsch.* **67b**, 893 (2012).

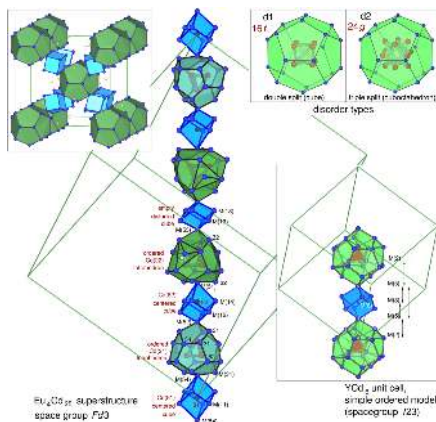


Figure 1. Details of the disorder (top right) and several ordered variants of the cubic YCd_6 -type structure in mixed calcium and strontium Zn/Cd/Hg compounds.

Keywords: Intermetallics, Zinc, Mercurides, Cadmides, Bandstructure calculation

MS29-P3 Estimation of the flip ratio from the diffraction pattern of 1D quasicrystalIreneusz Buganski¹, Radosław Strzalka¹, Janusz Wolny¹¹. AGH University of Science and Technology, Faculty of Physics and Applied Computer Science, Krakow, Poland

email: irek910329@gmail.com

We estimate the number of phason flips randomly applied to atomic positions of the model 1D quasicrystal based on the Average Unit Cell concept within the statistical approach. Phasons can be understood in many different ways in terms of aperiodic crystals [1]. In this work we understand phasons as local rearrangements of structure units. They are known in literature as phason flips [2]. We use the Fibonacci chain built of long L and short S unit tiles as a model 1D quasicrystal. As a phason flip we consider LS→SL swap in the Fibonacci chain sequence. As a consequence of flip occurrence, the change in intensities of the diffraction peaks is observed. The standard correction to the intensity loss in calculated diffraction pattern during the structure refinement process is the Debye-Waller factor defined in perpendicular space. What we propose is to analyze phasons in the physical space using the statistical approach. Here, the atomic structure is modeled by a statistical distribution of atomic positions in physical space (so-called Average unit Cell concept [3-5]). Each single flip of the unit tiles influences the distribution, respectively for different structures. The deviation from the ideal distribution, where no phasons flips are applied, can be easily designated and by that the number of flips can be quantified. In order to retrieve the number of flips we develop yet more precise analysis, which is based on power series expansion of the characteristic function for statistical distribution. This characteristic function for quasicrystals is the structure factor expressed within statistical approach. The moments of the distribution are fitted against diffraction (reference) data. It can be shown that the value of the second moment gives full information about the number of flips. This statement is based on the relation between moment value and flip ratio α , which can be calculated analytically. Higher-order moments tend to differ from the theoretically derived curve (Fig. 1).

References

- [1] T. Janssen, O. Radulescu, *Feoroelectrics* 305, 179-184, (2004)
- [2] M. de Boissieu et al., *Phys. Rev. Lett.* 95, 105503, (2005)
- [3] J. Wolny, *Philos. Mag.* A77, 395-412 (1998)
- [4] J. Wolny, *Acta Cryst.* A54, 1014-1018 (1998)
- [5] J. Wolny, L. Pytlik, *Acta Cryst.* A56, 11-14, (2000)

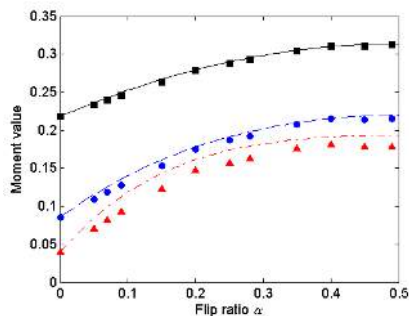


Figure 1. The values of the second- (black square), fourth- (blue circle) and sixth moment (red triangle) fitted with respect to the flip ratio α . The deviation from the theoretical curve (solid, dashed, dash-dotted respectively) is observable for higher-order moments

Keywords: quasicrystal, phasons, AUC

MS29-P4 Structure factor for generalized Penrose tilingMaciej Chodyn¹, Paweł Kuczera^{1,2}, Janusz Wolny¹

1. Faculty of Physics and Applied Computer Science, AGH University of Science and Technology, Krakow, Poland

2. Laboratory of Crystallography, ETH Zurich, Zurich, Switzerland

email: maciej.chodyn@gmail.com

The Generalized Penrose Tiling (GPT) [1,2] can be considered a promising alternative for Penrose Tiling (PT) as a model for decagonal quasicrystal refinement procedure, particularly in the statistical approach (also called the Average Unit Cell (AUC) approach) [3]. The statistical method using PT has been successfully applied to the structure optimization of various decagonal phases [4]. The application of the AUC concept to the GPT will be presented.

In the higher dimensional (*n*D) approach, PT is obtained by projecting a 5D hypercubic lattice through a window consisting of four pentagons, called the atomic surfaces (ASs), in the perpendicular space. The vertices of these pentagons together with two additional points form a rhombic icosahedron. The GPT is created by projecting the 5D hypercubic lattice through a window consisting of five polygons, generated by shifting the ASs along the body diagonal of the rhombic icosahedron. Three of the previously pentagonal ASs will become decagon, one will remain pentagonal and one more pentagon will be created (for PT it is a single point). The structure of GPT will depend on the shift parameter, its building units are still thick and thin rhombuses, but the matching rules and the tiling changes. Diffraction pattern of GPT have peaks in the same positions as regular PT, however their intensities are different.

Binary decagonal quasicrystal structure with arbitrary decoration for a given shift value was simulated. Its diffraction pattern was calculated using AUC method [5,6]. Generated diffraction pattern were used as "experimental data set" in structure refinement algorithm made to test the refining of shift parameter.

Literature

- [1] K. N. Ishihara, A. Yamamoto, *Acta Cryst.* (1988), A44, 508-516
- [2] A. Pavlovitch, M. Kleman, *J Phys a-Math Gen.* (1987), 20, 687-702
- [3] J. Wolny, *Phil. Mag.* (1998), 77, 395-414
- [4] P. Kuczera, J. Wolny, W. Steurer, *Acta Cryst.* (2012), B68, 578-589
- [5] B. Kozakowski, J. Wolny, *Acta Cryst.* (2010), A66, 489-498
- [6] M. Chodyn, P. Kuczera, J. Wolny, *Acta Cryst.* (2015), A71, 161-168

Keywords: quasicrystals, structure factor, Generalized Penrose Tiling

MS30. Structure and function in coordination compounds

Chairs: Marijana Đaković, Janusz Lipkowski

MS30-P1 Synthesis and structural studies of dioxomolybdenum(VI) complexes with isoniazid-related hydrazonesBiserka Prugovečki¹, Višnja Vrdoljak¹, Marina Cindrić¹, Ivana Puljić¹, Dubravka Matković-Čalogović¹

1. Division of General and Inorganic Chemistry, Department of Chemistry, Faculty of Science, University of Zagreb, Croatia

email: biserka@chem.pmf.hr

The chemistry of hydrazones is continuing to be an interesting area of research because of their modularity, easiness of synthesis and stability towards hydrolysis. [1–3] Synthesis of the dioxomolybdenum(VI) complexes $[\text{MoO}_2(\text{HL}^{\text{R}})(\text{MeOH})]\text{Cl}$ (**1–3**), was carried out using MoO_3Cl_2 and the corresponding aroylhydrazone ligand $\text{H}_2\text{L}^{\text{R}}$ (salicylaldehyde isonicotinoylhydrazone ($\text{H}_2\text{L}^{\text{SIH}}$), 2-hydroxy-naphthaldehyde isonicotinoylhydrazone ($\text{H}_2\text{L}^{\text{NIH}}$), or *p*-(*N,N'*-diethylaminosalicylaldehyde isonicotinoylhydrazone ($\text{H}_2\text{L}^{\text{E2NSIH}}$)) in methanol. Compounds $[\text{MoO}_2(\text{HL}^{\text{R}})(\text{H}_2\text{O})]\text{Cl}$ (**1a–3a**) obtained upon exposure of the corresponding mononuclear complexes **1–3** to moisture were also investigated. Deprotonation of the mononuclear complexes $[\text{MoO}_2(\text{HL}^{\text{R}})(\text{MeOH})]\text{Cl}$ (**1–3**), was performed using Et_3N as a base (by conventional solution based-method and mechanochemical approach) as well as by UV-light assisted reactions yielding $[\text{MoO}_2(\text{L}^{\text{SIH}})(\text{MeOH})]$ (**4**) [4], $[\text{MoO}_2(\text{L}^{\text{NIH}})(\text{MeOH})]$ (**5**) and $[\text{MoO}_2(\text{L}^{\text{E2NSIH}})]_n$ (**6**), respectively. Crystal and molecular structures of all complexes were solved by the single-crystal X-ray diffraction method. In all complexes the ligand coordinates the metal centre of the *cis*- MoO_2 core tridentately via phenolic-oxygen, azomethine-nitrogen and keto-hydrazone oxygen forming five and six member chelate rings. The remaining sixth coordination site of the distorted octahedron is occupied by the oxygen atom of the solvent molecule (methanol in **1–3** and **5**, water in **1a–3a**) or nitrogen atom of the bridging isonicotinyl moiety of the neighboring complex (in **6**). We were interested to investigate importance of nonbonding interactions in the structures, especially the ability of these complexes to form different hydrogen bonding motifs depending on the protonation state of the complexes.

[1] S. Banerjee, A. Ray, S. Sen, S. Mitra, D. L. Hughes, R. J. Butcher, S. R. Batten and D. R. Turner, *Inorg. Chim. Acta.*, 2008, **361**, 2692.

[2] J. G. Vos and M. T. Pryce, *Coord. Chem. Rev.*, 2010, **254**, 2519.

[3] A. Kobayashi, D. Yamamoto, H. Horiki, K. Sawaguchi, T. Matsumoto, K. Nakajima, H.-C. Chang and M. Kato, *Inorg. Chem.*, 2014, **53**, 2573.

[4] S. Gao, L.-H. Huo, H. Zhao and S. W. Ng, *Acta Cryst.* 2004, **E60**, m1757.

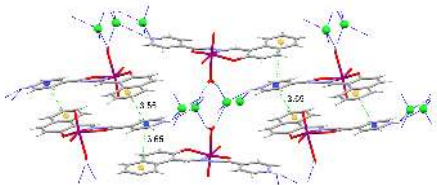


Figure 1. Layers of complex ions in 2a. Hydrogen bonds are shown by blue dotted lines and $\pi\cdots\pi$ interactions by green dashed lines. The distance between centroids is given in Å.

Keywords: dioxomolybdenum(VI) complexes, deprotonation, structural studies, hidrazones

MS30-P2 Oxo-bridged dinuclearCr^{III}-Ta^V complex: structural and spectroscopic characterization

Lidija Androš Dubraja¹, Marijana Jurić¹

¹ I. Ruder Bošković Institute, Bijenička cesta 54, 10000 Zagreb, Croatia

email: Lidija.Andros@irb.hr

The oxo-bridged metal units are interesting intramolecular motifs appearing in several bioinorganic molecules such as metalloproteins (Fe–O–Fe core) and in various inorganic systems, especially as polyoxometallates, materials with outstanding properties and functions.[1,2] Recently, unusual behaviour that causes the changes in material color and magnetic properties has been observed in structures with Cr–O–Cr bridges, referred as metal-to-metal-charge transfer (MMCT).[3] Even though there are several reports of light- and heat-induced MMCT, the occurrence of this intriguing phenomena is hard to predict and the relationship between electron transfer and molecular structure is not yet understood.[4]

In the recent years our research group has been involved in intensive studies related to tris(oxalato)oxotantalate(V) anion, with the aim of obtaining new metal-organic coordination systems with specific (electrical, optical, catalytic and/or magnetic) properties. It was found that this type of anion is prone to form heterometallic complexes with different topologies and nuclearities.[5] Depending on reaction conditions and reagents, the oxo group in $[\text{TaO}(\text{C}_2\text{O}_4)_3]^{3-}$ can be protonated or replaced with other ligand in the coordination sphere of tantalum.[6] Reaction of water solutions of complex $[\text{Cr}(\text{bpy})_2(\text{OH})_2]^{3+}$ cations and $[\text{TaO}(\text{C}_2\text{O}_4)_3]^{3-}$ anions yielded compound with new bonding topology of this anion – dinuclear oxo-bridged complex $[\text{Cr}(\text{bpy})_2(\text{OH})_2(\mu\text{-O})\text{Ta}(\text{C}_2\text{O}_4)_3]_2 \cdot 7\text{H}_2\text{O}$ (**1**) (bpy = 2,2'-bipyridine). Compound **1** was characterized by single-crystal X-ray diffraction, IR and UV/Vis spectroscopy. Figure 1 shows dinuclear $[\text{Cr}(\text{bpy})_2(\text{OH})_2(\mu\text{-O})\text{Ta}(\text{C}_2\text{O}_4)_3]$ unit, with chromium in octahedral geometry and tantalum in distorted pentagonal bipyramidal geometry. Single crystal measurements at room temperature and at 100 K have shown some differences in the unit cell parameters, as well as in the M–(O, N) bond lengths, which may indicate the change of oxidation state of metal centres. Further magnetic and MMCT studies of **1** are in progress.

[1] J. B. Vincent *et al.*, *Chem. Rev.*, 1990, **90**, 1447–1467; [2] D.-L. Long *et al.*, *Angew. Chem. Int. Ed.*, 2010, **49**, 1736–1758; [3] T. J. Morsing *et al.*, *Inorg. Chem.*, 2014, **53**, 2996–3003; [4] E. S. Koumoussi *et al.*, *J. Am. Chem. Soc.*, 2014, **136**, 15461–15464; [5] a) L. Androš *et al.*, *Inorg. Chem.*, 2013, **52**, 14299–14308; b) L. Androš Dubraja *et al.*, *CrystEngComm*, 2015, **17**, 2021–2029; [6] L. Androš *et al.*, *CrystEngComm*, 2013, **15**, 533–543.

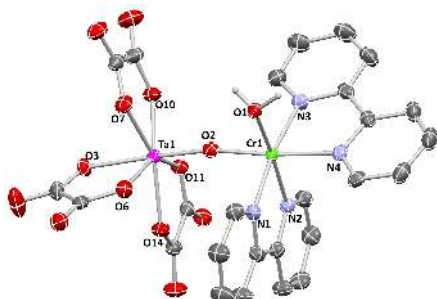


Figure 1. Dinuclear Cr^{III}-Ta^V unit in compound [Cr(bpy)₂(OH)₂(μ-O)Ta(C₂O₄)₂]_n·7H₂O (100 K) showing displacement ellipsoids at 50% probability. Hydrogen atoms on coordinated water molecule are depicted as spheres of arbitrary radii and those on the aromatic rings are omitted for clarity.

Keywords: oxo-bridged complex, tantalum, chromium, metal-to-metal charge transfer

MS30-P3 Crystal structure determination of four new copper (II) complexes containing *ono* type Schiff base ligands

Duygu Barut¹, Neslihan Korkmaz², Stephen T. Astley², Muhittin Aygün¹

1. Department of Physics, Dokuz Eylul University, 35160 Buca, İzmir, Turkey

2. Department of Chemistry, Ege University, 35100 Bornova, İzmir, Turkey

email: duygu.barut@hotmail.com

Schiff base ligands are considered as ‘privileged ligands’ because they are easily prepared by condensation between aldehydes and primary amines. These ligands are able to coordinate many different metals and to stabilize them in various oxidation states. The chemistry of transition metal complexes with Schiff bases has played an important role in the development of coordination chemistry as a whole. Multidentate Schiff bases have been widely used as ligands, because they can be easily attached to metal ions due to the formation of highly stable coordination compounds. These complexes show a large variety of catalytic, biological, antifungal, anti tumor and anti HIV activities [1].

In the present study, we were interested in the investigation of four new copper(II) complexes synthesized by tridentate Schiff base ligand, have different coordination environments. Single-crystal X-ray data were collected on an Agilent Diffraction Xcalibur diffractometer equipped with an Eos-CCD detector. Data analysis were carried out with the CrysAlis program [2]. Structures were solved by SHELXS-97 and olex2.solve, refined by means of SHELXL-97 programs [3] incorporated in the OLEX2 program package [4].

References

- [1] S. M. Saadeh, *Arabian Journal of Chemistry*, 2013, 6, 191-196.
- [2] CrysAlis PRO and CrysAlis RED. Agilent Technologies, Yarnton, Oxfordshire, England, 2002.
- [3] G. M. Sheldrick, *Acta Crystallogr. Sect. A* 2008, 64, 112-122.
- [4] O. V. Dolomanov, L. J. Bourhis, R. J. Gildea, J. A. K. Howard, H. Puschmann, *J. Appl. Cryst.* 2009, 42, 339-341.

Keywords: Cu(II) Complex, Schiff Base, Crystal structure

MS30-P4 Synthesis and crystal structures of new di- and polynuclear silver(I) saccharinate complexes with tertiary monophosphanes

Orhan Buyukgungor¹, Veyisel T. Yilmaz²

1. Department of Physics, Faculty of Arts and Sciences, Ondokuz Mayis University, 55159 Samsun, Turkey.

2. Department of Chemistry, Faculty of Arts and Sciences, Uludag University, 16059 Bursa, Turkey.

email: orhanb@omu.edu.tr

Over the years there has been a continuous interest in the biological activity of silver(I) metal complexes. Recently, we reported a number of silver(I) sac and found that these complexes have significant antibacterial and anticancer activities [1]. As an extension of our studies, in this work we synthesized and studied the crystal structures of four new silver(I) sac complexes containing the monophosphane ligands, namely $[\text{Ag}(\mu\text{-sac})(\text{PPh}_3)]_2$ (**1**), $[\text{Ag}(\mu\text{-sac})(\text{PPh}_2\text{Cy})]_2$ (**2**), $[\text{Ag}(\mu\text{-sac})(\text{PPhCy}_2)]_2$ (**3**) and $[\text{Ag}(\mu\text{-sac})(\text{PCy}_3)]_n$ (**4**), where PPh_3 = triphenylphosphane, PPh_2Cy = cyclohexyldiphenylphosphane, PPhCy_2 = dicyclohexylphenylphosphane and PCy_3 = tricyclohexylphosphane (see Figure.) The silver(I) ion in complex **1** is coordinated by a sac ligand via the N atom and a PPh_3 ligand, forming a $[\text{Ag}(\text{sac})(\text{PPh}_3)]$ unit and the $[\text{Ag}(\text{sac})(\text{PPh}_3)]$ units are further doubly bridged by relatively long Ag-O_{sulf} bonds, leading to a dinuclear structure $[\text{Ag}(\text{sac})(\text{PPh}_3)]_2$. The dimeric units of complex **1** are connected by weak intermolecular interactions such as C-H...O, $\pi(\text{sac})\dots\pi(\text{PPh}_3)$ and CH... $\pi(\text{sac}$ and $\text{PPh}_3)$. Complexes **2** and **3** show a structural similarity. Each complex also exhibits significant interactions between the silver(I) centers. The Ag-Ag distances are comparable with literature but significantly smaller than that found in other dinuclear sac complexes showing strong argentophilic interactions with Ag - Ag distances around 2.90 Å. Complex **4** is a one-dimensional metallopolymer in which the silver(I) ions are bridged by the sac ligands through the imino N and the carbonyl O atoms, leading to a linear one dimensional polymeric chain running along the b-axis. In all four crystal structures, the di- and polynuclear structures are achieved by the N/O bridging mode of the sac ligand. All phosphane ligands act as a monodentate donor through the P atom. Complexes **2** and **3** exhibit strong argentophilic interactions.

References:

[1] V.T. Yilmaz, E. Gocmen, C. Icel, M. Cengiz, S.Y. Susluer, O. Buyukgungor, J. Biol. Inorg. Chem. 19 (2014)

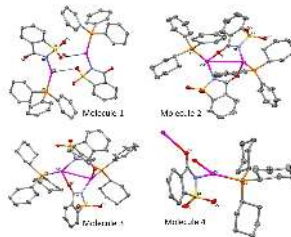


Figure 1. View of the molecular structures. Hydrogen atoms were omitted for clarity. The probability level of thermal ellipsoids are 30%.

Keywords: Crystal structure, Saccharinate, Phosphine

MS30-P5 Ruthenium quinazoline complexesPetra Kuzman¹, Anton Meden¹, Bogdan Štefane¹¹. Faculty of Chemistry and Chemical Technology, University of Ljubljana, Večna pot 113, SI-1000 Ljubljana, Slovenia

email: pkuzman1@gmail.com

Our research is based on the synthesis, characterization and evaluation of ruthenium quinazoline coordination compounds. We have successfully synthesized quinazoline derivatives **4** that were further used as ligands for the synthesis of ruthenium complexes **5** (Scheme 1). Successfully synthesized ruthenium complexes were fully characterized using X-ray single crystal analysis. A detailed kinetic studies of C-H activation reaction were carried out. Cyclometallation of ligands by transition metals is a very important reaction since it enables the synthesis of organometallic complexes with a carbon-metal bond. The most commonly used methods for the synthesis of cyclometallated complexes are (a) transmetallation (transfer of ligands from one metal to another) and (b) metallation with selective C-H activation.^{1,2} Organometallic reagents that are used in transmetallation reaction are expensive and often commercially unavailable. C-H activation allows the selective and direct functionalization of the non-reactive (hetero)aromatic C-H bonds, which leads to economically and ecologically friendly synthesis.³

Keywords: Organometallic complexes, ruthenium, X-ray crystallography

MS30-P6 Near-infrared to visible light-upconversion in molecular coordination complexesLaure Guenée¹, Davood Zare², Yan Suffren³, Andreas Hauser³, Claude Piguet²¹. Laboratory of Crystallography, University of Geneva, 24 quai Ernest Ensermet, 1211 Geneva 4, Switzerland². Department of Inorganic and Analytical Chemistry, University of Geneva, 30 quai Ernest Ensermet, 1211 Geneva 4, Switzerland³. Department of Physical Chemistry, University of Geneva, 30 quai Ernest Ensermet, 1211 Geneva 4, Switzerland

email: laure.guenee@unige.ch

Light-upconversion via stepwise energy transfer from a sensitizer to an activator exploits linear optics for converting low-energy infrared or near-infrared incident photons to higher energy emission. This phenomenon could be of potential use in solar cell technology [1] and for in situ biological probes and sensor [2]. Generally, this light-upconversion approach is restricted to activators possessing intermediate long-lived excited states such as those found for trivalent lanthanide cations dispersed in solid-state matrices. When the activator is embedded in a molecular complex, efficient nonradiative relaxation processes usually reduce excited state lifetimes to such an extent that upconversion becomes too inefficient to be detected under practical excitation intensities. However, with the development of the supramolecular chemistry of lanthanide complexes, using specially designed ligands, assemblies can be made where the geometry of the metal centre is controlled. We present here studies of crystallographic and photophysical properties on a series of isostructural trinuclear dimetallic helicates [MLnM(L1)₃](CF₃SO₃)₃ with M=Ga(III) or Cr(III) and Ln= Y(III) or Er(III), leading to a detailed rational analysis of the energy transfer upconversion (ETU) mechanism. A novel upconversion pathway is presented and we demonstrate that strong-field trivalent chromium chromophores irradiated with near-infrared photons produce upconverted green erbium-centered emission in discrete polynuclear triple-stranded helicates [3]. [1] Huang, X.; Han, S.; Huang, W.; Liu, X. *Chem. Soc. Rev.* 2013, 42, 173–201. [2] Liu, Y.; Tu, D.; Zhu, H.; Chen, X. *Chem. Soc. Rev.* 2013, 42, 6924–6958. [3] (a) Aboshyan-Sorgho, L.; Besnard, C.; Pattison, P.; Kittilstved, K. R.; Aebischer, A.; Bünzli, J.-C. G.; Hauser, A.; Piguet, C. *Angew. Chem., Int. Ed.* 2011, 50, 4108–4112. (b) Aboshyan-Sorgho, L.; Nozary, H.; Aebischer, A.; Bünzli, J.-C. G.; Morgantini, P.-Y.; Kittilstved, K. R.; Hauser, A.; Eliseeva, S. V.; Petoud, S.; Piguet, C. *Am. Chem. Soc.* 2012, 134, 12675–12684 and references therein. (c) Y. Suffren, D. Zare, S. V. Eliseeva, L. Guénée, H. Nozary, T. Lathion, L. Aboshyan-Sorgho, S. Petoud, A. Hauser and C. Piguet, *J. Phys. Chem. C*, 2013, 117, 26957–26963. (d) Y. Suffren, D. Zare, L. Guénée, S. V. Eliseeva, H. Nozary, L. Aboshyan-Sorgho, S. Petoud, A. Hauser and C. Piguet, *Dalton Trans.*, 2015, 44, 2529–2540.

Keywords: Light-upconversion, lanthanide complexes

MS30-P7 The synthesis and crystal structure of Cd(II)-Azoxybenzenetetracarboxylate with 1,4-bis(2-methylimidazol-1yl)butane

Murat TAŞ¹, Mürsel Arıç², Okan Zafer Yeşil²

1. Department of Science Education, Ondokuz Mayıs University, 55139, Samsun, Turkey

2. Department of Chemistry, Eskişehir Osmangazi University, 26480 Eskişehir, Turkey

email: murat.tas@omu.edu.tr

During the last decades, there is a continued interest in the rational design and synthesis of coordination polymers due to not only their application fields such as gas storage/separation, catalysis, luminescence, sensor, but also their fascinating topological structures [1]. Despite the syntheses of a great deal of coordination polymers, it has been still difficult the controllable synthesis of coordination polymers. In the assembly of coordination polymers, several factors, such as, organic ligands, metal ions, pH, solvents, temperature are the key factors [2]. Hence, it is important to choose the organic ligands, metal ions and regulate the reaction conditions for desired structures. In this study, $[\text{Cd}_2(\mu_6\text{-ao}_2\text{btc})(\mu\text{-1,4-bmeib})(\text{H}_2\text{O})_2]_n$ ($\text{H}_4\text{ao}_2\text{btc} = 3,3',5,5'\text{-azoxybenzenetetracarboxylic acid}$, 1,4-bmeib: 1,4-bis(2-methylimidazol-1yl)butane) was synthesized and characterized by elemental analysis, IR spectrum, single crystal X-ray diffraction. Complex **1** was prepared by the solvothermal reaction of $\text{H}_4\text{ao}_2\text{btc}$ (0.1 g, 0.279 mmol), $\text{CdCl}_2 \cdot 2.5\text{H}_2\text{O}$ (0.127 g, 0.558 mmol) and 1,4-bmeib ligand (0.061 g, 0.279 mmol) at 100 °C in the mixture of DMF: H_2O (10:2, v:v) in the presence of HNO_3 . The crystal structure of **1** with atom numbering scheme is shown in Fig. 1a. X-ray single-crystal diffraction analysis indicates that complex **1** crystallizes in the triclinic space group *P*. The asymmetric unit of **1** consists of one Cd(II) ion, one half 1,4-bmeib, one half ao_2btc and one aqua ligands. Ao_2btc ligand displays new coordination mode in **1** and each ao_2btc ligand acts a decadentate ligand in which 3,3'-carboxyl groups display bidentate chelating mode and 5,5'-carboxyl groups exhibit bidentate chelating and monodentate bridging modes, connecting to six metal centers. Each Cd(II) ions are bridging by 3,3'-and 5,5'-carboxylate oxygen atoms of ao_2btc ligand to form 1D double chains with the 26-membered rings. Adjacent 1D double chains are linked by 5,5'-carboxy groups of ao_2btc with $\text{Cd} \cdots \text{Cd}$ distance of 3.876 Å to generate 2D planar structures. 2D structures are extended to 3D porous structure by the coordination of 1,4-bmeib ligand (Fig. 1b).

Acknowledgements This work has been supported by The Scientific and Technological Research Council of Turkey (TUBITAK, No: 113Z313).

References

[1] He, Y.; Zhou, W.; Qian, G.; Chen, B., *Chem. Soc. Rev.* **2014**, 43, (16), 5657-5678.

[2] Erer, H.; Yeşil, O. Z.; Arıcı, M.; Keskin, S.; Büyükgüngör, O., *J. Solid State Chem.* **2014**, 210, (1), 261-266.



Figure 1. (a) The crystal structure of **1** with the atom labeling and (b) 3D structure of **1**

Keywords: Coordination polymers, azoxybenzenetetracarboxylate

MS30-P8 Three dimensional Zinc(II) and Cadmium(II)-Metal Organic Frameworks (MOFs) based on 3,3',5,5'-Azobenzenetetracarboxylate and bis(imidazole) ligands

Okan Zafer YEŞİLEL¹, Mürsel ARICI¹, Murat TAŞ², Hakan ERER¹

1. Department of Chemistry, Eskişehir Osmangazi University, 26480 Eskişehir, Turkey

2. Department of Science Education, Ondokuz Mayıs University, 55139, Samsun, Turkey

email: yesilel@ogu.edu.tr

The design and synthesis of coordination polymers have attracted attention due to their potential applications in the fields such as gas adsorption/separation, catalysis, conductivity, luminescence, magnetism and fascinating topologies [1]. Organic linkers and metal clusters containing secondary building units (SBUs) are very important to obtain three dimensional (3D) coordination polymers with the desired structures [2]. In this study, two novel coordination polymers, namely $\{[Zn_2(abtc)(1,4\text{-betib})]\cdot DMF\}_n$ (**1**) and $\{[Cd_2(abtc)(1,4\text{-betix})]\cdot DMF\}_n$ (**2**) (H₄abtc=3,3',5,5'-azobenzenetetracarboxylic acid, 1,4-betib = 1,4-bis(2-ethylimidazole-1-yl)butane and 1,4-betix = 1,4-bis(2-ethylimidazole-1-ylmethyl)benzene) were synthesized and structurally characterized by elemental analysis, IR spectra, single crystal X-ray diffraction. Complexes **1** and **2** were synthesized by the solvothermal methods at 100 °C in the presence of HNO₃. Single crystal X-ray diffraction analyses reveal that **1** and **2** crystallize in the monoclinic and orthorhombic systems with the space groups C2/c, P2₁2₁2₁, respectively. The crystal structures of **1** and **2** with the atom labeling are shown in Fig. 1. As seen in Fig 1, the Zn(II) and Cd(II) ions are five coordinated with a distorted square pyramidal geometry by four oxygen atoms from four different abtc ligands and one nitrogen atom from bis(imidazole) ligands. Each abtc ligand acts as an octadentate ligand, 3,3'-carboxyl and 5,5'-carboxyl groups display bis(monodentate) bridging modes to connect to eight metal centers. Topological analysis revealed that both complexes are 3,6 connected sqc5381 net. Thermal and photoluminescence properties of the complexes were investigated in detail.

Acknowledgements

This work has been supported by The Scientific and Technological Research Council of Turkey (TUBITAK, project no: 113Z313).

References

- [1] J. R. Li, Y. G. Ma, M. C. McCarthy, J. Sculley, J. M. Yu, H. K. Jeong, P. B. Balbuena, H. C. Zhou, *Coord. Chem. Rev.* 255 (2011) 1791-1823.
- [2] C. Raptopoulou, Y. Sanakis, K. Lazarou, A. Georgopoulou, M. Pissas and V. Psycharis, *Polyhedron* 34 (2015) 783-788.

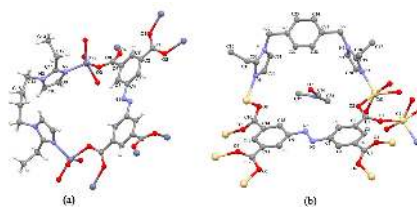


Figure 1. The crystal structures of **1** (a) and **2** (b) with the atom labeling

Keywords: Coordination polymers, azobenzenetetracarboxylate, bis(imidazole) ligands

MS30-P9 Na₃CoS₃: A new sulfido cobaltate with simple formula, but complex structure

Pirmin Stübke¹, Jan Kägi¹, Caroline Röhr¹

¹ Albert-Ludwigs-Universität Freiburg, Germany

email: pirmin@pyrite.chemie.uni-freiburg.de

Alkali sulfido metallates have been extensively investigated by the Bronger group in the 1980s [1]. In the case of the sodium cobaltates, Na₆[CoS₄] containing isolated tetrahedra [2], and the 'chain' compounds Na₃[CoS₂] [3] and Na₃[Co₂S₄][S] [4] are the only compounds obtained in these studies.

Applying an alternative synthetic route in directly reacting the pure transition metals and elemental sulfur with the alkali metals (or their previously prepared sulfides), the structure family of the respective ferrates has been substantially extended in the last years [5-6]. Accordingly, the new sulfido cobaltate(II) Na₃CoS₃, which forms dark grey xenomorphic crystals, was synthesized from the pure elements, with a small amount of CoS₂ and Na₆[CoS₄] as by-products, in melt flux reactions from a sulfur rich sample with the composition like e.g. Na:Co:S = 2.4:1:6.6 at a maximum temperature of 760 °C.

Contrary to the initial assumption based on the formula, the new compound does not contain Co(III), but is a quite complex sulfido cobaltate(II), which exhibits both sulfido and disulfido ligands besides each other. According to Na₃[Co₂S₆][Co₂S₄], the acentric orthorhombic structure (space group *Cmca*) with a large unit cell (*a*=884.24(2), *b*=2177.38(5), *c*=1193.20(3) pm, *Z*=12), which has been determined by mean of single crystal X-ray data (*R*₁=0.0205), contains two different, both yet unknown sulfido cobaltate ions: The oligomeric anions [Co₂S₆]⁸⁻ are built up from two edges sharing [CoS₄] tetrahedra. In contrast to common disulfido metallates, one of the terminal sulfido ligands S₂²⁻ is substituted by a η¹-disulfido ligand S₂²⁻ ([Co₂S₄(S₂)]⁸⁻). Chains of [CoS₄] tetrahedra, which are alternatingly connected via edges and corners, form the second building block. Herein, the disulfido ions as μ²-ligands are connecting two corner-sharing tetrahedra. Similar anions are yet only observed in the selenido gallate Cs₃Ga₂Se₅ [7]. The seven different Na cations are arranged inbetween the layers at heights *x* = 1/4 and 3/4 (CN = 5 - 8).

[1] W. Bronger, *Angew. Chem. Int. Ed. Engl.* **20**, 52 (1981).

[2] K. Klepp, W. Bronger, *Z. Naturforsch.* **38b**, 12 (1983).

[3] K. O. Klepp, W. Bronger, *J. Less-Common Met.* **98**, 165 (1984).

[4] W. Bronger, C. Bomba, *J. Less-Common Met.* **158**, 169 (1990).

[5] M. Schwarz, C. Röhr, *Inorg. Chem.* **54**, 1038 (2015).

[6] M. Schwarz, M. Haas, C. Röhr, *Z. Anorg. Allg. Chem.* **639**, 360 (2013).

[7] D. Friedrich, M. Schlosser, A. Pfitzner, *Z. Anorg. Allg. Chem.* **640**, 826 (2014).

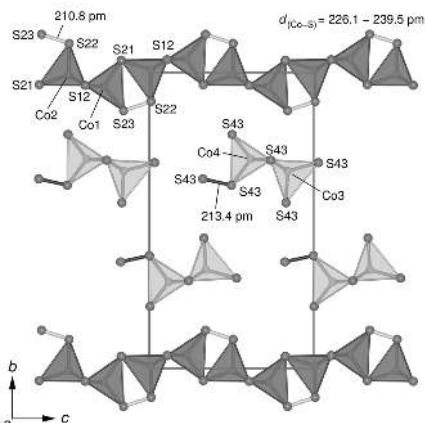


Figure 1. Arrangement of the two anions to form layers in the *b-c* plane. Chains Niggli formula: $^{1}_{\infty}[\text{CoS}_2\text{S}_{1/2}(\text{S}_{1/2})]^{4-} = [\text{Co}_2\text{S}_5]^{4-}$. Dimere formula: $[\text{Co}_2\text{S}_6(\text{S}_2)]^{8-}$.

Keywords: sulfido cobaltates, thiocobaltates, disulfide, synthesis

MS30-P10 New copper(II) halogenobenzoate complexes with nicotinamide: isomerism and supramolecular structure

Jan Moncol¹, Jozef Halaska¹

1. Institute of Inorganic Chemistry, FCHPT, Slovak University of Technology, Radlinského 9, SK-812 37 Bratislava, Slovakia

email: jan.moncol@stuba.sk

Nicotinamide (nia) has been employed as a supramolecular reagent [1,2]. Some copper(II) carboxylate complexes have shown that the intermolecular H-bonds can alter their magnetic properties. We have recently published mononuclear molecular complex [3] and binuclear molecular complex [4], which exhibit similar magnetic properties. These very similar magnetic properties of mononuclear as well as binuclear complexes could be explained by the presence of very similar H-bond systems, supramolecular synthons, that are pathway for antiferromagnetic interactions. In this report we present various crystal structures of new copper(II) halogenobenzoate complexes with nicotinamide of formulas $[\text{Cu}(\text{X-bz})_2(\text{nia})_2]$ and $[\text{Cu}(\text{X-bz})_2(\text{nia})_2(\text{H}_2\text{O})_2]$. The two polymorphs of $[\text{Cu}(\text{2,6-Cl}_2\text{bz})_2(\text{nia})_2]$ are examples of coordination compounds, which are conformation and supramolecular isomers. Additionally, the $[\text{Cu}(\text{X-bz})_2(\text{nia})_2(\text{H}_2\text{O})_2]$ and $[\text{Cu}(\text{X-bz})_2(\text{nia})_2] \cdot 2\text{H}_2\text{O}$ present examples of coordination isomerism. The molecules of all compounds are connected by $\text{N} \cdots \text{H} \cdots \text{O}$ and/or $\text{O} \cdots \text{H} \cdots \text{O}$ hydrogen bonds from NH_2 groups of nicotinamide and water molecules, which create supramolecular hydrogen-bonding-coordination chains and networks.

[1] J. Halaska, A. Pevec, P. Strauch, B. Kozlevcar, M. Koman, J. Moncol, *Polyhedron* **2013**, 61, 20. [2] J. Moncol, J. Mmaroszova, M. Koman, M. Mazur, T. Lis, *J. Coord. Chem.* **2008**, 61, 3740. [3] Z. Vaskova, J. Moncol, M. Korabik, D. Valigura, J. Svorec, T. Lis, M. Valko, M. Melnik, *Polyhedron* **2010**, 29, 154. [4] D. Valigura, J. Moncol, Z. Pucekova, T. Lis, J. Mrozinski, M. Melnik, *Eur. J. Inorg. Chem.* **2006**, 3813.

Keywords: nicotinamide, isomerism, hydrogen bonds, copper(II) benzoate

MS30-P11 Tailoring supramolecular assemblies of β -diketonato Co(II) and Ni(II) complexes

Mladen Borovina¹, Magdalena Malik^{1,2}, Toni Lijić¹, Gregor Talajić¹, Ivan Kodrin¹, Boris-Marko Kukovec¹, Marijana Đaković¹

1. Department of Chemistry, Faculty of Science, University of Zagreb; Horvátovac 102a; 10000 Zagreb, Croatia

2. Faculty of Chemistry, Wrocław University of Technology; Smoluchowskiego 23, 50-370 Wrocław, Poland

email: mborovina@chem.pmf.hr

In order not to rely on serendipity when targeting a desired physical property, we need an improved understanding of how metal-complexes can be organized and assembled into 3D solids using relatively weak and reversible interactions. Certain supramolecular synthons have already proved to be promising and reliable tools in engineering of crystalline organic substances. To examine the robustness and reliability of those synthons in metal-organic systems we have opted for β -diketonato complexes. β -Diketonates are a promising class of chelating ligands that eliminate the need for involvement of additional anions into the building of supramolecular assemblies. In this way, the functionalities are not exposed to the (usually) disruptive nature of counter ions commonly encountered in metal-organic systems, and are expected to communicate and interact with each other in the same manner as they do in purely organic systems. Nevertheless, the outcomes of our best theoretical and experimental efforts are often surprising.

Here, we report on a series of β -diketonato complexes of Co(II) and Ni(II) with selected structure directing N-heterocyclic ligands with the intention of giving an insight into the requirements that have to be met by the ligand itself, as well as by the complex as a whole, for the expected supramolecular behaviour to be achieved. The data are complemented by CSD data mining and extensive computational methods are used to facilitate the interpretation of the experimental efforts.

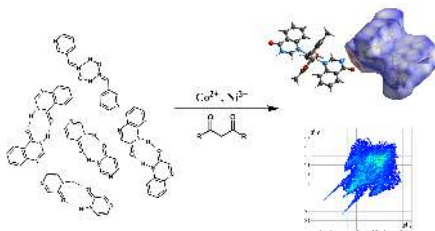


Figure 1. From selected ligands to final products and results.

Keywords: Metal Complexes, Crystal Engineering

MS30-P12 Novel complexes of copper(II) with $[\text{MnCl}_4]^{2-}$ anionJuraj Kuchár¹, Erika Samolová¹¹. Institute of Chemistry, Department of Inorganic Chemistry, P. J. Šafárik University in Košice, Košice, Slovakia

email: juraj.kuchar@upjs.sk

At present, hydrogen bonding mediated magnetism is a well-documented phenomenon [1] and the results of magnetic studies have shown that the exchange parameter J can reach as high values as 38.3 K [2]. The study of magnetic and thermodynamic properties of structurally 1D compound $\text{Cu}(\text{en})_2\text{Ni}(\text{CN})_4$ (en = 1,2-diaminoethane) in the very low temperature region (below 0.5 K) corroborated its magnetically 2D character; as additional exchange paths to the covalent bonds the present HBs of the N-H...N type were suggested. The character of the magnetic exchange interactions is very weak and is in line with long exchange path through the diamagnetic -NC-M-CN- five-atomic bridge. In order to shorten this five-atomic bridge we have undertaken a study of a series copper(II) compounds in which $[\text{M}(\text{CN})_4]^{2-}$ bridging species were replaced by $[\text{MnCl}_4]^{2-}$ anion. The use of this anion as a bridging unit enhances the attractiveness of these Cu(II)-Mn(II) bimetallic chain systems from magnetic properties point of view. The use of ethylenediamine's methyl derivatives lead to structurally similar 1D compounds as it was in the case of $\text{Cu}(\text{en})_2\text{Ni}(\text{CN})_4$ in which copper(II) atoms are linked by anion species. Surprisingly the use of the macrocyclic ligand *cyclam* (*cyclam* = 1,4,8,11-tetraazacyclotetradecane) led to different structural arrangement and the crystal structure analysis reveal 3D character of the structure, where besides the expected chains of -Cu-Cl-Mn-Cl-Cu- type another chain of -Mn-Cl-Mn-Cl-Mn- type that connecting them appeared. In order to investigate this phenomena we have prepared and characterized several new derivatives of the *cyclam* and used them for preparation of new complexes. The results of the crystal structure determination have shown formation of 1D chains; the hexa-coordinated Cu(II) atoms are surrounded by one molecule of blocking ligands and two chlorine atoms in *trans* position linking Cu(II) atoms with Mn(II) atoms as it was in above mentioned compounds. Further details of the synthesis, characterization and molecular and crystal structures of all compounds will be given.

This work was supported by the Slovak grant agency APVV under contract Nos. APVV-0132-11 and by grant agency VEGA (grant 1/0075/13).

[1] Costa J.S., Bandeira N.A.G., Guennic B.L., Robert V., Gamez P., Chastanet G., Ortiz-Frade L., Gasque L., *Inorg. Chem.* 50 (2011) 5696–5705. [2] Baran P., Boča R., Breza M., Elias H., Fuess H., Jorík V., Klement R., Svoboda I., *Polyhedron*, 21 (2002) 1561–1571.

Keywords: hydrogen bonds, copper and manganese compounds

MS30-P13 Crystallographic analysis of iridium(I) N-heterocyclic carbene complexes of benzimidazol-2-ylideneMerve İzmirli¹, Aytac G. Gökçe¹, Süleyman Gülcemal², Muhittin Aygün¹¹. Department of Physics, Dokuz Eylül University, 35160 Buca, İzmir, Turkey.². Department of Chemistry, Ege University, 35100 Bornova, İzmir, Turkey

email: izmirli.merve@yahoo.com

The transition metal complexes of N-heterocyclic carbenes (NHCs) based on imidazol, imidazolin and benzimidazole framework have been the focus of intense research in organometallic chemistry and homogeneous catalysis.^{1–4} The crystal and molecular structures of Ir(I) NHC complexes have been determined by single crystal x-ray diffraction technique. In both complexes, iridium atoms lie in a slightly distorted square-planar coordination environments defined by the coordination of the metal to the two olefinic bonds of the cyclooctadiene ligand, the carbon atom of the NHC ligand and the chlorine atom (Figure 1). The iridium–NHC bond lengths agreed (COD) well with the values found in other NHC-supported $[\text{Ir}(\text{COD})\text{Cl}]$ complexes.

¹ N-heterocyclic carbenes: From laboratory curiosities to efficient synthetic tools, ed. S. Díez-González, RSC Catalysis Series No. 6, Royal Society of Chemistry, Cambridge, 2011.

² F.E. Hahn and M.C. Jahnke, *Angew. Chem., Int. Ed.*, 2008, 47, 3122.

³ W.A. Herrmann, *Angew. Chem., Int. Ed.*, 2002, 41, 1290.

⁴ K.J. Cavell and D.S. McGuinness, *Coord. Chem. Rev.*, 2004, 248, 671.

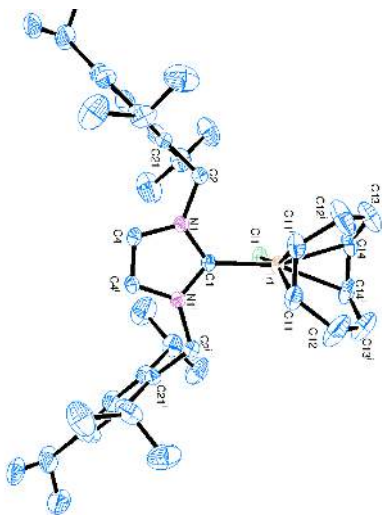


Figure 1. The molecular structure of the complex with displacement ellipsoids drawn at the 30% probability level and hydrogen atoms have been omitted for clarity.

Keywords: N-heterocyclic carbene, Ir(I) complex, benzimidazol-2-ylidene, crystal structure

MS30-P14 Ligand type and synthetic approach induced variability of supramolecular topologies of $[\text{Ni}_4\text{L}_4(\text{ROH})_4]$ AND $[\text{Ni}_4\text{L}_4(\text{ROH})_X(\text{R}'\text{OH})_Y]$; $X+Y=4$

Gordana Pavlović¹, Mirta Rubčić², Višnja Vrdoljak², Marina Cindrić²

1. University of Zagreb, Faculty of Textile Technology, Department of Applied Chemistry Prilaz baruna Filipovića 28a, HR-10000 Zagreb, Croatia

2. University of Zagreb, Faculty of Science, Department of Chemistry, Horvátovac 102a, HR-10000 Zagreb, Croatia

email: gordana.pavlovic@ttf.hr

The synthesis of polynuclear cluster compounds of the Mn, Fe, Ni, V and Co or mixed metals represents a number of challenges. Often it is difficult to predict the exact cluster structure due to potentially variable outcomes of self-assembly process. Owing to a wide range of their potential applications, *e.g.* in data storage, memory devices, switches and sensors, considerable attention has been devoted to the targeted synthesis of such systems. The impact of reversible release and reabsorption of both coordinated and uncoordinated solvent molecules on the cluster properties is well documented in the literature.¹ These processes are accompanied by the structural changes related to a cleavage/formation of the coordination bonds.^{2,3} Among different cluster types that can exhibit those features, cubane-like clusters with $[\text{Ni}_4(\mu_3\text{-O})_4]$ core are especially well studied class. The cubane-like core of nearly all investigated tetranuclear Ni(II) complexes consists of four identical $\mu_3\text{-O}$ bridges originating from -OH or -OR moieties. The symmetry of $[\text{Ni}_4\text{O}_4]$ core and the differences in the $\text{Ni}-\mu_3\text{-O}-\text{Ni}$ angles often have a decisive role in establishing intramolecular magnetic interactions. $[\text{Ni}_4\text{L}_4(\text{solv})_4]$ type of complexes can undergo reversible exchange of the coordinated solvent molecules (MeOH vs. H_2O).⁴ Although the structural alterations induced by such solvent exchange were subtle, substantial changes of the physical and chemical properties have been established. This study unveiled novel synthetic aspects and interesting structural features of a new family of Ni(II) compounds based on cubane-like clusters. Depending on reaction conditions different cubane-like clusters of the type $[\text{Ni}_4\text{L}_4(\text{ROH})_4]$ and $[\text{Ni}_4\text{L}_4(\text{ROH})_X(\text{R}'\text{OH})_Y]$ (H_2L = tridentate Schiff base ligand,

N -(2-hydroxy-5-methylphenyl)salicylideneimine, $\text{R} = \text{-CH}_3$, $\text{-C}_2\text{H}_5$, $\text{-C}_3\text{H}_7$, $\text{-C}_4\text{H}_9$ i $\text{-C}_5\text{H}_{11}$) were isolated (Fig.1). The various supramolecular phenomena such as polymorphism, conformational isomorphism and synmorphism were established. These phenomena will be discussed in detail on the basis of structure-property relationships. ¹ H. Zheng–Ming, X.–M. Zhang, *Dalton Trans.* 2011, 40, 2092–2098. ² E.–C. Yang, *et. al.*, *Polyhedron* 2003, 22, 1727–1733. ³ M. Moragues–Cánovas, *et. al.*, *Eur. J. Inorg. Chem.* 2004, 2219–2222. ⁴ A. Das, *et. al.*, *Inorg. Chem.* 2012, 51, 8141–8149.

Keywords: cubane-like clusters $[\text{Ni}_4\text{L}_4(\text{solv})_4]$; solv = ROH, tridentate Schiff base ligand, synthesis, supramolecular topologies

MS30-P15 Crystal structure and synthesis of two complexes: bis[(2-amino benzamide)(benzoate)]copper(II) and bis[(2-amino benzamide)(benzoate)]cobalt(II)

Canan Aytuğ Ava¹, Ömer Çelik^{1,2}, Tuba Kiyak³, Akif Arslan⁴, Mehmet Aslantaş⁵

1. Dicle University Science and Tecnology Application and Research Center, Dicle University, 21280 Diyarbakır, TURKEY
2. Physics Education Department, Ziya Gökalp Education Faculty, Dicle University, 21280
3. Physics Department, KSÜ, Avsar Campus, 46100 Kahramanmaraş, TURKEY
4. Düziçi Vocational School, Osmaniye Korkut Ata University, Osmaniye, TURKEY

email: cananaytug@hotmail.com

In this study, we describe the synthesis and X-ray structural determination of two complexes: bis[(2-amino benzamide)(benzoate)]copper(II) and bis[(2-amino benzamide)(benzoate)]cobalt(II), (**1** and **2**). Both Cu(II) and Co(II) ions in **1** and **2** have distorted octahedral geometry environments, and also forming four six-membered chelate rings. For the puckering-parameters values (Q , θ , and φ), the A, B, C, and D rings for the complex molecules **1** and **2** are almost boat conformations. In both complexes, the molecules are linked by O-H...O, N-H...O, C-H...O, C-H...N interactions and van der Waals forces.

We would like to thank Dr.Şemistan Karabuğa at Chemistry Department, KSU and DÜBTAM, University of Dicle, staff for their assistance without which this work could not have been accomplished.

Keywords: Metal Complex, Benzoic Acid, X-ray Crystallography.

MS30-P16 Synthesis, structural characterization, and biological analyses of $[C_{21}H_{23}Cu(II)N_2O_{12}]$ complex

Ömer Çelik^{1,2}, Akif Arslan³, Uğur Çömlekçioglu⁴, Ashabil Aygan⁴, Mehmet Aslantaş⁵

1. Physics Education Department, Ziya Gökalp Education Faculty, Dicle University, 21280 Diyarbakır, TURKEY
2. Dicle university DUBTAM X-ray lab. Sur, 21280, Diyarbakır, Turkey
3. Düziçi Vocational School, Osmaniye Korkut Ata University, Osmaniye, TURKEY
4. Biology Department, KSÜ, Avsar Campus, 46100 Kahramanmaraş, TURKEY
5. Physics Department, KSÜ, Avsar Campus, 46100 Kahramanmaraş, TURKEY

email: celiko21@yahoo.com

The title compound, $[C_{21}H_{23}Cu(II)N_2O_{12}]$, was synthesized from the reaction between 3,5-dihidroksibenzoic acid and 2-aminobenzamide in the presence of copper(II) sulfate, and characterized by means of X-ray single crystal diffraction method. The crystallographic analysis reveals that the geometry around the copper ion has a distorted pyramidal geometry by two O atoms, two N atoms and an O atom of H₂O molecule. The N-H...O strong intra- and O-H...O, N-H...O and C-H...O inter-molecular hydrogen bonding interactions mainly stabilize the crystal structure and form an infinite 3-dimensional network. Besides weak X-H... π and π ... π stacking interactions involving neighboring chains are also observed. Additionally, some effects of the metal complex on hydrolytic enzymes which are *Endo-1,4- β -Ksilanaz* and *Endo-1,4- β -Glukanaz*, and antimicrobial activity studies of the complex were carried out by using the various bacteria and fungi.

Keywords: Metal Complex, Benzoic Acid, X-ray Crystallography, Antimicrobial, Enzymatic Activity.

MS30-P17 Two-step spin transition and superstructure in an iron(II) coordination network based on flexible bitopic ligand 1-(tetrazol-1-yl)-3-(1,2,3-triazol-1-yl)propane

Joachim Kusz¹, Maria Ksiazek¹, Robert Bronisz², Marek Weselski²

1. Institute of Physics, University of Silesia, 40007 Katowice, Poland

2. Faculty of Chemistry, University of Wrocław, F. Joliot-Curie 14, 50383 Wrocław, Poland

email: joachim.kusz@us.edu.pl

The spin crossover (SCO) in iron(II) systems bring a lot of attention due to the possibility of switching between high (HS, S=2) and low (LS, S=0) spin state using different stimuli like temperature, pressure, AC magnetic field or light. The SCO is usually accompanied by change of other properties like: magnetic, optical, structural, dielectric, etc. In particular, it is connected with the step change of the Fe-ligand bond lengths. The structural distortion caused by the modification of structural parameters of chromophore FeN_6 propagates further, changing also the second coordination sphere. The spread of the deformation on the whole crystal leads to the appearance of the cooperative effects, including structural bistability, which is a basis for the potential applications in molecular electronics [1].

A majority of the structural studies concentrate only on the investigations of the two stable states LS and HS. The knowledge only of the crystal structures of the initial and final phases is not sufficient to establish correlations between the structural and magnetic properties of the SCO system.

$[\text{Fe}(\text{pttrz})_3](\text{ClO}_4)_2 \cdot \text{CH}_3\text{CN}$ (where $\text{pttrz}=1-(1,2,3\text{-triazol-1-yl})-3-(\text{tetrazol-1-yl})\text{propane}$) is a interesting SCO compound with 2D coordinated network, because exhibits two step complete SCO and only 25% of iron(II) ions undergo HSgLS transition during the first step [2].

A detailed inspection of the diffraction data provides very weak satellite reflections ($h + 1/2$, $k + 1/2$, $l + 1/2$) what is evidence for long-range ordering of the HS and LS Fe(II) iron ions within chains. Research of the superstructure of $[\text{Fe}(\text{pttrz})_3](\text{ClO}_4)_2 \cdot \text{CH}_3\text{CN}$ will increase the understanding of propagation processes of the structural distortions and as a result allow to rationally design new materials. In particular, it will aid in increasing of the cooperative character of SCO in the polymeric systems by the choice of proper ligands bridging the SCO centres.

The work was supported by the Polish National Science Centre (grant number DEC 2011/01/B/ST5/06311).

[1] P. Gutlich, H. A. Goodwin, *Top. Curr. Chem.* **2004**

[2] A. Bialonska, R. Bronisz, J. Kusz, M. Zubko, *Eur. J. Inorg. Chem.* **2013**, 884–893

Keywords: iron(II) compounds, two-step spin transition, superstructure

MS30-P18 Synthesis and structure characterization of biologically active triphenyltin complexes with thioamides

Agata Owczarzak¹, Anita Owczarzak¹, Maciej Kubicki¹, Marek Murias², Małgorzata Kucińska²

1. Adam Mickiewicz University

2. Poznań University of Medical Sciences

email: agataowczarzak@gmail.com

It has been proved that organotin compounds have anticancer properties but the exact mechanism of antitumor action is still unknown^[1,2]. Analysis of relationships between drug structure and the biological response can be a key to understanding cytotoxic activity. New organotin (IV) complexes with heterocyclic thioamides 2-mercaptoimidazoline (thimt) and 4,6-diamino-2-mercaptopyrimidine (4,6-dapmt) of formulae $[\text{Ph}_3\text{SnCl}(\text{thimt})]$ (**1**) and $[\text{Ph}_3\text{Sn}(4,6\text{-dapmt})]$ (**2**) have been synthesized and characterized by FT-IR, NMR, and X-ray diffraction. Deprotonated ligands bond to a metal through the sulfur atom. In both complexes of tin centers are 5-coordinated in less (1) or more (2) distorted (fig. 1). In **1** the coordination is by three carbon (equatorial plane), one chlorine and one sulphur atoms. In **2** weak Sn–N interactions complete the coordination sphere around the tin. It's the unique example of the structure of Ph_3SnXY system with axial-equatorial arrangement of the phenyl groups. Alternatively structure might be viewed as very distorted tetrahedron.^[3]

The complexes **1** and **2** were tested for in vitro cytotoxic activity against LMS (leiomyosarcoma cells), MCF7 (breast), HeLa (cervical) and CCD39LU (normal human lung fibroblast). Both complexes showed a better cytotoxic activity then clinically established chemotherapeutic cisplatin for all three cancer cell lines. Triphenyltin derivatives exhibit different chemosensitivity of all cell lines, but the best cytotoxic activity was established for LMS cell lines. Moreover, compounds **1** and **2** have less effect on the proliferation of normal cell types. These results showed that these complexes can be novel antitumor drug candidates.

References

[1] S.Tabassum C. Pettinari, *Journal of Organometallic Chemistry* Volume 691, 2006, 1761–1766

[2] P. J. Smith, *Chemistry of Tin*, Black Academic& Professional: London, 1998

[3] M. N. Xanthopoulou, S.K. Hadjikakou, N. Hadjilias, M.Kubicki, *Inorg. Chem.*, 2007, 46 (4), 1187–1195

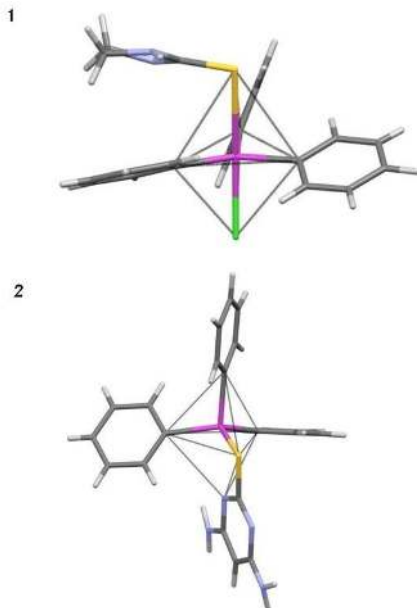


Figure 1. Coordination models of tin cations in (1) and in (2)

Keywords: X-ray crystallography, organotin(IV) complexes, heterocyclic thioamides, antitumor activity,

MS30-P19 X-ray structural analysis and catalytic properties of new thiazoline - carboxylate ruthenium complexes

Betül Şen¹, Serpil Denizaltı², Aytaç Gürhan Gökçe¹, Muhittin Aygün¹

1. Department of Physics, Dokuz Eylül University, 35160 Buca, İzmir, Turkey

2. Department of Chemistry, Ege University, 35100 Bornova, İzmir, Turkey

email: senbetulsen@gmail.com

X-ray Structural Analysis and Catalytic Properties of New Thiazoline - Carboxylate Ruthenium Complexes

Heterocyclic compounds such as thiazol(in)es, thiazolidines, oxazol(in)es have received large attention. These heterocycles are of importance as pharmaceuticals and ligands for catalysis. The thiazol(in)e ring is present in many biological active natural and synthetic products. There is a great number of publications related to biological activities of thiazoline scaffold. Metal complexes of carboxylate ligands such as picolinic acid, proline, quinoline or isoquinoline carboxylic acid, thiazole or thiazolidine carboxylic acid, bipyridine carboxylic acid are known and investigated their luminescence, structural properties, biological activities [1].

In the proposed study, X-ray diffraction analysis of Ruthenium complexes were performed using an Agilent Diffraction Xcalibur diffractometer equipped with an Eos-CCD detector. Data were absorption-corrected within the CrysAlis program [2]. Structures were solved by SHELXS-97 and refined by means of SHELXL-97 programs [3] incorporated in the OLEX2 program package [4]. Their catalytic activities were evaluated for ATH. These catalyst systems showed excellent activity for a range of ketone and aldehyde substrates tested. Attempts to obtain enantioselective products by lowering the temperature or increasing the catalyst loading, failed the *ee* values. In this work, high yields were obtained in the transfer hydrogenation reaction.

References

- [1] R. Staehle, L. Tong, L. Wang, L. Duan, A. Fischer, M. S. G. Ahlquist, L. Sun, S. Rau, *Inorg. Chem.* 2014, 53, 1307-1319.
- [2] CrysAlis^{Pro} Software system, Version 1.171.35.11, Agilent Technologies UK Ltd, 2011.
- [3] G. M. Sheldrick, *Acta Crystallogr. Sect. A* 2008, 64, 112-122.
- [4] O. V. Dolomanov, L. J. Bourhis, R. J. Gildea, J. A. K.. Howard, H. Puschmann, *J. Appl. Cryst.* 2009, 42, 339-341.

Keywords: Thiazoline, Ruthenium complexes, Crystal structure, Catalytic analysis

MS30-P20 Synthesis, structure and reactivity of $[\text{Cu}(\text{phen})_2]\text{BrO}_2$ aerobic oxidation of Br^- to BrO_2^- at room temperature

Shin-Guang Shyu¹, Md.Munkir Hossain¹, Chi-Rung Lee², Mei-Chun Tseng¹

1. Institute of Chemistry, Academia Sinica

2. Department of Chemical Engineering, Minghsin University of Science and Technology, Taiwan

email: sgshyu@gate.sinica.edu.tw

Unusual $4e^-$ oxidation of Br^- ion into a BrO_2^- ion occurred during the reaction between CuBr_2 and phenanthroline under air to form $[\text{Cu}(\text{phen})_2]\text{BrO}_2$ complex. ESI-MS of the compound confirm the presence of BrO_2^- in the solution. Its oxidation reactivity is different from its analogue $[\text{Cu}(\text{phen})_2]\text{ClO}_2$

Keywords: Aerobic oxidation / Bromide ion / Bromite ion / Copper

MS30-P21 The effect of weak interactions on the shape of cadmium(II) coordination polymers with pyridine-based hydrazines

Boris-Marko Kukovec¹, Nikolina Penić¹, Nives Matijaković¹, Marijana Đaković¹

1. Division of General and Inorganic Chemistry, Department of Chemistry, Faculty of Science, University of Zagreb, Horvátovac 102a, HR-10000 Zagreb, Croatia

email: bkukovec@chem.pmf.hr

Coordination polymers are infinite systems build up from metal ions and organic ligands (linkers) as the main units assembled via coordination bonds and weak interactions (hydrogen bonds, π - π interactions, metal-metal interactions, metal-aromatic interactions) [1]. Coordination polymers can extend in one, two or three dimensions. The 1D motif can be represented by linear, zigzag, double, ladder-like chains or helices. 2D and 3D coordination polymers are often called metal-organic frameworks (MOF). These materials have been used in crystal engineering due to their structural diversity and their applications as porous materials, in catalysis, ion exchange and gas storage [2]. Coordination polymers can also have other interesting properties e. g. nonlinear optics, luminescence and magnetism. We have prepared a series of cadmium(II) coordination polymers with isoniazid and niazid and various counterions (chloride, bromide, iodide, thiocyanate). Isonicotinylhydrazine (isoniazid) and nicotinylhydrazine (niazid) are suitable linkers for construction of coordination polymers as they are multidentate ligands - *N,O*-bidentate and *N*-bridging. They are capable of satisfying cadmium(II) coordination number (usually 5-7) by acting as *N,O*-bidentate ligands and they bridge the metal ions at the same time (via pyridine N atom). The aim of our study was to determine the effect of the counterions size, shape and their involvement in weak interactions on dimensionality of cadmium(II) polymers with isoniazid and niazid. In case of chloride and bromide use, we obtained 1D polymers with double chains, linked via chloride/bromide bridging atoms (Fig. 1a), while in case of iodide use, a 1D polymer with zigzag chain was formed, containing terminal iodide ions only. A 2D polymer was obtained by using thiocyanate ion, as it is an ambidentate ligand with N and S donor atoms, enabling the formation of a network (Fig. 1b). The polymers were also studied by IR spectroscopy, PXRD and thermal methods (TG/DTA, DSC) and various crystallization techniques were employed to get suitable single crystals for X-ray structure analysis.

References: [1] A. Y. Robin, K. M. Fromm, *Coord. Chem. Rev.* 250 (2006) 2127.; [2] U. Mueller, M. Schubert, F. Teich, H. Puetter, K. Schierle-Arndt, J. Pastré, J. Mater. Chem. 16 (2006) 626.

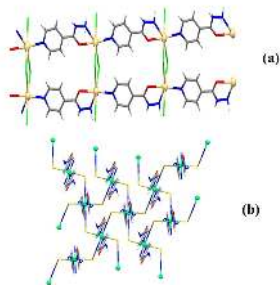


Figure 1. Cadmium(II) 1D coordination polymer with chloride and isoniazid (a) and 2D coordination polymer with thiocyanate and isoniazid (b)

Keywords: coordination polymer, cadmium, isoniazid, niiazid, crystal structure, weak interactions

MS30-P22 Structural, spectroscopic and activity studies of biomimetic resorcinarene-based zinc and copper complexes

Aleksandar Višnjevac¹, Jérôme Gout², Olivia Bistri², Olivia Reinaud²

1. Institut "Ruder Bošković", Bijenička 54, 10000 Zagreb, Croatia

2. Université Paris Descartes, CNRS UMR 8601, 45, Rue des Saints Pères, F-75006 Paris, France

email: aleksandar.visnjevac@irb.hr

The syntheses, chemical characterizations, and activity studies of Zn(II), Cu(I) and Cu(II) "bowl" complexes, based on the resorcin[4]arene scaffold with three imidazole-containing coordinating arms at the large rim, is presented. These complexes are biomimetic models of a mononuclear active site where cofacial triade of amino-acid residues holds the metal coordinated. The trisimidazole ligand RIm3 was prepared in a seven-steps procedure. The complexes of Zn(II), Cu(I) and Cu(II) were prepared by simple reactions of the ligand with stoichiometric amounts of corresponding salts. Spectroscopic studies [and X-ray single crystal analysis in case of the Cu(II) acetato complex] revealed a 5-coordinate SBP environment for the Zn(II) and Cu(II) centres provided by three imidazole arms, and two extra donors, one embedded inside the resorcinarene cavity, the other in exo position. These two labile sites are occupied by solvent molecules or residual water, and are readily displaced by carboxylate donors, the position of which (endo or exo) is under tight control of the cavity. The reaction of RIm3 ligand with Zn(II) or Cu(II) acetates led to the formation of the acetato complexes with the acetate irreversibly embedded inside the cavity. The molecular structure of the Cu(II) acetato complex features a rigidified resorcinarene bowl. The isolated resorcinarene basket possess a non-crystallographic, $4mm$ point symmetry, and can easily host small guest molecules. Three methylimidazole-containing coordinating arms at the large rim coordinate the Cu (II) ion. Its coordination sphere is completed by two O atoms from the intra-cavity bound acetate. The electron donors form a distorted square pyramide, where one of the nitrogens is at the apical position. The endo-coordination of the acetate is supported by an extensive network of intramolecular C-H...O and C-H... π interactions. Complex crystallizes in $P2_1/c$ space group; $a = 32.3310$ (4) Å, $b = 11.5490$ (1) Å, $c = 21.6020$ (2) Å, $\beta = 102.281$ (3)°.

[1] Višnjevac, A.; Gout, J.; Ingert, N.; Bistri, O.; Reinaud, O. (2010) *Org. Lett.* **12**, 2044 - 2047.

[2] Gout, J., Višnjevac, A., Rat, S., Bistri, O., Le Poul, N., Le Mest, Y. & Reinaud, O. (2013) *Eur. J. Inorg. Chem.* 5171 – 5180.

[3] Gout, J., Višnjevac, A., Rat, S., Parrot, A., Hessani, A., Bistri, O., Le Poul, N., Le Mest, Y. & Reinaud, O. (2014) *Inorg. Chem.* **53**, 6224 – 6234.

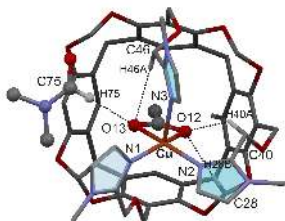


Figure 1. Structure of [Rlm₃Cu(II)CH₃COO]ClO₄, top view

Keywords: resorcinarene, biomimetic, zinc, copper, X-ray single crystal diffraction, IR, NMR, EPR

MS30-P23 Through the looking glass: anomalies and packing

Alice Brink¹

¹ University of the Free State, Chemistry Department, P.O. Box 339, Bloemfontein, 9301, South Africa

email: alice.brink@gmail.com

The formation and substitution of mono-, bi- and tridentate ligand substituted organometallic complexes to tailor the reactivity and biological activity of potential radiopharmaceuticals is filled with unexpected developments. X-ray crystallography grants undeniable advantages to “peer through the looking glass” in understanding the chemical trends in Group 7 (I) tricarbonyl complexes.

Our interest in the variation induced by ligand systems on *fac*-[M(CO)₃]⁺ complexes allows for interesting solid state as well as solution mechanistic studies utilising a range of spectroscopic techniques in addition to crystallography. The mixed ligand concept supports the platform of labelling the bioactive molecules to the transition metal complex utilising various bifunctional chelators. The solid state behaviour and the kinetic rate of substitution are widely influenced by the charge of the coordinated ligand system and the effects of the substituted monodentate incoming ligand. Isostructural and polymorphic crystallization effects will be described in addition to the substitution effects caused by incoming ligands with various acid/ base characteristics.

Keywords: Radiopharmaceutical design, substitution kinetics

MS30-P24 Molecular and crystal structures of hydroxyl and ester functionalized N-heterocyclic carbene complexes of iridium(I)

Merve İzmirli¹, Aytaç G. Gökçe¹, Derya Gülcemal², Süleyman Gülcemal², Muhittin Aygün¹

1. Department of Physics, Dokuz Eylül University, 35160 Buca, İzmir, Turkey.

2. Department of Chemistry, Ege University, 35100 Bornova, İzmir, Turkey

email: muhittin.aygun@deu.edu.tr

Because of their extraordinary properties, N-heterocyclic carbenes (NHCs) have found access to a great variety of catalytic processes which include C-C coupling reactions, formation of furans, cyclopropanation, olefin metathesis, hydroformylation, polymerization and hydrosilylation reactions.¹⁻⁵ The crystal and molecular structures of Ir(I) NHC complexes have been determined by single crystal x-ray diffraction technique. In both complexes, the coordination geometries around the iridium centers, formed by the coordination to the metal of the two olefinic bonds of the cyclooctadiene ligand, the carbon atom of the NHC ligand and the chlorine atom, are slightly distorted square-planar (Figure 1). The Ir-C(NHC) distances are within the expected range and consistent with other NHC-supported [Ir(COD)Cl] complexes.

¹ N-heterocyclic carbenes: From laboratory curiosities to efficient synthetic tools, ed. S. Díez-González, RSC Catalysis Series No. 6, Royal Society of Chemistry, Cambridge, 2011.

² F.E. Hahn, *Angew. Chem., Int. Ed.*, 2006, 45, 1348.

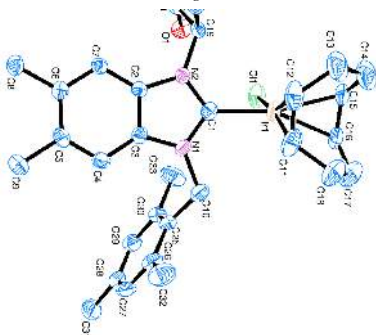
³ V. César, S. Bellemin-Lapponnaz and L.H. Gade, *Chem. Soc. Rev.*, 2004, 33, 619.

⁴ C.M. Crudden and D.P. Allen, *Coord. Chem. Rev.*, 2004, 248, 2247.

⁵ W.A. Herrmann, *Adv. Organomet. Chem.*, 2002, 48, 1.

Figure 1. The molecular structure of the complex with displacement ellipsoids drawn at the 30% probability level and hydrogen atoms have been omitted for clarity.

Keywords: N-heterocyclic carbene, Ir(I) complex, hydroxyl and ester functionalization, crystal structure



MS30-P25 Structure and activity study of gold(I) catalysts in the presence of thiols and amines

Georgina M. Rosair¹, Ai-Lan Lee¹, Paul C. Young¹, Samantha L. Green¹

1. Institute of Chemical Sciences, Heriot-Watt University, Edinburgh, EH14 4AS, United Kingdom

email: g.m.rosair@hw.ac.uk

Homogenous Gold catalysis has evolved from the rare and unusual to a rapidly evolving area of research. Gold catalysts act as π -Lewis acids for activating C-C π bonds but it is their capacity for fine tuning to control the selectivity and activity of reactions as well as their ready availability and robustness to oxygen that makes gold catalysts shine¹.

This work describes the quest to find the identity and activity of gold species present in gold catalysed reactions with cyclopropenes, allenes and allylic alcohols. A range of common nucleophiles, namely alcohols, thiols and amines have been employed in these reactions. Yet the presence of these nucleophiles could dramatically alter both selectivity and reactivity of the gold catalyst. Therefore we needed to identify the gold species present in these reactions to understand what was happening².

A pattern emerged of nucleophilicity and gold centre nuclearity in the degree of activity and identity of the gold species in these gold catalysed reactions.

1.M. Jia and M. Bandini, *ACS Catal.* 2015, **5**, 1638–1652

2.P. C. Young, S.L.J. Green, G.M.Rosair and A-L. Lee, *Dalton Trans.*, 2013, **42**, 9645

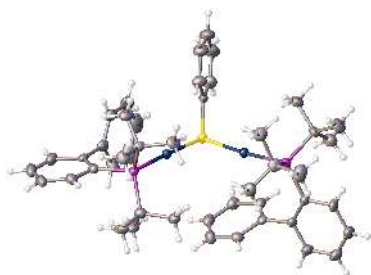


Figure 1. Gold complex in the presence of thiols. Counterion omitted for clarity

Keywords: gold catalysis, activity, nucleophile

MS30-P26 A heterometallic oxalate compound with square $\{\text{Cr}_2\text{Nb}_2(\mu\text{-O})_4\}$ core as precursor for mixed oxide

Marijana Jurić¹, Lidija Androš Dubraja¹, Jasminka Popović¹

1. Ruder Bošković Institute, Bijenička cesta 54, 10000 Zagreb, Croatia

email: Marijana.Juric@irb.hr

Recent research related to the multicomponent Nb-containing oxide materials revealed their very appealing structural and physical properties, leading to their development for a wide range of technological applications, such as ferroelectric and piezoelectric materials, ion conductors, and also as promising catalysts in several highly challenging processes.^[1] Lately, metal–organic coordination systems have been used as single-source precursors for the preparation of mixed-metal oxides through thermal decomposition. This method, compared with conventional methods, has several advantages: (i) the obtained material is more homogeneous because the metals are mixed at the molecular level; (ii) the resulting materials have relatively high specific surface areas because the oxides are formed under significantly milder conditions; (iii) there is much greater control of the metal stoichiometry in the final products; and (iv) there are no long-term and repeated grinding procedures. The oxalate anion, $\text{C}_2\text{O}_4^{2-}$ easily decomposes to the vapor phases CO_2 and CO through the low-temperature routes, and hence, the heterometallic oxalate-based compounds are suitable for the use as molecular precursors for mixed oxides.^[1–3]

Hence, due to the growing need for Nb-based oxides, further investigation of the Nb-containing heterometallic oxalate compounds that could serve as single-source precursors is of great importance. As a continuation of our studies,^[1–3] novel compound $[\text{Cr}(\text{bpy})_2(\mu\text{-O})_2\text{Nb}(\text{C}_2\text{O}_4)_2]_2 \cdot 3\text{H}_2\text{O}$ (**1**) (bpy = 2,2'-bipyridine) was synthesized and characterized by single-crystal X-ray diffraction, IR and UV/Vis spectroscopy and thermal analysis. The molecular structure of **1** exhibits a square shaped $\{\text{Cr}_2\text{Nb}_2(\mu\text{-O})_4\}$ core in which oxo-bridged Cr^{3+} and Nb^{5+} ions reside in alternate corners (Figure 1). Both metal ions display the octahedral coordination geometry. Thermal treatment of **1** at 1000 °C leads to molecular precursor-to-material conversion that yields the mixed-metal CrNbO_4 oxide, explored by powder X-ray diffraction.

[1] M. Jurić, J. Popović, A. Šantić, K. Molčanov, N. Brničević, P. Planinić, *Inorg. Chem.*, 2013, **52**, 1832–1842; [2] L. Androš, M. Jurić, J. Popović, A. Šantić, P. Lazić, M. Benčina, M. Valant, N. Brničević, P. Planinić, *Inorg. Chem.*, 2013, **52**, 14299–14308; [3] J. Habjanić, M. Jurić, J. Popović, K. Molčanov, D. Pajić, *Inorg. Chem.*, 2014, **53**, 9633–9643.

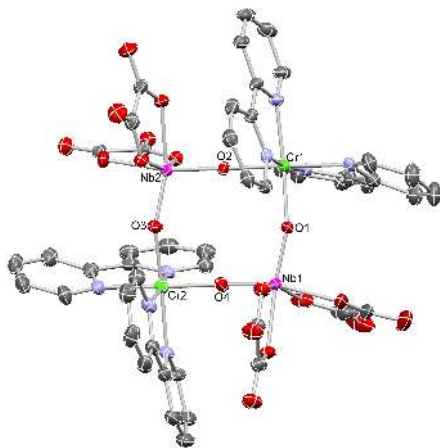


Figure 1. A view of the tetranuclear $[\text{Cr}_2(\text{bpy})(\mu\text{-O})\text{Nb}_2(\text{C}_2\text{O}_4)_3]$ molecule in 1. Displacement ellipsoids are drawn at the 30% probability level. Hydrogen atoms on the aromatic rings are omitted for clarity.

Keywords: heterometallic complex, oxalate ligand, oxo bridges, molecular precursor-to-material conversion, chromium niobate

MS30-P27 Isoquinoline-based Werner clathrates with xylene isomers: Aromatic interactions vs. molecular flexibility

Merrill M. Wicht¹, Nikolett B. Bathori¹, Luigi R. Nassimbeni²

1. Department of Chemistry, Cape Peninsula University of Technology, P.O.Box 652, Cape Town. 8000. South Africa

2. Department of Chemistry, University of Cape Town, Rondebosch, Cape Town. 7700. South Africa

email: wichtm@cput.ac.za

Werner clathrates are inclusion compounds of general formula $\text{MX}_2\text{L}_4\cdot n\text{G}$, where M is a divalent metal cation (typically Ni(II), Co(II), Fe(II), Cu(II) and Mn(II)), X is an anionic ligand (NCS^- , NCO^- , CN^- , NO_3^- or halide), L is a substituted pyridine or α -arylalkylamine, and G is a Guest, usually an organic aromatic compound. The separation of isomers, with similar boiling points, melting points and other physical properties, is difficult to accomplish by classical separation methods. In pursuit of a Werner clathrate which would provide a better system of aromatic interaction between the host and the guest, but simultaneously be selective for xylene isomers,¹ an isoquinoline-based clathrate was made.

The crystal structures of the Werner clathrates $\text{Ni}(\text{NCS})_2(\text{isoquinoline})_4$ (**H**) with *para*-xylene (**px**), *meta*-xylene (**mx**) and *ortho*-xylene (**ox**) have been elucidated. The kinetics of thermal decomposition of the three inclusion compounds were performed. Selectivity of **H** for the xylene isomers was determined by headspace gas chromatography for both the liquid and vapour phase binary mixtures of the xylenes.² Hirshfeld surfaces and fingerprint plots of **H** with the three guests were projected to illustrate the interactions between the host and guest. The chosen ligand has two fused rings which give it a larger aromatic system to improve the possible π interactions between **H** and the selected guests. The rigidity of the isoquinoline ligand, however, causes its lack of selectivity compared to a related Werner complex containing torsional flexibility of the phenyl moieties in the 4-phenylpyridine ligands.³

1. Lipkowski J. et al., Werner Clathrates in *Comprehensive Supramolecular Chemistry*. 20: 6 (1996) 691-714

2. Wicht, M.M., Báthori, N.B. and Nassimbeni, L.R., 2015, *Dalton Trans.*, DOI:10.1039/c5dt0084

3. Lusi M. and Barbour L.J. *Angew.Chem.Int.Ed.* 51 (2012) 1-5

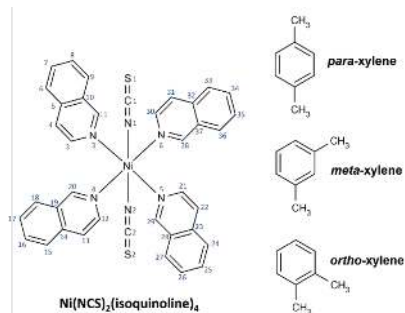


Figure 1. Scheme 1 Structural line diagrams and atomic numbering scheme of the host, $\text{Ni}(\text{NCS})_2(\text{isoquinoline})_4$, and the xylene isomers

Keywords: Werner clathrate, selectivity, torsional flexibility

MS30-P28 Interactions in rare-earth coordinated complexes grown from ionic liquids: application to the extraction and separation of rare earths

Jeroen Jacobs¹, Binnemans Koen², Van Meervelt Luc¹

1. Biomolecular Architecture, KU Leuven, Celestijnenlaan 200F, 3001 Leuven

2. Laboratory of Inorganic Chemistry, KU Leuven, Celestijnenlaan 200F, 3001 Leuven

email: jeroen.jacobs@chem.kuleuven.be

Extracting and separating the rare earths is a highly demanding process due to their similar chemical properties. The topic to recycle and separate mixtures of rare earths from scrap has been a major research topic over the last few years [1] due to the diminishing of the rare earth reserves and safekeeping of own stock. Since 1970, industry uses a liquid-liquid solvent extraction mechanism by coordinating the mixtures of rare earths with an extracting agent. Each entity is distributed over the aqueous and organic phase, with each consecutive extraction improving the separation and purity of the elements. Our research focuses on improving this process by using ionic liquids as extracting agents and looking at the formed entities at a structural level as current research is solely based on calculating thermodynamical parameters of the extraction/separation process. When dissolving a rare-earth salt into an ionic liquid, the elements are coordinated by the anionic entities of the ionic liquid to form an anionic complex. The organic cation of the ionic liquid neutralizes this and migrates the rare earth to the organic phase. Disturbances in interactions between the anion and cation can change the level of migration. By studying these key interactions, we try to relate them to the overall extraction process.

Different rare-earth salts were dissolved in ionic liquids containing β -diketonate anions and large organic cations such as 1-alkyl-3-methylimidazolium or tetraalkylammonium. After extraction, crystals were grown from the organic phase and measured. Current research results show that a non-classical hydrogen bond is persistent across the different molecules, whilst C-H...F interactions between the cation side chain and halogens on the β -diketonate add extra stability to the crystal structure. When comparing these side chain interactions with solubility data we noticed that these have a major impact on the stability and therefore extractability in the organic phase. Structures formed with 2-thenyltrifluoroacetate anions have little to no intention to form side chain interactions, leaving the alkyl chains of the cation disordered, whilst structures formed with hexafluoroacetylacetonate have strong side chain interactions, which leads to a better packing and crystal stability.

[1] Dupont, D.; Binnemans K., *Green Chemistry*, 2015, 17, 856–868

Keywords: Rare-earths, Ionic liquids, interactions

MS30-P29 Structure of carbonyl isocyanide complexes with Rhenium and Manganese: carbon monoxide releasing molecules for biological applications

Emmanuel Kottelat¹, Aurélien Crochet¹, Fabio Zobi¹

1. University of Fribourg, Switzerland

email: emmanuel.kottelat@unifr.ch

CO releasing molecules (CORMs) are widely investigated in synthetic and medicinal chemistry owing to the potential therapeutic applications of the gas. Medical scrutiny of CORMs pivots around treatment of inflammations, microbial infections and organ injuries. Organometallic carbonyl complexes are best suited to play the role of CO carriers as they allow the exogenous release of CO under controlled conditions and permit to overcome the toxicity of the gas. With the long-term goal of developing CORMs with similar properties to those of the *sesta*-methoxyisobutylisonitrile (MIBI) ^{99m}Tc complex (Cardiolite), we have studied the reactivity of isocyanide ligands (namely *tert*-butyl (tbu), isopropyl (ipp), cyclohexyl (chx), *S*-methylbenzyl (smb), tetramethylbutyl (tmb), and MIBI) towards 16-, 17-electron *cis*-[Re(CO)₂Br₄]⁻²⁻ species and the [Mn(CO)₅Br] complex. Group 5 metal ions were selected as Re and Mn-based CORMs show low cytotoxicity and demonstrated a protective action against ischemia-reperfusion injuries. A total of 6 different isocyanide ancillary ligands (CNR's), including MIBI, were selected for this study. Their reaction with the *cis*-dicarbonyl Re(III) and Re(II) complexes was accompanied by a 2 or 1 electron reduction of the metal center and resulted in the formation of stable *cis-mer*-[Re(CO)₂L₃Br] species (where L = CNR), while the same reactions with [Mn(CO)₅Br] gave *fac*-[Mn(CO)₃L₂Br] compounds. All complexes were characterized including single-crystal X-ray diffraction structure determinations. In addition, unique monocarbonyl species were obtained from the reactions of *cis*-[Re(CO)₂Br₄]⁻ with *tert*-butyl-isocyanide and *cis*-[Re(CO)₂Br₄]⁻²⁻ with MIBI. The species, an heptacoordinated Re(III) and a hexacoordinated Re(II) complex, could also be isolated and structurally characterized. The CO releasing, the cytotoxicity and antibacterial properties of the compounds were also investigated.

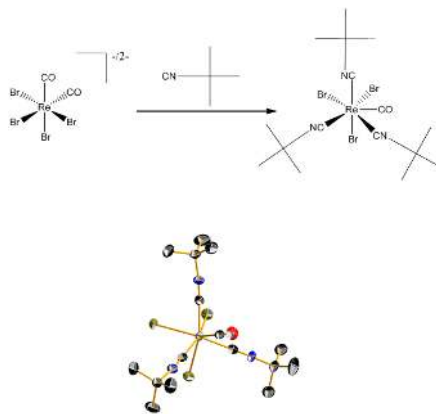


Figure 1. Reaction of [Re(CO)₂Br₄]⁻²⁻ with *tert*-butyl isocyanide ligand, giving the heptacoordinated d⁴, 18e⁻ complex

Keywords: CORM, isocyanide, rhenium, manganese, biocompatible

MS30-P30 Metal-organic frameworks assembled from lanthanide and 2,5-pyridinedicarboxylate with cubane-like $[Ln_4(OH)_4]$ building units

Mohammed Said Mohammed Abdelbaky¹, Mohammed S. M. Abdelbaky¹, Zakariae Amghouz^{1,2}, Santiago García-Granda¹, José Ruben García¹

1. Departamentos de Química Física y Analítica y Química Orgánica e Inorgánica, Universidad de Oviedo-CINN, 33006 Oviedo, Spain

2. Servicios Científico Técnicos, Universidad de Oviedo-CINN, 33006 Oviedo, Spain

email: saidmohammed.uo@uniovi.es

Lanthanide-organic frameworks (LOFs) have recently gained tremendous attention due to their luminescence¹ and magnetic properties². However, the unique features of Ln^{3+} make them ideal for developing new multifunctional materials. Herein, three novel LOFs based on 2,5-pyridinedicarboxylate (**25p**) ligand, formulated as $[Yb_4(OH)_4(25p)_4(H_2O)_3] \cdot H_2O$ (**25pYb**), $[Y_4(OH)_4(25p)_4(H_2O)_3] \cdot H_2O$ (**25pY-1**) and $[Y_4(OH)_4(25p)_4(H_2O)_3] \cdot H_2O$ (**25pY-2**), have been obtained as single phases under hydrothermal conditions. **25pYb** and **25pY-1** crystallize in the triclinic space group, $P\bar{1}$, with $a = 8.6075(5)$ Å, $b = 14.8478(7)$ Å, $c = 15.9164(9)$ Å, $\alpha = 86.277(4)^\circ$, $\beta = 80.196(5)^\circ$, $\gamma = 81.785(4)^\circ$ for **25pYb**, and $a = 8.7166(6)$ Å, $b = 14.966(1)$ Å, $c = 15.966(1)$ Å, $\alpha = 86.260(6)^\circ$, $\beta = 80.036(6)^\circ$, $\gamma = 81.599(6)^\circ$ for **25pY-1**, while, **25pY-2** crystallizes in the monoclinic space group, $P2_1/c$, with $a = 24.912(7)$ Å, $b = 13.7340(8)$ Å, $c = 14.3385(10)$ Å, $\beta = 100.551(7)^\circ$. The compounds have been characterized by single-crystal X-ray diffraction, X-ray powder diffraction, thermal analyses (TG-MS), scanning electron microscopy (SEM-EDX), and powder X-ray thermogravimetric analysis. **25pYb** is isostructural to **25pY-1** and their structures are based on isolated tetranuclear cubane-like $[Ln_4(OH)_4]^{8+}$ clusters, which are interconnected to eight neighbouring clusters through **25p** ligands leading to neutral 3D framework. While **25pY-2** is based on two independent cubane-like $[Y_4(OH)_4]^{8+}$ clusters, which are joined together through Y cation leading to the formation of a hexanuclear $[Y_6(OH)_6]^{10+}$ clusters, which in turn are joined via Y_2 cation resulting in infinite inorganic chain extending along c -axis, and these chains are connected through **25p** ligands leading finally to 3D framework. The luminescence properties of Eu^{3+} and Tb^{3+} doped **25pY-1** and **25pY-2** compounds have also been investigated and exhibit, respectively, strong red and green light emissions which are due to the efficient energy transfer process from the **25p** ligand to Eu^{3+} and Tb^{3+} .

References: (1) Z. Amghouz, S. G. Granda, J.-R. García, R.A.S. Ferreira, L. Mafra, L. D. Carlos, J. Rocha, *Inorg. Chem.* 51(2012), 1703-1716. (2) X. Feng, L.F. Ma, L. Liu, L.Y. Wang, H.L. Song, S.Y. Xie, *Cryst. Growth Des.* 13(2013) 4469-4479.

Acknowledgments: We thank financial support from Spanish Ministerio de Economía y Competitividad (MINECO-13-MAT2013-40950-R, FPI grant BES-2011-046948 to MSM-A and *Técnicos de Infraestructuras Científico-Tecnológicas* grant PTA2011-4903-I to Z-A) and ERDF.

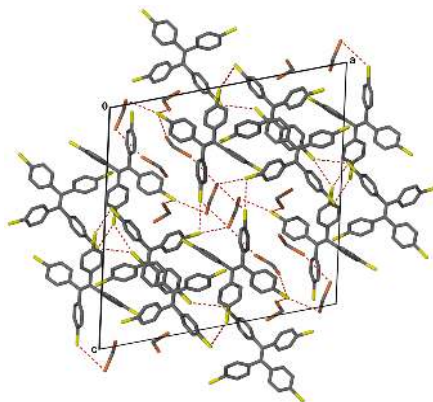


Figure 1. Cubane-like $[Yb(OH)_4]^{8+}$ cluster (a). The two independent cubane-like clusters (b). Projection of **25pYb** along the a -axis (c). Perspective view of the **25pY-2** along b -axis (d). Green emission for **25pYb-Tb-1** (e) and red emission for **25pYb-Eu-2** (f) upon UV light excitation.

Keywords: LOFs, Clusters, Luminescence

MS30-P31 Coordination polymers of the types $[MX_2(4\text{-cypy})_x]_n$ and $[MX_2py_x]_n$: syntheses, polymorphism and structure relations

Alexander Bodach¹, Haishuang Zhao², Yasar Krysiak², Lothar Fink¹, Miriam Heine¹, Jürgen Glinnemann¹, Edith Alig¹, Martin U. Schmidt¹

1. Institute of Inorganic and Analytical Chemistry, Goethe University, Max-von-Laue-Str. 7, 60438 Frankfurt/Main, Germany
2. Institute of Physical Chemistry, Johannes Gutenberg University, Jakob-Welder-Weg 11, 55128 Mainz, Germany

email: ax.bodach@yahoo.com

Syntheses and structural characterizations of coordination polymers have constituted a rapidly expanding field of research in the last decades, due to their interesting physical properties and potential applications. [1]

We report on the polymorphism of $[\text{CoBr}_2(4\text{-cypy})_2]_n$ and $[\text{NiCl}_2(4\text{-cypy})_2]_n$ (4-cypy = 4-cyanoipyridine). Both phases show octahedral coordination of the M^{II} ions, which is built up by two N-donor ligands and completed by bridging halide ions in the equatorial plane. This motif typically leads to chains in the $[MX_2(4\text{-cypy})_x]_n$ and the $[MX_2py_x]_n$ phases with $M^{\text{II}} = \text{Mn, Co, Ni, Cu, Pd, X} = \text{Cl, Br}$.

For the phases of the types $[MX_2(4\text{-cypy})_x]_n$ and $[MX_2py_x]_n$, ($x < 2$), the degree of polymerization increases with decreasing x which results in the constitution of double chains, bands or planes, depending on the structural requirements of the bridging halide ions and the potential bidentate co-ligand 4-cyanopyridine.

The structure relations of the above mentioned coordination polymers with different values of x are discussed. [2–5]

References:

- [1] S. R. Batten et al., *Pure Appl. Chem.* **85**(8),1715, **2013**
- [2] Y. Krysiak et al., *ZAAC* **640**(15), 3190, **2014**
- [3] H. Zhao et al., **2015**, in preparation
- [4] H. Zhao, *Master thesis*, Frankfurt/Main **2014**
- [5] A. Bodach, *Bachelor thesis*, Frankfurt/Main **2015**

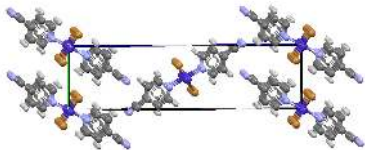


Figure 1. Crystal structure of $[\text{CoBr}_2(4\text{-cypy})_2]_n$ projected along a . Monoclinic space group $P 1 2_1/n 1$. Pseudo orthorhombic, minimal non-isomorphic supergroup $P 2/m 2_1/n 2_1/n$.

Keywords: Coordination polymers, structure relations, crystal engineering, polymorphism, condensed networks, substituted pyridine ligands

MS30-P32 A row of $(\text{XeF}_5^+)\text{M}_2^+(\text{SbF}_6^-)_3$ ($\text{M} = \text{Mg, Ni, Mn, Co, Cu, Zn}$) compounds: peculiarities of crystal structure, limit of isomorphic substitution, merohedral twinning

Evgeny Goreshnik¹, Zoran Mazej¹

1. Department of Inorganic Chemistry and Technology Jožef Stefan Institute Jamova 39 1000 Ljubljana Slovenia

email: evgeny.goreshnik@ijs.si

Mixed-cation compounds of general formula $(\text{XeF}_5^+)\text{M}_2^+(\text{SbF}_6^-)_3$ ($\text{M} = \text{Mg, Ni, Mn, Co, Cu, Zn}$) have been synthesized and structurally investigated using single crystal diffraction technique. A wide row ($\text{Mg, Mn, Co, Cu, Zn}$) derivatives are isotopic and crystallize in a monoclinic $P2_1/n$ space group with a β angle varying from 90.064(3) (Zn) to 90.432(2) (Co). Apex-shared MF_6 and SbF_6 octahedra are interconnected into infinite tridimensional framework with cavities, occupied by XeF_5^+ cations (Fig. 1). All investigated $(\text{XeF}_5^+)\text{M}_2^+(\text{SbF}_6^-)_3$ salts demonstrate more or less pronounced merohedral twinning with the same twinning law. Increasing of ionic radii (Hg) has led to a formation of completely different $(\text{XeF}_5)_3[\text{Hg}(\text{HF})]_2(\text{SbF}_6)_7$ compound.

Keywords: Mixed-cation compounds

MS30-P33 Structural diversities of manganese(II) complexes based on benzenedicarboxylate ions and 2,2'-dipyridylamine

Jelena R. Rogan¹, Lidija D. Radovanović², Dejan D. Poletić¹, Marko V. Rodić³

1. Faculty of Technology and Metallurgy, University of Belgrade, Karnegijeva 4, 11000 Belgrade, Serbia
2. Innovation Centre of Faculty of Technology and Metallurgy, University of Belgrade, Karnegijeva 4, 11000 Belgrade, Serbia
3. Faculty of Sciences, University of Novi Sad, Trg Dositeja Obradovića 3, 21000 Novi Sad, Serbia

email: rogan@tmf.bg.ac.rs

In crystal engineering, the anions of benzenedicarboxylic acids (BDC) are commonly used building blocks as they offer a broad array of possible coordination modes to a metal centers. The coordination capacity of BDCs is ranging from mono- to octadentate, resulting in the formation of fascinating metal-organic structures of various dimensionality and potential applications in many fields [1].

In our continual synthetic strategy of ternary transition metal complexes with BDCs [2], a new ongoing challenge is design of Mn(II) complexes. Two novel compounds, $[\text{Mn}(\text{dipya})(\text{pht})(\text{H}_2\text{O})_2]_2$, **1**, and $[\text{Mn}(\text{dipya})(\text{H}_2\text{O})_4](\text{tpht})$, **2**, with dianion of phthalic (pht) and terephthalic (tpht) acid and 2,2'-dipyridylamine (dipya) were hydrothermally prepared and characterized by single crystal X-ray diffraction, TG/DSC analysis and FT-IR spectroscopy.

1 crystallize in triclinic system, $P\bar{1}$ ($a=8.361(2)$, $b=9.126(2)$, $c=11.855(2)$ Å, $\alpha=69.31(3)$, $\beta=77.47(3)$, $\gamma=79.89(3)$ °, $R_1[I>2\sigma(I)]=0.0458$). **2** crystallize in monoclinic system, $P2_1/c$ ($a=7.617(2)$, $b=23.827(5)$, $c=11.087(2)$ Å, $\beta=102.31(3)$ °, $R_1[I>2\sigma(I)]=0.028$).

The coordination numbers of Mn(II) in **1** and **2** are 7 and 6, respectively. The major difference between **1** and **2** is in BDC coordination: the pht in **1** is coordinated as a bridging ligand with bis-chelate COO groups, while the tpht is only a counter ion in **2**. In both structures there are strong non-covalent interactions. In the packing arrangement of **1**, binuclear units are connected by intermolecular hydrogen bonds, forming layers parallel to the *ac*-plane and strengthened by face-to-face π - π interactions (at 3.689 Å). The discrete complex units of **2** are assembled in hydrophobic and hydrophilic pseudo-layers. The hydrogen bonds exist within the pseudo-layers and between them. Finally, 3D architecture is achieved through the π - π stacking interactions (at 3.896 Å) between dipya ligands from the adjacent layers.

[1] S. G. Baca, S. Decurtins, (2012). Phthalates: Chemical Properties, Impacts on Health and the Environment, edited by G. L. Moretti & D. Romano, pp. 1–60. Hauppauge, New York: Nova Science Publishers.

[2] D. Poletić, J. Rogan, M. V. Rodić, L. Radovanović, Acta Cryst. (2015) C71, 110–115; J. Rogan, D. Poletić, Lj. Karanović, Acta Cryst. (2011) C67, m230–m233, J. Rogan, D. Poletić, Lj. Karanović, G. Bogdanović, A. Spasojević-de Biré, D. M. Petrović, Polyhedron (2000) 19, 1415–1421.

Keywords: crystal structure, manganese(II) complex, phthalate ion, terephthalate ion, 2,2'-dipyridylamine

MS30-P34 Co(II) complexes with abpt ligands and pseudohalide anions exhibiting single-ion magnet behavior

Ivan Potočník¹, Lucia Váhovská¹, Svitlana Vitushkina^{1,2}

1. Department of Inorganic Chemistry, Faculty of Science, P.J. Šafárik University, Moyzesova 11, SK-041 54 Košice, Slovakia.

2. Department of Applied Chemistry, V.N. Karazin Kharkiv National University, Svobody sq. 4, UA-61077 Kharkiv, Ukraine.

email: ivan.potocnak@upjs.sk

The early examples of nanomagnets exhibiting slow relaxation of the magnetization (single-molecule magnets (SMMs)) were clusters of transition metal ions but recently mononuclear complexes (called single-ion magnets, SIMs) have been reported [1], even with the positive axial parameter of zero-field splitting (D) [2]. Nevertheless, the origin of SIM properties in mononuclear Co(II) complexes with D>0 remains rather unclear and more examples of this type of compounds are needed to shed light on the subject. With these ideas in mind, we have prepared five centrosymmetric pseudooctahedral mononuclear Co(II) complexes with 4-amino-3,5-bis(2-pyridyl)-1,2,4-triazole (abpt) ligand and nonlinear pseudohalide anions: tricyanomethanide (tcm), nitrocyanamide (nca), nitrodicyanomethanide (nodcm), tetracyanoazapropenide (tcap), and pentacyanoazapropenide (pcp).

Equatorial plane in the [Co(abpt)₂(tcm)₂] complex (**1**) is occupied by pairs of N2 and N3 atoms of two abpt and tcm ligands (Co1–N2 = 2.125(2) and Co1–N3 = 2.133(2) Å), pair of N1 atoms occupy axial positions at 2.109(2) Å (Fig. 1). This slightly compressed octahedral complex shows field-induced slow relaxation of magnetization with large axial single-ion zero-field-splitting parameter D = +48(2) cm⁻¹ [3]. Similar structure exhibits [Co(abpt)₂(nca)₂] (**2**) complex, with N2 and N3 atoms coordinated at 2.144(2) and 2.121(2) Å, respectively and N1 atoms coordinated at 2.086(2) Å. On the other hands, [Co(abpt)₂(H₂O)₂]X₂ (X = nodcm (**3**) and tcap (**4**)) and [Co(abpt)₂(MeOH)₂](pcp) (**5**) complexes exhibit slightly elongated octahedral structures with equatorial planes occupied by pairs of N2 atoms of abpt and O3 atoms of water/methanol ligands at 2.112(2) and 2.118(2) Å (**3**), 2.081(1) and 2.102(1) Å (**4**), and 2.058(1) and 2.109(1) Å (**5**), respectively. N1 atoms occupy axial positions at 2.146(2) (**3**), 2.166(1) (**4**) and 2.151(1) Å. Nodcm (**3**), tcap (**4**) and pcp (**5**) anions remain uncoordinated.

This work was supported by APVV-00014-11, VEGA 1/0598/14 and I-12-001-03. S.V. thanks The National Scholarship Programme of the Slovak Republic for the financial support during her stay at P.J. Šafárik University in Košice.

[1] Woodruff, D.N.; Winpenny, R.E.P.; Layfield, R.A. *Chem. Rev.* **2013**, 113, 5110.

[2] Colacio, E.; Ruiz, J.; Ruiz, E.; Cremades, E.; Krzystek, J.; Carretta, S.; Cano, J.; Guidi, T.; et al. *Angew. Chem., Int. Ed.* **2013**, 52, 9130.

[3] Herchel, R.; Váhovská, L.; Potočník, I.; Trávníček, Z. *Inorg. Chem.* **2014**, 53, 5896.

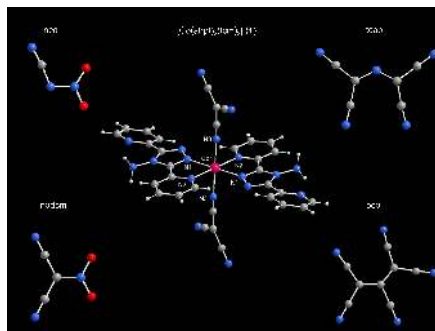


Figure 1. Structure of [Co(abpt)₂(tcm)₂] complex (**1**) along with structures of nitrocyanamide⁻ (nca), nitrodicyanomethanide (nodcm), tetracyanoazapropenide (tcap), and pentacyanoazapropenide (pcp) anions used in complexes **2** – **5**, respectively.

Keywords: Co(II) complexes, abpt, pseudohalides, single-ion magnets

MS30-P35 Novel coordination modes of
2,6-diacetylpyridine
bis(*S*-methylisothiosemicarbazone)

Marko V. Rodić¹, Vukadin M. Leovac¹, Ljiljana S.
Vojinović-Ješić¹

¹. Faculty of Sciences, University of Novi Sad, Trg Dositeja
Obradovića 3, 21000 Novi Sad, Serbia

email: marko.rodic@dh.uns.ac.rs

Thiosemicarbazones (tsc) are important class of *S*-donor ligands [1]. Their transition- and non-transition metal complexes are studied for many years, mainly due to wide variety of their biological activity. Their *S*-alkylated derivatives—*isothiosemicarbazones* (itsc)—are less studied, although they show interesting structural and electrochemical features. As a rule, *isothiosemicarbazones* are coordinated through the azomethine and isothioamide nitrogen atoms, which was also the case with pentadentate (*N*₅) 2,6-diacetylpyridine bis(*S*-methylisothiosemicarbazone) (*H*₂*L*) [2]. However, in [Ni(*HL*)] [3], one *isothiosemicarbazide* moiety of the tetradentate *HL* is coordinated in described way, whereas the other uses nitrogen N3 instead of azomethine nitrogen.

Here we present crystal structures of two copper complexes with this ligand of the formula [Cu(*H*₂*L*)Cl₂Py] (1) and [Cu^{II}₂(*H*₂*L*)₂Br₁₀Cu^I₆] (2) (Fig. 1), where novel coordination modes of this ligand are observed. In 1, ligand acts as *NNN* tridentate through the pyridine and both azomethine nitrogen atoms, so that both isothioamide nitrogen atoms remain uncoordinated. The distorted octahedral coordination polyhedron of Cu(II) is completed by coordination of the pyridine in equatorial, and chloride ligands in axial positions. Unsymmetrical coordination of *H*₂*L* is observed in 2: one *itsc* moiety is coordinated usually through the azomethine and isothioamide nitrogen atoms, whereas the other uses azomethine nitrogen to bind to the Cu(II) atom, and methylated sulfur to bind to the other Cu(I) atom. This complex has centrosymmetrical octanuclear structure, with Cu(II) atoms in square-pyramidal environment, and Cu(I) atoms in trigonal planar environment. It appears that coordination of terminal isothioamide groups can be avoided by introducing co-ligands with good donor capabilities; that coordination of alkylated sulfur atom is possible when acceptors are soft Pearson acids.

[1] T. S. Lobana, R. Sharma, G. Bawa, S. Khanna, *Coord. Chem. Rev.* (2009) 253, 977.

[2] V. M. Leovac, V. Divjaković, V. I. Češljević, R. Fazlić, *J. Serb. Chem. Soc.* (2003) 68, 425; V. M. Leovac, E. Ivegeš, V. I. Češljević, V. Divjaković, U. Klement, *J. Serb. Chem. Soc.* (1997) 62, 837.

[3] V. M. Leovac, G. A. Bogdanović, V. I. Češljević, V. Divjaković, *Acta Cryst.* (2000) C56, 936.

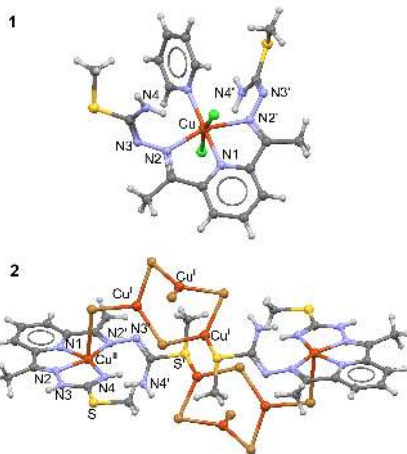


Figure 1. Molecular structures of the complexes Cu(*H*₂*L*)Cl₂Py] (1) and [Cu^{II}₂(*H*₂*L*)₂Br₁₀Cu^I₆] (2)

Keywords: crystal structure, Copper(II) complex, isothiosemicarbazone, 2,6-diacetylpyridine

MS30-P36 Crystal structure and hydrogen bonds pattern of a new hydrated hexafluoridosilicate based on adeninium

Belhouas Ratiba¹, Bouacida Sofiane^{1,2}, Boudaren Chaouki¹

1. Unité de recherche CHEMS, Université Mentouri Constantine, 25000, Algeria.

2. Département SM, Université LBM, Oum El Bouaghi, Algeria.

email: belhouas.ratiba@yahoo.fr

A new hybrid compound based on aminopurinium and hexafluoridosilicate(IV) was synthesized by aqueous solution reaction and characterized by X-ray diffraction. The asymmetric unit of $2C_5H_6N_5^+ \cdot SiF_6^{2-} \cdot 2H_2O$ contains one adeninium cation, half of a hexafluoridosilicate anion located on an inversion centre and one lattice water molecule. The aminopurinium cations are connected through N—H...N hydrogen bonds involving one H atom of the $-NH_2$ group and the H atom of the protonated N atom of the adenine ring system. The overall connection of the cation leads to the formation of planar ribbons parallel to (122). The hexafluoridosilicate anion and the water molecule are linked through O—H...F hydrogen bonds into chains parallel to [100]. The cationic ribbons and anionic chains are finally connected through additional N—H...O, N—H...F and O—H...F hydrogen bonds into a three-dimensional network in which layers of adeninium cations and fluoridosilicate anions alternate parallel to (001).

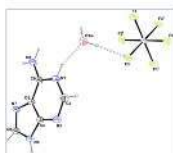


Figure 1. The principal structural units in the title compound. Displacement ellipsoids are drawn at the 30% probability level. H atoms are represented as small spheres of arbitrary radius. Hydrogen bonds are shown as dashed lines. [Symmetry code : (i) $-x, -y, z$]

Keywords: crystal structure, purinium cation, hexafluoridosilicate anion, hydrogen bond.

MS30-P37 Syntheses, structures, thermal stabilities and magnetic behaviors of two oxo-bridged lanthanide frameworks built up from dinuclear units

Belkacem Benmerad¹, Khadidja Aliouane², Narimene Rahahlia², Achoura Guehria-Laidoudi², Slimane Dahaoui³, Claude Lecomte³

1. Laboratoire de Physico-Chimie des Matériaux et Catalyse Faculté des Sciences Exactes, Université de Bejaia, 06000 Bejaia, (Algeria)

2. Laboratoire de Cristallographie et Thermodynamique, USTHB, BP 32, El-Alia, Bab-Ezzouar, Alger, (Algeria)

3. CRM2, UMR-CNRS 7036, Institut Jean Barriol, Université de Nancy 1, BP 230, 54506, Vandoeuvre-les-Nancy cedex, (France)

email: belkacem.benmerad@univ-bejaia.dz

Two three-dimensional polymeric lanthanides $\{Ln_2(C_4H_2O_4)_2(H_2O)_4 \cdot 3H_2O\}_n$, with $Ln = Ho^{3+}$; Gd^{3+} , have been synthesized, characterized by IR spectroscopy, and studied by single crystal X-ray diffraction. Their magnetic and thermal behaviors have been investigated on the light of their structures. These isomorphous compounds, of layer-type structure, contain a non-centrosymmetric dinuclear unit $Ln_2O_2(H_2O)_4$, beside three lattice water molecules stabilizing the 3D open-framework. The building entities are linked together through one classical syn-anti μ_2 -carboxylato- $\kappa_1 O$: $\kappa_1 O'$ bridge and the semi-rigid carbon backbone of the two pentadentate independent ligands. Within the bi-polyhedra, two double μ_2 -O'; $\kappa_2 O, O'$ bridges and a syn-syn classical one, support the magnetic measurements indicating relatively weak and concomitant ferromagnetic/anti-ferromagnetic interactions. The two distinct thermal behaviors evidence the higher metal-water bond strength with the smaller cation, and reveal the great supramolecular effects generated by hydrogen-bonding patterns.

Keywords: lanthanide organic frameworks, dinuclear building unit, thermal stability, supramolecular interactions, magnetic behavior.

MS30-P38 Synthesis and X-ray structural study of two new polymorphs coordination complexes based on imidazol derivative

Bouacida Sofiane^{1,2}, Bouchouit Mehdi², Bouraoui Abdelmalek², Merazig Hocine², Belfaitah Ali³

1. Département sciences de la matière, université Oum El Bouaghi, 04000 Oum El Bouaghi Algeria

2. Unité de Recherche de Chimie de l'Environnement et Moléculaire Structurale, Université Constantine 1, Constantine 25000, Algérie.

3. Equipe de Synthèse de Molécules à Objectif Thérapeutique, Laboratoire des Produits Naturels d'Origine Végétale et de Synthèse Organique, Université Constantine 1, Constantine 25000, Algérie.

email: bouacida_sofiane@yahoo.fr

Polymorphism is very common among pharmaceutical substances. As the polymorphs possess different internal organization within the solid, they often show different melting points, solubilities, chemical reactivity or stability. These can appreciably influence pharmaceutical properties such as dissolution rate and bioavailability. It is therefore important to evaluate the polymorphism in early stages of new formulation studies.

We report here the synthesis, crystallographic study and hydrogen bond interactions of two new polymorph coordination complexes based on imidazol derivative and Cobalt.

Polymorph (I) is triclinic with space group P-1 and cell parameters $a = 7.0882(8)$ Å, $b = 11.9322(12)$ Å, $c = 14.1882(15)$ Å, $\alpha = 71.417(5)^\circ$, $\beta = 86.927(5)^\circ$, $\gamma = 83.489(5)^\circ$, $V = 1129.9(2)$ Å³, and $Z = 2$. Polymorph (II) is monoclinic with space group P 21/n and cell parameters $a = 7.5554(2)$ Å, $b = 13.0466(5)$ Å, $c = 23.3958(9)$ Å, $\beta = 94.405(2)^\circ$, $V = 2299.36(14)$ Å³, and $Z = 4$.

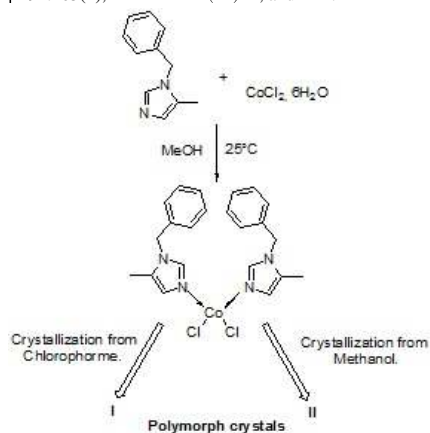


Figure 1. Scheme

Keywords: Polymorphism, single crystal, hydrogen bond, imidazol derivatives

MS30-P39 The role of methanol molecule in supramolecular assembling of [MoO₂L(CH₃OH)] · CH₃OH and [MoO₂L(CH₃OH)] Schiff base type complexes

Robert Katava¹, Gordana Pavlović¹, Marina Cindrić²

1. Department of Applied Chemistry, Faculty of Textile Technology, University of Zagreb, Prilaz baruna Filipovića 28a, Zagreb 10000, Croatia

2. Department of Chemistry, Faculty of Science, University of Zagreb, Horvatovac 102a, HR-10000 Zagreb, Croatia

email: robert.katava@ttf.hr

Investigations of Schiff base molybdenum(VI) complexes have been stimulated by discovery of molybdenum in a number of redox enzymes and their efficiency as catalysts both in heterogeneous and homogenous reactions. Reactions of tridentate O,N,O Schiff base ligands H₃L with [MoO₂(acac)₂] afforded a series of distorted octahedral *cis*-MoO₂²⁺ complexes of the [MoO₂L(CH₃OH)] · CH₃OH (**1-4**) and [MoO₂L(CH₃OH)]₂ (**5**) type. Coordinated CH₃OH molecule, positioned *trans* to oxido oxygen atom, could be readily removed from first coordination sphere of molybdenum(VI) cation, yielding a [MoO₂(L)] intermediate responsible for catalytic activation of substrates during Lewis acid catalyzed transformations.

The supramolecular architecture of complexes is dominated by two types of hydrogen bonds (HB): O–H...O and C–H...O. The supramolecular motif shaped by O–H...O HB in **2, 3** and **4** differs in comparison with that formed by the same type of HB in **1** and **5**.

The infinite chains in **2, 3** and **4** are shaped via the O–H...O HB which include the coordinated CH₃OH oxygen atom, CH₃OH solvent molecule and the oxido oxygen atom of the complex molecule (Fig. 1a). On the contrary, the supramolecular dimers in **1** are formed by two molecules of solvent CH₃OH and two complex molecules via the phenolate oxygen atom and oxygen atom from coordinated CH₃OH (Fig. 1b). Formed dimers are condensed with complex molecules via C–H...O intermolecular hydrogen bond which form centrosymmetric puckered 15-membered ring. (Figure 1b). Complex **5** does not contain solvent molecule of crystallization and the main supramolecular synthon formed via O–H...O hydrogen bond is centrosymmetric dimer between the –OH group of coordinated methanol and the oxygen donor atom of five-membered chelate ring of another complex molecule (Fig. 1c).

The determination of supramolecular role of CH₃OH molecules is essential in the context of complexes solubility and their catalytic activity in the conditions of epoxidation.

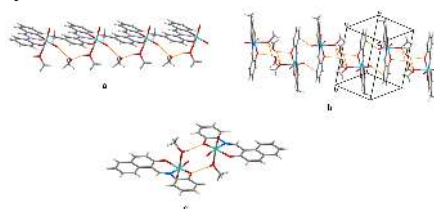


Figure 1. Supramolecular motifs in complexes: 3 (a), 1 (b) and 5 (c).

Keywords: molybdenum(VI) complexes, Schiff bases, supramolecular assembling

MS30-P40 Novel complexes of copper(II) with tridentate hydrazone ligands

Alen Bjelopetrović¹, Marina Cindrić¹, Višnja Vrdoljak¹, Gordana Pavlović²

1. University of Zagreb, Faculty of Science, Chemistry Department
2. University of Zagreb, Faculty of Textile Technology

email: alen.bjelopetrovic@mail.com

New complexes with different structures and properties were obtained by the reaction of *tetrakis*(μ -acetato)diaquadicopper(II) with appropriate hydrazone ligand.

Hydrazones represent the most common type of tridentate ONO donors. They are stabilized by ketamine-enolimine tautomerization as shown by scheme 1.

Hydrazone ligands H_2L^1 , H_2L^2 and H_2L^3 , used in this investigation, were prepared by condensation of benzohydrazide with different aldehydes: salicylaldehyde ($R_1 = H$, $R_2 = H$), 3-metoxysalicylaldehyde ($R_1 = OCH_3$, $R_2 = H$) and 4-metoxysalicylaldehyde ($R_1 = H$, $R_2 = OCH_3$), respectively.

Reactions of *tetrakis*(μ -acetato)diaquadicopper(II) with H_2L^1 , H_2L^2 or H_2L^3 in methanol resulted in formation of polymers of the general formula $[Cu(L)]_n$ while in the case of reaction with H_2L^2 a cuban type tetranuclear cluster $[Cu(L)]_4$ is also obtained. Addition of pyridine to the reaction mixtures of $[Cu(OAc)_2(H_2O)]_2$ and H_2L^1 , H_2L^2 and H_2L^3 resulted in formation of dimeric complexes $[Cu(L)(py)]_2$ with pyridine molecules coordinated to copper atoms. Mononuclear complex $[Cu(L^3)(D)]$ was isolated when in reaction mixture 1,10-phenantroline was added. These complexes are unstable and upon standing at room temperature lose pyridine molecules yielding $[Cu(L)]_2$. After exposure of $[Cu(L)]_2$ to pyridine vapours, it is possible to recover the starting complex. This is accompanied with colour change from pale green to original dark green.

Preliminary magnetochemical measurements of prepared dinuclear and tetranuclear complexes indicate antiferromagnetic arrangement of spins at low temperatures.

All isolated complexes were identified by elemental and thermogravimetric analysis, IR spectroscopy and powder X-ray diffraction method. In case of $[Cu(L)(py)]_2$ ($L = L^1$, L^2 or L^3), $[Cu(L^3)]_4$ and $[Cu(L^3)(D)]$, single crystal X-ray diffraction was additionally used.



Figure 1. Scheme 1. Ketamine-enolimine tautomerization of hydrazones

Keywords: hydrazones, dimeric complexes, cuban type clusters

MS31. Tailored physical properties in molecular crystals

MS31-P2 Crystal structure and gelation properties of naphthalene bioconjugates

Zoran Kokan¹, Berislav Perić¹, Janja Makarević², Goran Štefanić¹,
Leo Frkanec², Srećko I. Kirin¹

1. Materials Chemistry Department, Ruđer Bošković Institute, Bijenička c. 54, Croatia

2. Organic and Biochemistry Department, Ruđer Bošković Institute, Bijenička c. 54, Croatia

email: zoran.kokan@gmail.com

Low molecular mass gelators have been intensively researched in the past decade due to their ease of preparation and potential application in the field of soft and optical materials, transportation media, and as active media for organic reactions and catalysis.¹ Of special interests are chiral gelators where amplification of chiral or luminescent properties can be achieved via gelation.² We have successfully applied amino acid substituted benzene derivatives bearing phosphine moiety as ligands in Rh-catalyzed enantioselective hydrogenation reactions;³ it was shown that the enantioselectivity is strongly dependant of the amino acids used as well as the benzene substitution (*meta*- or *para*-). As an expansion of our research towards the field of soft materials, here we present an ongoing work on amino acid disubstituted naphthalene bioconjugates where solid state and gelation properties are influenced by small modifications of the molecule. Several crystal structures of bioconjugates were obtained. All compounds exhibit hydrogen bonding in their but no π - π stacking was observed. In the case of nonchiral glycine methyl ester derivative, two polymorphs were obtained by slow evaporation of different solvent solutions. It was shown by means of polycrystalline X-ray diffraction that in THF, a single phase is formed whilst in ethanol, both phases are present. The two polymorphs differ only in their characteristic torsion angles of the amide group. All derivatives were tested as gelators in various organic solvents. The results have shown that alanine derivative (Figure 1) with C6-aliphatic chains exhibit super-gelation of nonpolar aromatic solvents.

1. (a) N. M. Sangeetha and U. Maitra, *Chem. Soc. Rev.* **34** (2005) 821–836; (b) L. Frkanec and M. Žinić, *Chem. Commun.* (2010) 522–537; (c) J. Makarević *et al.* *Chem. Eur. J.* **7** (2001) 3328–3341; (d) B. Escuder *et al.* *New J. Chem.* **34** (2010) 1044–1054.2. (a) A. R. A. Palmans and E. W. Meijer, *Angew. Chem. Int. Ed.* **46** (2007) 8948–8968; (b) Z. Zhao, *et al.* *Soft Mater.* **9** (2013) 4564–4579.3. Z. Kokan *et al.* *Organometallics* **33** (2014) 4005–4015.

Chairs: Sebastian Pillet, Pilar Gomez-Sal

MS31-P1 Adaptive structural changes for increased sorption capacity

Vincent J. Smith¹

1. Department of Chemistry and Polymer Science, University of Stellenbosch, Stellenbosch 7600, South Africa

email: vjs@sun.ac.za

A two-dimensional (2-D) metal-organic framework $\{[\text{Zn}(\text{L})_2] \cdot \text{DMF} \cdot \text{H}_2\text{O}\}_n$ (**1**), prepared by the reaction of 4-(1*H*-benzo[d]imidazol-1-yl)benzoic acid (**L**) with $\text{Zn}(\text{NO}_3)_2 \cdot 4\text{H}_2\text{O}$ under solvothermal conditions, can adapt its structure during supercritical carbon dioxide (CO_2) guest-exchange and CO_2 sorption. The 2-D layers of the framework are associated by weak interactions that enable the framework to undergo guest-induced expansion and contraction. At high pressure, additional space is created between adjacent layers resulting in a significant increase in the CO_2 sorption capacity (Figure 1). Moreover, the structural changes and gas uptake by the host occur preferentially for CO_2 at 25 °C while nitrogen (N_2) and methane (CH_4) are not adsorbed under the same conditions. Pressure differential scanning calorimetry (PDSC) and in situ single-crystal X-ray diffraction (SCD) experiments under gas loading were carried out to obtain insight into the dynamic behaviour of the framework.

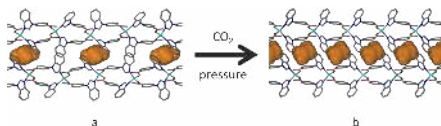


Figure 1. The framework viewed along [100]. a) Discrete mid-sized pockets of the structure observed at low pressure and b) the larger pockets observed at high pressure. Hydrogen atoms and guest molecules have been omitted for clarity.

Keywords: sorption, flexibility, carbon dioxide and hysteresis

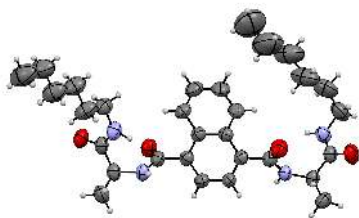


Figure 1. Molecular structure of the alanine bioconjugate.

Keywords: naphthalene, amino acid, bioconjugates, hydrogen bond

MS31-P3 New hybrid materials via a combination of imidazoles and complex hydrides: first compounds and further perspectives

Fabrice J. Morelle¹, Voraksmey Ban¹, Anna Miglio¹, Roman Skoryunov², Alexander Skripov², Geoffroy Hautier¹, Yaroslav Filinchuk¹

1. Institute of Condensed Matter and Nanosciences, Université Catholique de Louvain, Place L. Pasteur 1, 1348 Louvain-la-Neuve, Belgium

2. Institute of Metal Physics, Ural Branch of the Russian Academy of Sciences, Ekaterinburg 620137, Russia

email: fabrice.morelle@uclouvain.be

Since the discovery of zeolites by Axel Frederik Cronstedt in 1756, microporous materials have received an always increasing attention. In this field, the great challenges for chemists were, and still are, to tune the pore size and the pore's surface chemical nature in order to obtain materials with targeted properties while keeping the stability window as large as possible to allow practical applications. Over the past 15 years, Metal-Organic Frameworks (MOFs) received most of the attention in this field thanks to the ease of synthesizing linkers with various sizes, chemical properties, or number of coordination sites.

The recently discovered porous polymorphs of magnesium and manganese borohydride show that the tetrahydroborate anion can also have a structure directing effect as many organic ligands by preferentially making linear metal-BH₄-metal units[1], [2]. The formation of compounds containing both an organic ligand, in this case imidazolate and BH₄ group could lead to the formation of new porous hydrides having the easily tunable properties of imidazolate frameworks.

Li₂ImBH₄ (Im = imidazolate) and Li₂bImBH₄ (bIm = benzimidazolate) were successfully synthesized by liquid assisted grinding and liquid synthesis. Both structures were solved using synchrotron radiation powder diffraction and neutron powder diffraction in the case of LiImBH₄. The main features of these structures are the formation of parallel positively charged [Li₂(b)Im]₂ fibers extending perpendicular to the (benz)imidazolate plane. The charge balancing BH₄ units are located in between these fibers and coordinate to four Li atoms in a square planar environment. Anisotropic temperature factors refined from neutron diffraction data suggests high rotational disorder of the BH₄ unit perpendicular to the square plane. This disorder was investigated and confirmed by solid state NMR and theoretical studies.

This work clearly proves that it is possible to combine hydride and classical ligands in the same structure and that the resulting materials have original and unique properties compared to the pure borohydride or imidazolate compound.

[1] Y. Filinchuk, B. Richter, T. R. Jensen, V. Dmitriev, D. Chernyshov, and H. Hagemann, *Angew. Chem. Int. Ed.*, vol. 50, no. 47, pp. 11162–11166, Nov. 2011.

[2] B. Richter, D. B. Ravnsbæk, N. Tumanov, Y. Filinchuk, and T. R. Jensen, *Dalton Trans.*, vol. 44, no. 9, pp. 3988–3996, 2015.

Keywords: metal-organic frameworks, zeolitic imidazolate frameworks, borohydride, hydrogen storage, hybrid compounds

MS31-P4 Halogen-bond mediated assembly of metal-containing architectures

Marijana Đaković¹, Željka Soldin¹, Ivan Kodrin¹, Christer B. Aakeröy²

1. Department of Chemistry, Faculty of Science, University of Zagreb, Horvátovac 102a, Zagreb, Croatia

2. Department of Chemistry, Kansas State University, Manhattan, KS, 66506, USA

email: mdjakovic@chem.pmf.hr

There is still a shortage of robust and transferable guidelines for deliberate supramolecular synthesis of metal-containing structures with precise and desirable metrics and topologies. Of the plethora of non-covalent interactions that can determine the assembly of a solid-state structure, the halogen bond is currently receiving considerable attention as a potentially important actor on the supramolecular stage. Similar yet different to its hydrogen bonding counterpart, the halogen bond is becoming a valuable tool in the crystal engineering toolbox.[1] In fact, in many organic materials the halogen bond is used as the primary intermolecular interaction to dictate supramolecular self-assembly due to its strength, directionality and possibility for electrostatic fine-tuning of both the donor- and the acceptor moiety.[2] On the other hand, relatively few metal-organic frameworks that rely on XBs have not received anywhere near the same attention. Therefore, we opted to employ a set of guidelines that has emerged from the engineering of organic solid-state systems and transfer them to the assembly of desirable metal-containing motifs. In this contribution we demonstrate how that principle can successfully be utilised in the rational design of a series of copper(II) and cadmium(II) coordination compounds. In addition, several structure-property correlations are presented (e.g. solubility, thermal stability, elasticity), and structural, thermal and spectroscopic data are complemented by CSD data mining. Extensive computational methods are used to facilitate the interpretation of the experimental efforts.

[1] A. Mukherjee, S. Tohadi, G.R. Desiraju, *Acc. Chem. Res.*, 2014, 47, 2514.

[2] C. B. Aakeröy, M. Baldrighi, J. Desper, P. Metrangola, G. Resnati, *Chem. Eur. J.*, 2013, 19, 16240.



Figure 1. Hirshfeld surface mapped with d_{norm} for visualizing halogen bonds in $\text{CuCl}_2(\text{l-pz})_2$.

Keywords: halogen bond, crystal engineering, coordination compounds

MS32. Halogen bonding in the solid state

Chairs: Christer Aakeröy, Lee Brammer

MS32-P1 Back to the Future: applying 2000's interactions to explain supramolecular arrangements in 1950's compounds

Joao L.F. Silva¹, Karina Shimizu¹, Maria T. Duarte¹

1. Centro de Química Estrutural, Instituto Superior Técnico, U. Lisbon, Av. Rovisco Pais, 1049-001 Lisboa, Portugal

email: joao.luis@ist.utl.pt

The majority of papers published on halogen bonding are focused on molecules with isolated C-X bonds. In this work we tried to examine if the conclusions observed for this recent type of interactions also apply to a situation where two halogens are bonded to the same atom. To achieve this goal we choose a family of compounds, Cp_2TiX_2 , that was first prepared in the 1950's¹ and whose crystal packing could not at the time be analyzed in terms of halogen bonds.

As this type of interactions is the result of anisotropy in electron distribution around the halogen atoms^{2,3} we used DFT calculations to draw electron density maps for the various compounds. These maps showed that, in contrast with the halogens involved in isolated C-X bonds (the σ -hole model), the electron scattering is concentrated in the zone amidst the bonds, creating not only anisotropy but also asymmetry. Despite this asymmetry the parameters obtained for the type I halogen bonds encountered do not show large differences to those expected for C-X isolated bonds. However, the location of this large concentration of electronic charge in between the M-X bonds eliminates the possibility of type II halogen bonds.⁴

Another characteristic that is similar is the increase in significance of these halogen bonds with the atom polarizability: from fluorine (where they do not exist) to iodine (where all halogen atoms participate in $\text{X}\cdots\text{X}$ bonds).

In all compounds containing halogen atom there is always a competition between $\text{D-H}\cdots\text{X}$ and $\text{X}\cdots\text{X}$ interactions in the definition of the crystal packing. Independently of their relative number and significance, the presence of type I halogen bonds strongly affects the arrangement of the primary motif (chains of molecules formed through $\text{C-H}\cdots\text{X}$ hydrogen bonds) of these crystals: in the absence of $\text{X}\cdots\text{X}$ bonds the chains are parallel; when they are present the chains are antiparallel.

1 – G. Wilkinson, J.M Birmingham, *J. Am. Chem. Soc.*, 1954, 76, 4281-4

2 – T. Clark, M. Hennemann, J.S. Murray, P. Politzer, *J. Mol. Model.*, 2007, 13, 291-6

3 – P. Metrangolo, T. Pilati, G. Resnati, *CrystEngComm.*, 2006, 8, 946-7

4 – T.T.T. Bui, S. Dahaoui, C. Lecomte, G.R. Desiraju, E. Espinosa, *Angew. Chem.* 2009, 121, 389-9

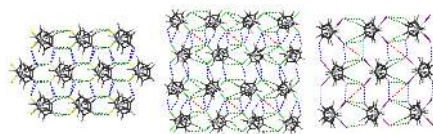


Figure 1. Crystal packing of Cp_2TiF_2 (left), Cp_2TiCl_2 (centre), and Cp_2TiI_2 (right): intrachain $\text{C-H}\cdots\text{X}$ (green), interchain $\text{C-H}\cdots\text{X}$ (blue) and $\text{X}\cdots\text{X}$ (red) interactions.

Keywords: Halogen bonding, Organometallic compounds

MS32-P2 Hydrogen bonds chains supported by halogen-halogen interactions in di- and trihaloimidazoles

Kacper W. Rajewski¹, Michał Andrzejewski¹, Jędrzej Marciniak¹, Andrzej Katrusiak¹

¹. Adam Mickiewicz University, Department of Materials Chemistry, Umultowska 89b, 61-614 Poznań, Poland

email: kacper.rajewski@gmail.com

Switchable polarization of $\text{NH}\cdots\text{N}$ hydrogen bonds remains in a great interest of crystallographers due to their ferroelectric properties. This effect has been recently reported for dabco salts and halobenzenimidazoles. Halogen interactions are kind of electrostatic interaction that can be as strong as hydrogen bonds and may force different molecules arrangement in space. What is more $\text{X}\cdots\text{X}$ interactions can significantly shorten $\text{NH}\cdots\text{N}$ bond length and allow proton transfer along hydrogen bond chains. During our studies we synthesized several haloderivatives of imidazole. Collected X-ray diffraction data at ambient conditions allowed us to determine five novel structures of double and triple substituted imidazoles at ambient conditions as an introduction for further high-pressure studies. The main structural features of all investigated haloimidazoles are: molecules arranged in sheets made of chains linked by $\text{NH}\cdots\text{N}$ bonds with $\text{X}\cdots\text{X}$ interactions holding sheets together. Halogen substitution causes steric hindrances which has major effect to the molecules arrangement. What is more, electronegative halogen atoms withdraw more electrons of the imidazole ring than H-atoms strengthening $\text{NH}\cdots\text{N}$ bonds.

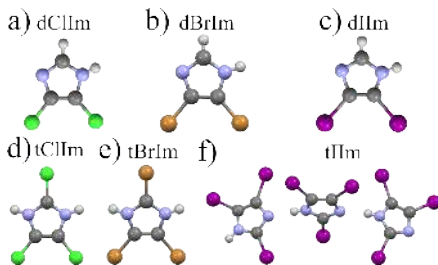


Figure 1. Haloimidazoles studied during research and their acronym symbols: (a) 4,5-dichloroimidazole (b) 4,5-dibromoimidazole (c) 4,5-diiodoimidazole (d) 2,4,5-trichloroimidazole (e) 2,4,5-tribromoimidazole (f) 2,4,5-triiodoimidazole.

Keywords: halogen-halogen interactions, hydrogen bond, imidazole.

MS32-P3 On the relation between topology of halogen-bonded molecular crystals and type of halogen-halogen contactsNikita S. Zakharov^{1,2}, Davide M. Proserpio^{1,3}, Vladislav A. Blatov^{1,2}

1. Samara Center for Theoretical Materials Science, Samara State University, Samara, Russia

2. Chemistry Department, Samara State University, Samara, Russia

3. Dipartimento di Chimica, Università degli Studi di Milano, Milano, Italy

email: nikitarui@mail.ru

We have studied 3722 monomolecular crystal structures of organic compounds comprising halogen bonds (XB). The structural information was taken from the Cambridge Structural Database (release 5.36). We have described the structures by infinite periodic graphs (underlying nets), whose vertices and edges correspond to molecular centers of mass and intermolecular halogen bonds, respectively. To describe the topology of supramolecular complexes formed by molecules connected by halogen bonds we have used the concept of molecular connection type that was formalized with molecular connection type symbol (MCTS) [1]. Topological classification of molecular connection types and underlying nets has been performed with the ToposPro package [2]; for determination of the type of halogen-halogen contacts [3] we have developed a special procedure and implemented it into ToposPro. As a result, the distributions of topological types and MCTSs were built for all halogen-bond patterns. The most frequent connection types of molecules are K^4 , B^4 , T^4 for the 2D halogen-bonded motifs and K^4 , G^{82} , P^6 , G^6 for the 3D ones. Separately, for the structures containing symmetrical halogen bonds we have found correlations between the XB type and the local topology of the supramolecular complexes. For example, type II contacts are typical in structures with MCTS B^2 , while type I contacts are inherent for the M^1 connection types.

The work was supported by the Russian government (grant No. 14.B25.31.0005).

References

[1] Aman F., Asiri A. M., Siddiqui W. A., Arshad M. N., Ashraf A., Zakharov N. S., Blatov V. A. *CrystEngComm*, **2014**, *16*, 1963-1970.

[2] Blatov V.A., Shevchenko A.P., Proserpio D.M. *Cryst. Growth Des.* **2014**, *14*, 3576.

[3] Tothadi S., Joseph S., Desiraju G. R. *Cryst. Growth Des.* **2013**, *13*, 3242-3254.

Keywords: halogen bond, topological properties, molecular crystals, supramolecular complexes

MS32-P4 Crystal engineering of metalloporphyrin assemblies by concerted halogen and hydrogen bonding interactionsHatem M. Titi¹, Israel Goldberg¹

1. School of Chemistry, Faculty of Exact Sciences, Tel Aviv University, Tel Aviv 69978, Israel

email: hat22t@hotmail.com

Metalloporphyrins have unique structural, photochemical, catalytic and electronic properties, and they provide magnificent building blocks for the construction of attractive supramolecular architectures.¹ The functional diversity that can be imparted to these tectons on the peripheral and axial sites of the porphyrin framework allows us to formulate supramolecular arrays of different topological features. The toolbox for obtaining materials of the desired structure contains in addition to the well characterized coordination and hydrogen bonds, newly exploited halogen bonding motifs. Concerted utilization of the non-covalent (and often competing) interactions in the porphyrin assembly process provides a new challenge in crystal engineering. In this presentation, we will highlight primarily the self-assembly of suitably functionalized metalloporphyrin scaffolds into halogen-bonds-driven networks. Successful designs of such architectures involved the use of di- and tetra-iodophenyl porphyrins metallated with either oxo-Mo^{VI} (L=axial ligand) or Sn^{IV}(L)₂ centers, with halogen bond donors and acceptors positioned in a complementary manner on 'L' and the *meso*-aryl groups. Then, we will shed light on new systems where hydrogen and halogen bonds act in concert in stabilizing the assembled architectures.²

1. I. Goldberg, *CrystEngComm*, **2008**, *10*, 637-645; W. M. Campbell, A. K. Burrell, D. L. Officer, K. W. Jolley, *Coord. Chem. Rev.*, **2004**, 1363-1379.

2. H. M. Titi, R. Patra, I. Goldberg, *Chem. Eur. J.*, **2013**, *19*, 14941-14949; G. Nandi, H. M. Titi, I. Goldberg, *Cryst. Growth Des.*, **2014**, *14*, 3557-3566; H. M. Titi, I. Goldberg, **2015** unpublished results

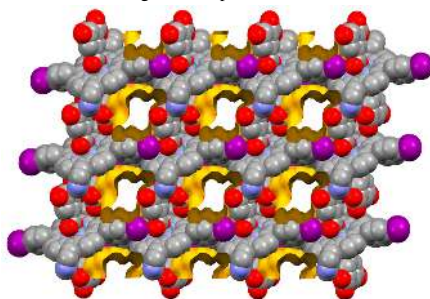


Figure 1. Supramolecular assembly of porphyrin moieties by directional non-covalent interactions

Keywords: Halogen Bonding, Hydrogen Bonding, Porphyrins

MS33. Mechanical effects and properties of ordered matter

Chairs: Panče Naumov, Helena Shepherd

MS33-P1 Thermoslient effect of an organic aminonitrile and its derivatives

Lukman O. Alimi¹, Vincent J. Smith¹, Leonard J. Barbour¹

1. Department of Chemistry, Stellenbosch University, South Africa.

email: lukman@sun.ac.za

The thermoslient effect is an extremely rare propensity of certain crystalline solids for self-actuation by elastic deformation or a ballistic event. Thermoslient compounds, colloquially known as “jumping crystals” are promising materials for fabrication of actuators that are also being considered as materials for clean energy conversion because of their capabilities to convert thermal energy into mechanical motion directly. Herein, an organic aminonitrile and its derivatives have been probed by a combination of structural, microscopic and thermoanalytical techniques. Crystals of these compounds were analysed by means of single crystal XRD and hotstage microscopy in the temperature range of 100 to 298 K and found to exhibit the thermoslient effect. We also carried out differential scanning calorimetric analysis at the temperature corresponding to that at which the crystal jumps as observed under a hotstage microscope.



Figure 1. Hotstage micrographs showing the thermoslient effect from 100 to 298 K

Keywords: actuation, jumping crystals, hotstage microscope, temperature, thermoslient effect

MS33-P2 Thermoslient shuttle: N'-2-propylidene-4-hydroxybenzohydrazide

Željko Skoko¹, Dean Popović², Jasminka Popović³

1. Department of Physics, Faculty of Science, University of Zagreb, Bijenička c. 32, 10000 Zagreb, Croatia

2. Institute of Physics, Bijenička c. 46, 10000 Zagreb, Croatia

3. Institute Ruder Bošković, Bijenička c. 54, 10000 Zagreb, Croatia

email: zskoko@phy.hr

Systems providing mechanical response to external stimuli (heat or light) are rapidly becoming one of the focuses of material science investigations, since these materials are very promising in the sense of conversion of thermal (or light) energy into mechanical work on the nanoscale. One class of such materials are thermoslient materials, or colloquially commonly called “jumping crystals”. These materials, when heated or cooled, undergo a sudden and sharp topotactic phase transition. During the transition, the crystals experience a change in their shape, as well as in the size of the unit-cell, that is so energetic that crystals literally jump off the stage to distances several times bigger than their dimensions [1].

It was reported [2] that N'-2-propylidene-4-hydroxybenzohydrazide behaved similarly as the jumping crystals. This system exhibited three polymorphic modifications (I, II and III), all having the same polar space group $Pna2_1$, with the phase transitions I to II and III to II reported as topotactic. It was also reported that during the irreversible phase transition from I to II single crystals of the phase I were violently disintegrated into single crystal fragments of the phase II (without jumping), while in the reversible phase transition III to II the periodicity along the polar axis expanded (approximately 14%) and the integrity of the single crystals was preserved, i.e. no movement of crystals was observed.

Our measurements showed a somewhat different behaviour. During the irreversible phase transition from I to II some of the crystals did indeed disintegrate into smaller fragments, but a large number remained intact and showed a typical jumping crystal behaviour – jumping all around over large distances (several cm). Also, during the reversible phase transition II to III, and III to II, crystals exhibited the jumping behaviour, perhaps somewhat weaker than during the phase transition I to II. This is in contrast to the statements reported previously. We performed detailed structural and mechanical measurements, with special emphasis on the strain evolution in the crystal lattice during heating/cooling and on basis of that propose a new mechanism for jumping crystals phenomenon in this system.

References:

[1] Skoko, Ž., Zamir, S., Naumov, P. & Bernstein, J. (2010), *J. Am. Chem. Soc.* **132**, 14191.

[2] Centore, R., Jazbinsek, M., Tuzi, A., Roviello, A., Capobianco, A. & Peluso, A. (2012) *CrystEngComm* **14**, 2645.

Keywords: thermoslient effect, polymorphism, topotactic

MS34. Growth, structure and application of multi-component crystals

The research was founded by the National Science Centre (grant No. NCN 2011/03/B/ST4/02591). Calculations have been carried out in Wrocław Centre for Networking and Supercomputing grant No. 285.

[1] N. Miyaoura, A. Suzuki, *Chem. Rev.*, **1995**, 95, 2457.

[2] A. Albini, S. Pietra, *Heterocyclic N-oxides*, CRC Press: Boca Raton, USA, **1991**.

Keywords: co-crystals, phenylenediboronic acid, hydrogen bonds

Chairs: Christopher Frampton, Tomislav Friščić

MS34-P1 Structure, stability and physicochemical properties of phenyleneboronic acids cocrystals with NO-compounds

Sylwia E. Kutyla¹, Dorota Stepień¹, Katarzyna N. Jarzemska¹, Radosław Kamiński¹, Łukasz Dobrzycki¹, Roland Boese², Jacek Młochowski³, Michał K. Cyrański¹

1. Czocharlski Laboratory of Advanced Crystal Engineering, Biological and Chemical Research Centre, Department of Chemistry, University of Warsaw, Żwirki i Wigury 101, 02-089 Warsaw, Poland

2. Department of Chemistry, University of Duisburg-Essen, 45117 Essen, Germany

3. Department of Chemistry, Wrocław University of Technology, Wybrzeże Wyspiańskiego 27, 50-370 Wrocław, Poland

email: sylwia.kutyla@student.uw.edu.pl

Organoboron compounds have been known for about 150 years and found a widespread use in synthetic organic chemistry,[1] in supramolecular chemistry, or medicine. In turn, N-oxides of various heterocyclic compounds are important due to their vast applications as protective groups, oxidants or ligands in coordination complexes.[2] Both classes of compounds are eager to form hydrogen bonds. It is therefore interesting to testify whether it is possible to combine them together into solid-state systems of desired properties (e.g. increased biological activity or solubility). Consequently, the purpose of this study was to co-crystallize phenylenediboronic acids with a series of aromatic N-oxides. 12 new cocrystals were obtained and structurally characterized. Their crystal networks are stabilized by an extended net of hydrogen bonds usually forming layers further interacting via pi-stacking. Most of the structures contain water molecules biding acid and N-oxide molecules together. Ortho- diphenyloboronic acid is much more resistant to form cocrystals with N-oxides than its para-analogue and creates much less predictable cocrystal structures. A truly remarkable result of the fused ortho-phenylenediboronic acid and its semi-anhydride incorporated into the cocrystal structure is reported. For all of the studied systems a comprehensive analysis of crystal packing and energetic features was conducted. The nature of intermolecular interactions was additionally investigated via the Hirshfeld surface approach. The obtained theoretical results were confronted with that of the TGA-DSC experiments.

MS34-P2 Formation of chiral and racemic multi-component crystals *via* solvent assisted ball millingChristian W. Lehmann¹, Nöthling Nils¹¹ Max-Planck-Institut für Kohlenforschung, Mülheim an der Ruhr, Germany

email: lehmann@kofo.mpg.de

Solvent assisted ball milling has been shown to enable the formation of multi-component crystals in cases where conventional solvent based crystallisation fails. In this study chiral starting materials, both enantiopure and racemic, are employed in co-crystal formation via ball milling. Previously we could show, that competitive ball milling of racemic mandelic acid and racemic proline amide resulted exclusively in the formation of the thermodynamically more stable diastereomeric co-crystal. This approach has now been extended to other carboxylic acids and carboxylic amides which did not form co-crystals, if only the pure enantiomers were involved.

Keywords: co-crystals, chirality, powder diffraction**MS34-P3** Growing cocrystals by stoichiometric cosublimationJan Čejka¹, Martin Lenz¹¹ Department of Solid State Chemistry, University of Chemistry and Technology Prague, Technická 5, 166 28 Prague, Czech Republic

email: jan.cejka@vscht.cz

We have designed a cosublimation device, which allows for separate heating of multiple compounds sharing one water-cooled condenser as a crystallization target under vacuum. This apparatus allows scientist to optimize vapour stoichiometry of the sublimed compounds. Obviously, it is capable to cocrystallize compounds with high difference between temperatures of sublimation, which is impossible when heating a mixture or sensitive compounds. Interchangeable condensers of various shapes can be used. The temperature of each component can be optimized to reach desired stoichiometry of sublimation, which we believe is the key to reach proper crystal growth conditions. Our “home-made” apparatus is easily built and effortlessly maintained.

Multi-component crystals offer a variety of properties, which allow pharmaceutical industry to tune up many parameters like crystal morphology, stability or solubility rate. While the world of solvated structures is limited to a couple of FDA acceptable solvents, the reign of cocrystals covers dozens of acceptable compounds. Aside from routine methods for preparation of cocrystals, sublimation is the least used technique. Only few fruitful experiments were published, in which a mixture of active pharmaceutical ingredient (API) with relevant cofomer was heated. In such arrangement only the compounds with similar temperature and rate of sublimation, or those having high affinity to each other, would form multi-component crystals. The effectivity of the process should improve with optimization of the vapour stoichiometry, which is usually “maintained” by empiric adjustments of the solid mixture stoichiometry. Hence, the ratio of compounds in the mixture and in the vapour is time dependent. The stoichiometry gets out of control, when the difference between temperatures of sublimation is too high. Heating the components separately allows to work under different and optimized sublimation temperatures, protects sensitive compounds and stabilizes vapour stoichiometry.

Our cosublimator and the results of cocrystallization experiments of APIs with suitable cofomers will be presented.

This work was supported by the Grant Agency of Czech Republic, Grant no. 106/14/03636S.

Keywords: multi-component crystals, cocrystals, crystal growth, sublimation

MS34-P4 Solubility-based solvate screening of pharmaceutical substance trospium chlorideVeronika Sládková¹, Tereza Skalická¹, Eliška Skořepová¹, Jan Čejka¹, Václav Eigner^{1,2}, Bohumil Kratochvíl¹¹. Department of Solid State Chemistry, University of Chemistry and Technology, Prague, Technická 5, 16628, Prague 6, Czech Republic². Institute of Physics AS CR, v.v.i., Na Slovance 2, 182 21 Prague 8, Czech Republic

email: sladkovv@vscht.cz

The ability of long-established pharmaceutical compound trospium chloride (TCl) to form solvates was investigated. Taking into account the solubility of TCl (and, therefore, material consumption), different solvate screening approaches were considered: slow evaporation, slurring and anti-solvent addition. We applied them on 20 polar solvents. Five solvates, with solvents methanol, acetonitrile, propionitrile, *N,N*-dimethylformamide, nitromethane and a dihydrate were identified and characterized by various analytical techniques. The structures of all solvates were determined by single-crystal X-ray diffraction. The reproducible forms were further characterized by powder X-ray diffraction, desolvation behaviour was observed by thermoanalytical (TGA/DSC) methods and solubility in particular solvents was determined via UV-Vis spectrophotometry or gravimetric measurements. Structural features of novel solvates and of previously described polymorphs and cocrystals of TCl were compared, presented by a tree diagram which classifies the structures according to their molecular packing.

This work was supported by the Grant Agency of Czech Republic, Grant no. 106/14/03636S and received financial support from specific university research (MSMT No 20/2015).

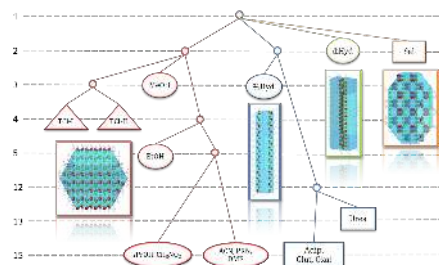


Figure 1. Tree diagram of trospium chloride solid forms

Keywords: pharmaceuticals, solvates, screening, X-ray crystallography

MS34-P5 Molecular dynamics of supersaturated indometacin-nicotinamide solutionsLászló Fábián¹, Karol P. Nartowski¹, Yaroslav Z. Khimyak¹¹. School of Pharmacy, University of East Anglia, Norwich, UK

email: l.fabian@uea.ac.uk

Recently, co-crystallisation has been shown to allow the growth of single crystals from compounds that could not be crystallised on their own [1]. This observation directed our attention towards the role of solution-state supramolecular assemblies in the formation of cocrystals. A relatively simple and experimentally well-characterised system, the indometacin-nicotinamide co-crystal [2] dissolved in alcohols or acetonitrile was selected for preliminary investigations.

The formation and stability of molecular aggregates were studied through a series of molecular dynamics simulations. As starting points, pre-aligned supramolecular synthons from the crystal structure or randomly placed solutes in cubic solvent boxes were used. The behaviours of dilute, saturated and supersaturated solutions were compared. Trajectories were simulated and analysed using the Gromacs package [3] and the general amber force field [4].

The results show that simple hydrogen-bonded dimers are not stable in these solutions, but pairs of molecules often remain in close proximity even when there are no longer hydrogen bonds between them. Indometacin-indometacin and indometacin-nicotinamide contacts are more persistent than nicotinamide-nicotinamide contacts. In both saturated and the supersaturated solutions, a dynamic set of clusters is formed, with the mean cluster size being bigger in the supersaturated solutions. This result is qualitatively consistent with the observed gradual decrease of the diffusion coefficients with increasing concentration, which was measured by solution PFG NMR spectroscopy. Further changes in the ¹H chemical shifts of the dissolved species with increasing solute concentration indicate changes in the local environment of the aggregating molecules. The clusters are dynamic both in terms of their size and structure, i.e., no crystal-like aggregates are observed. Both the mean and maximum cluster size show a marked fluctuation, but no appreciable drift towards larger sizes.

1. K. S. Eccles, R. E. Deasy, L. Fábián, A. R. Maguire and S. E. Lawrence, *J. Org. Chem.*, 2011, 76, 1159.

2. A. Alhalaweh, A. Sokolowski, N. Rodríguez-Hornedo and S. P. Velaga, *Cryst. Growth. Des.*, 2011, 11, 3923.

3. B. Hess, C. Kutzner, D. van der Spoel and E. Lindahl, *J. Chem. Theory Comput.*, 2008, 4, 435.

4. J. Wang, R. M. Wolf, J. W. Caldwell, P. A. Kollman and D. A. Case, *J. Comput. Chem.*, 2004, 25, 1157.

Keywords: cocrystal; molecular dynamics; pre-nucleation assemblies

MS34-P6 Crystal engineering of the Drotaverin saltsTamás Holczbauer¹, Máté Szabó¹, Mátys Czugler¹

1. Research Group of Chemical Crystallography, Institute of Organic Chemistry, Research Centre of Natural Sciences, Hungarian Academy of Sciences, Magyar Tudósok körútja 2., Budapest, H-1117, Hungary

email: holczbauer.tamas@tk.mta.hu

Structure determinations of drug molecules are essential for the exploration of their physical and chemical properties. Their crystalline state controls their solubility, absorption and other solid state properties thus their structures may provide a wealth of further information.

Drotaverin salts are exemplary for their good inclusion ability of crystallization solvents, so they could provide some interesting contexts by their solubility and also by the rationalization of their solid state structures. The structure was analysed by X-ray diffraction, providing the basic scrutiny in the solid state.

Starting from the drotaverin hydrochloride salt we made more than a dozen crystalline complexes. Besides the numerous solvent crystals we determined the crystal structures of co-crystals and the crystal structure of the hitherto unknown pure salt even. Anion metathesis reactions were also observed during some crystallization.

These crystal structures may provide basis not only for systematization but also means for a conscientious manipulation of salt – like drug forms in general.

These crystal structures give opportunity to observe the conformational changes and the idiosyncrasy of secondary interaction. Maybe these monitorings forecast the new partners of crystallisation.

Keywords: crystal engineering, secondary interactions, salts

MS34-P7 Structural diversity in pharmaceuticals: various sulfonate salts of agomelatineEliška Skořepová¹, Michal Hušák¹, Luděk Ridvan²

1. Department of Solid State Chemistry, University of Chemistry and Technology Prague, Technická 5, Prague 6, Czech Republic

2. Solid State Development, Zentiva k.s., U Kabelovny 130, Prague 10, Czech Republic

email: eliska.skorepova@vscht.cz

The search for new solid forms of an active pharmaceutical ingredient (API) is an important step in a drug development. Often, an API has a low water solubility, which then leads to a low oral bioavailability. The problem can be solved by salt formation. One such API is agomelatine (AG), a melatonergic antidepressant. However, agomelatine is an amidic compound and, since amides are considered very neutral, it was quite a surprise, when agomelatine, in the combination with three different sulfonate acids, produced salts. The five novel resulting crystalline forms were AG hydrogensulfate, AG hydrogensulfate methanol solvate hemihydrate, AG mesylate, AG mesylate monohydrate and AG besylate. Their structures were solved either from single-crystal or powder x-ray diffraction data. Interestingly, the structures of the two hydrogensulfates were determined from the same crystal via *single-crystal to single-crystal* transformation. In all of the structures, the agomelatine molecule was positively charged. Specifically, the amide oxygen was protonated. The proton transfer and the salt formation were also confirmed by solid state NMR and the ΔpK_A calculation.

This work was supported by the Grant Agency of Czech Republic, Grant no. 106/14/03636S and received financial support from specific university research (MSMT No 20/2015).

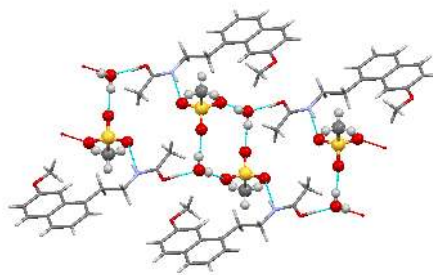


Figure 1. H-bonding in agomelatine mesylate monohydrate

Keywords: x-ray crystallography, pharmaceuticals, salt formation

MS34-P8 Cavity analysis in preparation of new solid-state phases of small molecules

Radka Zajíčková¹, Jan Čejka¹, Alexandr Jegorov²

1. Department of Solid State Chemistry, University of Chemistry and Technology Prague, Technická 5, Prague 6, Czech Republic
2. Teva Czech Industries s.r.o., Research Unit, Branišovská 31, 370 05 České Budějovice, Czech Republic

email: zajicovr@vscht.cz

Most solid substances exist in various forms, either polymorph or multi-component phases. The particular forms often differ in structure and physico-chemical properties. Plenty of ways are available to analyse and characterize solid phases. Even more points of view and software methods are used to examine and compare the obtained data sets. Cavity analysis of solid substances is a typical research area for biological macromolecules, zeolites and MOFs. Nevertheless it proves a great instrument in small molecules crystallography. Voids in crystal structures of small molecules are generated by packing of molecules of interest. Frequently, the primary molecules build voids, which can be occupied by solvent or co-former molecule, or just remain empty. The resulting molecular packing depends on crystal growth conditions and stability of the substance. The most important tracked parameters are: size, shape and position of each particular void in unit cell or in neighbour unit cells. This study applies cavity analysis in looking for new solid-state phases when at least one solid form is known. It is based on similarities of shape and size of cavities and shape and size of incorporated molecules (i.e. solvents) defined by different approaches. This work is supported by the Grant Agency of Czech Republic, Grant no. 106/14/03636S.

Keywords: multi-component phases, cavity analysis

MS34-P9 Inclusion compounds of a borneol dumb-bell host with methylcyclohexanones and 2-butanols: Structures and resolutions

Eustina Batisai¹, Luigi R. Nassimbini¹, Edwin Weber²

1. Department of Chemistry, University of Cape Town, Rondebosch 7700, South Africa
2. Institut für Organische Chemie TU Bergakademie Freiberg Leipziger Strasse 29, D- 09596 Freiberg/Sachs., Germany

email: ebatisai@gmail.com

Functionality and bulkiness are structural criteria typical of host molecules designed for crystalline inclusion formation.¹ Molecules meeting these requirements have been developed in a variety of geometric structures² including those resembling the shape of a wheel-and-axle³ or a dumb-bell.⁴ In a special kind of purpose-built host structures of the dumb-bell kind, chiral borneol moieties were used as bulky terminal substituent groups, thus providing chirality and hydrogen bonding sites. In this work, the host 2,2'-(benzene-1,4-diyl-diethynylene) diborneol has been employed to resolve racemic methylcyclohexanones and 2-butanols. For 2-methylcyclohexanone, the resultant inclusion compound yielded an enantiomeric excess of 72% (*S*) while with 3-methylcyclohexanone the enantiomeric excess was 57% (*S*). The host failed to resolve (*R*, *S*)- 2-butanol, and the inclusion compounds derived from (*R,S*)-, (*R*)- and (*S*)- 2-butanol are isostructural, being dominated by a stable framework of host•••host hydrogen bonds. The non templating effect of the 2-butanols was explained in terms of the secondary interactions occurring in the structures which were also analysed by the program CrystalExplorer.

1. E. Weber In: *Inclusion Compounds*; Eds., J. L. Atwood, J. E. D. Davies, D. D. MacNicol Oxford University Press: Oxford, 1991, vol. 4, pp. 188-262
2. R. Bishop, *Chem. Soc. Rev.* **1996**, 311
3. L. R. Nassimbini, H. Su, T-L Curtin, *Chem. Commun.* **2012**, 48, 8526
4. T. Müller, J. Hulliger, W. Seichter, E. Weber, T. Weber, M. Wübbenhorst, *Chem. Eur. J.*, **2000**, 6, 54

Keywords: Chiral host, resolution, methylcyclohexanones, 2-butanols

MS34-P10 Multitopic precursors for oxide materials' synthesisAlba Finelli¹, Aurélien Crochet¹, Katharina M. Fromm¹

1. University of Fribourg, Switzerland

email: alba.finelli@unifr.ch

Research interest in mixed metal oxide is increasing in material science. They have multiple applications, such as batteries, ceramics, pigments, high-Tc superconductors or transparent conductors. However, the two main challenges for the synthesis of such compounds are the lack of control on the ratio of the different metal components and the extreme conditions (up to 900 °C) that many of these oxides require during the synthesis. To overcome these kinds of issues we propose a new strategy for the synthesis of mixed metal complexes, a "multitopic ligand approach". The aim is to design specific ligands with selective coordination sites to bind different metal ions. Due to the metal ion preorganization in the precursor thus formed, the stoichiometry of the final oxide material can be controlled and the extreme synthesis conditions diminished (pressure or temperature). These new mixed metal complexes will be finally combusted to oxide materials with possible new features and ideally at the nanoscale.

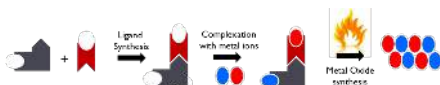


Figure 1. Multitopic ligand approach

Keywords: Multitopic ligand, coordination chemistry, oxides**MS34-P11** Co-crystals of vanillic acid with methylated xanthenesAyesha Jacobs¹, Francoise M. Amombo Noa¹

1. Cape Peninsula University of Technology

email: jacobsa@cput.ac.za

Vanillic acid (VA) forms co-crystals with caffeine (CAF) and theophylline (THP) of the form **VA•2CAF** and **2VA•THP** respectively. VA also forms a co-crystal hydrate with theobromine (THB), **VA•THB•2H₂O**. The structures of the co-crystals were determined. For **VA•2CAF**, each VA molecule is hydrogen bonded to two CAF molecules to form a unit. The units are linked *via* weak CH...N and CH...O interactions. The hydrogen bond network observed for **2VA•THP** is more extensive due to the additional N-H donor group of the THP. The hydrogen bonded ring networks pack to form layers with $\pi\cdots\pi$ interactions between the layers. The packing for **VA•THB•2H₂O** also presents with hydrogen bonded layers with the water molecules acting as bridges linking the VA-THB dimers. **VA•2CAF** was successfully prepared *via* the slurry method and *via* neat grinding. **VA•THB•2H₂O** could not be prepared *via* the previous two methods, however liquid assisted grinding was successful. Grinding experiments utilising 2: 1 mixtures of VA: THP resulted in the dihydrate, **2VA•THP•2H₂O**.

Keywords: vanillic acid, caffeine, theobromine, theophylline, co-crystals, grinding

MS34-P12 From homonuclear metal string complexes to heteronuclear metal string complexes

Shie-Ming Peng^{1,2}, Shao-An Hua¹, Ming-Chuan Cheng²

1. Department of Chemistry, National Taiwan University, Taipei, Taiwan

2. Institute of Chemistry, Academia Sinica, Taipei, Taiwan

email: smpeng@ntu.edu.tw

The study of metal string complexes with 1-D transition metal frameworks began in the early 1990s. Since these complexes provide great insight into multiple metal-metal bonds, and may have potential applications as molecular wires, this field of research has grown in the past 20 years. As such, the electronic structure of the simplest trinuclear complexes, the supporting ligand systems, and single molecular conductance of metal string complexes are discussed. This review will introduce the development of this field and summarize some important results in the newly designed heteronuclear metal string complexes (HMSCs). These molecules may be of great interest in studying the nature of heterometallic electronic effects and molecular electronic applications.

REFERENCES

- [1] Ismayilov RH, Wang WZ, Lee GH, Yeh CY, Hua SA, Song Y, Rohmer MM, Bénard M, S-M Peng *Angew. Chem. Int. Ed.*, **2011**, *50*, 2045-2048.
- [2] M-C Cheng, C-L Mai, C-Y Yeh, G-H Lee and S-M Peng *Chem. Commun.* **2013**, *49*, 7938-7940.
- [3] M-J Huang, S-A Hua, M-D Fu, G-C Huang, C Yin, C-H Ko, C-K Kuo, C-H Hsu, G-H Lee; K-Y Ho, C-H Wang, Y-W Yang, I-C Chen, S-M Peng, C-h Chen *Chemistry-A European Journal* **2014**, *20*(16), 4526-4531.
- [4] S-A Hua, M-C Cheng, C-h Chen, and S-M Peng *European Journal of Inorganic Chemistry* **2015**, *Micro Review*, "From Homonuclear Metal String Complexes to Heteronuclear Metal String Complexes" DOI:10.1002/ejic.201403237.

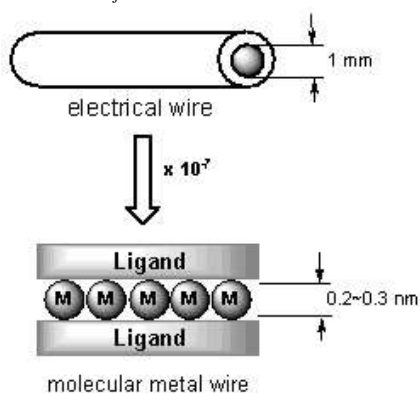


Figure 1. An electric wire and a miniature molecular wire.

Keywords: Metal String Complexes

MS35. Dynamics in nanoporous molecular crystals

Chairs: Angiolina Comotti, Len Barbour

MS35-P1 Control of porosity through temperature and pressure

Jan A. Gertenbach¹, Simon A. Herbert², Tia Jacobs², Agnieszka Janiak², Len J. Barbour²

1. PANalytical B.V., Almelo, The Netherlands

2. Stellenbosch University, Stellenbosch, South Africa

email: jan.gertenbach@panalytical.com

Gaining control of phase transformations offers the possibility of tailoring the properties of polymorphic materials.¹ X-ray powder diffraction is ideally suited to studying such structural modifications, particularly since the bulk material is analysed, allowing the averaged structural features of the material to be correlated with its bulk physical properties, in this case the porosity. In addition, rapid X-ray diffraction data collection allows the determination of intermediate phases, onset points of reactions and information about the reversibility of processes involved.

The material studied here exists in four distinct polymorphic forms, each porous to a differing extent. Control of the desired polymorph, and hence the desired porosity is achieved by manipulation of temperature and pressure. The X-ray diffractograms were modelled by Rietveld refinement using the HighScore Plus software² to study the structural processes during the phase transformations. The physical properties determined by sorption measurements were modelled using Partial Least Squares Regression (PLSR) analysis, and this data compared to the output from the Rietveld structural study.

1. see for example Herbert, S.A. *et al. J. Am. Chem. Soc.* (2013) *135*, 6411-6414.
2. Degen, T. *et al. Powder Diffr.* (2014) *29*, S13-S18.

Keywords: porosity, Rietveld, polymorph

MS35-P2 Using PIXEL to investigate as adsorption in metal-organic frameworksAndrew G.P. Maloney^{1,2}, Peter A. Wood¹, Simon Parsons²

1. Cambridge Crystallographic Data Centre, 12 Union Road, Cambridge, UK, CB2 1EZ

2. School of Chemistry, University of Edinburgh, Edinburgh, UK, EH9 3JJ

email: maloney@ccdc.cam.ac.uk

Over the last decade, the study of metal-organic frameworks (MOFs) has become a very popular avenue of research, with particular focus on their potential uses for gas storage and separation. Structurally, MOFs are made up of metal-ligand nodes that are connected by organic bridging ligands to form 3-dimensional porous frameworks. Synthesis of such frameworks can be achieved by combinations of these nodes and linkers to give a variety of structures with different pore sizes, topologies and chemical functionalities.¹ This so-called "modular synthesis" means that it is theoretically possible to create a vast catalogue of metal-organic frameworks for specific applications that is not possible for other porous materials such as zeolites.²

To date, there are over 10,000 MOF structures recorded in the Cambridge Structural Database (CSD).³ However, comparatively little work has been done to investigate the precise locations of adsorption sites in these structures since such experiments can be difficult to carry out and require specialist equipment.⁴ Additionally, the time taken to determine these positions for such a large number of structures experimentally renders such experimental methods impractical. Consequently, computational modelling of gas adsorption in metal-organic frameworks is a very appealing alternative, as calculations can be performed under a range of different simulated conditions, and additionally theoretical MOFs can be tested for suitability before any synthetic work is undertaken.

This presentation, timed to coincide with the 50th anniversary of the Cambridge Structural Database, demonstrates how geometric analysis and PIXEL⁵ energy calculations have been used to investigate adsorbate-adsorbent interactions in a range of metal-organic frameworks and gas molecules. Results are reported for adsorption between MOF-5 and Ar, MOF-5 and N₂, and HKUST-1 and CO₂. The locations of the adsorption sites and the calculated energies, which show differences in the Coulombic or dispersion characteristic of the interaction, are compared to experimental data and literature energy values calculated using standard computational methods of analysis for adsorption in metal-organic frameworks.

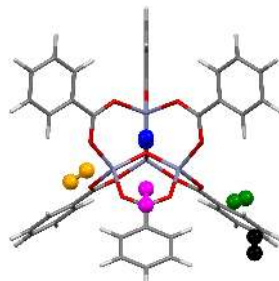
1. S. L. James, (2003) *Chem. Soc. Rev.*, **32**, 276-288.2. U. Mueller *et al.*, (2006) *J. Mat. Chem.*, **16**, 626-636.3. F. H. Allen, *Acta Cryst.*, **B58**, 380-388, 2002.4. N. Nijem *et al.*, (2010) *J. Am. Chem. Soc.*, **132**, 1654-1664.5. A. Gavezzotti, *New J. Chem.*, **35**, 1360-1368, 2011.

Figure 1. Nitrogen adsorption sites in MOF-5 calculated using PIXEL

Keywords: Gas adsorption, metal-organic frameworks, PIXEL

MS35-P3 Elucidating the mechanism responsible for anisotropic thermal expansion in a Metal-Organic Framework

Dewald P. van Heerden¹, Catharine Esterhuysen¹, Leonard J. Barbour¹

1. Supramolecular Materials Chemistry, Department of Chemistry and Polymer Science, Stellenbosch University, South Africa.

email: dpvh@sun.ac.za

Anomalous thermal expansion of a three-dimensional metal-organic framework (compound **1**) is examined by means of theoretical calculations. The methanol solvate ($[\text{Zn}(\text{L})(\text{OH})] \cdot n\text{CH}_3\text{OH}$, **1_{meth}**) = 4,4'-bis(2-methylimidazol-1-ylmethyl)-1,1'-biphenyl) was obtained following the procedure developed by Grobler *et al.* and subsequently desolvated in a single-crystal to single-crystal transformation to yield the apohost form, **1_{apo}**. [1] Variable temperature single crystal X-ray diffraction (SCD) analysis on the same crystal of **1_{apo}** under static vacuum revealed colossal positive thermal expansion along the *c* axis ($\alpha = 123 \times 10^{-6} \text{ K}^{-1}$) and biaxial negative thermal expansion along the *a* and *b* axes ($\alpha = -21 \times 10^{-6} \text{ K}^{-1}$). Inspection of the 100, 190, 280 and 370 K SCD structures pointed towards a concerted change in the labile coordination sphere of the zinc centre so as to elongate the coordination spiral in the *c* direction ($\text{Zn}-\text{O}(\text{H})-\text{Zn}$ angles enlarge), while the largely unaltered ligands ($\text{Zn} \cdots (\text{L}) \cdots \text{Zn}$ distance constant) are pulled closer together in the *ab* plane.

In this study Molecular Dynamics simulations in the NPT ensemble successfully reproduce the observed trend in unit cell parameters of **1_{apo}**. Computed internal coordinates involving zinc are, however, generally underestimated owing to shortcomings of the DREIDING force field. A mechanistic model that reproduces the convergent expansion of the material's coordination spiral is developed and evaluated at the DFT level of theory. The linear increase in energy calculated for the extension of a model consisting of six zinc centres and truncated ligands compares favourably to results obtained from a periodic DFT evaluation of the SCD structures.

[1] I. Grobler, V.J. Smith, P.M. Bhatt, S.A. Herbert, L.J. Barbour *J. Am. Chem. Soc.* (2013), 135, 6411.

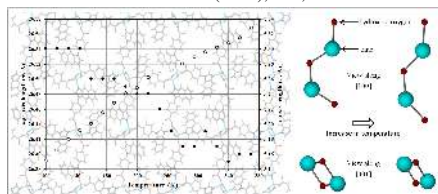


Figure 1. Left: Graph of unit cell lengths determined by variable temperature SCD on the same crystal of **1_{apo}** under static vacuum. [1] Right: schematic representation of the convergent expansion mechanism of the coordination spiral of **1** showing elongation in the *c* direction and contraction in the *ab* plane.

Keywords: Thermal Expansion, DFT

MS36. Molecular crystals offering new insight into intermolecular interactions

Chairs: Paola Gilli, Carl Henrik Gørbitz

MS36-P1 Solvent-free and solution based synthesis of *o*-hydroxy imines with non-planar molecular geometry

Marija Zbačnik^{1,2}, Linette Twigge², Andreas Roodt², Dominik Cincić¹

1. Laboratory of General and Inorganic Chemistry, Department of Chemistry, University of Zagreb, 10002 Zagreb, Croatia

2. Department of Chemistry, University of the Free State, 9301 Bloemfontein, South Africa

email: mzbacnik@chem.pmf.hr

Solvent-free methods of synthesis (neat, liquid-, seeding-, ion-assisted grinding) have been recognised as faster, environmentally more friendly and economically more acceptable ways to prepare new but also already known compounds. [1] *o*-Hydroxy Schiff bases are well known organic compounds that can possess photo- and/or thermochromic properties in the solid state due to possibility of keto-enol tautomeric change *via* intramolecular O...N hydrogen bond. [2] They can be easily obtained by condensation of aldehydes (or ketones) and primary amines [3] and thereafter used as ligands in coordination chemistry of transition metals. [4] For the reason of their ability to reversibly change their colour upon changing external conditions their structure-property correlation has been extensively studied. For almost 30 years it was thought that Schiff bases with non-planar molecular geometry cannot show thermochromism [2] so much work was done in the past 20 years to find ones that do. [5] Herein, we report solvent-free and solution based syntheses of *o*-hydroxy Schiff bases with non-planar molecular geometry obtained from salicylaldehyde and its derivatives and α -aminodiphenylmethane. The successfulness of method used was studied by means of PXRD, DSC and TG thermal analysis and NMR. Their thermochromic properties were checked by repeated exposure to temperature change from room to liquid-nitrogen temperature. The supramolecular impact on the keto-enol tautomerism (Figure 1) was studied using SCXRD.

[1] S.L. James, C.J. Adams, C. Bolm, D. Braga, P. Collier, T. Friščić, F. Grepioni, K.D.M. Harris, G. Hyett, W. Jones, A. Krebs, J. Mack, L. Maini, A. Guy Orpen, I.P. Parkin, W.C. Shearouse, J.W. Steed and D.C. Waddell, *Chem. Soc. Rev.*, 2012, **41**, 413. [2] M.D. Cohen and G.M.J. Schmidt, *J. Phys. Chem.*, 1962, **66**, 2442; M.D. Cohen, G.M.J. Schmidt and S. Flavian, *J. Chem. Soc.*, 1964, 2041; M.D. Cohen, Y. Hirshberg and G.M.J. Schmidt, *J. Chem. Soc.*, 1964, 2051. [3] Schiff, H; *Ann. Chim.*, 1864, **131**, 118. [4] A. Blagus, D. Cincić, T.

Friščić, B. Kaitner and V. Stilić, *Maced. J. Chem. Int. Ed.*, 2010, **29**, 117. [5] E. Hadjoudis, M. Vittorakis and I.M. Mavridis, *Tetrahedron*, 1987, **43**, 1345; F. Robert, A.D. Naik, B. Tinant, R. Robiette and Y. Garcia, *Chem. - Eur. J.*, 2009, **15**, 4327; F. Robert, P.-L. Jacquemin, B. Tinant and Y. Garcia, *CrystEngComm*, 2012, **14**, 4396; B. Kaitner and M. Zbačnik, *Acta Chim. Slov.*, 2012, **59**, 670; M. Zbačnik and B. Kaitner, *CrystEngComm*, 2014, **16**, 4162.

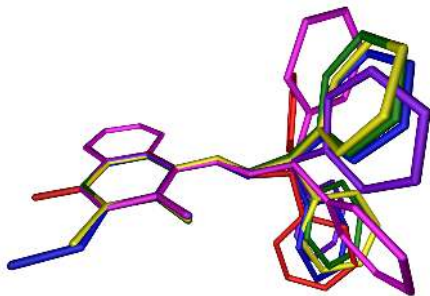


Figure 1. Overlapping pictures of non-planar *o*-hydroxy imines.

Keywords: Solvent-free synthesis, *o*-Hydroxy Schiff bases, Structure-property correlation, Thermochromism

MS36-P2 Structural features of the intermolecular interactions between PTA and nutraceutical acids in salts and platinum complexes

Valeria Ferretti¹, Paola Bergamini¹, Lorenza Marvelli¹, Luca Bretta¹

1. Department of Chemical and Pharmaceutical Sciences, University of Ferrara, Ferrara, Italy

email: frt@unife.it

The cage-like phosphine 1,3,5-triaza-7-phosphaadamantane (PTA) is attracting a lot of attention in coordination chemistry due to its favorable properties like stability to oxidation, small dimensions, solubility in water. Actually, Ru, Pd, Pt, Au, Ag complexes containing PTA are under investigation for aqueous phase or biphasic homogeneous catalysis, anticancer activity, photoluminescence experiments as well as crystal engineering. PTA molecule has a basic character, and it undergoes a selective nitrogen protonation, while the preferred coordination site is phosphorus. However, unlike the related compound hexamethylenetetramine, very few structural studies on PTA salts have been reported so far. We have therefore undertaken a systematic synthetic-structural study on PTA- nutraceutical acids salts, aimed at exploring the structural features of the interactions between the different molecules. In all the obtained crystals the two partners are connected through a strong hydrogen bond of N-H...O type, as shown in figure 1a; for this reason, we hypothesized that such an interaction could be maintained when PTA is bound to a transition metal, even if the pKa values of the N-sites are in general modified by the coordination. The synthetic approach was then focused on platinum complexes, which are good candidates in medicinal applications as anticancer drugs, obtaining experimental evidences of the formation of supramolecular complex-acid adducts, in which it is still present an hydrogen bond involving one nitrogen atom of the coordinated PTA and the acidic carboxylic group. As an example, the *cis*-[PtCl₂(PTA)₂]/vanillic acid molecular couple is shown in Figure 1b.

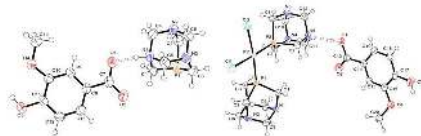


Figure 1. ORTEP views of a) PTA-vanillic acid salt and b) the *cis*-[PtCl₂(PTA)₂]/vanillic acid cocrystal

Keywords: PTA salts, Pt complexes, intermolecular interactions

MS36-P3 Inter- and intramolecular interactions of a series of oligoamide foldamers

Aku Suhonen¹, Riia Annala¹, Heikki Laakkonen¹, Elisa Nauha¹, Kaisa Helttunen¹, Maija Nissinen¹

1. Nanoscience Center (NSC), Department of Chemistry, University of Jyväskylä PO Box 35, FI-40014 University of Jyväskylä, Finland.

email: aku.suhonen@jyu.fi

Foldamers are synthetic biomimetic molecules composed of simple repeating units. They have been widely studied because of their vast potential as efficient and even stereoselective organocatalysts and as bioreceptor mimics.¹

We have prepared and crystallized three aromatic oligoamide foldamers of varying sizes, and analyzed their conformational and crystal packing properties.² As expected, hydrogen bonding is the most important non-covalent interaction affecting the molecular conformation and the crystal packing preferences. In addition, aromatic interactions play a stabilizing role.

The oligoamide foldamers adopt two distinct conformations, a helical @-conformation (Fig. 1) stabilized by intramolecular hydrogen bonds, and in the case of the longer molecules also by aromatic interactions, and a more open S-conformation. The choice between these two conformations seems to depend on the crystallization solvent; polar solvents facilitate the folding to an @-conformation whereas the S-conformation is obtained in non-polar solvents. As the molecules have several hydrogen bond donor and acceptor moieties they also display a wide array of crystal packing motifs, including molecular pairs, chains and solvent molecule assisted networks.

References

1. S. H. Gellman, *Acc. Chem. Res.* **1998**, *31*, 173-180.
2. a) A. Suhonen, E. Nauha, K. Salorinne, K. Helttunen and M. Nissinen, *CrystEngComm* **14** (2012), 7398-7407., b) A. Suhonen, M. Kortelainen, E. Nauha, S. Yliniemelä-Sipari, P. Pihko and M. Nissinen, *manuscript in preparation*, c) A. Suhonen, R. Annala, H. Laakkonen and M. Nissinen, *manuscript in preparation*.

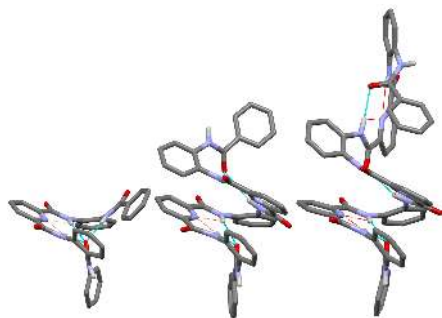


Figure 1. A series of three oligoamide foldamers with one, two and three pyridine core units.

Keywords: Foldamers, hydrogen bonding

MS36-P4 Different compounds from the same reactants: serendipity, misfortune or different reaction conditions?

Marisa Esterhuysen¹, Phillipus C. W. van den Berg¹, Hendrik G. Visser¹, Alice Brink¹, Marij a Zbačnik², Andreas Roodt¹

1. Department of Chemistry, University of the Free State, 9301 Bloemfontein, South Africa

2. Laboratory of General and Inorganic Chemistry, Department of Chemistry, University of Zagreb, 10002 Zagreb, Croatia

email: 2008005060@ufs4life.ac.za

The synthesis of chemical entities (pharmaceuticals, ligands, complexes, assemblies, etc.) is classically performed in solution (solvothermal). For example, in the case of Schiff base systems, Lin *et al.* [1] reported that in the solvothermal method of the synthesis of a carboxamide (*opda2pica*) derived from *o*-phenylenediamine (*opda*) and 2-picolinic acid (*2pica*), 70 mL of different solvents (pyridine, methanol, triphenylphosphate) was used. The reactants were dissolved, mixed and heated for more than 24 hours. The carboxamide was subsequently also coordinated to gallium(III) by means of the same solvothermal method using 40 mL of solvents. The total time required for this procedure was 24 hours yielding only 29% of the [Ga(*opda2pica*)₂] coordination compound.

In order to investigate these systems for biological and possible radiopharmaceutical evaluation but to use as little solvents as possible, we have applied a simple solution based method. Only 7 mL of methanol was used and the solutions were mixed and incubated at room temperature. After few hours serendipity played its role in chemistry and only a 1:2 co-crystal of *opda* and *2pica* was obtained. As (almost) solvent-free methods of synthesis (neat, liquid-, seeding-, ion-assisted grinding) have been recognised as potentially faster, environmentally friendly and economically acceptable ways to prepare new but also already known compounds, we re-evaluated the synthesis of the carboxamide and/or co-crystals of *opda* and *2pica* in few stoichiometric ratios.[2]

The success of the methods used was evaluated by means of FT-IR, PXRD, DSC and TG thermal analysis and NMR. Molecular and crystal structures were studied using SCXRD. This presentation will discuss the data obtained from this study to elucidate the reasons that lead to formation of co-crystals and/or carboxamide derived from *opda* and *2pica*.

[1] J. Lin, J.-Y. Zhang, T. Xu, X.-K. Ke, Z. Guo, *Acta Cryst.*, **C57**, 192-194, 2001.

[2] S. L. James, C. J. Adams, C. Bolm, D. Braga, P. Collier, T. Friščić, F. Grepioni, K. D. M. Harris, G. Hyett, W. Jones, A. Krebs, J. Mack, L. Maini, A. Guy Orpen, I. P. Parkin, W. C. Shearouse, J. W. Steed and D. C. Waddelli, *Chem. Soc. Rev.*, 2012, **41**, 413

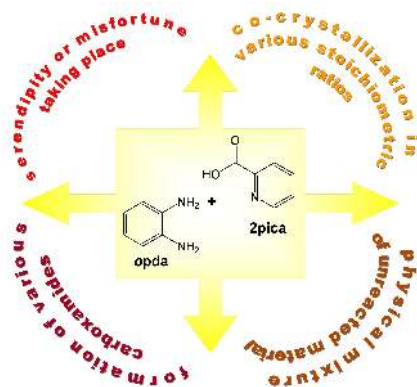


Figure 1. Schematic view of several possibilities of reaction of o-phenylenediamine (opda) and 2-picolinic acid (2pica).

Keywords: Carboxamide, Co-crystal, Solvothermal method, Solution based method, Grinding

MS36-P5 Intermolecular interactions of benzimidazole derivatives

Petra Bombicz¹, Gyula Tamás Gál¹, Ádám Lovász¹, Nóra V. Nagy¹, Tamás Holczbauer¹

1. Research Centre for Natural Sciences, Hungarian Academy of Sciences, POB 206, 1519 Budapest, Hungary

email: bombicz.petra@ttk.mta.hu

Imidazole is a constituent of the essential amino acid histidine what is present in many proteins and enzymes and plays a vital part in the structure and binding functions of hemoglobin. Imidazole is present in many pharmaceuticals, in antifungal, antiprotozoal and antihypertensive medications. It is a constituent of mercaptopurine, an immunosuppressive drug. There is benzimidazole moiety in vitamin B₁₂. A number of substituted imidazoles are selective inhibitors of nitric oxide synthase, which makes drug targets in inflammation, neurodegenerative diseases and tumors of the nervous system. The thermostable polybenzimidazole contains imidazole fused to a benzene ring, and acts as a fire retardant. Imidazole has been used extensively as a corrosion inhibitor on certain transition metals, such as copper.

The way to the aim to produce new substances with required properties is based on the knowledge of the structural properties of widely characterised solids. There is a long time effort to influence or favourably fine tune structural properties of solid materials by substituents and / or guest molecules. Their different sizes, shapes and chemical composition consequently alter the physico-chemical properties. In a crystal both steric requirements and electrostatic forces play a role in the architecture. A given packing arrangement may tolerate small changes caused either by the gradual change in site and/or size of substitution or in guest molecules incorporated into a host lattice. When the tolerance is terminated a different packing arrangement and/or a different molecular conformation appears. Occasionally the packing motifs may still remain but the motifs are moved relative to each other. The non-covalent interactions have an influence on the packing arrangement and the molecular recognition processes.

We present on the example of a series of benzimidazole derivatives how the balanced spatial requirements and electrostatic forces play a role in the arrangement of packing motifs in the crystals. Influencing the intermolecular interactions shows how the supramolecular synthon can be engineered.

Keywords: intermolecular interactions, isomorphy, packing arrangement

MS36-P6 The intramolecular hydrogen bond analysis in biologically active 5-fluoro-1*h*-indole-2,3-dione-3-thiosemicarbazones derivatives by experimental and theoretical methods

Arzu Karayel¹, F. Betül Kaynak², Nilgün Karalı³, Süheyla Özbey²

1. Department of Physics, Faculty of Arts and Sciences, Hitit University, 19030 Corum, Turkey

2. Physics Engineering Department, Faculty of Engineering, Hacettepe University, 06800 Ankara, Turkey

3. Department of Pharmaceutical Chemistry, Faculty of Pharmacy, Istanbul University, 34116 Beyazıt, Istanbul, Turkey

email: karayelarzu@gmail.com

There are several reports on the anticancer, antiviral and antibacterial activities of isatin-3-thiosemicarbazone derivatives (1-5). Investigations regarding the structure-activity relationships of 2-indolinones revealed that 5-halojenation and 3-thiosemicarbazone formations were efficient in increasing activity against a range of human cancer cells and various bacteria and viruses (3-8). In the light of these findings, 5-fluoro-1*h*-indole-2,3-dione 3-thiosemicarbazone derivatives were synthesized by reaction of *N*-substituted thiosemicarbazids with 5-fluoro-1*h*-indole-2,3-dione and evaluated for in vitro antituberculosis activity against *Mycobacterium tuberculosis* H37Rv. Their structures were confirmed by the spectral data elemental analysis and three of them were analysed by X-ray diffraction method. Due to playing a central role in the molecular structure and interactions of biologically molecules, the intramolecular hydrogen bonds (IHBs) were also calculated at the DFT level. Natural bond orbitals (NBO) calculations were used to examine the electronic characteristics of the intra-molecular hydrogen bonds. Experimental X-ray and NMR data were correlated with theoretical results. NBO energies show that the main contributions to energy stabilization correspond to LP → σ^* interactions for IHBs, O1...N3-H3 and N2...N4-H4; the delocalization LP → π^* for N₃-N₂=C₂ and N₃-C₉=S₁.

1. Teitz Y, Ronen D, Vansover A, Stematsky T, Riggs JL. Antiviral Res. 1994; 24: 305-314. 2. Karalı N. Eur J Med Chem 2002; 37: 909-918. 3. Hall MD, Salam NK, Hellawell JL, Fales HM, Kensler CB, Ludwig JA, Szakács G, Hibbs DE, Gottesman MM. J Med Chem. 2009; 52: 3191-3204. 4. Hall MD, Brimacombe KR, Varonka MS, Pluchino KM, Monda JK, Li J, Walsh MJ, Boxer MB, Warren TH, Fales HM, Gottesman MM. J Med Chem. 2011; 54: 5878-5889. 5. Kang I-J, Wang L-W, Hsu T-A, Yueh A, Lee C-C, Lee Y-C, Lee C-Y, Chao Y-S, Shih S-R, Chern J-H. Chem Lett 2011; 21: 1948-1952. 6. Güzel Ö, Karalı N, Salman, A. Bioorg Med Chem. 2008; 16: 8976-8987. 7. Sabet R, Mohammadpour M, et. al. Eur J Med Chem. 2010; 45: 1113-1118. 8. Karalı N, Gürsoy A, Kandemirli F, Shvetc N, Kaynak FB, Özbey S, et. al. Bioorg Med Chem. 2007; 15: 5888-5904.

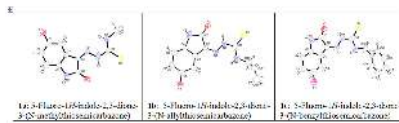


Figure 1. X-Ray Structures of 1a, 1b and 1c.

Keywords: 5-fluoro-1*h*-indole-2,3-dione, thiosemicarbazone, intramolecular hydrogen bonds, DFT, NBO

MS36-P7 Solid form control and design through structural informaticsGhazala Sadiq¹, Neil Feeder¹

1. The Cambridge Crystallographic Data Centre

email: sadiq@ccdc.cam.ac.uk

Uncontrolled crystal form polymorphism can have a critical impact on pharmaceutical drug product robustness, exemplified by NorvirTM [1] and NeuproTM [2]. The NorvirTM example illustrates how such polymorphism can be driven by a stronger set of hydrogen bonds in the stable form. At the CCDC we are developing structural informatics approaches to solid form design, including the Hydrogen-Bonding Propensity method which would have predicted the likely existence of the more stable polymorph of ritonavir (NorvirTM)[3].

Software including such methodologies is being developed under the guidance of the Crystal Form Consortium (CFC); a partnership between the CCDC and eleven global pharmaceutical companies. Here we will describe the potential application of these methodologies to minimise risk in solid form design.

Keywords: Polymorphism, Interaction, Pharmaceutical, Solid Form

MS36-P8 Cocrystallization out of the blue: DL-mandelic acid/ethyl-DL-mandelate cocrystalNatalia Tumanova¹, Natalia Tumanova¹, Géraldine Springuel¹, Bernadette Nornberg², Johan Wouters², Tom Leyssens¹

1. Université catholique de Louvain, Louvain-la-Neuve, Belgium

2. University of Namur, Namur, Belgium

email: natalia.tumanova@uclouvain.be

We present exceptional behavior of racemic mandelic acid in an ethanol solution. Dissolution of racemic mandelic acid in ethanol followed by evaporation to dryness results in a DL-mandelic acid/ethyl-DL-mandelate cocrystal. This behavior indicates that racemic mandelic acid tends not only to transform into an ester in ethanol, but also to immediately cocrystallize with untransformed acid molecules, thereby preventing a complete conversion of the acid into the ester. Cocrystal formation in ethanol was found to be reproducible under various conditions. DL-tropic acid and DL-phenyllactic acid that contain similar functional groups were tested as well, but no cocrystal formation was detected. The DL-mandelic acid/ethyl-DL-mandelate system has four chiral centers and presents a crystalline system with one of the co-formers being an ester, which is quite a rare phenomenon for cocrystals. Moreover, such an unexpected behavior of DL-mandelic acid should warn us that cocrystallization should be taken into account not only in the field of crystal engineering, but may even emerge as a byproduct in organic synthesis.

Keywords: cocrystallization, cocrystals, DL-mandelic acid

MS36-P9 Hydrogen bonding in a benzimidazole derivate - what is in a name ? A combined use of powder diffraction, solid state and molecular DFT study.

Lubo Smrček¹, Pavel Mach¹

1. Institute of Inorganic Chemistry, Slovak Academy of Sciences, Dubravská cesta 9, SK-845 36 Bratislava, Slovak Republic

email: uachsmrk@savba.sk

Apart for obvious electrostatic interactions the molecules of methyl 3-((benzimidazol-4(7)-yl)amino)-2-cyano-prop-2-enoate are in the structure (solved from powder diffraction data and refined by high quality energy minimization in the solid state) also held by N-H...N and C-H...N hydrogen bonds, remarkably differing in their strengths and roles. To evaluate the strength of these hydrogen bonds in the structure molecular DFT calculations applying dispersion corrected functional B97-D3 (environment-dependent D3 scheme with haVDZ basis set) as well as wave-function based SCS-MP2 method with def2-TZVPP basis set were done. Because wave-function based methods treat intermolecular electron correlation (a quantum-mechanical origin of dispersion interaction) in a different way than DFT does, application of the methods differing in their nature provides a stringent test of consistency of the resulting values. To estimate the interaction energy of infinite chain of N-H...N hydrogen bonded molecules a standard procedure based on extrapolation to infinity was applied. First, the interaction energies in a dimer, a trimer and in a tetramer of molecules of linked by one, two and three N-H...N bonds, were calculated. However, rather than the absolute value of the interaction energy it is the size of one its ingredients, of a dispersion interaction, which is of main interest here. For a dimer this contribution represents 78% of the interaction energy and this share slightly increases for the trimer (83%) and than just marginally for the tetramer (86%). Dispersion interaction calculated for pairs of molecules bound by the weaker C-H...N hydrogen bond is at DFT level of theory also relatively large, ~55%. It can be thus concluded that although from pure formal geometrical point of view the ribbons of the molecules in the structure are connected by hydrogen bonds, it should be clearly understood that in addition to the "pure" H-bond mechanism of interaction, it is dispersion interaction, which plays important role.

This work was supported by the Slovak Research and Development Agency under the contract No. APVV-0038-11.

Keywords: Weak interactions, hydrogen bonds, DFT, SCS-MP2

MS36-P10 Structural diversity in supramolecular compounds of para-sulfonatocalix[8]arene with phenanthroline

Barbara Lesniewska¹, Kinga Suwinska², Anthony W. Coleman³

1. Institute of Physical Chemistry PAS, ul. Kasprzaka 44/52, PL-01-224 Warszawa, Poland

2. Faculty of Mathematics and Natural Sciences, Cardinal Stefan Wyszyński University, Wóycickiego 1/3, PL-01 938 Warszawa, Poland

3. LMI, Universit_e Lyon 1 CNRS UMR 5615, 43 bvd 11 novembre, 69622 Villeurbanne, France

email: blesniewska@ichf.edu.pl

para-Sulfonatocalix[*n*]arenes are anionic, water soluble derivatives of calix[*n*]arenes, which are supramolecular hosts and 'building blocks' in crystal engineering. An important feature of these compounds is their ability to co-crystallize with variety of molecular species. They form a series of complexes with polar and non-polar molecules and/or metal cations both in solution and solid-state. They create a variety of supramolecular architectures such as bilayers, molecular capsules, polymers stabilized by hydrogen bonds, one or two-dimensional coordination polymers, motifs like 'ferris wheel' and 'Russian doll', helical arrays, channels filled with water molecules as well as nanometer-sized spheres or tubes¹.

Calix[8]arenes themselves may adopt sixteen 'up-down' conformations¹ and numerous others in which one or more of the aryl rings projects outward from the average plane of the molecule, depending on the functionalization of the macrocycle, the solvent used for the crystallization or the shape and nature of complexed guest molecules. The most common conformation, both in solution and in the solid state, is pleated loop conformation (Fig.1), stabilized by intramolecular hydrogen bonds O-H...O.

Calixarenes, due to their diversity and conformational mobility are important receptors in molecular recognition. The goal of this paper is to show structural diversity of *para*-sulfonatocalix[8]arene in complexes with 1,10-phenanthroline in solid state.

¹C. D. Gutsche. *Calixarenes: An Introduction*, 2nd ed., Royal Society of Chemistry, 2008.

²F. Perret, V. Bonnard, O. Danylyuk, K. Suwinska, A. W. Coleman. 2006, *New J. Chem.*, 30, 987.

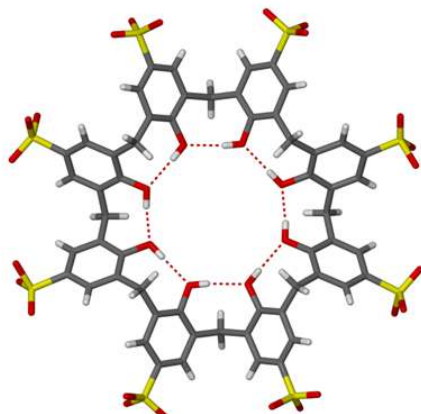


Figure 1. Pleated loop conformation of *para*-sulfonatocalix[8]arene².

Keywords: calixarenes, host-guest complexes, molecular recognition

MS36-P11 Hydrogen-bonded dimers of resorcinarene-based oxalamido-containing cavitands

Mario Cetina^{1,2}, N. Kodiah Beyeh¹, Zoran Džolić¹, Kari Rissanen¹

1. Department of Chemistry, University of Jyväskylä, P.O. Box 35, 40014 Jyväskylä, Finland

2. Department of Applied Chemistry, Faculty of Textile Technology, University of Zagreb, Zagreb, Croatia

email: m Cetina@tff.hr

The rational design of organic compounds and their controlled self-assembly through non-covalent associations to give defined supramolecular nano-structures is a stimulative and innovative approach for the development of smart structures and materials with extensive structural diversity and applications. Recently, much attention has been paid to researches on molecular systems containing self-complementary groups with the potential to construct cages, bowls and capsules [1,2].

Herein, we present the crystal structures of two resorcinarene-based oxalamido-containing cavitands featuring extended sides and self-complementary hydrogen bonding sites that form capsular-like structures. The hydrogen bonding interactions in these structures give rise to the formation of dimers. The self-included dimers are linked by numerous intermolecular interactions so forming firstly one-dimensional polymer structures, which are further linked into three-dimensional networks. In the construction of such supramolecular architectures participates various types of interactions, from strong hydrogen bonds (N–H···O, N–H···N) to weak C–H··· π interactions which also play important role in their formation.

[1] Beyeh, N.K.; Rissanen, K. (2011) *Isr. J. Chem.*, **51**, 769-780.

[2] Jędrzejewska, H.; Wierzbicki, M.; Cmoch, P.; Rissanen, K.; Szumna, A. (2014) *Angew. Chem. Int. Ed.*, **53**, 13760-13764.

Keywords: cavitands, resorcinarenes, non-covalent interactions

MS36-P12 Effect of methyl and hydroxyl substitution to the single crystal formation of some hydroxypyridinecarboxylic acids and their copper(II) complexes

Nóra V. Nagy¹, Nóra V. Nagy¹, Valerio B. Di Marco², Tamás Holczbauer¹, Petra Bombicz¹

1. Institute of Organic Chemistry, Research Centre for Natural Sciences HAS, Magyar tudósok körútja 2, 1117 Budapest, Hungary
2. Department of Chemical Sciences, University of Padova, via Marzolo 1, 35131 Padova, Italy

email: may.nora@ttk.mta.hu

A few methyl and hydroxyl substituted hydroxypyridinecarboxylic acids (HPC's) and their copper(II) complexes have been synthesized, crystallized and their structure were investigated by single crystal X-ray diffraction. These compounds are part of a series of HPC compounds which were developed as potential metal chelators for the treatment of metal overload. Redox active metals, like iron and copper, can undergo redox cycling and cause oxidative stress by increasing the formation of reactive oxygen species (ROS), resulting in the damage of many biomolecules in the cells. Copper overload is implicated in the pathogenesis of a variety of human diseases like cancer, cirrhosis, atherogenesis and neurodegenerative diseases, and it plays a key role in the copper metabolism disorders as Menkes and Wilson diseases. Similarly, iron overload is one of the most common metal toxicity diseases worldwide. Chelation therapy aims to remove toxic metal ions from human body or attenuate of their toxicity by transforming them into less toxic compounds. The basic requirement of a chelator is the stability of its complexes, which must be completely formed before their excretion. As the chelators should fulfill specific bio-chemical properties (high complex stability, fast formation kinetics, high selectivity for specified ion, good bioavailability, low toxicity), the design of non-toxic but metal-selective ligands is extremely difficult. Structural information about these ligands and their metal complexes can significantly support the drug developing. As a systematic series of HPC' with slightly altered molecules are investigated, the understanding of the supramolecular interactions (H-bridge, electrostatic coupling and other secondary interactions) exhibited in solid state will facilitate the fine-tuning of the structural properties in order to produce new substances with required properties. Our goal is to investigate the structure of these ligand molecules and their metal complexes (especially with copper(II)) by single crystal X-ray diffraction. The structure of two free ligands (space groups *Pna*2₁ and *P2*₁/*c*), one of them also as HCl salt (space group *P2*₁/*n*) and two polymorphic forms of a copper(II) complex (space groups *P*-1 and *P2*₁/*n*) have been revealed and studied so far.

$R_1, R_3, R_4 = \text{H}, \text{CH}_3, \text{COOH}$

$R_2 = \text{CH}_3, \text{CH}_2\text{CH}_2\text{OH}$

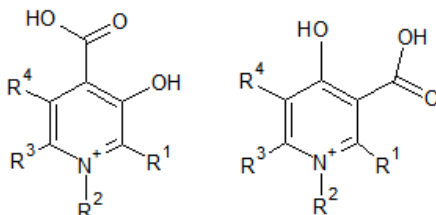


Figure 1. General formula of hydroxypyridinecarboxylic acid derivatives

Keywords: hydroxypyridinecarboxylic acid, chelat therapy, copper(II) complexes, secondary interactions

MS36-P13 High-pressure phase transitions in the family of photosensitive Co(III) complexesBoris A. Zakharov^{1,2}, Alexander S. Marchuk², Elena V. Boldyreva^{1,2}

1. Institute of Solid State Chemistry and Mechanochemistry, Siberian Branch of the Russian Academy of Sciences, Kutateladze 18, Novosibirsk 630128, Russia
 2. Novosibirsk State University, Pirogova 2, Novosibirsk 630090, Russia

email: b.zakharov@yahoo.com

It is known that mechanical stresses arise during any reaction in solid state. Stresses and strain influence reaction kinetics, reaction course, spatial propagation and sometimes chemical composition of reaction products. It is much easier to study interrelation between chemical reaction and strain in a crystal if the reaction is homogeneous. There are only few examples of homogeneous solid state reactions and one of the best studied examples is reversible nitro-nitrito linkage isomerisation in $[\text{Co}(\text{NH}_3)_5\text{NO}_2]\text{XY}$ ($\text{X}, \text{Y} = \text{Cl}, \text{Br}, \text{I}, \text{NO}_3$) complexes. These compounds were extensively studied during the last decades [1–4]. It is therefore very important to know mechanical properties of each crystal structure, in order to interpret and control various photomechanical effects, including the recently studied that could help us to explain mechanism of linkage isomerisation in details and can also help us to understand “photosalient effect” [5].

The aim of the present study was to follow high-pressure behavior of several compounds from $[\text{Co}(\text{NH}_3)_5\text{NO}_2]\text{XY}$ family. We have re-visited phase transition in $[\text{Co}(\text{NH}_3)_5\text{NO}_2]\text{I}_2$ at 0.7 GPa [6] using single-crystal X-ray diffraction technique. We have also found high-pressure phase transitions in $[\text{Co}(\text{NH}_3)_5\text{NO}_2]\text{Br}$, and $[\text{Co}(\text{NH}_3)_5\text{NO}_2]\text{BrNO}_3$ at 6.8 and 3.0 GPa respectively. In contrast to other studied compounds, phase transition in $[\text{Co}(\text{NH}_3)_5\text{NO}_2]\text{Br}$, was shown to be of single crystal – single crystal type and reversible without crystal breaking. We have also compared the results with high-pressure data for the compounds from the same family $[\text{Co}(\text{NH}_3)_5\text{NO}_2]\text{XY}$ ($\text{X}, \text{Y} = \text{Cl}, \text{Br}, \text{I}, \text{NO}_3$) which are stable in the studied pressure range.

The work was supported by grant from RFBR 14-03-00902.

1) Boldyreva E.V., Sidelnikov A.A., Chupakhin A.P., Lyakhov N.Z., Boldyrev V.V., *Proceed. Acad. Sci. USSR* 1984, 277, 893–896. 2) Boldyreva E.V., *Mol. Cryst. Liq. Cryst. Inc. Non-Lin. Opt.* 1994, 242, 17–52. 3) Boldyreva E.V. *Coord. Chem. Russ.*, 2001, 27(5), 323–350. 4) Nath N.K., Panda M.K., Sahoo S.C., Naumov P., *CrystEngComm*, 2014, 16, 1850–1858. 5) Naumov P., Sahoo S.C., Zakharov B.A., Boldyreva E.V., *Angew. Chem. Int. Ed.*, 2013, 52, 9990–9995. 6) Boldyreva E.V., Ahsbahs H., Uchtmann H., Kascheeva N. E., *High Pressure Research*, 2000, 17(2), 79–99.

Keywords: high pressure, X-ray diffraction, phase transitions, reactivity of solids

MS36-P14 A Kryptoracemate: a rare example of a racemic solution crystallizing in a Sohnke space groupReik Laubenstein¹, Beatrice Braun¹, Thomas Braun¹

1. Humboldt-Universität zu Berlin, Brook-Taylor-Str. 2, 12489 Berlin, Germany

email: laubensr@cms.hu-berlin.de

A rare outcome of the crystallization of a racemic solution is the formation of a kryptoracemate^{1,2} (also named false conglomerate³), in which a racemic solution produces enantiomorphic crystals which consist, however, of a racemic pair. We were fortunate to come across such well-ordered racemic crystal structure (*kryptorac*-1) crystallizing in the Sohnke space group $P2_12_12_1$ with two independent molecules of opposite chirality in the asymmetric unit which show no pseudosymmetry and which differ significantly with respect to soft conformational degrees of freedom. Our kryptoracemate is particularly interesting, since often the pairs of enantiomers in kryptoracemates have very similar conformations and they show pseudosymmetry.¹ Figure below shows an overlap of the two independent molecules in the asymmetric unit of *kryptorac*-1.

A polymorphic structure of the kryptoracemate crystallizes as a monoclinic twin with β approximately 90° in the centrosymmetric space group $P2_1/c$ (*rac*-1) with two independent molecules of the same chirality in the asymmetric unit and with similar lattice parameters as the kryptoracemate. Powder diffraction performed on bulk material revealed that *rac*-1 and *kryptorac*-1 co-exist.

Due to its free movement along three different bonds, this class of molecules can adopt several conformations, some of them being more abundant than others. A large number of similar compounds were prepared and structurally characterized. Their conformations, packing, hydrogen and halogen bonding and π stacking interactions are further discussed in order to understand the driving force for the formation of the kryptoracemate

Note that the Cambridge Structural Database is approaching 745,000 entries (CSD Version 5.36 and the updates, November 2014). Out of them, only a number of approximately 200 credible kryptoracemates were identified.^{1,2} An exhaustive search for this kind of compounds is rather difficult to undertake.

1. L. Fábíán and C. Pratt Brock, *Acta Crystallographica Section B*, **2010**, B66, 94–103 and references therein. 2. I. Bernal, S. Watkins, *Acta Crystallographica Section C*, **2015**, C71, 216–221 and references therein. 3. R. Bishop, M. L. Scudder, *Crystal Growth & Design*, **2009**, 9(6), 2890–2894.

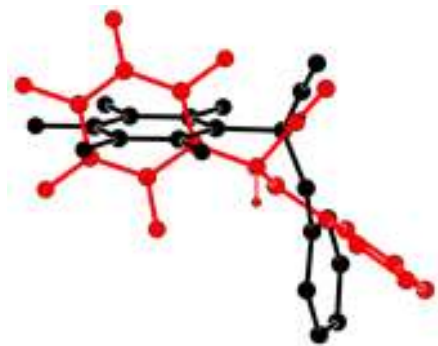


Figure 1.

Keywords: kryptoracemate, false conglomerate, chiral solids, polymorphism, intermolecular interactions, halogen bonding, H bonding, π stacking interactions

MS36-P15 A technique for the comparison and analysis of decorated molecular surfaces

Peter R. Spackman¹, Dylan Jayatilaka¹

¹. University of Western Australia

email: 20265845@student.uwa.edu.au

Molecular surfaces of various types are of immense value in chemistry. Typically, comparison and analysis of such surfaces relies upon human intuition and understanding which is inherently subjective.

We present a technique to describe the shape of the surface, and any associated properties on the surface (so-called decorations) which preserves relative location information while remaining translation and rotation invariant. The technique relies on a spherical harmonic decomposition followed by manipulation of the expansion coefficients in order to generate any number of rotation-invariant descriptors. [1] Although others have employed spherical harmonic decompositions for shape (see [2], [3]), the generation of rotation-invariant descriptors for shape and properties mapped on the surface is new in this context.

Importantly, the technique provides the capability to greatly reduce the amount of information which is invaluable for efficient large-scale algorithmic classification. An example of shape reconstruction is shown Figure 1 dependent only on the highest angular momentum l_{\max} of the spherical harmonics used in the process.

The technique will be applied on several sets of decorated Hirshfeld surfaces. Conclusions will be drawn from cluster analysis to objectively examine questions related to, for example, shape and interaction-dependent factors affecting crystal packing; and binding-pocket correlations for drug-search and co-crystallisation applications.

References

1. Burel, G. and H. Henocq, *3-DIMENSIONAL INVARIANTS AND THEIR APPLICATION TO OBJECT RECOGNITION*. Signal Processing, 1995. **45**(1): p. 1-22.
2. Morris, R.J., et al., *Real spherical harmonic expansion coefficients as 3D shape descriptors for protein binding pocket and ligand comparisons*. Bioinformatics, 2005. **21**(10): p. 2347-2355.
3. Venkatraman, V., et al. "Potential for Protein Surface Shape Analysis Using Spherical Harmonics and 3D Zernike Descriptors." *Cell Biochemistry and Biophysics*, 2009. **54**(1-3): 23-32.

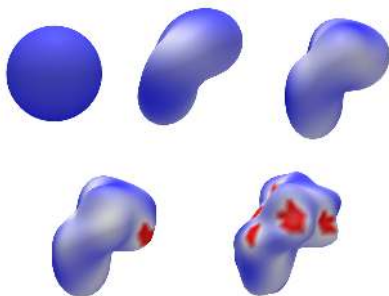


Figure 1. Reconstruction (from the resultant shape coefficients) of a sucrose molecule Hirshfeld surface along with a property on the surface (in this case d_{norm}) for angular momentum $l = 1, 4, 6, 8, 9$

Keywords: spherical harmonics, Hirshfeld surface, crystal packing, intermolecular interactions, cluster analysis

MS36-P16 Cyclohexylhemicucurbit[8]uril - a chiral macrocyclic host for anionic guests

Sandra Kaabel^{1,2}, Filip Topić², Elena Prigorchenko¹, Marina Kudrjašova¹, Elina Kalenius², Lauri Kivijärvi², Riina Aav¹, Kari Rissanen²

1. Department of Chemistry, Tallinn University of Technology, Akadeemia tee 15, 12618 Tallinn, Estonia

2. University of Jyväskylä, Department of Chemistry, Nanoscience Center, P.O. Box. 35, FI-40014 University of Jyväskylä, Finland

email: sandra.kaabel@ttu.ee

Cucurbituril chemistry has gained considerable interest over the last decades. Classical cucurbit[n]uril (CB[n]) homologues, known to encapsulate neutral or positively charged molecules, have already been employed in stimuli responsive systems and in CB[n] mediated catalysis.^{[1][2]} Accounts of anion binding within CB[n] homologues are scarce, with the exception of hemicucurbit[n]urils (HC[n]), a sub-group of the CB[n] family, known to preferentially bind anions.^{[3][4]}

Chiral cyclohexylhemicucurbit[n]urils (cycHC[n]) have been synthesized and investigated by our group.^{[5][6]} The electron-poor cavity of cycHC[n] renders these macrocycles capable of anion recognition.^[7] Our recent efforts to gain insight into the binding of anionic guests by cycHC[8] have resulted in a number of successfully crystallized and structurally characterized complexes. Crystal structures of 1:1 complexes with a number of singly charged tetrahedral and octahedral anions have been successfully obtained, demonstrating the remarkable ability of cycHC[8] to accommodate guests of different shapes and sizes. The flexible nature of the cycHC[8] portals allows for tight sealing of the encapsulated guests. Additionally, the binding of anionic guests to cycHC[8] has been complementarily evaluated by ESI-TOF MS and NMR spectroscopy.

[1] L. Isaacs, *Acc. Chem. Res.* **2014**, *47*, 2052–2062. [2] K. I. Assaf, W. M. Nau, *Chem. Soc. Rev.* **2014**, *44*, 394–418. [3] Y. Miyahara, K. Goto, M. Oka, T. Inazu, *Angew. Chem. Int. Ed. Engl.* **2004**, *43*, 5019–5022. [4] M. A. Yawer, V. Havel, V. Sindelar, *Angew. Chem. Int. Ed. Engl.* **2015**, *54*, 276–279. [5] R. Aav, E. Shmatova, I. Reile, M. Borissova, F. Topić, K. Rissanen, *Org. Lett.* **2013**, *15*, 3786–3789. [6] M. Fomitsenko, E. Shmatova, M. Ören, I. Järving, R. Aav, *Supramol. Chem.* **2014**, *26*, 698–703. [7] M. Ören, E. Shmatova, T. Tamm, R. Aav, *Phys. Chem. Chem. Phys.* **2014**, *16*, 19198–19205.

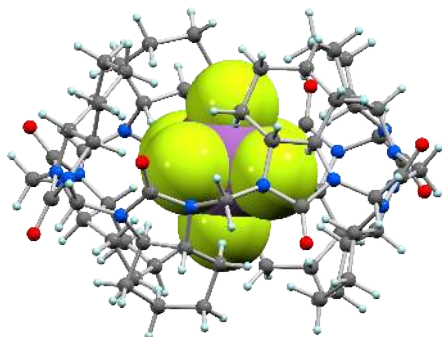


Figure 1. The structure of an inclusion complex of cycHC[8]:SbF₆⁺ from X-ray diffraction analysis

Keywords: hemicucurbiturils, host-guest chemistry, anion binding

MS36-P17 Shortest intermolecular contacts in crystals of organic compounds

Michał Kaźmierczak¹, Andrzej Katrusiak¹

¹. Department of Materials Chemistry, Faculty of Chemistry, Adam Mickiewicz University in Poznań, Umultowska 89b, 61-614 Poznań, Poland

email: kax@amu.edu.pl

The intermolecular interactions are one of the most important factor governing the formation of crystal structures.[i],[iii] Therefore characterization of the shortest contacts is extremely important for understanding this process, developing methods of crystal engineering[iiii] and predicting the crystal structures.[iv] The investigation of the shortest contacts population reveals bimodal distribution and a clear distinction between strong and weak interactions. Further deconvolution, show that populations are sum of Gaussian-like distributions for specific intermolecular contacts (Fig. 1).[v] Fitting to correct function gave parameters, like mean distance and standard deviation, very useful for validating crystal structures. Moreover, we have found group of crystal structures which does not have any van der Waals contacts,[vi] according to Bondi.[vii] The existence of such population is an important input in discussion of van der Waals radii values, and can be starting point for their recalculation.

[i] Desiraju, G. R. *Crystal Engineering: The Design of Organic Solids*; Elsevier: Amsterdam, 1989.

[ii] Desiraju, G. R. *A Bond by Any Other Name* *Angew. Chem., Int. Ed.* 2011, 50, 52–59.

[iii] Nalini, V.; Desiraju, G. R. *The Role of Non-bonded Interactions Involving Sulphur in the Crystal Engineering of 4 Å Short Axis Structures. Unusual Topochemical Reactivity of 4-(4-chlorophenyl)-thiazole-2(1H)-thione*. *J. Chem. Soc., Chem. Commun.* 1986, 1030–1032.

[iv] Price, S. L. *Computed Crystal Energy Landscapes for Understanding and Predicting Organic Crystal Structures and Polymorphism*. *Acc. Chem. Res.* 2009, 42, 117–126.

[v] Kaźmierczak, M. and Katrusiak, A. *Bimodal Distribution of the Shortest Intermolecular Contacts in Crystals of Organic Compounds* *Crystal Growth & Design* 2014 14 (5), 2223–2229.

[vi] Kaźmierczak, M.; Katrusiak, A. *The Most Loose Crystals of Organic Compounds* *J. Phys. Chem. C* 2013, 117, 1441–1446.

[vii] Bondi, A. *van der Waals Volumes and Radii*. *J. Phys. Chem.* 1964, 68, 441–451.

[viii] Allen, F. H. *The Cambridge Structural Database: A Quarter of a Million Crystal Structures and Rising*. *Acta Crystallogr., Sect. B: Struct. Sci.* 2002, 58, 380–388.

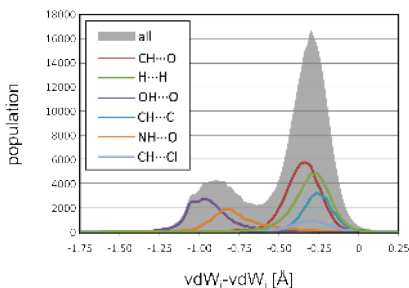


Figure 1. Distribution of six most popular types of shortest contacts in the CSD[viii] in function of small distances between van der Waals spheres.

Keywords: Intermolecular Interactions, Crystal Engineering

MS36-P18 [C₁₀mim][Cl]: An ionic liquid, a liquid crystal and a crystallisation solvent

Sofiane Saouane¹, Francesca P. A. Fabbiani¹

¹. GZG, Abteilung Kristallographie, Georg-August-Universität Göttingen, Göttingen, Germany

email: ssaouan@gwdg.de

Ionic liquids (ILs) are molten salts below the boiling point of water.¹ ILs are referred to as “designer solvents”:² they can be pre-tuned to desired physical and chemical properties through the numerous combinations of cations and anions. The sphere of interest in ILs has increased in the last decades. ILs’ versatile properties enable their application in several fields, among them the pharmaceutical research where ILs are starting to attract interest as crystallisation solvents.³

In a series of investigations of imidazolium-based ILs,⁴ the solid state behaviour of 1-decyl-3-methylimidazolium chloride, [C₁₀mim][Cl], has been studied using crystallisation and diffraction techniques at non-ambient conditions. The characterisation of the rich, hitherto unknown solid-state behaviour of [C₁₀mim][Cl] hydrates and liquid crystal phases are presented herein, along with preliminary results of adopting ILs as high-pressure crystallisation media for investigating drug polymorphism.

Keywords: ionic liquids, intermolecular interactions, high pressure, low temperature, crystallisation, hydrates.

MS37. Molecular crystalline processes at ambient and non-ambient conditions

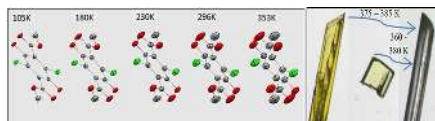


Figure 1. To the left 5 structures of Y with displayed ADPs in temperature steps 105K, 180K, 230K, 296K and 353K. The right image is of the three different coloured polymorphs from left yellow, light yellow and White and with their phase transition temperatures.

Chairs: Elena Boldyreva, Gareth Lloyd

Keywords: Polymorphism, thermostability, ab-initio, chromomorphism, phase transition

MS37-P1 Thermostability of the chromomorph

dimethyl3,6-dichloro-2,5-dihydroxyterephthalate

Philip Miguel Kofoed¹, Anna Hoser², Anders Madsen²

1. Nano-Science Center, University of Copenhagen

2. Department of Chemistry, University of Copenhagen

email: vrj813@alumni.ku.dk

A century ago Hantzsch[1] observed that dimethyl 3,6-dichloro-2,5-dihydroxyterephthalate (MCHTEP) exhibited chromomorphism, upon heating yellow single crystals (Y) to 430K they entered a solid state phase transformation and change into white crystals (W). Later a third light yellow (LY) form was discovered by Yang, Richardson & Dunitz[2] a light yellow (LY). By a multi-temperature study they investigated how the structural differences between the different polymorphs could lead to colour change and phase transformation. Especially the thermal parameters were probed as a function of temperatures. With this information they formulated a model of the thermostability of the three known forms based on vibrational energies and entropies. In the publication by Yang et al. they concludingly write the following statement: *Why has our intuition led us astray in expecting that the crystals with the larger atomic ADP's should have the greater entropy? ... The problem is left to the theoreticians.*

We investigate the system once more by introducing modern periodic ab-initio calculations as well as making a diffraction study of the system at approximately 10K. The ab-initio calculations in combination with the multi-temperature diffraction measurements allow us to assess the vibrational contribution to crystal stability in much more detail than previously done. This will be evaluated by calculation of cohesive energies with Crystal09[3,4] and comparison with other energy calculations programs like Pixel[5,6]. From Crystal09 we additionally derive lattice-dynamical information, and use this information to perform a normal mode refinement to obtain the vibrational energies and entropies[7], and thereby explain the phase transformations in this interesting chromomorphous system.

MS37-P2 Transformation of α -cyclodextrin hydrates at high pressure: a combined X-ray diffraction and molecular dynamics study

Rubén Granero-García¹, Ben Corry², Francesca P.A. Fabbiani¹

1. Crystallography Department, GZG, Georg-August-Universität Göttingen, Göttingen, Germany
2. Research School of Biology, Australian National University, ACT, Australia

email: ruben.granero@geo.uni-goettingen.de

The application of moderately high pressures is a powerful tool to induce structural changes in crystals of organic compounds. We are particularly interested in a detailed understanding of how and why structural transformations take place as a function of pressure. To provide a better answer to these questions we have complemented some of our single-crystal X-ray diffraction studies with molecular dynamics simulations.

One of the hydrates (form I) of α -cyclodextrin, a cyclic derivative of starch composed of six glucose units, incorporates additional water molecules in its cavity under compression up to 0.65 GPa. Concomitantly, one of the terminal hydroxyl groups becomes increasingly disordered as pressure is applied, expanding the available volume in the cavity [1]. Usually, compression of a molecular material enhances order and reduces the void volume [2–6], opposite to our experimental findings. This has motivated us to further explore the system using molecular dynamics.

First, we have performed simulations of the crystal in the absence of solvent at different pressures to study whether pressure has a direct effect on the disorder of the terminal hydroxyl groups. Second, we have carried out simulations on a cluster of unit cells immersed in water to study possible relationships between disorder, water content and pressure. From these simulations we have also been able to explore how the inclusion of water in the cavities takes place. Third, we have performed free energy calculations to better understand the rotation of the terminal hydroxyl groups and the movement of water through the crystal. Combining all our findings we propose a mechanism for the inclusion of water in α -cyclodextrin in the solid state at high pressure, which differs from the induced-fit mechanism that operates in solution at ambient pressure [7].

References

- [1] R. Granero-García, F. J. Lahoz, C. Paulmann, S. Saouane, F. P. A. Fabbiani, *CrystEngComm*, **2012**, *14*, 8664–8670
- [2] A. Olejniczak, A. Katrusiak, A. Vij, *CrystEngComm*, **2009**, *11*, 1073–1080
- [3] F. P. A. Fabbiani, G. Buth, B. Dittrich, H. Sowa, *CrystEngComm*, **2010**, *12*, 2541–2550
- [4] S. A. Moggach, C. H. Göbbitz, J. E. Warren, *CrystEngComm*, **2010**, *12*, 2322–2324
- [5] E. V. Boldyreva, *Acta Crystallogr. Sect. A*, **2008**, *64*, 218–231
- [6] P. A. Wood, J. J. McKinnon, S. Parsons, E. Pidcoc, M. A. Spackman, *CrystEngComm*, **2008**, *10*, 368–376
- [7] W. Saenger, N. Noltenmeyer, P. C. Manor, B. Hingert, B. Klar, *Bioorg. Chem.*, **1976**, *5*, 187–195

Keywords: Molecular crystals, High pressure, Molecular dynamics

MS37-P3 Radiation damage in chemical crystallography

Peter N. Horton¹, Simon J. Coles¹, Mateusz B. Pitak¹, Graham J. Tizzard¹, Claire Wilson²

1. UK National Crystallography Service, Chemistry, University of Southampton, Southampton, SO17 1BJ, U.K.
2. School of Chemistry, University of Glasgow, Glasgow, G12 8QQ, U.K.

email: pnh@soton.ac.uk

Although crystals suffering radiation damage is a well-known and studied phenomena for macromolecular crystallography¹, as far as we are aware there still appears to be no such published work relating to chemical crystallography. However, there are numerous anecdotal accounts of disintegrating crystals and resolution progressively dropping off that have been ascribed to radiation damage. Since the start of operations on the small molecule synchrotron beamline I19² at Diamond Light Source, there have been repeated comments from multiple users observing sample damage in the beam.

The UK National Crystallography Service³ handles a wide variety of samples and a number of these have experienced radiation damage. In order to understand the causes and symptoms of this effect in greater detail some controlled experiments were performed. A series of experiments were conducted on crystals that were known to undergo radiation damage in order to determine some quantification of the effect. Additionally the aim is to understand what one might be able to do to mitigate against the damage caused and determine whether the effects observed are similar to those of macromolecular crystallography. The effects of varying the collection temperature, overall dose, dose rate and wavelength of X-ray used were all tested and normalised for each sample.

Samples where radiation damage has been observed were chosen and were also required to be air stable and preferably not suffer from solvent loss, in order to minimize problems of non-reproducibility. Those chosen to probe this effect were:

1. A gold complex – has potential to suffer heavily from absorption effects.
2. A nickel complex with significant solvent water – this could to some extent mimic the behaviour exhibited by proteins.
3. A small organic compound – an example of unexpected decay. The poster will summarise the results of these experiments and contrast them with data collected on a high intensity rotating anode laboratory source.

[1] B. G. Ravelli, E. F. Garman, *Current Opinion of Structural Biology*, (2006), *16*, 624–629

[2] H. Nowell, S. A. Barnett, K.E. Christensen, S. J. Teat, D. R. Allan, *J. Synchrotron Rad.*, (2012), **19**, 435–441

[3] S. J. Coles and P. A. Gale, *Chem. Sci.*, 2012, **3**(3), 683–689

Keywords: Radiation Damage,

MS37-P4 Understanding phase transformation behaviour in aliphatic amino acids

Mateusz B. Pitak¹, Terry L. Threlfall¹, Claire Wilson², Simon J. Coles¹

1. Chemistry, University of Southampton, Highfield Campus, Southampton SO17 1BJ, UK

2. School of Chemistry, University of Glasgow, Joseph Black Building, Glasgow G12 8QQ, UK

email: m.pitak@soton.ac.uk

Polymorphism in DL-methionine and DL-norleucine was reported in the early 1950's in pioneer X-ray studies by Mathieson¹ and since then it has been subject to many detailed structural, thermoanalytical and spectroscopic studies. Amino acids with aliphatic side chains are particularly suitable for systematic study as they form sets of highly related structures which contain well-defined hydrogen bonded bilayers. The bilayers arrange to form structures where the hydrophobic side chains interact with each other through van der Waals interactions only. They exhibit remarkable thermal behaviour. Phase transformations in these materials are fully reversible and involve concerted molecular displacements and can therefore exhibit several forms, but their presence may be elusive and extremely hard to record. Even small degrees of rotation about bonds in the aliphatic chain can result in the formation of new phases. In a previous study², we presented the crystal structure of the elusive high temperature form of DL-norleucine. This material undergoes two single crystal to single crystal transformations leading to three unique forms at different temperatures. We showed that concerted translation of each bilayer in the crystal led to a sequence of $C2/c > P2_1/c > C2/c$ transformations. It has been shown that related amino acids (DL-norvaline & DL-aminobutanic acid) exhibit similar transformation patterns^{3,4}. The low temperature phase of DL-norvaline has not been successfully determined, but it can be assumed that it should be $C2/c$. In fact, recently re-determined high and low temperature phases of DL-aminobutanic acid are shown to be a mixture of $P2_1/c$ and $C2/c$ forms⁵. To understand the driving force behind these phase transition phenomena we have extended our studies to other aliphatic amino-acids. Our recent X-ray diffraction studies, complemented by DSC and Hot-stage Microscopy, on 2-aminoheptanoic acid ($C_7H_{15}NO_2$) show complex thermal behaviour over a wider temperature range. We examined the 30K - 400K range and found five possible forms. Three of these forms follow fully reversible $C2/c > P2_1/c > C2/c$ transformations. The remaining two low temperature forms are even more complicated and are currently under investigation.

1. A. Mathieson, *Acta Cryst.* 6, 1953, 399

2. S.J.Coles, et.al, *Crystal Growth & Des.* 2009, 4610

3. C.H.Göribitz, *J. Phys.Chem.B*, 2011, 115, 2447

4. T. Ichikawa, et.al, *Acta Cryst.* B24, 1968, 1488

5. C.H.Göribitz, et.al, *J.Phys.Chem.B*, 2012, 116, 10715



Figure 1. Hot-stage polarised optical microscopy of the highly reversible transformation of 2-aminobutanic acid in the range of 393K to 400 K.

Keywords: polymorphism, phase transformations, thermal analysis, crystallisation

MS37-P5 A racemic solution of an organometallic complex crystallizing as a disordered crystal structure of opposite enantiomers (pseudoracemate) in a chiral space group

Roy Herrmann¹, Beatrice Braun¹, Thomas Braun¹

1. Humboldt-Universität zu Berlin, Brook-Taylor-Str. 2, 12489 Berlin (Germany)

email: roy.herrmann@chemie.hu-berlin.de

The crystallization of a racemic solution results generally in three types of crystalline racemates: racemic compounds, racemic conglomerates, or pseudoracemates (see Figure). The most encountered type of crystalline racemates are racemic crystals (heterochiral) in which both *S* and *R* enantiomers are present in an equal amount in the unit cell in a well-ordered manner. Additionally, as a result of spontaneous resolution in *S* and *R* handed crystals, conglomerates (homochiral) can be obtained. A rare outcome of the crystallization of a racemic solution is the formation of pseudoracemic crystals (heterochiral), in which both *S* and *R* enantiomers are present in the crystal structure in a disordered manner.^[1] A Pseudoracemate is a solid solution of opposite enantiomers which can crystallize in any space group. Their existence was first formulated by Kipping and Pope.^[2]

All three types of crystalline racemates differ in their melting point diagrams and properties. That is why their accurate characterization is crucial for the pharma industry in the context of chiral drug design. Due to the fact that in general, only one of the enantiomers has biological activity, the other being inactive, inhibiting the desired effect or even being toxic. We were fortunate to come across such structure with a 1:1 stoichiometry of opposite enantiomers. Particularly interesting and extraordinarily rare is the fact that our pseudoracemate crystallizes in a Sohncke space group, therefore making a heterochiral crystal crystallize in a chiral space group. The compound under discussion is an organometallic complex crystallizing as a THF solvate in the monoclinic chiral space group $P2_1$. The asymmetric unit contains one independent complex¹ molecule on general position, whereas no other particularly interesting intra- or intermolecular interactions are present.

[1] H. D. Flack, *Helv. Chim. Acta* **2003**, *86*, 905–921.

[2] F. S. Kipping, W. J. Pope, *J. Chem. Soc. Trans.* **1897**, *71*, 989–1001.

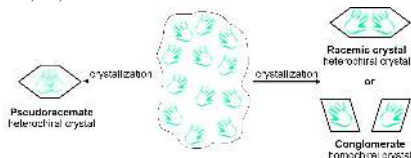


Figure 1. Crystallization types of a racemic solution.

Keywords: chirality, racemate, pseudoracemate, organometallic compounds

MS37-P6 X and N multi-temperature study on rotational disorder in crystalline N-Acetyl-L4-hydroxyproline

Jens Luebben^{1,2}, Birger Dittrich², Alison Edwards³

1. Georg-August-University Goettingen, Tammanstrasse 4, 37077 Goettingen, Germany

2. University Hamburg, Martin-Luther-King-Platz 6, 20146 Hamburg, Germany

3. Australian Nuclear Science and Technology Organisation, New Illawarra Road, Lucas Heights, Australia

email: jens.luebben@stud.uni-goettingen.de

Molecular crystals of N-Acetyl-L4-hydroxyproline and N-Acetyl-L4-hydroxyproline monohydrate show rotational disorder of acetyl hydrogen atoms at different temperatures. [1, 2] The anhydrate is disordered at temperatures above 200 K while the monohydrate form shows disorder at temperature above 100 K. A multi temperature study using X-Ray and neutron diffraction was carried out to understand better the conditions that cause this effect and the effect of disorder in general.

The identical chemical bonding in both compounds and the similar crystal packing make N-Acetyl-L4-hydroxyproline an ideal candidate for this study.

Several neutron data sets between 9 K and 250 K of both forms were collected [3] and studied along with their X-Ray counterparts and molecular dynamics simulations to gain in-depth understanding of the dynamic processes in the crystalline state.

[1] M. Hospital, C. Courseille, F. Leroy, B. P. Roques, *Biopolymers* **18**, 1141–1148 (1979).

[2] B. Dittrich, J. E. Warren, F. P. A. Fabbiani, W. Morgenroth, B. Cory, *Phys. Chem. Chem. Phys.*, **11**, 2601–2609 (2009).

[3] J. Lubben, C. Volkmann, S. Grabowsky, A. Edwards, W. Morgenroth, F. P. A. Fabbiani, G. M. Sheldrick and B. Dittrich, *Acta Cryst. A70*, 309–316 (2014).

Keywords: Neutron Diffraction, Low Temperature, Disorder

MS38. Combining crystallographic information with other methods

Chairs: Marco Milanese, Poul Norby

MS38-P1 Polymorph screening and crystal structure solution of 3-methylglutaric acid

Lukas Tapmeyer¹, Martin U. Schmidt¹, Michael Bolte¹

¹ Goethe University, Frankfurt am Main, Germany

email: lukas.tapmeyer@stud.uni-frankfurt.de

In solid-state NMR, as in almost every analytic technique, standard samples are needed to calibrate equipment in order to validate routine data collection. 3-Methylglutaric acid is a potential reference substance even though its crystal structure is unknown. [1]

As the crystal structure can influence the solid state NMR spectrum, the occurrence of polymorphs under the usual experimental conditions has to be investigated.

3-Methylglutaric acid crystallizes readily from a variety of solvents. A representative set of commonly used solvents was selected and the crystallisation performed at room temperature and at elevated temperature. To exclude phase changes at higher temperatures DTA-TG was employed. As no diverging phases were identified by X-ray powder diffraction, the structure was determined by single crystal X-ray diffraction.

To obtain data matching the experimental conditions of solid-state NMR, the diffraction measurement was carried out at -100 °C as well as at 20 °C. The determined structures were identical within the thermal expansion as expected, similar to the results of earlier executed differential thermal analysis.

3-Methylglutaric acid crystallises in the space group $P2_1/c$ with four molecules per unit cell (general position) and the lattice parameters

$a = 13.849$, $b = 5.323$, $c = 10.128$ and $\beta = 110.284$ ($R = 7.73$) at -100 °C and

$a = 13.909$, $b = 5.367$, $c = 10.307$ and $\beta = 110.555$ ($R = 5.29$) at room temperature (Fig. 1).

[1] D. H. Barich *et al.*, *Solid State Nucl. Magn. Reson.* 2006, 30, 125-129.

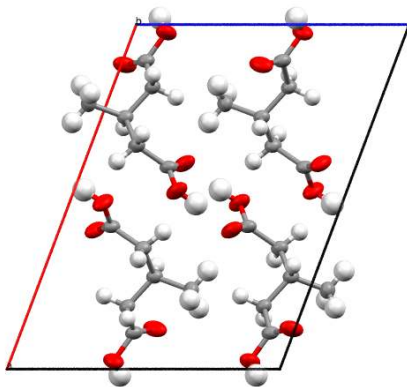


Figure 1. View along b axis (at room temperature).

Keywords: structure determination, NMR, organic compounds, polymorph screening

MS38-P2 Combining the powers of electron diffraction, electron microscopy, PXRD and NMR for structure determination of complex disordered zeolites

Tom Willhammar^{1,2}, Xiaodong Zou¹, Junliang Sun¹, Wei Wan¹,
Peter Oleynikov¹, Daliang Zhang¹

1. Department of Materials and Environmental Chemistry, Stockholm University, SE-106 91 Stockholm, Sweden
2. Electron Microscopy for Materials Science (EMAT), University of Antwerp, Groenenborgerlaan 171, B-2020 Antwerp, Belgium

email: tom.willhammar@uantwerpen.be

Intergrowth and stacking disorders are common in inorganic materials in general and within zeolites in particular. Severe disorder makes structure determination a great challenge. Recent developments in electron crystallography facilitate the study of disordered materials greatly. In combination with powder x-ray diffraction and NMR these methods have proven to be successful in the structure determination of the new heavily disordered zeolite structure ITQ-39 [1].

Electron crystallography is highly complementary to x-ray diffraction with two big advantages. Firstly single crystal diffraction data can be obtained from crystals smaller than 50 nm by utilizing the Rotation Electron Diffraction (RED) method [2]. Single crystal data makes it much easier to analyze material and obtain information such as the unit cell, symmetry and also general knowledge about the nature of the disorder. A second great benefit of electron crystallography is the possibility to obtain high resolution transmission electron microscopy (HRTEM) images; images which reveal the local arrangement of atoms in the material without averaging and are of huge importance in the study of disordered materials.

The zeolite ITQ-39 exhibits a PXRD pattern with few and broad features, Fig 1, due to disorder and small crystal size, 30x30x500 nm. RED data indicated presence of stacking disorder, as diffusely scattered lines, and twinning. HRTEM images along two perpendicular directions revealed the local atomic arrangement and confirm the stacking disorder and twinning. Crystallographic structure factors were extracted from ordered regions of the images, regions as small as a few unit cells. The structure factors were merged into a 3D potential map from which the atomic structure could be determined. The material turned out to be a new zeolite family built from a random intergrowth of three different polytypes.

The material was synthesized in the presence of F⁻ ions which are trapped inside small cages of the structure. ¹⁹F NMR can provide a fingerprint for the type of cages present in the structure showed the presence of two different types of cages, the 4⁶ and the 4⁵5¹ cages. The two cages can be assigned to the different polytypes and confirm their presence.

References

[1] Willhammar T, Sun JL, Wan W, Oleynikov P, Zhang DL, Zou XD, Moliner M, Gonzalez J, Martínez C, Rey F, Corma A, *Nature Chem.* 4 (2012) 188–194

[2] Zhang, DL, Oleynikov P, Hövmöller, S, Zou, XD Z. *Kristallogr.* 225 (2010) 94–102

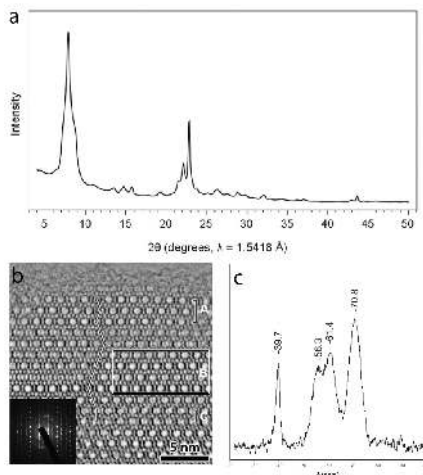


Figure 1. (a) PXRD pattern of the disordered zeolite ITQ-39 shows few and broad features. (b) A structure projection image reconstructed from HRTEM images reveals the local arrangement of atoms. (c) ¹⁹F NMR spectrum from ITQ-39 shows a fingerprint of 4⁶, 39.7 ppm, and 4⁵5¹, the other peaks.

Keywords: electron crystallography, zeolite, nmr

MS38-P3 Crystal structure of hydrated fluorides MF₂·4H₂O (M= Zn, Ni, Co): a combined approach

K. Forsberg¹, G. Nénert², T. Tao³, P. S. Halasyamani³

1. School of Chemical Science and Engineering, KTH Royal Institute of Technology, Teknikringen 42, 100 44 Stockholm, Sweden
2. PANalytical B.V., Lelyweg 1, 7602 EA, Almelo, The Netherlands
3. Department of Chemistry, University of Houston, Houston, Texas 77204-5003, USA

email: kerstino@kth.se

Inorganic metal fluorides and oxide-fluorides have significant importance in the development of many new technologies within for example energy production and storage, microelectronics and photonics, catalysis and the automotive industry. There is a need for better knowledge of the relationships between the structure of these compounds and some pertinent physical properties [1].

Based on single crystal X-ray work, ZnF₂·4H₂O has been suggested to crystallize in the polar space group Pca2₁ [2]. The possibility for non-linear optical properties of this compound and related phases motivated us to investigate this family further. Very little is known about the crystallography of the MF₂·4H₂O family. Compositions such as MF₂·4H₂O (M: Co, Ni, Fe) have been reported but not characterised structurally [3]. The crystal structure determination of such materials is particularly complicated as oxygen and fluorine atoms exhibit very similar scattering cross sections irrespective of the source (X-ray or neutron).

Using a combined approach of X-ray, neutron and second harmonic generation, we show that actually the crystal structure of these materials is centrosymmetric, in contradiction with previous reports. We discuss the crystal structure of these materials (MF₂·4H₂O, M= Zn, Co, Ni) using combined refinements using neutron and X-ray diffraction data. The use of complementary techniques was a key to determine the correct structure of these materials.

[1] Leblanc M., Maisonneuve, Tressaud A., *Chem. Rev.*, **115**(2), pp 1191- 1254 (2015).

[2] Bukvetskii B.V., Polishchuk S.A., Simonov V.I., *Sov. Phys. Crystallogr.*, **18**(5), pp 600-602 (1974).

[3] Lange B.A., Haendler H.M., *J. Inorg. Nucl. Chem.*, **35**, pp 3129- 3133 (1973); Swanepoel J., Heyns A.M., *Spectrochimica Acta*, **47A**(2), pp 243-253 (1991).

Keywords: fluorides; crystal structure; X-ray diffraction; second harmonic generation

MS38-P4 Investigation of the ultra-fast structural changes in metal-organic complexes: comparison spectroscopy and time-resolved XRD

Dirk Raiser¹, Darina Storozhuk ², Sreevidya Thekku Veedu², Simone Techert^{1,2,3}

1. Structural Dynamics of (Bio)chemical Systems, Max-Planck-Institute for biophysical chemistry, Am Faßberg 11, 37077 Göttingen, Germany
2. Structural Dynamics in Chemical Systems, Deutsches Elektronen-Synchrotron DESY, Notkestraße 85, 22607 Hamburg, Germany
3. Institute for X-Ray Physics, Faculty of Physics of the Georg-August-Universität Göttingen, Friedrich-Hund-Platz 1, 37077 Göttingen, Germany

email: dirk.raiser@mpibpc.mpg.de

Our aim is a detailed understanding of the ultrafast structural dynamics and the underlying basic mechanisms of molecular switches under optical excitation, which are still not fully understood in its variety. In order to monitor the occurring structural changes in molecules and alloys we are taking advantage of time-resolved x-ray diffraction measurements. But since the important electronic changes due to optical excitation take place on very short ps- and sub-ps timescales it gives rise to the necessity of faster time-resolved measurements than those which are currently possible at third generation synchrotrons. Besides new attempts of directly monitoring the structural changes with shorter x-ray pulses by femtosecond FEL- and XPS-pump-probe experiments, we are currently gaining more insight in the structural dynamics by indirect measurements using our fs-time-resolved transient absorption spectroscopy. Therefore we will present our recent spectroscopic data of a metal-organic complex which will be related to certain structural changes, while the near future aim is to prove these by further x-ray experiments.

Keywords: ultra-fast structural changes, metal-organic complex, transient absorption spectroscopy, time-resolved XRD

MS38-P5 Triel-rich mixed potassium
indides/gallides: Ternary variants of binary
trielides and the new 3:1:1 compound



Carolin Meyer¹, Martha Falk¹, Caroline Röhr¹

¹ Universität Freiburg, Institut für Anorganische und Analytische Chemie

email: carolin@magnetite.chemie.uni-freiburg.de

Alkali gallides and indides exhibit a fascinating complex structural chemistry inbetween electron-precise Zintl phases (e.g. NaIn), Wade cluster compounds (e.g. KGa_3), boron-analogs (e.g. $\text{K}_{17}\text{In}_{11}$) and simple intermetallics (like e.g. KIn_3). In a systematic experimental study, mixed In/Ga trielides have been synthesized from the elements to i. explore the 'coloring' of the polyanions with the two triels differing both in size and electronegativity and to ii. explore additional new polyanion topologies.

In the most In-rich indide KIn_3 [2,3] indium can be substituted by up to 1.12 atoms of Ga, which takes the more negatively charged tips of pyramids in the BaAl_3 -type structure [1]. Starting from KGa_3 [4] which is a Zintl phase in containing exo-bond *closo* dodecahedra Ga_3^{2-} and one 4-bonded Ga' per tripled formula unit, an only small amount of Ga can be substituted against In. This also holds for the related gallide K_3Ga_{13} . The new cluster compound of overall composition $\text{K}_{15}(\text{Ga}/\text{In})_{11}$ with an In proportion of $\approx 20\%$ and a very small In/Ga phase width crystallizes in a singular orthorhombic structure type (*Cmmm*, $a=1577.39$, $b=3354.71$, $c=654.97$ pm), which has been determined by means of single crystal X-ray data ($R1=4.8\%$). It contains 6 K and 13 triel positions, of which one [In(1)] is a pure In site, four (denoted *M*) are mixed Ga-rich positions (82-92% Ga) and the remaining sites are occupied by Ga only. The In/Ga atoms form two crystallographically different icosahedra [M^1_{12}] [built up from $M(1)/\text{Ga}(2)/M(6)/\text{Ga}(8)$] and [M^2_{12}] [$M(4)/M(9)/\text{Ga}(11)$] (dark gray polyhedra) in a 2:1 ratio and the new [Ga_3] cluster [formed by $\text{Ga}(5/7/10/13)$, light gray]. The latter consists of two pentagonal pyramids sharing one corner. The clusters are connected among each other and the 4-bonded $M(3)$ and $\text{Ga}(12)$ atoms. According to $\text{K}_{15}\text{M}_{55}=15 \text{ K}^+ + 2 [M^1_{12}]^{2-} + [M^2_{12}]^{2-} + [M^3_{13}]^{3-} + [M^4_6]$ the compound obeys the Zintl concept extended by the Jemmis electron counting rules, if the new double cluster is counted as 'intermediately' connected [5]. The experimental studies are accompanied by DFT band structure calculations.

[1] V. Müller, PhD thesis, TH Darmstadt (1995).

[2] G. Bruzzone, *Acta Crystallogr.* **B25**, 1206 (1969).

[3] M. Wendorff, C. Röhr, *Z. Anorg. Allg. Chem.* **631**, 338 (2005).

[4] S. P. Yatsenko, E. I. Gladyshevskii, K. A. Chuntunov, Y. P. Yarmolyuk, Y. N. Grin, *Kristallografiya* **28**, 809 (1983).

[5] E. D. Jemmis, M. M. Balakrishnarajan, P. D. Pancharatna, *Chem. Rev.* **102**, 93 (2002).

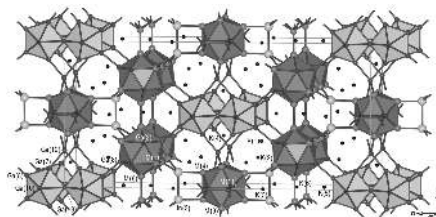


Figure 1. Crystal structure of the new mixed potassium Ga/In trielide $\text{K}_{15}\text{Ga}_{45(2)}\text{In}_{10(2)}$

Keywords: Indides, Gallides, Intermetallics, Bandstructure calculation

MS38-P6 The influence of oxime group substitution on hydrogen bonding patterns in pyridine-based complexes of Cd(II)

Ivan Kodrin¹, Vedran Barbarić¹, Ina Erceg¹, Aleksandar Višnjevac², Marijana Đaković¹

1. Department of Chemistry, Faculty of Science, University of Zagreb, Horvátovac 102A, 10000 Zagreb, Croatia

2. Laboratory for chemical and biological crystallography, Division of Physical Chemistry, Ruđer Bošković Institute, Bijenička cesta 54, 10000 Zagreb, Croatia

email: ikodrin@chem.pmf.hr

The synthesis and characterization of new materials together with the investigation of their physical properties represent areas of the greatest interest in chemistry today. Our knowledge about controlling the way in which metal-complexes, ligands and counter-ions assemble into more complex structures is rising every day. Even though each new discovery about the very intriguing and sometimes ambiguous relationship between a chemical structure of single molecules and non-covalent interactions that might govern their formation into higher-order structures is a one step closer to the successful design of new materials with desired properties. Moreover, even the simplest variations in chemical structure like exchange of hydrogen bond donors and acceptors, halide counter-ions may influence propensity toward specific hydrogen bond patterns.

Followed by the same idea, we have examined newly synthesized cadmium-based complexes linked to polymeric chains capable of acting as robust supramolecular synthons, yet enough flexible to accommodate to slight variations in molecular structure. Transformed pyridine-based ligands have at least two functionalities – they are able to complexate metals and form intermolecular interactions depending on substituents of aromatic ring. Therefore, they have already been well documented in literature as plausible building blocks and a logical joint between solely organic- and solely inorganic-based three-dimensional architectures.

This research work utilizes an experimental and theoretical approach in order to gain new insights about the supramolecular behavior of cadmium halide complexes with pyridine-based ligands functionalized in positions three and four with an oxime group. We report a synthesis of ligands and the derived complexes including description of crystallization techniques, spectral characterization, and determination of thermal properties. A computational study help us in further analysis of intermolecular interactions important for assembly of molecules in three-dimensional networks and to rationalize whether a dimeric supramolecular motif labeled as $R^2_2(6)$ according to graph-set theory prevails over $R^2_2(8)$, or *vice versa*.

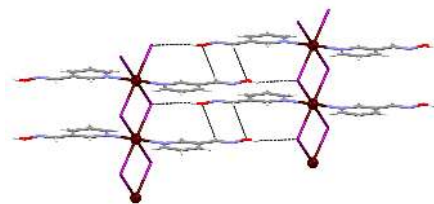


Figure 1. Intermolecular interactions between neighbouring polymeric chains, $[CdL_2(3\text{-oxpy})]_n$.

Keywords: Density Functional Theory (DFT), supramolecular interactions, Cd(II) complexes

MS38-P7 XRD analysis as a complementary tool of phase analysis in a forensic fieldMarek Kotrly^{1,2}

1. Institute of Criminalistics Prague, Bartolomejska 12, Praha 1, Czech Republic
2. Charles University in Prague, Faculty of Science, Albertov 6, Praha 2, Czech Republic

email: kotrly_kup@email.cz

Analyses of materials from an extremely wide spectrum are performed in a forensic field, but a number of which can be potentially dangerous - biological substances, explosives, poisons, etc. It is also often necessary to analyze materials that include organic and inorganic components and here is the role of XRD phase analysis irreplaceable.

In a forensic field, a broad range of analytical methods, such as optical microscopy, SEM/EDS/WDS, XRF, ion chromatography, Raman spectroscopy, FTIR, ICP MS, GC-MS, MS/MS, MSn, NMR, etc., are used for identification of unknown materials and by phase analysis. A needed synergic effect arises by combination of these methods and XRD techniques, which leads to a successful acquisition of evidence material applicable at trial.

XRD techniques are currently used for soil analysis, mineralogical and petrological objects, precious stones and other gemmological objects, pigment phases in the broadest sense, postblast residues, components of explosives and pyrotechnic compositions (inorganic and organic phases), plastics and polymers, pharmaceutical and cosmetic products (including narcotics), building materials, alloys and metals, fillers and additives (polymers, paper products, etc.), fillers of safes, "unknown" samples (in the broadest sense). X-ray powder diffraction in reflection and transmission mode and microdiffraction are usually applied. Gandolfi chamber is used in special cases and monocrystal methods are employed exceptionally.

So called "Legal Highs" - new synthetic drugs, which began appearing on the world market, currently pose a significant problem. These are structural variations of known substances with psychotomimetic effects, which have not been yet registered on the list of state controlled substances and are synthesized to evade the law. Many of the substances are temporarily sold legally. Analysis, identification and quantification of these substances are rather complex because they are not entered to identification databases. The methods of X-ray diffraction are a very convenient complementary technique to common methods of sophisticated organic analysis. The occurrence of Legal Highs on the market can be also considered very dangerous, since the toxicity in most of these substances has not been yet known.

Acknowledgements - Microanalytical methods at ICP were supported by projects: VD20062008B10, VD20072010B15, VG20102015065, VF20112015016, VF20122015027.

Keywords: forensic science, X-ray powder diffraction, microdiffraction, electron microscopy

MS38-P8 High-resolution crystallographic investigations of organometallic compoundsDarina Storozhuk¹, Dirk Raiser², Simone Techert^{1,2,3}

1. FS-SCS, Deutsches Elektronen-Synchrotron (DESY), Notkestr. 85, 22607 Hamburg, Germany
2. Max Planck Institute for Biophysical Chemistry, Am Fassberg 11, 37077 Göttingen, Germany
3. Institute for X-Ray Physics, Georg-August-Universität, Friedrich-Hund-Platz 1, 37077 Göttingen, Germany

email: darina.storozhuk@desy.de

Our motivation is to shed more light into the ultrafast dynamics of some organometallic molecules and study the mechanism underlying, drawing the complete picture of the system under investigation. But since the important electronic changes due to optical excitation take place on very short ps- and sub-ps timescales it gives rise to the necessity of faster time-resolved measurements than those, which are currently possible at third generation synchrotrons. We performed high-resolution crystallographic measurements at various temperatures and study the dynamics of the system as the function of temperature and will be presented.

Keywords: organometallic molecules, time-resolved measurements, high-resolution

MS38-P9 Adsorption of PVP polymer onto hydroxyapatite using a co-precipitation technique

Mongi Debbabi¹, Hassen Agougui¹

1. Laboratoire de Physico-chimie des Matériaux, Université de Monastir, Faculté des Sciences, 5019 Monastir, Tunisia.

email: m.debbabi@yahoo.fr

The hybrids compounds hydroxyapatite-polymer has interesting applications in biomedical domain, such as artificial bones and dental implants. In this scope, calcium hydroxyapatite was prepared in the presence of polyvinylpyrrolidone (PVP), at room temperature for 72 h. The synthesized samples were characterized by X-ray diffraction (XRD), Fourier transform infrared spectroscopy (FTIR), chemical analysis, atomic force microscopy (AFM) and scanning electron microscope (SEM). The X-ray powder analysis showed that the crystallinity is sensibly affected by the presence of polymer. IR spectra display the vibration modes of PO_4^{3-} and new vibration modes related to PVP, essentially at 2930, 1315, 945, 764 and 514 cm^{-1} . In addition, the conservation of (P-OH) band, suggested the formation of organic-inorganic bond between the PVP and Ca^{2+} ions of apatite. Atomic Force Microscopy (AFM) showed that the texture surface was changed by grafting.

Keywords: Hydroxyapatite, PVP, SEM, AFM.

MS38-P10 Local atomic and magnetic structure of 1D spin-chains in multiferroic copper guanidinium formate

Anthony E. Phillips¹, Alan J. Drew¹

1. Queen Mary University of London

email: a.e.phillips@qmul.ac.uk

The metal-organic framework copper guanidinium formate, $\text{C}(\text{NH}_2)_3[\text{Cu}(\text{HCO}_2)_3]$, is of interest for its multiferroic properties, recently shown to include hybrid improper ferroelectricity and substantial magnetoelectric coupling [1]. This material's structure is analogous to the well-known inorganic perovskite KCuF_3 , with guanidinium ions in the pores of a pseudo-cubic copper-formate framework. As in the inorganic counterpart, cooperative Jahn-Teller distortion results in one-dimensional antiferromagnetic Heisenberg spin chains containing short Cu coordination lengths. These chains interact only weakly with one another through longer bonds, and hence 3D magnetic order freezes in only at very low temperatures.

The Jahn-Teller distortion in this material does not directly cause ferroelectric ordering but is coupled to it via hydrogen bonding between the framework and guest ions. In order to determine the origins of this material's multiferroicity, it is therefore important to understand the origin of the cooperative distortion. Even in the well-studied inorganic analogue KCuF_3 , however, this remains obscure, with recent studies suggesting that the true behaviour of that system involves fluctuations about a lower-symmetry structure [2]. Modelling the behaviour of the title framework, which may involve coupling between lattice, orbital, and spin degrees of freedom, thus requires an understanding of fluctuations in both the atomic and magnetic structures in both space and time. To this end we here complement neutron crystallographic studies of this material with muon spin resonance and inelastic neutron scattering measurements on mosaic samples.

The muon sites in this material are close to the formate oxygen atoms and, given the Jahn-Teller distortion of the CuO_6 octahedra, are therefore located at a range of convenient distances from the Cu to measure its local magnetic field. We report studies under transverse and longitudinal magnetic fields, yielding information about the short-range correlations in the 1D chains and critical exponents for the magnetic phase transition. Inelastic neutron scattering measurements reveal the magnetic excitation spectrum of the 1D and 3D regions, including the spinon continuum and longitudinal mode. Our results provide direct experimental confirmation of the local magnetic structure of this material.

[1] Y. Tian *et al.* (2015) *Physica Status Solidi RRL* **9**, 1, 62

[2] J. Deisenhofer *et al.* (2011) *Ann. Phys.* **523**, 8, 645

Keywords: metal-organic framework, 1D magnetism, μSR , inelastic neutron scattering, Jahn-Teller distortion, multiferroic

MS38-P11 Combining X-ray crystallography and *in situ* single-crystal UV-Vis and Raman spectroscopy to study haem- and flavoproteins

Hans-Petter Hersleth¹, Åsmund K. Røhr¹, Wouter van Beek²,
Guillaume Pompidor³, K. Kristoffer Andersson¹

1. Department of Biosciences, Section for Biochemistry and Molecular Biology, University of Oslo, P.O. Box 1066 Blindern, NO-0316 Oslo, Norway

2. Swiss-Norwegian Beam Lines, European Synchrotron Radiation Facility, BP 220, Grenoble 38043, France

3. Swiss Light Source, Paul Scherrer Institute, CH-5232 Villigen PSI, Switzerland

email: h.p.hersleth@ibv.uio.no

X-ray crystallography is the central methods for studying the structure-function relation of redox proteins, however the crystal structures are missing key information. This includes oxidation state, protonation and spin state, which are essential for understanding the reaction mechanisms of these redox protein systems. Therefore, a combination of crystallographic and spectroscopic methods is vital for a more fully characterisation. Additionally, the redox sites are very labile for X-ray induced radiation damage and reduction during crystallographic data collection at synchrotrons. Therefore combining X-ray crystallography with *in situ* UV-Vis and Raman spectroscopy is important for both characterisation and radiation damage monitoring. We have used *in situ* spectroscopy setups at both X10SA at SLS, the Cryobench at ESRF and at the Swiss-Norwegian Beam Lines at ESRF. We have studied several haem- and flavonproteins such as myoglobin, cytochrome *c*, catalase-peroxidase, flavodoxin like protein NrdI, and several flavodoxins and flavodoxin reductases. These studies have resulted in complementary structural information, and shown the redox state of the solved crystal structures. With respect to radiation induced changes, we have observed for haem proteins a lengthening of the iron-oxygen bond, and for flavoproteins a bending of the flavin ring during X-ray induced radiation damage. We have been able to estimate the lifedose of different states, and these results have lead to the use of composite data collection to obtain the unreduced crystal structures of some of these redox proteins.

References: H.-P. Hersleth & K.K. Andersson. How different oxidation states of crystalline myoglobin are influenced by X-rays. *Biochim. Biophys. Acta, Proteins Proteomics* (2011), **1814**, 785-796. Å.K. Røhr, H.-P. Hersleth & K.K. Andersson. Tracking Flavin Conformations in Protein Crystal Structures with Raman Spectroscopy and QM/MM Calculations. *Angew. Chem. Int. Ed.* (2010), **49**, 2324-2327.

Acknowledgements. Financial support by the Norwegian Research Council through projects 214239/F20 / 218412/F50 / 231669/F20.

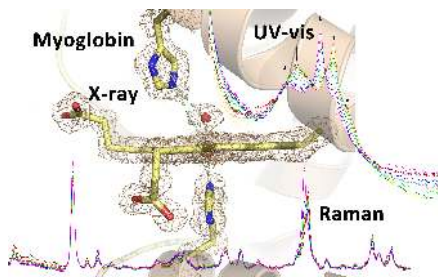


Figure 1.

Keywords: protein crystallography, single-crystal spectroscopy, haemproteins, flavoproteins, radiation damage

MS38-P12 Approaching the structure of tetranuclear Ni-complex: a journey through the maze of non-crystallographic information

Dubravka Sisak Jung¹, Ana Belen Pinar Prieto², Predrag Lazic³, Gordana Pavlovic⁴, Marina Cindric⁵

1. DECTRIS Ltd, Baden, Switzerland
2. ETH Zurich, Switzerland
3. Institute Rudjer Boskovic, Zagreb, Croatia
4. Faculty of Textile Technology
5. Faculty of Natural Sciences and Mathematics, Zagreb, Croatia

email: dubravka.sisak@dectris.com

As a result of various synthetic paths, a cubane-type Ni-complex was obtained. Its single-crystal structural analysis revealed four nickel atoms coordinated with five donors from organic ligand and one methanol molecule. Heating this sample to 180°C led to a change of magnetic properties from ferro- to antiferromagnetic, and of color from green to red. For clarity, the former sample will be referred to as cubane-Ni, and the latter as cubane-Ni-180. In order to solve the structure of cubane-Ni-180, X-Ray Powder Diffraction (XRPD) data were measured using the MYTHEN detector installed at Swiss Light Source. Any radiation damage was avoided by collecting 120° of data within ten seconds. However, the data resolution was only 3 Å. This, combined with lack of molecular model hindered classical structure determination, so additional information had to be considered. Thermogravimetric analysis showed a single weight loss, indicating that all methanol molecules were removed from the cubane-Ni structure upon heating. In fact, when the cubane-Ni-180 was exposed to a methanol atmosphere, it transformed back to cubane-Ni. These observations, supported by IR spectroscopy results, suggested that the Ni-ligand moiety was preserved. The XRPD patterns of both samples were found to be similar, so the unit cell parameters of the cubane-Ni could be used to facilitate the indexing of the cubane-Ni-180 pattern, which exhibited very few peaks. Quantum mechanical methods were subsequently used to assist in the structure solution. First, a starting structural model was built by removing the methanol ligands from the cubane-Ni structure. This model was subjected to series of energy optimizations, all resulting in clusters of four square-planar coordinated Ni-centers. This geometry was found to comply with the antiferromagnetic properties of the sample. Notwithstanding that the molecular structure was reasonable, the fit between the calculated and measured XRPD patterns was not satisfactory. In order to exclude the possibility of a strong model-bias, direct-space optimization of the modified molecular structure of cubane-Ni was tried. The last obstacle, preferred orientation of the crystallites, was addressed by adding geometrical restraints to the optimization. This way, solutions with chemically reasonable intermolecular distances could be favored. Finally, examination of the structures obtained by both approaches allowed the most likely structure of cubane-Ni-180 to be proposed.

Keywords: X-ray Powder Diffraction, structure determination, TG, quantum mechanics, Nickel complex, combining methods

MS38-P13 On element sensitive determination of local atomic structure with white beam x-ray fluorescence holography

Dawid T. Dul¹, Paweł Korecki¹

1. Institute of Physics, Jagiellonian University, Łojasiewicza 11, 30-348 Kraków, Poland

email: dawid.dul@gmail.com

White beam x-ray fluorescence holography (white beam XFH) enables local atomic structure determination around particularly chosen elements in the sample. It combines x-ray diffraction and x-ray fluorescence spectroscopy to obtain a hologram of the crystal structure around the element of interest. The hologram is formed as a result of the interference of the incident x-ray wave with waves scattered from atoms inside the sample. It is probed at the positions of absorbing atoms which work as internal detectors by measuring x-ray fluorescence photons. Structure information can be obtained directly from the holograms, since due to the short coherence length of white x-rays they can be interpreted as quasi-real space projections of the crystal structure, or through the application of reconstruction procedures [1, 2].

In this work, by employing analytic and numerical calculations, we show that element sensitive determination of local atomic structure with white beam XFH is generally only possible if so called matrix effects i.e. beam attenuation and indirect excitation are properly tackled [3]. We argue that these effects may lead to distortions in the holographic signal and/or spurious maxima in the reconstruction. Furthermore, we demonstrate that the effect of beam attenuation on the holograms is very weak for high incident beam energies whereas indirect excitation is important regardless of the energy range. We use these findings and propose an approximate, yet efficient method of correction for matrix effects [4].

This work was supported by the Polish National Science Center (DEC-2013/09/N/ST3/04111) and in part by the KNOW Research Consortium through the Marian Smoluchowski fellowship.

[1] P. Korecki, et al., Physical Review Letters 96, 035502 (2006)

[2] P. Korecki, et al., Journal of Synchrotron Radiation 18, 851 (2011).

[3] D. T. Dul, et al., EPL (Europhysics Letters) 104, 66001 (2013)

[4] D. T. Dul, et al., Journal of Applied Crystallography, in press (2015).

Keywords: x-ray diffraction, x-ray fluorescence, local atomic structure

MS38-P14 Combination of solid state NMR, DFT and XRPD for determination of a theophylline : 4-aminobenzoic acid cocrystal phase

José A.P. Fernandes¹, Mariana Sardo¹, Luís Mafrá¹, Duane Choquesillo-Lazarte², Norberto Masciocchi³

1. CICECO, Universidade de Aveiro, Campus de Santiago, 3810-193 Aveiro, Portugal
2. Laboratorio de Estudios Cristalográficos, IACT, CSIC-Universidad de Granada, Av. de las Palmeras 4, E-18100 Armilla, Granada, Spain
3. Dipartimento di Scienza e Alta Tecnologia, Università dell'Insubria, 22100 Como, Italy

email: jafernandes@ua.pt

Theophylline and 4-aminobenzoic acid in 1:1 ratio selectively, and quantitatively, generate, by Liquid Assisted Grinding (LAG), a new cocrystal phase (I). Its structure was retrieved by conventional laboratory X-ray powder diffraction methods, using the programme TOPAS academic for solving and refining the structure. The unusual absence of hydrogen-bond interactions involving the amino groups required further validation, performed by solid state NMR and IR characterization.

The use of 1D/2D ¹H high-resolution solid-state NMR techniques provided structural insight on local length scales revealing internuclear proximities and relative orientations between the building blocks of the title compound, thus providing information on the type of hydrogen bond synthons formed. DFT calculations were also employed to generate meaningful structures and calculate NMR ¹H and ¹³C chemical shifts to further validate the XRPD model.

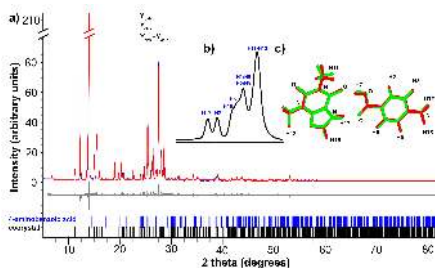


Figure 1. a) Final Rietveld refinement plot. Blue and black bars refer to the angular positions of Bragg reflections for 1 and the minor 4-aminobenzoic acid (<5%) contaminant, respectively; b) ¹H MAS NMR spectrum of 1 ($B_0=16.4$ T; 30 kHz MAS); c) Overlap of the structures obtained by XRPD and DFT.

Keywords: powder diffraction, solid state nuclear magnetic resonance, DFT, TOPAS, CASTEP

MS38-P15 ADPs simulations as an additional source of fine structural information

Francesco Punzo¹, Giuseppe M. Lombardo²

1. Dipartimento di Scienze del Farmaco Università degli Studi di Catania
2. Dipartimento di Scienze del Farmaco Università degli Studi di Catania

email: fpunzo@unict.it

The effect of the atomic thermal motion about their equilibrium positions, **u**, enters in the calculation of the structure-factor, which is a function of the Miller indexes defined by the vector **h**, as the Debye-Waller factor, $T(\mathbf{h})$. The calculation of the ADPs from the MD simulation ($U_{MD, cif}^*$) was carried out as follows: the first step involved the calculation of the symmetric tensor U^* from the MD trajectory by converting, in each of the N snapshots, the atomic Cartesian coordinates (*r*) into fractional coordinates (*r*^{*}), and applying to the fractional coordinates the usual definitions of mean coordinates and variance-covariance matrix; thereafter, the calculation of the average values of the cell parameters and the determination of the averaged reciprocal lattice parameters lengths were carried out. These values, as calculated from the MD trajectory, were used to finally obtain $U_{MD, cif}^*$. Apart from the possible comparison between X-ray and neutron inferred ADP data – the latter being more trustworthy for several physical reasons – valuable information could be obtained from their detailed analysis with a particular emphasis not only on their size but on their shape and spatial distribution. In this contribution we provide several examples – spanning, among others, from the study of polymorphism and pseudosymmetry to the energy ranking and stability of crystalline arrangements (1-4) – on extremely different chemical species thus confirming the wide pertinence of the proposed approach.

1. Lombardo G. M., Rescifina A., Punzo F. Functional hybrid co-crystals of humic substances: a growth forecast. *CrystEngComm* 2014, 16, 5917-5923.
2. Lombardo G. M., Punzo F. False asymmetry, pseudosymmetry, disorder, polymorphism and atomic displacement parameters. *J. Mol. Struct.* 2014, 1078, 158–164.
3. Lombardo G. M., Portalone G., Chiacchio U., Rescifina A., Punzo F. Potassium caffeate/caffeic acid co-crystal: the rat race between catecholic and carboxylic moiety in an atypical co-crystal. *Dalton Trans.*, 2012, 41, 14337–14344.
4. Lombardo G. M., Thompson A. L., Ballistreri F. P., Pappalardo A., Trusso Sfrassetto G., Tomaselli G. A., Toscano R. M., Punzo F. An integrated X-ray and Molecular Dynamics study of uranyl-salens structures and properties. *Dalton Trans.* 2012, 41, 1951-1960.

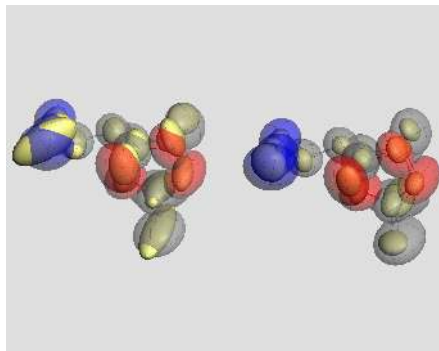


Figure 1. An example of adp qualitative comparison between computed, on the left (single cell, yellowish and supercell, coloured), and between computed and experimental, on the right (experimental, yellowish and supercell, coloured).

Keywords: adp, Molecular Dynamics, polymorphism, symmetry, pseudosymmetry, Shannon entropy

MS38-P16 Combining X-ray crystallography and ultrafast infrared spectroscopy – monitoring photo-induced guanine oxidation by $[\text{Ru}(\text{TAP})_2(\text{dppz})]^{2+}$

James P. Hall^{1,2}, Fergus E. Poynton³, Pádraic M. Keane^{1,2,3}, Sarah P. Gurung^{1,2}, John A. Brazier⁴, David J. Cardin¹, Graeme Winter², Thorfinnur Gunnlaugsson¹, Igor V. Sazanovich², Michael Towrie², Christine J. Cardin¹, John M. Kelly², Susan J. Quinn⁶

1. Department of Chemistry, University of Reading, Reading, UK
2. Diamond Light Source, Harwell Science and Innovation Campus, Didcot, UK
3. School of Chemistry, Trinity College, Dublin, Ireland
4. Department of Pharmacy, University of Reading, Reading, UK
5. Central Laser Facility, Research Complex at Harwell, Didcot, UK
6. School of Chemistry and Chemical Biology, University College Dublin, Dublin, Ireland

email: j.hall2@reading.ac.uk

Time resolved spectroscopy can be used to study reaction processes on a short timescale (as low as fs). Time-Resolved Infra-Red (TRIR) is a particularly powerful technique as it can be used to monitor the formation and breakage of individual chemical bonds, and therefore can be used to study fundamental chemical processes in biological¹ and chemical systems. However, whilst this technique is very powerful, interpretation of the results can be hampered by a lack of information about the local chemical environment of the group of interest as the sample is usually in solution. This means that, when studying biomolecules and in particular nucleic acids, there may be multiple conformations or binding sites present² which can be very difficult to assign.

In contrast, X-ray crystallography allows us to determine the position of every ordered atom or group within a crystal, providing unparalleled structural information about the environment within the sample. However, whilst facilities are available for time resolved experiments, it is difficult to reach into the sub-ns time domain without the use of specialised Laue or FEL sources.

Here we present the adaptation of pump-probe TRIR to measure data, in the ns and ps time domain, from samples consisting of 5µm crystal fragments. This technique was used to monitor the one electron photooxidation of guanine by a Ruthenium polypyridyl bound to a DNA duplex, the crystal structure of which we have previously reported³ (Figure 1). By assigning the spectroscopic result to a known structure, we are able to propose an individual base as the site of oxidation. Additionally, the spectroscopic fingerprint (reaction rate, relative yield, peak position) obtained from a crystal sample allows us to compare with that found in solution.

1. Towrie, M., Doorley, G.W., George, M.W., Parker, A.W., Quinn, S.J. & Kelly, J.M. *Analyst*. 2009, **134**, 1265-1273.

2. Keane, P.M., Poynton, F.E., Hall, J.P., Clark, I.P., Sazanovich, I.V., Towrie, M., Gunnlaugsson, T., Quinn, S.J., Cardin, C.J. & Kelly, J.M. *J. Phys. Chem. Lett.*, 2015, **6**, 734-738.

3. Hall, J.P., O'Sullivan, K., Naseer, A., Smith, J.A., Kelly, J.M. & Cardin, C.J. *Proc. Natl. Acad. Sci. USA*. 2011, **108**, 17610-17614.

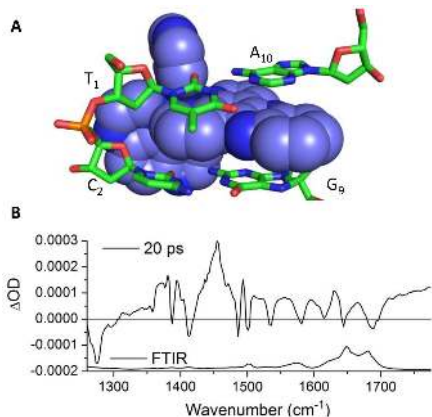


Figure 1. A- $[\text{Ru}(\text{TAP})_2(\text{dppz})]^{2+}$ (purple) intercalates into d(TCGGC GCCGA) at the terminal GA step in the duplex. (B) TRIR spectra were at multiple time delays, including 20 ps. By fitting the data at multiple time delays, the lifetimes of different excited states can be determined.

Keywords: Photochemistry, ultrafast spectroscopy, DNA

MS38-P17 Theoretical analysis (NBO, NPA, Mulliken Population Method) and molecular orbital studies (hardness, chemical potential, electrophilicity and Fukui Function Analysis) of (E)-2-((4-hydroxy-2-methylphenylimino)methyl)-3-methoxyphenol

Zeynep Demircioğlu¹, Çiğdem Albayrak Kaşas², Orhan Büyükgüngör¹

1. Department of Physics, Faculty of Arts and Sciences, Ondokuz Mayıs University, TR-55139 Samsun, Turkey

2. Department of Chemistry, Faculty of Arts and Science, Sinop University, TR-57000 Sinop, Turkey

email: zeynep.kelesoglu@omu.edu.tr

The molecular structure and spectroscopic properties of (E)-2-((4-hydroxy-2-methylphenylimino)methyl)-3-methoxyphenol, were characterized by X-ray diffraction, FT-IR and UV-Vis spectroscopy. All of theoretical calculations and optimized geometric parameters have been calculated by using density functional theory (DFT) with hybrid method B3LYP by 6-31G(d,p) basis set. The title compound of $\text{C}_{15}\text{H}_{15}\text{N}_2\text{O}_3$ have been analyzed according to electronic and energetics behaviors for enol-imine and keto-amine tautomers. Both these tautomers engender six-membered ring due to intramolecular hydrogen bonded interactions. The theoretical vibrational frequencies have been found in good agreement with the corresponding experimental data. A study on the electronic and optical properties, absorption wavelengths, excitation energy, dipole moment, molecular electrostatic potential (MEP) and frontier molecular orbital energies are performed using DFT method. Additionally, geometry optimizations in solvent media were performed with the same level of theory by the polarizable continuum model (PCM). The effect of solvents on the tautomeric stability has been investigated. Mulliken population method and natural population analysis (NPA) have been studied. NBO analysis is carried out to picture the charge transfer between the localized bonds and lone pairs. The local reactivity of the molecule has been studied using the Fukui function. NLO properties related to polarizability and hyperpolarizability are also discussed.

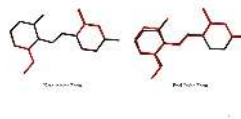


Figure 1. Superimposition of the X-ray structure (red) and calculated structure (black) of the enol-imine and keto amine forms of the title molecule.

Keywords: Natural Population Analysis (NPA), Fukui Function Analysis, Natural Bond Orbital Analysis (NBO)

MS38-P18 Integration of theoretical crystallography open database and AiiDA

Andrius Merkys^{1,2}, Giovanni Pizzi¹, Andrea Cepellotti¹, Nicolas Mounet¹, Saulius Gražulis², Nicola Marzari¹

1. Theory and Simulation of Materials (THEOS) and National Center for Computational Design and Discovery of Novel Materials (MARVEL), École Polytechnique Fédérale de Lausanne, 1015 Lausanne, Switzerland
2. Vilnius University Institute of Biotechnology, Graičiūno 8, LT-02241 Vilnius, Lithuania

email: andrius.merkys@gmail.com

Over almost a quarter of century of existence, Crystallographic Information Framework (CIF) format – an unified format for reporting and storage of the results of experimental crystal structure solutions – has been widely adopted and used as a de facto standard by most of crystallographic journals as well as structural databases (Inorganic Crystal Structure Database, Crystallography Open Database (COD, <http://www.crystallography.net>)). New CIF dictionaries are being developed with the aim of unambiguously defining ontologies in order to homogenize the data in various fields of crystallography. However, much effort is still needed to be put in for the field of theoretical crystallography, which is expanding quickly thanks to the unprecedented developments of electronic structure methods, the increase of computer power and the decrease of the price/performance ratio. The Theoretical Crystallography Open Database (TCOD, <http://www.crystallography.net/tcod/>) has been launched in order to collect the results of calculations, performed by the plethora of theoretical calculation groups using various modern theoretical approaches (DFT, post-HF, QM/MM, etc.), into an open-access resource. TCOD, together with the large set of experimental structures in the COD, opens the possibility for experimental-theoretical data cross-validation. TCOD has adopted the best practice of using the CIF format, approach-specific dictionaries and defining data validation criteria for automated checks. Furthermore, TCOD puts an emphasis on the provenance and reproducibility of the results by devising a special dictionary for related metadata. Recently, this dictionary was used as an interface for the integration of the TCOD with the AiiDA framework (<http://www.aiida.net>), a high-throughput infrastructure that provides a high-level research environment to automate the execution of computations, automatically store inputs and results in a tailored database (with particular care in always keeping track of the full provenance of all data) and share the results. Such an integration of calculation automation frameworks and database storage allows for deposition of simulation results with automatically recorded metadata, guaranteeing the reproducibility of each calculation as well as the full data provenance for each item in the database. Moreover, data from the TCOD database can be easily retrieved and imported back into the AiiDA framework as an input for further calculations and analyses.

Keywords: theoretical crystallography, structural databases, research environment software

MS38-P19 Structural characterization of complex LDH samples and TGA-GC-MS study of thermal response and carbonate contamination in nitrate and organic-exchanged hydrotalcites

Marco Milanesio¹, Eleonora Conteroso¹, Luca Palin¹, Valentina Gianotti¹, Luana Peroli², Enrico Mugnaioli³, Ute Kolb⁴, Davide Viterbo¹, Diego Antonioli¹

1. Dipartimento di Scienze e Innovazione Tecnologica, Università del Piemonte Orientale “A. Avogadro” Via Michel 11, I-15121 Alessandria, Italy
2. Dipartimento di Scienze Farmaceutiche Università degli Studi di Perugia Via del Liceo 1, I-06123 Perugia, Italy
3. Dipartimento di Scienze Fisiche, della Terra e dell’Ambiente, Università degli Studi di Siena Via Laterino 8, 53100 Siena, Italy
4. Institut für Physikalische Chemie, Johannes Gutenberg Universität, Jakob-Welder-Weg 11, 55099 Mainz, Germany

email: marco.milanesio@unipmn.it

Layered double hydroxides (LDH) are versatile materials used for intercalating bioactive molecules, both in pharmaceutical, nutraceutical and cosmetic fields, with the purpose of protecting them from degradation, enhancing their water solubility to increase bioavailability, to improve pharmacokinetics properties and formulation stability. The crystal chemistry of hydrotalcite-like compounds is investigated by X-ray powder diffraction (XRPD), automated electron diffraction tomography (ADT) and hyphenated TGA-GC-MS to shed light on the mechanisms involved in ion exchange and absorption of contaminants, mainly carbonate anions. For the first time ADT allowed to obtain a structural model of LDH-NO₃ from experiment, shedding light on the conformation of nitrate inside LDH and on the loss of crystallinity due to the layer morphology. The ADT analysis of a hybrid LDH sample (LDH-EUS) clearly revealed the increase of defectivity in this material. XRPD demonstrated that the presence of carbonate is able to drive the intercalation of organic molecules into LDH, since CO₂ contaminated samples tend to assume d-spacings roughly multiples of LDH-CO₃ d-spacing. TGA-GC-MS allowed distinguishing and quantifying intercalated and surface adsorbed organic molecules, confirming the presence and amount of carbonate, especially at low (below 2% in weight) concentrations and separating the different types and strength of adsorption, in relation with the temperature of elimination.

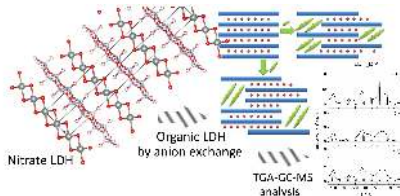


Figure 1. A model for ion exchange in hydrotalcite by combining XRPD, ED/ADT and TGA-GC-MS

Keywords: LDH thermal response, TGA-GC-MS, automated electron diffraction tomography, ionic exchange mechanism

MS39. Recent advances in diffraction instruments, detectors and data processing

Chairs: Trevor Forsyth, Rosanna Rizzi

MS39-P1 Novel powder diffractometry concepts using Mo and Ag radiation: see more!

Martijn Fransen¹, Milen Gataeshki¹, Roelof de Vries¹, Detlev Goetz¹, Marco Sommariva¹

1. PANalytical B.V., Lelyweg 1, 7602 EA Almelo, The Netherlands

email: martijn.fransen@panalytical.com

In the vast majority of powder diffractometers, Cu K-Alpha radiation is used. For certain applications, however, the 8 keV photons are not ideal, e.g. for *in operando* studies on electrochemical cells. Also new applications, like Pair Distribution Function analysis, or X-ray imaging applications like Computed Tomography require shorter wavelength radiation. Most standard laboratory diffractometers are not optimized for 'hard' radiation, however, as this more penetrating radiation puts additional demands on the beam path (optical elements and detectors). Therefore, many of these studies are done at synchrotron beamlines.

In this contribution, we'll present the striking results that can be obtained with optimized optics and large monolithic hybrid pixel detectors with unique CdTe sensors for hard radiation, showing that the lab diffractometer can sometimes be a preferred alternative over synchrotron beam time.

Keywords: Instrumentation, detectors, powder diffraction, in operando, PDF

MS39-P2 New possibilities in structural studies using inside x-ray sources

Gyula Faigel¹, Gabor Bortel¹, Miklos Tegze¹

1. Solid State Physics Institute, Wigner Research Center, H-1525, POB 49, Budapest, Hungary

email: gfa@szfki.hu

Traditionally, structure determination of crystalline substances is done by x-ray diffraction experiments. The source in these experiments is well separated from the sample and usually an almost parallel probe beam is used. Further, the sample has to be rotated to many orientations to fulfill Bragg condition and to measure enough reflections for structure determination. This arrangement makes the study of time dependent structural changes, and experiments at non-ambient conditions very difficult, especially in the short time scale. In addition, in these traditional diffraction experiments the phase of the scattered wave is lost, which makes structure solution non trivial. These difficulties could be overcome by using inside x-ray sources within the sample. In the early days of x-ray crystallography Max von Laue worked out the theory of diffraction for sources located in the sample [1]. At the same time this was also experimentally demonstrated by W. Kossel [2]. The pattern obtained this way is called Kossel pattern. Later, it was theoretically shown that not only the position and magnitude of Bragg reflections, but also their phase can be determined by measuring the fine structure of Kossel lines [3,4]. In spite of these advantages Kossel cone analysis is not wide spread. There are some experiments using electron microscopes for excitation of x-ray fluorescence, but almost no work using x-ray excitation. X-ray excitation is advantageous if bulk structural properties have to be determined. Further, in Kossel pattern studies no qualitative phase determination was demonstrated so far. Here we describe a setup built for the measurement of Kossel patterns, excited by synchrotron radiation. We also show that the resolution of this setup is enough for the determination of the phase of Bragg reflections.

[1] Laue M. Von, (1935). Ann. Phys., Lpz. **23**, 705.

[2] Kossel W, Loeck V and Voges H, (1935) *Z. Physik* **94** 139

[3] J. M. Cowley, Acta Cryst. (1964). **17**, 33

[4] J. T. Hutton, G.T. Trammell J.P. Hannon, Phys Rev. (1985), **B31**, 743

Keywords: Phase determination, Kossel lines

MS39-P3 CrysAlisPro 38: Data quality, fast experimentation, AutoChem 2.1 & StructureExplorer

Mathias Meyer¹

1. Agilent Technologies Poland Sp. z o.o., Ul. Szarskiego 3, PL-54-609 Wrocław

email: Mathias.Meyer@agilent.com

Data quality critically relies on proper instrument calibration. Our new version 38 of CrysAlisPro features a new approach to calibration enhancing the instrument description and thus giving better data quality. Improved hardware and software allow high speed data acquisition. Multi-threaded acquisition and reduction pipelines allow fast concurrent data reduction. The 'What is this?' tool gives chemical connectivity information in less than 1 min. AutoChem 2.1 offers a fine tuned structure completion algorithm and integrates the latest structure solution and refinement tools. It also offers a new structure visualizer called 'StructureExplorer'. It tightly links with the AutoChem 2.1, the external Olex2 program and internal data processing offering the user an easy handling of the structure from solution to report.

Keywords: Data processing, area detectors, automation

MS39-P4 Powder diffraction in Bragg-Brentano geometry with straight linear detectors

Dominik Kriegner¹, Zdenek Matej^{1,2}, Radomír Kuzel¹, Václav Holý¹

1. Department of Condensed Matter Physics, Charles University in Prague, Ke Karlovu 5, 121 16 Prague 2, Czech Republic

2. Max IV Laboratory, Lund University, Öle Rörers väg 1, 223 63 Lund, Sweden

email: dominik.kriegner@gmail.com

Powder diffraction as one of the most common material characterization tools is significantly benefiting from the recent developments in detector technology. One and two-dimensional detectors are nowadays commonly used to speed up the acquisition of powder diffraction data. This usually goes hand in hand with worse resolution and asymmetric peak profiles [1, 2]. In our presentation the influence of a straight linear detector on the resolution function in the Bragg-Brentano focusing geometry is discussed [3]. Because of the straight nature of most modern detectors geometrical defocusing occurs, which heavily influences the line shape of diffraction lines at low angles. To circumvent this problem we suggest an easy approach in which an adaptive range of channels of the linear detector is used at low angles. This results in an improved resolution especially at low angles. At higher angles the whole linear detector is used and the data collection remains fast. Using this algorithm a well behaved resolution function is obtained in the full angular range, whereas simply using the full linear detector the resolution function varies within one pattern, which hinders line-shape and Rietveld analysis.

[1] R. W. Cheary and A. Coelho, *J. Appl. Cryst.* **27**, 673-681 (1994)

[2] J. Slowik and A. Zieba, *J. Appl. Cryst.* **34**, 458-464 (2001)

[3] D. Kriegner, Z. Matej, R. Kuzel and V. Holý, *J. Appl. Cryst.* **48**, 613-618 (2015)

Keywords: powder diffraction, linear detector, Bragg Brentano, resolution function

MS39-P5 Neutron macromolecular crystallography at the FRM II - The neutron single crystal diffractometer BIODIFF

Andreas Ostermann¹, Tobias E. Schrader², Michael Monkenbusch^{2,3}, Bernhard Laatsch⁴, Philipp Jüttner⁴, Winfried Petry¹, Dieter Richter^{2,3}

1. Heinz Maier-Leibnitz Zentrum (MLZ), Technische Universität München, Lichtenbergstr. 1, 85748 Garching, Germany
2. Jülich Centre for Neutron Science JCNS, Forschungszentrum Jülich GmbH, Outstation at MLZ, Lichtenbergstr. 1, 85747 Garching, Germany
3. Institute for Complex Systems ICS, Forschungszentrum Jülich GmbH, 52425 Jülich, Germany
4. Forschungszentrum Jülich GmbH, Engineering and Technology (ZEA-1), 52425 Jülich, Germany
5. Forschungs-Neutronenquelle Heinz Maier-Leibnitz (FRM II), Technische Universität München, Lichtenbergstrasse 1, 85748 Garching

email: Andreas.Ostermann@frm2.tum.de

The research reactor Heinz Maier-Leibnitz (FRM II) is a modern high flux neutron source which feeds at the present 27 state of the art instruments. The newly build neutron single crystal diffractometer BIODIFF is especially designed to collect data from crystals with large unit cells. The main field of application is the structure analysis of proteins, especially the determination of hydrogen atom positions. BIODIFF is a joint project of the Forschungszentrum Jülich (FZJ/JCNS) and the Forschungs-Neutronenquelle Heinz Maier-Leibnitz (FRM II). Typical scientific questions addressed are the determination of protonation states of amino acid side chains and the characterization of the hydrogen bonding network between the protein and an inhibitor or substrate. BIODIFF is designed as a monochromatic instrument. By using a highly orientated pyrolytic graphite monochromator (PG002) the diffractometer is able to operate in the wavelength range of 2.4 Å to about 5.6 Å. Contaminations of higher order wavelengths are removed by a neutron velocity selector. To cover a large solid angle and thus to minimize the data collection time the main detector of BIODIFF consists of a neutron imaging plate system in a cylindrical geometry. A Li/ZnS scintillator CCD camera is available for additional detection abilities. The main advantage of BIODIFF is the possibility to adapt the wavelength to the size of the unit cell of the sample crystal while operating with a clean monochromatic beam that keeps the background level low. BIODIFF is equipped with a standard Oxford Cryosystem "Cryostream 7004" which allows measurements in the temperature regime from 90K up to 500K.

Keywords: Neutron protein crystallography, hydrogen atom positions, protonation states, hydrogen bonds, ligand binding, hydration structure

MS39-P6 Upgrading home-lab X-ray diffractometers with Incoatec's unique microfocus source IpS

André Beerlink¹, Jürgen Graf¹, Jörg Wiesmann¹, Carsten Michaelensen¹

1. Incoatec GmbH, Max-Planck-Str. 2, 21502 Geesthacht, Germany

email: beerlink@incoatec.de

Modern microfocus X-ray sources define the state-of-the-art for a broad spectrum of applications in home laboratories, such as protein and small molecule crystallography, and small-angle scattering. These sources are combined with multilayer Montel optics to image the source spot onto the sample. These optics provide a parallel or focused monochromatic X-ray beam, magnified to a suitable size.

Low power sealed microfocus sources, such as Incoatec's IpS represent an attractive alternative to rotating anodes, with a significant reduction in cost and maintenance. Power loads of a few kW/mm² in anode spot sizes below 50 micrometer diameter deliver a compact and very brilliant beam. For example, the IpS^{HighBrilliance} delivers more than $2 \cdot 10^{10}$ photons/s/mm² in a focal spot size of below 100 micrometer diameter at the sample position. It is available for Cu, Mo, Ag, Cr and Co anodes. Since the launch in 2006 nearly 600 IpS systems are now in operation worldwide for a large variety of applications in biology, chemistry, physics and material science.

Are you tired of getting spare parts for an ancient rotating anode or is your detector performance only limited by your x-ray source that lacks intensity? We will demonstrate how to bring former high end diffractometers back to a superb performance for cutting edge science after an upgrade with a high performance IpS source. Incoatec ensures full software and safety integration, and an installation hand in hand with your local service responsible, providing a constant service support by your partners on site.

In addition to all Bruker and Nonius systems, Incoatec also offers integrations into a wide range of instruments, e.g. Rigaku, marXperts, STOE, also together with Dectris or Huber components and we also provide customized special engineering solutions.

Keywords: microfocus, X-ray source, Incoatec, Scatex, brilliance, crystallography, protein, chemical

MS39-P7 Precise determination of lattice constants by energy dispersive Laue experiments with a PILATUS detector

Kurdzesau Fiodar¹, Schneebeli Matthias², Pilipp Volker², Mueller Marcus², Weber Thomas¹

1. Laboratorium für Kristallographie, ETH Zurich, Vladimir-Prelog-Weg 5, Zurich 8093, Switzerland
2. DECTRIS Ltd., Neuenhofstrasse 107, Baden 5400, Switzerland

email: fiodar.kurdzesau@mat.ethz.ch

The most common application of traditional (energy integrative) Laue technique is certainly identification of crystal orientations [1]. For obtaining further information such as lattice constants or integral Bragg intensities complementary experiments are required, which frequently cannot be performed without violating the integrity of bulky samples or moving the crystals. The later is of particular nuisance in cases of non-ambient experiments where the possibility of stationary measurements would heavily simplify experimental setups. Modern energy discriminating pixel detectors (e.g. PILATUS [2], frame store pnCCD [3] etc.) allow overcoming this problem providing the full information about bulky and/or stationary crystals via energy-dispersive Laue diffraction (EDLD) experiments.

In this study EDLD measurements are performed with a four-circle Eulerian geometry diffractometer equipped with a conventional X-ray source (Mo sealed tube) and a PILATUS 300 K detector [2]. The flexibility of the diffractometer is utilized for testing various experimental configurations (forward, back scattering etc.), while the crystal itself was not moved during the experiments. Parallax measurements of primary and diffracted radiation are used for determining experimental errors directly with the crystal under investigation, which allow correcting unavoidable misalignments of large samples. The PILATUS detector's energy resolution (<0.12 keV) is sufficient for a proper determination of the scattering vector lengths of recorded reflections, i.e. three-dimensional reciprocal space reconstructions, where the orientation and lattice constant determination become possible following standard procedures [4].

The developed technique was tested with several bulky samples (silicon, quartz, MgZn_2 etc.). The crystal orientation and lattice parameters could be identified with a satisfying precision (0.05° and 0.01 Å, or better). Possible applications of this method and its further developments (quantitative structure determination of stationary and/or bulky crystals) will be discussed.

[1] Z. Ren, D. Bourgeois, J.R. Helliwell et al, J. Synchrotron Rad., 1999, **6**, 891-917

[2] P. Kraft, A. Bergamaschi, Ch. Brönnimann et al, IEEE Trans.Nucl.Sci., 2009, **56**(3), 758-764

[3] S. Send, M. von Kozierowski, T. Panzner et al, J.Appl.Cryst., 2009, **42**, 1139-1146

[4] W. Kabsch, J.Appl.Cryst., 1988, **21**, 916-924

Keywords: Energy-dispersive X-ray diffraction analysis, Laue diffraction, PILATUS detectors.

MS39-P8 ISX stage: from automated *in situ* screening to structure solution

Severine Freisz¹, Freisz Severine¹, Benning Matthew²

1. Bruker AXS GmbH Oestliche Rheinbrueckenstrasse 49, 76187 Karlsruhe, Germany

2. Bruker AXS Inc. 5465 E. Cheryl Parkway Madison, WI 53711 United States

email: severine.freisz@bruker.com

Recent developments in hardware and software are greatly increasing the capabilities of in-house diffraction systems, making it more routine to obtain *de novo* structural information in the home lab. We have now introduced the D8-VENTURE solution for structural biology with the PHOTON 100 detector, featuring the first CMOS active pixel sensor for X-ray crystallography. Our new microfocus source, the METALJET delivers beam intensity exceeding those of typical bending-magnet beamlines.

Very recently, we developed a fully automated solution for *in situ* crystal screening in plates, the ISX stage. This stage facilitates the investigation of a large number of crystals within the routine workflow of the crystallization lab.

The combination of the sensitive PHOTON 100 detector and a high-intensity X-ray source maximizes the diffraction signal from even the smallest, most weakly diffracting crystals. The ISX software provides an intuitive user environment to maximize the productivity of even occasional users.

The system can be quickly converted from the typical single-crystal diffractometer to the completely motorized *in situ* crystal screening device, leaving the KAPPA untouched. The system can be reverted to the standard diffractometer just as quickly, after a favorite crystal has been identified for data collection.

Here we present all the ISX stage features and data we collected in house.

Keywords: In situ screening, Structural Biology

MS39-P9 Current status of the liquid-metal-jet X-ray source technology

Emil Espes¹, Björn Hansson¹, Oscar Hemberg¹, Mikael Otendal¹,
Tomi Tuohimaa¹, Per Takman¹

1. Excillum AB

email: emil.espes@excillum.com

High-end x-ray diffraction and scattering techniques such as high-resolution XRD, protein crystallography, and SAXS rely heavily on the x-ray source brightness for resolution and exposure time. Traditional solid or rotating anode x-ray tubes are typically limited in brightness by when the e-beam power density melts the anode. The liquid-metal-jet technology has overcome this limitation by using an anode that is already in the molten state.

We have previously demonstrated prototype performance of a metal-jet anode x-ray source concept [1-3] with unprecedented brightness in the range of one order of magnitude above current state-of-the art sources. Over the last years, the MetalJet technology has developed from prototypes into fully operational and stable X-ray tubes running in many labs over the world.

This presentation will review the current status of the technology specifically in terms of stability, lifetime, flux and brightness. It will also discuss details of the liquid-metal-jet technology with a focus on the fundamental limitations of the technology. It will furthermore refer to some recent data from applications within x-ray diffraction and SAXS.

[1] O. Hemberg, M. Otendal, and H. M. Hertz, *Appl. Phys. Lett.*, **2003**, 83, 1483.

[2] M. Otendal, T. Tuohimaa, U. Vogt, and H. M. Hertz, *Rev. Sci. Instr.*, **2008**, 79, 016102.

[3] T. Tuohimaa, M. Otendal, and H. M. Hertz, *Appl. Phys. Lett.*, **2007**, 91, 074104

Keywords: x-ray tube, x-ray source, microfocus, gallium, copper, silver, indium, brightness

MS39-P10 Software solutions for custom-built X-ray diffractometers and non-standard experimental setups

Pascal Parois¹, Mark R. Warren², Dominik Schaniel³, Richard I. Cooper¹

1. Chemical Crystallography, Department of Chemistry, University of Oxford, OX1 3TA Oxford, U.K.

2. Diamond Light Source, Harwell Science & Innovation Campus, Didcot OX11 0DE, U.K.

3. Université de Lorraine, CRM2, UMR 7036, Vandoeuvre-les-Nancy F-54506, Fr

email: pascal.parois@chem.ox.ac.uk

Commercially produced X-ray diffractometers are widely available and supplied with all the required software to plan, carry out and process data from routine experiments. However, they can be inadequate for experiments which require specialised sample environments *e.g.* photo-crystallography and other in-situ measurements, and there can be delays before certain hardware like pixel detectors become available. It is therefore sometimes necessary to build an instrument from scratch or modify an existing one which not only involves assembly of mechanical parts but also electronic synchronisation and software to coordinate the whole instrument and control the related experiment. Because parts are from different manufacturers it is very often challenging to write the software controlling the new instrument and fit the process in an existing workflow for data processing.

We present here different software which have been used in the Laboratoire de Cristallographie, Résonance Magnétique et Modélisations at université de Lorraine, Fr and the I19 beamline at the Diamond Light Source, Uk for instrument control, strategy and data processing.

Keywords: Software, X-ray intruments, Computer programming

MS39-P11 EIGER: The next generation of Hybrid Photon Counting detectors

Marcus Mueller¹, Arnau Casañes², Meitian Wang²

1. DECTRIS Ltd., Switzerland

2. Swiss Light Source at Paul Scherrer Institut, Switzerland

email: marcus.mueller@dectris.com

PILATUS detectors have set new standards for data quality and collection efficiency in crystallographic data acquisition. EIGER, the next generation of Hybrid Photon Counting (HPC) detectors, takes a great leap towards smaller pixel size and substantially shorter readout times. The first EIGER detectors start operation at various synchrotron beamlines in 2015 and are also available for laboratory instruments.

This presentation will describe the novel features of EIGER and how crystallographers can benefit from these. Furthermore, first results obtained with EIGER detectors will be presented.

Keywords: Hybrid Pixel Detectors, X-ray detectors, Hybrid Photon Counting detectors

MS39-P12 Application of a pnCCD for energy-dispersive Laue diffraction with ultra-hard X-rays

Sebastian Send¹, Ali Abboud¹, Nadja Wiesner¹, Mohammad Shokr¹, Tuba Conka-Nurdan², Manuela Klaus³, Christoph Genzel³, Dieter Schlosser⁴, Martin Huth⁴, Robert Hartmann⁴, Lothar Strüder⁴, Ullrich Pietsch¹

1. University of Siegen, Germany

2. Türk-Alman Üniversitesi, Istanbul, Turkey

3. Helmholtz-Zentrum Berlin, Germany

4. PnSensor GmbH, Munich, Germany

email: send@physik.uni-siegen.de

The use of highly brilliant synchrotron radiation allows precise analyses of crystalline materials by means of diffraction experiments. However, in a variety of applications, the availability of structural information is limited due to the insufficient performance of conventional detector systems for X-ray spectroscopy. New experimental possibilities are offered by energy-resolving area detectors based on the concept of the pn-junction charge coupled device (pnCCD). In particular, structure determination can be achieved in a single-shot exposure of the crystal to white synchrotron radiation in an energy-dispersive Laue diffraction experiment. Until now pnCCDs have successfully been applied for analyses of inorganic crystals and fast screening techniques quantifying polycrystallinity in organic samples of macromolecules with white X-rays between 10 keV and 35 keV.

In this work the spectroscopic performance of a pnCCD detector in the ultra-hard energy range between 40 keV and 140 keV is tested by means of an energy-dispersive Laue diffraction experiment on a GaAs crystal. About 100 Bragg peaks were collected in a single-shot exposure of the arbitrarily oriented sample to white synchrotron radiation provided by a wiggler and resolved in a large reciprocal-space volume. The positions and energies of individual Laue spots could be determined with a spatial accuracy of less than one pixel and a relative energy resolution below 1%. In this way the unit-cell parameters of GaAs were extracted with high accuracy allowing for a complete indexing of the recorded Laue pattern. Experimental structure-factor amplitudes could be obtained from the three-dimensional data sets taking into account photoelectric absorption as well as Compton scattering processes inside the detector. The agreement between measured and theoretical kinematical structure-factor amplitudes calculated from the known crystal structure is in the range of 10%. The results of this experiment demonstrate the potential of pnCCD detectors for applications in X-ray structure analysis using the complete energy spectrum of synchrotron radiation.

References:

- S. Send et al., *Nucl. Instrum. Meth. A*, 711 (2013), 132-142
- A. Abboud et al., *J. Instrum.* 8 (2013), P05005
- S. Send et al., *J. Appl. Cryst.* 45 (2012), 517-522
- S. Send et al., *J. Appl. Cryst.* 42 (2009), 1139-1146

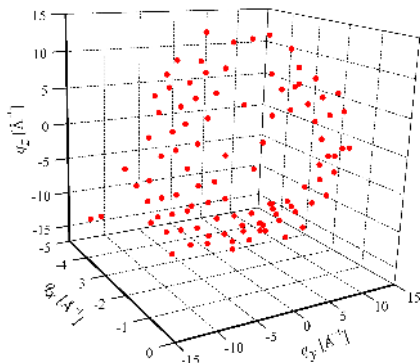


Figure 1. The recorded Laue pattern of GaAs after resolving the Laue spots' energies and converting the three-dimensional information into reciprocal-space coordinates. 101 Bragg peaks were collected in a single X-ray shot occupying reciprocal lattice points of GaAs in the defined coordinate system.

Keywords: energy-dispersive Laue diffraction, X-ray structure analysis, X-ray spectroscopy, white synchrotron radiation, pnCCD

MS39-P13 The DIALS framework

James M. Parkhurst^{1,2}, Graeme Winter¹, David Waterman³,
Richard Gildea¹, Luis Fuentes-Montero¹, Gwyndaf Evans¹

1. Diamond Light Source
2. MRC LMB
3. CCP4

email: james.parkhurst@diamond.ac.uk

Recent technological advances and changes in methodology in X-ray crystallography, such as high frame-rate pixel array detectors and serial femtosecond crystallography have created a need for the development of new algorithms; however, current integration programs for X-ray diffraction data are limited by their lack of openness or extensibility, resulting in a barrier between the development of new integration algorithms and their deployment on the beamline.

Here we present the DIALS (diffraction integration for advanced light sources) framework and integration package which is both a standalone application for the integration of X-ray diffraction data and a modular framework for developing new integration programs. The aim of the DIALS framework is to provide an extensible architecture within which new integration algorithms may be developed and quickly deployed without developers being required to write and maintain large amounts of high-level application source code. Rather, it is the aim of DIALS to liberate developers to allow them to concentrate solely on the scientific content of the algorithms themselves.

The DIALS framework implements a simple plugin system that allows algorithms to be loaded at runtime to perform certain tasks such as spot finding, indexing, refinement, background subtraction and integration. At the cost of writing a small amount of Python code, the developer can add an algorithm that can be loaded and selected at runtime without any modification of the DIALS framework itself. This design allows DIALS to be flexible with respect to the experiment being performed. For example, different algorithms can be used for data obtained using the rotation method or serial femtosecond crystallography.

DIALS provides a comprehensive suite of command line applications for the analysis of X-ray diffraction data as well as providing tools for visual inspection of the raw data and processing results. DIALS is written in a mixture of Python and C++ and is available for download from <http://sourceforge.net/projects/dials>; the source code is available under an open-source BSD license.

Keywords: Integration, data processing, X-ray crystallography, software

MS39-P14 Trends on multilayer X-ray optics and scatterless pinholes

Jörg Wiesmann¹, Frank Hertlein¹, Andreas Kleine¹, Carsten Michaelsen¹, Uwe Heidorn¹, Christopher Umland¹, Michael Störmer²

1. Incoatec GmbH, Max-Planck-Strasse 2, 21502 Geesthacht, Germany
2. Helmholtzzentrum Geesthacht, Max-Planck-Strasse 1, 21502 Geesthacht, Germany

email: wiesmann@incoatec.de

A large variety of X-ray optics is required for beam alignment, guidance or monochromator applications at synchrotron beamlines. We investigated various types of multilayer optics for energy ranges between several keV and up to 80 keV. For high-brightness laboratory sources like the latest Incoatec Microfocus Source IqS or metaljet based sources, optics with similar shape errors are nowadays needed. They are used as monochromators and beam shaping devices in protein and small molecule crystallography, as well as in powder diffraction and small angle scattering.

We will present new developments of 2-dim beam shaping Montel Optics for synchrotron applications and for high-brilliance laboratory equipment. At synchrotrons such as DLS, NSLS and APS, different types of these optics are now used, for example in analyzer systems for inelastic scattering. For the optics a perfect multilayer coating have to be produced with a precision within $\pm 1\%$ of the single layer spacing. Very low shape errors below 100 nm and figure errors below 5 arcsec are required for the substrates. In summary, this ensures also for laboratory sources superb flux densities of above 4×10^{11} ph/s/mm².

In this contribution we will also present cutting-edge results of a 50 cm laterally graded multilayer optics, developed for special mini-synchrotrons with a deviation to a specified film shape of less than 0.3 %.

Besides the multilayeroptics, other components shape the X-ray beam. For many experimental set-ups, the collimator and pinhole system plays a significant role. Parasitic aperture scattering causes loss in data quality especially in SAXS and GISAXS applications. Various measurement results will be presented showing the improvement of data quality with Incoatec's scatterless pinholes called SCATEX. These pinholes are either made of Germanium for energies < 11.2 keV or of Tantalum for energies > 11.2 keV and are available with diameters from 2 mm down to 20 μ m and below.

Keywords: Multilayer Optics; Scatterless Pinholes; Montel Optics; Metaljet; Microfocus Source; Synchrotron Beamline

MS39-P15 Fast and efficient - experiments with modern X-ray sources and CMOS APS detectors

Holger Ott¹, Bruce C. Noll²

1. Bruker AXS GmbH
2. Bruker AXS Inc.

email: holger.ott@bruker.com

New techniques for experimental design become available with the PHOTON detector's continuous-scans in shutterless mode. Until today, crystal screening has been a time-consuming task that hardly revealed more than the unit-cell dimensions. For one second exposures in shutterless mode, overall data collection times are reduced by as much as 75 % as long overhead times of CCD detectors are eliminated. Modern high-flux X-ray sources also generally lead to shorter exposure times per degree for a given sample. Consequently, the combination of the PHOTON detector with the new X-ray sources allows collecting often complete data sets in as little as 60 s.

These scans provide impressively more reflections for indexing than traditional matrix scans in far less time. The huge amount of information enables the sophisticated analysis of the diffraction pattern, e.g. for multifold twinning or modulation, using the powerful tools available in the newly released APEX3 software suite. Based on this examination, crystal defects are quickly identified, which may suggest the merit of picking another crystal. As an additional benefit, even the structure determination can be performed, revealing the chemical constitution of the crystal. This facilitates an easy decision-making to discontinue or continue the experiment with improved knowledge for an eventually desired more exhaustive data collection.

Typical day to day examples will be presented taking advantage of the latest PHOTON APS detector and X-ray source combinations showing how complete data collections can be finished in the time frame of a traditional pre-experiment.

Keywords: CMOS APS Detectors, Modern X-ray Sources, Fast and Efficient Data Collections

MS39-P16 VMXi – Development of an *in situ* MX beamline at Diamond Light Source

James Sandy¹, Juan Sanchez-Weatherby¹, Carina M.C. Lobley¹,
Marco Mazzorana¹, Jon Kelly¹, Geoff Preece¹, Andy Foster¹,
Andy Male¹, David Butler¹, Mic Harding¹, Adam Prescott¹,
Thomas Hartrampf¹, Dave Butler¹, Adam Taylor¹, Toby Hill¹,
Thomas Sorensen¹

1. Diamond Light Source Ltd, Harwell Science & Innovation Campus, Chilton, UK, OX11 0DE

email: james.sandy@diamond.ac.uk

For protein crystallographers, one of the bottlenecks in the structure solving process is the harvesting of protein crystals and finding appropriate cryo-protectants. This may be early on in the life of a project where the experimenter wishes to identify whether crystals are salt, protein or some other crystallisable object, or later when protein crystallisation conditions are being optimised to achieve the best possible resolution from the X-ray diffraction experiment. Additionally, some protein samples are either too small to harvest, are too fragile to manipulate, or do not permit cryo-cooling.

At the Diamond Light Source we are developing an *in-situ* MX beamline specifically designed to take the crystallisation support, be it a crystallisation plate, or an LCP plate, and collect useful data which will aid the crystallographer in their experiment. We will be able to remove this bottleneck by providing a very high flux, tunable micro-focus beamline to allow extremely rapid screening and data collection of samples at room temperature.

Users of this beamline will be able to deliver or post their plates to Diamond and have the plates stored at either 20° C or 4° C. The plates will be imaged and the user will identify objects that they wish to investigate. The user will interact with the VMXi beamline via a web interface which will give them the ability to mark objects, determine what kind of experiment they want i.e. screening, data collection, fluorescence etc and will give access to results from data previously collected.

Construction of the experimental area is now complete and the endstation is being designed by in-house engineers to make a very efficient and effective *in-situ* beamline. Due to the staged construction process we are able to keep the I02 beamline operational whilst building and commissioning the new endstation. The new VMXi beamline is scheduled to open in 2016 when I02 will cease operations.

Keywords: *in-situ*, beamline, macromolecular crystallography

MS39-P17 Single crystal neutron diffractometer for Biological macromolecules iBIX at J-PARC

Katsuhiko Kusaka¹, Taro Yamada¹, Naomine Yano¹, Takaaki Hosoya¹, Takashi Ohhara², Ichiro Tanaka¹, Masaki Katagiri¹

1. Frontier Research Center for Applied Atomic Sciences, Ibaraki University

2. J-PARC center, Japna atomic energy agency

email: kusakats@mx.ibaraki.ac.jp

Single crystal neutron diffraction is one of the powerful methods to obtain the structure information including the hydrogen atoms. IBARAKI biological crystal diffractometer called iBIX is a high performance time of flight single crystal neutron diffractometer to elucidate the hydrogen, protonation and hydration structures of organic compound and biological macromolecules in various life processes. iBIX is installed on BL03 in Material and Life Science Facility, J-PARC. Since the end of 2008, iBIX has been available to user experiments supported by Ibaraki University. In FY2012, we have succeeded to upgrade the 14 existing detectors and install the 16 new detectors for diffractometer of iBIX. The total measurement efficiency of the present diffractometer was on one order of magnitude from the previous one coupled with the increasing of accelerator power. In the end of FY2012, iBIX could be started to user experiments for biological macromolecules in earnest. In FY2014, the accelerator power of J-PARC is 300kW. We can collect a full data set of biological macromolecules for neutron structure analysis with around 2.0Å resolution in 10 days by using iBIX. The size of sample measured by iBIX is from 1 to 6mm³ in volume. If the accelerator power will become 1MW, the total measurement time or the sample size will be reduced to a one-third. In the beginning of FY2014, we have succeeded to collect the diffraction data sets of 6 biological macromolecules for about 4 months. Some interesting results obtained from these experiments which make the most of the merit of the neutron diffraction experiment will be reported in the poster. We started to upgrade the data reduction method and the diffractometer instruments in order to improve the data accuracy for the integrated intensities of Bragg reflections and to become user friendly system in the next phase, for example background extraction, the data correction method, integration method and profile fitting method. In the case of the diffraction data from larger unit cell crystals measured by iBIX, the some neighbor Bragg spots will overlap partially each other because iBIX was installed on the coupled moderator with the wide pulse shape. It is necessary to de-convolute the overlapped spots in order to obtain the integrated intensity of them. The profile fitting method can be applied for de-convolution of overlapping reflections. We will report also the development status of iBIX in the poster.

Keywords: Single crystal neutron diffraction, Biological macromolecule, pulse neutron

MS39-P18 DIALS – a new toolbox for diffraction image integration

David G. Waterman^{1,2}, Graeme Winter³, James M. Parkhurst³, Luis Fuentes-Montero³, Richard J. Gildea³, Aaron S. Brewster⁴, Nicholas K. Sauter⁴, Gwyndaf Evans³

1. CCP4, STFC
2. RCaH, Rutherford Appleton Laboratory
3. Diamond Light Source
4. Lawrence Berkeley National Laboratory

email: david.waterman@stfc.ac.uk

DIALS is a collaborative initiative to produce an open source software toolbox, built on top of the cctbx, to address tasks in diffraction image integration. The toolbox has been developed with a flexible, modular design and can be used at various levels: as a library, via a comprehensive set of command-line tools, or driven by a high-level script or expert system such as xia2. The motivation behind the development of DIALS is discussed and the structure of the software is explained. In particular, the use of DIALS for fast, high quality integration by 3D profile fitting in the context of synchrotron rotation experiments is covered in detail. Key features of DIALS are explored, including a powerful indexing program that utilises a choice of methods for identifying candidate basis vectors, and global multi-experiment geometry refinement with smoothly varying crystal models. The use of DIALS in different experimental contexts such as serial snapshot crystallography is touched upon. Potential users are encouraged to get involved with the project, and a timeline of development plans culminating in beta release of the software in the CCP4 suite is presented.

Keywords: integration, software, cctbx, ccp4, open source

MS39-P19 High resolution powder X-ray diffraction beamline at Taiwan Photon Source

Hwo-Shuenn Shue¹, Yu-Chun Chuang¹, Chung-Kai Chang¹, Kuan-Li Yu¹, Longlife Lee¹

1. National Synchrotron Radiation Research Center, Taiwan

email: hshue@nsrrc.org.tw

The low emittance (1.6 nm-rad) synchrotron radiation ring, Taiwan Photon Source (TPS), has reached the design goal of 3 GeV electron beam stored and delivered its first synchrotron light on the last day of 2014. The first 1.5 GeV synchrotron radiation ring in Taiwan, Taiwan Light source (TLS), has been operated for 21 years. TLS serves more than 2000 scientists and students every year now. To response the highly demanding of hard X-ray users, the medium energy 3 GeV synchrotron ring, TPS, has been constructed since 2010. In phase I, seven frontier beamlines will be constructed by the end of 2015. A dedicated high resolution powder diffraction beamline will be built after then. A highly collimated and intense X-ray source will be produced by an in-vacuum undulator (IU22) to obtain the highest possible brilliance in the range of 5-30 keV. To meet the versatile researchers in chemistry, physics and materials, a large concentric 3-circle diffractometer (Newport) equipped with a multi-crystal analyzer system and a fast position sensitive detector (MYTHEN 24K) were designed for high angular resolution and time-resolved studies respectively. The polycrystalline materials under non-ambient conditions, such as high/low temperature, high pressure and gas de/adsorption, will be investigated by PXRD techniques. In addition, to satisfy the high demanding of powder users, large amount of samples and increase the beamtime efficiency, a high throughput robot will be installed to allow automated sample mounting. The *in situ* and time resolved experiments as well as structure determination from powder diffraction data will be emphasized in this beamline.

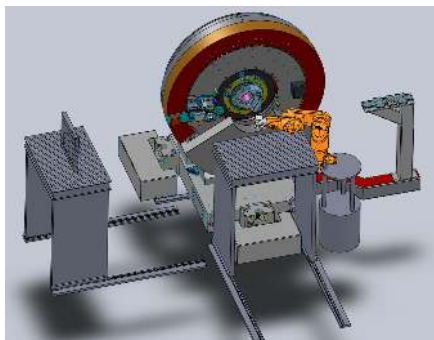


Figure 1. A large three circle powder diffractometer equipped with a multi-crystal analyzer, strip detector and flat area detector will be installed in TPS.

Keywords: Synchrotron Radiation, Powder X-ray Diffraction

MS39-P20 Designing a powder diffraction instrument optimised for hydrogenous materials. HOD - the Hydrogen Observation Diffractometer concept for ESS

Paul F. Henry^{1,2}, Mark T. Weller³, Chick C. Wilson³, Paul R. Raithby³, Holger Kohlmann⁴, Sten Eriksson², Chris Kneez²

1. European Spallation Source (ESS) AB, PO Box 176, Lund, Sweden
2. Chemical Engineering Dept., Chalmers University of Technology, Gothenburg, Sweden
3. Department of Chemistry, University of Bath, Bath, UK
4. University of Leipzig, Leipzig, Germany

email: paul.henry@ess.se

Hydrogen is the most important element on Earth and has arguably, over recent years, become even more important in the context of for the Grand Challenges facing Humankind; it is pervasive and unique in materials science, chemistry and biological systems. In addition to its strong structure and property directing role, it has itself become an increasingly important "guest" in materials, for example in relation to its huge potential in energy storage and energy vector applications. Therefore, understanding both the fundamental and applied behaviour and function of hydrogen – its location and its motion – in determining the properties of a system, will lie at the core of the majority of technological advances of the next few decades.

The problem facing the experimentalist is that hydrogen is a very weak X-ray scatterer and, even with the brightest synchrotron sources, it is almost impossible to accurately determine hydrogen positions. Neutron scattering potentially offers the solution, but is complicated by the high incoherent scattering cross section of ¹H, which gives very high backgrounds. While deuteration is often used, the positive / negative scattering contrast of D / ¹H becomes an issue if deuteration is incomplete, it is expensive or impossible to deuterate materials and deuteration often changes the physical properties of the material. Some progress has been made in this area over the last several years and techniques are under development that can significantly reduce and even control the scattering properties of hydrogen in neutron scattering.

However, no current generation instrument can deliver these to the experimentalist. The ESS, currently in the initial stages of construction in Lund, Sweden is a new type of spallation source, using a long pulse. This offers new possibilities for instrument design combining the features from reactor-based, continuous sources with time-of-flight energy sensitivity afforded by the pulsed nature of the source. HOD - the hydrogen observation diffractometer is the result of several years of development work aimed at delivering an optimised instrument for hydrogenous materials without the need to deuterate.

Keywords: powder, neutron, hydrogen, diffractometer

MS39-P21 How to determine the space group of a twinned crystal or one with metric specialization

Howard D. Flack¹

1. Chimie minérale, analytique et appliquée, University of Geneva, Switzerland

email: crystal@flack.ch

The excellent text *Determination of Space Group* by Looijenga-Vos & Buerger in the 5th edition of *International Tables for Crystallography* Volume A *Space-group symmetry* is dated. It will be replaced in the 6th edition by the text *Methods of space-group determination* by Shmueli, Flack & Spence. A major limitation of both of these texts is that the tables of values only apply to single-crystal samples. Using established theory available in the literature, tables of values applicable to many twinned crystals and many cases of metric specialization have been produced. The tables are arranged by observed Bravais-lattice type. For each observed Bravais-lattice type, the values are arranged horizontally by Laue and crystal class, and vertically by reflection conditions. The tables indicate those space groups obeying the observed Bravais-lattice type, the observed Laue and crystal classes, and the observed reflection conditions. The tables have been implemented in a commercially-available spreadsheet on a pc and will be available for demonstration.

Keywords: space group, twin, metric specialization

MS39-P22 XPAD, a hybrid pixel detector for accurate and time resolved X-ray data collection at laboratory

Paul ALLE¹, Pierre Delpierre², Emmanuel Wenger¹, Frédéric Bompard², Pierre Fertey², Slimane Dahaoui¹, Dominik Schaniel¹, Claude Lecomte¹

1. CRM2 Laboratory / Institut Jean Barriol / Université de Lorraine / CNRS. Faculté des sciences et technologies, 54506 Vandœuvre cedex. France.

2. imXpad 297 Av du Mistral, 13600 La Ciotat. France.

3. Synchrotron SOLEIL, l'Orme des Merisiers, 91190 Saint-Aubin. France.

email: paul.alle@univ-lorraine.fr

The new generation of X-ray detectors, the hybrid pixel area detectors known as 'pixel detectors', is based on direct detection and single-photon counting processes that leads to noise immunity and very high counting dynamic. Moreover their electronic architecture allows for an electronic shutter and fast readout time. These characteristics render them very attractive and explain their broad use on synchrotron beam lines since a few years. A long-standing collaboration between the CRM2 laboratory and the society imXPAD led us to develop an original laboratory diffractometer made from a Nonius Mach3 goniometer equipped with an Incoatec Mo micro source and a XPAD pixel area detector at the CRM2 laboratory four years ago. In this poster we will present the detector and the first laboratory applications: pump-probe (time resolved) experiments and accurate electron density measurements.

For the pump-probe experiment [1], we have developed a dedicated firmware for the FPGA (Field-Programmable Gate Array) inside the detector (a firmware allows programming the electronic architecture inside the FPGA to build any complex function). This particular flexibility of the XPAD detector was used to multiplex and sum the images inside the detector, synchronous with the pump-probe experiment, enabling the rapid data collection (independent of the image size) over thousands of cycles under external constraints whereby the measurement (and constraint) windows can be adjusted in the range of a few milliseconds to a few tens of milliseconds.

The capacity of this detector to perform very accurate data collection [2] will also be shown by comparison between charge density models obtained after multipolar refinements with identical strategies on data collected with three diffractometers, Mach3 XPAD, Agilent Atlas CCD and BRUKER PHOTON100 CMOS, on the same crystal of a relatively weakly scattering organic compound ($C_{15}H_{14}O_3$) to a maximum resolution of 0.96 \AA^{-1} .

[1] Diffraction studies under in-situ electric field using a 2D hybrid pixel XPAD detector : P. Fertey, P. Allé, E. Wenger, B. Dinkespiler, S. Hustache, K. Medjoubi, F. Picca, C. Lecomte and C. Mazzoli, *Journal of Applied*

Crystallography, **46**, 1151-1161, 2013.

[2] XPAD X-ray hybrid pixel detector for charge density quality diffracted intensities on a laboratory equipment : E. Wenger, S. Dahaoui, P. Allé, P. Parois, C. Palin, C. Lecomte and D. Schaniel, *Acta Crystallographica B*, **70**, 5, 783-791, 2014.

Keywords: Hybrid pixels detector, time resolved diffraction study, pump-probe experiment, charge density study, accurate X-ray diffraction data.

MS40. X-ray diffraction from microsecond to femtosecond time range (including FELs)

Chairs: Christian Betzel, Anton Barty

MS40-P1 Time-resolved X-ray diffraction study of inhomogeneous deformations in piezoelectric single crystals, induced by a nanosecond electric pulse

Hyeokmin Choe¹, Semën Gorfman¹, Michael Ziolkowski¹, Marco Vogt¹, Stefan Heidbrink¹, Ullrich Pietsch¹

¹. Department of Physics, University of Siegen, Walter-Flex Str. 3, D-57072 Siegen, Germany

email: choe@physik.uni-siegen.de

Electromechanical coupling (piezoelectric effect) is the physical property describing the ability of some materials to convert electrical energy to mechanical energy or vice versa. Despite the great technological importance of piezoelectric materials, many fundamental aspects of piezoelectricity are still quite poorly understood. For instance, very little are known about a reaction of piezoelectric crystals to ultra-short (e.g. nanosecond) and strong electric pulses on the microscopic and mesoscopic length scales. The aim of this work is to investigate the reaction of lithium niobate (LiNbO_3) and α -quartz ($\alpha\text{-SiO}_2$) single crystals to a nanosecond electric pulse by time-resolved X-ray diffraction.

We report on the measurement of time-dependent rocking curves of selected Bragg reflections from the $\sim 0.05\text{mm}$ thin single crystal plates. We applied 2ns electric pulse reaching the maximum amplitude of 30kV/mm and collected diffraction intensity as a function of time delay after the applied pulse. The measurement was performed using the specially developed stroboscopic data-acquisition system [1-3]. Figure 1 shows dynamics of 0 0 12 Bragg rocking curve of LiNbO_3 as a function of time (passed after the pulse). We observed the range of phenomena, corresponding to the changes on different time and length scales, including: (1) the change of integrated intensity, and (2) change of full width half maxima. The change of integrated intensity can be caused by both, the rearrangement within the unit cell (change of the structure factors) or alternatively by the change induced of the mosaicity (change of the extinction parameter).

[1] S. Gorfman, O. Schmidt, M. Ziolkowski, M. Kozierowski, and U. Pietsch, J. Appl. Phys. 108, 064911 (2010)

[2] S. Gorfman, O. Schmidt, V. Tsirelson, M. Ziolkowski, and U. Pietsch, Z. Anorg. Allgem. Chem. 639(11), 1953-1962 (2013)

[3] S. Gorfman, Crystallogr. Rev. 20(3), 210-232 (2014)

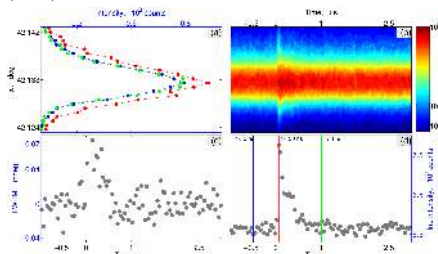


Figure 1. Time-resolved X-ray diffraction of LiNbO_3 single crystal, impacted by nanosecond high electric pulse: (a) dynamics of 0 0 12 Bragg rocking curves as selected time ranges, (b) time-resolved intensity map, (c) change of peak width, and (d) change of integrated intensity after applied electric pulse

Keywords: time-resolved X-ray diffraction, piezoelectric materials, nanosecond electric pulse

MS41. Advanced powder diffraction

Chairs: Radovan Černý, Michela Brunelli

MS41-P1 Characterization of cellulose fibers by powder diffraction

Kenny Stahl¹, Christian G. Frankær¹, Theis K. Guldbech¹, Anders Thygesen²

1. Department of Chemistry, Technical University of Denmark

2. Department of Chemical and Biochemical Engineering, Technical University of Denmark

email: kenny@kemi.dtu.dk

Increasing concerns about the pile-up of plastic garbage on land as well as at sea, have created a growing interest in biodegradable polymer materials. For construction purposes these materials require reinforcement. Here cellulose fibers represent biodegradable alternatives to glass and carbon fibers. This project is focusing on how to extract cellulose fibers from hemp and flax, while retaining the maximum strength of the fibers. The observed strength of cellulose fibers is typically 300 – 1500 MPa, while the theoretical strength is 8000 MPa. Microbial, enzymatic and chemical pre-treatments to remove lignin, pectin and hemicellulose are being tested with respect to effects on strength and interface bonding. An important and traditional method for characterization of cellulose is powder diffraction, which can reveal crystallinity and crystalline domain sizes. However, several problems complicate the evaluation of cellulose powder diffraction patterns: Small crystallite size, typically 4*15 nm, giving very broad and overlapping reflections; preferred orientation due to the fibrous nature of the sample; and transparency effects giving peak shifts and additional asymmetry. As a result a typical powder diffraction pattern will show only a few distinct features (Fig. 1). Several evaluation methods have been used over the years, but since the presentation of the crystal structure of cellulose I β [1], the Rietveld method is the preferred one [2]. Due to the few features in the diffraction patterns the challenge is to minimize the number of refined parameters and thereby correlations between parameters. The transparency peak shift and asymmetry effects have been studied using an internal Si-standard, and crystal domain sizes using pre-oriented samples. We will discuss the effects of sample preparation, peak overlap, transparency effects and preferred orientation, with the overall aim of getting reliable results for crystallinity and crystal domain sizes. The results will be compared to different pre-treatments and fiber strength measurements.

[1] Nishiyama, Y., Langan, P. and Chanzy, H. (2002) J. Am. Chem. Society 124, 9074 –9082. [2] Thygesen, A., Oddershede, J., Lilholt, H., Thomsen, A.B. and Ståhl, K. (2005) Cellulose 12, 563-576.

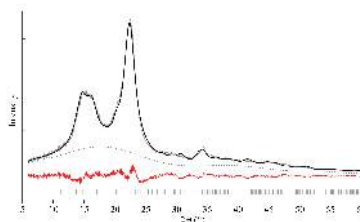


Figure 1. Powder diffraction pattern from raw hemp, 0.5 mm size fraction. Grey: raw data; black: calculated; red: difference, broken: refined background and Bragg peak markers at the bottom.

Keywords: Cellulose, powder diffraction

MS41-P2 New peroxy-compounds of Mo(VI). Completeness of structural research by powder diffraction studies

Wiesław Lasocha^{1,2}, Alicja Rafańska-Lasocha¹, Adrianna Borowiec¹

1. Faculty of Chemistry, Jagiellonian University, Ingardena 3, 30-060 Krakow, Poland

2. Institute of Catalysis PAS, Niezapominajek 8, 30-239 Krakow, Poland

email: lasocha@chemia.uj.edu.pl

The new peroxy- compounds of Mo(VI), W(VI), or V(V) are important in pharmacy, oxidation processes, removal of impurities and many other applications. Synthesis of new peroxy- compounds provides materials for scientific research, and allows finding new materials having certain oxygen content, given stability, and other tailored properties. In this project a group of molybdenum and pyridine carboxylic acids (pimelic acid and nicotinic acid) compounds were investigated. These compounds exhibit varying stability, from a few minutes (with a tendency to explosive decomposition) to several months. Due to the extremely low stability, part of the obtained compounds can be investigated solely immediately after the synthesis process. Chemical syntheses of these compounds were carried out at low temperatures. Due to their good solubility in water the excess of sediment reagents was used to precipitate them. In these syntheses both pyridine-carboxylic acids and their N-oxides were used. In the presented research we have obtained and determined crystal structures of 5 new compounds, two of them were examined only by powder diffractometry techniques. Only the simultaneous application of single crystal and powder diffraction methods enabled the structural characterization of the family peroxy compounds formed by isomeric pyridine carboxylic acids. The structural studies were performed with the use of global optimization methods (parallel tempering [1]) and laboratory diffractometers. In near future the obtained compounds will be tested in the reactions of catalytic oxidation of hydrocarbons.

Crystallographic data for some investigated compounds: (formula, sg, abc,abg, Vol.).

1. $\text{Na}[\text{MoO}(\text{O}_2)_2\text{ONC}_5\text{H}_4\text{COO}]\cdot 2\text{H}_2\text{O}$; C2/c; 25.070, 6.315, 14.588 Å, $^{-92.76^\circ}$, 2307Å^3 2. $\text{K}[\text{MoO}(\text{O}_2)_2\text{ONC}_5\text{H}_4\text{COO}]$; Cc; 7.496, 17.692, 7.5605, 101.45°, 982.68Å^3 3. $\text{NH}_4\{(\text{C}_5\text{H}_4\text{NOCO})\text{MoO}(\text{O}_2)_2\}$; P-1, 6.169, 6.314, 12.764, 77.99° , 81.45, 86.47°, 480.66Å^3 4. $\text{K}_2[\text{MoO}(\text{O}_2)_2\text{ONC}_5\text{H}_4\text{COO}]$; P-1, 9.138, 10.132, 6.908, 95.66, 110.41°, 74.34° , 577.18Å^3 .

Reference *J. Appl. Cryst.* **35** (2002), 734-743, V. Favre-Nicolin and R. Cerny

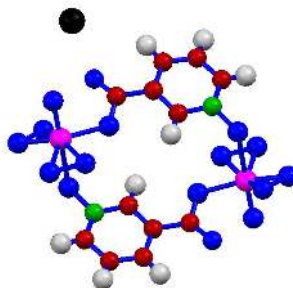


Figure 1. Potassium cation and cyclic anion of oxodiperoxomolybdate nicotinic acid N-oxide salt (4). Colors indicate: magenta Mo, green N, blue O, black K, brown C, gray H.

Keywords: peroxomolybdates, powder diffraction, global optimization techniques

MS41-P3 Self-checking bond restraints for Rietveld refinement

Ivan S. Bushmarinov¹, Artem O. Dmitrienko¹

1. A.N. Nesmeyanov Institute of Organoelement Compounds RAS

email: ib@xrlab.ru

The current development of structure determination from powder diffraction (SDPD) approaches has made such structures relatively accessible, with up to 300 Rietveld refined small-molecule structures published each year. However, unlike single-crystal XRD, the R-values for powder XRD data are highly unreliable [1], and the e.s.d. values of structural parameters are well-known [2] to be misleading. In addition, typical Rietveld refinements are heavily restrained, making it difficult to estimate the precision of the resulting structural parameters.

Here, we present a method for checking the validity and accuracy of a Rietveld refined structure requiring only the ability to change the individual values and the overall weight of the restraints. Previously we have found that the use of a custom bond restraint equation [3] in TOPAS helps identifying the "outlying" bonds (more deviating from the restraint value than others). The presence of such "outliers" indicates major errors in structural model. We have successfully applied this approach to structures ranging from organics to uranyl complexes.

In the current study, we consider a statistical model of restraint behavior to tailor the boxplot method for the specific task of outlier detection among bond length deviations. We designed this new method to utilize only classic parabolic restraints readily available in all refinement codes.

We propose an automated refinement protocol providing both initial detection of model errors and a self-check for the final structure. During the latter procedure, each restraint value is varied until it starts producing outliers. The average half-width (AHW) of the obtained restraint ranges represents the absolute extent of bond distortion tolerated by the particular combination of restraints, refinement strategy and powder pattern (typically ≈ 0.1 Å, but reaching 0.03 Å for high-quality lab data, according to a small international round robin).

We utilize the developed protocol to study and verify structures inaccessible to both SC-XRD and periodic DFT calculations, in particular Co complexes with strong spin-crossover and oligosiloxanes exhibiting full-molecule disorder.

This research has been supported by the Russian Presidential grant MK-7267.2015.3.

[1] C. Buchsbaum, M.U. Schmidt, *Acta Cryst. Sect. B* 63 (2007) 926.

[2] R.J. Hill, I.C. Madsen, *J. Appl. Cryst.* 19 (1986) 10.

[3] I.S. Bushmarinov, A.O. Dmitrienko, A.A. Korlyukov, M.Y. Antipin, *J. Appl. Cryst.* 45 (2012) 1187.

Keywords: powder diffraction, Rietveld refinement, restraints

MS41-P4 Humidity induced phase transitions of hewlysozyme investigated by microcrystalline powder diffraction on a laboratory system

Detlef Beckers¹, T. Degen¹, G. Németh¹, S. Saslis², S. Logotheti², F. Karavassili², A. Valmas², I. Margiolaki²

1. PANalytical B.V., Almelo, The Netherlands

2. University of Patras, Greece

email: detlef.beckers@panalytical.com

Proteins often crystallize in microcrystalline precipitates. The protein molecules are then surrounded by solvent and their packing arrangement is retained by limited intermolecular contacts. A change in the crystal environment first affects the bulk solvent that fills the intermolecular space, with resulting changes in the crystal structure. In literature it is reported that protein crystals in controlled humidity environments show a large change in unit-cell parameters when the humidity is decreased [1-2]. When a protein crystal is carefully dehydrated, it is in a metastable state in which the crystal initially still retains the original packing structure [2]. Further dehydration may cause the collapse of the crystal lattice: the crystal no longer maintains its packing structure because of the loss of a large amount of bulk solvent. However in some crystals, the dehydration induces a molecular arrangement change resulting in a new crystal structure. This has been already reported for hen egg-white (HEW) lysozyme [3]. While dehydration can induce structural changes, this is also likely to happen upon hydration of the same crystals.

Here, we present our results of microcrystalline protein samples on a laboratory X-ray powder diffractometer including in situ measurements under variable relative humidity conditions. The observed gradual structural changes as well as phase transitions upon dehydration and hydration of HEW lysozyme are analyzed in the relative humidity range 50% - 95%. We discuss and compare our results with related literature which is so far based on synchrotron studies only.

[1] Kiefersauer, R., et al. (2000). *J. Appl. Cryst.* 33, 1223-1230.

[2] Dobrianov, I., et al. (1999). *J. Cryst. Growth*, 196, 511-523.

[3] K. Harata, T. Akiba, *Acta Cryst.* (2007). D63, 1016-1021

Keywords: Protein powder diffraction, humidity , laboratory system

MS41-P5 Advanced materials analysis with the powder diffraction file™

Timothy G. Fawcett¹, Timothy G. Fawcett¹, Soorya N. Kabekkodu¹, Justin R. Blanton¹, Cyrus E. Crowder¹, Thomas N. Blanton¹

1. International Centre for Diffraction Data, Newtown Square, PA, USA

email: fawcett@icdd.com

Ten years ago the ICDD launched a new family of database products PDF-4. The purpose of these new databases were to provide researchers with an array of solid state analysis tools based on the powerful combination of single crystal and powder reference data, housed in a relational database format that could provide flexibility and powerful data mining. The ICDD has developed reference data and editorial procedures for experimental nanomaterials as well as amorphous materials. PDF-4 products now contain both amorphous and nanomaterial references. The use of digital patterns for both the material being analyzed and reference materials allows us to study crystallite size [1], molecular orientation and various instrumental and specimen contributions to the coherent and incoherent scatter, allowing for the analysis of crystallinity. Digital simulation tools are used to make the analyses radiation independent so that we can use experimental x-ray, neutron[2], electron [3] or synchrotron diffraction data for the analyses. We continue to work with our global membership to develop new methods and procedures. Most recently we have reviewed and published the largest collection of modulated structures, properly described by superspace groups, with up to 6-dimensional indexing and modulation vectors [4]. For improved quantitative analyses we have added massive numbers of atomic coordinates, digitized all patterns and calculated I/Ic scaling factors for both X-rays and neutron analyses.

References

[1] Scardi, P., Leoni, M. and Faber J., **2006**, "Diffraction Line Profile from a Disperse System: A Simple Alternative to Voightian Profiles", Powder Diffraction, Vol. 21, No. 4, p 270

[2] Faber, J., Crowder, C.E., Blanton, J., Kabekkodu, S., Gourdon, O., Blanton, T., Fawcett, T. G., "New Neutron Diffraction Data Capability in the PDF-4, 2014 Relational Database", **2015**, accepted for publication in Adv. In X-ray Anal. Vol. 58

[3] Reid, J., Crane, D., Blanton, J., Crowder, C., Kabekkodu, S., and Fawcett, T., **2011**, "Tools for Electron Diffraction Pattern Simulation for the Powder Diffraction File", Microscopy Today, January, 38-42.

[4] <http://www.icdd.com/products/2014/modulatedstructures.htm> and <https://www.youtube.com/user/TheICDD>

Keywords: powder diffraction file, database, diffraction

MS41-P6 What pushes some molecular materials beyond the edge of crystallinity : an experimental study based on machine-learning predictive models

Jerome G.P. Wicker¹, Max Pillong², Trixie Wagner², William I.F. David^{1,3}, Richard I. Cooper¹

1. University of Oxford, Department of Chemistry, Oxford, UK

2. Novartis Institutes for BioMedical Research, Basel, Switzerland

3. ISIS Facility, Rutherford Appleton Laboratory, Chilton, UK

email: jerome.wicker@chem.ox.ac.uk

Many molecular systems, perhaps a substantial minority, exist near the 'edge of crystallinity'. Often, despite repeated crystallisation attempts, these materials, at best, form polycrystalline solids and frequently exhibit substantial defects in crystal growth. Why is long-range order facile in some organic materials while others exhibit significant build-ups of defects and lattice strain?¹

We have recently established predictive models, developed using machine learning algorithms,² that provide a set of chemical and geometrical reasons why some materials crystallise more straightforwardly than others. Here, we present our initial experimental results from a set of 200 materials with unknown crystal structure that we predict using our machine learning algorithms to span the boundary between poorly crystallising materials and those which form single crystals.

Using the high resolution MAC detectors on ESRF beamline ID22, we have measured the powder diffraction patterns of all 200 structures. The materials are constituted into thirteen families, each containing a set of chemically similar derivatives. A substantial number of potential pharmaceutical materials are included in the study. While some structures are amorphous, most of the data are of sufficient quality to determine not only the crystal structure but also the extent and nature of microstructural imperfections such as lattice strain and stacking defects which are common and clearly visible.

Here, we will present an overview of the results, which includes analysis of *hkl*-dependent anisotropic and asymmetrical line broadening as well as particle-size distributions. With 200 organic materials, in thirteen chemical families, we have a substantial body of information that allows us to rationalise the difference in behaviour across families as functional group derivatives vary, and enables us to correlate the propensity for crystallisation with the degree of microstructural imperfection.

1. Hursthouse, M. B., Huth, L. S. & Threlfall, T. L. Why Do Organic Compounds Crystallise Well or Badly or Ever so Slowly ? Why Is Crystallisation Nevertheless Such a Good Purification Technique ? *Org. Process Res. Dev.* **13**, 1231–1240 (2009).

2. Wicker, J. & Cooper, R. Will it crystallise? Predicting crystallinity of molecular materials. *CrystEngComm* **17**, 1927–1934 (2014).

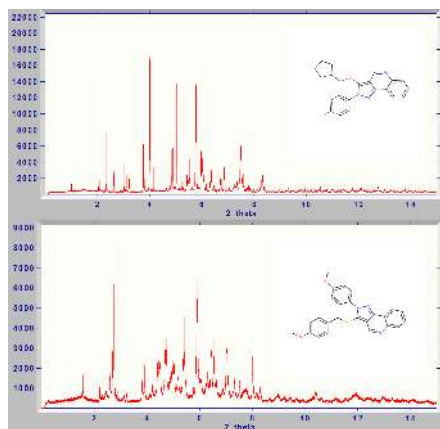


Figure 1. High resolution powder diffraction data of (a) crystalline and (b) poorly crystalline organic materials collected using ESRF beamline ID22.

Keywords: crystallization, prediction, powder diffraction, microstructure, machine learning

MS41-P7 Structural characterization of Re-substituted lanthanum tungstates $\text{La}_{5.4}\text{W}_{1-x}\text{Re}_x\text{O}_{12.6}$ ($0 \leq x \leq 0.2$) with Neutron and X-Ray Diffraction

Andrea Fantin¹, Tobias Scherb¹, Janka Seeger², Gerhard Schumacher¹, Wilhelm A. Meulenber²

1. Helmholtz-Zentrum Berlin für Materialien und Energie GmbH, Hahn-Meitner-Platz 1, D-14109, Berlin, Germany
2. Forschungszentrum Jülich GmbH, Institute of Energy and Climate Research IEK-1, D-52425 Jülich, Germany

email: andrea.fantin@helmholtz-berlin.de

The presented work on proton conducting materials will show new results on the structural characterization of a substituted lanthanum tungstate: $\text{La}_{5.4}\text{W}_{1-x}\text{Re}_x\text{O}_{12.6}$ with $0 \leq x \leq 0.2$ in two different conditions (dry-Ar, wet-D2O). Among the eight specimens measured, the one without substitution ($\text{La}_{5.4}\text{WO}_{12.6}$) and the other with highest Re-substitution level ($x=0.2$) will be in the focus of the presentation and compared throughout the whole talk.

Their comparison will be achieved considering Neutron Diffraction results, due to the insufficient contrast between W ($Z=74$, $b=4.86\text{fm}$) and Re ($Z=75$, $b=9.2\text{fm}$) against X-Rays. The structural model of the undoped system $\text{La}_{5.4}\text{WO}_{12.6}$, as suggested recently by a coauthor [1] will be independently confirmed and taken as starting point to determine the position of Re-atoms in the crystal structure.

Neutron Diffraction data was obtained from D2B (ILL, Grenoble) and HRPT (SINQ, Villigen). At D2B, High-Resolution mode was employed for the two above-mentioned samples, measuring many temperature steps with a Displex-device (5K – 200 K range). At SINQ, 1.5K was reached in High-Intensity mode, using their peculiar orange cryostat ORI4.

Three models will be finally presented for the Re-substituted system within the Fm-3m space group: Re substituting W on the main W position (Wyckoff site 4a), Re substituting W on the shared La/W position (Wyckoff site 48h) and Re substituting W statistically on both sites. As low temperature minimizes thermal vibrations, structural modeling may exclude positional disorder contribution. Substitution amount in the shared sites is reached refining occupancies in a single-atom-per-site approach (average neutron scattering length). Results match with composition obtained from Electron-Micro-Probe-Analysis.

Due to the low Re amount (~1 atom per unit cell out of 32 cations and 55 oxygen anions) and the close neutron scattering length of Re to the main element La ($Z=57$, $b=8.24\text{fm}$) it is hard to determine unambiguously the very details of the structure. Finally, special importance is given to the refined oxygen occupancies in wet and dry condition and compared to thermo-gravimetric results.

[1] T. Scherb, PhD Thesis. Technische Universität Berlin, 2011, doi: <http://dx.doi.org/10.5442/d0014>.

Keywords: Proton Conductors, Lanthanum Tungstates, Neutron Diffraction

MS43. Thin films, stresses and textures

Chairs: Fabiola Liscio, Magali Morales

MS43-P1 Rapid thermal annealing induced formation of Ge nanoparticles in ZnO thin films: A detailed SAXS study

Leyla T. Yildirim¹, Abdullah Ceylan¹, Sadan Ozcan¹, S. Ismat SHAH²

1. Department of Physics Engineering, Hacettepe University, 06800, Ankara, Turkey.

2. Department of Materials Science and Engineering, University of Delaware, Newark, DE19716, USA.

email: tatar@hacettepe.edu.tr

In this study, germanium nanoparticles (Ge-np) embedded ZnO multilayered thin films were produced on z-cut quartz and Si substrates by sequential r.f. sputtering of ZnO and d.c. sputtering of Ge targets followed by an ex-situ rapid thermal annealing (RTA) process performed at 600°C for 30, 60, and 90 s. Evolution of Ge-np via RTA process have been investigated in detail especially by using small angle x-ray scattering (SAXS) technique. X-ray diffraction (XRD) patterns showed that fcc diamond phase Ge-np were successfully formed in c-axis oriented ZnO host. Crystallite sizes of diamond phase Ge-np calculated by Scherrer formula were in the range of 18-27 nm. Analysis of SAXS patterns revealed that optimum RTA time at 600°C to form monodispersed Ge-np is 60 s. Moreover, 30 s RTA was inadequate for the complete crystallization and segregation of crystalline Ge-np, 90 s RTA turned out to be improving the crystallite size as well as deteriorating the isolation of Ge-np possibly by inter diffusion of Ge atoms back to ZnO host. These results suggest that RTA applied under certain conditions is a robust and scalable route to form monodispersed well crystallized Ge-np in ZnO multilayered thin films for various applications.

Keywords: Ge nanoparticles, ZnO thin film, SAXS, Sputtering.

MS43-P2 Evidence of Ferroelectricity in La₂Zr₂O₇ thin films with a frustrated pyrochlore-type structure

Pascal Roussel¹, Bayart Alexandre¹, Saitzek Sébastien¹, Shao ZhenMian¹, Ferri Anthony¹, Huvé Marielle¹, Desfeux Rachel¹

1. Unité de Catalyse et Chimie du Solide (UCCS) - CNRS UMR 8181 - 59652 Villeneuve d'Ascq - France

email: pascal.roussel@ensc-lille.fr

Thin films of lanthanum zirconate (La₂Zr₂O₇) have been grown by an easy sol-gel route on (110)-oriented SrTiO₃ substrates. Electrical measurements, locally performed by piezoresponse force microscopy, evidence unambiguously the ferroelectric state of the films at the nanoscale level. In the La₂Zr₂O₇ bulk material, ferroelectricity is absent due to the centro-symmetric cubic pyrochlore structure. In thin films, the extensive study carried out by high resolution X-ray diffraction highlights a lowering of the cubic symmetry that may explain the emergence of ferroelectricity. This slight structural modification is interpreted as a geometrical frustration induced by the substrate's strains during the film growth. In addition, pole figure experiments are used to give epitaxial relationships between the La₂Zr₂O₇ film and the SrTiO₃ substrate. Finally, high-resolution transmission electron microscopy images obtained on a cross-section of the film will be presented.

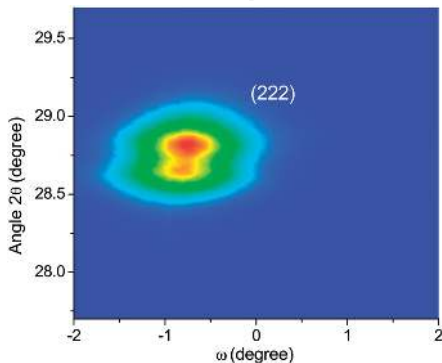


Figure 1. Reciprocal space map around the (222) reflection for the La₂Zr₂O₇ film grown on the (110)-oriented SrTiO₃ substrate

Keywords: ferroelectricity, piezoelectric force microscopy, reciprocal space mapping, pole figure

MS43-P3 Structural characterization of a [1]benzothieno [3,2-b]benzothiophene (btbt) derivative in bulk and thin films

Gabin Gbabode¹, Aurelien Blangenois¹, Philippe Négrier², Denise Mondieig³, Gérard Coquerel¹, Yves Geerts³, Michele Sferrazza⁴

1. Unité de Cristallogénèse, SMS, EA 3233, Normandie Université, Université de Rouen, 1 rue Lucien Tesnière, F-76821 Mont-Saint-Aignan, France

2. Université Bordeaux, LOMA, UMR 5798, 351 Cours de la Libération, F-33400 Talence, France

3. Laboratoire de Chimie des Polymères, Faculté des Sciences, Université Libre de Bruxelles CP206/1, Campus de la Plaine, B-1050 Brussels, Belgium

4. Département de Physique, Faculté des Sciences, Université Libre de Bruxelles CP223, Campus de la Plaine, B-1050 Brussels, Belgium

email: gabin.gbabode@univ-rouen.fr

In the past decades, particular attention has been paid onto organic molecules comprising π -conjugated moieties owing to their potential applications in the promising field of organic electronics [1]. In this framework, knowledge of the crystal packing of target molecules is of prime importance since charge transport properties are highly dependent on the structural arrangement. Furthermore, it has been demonstrated that charge transport is effectively driven by the first molecular layers close to the underlying substrate in the case of Organic Field-Effect Transistors (OFETs) [2]. Then, structural characterization studies aiming at seeking eventual polymorphism in thin films and understanding its occurrence are mandatory for a rational design of devices architecture.

In this presentation, we will show results on the polymorphism of a mono-alkylated (with an octyl chain) [1]benzothieno[3,2-b]benzothiophene molecule (hereafter called C8-BTBT) in bulk samples and thin films. Alkylated BTBT molecules are currently among the most promising candidates to be used as solution-processed air-stable high-performance organic semiconductors [3].

We proved the existence of three distinct polymorphs for C8-BTBT bulk samples, called forms I, II and III, forms I and III being observed at room temperature and form II at high temperature. The crystal structures of forms I and III have been determined from X-ray powder diffraction data and both consist in lamellar arrangement composed of bi-layers of "head-to-head" (or "tail-to-tail") stacked molecules.

Grazing incidence X-ray diffraction measurements on C8-BTBT thin films showed that the same structural arrangement is revealed in all thin films independently of film thickness and corresponds to form III observed for bulk samples, then discarding the possibility of a substrate-induced phase [4] for this compound. A tentative explanation of this result will be given in our presentation based on the crystal structure determined for form III.

References.

- [1] A. Facchetti, *Materials Today* 2007, 10, 28-37.
- [2] F. Dinelli, M. Murgia, P. Levy, M. Cavallini, F. Biscarini, D. M. de Leeuw, *Phys. Rev. Lett.* 2004, 92, 116802.
- [3] Y. Yuan, G. Giri, A. L. Ayzner, A. P. Zoombelt, S. C. B. Mannsfeld, J. Chen, D. Nordlund, M. F. Toney, J. Huang, Z. Bao, *Nat. Commun* 2014, 5, 3005-3013.

- [4] G. Gbabode, N. Dumont, F. Quist, G. Schweicher, A. Moser, P. Viville, R. Lazzaroni, Y. H. Geerts, *Adv. Mater.* 2012, 24, 658-662.

Keywords: polymorphism, thin films, grazing incidence X-ray diffraction, crystal structure determination, organic electronics.

MS43-P4 Polymorphic phases of an organic semiconductor: a combined raman and grazing incidence X-ray diffraction study

Andrew O.F. Jones^{1,2}, Benedikt Schroe¹, Michele Sferrazza², Roland Resel¹

1. Institute of Solid State Physics, Graz University of Technology, 8010 Graz, Austria

2. Département de Physique, Faculté des Sciences, Université Libre de Bruxelles, 1050 Brussels, Belgium

email: andrew.jones@tugraz.at

There is currently a great interest in solution-processable organic molecular semiconductors due to their potential to produce cheap, efficient and flexible organic devices. Polymorphism has already been observed in several molecular semiconductors, notably pentacene, and this can have an effect on the key physicals properties of these materials, such as the charge transport mobility. Understanding the structure of these systems when coated onto a gate dielectric is therefore of prime importance, especially as charge transport has been shown to primarily occur in the first molecular layers at the interface with the dielectric, meaning knowledge of the molecular arrangement in this region is essential. Excellent charge transport mobilities of up to $43 \text{ cm}^2 \text{ V}^{-1} \text{ s}^{-1}$ have been observed for solution processed films from the family of alkylated [1]benzothieno[3,2-b]benzothiophenes (BTBT),^[1] making them of importance for the future production of high performance organic devices. Here, we present structural investigations of the BTBT derivative, 2,7-dioctyloxy-BTBT ($\text{C}_{18}\text{O-BTBT-OC}_8$). Unusually, $\text{C}_{18}\text{O-BTBT-OC}_8$ shows a different polymorphic phase to that of the single crystal structure when spin-coated as a thin film (herringbone packing in films vs. layered π - π stacking in the single crystal).^[2] This type of polymorphic phase, which is only observed in thin films, is termed a substrate-induced phase (SIP) and understanding the formation and structure of such phases is an important challenge when dealing with organic semiconductor thin films. The phase behaviour of $\text{C}_{18}\text{O-BTBT-OC}_8$ in single crystals and also thin and thick films has been investigated extensively by X-ray diffraction (specular and grazing incidence), Raman spectroscopy and AFM. The temperature dependent phase behaviour is also investigated, revealing new polymorphic phases, while solvent vapour annealing and aging of the films is also shown to alter the phase which is present. The structure and origins of these different phases of an organic semiconductor with a rich polymorphic landscape will be discussed, with the implications for the control of film structure and morphology highlighted.

[1] Y. Yuan, G. Giri, A. L. Ayzner, A. P. Zoombelt, S. C. B. Mannsfeld, J. Chen, D. Nordlund, M. F. Toney, J. Huang, Z. Bao, *Nat. Commun.* **2014**, *5*, 3005.

[2] A. O. F. Jones, Y. H. Geerts, J. Karpinska, A. R. Kennedy, R. Resel, C. Röthel, C. Ruzié, O. Werzer, M.

Sferrazza, *ACS Appl. Mater. Interfaces* **2015**, *7*, 1868.

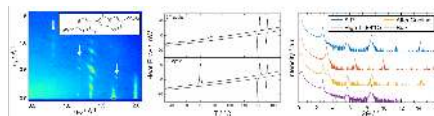


Figure 1. Left: Reciprocal space map from a film of $\text{C}_{18}\text{O-BTBT-OC}_8$ with structure inset; white arrows show peaks belonging to the bulk, other peaks correspond to the SIP. Centre: DSC measurement of bulk $\text{C}_{18}\text{O-BTBT-OC}_8$. Right: Specular X-ray diffraction of the different phases in films of $\text{C}_{18}\text{O-BTBT-OC}_8$.

Keywords: Organic semiconductors, thin films, polymorphism, substrate-induced phase.

MS43-P5 Novel *transrotational* solid state order discovered by TEM in crystallizing amorphous films

Vladimir Y. Kolosov¹

I. Ural Federal University

email: kolosov@urfu.ru

Novel microstructure with unexpected, dislocation independent, regular internal bending of the crystal lattice planes [1] are formed in thin films/layers as a result of amorphous – crystalline transitions. Such **perfect crystals/grains with regularly curved lattice** (built up by simultaneous translation and small regular rotation of the unit cell) **demonstrate a new “transrotational” [2] type of solid state order realized in thin films**. It is primarily dislocation independent and takes place round an axis lying in the film plane of the growing crystal, **Fig.1**. The maximal values correspond to essential lattice orientation gradients accumulated at the mesoscale (up to 300 degrees per μm). The main data have been obtained by diffraction transmission electron microscopy (TEM), primarily bend-contour method [3], including in situ studies, HREM. Thin films studied were prepared by laser, e-beam and thermal evaporation mostly with thickness or/and composition gradients across TEM grids (to learn these factors directly), solid state amorphization, pyrolysis.

Thin (10 - 100 nm) crystallized areas we examine vary from small crystals (0.1 - 100 μm), ribbons, whiskers or spherulites to large-scaled polycrystalline areas with a complex texture. They can be grown with the help of aging, heat treatment and local annealing by focused electron (or laser beam) in amorphous films of substances of different chemical nature including oxides, chalcogenides, some metals and alloys and are stable with years. Unlike other unusual regular nano aggregations of atoms widely recognized by the community in recent 30 years (quasi-crystals, fullerenes, nanotubes and other nano derivatives) these less known “transrotational” crystals/structures are less confined in dimensions and have much less curvature in atoms plane packing. Transrotational micro crystals have been eventually recognized/studied also by other authors in some vital thin film materials, i.e. PCMs (phase-change materials) for memory [4], silicides [5], SrTiO₃ [6].

[1] I. E. Bolotov, V. Yu. Kolosov and A. V. Kozhyn, Phys. Stat. Sol. 72a (1982), p.645.

[2] V. Yu. Kolosov and A. R. Thölen, Acta Mat. 48, (2000), p.1829.

[3] I. E. Bolotov and V. Yu. Kolosov, Phys. Stat. Sol. 69a (1982), p.85.

[4] B. J. Kooi and J. T. M. De Hosson, J. App. Phys. 95 (2004), p.4714.

[5] E. Rimini et. al., J. App. Phys. 105 (2009), p.123502.

[6] V. Longo et. al., ECS SSS Techn. 2 (2013), N120.

Funding of the Ed. & Sci. RF Ministry is acknowledged

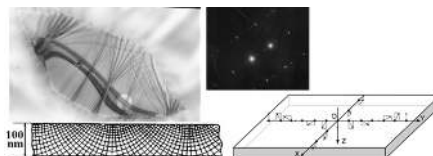


Figure 1. TEM of transrotational Se crystal (upper left) with one of the SAED patterns from the zone-axis pattern marked by 1 μm SA aperture. Schemes of internal lattice bending (lower left) shown in film cross section and regular rotation of the unit cell - 2-axes lattice bending (lower right).

Keywords: novel aperiodic crystals, electron diffraction, TEM, in situ, thin films, complex texture

MS43-P6 Characterization of Zinc Oxide thin films grown on different substratesBEATRICE G. SBARCEA¹, Carmen PARASCHIV¹, Delia PATROI¹, Virgil E. MARINESCU¹, Sorina A. MITREA¹¹. National Institute for R&D in Electrical Engineering ICPE-CA Bucharest

email: gabi_bea@yahoo.com

Al doped ZnO films were grown by Pulsed Laser Deposition. Doped ZnO films were characterized structural and optical. X-ray diffraction measurements reveal a polycrystalline structure of films and a hexagonal wurtzite crystal structure. The crystallite size for all the samples is less than 20 nm. Doped ZnO films were also characterized using Scanning Electron Microscopy and Atomic Force Microscopy. The optical transmittances of Al doped ZnO films are over 70%. Pulsed laser deposited for n-type ZnO can be applied to optoelectronic devices in order to replace the conventional ITO films.

Keywords: ZnO, X-ray diffraction, PLD**MS43-P7** Combined Analysis in 2015: XRD (Texture, Residual Stresses, Microstructure) complemented by fluorescence (XRF and GiXRF) and Electron DiffractionDaniel Chateigner¹, Luca Lutterotti², Béranger Caby³, Magali Morales⁴, Giancarlo Pepponi⁵, Olivier Pérez¹, Philippe Boullay¹, Emmanuel Nlot³¹. CRISMAT, CNRS 6508, and IUT, Univ. Caen Basse Normandie, France². Univ Trento, Italy³. LETI, CEA Grenoble, France⁴. CIMAP, Univ Caen Basse Normandie⁵. Fondazione B. Kessler, Trento, Italy

email: daniel.chateigner@ensicaen.fr

The 12-years old methodology called Combined Analysis using rays (x-rays, neutrons, electrons) has proved its efficiency in particular in treating QTA from diffraction spectra using x-rays, neutrons and electrons.

Its success concerning Quantitative Texture Analysis summarises as three main points:

- it avoids tricky data reductions and corrections, that depend on more or less uncontrolled parameters, these latter becoming fitted parameters that are then better estimated
- it solves the difficult overlapping peaks problem (intra- and interphases), with the use of an extended Rietveld approach
- it includes the determination of other important quantities, like residual stresses, crystal sizes and microstrains, structures ...

Not only Combined Analysis avoids false minima in the refinements when e.g. texture or structure is the only targeted aspect, but it also allows to benefit from anisotropies in real samples rather than to suffer for them during characterizations.

We will show on an In₂O₃/Ag/In₂O₃ stack, that Combined Analysis can be generalized to more characterization techniques. X-ray Specular Reflectivity is one of them, implemented for more than 10 years, and recently X-ray Fluorescence got incorporated, allowing another view of materials' elemental compositions, from low-angles oscillations and total fluorescence.

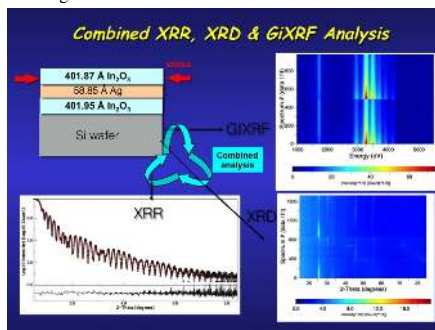


Figure 1. A XRF-GiXRF-QTA-RSA-QMA combined analysis of an In₂O₃/Ag/In₂O₃ stack

Keywords: In₂O₃ film, texture, stress, combined analysis

MS43-P8 Efficient sensing of explosives by using highly textured fluorescent nonporous films of oligophenyleneethynylene derivatives

Arie van der Lee¹, Thomas Caron², Eric Pasquier², Robert Pansu³, Vincent Rouessac¹, Simon Clavaguera², Myriam Bouhadid², Françoise Serein-Spirau⁴, Jean-Pierre Lère-Porte⁴, Pierre Montméat²

1. Institut Européen des Membranes, Montpellier, France
2. CEA-DAM Le Ripault, Monts, France
3. ENS, Cachan, France
4. Institut Charles Gerhardt, Montpellier, France

email: avderlee@univ-montp2.fr

The fluorescence of thin films of diimine-substituted phenyleneethynylene can be efficiently quenched by nitroaromatic vapors, which is not the case for the unsubstituted parent compound. Thin film porosity is usually considered to be an essential factor for efficient quenching, but in the present case the origin is completely different, as both films are non-porous and hermetic to DNT/TNT molecules. The explanation for this very efficient sensing comes from the molecular organization in the two crystallized thin films. By combining the information from single-crystal and thin film diffraction experiments it is shown that π -stacking in the structure of both the substituted and the non-substituted compound is not very pronounced, but that the orientation of the phenyleneethynylene fluorophore differs markedly with respect to the surface of the film. For the substituted compound, the fluorophore is almost parallel to the surface, thus making it readily available to molecules of a nitroaromatic quencher. This rationale is also observed in the case of a related compound bearing methoxy side chains instead of the long octyloxy moieties. Fluorescence lifetime experiments show that the efficient quenching process in the non-porous, crystallized films of the substituted compound is due to a fast (<70ps) diffusion of excitons from the bulk of the film toward its surface where they are quenched.

Keywords: thin films, explosives, diffraction, fluorescence

MS43-P9 Cathodic arc evaporation of oxide coatings: investigation of the phase transformation at the target surface and deposition of Al and Hf oxides

Antonia Neels¹, Xavier Maeder², Max Döbeli³, Alex Dommann⁴, Hans Rudigier⁵, Beno Widrig⁵, Jürgen Ramm⁵

1. Center for X-ray Analytics, Empa, Überlandstrasse 129, 8600 Dübendorf, Switzerland.
2. Laboratory for Mechanics of Materials and Nanostructures, Empa, Feuerwerkerstrasse 39, 3602 Thun, Switzerland.
3. Ion Beam Physics, ETH Zurich, Otto-Stern-Weg 5, CH-8093 Zürich, Switzerland.
4. Département 'Materials meet Life', Empa, Lerchenfeldstr. 5, CH-9014 St. Gallen, Switzerland.
5. Oerlikon Surface Solution AG, Iramali 18, LI-9496 Balzers, Liechtenstein.

email: antonia.neels@empa.ch

Reactive cathodic arc evaporation is an attractive method to produce oxide coatings for a wide variety of applications, e.g. for oxidation and chemical protective coatings, diffusion barriers, or for wear protection in tribological systems [1]. One reason for this is the possibility to control the phases and phase compositions of the synthesized oxides by the chemical composition of compound targets utilized as cathodes for the evaporation. The oxygen flow influences the evaporation rates of the cathode material as well as the conditions under which the metallic vapour condenses and reacts at the substrate surface. To control these parameters, it is necessary to understand the process related to the oxide synthesis. We are therefore active in studying the phase transformation at the target (cathode) surface after the arc process and to correlate the results with the phases obtained in the coating [2]. The example of the Al-Hf system is given in Fig. 1.

The targets were operated with and without oxygen reactive gas. The phase composition at the target surface was determined by X-ray diffraction (XRD) analyses and compared for the different process conditions. Coatings were deposited for each process parameter set utilized for surface treatment of the targets. The compositions of the layers were determined by Rutherford backscattering spectrometry. XRD was used to determine the metallic and oxide phases in the layers. A comparison of the phase composition between layers and target surface is given and the possible processes during target surface modifications are discussed. In addition, high temperature in-situ XRD measurements up to 1290°C were performed to study the process of oxide formation from intermetallic compounds in the layers [2]. As a result, the oxide coatings produced by this state-of the art reactive cathodic arc evaporation process are well suited for applications in high temperature environment, especially as oxidation and diffusion barriers.

References:

- [1] X. Maeder, M. Döbeli, A. Dommann, A. Neels, P. Polcik, R. Rachbauer, H. Rudigier, B. Widrig,

J.Ramm. *Proceeding of the 18th Plansee Seminar*, L.S. Sigl, H. Kestler and J. Wagner (Eds.), *PLANSEE SE, Tyrol/Austria*, **2013**, HM45, 1381.

[2] X. Maeder, M. Döbeli, A. Dommann, A. Neels, H. Rudigier, B. Widrig, J. Ramm. (2014) *Surface and Coatings Technology*, DOI: 10.1016/j.surfcoat.2014.07.095, in press.

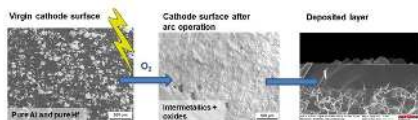


Figure 1. SEM images of a composite Al-Hf cathode surface before (left) and after the arc operation (middle) and the associated deposited layer (right).

Keywords: in-situ XRD, hard coatings, intermetallics, target processes, layers

MS43-P10 Thin film polymorphism in organic semiconductors

Basab Chattopadhyay¹, Yves H. Geerts¹

¹ Université Libre de Bruxelles (ULB), Faculté des Sciences, Laboratoire Chimie des Polymères, CP 206/1, Boulevard du Triomphe, 1050 Bruxelles, Belgium

email: Basab.Chattopadhyay@ulb.ac.be

Polymorphism is a phenomenon which is crucial to the understanding of crystal nucleation and growth, and establishment of structure–property correlation.¹ It is a phenomenon with high industrial significance particularly in pharmaceutical industry. Given the importance of polymorphism in determining the property of materials, a topic of recent interest is to study how it affects the performance of functional materials in the field of organic electronics. Although, presence of several polymorphic forms facilitates the study of charge-transport behaviour with respect to crystal packing, it may hinder the reproducibility, reliability, and stability of the devices fabricated using such materials. Research is being carried out to identify specific polymorphic phases of organic thin films, where the polymorphism exists near the substrate.² Depending on film thickness, deposition methodologies, temperature etc, a particular phase may exist. Under certain circumstances it may be possible to induce transformation from one phase to another. The physical and chemical factors that drive such a process are not yet clearly understood. Hence, it is of utmost importance to identify the phases and to control the formation of the different forms. In particular, this is really crucial in the field of organic electronics, where the charge-transport properties are highly dependent on crystal packing, especially for organic field-effect transistors where charge transport occurs at the interface between the organic semiconductor and the dielectric. In this presentation, we present an overview of the recent advances done in our group in this topic. Especially, [1]benzothieno[3,2-b][1]benzothiophene (**BTBT**) based semiconductors which are gradually emerging as the most promising organic semiconductor are the principal objects of our study. Structural and morphological studies of library of BTBT-based compounds are presented to gain more insights into the phenomenon.

[1] Bernstein, J. *Polymorphism – a Perspective. Cryst. Growth Des.* 2011, 11, 632–650.

[2] S. T. Salammal, J.-Y. Balandier, J.-B. Arlin, Y. Olivier, V. Lemaire, L. Wang, D. Beljonne, J. Cornil, A. R. Kennedy, Y. H. Geerts, B. Chattopadhyay, *The Journal of Physical Chemistry C*, 2014, 118, 657–669; Moser, A.; Salzmann, I.; Oehzelt, M.; Neuhold, A.; Flesch, H.-G.; Ivanco, J.; Pop, S.; Toader, T.; Zahn, D. R. T.; Smilgies, D.-M.; et al. *Chem. Phys. Lett.* 2013, 574, 51–55.

Keywords: Polymorphism, Thin Films, X-ray diffraction,

MS43-P11 Structure characterization of lattice-matched rutile and TiO₂-II phases grown by atomic layer deposition on α -Al₂O₃(0 0 1)

Kristel Möldre¹, Hugo Mändar¹, Lauri Aarik¹, Aivar Tarre¹, Jaan Aarik¹

¹. Institute of physics, University of Tartu, Ravila 14c, 50411, Tartu, Estonia

email: kristel.moldre@ut.ee

Atomic layer deposition of TiO₂ from TiCl₄ and ozone on single crystal α -Al₂O₃(0 0 1) substrates was investigated. The structure of films was characterized using X-ray reflection (XRR) and X-ray diffraction (XRD) in high resolution (HR), in-plane (IP) and reciprocal space mapping (RSM) modes.

HR-XRD θ -2 θ diffraction patterns of the films deposited on c-sapphire at 400–600°C, showed two reflections together with their Pendellösung fringes, which implied that (1 0 0)-oriented high-pressure TiO₂-II or strained rutile was formed. X-ray crystallite sizes in direction of surface normal, determined from boardening analysis of the reflections were comparable to the film thicknesses (XRR) at $T_G \geq 400^\circ\text{C}$.

IP-XRD analysis revealed that at 400–600°C both rutile and TiO₂-II were epitaxially grown in the films with epitaxial relationships of $[0\ 1\ 0]_R/[1\ 0\ 0]_S$ and $[0\ 0\ 1]_R/[1\ 2\ 0]_S$ for rutile and sapphire, and $[0\ 0\ 1]_R/[1\ 0\ 0]_S$ and $[0\ -1\ 0]_R/[1\ 2\ 0]_S$ for TiO₂-II and sapphire. It is worth noting that the $(0\ 0\ 1)_R/(0\ 1\ 0)_R$ in-plane relationship for rutile and TiO₂-II in our films differed from the $(0\ 0\ 1)_R/(0\ 1\ 1)_R$ relationship reported earlier for TiO₂-II and rutile in a natural form of TiO₂ [1].

Lattice parameters were determined by IP-XRD analysis of reflections 0 2 0, 0 0 2 of TiO₂-II and 0 1 1 of rutile and by RSM of reflection 3 1 1 of TiO₂-II and reflections 3 1 0 and 3 0 1 of rutile. The parameters of TiO₂-II were $a_H = 0.4531 \pm 0.0002$ nm, $b_H = 0.546 \pm 0.003$ nm and $c_H = 0.482 \pm 0.006$ nm while those of rutile equaled to $a_R = 0.4531 \pm 0.0002$ nm, $b_R = 0.475 \pm 0.006$ nm and $c_R = 0.29 \pm 0.01$ nm. According to these results the crystallites with TiO₂-II and highly strained rutile structures were evidently lattice-matched to each other in the films. Comparison of the in-plane atomic arrangements in 2D unit cells of α -Al₂O₃(0 0 1), rutile (1 0 0) and TiO₂-II (1 0 0) (Fig. 1) demonstrated relatively good lattice match explaining the epitaxial growth observed in our experiments.

From boardening analysis of reflections 1 1 0 and 1 1 1 for TiO₂-II and 1 1 0, 1 0 1, 3 0 1 for rutile the in-plane X-ray crystallite sizes were estimated to be 4.0 nm for TiO₂-II and 3.6 nm for rutile.

[1] D.W. Meng, X.L. Wu, F. Sun, L.W. Huang, F. Liu, Y.J. Han, J.P. Zheng, X. Meng, R. Mason, High-pressure polymorphic transformation of rutile to α -PbO₂-type TiO₂ at $\{0\ 1\ 1\}_R$ twin boundaries, *Micron* 39 (2008) 280–286.

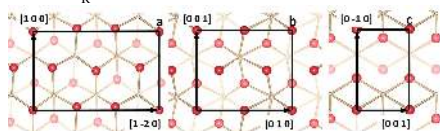


Figure 1. Structure models of in-plane unit cells and atomic arrangements for (a) α -Al₂O₃(0 0 1), (b) TiO₂-II(1 0 0) and (c) rutile(1 0 0) atomic planes. Large spheres designate positions of oxygen and small spheres show location of Al or Ti. Labels at arrows show crystallographic directions.

Keywords: Titanium Dioxide, Thin Films, Atomic Layer Deposition, Crystal Structure, Epitaxy, TiO₂-II, Rutile

MS43-P12 Also disorder can improve thin film transistor performance

Laura Ferlauto¹, Fabiola Liscio¹, Emanuele Orgiu², Norberto Masciocchi³, Antonietta Guagliardi⁴, Fabio Biscarini⁵, Paolo Samori², Silvia Milita¹

1. Istituto di Microelettronica e Microsistemi (IMM)-CNR, via Piero Gobetti 101, I-40129, Bologna, Italy
2. ISIS & icFRC, Université de Strasbourg & CNRS, 8 allée Gaspard Monge 67000, Strasbourg, France
3. Dip. Scienza e Alta Tecnologia, Università dell'Insubria & To.Sca.Lab, via Valleggio 11, I-22100 Como, Italy
4. Istituto di Cristallografia-CNR & To.Sca.Lab, via Lucini 3, I-22100 Como, Italy
5. Dip. Scienze della Vita, Università di Modena e Reggio Emilia, via Campi 183, 41125, Modena, Italy

email: ferlauto@bo.imm.cnr.it

The relentless progress in Organic Electronics has catalyzed the attention to the design of novel materials combining structural and functional complexity. Despite this, the development of highly performing solution processed n-type Organic Field-Effect Transistors is still a great challenge due to the difficulty of achieving high solubility and good air stability without undermining electrical properties. Among n-type organic semiconductors, perylene alkyldiimide derivatives have demonstrated good electrical performance as well as excellent processability and air stability. In particular, the functionalization of the perylene core by means of cyano-groups increases the ambient stability by lowering the energy of the lowest unoccupied molecular orbital, while the presence of alkyl chains enhances the solubility of the molecules by decreasing the core planarity. Since the introduction of side chains also affects the self-assembly at the supramolecular level and consequently also the efficiency of charge transport in the material, a cautious design which aims to optimize the intermolecular interactions between π -conjugated molecules must be implemented. This study emphasizes how the introduction of molecular disorder can be the key for enhanced transport properties once the devices are treated via thermal annealing. In this work we report a multiscale structural analysis performed by X-ray diffraction, X-ray reflectivity and atomic force microscopy on thin-films of dicyanoperylene molecules decorated with either linear or asymmetric branched alkyl-side chains. The synthesis of the branched species leads to the formation of a mixture of four “distinct” stereoisomers, two RR/SS and RS/SR enantiomeric pairs. This conformational disorder not only increases the material solubility and makes the crystallization process more difficult with respect to the case of molecules with linear side-chains, but also favors the 2D-growth mode. Optimized post-deposition thermal annealing leads then to a structural transition towards the bulk-phase for molecules exposing branched chains, still preserving the 2D morphology and improving the transport properties of thin-film devices. These findings suggest that the synthesis of highly processable molecules capable of undergoing strong supramolecular rearrangement during optimized classical post-growth processes can be more efficient than improving the charge carrier mobility at the expense of solubility.

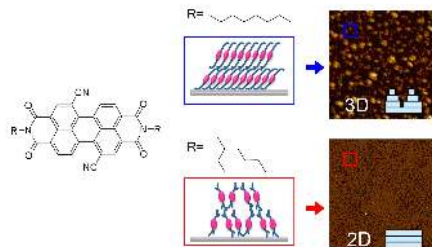


Figure 1. Chemical formula, sketch of molecular self-assembly and AFM images of the two perylene di-imide isomers.

Keywords: organic field-effect transistors, organic thin films, X-ray diffraction, perylene derivatives

MS43-P13 Changes of the molecular structure in organic thin film transistors during operation

Fabiola Liscio¹, Laura Ferlauto¹, Micaela Matta², Rafael Pfattner³, Mauro Murgia⁴, Conceptio Rovira⁵, Marta Mas-Torrent⁵, Francesco Zerbetto², Silvia Milita¹, Fabio Biscarini⁵

1. CNR - IMM Sezione di Bologna, Via P. Gobetti 101, 40129 Bologna, Italy
2. Dip. di Chimica "G. Ciamician", Università di Bologna, 40126 Bologna, Italy
3. Institut de Ciència de Materials de Barcelona (ICMAB-CSIC) and Networking Research Center on Bioengineering, Biomaterials and Nanomedicine (CIBER-BBN), 08193 Bellaterra, Spain
4. CNR - ISMN Sezione di Bologna, Via P. Gobetti 101, 40129 Bologna, Italy
5. Dip. Scienze della Vita, Università di Modena e Reggio Emilia, 41125 Modena, Italy

email: liscio@bo.imm.cnr.it

Thin film of organic semiconductors have been widely studied at different length scales, for improving the electrical response of devices based on them. Up to now, a lot of knowledge has been gained about how molecular packing, morphology, grain boundaries and defects affect the charge transport in Organic Field Effect Transistors (OFETs) [1-3]. However, in real application, the impact of an electric field on the organic semiconductor and thus the transport parameters needs to be taken into account in order to develop high-performance organic device. Here, we present for the first time the structural evolution of pentacene thin film observed during the OFET operation. This investigation was achieved by performing X-Ray Diffraction measurements, both in out-of-plane and grazing incidence geometries, in real time, i.e. during the application of drain-source (V_{DS}) and gate (V_G) voltages. In particular, Selected Bragg reflections characteristic of the lattice planes perpendicular and parallel to the dielectric surface were monitored during OFET operation. The effect of V_{GS} on the pentacene crystal structure was calculated by Molecular Dynamics and Density Functional Theory simulations. The interplay between the calculated changes of the structure and the experimental results provide an understanding of the structural evolution of operating transistors. The transversal field induces a slight change of orientation of the molecules within the crystalline domains, whereas it may be more relevant for a small fraction of molecules located at the grain boundaries or nearby whose re-orientation is substantial and leads to a significant energetic lowering of the charges. This implies that the re-oriented molecules at grain boundaries might act as shallow traps for charge carriers, opening a new unexplored route for understanding the relationship between structure and electrical properties of OFET devices.

[1] A. Shehu, S. D. Quiroga, P. D'Angelo, et al., *Phys. Rev. Lett.* **2010**, *104*, 246602

[2] J. Rivnay, L. H. Jimison, J. E. Northrup et al. *Nat. Materials* **2009**, *8*, 952

[3] F. Liscio, C. Albonetti, K. Broche et al., *ACS Nano*, **2013**, *7*, 1257

Keywords: real time X-ray diffraction, lattice strain, organic field-effect transistors, bias stress, pentacene

MS44. New applications of old algorithms in crystallography

Chairs: George Sheldrick, Isabel Uson

MS44-P1 Macromolecular diffraction data: Maximum entropy Patterson calculation used to estimate unobserved data

Anders Kadziola¹

1. Department of Chemistry, University of Copenhagen

email: kadziola@chem.ku.dk

The principle of maximum entropy has been applied to the Patterson function. Patterson functions are used in classical molecular replacement rotation functions as Patterson overlap functions. Larger portions of reciprocal space with unobserved data are likely to introduce serious errors in such overlap function calculations. Inclusion of maximum entropy estimates for missing intensities are shown to reduce these errors considerably. As a prior in the maximum entropy calculation, a Fourier transform of a parameterized fit to the average intensity as a function of resolution is used. The calculations are fully CCP4-compatible, reading and writing the mtz- and map-file format.

Keywords: maximum entropy, Patterson, molecular replacement

MS44-P2 The use of your model to assess the features of a diffraction patternDavid Rae¹¹. Research School of Chemistry, The Australian National University, Canberra, ACT 2601, Australia

email: rae@rsc.anu.edu.au

The model for the diffraction pattern of a crystal structure tries to describe intensities at various points \mathbf{h} in reciprocal space. Any particular quantum sees a phased quantity $\sum_n a_n(\mathbf{h}) F_n(\mathbf{h})$ where the $a_n(\mathbf{h})$ are complex and the $F_n(\mathbf{h})$ are real. The observed intensity $I(\mathbf{h}) = Y_{\text{obs}}(\mathbf{h})^2$ is then an averaged quantity

$$Y_{\text{obs}}(\mathbf{h})^2 = \sum_{m,n} F_m(\mathbf{h}) F_n(\mathbf{h}) \langle a_m(\mathbf{h}) a_n(\mathbf{h})^* \rangle / 2 = \sum_{m,n} g_{mn}(\mathbf{h}) F_m(\mathbf{h}) F_n(\mathbf{h}).$$

A count of $n(\mathbf{h}) \pm \sqrt{n(\mathbf{h})}$ associated with $Y_{\text{obs}}(\mathbf{h})^2$ corresponds to $\sqrt{n(\mathbf{h})} \pm 1/2$ associated with $Y_{\text{obs}}(\mathbf{h})$. $Y_{\text{obs}}(\mathbf{h})$ can be described as a vector $\mathbf{Y}(\mathbf{h})$ in an M dimensional space with the same variance in any direction.

$\mathbf{Y}(\mathbf{h}) = \sum_n \sqrt{g_{nn}(\mathbf{h})} F_n(\mathbf{h}) \mathbf{i}_n$ where $\mathbf{i}_m \cdot \mathbf{i}_n = g_{mn}(\mathbf{h}) / \sqrt{[g_{mm}(\mathbf{h}) g_{nn}(\mathbf{h})]}$ so that $\mathbf{i}_m \cdot \mathbf{i}_m = \mathbf{i}_n \cdot \mathbf{i}_n = 1$.

The angle between \mathbf{i}_m and $\mathbf{Y}(\mathbf{h})$ is given by $\cos(\epsilon_m(\mathbf{h})) = \sum_n g_{mn}(\mathbf{h}) F_n(\mathbf{h}) / [Y(\mathbf{h}) \sqrt{g_{mm}(\mathbf{h})}]$.

Least squares refinement evaluates change in the direction of an initial model $\mathbf{Y}_{\text{calc}}(\mathbf{h})$ that is assumed to be the direction of $\mathbf{Y}_{\text{obs}}(\mathbf{h})$. The expressions for $g_{mn}(\mathbf{h})$ can be chosen so that stacking faults, twins and allo twins are simply special cases of a more general description, ie one where the crystal is not the same everywhere. The fraction of $Y_{\text{obs}}(\mathbf{h})^2$ associated with $\sqrt{g_{mm}(\mathbf{h})} F_m(\mathbf{h})$ is then $\cos^2(\epsilon_m(\mathbf{h}))$ with an associated partial residual $\cos(\epsilon_m(\mathbf{h})) [Y_{\text{obs}}(\mathbf{h}) - Y_{\text{calc}}(\mathbf{h})] \cdot \mathbf{i}_m$.

The variance of $\mathbf{Y}_{\text{calc}}(\mathbf{h})$ can also be evaluated in terms of known or assumed variances and covariances of the parameters describing the model. Thus partial observations of variables can also be obtained [1]. The least squares refinement of the parameters describing the $g_{mn}(\mathbf{h})$ can be separated from the refinement of the parameters describing the $F(\mathbf{h})$. Peak positions and profiles are associated with changes in the $g_{mn}(\mathbf{h})$ for the same $F_m(\mathbf{h})$ and $F_n(\mathbf{h})$. There is thus an implicit merging of $F_m(\mathbf{h})$ values with an associated best least squares value, variance and effective partial observation coefficient $\langle \cos^2(\epsilon_m(\mathbf{h})) \rangle$.

The background is part of the model of any intensity or linear combination of intensities and intensity data should have sufficient information for this to be known. The evaluation of the statistics for components of observations should assist the identification of sources of systematic error.

References

Rae, A.D., (2013) "The use of partial observations, partial models, and partial residuals to improve the least squares refinement of crystal structures", *Crystallography Reviews*, Vol. 20, 155-229, Taylor & Francis.

Keywords: partial observations, least squares, error distribution

MS44-P3 Speeding up accurate scattering factors calculation for macromolecules. Algorithms for aspherical atom formalism and direct summationMichał L. Chodkiewicz¹, Paulina M. Dominiak¹, Anna Makal¹, Szymon Migacz², Witold R. Rudnicki^{2,3}, Krzysztof Woźniak¹¹. Biological and Chemical Research Centre, Chemistry Department, University of Warsaw, Żwirki i Wigury 101, 02-089 Warszawa, Poland². Interdisciplinary Centre for Mathematical and Computational Modelling, University of Warsaw, Pawińskiego 5A, 02-106 Warsaw, Poland.³. Department of Bioinformatics, University of Białystok, Ciołkowskiego 1M, 15-245 Białystok, Poland.

email: mchodkiewicz@chem.uw.edu.pl

The most popular method of calculation of scattering factors (SF) for macromolecules is based on fast Fourier transform (FFT) of dynamic electron density of spherical atoms. With increasing number of high resolution data for large molecular systems a need for efficient implementation of more accurate methods of SF calculation emerges. We have developed a code combining improved description of atomic electron densities via aspherical atom model with accurate calculation of Fourier transform via direct summation. Such a combination can result in relatively slow calculation of SF. Therefore we have proposed few algorithms facilitating efficient calculation of SF. Some of them apply also for spherical atom model. The influence of the developments on execution time is discussed for model macromolecules. University at Buffalo Pseudoatom Databank (UBDB) [1] was used for parameterization of aspherical atom model.

[1] Jarzemska, K. N. & Dominiak, P. M. (2012) *Acta Cryst.* A68, 139-147.

Keywords: scattering factors, aspherical atom, pseudoatom databank

MS44-P4 Cross-correlation functions used for structure determination from powder patterns – Method development and application scenarios

Stefan Habermehl¹, Lea Totzauer¹, Philipp Mörschel¹, Pierre Eisenbrandt¹, Martin U. Schmidt¹

1. Goethe University, Frankfurt am Main, Germany

email: habermehl@chemie.uni-frankfurt.de

A new method for the determination of organic crystal structures from powder diffraction data has been developed and implemented in the program FIDEL (Fit with DEviating Lattice parameters) [1]. The approach taken relies on a robust fitting algorithm, which uses the normalized integral of a weighted cross-correlation function for the comparison of powder patterns. This generalized similarity measure, originally introduced by de Gelder *et. al* [2] has been successfully deployed for fitting, clustering and comparison of crystal structures. The lattice parameters, molecular position, molecular orientation and selected intramolecular degrees of freedom of a start structure are fitted to the powder pattern in a robust and scalable procedure that is suited both for visibly strongly deviating structure models and experimental patterns of very low quality. This allows for a wide range of highly automated applications:

- 1) Testing the similarity of powder patterns and crystal structures with different space group settings
- 2) Preprocessor for Rietveld refinements starting with significantly deviating structural models, e.g. from (a) structure data of an isostructural chemical derivative; (b) structure data of an isostructural hydrate or solvate; (c) structure data from measurements at another temperature. FIDEL includes capabilities for an automatic Rietveld refinement sequence using the program TOPAS [3].
- 3) Automated clustering and screening of large numbers of possible structure candidates. This has been demonstrated using the results from crystal structure predictions based on lattice-energy minimizations by force-field methods.
- 4) Structure determination from unindexed powder patterns from scratch using an iterative fitting procedure in various space groups based on a Monte Carlo approach. The method can even be applied to powder patterns of disordered structures or non-phase-pure samples providing best matching structural candidates for further analysis.

[1] S. Habermehl, P. Mörschel, P. Eisenbrandt, S.M. Hammer, M.U. Schmidt, *Acta Cryst.* **2014**, B70, 347-359.

[2] R. de Gelder, R. Wehrens, J.A. Hageman, *J. Comput. Chem.* **2001**, 22, 273-289.

[3] A.A. Coelho, *TOPAS-Academic, Version 4.1*, **2007**, Coelho Software, Brisbane, Australia.

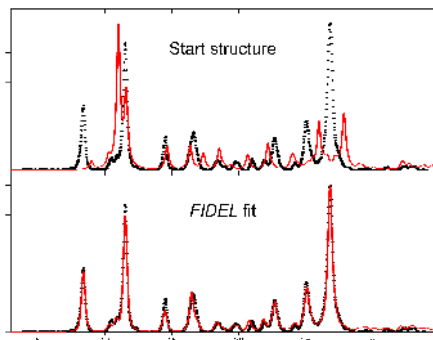


Figure 1. Background corrected X-ray powder diagram of Pigment Yellow 14 (dots) and simulated diagrams (red lines) of a strongly deviating structural model (a) before optimization with FIDEL, (b) after optimization with FIDEL.

Keywords: cross-correlation functions, similarity measure, crystal structure fitting, SDPD, powder diffraction, organic compounds

MS45. Chemical information as prior knowledge in crystallography

Chairs: Anthony Linden, Rob Nicholls

MS45-P1 X-ray origins: protection or paranoia?

Natalie Johnson¹, Michael R. Probert¹

¹. School of Chemistry, Bedson Building, Newcastle University, Newcastle upon Tyne, NE1 7RU, UK

email: N.Johnson5@newcastle.ac.uk

Deliberate fabrication of crystallographic data has previously led to falsified structures being published and then later retracted from respected scientific journals¹⁻³. Identified perpetrators, in these cases, had made very simple modifications to structural files, such as manually changing unit cell sizes and atom types, to produce adjusted data. Fortunately they were found to be unable to produce raw experimental data to support their claims. Kroon-Batenburg and Helliwell⁴ proposed that the requirement for the deposition of raw crystallographic data may be a potential method of preventing the submission of counterfeit structures. However we can show that the recreation of raw diffraction images is no longer difficult, opening the doors for those less scrupulous to take advantage, if this is not already occurring!

Detector frame formats from many manufacturers are well documented and this information can be reverse-engineered to encode synthetic diffraction data. This process was brought to light as a product of research into optimising data collection parameters for charge density studies. The chosen method required us to produce an algorithm which takes data from integrated *.raw* files as a starting point to create replicas of experimental images. A simple misuse of this code could take structure factors calculated for an entirely fabricated compound and produce diffraction images that, when processed, return the artificial structure. The frames are not visually distinguishable from authentic, experimentally determined, ones and can be fully integrated using standard protocols. The authors find this situation potentially alarming and requiring immediate attention.

A structure refined from data processed from these artificial diffraction images pass all IUCr checkCIF⁵ protocols without raising alerts. We will present such a structure, full details of the algorithms employed and propose methodologies that may safeguard against this approach going undetected.

References

1. T. Liu et al., *Acta Crystallogr., Sect. E: Struct. Rep. Online*, 2010, **66**, e13-e14.

2. H. Zhong et al., *Acta Crystallogr., Sect. E: Struct. Rep. Online*, 2010, **66**, e11-e12.

3. International Union of Crystallography, *Acta Crystallogr., Sect. D: Biol. Crystallogr.*, 2010, **66**, 222.

4. L.M. Kroon-Batenburg, J. R. Helliwell, *Acta Crystallogr., Sect. D: Biol. Crystallogr.*, 2014, **70**, 2502-2509.

5. A. L. Spek, *Acta Crystallogr., Sect. D: Biol. Crystallogr.*, 2009, **65**, 148-155

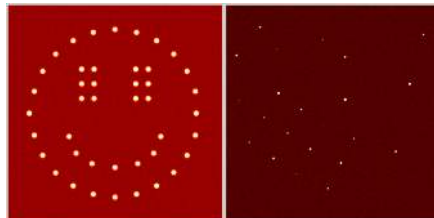


Figure 1. Two diffraction images - which is real?

Keywords: Data, Simulation, Software,

MS47. History of crystallography and ECA

Chairs: Sine Larsen, Howard Flack

MS47-P1 Finding your place in the world – using the CSD to benchmark your research

Amy A. Sarjeant¹, Seth Wiggin¹, Suzanna C. Ward¹, Peter A. Wood¹, Colin R. Groom¹

¹. Cambridge Crystallographic Data Centre, Cambridge, United Kingdom

email: sarjeant@ccdc.cam.ac.uk

All researchers hope to leave a mark on the world with their work. Everyone wants his or her latest opus to be ground breaking, record setting or expectation shattering. If one is lucky enough to hit upon such a success, what happens when it is published into the common consciousness? Does it rise meteorically to the headlines and covers of every journal only to burn out a few years later, or does it become a staple of research projects for years to come? The vast archive that is the Cambridge Structural Database can help us track molecular and structural phenomena, giving us a sense of perspective on when our research darlings were born, and how the work surrounding them has evolved over time. In addition, we can map our current favorites against older trends to judge where we are in the research cycle. Here we take a look through the CSD, charting the course of “famous” molecules such as fullerenes and metallocenes from initial structure determinations to the latest reports. We then compare these trends against current hot topics such as the ubiquitous Metal–Organic Frameworks. Do the trends suggest we are at the zenith of this research, or do they point to many fruitful years in the future?

Keywords: databases, crystallography, publications

MS47-P2 Kathleen Lonsdale & Helen Megaw

Mike Glazer¹

¹. Clarendon Laboratory, Parks Road, University of Oxford, OX1 3PU, UK

email: glazer@physics.ox.ac.uk

In this talk I shall give a brief description of the work and personalities of two famous female crystallographers, Professor Dame Kathleen Lonsdale and Dr. Helen Megaw, both of whom have influenced my own career. Kathleen Lonsdale was trained as a physicist originally but became a Professor in the Department of Chemistry at University College London. Her last two research students were myself and Howard Flack. Helen Megaw worked in the Cavendish Laboratory, Cambridge, where I was her last postdoctoral assistant.



Figure 1. Kathleen Lonsdale and Helen Megaw

Keywords: Lonsdale, Megaw

MS48. Teaching and outreach of crystallography

Chairs: Krešimir Molčanov, Bart Kahr

MS48-P1 Olex2 and IYCr OpenLabs

Horst Puschmann¹, Oleg Dolomanov¹

1. Durham University, South Road, Durham, DH1 3LE, UK

email: horst.puschmann@gmail.com

Olex2[1,2] is a powerful crystallographic package that combines ease-of-use with the powerful tools required for mastering even the most demanding tasks in small-molecule crystallography.

Interested students and novices can achieve remarkable results with a minimum amount of prior knowledge, while more experienced crystallographer will find many tools that make working with structures intuitive and efficient.

This combination leads to the ideal teaching package, where the focus of crystallographic teaching is naturally shifting away from a particular (and often peculiar!) syntax towards a deeper understanding of the underlying principles of crystallographic model building and refinement.

While novices can focus on the actual crystallography at hand, instructors and those with prior crystallographic experience can equally embark on a learning journey: time has not stood still and exciting and developments in the area of small-molecule software is actively happening.

Olex2 has been used extensively in three teaching events during the Open Labs that were organised during the IYCr: Remotely in Buenos Aires (Argentina) and in person in Izmir (Turkey) and Hong Kong. This contribution will draw on the experiences at these Open Labs and reach the conclusion that has been reached by almost all of the participants: Small-Molecule Crystallography is an exciting area for everyone to get involved in – and one that is no longer firmly in the hand of dedicated structural analysts.

[1] **OLEX2**: a complete structure solution, refinement and analysis program, *J. Appl. Cryst.* (2009), 42, 339-341.

[2] The anatomy of a comprehensive constrained, restrained refinement program for the modern computing environment - Olex2 dissected, *Acta Cryst.* (2015). A71

Keywords: small-molecule, refinement, model, teaching, solution, analysis

MS48-P2 The Nosy Monster and the Carbon Stars. Teaching crystallography through children's literature

Laura Rocas¹, Jessica Gómez Álvarez², Santiago García-Granda¹

1. Department of Physical and Analytical Chemistry, University of Oviedo - F.UO - CINN, Spain

2. Háblame Bajito, www.hablamebajito.com, Spain

email: laura.uniovi@gmail.com

The University of Oviedo has been actively involved in several crystallography outreach activities during the last few years, particularly last year in connection with the IYCr2014, and some successful projects are being developed to make crystallography close to the public [1]. In this contribution we will introduce one of these activities: *The Nosy Monster and the Carbon Stars* [2]. A story about particles, matter and crystals, created for children (age from 4 to 8 approximately). The main objective of this project is to show the beauty of crystals and to integrate some crystallography concepts in the absorbent mind of the youngest children.

Recent trends in education have focused on an integrated curriculum. Children learn best when subject matter is meaningful and useful, and when it is integrated with other areas of the curriculum such as reading, hands-on experimentation or maths. This includes reading or listening to any kind of story. Regarding science, this is specially true. Moreover, knowledge acquisition is even more reinforced when an inquiry-based, discovery-focused approach is used. In this sense, literature is a great tool to transmit knowledge to children.

The Nosy Monster and the Carbon Stars is an illustrated book (hardcover, 23x23 cm, 34 pages). A digital edition of the book, both in English and Spanish, is being distributed free of charge [2]. The book can be used in a classroom or at home to introduce the following basic concepts to children: i) Matter is made of particles; ii) Crystals are built up of perfectly ordered particles; iii) Different arrangement of these particles lead to different kind of crystals with distinct properties. The story with not only introduce a topic, but it will hook listeners and serve to demonstrate abstract ideas. It is ideal to use it to lead off a hands on activity about matter and crystals.

"Mati is a monster but, above all, he is a child, and as a child he's got an inner world which is full of curiosity and color. When he asks his mum what monsters are made of, his mum goes back to the Big Bang to explain him that everything we know comes from the same place, including carbon, of which diamonds, coal, pencils and even us are made!"

Acknowledgements: Financial support from Ministerio de Economía y Competitividad de España (FCT-14-8647 and MAT2013-40950-R)

[1] Acta Cryst. (2011) A67, C803-C804; Acta Cryst. (2013). A69, s253-s254; Acta Cryst. (2014). A70, C1300.

[2] <http://elmonstruocurioso.org>

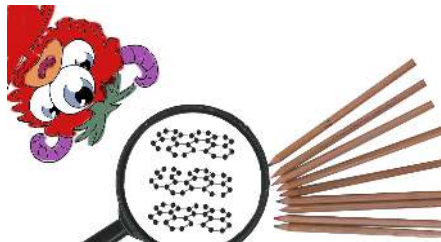


Figure 1. The Nosy Monster and the Carbon Stars - Graphite

Keywords: Crystallography for children, outreach, carbon crystals

MS48-P3 Growing crystals - lighting up dreams - crystal growing competition in Vietnam

Ngan Nguyen Bich¹, Luc Van Meervelt²

1. Chemistry Department, Hanoi National University of Education (HNUE), Vietnam

2. Chemistry Department, KU Leuven, Belgium

email: ngannb@hnue.edu.vn

In the framework of the project “**A joint structural research on platinum(II) complexes for antitumor activity and elaboration of the framework for training in crystallography**”, funded by VLIR-UOS in Belgium, single crystal crystallography has been introduced at the Chemistry Department of HNUE in Vietnam. On the other hand, the first edition of a Crystal Growing Competition was organized in Vietnam in 2014. When announced many participants, varying from undergraduate students to high school students were very motivated to grow their own crystals.

Initially, students from a few high schools in Hanoi and the Chemistry Department (HNUE) were selected to participate at this first edition. However, members of some Scientific Clubs also asked to attend the competition, and finally more than 100 student groups were registered. Packages with starting material and description of the procedure how to grow a single crystal were delivered to each group. Alum and copper sulfate were used as materials for crystallization.

The final results were evaluated by the organizers as very positive (Figure 1). An official prize awarding ceremony took place in December 2014. Also a video showing the process of the crystal growth was submitted by one of the participating groups illustrating their motivation and enthusiasm.

A small poll among participants illustrated that the students appreciated the new skills they acquired during the competition and showed the need for a next edition. One of the participants has written a news item at the website of her high school and referred to the competition as “*Growing Crystals – Lighting up Dreams*”. This turns out to be the slogan of the 2015 edition of the Crystal Growing Competition in Vietnam, which is now integrated in the IUCr Crystal Growing Competition 2015.

Acknowledgement: We would like to thank VLIR-UOS (project ZEIN2014Z182), IUCr, KU Leuven and HNUE for supporting the Crystal Growing Competition in Vietnam.

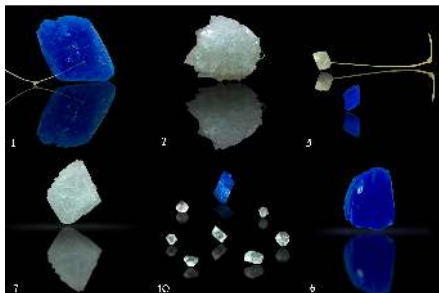


Figure 1. Selected crystals of alum and copper sulfate submitted to the Crystal Growing Competition in Vietnam, edition 2014

Keywords: Crystal growing competition, Vietnam.

MS50. Cultural and historical aspects of crystallography

Chairs: Aleksandar Višnjevac, Petr Bezdička

MS50-P1 Naturally irradiated fluorite as a historic violet pigment: X-ray diffraction and Raman spectroscopic study

Petr Bezdička^{1,2}, Zdeňka Čermáková^{1,2}, Ivan Němec³, Janka Hradilová¹, David Hradil^{1,2}

1. Academy of Fine Arts in Prague, ALMA laboratory, U Akademie 4, 170 22 Prague 7, Czech Republic

2. Institute of Inorganic Chemistry of the ASCR, v.v.i., ALMA laboratory, 250 68 Husinec - Řež, Czech Republic

3. Department of Inorganic Chemistry, Faculty of Science, Charles University in Prague, Hlavova 8, 128 00 Prague 2, Czech Republic

email: petrb@iic.cas.cz

Naturally irradiated violet fluorite, a cubic CaF_2 mineral, is a rare historic pigment. Its documented usage in Europe stretches from ca. 1450 to ca. 1550. The intensely coloured violetish black naturally irradiated fluorite is commonly called antozonite, which is only vaguely defined based on its dark colour and specific odour emanated during grinding. In the published literature, there have been some discrepancies about its physico - chemical properties. Therefore, sixteen samples of antozonite were analysed by X-ray powder diffraction in transmission mode and Raman (micro-) spectroscopy using five different excitation laser wavelengths (445, 532, 633, 780 and 1064 nm).

The structural damage of antozonite samples has been assessed by X-ray diffraction and related to their lightness using analysis of image histograms. The XRD study confirmed that the structural disorder caused by natural irradiation may be expressed by broadening of its diffraction lines. The higher is their full-width half-maxima, the lower is the sample's lightness. On the other hand, the reported increase of antozonite's unit cell parameter (and the unit cell volume) is not so straightforward. The studied antozonite samples did not exhibit positive correlation of the parameter and the observed increase of the FWHMs. Still, the sample with the highest full-width half-maxima had also one of the highest values of the unit cell parameter.

Raman spectroscopy revealed specific bands located below 500 cm^{-1} probably related to radiation-caused defects. Their intensity increased with increasing violet colour saturation, thus providing a specification for antozonite's definition. Spectra excited at 445 and 780 nm contained also numerous broad bands above 500 cm^{-1} , which seem to be caused by the presence of rare earth elements.

The obtained results have been applied in the analysis of micro-samples of a Late Gothic altarpiece located in an Italian Court in UNESCO city Kutná Hora, Czech

Republic, which contained exceptionally large grains of deep violet fluorite identified as antozonite.

Keywords: Antozonite, Fluorite, X-ray powder diffraction, Raman spectroscopy

MS50-P2 Pattern zoo part I: on the choices and number of asymmetric units for the 17 plane groups

Manfred Wildner¹

¹. Institut für Mineralogie und Kristallographie, Universität Wien, Althanstr. 14, A-1090 Wien, Austria

email: manfred.wildner@univie.ac.at

The 17 plane groups (PGs, often better known as ‘wallpaper groups’) and related periodic tilings and patterns played – and still play – an important role in arts and cultural history over the centuries. Even in palaeolithic caves, simple patterns and grids (probably for testing pigments) have been found along with the famous cave paintings. Starting with Kepler’s *Harmonice Mundi* from 1619, they also form an outstanding object of vivid interdisciplinary research, mainly concentrated in the mathematical sciences.

A basic concept of PGs and tilings is the asymmetric unit (ASU) (or ‘fundamental domain’, ‘generating region’). According to the *International Tables Vol. A*, “An asymmetric unit ... is a (simply connected) smallest closed part ... from which, by application of all symmetry operations ..., the whole of space is filled”. It is clear that – except in four PGs – the choice of the ASU, and hence the generated tiling, is not unique. Although this fact is often mentioned in literature, there seem to exist no published enumerations of possible ASUs for the PGs, according to any classification scheme whatsoever.

To enumerate choices of ASUs for the PGs, basic prerequisites are: 1) ASUs (or rather the tile representing an ASU) have to be asymmetric (of course) and by applying symmetry elements the resulting tiling has to fill the plane isohedrally – and thus monohedrally – without overlaps or gaps. From this follows that 2a) mirror planes or rotation axes must not occur inside an ASU; 2b) mirror planes may form edges of an ASU; 2c) rotation axes may occur on corners (all axes) or edges (2-fold axes only) of an ASU; and 2d) glide planes may occur inside ASUs, but their partial lengths underlie restrictions.

In the present attempt to enumerate, but also to limit, the number of possible ASUs, we will adhere to the following further conditions: 1) we will use only convex straight-line bordered polygons as ASU, i.e. ‘Escher-like’ ASUs are not considered; 2) to assure that the symmetry of a PG is maintained in the resulting tiling, ASUs are graphically marked as asymmetric (the ‘zoo mission’); but, we shall allow for ‘symmetrized’ ASUs, if the unmarked tiling belongs to a smaller cell or to a supergroup within the same crystal system; 3) we will distinguish cell-confined and non-cell-confined ASUs.

Tilings corresponding to all enumerated ASUs of the 17 PGs will be presented graphically, and, where applicable, references to higher symmetric unmarked tilings will be given.

Keywords: plane groups, asymmetric unit, wallpaper groups, tilings, patterns, polygon tilings, isohedral tilings

MS51. Methods and results in chemical crystallography

MS51-P1 Crystal structure and synthesis of 2,2-dimethyl-5-(prop-2-yn-1-yloxy)-4H-benzo[d][1,3]dioxin-4-one

Çiğdem Akmansoy¹, Çiğdem Akmansoy¹, Ömer Çelik^{2,3}, Cumali Çelik⁴, Tuba Şimşir⁵, Mehmet Aslantaş⁵

1. Dicle University, 21280 Diyarbakır, TURKEY
2. Physics Education Department, Ziya Gökalp Education Faculty, Dicle University, 21280 Diyarbakır, TURKEY
3. Dicle University Science and Technology Applied and Research Center, X-ray Lab. 21280, Diyarbakır / TURKEY
4. Yalova Community College, Yalova University, 77200 Yalova, TURKEY
5. Physics Department, KSÜ, Aysar Campus, 46100 Kahramanmaraş, TURKEY

email: c.akmansoy62@gmail.com

The title compound, 2,2-dimethyl-5-(prop-2-yn-1-yloxy)-4H-benzo[d][1,3]dioxin-4-one, ($C_{13}H_{12}O_4$), has been synthesized and characterized by spectroscopic and single crystal X-ray diffraction techniques. The compound (I) is in triclinic form and the unit-cell dimensions for (I) at 296(2)K are $a=6.7498(1)\text{Å}$, $b=7.8207(2)\text{Å}$, $c=11.6311(2)\text{Å}$, $\alpha=87.1780(10)^\circ$, $\beta=83.1690(10)^\circ$, $\gamma=68.2250(10)^\circ$, $V=566.119(19)\text{Å}^3$, $D_x=1.362\text{ g/cm}^3$, and $Z=2$. The R and GOF values for the compound are 0.0388 and 1.078, respectively, for the number of 2311 reflections. The whole molecule is not planar and all the bond lengths and angles are within normal ranges. In the crystal there is a number of strong C-H...O inter-molecular hydrogen bonds present. In addition, three C-H...Cg (min H...Cg=3.031Å and C-H...Cg=141.00°) and an aromatic Cg2...Cg2 [1-x, 1-y, 1-z; Cg2 is the centroid of the (C4-C9) ring] stacking interactions [centroid-centroid distance =5.8212(7)Å] involving neighboring molecules are also observed.

We would like to thank DÜPTAM, University of Dicle, for X-ray data collection and also staff for their assistance without which this work could not have been accomplished.

Keywords: X-ray Crystallography, NMR, IR.

MS51-P2 The synthesis, characterization and crystal structure of 4-((E)-4-bromophenyl)diazenyl)-2-((E)-(phenylimino)methyl)phenol

Fırat Anğay¹, Ömer Çelik¹, Mesut İkiz², Esin İspir²

1. Dept of Physics, Dicle University, Diyarbakır, Turkey
2. Dept of Chemistry, K. Maraş Sütçü İmam University, Kahramanmaraş, Turkey

email: firat86@yahoo.com

Apart from their purely chemical interest, azo-azomethine dyes are being increasingly used in the textile, leather and plastic industries [1]. Regarding the industrial importance of metallized azo dyes relative to their structures, they can be classified into two main types: those in which the azo group participates in the coordination to the metal ion with formation of the chelate ring and those in which it is not [2].

In this study, the synthesis and characterization of 4-((E)-4-bromophenyl)diazenyl)-2-((E)-(phenylimino)methyl)phenol which synthesized from the reaction of (E)-1-(5-((4-bromophenyl)diazenyl)-2-hydroxyphenyl)ethanone with aniline is reported. The structure of the compound, $[C_{21}H_{14}BrN_2O]$, is characterized by single-crystal X-ray diffraction analysis. Its crystallizes in a monoclinic system C1/c space group, with $a=37.4840$, $b=7.0935$, $c=6.2089$, $\beta=97.497^\circ$, $V=1636.79$, $Z=4$, $m(MoK\alpha)=2.522\text{ mm}^{-1}$. The structure was solved by direct methods SHELXS-97 [3], and refined by full matrix least squares techniques on F^2 using SHELXL-97[3] with refinement of F^2 against all reflections. There is an intermolecular O-H...N hydrogen bond and molecules are linked by C-H...pi and hydrogen bonds and weak pi-pi stacking interactions in the crystal structure. All Bond lengths, bond angles, torsion angles and dihedral angles are determined. ORTEP III [4] drawing of completed molecule and atom labelling-scheme are drawn.

[1] Karaer, H.; Gümrükçüoğlu, İ. E., Turk. J. Chem. **1999**, 23, 67-71.

[2] Soliman, E. M.; El-Shabasy, M., Journal Material Science **1994**, 29, 5405-4509.

[3] Sheldrick, G. M., ActaCryst. **2008** A64, 112-122.

[4] Farrugia, L. J., J. Appl. Cryst. **2012** 45, 849-854.

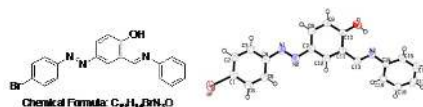


Figure 1. Crystal form of 4-((E)-4-bromophenyl)diazenyl)-2-((E)-(phenylimino)methyl)phenol

Keywords: Azogroup, schiffbase, X-Ray study

MS51-P3 Disulfide complexes: their interaction with silver(I) and copper(II)

Massimo Varisco¹, Aurelien Crochet¹, Katharina M. Fromm¹

1. University of Fribourg, Switzerland

email: massimo.varisco@unifr.ch

Bisisonicotinate disulphide (isoDiS, Figure 1) was widely used in our research group for Au(111) surface pre-treatment in combination with antibacterial complexes[1, 2]. In order to increase our knowledge of the interactions taking place on the surface, crystallographic studies were performed using the metal ions that were coated on the surface during the above-mentioned studies. These ions are silver(I) nitrate and copper(II) nitrate, both have interesting antibacterial properties, but can interact with the sulphur atoms taking the place of the gold surface. Two similar ligands were also taken into account in order to look for a better alternative, thus improving the quality of the developed materials.

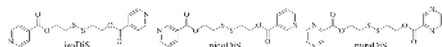


Figure 1. the three different ligands.

Keywords: coordination chemistry, biomaterials

MS51-P4 Chemical composition range and flux crystal growth of $\text{Ca}_{2-x}\text{Li}_{2x}\text{GeO}_4$ solid solutions

Vladimir A. Ivanov¹, Mikhail O. Marychev¹, Pavel V. Andreev¹, Vladimir A. Lykov¹, Mikhail A. Faddeev¹, Iovka Koseva², Velin Nikolov¹

1. N.I. Lobachevsky State University of Nizhni Novgorod, Nizhni Novgorod, Russia

2. Bulgarian Academy of Science, Institute of General and Inorganic Chemistry, Sofia, Bulgaria

email: iv-vlad@yandex.ru

The present studies included: solid state synthesis of $\text{Ca}_{2-x}\text{Li}_{2x}\text{GeO}_4$ where $2x$ varied from 0 to 2; crystal growth from different solutions with Ca_2GeO_4 concentration in the range from 8 to 40 wt. %; X-ray phase analysis for determining the primary crystallizing phase and its cell parameters; elemental analysis of the obtained crystals.

A series of $\text{Ca}_{2-x}\text{Li}_{2x}\text{GeO}_4$ solid solutions with $0 < 2x < 2$, were synthesized by the classical solid state method. X-ray analysis revealed that for $0 < 2x < 0.6$ only $\text{Ca}_2\text{Li}_2\text{GeO}_4$ solid solutions of Ca_2GeO_4 structure crystallized. The cell parameters of this phase linearly decreased upon increasing the lithium concentration, which means that the solutions are in accordance with the Vegard's law. For $2x > 0.6$ the specimens contained two phases: (i) $\text{Ca}_2\text{Li}_2\text{GeO}_4$ with maximum lithium concentration approximately equal to that for $2x = 0.6$ and minimum values of the cell parameters and (ii) $\text{Li}_2\text{CaGeO}_4$.

Both $\text{Li}_2\text{CaGeO}_4$ and Ca_2GeO_4 doped with chromium are promising laser materials with Cr^{4+} emission in the 1.1 – 1.6 μm range. From this point of view it was important to find suitable conditions for the crystal growth from $\text{Li}_2\text{CaGeO}_4$ and from $\text{Ca}_2\text{Li}_2\text{GeO}_4$ solid solutions in order to obtain good-quality crystals with the required dimensions.

High temperature solutions were used for $\text{Li}_2\text{CaGeO}_4$ and $\text{Ca}_2\text{Li}_2\text{GeO}_4$ crystal growth by spontaneous crystallization. $\text{Li}_2\text{CaGeO}_4$ crystals were grown in the concentration range 8-26 wt. % Ca_2GeO_4 in the temperature range 830-980 °C. Crystals with chemical compositions different from those of the $\text{Ca}_{2-x}\text{Li}_{2x}\text{GeO}_4$ solid solutions were grown in the concentration range 26-40 wt % Ca_2GeO_4 in the temperature range 980-1090 °C.

The cell volumes calculated on the basis of the XRD measurements and the lithium concentrations obtained by ICP-OES analysis for some crystals were plotted on the linear dependence between the cell volumes and the lithium concentrations of the $\text{Ca}_{2-x}\text{Li}_{2x}\text{GeO}_4$ solid solutions obtained after solid state synthesis (Fig.). As can be seen, all crystal specimens grown from the high temperature system are $\text{Ca}_2\text{Li}_2\text{GeO}_4$ solid solutions with cell volumes and lithium concentrations similar to those obtained by solid state synthesis.

The research is partly supported by the grant (the agreement of August 27, 2013 № 02.B.49.21.0003 between the Ministry of Education and Science of the Russian Federation and N.I. Lobachevsky State University of Nizhni Novgorod).

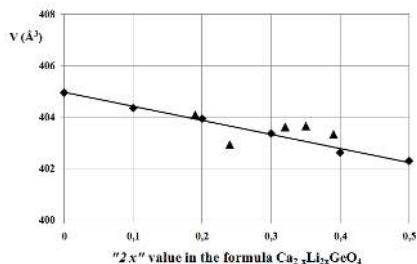


Figure 1. Dependence between the cell volume calculated from X-ray data and Li concentration in $\text{Ca}_{2-x}\text{Li}_x\text{GeO}_4$ solid solutions "square" – solid state synthesis, \blacktriangle (triangle) – single crystals grown from high-temperature $\text{Li}_2\text{MoO}_4\text{-Ca}_2\text{GeO}_4$ solutions.

Keywords: oxide materials, solid state reactions, crystal growth, X-ray diffraction

MS51-P5 Growth crystals KDP from water solutions with KMnO_4

Anna E. Egorova¹, Vadim N. Portnov¹

1. N.I. Lobachevsky State University of Nizhni Novgorod, Nizhni Novgorod, Russia

email: ae-egorova@yandex.ru

Crystals of potassium dihydrogen phosphate are widely applied in science and techniques, medicine and industry. In this work we grew up crystals of potassium dihydrogen phosphate with potassium permanganate up by the temperature differential method with concentration convention condition in thermostat with constant degree of supercooling 3.5-4 °C. It was established KMnO_4 influence on the growth of KDP. The grown crystals have prismatic habit without pinching. Crystals got brown coloring, and it was visible that in sector of growth of a side of a prism concentration of manganese more than in sector of growth of a bipyramid. The structure of this crystal was defined by single crystal X-ray diffraction. X-ray diffraction data for this sample were obtained with Oxford Diffraction (Gemini S) diffractometer on graphite monochromatic Mo-K α radiation ($\lambda=0.71073$ Å) and with CCD Sapphire III detector in the ω -scan mode at a room temperature. The crystal structure was solved by direct methods (Shelx97) and refined by full matrix method (Shelx97). The reflection data were processed by using an analytical absorption correction algorithm. The crystal structure was solved by direct methods and refined by full matrix method. All non-hydrogen atoms were refined with anisotropic correction. Hydrogen atoms were located from difference Fourier synthesis and refined isotropically. Potassium permanganate (KMnO_4) addition to the KDP (KH_2PO_4) solution increases the growth rate of the {100} faces and decreases that of the {101} ones. The complex ion MnHPO_4^{3+} is an impurity affecting {101} face growth rate. The manganese-ion Mn^{3+} replaces the K^+ ion in the KDP structure and causes the change of hydrogen positions. The increase of the {100} face growth rate is connected with the capture of MnO_2 particles. The doping of KDP crystals by manganese decreases the effective quadratic nonlinear sensitivity of crystals [D.A. Vorontsov, A.E. Egorova, E.L. Kim, M.O. Marychev, A.A. Petrova, V.N. Portnov, N.V. Somov. Vestnik of Lobachevsky State University of Nizhni Novgorod, 2010, №5(2), p. 210–213.]. The analysis of element structure of crystals was carried out on a Wavelength Dispersive X-Ray Fluorescence Spectrometer of Shimadzu Lab Center XRF-1800 on intensity K α -line of characteristic x-ray radiation (HRI) of potassium and manganese. So concentration of atoms Mn was measured by Optical Emission Spectrometer Varian ICP-OES.

Keywords: growth crystal, KDP (KH_2PO_4), X-ray

